

RNA modification and non-coding RNAs in human disease

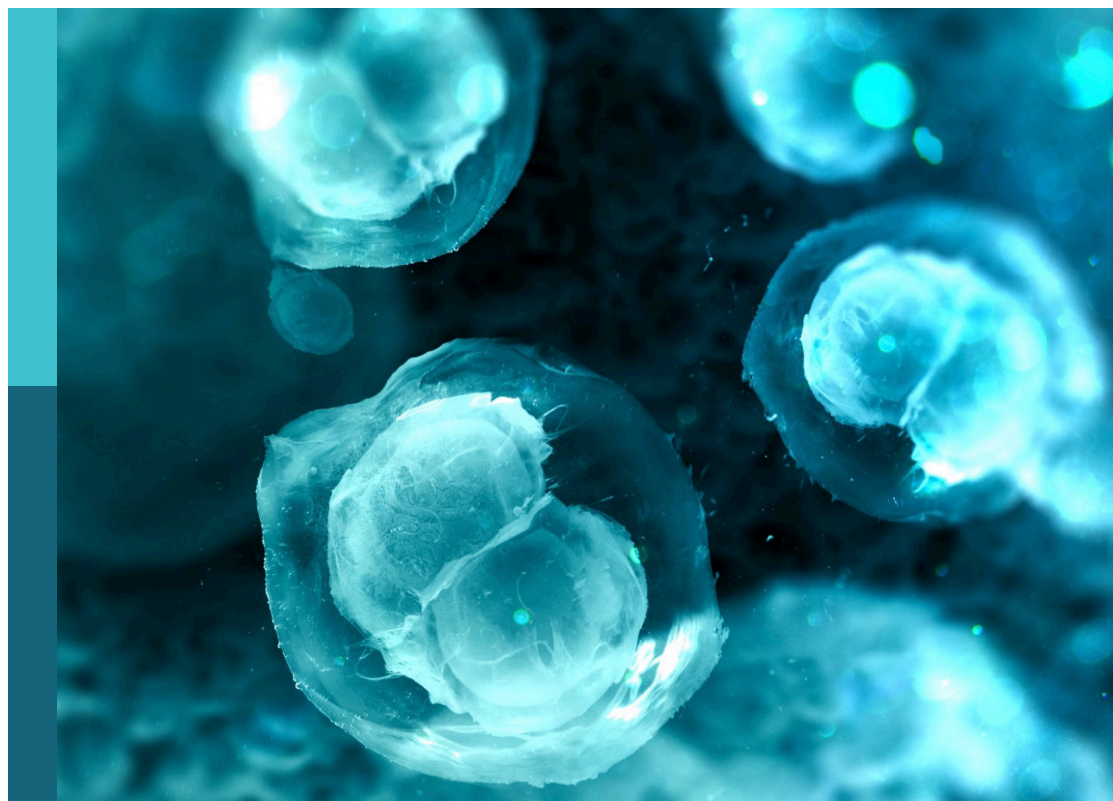
Edited by

Jing Zhang, Jingmin Ou, Tao Zeng, Xiang Zhang, Song Zhao and Jinshui Zhu

Published in

Frontiers in Cell and Developmental Biology

Frontiers in Genetics



FRONTIERS EBOOK COPYRIGHT STATEMENT

The copyright in the text of individual articles in this ebook is the property of their respective authors or their respective institutions or funders. The copyright in graphics and images within each article may be subject to copyright of other parties. In both cases this is subject to a license granted to Frontiers.

The compilation of articles constituting this ebook is the property of Frontiers.

Each article within this ebook, and the ebook itself, are published under the most recent version of the Creative Commons CC-BY licence. The version current at the date of publication of this ebook is CC-BY 4.0. If the CC-BY licence is updated, the licence granted by Frontiers is automatically updated to the new version.

When exercising any right under the CC-BY licence, Frontiers must be attributed as the original publisher of the article or ebook, as applicable.

Authors have the responsibility of ensuring that any graphics or other materials which are the property of others may be included in the CC-BY licence, but this should be checked before relying on the CC-BY licence to reproduce those materials. Any copyright notices relating to those materials must be complied with.

Copyright and source acknowledgement notices may not be removed and must be displayed in any copy, derivative work or partial copy which includes the elements in question.

All copyright, and all rights therein, are protected by national and international copyright laws. The above represents a summary only. For further information please read Frontiers' Conditions for Website Use and Copyright Statement, and the applicable CC-BY licence.

ISSN 1664-8714
ISBN 978-2-83252-080-2
DOI 10.3389/978-2-83252-080-2

About Frontiers

Frontiers is more than just an open access publisher of scholarly articles: it is a pioneering approach to the world of academia, radically improving the way scholarly research is managed. The grand vision of Frontiers is a world where all people have an equal opportunity to seek, share and generate knowledge. Frontiers provides immediate and permanent online open access to all its publications, but this alone is not enough to realize our grand goals.

Frontiers journal series

The Frontiers journal series is a multi-tier and interdisciplinary set of open-access, online journals, promising a paradigm shift from the current review, selection and dissemination processes in academic publishing. All Frontiers journals are driven by researchers for researchers; therefore, they constitute a service to the scholarly community. At the same time, the *Frontiers journal series* operates on a revolutionary invention, the tiered publishing system, initially addressing specific communities of scholars, and gradually climbing up to broader public understanding, thus serving the interests of the lay society, too.

Dedication to quality

Each Frontiers article is a landmark of the highest quality, thanks to genuinely collaborative interactions between authors and review editors, who include some of the world's best academicians. Research must be certified by peers before entering a stream of knowledge that may eventually reach the public - and shape society; therefore, Frontiers only applies the most rigorous and unbiased reviews. Frontiers revolutionizes research publishing by freely delivering the most outstanding research, evaluated with no bias from both the academic and social point of view. By applying the most advanced information technologies, Frontiers is catapulting scholarly publishing into a new generation.

What are Frontiers Research Topics?

Frontiers Research Topics are very popular trademarks of the *Frontiers journals series*: they are collections of at least ten articles, all centered on a particular subject. With their unique mix of varied contributions from Original Research to Review Articles, Frontiers Research Topics unify the most influential researchers, the latest key findings and historical advances in a hot research area.

Find out more on how to host your own Frontiers Research Topic or contribute to one as an author by contacting the Frontiers editorial office: frontiersin.org/about/contact

RNA modification and non-coding RNAs in human disease

Topic editors

Jing Zhang — Shanghai Jiao Tong University, China

Jingmin Ou — Shanghai Jiao Tong University, China

Tao Zeng — Guangzhou laboratory, China

Xiang Zhang — The Chinese University of Hong Kong, China

Song Zhao — First Affiliated Hospital of Zhengzhou University, China

Jinshui Zhu — Shanghai Jiao Tong University, China

Citation

Zhang, J., Ou, J., Zeng, T., Zhang, X., Zhao, S., Zhu, J., eds. (2023). *RNA modification and non-coding RNAs in human disease*.

Lausanne: Frontiers Media SA. doi: 10.3389/978-2-83252-080-2

Table of contents

- 06 **The Methylation Pattern for Knee and Hip Osteoarthritis**
Zhen Wu, Lu Shou, Jian Wang, Tao Huang and Xinwei Xu
- 15 **Hsa_circ_0020095 Promotes Oncogenesis and Cisplatin Resistance in Colon Cancer by Sponging miR-487a-3p and Modulating SOX9**
Yanlai Sun, Zhen Cao, Junqi Shan, Yang Gao, Xin Liu, Dejian Ma and Zengjun Li
- 28 **Circular RNA CircCOL5A1 Sponges the MiR-7-5p/Epac1 Axis to Promote the Progression of Keloids Through Regulating PI3K/Akt Signaling Pathway**
Wenchang Lv, Shengxuan Liu, Qi Zhang, Weijie Hu, Yiping Wu and Yuping Ren
- 45 **Decitabine Induces Change of Biological Traits in Myelodysplastic Syndromes via FOXO1 Activation**
Zheng Zhang, Yan Jia, Feng Xv, Lu-xi Song, Lei Shi, Juan Guo and Chun-kang Chang
- 59 **Circular RNA_PDHx Promotes the Proliferation and Invasion of Prostate Cancer by Sponging MiR-378a-3p**
Yuanshen Mao, Wenfeng Li, Bao Hua, Xin Gu, Weixin Pan, Qi Chen, Bin Xu, Chao Lu and Zhong Wang
- 71 **Insights Into circRNAs: Functional Roles in Lung Cancer Management and the Potential Mechanisms**
Bing Feng, Hao Zhou, Ting Wang, Xinrong Lin, Yongting Lai, Xiaoyuan Chu and Rui Wang
- 83 **The m⁶A Reader YTHDF1 Facilitates the Tumorigenesis and Metastasis of Gastric Cancer via USP14 Translation in an m⁶A-Dependent Manner**
Xiao-Yu Chen, Rui Liang, You-Cai Yi, Hui-Ning Fan, Ming Chen, Jing Zhang and Jin-Shui Zhu
- 98 **miRNA Landscape in Pathogenesis and Treatment of Vogt–Koyanagi–Harada Disease**
Fabian Vega-Tapia, Mario Bustamante, Rodrigo A. Valenzuela, Cristhian A. Urzua and Loreto Cuitino
- 107 **Melatonin Attenuates Chromium (VI)-Induced Spermatogonial Stem Cell/Progenitor Mitophagy by Restoration of METTL3-Mediated RNA N⁶-Methyladenosine Modification**
Yinghua Lv, Tianjiao Li, Manman Yang, Lihong Su, Zhendong Zhu, Sihang Zhao, Wenxian Zeng and Yi Zheng
- 126 **LOC550643, a Long Non-coding RNA, Acts as Novel Oncogene in Regulating Breast Cancer Growth and Metastasis**
Kuo-Wang Tsai, Kian-Hwee Chong, Chao-Hsu Li, Ya-Ting Tu, Yi-Ru Chen, Ming-Cheng Lee, Shih-Hsuan Chan, Lu-Hai Wang and Yao-Jen Chang

- 143 **N6-Methyladenosine Modification Opens a New Chapter in Circular RNA Biology**
Jun Wu, Xin Guo, Yi Wen, Shangqing Huang, Xiaohui Yuan, Lijun Tang and Hongyu Sun
- 156 **KIAA1429 and ALKBH5 Oppositely Influence Aortic Dissection Progression *via* Regulating the Maturation of Pri-miR-143-3p in an m6A-Dependent Manner**
Peng Wang, Zhiwei Wang, Min Zhang, Qi Wu, Feng Shi and Shun Yuan
- 171 **LncRNA RNA Component of Mitochondrial RNA-Processing Endoribonuclease Promotes AKT-Dependent Breast Cancer Growth and Migration by Trapping MicroRNA-206**
Yingdan Huang, Bangxiang Xie, Mingming Cao, Hua Lu, Xiaohua Wu, Qian Hao and Xiang Zhou
- 184 **Expression Profile Analysis of Long Non-coding RNA in OVX Models-Derived BMSCs for Postmenopausal Osteoporosis by RNA Sequencing and Bioinformatics**
Huijie Gu, Zhongyue Huang, Kaifeng Zhou, Guangnan Chen, Chong Bian, Jun Xu and Xiaofan Yin
- 197 **Crosstalk Between MicroRNAs and Circular RNAs in Human Diseases: A Bibliographic Study**
Yu-Meng Chen, Yi-Li Zheng, Xuan Su and Xue-Qiang Wang
- 207 **Expression Profile and Potential Function of Circular RNAs in Peripheral Blood Mononuclear Cells in Male Patients With Primary Gout**
Fei Dai, Quan-Bo Zhang, Yi-Ping Tang, Yi-Xi He, Ting Yi and Yu-Feng Qing
- 220 **Research Progress of circRNAs in Glioblastoma**
Xu Guo and Haozhe Piao
- 234 **Crosstalk Among circRNA/lncRNA, miRNA, and mRNA in Osteoarthritis**
Hui Kong, Ming-Li Sun, Xin-An Zhang and Xue-Qiang Wang
- 265 **Potential Prognostic Value of a Seven m6A-Related LncRNAs Signature and the Correlative Immune Infiltration in Colon Adenocarcinoma**
Xiu-kun Chai, Wei Qi, Chun-Yan Zou, Chen-Xi He, Miao Su and Dong-Qiang Zhao
- 280 **Non-Coding RNAs and Brain Tumors: Insights Into Their Roles in Apoptosis**
Omid Reza Tamtaji, Maryam Derakhshan, Fatemeh Zahra Rashidi Noshabad, Javad Razaviyan, Razie Hadavi, Hamed Jafarpour, Ameneh Jafari, Ali Rajabi, Michael R. Hamblin, Mahmood Khaksary Mahabady, Mohammad Taghizadieh and Hamed Mirzaei

- 298 **Emerging Role and Mechanism of circRNAs in Pediatric Malignant Solid Tumors**
Qiyang Shen, Xingyu Liu, Wei Li, Xu Zhao, Tao Li, Kai Zhou and Jianfeng Zhou
- 311 **Establishment of m7G-related gene pair signature to predict overall survival in colorectal cancer**
Kai Li and Weixing Wang



The Methylation Pattern for Knee and Hip Osteoarthritis

Zhen Wu¹, Lu Shou², Jian Wang¹, Tao Huang^{3*} and Xinwei Xu^{1*}

¹ Department of Orthopaedics, Tongde Hospital of Zhejiang Province, Hangzhou, China, ² Department of Pneumology, Tongde Hospital of Zhejiang Province, Hangzhou, China, ³ Shanghai Institute of Nutrition and Health, Chinese Academy of Sciences, Shanghai, China

OPEN ACCESS

Edited by:

Jing Zhang,
Shanghai Jiao Tong University, China

Reviewed by:

Jun Xu,
Shanghai Jiao Tong University, China
Hongting Jin,
Zhejiang Chinese Medical University,
China

*Correspondence:

Xinwei Xu
xuxinwei011@163.com
Tao Huang
tohuangtao@126.com

Specialty section:

This article was submitted to
Epigenomics and Epigenetics,
a section of the journal
Frontiers in Cell and Developmental
Biology

Received: 02 September 2020

Accepted: 22 October 2020

Published: 06 November 2020

Citation:

Wu Z, Shou L, Wang J, Huang T
and Xu X (2020) The Methylation
Pattern for Knee and Hip
Osteoarthritis.
Front. Cell Dev. Biol. 8:602024.
doi: 10.3389/fcell.2020.602024

Osteoarthritis is one of the most prevalent chronic joint diseases for middle-aged and elderly people. But in recent years, the number of young people suffering from the disease increases quickly. It is known that osteoarthritis is a common degenerative disease caused by the combination and interaction of many factors such as natural and environmental factors. DNA methylations reflect the effects of environmental factors. Several researches on DNA methylation at specific genes in OA cartilage indicated the great potential roles of DNA methylation in OA. To systematically investigate the methylation pattern in knee and hip osteoarthritis, we analyzed the methylation profiles in cartilage of 16 OA hip samples, 19 control hip samples and 62 OA knee samples. 12 discriminative methylation sites were identified using advanced minimal Redundancy Maximal Relevance (mRMR) and Incremental Feature Selection (IFS) methods. The SVM classifier of these 12 methylation sites from genes like MEIS1, GABRG3, RXRA, and EN1, can perfectly classify the OA hip samples, control hip samples and OA knee samples evaluated with LOOCV (Leave-One Out-Cross Validation). These 12 methylation sites can not only serve as biomarker, but also provide underlying mechanism of OA.

Keywords: osteoarthritis, methylation, Support Vector Machine, minimal Redundancy Maximal Relevance, Incremental Feature Selection

INTRODUCTION

Osteoarthritis is one of the most prevalent chronic joint diseases, characterized by the loss, degeneration and calcification of articular cartilage (Im and Choi, 2013). It often occurs in middle-aged and elderly people, and the incidence in females is significantly higher than that in males (Rushton et al., 2014). Research shows that in recent years, with the quickening pace of life, the number of young people suffering from the disease began to increase, ultimately resulting in sustained growth in the social burden (den Hollander and Meulenbelt, 2015).

Despite the unremitting efforts of many scholars, the pathogenesis of osteoarthritis is still not clear yet. Current studies indicate that osteoarthritis is a common degenerative disease caused by the combination and interaction of many factors such as natural and environmental factors (Felson, 2004). The increase in age, damage of tissue and cell, obesity, the overuse of joints and genetic susceptibility are known as OA major risk factors (Hunter et al., 2002).

Osteoarthritis mainly involves the cartilage of the weight-bearing joints, followed by the synovium. At present, it is generally believed that the central part of OA mechanism is the degeneration of articular cartilage, resulting from the imbalance between anabolism and catabolism

in the cartilage extracellular matrix caused by mechanical and biological factors (Martel-Pelletier et al., 2008). Since these changes are reported to be caused by genetic changes in the chondrocyte associated with the OA epigenetic mechanism, it's assumed that the epigenetic changes of chondrocytes may be a key driver in osteoarthritis (Reynard and Loughlin, 2012).

Studies on epigenetic of OA have suggested that these mechanisms is very significant during the onset and progression of disease (Barter and Young, 2013). Despite the fact that there exist many epigenetic mechanisms like DNA methylation, miRNA and histone modifications (Aref-Eshghi et al., 2015), the involvement of DNA methylation in OA pathophysiology is the most studied subject (Rice et al., 2020; Sun et al., 2020; Zhou et al., 2020). DNA methylation mainly occurs at CpG dinucleotides, selectively adding a methyl group to cytosine to form 5-methylcytosine under the catalysis of DNA methyltransferase (DNMT). DNA methylation is involved with transcriptional inhibition by preventing the binding of proteins to gene promoters and changing chromatin structure (Loeser, 2008). The changes of methylation status can accelerate the development of OA (Miranda-Duarte, 2018). Thus, further studies on the mechanisms involved in DNA methylation is another way to develop new OA therapy strategies.

There have been several researches on DNA methylation at specific genes in OA cartilage. For instance, the expression of matrix metalloproteinase genes has been reported to be upregulated in OA chondrocytes, resulting in extracellular matrix degradation (Kevorkian et al., 2004). In addition, genes associated with OA chondrocytes like GDF-5, SOX-9, DIO-2, and ADAMTS-4 were also suggested to be differentially expressed between OA cartilage and control group (Reynard and Loughlin, 2012). It has also been reported that the IL1B promoter is demethylated in articular chondrocytes as a response to inflammatory cytokine signaling (Hashimoto et al., 2009).

OA happens in knees and hips mostly. But knee OA is more common than hip OA. Although articular cartilage of hip and knee joints have substantial similar characters and functions, the disease progression and subsequent treatment may be different between the two joints (Pereira et al., 2016). Transcriptomic studies have indicated that genes dysregulated in hip and knee OA have great difference (Loughlin and Reynard, 2015), so does the methylation patterns in hip and knee OA samples (Rushton et al., 2014). These findings highlight the importance of the separation of OA researches from skeletal sites and help us understand the cartilage homeostasis.

The cure for osteoarthritis is mainly to mitigate pain, improve the function of the joints and avoid the side effects of the treatment as far as possible. However, due to the slow progress of osteoarthritis and the lack of sensitive detection methods to identify early OA changes, it is difficult to find disease-modifying drugs at present. Epigenetic markers mentioned above can detect the phenotypes of various chondrocytes, including articular cartilage homeostasis, chondrogenic differentiation and

the development of OA, which may provide new targets and strategies for drug treatment of OA.

To systematically investigate the methylation pattern in knee and hip osteoarthritis, we analyzed the methylation profiles in cartilage of 16 OA hip samples, 19 control hip samples and 62 OA knee samples. 12 discriminative methylation sites were identified based on minimal Redundancy Maximal Relevance (mRMR) and Incremental Feature Selection (IFS). mRMR is a widely used power feature selection method (Chen et al., 2017b, 2018b, 2019c; Cai et al., 2018; Li and Huang, 2018; Li et al., 2019a) which considers not only the relevance with OA status but also the redundancy among methylation status. It can identify a small but well performed methylation signature. What's more, an SVM (Support Vector Machine) (Chen et al., 2017c, 2019a,b,d; Sun et al., 2018; Li et al., 2019b; Pan et al., 2019) OA classifier was built based on these 12 methylation sites and it can perfectly classify the OA hip samples, control hip samples and OA knee samples evaluated with LOOCV (Leave-One Out-Cross Validation) (Chen et al., 2014; Zhang N. et al., 2015; Cheng et al., 2016; Li et al., 2018; Wang and Huang, 2019). Although the model needs to be validated on independent large dataset, these 12 methylation sites provided clues for the mechanisms of OA.

MATERIALS AND METHODS

The Cartilage DNA Methylation Profiles of OA Hips, Control Hips and OA Knees

We downloaded the cartilage DNA methylation profiles of 16 OA hip samples, 19 control hip samples and 62 OA knee samples from publicly available GEO (Transcript Expression Omnibus) database under accession number of GSE63695 (Rushton et al., 2014). The DNA methylations were measured using Illumina Human Methylation 450 Array. There were 4,82,421 probes corresponding to methylation sites. The processed beta values that were normalized with preprocess Funnorm function from R package minfi were used for further analysis.

Identify the Representative OA Methylation Sites

To identify the most discriminative features among different groups, many analysis methods have been developed (Huang et al., 2008; Cai et al., 2010; Zhang et al., 2012, 2016, 2017; Li et al., 2014; Zhang P.W. et al., 2015; Chen et al., 2018a; Wang et al., 2018). ANOVA (Analysis of Variance) is an obvious choice. But such statistical methods don't consider the relationship between features, therefore a lot of redundant features will be selected.

In our study, the number of features, i.e., methylation sites, was extremely large. Obviously, many of them were redundant. To select the representative features, we adopted mRMR method developed by Peng et al. (2005) to reduce redundancy of selected genes. This method has been widely used and proven to be very effective in handling high dimensional data (Niu et al., 2013; Zhao et al., 2013; Zhou et al., 2015; Zhang et al., 2016; Li and Huang, 2017; Liu et al., 2017). The C++ version

Abbreviations: mRMR, minimal Redundancy Maximal Relevance; SVM, Support Vector Machine; IFS, Incremental Feature Selection; DNMT, DNA methyltransferase; LOOCV, Leave-One Out-Cross Validation; GEO, Transcript Expression Omnibus.

mRMR program downloaded from <http://home.penglab.com/proj/mRMR/> was used in this study.

Its idea is simple and clear. Let us use Ω to denote all the 4,82,421 methylation sites, Ω_s to denote the selected m sites, and Ω_g to denote the n sites to be selected.

First, we evaluated the relevance of site g from Ω_g with three-class sample labels l (OA hips, control hips and OA knees) was calculated with mutual information (I) equation (Sun et al., 2012; Huang and Cai, 2013):

$$I(g, l) \quad (1)$$

Meanwhile, the redundancy of site g with the m selected sites g_i ($i = 1, 2, \dots, m$) in Ω_s can also be calculated based on mutual information:

$$\frac{1}{m} \left(\sum_{g_i \in \Omega_s} I(g, g_i) \right) \quad (2)$$

The goal can be characterized as maximizing the function which balances the relevance and redundancy:

$$\max_{g_j \in \Omega_g} \left[I(g_j, l) - \frac{1}{m} \left(\sum_{g_i \in \Omega_s} I(g_j, g_i) \right) \right] \quad (j = 1, 2, \dots, n) \quad (3)$$

Each time, one best site that maximized this function will be moved from Ω_g to Ω_s . Eventually, all the sites will be ranked based on their relevance with sample labels and redundancy between each other. The ranked methylation sites from large to small can be represented as:

$$S = \{g'_1, g'_2, \dots, g'_r, \dots, g'_N\} \quad (4)$$

The top ranked methylation sites have better discriminative ability.

To reduce the computational complexity, we focused on the top 300 mRMR sites for further analysis which should be enough to classify the samples and suitable as biomarkers.

Optimize the Discriminative Methylation Sites for OA

Although we identified the non-redundant OA sites using mRMR method, we still wanted to obtain the methylation site combinations which can classify the OA hips, control hips and OA knees. To do so, we applied a widely used optimization method, IFS (Jiang et al., 2013; Li et al., 2014; Shu et al., 2014; Zhang et al., 2014; Huang et al., 2015; Zhang P.W. et al., 2015; Chen et al., 2017a).

Based on the ranked mRMR site list, each time, the top r sites $\{g'_1, g'_2, \dots, g'_r\}$ were chosen to construct a SVM (Support Vector Machine) classifier and its accuracy evaluated with LOOCV (Chen et al., 2014; Zhang N. et al., 2015; Cheng et al., 2016; Li et al., 2018; Wang and Huang, 2019) was recorded. SVM is classical machine learning classifier with a wide range of applications in biomedicine (Chen et al., 2017c, 2019b; Li et al., 2018, 2019b; Sun et al., 2018; Pan et al., 2019). The R function `svm` in package `e1071`¹ was used to apply the SVM method. LOOCV,

¹<https://CRAN.R-project.org/package=e1071>

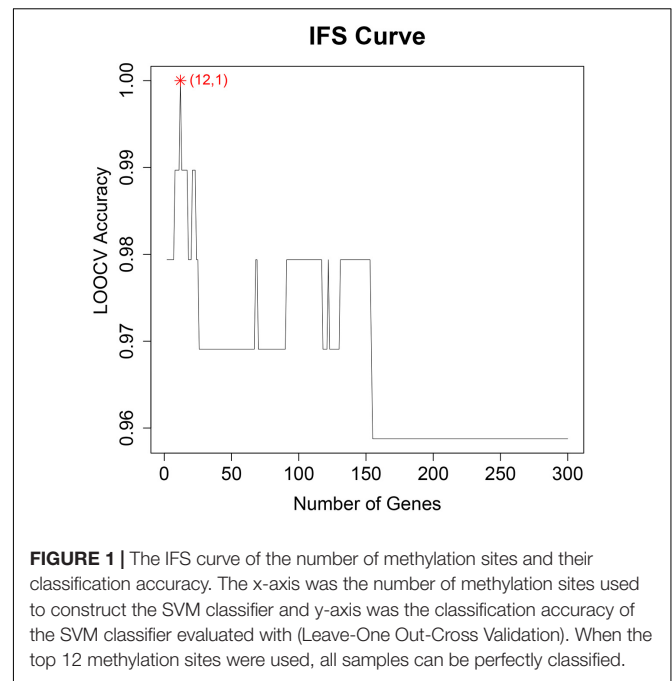


FIGURE 1 | The IFS curve of the number of methylation sites and their classification accuracy. The x-axis was the number of methylation sites used to construct the SVM classifier and y-axis was the classification accuracy of the SVM classifier evaluated with (Leave-One Out-Cross Validation). When the top 12 methylation sites were used, all samples can be perfectly classified.

as known as Jackknife test, is a widely used objective method to evaluate the prediction performance of classifiers (Chou, 2011). Each time, one sample was treated as test sample while the other samples were used to train the model. At last, each sample had been tested for once and the classes of all samples were predicted. By comparing the predicted classes and actual classes, we can calculate the LOOCV accuracy.

After 300 rounds, the performances of the 300 methylation subsets were tested. By analyzing the number of used methylation sites and the performance of corresponding classifier, we can easily find the best methylation sites.

RESULTS AND DISCUSSION

The Representative OA Methylation Sites

In the OA methylation dataset, there were 4,82,421 features. On one hand, the number of features was large; on the other hand, there were redundancy among these methylation sites. To reduce the number of features to a reasonable number for further study, we adopted the mRMR method.

The methylation sites were ranked based on both their relevance with the sample labels, i.e., OA hips, control hips or OA knees, and their redundancy with each other. In other words, only the methylation site that exhibited different pattern with already selected sites will be selected from the candidate methylation site pool. With the mRMR analysis, we identified the top 300 most representative OA methylation sites.

The Discriminative Methylation Sites for OA

Although the mRMR method considered the relevance between features and sample labels, but it was balanced with redundancy.

TABLE 1 | The 12 discriminative methylation sites for OA.

Rank	Probe	Chromosome	Coordinate	Gene	mRMR score
1	cg09462924	2	66666470	MEIS1	0.943
2	cg22118147	5	172144013	-	0.263
3	cg18576667	15	27597409	GABRG3	0.328
4	cg07533951	12	114879558	-	0.284
5	cg14545975	9	137297213	FXRA	0.245
6	cg05877497	2	66667946	MEIS1	0.264
7	cg21811143	2	119599748	EN1	0.219
8	cg09989996	1	753376	FAM87B	0.235
9	cg19738283	2	176976802	HOXD10	0.244
10	cg02824888	12	115129011	-	0.226
11	cg04288999	2	66667852	MEIS1	0.238
12	cg00995986	2	66665428	MEIS1	0.214

We would like to find the methylation sites that can best classify different OA samples. These sites not only should be concise, but also have great discriminative ability.

To find the best discriminative methylation sites for OA, we plotted the IFS results in **Figure 1** in which, the *x*-axis was the number of methylation sites and the *y*-axis was the LOOCV accuracy of the SVM classifier based these sites. It can be seen that when the top 12 mRMR sites was used, the ACC was the highest. All samples were correctly classified. The 12 chosen methylation sites were given in **Table 1**. The chromosome positions were from Genome Build 37 (hg19). We must be cautious that this accuracy

needs to be validated on an independent large OA cohort. But since there is no other similar dataset, we can only try our best and evaluate it with objective LOOCV method. The results provided clues about the difference between OA and control and the difference between hip OA and knee OA and worth to be further investigated.

To explore the methylation levels of the 12 sites in different disease status, we plotted the heatmap of them in all samples in **Figure 2**. It can be seen that OA hip were more similar with OA knee than with control hip. The disease status surpassed the tissue specificity. As for OA hip and OA knee, there were nine highly methylated sites in OA knee (cg21811143, cg19738283, cg00995986, cg09462924, cg05877497, cg04288999, cg07533951, cg14545975, and cg02824888) while there were three highly methylated sites in OA hip (cg18576667, cg22118147, and cg09989996).

The Relationship Between the Methylation Signature of Cartilage Tissue and Gene Expression Signature of Blood in OA

There have been studies of blood expression profiles of OA (Ramos et al., 2014; Li et al., 2018). Ramos et al. identified 27 blood expression signature genes of OA (Ramos et al., 2014) and Li et al. (2018) identified 23 blood expression signature genes. By combining them, we obtain 46 blood expression signature genes. There was no overlap between the 46 blood

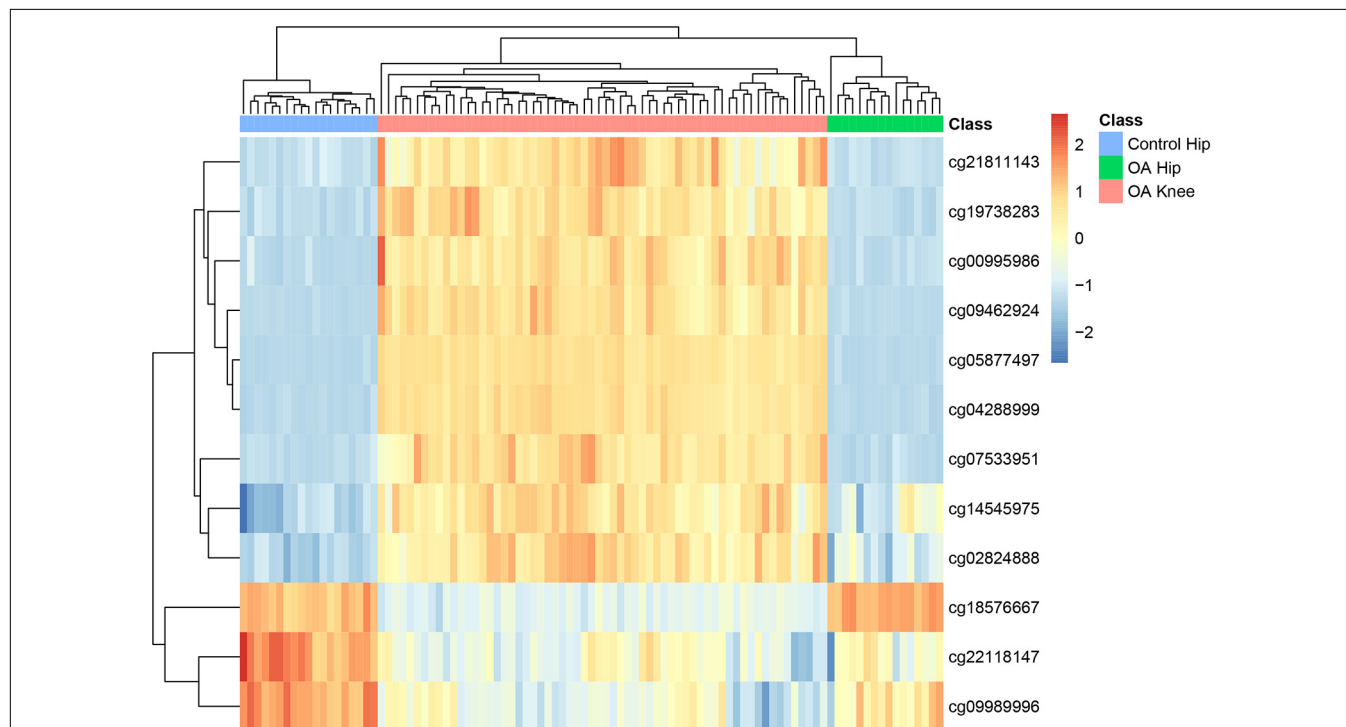
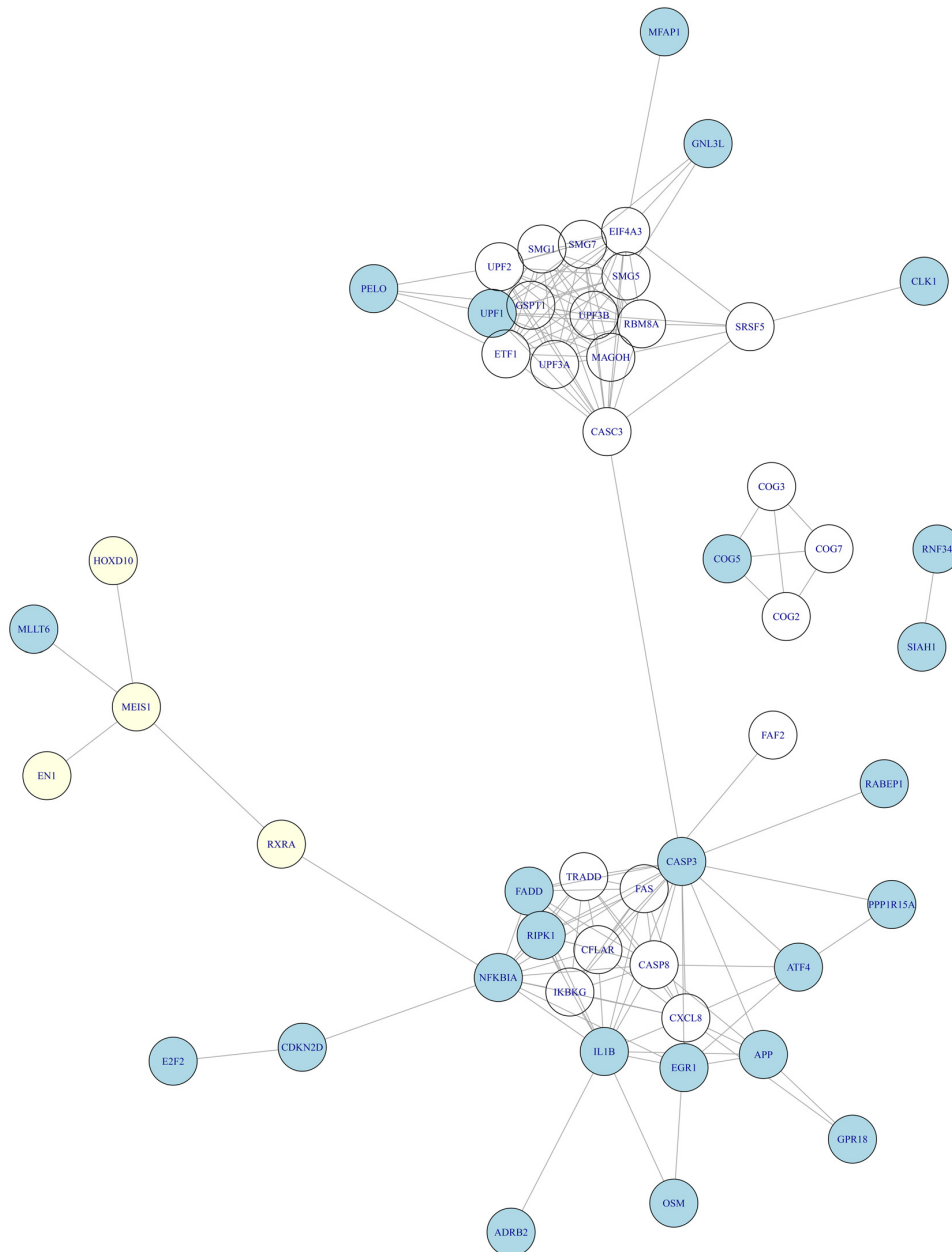


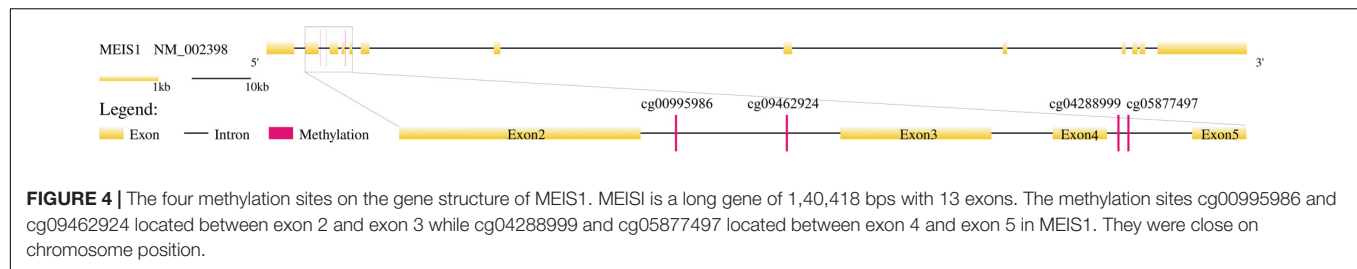
FIGURE 2 | The heatmap of the 12 methylation sites in OA hips, control hips and OA knees. Each row corresponded to the scaled methylation level of one site and each column corresponded to a sample which could be OA hip, control hip or OA knee. It can be seen that all samples were clustered into the right groups.



expression signature genes and our cartilage tissue methylation signature genes. But when we mapped them onto STRING network² (Szklarczyk et al., 2018), the network relationship between tissue methylation genes and blood expression genes (**Figure 3**) was clear. It can be seen that MEIS1 was the hub of methylation signature which can interact with the other three methylation genes (EN1, RXRA, and HOXD10) and the

The Biological Functions of the Discriminative Methylation Sites for OA

²<http://string-db.org>, version: 11.0



to the same gene, MEIS1 (Meis Homeobox 1). We checked the consistency of these four MEIS1 methylation sites in OA hips, control hips and OA knees in **Figure 2** and we found they shared similar pattern although they were not identical. MEIS1 is a long gene of 1,40,418 bps with 13 exons. We mapped the four methylation sites onto the gene structure of MEIS1 (**Figure 4**). The methylation sites cg00995986 and cg09462924 located between exon 2 and exon 3 while cg04288999 and cg05877497 located between exon 4 and exon 5. They were close on chromosome position. There have been reports that MEIS1 was associated with blood and epithelial cancers, such as acute leukemia and skin cancer (Okumura et al., 2014; Wang et al., 2014). As a transcription factor, MEIS1 can bind chromatin DNA and regulate pluripotency of stem cells (Okumura et al., 2014). It is generally considered as an oncogene which accelerate development (Wang et al., 2014). There are no reported associations between MEIS1 and osteoarthritis. MEIS1 may serve as a novel OA biomarker, especially for distinguishing the difference between hip OA and knee OA.

Another interesting methylation site was cg21811143 which locate in EN1 (Engrailed Homeobox 1). It plays a role in controlling development of the central nervous system (CNS) (Webb et al., 2008) and segmentation course, where it is required for the formation of posterior compartments (Lawrence and Johnston, 1984). Recent studies have identified EN1 gene as a decisive factor of bone mineral density (BMD) via whole-genome sequencing (Zheng et al., 2015), while higher BMD was considered to be involved with OA in many cross-sectional and longitudinal epidemiological studies (Belmonte-Serrano et al., 1993). SNP rs4144782 in EN1 was reported to be significantly associated with increased risk of knee OA (OR = 1.26; 95% CI: 1.05–1.50, p -value = 0.012) (Li et al., 2017). What's more, the EN1 mRNA levels were differentially expressed between Knee and hip Intra-articular adipose tissues (IAATs) and Subcutaneous adipose tissue (SCAT) (Eymard et al., 2017). Its expression was strongly decreased in all IAATs compared with SCAT (Infrapatellar fat pad, IFP: 0.3-fold, p = 0.006; Suprapatellar fat pad, SPFP: 0.2-fold, p = 0.006; and Acetabular fat pad, AFP: 0.3-fold, p = 0.046) (Eymard et al., 2017). The genomic, methylation and transcriptomic evidences of the association between EN1 and OA make it a strong candidate OA gene worth further experimental validation.

GABRG3 and RXRA, were gamma-aminobutyric acid (GABA) receptor and retinoid X receptor, respectively. Beside autistic disorder (Menold et al., 2001) and Alzheimer's disease (Iwakiri et al., 2009), GABRG3 is associated with alcohol

dependence by affecting disinhibition and hyperexcitability of CNS (Dick et al., 2004; Edenberg and Foroud, 2006). Maybe it can also affect how OA patients feel about pain. For RXRA, its methylation status was reported to be associated with childhood bone mineral content (BMC) (Harvey et al., 2014).

The methylation sites that can't be annotated to genes may functions through trans-regulation (van Eijk et al., 2012). Their roles can be investigated with integrative analysis of multi-omics OA data in the future.

Another issue of this work was the small sample size. It will overestimate the prediction performance. The confounding factors and disease heterogeneity will be difficult to detect in such small dataset. The signature needs to be validated on large cohorts from different medical centers.

CONCLUSION

As a chronic joint disease, osteoarthritis is very common in elder people. Even young people are more and more likely to have OA symptoms due to the quickening pace of life. OA happens in knees and hips mostly, but knee OA is more common than hip OA. The disease progression and treatment of hip and knee OA are different. Since the epigenetic factor plays key roles in OA, we systematically analyzed the DNA methylation profiles of cartilage from 16 OA hip samples, 19 control hip samples and 62 OA knee samples. With advanced feature selection methods, 12 OA discriminative methylation sites were selected from a total of 4,82,421 sites. These sites corresponded to genes like MEIS1, EN1, GABRG3, and RXRA. These results provided not only novel OA biomarkers, but also possible mechanisms that worth further investigation in an independent large cohort.

DATA AVAILABILITY STATEMENT

Publicly available datasets were analyzed in this study. This data can be found here: <https://www.ncbi.nlm.nih.gov/geo/query/acc.cgi?acc=GSE63695>.

AUTHOR CONTRIBUTIONS

TH and XX designed the experiment. ZW performed the experiment. LS and JW participant in the data analysis. ZW, TH, and XX wrote the manuscript. All authors contributed to the article and approved the submitted version.

FUNDING

This work was supported by the National Natural Science Foundation of China (31701151), National Key R&D Program of China (2018YFC0910403),

Shanghai Municipal Science and Technology Major Project (Grant No. 2017SHZDZX01), Shanghai Sailing Program (16YF1413800), and the Youth Innovation Promotion Association of Chinese Academy of Sciences (CAS) (2016245).

REFERENCES

- Aref-Eshghi, E., Zhang, Y., Liu, M., Harper, P. E., Martin G., Furey, A. (2015). Genome-wide DNA methylation study of hip and knee cartilage reveals embryonic organ and skeletal system morphogenesis as major pathways involved in osteoarthritis. *BMC Musculoskelet. Disord.* 16:287. doi: 10.1186/s12891-015-0745-5
- Barter, M. J., and Young, D. A. (2013). Epigenetic mechanisms and non-coding RNAs in osteoarthritis. *Curr. Rheumatol. Rep.* 15:353. doi: 10.1007/s11926-013-0353-z
- Belmonte-Serrano, M. A., Bloch, D. A., Lane, N. E., Michel, B. E., and Fries, J. F. (1993). The relationship between spinal and peripheral osteoarthritis and bone density measurements. *J. Rheumatol.* 20, 1005–1013.
- Cai, L., Huang, T., Su, J., Zhang, X., Chen, W., Zhang, F., et al. (2018). Implications of newly identified brain eQTL genes and their interactors in schizophrenia. *Mol. Ther. Nucleic Acids* 12, 433–442. doi: 10.1016/j.omtn.2018.05.026
- Cai, Y. D., Huang, T., Feng, K. Y., Hu, L., and Xie, L. (2010). A unified 35-gene signature for both subtype classification and survival prediction in diffuse large B-cell lymphomas. *PLoS One* 5:e12726. doi: 10.1371/journal.pone.0012726
- Chen, L., Li, J., Zhang, Y. H., Feng, K., Wang, S., Zhang, Y., et al. (2017a). Identification of gene expression signatures across different types of neural stem cells with the Monte-Carlo feature selection method. *J. Cell. Biochem.* 119, 3394–3403.
- Chen, L., Wang, S., Zhang, Y. H., Li, J., Xing, Z. H., Yang, J., et al. (2017b). Identify key sequence features to improve CRISPR sgRNA efficacy. *IEEE Access* 5, 26582–26590. doi: 10.1109/ACCESS.2017.2775703
- Chen, L., Zhang, Y.-H., Wang, S., Zhang, Y., Huang, T., and Cai, Y.-D. (2017c). Prediction and analysis of essential genes using the enrichments of gene ontology and KEGG pathways. *PLoS One* 12:e0184129. doi: 10.1371/journal.pone.0184129
- Chen, L., Li, J., Zhang, Y. H., Feng, K., Wang, S., Zhang, Y., et al. (2018a). Identification of gene expression signatures across different types of neural stem cells with the Monte-Carlo feature selection method. *J. Cell. Biochem.* 119, 3394–3403. doi: 10.1002/jcb.26507
- Chen, L., Zhang, Y. H., Huang, G., Pan, X., Wang, S., Huang, T., et al. (2018b). Discriminating cirRNAs from other lncRNAs using a hierarchical extreme learning machine (H-ELM) algorithm with feature selection. *Mol. Genet. Genomics* 293, 137–149. doi: 10.1007/s00438-017-1372-7
- Chen, L., Lu, J., Zhang, N., Huang, T., and Cai, Y. D. (2014). A hybrid method for prediction and repositioning of drug anatomical therapeutic chemical classes. *Mol. Biosyst.* 10, 868–877. doi: 10.1039/c3mb70490d
- Chen, L., Pan, X., Zeng, T., Zhang, Y., Huang, T., and Cai, Y. (2019a). Identifying essential signature genes and expression rules associated with distinctive development stages of early embryonic cells. *IEEE Access* 7, 128570–128578. doi: 10.1109/ACCESS.2019.2939556
- Chen, L., Pan, X., Zhang, Y.-H., Kong, X., Huang, T., and Cai, Y.-D. (2019b). Tissue differences revealed by gene expression profiles of various cell lines. *J. Cell. Biochem.* 120, 7068–7081. doi: 10.1002/jcb.27977
- Chen, L., Pan, X., Zhang, Y.-H., Liu, M., Huang, T., and Cai, Y.-D. (2019c). Classification of widely and rarely expressed genes with recurrent neural network. *Comput. Struct. Biotechnol. J.* 17, 49–60. doi: 10.1016/j.csbj.2018.12.002
- Chen, L., Pan, X., Zhang, Y. H., Hu, X., Feng, K., Huang, T., et al. (2019d). Primary tumor site specificity is preserved in patient-derived tumor xenograft models. *Front. Genet.* 10:738. doi: 10.3389/fgene.2019.00738
- Cheng, S., Zhu, C., Chu, C., Huang, T., Kong, X., and Zhu, L. C. (2016). Prediction of bioactive compound pathways using chemical interaction and structural information. *Comb. Chem. High Throughput Screen.* 19, 161–169. doi: 10.2174/1386207319666151110123611
- Chou, K. C. (2011). Some remarks on protein attribute prediction and pseudo amino acid composition. *J. Theor. Biol.* 273, 236–247. doi: 10.1016/j.jtbi.2010.12.024
- den Hollander, W., and Meulenbelt, I. (2015). DNA methylation in osteoarthritis. *Curr. Genomics* 16, 419–426. doi: 10.2174/1389202916666150817212711
- Dick, D. M., Edenberg, H. J., Xuei, X., Goate, A., Kuperman, S., Schuckit, M., et al. (2004). Association of GABRG3 with alcohol dependence. *Alcohol. Clin. Exp. Res.* 28, 4–9. doi: 10.1097/01.alc.0000108645.54345.98
- Edenberg, H. J., and Foroud, T. (2006). The genetics of alcoholism: identifying specific genes through family studies. *Addict. Biol.* 11, 386–396. doi: 10.1111/j.1369-1600.2006.00035.x
- Eymard, F., Pigenet, A., Citadelle, D., Tordjman, J., Foucher, L., Rose, C., et al. (2017). Knee and hip intra-articular adipose tissues (IAATs) compared with autologous subcutaneous adipose tissue: a specific phenotype for a central player in osteoarthritis. *Ann. Rheum. Dis.* 76, 1142–1148. doi: 10.1136/annrheumdis-2016-210478
- Felson, D. T. (2004). An update on the pathogenesis and epidemiology of osteoarthritis. *Radiol. Clin. North Am.* 42, 1–9. doi: 10.1016/s0033-8389(03)00161-1
- Harvey, N. C., Sheppard, A., Godfrey, K. M., McLean, C., Garratt, E., Ntani, G., et al. (2014). Childhood bone mineral content is associated with methylation status of the RXRA promoter at birth. *J. Bone Miner. Res.* 29, 600–607. doi: 10.1002/jbmr.2056
- Hashimoto, K., Oreffo, R. O., Gibson, M. B., Goldring, M. B., and Roach, H. I. (2009). DNA demethylation at specific CpG sites in the IL1B promoter in response to inflammatory cytokines in human articular chondrocytes. *Arthritis Rheum* 60, 3303–3313. doi: 10.1002/art.24882
- Huang, T., and Cai, Y.-D. (2013). An information-theoretic machine learning approach to expression QTL analysis. *PLoS One* 8:e67899. doi: 10.1371/journal.pone.0067899
- Huang, T., Shu, Y., and Cai, Y.-D. (2015). Genetic differences among ethnic groups. *BMC Genomics* 16:1093. doi: 10.1186/s12864-015-2328-0
- Huang, T., Tu, K., Shyr, Y., Wei, C. C., Xie, L., and Li, Y. X. (2008). The prediction of interferon treatment effects based on time series microarray gene expression profiles. *J. Transl. Med.* 6:44. doi: 10.1186/1479-5876-6-44
- Hunter, D. J., March, L., and Sambrook, P. N. (2002). Knee osteoarthritis: the influence of environmental factors. *Clin. Exp. Rheumatol.* 20, 93–100.
- Im, G. I., and Choi, Y. J. (2013). Epigenetics in osteoarthritis and its implication for future therapeutics. *Expert Opin. Biol. Ther.* 13, 713–721. doi: 10.1517/14712598.2013.764410
- Iwakiri, M., Mizukami, K., Ikonovic, M. D., Ishikawa, M., Abrahamson, E. E., DeKosky, S. T., et al. (2009). An immunohistochemical study of GABA A receptor gamma subunits in Alzheimer's disease hippocampus: relationship to neurofibrillary tangle progression. *Neuropathology* 29, 263–269. doi: 10.1111/j.1440-1789.2008.00978.x
- Jiang, Y., Huang, T., Chen, L., Gao, Y. F., Cai, Y., and Chou, K. C. (2013). Signal propagation in protein interaction network during colorectal cancer progression. *Biomed Res. Int.* 2013:287019. doi: 10.1155/2013/287019
- Kevorkian, L., Young, D. A., Darrah, C., Donnell, S. T., Shepstone, L., Porter, S., et al. (2004). Expression profiling of metalloproteinases and their inhibitors in cartilage. *Arthritis Rheum* 50, 131–141. doi: 10.1002/art.11433
- Lawrence, P. A., and Johnston, P. (1984). On the role of the engrailed+ gene in the internal organs of Drosophila. *EMBO J.* 3, 2839–2844. doi: 10.1002/j.1460-2075.1984.tb02217.x

- Li, B. Q., You, J., Huang, T., and Cai, Y. D. (2014). Classification of non-small cell lung cancer based on copy number alterations. *PLoS One* 9:e88300. doi: 10.1371/journal.pone.0088300
- Li, H., Zhang, X., Cao, Y., Hu, S., Peng, F., Zhou, J., et al. (2017). Association between EN1 rs4144782 and susceptibility of knee osteoarthritis: a case-control study. *Oncotarget* 8, 36650–36657. doi: 10.18632/oncotarget.16842
- Li, J., and Huang, T. (2017). Predicting and analyzing early wake-up associated gene expressions by integrating GWAS and eQTL studies. *Biochim. Biophys. Acta Mol. Basis Dis.* 1864(6 Pt B), 2241–2246. doi: 10.1016/j.bbadis.2017.10.036
- Li, J., and Huang, T. (2018). Predicting and analyzing early wake-up associated gene expressions by integrating GWAS and eQTL studies. *Biochim. Biophys. Acta* 1864(6 Pt B), 2241–2246. doi: 10.1016/j.bbadis.2017.10.036
- Li, J., Lan, C.-N., Kong, Y., Feng, S.-S., and Huang, T. (2018). Identification and analysis of blood gene expression signature for osteoarthritis with advanced feature selection methods. *Front. Genet.* 9:246. doi: 10.3389/fgene.2018.00246
- Li, J., Lu, L., Zhang, Y. H., Liu, M., Chen, L., Huang, T., et al. (2019a). Identification of synthetic lethality based on a functional network by using machine learning algorithms. *J. Cell. Biochem.* 120, 405–416. doi: 10.1002/jcb.27395
- Li, J., Lu, L., Zhang, Y.-H., Xu, Y., Liu, M., Feng, K., et al. (2019b). Identification of leukemia stem cell expression signatures through Monte Carlo feature selection strategy and support vector machine. *Cancer Gene Ther.* 27, 56–69. doi: 10.1038/s41417-019-0105-y
- Liu, L., Chen, L., Zhang, Y. H., Wei, L., Cheng, S., Kong, X., et al. (2017). Analysis and prediction of drug-drug interaction by minimum redundancy maximum relevance and incremental feature selection. *J. Biomol. Struct. Dyn.* 35, 312–329. doi: 10.1080/07391102.2016.1138142
- Loeser, R. F. (2008). Molecular mechanisms of cartilage destruction in osteoarthritis. *J. Musculoskelet. Neuronal Interact.* 8, 303–306.
- Loughlin, J., and Reynard, L. N. (2015). Osteoarthritis: epigenetics of articular cartilage in knee and hip OA. *Nat. Rev. Rheumatol.* 11, 6–7. doi: 10.1038/nrrheum.2014.189
- Martel-Pelletier, J., Boileau, C., Pelletier, J. P., and Roughley, P. J. (2008). Cartilage in normal and osteoarthritis conditions. *Best Pract. Res. Clin. Rheumatol.* 22, 351–384. doi: 10.1016/j.berh.2008.02.001
- Menold, M. M., Shao, Y., Wolpert, C. M., Donnelly, S. L., Raiford, K. L., Martin, E. R., et al. (2001). Association analysis of chromosome 15 GABAA receptor subunit genes in autistic disorder. *J. Neurogenet.* 15, 245–259. doi: 10.3109/01677060109167380
- Miranda-Duarte, A. (2018). DNA methylation in osteoarthritis: current status and therapeutic implications. *Open Rheumatol. J.* 12, 37–49. doi: 10.2174/1874312901812010037
- Niu, B., Huang, G., Zheng, L., Wang, X., Chen, F., Zhang, Y., et al. (2013). Prediction of substrate-enzyme-product interaction based on molecular descriptors and physicochemical properties. *Biomed Res. Int.* 2013:674215. doi: 10.1155/2013/674215
- Okumura, K., Saito, M., Isogai, E., Aoto, Y., Hachiya, T., Sakakibara, Y., et al. (2014). Meis1 regulates epidermal stem cells and is required for skin tumorigenesis. *PLoS One* 9:e102111. doi: 10.1371/journal.pone.0102111
- Pan, X., Chen, L., Feng, K. Y., Hu, X. H., Zhang, Y. H., Kong, X. Y., et al. (2019). Analysis of expression pattern of snoRNAs in different cancer types with machine learning algorithms. *Int. J. Mol. Sci.* 20:2185. doi: 10.3390/ijms20092185
- Peng, H., Long, F., and Ding, C. (2005). Feature selection based on mutual information: criteria of max-dependency, max-relevance, and min-redundancy. *IEEE Trans. Pattern Anal. Mach. Intell.* 27, 1226–1238. doi: 10.1109/tpami.2005.159
- Pereira, D., Severo, M., Santos, R. A., Barros, H., Branco, J., Lucas, R., et al. (2016). Knee and hip radiographic osteoarthritis features: differences on pain, function and quality of life. *Clin. Rheumatol.* 35, 1555–1564. doi: 10.1007/s10067-015-3087-7
- Ramos, Y. F., Bos, S. D., Lakenberg, N., Böhringer, S., den Hollander, W. J., Kloppenburg, M., et al. (2014). Genes expressed in blood link osteoarthritis with apoptotic pathways. *Ann. Rheum. Dis.* 73, 1844–1853. doi: 10.1136/annrheumdis-2013-203405
- Reynard, L. N., and Loughlin, J. (2012). Genetics and epigenetics of osteoarthritis. *Maturitas* 71, 200–204. doi: 10.1016/j.maturitas.2011.12.001
- Rice, S. J., Beier, F., Young, D. A., and Loughlin, J. (2020). Interplay between genetics and epigenetics in osteoarthritis. *Nat. Rev. Rheumatol.* 16, 268–281. doi: 10.1038/s41584-020-0407-3
- Rushton, M. D., Reynard, L. N., Barter, M. J., Refaie, R., Rankin, K. S., Young, D. A., et al. (2014). Characterization of the cartilage DNA methylome in knee and hip osteoarthritis. *Arthritis Rheumatol.* 66, 2450–2460. doi: 10.1002/art.38713
- Shu, Y., Zhang, N., Kong, X., Huang, T., and Cai, Y. D. (2014). Predicting A-to-I RNA editing by feature selection and random forest. *PLoS One* 9:e110607. doi: 10.1371/journal.pone.0110607
- Sun, L., Yu, Y., Huang, T., An, P., Yu, D., Yu, Z., et al. (2012). Associations between ionomic profile and metabolic abnormalities in human population. *PLoS One* 7:e38845. doi: 10.1371/journal.pone.0038845
- Sun, X., Li, J., Gu, L., Wang, S., Zhang, Y., Huang, T., et al. (2018). Identifying the characteristics of the hypusine sites using SMOTE and SVM algorithm with feature selection. *Curr. Proteomics* 15, 111–118. doi: 10.2174/1570164614666171109120615
- Sun, X., Xiao, L., Chen, J., Chen, X., Chen, X., Yao, S., et al. (2020). DNA methylation is involved in the pathogenesis of osteoarthritis by regulating CtBP expression and CtBP-mediated signaling. *Int. J. Biol. Sci.* 16, 994–1009. doi: 10.7150/ijbs.39945
- Szklarczyk, D., Gable, A. L., Lyon, D., Junge, A., Wyder, S., Huerta-Cepas, J., et al. (2018). STRING v11: protein-protein association networks with increased coverage, supporting functional discovery in genome-wide experimental datasets. *Nucleic Acids Res.* 47, D607–D613. doi: 10.1093/nar/gky1131
- van Eijk, K. R., de Jong, S., Boks, M. P., Langeveld, T., Colas, F., Veldink, J. H., et al. (2012). Genetic analysis of DNA methylation and gene expression levels in whole blood of healthy human subjects. *BMC Genomics* 13:636. doi: 10.1186/1471-2164-13-636
- Wang, D., Li, J.-R., Zhang, Y.-H., Chen, L., Huang, T., and Cai, Y.-D. (2018). Identification of differentially expressed genes between original breast cancer and xenograft using machine learning algorithms. *Genes* 9:155. doi: 10.3390/genes9030155
- Wang, Q. F., Li, Y. J., Dong, J. F., Li, B., Kaberlein, J. J., Zhang, L., et al. (2014). Regulation of MEIS1 by distal enhancer elements in acute leukemia. *Leukemia* 28, 138–146. doi: 10.1038/leu.2013.260
- Wang, S. B., and Huang, T. (2019). The early detection of asthma based on blood gene expression. *Mol. Biol. Rep.* 46, 217–223. doi: 10.1007/s11033-018-4463-6
- Webb, B. T., Sullivan, P. F., Skelly, T., and van den Oord, E. J. (2008). Model-based gene selection shows engrailed 1 is associated with antipsychotic response. *Pharmacogenet. Genomics* 18, 751–759. doi: 10.1097/FPC.0b013e32830162bc
- Zhang, N., Huang, T., and Cai, Y. D. (2014). Discriminating between deleterious and neutral non-frameshifting indels based on protein interaction networks and hybrid properties. *Mol. Genet. Genomics* 290, 343–352.
- Zhang, N., Huang, T., and Cai, Y. D. (2015). Discriminating between deleterious and neutral non-frameshifting indels based on protein interaction networks and hybrid properties. *Mol. Genet. Genomics* 290, 343–352. doi: 10.1007/s00438-014-0922-5
- Zhang, N., Wang, M., Zhang, P., and Huang, T. (2016). Classification of cancers based on copy number variation landscapes. *Biochim. Biophys. Acta Gen. Subj.* 1860(11 Part B), 2750–2755. doi: 10.1016/j.bbagen.2016.06.003
- Zhang, P. W., Chen, L., Huang, T., Zhang, N., Kong, X. Y., and Cai, Y. D. (2015). Classifying ten types of major cancers based on reverse phase protein array profiles. *PLoS One* 10:e0123147. doi: 10.1371/journal.pone.0123147
- Zhang, X., Chen, C., Wu, M., Chen, L., Zhang, J., Zhang, X., et al. (2012). Plasma microRNA profile as a predictor of early virological response to interferon treatment in chronic hepatitis B patients. *Antivir. Ther.* 17, 1243–1253. doi: 10.3851/imp2401
- Zhang, Y. H., Huang, T., Chen, L., Xu, Y., Hu, Y., Hu, L. D., et al. (2017). Identifying and analyzing different cancer subtypes using RNA-seq data of blood platelets. *Oncotarget* 8, 87494–87511. doi: 10.18632/oncotarget.20903
- Zhao, T. H., Jiang, M., Huang, T., Li, B. Q., Zhang, N., Li, H. P., et al. (2013). A novel method of predicting protein disordered regions based on sequence features. *Biomed Res. Int.* 2013:414327. doi: 10.1155/2013/414327
- Zheng, H. F., Forgetta, V., Hsu, Y. H., Estrada, K., Rosello-Diez, A., Leo, P. J., et al. (2015). Whole-genome sequencing identifies EN1 as a determinant of bone density and fracture. *Nature* 526, 112–117. doi: 10.1038/nature14878

- Zhou, Y., Yang, L., Wang, H., Chen, X., Jiang, W., Wang, Z., et al. (2020). Alterations in DNA methylation profiles in cancellous bone of postmenopausal women with osteoporosis. *FEBS Open Bio* 10, 1516–1531. doi: 10.1002/2211-5463.12907
- Zhou, Y., Zhang, N., Li, B. Q., Huang, T., Cai, Y. D., and Kong, X. Y. (2015). A method to distinguish between lysine acetylation and lysine ubiquitination with feature selection and analysis. *J. Biomol. Struct. Dyn.* 33, 2479–2490. doi: 10.1080/07391102.2014.1001793

Conflict of Interest: The authors declare that the research was conducted in the absence of any commercial or financial relationships that could be construed as a potential conflict of interest.

Copyright © 2020 Wu, Shou, Wang, Huang and Xu. This is an open-access article distributed under the terms of the Creative Commons Attribution License (CC BY). The use, distribution or reproduction in other forums is permitted, provided the original author(s) and the copyright owner(s) are credited and that the original publication in this journal is cited, in accordance with accepted academic practice. No use, distribution or reproduction is permitted which does not comply with these terms.



Hsa_circ_0020095 Promotes Oncogenesis and Cisplatin Resistance in Colon Cancer by Sponging miR-487a-3p and Modulating SOX9

Yanlai Sun¹, Zhen Cao^{1,2}, Junqi Shan¹, Yang Gao¹, Xin Liu¹, Dejian Ma² and Zengjun Li^{1*}

¹ Department of Gastrointestinal Cancer Surgery, Shandong Cancer Hospital and Institute, Shandong First Medical University and Shandong Academy of Medical Sciences, Jinan, China, ² Shandong First Medical University and Shandong Academy of Medical Sciences, Jinan, China

OPEN ACCESS

Edited by:

Song Zhao,
First Affiliated Hospital of Zhengzhou
University, China

Reviewed by:

Lei Zhao,
University of Wisconsin-Madison,
United States
Ling-Qing Yuan,
Central South University, China

*Correspondence:

Zengjun Li
lizengjun16@outlook.com

Specialty section:

This article was submitted to
Epigenomics and Epigenetics,
a section of the journal
Frontiers in Cell and Developmental
Biology

Received: 10 September 2020

Accepted: 07 December 2020

Published: 15 January 2021

Citation:

Sun Y, Cao Z, Shan J, Gao Y,
Liu X, Ma D and Li Z (2021)
Hsa_circ_0020095 Promotes
Oncogenesis and Cisplatin
Resistance in Colon Cancer by
Sponging miR-487a-3p
and Modulating SOX9.
Front. Cell Dev. Biol. 8:604869.
doi: 10.3389/fcell.2020.604869

Objectives: Colon cancer (CC) currently ranks as the third most common human cancer worldwide with an increasing incidence and a poor prognosis. Recently, circular RNAs have been reported to regulate the progression of diverse human cancers. However, the role of circRNA hsa_circ_0020095 in CC remains largely unclear.

Methods: Expression levels of the related circRNAs, microRNAs and mRNA in CC tissues and cells were determined. The impacts of circ_0020095 or miR-487a-3p on CC cells were examined at the indicated times after transfection. Meanwhile, a luciferase-reporter experiment was employed to validate the interplay between miR-487a-3p and circ_0020095 or SOX9. Moreover, the *in vivo* tumor growth assay was applied to further evaluate the effects of circ_0020095 knockdown on CC progression.

Results: We demonstrated that circ_0020095 was highly expressed in CC tissues and cells. The proliferation, migration, invasion, and cisplatin resistance of CC were suppressed by silencing circ_0020095 *in vitro* and *in vivo* or by ectopic expression of miR-487a-3p *in vitro*. Mechanistically, circ_0020095 could directly bind to miR-487a-3p and subsequently act as a miR-487a-3p sponge to modulate the activity by targeting the 3'-UTR of SOX9. Interestingly, overexpression of circ_0020095 dramatically reversed the suppressive effects of miR-487a-3p mimics on CC cells.

Conclusion: Circ_0020095 functions as an oncogene to accelerate CC cell proliferation, invasion, migration and cisplatin resistance through the miR-487a-3p/SOX9 axis, which could be a promising target for CC treatment.

Keywords: colon cancer, circ_0020095, miR-487a-3p, SOX9, proliferation

Abbreviations: CC, colon cancer; CCND1, cyclin D1; CircRNAs, circular RNAs; CRC, colorectal cancer; miRNAs, microRNAs; MTT, 3-[4,5-dimethylthiazol-2-yl]-2,5-diphenyl tetrazolium bromide; qRT-PCR, quantitative real-time PCR; SH2B1, SH2B adaptor protein 1; SOX9, SRY-box transcription factor 9; T1D, type 1 diabetes; 5-FU, 5-fluorouracil.

INTRODUCTION

Colon cancer (CC) is known as one of the most frequent digestive cancers in the world with a high incidence and poor prognosis (Weinberg and Marshall, 2019). Despite the huge progress of therapeutic modalities, CC still ranks as the third primary cause of tumor-associated death (Banerjee et al., 2017). At present, CC incidence rises dramatically with age due to the accumulation of random somatic mutations, and more than ninety percent of CC cases occur after 50 years of age (Cappell, 2003). Multiple therapeutic options, including surgical removal, radiotherapy and chemotherapy, can be used for the treatment of CC patients. The mortality of CC has been decreased by more than 30% in recent decades (Howe et al., 2006). Nevertheless, the 5-year survival rate of CC patients at advanced stages is still only approximately 10%, which is mainly related to the multidrug resistance to chemotherapy drugs in advanced patients (Wang et al., 2014). In addition, recurrence has been observed in a substantial proportion of advanced CC patients after surgery (Gerner et al., 2018; Weinberg and Marshall, 2019). Therefore, it is essential to better understand the molecular mechanisms of CC to develop more effective approaches for the treatment of CC.

It is generally known that only approximately two percent of the human genome possesses protein-coding capacity, and most transcripts are generated as non-coding RNAs, which used to be considered transcriptional noise (Yang et al., 2019). As one of the most common subtypes, circular RNAs (circRNAs), which have a stable circular structure, were recently found to be widely expressed in mammalian cells (Qu and Adelson, 2012). Since the first report was published, circRNAs have been found to play a role in various cellular physiological processes, such as cell proliferation, apoptosis and differentiation (Holdt et al., 2018; Patop and Kadener, 2018). Dysregulation of circRNA expression has been observed in multiple human diseases, such as cancers, neurodegenerative disorders, and metabolic diseases (Haq and Harries, 2017). Recently, a number of circRNAs have been reported to contribute to the progression of CC (Ju et al., 2019). However, the pathogenesis of CC is still not completely understood. Circ_0020095 originates from the ATRNL1 gene and consists of the head-to-tail splicing of exons 9–18. It is a novel circRNA that was identified to be dysregulated in CC tissues in a microarray analysis (Zhang et al., 2019). Its functional role in CC remains undetermined.

Other studies have also elucidated that circRNAs suppress the inhibitory effects of miRNAs on target RNAs by competitively binding miRNAs (Militello et al., 2016). This competitive relationship represents a novel mechanism of gene regulation that has a major role in the physiology and development of cancer (Kulcheski et al., 2016). In our preliminary experiments, we screened and identified five potential target miRNAs and found that the level of miR-487a-3p was significantly regulated by circ_0020095 in CC cells. Therefore, we speculated that circ_0020095 may influence the CC process by regulating miR-487a-3p. MicroRNAs (miRNAs) can be widely involved in a variety of biological processes, such as cell differentiation, proliferation, apoptosis and metastasis, by translation inhibition or direct degradation of mRNAs to negatively regulate specific

target genes (Hammond, 2015; Peng and Croce, 2016). Currently, an increasing number of miRNAs, such as miR-193a (Teng et al., 2017), miR-137 (Sakaguchi et al., 2016), miR-34a (Bu et al., 2016) and miR-143 (Gomes et al., 2018), have been found to be associated with the occurrence and development of CC by promoting or preventing the malignant biological behavior of CC. MiRNAs are expected to become novel markers for the diagnosis, treatment and prognosis of CC (Slattery et al., 2018). Studies have demonstrated that miR-487a-3p is a vital biomolecule regulating prostate cancer, breast cancer and other cancers (Yang et al., 2018; Wang et al., 2019). SRY-box transcription factor 9 (SOX9), as a chemoradiotherapy-sensitive gene in colorectal cancer patients, could be a suitable biomarker to predict the relapse after the treatment (Du et al., 2019). In human non-small cell lung cancer, miR-592 functions as a tumor suppressor by targeting SOX9 (Li et al., 2017). Therefore, we speculated that miR-487a-3p might also be a crucial therapeutic target for CC.

In this study, we aimed to investigate the biological functions of circ_0020095/miR-487a-3p and further elucidate the underlying molecular mechanisms in CC which may become a promising therapeutic target for CC patients.

MATERIALS AND METHODS

Collection of CC Tissues and Cell Lines

Twenty CC tissues and their paired normal tissues were obtained from patients who received treatment at Shandong Cancer Hospital and Institute between 2013 and 2018, and written informed consent was obtained from every patient. This study was approved by the ethics committee of Shandong Cancer Hospital and Institute. A healthy human colon cell line (NCM460) and CC cell lines (HT29, SW480, SW620, and HCT116) were provided by the Type Culture Collection of the Chinese Academy of Sciences (Shanghai, China). Cells were cultured in RPMI-1640 medium (HyClone, United States) containing 10% fetal bovine serum (FBS) and kept at 37°C in a cell incubator with 5% CO₂ and 95% air.

RNA Extraction and Quantitative Real-Time PCR (RT-PCR) Assay

RNA extraction from CC tissues and cells was carried out using TRIzol reagent (Invitrogen, United States) following the manufacturer's instructions. After the concentration of RNA was determined via a NanoDrop 2000c (Thermo Scientific, United States), 3 µg of RNA was used as template to produce cDNA using a Bestar qPCR RT kit (DBI Bioscience, China). The RT-PCR of circRNAs, miRNAs and mRNAs was completed using Bestar qPCR MasterMix (DBI Bioscience) on an ABI 7500 system (ABI Biosystems, United States). The sequences of the primers used in this study are shown in Table 1.

RNase R Resistance Analysis

Circ_0020095 and its linear isoform were incubated at 37°C with RNase R (5 U/mg, Epicenter) for half an hour. Subsequently, the

TABLE 1 | All primers of qRT-PCR analysis used in the current study.

Gene	Primers	
	Forward (5'-3')	Reverse (5'-3')
GAPDH	TGTTGTCATGGGTGTGAAC	ATGGCATGGACTGTGGTCAT
Circ_0020095	GCTTATTGGAATGCACCACA	GTTTCTGGAACAAGC
miR-487a-3p	AATCATACAGGGACATC	CAAGTG
SOX9	AGGAAGTCGGTGAAGAACGG	TGCGTGTGCTGGAGTC
miR-485-3p	CCGCTCGAGATGCGGCTT	CGCCTTGAAGATGGCGTTG
miR-338-3p	TGGG AAGC	CGGGGTACCAAGATGCTT
miR-656-3p	TGCGGTCCAGCATCAGTGAT	CTA GATGCC
miR-660-5p	ACACTCCAGCTGGGAAT	CCAGTGCAGGGTCCGAGGT
U6	ATTATA CAGTCA	CTCAACTGGTGTGCTGGA
	TACCCATTGCATAT	GTCG
	CGGAGTTG	GCAATTCAGTTGAGAGA
	CTCGCTTCG GCAGCACA	GGUUG
		GTGCAGGGTCCGAGGT
		AACGCTTACGAATTTGCGT

treated RNAs were reverse transcribed with the indicated primers and analyzed by qRT-PCR.

Fluorescence *in situ* Hybridization (FISH)

Biotin-labeled specific RNA probe of circ_0020095 was obtained from RiboBio (Shanghai, China). Exponentially growing HT29 cells were collected and fixed in 4% formalin and then hybridized in hybridization buffer containing biotin-labeled circ_0020095. Signals were detected via a tyramide-conjugated Alexa 488 fluorochrome TSA kit.

RNA Transfection

Two specific siRNAs against circ_0020095 (siRNA#1 and siRNA#2) and a negative control (siRNA-NC) and a miR-487a-3p mimics, inhibitor and miR-NC were all synthesized by RiboBio (Shanghai, China). Transfection into HT29 and SW480 cells was carried out using Lipofectamine 3000 (Invitrogen) following the manufacturer's protocol.

Cell Counting Kit-8 (CCK-8) Assay

Cell Counting Kit-8 (Dojindo, Rockville, MD, United States) reagent was added to HT29 and SW480 cells to determine cell proliferation. In brief, 2×10^4 HT29 and SW480 cells were seeded into 96-well plates. After 24 h of culture, 10 μ l CCK-8 solution was added into each well and incubated for 10 min. Subsequently, absorbance was measured at 450 nm.

Cisplatin Treatment

Treated HT29 and SW480 cells were collected at exponential growth phase and seeded into 96-well plates, followed by incubation with cisplatin (0, 5, 10, 15, and 25 μ g/ml) for the indicated times. Then, cell proliferation activity was examined by the CCK-8 assay.

Colony Formation Assay

Treated HT29 and SW480 cells were collected at exponential growth phase and seeded into 96-well plates at a concentration of 2×10^4 cells per well. After 2 weeks of culture at 37°C, visible

colonies were fixed in 4% paraformaldehyde followed by staining with Giemsa solution. The number of colonies in both the control and experimental groups was counted under a microscope at 10 \times magnification.

Cell Apoptosis Analysis (Flow Cytometry Analysis)

Treated HT29 and SW480 cells were collected at exponential growth phase and seeded into 96-well plates at a concentration of 2×10^4 cells per well. After staining with propidium iodide and Annexin V, HT29 and SW480 cells were subjected to cell apoptosis using a flow cytometer (FACScan, United States), and the results were analyzed by CELL Quest 3.0 software.

Wound-Healing Assay

Treated HT29 and SW480 cells were harvested and seeded into 35-mm dishes at a concentration of 1×10^5 cells per well and cultured at 37°C until confluence. A straight scratch was made on the cell surface using a sterile pipette tip. Images were taken 0 and 24 h after scratching, and the width of the scratch was measured under a microscope.

Transwell Assay

Transwell chambers coated with or without Matrigel matrix (BD Bioscience, United States) were employed to estimate the cell migration and invasion of HT29 and SW480 cells. Treated HT29 and SW480 cells were harvested and resuspended in culture medium to a final concentration of 1×10^5 cells/ml. The upper chamber was filled with 200 μ l of cell suspension, and the lower chamber was filled with 500 μ l FBS-containing culture medium. After 24 h of incubation at 37°C, migratory and invasive CC cells were fixed with 70% ethanol and stained with crystal violet. The number of migratory and invasive cells was counted under a microscope.

Dual Luciferase Reporter Assay

Circ_0020095 sequence containing wild-type (WT) or mutated (MUT) miR-487a-3p binding site was synthesized and inserted into the pmirGLO Dual-luciferase miRNA Target Expression Vector (Promega, WI, United States). The recombinant reporter plasmid was named circ_0020095-WT or circ_0020095-MUT. circ_0020095-WT or circ_0020095-MUT was cotransfected with miR-487a-3p or miR-NC into HT29 and SW480 cells using Lipofectamine 3000 (Invitrogen, United States). Luciferase activities of HT29 and SW480 cells were measured after 48 h of cotransfection by using the Luciferase Reporter Assay System (Promega, WI, United States). Similar to the above, a SOX9 sequence containing the WT or MUT miR-487a-3p binding site was amplified and subcloned into the pmirGLO vector to generate SOX9-WT or SOX9-MUT reporter plasmid. The transfection procedure was carried out as described above.

In vivo Tumor Growth Assay

HT29 cells stably expressing circ_0020095 siRNAs or si-NC were harvested and resuspended in culture medium at a concentration

of 2×10^5 cells/ml. Next, 200 μ l HT cell suspension was inoculated into the right flanks of nude mice (male, 8 weeks old). Animals were obtained from the University of Jinan-Shandong Academy of Medical Sciences. Animal manipulations were approved by the Institutional Animal Care and Use Committee of the Hospital. Tumor volume and weight were examined every week until 4 weeks after inoculation.

Statistical Analysis

Data in this study are shown as the means \pm standard deviation (SD) and were analyzed with SPSS (version 20.0, SPSS, Chicago, United States). The significance of the difference between the control and experimental groups was estimated via Student's *t* test, and *P* less than 0.05 was considered statistically significant.

RESULTS

Circ_0020095 Was Identified to Be Increased in CC

A previous study identified 334 dysregulated circRNAs in CC tissues by microarray analysis; and we focus on the top 11 upregulated circular RNAs that may involve in the carcinogenesis of CC (Zhang et al., 2019). **Figure 1A** indicates their genome location. In our cohort, we randomly selected 6 paired CC tumor tissues and adjacent normal tissues and tested the expression of these 11 circular RNAs, and we found that circ_0020095 was the most dysregulated circRNA between the CC tumor tissues and paired normal tissues (**Figure 1B**). Circ_0020095 originates from the ATRNL1 gene and consists of the head-to-tail splicing of exons 9–18, and Sanger sequencing was used to validate its circular structure (**Figure 1C**). Convergent and divergent primers were designed to amplify linear and circular RNA isoforms based on templates of cDNA and gDNA extracted from three CC tissues and HT29 and SW480 cell lines using semiquantitative PCR. The results indicated that convergent primers could only amplify linear RNAs (the band close to 200 bp) in the cDNA and gDNA groups while circ_0020095 (the band close to 500 bp) could only be produced in the cDNA group but not in the gDNA group by divergent primers (**Figure 1D**). Moreover, in HT29 and SW480 cells, we found that the circular isoform was resistant to RNase R treatment, while the linear isoform was clearly digested by RNase R (**Figure 1E**). In addition, the FISH assay indicated that circ_0020095 was predominantly located in the cytoplasm, while its isoform was located in both the cytoplasm and nucleus (**Figure 1F**). Two siRNAs (siRNA#1 and siRNA#2) against circ_0020095 were synthesized to silence the expression of circ_0020095 in HT29 and SW480 cells (**Figure 1G**). Northern blots analysis of circ_0020095 indicated that siRNA#1 and siRNA#2 transfection resulted in a significant downregulation of circ_0020095 in HT29 and SW480 cells (**Figures 1H,I**). Subsequently, we found that circ_0020095 was significantly increased in four CC cell lines, HT29, SW480, SW620, and HCT116, compared to the healthy human colon cell line NCM460 (**Figure 1J**). We further verified its upregulation in 20 CC tissue samples compared

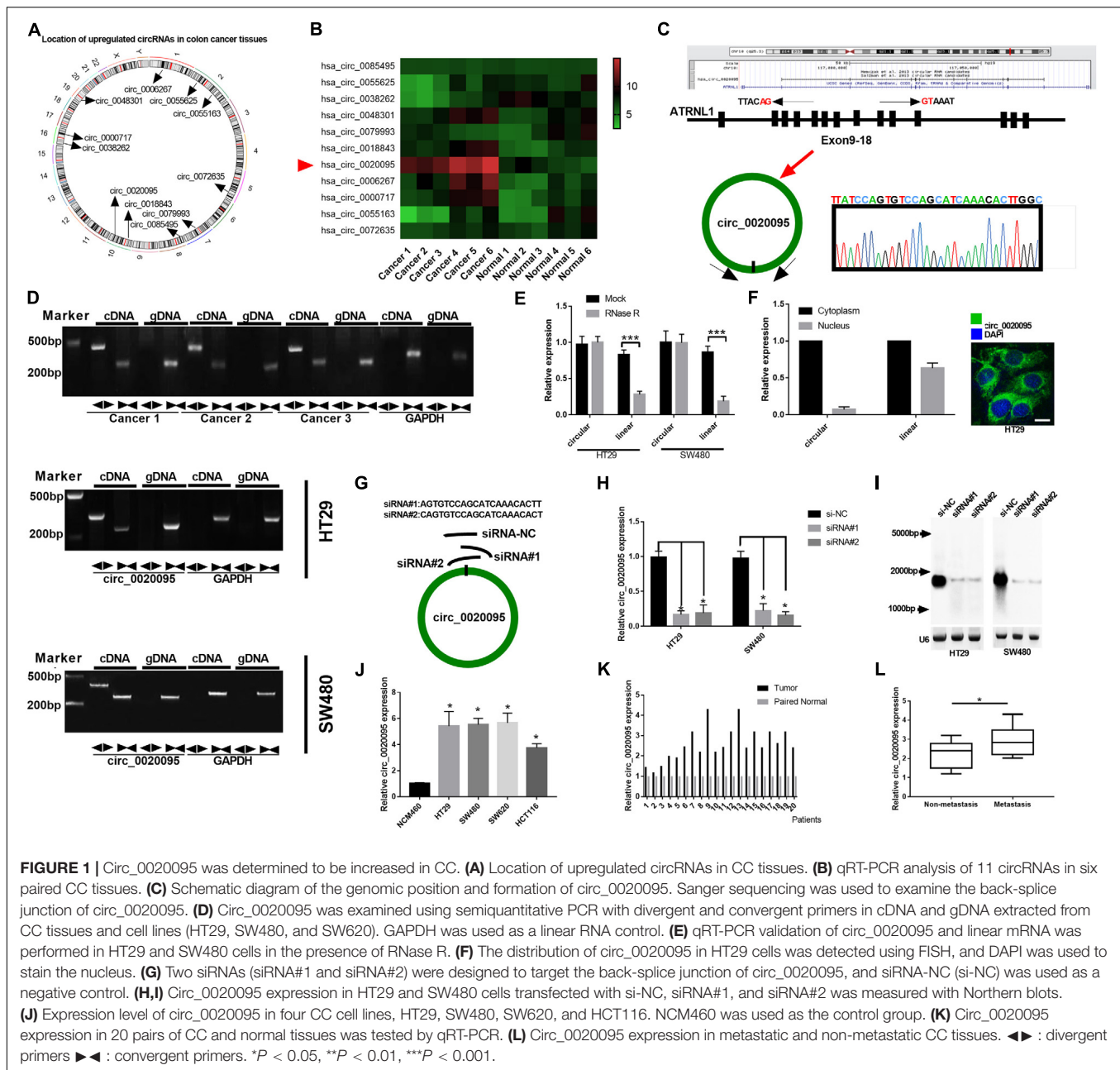
to matched normal samples through qRT-PCR (**Figure 1K**). In addition, we revealed that circ_0020095 expression was higher in metastatic CC tissues than in non-metastatic tissues (**Figure 1L**). These results suggested that circ_0020095 was increased in CC, indicating that it might be involved in the pathogenesis of CC.

Silencing of Circ_0020095 Suppressed CC Cell Growth *in vitro*

To investigate the functions of circ_0020095 in CC, siRNA#1 and siRNA#2 were stably transfected into HT29 and SW480 cells, followed by analysis of cell proliferation, apoptosis, migration, and invasion. The CCK-8 assay indicated that circ_0020095 knockdown remarkably reduced the viability of HT29 and SW480 cells (**Figure 2A**). The results from the colony formation assay showed a significant downregulation of the colony formation rate of the siRNA pool groups compared to the si-NC groups (**Figure 2B**). The soft agar colony formation assay also revealed an inhibition of colony numbers in siRNA pool-transfected HT29 and SW480 cells (**Figure 2C**). On the other hand, circ_0020095 silencing was demonstrated to cause a dramatic increase in the apoptosis of HT29 and SW480 cells (**Figure 2D**). The effects of circ_0020095 knockdown on cell migratory capacity were assessed through transwell and wound-healing experiments in HT29 and SW480 cells. The results showed that the migratory capacity of HT29 and SW480 cells was dramatically suppressed in the siRNA pool group compared to the si-NC group (**Figures 2E,F**). Moreover, by using a Matrigel-coated transwell chamber, we demonstrated that circ_0020095 knockdown resulted in a significant decrease in the number of invasive HT29 and SW480 cells (**Figure 2G**). To explore the role of circ_0020095 in the chemoresistance of CC cells, HT29 and SW480 cells were treated with different concentrations of cisplatin followed by viability examination using the CCK-8 assay. In the presence of different concentrations of cisplatin (0, 5, 10, 15, and 25 μ g/ml), the viability of HT29 and SW480 cells that were transfected with the siRNA pool was markedly suppressed compared to that of cells transfected with si-NC (**Figure 2H**). Moreover, we found that the viability of HT29 and SW480 cells treated with the siRNA pool was significantly attenuated after 24 and 48 h of cisplatin treatment (5 μ g/ml) (**Figure 2I**). Overall, silencing of circ_0020095 was demonstrated to inhibit CC cell growth *in vitro*.

Circ_0020095 Acted as a Sponge of miR-487a-3p

To determine whether circ_0020095 could sponge miRNAs in CC cells, we selected five candidate miRNAs by overlapping the results of the predicted miRNA binding sites in the circ_0020095 sequence by StarBase and Circular RNA interactome (**Figure 3A**). We then examined whether the identified miRNAs could directly bind circ_0020095. A specific biotin-labeled circ_0020095 probe was designed and used to pull down circ_0020095 in HT29 and SW480 cells. The pulldown efficiency was dramatically increased in HT29 and SW480 cells with stable

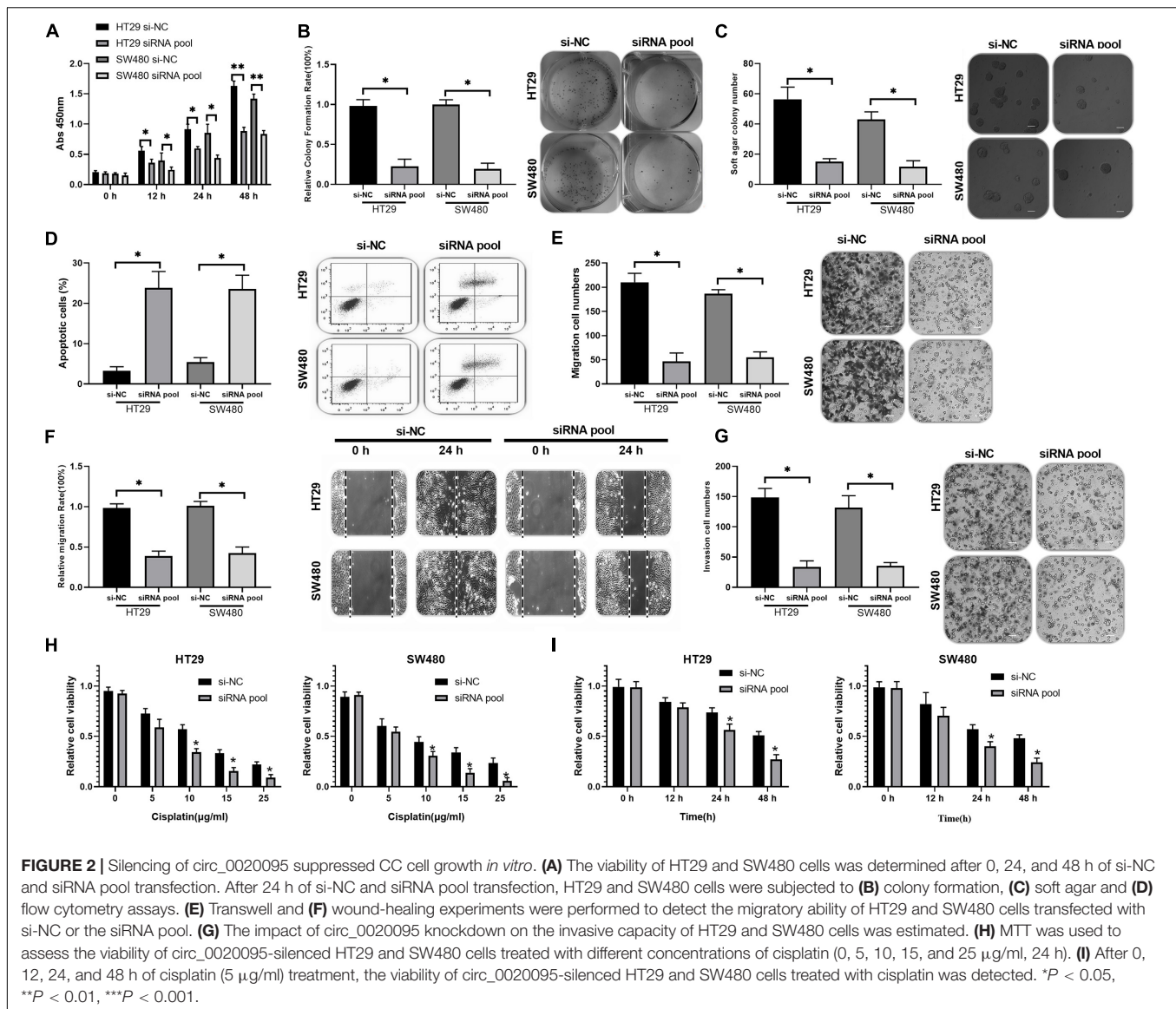


circ_0020095 overexpression (Figures 3B,C). After pulldown, miRNAs were isolated, and the five candidate miRNAs were analyzed via qRT-PCR. The results indicated that in both HT29 and SW480 cells, miR-487a-3p, and miR-338-3p were abundantly pulled down by the circ_0020095 probe (Figures 3D,E). On the other hand, we found a significant upregulation of circ_0020095 in HT29 and SW480 cells treated with biotin-labeled miR-487a-3p wt compared to those cells treated with biotin-labeled miR-487a-3p mut (Figure 3F). We further performed a luciferase reporter assay to determine whether miR-487a-3p directly interacts with circ_0020095 (Figure 3G). HT29 and SW480 cells cotransfected with miR-487a-3p mimics and a circ_0020095 wt reporter plasmid

exhibited reduced luciferase activity (Figures 3H,I). These findings suggested that circ_0020095 acted as a sponge of miR-487a-3p in CC cells.

Transfection of miR-487a-3p Suppressed CC Cell Growth *in vitro*

Kaplan-Meier analysis indicated that CC patients with low miR-487a-3p expression exhibited a worse prognosis (Figure 4A). By analyzing the expression level of miR-487a-3p with qRT-PCR, we revealed that miR-487a-3p was significantly decreased in both CC tissues and cell lines (HT29, SW480, SW620, and HCT116) compared to normal tissues and the NCM460 cell line,

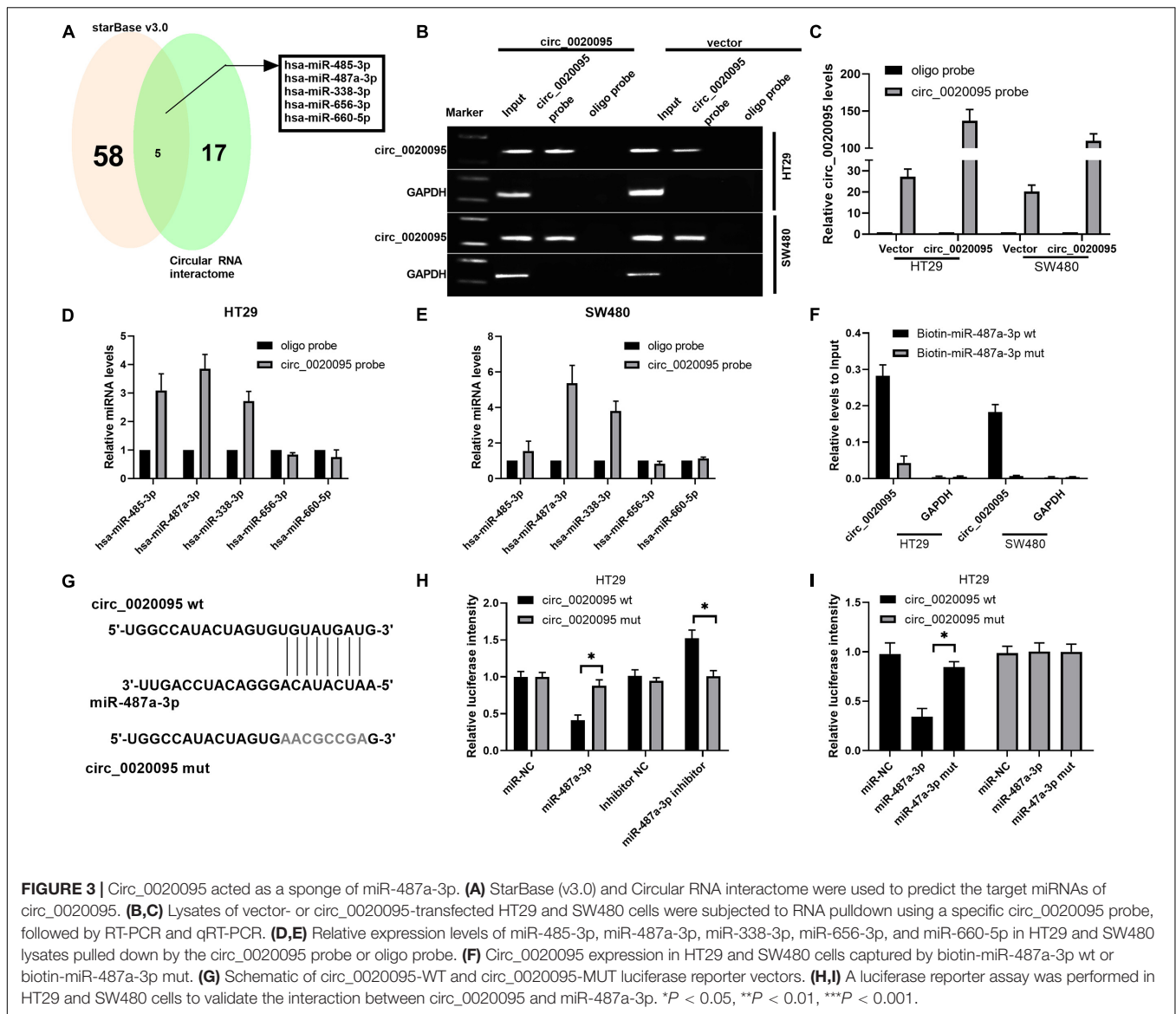


respectively (Figures 4B,C). Next, we estimated the effects of miR-487a-3p overexpression on cell proliferation, invasion and migration. In the colony formation assay, we observed that miR-487a-3p transfection resulted in a significant suppression of the colony formation rate of HT29 and SW480 cells (Figure 4D). Similarly, miR-487a-3p transfection also caused a decrease in the soft agar colony number of HT29 and SW480 cells (Figure 4E). In the transwell assay, we found that miR-487a-3p transfection led to a dramatic suppression of the invasive and migratory abilities of HT29 and SW480 cells compared to miR-NC transfection (Figures 4F,G). In addition, we also investigated the role of miR-487a-3p in the cisplatin resistance of CC cells. The results indicated that miR-487a-3p transfection significantly enhanced the sensitivity of HT29 and SW480 cells to 15 and 25 $\mu\text{g/ml}$ cisplatin compared to the miR-NC transfection (Figures 4H,I). Moreover, the viability of HT29 and SW480 cells was found to be significantly attenuated by overexpressing miR-487a-3p after

24 and 48 h of 5 $\mu\text{g/ml}$ cisplatin treatment (Figures 4J,K). These results demonstrated that miR-487a-3p overexpression remarkably suppressed CC cell growth *in vitro*.

miR-487a-3p Repressed SOX9 Expression by Directly Binding Its 3'UTR

To determine the target gene of miR-487a-3p in CC cells, we selected two candidate genes, SOX9 and TMEM178B, by overlapping the results of TargetScan, miRDB and miRMap analyses (Figure 5A). To confirm whether miR-487a-3p physically interacts with these two candidate genes, dual-luciferase reporter assays were carried out in HT29 and SW480 cells. The results indicated that the luciferase activity of CC cells was dramatically attenuated after cotransfection with miR-487a-3p and the SOX9 plasmid but not with the TMEM178B plasmid (Figures 5B,C). We further validated the interaction



between miR-487a-3p and SOX9 using SOX9 wt and SOX9 mut reporter plasmids (**Figure 5D**). The luciferase activity of HT29 and SW480 cells driven by SOX9 wt was obviously reduced by miR-487a-3p, while the luciferase activity driven by SOX9 mut was not affected by miR-487a-3p transfection (**Figures 5E,F**). In addition, a significant downregulation of SOX9 mRNA and protein levels was observed in miR-487a-3p-overexpressing HT29 and SW480 cells (**Figures 5G,H**). These findings suggested that miR-487a-3p could suppress the expression of SOX9 in HT29 and SW480 cells by directly binding to SOX9.

Circ_0020095 Promotes Oncogenesis of Colon Cancer by Sponging Multiple miRNAs

Due to the association of circ_0020095 and miR-487a-3p in CC, we next investigated whether circ_0020095 could abolish

the inhibitory effects of miR-487a-3p on SOX9 expression and CC cell proliferation, invasion and migration. The results from qRT-PCR and western blot experiments indicated that miR-487a-3p-induced downregulation of SOX9 mRNA and protein was abolished by the cotransfection of miR-487a-3p and circ_0020095 in HT29 and SW480 cells (**Figures 6A–C**). In the colony formation assay, we observed that ectopic expression of circ_0020095 in HT29 and SW480 cells restored the cell proliferation activity suppressed by miR-487a-3p (**Figure 6D**). Moreover, by using a transwell assay, we found that circ_0020095 transfection in HT29 and SW480 cells could restore the cell invasion and migration abilities, which were suppressed by overexpression of miR-487a-3p (**Figures 6E,F**). These results indicated that circ_0020095 could regulate CC cell proliferation, migration and invasion by sponging multiple miRNAs, we also

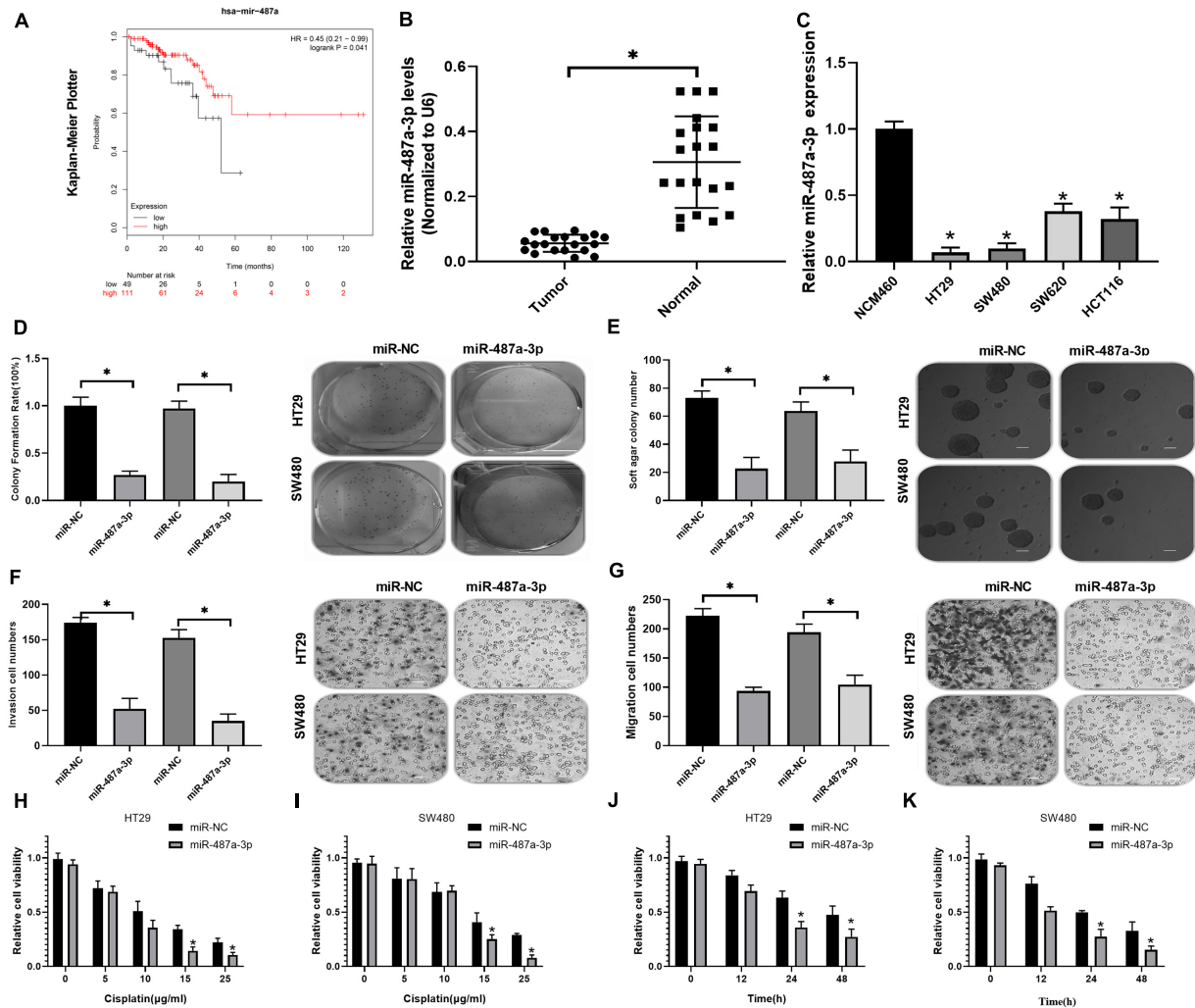


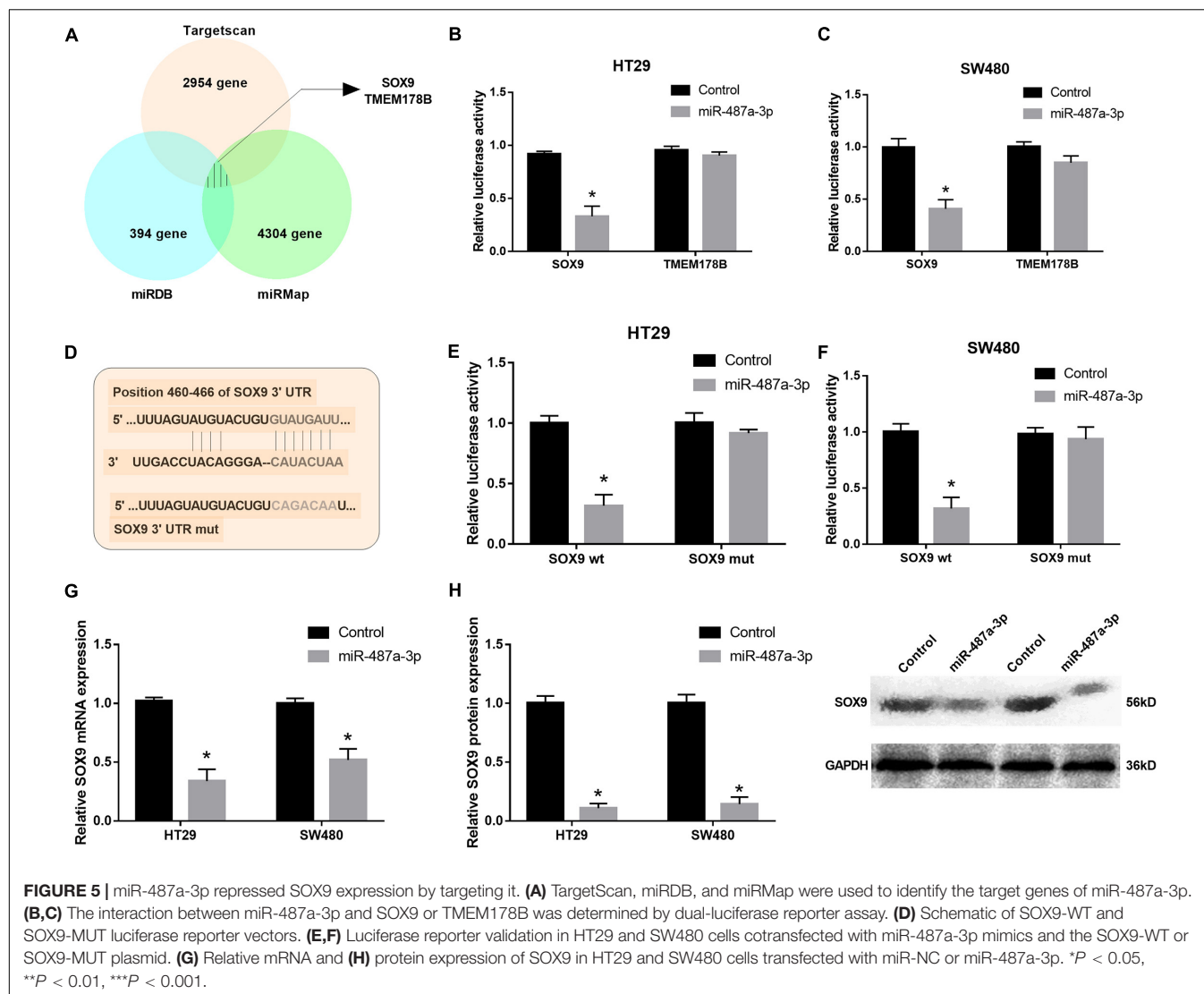
FIGURE 4 | Transfection of miR-487a-3p suppressed CC cell growth *in vitro*. **(A)** Kaplan-Meier analysis of the prognosis of CC patients with high or low miR-487a-3p expression. **(B)** Relative expression level of miR-487a-3p in CC tissue samples and matched normal samples. **(C)** Relative expression level of miR-487a-3p in CC cell lines HT29, SW480, SW620, and HCT116. NCM460 was used as a control. After 24 h of miR-NC and miR-487a-3p mimic transfection, HT29 and SW480 cells were subjected to analysis of proliferation, invasion and migration through **(D)** colony formation, **(E)** soft agar **(F,G)** and transwell assays. **(H,I)** The viability of HT29 and SW480 cells transfected with miR-487a-3p or miR-NC was detected in the presence of various concentrations of cisplatin (0, 5, 10, 15, and 25 $\mu\text{g/ml}$). **(J,K)** After 0, 12, 24, and 48 h of cisplatin (5 $\mu\text{g/ml}$) treatment, the viability of HT29 and SW480 cells treated with miR-487a-3p or miR-NC was detected. * $P < 0.05$, ** $P < 0.01$, *** $P < 0.001$.

showed that circ_0020095 regulated Met expression through miR-338-3p (**Supplementary Figure 1**). These data indicated that circ_0020095 promotes tumorigenesis of CC by sponging multiple miRNAs.

Silencing of Circ_0020095 Suppressed CC Tumor Growth *in vivo*

To further examine whether circ_0020095 silencing could inhibit CC tumor growth *in vivo*, HT29 cells stably transfected with an siRNA pool or si-NC were inoculated into nude mice. Xenograft tumors were examined 4 weeks after inoculation. The results showed that the tumor volumes and weights in the siRNA pool-transfected group were dramatically decreased

than those in the si-NC group (**Figures 7A–D**). The expression levels of miR-487a-3p and circ_0020095 were determined in the xenograft tumors collected from the siRNA pool and si-NC groups. Compared to that in the si-NC group, the expression level of miR-487a-3p was remarkably upregulated, while circ_0020095 was significantly downregulated, in the siRNA pool group (**Figures 7E,F**). Moreover, by using IHC analysis, we found that the staining intensity of SOX9 was obviously weaker in the tumor sections of the siRNA pool group than in those of the si-NC group (**Figure 7G**). In addition, in xenograft tumors, a negative correlation was observed between the expression levels of miR-487a-3p and circ_0020095 or SOX9 (**Figures 7H,I**), while a positive correlation was revealed between the expression levels of circ_0020095 and SOX9 (**Figures 7J,K**). These results



demonstrated that silencing circ_0020095 suppressed CC tumor growth *in vivo*.

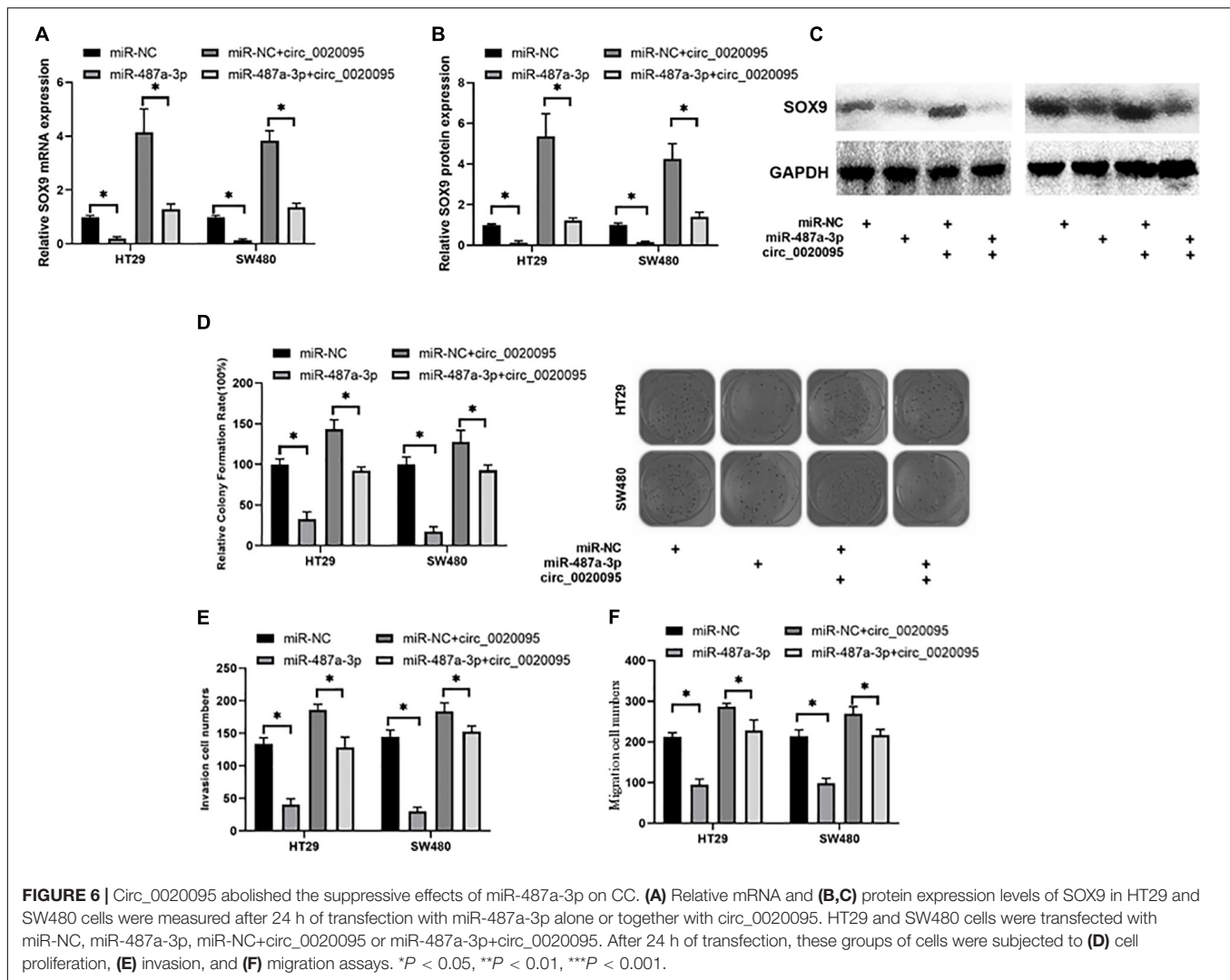
DISCUSSION

Hsa_circ_0020095 was abundantly expressed in CC tissues and CC cell lines. Via *in vitro* and *in vivo* experiments, we have found that circ_0020095 promotes the proliferation, migration and invasion activities in CC, while the circ_0020095/ miR-487a-3p sponge structure alleviates these activities in CC. Meanwhile, the expression of SOX9 was in line with the effects by circ_0020095 and circ_0020095/ miR-487a-3p sponge structure.

CircRNAs widely exist in the eukaryotic transcriptome and are involved in the modulation of gene expression; therefore, circRNAs have been a research hotspot in recent decades. Circ_0020095 is encoded by the ATRNL1 gene, which might play a role in the melanocortin cascade that modulates energy homeostasis (Stark et al., 2010). The involvement

of circRNAs in the initiation and development of human cancers has been well demonstrated by *in vitro* and *in vivo* evidence (Meng et al., 2017). Whether circ_0020095 can affect the progression of CC remains undetermined. Therefore, investigating circRNA regulatory mechanisms to cancer progression will provide insights into future tumor prevention and therapy strategies.

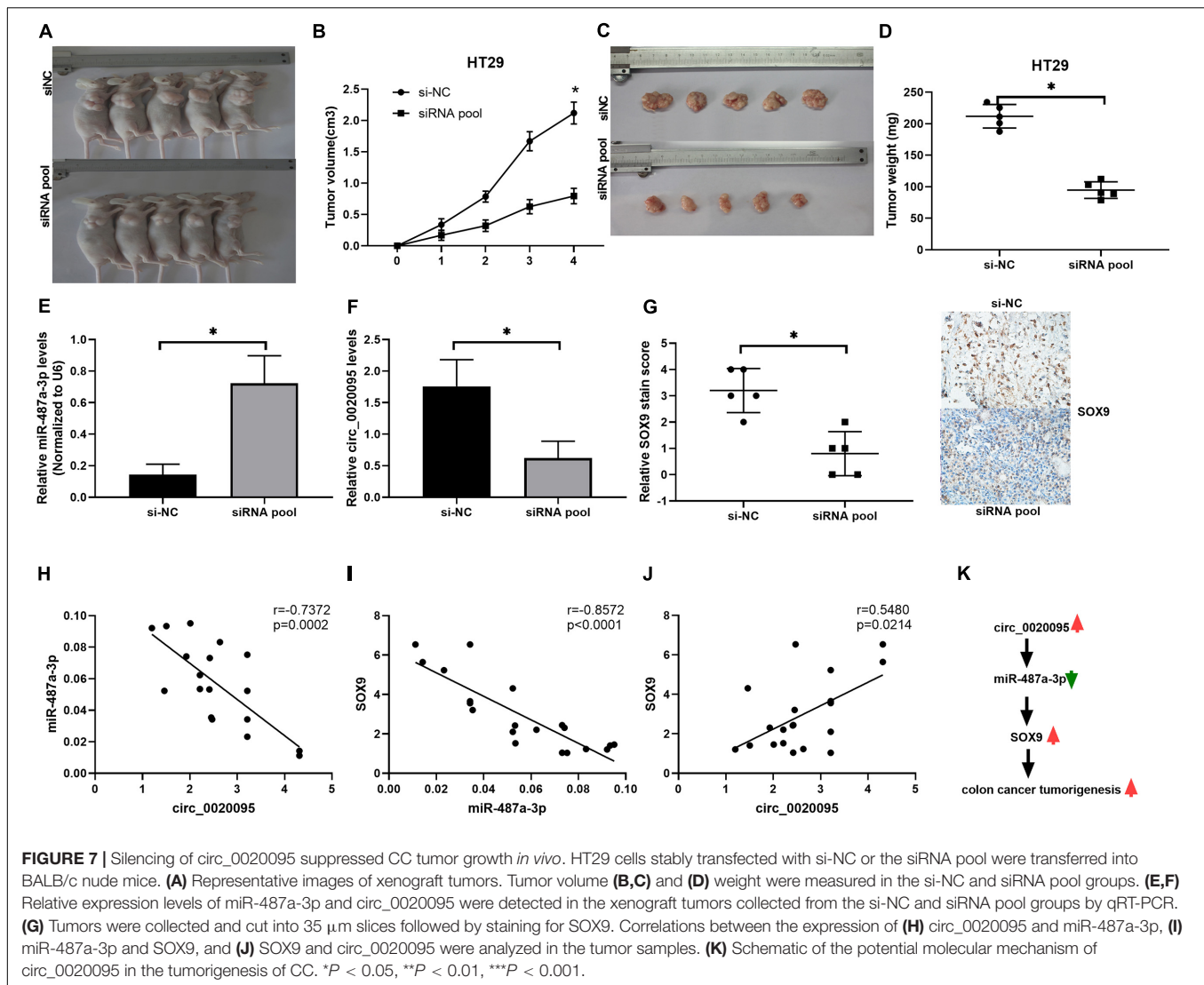
Many circRNAs have been reported in CC thus far. For example, circRNA CCDC66 is identified to be strongly increased in the colon and associated with a poor prognosis. Gain- and loss-of-function studies show that it could promote CC cell growth and metastasis (Hsiao et al., 2017). Similarly, circ_000984 is strongly increased in CC, and its knockdown results in suppression of CC cell proliferation, migration and invasion *in vivo* and *in vitro* (Xu et al., 2017). Moreover, hsa_circ_0136666 is highly expressed in CRC and the silence of hsa_circ_0136666 regulates the proliferation and migration of colorectal cancer (CRC) cells by sponging miR-136, thus modulating the expression of SH2B adaptor protein 1



(SH2B1) (Jin et al., 2019). In accordance with our findings, circ_0020095 was identified to be strongly upregulated in CC tissues and cell lines (HT29 and SW480). After silencing of circ_0020095 with siRNA, CC cell proliferation, migration and invasion were significantly reduced, while the apoptosis was dramatically increased in HT29 and SW480 cells. Similarly, the silence of hsa_circ_0007534 by siRNA remarkably reduces the proliferation and increases apoptosis of CRC cells (Zhang et al., 2018). Moreover, we have found that the cisplatin resistance of circ_0020095 was in a dose- and time-dependent manner (Figures 2H,I). Accumulating evidence has proved that the dysregulation of circRNAs is correlated with drug resistance in various tumors (Hua et al., 2019). Taking CRC as an example, the upregulated hsa_circ_000504 promotes 5-fluorouracil (5-FU) resistance by modulating the circRNA/miR-485-5p/STAT3/AKT3/BCL2 signaling pathway (Xiong et al., 2017). Taken together, these findings substantiated that circ_0020095 exerted oncogenic effects on CC.

In terms of the mechanism, we chose miR-487a-3p as a potential target miRNA of circ_0020095 by bioinformatics

prediction analysis. By searching the literature, we found that miR-487a-3p was only reported in a few studies. In 2018, miR-487a-3p is identified as a lymph node metastasis-associated miRNA in The Cancer Genome Atlas lung adenocarcinoma patient cohort, and a high level of miR-487a-3p was demonstrated to be related to a worse prognosis (Gonzalez-Vallinas et al., 2018). In the same year, miR-487a-3p is revealed to be overexpressed in type 1 diabetes (T1D) by using microarray analysis in the peripheral blood samples of T1D pediatric patients, however, a functional study is not performed (Zurawek et al., 2018). Recently, miR-487a-3p is found to function as a novel tumor repressor in prostate cancer by targeting cyclin D1 (CCND1) (Wang et al., 2020). However, a low level of miR-487a-3p is linked to a high metastasis rate and poor prognosis by targeting SMAD7 in pancreatic cancer tissues (Zhou et al., 2020). To the best of our knowledge, the role of miR-487a-3p in CC has not been reported until now. Through a dual-luciferase reporter assay, we confirmed that in CC cells, circ_0020095 directly binds to miR-487a-3p as a sponge structure which directly targets the 3'-UTR of SOX9 by comparing



wt with mut of SOX9 reporter plasmids. Similarly, circRNA-ACAP2 could regulate Tiam1 expression by abolishing the suppressive effect of miR-21-5p on Tiam1 expression by sponging with a miRNA in SW480 cells (He et al., 2018). Moreover, overexpression of miR-487a-3p could suppress CC cell growth. This is the first evidence that miR-487a-3p acts as a tumor suppressor in CC.

SOX9 is a high mobility group box transcription factor that has been shown to be increased in multiple human tissues and acts as an oncogenic agent in tumor progression (Huang and Guo, 2017). A relationship between SOX9 and CC cell growth and development has been observed by a number of studies (Marcker Espersen et al., 2016; Prevostel and Blache, 2017). For this relationship, Shen et al. have found that SOX9 was overexpressed in colon cancer. Knockdown of SOX9 expression results in reduced invasiveness and metastasis of colon cancer cells and inhibits the tumor growth and peritoneal metastasis in nude mice by inhibiting the S100P/RAGE/ERK/EMT signaling pathway (Shen et al., 2015). Similarly, SOX9 regulates migration

and invasion in SW480 and SW620 cells and triggers the transition between epithelial and mesenchymal states (Carrasco-Garcia et al., 2016). The expression level of SOX9 could be used to predict relapse in CC patients with stage II disease; a high level predicted a low risk of relapse, and a low level predicted a high risk of relapse (Marcker Espersen et al., 2016). Moreover, miR-133b directly targets the protein level of WAVE2/Sox9/c-Met in clinical samples (Wang et al., 2018). Based on these findings, the potential mechanism of SOX9/c-Met may play an important role during relapse in CC patients. Similarly, we have found miR-487a-3p regulated the protein expression of SOX9 in our experiments. Taken together, circ_0020095 not only indirectly regulated the expression of SOX9 through miR-487a-3p but also reversed the inhibitory effects of miR-487a-3p on CC cells. In our future research, we aim to investigate the mutual effects of SOX9 and C-Met on CC patients with different stages.

There are some limitations to our study. Firstly, Considering the low expression of miR-487a-3p in both CC tissues and cell lines (HT29, SW480, SW620, and HCT116) compared to

normal tissues and the NCM460 cell line, there is another possibility that Sox9 is directly regulated by circ_0020095, or through other targets. However, we have confirmed the finding that circ_0020095 could downregulate the mRNA and protein expression of Sox9 by sponging miR-487a-3p. Secondly, we have only randomly chosen 6 paired CC tumor tissues and adjacent normal tissues to test the expression of 11 circular RNAs. Although the number size is small, we have proved the increased circ_0020095 in tissues (**Figure 1K**) and cell lines through semiquantitative PCR, FISH assay and qRT-PCR which was consistent with the result in **Figure 1B**.

CONCLUSION

Our results showed that the circ_0020095/miR-487a-3p/SOX9 axis plays a critical role in the progression of CC cells, not only improving our understanding of the tumorigenesis of CC but also offering a novel therapeutic strategy for CC patients.

DATA AVAILABILITY STATEMENT

The raw data supporting the conclusions of this article will be made available by the authors, without undue reservation.

ETHICS STATEMENT

The studies involving human participants were reviewed and approved by the Research Ethics Committee of Shandong Cancer Hospital and Institute, Shandong First Medical University and Shandong Academy of Medical Sciences. The patients/participants provided their written informed consent to participate in this study. The animal study was reviewed and approved by the Research Ethics Committee of Shandong Cancer Hospital and Institute, Shandong First Medical University and Shandong Academy of Medical Sciences.

REFERENCES

- Banerjee, A., Pathak, S., Subramaniam, V. D., Dharanivasan, G., Murugesan, R., and Verma, R. S. (2017). Strategies for targeted drug delivery in treatment of colon cancer: current trends and future perspectives. *Drug Discov. Today* 22, 1224–1232. doi: 10.1016/j.drudis.2017.05.006
- Bu, P., Wang, L., Chen, K. Y., Srinivasan, T., Murthy, P. K., Tung, K. L., et al. (2016). A miR-34a-Numb feedforward loop triggered by inflammation regulates asymmetric stem cell division in intestine and colon cancer. *Cell Stem Cell* 18, 189–202. doi: 10.1016/j.stem.2016.01.006
- Cappell, M. S. (2003). Colon cancer during pregnancy. *Gastroenterol. Clin. North Am.* 32, 341–383. doi: 10.1016/s0889-8553(02)00066-3
- Carrasco-Garcia, E., Lopez, L., Aldaz, P., Arevalo, S., Aldaregia, J., Egaña, L., et al. (2016). SOX9-regulated cell plasticity in colorectal metastasis is attenuated by rapamycin. *Sci. Rep.* 6:32350.
- Du, B., Wang, T., Yang, X., Wang, J., Shi, X., Wang, X., et al. (2019). SOX9, miR-495, miR-590-3p, and miR-320d were identified as chemoradiotherapy-sensitive genes and miRNAs in colorectal cancer patients based on a microarray dataset. *Neoplasma* 66, 8–19. doi: 10.4149/neo_2018_170324n214

AUTHOR CONTRIBUTIONS

DM and YS conceived and designed the experiments. DM, ZC, JS, YG, and XL performed the data analysis and interpretation. ZL performed the bioinformatics analysis. YS contributed to clinical materials. DM and ZC were involved in the manuscript preparation. ZL, JS, YG, and XL were responsible for the writing revision and modifications of figures. All authors read and approved the final manuscript.

FUNDING

This experiment was funded by an independent established funding source from Department of Gastrointestinal Cancer Surgery, Shandong Cancer Hospital and Institute, Shandong First Medical University and Shandong Academy of Medical Sciences. Additionally, we thank Professor Sun from Shandong Cancer Hospital and Institute, Shandong First Medical University and Shandong Academy of Medical Sciences for his help with the bioinformatic analysis for free. This article was completed by DM, ZC, JS, YG, XL, and ZL and it was not paid by a pharmaceutical company or other agency. ZL had full access to all the data in the study and had final responsibility for the decision to submit for publication.

SUPPLEMENTARY MATERIAL

The Supplementary Material for this article can be found online at: <https://www.frontiersin.org/articles/10.3389/fcell.2020.604869/full#supplementary-material>

Supplementary Figure 1 | Circ_0020095 functions as an efficient miR-338-3p sponge and regulates Met expression in colon cancer cells. **(A)** Schematic of the circ_0020095-WT and circ_0020095-MUT luciferase reporter vectors. **(B,C)** A luciferase reporter assay was performed in HT29 and SW480 cells to validate the interaction between circ_0020095 and miR-338-3p. **(D)** The protein expression of Met in HT29 and SW480 cells was measured after 24 h of transfection with miR-338-3p alone or together with circ_0020095. Data in **(B,C)** are the mean \pm SEM. of three experiments, * $P < 0.05$, Student's *t*-test.

- Gerner, E. W., Bruckheimer, E., and Cohen, A. (2018). Cancer pharmacoprevention: targeting polyamine metabolism to manage risk factors for colon cancer. *J. Biol. Chem.* 293, 18770–18778. doi: 10.1074/jbc.tm118.003343
- Gomes, S. E., Pereira, D. M., Roma-Rodrigues, C., Fernandes, A. R., Borralho, P. M., and Rodrigues, C. M. P. (2018). Convergence of miR-143 overexpression, oxidative stress and cell death in HCT116 human colon cancer cells. *PLoS One* 13:e0191607. doi: 10.1371/journal.pone.0191607
- Gonzalez-Vallinas, M., Rodriguez-Paredes, M., Albrecht, M., Sticht, C., Stichel, D., Gutekunst, J., et al. (2018). Epigenetically regulated chromosome 14q32 miRNA cluster induces metastasis and predicts poor prognosis in lung adenocarcinoma patients. *Mol. Cancer Res.* 16, 390–402. doi: 10.1158/1541-7786.mcr-17-0334
- Hammond, S. M. (2015). An overview of microRNAs. *Adv. Drug Deliv. Rev.* 87, 3–14. doi: 10.1007/978-3-319-03725-7_1
- Haque, S., and Harries, L. W. (2017). Circular RNAs (circRNAs) in health and disease. *Genes (Basel)* 8:353. doi: 10.3390/genes8120353
- He, J. H., Li, Y. G., Han, Z. P., Zhou, J. B., Chen, W. M., Lv, Y. B., et al. (2018). The CircRNA-ACAP2/Hsa-miR-21-5p/ Tiam1 regulatory feedback circuit affects

- the proliferation, migration, and invasion of colon cancer SW480 cells. *Cell. Physiol. Biochem.* 49, 1539–1550. doi: 10.1159/000493457
- Holdt, L. M., Kohlmaier, A., and Teupser, D. (2018). Molecular roles and function of circular RNAs in eukaryotic cells. *Cell. Mol. Life Sci.* 75, 1071–1098. doi: 10.1007/s00018-017-2688-5
- Howe, H. L., Wu, X., Ries, L. A., Cokkinides, V., Ahmed, F., Jemal, A., et al. (2006). Annual report to the nation on the status of cancer, 1975–2003, featuring cancer among U.S. Hispanic/Latino populations. *Cancer* 107, 1711–1742. doi: 10.1002/cncr.22193
- Hsiao, K. Y., Lin, Y. C., Gupta, S. K., Chang, N., Yen, L., Sun, H. S., et al. (2017). Noncoding effects of circular RNA CCDC66 promote colon cancer growth and metastasis. *Cancer Res.* 77, 2339–2350. doi: 10.1158/0008-5472.can-16-1883
- Hua, X., Sun, Y., Chen, J., Wu, Y., Sha, J., Han, S., et al. (2019). Circular RNAs in drug resistant tumors. *Biomed. Pharmacother.* 118:109233. doi: 10.1016/j.biopha.2019.109233
- Huang, J., and Guo, L. (2017). Knockdown of SOX9 Inhibits the proliferation, invasion, and EMT in thyroid cancer cells. *Oncol. Res.* 25, 167–176. doi: 10.3727/096504016x14732772150307
- Jin, C., Wang, A., Liu, L., Wang, G., and Li, G. (2019). Hsa_circ_0136666 promotes the proliferation and invasion of colorectal cancer through miR-136/SH2B1 axis. *J. Cell. Physiol.* 234, 7247–7256. doi: 10.1002/jcp.27482
- Ju, H. Q., Zhao, Q., Wang, F., Lan, P., Wang, Z., Zuo, Z. X., et al. (2019). A circRNA signature predicts postoperative recurrence in stage II/III colon cancer. *EMBO Mol. Med.* 11:e10168.
- Kulcheski, F. R., Christoff, A. P., and Margis, R. (2016). Circular RNAs are miRNA sponges and can be used as a new class of biomarker. *J. Biotechnol.* 238, 42–51. doi: 10.1016/j.jbiotec.2016.09.011
- Li, Z., Li, B., Niu, L., and Ge, L. (2017). miR-592 functions as a tumor suppressor in human non-small cell lung cancer by targeting SOX9. *Oncol. Rep.* 37, 297–304. doi: 10.3892/or.2016.5275
- Marcker Espersen, M. L., Linnemann, D., Christensen, I. J., Alamili, M., Troelsen, J. T., and Høgdall, E. (2016). SOX9 expression predicts relapse of stage II colon cancer patients. *Hum. Pathol.* 52, 38–46. doi: 10.1016/j.humpath.2015.12.026
- Meng, S., Zhou, H., Feng, Z., Xu, Z., Tang, Y., Li, P., et al. (2017). CircRNA: functions and properties of a novel potential biomarker for cancer. *Mol. Cancer* 16:94.
- Militello, G., Weirick, T., John, D., Döring, C., Dimmeler, S., and Uchida, S. (2016). Screening and validation of lncRNAs and circRNAs as miRNA sponges. *Brief. Bioinform.* 18, 780–788.
- Patop, I. L., and Kadener, S. (2018). circRNAs in cancer. *Curr. Opin. Genet. Dev.* 48, 121–127.
- Peng, Y., and Croce, C. M. (2016). The role of MicroRNAs in human cancer. *Signal Transduct. Target. Ther.* 1:15004.
- Prevostel, C., and Blache, P. (2017). The dose-dependent effect of SOX9 and its incidence in colorectal cancer. *Eur. J. Cancer* 86, 150–157. doi: 10.1016/j.ejca.2017.08.037
- Qu, Z., and Adelson, D. L. (2012). Evolutionary conservation and functional roles of ncRNA. *Front. Genet.* 3:205. doi: 10.3389/fgene.2012.00205
- Sakaguchi, M., Hisamori, S., Oshima, N., Sato, F., Shimono, Y., and Sakai, Y. (2016). miR-137 regulates the tumorigenicity of colon cancer stem cells through the inhibition of DCLK1. *Mol. Cancer Res.* 14, 354–362. doi: 10.1158/1541-7786.mcr-15-0380
- Shen, Z., Deng, H., Fang, Y., Zhu, X., Ye, G. T., Yan, L., et al. (2015). Identification of the interplay between SOX9 and S100P in the metastasis and invasion of colon carcinoma. *Oncotarget* 6, 20672–20684. doi: 10.18632/oncotarget.3967
- Slattery, M. L., Mullany, L. E., Sakoda, L. C., Wolff, R. K., Samowitz, W. S., and Herrick, J. S. (2018). Dysregulated genes and miRNAs in the apoptosis pathway in colorectal cancer patients. *Apoptosis* 23, 237–250. doi: 10.1007/s10495-018-1451-1
- Stark, Z., Bruno, D. L., Mountford, H., Lockhart, P. J., and Amor, D. J. (2010). De novo 325 kb microdeletion in chromosome band 10q25.3 including ATRNL1 in a boy with cognitive impairment, autism and dysmorphic features. *Eur. J. Med. Genet.* 53, 337–339. doi: 10.1016/j.ejmg.2010.07.009
- Teng, Y., Ren, Y., Hu, X., Mu, J., Samykutty, A., Zhuang, X., et al. (2017). MVP-mediated exosomal sorting of miR-193a promotes colon cancer progression. *Nat. Commun.* 8:14448.
- Wang, M., Yu, W., Gao, J., Ma, W., Frentsch, M., Thiel, A., et al. (2019). MicroRNA-487a-3p functions as a new tumor suppressor in prostate cancer by targeting CCND1. *J. Cell. Physiol.* 235, 1588–1600. doi: 10.1002/jcp.29078
- Wang, M., Yu, W., Gao, J., Ma, W., Frentsch, M., Thiel, A., et al. (2020). MicroRNA-487a-3p functions as a new tumor suppressor in prostate cancer by targeting CCND1. *J. Cell. Physiol.* 235, 1588–1600. doi: 10.1002/jcp.29078
- Wang, Q. Y., Zhou, C. X., Zhan, M. N., Tang, J., Wang, C. L., Ma, C. N., et al. (2018). MiR-133b targets Sox9 to control pathogenesis and metastasis of breast cancer. *Cell Death Dis* 9:752.
- Wang, Z. X., Cao, J. X., Liu, Z. P., Cui, Y. X., Li, C. Y., Li, D., et al. (2014). Combination of chemotherapy and immunotherapy for colon cancer in China: a meta-analysis. *World J. Gastroenterol.* 20, 1095–1106. doi: 10.3748/wjg.v20.i4.1095
- Weinberg, B. A., and Marshall, J. L. (2019). Colon cancer in young adults: trends and their implications. *Curr. Oncol. Rep.* 21:3.
- Xiong, W., Ai, Y. Q., Li, Y. F., Ye, Q., Chen, Z. T., Qin, J. Y., et al. (2017). Microarray analysis of circular RNA expression profile associated with 5-fluorouracil-based chemoradiation resistance in colorectal cancer cells. *Biomed. Res. Int.* 2017:8421614.
- Xu, X. W., Zheng, B. A., Hu, Z. M., Qian, Z. Y., Huang, C. J., Liu, X. Q., et al. (2017). Circular RNA hsa_circ_000984 promotes colon cancer growth and metastasis by sponging miR-106b. *Oncotarget* 8, 91674–91683. doi: 10.18632/oncotarget.21748
- Yang, X., Wang, M., Dongjie Yao, B., Li, J., Tang, X., Li, S., et al. (2018). miR-487a promotes progression of gastric cancer by targeting TIA1. *Biochimie* 154, 119–126. doi: 10.1016/j.biochi.2018.08.006
- Yang, Z., Zhao, Y., Lin, G., Zhou, X., Jiang, X., and Zhao, H. (2019). Noncoding RNA activated by DNA damage (NORAD): biologic function and mechanisms in human cancers. *Clin. Chim. Acta* 489, 5–9. doi: 10.1016/j.cca.2018.11.025
- Zhang, J., Liu, H., Zhao, P., Zhou, H., and Mao, T. (2019). Has_circ_0055625 from circRNA profile increases colon cancer cell growth by sponging miR-106b-5p. *J. Cell. Biochem.* 120, 3027–3037. doi: 10.1002/jcb.27355
- Zhang, R., Xu, J., Zhao, J., and Wang, X. (2018). Silencing of hsa_circ_0007534 suppresses proliferation and induces apoptosis in colorectal cancer cells. *Eur. Rev. Med. Pharmacol. Sci.* 22, 118–126.
- Zhou, J., Qie, S., Fang, H., and Xi, J. (2020). MiR-487a-3p suppresses the malignant development of pancreatic cancer by targeting SMAD7. *Exp. Mol. Pathol.* 116:104489. doi: 10.1016/j.yexmp.2020.10.4489
- Zurawek, M., Dzikiewicz-Krawczyk, A., Izykowska, K., Ziolkowska-Suchanek, I., Skowronska, B., Czainska, M., et al. (2018). miR-487a-3p upregulated in type 1 diabetes targets CTLA4 and FOXO3. *Diabetes Res. Clin. Pract.* 142, 146–153. doi: 10.1016/j.diabres.2018.05.044

Conflict of Interest: The authors declare that the research was conducted in the absence of any commercial or financial relationships that could be construed as a potential conflict of interest.

Copyright © 2021 Sun, Cao, Shan, Gao, Liu, Ma and Li. This is an open-access article distributed under the terms of the Creative Commons Attribution License (CC BY). The use, distribution or reproduction in other forums is permitted, provided the original author(s) and the copyright owner(s) are credited and that the original publication in this journal is cited, in accordance with accepted academic practice. No use, distribution or reproduction is permitted which does not comply with these terms.



Circular RNA CircCOL5A1 Sponges the MiR-7-5p/Epac1 Axis to Promote the Progression of Keloids Through Regulating PI3K/Akt Signaling Pathway

OPEN ACCESS

Edited by:

Song Zhao,
First Affiliated Hospital of Zhengzhou
University, China

Reviewed by:

Albert Mellick,
University of New South Wales,
Australia
XiuKai Cao,
Yangzhou University, China

*Correspondence:

Yuping Ren
yprentj@163.com

[†] These authors have contributed
equally to this work and share first
authorship

Specialty section:

This article was submitted to
Epigenomics and Epigenetics,
a section of the journal
Frontiers in Cell and Developmental
Biology

Received: 04 November 2020

Accepted: 04 January 2021

Published: 21 January 2021

Citation:

Lv W, Liu S, Zhang Q, Hu W,
Wu Y and Ren Y (2021) Circular RNA
CircCOL5A1 Sponges the
MiR-7-5p/Epac1 Axis to Promote the
Progression of Keloids Through
Regulating PI3K/Akt Signaling
Pathway.
Front. Cell Dev. Biol. 9:626027.
doi: 10.3389/fcell.2021.626027

Wenchang Lv^{1†}, Shengxuan Liu^{2†}, Qi Zhang¹, Weijie Hu¹, Yiping Wu¹ and Yuping Ren^{1*}

¹ Department of Plastic and Aesthetic Surgery, Tongji Hospital, Tongji Medical College, Huazhong University of Science and Technology (HUST), Wuhan, China, ² Department of Pediatrics, Tongji Hospital, Tongji Medical College, Huazhong University of Science and Technology (HUST), Wuhan, China

Keloids, as a result of abnormal wound healing in susceptible individuals, are characterized by the hyper-proliferation of fibroblasts and exaggerated deposition of extracellular matrix. Current surgical and therapeutic modalities provide limited satisfactory results. Growing evidence has highlighted the roles of circRNAs in acting as miRNA sponges. However, up to date, the regulatory mechanism of circRNAs in the pathological process of keloids has rarely been reported. In this study, cell proliferation, cell migration, flow cytometry, western blotting, fluorescence *in situ* hybridization, dual-luciferase activity, and immunohistochemistry assays were applied to explore the roles and mechanisms of the circCOL5A1/miR-7-5p/Epac1 axis in the keloid. The therapeutic potential of circCOL5A1 was investigated by establishing keloid implantation models. The RT-qPCR result revealed that circCOL5A1 expression was obviously higher in keloid tissues and keloid fibroblasts. Subsequent cellular experiments demonstrated that circCOL5A1 knockdown repressed the proliferation, migration, extracellular matrix (ECM) deposition, whereas promoted cell apoptosis, through the PI3K/Akt signaling pathway. Furthermore, RNA-fluorescence *in situ* hybridization (RNA-FISH) illustrated that both circCOL5A1 and miR-7-5p were located in the cytoplasm. The luciferase reporter gene assay confirmed that exact binding sites were present between circCOL5A1 and miR-7-5p, as well as between miR-7-5p and Epac1. Collectively, the present study revealed that circCOL5A1 functioned as competing endogenous RNA (ceRNA) by adsorbing miR-7-5p to release Epac1, which contributed to pathological hyperplasia of keloids through activating the PI3K/Akt signaling pathway. Our data indicated that circCOL5A1 might serve as a novel promising therapeutic target and represent a new avenue to understand underlying pathogenesis for keloids.

Keywords: keloid, fibroblast, circCOL5A1, miR-7-5p, Epac1, PI3K/Akt pathway

INTRODUCTION

Keloids are a benign skin fibroproliferative tumor that generally serves as a result of abnormal wound healing in susceptible individuals and are unique to humans (Limandjaja et al., 2020). Keloids are often accompanied by severe pain, itching, skin deformities, and even joint movement dysfunction, which seriously affects the physiological and psychological health of patients. Keloids are characterized pathologically by the hyperproliferation of cells (e.g., fibroblasts) and excessive deposition of extracellular matrix (ECM) (e.g., type I and type III collagen) (Rippa et al., 2019). Keloid-derived fibroblasts, served as the main cellular components in keloid tissues, play a pivotal role in modulating the synthesis and re-modeling of ECM, indicating an association between the continuous aggressive growth and collagen production (Arjunan et al., 2020). Meanwhile, in keloid patients, the systemic balance between fibroblast proliferation and apoptosis is distorted, resulting in the continuous hyperplasia of keloids. Currently, there are a variety of treatment methods such as compression therapy, intralesional steroid therapy, cryotherapy, and the combination of surgical resection and radiotherapy for keloid prevention and treatment (Betarbet and Blalock, 2020). However, the recurrence rate remains high and none of these treatments provide satisfactory results in all patients. Therefore, an in-depth understanding of the molecular mechanisms of aggressive progression of keloid and exploring novel efficient therapeutic strategies is an urgent need.

Circular RNAs (circRNAs) are a relatively new RNA type and are commonly generated by back-splicing of primary transcripts (Artemaki et al., 2020). Unlike the linear RNA, circRNAs are a covalently closed single-stranded RNA, in which the junction of the 3' end and 5' end of the exon are tightly connected. Based on their peculiar structure, circRNAs exist in multiple species with high sequence conservation and are not easily degraded by exonuclease (Xu et al., 2020). Additionally, circRNA possesses multiple functions at the post-transcriptional level, including acting as a microRNA (miRNA) sponge, binding to RNA-binding proteins (RBPs), regulating transcription and translation (Di Timoteo et al., 2020). Recently, with the development of high-throughput sequencing technology and bioinformatics analysis, increasing pieces of evidence have demonstrated that circRNAs are emerging as a crucial role in various biological processes, including proliferation, migration, and apoptosis.

Most studies have indicated that circRNAs are able to serve as competitive endogenous RNAs (ceRNAs) or miRNA sponges, to regulate target gene expression. For example, circCCDC9 acts as a ceRNA of miR-6792-3p to suppress the proliferation and invasion of gastric cancer cell lines *in vitro* and tumor growth and metastasis *in vivo* (Luo et al., 2020). Yue et al. (2020) constructed a circHUWE1-associated ceRNA network and then determined that circHUWE1 could directly sponge miR-29b to relieve AKT3 suppression, via activating the AKT signaling pathway in skeletal muscle development. In this research, we have studied a previously reported circRNA, named as circCOL5A1, which was derived from the host gene COL5A1 and was cyclized with the head-to-tail splicing of exon 13 and exon 19 (Shi et al., 2020). COL5A1 encodes an alpha

chain for one of the low abundance fibrillar collagens, which is closely related to type V collagen and involves in the progression of many fibrotic diseases. For example, based on gene expression analysis of human osteoarthritis synovium, Remst et al. (2014) found that the COL5A1, as a TGF β -responsive gene, was significantly upregulated in humans with end-stage osteoarthritis. Besides, the histopathological features of skin and lung in a animal model of systemic sclerosis induced by type V collagen revealed that increased collagen V fibers and COL5A1 gene expression (Teodoro et al., 2019). The study by Yokota et al. (2020) demonstrated that type V collagen played a crucial role in scar size following myocardial infarction and induced fibroblast activation. Therefore, based on the regulatory role of COL5A1 in these fibrosis diseases, it could be speculated that COL5A1 might be associated with the pathogenesis of keloids and have the potential to serve as a novel therapeutic target. Moreover, in keloid, Shi et al. (2020) identified potential diagnostic and therapeutic circRNAs using a circRNA microarray assay, the results revealed that a total of five circRNAs, of which circCOL5A1 was markedly upregulated in keloid tissues. Subsequently, biological process analysis determined that these target genes might play vital roles in the positive regulation of cell proliferation and cell cycle pathways. However, the mechanism of circCOL5A1 as ceRNA in keloids has not been fully elucidated.

There is an increasing amount of evidence which highlights ncRNAs (mainly miRNAs and lncRNAs) key contribution to the pathogenesis of keloids through modulating the pathways of promoting and suppressing fibrosis. However, the pathological mechanism of circRNAs in keloid development has rarely been reported. It is key and feasible to better understand these novel RNA interactions and construct a circRNA-miRNA-mRNA network for further research on the specific pathogenesis of keloid. Therefore, in this study, based on a published circRNA microarray analysis, we first investigated the function and regulatory mechanism of circCOL5A1 in keloids. The results revealed that circCOL5A1 acted as a sponge of miR-7-5p to affect the expression of Epac1, and eventually modulated the human keloid fibroblasts (HKFs) functions including proliferation, migration, and apoptosis through PI3K/Akt signaling pathway. Collectively, our findings have provided evidence of the mechanism of circRNAs in the pathogenesis of keloids and offered novel insights into therapeutic targets for keloid treatment.

MATERIALS AND METHODS

Tissue Samples

Keloid tissue specimens were obtained from 15 patients who underwent cosmetic resection at the Department of Plastic Surgery, Tongji Hospital of Huazhong University of Science and Technology between June 2018 and September 2020. Meanwhile, the normal skin tissues of the control group were taken from 15 patients with circumcision. These samples were collected with consent from these patients, and the pathological characteristics of the samples had been confirmed by pathologists. Furthermore, this research was approved by the

ethical committee of Tongji Hospital of Huazhong University of Science and Technology (Wuhan, China).

The Primary Fibroblasts Culture and Transfection

Human keloid fibroblasts and human dermal fibroblasts (HDFs) were isolated from the center of freshly surgically removed keloid tissues and normal skin tissues, respectively, and were extracted by the collagenase digestion method (Pandamooz et al., 2012). The primary fibroblasts were cultured in Dulbecco's Modified Eagle's Medium: Nutrient Mixture F-12 (DMEM/F12, Gibco, Carlsbad, CA, United States) supplemented with 10% fetal bovine serum (FBS, Gibco, Carlsbad, CA, United States), penicillin, and streptomycin (100 IU/mL) at 37°C in 5% CO₂ atmosphere. HDFs and HKFs at 3–5 passages were used for further experiments.

The primary fibroblasts were seeded in 6-well plates at a density of 2×10^5 /well and incubated to 40–50% confluence before transfection. The small interfering RNAs (siRNAs) of circCOL5A1 (si-circCOL5A1), miR-7-3p mimics, miR-7-3p inhibitor, and the corresponding negative control (denoted as si-NC, mimics NC, and inhibitor NC group) were designed and synthesized by Ribo Biotech (Guangzhou, China). Meanwhile, according to the manufacturer's instruction, Lipofectamine 3000 Transfection Reagent (Invitrogen, United States) was regarded as the transfection medium. After 24 h, RT-qPCR analysis was applied to evaluate transfection efficiency.

Cell Proliferation Assay and 5-Ethynyl-20-Deoxyuridine (EdU) Incorporation Assay

The proliferation of HKFs was assessed using a cell counting kit-8 (CCK-8) assay (Dojindo, Kumamoto, Japan) according to the manufacturer protocol (Wu et al., 2020). Briefly, HKFs were plated in a 96-well plate at a density of 3×10^3 /well and incubated to 40% confluence. After transfection, 10 μ L CCK-8 reagent was directly added to each well of a 96-well plate at the specified time (0 h, 24 h, 48 h, 72 h, and 96 h), and then incubated for 2 h in a dark environment. Finally, a microplate reader (BioTek Instruments, United States) was applied to measure the optical density (OD) at a wavelength of 450 nm.

The proliferation of HKFs was also measured with an EdU DNA cell proliferation kit (RiboBio, Wuhan, China). After transfection, the HKFs were incubated with a medium containing 50 μ M EdU for 2 h. The HKFs were fixed with 4% paraformaldehyde for 30 min, and then the excess formaldehyde was neutralized with a 2 mg/mL glycine solution. Subsequently, the HKFs were, respectively, stained in Apollo reaction cocktail and Hoechst staining solution and then incubated for 30 min in the dark. A fluorescence microscope (IX35, Olympus, Japan) was used for capturing randomly selected areas to observe the ratio of proliferating cells (EdU positive) to the total number of cells (DAPI positive) (Bieg et al., 2019). Samples were prepared in triplicate.

Wound Healing Assay

After transfection, HKFs were seeded on the 6-well plate at a density of approximately 2×10^5 /well and grown to confluence until formed a single cell layer. Next, a 200 μ L pipette tip was employed to gently scratch the wound across the cell monolayer (Yun et al., 2015). Afterward, the detached cells and debris were removed by washing with phosphate-buffered saline (PBS) and replaced with serum-free DMEM/F12 medium. After routine culture for 0 h and 24 h, the cells that migrated to the scratched area were photographed with a microscope, respectively. In order to evaluate wound closure, Image J software was utilized to measure and calculate the horizontal distance of migrating cells from the initial wound. The experiment was performed in triplicate with the mean value calculated.

Transwell Migration Assay

The migratory ability of HKFs was also assessed by 24-well transwell migration chambers (8 μ m size, Corning, United States). In short, a total of 5×10^4 /well HKFs were resuspended in 200 μ L serum-free DMEM/F12 medium and inoculated evenly into the inner chambers. Meanwhile, the bottom chambers were replenished with 500 μ L DMEM/F12 medium containing 20% FBS as the attractant. After 24 h, the cells migrated to the lower chamber through the hole and were fixed with 4% paraformaldehyde and then stained with 0.1% crystal violet (Qiu et al., 2018). Finally, Image J software was employed to count the number of migrated cells.

Cell Apoptosis Assay

The apoptosis rate of HKFs was evaluated using the Annexin V-FITC/propidium iodide (PI) Apoptosis Detection Kit (KeyGen Biotech, Nanjing, China). Briefly, HKFs were seeded at a density of approximately 2×10^5 /well in 6-well plates. After transfection, cells were harvested using pancreatin without EDTA and washed with cold PBS. Subsequently, the cells were resuspended in 500 μ L binding buffer and incubated with 5 μ L Annexin V-FITC for 15 min and 5 μ L PI for 5 min in the dark (Lu et al., 2018). Finally, a flow cytometry (BD FACSCalibur, San Jose, CA, United States) was applied to detect the cell-apoptosis rate in each tube. In addition, the percentage of early (Annexin V-FITC+/PI-) and late (Annexin V-FITC+/PI+) apoptotic cells in each sample was calculated by FlowJo software version 8 (Ashland, OR, United States) to evaluate the influence of intervention factors on cell apoptosis.

RNA Isolation and Quantitative Reverse-Transcription PCR (RT-qPCR) Assay

TRIzol reagent kit (Invitrogen) was performed to extract circRNAs, miRNAs, and mRNAs from tissue specimens and cultured primary cells, respectively. Then, the concentration and purity of total RNA were evaluated using a NanoDrop 2000 spectrophotometer (Thermo Fisher Scientific, Wilmington, DE, United States). The PrimeScript RT kit (Takara, Japan) was performed to reverse transcription of RNA into complementary DNA (cDNA) at 103°C for 5 s, 37°C for 10 min, and 4°C for

TABLE 1 | All primer sequences used for RT-qPCR.

Gene name	Forward primer	Reverse primer
circCOL5A1	CACCAAATTCCTCGACCGCA	TGGCTGAGCTCAAACACCTCC
COL5A1	TACCCTGCGTCTGCATTTC	GCTCGTTGTAGATGGAGACCA
Epac1	GACCGGAAGTACCACCTTAGG	AGATTCCACAACCTTGGCTCC
miR-7-5p	CAG GGA GGC GTG GAT CAC TG	CGTCG GGG GCT CAT GGA GCGG
U6	CTCGCTTCGGCAGCACATATACT	ACGCTTCACGAATTTGCGTGTG
GAPDH	ACCACAGTCATGCCATCAC	TCCACCACCCCTGTTGCTGTA

15 min (Wang et al., 2018). The qRT-PCR analysis was performed a Power SYBR Green PCR master mix (Yeasen, Shanghai, China) in a real-time thermal cycler. All primer sequences used for RT-qPCR are summarized in **Table 1**. The expression of circRNA and mRNA was normalized to the GAPDH level, and the expression of miRNA was normalized to the U6 level. All data were collected and quantified using the $2^{-\Delta\Delta Ct}$ method to evaluate relative expression levels of circRNAs, miRNAs, and mRNAs. The RT-qPCR assay was performed using three independent replicates.

Western Blot Analysis

Total proteins were extracted using lysis buffer for radio-immunoprecipitation assay (RIPA) (Boster, Wuhan, China), and the protein concentration estimated with a bicinchoninic acid (BCA) protein assay kit (Boster, Wuhan, China). After boiling at 100°C for 5 min, the equal amounts of protein extract were electrophoresed in a 10% sodium dodecyl sulfate-polyacrylamide gel electrophoresis (SDS-PAGE) at 80 V for 20 min and then 120 V for 1 h. Subsequently, the protein extract was transferred to PVDF membranes (Biosharp, Shanghai, China) at 220 mA for 60 min. After repeated washing using tris-buffered saline containing Tween 20 (TBST), the PVDF membranes were blocked with 5% bull serum albumin (BSA) blocking buffer for 2 h at 37°C, and then incubated with primary antibody collagen I, 1:1,000; collagen III, 1:1,000; α -smooth muscle actin (α -SMA), 1:1,000; Epac1, 1:1,500; p-Akt, 1:1,000; t-Akt, 1:1,000; p-PI3K, 1:1,000; t-PI3K, 1:1,000; GAPDH, 1:2,500 overnight at 4°C. Afterward, the PVDF membranes were incubated with a secondary antibody (anti-rabbit IgG, HRP-linked antibody, 1:5,000; anti-mouse IgG, HRP-linked antibody, 1:5,000) for 1 h at 37°C (Wang et al., 2020b). Finally, signals were visualized using the enhanced chemiluminescence (ECL) detection kit (Yeasen, Shanghai, China), and the relative protein abundance was measured by ImageJ image analysis software (version 1.44p, National Institutes of Health, United States). All primary antibody was purchased from Abcam, Cambridge, MA, United States.

Fluorescence *in situ* Hybridization (FISH)

The FISH analysis was performed to observe and verify the intracellular localization of circCOL5A1 and miR-7-5p in primary HKFs. Cy3-labeled circCOL5A1 probes and FAM-labeled miR-7-5p were designed and synthesized by RiboBio (Wuhan, China). The probe sequences of circCOL5A1 and miR-7-5p for FISH were obtained on request. In short, after

rinsing with PBS, the cells were fixed in 4% formaldehyde solution at 37°C for 10 min, and then incubated with 0.5% Triton X-100 solution at 4°C for 5 min (Squassina et al., 2020). Specific probes for circCOL5A1 and miR-7-5p were performed *in situ* hybridization overnight in the dark. Finally, a fluorescence microscope (IX35, Olympus, Japan) was used to acquire and visualize the images at 200 × magnification and 400 × magnification.

Bioinformatic Analysis

Based on a circRNA published microarray, the Cytoscape software platform¹ was applied to construct and visualize a circRNA-miRNA-mRNA interaction network (Marazzi et al., 2020). Moreover, we performed an online prediction software Circular RNA Interactome² to predict the miRNAs binding sites of circCOL5A1. Similarly, three independent miRNA databases (TargetScan, miRWalk, and miRDIIP) were applied to predict mRNAs that may bind to miR-7-5p, respectively. Gene Ontology (GO) consisted of three structured ontologies such as biological processes (BP), cellular components (CC), and molecular functions (MF) (Yoneda et al., 2020). Kyoto Encyclopedia of Genes and Genomes (KEGG) database was applied for investigating worthwhile biological pathways of target genes (Zhou et al., 2020). Finally, the online website (DAVID)³ was used to perform GO annotation and KEGG pathway enrichment analysis on mRNA targeted by circRNA.

Dual-Luciferase Activity Assay

The recombinant luciferase reporter plasmid of circCOL5A1 (wild type-WT), circCOL5A1 (hsa-miR-7-5p, mutant-Mut, Mut1 + Mut2), and pRL-CMV (Promega) were designed and synthesized by Heyuan (Shanghai, China). When HEK293T cells grown to a confluency of 40–50%, the circCOL5A1 plasmid together with the miR-7-5p mimic were transfected into cells via Lipofectamine 3000 Transfection Reagent (Invitrogen). Analogously, the psiCHECK-Epac1-Wt or psiCHECK-Epac1-Mut plasmids were synthesized by Heyuan (Shanghai, China) and then co-transfected into cells with miR-7-5p mimics. After transfection, firefly luciferase activity and Rluc activity were evaluated using the dual-luciferase reporter gene (DLR) analysis system kit (Promega, United States). Firefly luciferase (Luc) was defined as a reference to assess the signal value of Renilla (Rluc) luciferase (Li et al., 2020).

Implantation of Keloid Tissue Into the Nude Mice

Animal experiments in this study were approved by the Animal Care and Use Committee of Huazhong University of Science and Technology (Wuhan, China). The keloid specimens obtained from the patients were manually divided into small pieces (5 mm × 3 mm × 3 mm). A total of 15 small pieces were randomly assigned to five groups and stored in DMAE/F12 medium. To explore the therapeutic effect of circCOL5A1 on

¹<http://www.cytoscape.org/>

²<https://circinteractome.nia.nih.gov/>

³<https://david.abcc.ncifcrf.gov>

keloids *in vivo* (**Scheme 1**), 6-week-old male BALB/C nude mice underwent general inhalation anesthesia ($n = 5$ for each group). Subsequently, within 3 h of keloid tissue resection, three small keloid tissue samples were implanted into each of the five nude mice (one on the upper back, one on the lower back, and one on the abdomen) (Fanous et al., 2019). Each transplantation site was at least 3 cm apart to prevent treatment diffusion and mutual influence. After the wound skin healed (1 week), each mouse was randomly divided into one of three treatment groups (control, si-NC, and si-COL5A1). To avoid potential confounding factors, especially the different mechanical tensile strengths of the skin in different sites, the sites chosen for different interventions were randomized. After 2 weeks of intervention, the keloid grafts were taken out from the nude mice and weighed, while the grafts volume was measured. The keloid grafts were used for the following western blot analysis and histological assessment.

Immunohistochemistry (IHC)

After obtaining the transplanted keloid tissues from nude mice, the keloid tissues were embedded in paraffin and prepared into 4 mm sections. The sections were deparaffinized in xylene and rehydrated in ethanol solutions. To eliminate non-specific binding, the dehydrated sections were blocked in normal goat serum for 30 min and then incubated overnight with primary antibodies (1:100 dilution; Santa Cruz Biotechnology, Santa Cruz, CA, United States) at 4°C. After incubating the secondary antibody in the next day, the sections are stained with diaminobenzidine (DAB) to facilitate visualization of positive signals and then the nuclei were counterstained with hematoxylin (Damjanovic et al., 2020). The immunoreactivity of type I and III collagen and α -SMA in each section were assessed semiquantitatively using MetaMorph image analysis software (Universal Image Corp., Buckinghamshire, United Kingdom). The result was a statistical analysis of the average signal intensity of three different digital images.

Statistical Analysis

All data were expressed as mean \pm standard deviation using GraphPad Prism Software (version 8.0.1, La Jolla, CA, United States). Comparison between two groups was analyzed using the Student *t*-test. Differences between the three or more groups of data were compared by one-way ANOVA. Pearson's test was applied for the correlation analysis between two groups. A value of $p < 0.05$ was considered statistically significant.

RESULTS

The Expression of circCOL5A1 in Keloid Tissues and HKFs

The previous sequencing study showed that circCOL5A1 was significantly upregulated in keloids compared with normal skin tissues through the microarray assay results. Afterward, the relative expression of circCOL5A1 was detected by qRT-PCR in keloid tissues and normal skin tissues. The expression level of circCOL5A1 was significantly upregulated in keloid

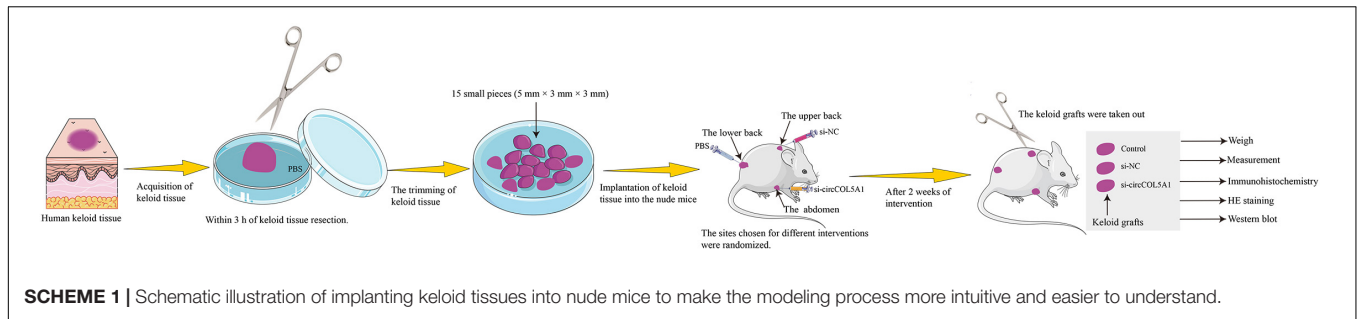
tissues, which was consistent with the microarray assay data (**Figure 1A**). Meanwhile, we applied collagenase digestion to extract primary fibroblasts, and the result of qPCR showed that circCOL5A1 was also significantly increased in human keloid fibroblasts (HKFs) compared with HDFs (**Figure 1B**). These data suggested that circCOL5A1 might be a circular molecular closely correlated with the progression of keloids. To investigate the regulatory effect of circCOL5A1, three circCOL5A1 siRNA and NC siRNA (the sequence is 5'-TTCTCCGAACGTGTCACGTdTdT-3') were designed and synthesized to specific silence circCOL5A1 without affecting the level of COL5A1 mRNA in the HKFs (**Figure 1C**). After detecting the silencing efficiency through qRT-PCR, si-circCOL5A1-2 (the sequence is 5'-GTGTTTGAGCTCAGCCAGC-3') was selected for subsequent experiments. Besides, circCOL5A1 was generated from the COL5A1 gene, which was located at chromosome 9 and consisted of the head-to-tail splicing of exon 13 and exon 19 (CircBase ID: hsa_circ_0007482, splicing sequence length: 545 nucleic acid base) (**Figure 1D**).

Construction of circRNA-miRNA-mRNA Network

Firstly, we performed an online prediction software Circular RNA Interactome (see text footnote 2) to predict many miRNAs (such as miR-7-5p, miR-604, miR-639, and miR-665) binding to circCOL5A1 (**Supplementary Table 1**). Secondly, the relative expressions of these miRNAs (such as miR-7-5p, miR-604, miR-639, and miR-665) were detected by qRT-PCR in keloid tissues and normal skin tissues. The results of qRT-PCR revealed that only miR-7-5p and miR-665 were significantly downregulated in keloid tissues compared with normal skin tissues, while miR-604 and miR-639 were not differentially expressed between keloid tissues and normal skin tissues (**Supplementary Figure 1**). Thirdly, previous study determined that miR-7 downregulation mediated excessive collagen expression in localized scleroderma, suggesting that miR-7 played some part in the pathogenesis of cutaneous fibrosis (Etoh et al., 2013). Therefore, miR-7-5p was selected as a potential binding target of circCOL5A1 for constructing circRNA-miRNA-mRNA network. Fourthly, target genes of miR-7-5p were detected by three independent miRNA databases (TargetScan, miRWalk, and mirDIP). Taken together, we screened out circCOL5A1 based on the published microarray assay results and then constructed a circRNA-miRNA-mRNA network according to the ceRNA theory and the presence of potential binding sites (**Figure 1E**).

GO and KEGG Pathway Enrichment Analyses

In this study, we initially explored the mechanism of circCOL5A1 through predicting its target mRNAs. To predict the potential target genes of miR-7-5p, we used three databases (TargetScan, miRWalk, and mirDIP) and then identified a total of 2262 target genes. We next determined the potential functions of these target genes, GO and pathway analyses were performed using the online website (DAVID, see text footnote 3). GO enrichment analysis suggested that the genes targeted by circCOL5A1 had



an effect on several biological processes, especially cell growth and histone modification (Figure 1F). KEGG pathway analysis demonstrated that these target genes were involved in the PI3K/Akt signaling pathway, mTOR signaling pathway, and cAMP signaling pathway that were all associated with the pathogenesis of keloids (Figure 1G).

Characteristics of circCOL5A1 in HKFs

In order to further confirm the stability of circCOL5A1, after treatment with or without RNase R, the expression levels of circCOL5A1 and linear COL5A1 were detected in HKFs by qRT-PCR. The results confirmed that RNase R treatment degraded the linear transcript of COL5A1, while circCOL5A1 could resist RNase R treatment (Figure 1H). Additionally, we found that the subcellular localization of circCOL5A1 was mainly located in the cytoplasm using a FISH assay. It indicated that circCOL5A1 might function in the cytoplasm (Figure 1I). Meanwhile, negative control was performed to determine that circCOL5A1 was mainly localized in the cytoplasm of HKFs with specific signal (Supplementary Figure 2). In summary, the above results determined that circCOL5A1 was mainly localized in the cytoplasm of HKFs with high abundance, high sequence conservation, and specific expression.

CircCOL5A1 Regulated HKFs Proliferation, Migration, Apoptosis, and ECM Deposition Through PI3K/Akt Signaling Pathway *in vitro*

To explore the role of circCOL5A1 in the proliferation of HKFs, CCK-8 assay, and EdU assay were performed. The CCK-8 analysis demonstrated that the silencing of circCOL5A1 observably suppressed the proliferation ability, especially 48 h after transfection (Figure 2A). Similarly, the EdU results revealed that silencing circCOL5A1 significantly reduced the percentage of EdU positive cells (Figure 2B). Meanwhile, wound healing and transwell assay was performed to investigate the effect of circCOL5A1 on HKFs migration. The results revealed that knockdown of circCOL5A1 could suppress the migration of HKFs (Figures 2C–E). As shown in Figure 2F, the downregulation of circCOL5A1 significantly increased the apoptotic ratio of HKFs, which was consistent with the results of CCK-8 assay and EdU assay.

Furthermore, to further explore the role of circCOL5A1 in promoting the pathological hyperplasia of keloid, the expression

of the main components of ECM were examined, including type I and III collagen, and α -SMA through western blot. The results indicated that si-circCOL5A1 transfection markedly reduced the protein expression levels of type I and III collagen, and α -SMA in HKFs (Figure 2G). Besides, the phosphorylation levels of PI3K and Akt were significantly suppressed after transfection with si-circCOL5A1 (Figure 2H). Taken together, these above data demonstrated that circCOL5A1 regulated HKFs proliferation, migration, apoptosis, and ECM deposition through PI3K/Akt signaling pathway.

MiR-7-5p Was Significantly Downregulated in Keloid Tissues and HKFs

Taking into account circCOL5A1 stable located in the cytoplasm, we also investigated the subcellular location of miR-7-5p in HKFs. The result of the FISH assay showed that miR-7-5p was also located in the cytoplasm (Figure 3A). Furthermore, we detected the expression of miR-7-5p both in keloid tissues and HKFs. The results of qRT-PCR suggested significant downregulation of miR-7-5p in keloid tissues and HKFs (Figures 3B,C), indicating that miR-7-5p itself was a fibrosis-inhibitor in the progress of keloids. After transfection with miR-7-5p mimics or miR-7-5p inhibitor, miR-7-5p expression was significantly enhanced in the miR-7-5p inhibitor group compared with the inhibitor NC group, whereas miR-7-5p expression was significantly decreased in the miR-7-5p mimics group (Figure 3D).

MiR-7-5p Regulated HKFs Proliferation, Migration, and Invasion *in vitro* by Targeting Epac1

As no studies have explored the role of miR-7-5p in the pathological process of keloids, we clarified for the first time the mechanism and biological functions of miR-7-5p in HKFs. Interestingly, bioinformatics analysis predicted the potential binding sites between miR-7-5p and Epac1. Simultaneously, our previous study had confirmed that Epac1 played an essential regulatory role in the occurrence and progression of keloids (Lv et al., 2021). Therefore, we choose Epac1 as the target gene of miR-7-5p for further functional verification.

In the following, the expression of miR-7-5p in HKFs was successfully knocked down in HKFs using transient transfection with specific miR-7-5p inhibitor and upregulated

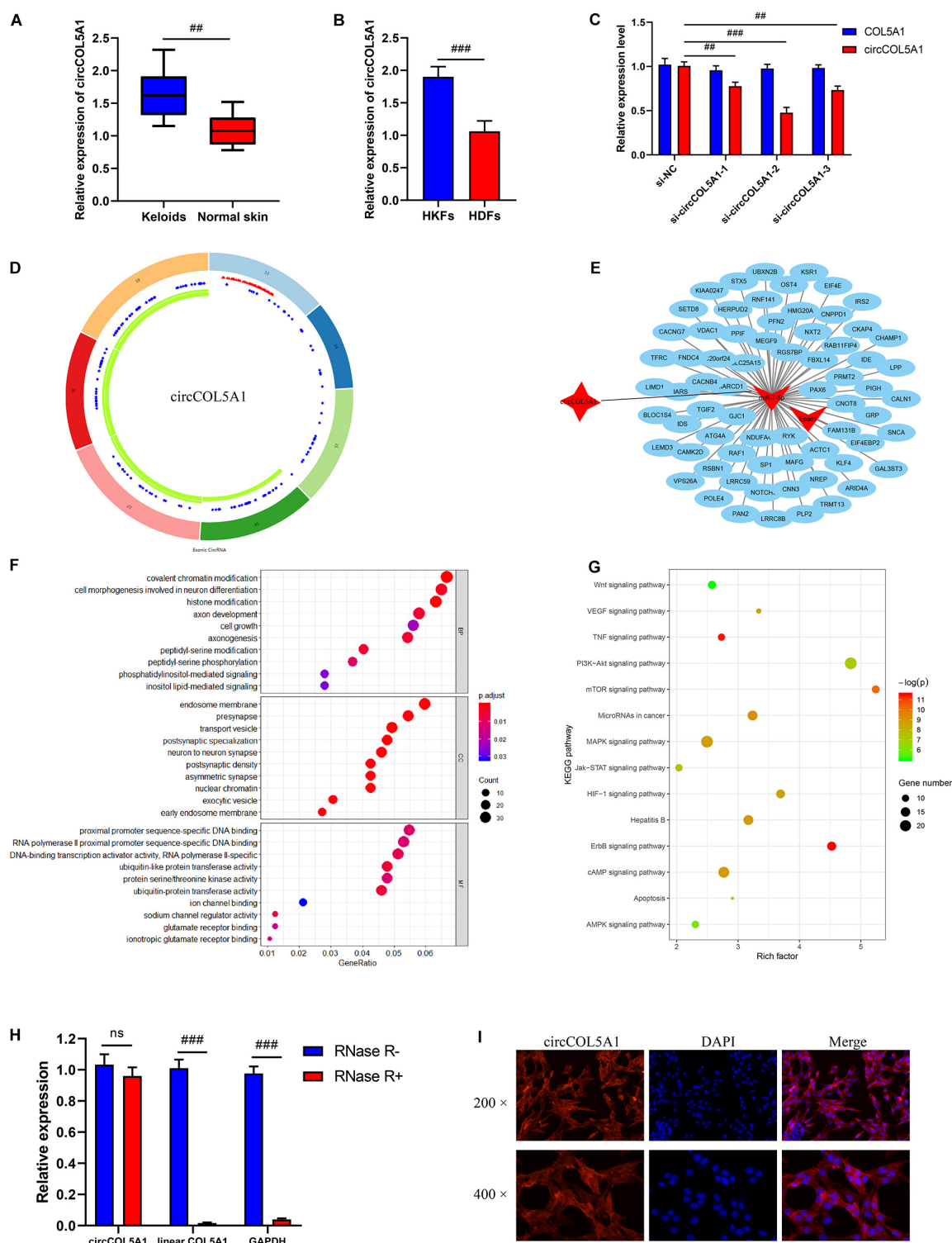
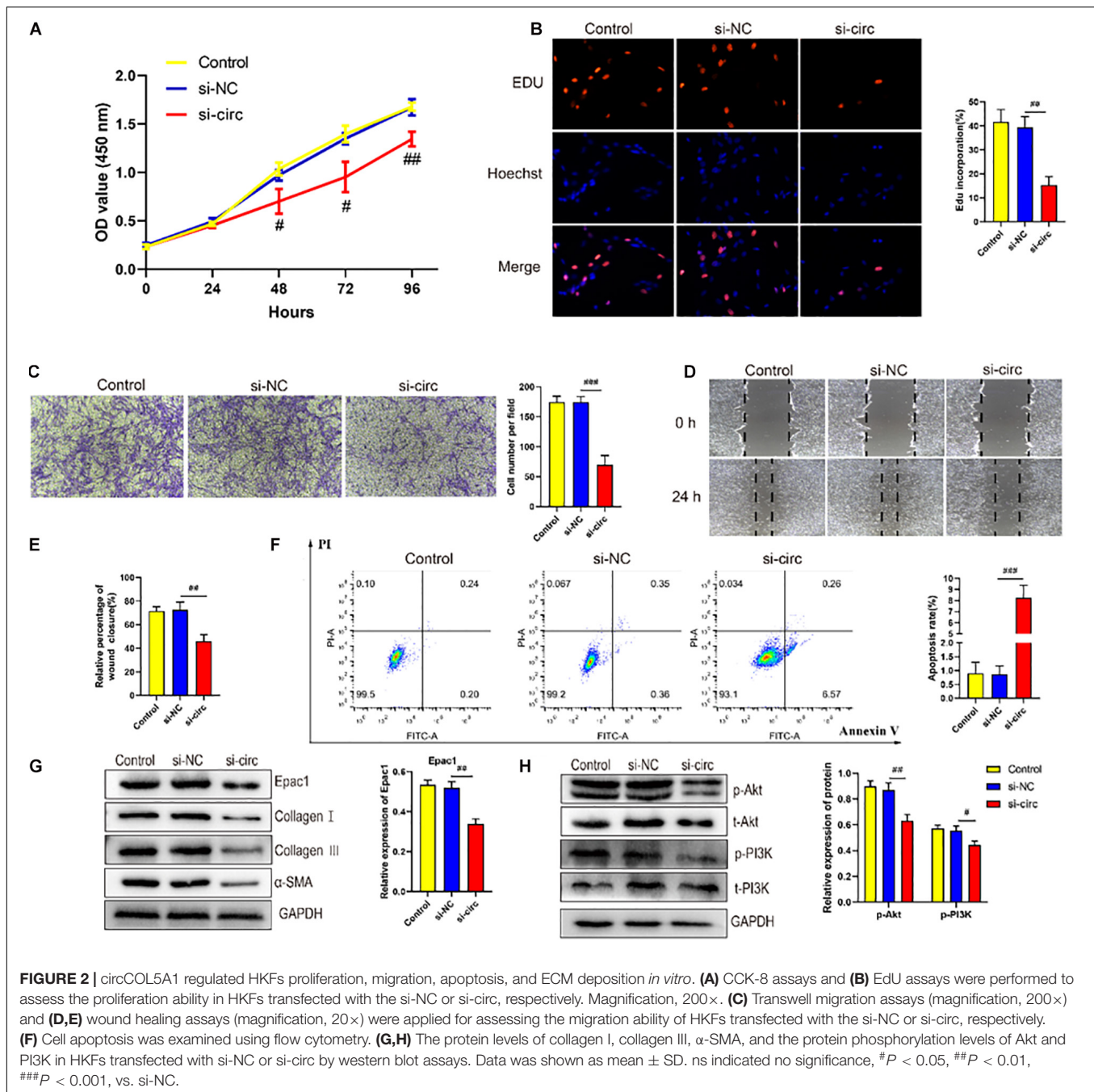


FIGURE 1 | Bioinformatics analysis and characterization of circCOL5A1. **(A)** The relative RNA levels of circCOL5A1 were evaluated by qRT-PCR between keloid tissues and normal skin. **(B)** The relative RNA levels of circCOL5A1 were evaluated by qRT-PCR between HKFs and HDFs. **(C)** The silent efficiency of circCOL5A1 was evaluated by qRT-PCR in HKFs transfected with si-NC or siRNAs, respectively. **(D)** The structure and binding sites of circCOL5A1. The red sites represented the microRNA response element. The blue sites represented RNA binding protein. The green sites represented an open reading frame. **(E)** Construction of circRNA-miRNA-mRNA network. GO **(F)** and KEGG **(G)** analysis of circCOL5A1 target genes. **(H)** The relative abundance of circCOL5A1 or linear COL5A1 in HKFs were detected by qRT-PCR after treatment with or without RNase R. **(I)** FISH assays were performed to observe the cellular location of circCOL5A1 (red) in HKFs (magnification, 200× and magnification, 400×). ## $p < 0.01$ and ### $p < 0.001$.



using specific miR-7-5p mimics (Figure 3D). The CCK-8 and EdU assay presented that knockdown of miR-7-5p could significantly promote the proliferation ability and increase the percentage of EdU positive cells, indicating that miR-7-5p in itself could prevent the cell proliferative potential (Figures 3E,F). Meanwhile, the results of wound healing and transwell assay revealed that the downregulation of miR-7-5p was able to promote the migration of HKFs. Inversely, substantially increased expression of miR-7-5p could slow down cell migration (Figures 3G,H). Concurrently, the apoptotic tendency of HKFs was promoted strongly

by miR-7-5p mimics, yet miR-7-5p inhibitor induced the opposite trend of cell apoptosis (Figure 3I). Besides, the results of western blot revealed that the Epac1 protein level prominently decreased after the transfection of miR-7-5p mimics, while Epac1 expression prominently increased in the miR-7-5p inhibitor group (Figure 3J). Meanwhile, the transfection of HKFs with miR-7-5p mimics resulted in the reduction of collagen I, collagen III, and α -SMA at protein levels, indicating that miR-7-5p itself could reverse the pathological phenotype of excessive ECM deposition in keloids (Figure 3J). Overexpression of miR-7-5p significantly suppressed the

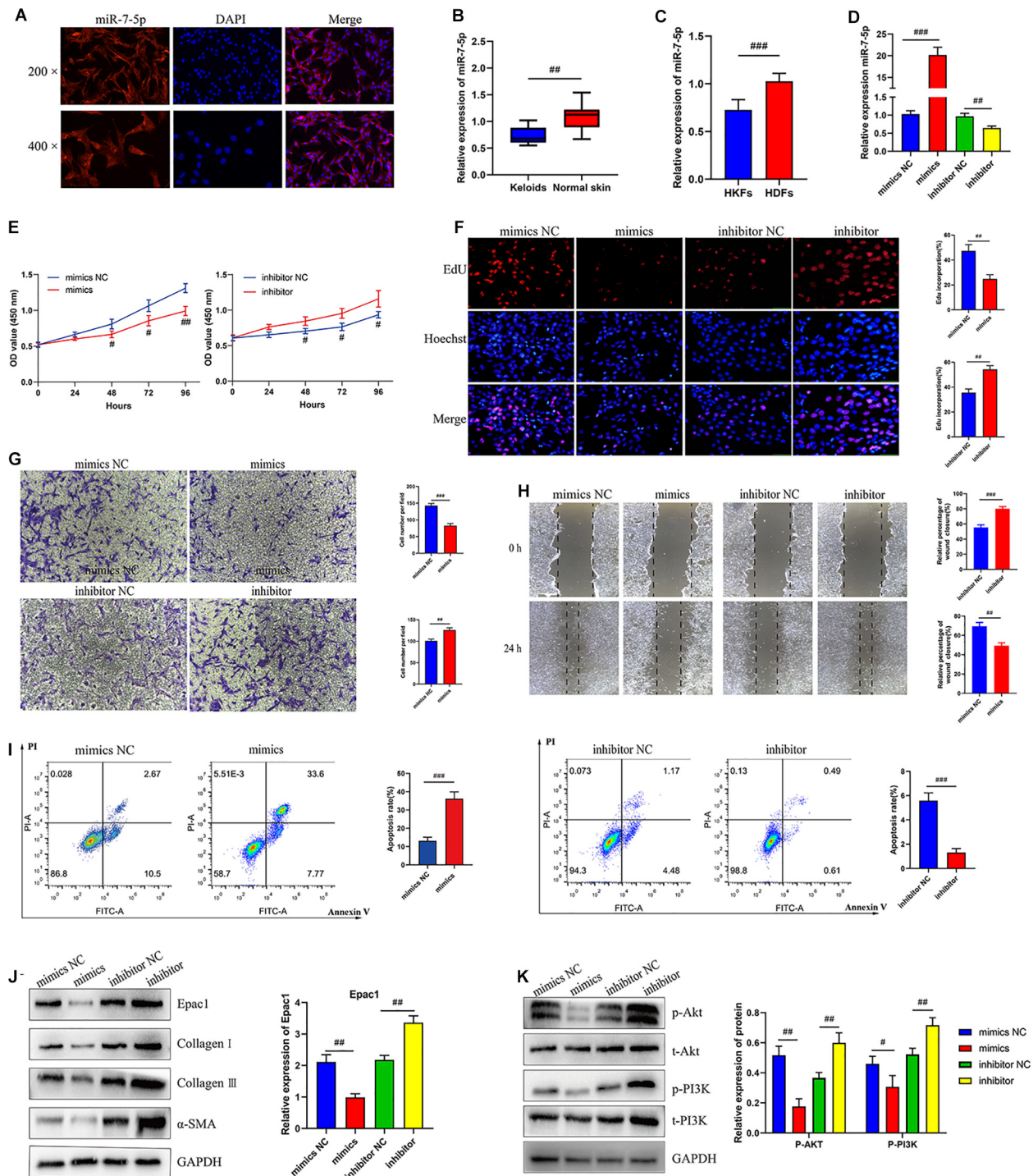


FIGURE 3 | MiR-7-5p regulated HKFs proliferation, migration, apoptosis, and ECM deposition *in vitro* by targeting Epac1. **(A)** FISH assays were performed to observe the cellular location of miR-7-5p (red) in HKFs (magnification, 200 \times and magnification, 400 \times). **(B)** The relative RNA levels of miR-7-5p were evaluated by qRT-PCR between keloid tissues and normal skin. **(C)** The relative RNA levels of miR-7-5p were evaluated by qRT-PCR between HKFs and HDFs. **(D)** The transfection efficiency of miR-7-5p was evaluated by qRT-PCR in HKFs transfected with the miR-7-5p mimics or inhibitor, respectively. **(E)** CCK-8 assays and **(F)** EdU assays were performed to evaluate the proliferation ability in HKFs transfected with the miR-7-5p mimics or inhibitor, respectively. Magnification, 200 \times . **(G)** Transwell migration assays (magnification, 200 \times) and **(H)** wound healing assays (magnification, 20 \times) were applied for assessing the migration ability of HKFs transfected with the miR-7-5p mimics or inhibitor, respectively. **(I)** Cell apoptosis was examined using flow cytometry. **(J,K)** The protein levels of Epac1, collagen I, collagen III, α -SMA, and the protein phosphorylation levels of Akt and PI3K in HKFs transfected with miR-7-5p mimics or inhibitor by western blot assays. Data was shown as mean \pm SD. ns indicated no significance, $^{\#}P < 0.05$, $^{##}P < 0.01$, $^{###}P < 0.001$, vs. NC.

PI3K/Akt signaling pathway activation (Figure 3K). Thus, the above data above demonstrated that miR-7-5p had an indispensable effect on regulating HKFs proliferation, migration, apoptosis, and ECM deposition through PI3K/Akt signaling pathway.

CircCOL5A1 Served as a miRNA Sponge of miR-7-5p to Regulate Epac1 Expression

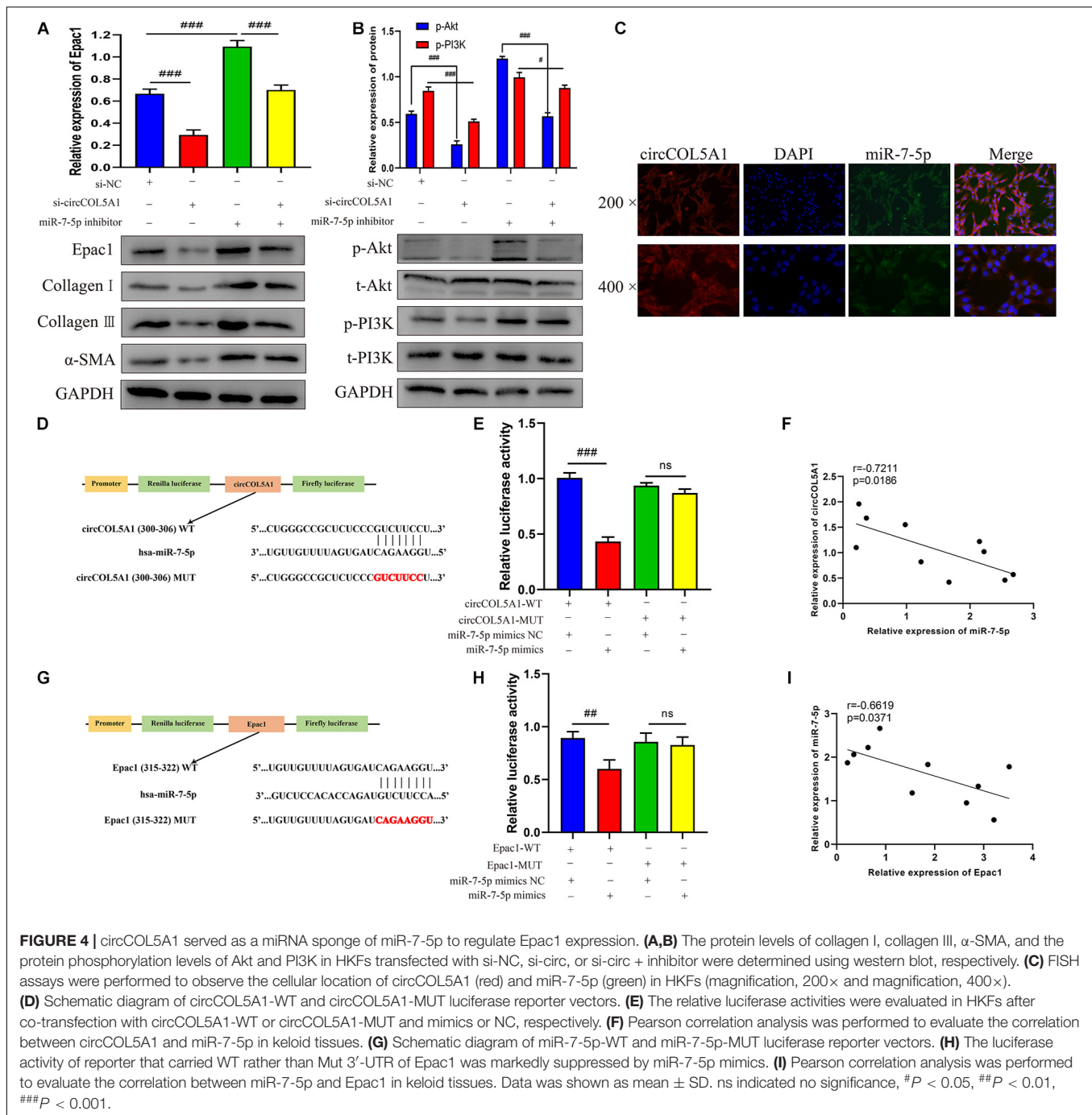
Growing studies have confirmed that circRNA has assumed the indispensable role of a miRNA sponge in the occurrence and development of fibrotic diseases, especially keloids (Jin et al., 2020). A series of experiments were performed to further investigate the interaction between circCOL5A1, miR-7-5p, and Epac1. Firstly, western blot analysis revealed that the downregulation of circCOL5A1 markedly reduced Epac1 protein level, while inhibiting miR-7-5p promoted the above level (Figure 4A). Interestingly, the co-transfection of si-circCOL5A1 and miR-7-5p inhibitor did not affect the expression of Epac1 in HKFs (Figure 4A). After transfection with si-NC, si-circ, or si-circ + inhibitor, respectively, the protein levels of ECM as well as the protein phosphorylation levels of Akt and PI3K in HKFs, were consistent with the above results (Figures 4A,B). Secondly, to investigate whether circCOL5A1 served as a miRNA sponge in the cytoplasm of HKFs, the FISH assay was applied to assess the subcellular co-location of circCOL5A1 and miR-7-5p. The results indicated that circCOL5A1 (red) and miR-7-5p (green) were mainly visualized in the cytoplasm (Figure 4C). Thirdly, we used an online software Circular RNA Interactome to predict the miRNAs binding sites of circCOL5A1. The prediction tool predicted a potential binding site where circCOL5A1 might sponge to the seed region of miR-7-5p (Figure 4D). To further confirm the interaction target predicted by bioinformatics, a dual-luciferase reporter assay was conducted. The results suggested that miR-7-5p mimics markedly reduced the luciferase activity of vector containing the full-length of circCOL5A1-WT sequences, but did not influence the luciferase activity of vector including mutant binding sites of miR-7-5p (Figure 4E). Subsequently, the online prediction website (TargetScan) was applied to define that Epac1 was a potential target gene of miR-7-5p (Figure 4G). In the luciferase reporter assay, the wild-type and mutant sequences were constructed and transfected, respectively. The luciferase activity analysis revealed that miR-7-5p tightly bound to Epac1 through covalent molecular conjunction (Figure 4H). These results indicated that there might be a direct interaction between circCOL5A1 and miR-7-5p as well as between miR-7-5p and Epac1. Furthermore, qRT-PCR was performed to evaluate the expression of circCOL5A1, miR-7-5p, and Epac1 from frozen keloid tissues. The results indicated that there was a significantly negative correlation between circCOL5A1 and miR-7-5p, as well as a highly negative correlation between miR-7-5p and Epac1 (Figures 4F,I). In summary, these above data determined that circCOL5A1 acted as a sponge of miR-7-5p in the cytoplasm, thereby promoting the expression of Epac1 in HKFs.

CircCOL5A1 Regulated HKFs Proliferation, Migration, and Invasion Through circCOL5A1/miR-7-5p/Epac1 Axis

To further investigate whether circCOL5A1 served as a fibrosis-inhibitor in HKFs by suppressing the activity of miR-7-5p to upregulate Epac1 protein expression, rescue experiments were performed using si-circCOL5A1 and miR-7-5p inhibitor. In addition, we attempted to investigate whether miR-7-5p inhibitor combined with si-circCOL5A1 could reverse the biological function and PI3K/Akt pathway activation induced by miR-7-5p inhibitor. The results demonstrated that miR-7-5p inhibitor reversed the proliferation, migration, and apoptosis regulation effects induced by circCOL5A1 knockdown in HKFs through CCK-8 and EdU assay, wound healing and transwell assay, apoptosis analysis, and western blot analysis (Figures 5A–F). Afterward, to observe whether circCOL5A1 could restore the expression level of Epac1 increased by miR-7-5p inhibitor, the western blot assay was used to detect Epac1 protein expression. The results revealed that the gray value of the Epac1 protein band in the si-circCOL5A1 + miR-7-5p inhibitor group was significantly lower than that of the miR-7-5p inhibitor group (Figure 5G). Simultaneously, the reduction of ECM deposition and the inhibition of the PI3K/Akt signaling pathway caused by silencing circCOL5A1 were reversed by a miR-7-5p inhibitor (Figure 5H). Collectively, these above data indicated that circCOL5A1 reversed miR-7-5p-induced enhancement of HKFs biological function, and could restore the expression of miR-7-5p target Epac1, forming the circCOL5A1/miR-7-5p/Epac1 regulating axis.

Downregulation of circCOL5A1 Suppressed the Growth and ECM Deposition of Keloids *in vivo*

To further elucidate the effects of circCOL5A1 on the growth and ECM deposition of keloids *in vivo*, fresh human keloid tissues were implanted under the skin of nude mice and intervened with three methods (PBS, si-NC, and si-circCOL5A1). The keloid grafts were intervention every 3 days and the volumes were measured with a vernier caliper. After 14 days, all the nude mice were killed, the weights of keloid graft were determined. Compared with the control and si-NC group, the circCOL5A1 siRNA group significantly reduced the tumor volume and weight (Figures 6A–C). These subcutaneously transplanted keloid tissues were further examined by HE staining, IHC, and WB analysis. HE staining displayed that the eosinophilic, refractory homogeneous lamellar collagen fibers of keloid tissues in the circCOL5A1 siRNA group became thinner, less dense, and loosely arranged, compared with the control and si-NC group (Figure 6D). Meanwhile, the results of IHC and WB revealed that the expression of type I and III collagen and α -SMA were markedly downregulated in the circCOL5A1 siRNA group (Figures 6E,F). Taken together, these findings demonstrated that si-circCOL5A1 could reverse the pathological phenotype of



keloids, and circCOL5A1 was expected to become a potential therapeutic target.

DISCUSSION

Cutaneous pathological keloids are an abnormal fibroproliferative wound healing reaction (Ekstein et al., 2020). The etiology of keloids remains unclear but may be closely involved in genetics and external system factors (Tan

et al., 2019). Epigenetics, representing the potential link of complex interactions between genetics and external risk factors, is currently under intense scrutiny (Hodjat et al., 2020). Recently, the ncRNA-based mechanism is a pivotal part of epigenetic modification and has accounted for the complexity of many diseases. Furthermore, accumulating evidence about the regulatory mechanism of circRNAs has determined that ceRNA crosstalk might be associated with the progression of tumors and fibrotic diseases (Dai et al., 2020). However, keloid-related circRNAs research only stayed at the stage of high-throughput

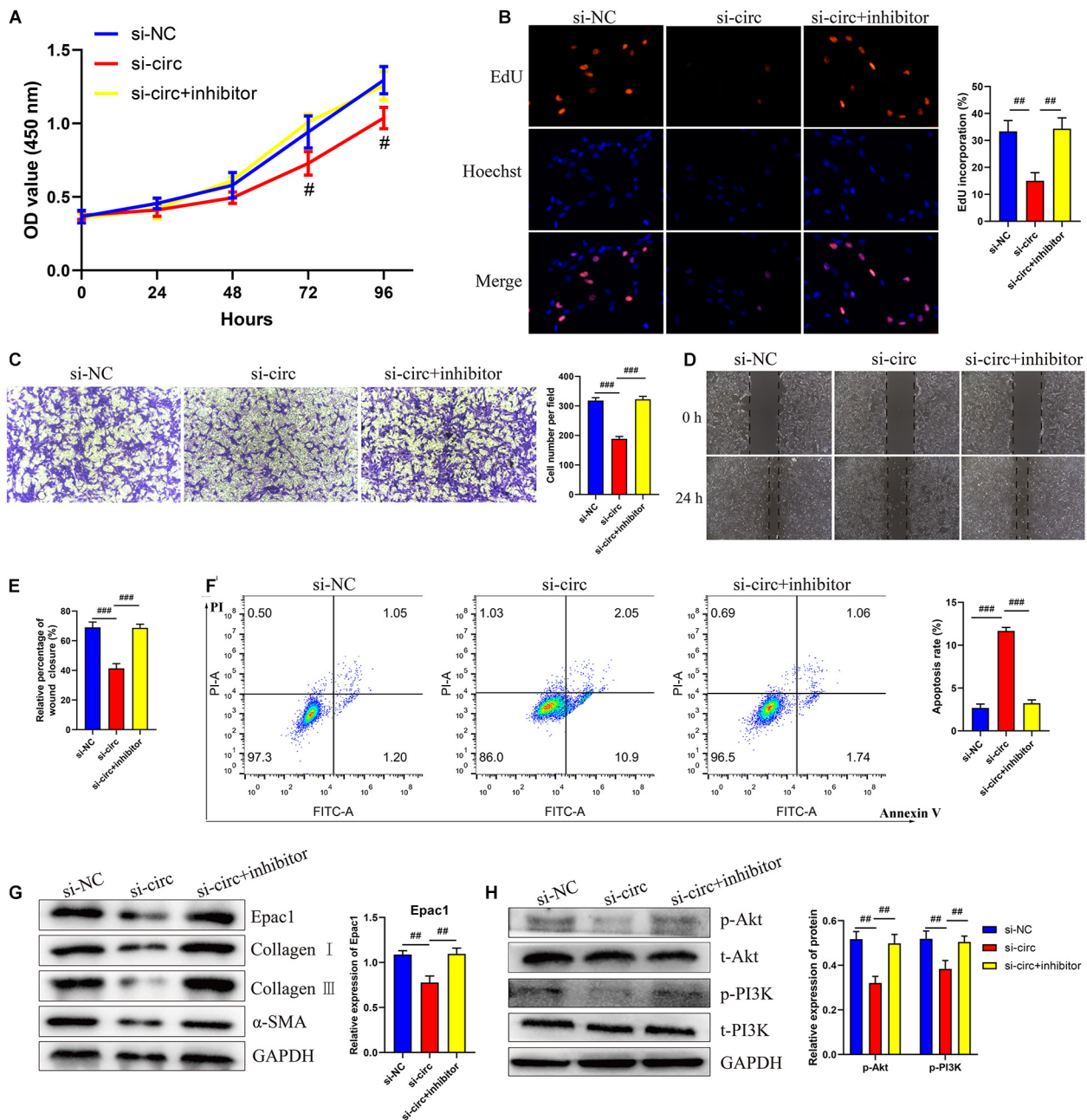
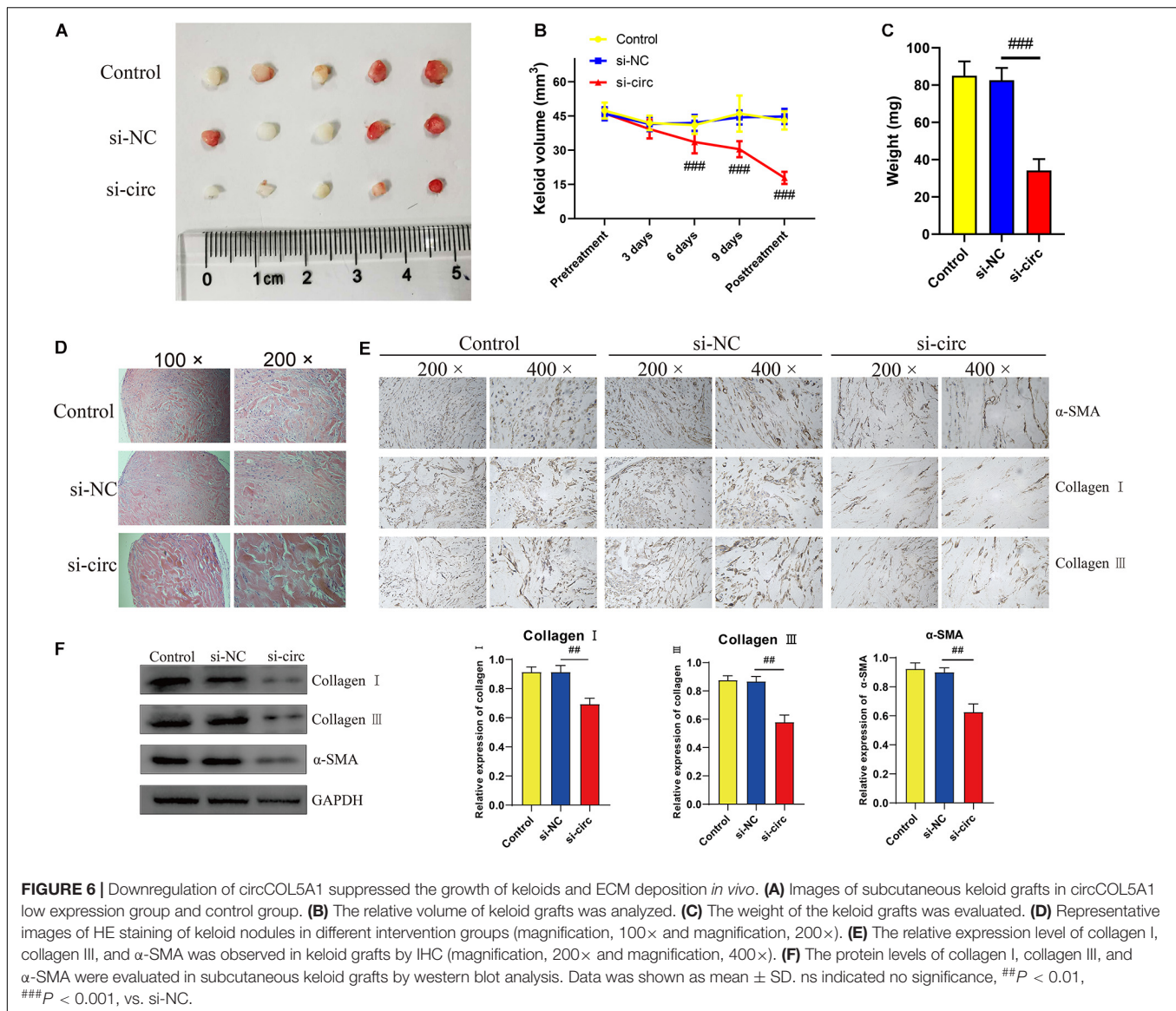


FIGURE 5 | circCOL5A1 regulated HKFs proliferation, migration, apoptosis, and ECM deposition through circCOL5A1/miR-7-5p/Epac1 axis. **(A)** CCK-8 assays and **(B)** EdU assays were performed to evaluate the proliferation ability in HKFs transfected with the si-NC, si-circ, or si-circ + inhibitor, respectively. Magnification, 200 \times . **(C)** Transwell migration assays (magnification, 200 \times) and **(D,E)** wound healing assays (magnification, 20 \times) were applied for assessing the migration ability of HKFs transfected with the si-NC, si-circ, or si-circ + inhibitor, respectively. **(F)** Cell apoptosis was examined using flow cytometry. **(G,H)** The protein levels of collagen I, collagen III, α -SMA, and the protein phosphorylation levels of Akt and PI3K in HKFs transfected with si-NC, si-circ, or si-circ + inhibitor by western blot assays. Data was shown as mean \pm SD. ns indicated no significance, # P < 0.05, ## P < 0.01, ### P < 0.001, vs. si-NC.

sequencing and the ceRNA function of circRNAs has not been well recognized to date. In the present study, we firstly confirmed that circCOL5A1/miR-7-5p/Epac1 axis was involved in keloid progression.

In this study, according to the published circRNA microarray assay, we demonstrated that circCOL5A1 was significantly

upregulated in keloids, which was consistent with the microarray assay results. Secondly, *in vitro* and *in vivo*, we found that circCOL5A1 acted as a fibrosis promoter to promote HKFs proliferation, migration, and ECM deposition, on the contrary, inhibit apoptosis. Thirdly, miR-7-5p was defined as a potential target of circCOL5A1 through bioinformatic analysis



and dual-luciferase reporter assay. Meanwhile, we identified a significant decrease in miR-7-5p expression and a negative correlation between circCOL5A1 and miR-7-5p expression levels in keloid tissues. Fourthly, mechanically, functional experiments revealed that circCOL5A1 functioned as a ceRNA by sponging with miR-7-5p to upregulate the target gene *Epac1* in keloid progression. Moreover, silencing circCOL5A1 could reverse the pathological phenotype of keloids via inhibiting PI3K/Akt pathway activity. Considering the above evidence, the results suggested a correlation between the circCOL5A1-associated ceRNA crosstalk and PI3K/Akt signaling pathway, referring as a potential regulatory mechanism in the pathogenesis of keloids.

Currently, circRNAs are involved in regulating the target gene at the posttranscriptional level via function as sponges of miRNAs and RBPs (Hansen et al., 2013). Inhibiting translation or participating in the degradation of target mRNA was deemed to be the most classic regulatory mechanism of miRNAs. Hence, the

circRNA/miRNA/mRNA axis was referred to as the competitive ceRNA mechanism in multiple biological processes. For example, Song et al. (2020) found that the high expression of circ0003998 in hepatocellular carcinoma (HCC) tissues correlated with the aggressive characteristics of HCC patients. Mechanically, circ0003998 could not only act as the ceRNA of microRNA-143-3p to reduce the inhibition of EMT-related *FOSL2* but also combine with PCBP1 protein to promote EMT-related CD44v6 expression (Song et al., 2020). Shi et al. (2020) constructed a circRNA-miRNA-mRNA interaction network using a circRNA microarray of keloids. Then the gene ontology (GO) analysis was performed to suggest that these ncRNAs might partly contribute to the etiology of keloids by affecting cAMP signaling and cell cycle pathways. Analogously, Wang et al. (2019) carried out high-throughput sequencing and bioinformatics to identify the alterations in circRNA and mRNA expression profiles and then to construct gene networks in keloids.

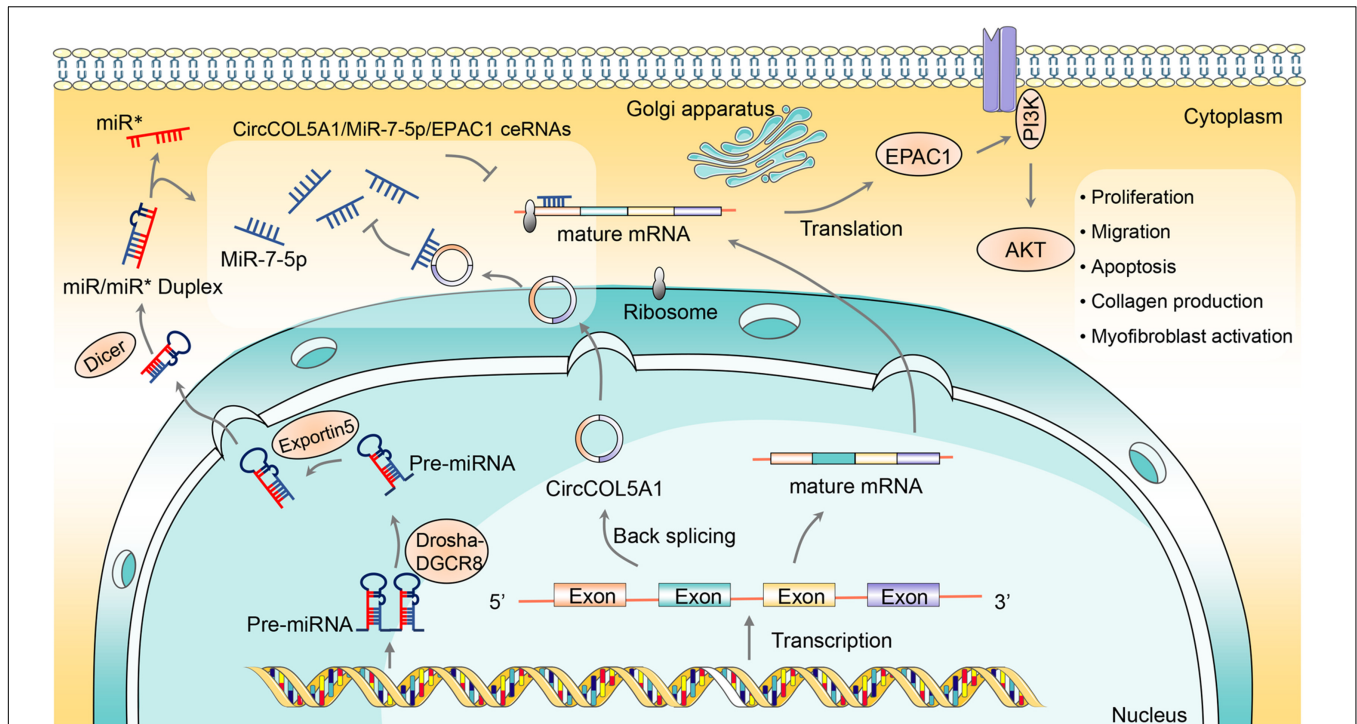


FIGURE 7 | The schematic diagram illustrates the role of circCOL5A1 as a ceRNA for miR-7-5p to release Epac1 in regulating the pathological phenotype of keloids. circCOL5A1 was generated by the head-to-tail splicing of COL5A1 in the nucleus and then functioned as ceRNA in the cytoplasm. circCOL5A1 reversed miR-7-5p-induced enhancement of HKFs biological function via the PI3K/Akt signaling pathway, including proliferation, migration, apoptosis, collagen production, and myofibroblast activation. Mechanismly, circRNAs could restore the expression of miR-7-5p target Epac1, forming the circCOL5A1/miR-7-5p/Epac1 regulating axis. The miR* represented a segment of RNA on the pre-miRNA, and its position happened to be opposite that of the mature miRNA.

Herein, circCOL5A1 was predicted to contain the miRNA binding site of miR-7-5p through the online prediction website Circular RNA Interactome⁴. Firstly, a series of functional experiments such as FISH and dual-luciferase reporter gene determined that circCOL5A1 and miR-7-5p were co-located in the cytoplasm of HKFs, and showed the potentiality of circCOL5A1 to sponge miR-7-5p. Secondly, the functional rescue experiments supported that circCOL5A1 reversed the effect of miR-7-5p on suppressing keloid hyperplasia. The results indicated that miR-7-5p inhibitor could reverse the suppressing effects of silencing circCOL5A1 on proliferation, migration, and ECM deposition. Inversely, miR-7-5p inhibitors could reverse the apoptosis-promoting effects of silencing circCOL5A1. Thirdly, we also discovered that miR-7-5p mimics inhibited the activation of Epac1 in HKFs, while miR-7-5p inhibitor promoted the activation of Epac1, indicating that miR-7-5p is a potent negative regulator of Epac1. Finally, we identified that knocking down circCOL5A1 could suppress the expression of Epac1 in HKFs, which was retarded by miR-7-5p inhibitor. Therefore, the above results provided sufficient evidence to support that circCOL5A1 functioned as a ceRNA by adsorbing miR-7-5p to release Epac1, which resulted in hyperproliferation and invasive growth of keloids.

⁴<https://circinteractome.nia.nih.gov/index.html>

Epac1, served as Rap guanine nucleotide exchange factor directly activated by cAMP, has been proved to participate in the progression of multiple tumors and fibrotic diseases through directly activating Akt/protein kinase B (Christensen et al., 2003). Our previous studies have confirmed that the fibrosis promoter Epac1 stimulated HKFs proliferation and migration, thereby playing a positive role in the pathological process of keloids. Interestingly, a study by Garcia-Morales et al. (2017) found that Epac1 reduction in a miR-7-mediated manner contributed to vascular endothelial permeability and eNOS uncoupling during retinopathy. Besides, Etoh et al. (2013) found that systemic or local downregulation of miR-7 could mediate excessive collagen expression in localized scleroderma. However, so far, it has remained ambiguous how circCOL5A1/miR-7-5p axis contributed to Epac1-induced progression in keloids. Strikingly, we systematically illuminated that circCOL5A1 directly bound to miR-7-5p to release Epac1. It emphasized that the novel mechanism of the crosstalk between circCOL5A1/miR-7-5p/Epac1 axis and PI3K/Akt signaling pathway in regulating the keloid process.

As representative members of anti-apoptotic and survival-promoting signaling pathways, PI3K and its downstream target Akt participated in regulating many cellular functions, especially proliferation, migration, transformation, and cell-cycle progression. For example, Zhang et al. (2018) confirmed that exosomes derived from adipose tissue stem cells promoted

scar-free wound healing through PI3K/Akt signaling pathway. Meanwhile, the PI3K/AKT pathway also mediated cutaneous wound contraction by regulating fibroblast migration and differentiation into myofibroblasts (Li et al., 2016). In our study, si-circCOL5A1 significantly decreased the phosphorylation of PI3K and Akt, while miR-7-5p inhibitor partially alleviated downregulated circCOL5A1-induced alterations. Therefore, the changes of total protein and phosphorylated protein levels of PI3K and Akt were detected by silencing or overexpressing circRNA and miRNA. In fact, many studies on the circRNA pathway have adopted this approach, that is, the expression of the terminal pathway was verified by regulating the circRNA/miRNA/mRNA axis (Luo et al., 2020; Wang et al., 2020a). Taken together, this evidence supported that PI3K/Akt signaling pathway functioned in accelerating full-thickness wound healing and attenuating keloid formation.

To our knowledge, this was the first study that comprehensively explored circCOL5A1 acted as a ceRNA in the regulation of keloid formation. Moreover, we investigated for the first time the miR-7-5p/Epac1 axis in keloid progression. Our findings might shed new light on the keloids treatment of ncRNAs epigenetic modification. However, there are several limitations to our study. On the one hand, it was well-known that keloids are unique to humans. Due to the absence of a suitable animal model, animal research of keloids generally relied on excised keloid tissues to construct subcutaneous transplantation models on nude mice. Regrettably, it was impossible to investigate the correlation between the immune system and keloid formation with these models. On the other hand, relatively few keloid patients need to undergo surgical resection within the limited period of this study. Therefore, it is difficult to collect a large number of samples, which is a general limitation of keloid research. The further large-scale analysis will be required in the future. Furthermore, whether circCOL5A1 involved in promoting the pathological phenotype of keloids through interacting with RBPs required further exploration.

In summary, we identified that circCOL5A1 was remarkably upregulated in keloids, while miR-7-5p was remarkably downregulated. Meanwhile, our research provided the first line of exhaustive evidence that circCOL5A1 acted as a ceRNA by adsorption of miR-7-5p to release Epac1 to regulate HKFs proliferation, migration, apoptosis, and ECM deposition. Furthermore, si-circCOL5A1 resulted in suppressing the Epac1-induced PI3K/Akt signaling pathway to partially reverse the pathological phenotype of hyperproliferation and invasive growth (Figure 7). Consequently, our findings elucidated the pivotal role of circCOL5A1 in the etiology and pathogenesis of keloids and might shed novel light on diagnostic and therapeutic strategies for keloids.

REFERENCES

- Arjunan, S., Gan, S. U., Choolani, M., Raj, V., Lim, J., Biswas, A., et al. (2020). Inhibition of growth of Asian keloid cells with human umbilical cord Wharton's jelly stem cell-conditioned medium. *Stem Cell. Res. Ther.* 11:78. doi: 10.1186/s13287-020-01609-7
- Artemaki, P. I., Scorilas, A., and Kontos, C. K. (2020). Circular RNAs: a new piece in the colorectal cancer puzzle. *Cancers* 12:2464. doi: 10.3390/cancers12092464

DATA AVAILABILITY STATEMENT

The original contributions presented in the study are included in the article/Supplementary Material, further inquiries can be directed to the corresponding author.

ETHICS STATEMENT

The studies involving human participants were reviewed and approved by the Ethical Committee of Tongji Hospital of Huazhong University of Science and Technology (Wuhan, China). The patients/participants provided their written informed consent to participate in this study. The animal study was reviewed and approved by the Animal Care and Use Committee of Huazhong University of Science and Technology (Wuhan, China).

AUTHOR CONTRIBUTIONS

WL and SL designed and performed the experiments and were a major contributor in writing the manuscript. YR was involved in drafting the manuscript and revising it critically for important intellectual content. QZ, WH, and YW provided a guide for the experiment technology and helped shape the manuscript. All authors read and approved the final manuscript.

FUNDING

This study was supported by the China Guanghua Science and Technology Foundation (Grant No. 2019JZX0001).

SUPPLEMENTARY MATERIAL

The Supplementary Material for this article can be found online at: <https://www.frontiersin.org/articles/10.3389/fcell.2021.626027/full#supplementary-material>

Supplementary Figure 1 | The expression of miR-665, miR-604, and miR-639 between keloid tissues and normal skin tissues. $^{\#}p < 0.05$.

Supplementary Figure 2 | Negative control was performed to determine that circCOL5A1 was mainly localized in the cytoplasm of HKFs with specific signal (magnification, 200 \times and magnification, 400 \times).

Supplementary Table 1 | An online prediction software Circular RNA Interactome was applied to predict many miRNAs binding to circCOL5A1.

- Betarbet, U., and Blalock, T. W. (2020). Keloids: a review of etiology, prevention, and treatment. *J. Clin. Aesthet. Dermatol.* 13, 33–43.
- Bieg, D., Sypniewski, D., Nowak, E., and Bednarek, I. (2019). MiR-424-3p suppresses galectin-3 expression and sensitizes ovarian cancer cells to cisplatin. *Arch. Gynecol. Obstet.* 299, 1077–1087. doi: 10.1007/s00404-018-4999-7
- Christensen, A. E., Selheim, F., de Rooij, J., Dremier, S., Schwede, F., Dao, K. K., et al. (2003). cAMP analog mapping of Epac1 and cAMP kinase. Discriminating analogs demonstrate that Epac and cAMP kinase act synergistically to promote

- PC-12 cell neurite extension. *J. Biol. Chem.* 278, 35394–35402. doi: 10.1074/jbc.M302179200
- Dai, F., Wu, Y., Lu, Y., An, C., Zheng, X., Dai, L., et al. (2020). Crosstalk between RNA m(6)a modification and non-coding RNA contributes to cancer growth and progression. *Mol. Ther. Nucleic Acids* 22, 62–71. doi: 10.1016/j.omtn.2020.08.004
- Damjanovic, S. S., Antic, J. A., Elezovic-Kovacevic, V. I., Dundjerovic, D. M., Milicevic, I. T., Beleslin-Cokic, B. B., et al. (2020). ARMC5 alterations in patients with sporadic neuroendocrine tumors and multiple endocrine neoplasia type 1 (MEN1). *J. Clin. Endocrinol. Metab.* 105, 4531–4542. doi: 10.1210/clinem/dgaa631
- Di Timoteo, G., Rossi, F., and Bozzoni, I. (2020). Circular RNAs in cell differentiation and development. *Development* 147:dev182725. doi: 10.1242/dev.182725
- Ekstein, S. F., Wyles, S. P., Moran, S. L., and Meves, A. (2020). Keloids: a review of therapeutic management. *Int. J. Dermatol.* 2020:32905614. doi: 10.1111/ijd.15159
- Etoh, M., Jinnin, M., Makino, K., Yamane, K., Nakayama, W., Aoi, J., et al. (2013). microRNA-7 down-regulation mediates excessive collagen expression in localized scleroderma. *Arch Dermatol. Res.* 305, 9–15. doi: 10.1007/s00403-012-1287-4
- Fanous, A., Bezdjian, A., Caglar, D., Mlynarek, A., Fanous, N., Lenhart, S. F., et al. (2019). Treatment of keloid scars with botulinum toxin type A versus triamcinolone in an athymic nude mouse model. *Plast Reconstr. Surg.* 143, 760–767. doi: 10.1097/PRS.0000000000005323
- Garcia-Morales, V., Friedrich, J., Jorna, L. M., Campos-Toimil, M., Hammes, H. P., Schmidt, M., et al. (2017). The microRNA-7-mediated reduction in EPAC-1 contributes to vascular endothelial permeability and eNOS uncoupling in murine experimental retinopathy. *Acta Diabetol.* 54, 581–591. doi: 10.1007/s00592-017-0985-y
- Hansen, T. B., Jensen, T. I., Clausen, B. H., Bramsen, J. B., Finsen, B., Damgaard, C. K., et al. (2013). Natural RNA circles function as efficient microRNA sponges. *Nature* 495, 384–388. doi: 10.1038/nature11993
- Hodjat, M., Khan, F., and Saadat, K. (2020). Epigenetic alterations in aging tooth and the reprogramming potential. *Ageing Res. Rev.* 63:101140. doi: 10.1016/j.arr.2020.101140
- Jin, H., Li, C., Dong, P., Huang, J., Yu, J., and Zheng, J. (2020). Circular RNA cMTO1 promotes PTEN expression through sponging miR-181b-5p in liver fibrosis. *Front. Cell. Dev. Biol.* 8:714. doi: 10.3389/fcell.2020.00714
- Li, G., Li, Y. Y., Sun, J. E., Lin, W. H., and Zhou, R. X. (2016). ILK-PI3K/AKT pathway participates in cutaneous wound contraction by regulating fibroblast migration and differentiation to myofibroblast. *Lab. Invest.* 96, 741–751. doi: 10.1038/labinvest.2016.48
- Li, X., Liao, J., Su, X., Li, W., Bi, Z., Wang, J., et al. (2020). Human urine-derived stem cells protect against renal ischemia/reperfusion injury in a rat model via exosomal miR-146a-5p which targets IRAK1. *Theranostics* 10, 9561–9578. doi: 10.7150/thno.42153
- Limandjaja, G. C., Niessen, F. B., Scheper, R. J., and Gibbs, S. (2020). The keloid disorder: heterogeneity, histopathology, mechanisms and models. *Front. Cell. Dev. Biol.* 8:360. doi: 10.3389/fcell.2020.00360
- Lu, C., Wang, H., Chen, S., Yang, R., Li, H., and Zhang, G. (2018). Baicalein inhibits cell growth and increases cisplatin sensitivity of A549 and H460 cells via miR-424-3p and targeting PTEN/PI3K/Akt pathway. *J. Cell. Mol. Med.* 22, 2478–2487. doi: 10.1111/jcmm.13556
- Luo, Z., Rong, Z., Zhang, J., Zhu, Z., Yu, Z., Li, T., et al. (2020). Circular RNA circCCDC9 acts as a miR-6792-3p sponge to suppress the progression of gastric cancer through regulating CAV1 expression. *Mol. Cancer* 19:86. doi: 10.1186/s12943-020-01203-8
- Lv, W., Liu, S., Zhang, Q., Yi, Z., Bao, X., Feng, Y., et al. (2021). Downregulation of epac reduces fibrosis and induces apoptosis through akt signaling in human keloid fibroblasts. *J. Surg. Res.* 257, 306–316. doi: 10.1016/j.jss.2019.12.026
- Marazzi, L., Gainer-Dewar, A., and Vera-Licona, P. (2020). OCSANA+: optimal control and simulation of signaling networks from network analysis. *Bioinformatics* 36, 4960–4962. doi: 10.1093/bioinformatics/btaa625
- Pandamooz, S., Hadipour, A., Akhavan-Niaki, H., Pourghasem, M., Abedian, Z., Ardekani, A. M., et al. (2012). Short exposure to collagenase and coculture with mouse embryonic pancreas improve human dermal fibroblast culture. *Biotechnol. Appl. Biochem.* 59, 254–261. doi: 10.1002/bab.1020
- Qiu, X., Feng, J. R., Qiu, J., Liu, L., Xie, Y., Zhang, Y. P., et al. (2018). ITGBL1 promotes migration, invasion and predicts a poor prognosis in colorectal cancer. *Biomed. Pharmacother.* 104, 172–180. doi: 10.1016/j.biopha.2018.05.033
- Remst, D. F., Blom, A. B., Vitters, E. L., Bank, R. A., van den Berg, W. B., Blaney Davidson, E. N., et al. (2014). Gene expression analysis of murine and human osteoarthritis synovium reveals elevation of transforming growth factor beta-responsive genes in osteoarthritis-related fibrosis. *Arthritis Rheumatol.* 66, 647–656. doi: 10.1002/art.38266
- Rippa, A. L., Kalabusheva, E. P., and Vorotelyak, E. A. (2019). Regeneration of dermis: scarring and cells involved. *Cells* 8:607. doi: 10.3390/cells8060607
- Shi, J., Yao, S., Chen, P., Yang, Y., Qian, M., Han, Y., et al. (2020). The integrative regulatory network of circRNA and microRNA in keloid scarring. *Mol. Biol. Rep.* 47, 201–209. doi: 10.1007/s11033-019-05120-y
- Song, L. N., Qiao, G. L., Yu, J., Yang, C. M., Chen, Y., Deng, Z. F., et al. (2020). Hsa_circ_0003998 promotes epithelial to mesenchymal transition of hepatocellular carcinoma by sponging miR-143-3p and PCBP1. *J. Exp. Clin. Cancer Res.* 39:114. doi: 10.1186/s13046-020-01576-0
- Squassina, A., Manchia, M., Pisanu, C., Ardu, R., Arzedi, C., Bocchetta, A., et al. (2020). Telomere attrition and inflammatory load in severe psychiatric disorders and in response to psychotropic medications. *Neuropsychopharmacology* 45, 2229–2238. doi: 10.1038/s41386-020-00844-z
- Tan, S., Khumalo, N., and Bayat, A. (2019). Understanding keloid pathobiology from a quasi-neoplastic perspective: less of a scar and more of a chronic inflammatory disease with cancer-like tendencies. *Front. Immunol.* 10:1810. doi: 10.3389/fimmu.2019.01810
- Teodoro, W. R., de Jesus Queiroz, Z. A., Dos Santos, L. A., Catanozi, S., Dos Santos Filho, A., Bueno, C., et al. (2019). Proposition of a novel animal model of systemic sclerosis induced by type V collagen in C57BL/6 mice that reproduces fibrosis, vasculopathy and autoimmunity. *Arthritis. Res. Ther.* 21:278. doi: 10.1186/s13075-019-2052-2
- Wang, H., Zhang, J., Xu, Z., Yang, J., Xu, Y., Liu, Y., et al. (2020a). Circular RNA hsa_circ_0000848 promotes trophoblast cell migration and invasion and inhibits cell apoptosis by sponging hsa-miR-6768-5p. *Front. Cell. Dev. Biol.* 8:278. doi: 10.3389/fcell.2020.00278
- Wang, M., Liu, J., Zhao, Y., He, R., Xu, X., Guo, X., et al. (2020b). Upregulation of METTL14 mediates the elevation of PERP mRNA N(6) adenosine methylation promoting the growth and metastasis of pancreatic cancer. *Mol. Cancer* 19:130. doi: 10.1186/s12943-020-01249-8
- Wang, J., Wu, H., Xiao, Z., and Dong, X. (2019). Expression Profiles of lncRNAs and circRNAs in Keloid. *Plast Reconstr. Surg. Glob. Open* 7:e2265. doi: 10.1097/GOX.0000000000002265
- Wang, X., Zhang, C., Wu, Z., Chen, Y., and Shi, W. (2018). CircIBTK inhibits DNA demethylation and activation of AKT signaling pathway via miR-29b in peripheral blood mononuclear cells in systemic lupus erythematosus. *Arthritis. Res. Ther.* 20:118. doi: 10.1186/s13075-018-1618-8
- Wu, Y., Xiao, H., Pi, J., Zhang, H., Pan, A., Pu, Y., et al. (2020). The circular RNA aplacirc_13267 upregulates duck granulosa cell apoptosis by the apla-miR-1-13/THBS1 signaling pathway. *J. Cell. Physiol.* 235, 5750–5763. doi: 10.1002/jcp.29509
- Xu, T., Wang, M., Jiang, L., Ma, L., Wan, L., Chen, Q., et al. (2020). CircRNAs in anticancer drug resistance: recent advances and future potential. *Mol. Cancer.* 19:127. doi: 10.1186/s12943-020-01240-3
- Yokota, T., McCourt, J., Ma, F., Ren, S., Li, S., Kim, T. H., et al. (2020). Type V collagen in scar tissue regulates the size of scar after heart injury. *Cell* 54:e523. doi: 10.1016/j.cell.2020.06.030
- Yoneda, K., Nagano, R., Mikami, T., Sakuraba, H., Fukui, K., Araki, T., et al. (2020). Catalytic properties and crystal structure of UDP-galactose 4-epimerase-like l-threonine 3-dehydrogenase from *Phytophthora infestans*. *Enzyme Microb. Technol.* 140:109627. doi: 10.1016/j.enzmictec.2020.109627
- Yue, B., Wang, J., Ru, W., Wu, J., Cao, X., Yang, H., et al. (2020). The circular RNA circHUWE1 sponges the miR-29b-AKT3 Axis to regulate myoblast development. *Mol. Ther. Nucleic Acids* 19, 1086–1097. doi: 10.1016/j.omtn.2019.12.039
- Yun, I. S., Lee, M. H., Rah, D. K., Lew, D. H., Park, J. C., and Lee, W. J. (2015). Heat shock protein 90 inhibitor (17-AAG) induces apoptosis and decreases

- cell migration/motility of keloid fibroblasts. *Plast Reconstr. Surg.* 136, 44–53. doi: 10.1097/PRS.0000000000001362
- Zhang, W., Bai, X., Zhao, B., Li, Y., Zhang, Y., Li, Z., et al. (2018). Cell-free therapy based on adipose tissue stem cell-derived exosomes promotes wound healing via the PI3K/Akt signaling pathway. *Exp. Cell. Res.* 370, 333–342. doi: 10.1016/j.yexcr.2018.06.035
- Zhou, J., Zhao, H., Huang, Z., Ye, X., Zhang, L., Li, Q., et al. (2020). Differential transcriptomic analysis of crayfish (*Procambarus clarkii*) from a rice coculture system challenged by *Vibrio parahaemolyticus*. *Comp. Biochem. Physiol. Part D Genom. Proteom.* 36:100741. doi: 10.1016/j.cbd.2020.100741

Conflict of Interest: The authors declare that the research was conducted in the absence of any commercial or financial relationships that could be construed as a potential conflict of interest.

Copyright © 2021 Lv, Liu, Zhang, Hu, Wu and Ren. This is an open-access article distributed under the terms of the Creative Commons Attribution License (CC BY). The use, distribution or reproduction in other forums is permitted, provided the original author(s) and the copyright owner(s) are credited and that the original publication in this journal is cited, in accordance with accepted academic practice. No use, distribution or reproduction is permitted which does not comply with these terms.



Decitabine Induces Change of Biological Traits in Myelodysplastic Syndromes via FOXO1 Activation

Zheng Zhang, Yan Jia, Feng Xv, Lu-xi Song, Lei Shi, Juan Guo and Chun-kang Chang*

Department of Hematology, Shanghai Jiao Tong University Affiliated Sixth People's Hospital, Shanghai, China

OPEN ACCESS

Edited by:

Song Zhao,
First Affiliated Hospital of Zhengzhou
University, China

Reviewed by:

Jian Zhou,
Henan Provincial Cancer Hospital,
China
Haizhou Xing,
First Affiliated Hospital of Zhengzhou
University, China

*Correspondence:

Chun-kang Chang
changchungkang@sjtu.edu.cn

Specialty section:

This article was submitted to
Epigenomics and Epigenetics,
a section of the journal
Frontiers in Genetics

Received: 08 September 2020

Accepted: 04 December 2020

Published: 27 January 2021

Citation:

Zhang Z, Jia Y, Xv F, Song L-x,
Shi L, Guo J and Chang C-k (2021)
Decitabine Induces Change
of Biological Traits in Myelodysplastic
Syndromes via FOXO1 Activation.
Front. Genet. 11:603956.
doi: 10.3389/fgene.2020.603956

Decitabine (DAC) is considered to be a profound global DNA demethylation, which can induce the re-expression of silenced tumor suppressor genes. Little is known about the function of tumor suppressor gene FOXO1 in myelodysplastic syndromes (MDS). To address this issue, the study firstly investigated differentially expressed genes (DEGs) for DAC treatment in MDS cell lines, then explored the role of FOXO1 through silencing its expression before DAC treatment in MDS. The results showed that FOXO1 exists in a hyperphosphorylated, inactive form in MDS-L cells. DAC treatment both induces FOXO1 expression and reactivates the protein in its low phosphorylation level. Additionally, the results also demonstrated that this FOXO1 activation is responsible for the DAC-induced apoptosis, cell cycle arrest, antigen differentiation, and immunoregulation in MDS-L cells. We also demonstrated DAC-induced FOXO1 activation upregulates anti-tumor immune response in higher-risk MDS specimens. Collectively, these results suggest that DAC induces FOXO1 activation, which plays an important role in anti-MDS tumors.

Keywords: myelodysplastic syndromes, DEGs, FOXO1, PTEN, TLR4

INTRODUCTION

Myelodysplastic syndrome (MDS) is a set of highly heterogeneous myeloid neoplasms, featured by variable cytopenias, inefficient hematopoiesis and a proportionable risk of progression to acute myeloid leukemia. The incidence of MDS in the elderly gradually increases with age, which is one of the main factors that threaten the quality of life and survival of the elderly. Although 3 therapies targeting MDS have been approved since 2004, the overall 5-year survival rate remains relatively poor at approximately 31% without a clear temporal improvement in outcomes (Zeidan et al., 2019). The heterogeneity of MDS requires a variety of complex and personalized treatments. Precision determination of prognosis is a key to select a suitable therapy and to forecast the prognosis of patients with MDS. According to the International Prognostic Scoring System (IPSS) or revised IPSS (IPSS-R), approximately 30% of patients are categorized as higher-risk groups (Greenberg et al., 1997, 2012). Hypomethylating agents (HMAs), such as decitabine (DAC), are approved as the first-line treatment option for higher-risk MDS. DAC has a wide range of therapeutic mechanisms for MDS, which reactivates silenced tumor suppressor genes, increases expression of cancer-testis antigens (CTAs), and regulates immune checkpoint molecules (Chang et al., 2017; Zhang et al., 2017a,b). Previous studies have shown that epigenetic silencing of tumor suppressor genes results in the growth advantage of a clonal subpopulation of MDS. This epigenetic modification is reversible, and methyltransferase inhibitors, such as DAC, will reverse the situation and reactivate the silenced tumor suppressor genes (Itzykson and Fenaux, 2014). The "O" subclass

of the forkhead transcription factors (FOX) family is considered important tumor suppressor genes. FOXO genes exist widely in various organisms, they play an important role in the lifespan of invertebrates and mammals, and they inhibit tumor proliferation and regulate energy metabolism and induce cellular responses (Link and Fernandez-Marcos, 2017). In fact, a study has studied the effects of DAC treatment on the myeloid MDS cell line SKM-1 and investigated the role of FOXO3A in DAC-dependent treatment (Zeng et al., 2017). Currently, no studies have investigated the pathogenesis of FOXO1 in MDS.

FOXO1, also known as forkhead in rhabdomyosarcoma-like protein 1 (FKHRL1), is another key transcription factor of the FOX family with important roles in anti-oxidative enzymes, cell cycle arrest, apoptosis, autophagy, metabolic and immune regulators, which make it a super transcription factor with complex activities it a super transcription factor with complex activities (Murtaza et al., 2017; Jiang et al., 2018). It is characterized by the existence of a unique forkhead DNA binding domain, a highly conserved wing-helix motif, and regulation the transcription of a variety of downstream genes (Chen et al., 2019). The function of FOXO1 is not only regulated by microRNAs, which play important roles in destabilizing or attenuating the translation of FOXO1 mRNA, but also by post-translational modifications (such as phosphorylation, acetylation, and ubiquitination), which ultimately affect its nuclear/cytoplasmic transport and thus its cellular localization (Xing et al., 2018). After FOXO1 is phosphorylated, p-FOXO1 binds to the cytoplasm by 14-3-3 proteins and is involved in the subsequent interaction with ubiquitin E3 ligases, which induces its degradation, FOXO1 is inactivated and its target gene is down-regulated (Brownawell et al., 2001). Furthermore, FOXO1 is directly or indirectly regulated by other protein kinases (such as AKT, MAPK1, and PTEN). FOXO1 is considered as a potential tumor suppressor gene that participates in regulating the differentiation of a variety of cells and plays a role in inhibiting tumor cell proliferation (Ushmorov and Wirth, 2018). An increasing number of studies have confirmed that the re-expression and activation of FOXO1 in tumor cells has great potential in anti-tumor therapy (Shi et al., 2018).

In this study, we investigated the effects of a low concentration of DAC (1 μ M) on differentially expressed genes (DEGs), cell apoptosis, cycle arrest, differentiation, and immunoregulation in MDS cell lines and patients. In addition, we also investigated the role of FOXO1 in DAC-dependent processes by measuring the expression level and activity of this gene and its downstream targets after DAC treatment.

RESULTS

Transcriptome Profiling of MDS Cell Lines Following DAC Treatment

The GEM analysis of MDS-L cell showed 1,745 differentially expressed genes compared with the control: 842 were upregulated, while 903 genes were downregulated. The GEM analysis of SKM-1 cell showed 1,303 differentially

expressed genes compared with the results of the control: 541 were upregulated, while 762 genes were downregulated. The overlap among the 2 cell lines contained 256 genes. Among them, 89 genes were upregulated together and 167 genes were downregulated together.

GO Terms and Pathways Enriched by DEGs

The GO analysis revealed that MDS cell line DEGs are involved in the process of immune-related response. Biological process (BP) was mainly enriched in defense response to virus, immune response, inflammatory response, intrinsic apoptotic signaling pathway in response to DNA damage, and positive regulation of inflammatory response (Figure 1A). For cellular component (CC), enrichment of DEGs was mainly enriched inside the chromosome, chromosomal part, and nuclear chromosome (Figure 1B). For molecular function (MF), enrichment of DEGs was primarily in transcription factor binding, identical protein binding, and protein dimerization binding (Figure 1C). KEGG pathway analysis showed that DEGs enrichment occurred principally in the FOXO signaling pathway, Epstein-Barr virus infection, cellular senescence, cell cycle, and hematopoietic cell lineage (Figure 1D). Overall, there were significantly altered transcripts participating in the FOXO signaling pathway, cell cycle, Toll-like receptor signaling pathway, hematopoietic cell differentiation, inflammatory response, and p53 signaling pathway (Figure 1E).

Functional Network of DAC-Induced Transcripts

The subnetwork enrichment analysis of DAC induced immune related transcripts in MDS cell lines identified TP53, FOXO1, TLR4, TLR8, S100A8, S100A9, CD14, and CXCL10 as highly interconnected genes, and are likely to be the potential hubs of the immunity functional network (Figure 2). The FOXO1 signaling pathway containing genes AKT3, ATM, BCL2L11, BCL6, BNIP3, CAT, CCND2, CDK2, FBXO32, FOXO1, HOMER1, IL6, IL7R, KLF2, MAPK11, MAPK14, MAPK8, MAPK9, PCK1, PCK2, PIK3CD, PIK3CG, PIK3R1, PTEN, SMAD2, SMAD3, and TNFSF10 are biologically linked to numerous signal pathways, including cell apoptosis, cell cycle, cell differentiation, and immune system. In this study, we concentrated especially on the effect of FOXO1 on biological characteristics in MDS.

DAC Induces Apoptosis in MDS-L Cells

As DAC exposure time expanded, the percentages of apoptotic cells increased significantly (Figure 3A). Annexin-V-FITC/PI double labeling confirmed the rate of apoptosis. The labeling showed a gradual increase in apoptosis on days 3rd and 5th day, confirming that with the increase in early apoptotic cells is the most significant rate (Figure 3B).

In the absence of DAC, the expression of activated FOXO1 was very low in MDS-L cells, but after the initiation of treatment on days 3 and 5, the expression of activated FOXO1 gradually increased, rather than the non-activated phosphorylated form

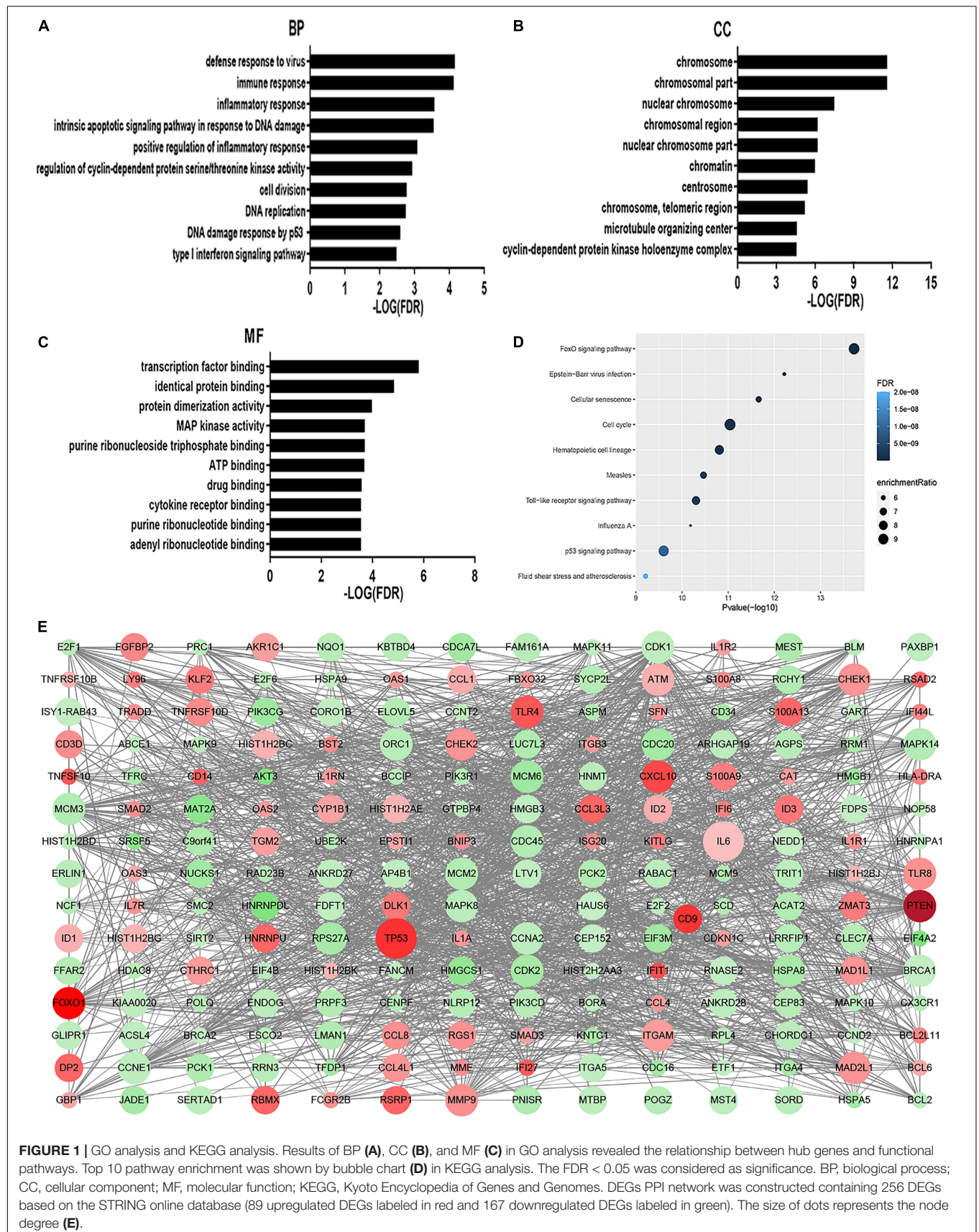


FIGURE 1 | GO analysis and KEGG analysis. Results of BP (A), CC (B), and MF (C) in GO analysis revealed the relationship between hub genes and functional pathways. Top 10 pathway enrichment was shown by bubble chart (D) in KEGG analysis. The FDR < 0.05 was considered as significance. BP, biological process; CC, cellular component; MF, molecular function; KEGG, Kyoto Encyclopedia of Genes and Genomes. DEGs PPI network was constructed containing 256 DEGs based on the STRING online database (89 upregulated DEGs labeled in red and 167 downregulated DEGs labeled in green). The size of dots represents the node degree (E).

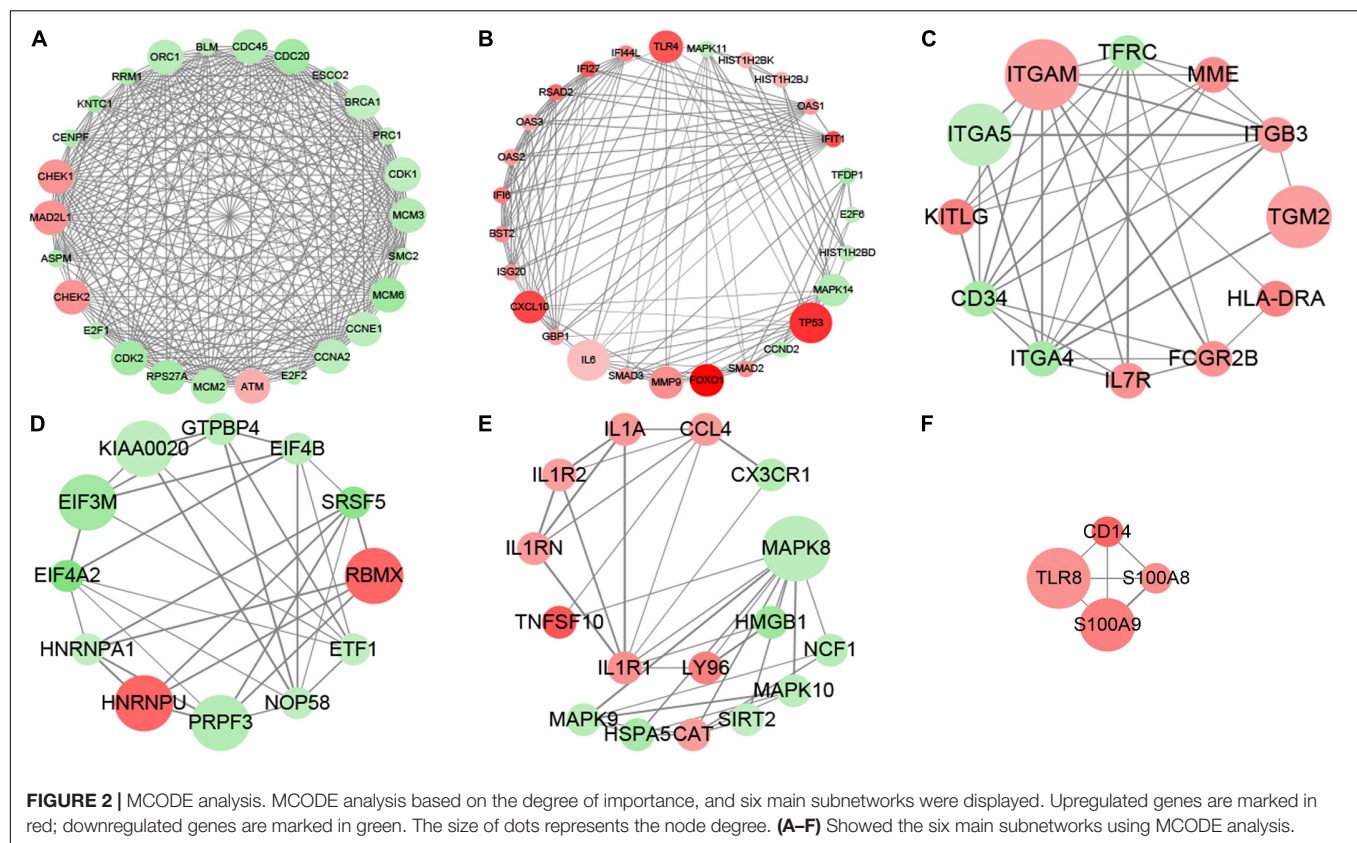


FIGURE 2 | MCODE analysis. MCODE analysis based on the degree of importance, and six main subnetworks were displayed. Upregulated genes are marked in red; downregulated genes are marked in green. The size of dots represents the node degree. (A–F) Showed the six main subnetworks using MCODE analysis.

(p-FOXO1). The expression of p-FOXO1 gradually decreased, indicating that FOXO1 mainly exists in an inactive form in MDS-L cells. With the prolonged action of the drug, DAC can induce FOXO1 activation in MDS-L cells (Figure 3C). The expression of target protein downstream of apoptosis-related FOXO1 was also detected. As shown in Figure 3C, measurable expression of apoptosis-related proteins Bim, Puma, and FasL was observed in untreated MDS-L cells. After DAC treatment, Bim, Puma, and FasL protein expression increased significantly with the increase of exposure time to drug (Figure 3C).

To investigate the role of FOXO1 in DAC-induced MDS-L cell apoptosis, we suppressed FOXO1 expression by targeting siRNA before DAC treatment. Western blot displayed that siRNA targeting FOXO1 decreased FOXO1 expression approximately 72% compared to negative control siRNA. After DAC treatment, FOXO1 expression increased obviously in negative control siRNA-treated MDS-L cells. In contrast, the expression of FOXO1 showed no significant increase when cells were treated with FOXO1-targeted siRNAs (Figure 3D). These data confirm that FOXO1 expression is inhibited by siRNA. We also observed that silencing FOXO1 expression helped to suppress Bim expression after DAC treatment, but not the expression of Puma and FasL protein, suggesting that the presence and activation of FOXO1 plays a crucial role in the activation of Bim (Figure 3D).

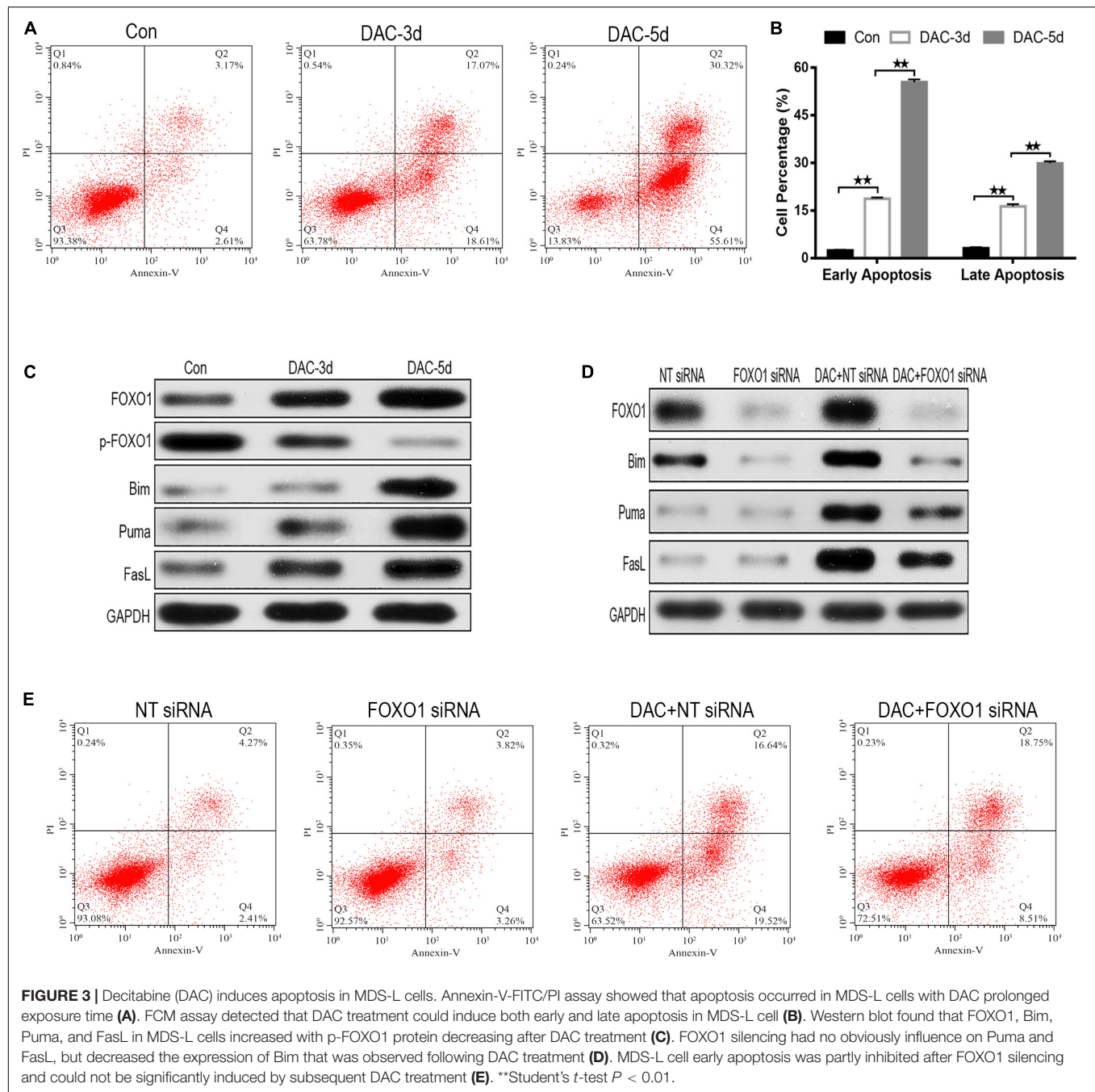
After knockdown of FOXO1, apoptosis assay indicated that silenced FOXO1 did not significantly affect the later apoptosis of MDS-L cells, but significantly decreased early apoptosis of

MDS-L cells, suggesting that FOXO 1 activation is involved mostly in the early stages of DAC-induced apoptosis (Figure 3E).

DAC Induces Cell Cycle Arrest in MDS-L Cells

After DAC treatment, the ratio of cells in S phase decreased significantly, while the proportion of cells in G0/G1 phase increased, indicating that cell cycle arrest was induced by G0/G1 blockade (Figures 4A,B). The influence of DAC treatment on cell cycle gene expression was also observed. CDKN1A, CDKN1B, CCND1, and CCND2 are downstream genes targeted by FOXO1 and are disordered in a multiple of tumors. As shown in Figure 4C, the expression of CDKN1A and CDKN1B was scarce in untreated MDS-L cells, but after DAC treatment, the expression of CDKN1A and CDKN1B was upregulated with drug maintenance application. Conversely, a significant decrease in CCND1 and CCND2 expression was observed in the presence of DAC (Figure 4C).

Then, we studied the effect of silent FOXO1 on CDKN1A, CDKN1B, CCND1, and CCND2. Compared with control siRNA, silencing FOXO1 had significant effects on the cell cycle. The expression of FOXO1 downstream targets CDKN1A and CCND1 were obviously affected, whereas silencing FOXO1 had no significant effect on CDKN1B and CCND2 (Figure 4D). In the presence of FOXO1 silencing, DAC showed no obviously ability to regulate either CDKN1B and CCND2 protein expression, indicating FOXO1 has a regulatory effect to CDKN1A and

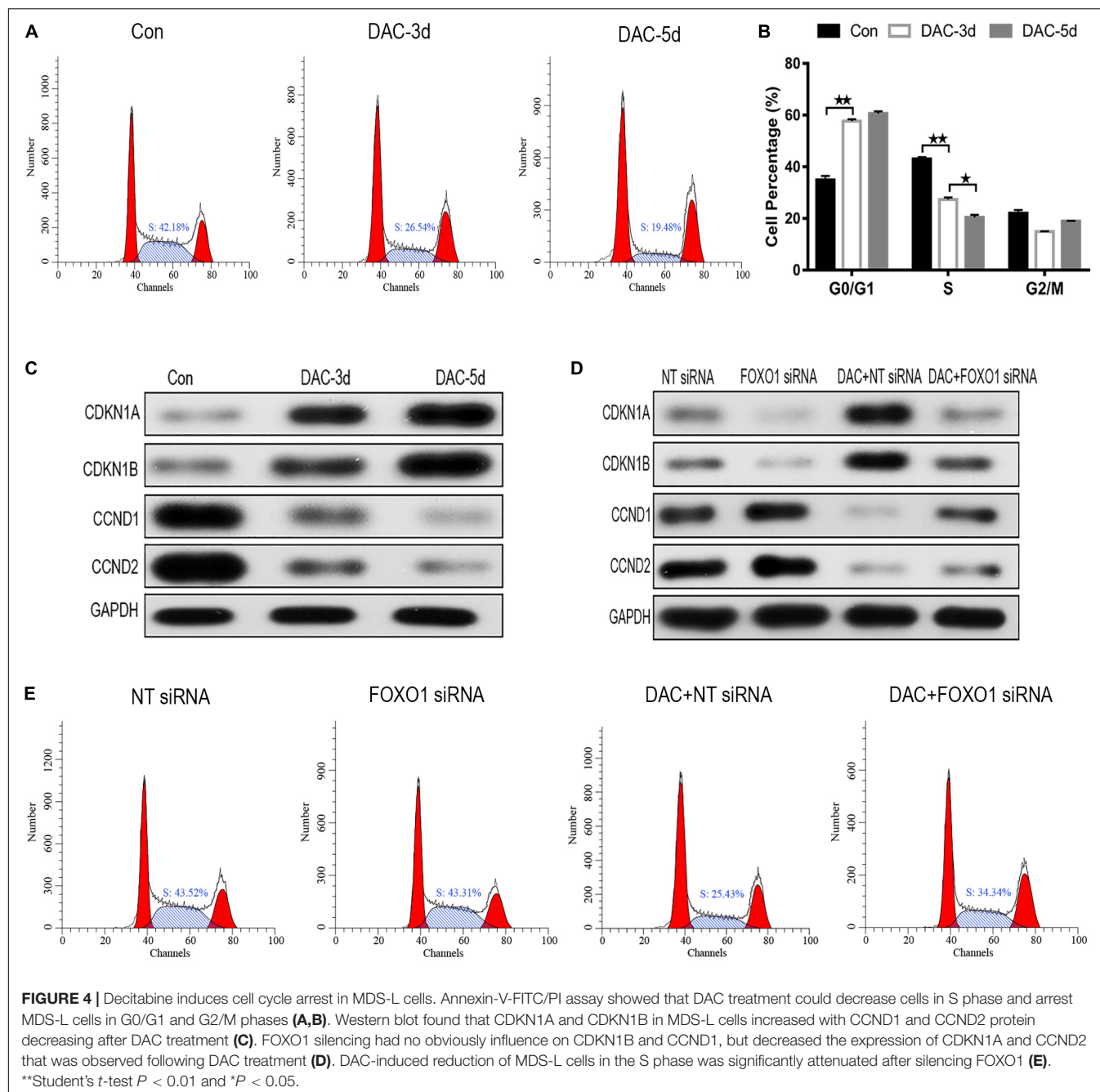


CCND1 (Figure 4D). The increase in the proportion of S phase cells in MDS-L following knockdown of FOXO1 was not totally reversed by subsequent DAC treatment, suggesting that FOXO1 activation plays an indispensable role in DAC-induced cell cycle arrest (Figure 4E).

FOXO1 Contributes to DAC-Induced MDS-L Cell Differentiation

MDS-L cells were positive for CD34, c-Kit, HLA-DR, CD13, and CD33, and partially positive for CD41 and negative for

CD3, CD14, CD20, and CD235a (Tohyama et al., 1994). The expression levels of myeloid cell antigen CD13, T lymphocyte cell marker CD3, monocyte differentiation marker CD14, B lymphocyte differentiation marker CD20, and erythroid cell differentiation marker CD235a on the surface of DAC treated MDS-L cells were detected. The expression levels of CD3, CD14, and CD20 on the surface of MDS-L cells increased after DAC treatment, accompanied by antigen changes, with CD13 showing a significant decrease after treatment, while the expression of CD235a showed no obvious change during DAC treatment. As DAC action



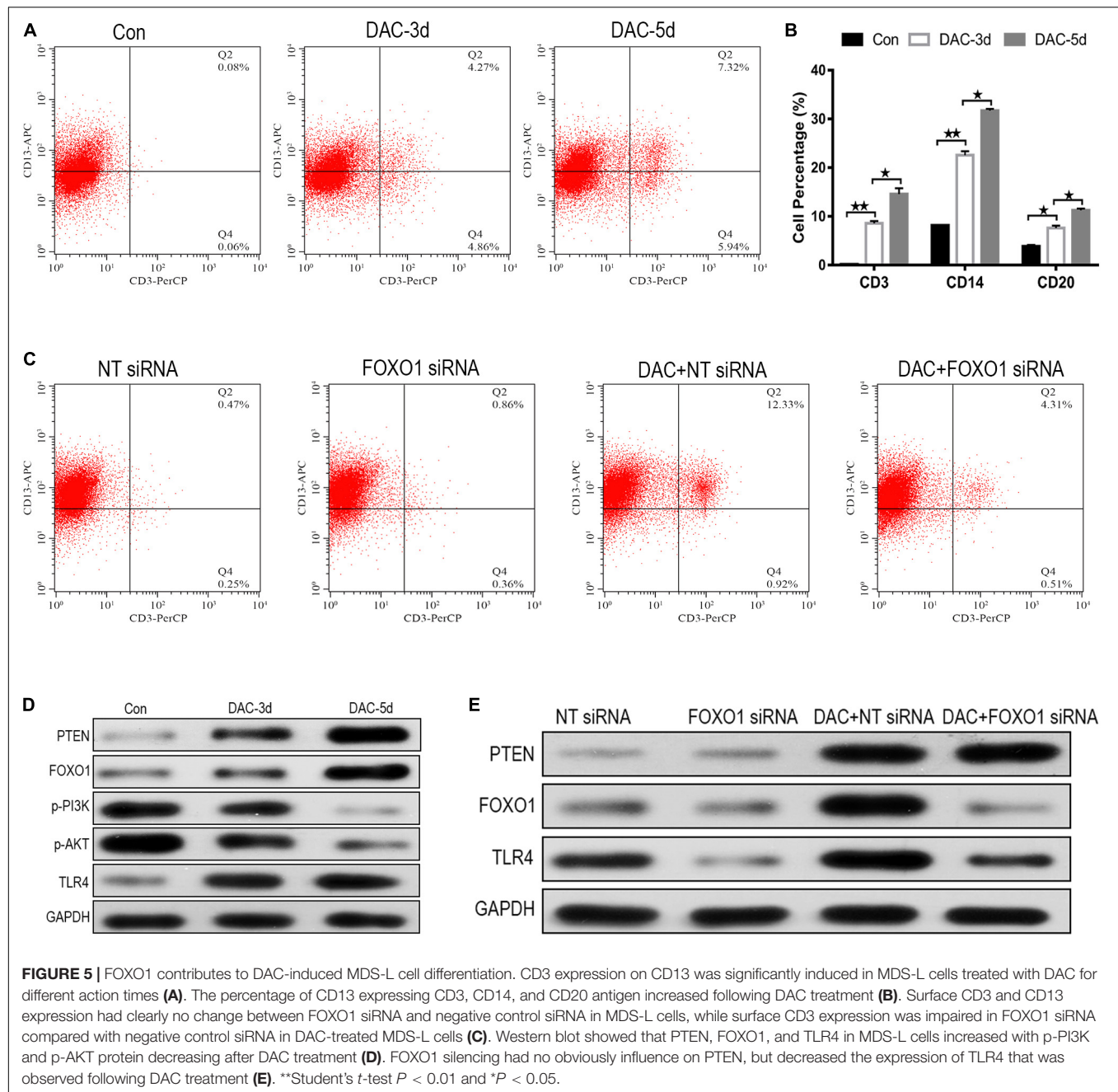
time was prolonged, the expression levels of CD3, CD14, and CD20 continued to increase in a time-dependent manner (Figures 5A,B).

No significant difference in cell differentiation antigen expression was observed between MDS-L cells in which FOXO1 was silenced and non-silenced control. However, when FOXO1 siRNA-MDS-L cells were treated with DAC, the observed increase in CD3-positive cells were significantly reduced compared to cells bearing negative control siRNA (Figure 5C), indicating that silencing FOXO1 before DAC treatment weakens, but does not eliminate the differentiation of

DAC-induced MDS-L cells into antigen molecules. Therefore, the above studies indicate that FOXO1 activation contributes to DAC-induced MDS cell differentiation.

FOXO1 Contributes to DAC-Mediated TLR-4 Augment in MDS-L Cells

The PTEN/PI3K/AKT/FOXO1 signaling pathway is a major signaling pathway involved in cell proliferation, apoptosis, metastasis, and immunoregulation, and its cascade reaction pathway occupies an important position in the signal



transduction process (Jiang et al., 2018). In this study, the protein expression of PTEN, FOXO1, p-PI3K, p-AKT, and TLR-4 was also detected employing western blot. The results showed that the protein expression of PTEN, FOXO1, and TLR-4 increased after DAC treatment, accompanied by significant decreases in p-PI3K, and p-AKT (Figure 5D). Compared with the negative control group, FOXO1 siRNA-MDS-L cells treated with DAC, the expression of PTEN showed significant upregulation, but the expression of FOXO1 and TLR-4 showed a significant decrease (Figure 5E). Thus, DAC induces PTEN, which in turn activates FOXO1

signaling, leading to the activation TLR4-driven innate immune response.

FOXO1 Contributes to DAC-Mediated Immune Activation in MDS Patients

Because MDS-L lacks innate and adaptive immune cells, MDS patient specimens were used to verify the effect of FOXO1 on innate and adaptive immunity *in vivo*. The transcriptional profiling of 84 genes involving innate and adaptive immune processes were evaluated after 4 courses DAC treatment in 3

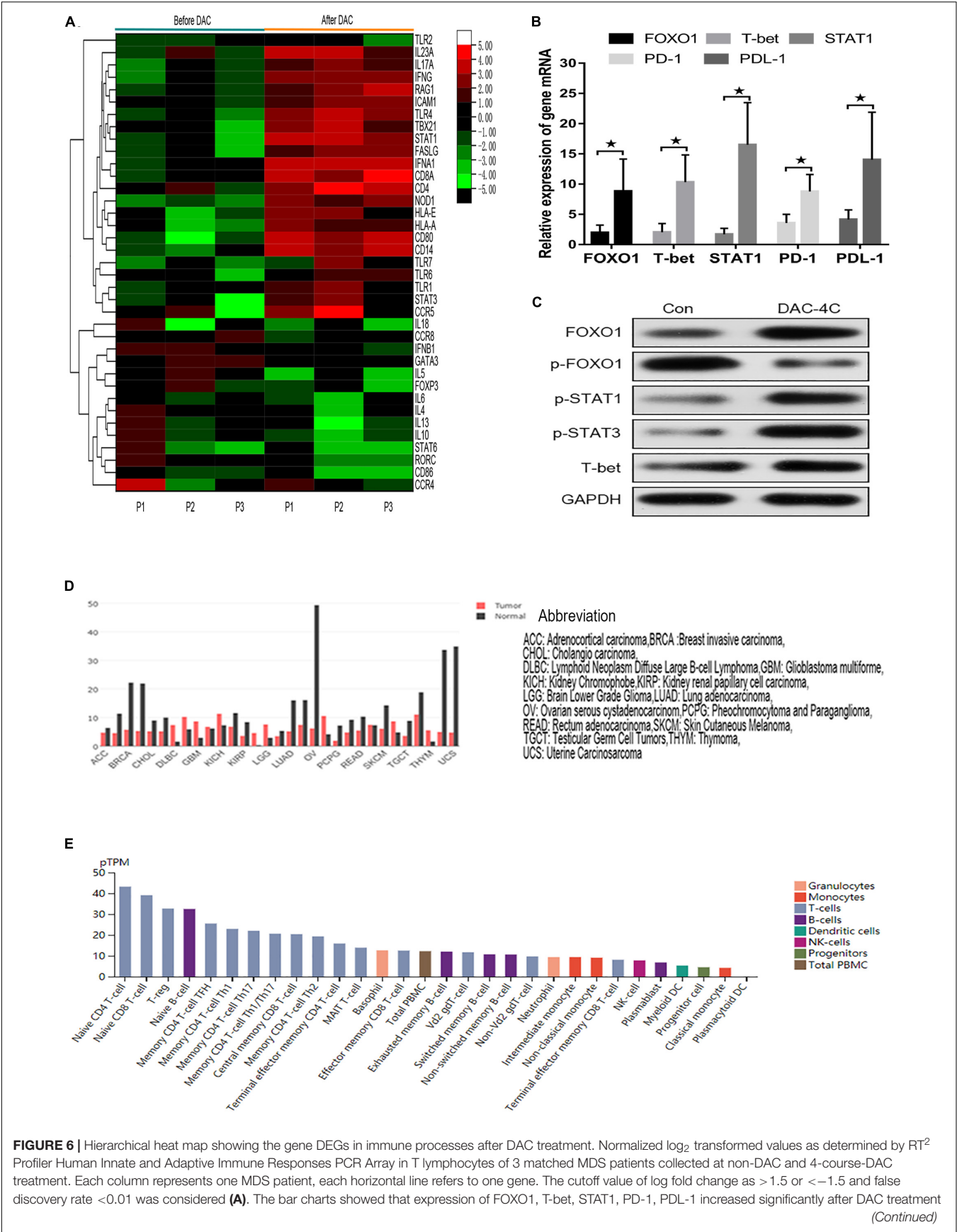


FIGURE 6 | Hierarchical heat map showing the gene DEGs in immune processes after DAC treatment. Normalized log₂ transformed values as determined by RT² Profiler Human Innate and Adaptive Immune Responses PCR Array in T lymphocytes of 3 matched MDS patients collected at non-DAC and 4-course-DAC treatment. Each column represents one MDS patient, each horizontal line refers to one gene. The cutoff value of log fold change as >1.5 or <-1.5 and false discovery rate <0.01 was considered **(A)**. The bar charts showed that expression of FOXO1, T-bet, STAT1, PD-1, PDL-1 increased significantly after DAC treatment **(Continued)**

FIGURE 6 | Continued

(B). Western blot showed that FOXO1, p-STAT1, p-STAT3, and T-bet in one MDS patient increased with p-FOXO1 protein decreasing after DAC treatment **(C)**. Using the GEPIA (Gene Expression Profiling Interactive Analysis) dataset (<http://gepia.cancer-pku.cn/>), we compared the mRNA expression of FOXO1 between different tumors and normal tissues. The results indicated that the expression levels of FOXO1 were obviously higher in normal tissues than in tumors. The gene expression profile across different tumor samples and paired normal tissues (Bar plot). The height of bar represents the median expression of certain tumor type or normal tissue **(D)**. Utilizing an online tool (The Human Protein Atlas which aim to map all the human proteins in cells, tissues and organs using integration of various omics technologies, <https://www.proteinatlas.org/>), we explored the mRNA expression of FOXO1 in immune cells. The results show FOXO1 plays an important role in immune cell development **(E)**. * means $P < 0.05$.

matched MDS patients ($n = 3$) (**Supplementary Table 1**). The transcriptional profiling analysis was performed on isolated T cells. A total of 37 (44%) genes were differentially expressed after DAC treatment with fold changes >2.5 (**Figure 6A**). Among these, a total of 23 (27.4%) innate and adaptive immunity genes were significantly upregulated. The altered transcriptional profiling of MDS T cells was characterized by the upregulation of innate and adaptive immunity genes. Meanwhile, the expression of FOXO1, STAT1, T-bet, PD-1, and PD-L1 was also detected in 12 paired MDS patients by RT-PCR due to the limiting amount of the panel. As shown in **Figure 6B**, the mRNA level of FOXO1, T-bet, STAT1, PD-1, and PD-L1 was highly upregulated after 4 courses of DAC treatment. Furthermore, the protein expression level of FOXO1, p-FOXO1, p-STAT3, and T-bet was detected by western blot in 1 MDS patient. As shown in **Figure 6C**, the expression of activated FOXO1, p-STAT1, p-STAT3, and T-bet increased, while the expression of non-activated p-FOXO1 reduced after DAC treatment. Therefore, the above studies demonstrate that FOXO1 activation contributes to DAC-induced immune activation in MDS.

DISCUSSION

Myelodysplastic syndromes indicates that the status of pre-leukemia with ineffective hematopoiesis, featured by bone marrow dysplasia that easily progresses into acute myeloid leukemia (Steensma, 2018). For higher-risk MDS patients who are not suitable for transplant, HMAs are most appropriate. DAC are therapeutic agents and have already been used in treatment of higher-risk MDS and acute myeloid leukemia for many years. DAC can play a role in decreasing MDS clonal burden, then resulting in improved hematopoiesis, but do not eradicating tumor stem cells, so relapse is inevitable tendency. The mechanism of action of DAC is still not fully understood, and may result from a combination of conventional cytotoxic, DNA hypomethylation and immune-related mechanisms including changes in interferon signaling and presentation of neoantigens as epitopes to the immune system (Licht, 2015; Chiappinelli et al., 2017). Once DAC fails due to intolerance, resistance, or relapse after a favorable response, the approved second-line therapy is limited, the outlook is poor, and the median survival time is less than 6 months (Jabbour et al., 2010; Prébet et al., 2011; Montalban-Bravo et al., 2018). Therefore, clarifying the mechanism underlying DAC is required to improve the treatment effect in MDS.

Decitabine is considered as a rapid and profound global DNA demethylation, as well as site-specific promoter demethylation

of many genes including cancer suppressor genes and immune-related genes (Wolff et al., 2017; Seelan et al., 2018). In this study, using the DEG analytical method, the data suggest that multiple genes and multigenic pathways were regulated by DAC. For example, DAC could activate the interferon signaling and p53 signaling pathway induce further biological process in pathway analysis as previous reports (Chang et al., 2017; Zhang et al., 2017a,b). However, this study focused on the mechanism of tumor suppressor gene FOXO1 in DAC-dependent processes. The results indicated that FOXO1 is hyperphosphorylated in MDS-L cells and thus inactivated. DAC treatment activates FOXO1 by increasing its gene expression and reducing its protein phosphorylation, leading to up-regulation of downstream effectors Bim, Puma, FasL, CDKN1A, and CDKN1B and down-regulation of downstream cell cycle effectors Cyclin D1 and Cyclin D2. Furthermore, DAC-induced differentiation of MDS-L cells into lymphocytes and monocytes, MDS-L cell cycle arrest, apoptosis, and immune activation were also observed.

Forkhead box O (FOXO) transcription factors, including FOXO1 (FKHR), FOXO3a (FKHRL1), FOXO4 (AFX), and FOXO6, have also been increasingly recognized as tumor suppressors through serving as pivotal connection points to allow stress signals, proliferative nutrient and diverse to cluster and integrate with distinct gene networks to control cell fate, metabolism, and cancer development (Farhan et al., 2017; Jiramongkol and Lam, 2020). As shown in **Figure 6D**, FOXO1 expression is reduced in most tumors and appears to act as a tumor suppressor gene. In this study, similar to the effect of FOXO3A activation in the SKM-1 cell line (Zeng et al., 2017), active FOXO1 also plays an important role in suppressing MDS-L by inducing apoptosis and by suppressing progression of cell cycle. In contrast to active FOXO3A, our research confirmed that activated FOXO1 tends to directly regulate Bim gene, which is consistent with previous research (Dijkers et al., 2000, 2002). That is, activated FOXO1 is translocated to the nucleus, binding to the Bim promoter and induces the transcription of the Bim gene. However, FOXO1 activation showed a limited regulation effect on Puma and FasL expression by silencing FOXO1, which shows that DAC may up-regulate the expression of Puma and FasL in other ways. Therefore, it is possible that the apoptosis induced by DAC is mainly mediated through the mitochondrial apoptosis pathway. Through a similar silencing FOXO1 gene function test, we also found that FOXO1 has a more closely regulatory effect on CDKN1A and CCND2 than on CDKN1B and CCND1 (Schmidt et al., 2002).

Next, we focused on the role of FOXO1 in the MDS immune microenvironment. As shown in **Figure 6E**, FOXO1 also inherently controls the anti-tumor immune response and

the homeostasis and development of immune cells, including T cells, B cells, natural killer (NK) cells, macrophages, and dendritic cells. However, the mechanism of FOXO1 in the MDS immune environment has not been reported so far. In the past decade, aberrant immune activation in lower risk MDS and impaired anti-leukemic immunity in higher risk Malignant clones as well as MDS in the bone marrow microenvironment were identified as key pathogenic drivers of MDS. Multiple mechanisms are involved in higher risk MDS to promote immune tolerance (Ivy and Brent, 2018; Sallman and List, 2019). Several reports have demonstrated that higher risk disease is accompanied by an increase in myeloid-derived suppressor cells (MDSCs), along with regulatory T cells (Tregs) augmentation (Gabrilovich and Nagaraj, 2009; Kittang et al., 2015). One effect of increasing suppressive cell subsets is to reduce cytotoxic anti-leukemia immunity. The activation and function of NK cells and cytotoxic T lymphocytes (CTL) play important cytotoxic activity in response to myeloid neoplasms, but their functions are reduced in high-risk MDS (Epling-Burnette et al., 2007; Kotsianidis et al., 2009). In our study, the results showed that DAC promotes the differentiation of MDS-L cell surface antigen into lymphocytes and monocytes through activating FOXO1. Further PTEN/PI3K/AKT/FOXO1 pathway study confirmed that DAC upregulates PTEN gene expression, thereby inhibiting the phosphorylation of PI3K and AKT and releasing FOXO1 inhibition. Activated FOXO1 can upregulate TLR4 expression, thereby activating the MDS innate immune system. The results were consistent with previous studies, FOXO1 is a key regulator of many inflammatory factors, such as TLR4, NF- κ B, tumor necrosis factor (TNF)- α , interleukin (IL)-1 β , and IL-18, via the TLR4/NF- κ B signaling pathway (Kamo et al., 2013; Li et al., 2016). In the specimens of MDS patients, we further verified that with the increased expression of FOXO1, there is a wide range of upregulation and activation of type I immune cell transcription factors and up-regulation of cellular immune functions, thereby enhancing anti-leukemia effects and inhibiting the growth of MDS malignant clones. All the results demonstrated that DAC can activate FOXO1 to enhance anti-tumor immune effect in higher risk MDS.

Accumulating evidence has shown the paradoxical intrinsic role of the FOXO1 in cancer, which can act as a tumor repressor while also maintaining cancer stem cells (Sykes et al., 2011; Long et al., 2020). The regulatory role of FOXO1 in tumor immunity is equally confusing (Deng et al., 2018). DAC also has a double-edged sword effect on the regulation of MDS immune function. The global demethylation of DNA can induce anti-tumor effects. It can also upregulate the expression of inhibitory immune checkpoint receptors and their ligands, resulting in secondary resistance to DAC (Wolff et al., 2017). Due to the limitation of conditions, we do not have a suitable animal model of MDS to further verify activated FOXO1 and their extracellular factors in cancer cells, stromal cells, and immune cells. These factors have a profound effect on promoting or inhibiting anti-cancer immunity in the tumor microenvironment. The effect of activated FOXO1 on the prognosis and survival of MDS disease also requires further long-term follow-up. Based on the above findings, we agree

with assumption of Wolff E, who proposed a role for FOXO1 as a rheostat, which regulates both immune homeostasis and the immune response in cancer immunity. In the future, further study is needed to better understand the role of FOXO1 in MDS pathogenesis. It will be interesting to better understand each molecule and each cell type regulated by FOXO1 directly in the settings of cancer patients or tumor models (Tirosh et al., 2016).

In conclusion, this study showed that silencing FOXO1 expression impaired DAC-induced apoptosis, cell cycle arrest, and cellular differentiation, which potentially may be due to the observed down-regulation of Bim, CDKN1A, and CCND1. DAC-induced TLR4 upregulation was mainly reversed by FOXO1 silencing, which could explain the partial reversal of DAC-induced immune activation observed when FOXO1 expression was knocked down. It was found that the up-regulation of innate and adaptive immunity genes after DAC treatment, as well as the subsequent increase in T-bet, p-FOXO1, and p-STAT3 in MDS samples, were related to the up-regulation and activation of FOXO1 induced by DAC. Collectively, DAC induces FOXO1 activation, which plays an important role in anti-MDS tumors.

MATERIALS AND METHODS

Cell Culture and DAC Treatment

MDS-L cells were donated by Prof. Tohyama (Tohyama et al., 1995). MDS-derived leukemia cell line SKM-1 cells were donated by Prof. Nakagawa (Nakagawa and Matozaki, 1995). Cell lines were cultured in RPMI 1640, which contained 10% heat-inactivated fetal bovine serum and 1% penicillin-streptomycin at 37°C in a humidified atmosphere containing 5% CO₂. Furthermore, IL-3 (100 U/ml) is essential for MDS-L cells. When cells reached the logarithmic growth phase, they were seeded at a density of 5×10^5 cells/well in 6-well plates and harvested with five 24-h pulses of 1 μ M DAC (Selleck Chemicals LLC, Houston TX, United States) and collected after the treatment (Zhang et al., 2017b).

RNA Preparation and Gene Expression Microarray (GEM)

As previously described, according to the manufacturer's instructions, total RNA was extracted from 10^5 cell lines using the RNeasy system (Qiagen, Valencia, CA, United States). A Genechip Primeview™ Human Gene Expression Array (Affymetrix, United States) was used for the GEM study. The signal intensities were obtained with a Genechip Scanner 3000 7G (Affymetrix) to generate cell intensity files (CEL). Statistical analysis was performed using Partek Genomics Suite software (Partek, Inc., St. Louis, MO, United States). The robust multiple array average (RMA) algorithm was used to normalize the data. The false discovery rate (FDR) was lower than 0.15 to minimize the misidentification of genes. Analyzed the changes of up-regulated or down-regulated genes greater than 1.0 times (Xu et al., 2014).

Functional Enrichment Analysis

WebGestalt¹ is an automated systematic-analysis tool that helps understand common and unique way within a set of orthogonal target discovery researches. The tool is free and well-maintained, user-friendly gene-list analysis for gene annotation and analysis. The gene ontology (GO) terms for biological process (BP), cellular component (CC), and molecular function (MF) categories, as well as Kyoto Encyclopedia of Genes and Genomes (KEGG) pathways was performed using the WebGestalt online tool. GraphPad (GraphPad Software, Inc., San Diego, CA, United States) was used to improve GO graphic analysis. Fisher's exact test was used to select the important approach, and the significance threshold was defined by FDR. *P*-value < 0.05 was considered statistically significant. STRING² was employed to construct protein-protein interaction (PPI) network of DEGs for DAC treatment MDS cell lines and the confidence score of the interaction > 0.4 was considered statistically significant. Cytoscape was employed to annotate and improve the up-down regulated genes of PPI. Further, molecular complex detection (MCODE) APP was applied to identify densely connected network components (Xu et al., 2014).

Cellular Transfection

MDS-L cells were transfected with either Silencer Select FOXO1 (cat. AM16708) or Silencer Select Negative Control (cat. AM4611) siRNAs, both of which were purchased from Thermo Fisher (Thermo Fisher Scientific, Waltham, MA, United States), and Lipofectamine 3000 reagent (Thermo Fisher Scientific, Waltham, MA, United States) according to previously reported literature (Zeng et al., 2017). The harvest time of these transfected cells was set to 24 h after transfection. Then, the transfected cells were either cultured or treated with 1 μ M of DAC as needed for 72 h.

Apoptosis Assessment

Cell apoptosis analysis was fulfilled by employing an annexin V-FITC/PI apoptosis detection kit (BD Biosciences) with a flow cytometer (FACS Calibur, BD Biosciences, Franklin Lakes, NJ, United States). According to different experimental manipulation, MDS-L cells were seeded and inoculated in a 6-well plate at a density of 10^5 cells per well. Subsequently, these cells were first suspended in the binding buffer, and then Annexin V-FITC (10 μ l) and PI (5 μ l) were, respectively, supplied to each well. Finally, The mixture was reacted in the dark for 15 min and then analyzed using flow cytometry (FCM) (Zhang et al., 2017b).

Cell Cycle Analysis

Wash 5×10^4 cells with cold phosphate-buffered saline (PBS), fix in 70% ethanol, wash once with PBS, and then re-suspend in 1 mL of propidium iodide (PI) staining reagent (50 mg/ml of propidium iodide and 1 mg/ml of RNase). Before performing cell cycle analysis, the samples were incubated in the dark for 30 min. The cell cycle was measured with FACS Calibur. The percentages

of cells in the G1, S, and G2 phases were calculated with the Cellquest software (Xu et al., 2014).

Detection of Cell Surface Markers

DAC-treated MDS-L cells were collected and stained for surface antigen, 10 μ l of PerCP-bound anti-CD3 antibody, APC-bound anti-CD13 antibody, FITC-bound anti-CD14 antibody, PE-bound anti-CD20 antibody or PE-bound anti-235a antibody (Becton Dickinson) was added to the cells and incubated for 15 min at room temperature in the darkness. Cells were then washed and resuspended in PBS, and surface markers were analyzed by FCM within 1 h.

Bone Marrow Mononuclear Cells and T Lymphocytes Preparation

Twelve MDS patients were administered with DAC (product name: Dacogen, DAC, Xian Janssen Pharmaceutical Ltd., 20 mg/M² \times 5 days for 4 courses) for immune research after obtaining informed consent according to the Declaration of Helsinki and Council for International Organizations of Medical Sciences International Ethical Guidelines, and ethical approval was obtained from the ethics review board at The Sixth Hospital Affiliated with Shanghai Jiao Tong University. All participants provided written informed consent prior to enrollment, and the privacy rights of human subjects were observed. MDS were diagnosed in accordance with the World Health Organization (WHO) 2016 criteria (Arber et al., 2016), and the detailed information regarding MDS patients is shown in **Supplementary Table 1**. Five milliliters of fresh bone marrow were aspirated from posterior iliac crests. Bone marrow mononuclear cells (BM-MNCs) were isolated using Ficoll-Hypaque gradient (Lymphoprep TM, Niergaard, Oslo, Norway) for mRNA expression by quantitative real-time polymerase chain reaction (PCR). BM-MNCs of some MDS patients were carefully separated into 2 portions, T cells of 1 part were isolated using MACS CD3+ T microbeads (Miltenyi Biotec), followed by RT² Profiler PCR Arrays and the rest of the BM-MNCs were used for western blot analysis (Zhang et al., 2017b).

Western Blot Analysis

Whole cell lysates were obtained from MDS-L cell line or BM-MNCs of MDS patients, and separate the same amount of protein by 12% sodium dodecyl sulfate polyacrylamide gel electrophoresis (SDS-PAGE), and then blotted onto a polyvinylidene difluoride (PVDF) membrane. The PVDF membranes were blocked with Tris-buffered saline (TBS) containing 5% skimmed milk powder for 1 h, and then incubated with the primary antibodies (**Supplementary Table 2**) at 4°C overnight. Membranes were incubated with either anti-mouse or anti-rabbit immunoglobulin G (IgG) horseradish peroxidase-conjugated secondary antibody (Amersham Biosciences, Piscataway, NJ, United States). Specific bands were visualized using ECL Western Blotting Detection Reagents (Amersham Biosciences, Piscataway, NJ, United States). The intensity of bands was quantified using Image Lab software version 2.0 (Bio-Rad Laboratories, Hercules, CA, United States), and

¹<http://www.webgestalt.org/option.php>

²<http://string-db.org>

glyceraldehyde 3-phosphate dehydrogenase (GAPDH) was used as an internal standard (Xu et al., 2014).

RT² Profiler PCR Arrays

According to the manufacturer's instructions, 3 matched MDS patients were isolated from 3×10^6 total T cells RNA using miRNeasy Micro Kit (Qiagen). RNA concentration and quality were evaluated by using Nanodrop-ND-1000 (Celbio). According to the manufacturer's instructions, cDNA was synthesized from 250 ng of total RNA using RT² First Strand Kit (SABiosciences Corp.), and the expression levels of 84 genes (Supplementary Table 3) were analyzed by RT² Profiler Human Innate and Adaptive Immune Response PCR Array (PAHS-052Z, SABiosciences Corp). Real-Time PCR amplification was performed on a 7500 Real-Time PCR System (Applied Biosystems). The online tool RT² Profiler data analysis software (Qiagen) was used for data standardization and statistical analyses. The threshold cut-off point was based on >2.5-fold differential expression. The Pheatmap package was used to investigate the differential expression of immune genes through PCR Arrays (Serena et al., 2018).

Quantitative Reverse-Transcription Polymerase Chain Reaction (qRT-PCR)

Total RNA was extracted from BM-MNCs of 12 matched MDS patients using the RNeasy Mini Kit (QIAGEN, Hilden, Germany) according to the manufacturer's instructions. Afterward, reverse transcription and qRT-PCR were, respectively, fulfilled by utilizing a Revert-AidTM First Strand cDNA Synthesis Kit (Fermentas, Burlington, ON, Canada) and SYBR Premix Ex TaqTM II (Tli RNaseH Plus) (TAKARA, Beijing, China). The threshold cycles were used to calculate relative expression levels according to the $2^{-\Delta\Delta C_t}$ method. Relative mRNA expression levels were normalized to the level of GAPDH. The primer sequences used in this investigation are shown in Supplementary Table 4 (Zhang et al., 2017a).

Statistical Analysis

All experiments were performed at least 3 times. The analysis of flow cytometry data was performed using CellQuest software. Continuous variables were expressed as mean \pm standard deviation (SD) or median. According to the distribution of each variable, the comparison was made according to parameters [Student's *t* test, analysis of variance (ANOVA)] or non-parametric (Mann-Whitney *U* Test, Kruskal-Wallis). Categorical variables were compared using Fisher's exact

tests. The difference was considered statistically significant at $P < 0.05$. Statistical analyses were performed using GraphPad Prism program (GraphPad Software, Inc., San Diego, CA, United States) or SPSS software (version 22.0).

DATA AVAILABILITY STATEMENT

The data presented in the study are deposited in the (<https://www.ncbi.nlm.nih.gov/geo/query/acc.cgi?acc=GSE164744>) repository, accession number: GSE164744.

ETHICS STATEMENT

The studies involving human participants were reviewed and approved by the Sixth Hospital Affiliated with Shanghai Jiao Tong University. The patients/participants provided their written informed consent to participate in this study.

AUTHOR CONTRIBUTIONS

ZZ and C-kC started the project, and conceived and designed the experiments. YJ, FX, and L-xS performed the experiments. LS and JG analyzed the data. C-kC took the primary responsibility for the final content. ZZ, YJ, FX, L-xS, LS, JG, and C-kC read and approved the final manuscript. All authors contributed to the article and approved the submitted version.

FUNDING

This work was supported by the National Natural Science Foundation of China (Grant Nos. 81400091 and 81770121).

ACKNOWLEDGMENTS

This manuscript has been released as a pre-print at: <https://www.researchsquare.com/article/rs-48006/v1>.

SUPPLEMENTARY MATERIAL

The Supplementary Material for this article can be found online at: <https://www.frontiersin.org/articles/10.3389/fgene.2020.603956/full#supplementary-material>

REFERENCES

- Arber, D. A., Orazi, A., Hasserjian, R., Thiele, J., Borowitz, M. J., Le Beau, M. M., et al. (2016). The 2016 revision to the World Health Organization classification of myeloid neoplasms and acute leukemia. *Blood* 127, 2391–2405. doi: 10.1182/blood-2016-03-643544
- Brownawell, A. M., Kops, G. J., Macara, I. G., and Burgering, B. M. (2001). Inhibition of nuclear import by protein kinase B (Akt) regulates the subcellular distribution and activity of the forkhead transcription factor AFX. *Mol. Cell Biol.* 21, 3534–3546. doi: 10.1128/MCB.21.10.3534-3546.2001
- Chang, C. K., Zhao, Y. S., Xu, F., Guo, J., Zhang, Z., He, Q., et al. (2017). TP53 mutations predict decitabine-induced complete responses in patients with myelodysplastic syndromes. *Br. J. Haematol.* 176, 600–608. doi: 10.1111/bjh.14455
- Chen, J., Lu, Y., Tian, M., and Huang, Q. (2019). Molecular mechanisms of FOXO1 in adipocyte differentiation. *J. Mol. Endocrinol.* 62, R239–R253. doi: 10.1530/JME-18-0178

- Chiappinelli, K. B., Strissel, P. L., Desrichard, A., Li, H., Henke, C., Akman, B., et al. (2017). Inhibiting DNA Methylation causes an interferon response in cancer via dsRNA including endogenous retroviruses. *Cell* 169:361. doi: 10.1016/j.cell.2017.03.036
- Deng, Y., Wang, F., Hughes, T., and Yu, J. (2018). FOXOs in cancer immunity: knowns and unknowns. *Semin. Cancer Biol.* 50, 53–64. doi: 10.1016/j.semcancer.2018.01.005
- Dijkers, P. F., Birkenkamp, K. U., Lam, E. W., Thomas, N. S., Lammers, J. W., Koenderman, L., et al. (2002). FKHR-L1 can act as a critical effector of cell death induced by cytokine withdrawal: protein kinase B-enhanced cell survival through maintenance of mitochondrial integrity. *J. Cell Biol.* 156, 531–542. doi: 10.1083/jcb.200108084
- Dijkers, P. F., Medema, R. H., Lammers, J. W., Koenderman, L., and Coffey, P. J. (2000). Expression of the pro-apoptotic Bcl-2 family member Bim is regulated by the forkhead transcription factor FKHR-L1. *Curr. Biol.* 10, 1201–1204. doi: 10.1016/S0960-9822(00)00728-4
- Epling-Burnette, P. K., Bai, F., Painter, J. S., Rollison, D. E., Salih, H. R., Krusch, M., et al. (2007). Reduced natural killer (NK) function associated with high-risk myelodysplastic syndrome (MDS) and reduced expression of activating NK receptors. *Blood* 109, 4816–4824. doi: 10.1182/blood-2006-07-035519
- Farhan, M., Wang, H., Gaur, U., Little, P. J., Xu, J., and Zheng, W. (2017). FOXO signaling pathways as therapeutic targets in cancer. *Int. J. Biol. Sci.* 13, 815–827. doi: 10.7150/ijbs.20052
- Gabrilovich, D. I., and Nagaraj, S. (2009). Myeloid-derived suppressor cells as regulators of the immune system. *Nat. Rev. Immunol.* 9, 162–174. doi: 10.1038/nri2506
- Greenberg, P., Cox, C., LeBeau, M. M., Fenaux, P., Morel, P., Sanz, G., et al. (1997). International scoring system for evaluating prognosis in myelodysplastic syndromes. *Blood* 89, 2079–2088.
- Greenberg, P. L., Tuechler, H., Schanz, J., Sanz, G., Garcia-Manero, G., Solé, F., et al. (2012). Revised international prognostic scoring system for myelodysplastic syndromes. *Blood* 120, 2454–2465. doi: 10.1182/blood-2012-03-420489
- Itzykson, R., and Fenaux, P. (2014). Epigenetics of myelodysplastic syndromes. *Leukemia* 28, 497–506. doi: 10.1038/leu.2013.343
- Ivy, K. S., and Brent, F. P. Jr. (2018). Disordered immune regulation and its therapeutic targeting in myelodysplastic syndromes. *Curr. Hematol. Malig. Rep.* 13, 244–255. doi: 10.1007/s11899-018-0463-9
- Jabbour, E., Garcia-Manero, G., Batty, N., Shan, J., O'Brien, S., Cortes, J., et al. (2010). Outcome of patients with myelodysplastic syndrome after failure of decitabine therapy. *Cancer* 116, 3830–3834. doi: 10.1002/cncr.25247
- Jiang, S., Li, T., Yang, Z., Hu, W., and Yang, Y. (2018). Deciphering the roles of FOXO1 in human neoplasms. *Int. J. Cancer* 143, 1560–1568. doi: 10.1002/ijc.31338
- Jiramongkol, Y., and Lam, E. W. (2020). FOXO transcription factor family in cancer and metastasis. *Cancer Metast. Rev.* 39, 681–709. doi: 10.1007/s10555-020-09883-w
- Kamo, N., Ke, B., Busuttill, R. W., and Kupiec-Weglinski, J. W. (2013). PTEN-mediated Akt/ β -catenin/Foxo1 signaling regulates innate immune responses in mouse liver ischemia/reperfusion injury. *Hepatology* 57, 289–298. doi: 10.1002/hep.25958
- Kittang, A. O., Kordasti, S., Sand, K. E., Costantini, B., Kramer, A. M., Perezabellan, P., et al. (2015). Expansion of myeloid derived suppressor cells correlates with number of T regulatory cells and disease progression in myelodysplastic syndrome. *Oncoimmunology* 5:e1062208. doi: 10.1080/2162402x.2015.1062208
- Kotsianidis, I., Bouchliou, I., Nakou, E., Spanoudakis, E., Margaritis, D., Christophoridou, A. V., et al. (2009). Kinetics, function and bone marrow trafficking of CD4+CD25+FOXP3+ regulatory T cells in myelodysplastic syndromes (MDS). *Leukemia* 23, 510–518. doi: 10.1038/leu.2008.333
- Li, Z., He, Q., Zhai, X., You, Y., Li, L., Hou, Y., et al. (2016). Foxo1-mediated inflammatory response after cerebral hemorrhage in rats. *Neurosci. Lett.* 629, 131–136. doi: 10.1016/j.neulet.2016.06.013
- Licht, J. D. (2015). DNA methylation inhibitors in cancer therapy: the immunity dimension. *Cell* 162, 938–939. doi: 10.1016/j.cell.2015.08.005
- Link, W., and Fernandez-Marcos, P. J. (2017). FOXO transcription factors at the interface of metabolism and cancer. *Int. J. Cancer* 141, 2379–2391. doi: 10.1002/ijc.30840
- Long, J., Jia, M. Y., Fang, W. Y., Chen, X. J., Mu, L. L., Wang, Z. Y., et al. (2020). FLT3 inhibition upregulates HDAC8 via FOXO to inactivate p53 and promote maintenance of FLT3-ITD+ acute myeloid leukemia. *Blood* 135, 1472–1483. doi: 10.1182/blood.2019003538
- Montalban-Bravo, G., Garcia-Manero, G., and Jabbour, E. (2018). Therapeutic choices after hypomethylating agent resistance for myelodysplastic syndromes. *Curr. Opin. Hematol.* 25, 146–153. doi: 10.1097/MOH.00000000000000400
- Murtaza, G., Khan, A. K., Rashid, R., Muneer, S., Hasan, S. M. F., and Chen, J. (2017). FOXO transcriptional factors and long-term living. *Oxid. Med. Cell Longev.* 2017:3494289. doi: 10.1155/2017/3494289
- Nakagawa, T., and Matozaki, S. (1995). The SKM-1 leukemic cell line established from a patient with progression to myelomonocytic leukemia in myelodysplastic syndrome (MDS)-contribution to better understanding of MDS. *Leuk. Lymphoma* 17, 335–339. doi: 10.3109/10428199509056841
- Prébet, T., Gore, S. D., Esterni, B., Gardin, C., Itzykson, R., Thepot, S., et al. (2011). Outcome of high-risk myelodysplastic syndrome after azacitidine treatment failure. *J. Clin. Oncol.* 29, 3322–3327. doi: 10.1200/JCO.2011.35.8135
- Sallman, D. A., and List, A. (2019). The central role of inflammatory signaling in the pathogenesis of myelodysplastic syndromes. *Blood* 133, 1039–1048. doi: 10.1182/blood-2018-10-844654
- Schmidt, M., Fernandez de Mattos, S., van der Horst, A., Klompmaier, R., Kops, G. J., Lam, E. W., et al. (2002). Cell cycle inhibition by FoxO forkhead transcription factors involves downregulation of Cyclin D. *Mol. Cell Biol.* 22, 7842–7852. doi: 10.1128/mcb.22.22.7842-7852.2002
- Seelan, R. S., Mukhopadhyay, P., Pisano, M. M., and Greene, R. M. (2018). Effects of 5-Aza-2'-deoxycytidine (decitabine) on gene expression. *Drug Metab. Rev.* 50, 193–207. doi: 10.1080/03602532.2018.1437446
- Serena, D. M., Chiara, M., Giulia, A., Tania, R., Roberta, N., Martina, G., et al. (2018). Immunosuppressive Treg cells acquire the phenotype of effector-T cells in chronic lymphocytic leukemia patients. *J. Transl. Med.* 16:172. doi: 10.1186/s12967-018-1545-0
- Shi, F., Li, T., Liu, Z., Qu, K., Shi, C., Li, Y., et al. (2018). FOXO1: another avenue for treating digestive malignancy? *Semin. Cancer Biol.* 50, 124–131. doi: 10.1016/j.semcancer.2017.09.009
- Steensma, D. P. (2018). Myelodysplastic syndromes current treatment algorithm 2018. *Blood Cancer J.* 8:47. doi: 10.1038/s41408-018-0085-4
- Sykes, S. M., Lane, S. W., Bullinger, L., Kalaitzidis, D., Yusuf, R., Saez, B., et al. (2011). AKT/FOXO signaling enforces reversible differentiation blockade in myeloid leukemias. *Cell* 146, 697–708. doi: 10.1016/j.cell.2011.07.032
- Tirosh, I., Izar, B., Prakadan, S. M., Wadsworth, M. H. II, Treacy, D., Trombetta, J. J., et al. (2016). Dissecting the multicellular ecosystem of metastatic melanoma by single-cell RNA-seq. *Science* 352, 189–196. doi: 10.1126/science.aad0501
- Tohyama, K., Tohyama, Y., Nakayama, T., Ueda, T., Nakamura, T., and Yoshida, Y. (1995). A novel factor-dependent human myelodysplastic cell line, MDS92, contains haemopoietic cells of several lineages. *Br. J. Haematol.* 91, 795–799. doi: 10.1111/j.1365-2141.1995.tb05391.x
- Tohyama, K., Tsutani, H., Ueda, T., Nakamura, T., and Yoshida, Y. (1994). Establishment and characterization of a novel myeloid cell line from the bone marrow of a patient with the myelodysplastic syndrome. *Br. J. Haematol.* 87, 235–242. doi: 10.1111/j.1365-2141.1994.tb04904.x
- Ushmorov, A., and Wirth, T. (2018). FOXO in B-cell lymphopoiesis and B cell neoplasia. *Semin. Cancer Biol.* 50, 132–141. doi: 10.1016/j.semcancer.2017.07.008
- Wolff, F., Leisch, M., Greil, R., Risch, A., and Pleyer, L. (2017). The double-edged sword of (re)expression of genes by hypomethylating agents: from viral mimicry to exploitation as priming agents for targeted immune checkpoint modulation. *Cell Commun. Signal.* 15:13. doi: 10.1186/s12964-017-0168-z
- Xing, Y. Q., Li, A., Yang, Y., Li, X. X., Zhang, L. N., and Guo, H. C. (2018). The regulation of FOXO1 and its role in disease progression. *Life Sci.* 193, 124–131. doi: 10.1016/j.lfs.2017.11.030
- Xu, F., He, Q., Li, X., Chang, C. K., Wu, L. Y., Zhang, Z., et al. (2014). Rigosertib as a selective anti-tumor agent can ameliorate multiple dysregulated signaling transduction pathways in high-grade myelodysplastic syndrome. *Sci. Rep.* 4:7310. doi: 10.1038/srep07310
- Zeidan, A. M., Shallis, R. M., Wang, R., Davidoff, A., and Ma, X. (2019). Epidemiology of myelodysplastic syndromes: why characterizing the beast is a prerequisite to taming it. *Blood Rev.* 34, 1–15.
- Zeng, W., Dai, H., Yan, M., Cai, X., Luo, H., Ke, M., et al. (2017). Decitabine-induced changes in human myelodysplastic syndrome cell line SKM-1 are

- mediated by FOXO3A activation. *J. Immunol. Res.* 2017:4302320. doi: 10.1155/2017/4302320
- Zhang, Z., Chang, C. K., He, Q., Guo, J., Tao, Y., Wu, L. Y., et al. (2017a). Increased PD-1/STAT1 ratio may account for the survival benefit in decitabine therapy for lower risk myelodysplastic syndrome. *Leuk. Lymphoma* 58, 969–978. doi: 10.1080/10428194
- Zhang, Z., He, Q., Tao, Y., Guo, J., Xu, F., Wu, L. Y., et al. (2017b). Decitabine treatment sensitizes tumor cells to T-cell-mediated cytotoxicity in patients with myelodysplastic syndromes. *Am. J. Transl. Res.* 9, 454–465.

Conflict of Interest: The authors declare that the research was conducted in the absence of any commercial or financial relationships that could be construed as a potential conflict of interest.

Copyright © 2021 Zhang, Jia, Xu, Song, Shi, Guo and Chang. This is an open-access article distributed under the terms of the Creative Commons Attribution License (CC BY). The use, distribution or reproduction in other forums is permitted, provided the original author(s) and the copyright owner(s) are credited and that the original publication in this journal is cited, in accordance with accepted academic practice. No use, distribution or reproduction is permitted which does not comply with these terms.



Circular RNA_PDHX Promotes the Proliferation and Invasion of Prostate Cancer by Sponging MiR-378a-3p

Yuanshen Mao[†], Wenfeng Li[†], Bao Hua, Xin Gu, Weixin Pan, Qi Chen, Bin Xu*, Chao Lu* and Zhong Wang*

Department of Urology, Shanghai Ninth People's Hospital, Shanghai Jiao Tong University School of Medicine, Shanghai, China

OPEN ACCESS

Edited by:

Jing Zhang,
Shanghai Jiao Tong University, China

Reviewed by:

Jinshui Zhu,
Shanghai Jiao Tong University, China
Jingmin Ou,
Shanghai Jiao Tong University, China
Xinxin Yan,
Tianjin Medical University, China

*Correspondence:

Bin Xu
chxb2004@126.com
Zhong Wang
zhongwang2010@sina.com
Chao Lu
luchao20190331@163.com

[†] These authors have contributed
equally to this work

Specialty section:

This article was submitted to
Epigenomics and Epigenetics,
a section of the journal
Frontiers in Cell and Developmental
Biology

Received: 04 September 2020

Accepted: 02 December 2020

Published: 28 January 2021

Citation:

Mao Y, Li W, Hua B, Gu X, Pan W,
Chen Q, Xu B, Lu C and Wang Z
(2021) Circular RNA_PDHX Promotes
the Proliferation and Invasion
of Prostate Cancer by Sponging
MiR-378a-3p.
Front. Cell Dev. Biol. 8:602707.
doi: 10.3389/fcell.2020.602707

The dysregulation of circular RNAs (circRNAs) is implicated in the pathogenesis of prostate cancer (PCa). However, the underlying mechanisms by which hsa_circ_0003768 (circPDHX) contributes to PCa remain elusive. The differentially expressed circRNAs between PCa and normal tissues were identified by Gene Expression Omnibus dataset. The association of circPDHX and miR-378a-3p expression with the clinicopathological parameters and prognosis in patients with PCa was analyzed by fluorescence *in situ* hybridization and The Cancer Genome Atlas dataset. 3-(4,5-Dimethylthiazol-2-yl)-2,5-diphenyltetrazolium bromide (MTT) and Transwell assays as well as a xenograft tumor model were used to assess the role of circPDHX in PCa cells. circPDHX-specific binding with miR-378a-3p was validated by bioinformatic analysis, luciferase gene reporter, and RNA immunoprecipitation assays. As a result, we found that increased expression of circPDHX was associated with Gleason score ($P = 0.001$) and pathogenic T stage ($P = 0.01$) and acted as an independent prognostic factor of poor survival ($P = 0.036$) in patients with PCa. Knockdown of circPDHX inhibited cell proliferation and invasion *in vitro* and *in vivo*, but ectopic expression of circPDHX reversed these effects. Furthermore, circPDHX could sponge miR-378a-3p to promote cell proliferation, but miR-378a-3p counteracted circPDHX-induced cell proliferation and insulin-like growth factor 1 receptor (IGF1R) expression in PCa cells. In conclusion, our findings demonstrated that circPDHX facilitated the proliferation and invasion of PCa cells by sponging miR-378a-3p.

Keywords: prostate cancer, circPDHX, miR-378a-3p, IGF1R, growth, invasion

INTRODUCTION

The morbidity of prostate cancer (PCa) ranks the first place, and it is a second cause of cancer-related mortality in male cancers in the United States (Siegel et al., 2017). Although more than 90% patients with PCa can be cured after surgical resection with a higher 5-year survival rate (Vis et al., 2006), the advanced cases still harbor an unfavorable prognosis due to the tumor dissemination and metastasis (Huang E. Y. et al., 2018). The aberrant expression of non-coding RNAs is associated with the pathogenesis of PCa (Shukla et al., 2016; Dong et al., 2018;

Huang W. et al., 2018). Therefore, identification of novel biomarkers is urgently needed to increase the early detection of PCa.

Circular RNAa (circRNAs) as a new subgroup of non-coding RNAs (ncRNAs) have covalently closed loop structures and more tissue stability when compared with the corresponding linear RNAs due to their resistance to RNase R (Qu et al., 2017). Increasing data indicate that aberrant expression of circRNAs is involved in the progression of PCa. Low expression of circ-ITCH is associated with pathologic T stage, lymph node metastasis, and poor survival in patients with PCa (Huang E. et al., 2019). Upregulation of circSMARCA5, hsa_circ_102004, and hsa_circ_0004870 favors the proliferation and enzalutamide resistance in PCa cells (Kong et al., 2017; Greene et al., 2019; Si-Tu et al., 2019), but hsa_circ_0001206 inhibits the proliferation and invasion of PCa cells (Song et al., 2019). Moreover, circFOXO3 acts as an oncogene by sponging miR-29a-3p (Kong et al., 2020), while circUCK2 functions as a tumor suppressor in PCa by sponging miR-767-5p (Xiang et al., 2019). Until now, the functional role of hsa_circ_0003768 in PCa remains undocumented.

MicroRNAs (miRNAs) as another subtype of ncRNAs act a crucial role in the tumorigenesis of PCa (Chen L. et al., 2019; Huang S. et al., 2019; Zhao et al., 2019), of which miR-378a-3p is initiated to act as a tumor suppressor in rhabdomyosarcoma (Megiorni et al., 2014) and facilitates tamoxifen sensitivity in breast cancer by targeting GOLT1A (Ikeda et al., 2015). In addition, miR-378a-3p represses myoblasts growth in skeletal muscle development by targeting HDAC4 (Wei et al., 2016) and the activation of hepatic stellate cells by targeting Gli3 (Hyun et al., 2016). The serum levels of miR-378-3p are decreased in PCa (Nguyen et al., 2013) and may be used as a therapeutic strategy for PCa.

Herein, we identified a differentially expressed hsa_circ_0003768 (circPDHX) between PCa and normal tissue samples and found that elevated expression of circPDHX was associated with Gleason score, pathogenic T stage, and poor survival in patients with PCa; circPDHX contributed to the PCa tumorigenesis by sponging miR-378a-3p and might provide a potential biomarker for PCa.

MATERIALS AND METHODS

Clinical Samples

The differentially expressed circRNAs between PCa and normal tissues were downloaded from the Gene Expression Omnibus (GEO) dataset¹. The tissue microarray (No. XT16-016) including 75 paired PCa samples was purchased from Alenabio Biotechnology (Xi'an, China). The clinicopathological data of PCa patients as well as the expression levels of miR-98-5p, miR-99a-5p, miR-99b-5p, miR-100-5p, miR-182-5p, miR-378a-3p, miR-494-3p, let-7a-5p, let-7b-5p, let-7c-5p, let-7d-5p, let-7e-5p, let-7f-5p, let-7g-5p, let-7i-5p, and insulin-like growth factor 1 receptor (IGF1R) were downloaded from The Cancer

Genome Atlas (TCGA) dataset². The patients did not receive any chemotherapy, and the protocols were approved by the Ethics Committee of Shanghai Ninth People's Hospital.

Fluorescence *in situ* Hybridization

The probe sequence for circPDHX (5'-TGGCTGTGGCAACAGATAAA-3') and biotin-labeled probe sequences for miR-378a-3p (5'-ACACAGGACCTGGAGTCAGGAG-3') were used to analyze the expression of circPDHX and miR-378a-3p in PCa tissue samples. The detailed description of fluorescence *in situ* hybridization (FISH) analysis was conducted as previously reported (Dong et al., 2018).

Plasmid Construction

The wild-type (WT) or mutant (Mut) 3' untranslated region (UTR) vectors of circPDHX and IGF1R, containing miR-378a-3p binding sites, were constructed by annealing double-stranded DNA and inserting it into the pmirGLO vector at the *Bam*HI and *Eco*RI sites. Lentivirus mediated si-circPDHX (5'-GACTCTGTAAAGGTTGAAGAA-3') or its negative control (si-NC) was constructed by Genechem (Shanghai, China), and circPDHX plasmids as well as miR-378a-3p mimic or inhibitor were offered by GenePharma (Shanghai, China).

Cell Culture

PCa cell lines (PC3 and 22RV1) used in these studies were provided by the Institute of Chemistry and Cell Biology (Shanghai, China) and were cultured in Dulbecco's modified Eagle's medium (DMEM) medium supplemented with 10% heat-inactivated fetal bovine serum (FBS) in a humidified atmosphere containing 5% CO₂ at 37°C.

Quantitative Real-Time PCR

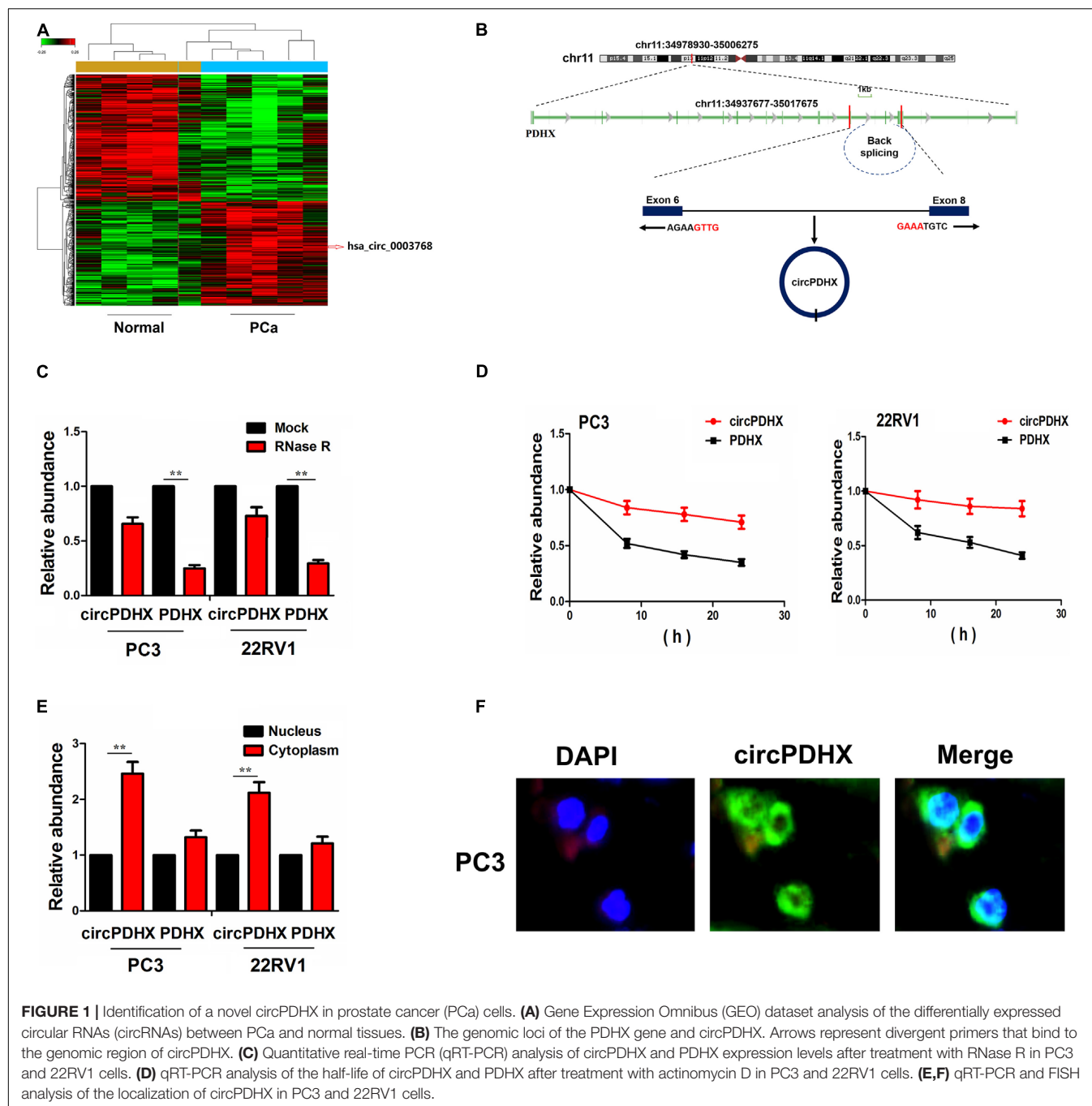
RNA was isolated from PCa cells using Trizol reagent (Invitrogen). One Step SYBR® PrimeScript™ PLUS RT-PCR Kit (TaKaRa, Beijing, China) was used to examine the expression of circPDHX and IGF1R. TaqMan® MicroRNA Reverse Transcription Kit and TaqMan Universal Master Mix II (Thermo Fisher Scientific, Runcorn, United Kingdom) were used to measure miR-378a-3p expression. U6 or β -actin was used as an internal parameter. The $2^{-\Delta\Delta CT}$ equation was used to quantify the data in triplicate. The primer sequences of circPDHX, miR-378a-3p, and IGF1R were indicated in **Supplementary Table 1**.

Western Blot Analysis

Prostate cancer cell lines were harvested, and protein was extracted using RNA immunoprecipitation assay (RIPA) lysis buffer (Beyotime) and protease inhibitor (Beyotime). Primary antibodies against IGF1R (Ab-1161, Signalway, Shanghai, China) and glyceraldehyde 3-phosphate dehydrogenase (GAPDH) (ab9485, Abcam) were diluted (1:1,000) and incubated overnight at 4°C. Secondary antibody of goat anti-rabbit

¹<https://www.ncbi.nlm.nih.gov/geo/>

²<http://xena.ucsc.edu/>



immunoglobulin G (IgG) (ab6721, Abcam, 1:10,000) was cultured for 1 h at room temperature. After rinsing, the polyvinylidene fluoride (PVDF) membrane of the antibodies was transferred onto the system. Captured signal was quantified by Image Lab Software 3.0 (Bio-Rad), and GAPDH was used as an internal parameter.

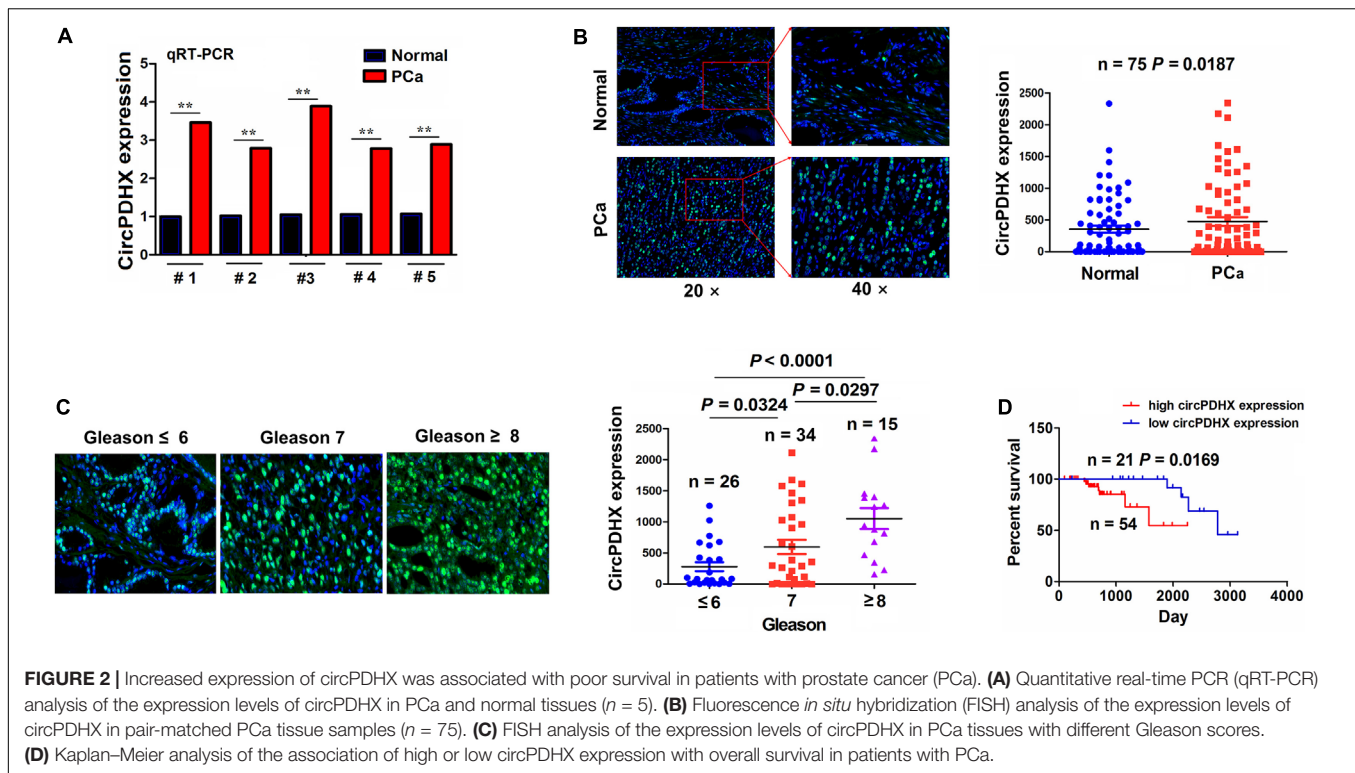
MTT and Transwell Assays

Cell viability and invasive potential were assessed by 3-(4,5-dimethylthiazol-2-yl)-2,5-diphenyltetrazolium bromide

(MTT) and Transwell assays according to the previous report (Dong et al., 2018).

Actinomycin D and RNase R Treatment

Transcription was prevented by the addition of 2 mg/ml actinomycin D, and dimethyl sulfoxide (DMSO) (Sigma-Aldrich, St. Louis, MO, United States) was used as the control group. Total RNA was incubated for 30 min at 37°C with 3 U/μg of RNase R (Epicentre Technologies, Madison, WI, United States).



Dual-Luciferase Reporter Assay

PCa cells were seeded into 24-well plates, and pmirGLO report vectors containing WT or Mut 3'UTR of circPDHX and IGF1R were cotransfected with miR-378a-3p mimic or inhibitor into PC3 and 22RV1 cell lines. After the transfection for 48 h, luciferase activities were detected with a dual-luciferase reporter system (Promega, Madison, WI, United States).

RNA Immunoprecipitation

RNA immunoprecipitation (RIP) assay was conducted using a Magna RIP RNA-Binding Protein Immunoprecipitation Kit (Millipore, Billerica, MA, United States) according to the manufacturer's instructions.

Animal Experiments

Six-week-old female immune-deficient nude mice (BALB/c-nu) were injected subcutaneously with 5×10^7 PC3 cells stably transfected with si-circPDHX or si-NC. Mice were monitored daily and developed a subcutaneous tumor. The tumor volume was detected every other day by using a formula: volume = length \times width²/2. This study was approved by Animal Ethics Committee of our hospital.

Statistical Analysis

Statistical analyses were conducted by SPSS 20.0 (IBM, SPSS, Chicago, IL, United States) and GraphPad Prism. Student's *t*-test or chi-square test was used to assess the statistical significance for comparisons of two groups. Pearson correlation analysis

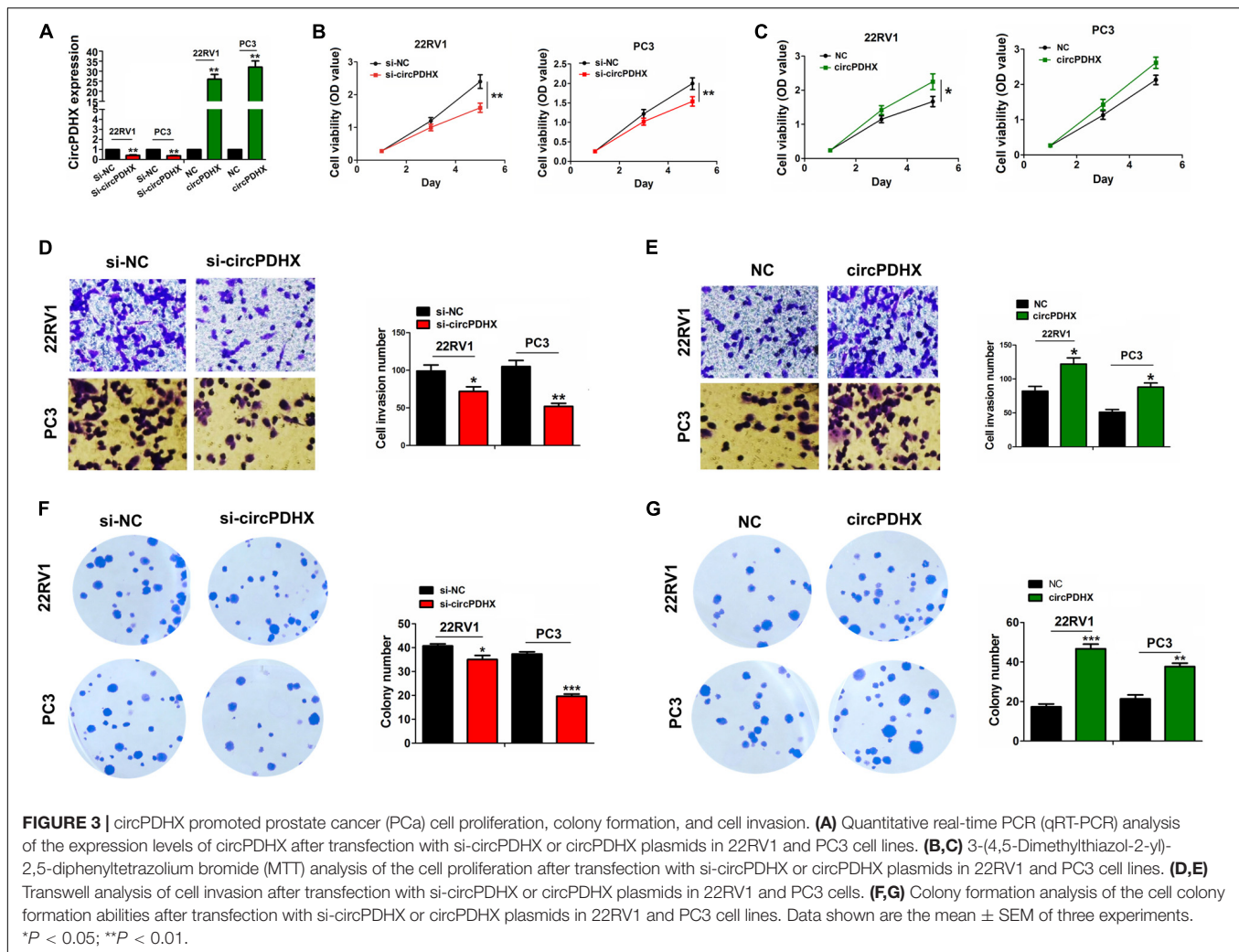
was used to analyze the correlations. Overall survival curve was analyzed with the Kaplan–Meier method and log-rank test. Univariate and multivariate analyses were implemented by a Cox proportional hazard regression model. $P < 0.05$ was considered statistical significance.

RESULTS

Identification of a Novel CircPDHX in PCa Cells

A microarray chip (GSE113124) was used to screen differentially expressed circRNAs between PCa and normal tissues. With the criteria of $P < 0.01$ and FC > 1.5 , 546 downregulated circRNAs and 432 upregulated circRNAs were identified in PCa tissue samples, of which hsa_circ_0003768 had a significantly increased expression in PCa tissues (FC = 2.63, $P = 0.0009$; **Figure 1A**).

We found that hsa_circ_0003768 (chr11:34978930-35006275) originated from exon 6, eight regions within the pyruvate dehydrogenase complex component X (PDHX) locus and is termed as circPDHX (**Figure 1B**). Compared with linear PDHX, circPDHX gave rise to a resistance to RNase R treatment in PC3 and 22RV1 cell lines, and circPDHX had a loop structure in PCa cells (**Figure 1C**). After PC3 and 22RV1 cell lines were treated by a transcription inhibitor actinomycin D, quantitative real-time PCR (qRT-PCR) analysis showed that the half-life of circPDHX reached more than 24 h, but that of PDHX was < 6 h in these two cells (**Figure 1D**). qRT-PCR and FISH analysis revealed that circPDHX was mainly localized in the cytoplasm of PCa cells (**Figures 1E,F**).



Elevated Expression of CircPDHX Was Associated With Poor Survival in Patients With PCa

The expression of circPDHX was examined in PCa tissues by qRT-PCR analysis, which indicated that circPDHX expression levels were increased in PCa tissue samples as compared with the pair-matched normal tissues ($P < 0.01$; **Figure 2A**). This result was further validated by FISH analysis in paired 75 PCa samples ($P = 0.0187$; **Figure 2B**). We then analyzed the association of circPDHX expression with Gleason scores in PCa and found that circPDHX expression levels were elevated gradually with increased Gleason scores ($P < 0.05$; **Figure 2C**).

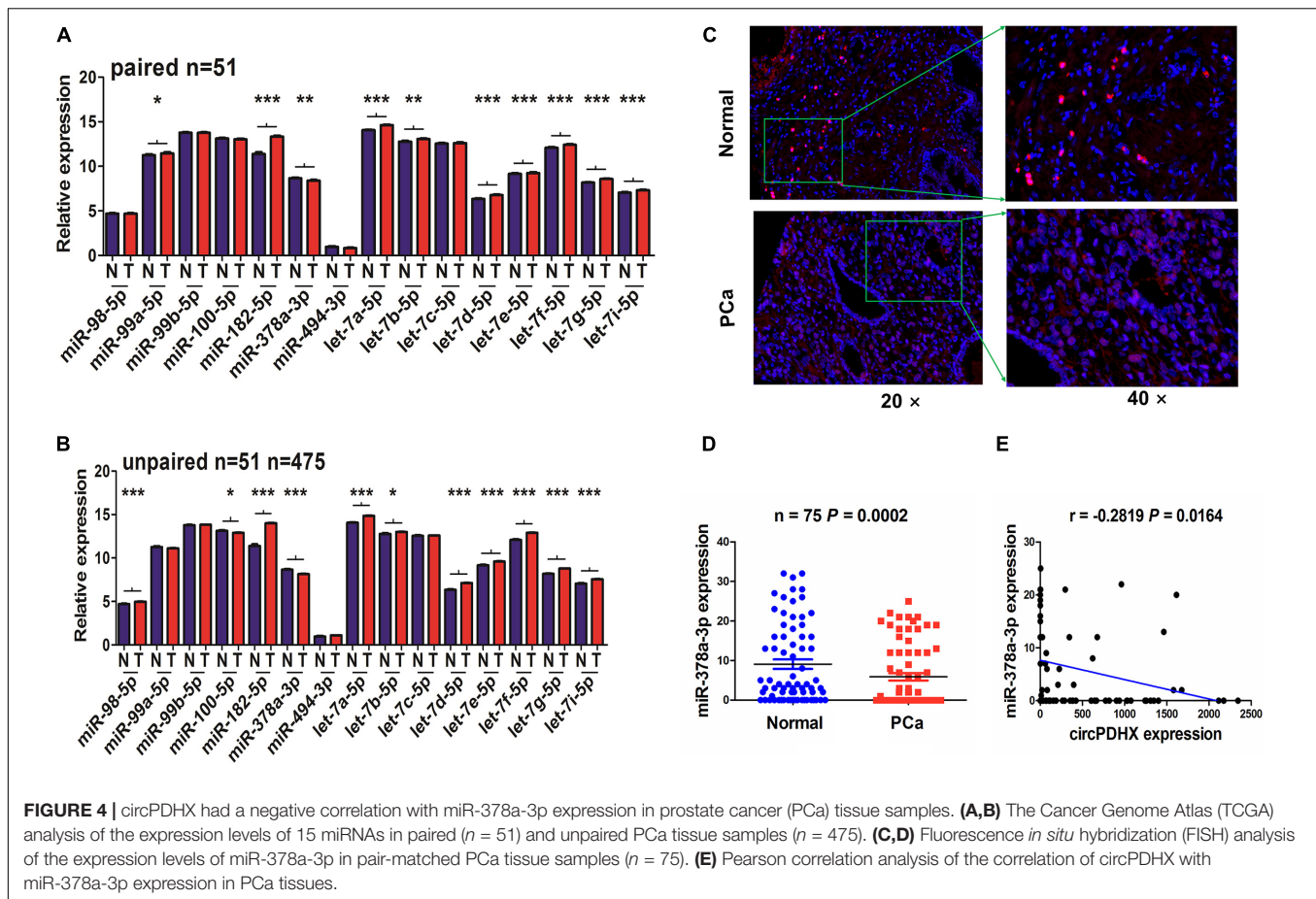
According to circPDHX expression levels, survival time, and status, cutoff value (495.56), area under curve (AUC) (0.64), sensitivity (80.0%), and specificity (58.7%) of circPDHX were achieved in patients with PCa (**Supplementary Figure 1**) by using a cutoff finder³. As indicated in **Supplementary Table 2**, the elevated expression of circPDHX was positively associated with

Gleason score ($P = 0.001$) and pathogenic T stage ($P = 0.01$) in patients with PCa. Kaplan–Meier analysis demonstrated that the patients with high circPDHX expression harbored a poorer survival as compared with those with low circPDHX expression ($P = 0.0169$; **Figure 2D**). Univariate and multivariate analyses unveiled that high circPDHX expression as well as higher Gleason score was an independent prognostic factor of poor survival in PCa patients ($P = 0.036$; **Supplementary Table 3**).

CircPDHX Promoted Proliferation, Colony Formation, and Invasion of PCa Cells

Elevated expression of circPDHX in PCa tissues indicated it as a tumor-promoting factor. To confirm this hypothesis, we assessed the functional role of circPDHX in PCa cells. The silencing efficiency of si-circPDHX or overexpression efficiency of circPDHX plasmids was confirmed in 22RV1 and PC3 cells by qRT-PCR analysis (**Figure 3A**). Consequently, we found that knockdown of circPDHX repressed cell viability (**Figure 3B**), invasive potential (**Figure 3D**), and

³<http://molpath.charite.de/cutoff/load.jsp>



colony formation (Figure 3F) in 22RV1 and PC3 cells, but restored circPDHX expression reversed these effects (Figures 3C,E,G).

CircPDHX Was Negatively Associated With MiR-378a-3p Expression in PCa Tissues

To elucidate the underlying mechanisms of circPDHX in PCa cells, we identified 15 miRNAs that may have the potential to bind with circPDHX by using Circular RNA Interactome⁴ and found that only miR-378a-3p had a decreased expression in paired ($n = 51$, Figure 4A) and unpaired PCa samples ($n = 475$, Figure 4B). Reduced expression of miR-378a-3p was further validated by FISH analysis in PCa samples ($n = 75$, $P = 0.0002$; Figures 4C,D). Pearson correlation analysis indicated that miR-378a-3p possessed a negative correlation with circPDHX expression in PCa samples ($r = -0.2819$, $P = 0.0164$; Figure 4E).

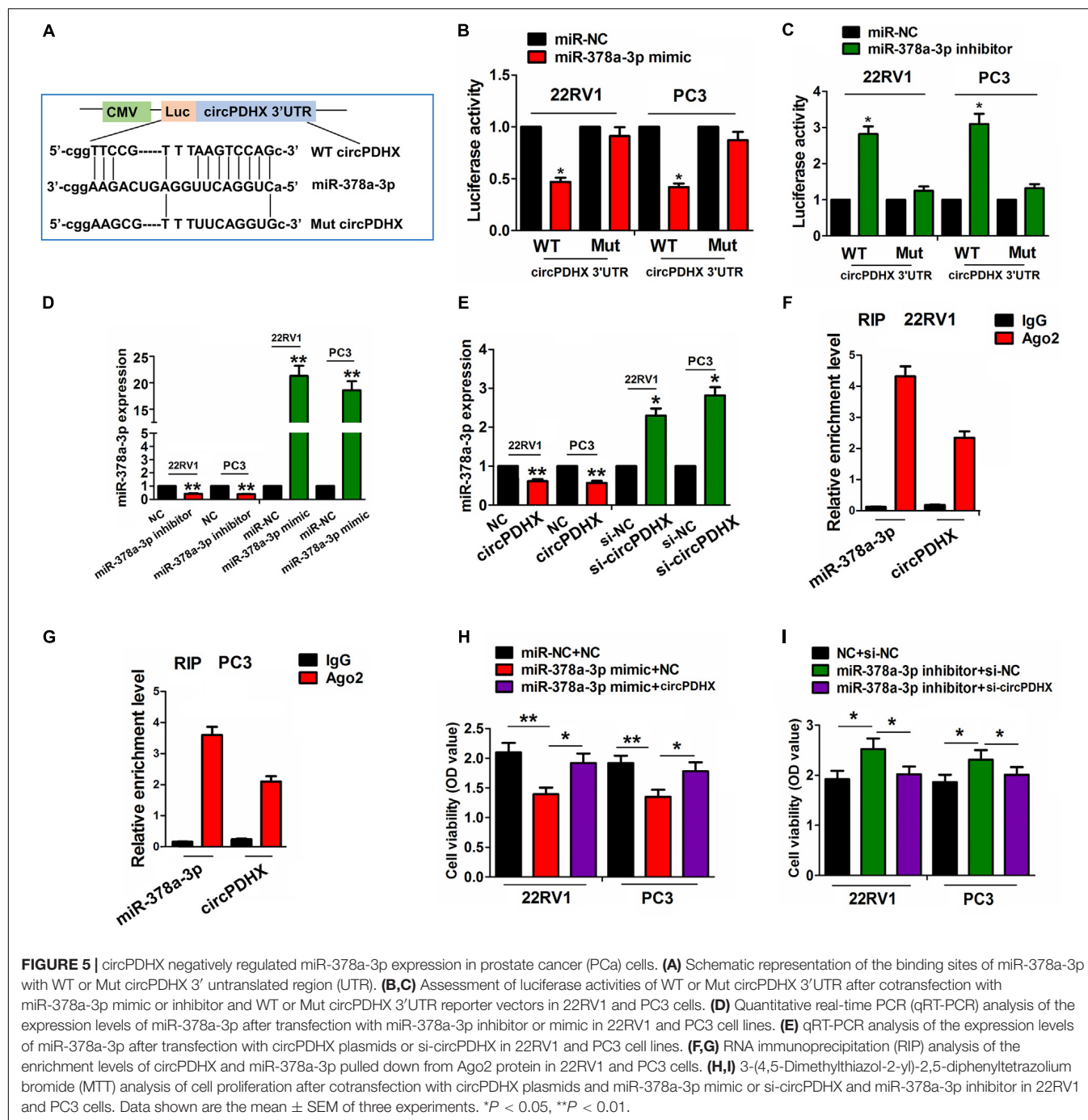
We then found that low expression of miR-378a-3p was associated with higher Gleason score ($P = 0.041$) and pathological N stage ($P = 0.036$) in PCa patients (Supplementary Table 4). However, the patients with low miR-378a-3p expression had

no difference in poor survival and tumor recurrence as compared with those with high miR-378a-3p expression (Supplementary Figure 2).

CircPDHX Could Sponge MiR-378a-3p in PCa Cells

The binding sites of miR-378a-3p with WT or Mut circPDHX 3'UTR are indicated in Figure 5A. To confirm whether circPDHX could bind with miR-378a-3p, we cotransfected 22RV1 and PC3 cells with WT or Mut circPDHX 3'UTR reporter vectors and the miR-378a-3p mimic or inhibitor and found that miR-378a-3p mimic reduced the luciferase activities of WT circPDHX 3'UTR in 22RV1 and PC3 cell lines (Figure 5B), while the miR-378a-3p inhibitor increased their luciferase activities (Figure 5C). However, the miR-378a-3p mimic or inhibitor exerted no effects on those of Mut circPDHX 3'UTR as compared with the control group (Figures 5B,C). Further investigations showed that the knockdown or overexpression efficiency of the miR-378a-3p inhibitor or mimic in 22RV1 and PC3 cell lines was determined by qRT-PCR analysis (Figure 5D), but the miR-378a-3p mimic or inhibitor had no effect on circPDHX expression levels (Supplementary Figure 3). It was noted that the restored expression of circPDHX decreased the expression of miR-378a-3p, while silencing circPDHX increased its expression

⁴<https://circinteractome.nia.nih.gov/index.html>

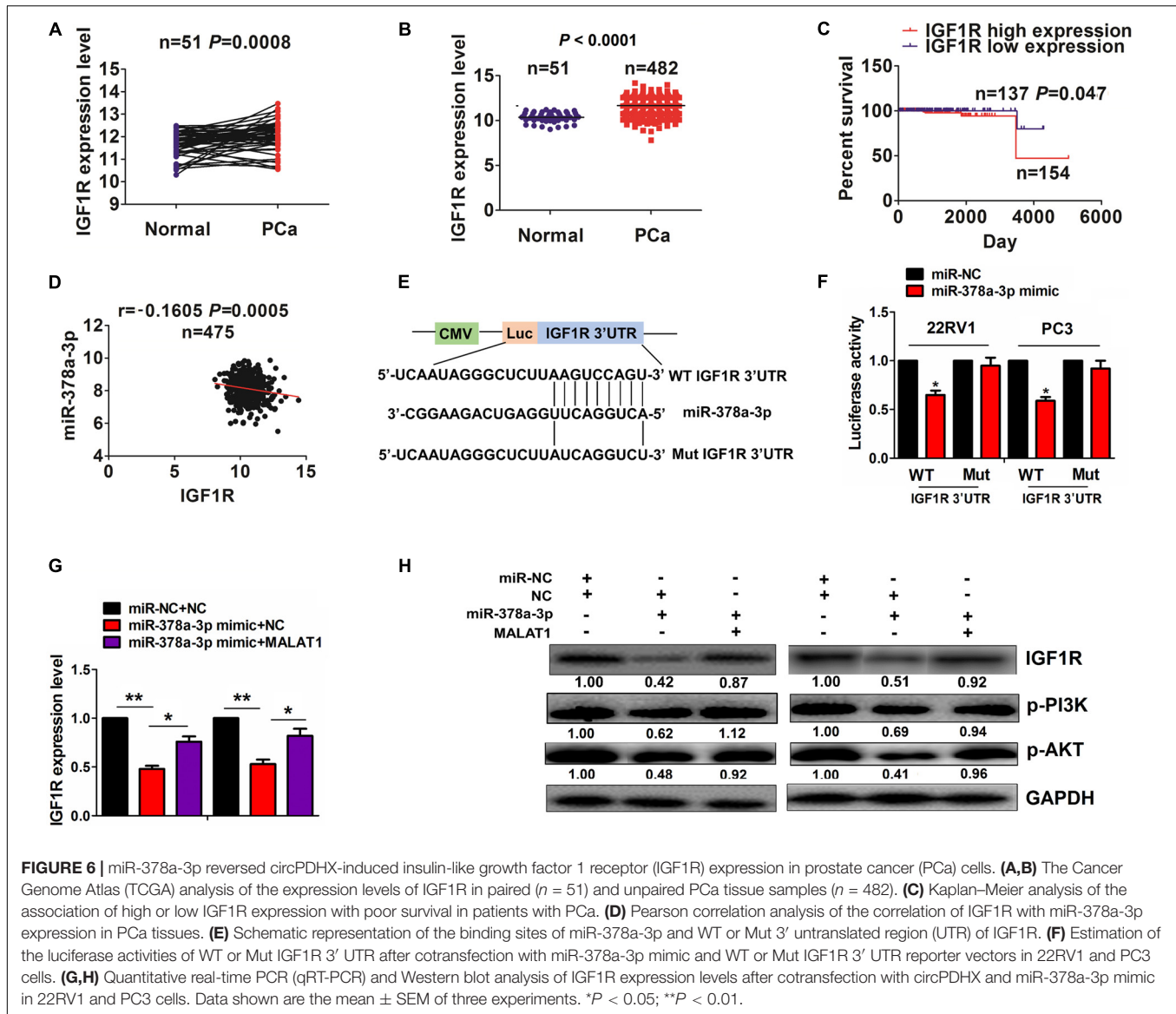


levels in these two cell lines (Figure 5E). Furthermore, RIP assay was conducted for Ago2 protein in 22RV1 and PC3 cells, and the expression of endogenous circPDHX and miR-378a-3p pulled down from Ago2-expressed 22RV1 and PC3 cells, indicated by qRT-PCR analysis, was enriched in Ago2 pellet in comparison with the input control (Figures 5F,G). After cotransfection with circPDHX plasmids and miR-378a-3p mimic or si-circPDHX and miR-378a-3p inhibitor in 22RV1 and PC3 cells, we found that the miR-378a-3p mimic inhibited cell viability and reversed circPDHX-induced cell proliferation

(Figure 5H), while the miR-378a-3p inhibitor showed the opposite effects (Figure 5I).

MiR-378a-3p Reversed CircPDHX-Induced IGF1R Expression in PCa Cells

We identified the targets of miR-378a-3p and found that miR-378a-3p might have the greatest potential to bind with 3'UTR of IGF1R by using the starBase v2.0 prediction tool



(⁵, **Supplementary Table 5**). TCGA cohort showed that IGF1R expression was increased in paired ($n = 51$, $P = 0.0008$; **Figure 6A**) and unpaired PCa samples ($n = 482$, $P < 0.0001$; **Figure 6B**). Then, high expression of IGF1R was associated with pathological T stage in PCa patients ($P = 0.034$, **Supplementary Table 6**), and the patients with high IGF1R expression harbored a poorer survival ($P = 0.047$, **Figure 6C**) as compared with those with low IGF1R expression. However, univariate and multivariate analyses uncovered that high IGF1R expression was not an independent prognostic factor of poor survival in PCa patients (**Supplementary Table 7**).

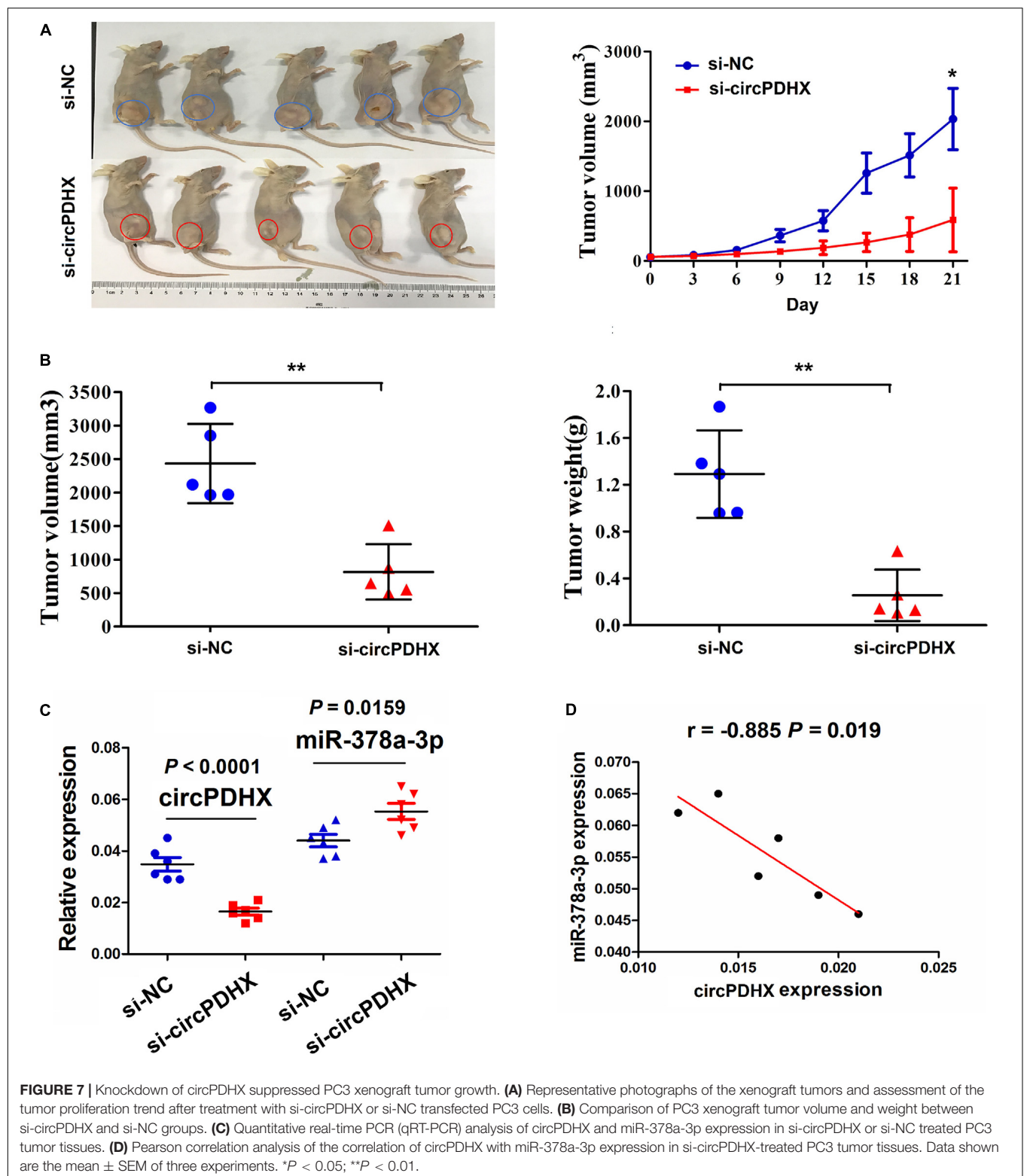
Pearson correlation analysis indicated that miR-378a-3p had a negative correlation with IGF1R expression in PCa tissues ($r = -0.1605$, $P = 0.0005$; **Figure 6D**). The binding sites of miR-378a-3p with WT or Mut 3' UTR of IGF1R were indicated

in **Figure 6E**. To confirm whether miR-378a-3p could bind with 3' UTR of IGF1R, we cotransfected 22RV1 and PC3 cell lines with WT or Mut IGF1R 3' UTR reporter vectors and miR-378a-3p mimic and found that miR-378a-3p mimic reduced the luciferase activities of WT IGF1R 3' UTR in these two cell lines but had no effects on those of Mut IGF1R 3' UTR as compared with the miR-NC group (**Figure 6F**). qRT-PCR and Western blot analysis indicated that miR-378a-3p inhibited the activation of IGF1R/PI3K/AKT signaling and reversed circPDHX-induced signaling activation in 22RV1 and PC3 cell lines (**Figures 6G,H**).

Knockdown of CircPDHX Inhibited the Tumorigenesis of PCa *in vivo*

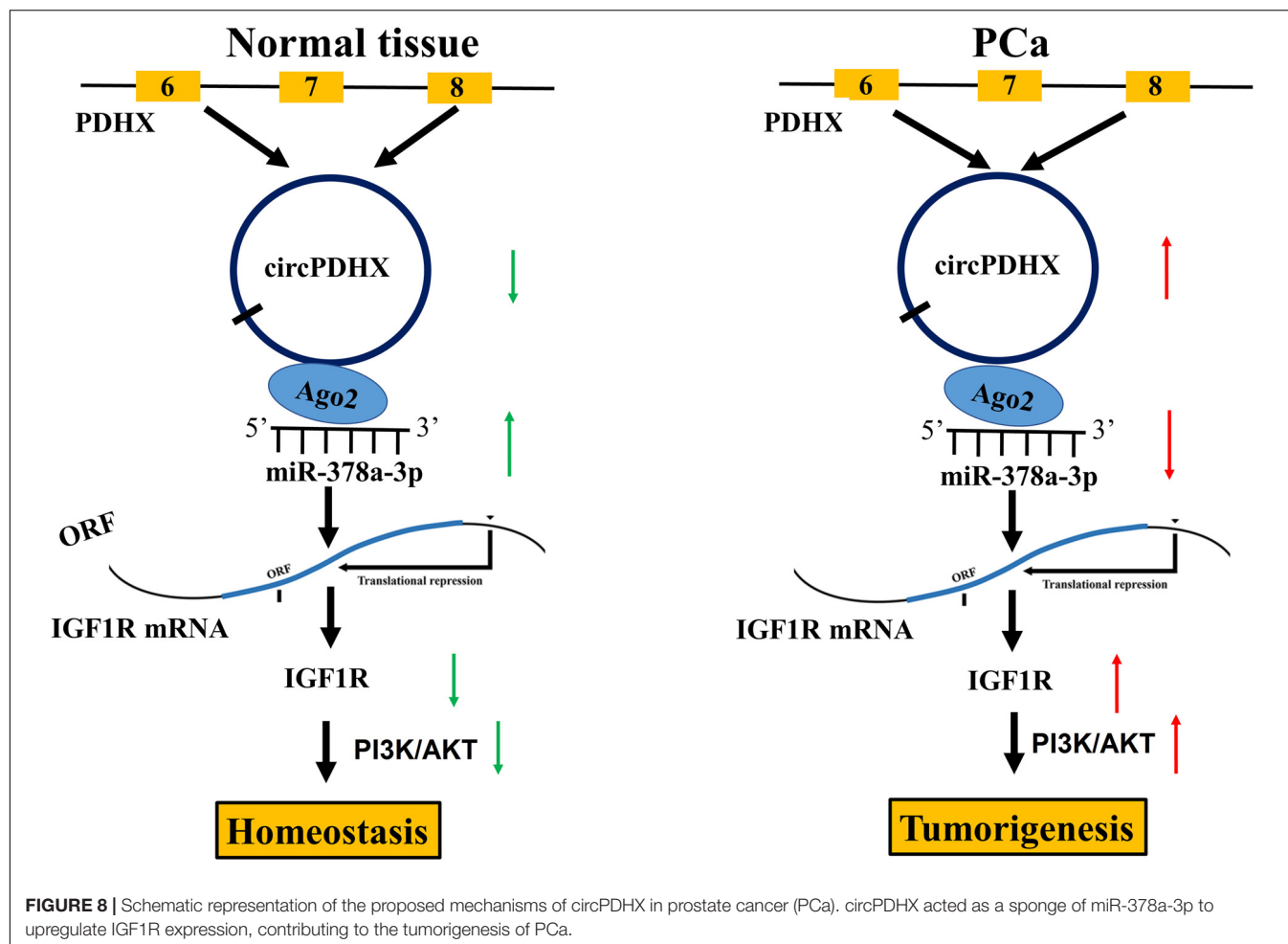
To confirm the effects of circPDHX on PCa tumor growth *in vivo*, a xenograft tumor model was constructed after

⁵<http://starbase.sysu.edu.cn/starbase2/index.php>



subcutaneous inoculation with si-circPDHX stably transfected PC3 cells. During the growth period, the length and weight of PCa tumors were measured. We found that the proliferative capabilities of PCa tumors were impeded by downregulation

of circPDHX in comparison with si-NC group (Figure 7A). After PCa tumor tissues were harvested, the average tumor volume and weight were smaller in the si-circPDHX group than those in the si-NC group (Figure 7B). qRT-PCR analysis



indicated that circPDHX expression was markedly reduced, while miR-378a-3p expression was increased in the si-circPDHX group as compared with the si-NC group (Figure 7C). Pearson correlation analysis showed that circPDHX had a negative correlation with miR-378a-3p expression in si-circPDHX group (Figure 7D).

DISCUSSION

circRNAs as a novel ncRNA have been implicated in the prognosis and progression of multiple malignancies including PCa (Wang et al., 2018; Zhang et al., 2019). The upregulation of circ-ITCH is associated with distant metastasis and poor prognosis in patients with PCa (Huang E. et al., 2019). Herein, we identified a differentially expressed circPDHX and found that high expression of circPDHX was associated with Gleason score and pathogenic T stage and acted as an independent prognostic factor of poor survival in PCa patients.

Previous studies showed that circRNAs can act as oncogenic factors (Kong et al., 2017; Si-Tu et al., 2019) or tumor suppressors in PCa (Song et al., 2019). Herein, we assess the functional role of circPDHX in PCa cells and found

that silencing circPDHX repressed the cell viability, colony formation, and cell invasion *in vitro* and *in vivo*, but ectopic expression of circPDHX indicated the tumor-promoting effects. Our results indicated that circPDHX might act as an oncogene in PCa.

Increasing investigations demonstrated that circRNAs can act as miRNA sponges to participate in cancer regulation (Chen Y. et al., 2019). circHIPK3 and circZNF609 enhance the proliferation and invasion of PCa by sponging miR-193a-3p/-338-3p or miR-186-5p (Cai et al., 2019; Chen D. et al., 2019; Jin et al., 2019), whereas circRNA17 and circUCK2 suppress the progression of PCa by sponging miR-181c-5p or miR-767-5p (Wu et al., 2019; Xiang et al., 2019). Herein, we found that circPDHX could bind with Ago2-miR-378a-3p complex and negatively regulate miR-378a-3p expression in PCa cells. Likewise, hsa_circ_0007059 suppresses cell proliferation and epithelial-mesenchymal transition in lung cancer by sponging miR-378a-3p (Gao et al., 2019). These studies indicated that circPDHX might act as a sponge of miR-378a-3p to promote PCa progression.

Some studies have shown that miR-378a-3p is downregulated in colorectal cancer (CRC), and its low expression indicates poor survival in patients with CRC (Li et al., 2014). It also

restrains melanoma growth via targeting PARVA (Velazquez-Torres et al., 2018) and acts as a chemosensitizer in ovarian cancer (Xu et al., 2018). In accordance, we found that low expression of miR-378a-3p was associated with Gleason score and pathogenic N stage in patients with PCa. IGF1R was further validated as a direct target of miR-378a-3p in PCa cells and indicated a poor survival in patients with PCa. In addition, miR-378a-3p displayed a negative correlation with circPDHX expression and attenuated circPDHX-induced cell proliferation and IGF1R expression in PCa cells. Our results suggested that circPDHX might act as a sponge of miR-378a-3p to upregulate IGF1R expression, contributing to the tumorigenesis of PCa (Figure 8).

Taken together, the increased expression of circPDHX was associated with Gleason score and pathogenic T stage and acted as an independent prognostic factor of poor survival in patients with PCa. circPDHX facilitated the tumorigenesis of PCa by sponging miR-378a-3p. This study might offer a potential biomarker for the detection of PCa.

DATA AVAILABILITY STATEMENT

The original contributions presented in the study are included in the article/Supplementary Material, further inquiries can be directed to the corresponding author/s.

REFERENCES

- Cai, C., Zhi, Y., Wang, K., Zhang, P., Ji, Z., Xie, C., et al. (2019). CircHIPK3 overexpression accelerates the proliferation and invasion of prostate cancer cells through regulating miRNA-338-3p. *Oncol. Targets Ther.* 12, 3363–3372. doi: 10.2147/OTT.S196931
- Chen, D., Lu, X., Yang, F., and Xing, N. (2019). Circular RNA circHIPK3 promotes cell proliferation and invasion of prostate cancer by sponging miR-193a-3p and regulating MCL1 expression. *Cancer Manag. Res.* 11, 1415–1423. doi: 10.2147/CMAR.S190669
- Chen, L., Hu, W., Li, G., Guo, Y., Wan, Z., and Yu, J. (2019). Inhibition of miR-9-5p suppresses prostate cancer progress by targeting StarD13. *Cell Mol. Biol. Lett.* 24:20. doi: 10.1186/s11658-019-0145-1
- Chen, Y., Yang, F., Fang, E., Xiao, W., Mei, H., Li, H., et al. (2019). Circular RNA circAGO2 drives cancer progression through facilitating HuR-repressed functions of AGO2-miRNA complexes. *Cell Death Differ.* 26, 1346–1364. doi: 10.1038/s41418-018-0220-6
- Dong, L., Ding, H., Li, Y., Xue, D., and Liu, Y. (2018). LncRNA TINCR is associated with clinical progression and serves as tumor suppressive role in prostate cancer. *Cancer Manag. Res.* 10, 2799–2807. doi: 10.2147/CMAR.S170526
- Gao, S., Yu, Y., Liu, L., Meng, J., and Li, G. (2019). Circular RNA hsa_circ_0007059 restrains proliferation and epithelial-mesenchymal transition in lung cancer cells via inhibiting microRNA-378. *Life Sci.* 233:116692. doi: 10.1016/j.lfs.2019.116692
- Greene, J., Baird, A. M., Casey, O., Brady, L., Blackshields, G., Lim, M., et al. (2019). Circular RNAs are differentially expressed in prostate cancer and are potentially associated with resistance to enzalutamide. *Sci. Rep.* 9:10739. doi: 10.1038/s41598-019-47189-2
- Huang, E., Chen, X., and Yuan, Y. (2019). Downregulated circular RNA itchy E3 ubiquitin protein ligase correlates with advanced pathologic T stage, high lymph node metastasis risk and poor survivals in prostate cancer patients. *Cancer Biomark.* 26, 41–50. doi: 10.3233/CBM-182111

ETHICS STATEMENT

The studies involving human participants were reviewed and approved by the protocols were approved by the Ethics Committee of Shanghai Ninth People's Hospital. The patients/participants provided their written informed consent to participate in this study. The animal study was reviewed and approved by this study was approved by the Animal Ethics Committee of Shanghai Ninth People's Hospital.

AUTHOR CONTRIBUTIONS

BX, CL, and ZW designed this study. YM and WL performed the experiments and wrote the manuscript. BX searched the literature. WP and QC collected the clinical samples. BH and XG assisted in conducting the experiments. CL revised the manuscript, and all authors read and approved the final manuscript. All authors contributed to the article and approved the submitted version.

SUPPLEMENTARY MATERIAL

The Supplementary Material for this article can be found online at: <https://www.frontiersin.org/articles/10.3389/fcell.2020.602707/full#supplementary-material>

- Huang, E. Y., Chang, Y. J., Huang, S. P., Lin, V. C., Yu, C. C., Huang, C. Y., et al. (2018). A common regulatory variant in SLC35B4 influences the recurrence and survival of prostate cancer. *J. Cell Mol. Med.* 22, 3661–3670. doi: 10.1111/jcmm.13649
- Huang, S., Zou, C., Tang, Y., Wa, Q., Peng, X., Chen, X., et al. (2019). miR-582-3p and miR-582-5p suppress prostate cancer metastasis to bone by repressing TGF- β signaling. *Mol. Ther. Nucleic Acids* 16, 91–104. doi: 10.1016/j.omtn.2019.01.004
- Huang, W., Su, X., Yan, W., Kong, Z., Wang, D., Huang, Y., et al. (2018). Overexpression of AR-regulated lncRNA TMPO-AS1 correlates with tumor progression and poor prognosis in prostate cancer. *Prostate* 78, 1248–1261. doi: 10.1002/pros.23700
- Hyun, J., Wang, S., Kim, J., Rao, K. M., Park, S. Y., Chung, I., et al. (2016). MicroRNA-378 limits activation of hepatic stellate cells and liver fibrosis by suppressing Gli3 expression. *Nat. Commun.* 7:10993. doi: 10.1038/ncomms10993
- Ikeda, K., Horie-Inoue, K., Ueno, T., Suzuki, T., Sato, W., Shigekawa, T., et al. (2015). miR-378a-3p modulates tamoxifen sensitivity in breast cancer MCF-7 cells through targeting GOLT1A. *Sci. Rep.* 5:13170. doi: 10.1038/srep13170
- Jin, C., Zhao, W., Zhang, Z., and Liu, W. (2019). Silencing circular RNA circZNF609 restrains growth, migration and invasion by up-regulating microRNA-186-5p in prostate cancer. *Artif. Cells Nanomed. Biotechnol.* 47, 3350–3358. doi: 10.1080/21691401.2019.1648281
- Kong, Z., Wan, X., Lu, Y., Zhang, Y., Huang, Y., Xu, Y., et al. (2020). Circular RNA circFOXO3 promotes prostate cancer progression through sponging miR-29a-3p. *J. Cell Mol. Med.* 24, 799–813. doi: 10.1111/jcmm.14791
- Kong, Z., Wan, X., Zhang, Y., Zhang, P., Zhang, Y., Zhang, X., et al. (2017). Androgen-responsive circular RNA circSMARCA5 is up-regulated and promotes cell proliferation in prostate cancer. *Biochem. Biophys. Res. Commun.* 493, 1217–1223. doi: 10.1016/j.bbrc.2017.07.162
- Li, H., Dai, S., Zhen, T., Shi, H., Zhang, F., Yang, Y., et al. (2014). Clinical and biological significance of miR-378a-3p and miR-378a-5p in colorectal cancer. *Eur. J. Cancer* 50, 1207–1221. doi: 10.1016/j.jejca.2013.12.010

- Megiorni, F., Cialfi, S., McDowell, H. P., Felsani, A., Camero, S., Guffanti, A., et al. (2014). Deep Sequencing the microRNA profile in rhabdomyosarcoma reveals down-regulation of miR-378 family members. *BMC Cancer* 14:880. doi: 10.1186/1471-2407-14-880
- Nguyen, H. C., Xie, W., Yang, M., Hsieh, C. L., Drouin, S., Lee, G. S., et al. (2013). Expression differences of circulating microRNAs in metastatic castration resistant prostate cancer and low-risk, localized prostate cancer. *Prostate* 73, 346–354. doi: 10.1002/pros.22572
- Qu, S., Zhong, Y., Shang, R., Zhang, X., Song, W., Kjems, J., et al. (2017). The emerging landscape of circular RNA in life processes. *RNA Biol.* 14, 992–999. doi: 10.1080/15476286.2016.1220473
- Shukla, S., Zhang, X., Niknafs, Y. S., Xiao, L., Mehra, R., Cieřlik, M., et al. (2016). Identification and validation of PCAT14 as prognostic biomarker in prostate cancer. *Neoplasia* 18, 489–499. doi: 10.1016/j.neo.2016.07.001
- Siegel, R. L., Miller, K. D., and Jemal, A. (2017). Cancer statistics, 2017. *CA Cancer J. Clin.* 67, 7–30. doi: 10.3322/caac.21387
- Si-Tu, J., Cai, Y., Feng, T., Yang, D., Yuan, S., Yang, X., et al. (2019). Upregulated circular RNA circ-102004 that promotes cell proliferation in prostate cancer. *Int. J. Biol. Macromol.* 122, 1235–1243. doi: 10.1016/j.ijbiomac.2018.09.076
- Song, Z., Zhuo, Z., Ma, Z., Hou, C., Chen, G., and Xu, G. (2019). Hsa_Circ_0001206 is downregulated and inhibits cell proliferation, migration and invasion in prostate cancer. *Artif. Cells Nanomed. Biotechnol.* 47, 2449–2464. doi: 10.1080/21691401.2019.1626866
- Velazquez-Torres, G., Shoshan, E., Ivan, C., Huang, L., Fuentes-Mattei, E., Paret, H., et al. (2018). A-to-I miR-378a-3p editing can prevent melanoma progression via regulation of PARVA expression. *Nat. Commun.* 9:461. doi: 10.1038/s41467-018-02851-7
- Vis, A. N., Schröder, F. H., and van der Kwast, T. H. (2006). The actual value of the surgical margin status as a predictor of disease progression in men with early prostate cancer. *Eur. Urol.* 50, 258–265. doi: 10.1016/j.eururo.2005.11.030
- Wang, H., Chen, W., Jin, M., Hou, L., Chen, X., Zhang, R., et al. (2018). CircSLC3A2 functions as an oncogenic factor in hepatocellular carcinoma by sponging miR-490-3p and regulating PPM1F expression. *Mol. Cancer* 17:165. doi: 10.1186/s12943-018-0909-7
- Wei, X., Li, H., Zhang, B., Li, C., Dong, D., Lan, X., et al. (2016). miR-378a-3p promotes differentiation and inhibits proliferation of myoblasts by targeting HDAC4 in skeletal muscle development. *RNA Biol.* 13, 1300–1309. doi: 10.1080/15476286.2016.1239008
- Wu, G., Sun, Y., Xiang, Z., Wang, K., Liu, B., Xiao, G., et al. (2019). Preclinical study using circular RNA 17 and micro RNA 181c-5p to suppress the enzalutamide-resistant prostate cancer progression. *Cell Death Dis.* 10:37. doi: 10.1038/s41419-018-1048-1
- Xiang, Z., Xu, C., Wu, G., Liu, B., and Wu, D. (2019). CircRNA-UCK2 increased TET1 inhibits proliferation and invasion of prostate cancer cells via sponge MiRNA-767-5p. *Open Med.* 14, 833–842. doi: 10.1515/med-2019-0097
- Xu, Z. H., Yao, T. Z., and Liu, W. (2018). miR-378a-3p sensitizes ovarian cancer cells to cisplatin through targeting MAPK1/GRB2. *Biomed. Pharmacother.* 107, 1410–1417. doi: 10.1016/j.biopha.2018.08.132
- Zhang, J., Hou, L., Liang, R., Chen, X., Zhang, R., Chen, W., et al. (2019). CircDLST promotes the tumorigenesis and metastasis of gastric cancer by sponging miR-502-5p and activating the NRAS/MEK1/ERK1/2 signaling. *Mol. Cancer* 18:80. doi: 10.1186/s12943-019-1015-1
- Zhao, H., Lai, X., Zhang, W., Zhu, H., Zhang, S., Wu, W., et al. (2019). MiR-30a-5p frequently downregulated in prostate cancer inhibits cell proliferation via targeting PCLAF. *Artif. Cells Nanomed. Biotechnol.* 47, 278–289. doi: 10.1080/21691401.2018.1553783

Conflict of Interest: The authors declare that the research was conducted in the absence of any commercial or financial relationships that could be construed as a potential conflict of interest.

Copyright © 2021 Mao, Li, Hua, Gu, Pan, Chen, Xu, Lu and Wang. This is an open-access article distributed under the terms of the Creative Commons Attribution License (CC BY). The use, distribution or reproduction in other forums is permitted, provided the original author(s) and the copyright owner(s) are credited and that the original publication in this journal is cited, in accordance with accepted academic practice. No use, distribution or reproduction is permitted which does not comply with these terms.



Insights Into circRNAs: Functional Roles in Lung Cancer Management and the Potential Mechanisms

Bing Feng^{1†}, Hao Zhou^{2†}, Ting Wang¹, Xinrong Lin¹, Yongting Lai³, Xiaoyuan Chu^{1,2,3} and Rui Wang^{1,2,3*}

¹ Department of Medical Oncology, Jinling Hospital, School of Medicine, Nanjing University, Nanjing, China, ² Department of Medical Oncology, Jinling Hospital, Nanjing Medical University, Nanjing, China, ³ Department of Medical Oncology, Nanjing School of Clinical Medicine, Jinling Hospital, Southern Medical University, Nanjing, China

OPEN ACCESS

Edited by:

Xiang Zhang,
The Chinese University of Hong Kong,
China

Reviewed by:

Jing Zhang,
Shanghai Jiao Tong University, China
Juqiang Han,
People's Liberation Army General
Hospital, China

*Correspondence:

Rui Wang
wangrui218@163.com

[†] These authors have contributed
equally to this work

Specialty section:

This article was submitted to
Epigenomics and Epigenetics,
a section of the journal
Frontiers in Cell and Developmental
Biology

Received: 02 December 2020

Accepted: 20 January 2021

Published: 09 February 2021

Citation:

Feng B, Zhou H, Wang T, Lin X,
Lai Y, Chu X and Wang R (2021)
Insights Into circRNAs: Functional
Roles in Lung Cancer Management
and the Potential Mechanisms.
Front. Cell Dev. Biol. 9:636913.
doi: 10.3389/fcell.2021.636913

Lung cancer is the most prevalent cancer globally. It is also the leading cause of cancer-related death because of the late diagnosis and the frequent resistance to therapeutics. Therefore, it is impending to identify novel biomarkers and effective therapeutic targets to improve the clinical outcomes. Identified as a new class of RNAs, circular RNAs (circRNAs) derive from pre-mRNA back splicing with considerable stability and conservation. Accumulating research reveal that circRNAs can function as microRNA (miRNA) sponges, regulators of gene transcription and alternative splicing, as well as interact with RNA-binding proteins (RBPs), or even be translated into proteins directly. Currently, a large body of circRNAs have been demonstrated differentially expressed in physiological and pathological processes including cancer. In lung cancer, circRNAs play multiple roles in carcinogenesis, development, and response to different therapies, indicating their potential as diagnostic and prognostic biomarkers as well as novel therapeutics. In this review, we summarize the multi-faceted functions of circRNAs in lung cancer and the underlying mechanisms, together with the possible future of these discoveries in clinical application.

Keywords: circular RNAs (circRNAs), microRNAs (miRNAs), lung cancer, biomarker, prognosis

Abbreviations: ADAR1, adenosine deaminase 1; CDK2, cyclin-dependent kinase 2; CDKN1, cyclin-dependent kinase inhibitor 1; ceRNA, competing endogenous RNA; circRNAs, circular RNAs; circrRNAs, circRNA rRNAs; ciRNAs, intronic circRNAs; CXCR4, C-X-C motif chemokine receptor 4; EcircRNAs, exonic circRNAs; EGF, epidermal growth factor; EGFR, epidermal growth factor receptor; EIF3, eukaryotic initiation factor 3; ElciRNAs, exonic circRNAs with introns; EMT, epithelial-to-mesenchymal transition; f-circRNAs, fusion circRNAs; FLI1, friend leukemia virus integration 1; FOXM1, Forkhead Box (Fox) transcription factor 1; HIF, hypoxia-inducible factor; IRES, internal ribosome entry site; lncRNA, long non-coding RNA; m6A, N6-methyladenosine; MBL, splicing factor muscleblind; miRNA, microRNA; NSCLC, non-small cell lung cancer; ORF, open reading frame; PD-1, programmed cell death-1; PD-L1, programmed cell death-1 ligand; PDPK, phosphoinositide-dependent protein kinase; PES1, pescadillo homolog 1; PFS, progression-free survival; Pol II, RNA polymerase II; PTEN, phosphatase and tensin homolog deleted on chromosome 10; QKI, RNA-binding protein quaking; RBP, RNA-binding protein; ROCK1, Rho-associated coiled-coil kinase 1; rRNA, ribosomal RNA; SCLC, small cell lung cancer; snRNA, small nuclear RNA; snRNP, small nuclear ribonucleoprotein; TGF- β , transforming growth factor- β ; TKI, tyrosine kinase inhibitor; TME, tumor microenvironment; TNM, tumor node metastasis; tricRNAs, tRNA intronic circRNAs.

INTRODUCTION

Nowadays, lung cancer is the most frequent cause of cancer-related mortality (Siegel et al., 2017). Non-small cell lung cancer (NSCLC), including lung adenocarcinoma, squamous cell lung carcinoma, and large cell lung carcinoma, constitutes about 85% of lung cancer cases. Although the novel therapeutic strategies such as targeting drugs toward the epidermal growth factor receptor (EGFR), anaplastic lymphoma kinase (ALK), and immune checkpoints programmed cell death-1 (PD-1) and/or programmed cell death-1 ligand (PD-L1) have led to an great progress of advanced NSCLC patients among the past decades, the long-term survival of lung cancer remains unfavorable because of the late diagnosis and the frequent resistance to therapeutics (Chansky et al., 2017; Kris et al., 2017). Therefore, the identification of sensitive biomarkers for early detection and prognosis estimation, as well as effective therapeutic targets is urgently needed to improve the clinical outcomes.

Circular RNAs (circRNAs) are identified as a new class of endogenous RNAs derived from back splicing. Lacking the 3'-poly(A) tails and 5'-end caps (Suzuki and Tsukahara, 2014), circRNAs have closed loop structures generated from the ligation of exons, introns, or both (Wang et al., 2019b), thus are divided into the three main subtypes as exonic circRNAs (EcircRNAs), intronic circRNAs (ciRNAs), and exonic circRNAs with introns (EIciRNAs), respectively. EcircRNAs exist in the eukaryotic cytoplasm, while ciRNAs and EIciRNAs are mainly in the nucleus. Other subtypes of circRNAs include intergenic circRNAs, tRNA intronic circRNAs (tricRNAs), antisense circRNAs, overlapping circRNAs, circRNA rRNAs (circrRNAs), and intragenic circRNAs (Liang et al., 2020). Owing to the absence of the 3' and 5' ends, circRNAs exhibit much more stability and conservation than the linear RNAs and are insusceptible to RNA exonuclease or RNase R-induced degradation. In general, circRNAs are expressed at lower levels than the host genes (Enuka et al., 2016). Although discovered half a century ago (Sanger et al., 1976), circRNAs are recently considered as the by-products from pre-mRNA back splicing without important biological functions. Currently, a large body of circRNAs have been demonstrated differentially expressed in physiological and pathological states including cancer due to the development of next-generation sequencing and bioinformatic technologies (Dragomir and Calin, 2018). In lung cancer, circRNAs reveal multiple roles in carcinogenesis, development, and response to therapies, implying their potential roles as not only the diagnostic and prognostic biomarkers but also novel therapeutics.

BIOGENESIS OF circRNAs

RNA alternative splicing is a basic gene expression event in eukaryotic cells. Unlike conventional splicing of mRNA, circRNAs are mainly produced from back-splicing process by ligating a downstream 5' site with an upstream 3' site and forming a single-strand closed loop (Jeck et al., 2013). After that, all or part of introns will be removed by the spliceosome

and the rest of sequences are to be connected, generating the corresponding subtypes of circRNAs. Exon-skipping is another mechanism for circRNA circularization. It is reported that exon-skipping promotes the shaping process of the spliced lariat containing the circularized exon (Kelly et al., 2015). Furthermore, RNA-binding proteins (RBPs) are demonstrated to be able to induce circRNAs formation. For example, splicing factor muscleblind (MBL) has binding sites on flanking introns of its pre-mRNA and is able to bring the two splicing sites close together and facilitate circularization (Ashwal-Fluss et al., 2014). Enzyme adenosine deaminase 1 (ADAR1) can inhibit circRNAs' expression by Adenosine-to-Inosine editing to diminish RNA pairing structure of flanking introns and diminish the back-splicing efficiency (Ivanov et al., 2015). RNA-binding protein quaking (QKI) is also proved to regulate circRNAs' biogenesis by binding to sites flanking circRNAs forming exons to induce exon circularization during epithelial-mesenchymal transition (EMT) (Conn et al., 2015).

FUNCTIONS AND MECHANISMS OF circRNAs

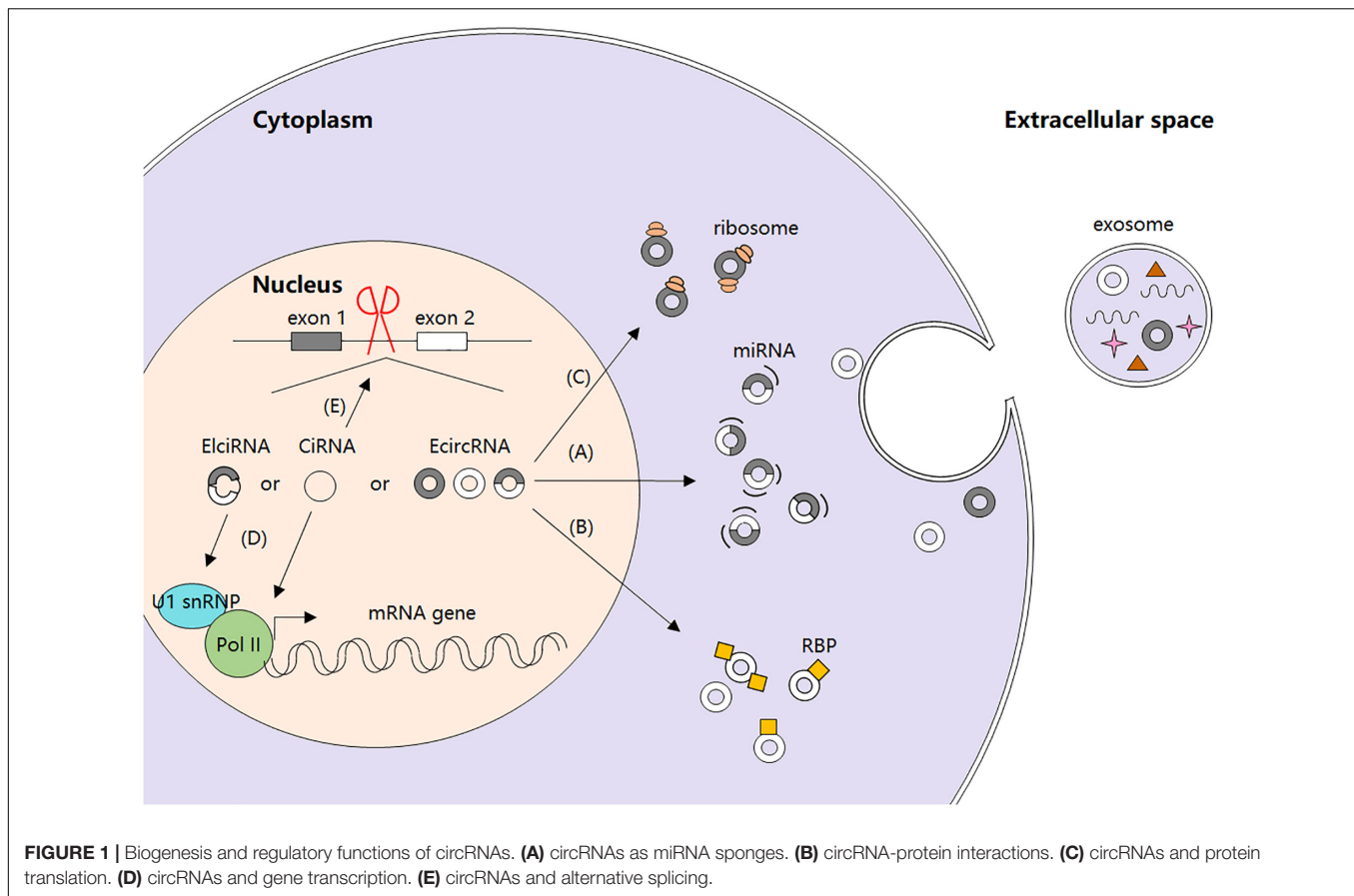
Recently, increasing studies have focused on circRNAs' biological functions and their regulation. It is confirmed that circRNAs can function as microRNA (miRNA) sponges to stop miRNAs from regulating gene expression via a circRNA-miRNA-mRNA pathway (Hansen et al., 2013). Moreover, circRNAs can act as regulators of gene transcription and alternative splicing, as well as interact with RBPs, or even be translated into peptides or full-length proteins directly (Liu et al., 2017) (Figure 1).

circRNAs as miRNA Sponges

miRNAs are small non-coding RNAs that post-transcriptionally regulate gene expression by base pairing with specific mRNA target sequences, thereby leading to translational inhibition or mRNA degradation (Salmanidis et al., 2014). They can be endogenously sponged by long non-coding RNAs (lncRNAs) owing to the presence of the miRNA response element (MRE) in lncRNA sequences (Cesana et al., 2011). It has been shown that some circRNAs located in cytoplasm also have complementary binding sites of miRNAs and can thus function as competing endogenous RNAs (ceRNAs) to compete with miRNAs and further regulate cellular functions (Zhong et al., 2018). For instance, EcircRNA ciRS-7 is reported to harbor more than 60 conserved miRNA seed match segments for miR-7, thereby antagonizing miR-7 biological activity and functions (Hansen et al., 2013). Subsequent studies confirm the importance of ciRS-7 as miR-7 sponges in many pathological processes including myocardial infarction, insulin secretion, and carcinogenesis (Pan et al., 2018).

circRNA-Protein Interactions

Recently, it is demonstrated that certain circRNAs can serve as protein decoys through binding to RBPs and regulate their interaction with DNAs, RNAs, and/or other proteins. For example, with several MBL binding sites, circMbl is able



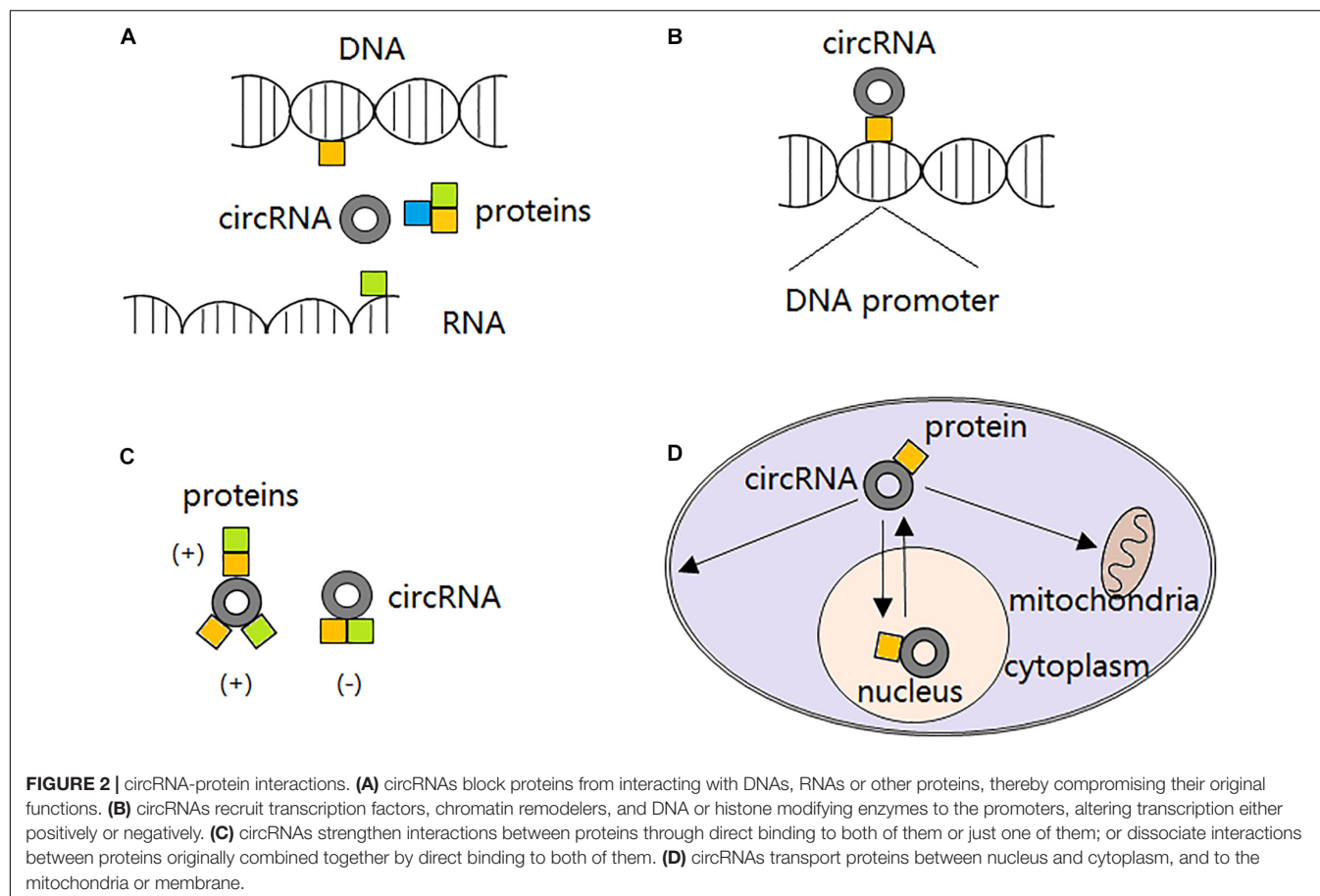
to sponge out the excessive MBL proteins and maintain its expression balance (Ashwal-Fluss et al., 2014). circANRIL can bind to pescadillo homolog 1 (PES1) and restrain exonuclease-mediated pre-rRNA (ribosomal RNA) processing (Holdt et al., 2016). circPABPN1 binds to HuR and prevents its binding to PABPN1 mRNA, resulting in PABPN1 translation attenuation (Abdelmohsen et al., 2017). circ-Foxo3 participates in the composition of a ternary complex by binding to cyclin-dependent kinase 2 (CDK2) and cyclin-dependent kinase inhibitor 1 (CDKN1), leading to impaired function of CDK2 and cell cycle arrest (Du et al., 2016). However, not all the circRNAs interacting with RBPs inhibit proteins functions. Particularly, circ-Amotl1 is reported to interact with and stabilize oncogene *c-myc* and upregulate *c-myc* targets, thereby promoting tumorigenesis (Yang Q. et al., 2017). The second action mode of circRNAs in interacting with proteins is to serve as protein recruiters. They can recruit not only transcription factors (Wang et al., 2019c), but also chromatin remodelers (Ding et al., 2019) and DNA or histone modifying enzymes (Chen N. et al., 2018) to the promoters and alter transcription either positively or negatively. Furthermore, circRNAs are able to alter interactions between proteins. In detail, circRNAs can strengthen interactions between proteins through direct binding to both of them (Huang S. et al., 2019) or just one of them (Fang et al., 2018), or dissociate interactions between proteins originally combined together by direct binding to both of them (Fang et al., 2019). Interestingly,

it is reported that some circRNAs can also serve as protein transporters. circRNAs transport proteins between nucleus and cytoplasm (Yang Z. et al., 2017; Wang et al., 2019e), and to the mitochondria (Liu et al., 2020) or membrane (Du et al., 2020) (Figure 2).

circRNAs and Protein Translation

Although initially considered as non-coding RNAs (Jeck et al., 2013), circRNAs are shown to be translatable in human transcriptome *in vivo* by ribosome footprinting and mass spectrometry analysis recently (Pamudurti et al., 2017). With the help of internal ribosome entry site (IRES) which is a non-circle structure, circRNA can be translated into either small peptides or full-length proteins. For example, circ-SHPRH is reported to encode the protein SHPRH-146aa, protect full-length SHPRH from degradation by the ubiquitin proteasome, and ultimately inhibit glioma tumorigenesis (Zhang et al., 2018a). An endogenous circFBXW7 can be encoded into a 21 kDa protein with suppressive roles in malignant phenotypes of human glioblastoma (Yang et al., 2018). Moreover, extensive N6-methyladenosine modification can drive the cap-independent translation of circRNAs together with m6A reader YTHDF3 and translation initiation factors eIF3A and eIF4G2 (Yang Y. et al., 2017).

Known circRNAs and their protein production are listed in Table 1.



circRNAs and Gene Transcription

It is demonstrated that certain ElciRNAs and ciRNAs may act as transcriptional regulators. For instance, ElciRNAs circEIF3J and circPAIP2 are reported to promote their parental genes promotion by a specific U1 small nuclear RNA (snRNA)-ElciRNA interaction. Mechanically, ElciRNAs bind to U1 small nuclear ribonucleoprotein (snRNP) through interaction with U1 snRNA and to form ElciRNA-U1 snRNP complexes, which will further interact with RNA polymerase II (Pol II) transcription complex of the parental gene and

enhance gene transcription (Li et al., 2015). Besides, ciRNA ci-ankrd52 is able to accumulate to its transcription sites and positively regulate elongation Pol II machinery, suggesting a *cis*-regulatory role of ciRNAs in expression of their parental genes (Zhang et al., 2013).

circRNAs and Alternative Splicing

RNA alternative splicing is a basic gene expression event in eukaryotic cells. During this process, the backsplicing of circRNAs competes with the linear splicing of pre-mRNAs for splicing sites. For example, derived from the second exon of splicing factor MBL, circMbl itself and its flanking introns have conserved MBL binding sites, indicating that MBL may have effects on alternative splicing and modulate the balance between the backsplicing of circRNAs and the linear splicing of pre-mRNAs (Ashwal-Fluss et al., 2014). Meanwhile, circRNAs can act as “mRNA traps” during the back-splicing process by sequestering the translation start site to prevent translation of certain normal linear transcripts and reduce the expression of the very proteins. For instance, EcircRNAs generated from Formin (Fmn) and Duchenne muscular dystrophies traps (DMD) genes are able to cause inactivation of RNA transcripts with certain deletion mutations, thereby diminishing the expression levels of the corresponding functional proteins (Chao et al., 1998; Gualandi et al., 2003).

TABLE 1 | circRNAs and protein translation.

circRNA	Peptide/protein	References
circSHPRH	SHPRH-146aa	Zhang et al., 2018a
circFBXW7	FBXW7-185aa	Yang et al., 2018
HPV16 circE7	E7 oncoprotein	Zhao et al., 2019
circ β -catenin	β -catenin-370aa	Liang et al., 2019
circAKT3	AKT3-174aa	Xia et al., 2019
circPPP1R12A	PPP1R12A-73aa	Zheng et al., 2019
circPIN-Texon2	PINT87aa	Zhang et al., 2018b
circGprc5a	circGprc5a-peptide	Gu et al., 2018
circLgr4	circLgr4-peptide	Zhi et al., 2019

circRNAs AND LUNG CANCER

Emerging evidence suggests that circRNAs are abnormally expressed and playing endogenous regulatory roles in carcinogenesis and development of lung cancer, including cell viability, apoptosis, autophagy, invasion, migration, tumor microenvironment (TME) regulation (such as tumor immunosuppression, angiogenesis, hypoxia, and metabolic abnormalities), and therapeutic sensitivities. Moreover, circRNAs own relative specificity and stability compared to other non-coding RNAs, making them more attractive as novel diagnostic and prognostic biomarkers as well as promising therapeutics in lung cancer management. With the development of high-throughput sequencing technology, circRNA expressions in cell lines, tissue samples, and liquid biopsies (especially blood) from lung cancer patients have been detected (Wang et al., 2019a; Zhang et al., 2020). Functional validation assays as well as bioinformatic analysis have been performed to reveal the interaction network of circRNAs and other regulatory factors in lung cancer tumorigenesis and development.

circRNAs as Diagnostic and Prognostic Biomarkers for Lung Cancer

With advantages such as non-invasion, specificity, reproducibility, and sensitivity, circRNAs can act as biomarkers for lung cancer pathological subtyping. For example, hsa_circ_0013958 is indicated to be used as a potential biomarker for screening and early detecting lung adenocarcinoma (Zhu et al., 2017). In a recent work, circRNA expressions are profiled in both lung adenocarcinoma and squamous cell carcinoma and the result indicates that the two subtypes exhibit distinct circRNA expression signatures (Wang et al., 2019a). Similarly, circNOL10 expression varies significantly between lung adenocarcinoma and lung squamous cell carcinoma and has close relationship with the degree of differentiation (Nan et al., 2018). Another study confirms that circ-STXBP5L is selectively expressed in small cell lung cancer (SCLC) samples compared with NSCLC (Zhang et al., 2020). These results highlight the important diagnostic value of circRNAs in pathological classification of lung cancer.

Moreover, mounting studies demonstrate that circRNAs can also serve as prognostic biomarkers for lung cancer occurrence, development, tumor node metastasis (TNM) staging, pathological grade, and lymphatic metastasis. Generally, many circRNAs are upregulated in lung cancer and are considered to be “onco-circRNAs” due to their positive roles in cancer cell proliferation, invasion, and migration, as well as the negative regulation on cancer cell apoptosis. Vice versa, circRNAs that are downregulated in lung cancer with tumor-suppressive functions are considered as “tumor-suppressive circRNAs.”

Onco-circRNAs in Lung Cancer

To date, a multitude of onco-circRNAs have been identified in lung cancer and proposed as potential biomarkers for prognosis.

As is well-known that metastasis is one of the main characteristics of malignant tumors including lung cancer. It is reported that friend leukemia virus integration 1 (FLI1) exonic

circRNA FECR1 can promote SCLC metastasis by increasing rho-associated coiled-coil kinase 1 (ROCK1) expressions through direct inhibition of miR584-3p (Li L. et al., 2019). It is described above that circ-STXBP5L participates in the carcinogenesis of SCLC as an onco-circRNA by sponging miR-224-3p and miR-512-3p and regulating a subset of target genes, including Akts, NFκB and Pik3ca (Zhang et al., 2020). As for NSCLC, the data are more detailed. For instance, over-expressed in EGFR-resistant H1975 cells, circRNA CCDC66 is regulated by HGF/c-Met to increase EMT process and drug resistance of lung adenocarcinoma (Joseph et al., 2018). Produced from the EML4-ALK fusion, circRNA F-circEA-2a reveals positive effect on cell invasion and migration in NSCLC, highlighting its critical role in EML4-ALK-positive NSCLC (Tan et al., 2018). circRNA_102231 promotes cellular proliferation, invasion, and migration in lung cancer. Highly expressed circRNA_102231 may serve as a biomarker for both diagnosis and prognosis for lung cancer patients (Zong et al., 2018). It is demonstrated that circHIPK3 can restore lung cancer cell survival and proliferation via sponging miR-124 and regulating expression of its potential targets such as SphK1, STAT3, and CDK4 (Yu et al., 2018). Particularly, circHIPK3 also functions as a negative autophagy regulator in lung cancer through the miR124-3p-STAT3-PRKAA pathway which is dependent on STK11 status (Chen et al., 2020). circHIPK3 regulates the EMT progress of NSCLC through miR-149-mediated Forkhead Box transcription factor FOXM1 expression regulation, closely correlated with the aggressive potential and unfavorable prognosis (Lu et al., 2020). CircPVT1 positively regulates NSCLC cell proliferation, invasion, and metastasis by sponging miR-125b and activating the corresponding E2F2 signaling pathway (Li X. et al., 2018). It can also act as a competing endogenous RNA for miR-497 and indirectly increase the expression of Bcl-2, leading to promoted NSCLC progression and predicting poor survival of the patients (Qin et al., 2019).

Hypoxia caused by the instability of the tumor-associated microvasculature is one of the key reasons for cancer progression. It is reported that circ_0000376 can promote NSCLC progression by regulating the miR-1182/NOVA2 axis and is relative to the poor overall survival of NSCLC patients. Hypoxia enhances circ_0000376 expression and promotes the glycolysis, viability, invasion and migration of NSCLC cells. Manipulated inhibition of circ_0000376 suppresses the progressive activities of hypoxia-induced NSCLC cells both *in vitro* and *in vivo* (Li C. et al., 2020).

Several circRNAs are verified to effect both cell proliferation and apoptosis in lung cancer. For instance, upregulated hsa_circ_0000064 demonstrates effect on cell proliferation, metastasis, and apoptosis by regulating target genes such as cell cycle regulators p21WAF1, cyclin D1, and CDK6, as well as apoptotic factors caspase-3, caspase-9, and bax (Luo et al., 2017). Serving as a sponge for miR-503, circ-BANP promotes proliferation, invasion, and migration while attenuates apoptosis of lung cancer cells through promotion of LARP1 expression (Han et al., 2018). circ-FOXM1 works as a ceRNA to target PDPF and MACC1 by sponging miR-1304-5p in NSCLC. It promotes cellular proliferation, invasion, and migration, and suppresses apoptosis, thus playing oncogenic roles in progression

of NSCLC. The elevation of circ-FOXO1 in NSCLC is proved to be strongly linked to advanced TNM stages, lymph node invasion, as well as dismal prognosis (Liu G. et al., 2019). Commonly upregulated in NSCLC tissues and cell lines, circ_0026134 facilitates NSCLC proliferation and metastatic properties and weakens cell apoptosis, dependent on the sponge and down-regulation of miR-1287 and miR-1256 (Chang et al., 2019). Similarly, circRNA 100146 is highly expressed and playing an oncogenic role in the progression of NSCLC. It enhances NSCLC cell proliferation and invasion and inhibits cell apoptosis through direct binding to miR-361-3p and miR-615-5p and affections on multiple downstream molecules such as NFAT5, COL1A1, TRAF3, and MEF2C (Chen L. et al., 2019).

It is shown that lung cancer progression is also promoted by increased glycolysis. For example, Enolase 1 (ENO1) is a glycolysis enzyme which performs crucial roles in glucose metabolism and contributes to progression of lung cancer. Recently, circ-ENO1 and its host gene ENO1 are reported to be upregulated in lung adenocarcinoma. Mechanistically, circ-ENO1 acts as a ceRNA of miR-22-3p and upregulates ENO1 expression, promoting glycolysis and tumor progression in lung adenocarcinoma. Silencing of circ-ENO1 inhibits glycolysis, cell proliferation, migration and EMT of lung adenocarcinoma (Zhou J. et al., 2019).

Tumor immune microenvironment is another pivotal factor for the development of lung cancer where cancer cells interact with immune cells to facilitate immune evasion. For example, NSCLC-derived intracellular and extracellular PD-L1 can not only promote cancer progression and drug resistance but also facilitate tumor immune evasion (Li Y. et al., 2019). It is recently demonstrated that circ-CPA4 is high-expressed in NSCLC and can regulate cell growth, metastasis, stemness and drug resistance as well as inactivate CD8⁺ T cells in tumor immune microenvironment through miRNA let-7/PD-L1 regulatory axis. Inhibition of circ-CPA4 suppresses NSCLC cell growth, mobility and EMT, while enhances cell death via downregulation of let-7/PD-L1 axis. Furthermore, circ-CPA4 can positively regulate the expression of exosomal PD-L1 which promotes NSCLC cell stemness and increases the resistance toward cisplatin (Hong et al., 2020).

Dysregulated onco-circRNAs in lung cancer, their functions, and the underlying mechanisms are listed in **Table 2**.

Tumor-Suppressive circRNAs in Lung Cancer

A series of circRNAs have been found downregulated in lung cancer and thus considered as tumor suppressors. For instance, downregulated in SCLC and chemo-resistant NSCLC cells, circRNA cESRP1 enhances drug sensitivity by directly binding to and repressing miR-93-5p, thereby up-regulating the expression of Smad7 and p21, forming a negative feedback loop to regulate EMT process dependent of transforming growth factor- β (TGF- β) (Huang W. et al., 2019).

In NSCLC, circRNA ITCH is reported markedly decreased in cancer tissues with negative regulation on the proliferation of cancer cells by down-regulating oncogenic miR-7 and miR-214 as well as up-regulating T-cell factor, β -catenin, c-Myc, and cyclin D1, thereby enhancing the activation of

the Wnt/ β -catenin signaling pathway (Wan et al., 2016). circ_0001649 is demonstrated to have a decreased expression in NSCLC tissues and cell lines with suppressive functions on cell growth and metastasis both *in vitro* and *in vivo* partially by sponging out miR-331-3p and miR-338-5p. The down-regulation of circ_0001649 is highly interrelated with advanced TNM stage, positive lymph node metastasis, and poor prognosis of NSCLC patients (Liu T. et al., 2018). circPTK2 promotes TIF1 γ expression and inhibits TGF- β -induced EMT and metastasis in NSCLC dependent on miR-429/miR-200b-3p sponging (Wang et al., 2018). circRNA-FOXO3 expression is also found decreased in NSCLC and correlated with clinical outcomes. circRNA-FOXO3 inhibits NSCLC cell proliferation, invasion, and migration by acting as a ceRNA to sponge miR-155 and release FOXO3 expression (Zhang et al., 2018c).

Cell apoptosis is also regulated by certain tumor-suppressive circRNAs in lung cancer. For example, acting as an endogenous sponge for miR-1252, has_circ_0043256 can upregulate the expression of ITCH and finally inhibit Wnt/ β -catenin pathway, leading to suppression of cell proliferation and enhancement of apoptosis in NSCLC (Tian et al., 2017). circNOL10 is downregulated in both lung cancer tissues and cells and conducive in differentiating lung adenocarcinoma and lung squamous cell carcinoma. Furthermore, circNOL10 inhibits lung cancer by enhancing transcriptional regulation of the HN polypeptide family, which exerts pivotal functions on biological processes such as proliferation, apoptosis, and cell cycle progression (Nan et al., 2018).

Dysregulated tumor-suppressive circRNAs in lung cancer, their functions, and the underlying mechanisms are listed in **Table 3**.

circRNAs and the Therapeutic Response of Lung Cancer

Except for chemotherapy, targeted therapies and immunotherapies have revolutionized the lung cancer management within the last decades. However, drug-resistance still develops after the treatment. Considering the multiple roles of circRNAs in lung cancer progression, it is not surprising to apply them as predictive biomarkers for the follow-up of patients. Furthermore, the detection of circRNAs in liquid biopsies has provided a more convenient method for the management of post-treatment follow-up.

Chemotherapy

With the assistance of a high-throughput circRNA microarray, a significant upregulation of 2,909 circRNAs as well as downregulation of 8,372 circRNAs are discovered in taxol-resistant A549 lung adenocarcinoma cells compared with the parental cells (Xu et al., 2018). Functional validation assays highlight the circRNA/miRNA networks in this context. The most pronouncedly enriched pathways for aberrant circRNA-related host genes include VEGFR, EGFR, integrin, and rho GTPase signaling, which are all involved in the progression of chemo-resistance.

Eukaryotic initiation factor 3 (EIF3) is one of the largest translation initiation factors. Previous studies have suggested

TABLE 2 | Dysregulated onco-circRNAs in lung cancer.

circRNA	Function	Mechanism	References
circFEER1	Metastasis of SCLC	miR584-3p/ROCK1	Li L. et al., 2019
circSTXBP5L	Carcinogenesis of SCLC	miR-224-3p and miR-512-3p/Akts, NFκB, and Pik3ca	Zhang et al., 2020
circ_100876	Prognosis values	?	Yao et al., 2017
circCCDC66	EMT and drug resistance of lung adenocarcinoma	?	Joseph et al., 2018
circF-circEA-2a	Invasion and migration of NSCLC	?	Tan et al., 2018
circRNA_102231	Proliferation, invasion, and migration of lung cancer	?	Zong et al., 2018
hsa_circRNA_103809	Proliferation and invasion of lung cancer	miR-4302/ZNF121/ MYC	Liu W. et al., 2018
circH1PK3	Cell survival and proliferation of lung cancer	miR-124/SphK1, STAT3, and CDK4	Yu et al., 2018
	Autophagy of lung cancer	miR124-3p/STAT3/PRKAA	Chen et al., 2020
	EMT and aggressiveness of NSCLC	miR-149/FOXO1	Lu et al., 2020
circPVT1	Proliferation, invasion, and metastasis of NSCLC	miR-125b/E2F2	Li X. et al., 2018
	NSCLC progression	miR-497/Bcl-2	Qin et al., 2019
circMAN2B2	Proliferation and invasion of lung cancer	miR-1275/FOXK1	Ma et al., 2018
circ_0067934	Tumorigenesis, EMT, and metastasis of NSCLC	?	Wang and Li, 2018
hsa_circ_0020123	Proliferation, invasion, and migration of NSCLC	miR-144/ZEB1 and EZH2	Qu et al., 2018
	Growth, invasion, migration, and apoptosis of NSCLC	miR-488e3p/ADAM9	Wan et al., 2019
circFADS2	Proliferation and invasion of lung cancer	miR-498/ FOXO1/KLF6	Zhao et al., 2018
circ_0016760	Progression of NSCLC	miR-1287/GAGE1	Li Y. et al., 2018
circPRKCI	Proliferation and tumorigenesis of lung adenocarcinoma	miR-545 and miR-589/E2F7	Qiu et al., 2018
circCMPK1	Cell proliferation of NSCLC	miR-302e/cyclin D1	Cui et al., 2020
circFGFR1	Proliferation, migration, invasion, and immune evasion abilities of NSCLC	miR-381-3p/CXCR4	Zhang P. et al., 2019
circP4HB	EMT and metastasis of NSCLC	miR-133a-5p/vimentin	Wang et al., 2019f
hsa_circ_000984	Proliferation and metastasis of NSCLC	Wnt/β-catenin signaling	Li X. et al., 2019
circ_0003645	NSCLC progression	miR-1179/TMEM14A	An et al., 2019
circZFR	NSCLC progression	miR-101-3p/CUL4B	Zhang H. et al., 2019
hsa_circ_0023404	Proliferation, invasion, and migration of NSCLC	miR-217/ZEB1	Liu C. et al., 2019
F-circSR1 and 2	Migration and invasion of NSCLC	?	Wu et al., 2019
circPRMT5	NSCLC progression	miR-377, miR-382, and miR-498/EZH2	Wang et al., 2019h
circPIP5K1A	Proliferation and metastasis of NSCLC	miR-600/HIF-1α	Chi et al., 2019
circATXN7	Proliferation and invasion abilities of NSCLC	?	Huang Q. et al., 2019
circFGFR3	Proliferation and invasion of NSCLC	miR-22-3p/Gal-1, p-AKT and p-ERK1/2	Qiu et al., 2019
circ_0043278	Proliferation, invasion and migration of NSCLC	miR-520f/ROCK1, CDKN1B and AKT3	Cui et al., 2019
circRAD23B	Progression of NSCLC	miR-593e3p/CCND2 and miR-653e5p/TIAM1	Han et al., 2019
circNT5E	Cell growth, proliferation, and migration of NSCLC	miR-134	Dong et al., 2020
hsa_circ_0013958	Proliferation, invasion, and apoptosis of lung adenocarcinoma	miR-134/cyclin D1	Zhu et al., 2017
circ_0000376	Glycolysis, cell viability, invasion and migration of NSCLC	miR-1182/NOVA2	Li Y. et al., 2020
hsa_circ_0000064	Proliferation, apoptosis, and metastasis of lung cancer	Cell cycle regulators (p21WAF1, cyclin D1, and CDK6) and apoptotic factors (caspase-3, caspase-9, and bax)	Luo et al., 2017
hsa_circ_0007385	NSCLC progression	miR-181/Bcl-2 and CDK1	Jiang et al., 2018
circBANP	Proliferation, invasion, migration, and apoptosis of lung cancer	miR-503/LARP1	Han et al., 2018
circVANG1	Proliferation, migration, invasion, and apoptosis of NSCLC	miR-195/Bcl-2 and Bax	Wang et al., 2019d
circFOXO1	Proliferation, invasion, migration, and apoptosis of NSCLC	miR-1304-5p/ PPDPF and MACC1	Liu G. et al., 2019
circ_0026134	Proliferation, metastasis, and apoptosis of NSCLC	miR-1287/PIK3R3 and miR-1256/TCTN1	Chang et al., 2019
circRNA 100146	Proliferation, invasion, and apoptosis of NSCLC	miR-361-3p and miR-615-5p/ NFAT5, COL1A1, TRAF3, and MEF2C	Chen L. et al., 2019
circCDR1	Cell viability, migration, invasion, and apoptosis of NSCLC	miR-219a-5p/SOX5	Li Y. et al., 2020
circ-ENO1	Glycolysis, proliferation, apoptosis, migration and EMT of lung adenocarcinoma	miR-22-3p/ENO1	Zhou J. et al., 2019
circ-CPA4	Cell growth, mobility, stemness, drug resistance, and CD8+ T cell inactivation in the tumor immune microenvironment of NSCLC	let-7/PD-L1	Hong et al., 2020

TABLE 3 | Dysregulated tumor-suppressive circRNAs in lung cancer.

circRNA	Function	Mechanism	References
circESRP1	EMT and drug sensitivity of SCLC	miR-93-5p/Smad7/p21(CDKN1A)/TGF- β	Huang W. et al., 2019
circITCH	proliferation of NSCLC	miR-7 and miR-214/ T-cell factor, β -catenin, c-Myc, and cyclin D1	Wan et al., 2016
circ_0001649	growth and metastasis of NSCLC	miR-331-3p and miR-338-5p	Liu T. et al., 2018
circPTK2	EMT and metastasis of NSCLC	miR-429 and miR-200b-3p/TIF1 γ /TGF- β	Wang et al., 2018
circFOXO3	Proliferation, invasion, and migration of NSCLC	miR-155/FOXO3	Zhang et al., 2018c
hsa_circ_100395	Proliferation, invasion, and migration of lung cancer	miR-1228/TCF21	Chen D. et al., 2018
hsa_circ_0033155	Proliferation and migration of NSCLC	PTEN	Gu et al., 2019
circSMARCA5	Proliferation and chemo-sensitivity of NSCLC	miR-19b-3p/HOXA9	Wang et al., 2019g; Tong, 2020
hsa_circ_0007059	Proliferation and EMT of lung cancer	miR-378/Wnt/ β -catenin and ERK1/2	Gao et al., 2019
circARHGAP10	NSCLC progression	miR-150-5p/GLUT1	Jin et al., 2019
circPTPRA	EMT and metastasis of NSCLC	miR-96-5p/RASSF8	Wei et al., 2019
has_circ_0043256	Proliferation and apoptosis of NSCLC	miR-1252/ITCH/Wnt/ β -catenin	Tian et al., 2017
circNOL10	Proliferation, apoptosis, and cell cycle progression of lung cancer	SCLM1/the HN polypeptide family	Nan et al., 2018

the involvement of EIF3a in tumorigenesis and drug resistance of lung cancer. Recently, it is found that the expression of hsa_circ_0004350 and hsa_circ_0092857, both derived from EIF3a, varies prominently in cisplatin-resistant lung cancer cell line and the parental cell line. Manipulated regulation of the two circEIF3as affects cisplatin sensitivity of lung cancer cells. Further bioinformatic analysis indicates that the two circEIF3as are not only related to translational regulation, but also showing functional synergy with their parental gene EIF3a, thus serving as potential therapeutic targets during lung cancer management (Huang M.S. et al., 2019).

Targeted Therapy

EGFR-tyrosine kinase inhibitors (EGFR-TKIs) have become important constituents for NSCLC treatment these years. Despite the good initial responses, tumor progression is systematically observed due to the emergence of acquire resistance. Furthermore, detection for EGFR driver mutation is hindered by problems such as cancer heterogeneity and lack of cancer tissues. By screening circRNAs expression profile via circRNA microarray, it is found that hsa_circ_0109320 and hsa_circ_0134501 are upregulated in gefitinib-effective NSCLC patients. Moreover, hsa_circ_0109320 expression is associated with better progression-free survival (PFS), indicating its potential role as a prognostic biomarker for gefitinib-treated NSCLC patients (Liu Y. et al., 2019). Similarly, hsa_circ_0004015 is identified to be highly expressed in NSCLC cells and tissues. Patients with high expression of hsa_circ_0004015 often have a worse overall survival rate. Further study indicates that hsa_circ_0004015 promotes NSCLC progression and gefitinib resistance through sponge for miR-1183 and induction of 3-phosphoinositide-dependent protein kinase 1 (PDPK) as well as the downstream AKT pathway (Zhou Y. et al., 2019). Recently, circRNA expression profiles have been explored in Osimertinib (AZD9291)-resistant NSCLC cells and the result shows that the most modulated circRNAs are involved in regulation of cancer-related pathways including proliferation, invasion, apoptosis,

and resistance to chemotherapeutic drugs as well as γ -radiation (Chen T. et al., 2019).

Another role of circRNAs during tumorigenesis is the formation of fusion circRNAs (f-circRNAs) derived from chromosomal translocations (Guarnerio et al., 2016). It is demonstrated that f-circEA-2a which derived from back splicing of the EML4-ALK fusion gene promotes cell invasion and migration but not cell proliferation in NSCLC. Interestingly, f-circEA-2a is detected in tumor tissues but not plasma of EML4-ALK-positive NSCLC patients (Tan et al., 2018).

Immunotherapy

Anti-PD-1-based immunotherapy has led to an effective response in multiple advanced cancers, lung cancer included. However, more than half of NSCLC patients lack a long-term response to this immunotherapy (Melosky et al., 2019). Emerging evidence show that dysregulated chemokine receptor expression is one of the critical intrinsic reasons for tumor-promotion and immune system evasion (Adrover et al., 2019). Recently, it is found that circFGFR1 may act as a sponge for miR-381-3p, thereby promoting NSCLC progression and resistance to anti-PD-1 therapy by up-regulating CXCR4 expression. CircFGFR1 is upregulated in NSCLC tissues with its expression closely correlated with unfavorable prognosis of NSCLC patients. Manipulated upregulation of circFGFR1 promotes the proliferation, invasion, migration, and immune evasion of NSCLC cells, while knockdown of CXCR4 resensitizes NSCLC cells to anti-PD-1 immunotherapy (Zhang P. et al., 2019). As is mentioned above, circ-CPA4 can regulate cell growth, mobility, stemness and drug resistance in NSCLC cells and inactivates CD8⁺ T cells in the tumor immune microenvironment through the let-7 miRNA/PD-L1 axis. On the one hand, PD-L1 selfregulates NSCLC cell malignant activities. On the other hand, secreted PD-L1 by exosomes inactivates CD8⁺ T cells by activating extracellular and intracellular pathways and mediates cell death to facilitate immune evasion (Hong et al., 2020).

circRNAs as Promising Therapeutics for Lung Cancer

Regarding the onco- and tumor suppressive- roles in lung cancer, circRNAs provide insight into the exploration of novel strategies in lung cancer management. Moreover, as mentioned above, circRNAs are more suitable for targeted molecular therapy because of their stable, tissue specific, and ceRNA-equivalent characteristics. Further investigation is needed to translate circRNAs into clinics and provide a foundation for developing novel potential therapeutic strategies for lung cancer and improve the prognosis of the patients.

DISCUSSION

Despite significant advances in diagnosis and treatment, lung cancer remains the leading cause of death worldwide with its underlying mechanisms remaining largely undiscovered. A major obstacle of improving clinical outcomes is to identify sensitive biomarkers and novel therapeutics for individualized diagnosis and treatment of lung cancer. In recent years, thousands of circRNAs have been identified with the rapid development of NGS technology and bioinformatics. Although considered as splicing by-products initially, circRNAs are now becoming a hotspot in the field of cancer owing to their conservation across species, the relative high stability and abundance, and the accessibility in body fluids, especially blood. They reveal diverse regulatory functions on genes and proteins involved in cancer cell proliferation, invasion, migration, cell cycle, apoptosis, and drug sensitivity. Moreover, recent studies have shown that the role of circRNAs in cancer is mainly dependent on the circRNA-miRNA-mRNA regulatory network, indicating their potential functions in the regulation of transcriptional and post-transcriptional levels. Other mechanisms include interacting with RBPs, translating into either peptides or full-length proteins, and regulating transcription. This provides novel biomarkers for lung cancer prognosis prediction, especially considering the lack of reliable clinical biomarkers in SCLC. In addition,

engineered circRNAs can be applied to effectively sequester not only RNAs (including miRNAs), but also DNAs and RBPs with specific sequences both *in vitro* and *in vivo*, providing promising molecular targets for the therapy of lung cancer (Lasda and Parker, 2014).

However, it should be noted that the study on circRNAs in lung cancer is still in the early stage. The functions and underlying mechanisms of circRNAs in the regulatory network of tumorigenesis and progression remains largely unknown and needs to be further studied in more cell lines and clinical samples. Moreover, problems such as the high cost of experiment, difficulties in detection and monitoring, and the potential side effects, are still limiting the application of circRNAs in clinic. We hope that in the future, with the rapid development of bioinformatic technology and universal studies in patient tissue samples, circRNAs could help to achieve better individualized diagnosis and treatment of lung cancer.

AUTHOR CONTRIBUTIONS

RW conceptualized the review. BF and HZ were the major contributors in writing the manuscript. TW designed the figures. XL and YL prepared the tables. XC critically reviewed and edited the manuscript. All the authors read and approved the final manuscript.

FUNDING

This study was supported by grants from the National Natural Science Foundation of China (Nos. 81772995 and 81472266); the Excellent Youth Foundation of Jiangsu Province, China (No. BK20140032); Jiangsu Province's Key Provincial Talents Program (No. ZDRCA2016090); Jiangsu Provincial Medical Youth Talent, The Project of Invigorating Health Care through Science, Technology and Education (No. QNRC2016886).

REFERENCES

- Abdelmohsen, K., Panda, A. C., Munk, R., Grammatikakis, I., Dudekula, D. B., De, S., et al. (2017). Identification of HuR target circular RNAs uncovers suppression of PABPN1 translation by CircPABPN1. *RNA Biol.* 14, 361–369. doi: 10.1080/15476286.2017.1279788
- Adrover, J. M., Fresno, C. D., Crainiciuc, G., Cuartero, M. I., Casanova-Acebes, M., Weiss, L. A., et al. (2019). A neutrophil timer coordinates immune defense and vascular protection. *Immunity* 51, 966–967. doi: 10.1016/j.immuni.2019.01.002
- An, J., Shi, H., Zhang, N., and Song, S. (2019). Elevation of circular RNA circ_0003645 forecasts unfavorable prognosis and facilitates cell progression via miR-1179/TMEM14A pathway in non-small cell lung cancer. *Biochem. Biophys. Res. Commun.* 511, 921–925. doi: 10.1016/j.bbrc.2019.03.011
- Ashwal-Fluss, R., Meyer, M., Pamudurti, N. R., Ivanov, A., Bartok, O., Hanan, M., et al. (2014). circRNA biogenesis competes with pre-mRNA splicing. *Mol. Cell* 56, 55–66. doi: 10.1016/j.molcel.2014.08.019
- Cesana, M., Cacchiarelli, D., Legnini, I., Santini, T., Sthandier, O., Chinappi, M., et al. (2011). A long noncoding RNA controls muscle differentiation by functioning as a competing endogenous RNA. *Cell* 147, 358–369. doi: 10.1016/j.cell.2011.09.028
- Chang, H., Qu, J., Wang, J., Liang, X., and Sun, W. (2019). Circular RNA circ_0026134 regulates non-small cell lung cancer cell proliferation and invasion via sponging miR-1256 and miR-1287. *Biomed. Pharmacother.* 112:108743. doi: 10.1016/j.biopha.2019.108743
- Chansky, K., Dettterbeck, F. C., Nicholson, A. G., Rusch, V. W., Vallières, E., Groome, P., et al. (2017). The IASLC lung cancer staging project: external validation of the revision of the TNM stage groupings in the eighth edition of the TNM classification of lung cancer. *J. Thorac. Oncol.* 12, 1109–1121. doi: 10.1016/j.jtho.2017.04.011
- Chao, C., Chan, D., Kuo, A., and Leder, P. (1998). The mouse formin (Fmn) gene: abundant circular RNA transcripts and gene-targeted deletion analysis. *Mol. Med.* 4, 614–628.
- Chen, D., Ma, W., Ke, Z., and Xie, F. (2018). CircRNA hsa_circ_100395 regulates miR-1228/TCF21 pathway to inhibit lung cancer progression. *Cell Cycle* 17, 2080–2090. doi: 10.1080/15384101.2018.1515553
- Chen, N., Zhao, G., Yan, X., Lv, Z., Yin, H., Zhang, S., et al. (2018). A novel FLI1 exonic circular RNA promotes metastasis in breast cancer by coordinately regulating TET1 and DNMT1. *Genome Biol.* 19:218. doi: 10.1186/s13059-018-1594-y
- Chen, L., Nan, A., Zhang, N., Jia, Y., Li, X., Ling, Y., et al. (2019). Circular RNA 100146 functions as an oncogene through direct binding to miR-361-3p and

- miR-615-5p in non-small cell lung cancer. *Mol. Cancer*. 18:13. doi: 10.1186/s12943-019-0943-0
- Chen, T., Luo, J., Gu, Y., Huang, J., Luo, Q., and Yang, Y. (2019). Comprehensive analysis of circular RNA profiling in AZD9291-resistant non-small cell lung cancer cell lines. *Thorac. Cancer* 10, 930–941. doi: 10.1111/1759-7714.13032
- Chen, X., Mao, R., Su, W., Yang, X., Geng, Q., Guo, C., et al. (2020). Circular RNA circHIPK3 modulates autophagy via MIR124-3p-STAT3-PRKAA/AMPK α signaling in STK11 mutant lung cancer. *Autophagy* 16, 659–671. doi: 10.1080/15548627.2019.1634945
- Chi, Y., Luo, Q., Song, Y., Yang, F., Wang, Y., Jin, M., et al. (2019). Circular RNA circPIP5K1A promotes non-small cell lung cancer proliferation and metastasis through miR-600/HIF-1 α regulation. *J. Cell Biochem.* 120, 19019–19030. doi: 10.1002/jcb.29225
- Conn, S. J., Pillman, K. A., Toubia, J., Conn, V. M., Salmanidis, M., Phillips, C. A., et al. (2015). The RNA binding protein quaking regulates formation of circRNAs. *Cell* 160, 1125–1134. doi: 10.1016/j.cell.2015.02.014
- Cui, D., Qian, R., and Li, Y. (2020). Circular RNA circ-CMPK1 contributes to cell proliferation of non-small cell lung cancer by elevating cyclin D1 via sponging miR-302e. *Mol. Genet. Genomic Med.* 8:e999. doi: 10.1002/mgg3.999
- Cui, J., Li, W., Liu, G., Chen, X., Gao, X., Lu, H., et al. (2019). A novel circular RNA, hsa_circ_0043278, acts as a potential biomarker and promotes non-small cell lung cancer cell proliferation and migration by regulating miR-520f. *Artif. Cells Nanomed. Biotechnol.* 47, 810–821. doi: 10.1080/21691401.2019.1575847
- Ding, L., Zhao, Y., Dang, S., Wang, Y., Li, X., Yu, X., et al. (2019). Circular RNA circ-DONSON facilitates gastric cancer growth and invasion via NURF complex dependent activation of transcription factor SOX4. *Mol. Cancer*. 18:45. doi: 10.1186/s12943-019-1006-2
- Dong, L., Zheng, J., Gao, Y., Zhou, X., Song, W., and Huang, J. (2020). The circular RNA NT5E promotes non-small cell lung cancer cell growth via sponging microRNA-134. *Aging* 12, 3936–3949. doi: 10.18632/aging.102861
- Dragomir, M., and Calin, G. A. (2018). Circular RNAs in cancer - lessons learned from microRNAs. *Front. Oncol.* 8:179. doi: 10.3389/fonc.2018.00179
- Du, W., Yang, W., Li, X., Fang, L., Wu, N., Li, F., et al. (2020). The circular RNA circSKA3 binds integrin β 1 to induce invadopodium formation enhancing breast cancer invasion. *Mol. Ther.* 28, 1287–1298. doi: 10.1016/j.yjmt.2020.03.002
- Du, W., Yang, W., Liu, E., Yang, Z., Dhaliwal, P., and Yang, B. (2016). Foxo3 circular RNA retards cell cycle progression via forming ternary complexes with p21 and CDK2. *Nucleic Acids Res.* 44, 2846–2858. doi: 10.1093/nar/gkw027
- Enuka, Y., Lauriola, M., Feldman, M. E., Sas-Chen, A., Ulitsky, I., and Yarden, Y. (2016). Circular RNAs are long-lived and display only minimal early alterations in response to a growth factor. *Nucleic Acids Res.* 44, 1370–1383. doi: 10.1093/nar/gkv1367
- Fang, L., Du, W., Awan, F., Dong, J., and Yang, B. (2019). The circular RNA circ-Ccnb1 dissociates Ccnb1/Cdk1 complex suppressing cell invasion and tumorigenesis. *Cancer Lett.* 459, 216–226. doi: 10.1016/j.canlet.2019.05.036
- Fang, L., Du, W., Lyu, J., Dong, J., Zhang, C., Yang, W., et al. (2018). Enhanced breast cancer progression by mutant p53 is inhibited by the circular RNA circ-Ccnb1. *Cell Death Differ.* 25, 2195–2208. doi: 10.1038/s41418-018-0115-6
- Gao, S., Yu, Y., Liu, L., Meng, J., and Li, G. (2019). Circular RNA hsa_circ_0007059 restrains proliferation and epithelial-mesenchymal transition in lung cancer cells via inhibiting microRNA-378. *Life Sci.* 233:116692. doi: 10.1016/j.lfs.2019.116692
- Gu, C., Zhou, N., Wang, Z., Li, G., Kou, Y., Yu, S., et al. (2018). CircGprc5a promoted bladder oncogenesis and metastasis through Gprc5a-targeting peptide. *Mol. Ther. Nucleic Acids* 13, 633–641.
- Gu, X., Wang, G., Shen, H., and Fei, X. (2019). Hsa_circ_0033155: a potential novel biomarker for non-small cell lung cancer. *Exp. Ther. Med.* 16, 3220–3226. doi: 10.3892/etm.2018.6565
- Gualandi, F., Trabanello, C., Rimessi, P., Calzolari, E., Toffolatti, L., Patarnello, T., et al. (2003). Multiple exon skipping and RNA circularisation contribute to the severe phenotypic expression of exon 5 dystrophin deletion. *J. Med. Genet.* 40:e100. doi: 10.1136/jmg.40.8.e100
- Guarnerio, J., Bezzi, M., Jeong, J. C., Paffenholz, S. V., Berry, K., Naldini, M. M., et al. (2016). Oncogenic role of fusion-circRNAs derived from cancer-associated chromosomal translocations. *Cell* 165, 289–302. doi: 10.1016/j.cell.2016.03.020
- Han, J., Zhao, G., Ma, X., Dong, Q., Zhang, H., Wang, Y., et al. (2018). CircRNA circ-BANP-mediated miR-503/LARP1 signaling contributes to lung cancer progression. *Biochem. Biophys. Res. Commun.* 503, 2429–2435. doi: 10.1016/j.bbrc.2018.06.172
- Han, W., Wang, L., Zhang, L., Wang, Y., and Li, Y. (2019). Circular RNA circ-RAD23B promotes cell growth and invasion by miR-593-3p/CCND2 and miR-653-5p/TIAM1 pathways in non-small cell lung cancer. *Biochem. Biophys. Res. Commun.* 510, 462–466. doi: 10.1016/j.bbrc.2019.01.131
- Hansen, T. B., Jensen, T. I., Clausen, B. H., Bramsen, J. B., Finsen, B., Damgaard, C. K., et al. (2013). Natural RNA circles function as efficient microRNA sponges. *Nature* 495, 384–388. doi: 10.1038/nature11993
- Holdt, L. M., Stahringer, A., Sassm, K., Pichler, G., Kulak, N. A., Wilfert, W., et al. (2016). Circular non-coding RNA ANRIL modulates ribosomal RNA maturation and atherosclerosis in humans. *Nat. Commun.* 7:12429. doi: 10.1038/ncomms12429
- Hong, W., Xue, M., Jiang, J., Zhang, Y., and Gao, X. (2020). Circular RNA circ-CPA4/let-7 miRNA/PD-L1 axis regulates cell growth, stemness, drug resistance and immune evasion in non-small cell lung cancer (NSCLC). *J. Exp. Clin. Cancer Res.* 39:149. doi: 10.1186/s13046-020-01648-1
- Huang, M. S., Yuan, F. Q., Gao, Y., Liu, J. Y., Chen, Y. X., Wang, C. J., et al. (2019). Circular RNA screening from EIF3a in lung cancer. *Cancer Med.* 8, 4159–4168. doi: 10.1002/cam4.2338
- Huang, Q., Wang, S., Li, X., Yang, F., Feng, C., Zhong, K., et al. (2019). Circular RNA ATXN7 is upregulated in non-small cell lung cancer and promotes disease progression. *Oncol. Lett.* 17, 4803–4810. doi: 10.3892/ol.2019.10168
- Huang, S., Li, X., Zheng, H., Si, X., Li, B., Wei, G., et al. (2019). Loss of super-enhancer-regulated circRNA Nfix induces cardiac regeneration after myocardial infarction in adult mice. *Circulation* 139, 2857–2876. doi: 10.1161/CIRCULATIONAHA.118.038361
- Huang, W., Yang, Y., Wu, J., Niu, Y., Yao, Y., Zhang, J., et al. (2019). Circular RNA cESRP1 sensitises small cell lung cancer cells to chemotherapy by sponging miR-93-5p to inhibit TGF- β signalling. *Cell Death Differ.* 27, 1709–1727. doi: 10.1038/s41418-019-0455-x
- Ivanov, A., Memczak, S., Wyler, E., Torti, F., Porath, H. T., Orejuela, M. R., et al. (2015). Analysis of intron sequences reveals hallmarks of circular RNA biogenesis in animals. *Cell Rep.* 10, 170–177. doi: 10.1016/j.celrep.2014.12.019
- Jeck, W. R., Sorrentino, J. A., Wang, K., Slevin, M. K., Burd, C. E., Liu, J., et al. (2013). Circular RNAs are abundant, conserved, and associated with ALU repeats. *RNA* 19, 141–157. doi: 10.1261/rna.035667.112
- Jiang, M., Mai, Z., Wan, S., Chi, Y., Zhang, X., Sun, B., et al. (2018). Microarray profiles reveal that circular RNA hsa_circ_0007385 functions as an oncogene in non-small cell lung cancer tumorigenesis. *J. Cancer Res. Clin. Oncol.* 144, 667–674. doi: 10.1007/s00432-017-2576-2
- Jin, M., Shi, C., Yang, C., Liu, J., and Huang, G. (2019). Upregulated circRNA ARHGAP10 predicts an unfavorable prognosis in NSCLC through regulation of the miR-150-5p/GLUT-1 Axis. *Mol. Ther. Nucleic Acids* 18, 219–231. doi: 10.1016/j.omtn.2019.08.016
- Joseph, N. A., Chiou, S. H., Lung, Z., Yang, C., Lin, T., Chang, H., et al. (2018). The role of HGF-MET pathway and CCDC66 circRNA expression in EGFR resistance and epithelial-to-mesenchymal transition of lung adenocarcinoma cells. *J. Hematol. Oncol.* 11:74. doi: 10.1186/s13045-018-0557-9
- Kelly, S., Greenman, C., Cook, P. R., and Papantonis, A. (2015). Exon skipping is correlated with exon circularization. *J. Mol. Biol.* 427, 2414–2417. doi: 10.1016/j.jmb.2015.02.018
- Kris, M. G., Gaspar, L. E., Chaft, J. E., Kennedy, E. B., Azzoli, C. G., Ellis, P. M., et al. (2017). Adjuvant systemic therapy and adjuvant radiation therapy for Stage I to IIIA completely resected non-small-cell lung cancers: american society of clinical oncology/cancer care ontario clinical practice guideline update. *J. Clin. Oncol.* 35, 2960–2974. doi: 10.1200/JCO.2017.72.4401
- Lasda, E., and Parker, R. (2014). Circular RNAs: diversity of form and function. *RNA* 20, 1829–1842. doi: 10.1261/rna.047126.114
- Li, C., Liu, H., Niu, Q., and Gao, J. (2020). Circ_0000376, a Novel circRNA, promotes the progression of non-small cell lung cancer through regulating the miR-1182/NOVA2 network. *Cancer Manag. Res.* 12, 7635–7647. doi: 10.2147/CMAR.S258340
- Li, Y., Zhang, J., Pan, S., Zhou, J., Diao, X., and Liu, S. (2020). CircRNA CDR1as knockdown inhibits progression of non-small-cell lung cancer by regulating miR-219a-5p/SOX5 axis. *Thorac. Cancer* 11, 537–548. doi: 10.1111/1759-7714.13274

- Li, L., Li, W., Chen, N., Zhao, H., Xu, G., Zhao, Y., et al. (2019). FLI1 exonic circular RNAs as a novel oncogenic driver to promote tumor metastasis in small cell lung cancer. *Clin. Cancer Res.* 25, 1302–1317. doi: 10.1158/1078-0432.CCR-18-1447
- Li, X., Liu, Y., Zhou, J., Li, W., Guo, H., and Ma, H. (2019). Enhanced expression of circular RNA hsa_circ_000984 promotes cells proliferation and metastasis in non-small cell lung cancer by modulating Wnt/ β -catenin pathway. *Eur. Rev. Med. Pharmacol. Sci.* 23, 3366–3374. doi: 10.26355/eurrev_201904_17700
- Li, Y., Yu, J., Liu, Z., Yang, H., Tang, J., and Chen, Z. (2019). Programmed death Ligand 1 indicates pre-existing adaptive immune response by tumor-infiltrating CD8+ T Cells in non-small cell lung cancer. *Int. J. Mol. Sci.* 20:5138. doi: 10.3390/ijms20205138
- Li, X., Zhang, Z., Jiang, H., Li, Q., Wang, R., Pan, H., et al. (2018). Circular RNA circPVT1 promotes proliferation and invasion through sponging miR-125b and activating E2F2 signaling in non-small cell lung cancer. *Cell Physiol. Biochem.* 51, 2324–2340. doi: 10.1159/000495876
- Li, Y., Hu, J., Li, L., Cai, S., Zhang, H., Zhu, X., et al. (2018). Upregulated circular RNA circ_0016760 indicates unfavorable prognosis in NSCLC and promotes cell progression through miR-1287/GAGE1 axis. *Biochem. Biophys. Res. Commun.* 503, 2089–2094. doi: 10.1016/j.bbrc.2018.07.164
- Li, Z., Huang, C., Bao, C., Chen, L., Lin, M., Wang, X., et al. (2015). Exon-intron circular RNAs regulate transcription in the nucleus. *Nat. Struct. Mol. Biol.* 22, 256–264. doi: 10.1038/nsmb.2959
- Liang, W. C., Wong, C. W., Liang, P. P., Shi, M., Cao, Y., Rao, S. T., et al. (2019). Translation of the circular RNA circ(β -catenin promotes liver cancer cell growth through activation of the Wnt pathway. *Genome Biol.* 20:84.
- Liang, Z., Guo, C., Zou, M., Meng, P., and Zhang, T. (2020). CircRNA-miRNA-mRNA regulatory network in human lung cancer: an update. *Cancer Cell Int.* 20:173. doi: 10.1186/s12935-020-01245-4
- Liu, C., Zhang, Z., and Qi, D. (2019). Circular RNA hsa_circ_0023404 promotes proliferation, migration and invasion in non-small cell lung cancer by regulating miR-217/ZEB1 axis. *Onco. Targets Ther.* 12, 6181–6189. doi: 10.2147/OTT.S201834
- Liu, G., Shi, H., Deng, L., Zheng, H., Kong, W., Wen, X., et al. (2019). Circular RNA circ-FOXO1 facilitates cell progression as ceRNA to target PDPF and MACC1 by sponging miR-1304-5p in non-small cell lung cancer. *Biochem. Biophys. Res. Commun.* 513, 207–212. doi: 10.1016/j.bbrc.2019.03.213
- Liu, Y., Han, X., Xing, P., Hu, X., Hao, X., Wang, Y., et al. (2019). Circular RNA profiling identified as a biomarker for predicting the efficacy of Gefitinib therapy for non-small cell lung cancer. *J. Thorac. Dis.* 11, 1779–1787. doi: 10.21037/jtd.2019.05.22
- Liu, L., Wang, J., Khanabadi, R., Kalionis, B., Tai, X., and Xia, S. (2017). Circular RNAs: isolation, characterization and their potential role in diseases. *RNA Biol.* 14, 1715–1721. doi: 10.1080/15476286.2017.1367886
- Liu, T., Song, Z., and Gai, Y. (2018). Circular RNA circ_0001649 acts as a prognostic biomarker and inhibits NSCLC progression via sponging miR-331-3p and miR-338-5p. *Biochem. Biophys. Res. Commun.* 503, 1503–1509. doi: 10.1016/j.bbrc.2018.07.070
- Liu, W., Ma, W., Yuan, Y., Zhang, Y., and Sun, S. (2018). Circular RNA hsa_circRNA_103809 promotes lung cancer progression via facilitating ZNF121-dependent MYC expression by sequestering miR-4302. *Biochem. Biophys. Res. Commun.* 500, 846–851. doi: 10.1016/j.bbrc.2018.04.172
- Liu, X., Wang, X., Li, J., Hu, S., Deng, Y., Yin, H., et al. (2020). Identification of mecciRNAs and their roles in the mitochondrial entry of proteins. *Sci. China Life Sci.* 63, 1429–1449. doi: 10.1007/s11427-020-1631-9
- Lu, H., Han, X., Ren, J., Ren, K., Li, Z., and Sun, Z. (2020). Circular RNA HIPK3 induces cell proliferation and inhibits apoptosis in non-small cell lung cancer through sponging miR-149. *Cancer Biol. Ther.* 21, 113–121. doi: 10.1080/15384047.2019.1669995
- Luo, Y., Zhu, X., Huang, K., Zhang, Q., Fan, Y., Yan, P., et al. (2017). Emerging roles of circular RNA hsa_circ_0000064 in the proliferation and metastasis of lung cancer. *Biomed. Pharmacother.* 96, 892–898. doi: 10.1016/j.biopha.2017.12.015
- Ma, X., Yang, X., Bao, W., Li, S., Liang, S., Sun, Y., et al. (2018). Circular RNA circMAN2B2 facilitates lung cancer cell proliferation and invasion via miR-1275/FOXK1 axis. *Biochem. Biophys. Res. Commun.* 498, 1009–1015. doi: 10.1016/j.bbrc.2018.03.105
- Melosky, B., Juergens, R., McLeod, D., Leighl, N., Brade, A., Card, P. B., et al. (2019). Immune checkpoint-inhibitors and chemoradiation in stage III unresectable non-small cell lung cancer. *Lung Cancer* 134, 259–267. doi: 10.1016/j.lungcan.2019.05.027
- Nan, A., Chen, L., Zhang, N., Jia, Y., Li, X., Zhou, H., et al. (2018). Circular RNA circNOL10 inhibits lung cancer development by promoting SCLM1-mediated transcriptional regulation of the humanin polypeptide family. *Adv. Sci.* 6:1800654. doi: 10.1002/adv.201800654
- Pamudurti, N. R., Bartok, O., Jens, M., Ashwal-Fluss, R., Stottmeister, C., Ruhe, L., et al. (2017). Translation of CircRNAs. *Mol. Cell.* 66, 9.e7–21.e7. doi: 10.1016/j.molcel.2017.02.021
- Pan, H., Li, T., Jiang, Y., Pan, C., Ding, Y., Huang, Z., et al. (2018). Overexpression of circular RNA ciRS-7 abrogates the tumor suppressive effect of miR-7 on gastric cancer via PTEN/PI3K/AKT signaling pathway. *J. Cell Biochem.* 119, 440–446. doi: 10.1002/jcb.26201
- Qin, S., Zhao, Y., Lim, G., Lin, H., Zhang, X., and Zhang, X. (2019). Circular RNA PVT1 acts as a competing endogenous RNA for miR-497 in promoting non-small cell lung cancer progression. *Biomed. Pharmacother.* 111, 244–250. doi: 10.1016/j.biopha.2018.12.007
- Qiu, B., Zhang, P., Xiong, D., Xu, J., Long, X., Zhu, S., et al. (2019). CircRNA fibroblast growth factor receptor 3 promotes tumor progression in non-small cell lung cancer by regulating Galectin-1-AKT/ERK1/2 signaling. *J. Cell Physiol.* 234, 11256–11264. doi: 10.1002/jcp.27783
- Qiu, M., Xia, W., Chen, R., Wang, S., Xu, Y., Ma, Z., et al. (2018). The circular RNA circPRKCI promotes tumor growth in lung adenocarcinoma. *Cancer Res.* 78, 2839–2851. doi: 10.1158/0008-5472.CAN-17-2808
- Qu, D., Yan, B., Xin, R., and Ma, T. (2018). A novel circular RNA hsa_circ_0020123 exerts oncogenic properties through suppression of miR-144 in non-small cell lung cancer. *Am. J. Cancer Res.* 8, 1387–1402.
- Salmanidis, M., Pillman, K., Goodall, G., and Bracken, C. (2014). Direct transcriptional regulation by nuclear microRNAs. *Int. J. Biochem. Cell Biol.* 54, 304–311. doi: 10.1016/j.biocel.2014.03.010
- Sanger, H. L., Klotz, G., Riesner, D., Gross, H. J., and Kleinschmidt, A. K. (1976). Viroids are single-stranded covalently closed circular RNA molecules existing as highly base-paired rod-like structures. *Proc. Natl. Acad. Sci. U.S.A.* 73, 3852–3856.
- Siegel, R. L., Miller, K. D., and Jemal, A. (2017). Cancer statistics, 2017. *CA Cancer J. Clin.* 67, 7–30. doi: 10.3322/caac.21387
- Suzuki, H., and Tsukahara, T. (2014). A view of pre-mRNA splicing from RNase R resistant RNAs. *Int. J. Mol. Sci.* 15, 9331–9342. doi: 10.3390/ijms15069331
- Tan, S., Sun, D., Pu, W., Gou, Q., Guo, C., Gong, Y., et al. (2018). Circular RNA F-circEA-2a derived from EML4-ALK fusion gene promotes cell migration and invasion in non-small cell lung cancer. *Mol. Cancer* 17:138. doi: 10.1186/s12943-018-0887-9
- Tian, F., Yu, C., Ye, W., and Wang, Q. (2017). Cinnamaldehyde induces cell apoptosis mediated by a novel circular RNA hsa_circ_0043256 in non-small cell lung cancer. *Biochem. Biophys. Res. Commun.* 493, 1260–1266. doi: 10.1016/j.bbrc.2017.09.136
- Tong, S. (2020). Circular RNA SMARCA5 may serve as a tumor suppressor in non-small cell lung cancer. *J. Clin. Lab Anal.* 34:e23195. doi: 10.1002/jcla.23195
- Wan, J., Hao, L., Zheng, X., and Li, Z. (2019). Circular RNA circ_0020123 promotes non-small cell lung cancer progression by acting as a ceRNA for miR-488-3p to regulate ADAM9 expression. *Biochem. Biophys. Res. Commun.* 515, 303–309. doi: 10.1016/j.bbrc.2019.05.158
- Wan, L., Zhang, L., Fan, K., Cheng, Z., Sun, Q., and Wang, J. (2016). Circular RNA-ITCH suppresses lung cancer proliferation via inhibiting the Wnt/ β -Catenin pathway. *Biomed. Res. Int.* 2016:1579490. doi: 10.1155/2016/1579490
- Wang, L., Tong, X., Zhou, Z., Wang, S., Lei, Z., Zhang, T., et al. (2018). Circular RNA hsa_circ_0008305 (circPTK2) inhibits TGF- β -induced epithelial-mesenchymal transition and metastasis by controlling TIF1 γ in non-small cell lung cancer. *Mol. Cancer* 17:140. doi: 10.1186/s12943-018-0889-7
- Wang, C., Tan, S., Liu, W., Lei, Q., Qiao, W., Wu, Y., et al. (2019a). RNA-Seq profiling of circular RNA in human lung adenocarcinoma and squamous cell carcinoma. *Mol. Cancer* 18:134. doi: 10.1186/s12943-019-1061-8
- Wang, J., Zhu, M., Pan, J., Chen, C., Xia, S., and Song, Y. (2019b). Circular RNAs: a rising star in respiratory diseases. *Respir. Res.* 20:3. doi: 10.1186/s12931-018-0962-1
- Wang, L., Long, H., Zheng, Q., Bo, X., Xiao, X., and Li, B. (2019c). Circular RNA circRHOT1 promotes hepatocellular carcinoma progression by initiation of NR2F6 expression. *Mol. Cancer* 18:119. doi: 10.1186/s12943-019-1046-7
- Wang, L., Ma, H., Kong, W., Liu, B., and Zhang, X. (2019d). Up-regulated circular RNA VANGL1 contributes to progression of non-small cell lung cancer through inhibition of miR-195 and activation of Bcl-2. *Biosci. Rep.* 39:BSR20182433. doi: 10.1042/BSR20182433

- Wang, S., Zhang, Y., Cai, Q., Ma, M., Jin, L., Weng, M., et al. (2019e). Circular RNA FOXP1 promotes tumor progression and Warburg effect in gallbladder cancer by regulating PKLR expression. *Mol. Cancer* 18:145. doi: 10.1186/s12943-019-1078-z
- Wang, T., Wang, X., Du, Q., Wu, N., Liu, X., Chen, Y., et al. (2019f). The circRNA circP4HB promotes NSCLC aggressiveness and metastasis by sponging miR-133a-5p. *Biochem. Biophys. Res. Commun.* 513, 904–911. doi: 10.1016/j.bbrc.2019.04.108
- Wang, Y., Li, H., Lu, H., and Qin, Y. (2019g). Circular RNA SMARCA5 inhibits the proliferation, migration, and invasion of non-small cell lung cancer by miR-19b-3p/HOXA9 axis. *Onco. Targets Ther.* 12, 7055–7065. doi: 10.2147/OTT.S216320
- Wang, Y., Li, Y., He, H., and Wang, F. (2019h). Circular RNA circ-PRMT5 facilitates non-small cell lung cancer proliferation through upregulating EZH2 via sponging miR-377/382/498. *Gene* 720:144099. doi: 10.1016/j.gene.2019.144099
- Wang, J., and Li, H. (2018). CircRNA circ_0067934 silencing inhibits the proliferation, migration and invasion of NSCLC cells and correlates with unfavorable prognosis in NSCLC. *Eur. Rev. Med. Pharmacol. Sci.* 22, 3053–3060. doi: 10.26355/eurrev_201805_15063
- Wei, S., Zheng, Y., Jiang, Y., Li, X., Geng, J., Shen, Y., et al. (2019). The circRNA circPTPRA suppresses epithelial-mesenchymal transitioning and metastasis of NSCLC cells by sponging miR-96-5p. *EBioMedicine*. 44, 182–193. doi: 10.1016/j.ebiom.2019.05.032
- Wu, K., Liao, X., Gong, Y., He, J., Zhou, J., Tan, S., et al. (2019). Circular RNA F-circSR derived from SLC34A2-ROS1 fusion gene promotes cell migration in non-small cell lung cancer. *Mol. Cancer* 18:98. doi: 10.1186/s12943-019-1028-9
- Xia, X., Li, X., Li, F., Wu, X., Zhang, M., Zhou, H., et al. (2019). A novel tumor suppressor protein encoded by circular AKT3 RNA inhibits glioblastoma tumorigenicity by competing with active phosphoinositide-dependent Kinase-1. *Mol. Cancer* 18:131.
- Xu, N., Chen, S., Liu, Y., Li, W., Liu, Z., Bian, X., et al. (2018). Profiles and bioinformatics analysis of differentially expressed circRNAs in taxol-resistant non-small cell lung cancer cells. *Cell Physiol. Biochem.* 48, 2046–2060. doi: 10.1159/000492543
- Yang, Q., Du, W., Wu, N., Yang, W., Awan, F. M., Fang, L., et al. (2017). A circular RNA promotes tumorigenesis by inducing c-myc nuclear translocation. *Cell Death Differ.* 24, 1609–1620. doi: 10.1038/cdd.2017.86
- Yang, Y., Fan, X., Mao, M., Song, X., Wu, P., Zhang, Y., et al. (2017). Extensive translation of circular RNAs driven by N6-methyladenosine. *Cell Res.* 27, 626–641. doi: 10.1038/cr.2017.31
- Yang, Z., Awan, F., Du, W., Zeng, Y., Lyu, J., Wu, D., et al. (2017). The circular RNA interacts with STAT3, increasing its nuclear translocation and wound repair by modulating Dnmt3a and miR-17 function. *Mol. Ther.* 25, 2062–2074. doi: 10.1016/j.yimthe.2017.05.022
- Yang, Y., Gao, X., Zhang, M., Yan, S., Sun, C., Xiao, F., et al. (2018). Novel role of FBXW7 circular RNA in repressing glioma tumorigenesis. *J. Natl. Cancer Inst.* 110, 304–315. doi: 10.1093/jnci/djx166
- Yao, J., Zhao, S., Liu, Q., Lv, M., Zhou, D., Liao, Z., et al. (2017). Over-expression of CircRNA_100876 in non-small cell lung cancer and its prognostic value. *Pathol. Res. Pract.* 213, 453–456. doi: 10.1016/j.prp.2017.02.011
- Yu, H., Chen, Y., and Jiang, P. (2018). Circular RNA HIPK3 exerts oncogenic properties through suppression of miR-124 in lung cancer. *Biochem. Biophys. Res. Commun.* 506, 455–462. doi: 10.1016/j.bbrc.2018.10.087
- Zhang, C., Zhang, B., Yuan, B., Chen, C., Zhou, Y., Zhang, Y., et al. (2020). RNA-Seq profiling of circular RNAs in human small cell lung cancer. *Epigenomics* 12, 685–700. doi: 10.2217/epi-2019-0382
- Zhang, H., Wang, X., Hu, B., Zhang, F., Wei, H., and Li, L. (2019). Circular RNA ZFR accelerates non-small cell lung cancer progression by acting as a miR-101-3p sponge to enhance CUL4B expression. *Artif. Cells Nanomed. Biotechnol.* 47, 3410–3416. doi: 10.1080/21691401.2019.1652623
- Zhang, P., Pei, X., Li, K., Jin, L., Wang, F., Wu, J., et al. (2019). Circular RNA circFGFR1 promotes progression and anti-PD-1 resistance by sponging miR-381-3p in non-small cell lung cancer cells. *Mol. Cancer* 18:179. doi: 10.1186/s12943-019-1111-2
- Zhang, M., Huang, N., Yang, X., Luo, J., Yan, S., Xiao, F., et al. (2018a). A novel protein encoded by the circular form of the SHPRH gene suppresses glioma tumorigenesis. *Oncogene* 37, 1805–1814. doi: 10.1038/s41388-017-0019-9
- Zhang, M., Zhao, K., Xu, X., Yang, Y., Yan, S., Wei, P., et al. (2018b). A peptide encoded by circular form of LINC-PINT suppresses oncogenic transcriptional elongation in glioblastoma. *Nat. Commun.* 9:4475.
- Zhang, Y., Zhao, H., and Zhang, L. (2018c). Identification of the tumor-suppressive function of circular RNA FOXO3 in non-small cell lung cancer through sponging miR-155. *Mol. Med. Rep.* 17, 7692–7700. doi: 10.3892/mmr.2018.8830
- Zhang, Y., Zhang, X., Chen, T., Xiang, J., Yin, Q., Xing, Y., et al. (2013). Circular intronic long noncoding RNAs. *Mol. Cell* 51, 792–806. doi: 10.1016/j.molcel.2013.08.017
- Zhao, F., Han, Y., Liu, Z., Zhao, Z., Li, Z., and Jia, K. (2018). circFADS2 regulates lung cancer cells proliferation and invasion via acting as a sponge of miR-498. *Biosci. Rep.* 38:BSR20180570. doi: 10.1042/BSR20180570
- Zhao, J., Lee, E. E., Kim, J., Yang, R., Chamseddin, B., Ni, C., et al. (2019). Transforming activity of an oncoprotein-encoding circular RNA from human papillomavirus. *Nat. Commun.* 10:2300.
- Zheng, X., Chen, L., Zhou, Y., Wang, Q., Zheng, Z., Xu, B., et al. (2019). A novel protein encoded by a circular RNA circPPP1R12A promotes tumor pathogenesis and metastasis of colon cancer via Hippo-YAP signaling. *Mol. Cancer* 18:47.
- Zhi, X., Zhang, J., Cheng, Z., Bian, L., and Qin, J. (2019). CircLgr4 drives colorectal tumorigenesis and invasion through Lgr4-targeting peptide. *Int. J. Cancer* [Epub ahead of print]. doi: 10.1002/ijc.32549
- Zhong, Y., Du, Y., Yang, X., Mo, Y., Fan, C., Xiong, F., et al. (2018). Circular RNAs function as ceRNAs to regulate and control human cancer progression. *Mol. Cancer* 17:79. doi: 10.1186/s12943-018-0827-8
- Zhou, J., Zhang, S., Chen, Z., He, Z., Xu, Y., and Li, Z. (2019). CircRNA-ENO1 promoted glycolysis and tumor progression in lung adenocarcinoma through upregulating its host gene ENO1. *Cell Death Dis.* 10:885. doi: 10.1038/s41419-019-2127-7
- Zhou, Y., Zheng, X., Xu, B., Chen, L., Wang, Q., Deng, H., et al. (2019). Circular RNA hsa_circ_0004015 regulates the proliferation, invasion, and TKI drug resistance of non-small cell lung cancer by miR-1183/PDPK1 signaling pathway. *Biochem. Biophys. Res. Commun.* 508, 527–535. doi: 10.1016/j.bbrc.2018.11.157
- Zhu, X., Wang, X., Wei, S., Chen, Y., Chen, Y., Fan, X., et al. (2017). hsa_circ_0013958: a circular RNA and potential novel biomarker for lung adenocarcinoma. *Febs J.* 284, 2170–2182. doi: 10.1111/febs.14132
- Zong, L., Sun, Q., Zhang, H., Chen, Z., Deng, Y., Li, D., et al. (2018). Increased expression of circRNA_102231 in lung cancer and its clinical significance. *Biomed. Pharmacother.* 102, 639–644. doi: 10.1016/j.biopha.2018.03.084

Conflict of Interest: The authors declare that the research was conducted in the absence of any commercial or financial relationships that could be construed as a potential conflict of interest.

Copyright © 2021 Feng, Zhou, Wang, Lin, Lai, Chu and Wang. This is an open-access article distributed under the terms of the Creative Commons Attribution License (CC BY). The use, distribution or reproduction in other forums is permitted, provided the original author(s) and the copyright owner(s) are credited and that the original publication in this journal is cited, in accordance with accepted academic practice. No use, distribution or reproduction is permitted which does not comply with these terms.



The m⁶A Reader YTHDF1 Facilitates the Tumorigenesis and Metastasis of Gastric Cancer via USP14 Translation in an m⁶A-Dependent Manner

Xiao-Yu Chen[†], Rui Liang[†], You-Cai Yi, Hui-Ning Fan, Ming Chen, Jing Zhang^{*†} and Jin-Shui Zhu^{*†}

Department of Gastroenterology, Shanghai Jiao Tong University Affiliated Sixth People's Hospital, Shanghai, China

OPEN ACCESS

Edited by:

Hehuang Xie,
Virginia Tech, United States

Reviewed by:

Jinghao Sheng,
Zhejiang University, China
Jiangbo Wei,
University of Chicago, United States

*Correspondence:

Jing Zhang
jing5522724@vip.163.com
Jin-Shui Zhu
zhujs1803@163.com

[†]These authors have contributed
equally to this work

[‡]These authors have contributed
equally to this work

Specialty section:

This article was submitted to
Epigenomics and Epigenetics,
a section of the journal
Frontiers in Cell and Developmental
Biology

Received: 30 December 2020

Accepted: 23 February 2021

Published: 15 March 2021

Citation:

Chen X-Y, Liang R, Yi Y-C,
Fan H-N, Chen M, Zhang J and
Zhu J-S (2021) The m⁶A Reader
YTHDF1 Facilitates the Tumorigenesis
and Metastasis of Gastric Cancer via
USP14 Translation in an
m⁶A-Dependent Manner.
Front. Cell Dev. Biol. 9:647702.
doi: 10.3389/fcell.2021.647702

Objectives: N⁶-methyladenosine (m⁶A) RNA methylation is implicated in the progression of multiple cancers via influencing mRNA modification. YTHDF1 can act as an oncogene in gastric cancer (GC), while the biological mechanisms via which YTHDF1 regulates gastric tumorigenesis through m⁶A modification remain largely unknown.

Methods: GEO and TCGA cohorts were analyzed for differentially expressed m⁶A modification components in GC clinical specimens and their association with clinical prognosis. Transwell and flow cytometry assays as well as subcutaneous xenograft and lung metastasis models were used to evaluate the phenotype of YTHDF1 in GC. Intersection of RNA/MeRIP-seq, luciferase assay, RIP-PCR, RNA pull-down and MeRIP-PCR was used to identify YTHDF1- modified USP14 and its m⁶A levels in GC cells.

Results: High-expressed YTHDF1 was found in GC tissues and was related to poor prognosis, acting as an independent prognostic factor of poor survival in GC patients. YTHDF1 deficiency inhibited cell proliferation and invasion (*in vitro*), and gastric tumorigenesis and lung metastasis (*in vivo*) and also induced cell apoptosis. Intersection assays revealed that YTHDF1 promoted USP14 protein translation in an m⁶A-dependent manner. USP14 upregulation was positively correlated with YTHDF1 expression and indicated a poor prognosis in GC.

Conclusion: Our data suggested that m⁶A reader YTHDF1 facilitated tumorigenesis and metastasis of GC by promoting USP14 protein translation in an m⁶A-dependent manner and might provide a potential target for GC treatment.

Keywords: tumorigenesis, N⁶-methyladenosine, metastasis, gastric cancer, YTHDF1, USP14

Abbreviations: 3'-UTR, 3'-prime untranslated region; AR, androgen receptor; DEGs, differentially expressed genes; Co-IP, Co-immunoprecipitation; GC, gastric cancer; GEO, Gene Expression Omnibus; GO, Gene ontology; GSEA, gene set enrichment analysis; IHC, immunohistochemistry; KEGG, Kyoto Encyclopedia of Genes and Genomes; m⁶A, N⁶-methyladenosine; MeRIP, Methylated RNA immune-precipitation; NC, negative control; PBS, phosphate buffered saline; RT-qPCR, quantitative real-time PCR; RIP, RNA immunoprecipitation; TCGA, The Cancer Genome Atlas; TMA, Tissue microarray; USP14, Ubiquitin-specific protease 14.

INTRODUCTION

According to the global cancer statistics, gastric cancer (GC) is regarded as one of the most invasive cancers and is the third leading factor of tumor-associated deaths (Bray et al., 2018). Past decades have witnessed great progress in diagnostic and therapeutic methods of GC including targeted therapy, and immunotherapy (Ajani et al., 2017). However, the prognosis of patients with GC, especially metastatic cases, is still unfavorable due to the aggressiveness of the tumor. Hence, we urgently need to obtain novel biomarkers for early screening and treatment of GC.

N⁶-methyladenosine (m⁶A) is a member of chemical modifications commonly and abundantly found in eukaryotic mRNAs, and its modification is a dynamic and reversible process (Jia et al., 2011). The m⁶A RNA modification is initiated by the m⁶A methyltransferases complex (“writers”) including METTL3/14, WTAP, RBM15/15B, and KIAA1429, reversed by demethylases (FTO and ALKBH5, named “erasers”), and identified by m⁶A binding proteins (YTHDF1/2/3, IGF2BP1, HNRNPA2B1, and BCDIN3D, termed as “readers”) (Chen et al., 2019). Recent studies have indicated that the m⁶A modification is involved in tumor progression and acts as tumor-promoting or suppressive factors in multiple malignancies (Lin et al., 2016; Ma et al., 2017; Liu J. et al., 2018; Chen et al., 2019). METTL3 enhances metastasis of GC by m⁶A modification of ZMYM1/E-cadherin signaling, and WTAP results in a poor clinical prognosis of GC through regulating tumor-related immune infiltration (Yue et al., 2019; Li H. et al., 2020). YTHDF1 (m⁶A “reader”) can be used to predict poor prognosis in breast cancer and promotes FDZ5 translation, leading to hepatocellular carcinoma progression (Anita et al., 2020; Liu X. et al., 2020). YTHDF1 can bind to mammalian mRNAs and alter the protein translation process in a m⁶A-dependent manner. For example, it can modulate the translational efficiency of cyclin-dependent kinases in lung adenocarcinomas (Shi et al., 2019), EIF3C in ovarian cancer (Liu T. et al., 2020), and lysosomal cathepsins in melanoma and colorectal cancer (Han D. et al., 2019).

YTHDF1 has been reported to facilitate gastric carcinogenesis by controlling FDZ7 translation (Pi et al., 2020). Herein, we observed the significant upregulation of YTHDF1 in GC tissue samples and its increased expression was associated with poor prognosis, acting as an independent prognostic factor in patients with GC. Knockdown of YTHDF1 repressed GC cell growth and metastasis *in vitro* and *in vivo*. Intersection co-analysis for RNA-seq, Methylated RNA immune-precipitation (MeRIP)-seq/qPCR, Co-immunoprecipitation (Co-IP), RNA immunoprecipitation (RIP)-qPCR, luciferase analysis and RNA pull-down revealed that YTHDF1 facilitated USP14 translation via a m⁶A-dependent way, and USP14 upregulation harbored a positive correlation with YTHDF1 expression and indicated a poor prognosis in GC.

MATERIALS AND METHODS

Clinical Data

The clinichological data of GC patients as well as the relative expression levels of YTHDF1, and proteasomal protein

catabolic process-related factors (USP14, ANKIB1, ARIH1, ATXN3, GABARAPL2, NUB1, PRKACA, PSMC1, SIRT2, TLK2, UBQLN1, and WAC) were obtained from Gene Expression Omnibus (GEO) database ($n = 592$, including datasets GSE29272, GSE14210, GSE15459, GSE22377, and GSE51105)¹ and The Cancer Genome Atlas (TCGA) RNA-seq database ($n = 292$)². The protocols used in our study were approved by the Ethics Committee of the Shanghai Sixth People's Hospital. The comprehensive clinical and pathological information of GC patients for YTHDF1 expression are summarized in **Tables 1, 2** and **Supplementary Tables S1, S2**.

Tissue Microarray and Immunohistochemistry Analysis

Human microarrays (TMA) from GC were purchased from Shanghai Outdo Biotech Co. Ltd. (Shanghai, China). TMA1 contained 80 pairs of tumors and matched adjacent tissues (**Supplementary Tables S3, S4**) and TMA2 included 28 tumors and matched adjacent tissues. Signed written informed consent was obtained and patient's personal data were deleted. The expression and cellular localization of YTHDF1 and USP14 in GC tissues were detected by immunohistochemistry (IHC) analysis. The GC tissues were stained with anti-YTHDF1 (ab230330, Abcam, United States) and anti-USP14 (ab71165, Abcam, United States) antibodies. The IHC assay involved the following steps: 3 mm thick sections were used in IHC examinations, and were unmasked with sodium citrate-hydrochloric acid buffer (10 mM, pH 6.0) at 90°C for 30 min. Afterward, the sections were incubated with 0.03% hydrogen peroxide for 10 min to eliminate the effect of endogenous peroxidase activity. Next, incubate the sections with blocking serum for 30 min at room temperature. The blocking serum was composed of 0.04% bovine serum albumin (A2153, Sigma-Aldrich, Shanghai, China) and 0.5% normal goat serum (X0907, Dako Corporation, Carpinteria, CA, United States) in phosphate buffered saline (PBS) solution. After dilution of anti-YTHDF1 (1:100, ab230330, Abcam, United States) and anti-USP14 (1:500, ab71165, Abcam, United States) antibodies, they were used for incubation of slides overnight at 4°C. Next, PBS was used to wash sections 3 times for 5 min each. Finally, 0.5% casein and 5% normal serum were added to block non-specific staining for 30 min at room temperature, and the sections were stained with diaminobenzidine substrate and hematoxylin. The tissue slides were evaluated under a microscope (Nikon ECLIPSE Ci) and pictures were scanned by PANNORAMIC MIDI (3DHISTECH, Hungary) and acquired using CaseViewer_2.0 (v2.0.2.61392, 3DHISTECH, Hungary). The histochemistry score as quantification of protein expression was analyzed using DensitoQuant 1.15.4 of QuantCenter (3DHISTECH, Hungary) (Azim et al., 2015; Yeo et al., 2015). IHC scoring was evaluated by two independent clinical pathologists.

¹<http://kmplot.com/analysis/>

²<https://genome-cancer.ucsc.edu>

RNA Extraction and Real-Time Quantitative PCR

Total RNA was extracted from GC cell lines using TRIzol reagent (Invitrogen, Thermo Fisher Scientific, United States). The cDNA was synthesized from RNA using the PrimeScript™ RT kit (RR037A, Takara, Japan). TB Green™ Premix Ex Taq™ II kit (RR820A, Takara, Japan) and QuantStudio 7 Flex were used in real-time quantitative PCR (RT-qPCR) based on the manufacturer's guidelines. The mRNA expression levels of target genes were measured using the $2^{-\Delta \Delta C_t}$ method. β -ACTIN was used as control to normalize mRNA expression. The primers used are listed in **Supplementary Table S5**.

Cell Culture

The human GC cell line AGS was purchased from Shanghai Institute of Biochemistry and Cell Biology. Other human GC cell lines (MKN-28, HGC-27, BGC-823, SGC-7901) and the normal human gastric epithelial cell line GES-1 were obtained from stocks at Digestive Disease Laboratory of Shanghai Sixth People's Hospital. These cell lines were tested to be free of Mycoplasma and were maintained in Ham's F-12K (Kaighn's) Medium (Gibco, United States) or Roswell Park Memorial Institute 1640 medium (Hyclone, Logan, Utah) supplemented with 10% heat-inactivated fetal bovine serum (Gibco, United States), 100 μ g/mL of streptomycin and 100 U/mL of penicillin (Penicillin-Streptomycin-Glutamine, Gibco, United States) in a humidified incubator containing 5% CO₂ at a temperature of 37°C. Cells were treated with 100 μ M IU1 (Selleck, Houston, TX, United States) wherever mentioned.

Western Blotting

GC cells were obtained and extracted using Radio Immunoprecipitation Assay Lysis buffer (Beyotime, Shanghai, China) and equal volumes of GC cells extracted solution were separated on 7.5 and 10% SDS-PAGE gels (EpiZyme, Shanghai, China). The protein bands were transferred from SDS-PAGE gels to PVDF membranes (Millipore PVDF 0.45 μ m). The primary antibodies anti-YTHDF1 (ab230330, Abcam, United States), anti-USP14 (ab71165, Abcam, United States), and anti- β -actin (Proteintech, IL, United States) were added at a dilution of 1:500 or 1:1,000 according to the manufacturer's instructions and incubated at 4°C overnight. The secondary antibodies (horseradish peroxidase [HRP] rabbit IgG) were diluted 1:3,000 and incubated with the membranes at room temperature for 2 h. The membranes were washed thrice with Tris-Buffered Saline with Tween-20, and the immunoreactive bands were developed using SuperSignal West Dura Extended Duration Substrate (Thermo Fisher Scientific, IL, United States) based on established protocols. These experiments were repeated more than three times.

Cell Transfection and Lentiviral Infection

The steps of transient transfection and lentiviral infection were performed as described previously (Liu H. et al., 2018). Plasmid-mediated USP14 (NM_005151) vector, and lentiviral vectors for YTHDF1 knockdown and overexpression (NM_017798)

TABLE 1 | Correlation of YTHDF1 expression with clinicopathological parameters in GC patients (GSE29272).

Variables	Cases (n)	YTHDF1 expression		P
		Low (%)	High (%)	
Age				
≤60	75	52 (69.3)	23 (30.7)	0.1675
>60	51	41 (80.4)	10 (19.6)	
Gender				
Male	99	75 (75.8)	24 (24.2)	0.3428
Female	27	18 (66.7)	9 (33.3)	
Tumor grade				
1~2	45	32 (71.1)	13 (28.9)	0.609
3	81	61 (75.3)	20 (24.7)	
Pathological stage				
I/II	10	10 (100.0)	0 (0.0)	0.0619
III/IV	116	83 (71.6)	33 (28.4)	
Lymph node metastasis				
No	26	21 (80.8)	5 (19.2)	0.333
Yes	98	70 (71.4)	28 (28.6)	
Unknown	2	2 (100.0)	0 (0.0)	
Family history of upper gastrointestinal cancer				
No	97	69 (71.1)	28 (28.9)	0.2134
Yes	29	24 (82.8)	5 (17.2)	
Lesion				
GNCA	71	60 (84.5)	11 (15.5)	0.002**
GCA	55	33 (60.0)	22 (40.0)	

**P < 0.01; GNCA, gastric non-cardia adenocarcinomas; GCA, gastric cardia adenocarcinomas.

were purchased from Genechem (Shanghai, China) and an empty vector was used as the negative control (NC). The m⁶A binding site mutated USP14 vector was obtained from RiboBio (Guangzhou, China) with mutation from A to C at No.721 sequence site. The additional details relative to overexpression plasmids of USP14 and YTHDF1 are presented in **Supplementary Table S6**. The target sequence of the two shRNA (shYTHDF1) were 5'-CGAAAGAGTTTGAGTGGAA-3' and 5'-TCGTTACATCAGAAGGATA-3' (**Supplementary Table S7**).

Cell Proliferation, Migration, and Invasion Assays

Transwell migration and invasion assays were conducted as previously described (Liu H. et al., 2018). Cell proliferation was detected using a CCK-8 assay kit (Dojindo Corp, Japan) and colony formation. These experiments were repeated at least three times. CCK-8 assay: 1×10^3 cells were seeded in a 96-well plate. After cells culture for 0, 24, 48, 72, and 96 h, dyeing solution containing 10 μ L CCK-8 reagent and 90 μ L culture medium were added directly to each well. The cells were then incubated at 37°C for 1 h, and the optional density was measured at 450 nm. Colony formation: GC tumor cells were trypsinized before collection for counting and a total of $1-3 \times 10^3$ cells were plated in 6-well plates and cultured at 37°C in an incubator for 7 days. After washing three times using PBS and fixed with 4% paraformaldehyde,

TABLE 2 | Cox regression analysis of YTHDF1 as potential overall survival predictor (GSE29272).

Variables	Univariate cox regression analysis		Multivariate cox regression analysis	
	RR (95% CI)	P-value	RR (95% CI)	P-value
Age (years, ≤ 60 vs. > 60)	0.777 (0.515–1.173)	0.229	NA	NA
Gender (Male vs. Female)	1.164 (0.715–1.895)	0.541	NA	NA
Tumor grade (I + II vs. III)	0.721 (0.467–1.111)	0.138	NA	NA
Pathological stage (I + II vs. III + IV)	0.777 (0.359–1.681)	0.522	NA	NA
Family history of upper gastrointestinal cancer (No vs. Yes)	0.831 (0.506–1.364)	0.463	NA	NA
Lesion (GNCA vs. GCA)	0.864 (0.572–1.304)	0.486	NA	NA
Lymph node metastasis (No vs. Yes)	0.355 (0.197–0.639)	0.001**	0.354 (0.196–0.639)	0.001**
YTHDF1 (Low vs. High)	0.607 (0.386–0.954)	0.03*	0.607 (0.386–0.955)	0.031*

* $P < 0.05$; ** $P < 0.01$.

RR, relative risk; NA, not analyzed; GNCA, gastric non-cardia adenocarcinomas; GCA, gastric cardia adenocarcinomas.

colonies were stained by 0.1% crystal violet solution. Cell colonies were then imaged, counted and analyzed.

Flow-Cytometric Analysis

Cell apoptosis assays and cell cycle assays were performed and three separate experiments were performed for each clone. For cell apoptosis assays: cells were trypsinized and washed with cold PBS (4°C), and then resuspended in Annexin V Binding Buffer in accordance with the manufacturer's instructions for the APC Annexin V Apoptosis Detection Kit with 7-AAD (Biolegend, San Diego, CA, United States). Five microliter APC Annexin and 7-AAD Viability Staining Solution were added to the cells in the dark conditions, respectively, and incubate at room temperature (25°C) for 15 min. A volume of 400 µL of Annexin V Binding Buffer was then added to each tube before the flow cytometry analysis on a CytoFLEX flow cytometer (Beckman Coulter, CA, United States). Cell apoptosis was analyzed using the CytoFLEX-CytExpert Software 2.4 (Beckman Coulter, CA, United States). For cell cycle assays: after washing cells twice in cold PBS and RNase incubation for 30 min at 37°C, the fixed cells were dyed by PI (Cell Cycle DNA Content Quantitation Assay, Solarbio, Beijing, China) for 30 min at room temperature in the dark. Each sample was then filtered through a 50 µm nylon strainer to obtain single-cell suspension. The samples were then analyzed on CytoFLEX flow cytometer (Beckman Coulter, CA, United States). FlowJo 10.4 software (Becton, Dickinson & Company, NJ, United States) was used for cell cycle analysis.

Animal Models

The animal experiments were approved by the Ethics Committee of Shanghai Jiao Tong University Affiliated Sixth People's Hospital. For the subcutaneous xenotransplanted tumor model, BALB/c nude mice (15 mice, 5–6 weeks old) were purchased from JRDUN Biotechnology (Shanghai, China) and fed in specific-pathogen-free animal houses. BGC-823 cells (5×10^6) with shRNAs targeting YTHDF1 (sh-YTHDF1) or shRNAs targeting control (sh-NC) were trypsinized and suspended in 0.1 mL PBS and injected subcutaneously into the BALB/c mice ($n = 5$ mice per group). For the subcutaneous-injected mice, the volume of xenograft growth was examined by measuring tumor width

and length every 3 days [volume = (length \times width²)/2]. After 5 weeks, mice were sacrificed, and the tumor weight was recorded. Tissues were paraffin-embedded, dissected, and stained with hematoxylin-eosin. For the pulmonary metastasis model, mice were randomly divided into 2 groups ($n = 4$ per group) and 2×10^6 cells were injected into the tail vein of the BALB/c nude mice. After 4 weeks, mice were sacrificed and lungs were extracted and fixed 4% paraformaldehyde in PBS. The number of metastatic lung tumors from GC cells was further counted. Tissues were paraffin-embedded, dissected, and stained with hematoxylin-eosin.

RNA-Seq

Total RNA was isolated from stable YTHDF1 control or knockdown AGS cells using Trizol reagent (Invitrogen) according to the manual's instruction. Poly(A) mRNA purification was followed and extracted from 50 to 100 ng total RNA using NEB Next® Poly(A) mRNA Magnetic Isolation Module. The library establishment and next generation sequencing (NGS) were performed by Aksomics (Shanghai, China). Every group was sequenced in triplicate.

RNA Immunoprecipitation (RIP) Assay

RIP assay was carried out by using a RNA Immunoprecipitation Kit (Genesee Biotech, Guangzhou, China). According to the manufacturer's instructions, BGC-823 cells were seeded in T75 flasks at 70–80% confluence. 5 µg of YTHDF1 (ab220162, Abcam) antibody and a corresponding control rabbit IgG (2729, Cell Signaling Technology) were conjugated to Dynabeads (11203D, Thermo Fisher Scientific) by incubation for 2 h at 4°C, followed by washing 2 times and incubation with 450 µL supernatants of BGC-823 cells and 350 µL RIP buffer A (provided by RIP Kit) for 2 h at 4°C. After washing with 1 mL RIP buffer B (provided by RIP Kit) for 5 times, beads were resuspended in 300 µL Buffer E (provided by RIP Kit), followed by DNA digestion through DR Columns (provided by RIP Kit). Input and co-immunoprecipitated RNAs were extracted by DR Columns (provided by RIP Kit) and analyzed by RT-qPCR.

Methylated RNA Immune-Precipitation (MeRIP)-Seq and MeRIP-qPCR

Total RNAs were extracted from sh-YTHDF1 and sh-NC transfected AGS cells by using TRIzol reagent (Invitrogen). Seq-StarTM poly(A) mRNA Isolation Kit (Arraystar, Rockville, United States) was used to obtain complete mRNA. After fragmenting, RNA (100 nucleotides) was incubated with m⁶A antibody (ABE572, Merck Millipore, Germany) for immunoprecipitation based on the instructions of the MeRIP m⁶A Kit (Merck Millipore, Germany). The mRNA with m⁶A enrichment was then assayed using NGS or RT-qPCR. For NGS, RNA fragments were purified from m⁶A-MeRIP and sequenced with Illumina HiSeq X-10 after building the library with the NEBNext Ultra RNA library Prep kit for Illumina (New England BioLabs). The library establishment and NGS were performed by Aksonomics (Shanghai, China). MeRIP-qPCR was executed to measure the m⁶A levels of USP14 in GC cells. Primers targeting the m⁶A negative/positive site of MAP2K4 were used as the negative/positive control (Supplementary Table S5).

Co-immunoprecipitation (Co-IP)

BGC-823 cells were washed with PBS and incubated in 200 μ L lysis buffer (50 mM Tris-HCl, pH 7.5, 150 mM NaCl, 15 mM MgCl₂, 5 mM EDTA, and 0.1% NP-40) containing protease inhibitor Cocktail (Roche, Mannheim, Germany) for subsequent Co-IP. The cell lysates were incubated with specific antibodies against USP14 (ab71165, Abcam, United States) and YTHDF1 (ab220162, Abcam, United States) at 4°C for 2 h, then incubated with 2.5 mg Dynabeads Protein G magnetic beads (Thermo Fisher Scientific, 10004D) at 4°C overnight. The beads were separated and washed with cold PBS, and Western blotting analysis was performed.

Luciferase Reporter Assay

The fragment of wild-type USP14 CDS (USP14) containing predicted YTHDF1 target sites was amplified by PCR and cloned into pGL3 vector (Promega, United States), which included Firefly luciferase reporter genes. The wild-type YTHDF1 (YTHDF1-WT) was amplified by PCR and cloned into pcDNA3.1 vector. The mutant YTHDF1 (YTHDF1-MUT) was then generated by mutating the YTH domain of YTHDF1 using Gene Mutation Kit (Takara, JAPAN). Next, the YTHDF1-MUT or YTHDF1-WT plasmid were co-transfected with USP14 and pRL-TK vector which included Renilla luciferase reporter genes (Promega, United States) into AGS cells. The pcDNA3.1 vector was used as negative control. After 48 h, the cells were harvested, and the Firefly and Renilla luciferase activities were measured based on a dual-luciferase reporter assay system (Promega, United States). The relative luciferase activity was normalized to Renilla luciferase activity (F-Luc/R-Luc).

Biotin-Coupled Probe RNA Pull Down Assay

To confirm whether YTHDF1 protein could be pulled down from USP14 mRNA in GC cells, biotinylated-USP14 probe was synthesized by RiboBio (Guangzhou, China)

(Supplementary Table S8). BGC-823 cells (1×10^7) were lysed and incubated with biotin-labeled USP14 probe. Next, the biotin-coupled RNA complex was pulled down using streptavidin-coated magnetic beads adsorption. The enriched YTHDF1 was analyzed by western blot analysis.

Statistical Analysis

Each experiment was repeated at least 3 times. Statistical tests were performed using SPSS 22.0 (IBM, SPSS, Chicago, IL, United States) and GraphPad version 8.0 Prism (GraphPad Software, La Jolla, CA, United States). The continuous variables were described as the mean \pm standard deviations. Significant differences were evaluated via Student's unpaired *t*-test or the chi-square test for comparisons of two groups. For multiple groups, significant differences were analyzed by one-way ANOVA (followed by Tukey's honest test). Pearson's correlation coefficient analysis was used for analyzing correlations. Survival curves were generated using the Kaplan-Meier method and log-rank testing. A *p*-value less than 0.05 was considered statistically significant.

RESULTS

High Expression of YTHDF1 Indicated Poor Prognosis in Patients With GC

Recent studies have revealed m⁶A methylation components can act as tumor-associated factors, including “writers” (METTL3/14, WTAP and KIAA1429), “erasers” (FTO and ALKBH5), and “readers” (YTHDF1/2/3, HNRNPA2B1, BCDIN3D) (Lin et al., 2016; Ma et al., 2017; Liu J. et al., 2018; Chen et al., 2019). We herein measured the expression of these m⁶A-related members in 418 patients with GC from TCGA (*n* = 292) and GSE29272 (*n* = 126) databases (clinicopathological data shown in Tables 1, 2 and Supplementary Tables S1, S2). Compared with the adjacent normal tissues, KIAA1429, YTHDF1, and HNRNPA2B1 were upregulated in GC tissues from TCGA (Figure 1A). Furthermore, YTHDF1 expression was significantly increased both in gastric cardia adenocarcinoma (GCA) and gastric non-cardia adenocarcinoma (GNCA) according to the GSE29272 dataset compared with their pair-matched normal tissues (Figure 1B and Supplementary Figure S1A). The genetic alterations and copy numbers of *YTHDF1* were analyzed using the cBioPortal (cBio Cancer Genomics Portal³) (Cerami et al., 2012; Gao et al., 2013), which indicated that the *YTHDF1* gene was frequently amplified and the mRNA expression of *YTHDF1* had a positive correlation with its copy number in TCGA cohort (*P* < 0.001, *r* = 0.7106, Figure 1C). The *YTHDF1* gene was altered in 12.09% of 612 cases, including mutation (3 cases, 4.05%), amplification (59 cases, 79.73%), and multiple alterations (1 case, 1.35%) (Supplementary Figure S1B).

Furthermore, Kaplan-Meier survival analysis demonstrated that GC patients with high YTHDF1 expression possessed poorer overall survival (*P* = 0.0352, Supplementary Figure S1C). Consistently, the cases with YTHDF1-high expression displayed poor survival (Figure 1D) and tumor recurrence (Figure 1E)

³<http://www.cbioportal.org>

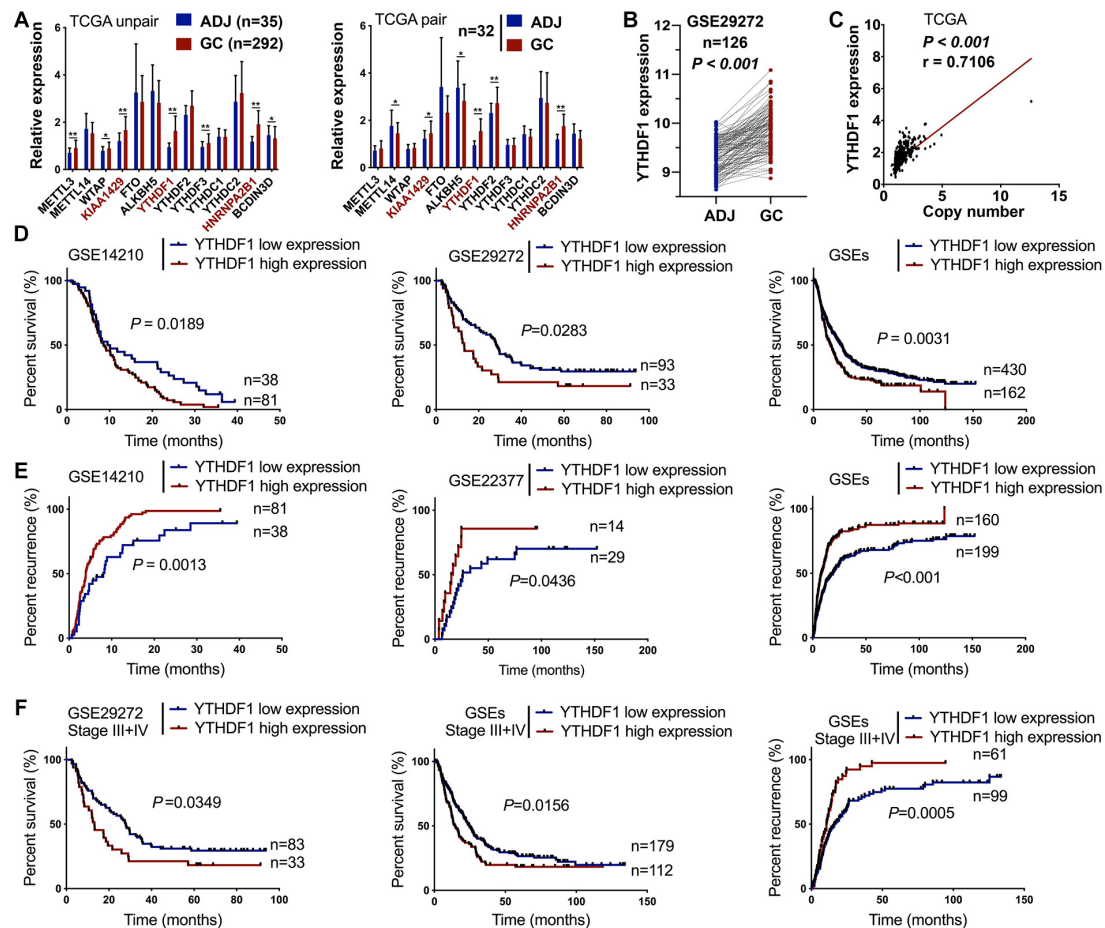


FIGURE 1 | High expression of YTHDF1 predicts a poor prognosis in patients with GC. **(A)** Gene expression of m⁶A-related compositions in patients with GC according to TCGA dataset (unpaired or paired). **(B)** Gene expression of YTHDF1 in patients with GC according to GSE29272 dataset (n = 126). **(C)** Correlation analysis between gene expression and the copy number status of YTHDF1 in TCGA-GC dataset. **(D,E)** Kaplan-Meier analysis of GC patients in GSEs dataset for the correlations between YTHDF1 expression and overall survival, as well as tumor recurrence. **(F)** Kaplan-Meier analysis of GC patients with Stage III and Stage IV in GSEs database. ADJ, adjacent normal; GC, gastric cancer. Data are shown as means \pm S.D. *P < 0.05, **P < 0.01.

as compared with those with low expression in GEO database. Although *YTHDF1* expression showed no significant differences at different stages both in TCGA and the GSE29272 dataset, GC patients in late stages (FIGO stage III or IV) rather than in early stages (FIGO stage I or II) with high *YTHDF1* expression tended to exhibit poor survival and tumor recurrence (Figure 1F and Supplementary Figures S2A–C). Therefore, these results indicated that YTHDF1 as a m⁶A reader was upregulated in GC tissues and was involved with a poor prognosis in GC patients.

Receiver operating characteristic (ROC) curve analysis was performed to determine the cutoff values of several m⁶A-related proteins (METTL3/14, YTHDF1/2, ALKBH5, FTO, and HNRNPAB1) in TCGA cohort (Supplementary Figure S1C). The area under the ROC curve (AUC), cutoff value, sensitivity, and specificity of YTHDF1 were 0.52, 10.16, 97.9, and 8.2%, respectively, in TCGA cohort (Supplementary Figure S1C), indicating that YTHDF1 was a promising clinical marker in GC patients. Up-expression of YTHDF1 was significantly associated with N stage (TCGA cohort, P = 0.019), cancer lesion (GEO

cohort, P = 0.002), and tumor size (TMA1, P = 0.015) in patients with GC (Table 1 and Supplementary Tables S1, S3). Moreover, univariate and multivariate Cox regression analyses suggested that YTHDF1 expression and lymph node metastasis were independent prognostic factors of poor survival in patients with GC from the GSE29272 dataset, while pathological stage and age were independent prognostic factors in TCGA cohort (Table 2 and Supplementary Tables S2, S4).

YTHDF1 Knockdown Repressed Proliferation and Invasion *in vivo* and *in vitro*

We analyzed the RNA expression level of *YTHDF1* using the Cancer Cell Line Encyclopedia⁴ database, in which AGS had the highest expression of YTHDF1 among GC cell lines (Supplementary Figure S3A). YTHDF1 protein expression

⁴<https://portals.broadinstitute.org/ccle>

was measured in various GC cell lines by western blotting analysis, which indicated that it was much higher in BGC-823, AGS, SGC-7901 cell lines than the normal gastric gland cell line GES-1 (Figure 2A). We then characterized the altered cellular phenotypes by establishing stable shRNA-expressing AGS and BGC-823 cell lines (Figure 2B). YTHDF1 silencing significantly impaired cell growth of AGS and BGC-823 cells as indicated by CCK-8 assays and colony formation assays (Figures 2C,D) and repressed cell migration and invasion abilities as indicated by the Transwell assay (Figures 2E,F). Flow-cytometric analysis showed that downregulation of YTHDF1 induced cell cycle arrest at the S phase (Supplementary Figure S3B) and cell apoptosis (Figure 2G and Supplementary Figure S3C) as compared with the sh-NC group in BGC-823 and AGS cells.

The oncogenic role of YTHDF1 in GC tumorigenesis was investigated by subcutaneous or tail vein injection with control cells or YTHDF1-deficient BGC-823 cells into immunocompromised nude mice (Figure 3A). Low YTHDF1 expression lead to delayed cell growth of BGC-823-engrafted tumors (Figures 3B,C), and the tumor weight and volume in YTHDF1 deficient tumors were reduced in comparison with the sh-NC group (Figures 3D,E). The effects of YTHDF1

knockdown on GC with lung metastasis were observed and the number of metastatic lung tumors from GC was markedly decreased in YTHDF1-deficient mice as compared with the sh-NC group (Figures 3F,G).

Transcriptome-Wide Identification of YTHDF1 Targets in GC Cells

In order to comprehensively discover the downstream mechanisms of YTHDF1 in GC tumorigenesis, we performed a RNA-seq analysis, which revealed obvious subsets of transcripts that were altered due to the downregulation of YTHDF1 in AGS cells ($P < 0.05$, Supplementary Table S9). Among these, 430 genes were altered with absolute value of $\log_2(\text{Fold Change}) > 0.585$, including 276 upregulated and 154 downregulated genes (Figure 4A and Supplementary Figures S4A,B). These altered genes were distributed in different position across chromosomes (Supplementary Figure S4C). Gene ontology (GO) analysis and gene set enrichment analysis (GSEA) were used to analyze the regulatory roles of YTHDF1 in GC. GO analysis revealed that the differentially-expressed genes (DEGs) regulated by YTHDF1 participated in cell proliferation, protease inhibitor complex activity, cell migration,

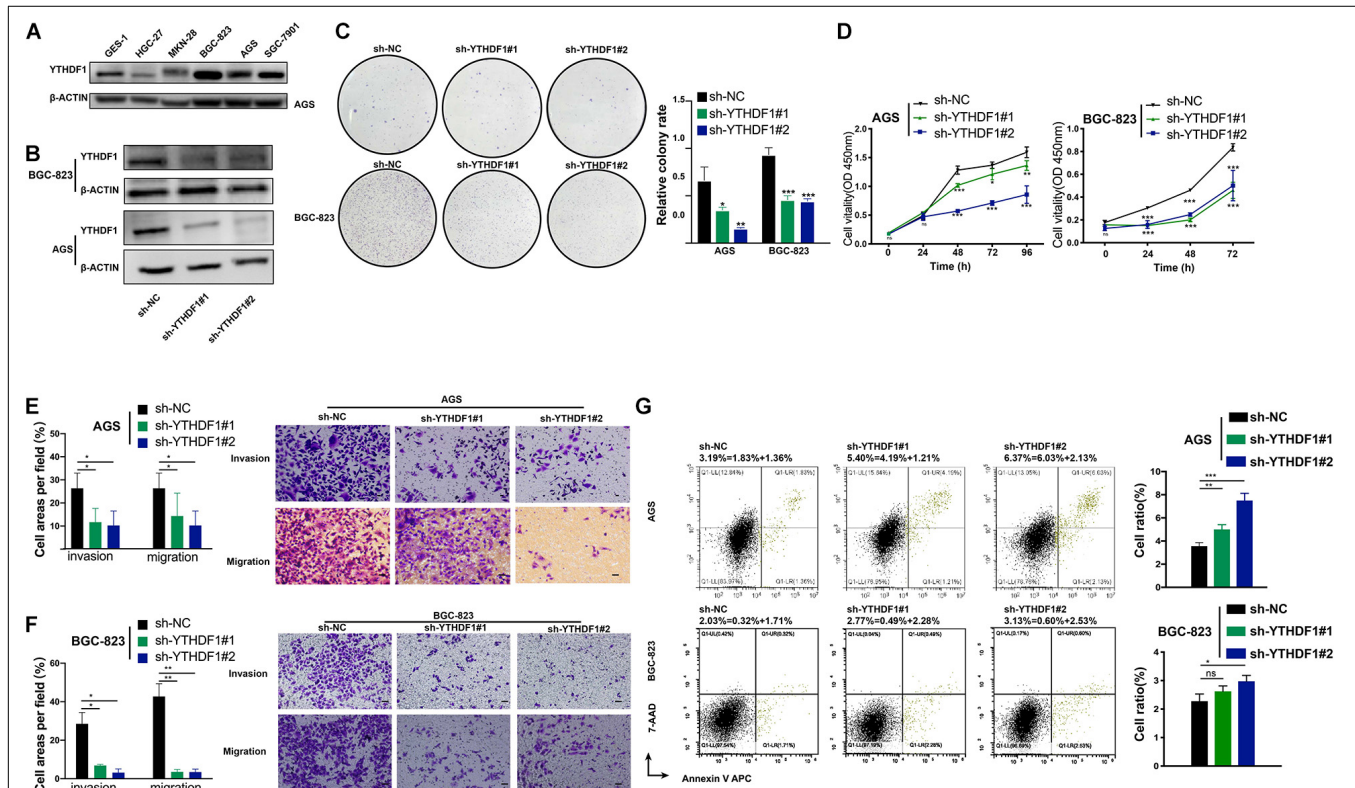
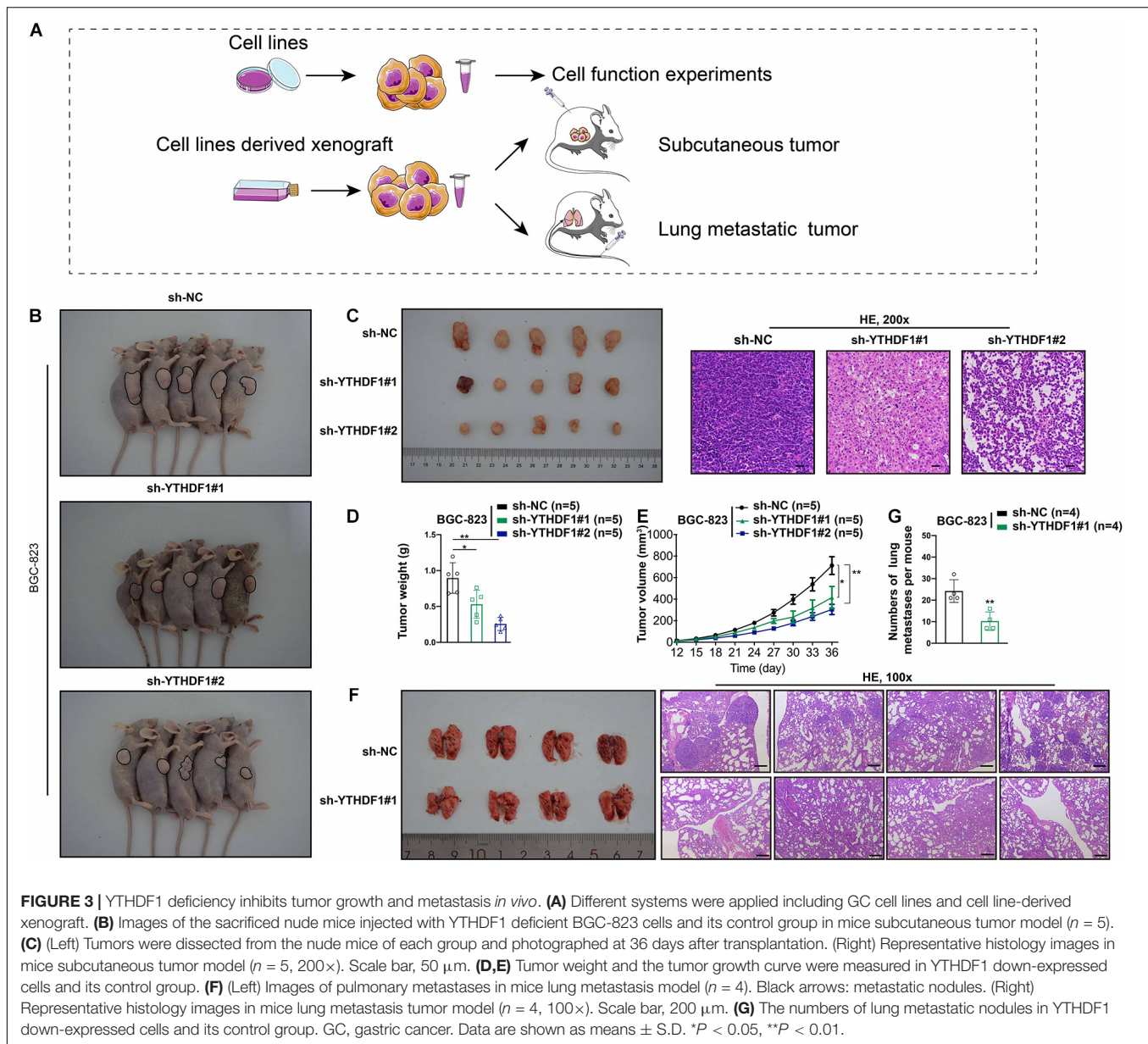


FIGURE 2 | Inhibition of YTHDF1 suppresses cell growth, migration and invasion *in vitro*. (A) Western blot analysis for YTHDF1 expression in GES-1 and GC cell lines (AGS, BGC-823, SGC-7901, MKN-28, and HGC-27). (B) Western blot analysis for YTHDF1 expression in AGS and BGC-823 cells infected with two independent shRNAs targeting YTHDF1 (sh-YTHDF1#1/2) or a control shRNA (sh-NC). (C) Colony formation assays of AGS and BGC-823 cells described in (B). (D) CCK8 assays were performed to determine cell growth in YTHDF1 deficient AGS and BGC-823 cells as described in (B). (E,F) Knockdown of YTHDF1 decreased the abilities of migration and invasion of AGS and BGC-823 cells. Scale bar, 50 μm . (G) Cell apoptosis analysis was used to compare down-expression of YTHDF1 (sh-YTHDF1#1/2) with the sh-NC group in BGC-823 and AGS cells. * $P < 0.05$, ** $P < 0.01$, *** $P < 0.001$; ns, no significance.



the Wnt signaling pathway, programmed cell death, ubiquitin-ubiquitin ligase activity and the ERK1 and ERK2 cascade (Figure 4B). GSEA analysis also indicated that YTHDF1 upregulated or downregulated target genes were related to mononuclear cell proliferation, phosphoprotein binding, protease binding, and epithelial cell migration (Figures 4C–G and Supplementary Figure S4D), suggesting that YTHDF1 could act as an oncogene in GC.

YTHDF1 can promote protein translation in a m⁶A-dependent manner (Wang et al., 2015). We then identified possible transcripts modified by m⁶A methylation in sh-YTHDF1 and sh-NC transfected AGS cells. Using m⁶A-seq analysis, we identified 6753 m⁶A peaks with significant dysregulation ($P < 0.05$, Supplementary Table S10). The m⁶A peaks were uniquely detected with the GUGAAACC

motifs ($P = 5.7 \times 10^{-13}$), mainly enriched in 3'UTR regions (Figures 4H,I), and were located on different chromosomes (Figure 4J). Functional annotation of these m⁶A-modified mRNAs suggested several obvious Kyoto Encyclopedia of Genes and Genomes (KEGG) gene clusters such as the Wnt signaling and MAPK signaling pathways (Supplementary Table S11).

USP14 Was a m⁶A Modification Target of YTHDF1 in GC Cells

RIP-seq has been used to screen YTHDF1-specific binding genes in Hela cells and 14,912 potential genes were found to bind with YTHDF1 (Wang et al., 2015). To explore the direct interactions between YTHDF1 and its targeted transcripts,

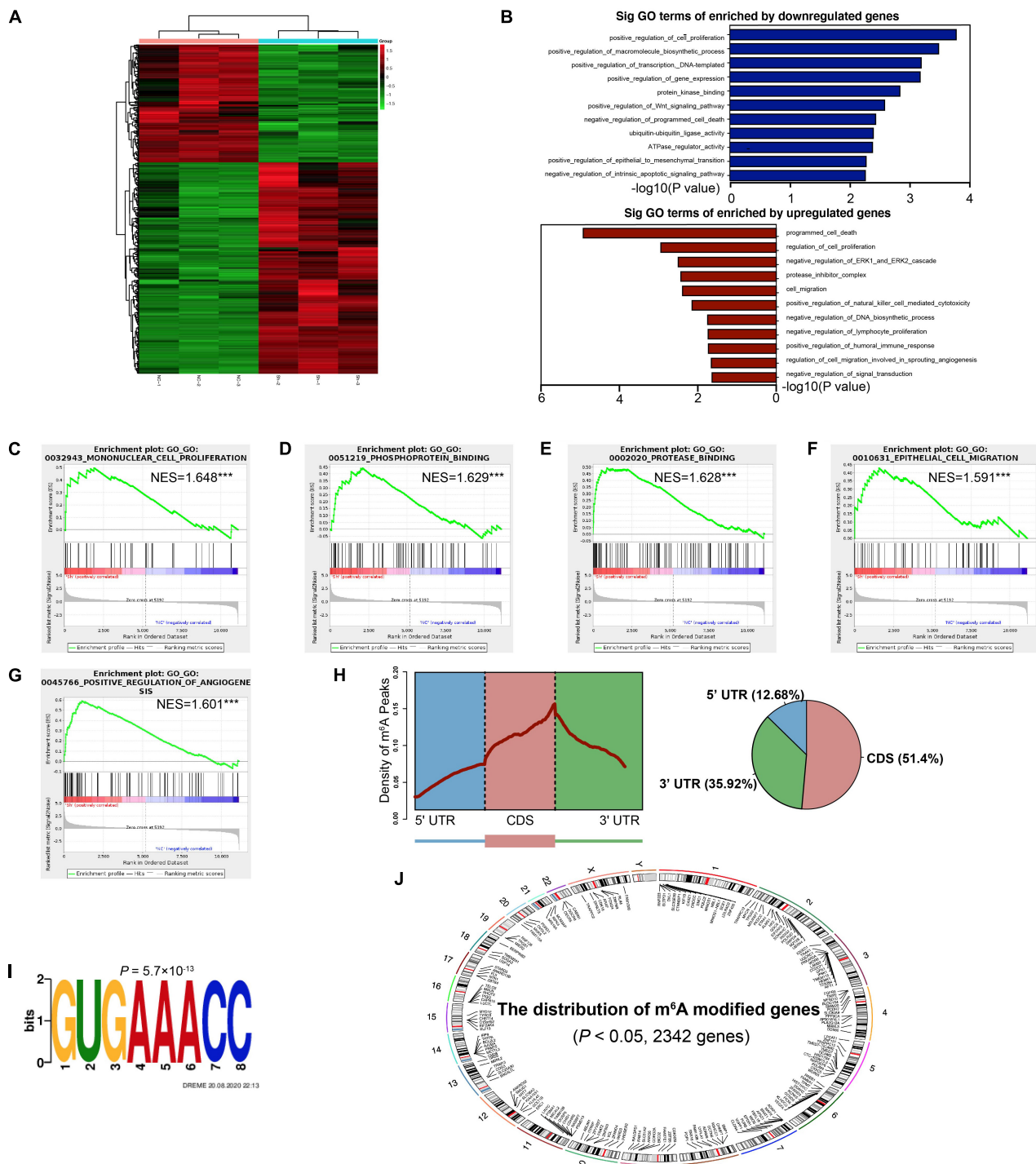


FIGURE 4 | Identification of the YTHDF1 targets in GC cells. **(A)** Heatmap of DEGs identified by RNA-seq. **(B)** GO enrichment analysis of DEGs. **(C–G)** GSEA plots showing the pathways of DEGs enriched by YTHDF1 were involved in GC cells. **(H)** Metagene profiles of m⁶A enrichment across mRNA transcriptome in BGC-823 cells. **(I)** The m⁶A motif detected by the DREME motif analysis with m⁶A-seq results. **(J)** The distribution of m⁶A peaks on different chromosomes. DEGs, differentially expressed genes; GC, gastric cancer; GO, Gene ontology; GSEA, gene set enrichment analysis. ****P* < 0.001.

the intersection co-analysis of RNA-seq, MeRIP-seq, and RIP-seq suggested that 2138 YTHDF1-binding genes were marked by m⁶A, among which 1,732 (81.01%) genes were not altered

under YTHDF1 deficiency as shown by RNA-seq (Figure 5A). These results demonstrated that YTHDF1 did not affect the RNA abundance of these 1732 targets in GC cells, which is

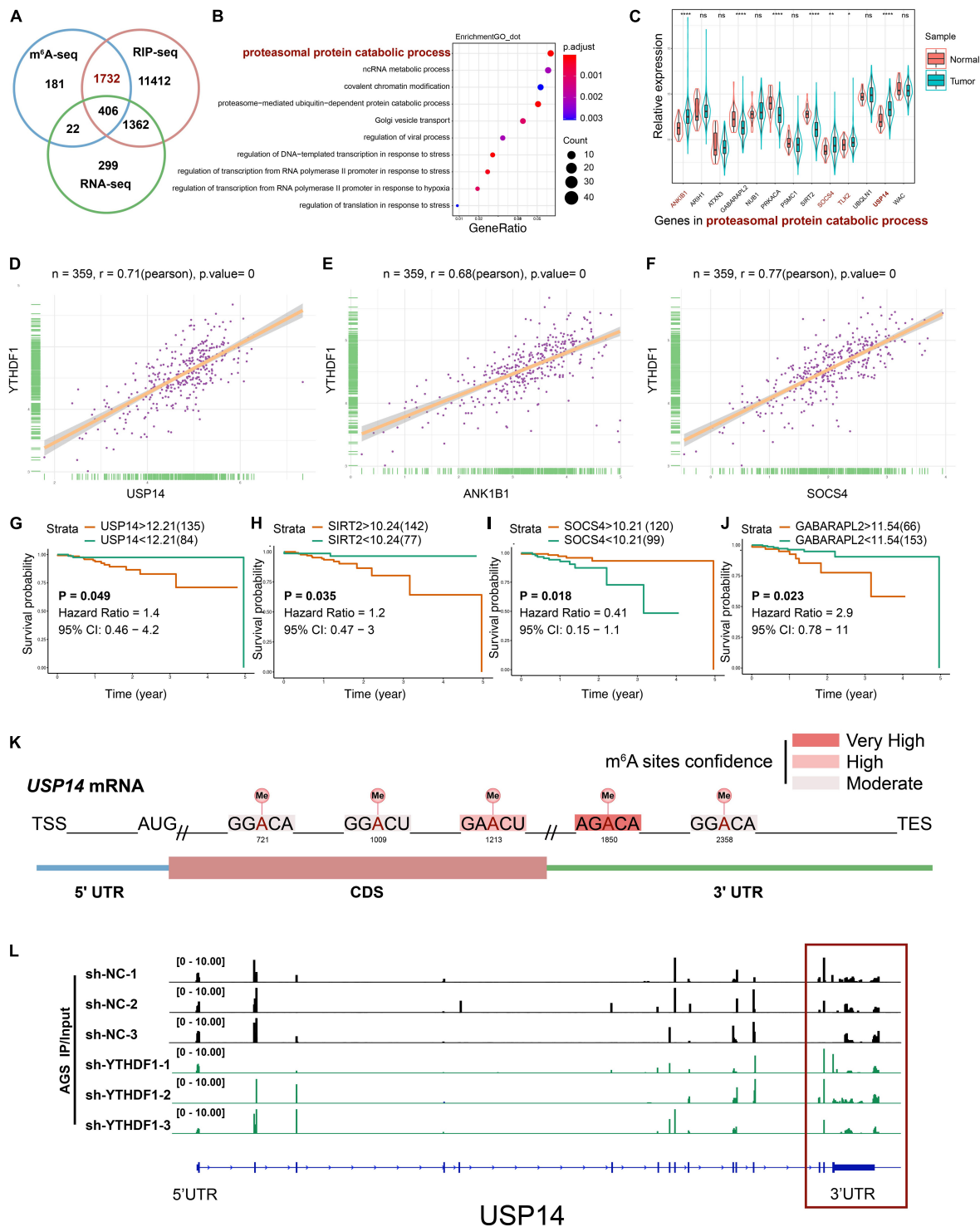


FIGURE 5 | USP14 as the m⁶A modification target of YTHDF1. **(A)** Overlapping analysis of genes identified by MeRIP-seq, RIP-seq, and RNA-seq. **(B)** GO analysis of genes described in (A). **(C)** The expression of genes related to proteasomal protein catabolic process in patients with GC according to TCGA dataset. **(D–F)** Correlation analysis between YTHDF1 expression and USP14, ANK1B1 and SOCS4 expression in TCGA-GC dataset. **(G–J)** Kaplan-Meier analysis of GC patients in TCGA dataset for the correlations between USP14/SIRT2/SOCS4/GABARAPL2 expression and overall survival. **(K)** Predicted m⁶A sites in USP14 mRNA by SRAMP program, especially in 3'UTR. **(L)** The m⁶A abundance on USP14 mRNA transcripts in sh-YTHDF1 and sh-NC infected AGS cells as examined by MeRIP-seq. Data represented the mean \pm SD. GC, gastric cancer; GO, Gene ontology; TCGA, The Cancer Genome Atlas; MeRIP, Methylated RNA immune-precipitation. Data are shown as means. * $P < 0.05$, ** $P < 0.01$, **** $P < 0.0001$; ns, no significance.

in accordance with previous findings that YTHDF1 regulates protein synthesis in a m⁶A-dependent manner in ovarian cancer (Liu T. et al., 2020). In addition, functional annotation confirmed the foregoing 1,732 genes were involved in multiple biological processes covering proteasomal protein catabolic processes (Figure 5B). The expression of these proteasomal protein catabolic process-related factors was analyzed in patients with GC according to TCGA dataset (Figure 5C). YTHDF1 exhibited a positive correlation with proteasomal protein catabolic process-related factors in GC tissue samples from TCGA cohort (Figures 5D–F and Supplementary Figure S5A), but showed an opposite tendency between gene expression and tumor prognosis, with only ubiquitin-specific protease 14 (USP14) upregulation indicating a shorter overall survival in patients with GC (Figures 5G–J and Supplementary Figure S5B). RNA m⁶A enrichment tended to locate at the 3'-UTR and near the stop codons of mRNA which contains the classic RRACH sequence (R = G/A and H = A/C/U) (Meyer et al., 2012; Yi et al., 2020). Analysis of USP14 mRNA with SRAMP program (Zhou et al., 2016) predicted the potential m⁶A sites on 3'UTR (Figure 5K and Supplementary Table S12), which was consistent with our results showing m⁶A peaks were located on USP14 mRNA in sh-YTHDF1 and sh-NC transfected AGS cells, especially on the 3'UTR as demonstrated by the MeRIP-seq findings (Figure 5L and Supplementary Figure S5C). USP14 as a component of proteasome-associated deubiquitinating enzyme complex can eliminate ubiquitins from proteasome-bound substrates and inhibit the proteasome non-catalytically (Chen et al., 2018). Consistently, StarBase2.0 predicted that USP14 mRNA can be enriched by YTHDF1 (ENCORI: The Encyclopedia of RNA Interactomes) (Li et al., 2014). These data suggested that USP14 was a m⁶A modification target of YTHDF1 in GC cells.

Upregulation of USP14 Reversed the Tumor Depressed Phenotype in YTHDF1-Knockdown GC Cells

In order to confirm whether YTHDF1 could affect USP14 protein translation in GC cells, we measured the effects of YTHDF1 on transcription and translation levels of USP14. We found that knockdown of YTHDF1 decreased the protein abundance of USP14 rather than its transcription levels in AGS and BGC-823 cells as expected by RT-qPCR and western blotting analysis (Figures 6A,B). Based on the Co-IP assay, YTHDF1 protein was not bound to USP14 protein in BGC-823 cells (Supplementary Figure S6A). Instead, RIP-qPCR of YTHDF1 was used to certify the interrelationship between YTHDF1 and USP14 mRNA and we found that USP14 RNA was enriched in YTHDF1 bound RNA in BGC-823 GC cells (Figure 6C). To further explore the effects of m⁶A modification on the status of USP14 mRNA, we used MeRIP-qPCR to indicate significant m⁶A enrichment sites in USP14 mRNA as compared with the control group in AGS cells (Figure 6D). To confirm the binding of USP14 mRNA with YTHDF1 protein, a RNA pull down assay was performed in BGC-823 cells using a biotinylated USP14 probe and showed that YTHDF1 was abundantly pulled down by the biotin-coupled

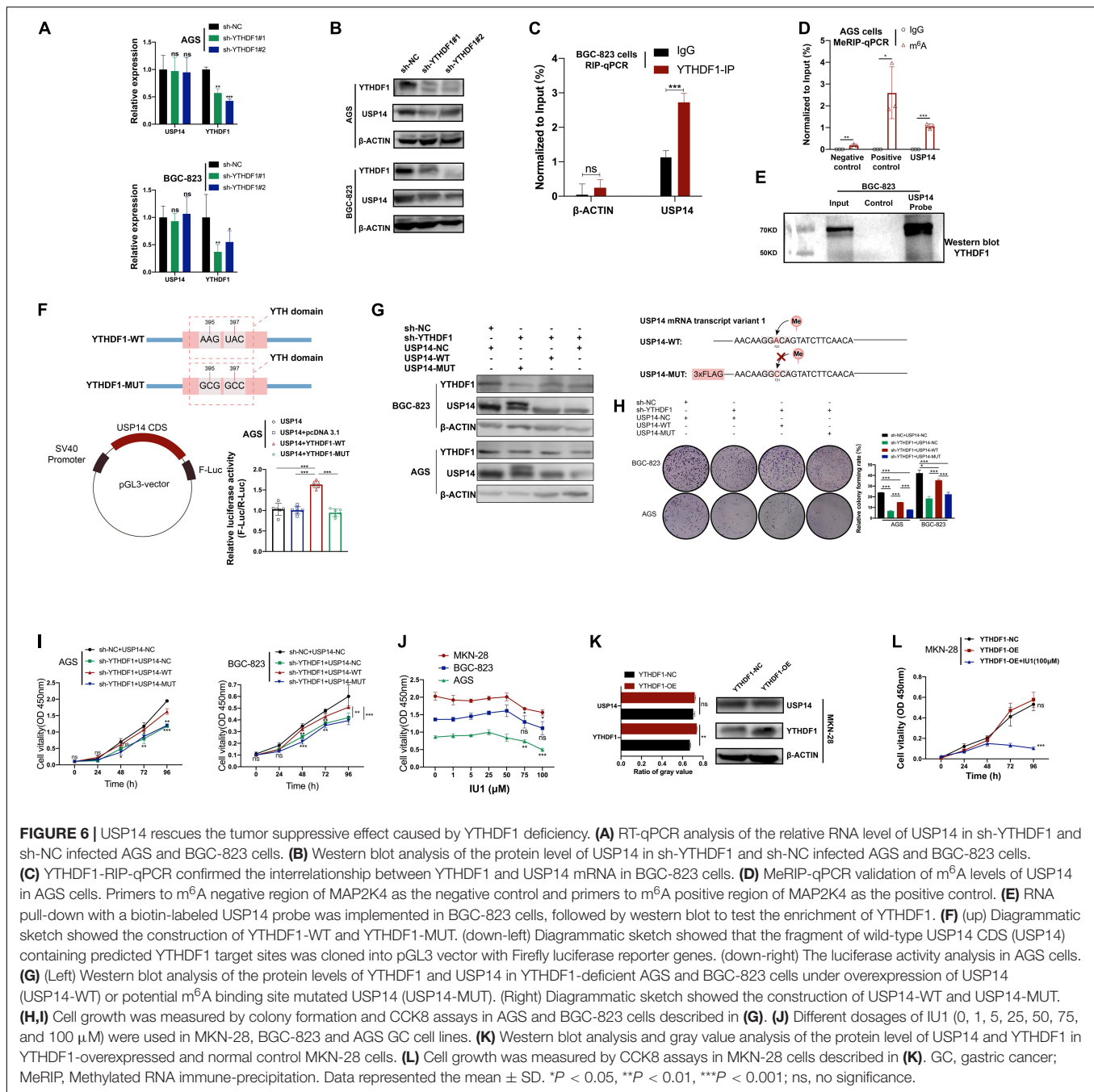
USP14 probe rather than the control probe in BGC-823 cells (Figure 6E). Additionally, we intended to construct a pGL3-USP14 vector with the USP14 CDS cloned into pGL3 vector with Firefly luciferase reporter genes. The luciferase assay showed that YTHDF1-WT rather than YTHDF1-MUT enhanced expression of USP14 in AGS cells (Figure 6F). These data illustrated that YTHDF1 could directly bind with USP14 mRNA and facilitated its protein translation in a m⁶A-dependent manner.

According to a previous study, silencing of USP14 induced GC cell apoptosis (Fu et al., 2018). We then investigated whether overexpression of USP14 could restore the delayed tumor progression phenotype in YTHDF1-deficient AGS and BGC-823 cells. The overexpression of USP14 in these two cell lines was determined by western blotting analysis (Supplementary Figure S6B). Knockdown of YTHDF1 suppressed cell growth and colony formation, while overexpression of USP14 could rescue sh-YTHDF1 expressing GC cells from these effects (Supplementary Figures S6C,D). Furthermore, according to SRAMP website prediction of m⁶A site on USP14 mRNA transcript variant 1 and the primer used in MeRIP-qPCR, we constructed the USP14-MUT vector linked with 3×FLAG (Figure 6G). Because of USP14-MUT vector with 3×FLAG (~2 kDa), two protein bands were endogenous USP14 and overexpressed USP14 protein with 3×FLAG, respectively (Figure 6G). We then used this potential m⁶A binding site mutated USP14 in the same experiments, which could not rescue the impaired effects caused by sh-YTHDF1 (Figures 6G–I). In addition, IU1, a small-molecule inhibitor of USP14, accelerated the degradation of a subset of proteasome substrates and suppressed cell proliferation, migration, and invasion in lung cancer and cervical cancer (Lee et al., 2010; Han K.H. et al., 2019; Xu et al., 2020). The IC₅₀ of IU1 is 4.7 μM⁵, and concentrations of 50–100 μM IU1 have been used in multiple cancer cells (Li H. et al., 2019; Xia et al., 2019; Sharma et al., 2020; Sharma and Almasan, 2020). We found that the viability of AGS and MKN-28 cells was remarkably suppressed by 75–100 μM IU1, while not in BGC-823 cells (Figure 6J). The cell migration and invasion induced by YTHDF1 overexpression were reversed by exposure to IU1 (100 μM) (Figures 6K,L and Supplementary Figure S6E).

YTHDF1 Harbored a Positive Correlation With USP14 Expression in GC Patients

To further investigate the expression of YTHDF1 or USP14 in GC patients, IHC analysis was performed within the TMA1 and TMA2 cohorts containing 80 and 28 pairs of GC samples, respectively (Figures 7A–F). We found that YTHDF1 expression was markedly elevated in GC tissues as compared with the normal tissues preferentially in the TMA1 cohort (Figures 7A,C) rather than in the TMA2 cohort (Supplementary Figures S6F,G), while USP14 was upregulated in GC tissues in the TMA2 cohort (Figures 7B,D). Pearson correlation analysis demonstrated that YTHDF1 harbored a positive correlation with USP14 expression in GC tissues in the TMA2 cohort ($P = 0.0273$, Figure 7E). Survival analysis suggested GC patients with high-regulated

⁵<https://www.selleck.cn/products/iu1.html>

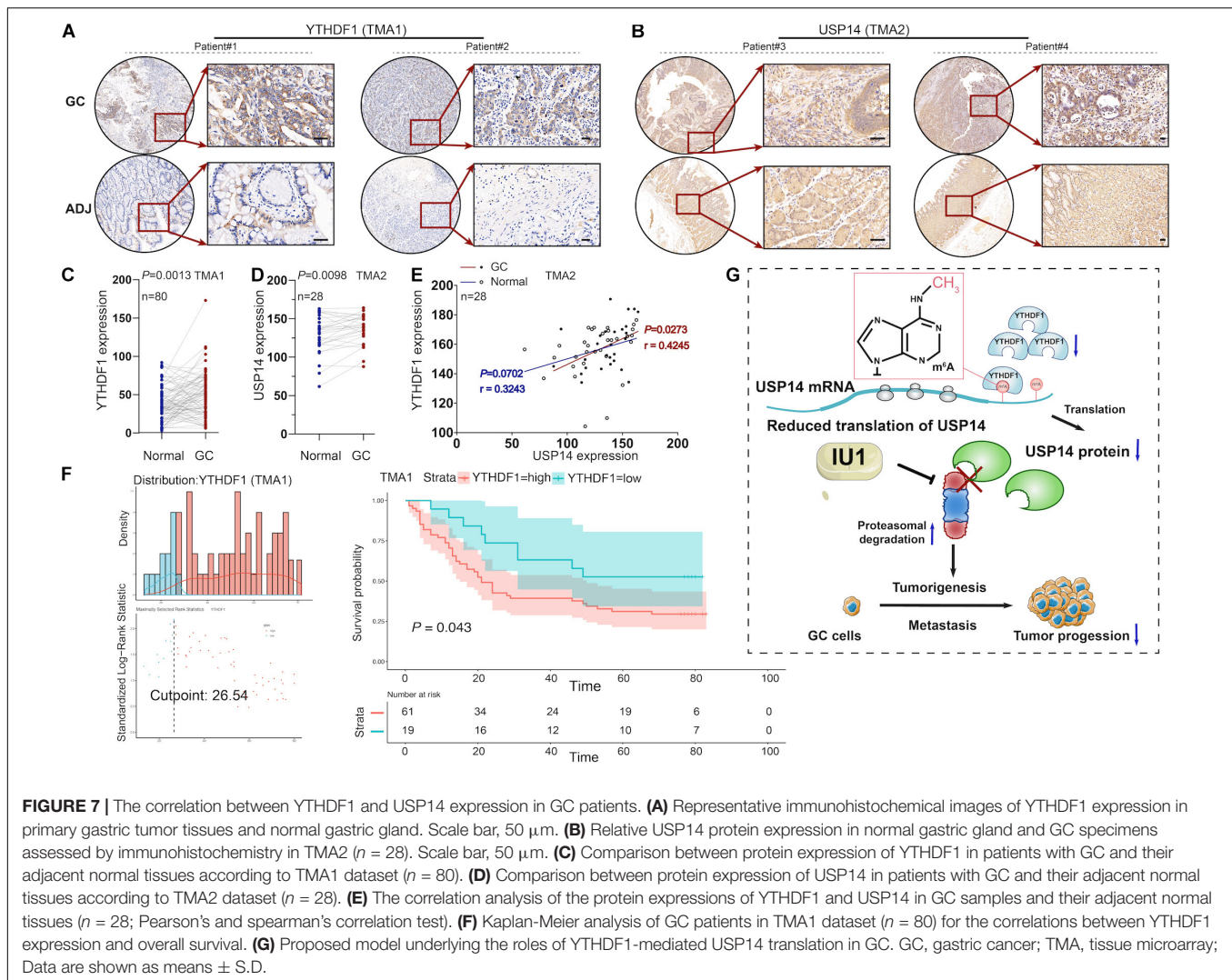


YTHDF1 (TMA1 cohort) or USP14 (TCGA cohort) expression exhibited worse overall survival as compared with patients having low YTHDF1 or USP14 expression (Figures 5G, 7F).

DISCUSSION

Increasing studies have revealed that m⁶A modification plays a role in both physio-biochemical and pathophysiological processes, including carcinogenesis (Cheng et al., 2019; Jin et al., 2019; Li T. et al., 2019). Tumor growth and invasion can be

effectively controlled by m⁶A-related “writers,” “readers,” and “erasers,” which determine the fate of m⁶A-modified mRNAs (Lin et al., 2016; Ma et al., 2017; Li N. et al., 2020; Wang et al., 2020). Higher expression of YTHDF1 is related to worse prognosis in patients with hepatocellular carcinoma (Liu X. et al., 2020). We herein found that YTHDF1 as a m⁶A “reader” was upregulated in GC tissues. About 93.8% of GC patients (Supplementary Figure S1C) exhibited relatively increased YTHDF1 expression, and its upregulation predicted a poor prognosis in patients with GC. A shortcoming of our clinical evidence is that we mainly use public database and



the sample size of TMA is limited. However, these findings illuminate us that the m⁶A might take part in GC tumorigenesis to a certain degree. In addition, YTHDF1 deficiency impaired GC cell growth and metastasis and induced cell apoptosis both *in vitro* and *in vivo*. The previous experiments indicated YTHDF1 likely represented a common oncogenic driver in gastric carcinogenesis.

RNA-seq and GO analyses indicated that YTHDF1-regulated DEGs were enriched in cell proliferation, migration and metastatic signaling pathways. Intersection co-analysis for RNA-seq, MeRIP-seq and RIP-seq revealed that YTHDF1 could mediate m⁶A methylation to affect proteasomal protein catabolic process, of which USP14 acted as an important target of YTHDF1. The inhibition of USP14 can be speculated to be particularly cytotoxic to cancer cells as it could block proteasome function and increase proteasomal substrates (D'Arcy et al., 2015). Moreover, USP14 is associated with tumorigenesis and drug resistance including breast cancer, lung cancer, and GC (Fu et al., 2018; Han K.H. et al., 2019; Xia et al., 2019). Recently, researches have revealed USP14 enhances cisplatin resistance

through affecting Akt/ERK signaling pathways and accelerates cell proliferation and migration in GC (Fu et al., 2018; Han K.H. et al., 2019; Xia et al., 2019). We herein found that USP14 was identified as a downstream target of YTHDF1, and had a positive correlation with YTHDF1 expression, which indicated poor prognosis in GC.

It has been demonstrated that inhibition of USP14-mediated androgen receptor (AR) deubiquitination contributes to the downregulation of AR proteins and suppression of AR-related signaling pathways, such as Wnt/ β -catenin in breast cancer (Liao et al., 2018; Xia et al., 2019). YTHDF1 can promote gastric carcinogenesis by controlling translation of Frizzled7 in GC (Pi et al., 2020). We herein found that YTHDF1 could promote USP14 protein translation in a m⁶A-dependent manner and USP14 overexpression reversed the tumor suppressive effects caused by YTHDF1 knockdown in GC cells.

In addition, the regulating or inhibiting factors of m⁶A modifications may act as potential strategies for cancer treatments, as observed for MA2 in glioblastoma multiforme, R-2HG/SPI1/FB23-2 in acute myeloid leukemia, and CA4 in

colorectal cancer (Zhang et al., 2016; Weng et al., 2017; Su et al., 2018; Huang et al., 2019). We herein found that IU1 as an inhibitor of USP14 could repress cell growth and restore the tumor-promoting effects induced by YTHDF1 in GC cells. Our findings indicated that YTHDF1 could promote USP14 protein translation in a m⁶A-dependent manner, leading to gastric carcinogenesis (Figure 7G).

YTHDF1 can promote GC progression via affecting translation of Frizzled7 in GC, which is an important receptor to transmit Wnt signaling (Pi et al., 2020). To our knowledge, we provides evidence that m⁶A RNA methylation can modulate not only the Wnt signaling but also the ubiquitin-related pathway to influence GC progression. Since the dysregulation of USP14 has been implicated in multiple human cancers (Li H. et al., 2019; Sharma et al., 2020), USP14 inhibitors may be also applicable to treat other cancers with altered USP14 activity. In conclusion, our results prove that YTHDF1 recognizes the m⁶A target on USP14 mRNA and subsequently promotes the translation of USP14. Based on our findings and the above research reports, we believe that the YTHDF1-USP14 expression mechanism has important significance in GC development, and should be forward investigated for GC prognosis, treatment or diagnosis.

DATA AVAILABILITY STATEMENT

The datasets presented in this study can be found in online repositories. The names of the repository and accession number(s) can be found below: GSE166972. The information can be found in the article/**Supplementary Material**.

ETHICS STATEMENT

The studies involving human participants were reviewed and approved by the Ethics Committee of the Shanghai Sixth

People's Hospital. The patients/participants provided their written informed consent to participate in this study. The animal study was reviewed and approved by the Ethics Committee of Shanghai Jiao Tong University Affiliated Sixth People's Hospital.

AUTHOR CONTRIBUTIONS

JZ and J-SZ designed this study. X-YC drafted the manuscript and conducted the statistical analysis. X-YC and RL performed the experiments. Y-CY, H-NF, and MC collected the data. JZ revised this manuscript. All authors read and approved the final manuscript.

FUNDING

This work was supported by the grants from the Double-Hundred Talent Plan of Shanghai Jiao Tong University School of Medicine (No. 20191831) and the National Natural Science Foundation of China (No. 81873143, 82074161).

ACKNOWLEDGMENTS

We thank Linguo Zhao and Jian Zhao for the technical support and Guozi for sharing codes and psychological support from Fangbo Liu.

SUPPLEMENTARY MATERIAL

The Supplementary Material for this article can be found online at: <https://www.frontiersin.org/articles/10.3389/fcell.2021.647702/full#supplementary-material>

REFERENCES

- Ajani, J. A., Lee, J., Sano, T., Janjigian, Y. Y., Fan, D., and Song, S. (2017). Gastric adenocarcinoma. *Nat. Rev. Dis. Primer* 3:17036. doi: 10.1038/nrdp.2017.36
- Anita, R., Paramasivam, A., Priyadharsini, J. V., and Chitra, S. (2020). The m⁶A readers YTHDF1 and YTHDF3 aberrations associated with metastasis and predict poor prognosis in breast cancer patients. *Am. J. Cancer Res.* 10, 2546–2554.
- Azim, H. A., Peccatori, F. A., Brohée, S., Branstetter, D., Loi, S., Viale, G., et al. (2015). RANK-ligand (RANKL) expression in young breast cancer patients and during pregnancy. *Breast Cancer Res. BCR* 17:24. doi: 10.1186/s13058-015-0538-7
- Bray, F., Ferlay, J., Soerjomataram, I., Siegel, R. L., Torre, L. A., and Jemal, A. (2018). Global cancer statistics 2018: GLOBOCAN estimates of incidence and mortality worldwide for 36 cancers in 185 countries. *CA Cancer J. Clin.* 68, 394–424. doi: 10.3322/caac.21492
- Cerami, E., Gao, J., Dogrusoz, U., Gross, B. E., Sumer, S. O., Aksoy, B. A., et al. (2012). The cBio cancer genomics portal: an open platform for exploring multidimensional cancer genomics data. *Cancer Discov.* 2, 401–404. doi: 10.1158/2159-8290.CD-12-0095
- Chen, L., Zhu, G., Johns, E. M., and Yang, X. (2018). TRIM11 activates the proteasome and promotes overall protein degradation by regulating USP14. *Nat. Commun.* 9:1223. doi: 10.1038/s41467-018-03499-z
- Chen, X.-Y., Zhang, J., and Zhu, J.-S. (2019). The role of m⁶A RNA methylation in human cancer. *Mol. Cancer* 18:103. doi: 10.1186/s12943-019-1033-z
- Cheng, M., Sheng, L., Gao, Q., Xiong, Q., Zhang, H., Wu, M., et al. (2019). The m⁶A methyltransferase METTL3 promotes bladder cancer progression via AFF4/NF-κB/MYC signaling network. *Oncogene* 38, 3667–3680. doi: 10.1038/s41388-019-0683-z
- D'Arcy, P., Wang, X., and Linder, S. (2015). Deubiquitinase inhibition as a cancer therapeutic strategy. *Pharmacol. Ther.* 147, 32–54. doi: 10.1016/j.pharmthera.2014.11.002
- Fu, Y., Ma, G., Liu, G., Li, B., Li, H., Hao, X., et al. (2018). USP14 as a novel prognostic marker promotes cisplatin resistance via Akt/ERK signaling pathways in gastric cancer. *Cancer Med.* 7, 5577–5588. doi: 10.1002/cam4.1770
- Gao, J., Aksoy, B. A., Dogrusoz, U., Dresdner, G., Gross, B., Sumer, S. O., et al. (2013). Integrative analysis of complex cancer genomics and clinical profiles using the cBioPortal. *Sci. Signal.* 6:11. doi: 10.1126/scisignal.2004088
- Han, D., Liu, J., Chen, C., Dong, L., Liu, Y., Chang, R., et al. (2019). Anti-tumour immunity controlled through mRNA m⁶A methylation and YTHDF1 in dendritic cells. *Nature* 566, 270–274. doi: 10.1038/s41586-019-0916-x
- Han, K. H., Kwak, M., Lee, T. H., Park, M.-S., Jeong, I.-H., Kim, M. J., et al. (2019). USP14 inhibition regulates tumorigenesis by inducing autophagy in lung cancer in vitro. *Int. J. Mol. Sci.* 20:5300. doi: 10.3390/ijms20215300
- Huang, Y., Su, R., Sheng, Y., Dong, L., Dong, Z., Xu, H., et al. (2019). Small-molecule targeting of oncogenic FTO demethylase in acute myeloid

- leukemia. *Cancer Cell* 35, 677.e10–691.e10. doi: 10.1016/j.ccell.2019.03.006
- Jia, G., Fu, Y., Zhao, X., Dai, Q., Zheng, G., Yang, Y., et al. (2011). N⁶-Methyladenosine in nuclear RNA is a major substrate of the obesity-associated FTO. *Nat. Chem. Biol.* 7, 885–887. doi: 10.1038/nchembio.687
- Jin, D., Guo, J., Wu, Y., Du, J., Yang, L., Wang, X., et al. (2019). m⁶A mRNA methylation initiated by METTL3 directly promotes YAP translation and increases YAP activity by regulating the MALAT1-miR-1914-3p-YAP axis to induce NSCLC drug resistance and metastasis. *J. Hematol. Oncol.* 12:135. doi: 10.1186/s13045-019-0830-6
- Lee, B.-H., Lee, M. J., Park, S., Oh, D.-C., Elsassner, S., Chen, P.-C., et al. (2010). Enhancement of proteasome activity by a small-molecule inhibitor of USP14. *Nature* 467, 179–184. doi: 10.1038/nature09299
- Li, H., Su, Q., Li, B., Lan, L., Wang, C., Li, W., et al. (2020). High expression of WTAP leads to poor prognosis of gastric cancer by influencing tumour-associated T lymphocyte infiltration. *J. Cell. Mol. Med.* 24, 4452–4465. doi: 10.1111/jcmm.15104
- Li, H., Zhao, Z., Ling, J., Pan, L., Zhao, X., Zhu, H., et al. (2019). USP14 promotes K63-linked RIG-I deubiquitination and suppresses antiviral immune responses. *Eur. J. Immunol.* 49, 42–53. doi: 10.1002/eji.201847603
- Li, J.-H., Liu, S., Zhou, H., Qu, L.-H., and Yang, J.-H. (2014). starBase v2.0: decoding miRNA-ceRNA, miRNA-ncRNA and protein-RNA interaction networks from large-scale CLIP-Seq data. *Nucleic Acids Res.* 42, D92–D97. doi: 10.1093/nar/gkt1248
- Li, N., Kang, Y., Wang, L., Huff, S., Tang, R., Hui, H., et al. (2020). ALKBH5 regulates anti-PD-1 therapy response by modulating lactate and suppressive immune cell accumulation in tumor microenvironment. *Proc. Natl. Acad. Sci. U.S.A.* 117, 20159–20170. doi: 10.1073/pnas.1918986117
- Li, T., Hu, P.-S., Zuo, Z., Lin, J.-F., Li, X., Wu, Q.-N., et al. (2019). METTL3 facilitates tumor progression via an m⁶A-IGF2BP2-dependent mechanism in colorectal carcinoma. *Mol. Cancer* 18:112. doi: 10.1186/s12943-019-1038-7
- Liao, Y., Xia, X., Liu, N., Cai, J., Guo, Z., Li, Y., et al. (2018). Growth arrest and apoptosis induction in androgen receptor-positive human breast cancer cells by inhibition of USP14-mediated androgen receptor deubiquitination. *Oncogene* 37, 1896–1910. doi: 10.1038/s41388-017-0069-z
- Lin, S., Choe, J., Du, P., Triboulet, R., and Gregory, R. I. (2016). The m⁶A methyltransferase METTL3 promotes translation in human cancer cells. *Mol. Cell* 62, 335–345. doi: 10.1016/j.molcel.2016.03.021
- Liu, H., Liu, Y., Bian, Z., Zhang, J., Zhang, R., Chen, X., et al. (2018). Circular RNA YAP1 inhibits the proliferation and invasion of gastric cancer cells by regulating the miR-367-5p/p27 Kip1 axis. *Mol. Cancer* 17:151. doi: 10.1186/s12943-018-0902-1
- Liu, J., Eckert, M. A., Harada, B. T., Liu, S.-M., Lu, Z., Yu, K., et al. (2018). m⁶A mRNA methylation regulates AKT activity to promote the proliferation and tumorigenicity of endometrial cancer. *Nat. Cell Biol.* 20, 1074–1083. doi: 10.1038/s41556-018-0174-4
- Liu, T., Wei, Q., Jin, J., Luo, Q., Liu, Y., Yang, Y., et al. (2020). The m⁶A reader YTHDF1 promotes ovarian cancer progression via augmenting EIF3C translation. *Nucleic Acids Res.* 48, 3816–3831. doi: 10.1093/nar/gkaa048
- Liu, X., Qin, J., Gao, T., Li, C., He, B., Pan, B., et al. (2020). YTHDF1 facilitates the progression of hepatocellular carcinoma by promoting FZD5 mRNA translation in an m⁶A-Dependent manner. *Mol. Ther. Nucleic Acids* 22, 750–765. doi: 10.1016/j.omtn.2020.09.036
- Ma, J. Z., Yang, F., Zhou, C. C., Liu, F., Yuan, J.-H., Wang, F., et al. (2017). METTL14 suppresses the metastatic potential of hepatocellular carcinoma by modulating N(6)-methyladenosine-dependent primary MicroRNA processing. *Hepatology* 65, 529–543. doi: 10.1002/hep.28885
- Meyer, K. D., Saletore, Y., Zumbo, P., Elemento, O., Mason, C. E., and Jaffrey, S. R. (2012). Comprehensive analysis of mRNA methylation reveals enrichment in 3' UTRs and near stop codons. *Cell* 149, 1635–1646. doi: 10.1016/j.cell.2012.05.003
- Pi, J., Wang, W., Ji, M., Wang, X., Wei, X., Jin, J., et al. (2020). YTHDF1 promotes gastric carcinogenesis by controlling translation of FZD7. *Cancer Res.* [Epub ahead of print]. doi: 10.1158/0008-5472.CAN-20-0066
- Sharma, A., and Almasan, A. (2020). USP14 regulates DNA damage response and is a target for radiosensitization in non-small cell lung cancer. *Int. J. Mol. Sci.* 21:6383. doi: 10.3390/ijms21176383
- Sharma, A., Alswillah, T., Kapoor, I., Debjani, P., Willard, B., Summers, M. K., et al. (2020). USP14 is a deubiquitinase for Ku70 and critical determinant of non-homologous end joining repair in autophagy and PTEN-deficient cells. *Nucleic Acids Res.* 48, 736–747. doi: 10.1093/nar/gkz1103
- Shi, Y., Fan, S., Wu, M., Zuo, Z., Li, X., Jiang, L., et al. (2019). YTHDF1 links hypoxia adaptation and non-small cell lung cancer progression. *Nat. Commun.* 10:4892. doi: 10.1038/s41467-019-12801-6
- Su, R., Dong, L., Li, C., Nachtergaele, S., Wunderlich, M., Qing, Y., et al. (2018). R-2HG exhibits anti-tumor activity by targeting FTO/m⁶A/MYC/CEBPA signaling. *Cell* 172, 90.e23–105.e23. doi: 10.1016/j.cell.2017.11.031
- Wang, Q., Chen, C., Ding, Q., Zhao, Y., Wang, Z., Chen, J., et al. (2020). METTL3-mediated m⁶A modification of HDGF mRNA promotes gastric cancer progression and has prognostic significance. *Gut* 69, 1193–1205. doi: 10.1136/gutjnl-2019-319639
- Wang, X., Zhao, B. S., Roundtree, I. A., Lu, Z., Han, D., Ma, H., et al. (2015). N⁶-methyladenosine modulates messenger RNA translation efficiency. *Cell* 161, 1388–1399. doi: 10.1016/j.cell.2015.05.014
- Weng, H., Huang, H., Wu, H., Qin, X., Zhao, B. S., Dong, L., et al. (2017). METTL14 inhibits hematopoietic stem/progenitor differentiation and promotes leukemogenesis via mRNA m⁶A modification. *Cell Stem Cell* 22, 191.e9–205.e9. doi: 10.1016/j.stem.2017.11.016
- Xia, X., Huang, C., Liao, Y., Liu, Y., He, J., Guo, Z., et al. (2019). Inhibition of USP14 enhances the sensitivity of breast cancer to enzalutamide. *J. Exp. Clin. Cancer Res.* CR 38:220. doi: 10.1186/s13046-019-1227-7
- Xu, L., Wang, J., Yuan, X., Yang, S., Xu, X., Li, K., et al. (2020). IU1 suppresses proliferation of cervical cancer cells through MDM2 degradation. *Int. J. Biol. Sci.* 16, 2951–2963. doi: 10.7150/ijbs.47999
- Yeo, W., Chan, S. L., Mo, F. K. F., Chu, C. M., Hui, J. W. Y., Tong, J. H. M., et al. (2015). Phase I/II study of temsirolimus for patients with unresectable Hepatocellular Carcinoma (HCC)- a correlative study to explore potential biomarkers for response. *BMC Cancer* 15:395. doi: 10.1186/s12885-015-1334-6
- Yi, Y.-C., Chen, X.-Y., Zhang, J., and Zhu, J.-S. (2020). Novel insights into the interplay between m⁶A modification and noncoding RNAs in cancer. *Mol. Cancer* 19:121. doi: 10.1186/s12943-020-01233-2
- Yue, B., Song, C., Yang, L., Cui, R., Cheng, X., Zhang, Z., et al. (2019). METTL3-mediated N⁶-methyladenosine modification is critical for epithelial-mesenchymal transition and metastasis of gastric cancer. *Mol. Cancer* 18:142. doi: 10.1186/s12943-019-1065-4
- Zhang, J., Tsoi, H., Li, X., Wang, H., Gao, J., Wang, K., et al. (2016). Carbonic anhydrase IV inhibits colon cancer development by inhibiting the Wnt signalling pathway through targeting the WTAP-WT1-TBL1 axis. *Gut* 65, 1482–1493. doi: 10.1136/gutjnl-2014-308614
- Zhou, Y., Zeng, P., Li, Y.-H., Zhang, Z., and Cui, Q. (2016). SRAMP: prediction of mammalian N⁶-methyladenosine (m⁶A) sites based on sequence-derived features. *Nucleic Acids Res.* 44:e91. doi: 10.1093/nar/gkw104

Conflict of Interest: The authors declare that the research was conducted in the absence of any commercial or financial relationships that could be construed as a potential conflict of interest.

Copyright © 2021 Chen, Liang, Yi, Fan, Chen, Zhang and Zhu. This is an open-access article distributed under the terms of the Creative Commons Attribution License (CC BY). The use, distribution or reproduction in other forums is permitted, provided the original author(s) and the copyright owner(s) are credited and that the original publication in this journal is cited, in accordance with accepted academic practice. No use, distribution or reproduction is permitted which does not comply with these terms.



miRNA Landscape in Pathogenesis and Treatment of Vogt–Koyanagi–Harada Disease

Fabian Vega-Tapia¹, Mario Bustamante^{1,2}, Rodrigo A. Valenzuela^{3,4},
Cristhian A. Urzua^{1,5,6*} and Loreto Cuitino^{1,7*}

¹ Laboratory of Ocular and Systemic Autoimmune Diseases, Faculty of Medicine, Universidad de Chile, Santiago, Chile, ² Núcleo de Ciencias Biológicas, Facultad de Estudios Interdisciplinarios, Universidad Mayor, Santiago, Chile, ³ Department of Health Science, Universidad de Aysén, Coyhaique, Chile, ⁴ Department of Chemical and Biological Sciences, Faculty of Health, Universidad Bernardo O'Higgins, Santiago, Chile, ⁵ Department of Ophthalmology, University of Chile, Santiago, Chile, ⁶ Faculty of Medicine, Clínica Alemana Universidad del Desarrollo, Santiago, Chile, ⁷ Servicio de Oftalmología, Hospital Clínico Universidad de Chile, Santiago, Chile

OPEN ACCESS

Edited by:

Jingmin Ou,
Shanghai Jiao Tong University, China

Reviewed by:

Girdhari Lal,
National Centre for Cell Science, India
Claire Joanne Stocker,
Aston University, United Kingdom

*Correspondence:

Cristhian A. Urzua
cristhian.urzua@uchile.cl
Loreto Cuitino
cuitinole@gmail.com

Specialty section:

This article was submitted to
Epigenomics and Epigenetics,
a section of the journal
Frontiers in Cell and Developmental
Biology

Received: 25 January 2021

Accepted: 22 March 2021

Published: 10 May 2021

Citation:

Vega-Tapia F, Bustamante M,
Valenzuela RA, Urzua CA and
Cuitino L (2021) miRNA Landscape
in Pathogenesis and Treatment
of Vogt–Koyanagi–Harada Disease.
Front. Cell Dev. Biol. 9:658514.
doi: 10.3389/fcell.2021.658514

miRNAs, one of the members of the noncoding RNA family, are regulators of gene expression in inflammatory and autoimmune diseases. Changes in miRNA pool expression have been associated with differentiation of CD4⁺ T cells toward an inflammatory phenotype and with loss of self-tolerance in autoimmune diseases. Vogt–Koyanagi–Harada (VKH) disease is a chronic multisystemic pathology, affecting the uvea, inner ear, central nervous system, and skin. Several lines of evidence support an autoimmune etiology for VKH, with loss of tolerance against retinal pigmented epithelium-related self-antigens. This deleterious reaction is characterized by exacerbated inflammation, due to an aberrant T_H1 and T_H17 polarization and secretion of their proinflammatory hallmark cytokines interleukin 6 (IL-6), IL-17, interferon γ , and tumor necrosis factor α , and an impaired CD4⁺ CD25^{high} FoxP3⁺ regulatory T cell function. To restrain inflammation, VKH is pharmacologically treated with corticosteroids and immunosuppressive drugs as first and second line of therapy, respectively. Changes in the expression of miRNAs related to immunoregulatory pathways have been associated with VKH development, whereas some genetic variants of miRNAs have been found to be risk modifiers of VKH. Furthermore, the drugs commonly used in VKH treatment have great influence on miRNA expression, including those miRNAs associated to VKH disease. This relationship between response to therapy and miRNA regulation suggests that these small noncoding molecules might be therapeutic targets for the development of more effective and specific pharmacological therapy for VKH. In this review, we discuss the latest evidence regarding regulation and alteration of miRNA associated with VKH disease and its treatment.

Keywords: miRNA, VKH, autoimmunity, inflammation, therapy

INTRODUCTION

miRNAs are short noncoding RNAs (20–23 nucleotides) that finely tune gene expression (Starega-Roslan et al., 2011). The best-known mechanism of action for gene regulation by miRNAs is post-transcriptional regulation through RISC-dependent binding or degradation of the target mRNAs, but other new functions have been described (Wu et al., 2010;

Ramchandran and Chaluvaly-Raghavan, 2017). Recognition of targets by the miRNA is based on the pairing of a short fragment (6–8 bases), which allows a single miRNA to bind to and regulate the activity of multiple targets, pathways, and, thus, cell function. This feature of miRNA also affects the immune system, and their dysregulation can lead to immune-related disorders such as autoimmunity.

The pathogenic role of miRNA in autoimmune diseases stems from their capability to regulate the activity of major immune-related pathways and immune cell function. For instance, Toll-like receptors (TLRs) and their signaling pathways are regulated by miRNAs, suggesting that miRNA dysregulation could reshape response toward endogenous DAMPs and foster autoimmunity (Nahid et al., 2011; He et al., 2014). Moreover, aberrant miRNA expression disrupts regulatory T cell (Treg) and tolerogenic dendritic cell function and phenotype stability (Li et al., 2014; Wu et al., 2018; Dekkema et al., 2019; Lyszkiewicz et al., 2019; Zhang et al., 2019; Chen et al., 2020; Geng et al., 2020; Tang et al., 2020). Involvement of miRNA in autoimmune diseases is also supported by the correlation of miRNA levels and many disease biomarkers. Let-7f expression is reduced in active systemic lupus erythematosus (SLE) and negatively correlates with disease activity index and proteinuria (Geng et al., 2020), whereas circulating exosomal miR-21 and miR-146a correlate with anti-SSA and anti-dsDNA levels, respectively (Li et al., 2020). Several miRNAs correlate with anti-citrullinated peptide antibodies levels and disease activity score in patients with rheumatoid arthritis (RA) (De La Rosa et al., 2020). miRNA may promote autoimmunity through direct binding to TLR-7/8 (Kim et al., 2016; Hegewald et al., 2020); therefore, general overexpression of miRNA may facilitate self-tolerance failure through mechanisms other than regulation on gene expression. In summary, miRNAs contribute to autoimmunity through the disruption of immune-related pathways, impairment of regulatory cell phenotype, or mounting immune response through TLR engagement.

VOGT-KOYANAGI-HARADA DISEASE

Vogt–Koyanagi–Harada (VKH) disease is a rare autoimmune disease with ocular and systemic compromise. Ocular manifestations are characterized mainly by severe bilateral granulomatous panuveitis, exudative retinal detachments, and optic nerve edema, with eventual development of ocular pigmentary changes as late features in advanced phases of the disease. Systemic symptoms include tinnitus, hearing loss, vertigo, meningismus, vitiligo, and poliosis (O'keefe and Rao, 2017). A recent study suggests that delayed diagnosis and inadequate treatment lead to iris deterioration in patients with chronic recurrent disease (Chee and Win, 2021). VKH disease generally affects young women and is the leading cause of noninfectious uveitis with a known etiological factor in many high-risk populations, including India, Thailand, and Chile, and a major cause of panuveitis in Tunisia, Iran, Japan, and the Hispanic population in the United States (Lieberman et al., 2015; O'keefe and Rao, 2017).

VKH etiopathogenesis is only partially understood; however, several studies provide evidence that the disease is caused by the immune reaction against pigmented cell-related autoantigens (Kobayashi et al., 1998; Otani et al., 2006). Therefore, understanding the mechanisms of immune dysregulation in the context of VKH is necessary to create more specific and effective therapies.

CD4⁺ T Cells and Their Role in VKH Pathogenesis

As an autoimmune disorder, immune response against self is an underlying pathogenic mechanism of VKH, leading to the destruction and functional impairment of the retinal pigment epithelium and adjacent layers of the eye. Failure of tolerogenic mechanisms lead to the activation of self-reactive immune cells, including CD4⁺ T cells, which are major contributors to VKH. Increased CD4⁺ T cell population has been observed in the aqueous humor and cerebrospinal fluid of VKH patients (Norose et al., 1990, 1994; Ohta and Yoshimura, 1998). Initial phenotypical characterization of CD4⁺ T cells in VKH revealed an immune response shifted toward the T_H1 subset with increased expression of activation markers CD25 and HLA-DR, the proinflammatory cytokine interferon γ (IFN- γ), and the transcription factor T-Bet (Norose and Yano, 1996; Li et al., 2005; Sugita et al., 2006). Notably, these T_H1 cells have cytolytic activity on melanoma cells and cells expressing peptides related with pigmented tissues and express memory T cell markers, suggesting that loss of tolerance toward pigmented epithelium and long-term T_H1 response are a crucial factor in VKH pathogenesis (Norose and Yano, 1996; Sugita et al., 2006). The introduction of the T_H17 subset expanded the knowledge of the role of CD4⁺ T cells in autoimmunity. Interleukin 23 (IL-23) is a cytokine of the IL-12 family that induces differentiation of CD4⁺ T cells into the T_H17 subpopulation to secrete the hallmark cytokine IL-17. IL-23 is increased in patients with active VKH (Wang et al., 2018) and is associated with active uveitis (Chi et al., 2008; Przepiera-Bedzak et al., 2016; Velez et al., 2016), and its administration enhances IFN- γ and IL-17 secretion in peripheral blood mononuclear cells (PBMCs) and isolated CD4⁺ T cells *in vitro* (Chi et al., 2007). Treatment-induced remission is associated with decreased expression of T_H1 and T_H17 cytokines and related transcription factors in PBMCs and CD4⁺ T cells (Liu et al., 2009).

Treg-inducing mechanisms seem to be defective in VKH; in a study published by Commodaro et al. (2010), no difference in the frequency of circulating Treg between controls and VKH patients, with or without active disease, was found. However, IL-10 and transforming growth factor β secretion was significantly stronger in the PBMCs from inactive VKH patients after *in vitro* stimulation, whereas IFN- γ was higher in active patients, without differences between control and inactive VKH groups (Commodaro et al., 2010). This study suggests that function, rather than number of Tregs, and maybe other regulatory cells, is impaired in VKH patients with active disease. In agreement with this, serum levels of the immunoregulatory cytokine IL-27 are decreased in patients with active VKH, which suppresses IL-17 expression and promotes IL-10 secretion in naive CD4⁺ T cells

(Wang et al., 2012). Another immunoregulatory cytokine, IL-35, is also decreased in VKH patients, and culturing PBMCs with anti-CD3 and anti-CD28 antibodies in presence of IL-35 inhibits secretion of IFN- γ and IL-17 but enhances IL-10 release (Hu et al., 2019). Altogether, data show that deregulation of CD4⁺ T cells is an important event in VKH pathophysiology; therefore, understanding the mechanisms that cause these changes might be key for the development of effective therapies for this disease.

Current Pharmacological Therapies for VKH

Systemic corticosteroids (CSs) (prednisolone) are the mainstay of clinical management of VKH, with evidence endorsing the use of high doses at early phases resulting in shorter treatment periods, reduced disease severity, and better subclinical manifestations (Chee et al., 2007; Jap et al., 2008; Kitaichi et al., 2008; Kawaguchi et al., 2010), whereas CS administration for at least 6 months is key to reduce the risk of recurrence (Lai et al., 2009; Errera et al., 2011). CS therapy is known to have several side effects, including systemic (diabetes, Cushing syndrome, osteoporosis) and eye-related features (cataract, glaucoma, visual impairment) (Valenzuela et al., 2020b).

Immunomodulatory therapy (IMT), including mycophenolate mofetil (MMF), methotrexate (MTX), cyclosporin A (CsA), and azathioprine, is usually used as a CS-sparing treatment with successful visual acuity improvement and reduction of sunset glow fundus development in some reports (Agarwal et al., 2006; Shen et al., 2016; Abu El-Asrar et al., 2017; Yang et al., 2018; Ei Ei Lin et al., 2020). Early use of CS and IMT combined as a first-line therapy increases the chances of remission and lowers the risk of chronic disease compared with CS monotherapy (Herbort et al., 2017, 2019).

Biologics have been introduced in uveitis management, and guidelines recommend them upon systemic CS/IMT treatment failure (Rosenbaum et al., 2019; Valenzuela et al., 2020b). Studies have shown that the use of adalimumab [anti-tumor necrosis factor α (TNF- α) antibody] (Couto et al., 2018; Hiyama et al., 2021) and rituximab (anti-CD20 antibody) (Abu El-Asrar et al., 2020) improves visual acuity, alleviates inflammation, and allows for CS tapering. Case reports have shown favorable results for the use of infliximab (anti-TNF- α) (Wang and Gaudio, 2008; Zmuda et al., 2013) and intravitreal bevacizumab (anti-VEGF-A) (Wu et al., 2009; Park et al., 2011) as treatment of VKH.

miRNAs AND THEIR ROLE IN VKH ETIOLOGY AND TREATMENT

miRNAs as Mediators of VKH Pathogenesis

miRNAs have been implicated in the development of VKH disease. Asakage and colleagues recently reported their results on differentially expressed miRNAs (DEmiRs) in the serum of patients with noninfectious uveitis, including VKH, using a microarray approach (Asakage et al., 2020). The results revealed a set of 188 DEmiRs in VKH patients when compared with

healthy controls (HCs), of which 59 DEmiRs were unique to VKH when compared with sarcoidosis and Behçet's disease (BD). The authors used several approaches such as unsupervised hierarchical analysis and principal component analysis to show that VKH is related with a distinctive miRNA expression profile compared with uveitis of different etiology. Differential expression and copy number variation (CNV) in several miRNAs between VKH and BD have been described, probably due to the difference in the nature of these immunological disorders (autoimmune/adaptive in VKH vs. autoinflammatory/innate in BD) (Qi et al., 2013; Zhou et al., 2014; Hou et al., 2016). This distinctive miRNA expression pattern suggests that a specific miRNA-mediated mechanism is central to VKH pathogenesis. A summary of the findings and a brief discussion on the role of miRNAs involved in VKH are provided in **Table 1**.

miR-20a: Patients with active VKH have lower expression of miR-20a-5p in CD4⁺ T cells compared to HC, which is associated with a hypermethylated miR-20a-5p promoter (Chang et al., 2018). Overexpression of miR-20a-5p indirectly decreases IL-17 expression in VKH CD4⁺ T cells through the regulation of oncostatin M and CCL1 expression (Chang et al., 2018). Accordingly, a comprehensive analysis based on literature-supported miRNA-mRNA interactions found that miR-20a may suppress T_H17 differentiation through the targeting of several regulators (Honardoost et al., 2015). Moreover, miR-20a expression increases upon T cell activation and inhibits T cell receptor signaling, while also decreasing the expression of CD69, IL-2, IL-8, and, especially, IL-10 (Reddycherla et al., 2015). Altogether, evidence suggests that miR-20a participates in a negative feedback loop that modulates CD4⁺ T cell activation and polarization.

miR-23a: A high copy number (>2) of the miR-23a coding gene is linked to VKH. This CNV directly correlates with

TABLE 1 | miRNAs associated with VKH.

miRNA	Association with VKH	Immunoregulatory effect	References
miR-20a	Hypermethylated promoter and downregulated in CD4 ⁺ T cells	Inhibits T _H 17 differentiation. Attenuates TCR signaling and regulates cytokine expression in activated CD4 ⁺ T cells.	Qi et al., 2013
miR-23a	Increased gene copy number	Correlates with IL-6 expression in PBMCs. Regulates the expression of IL-17 and HO-1.	Wu et al., 2009
miR-146a	Increased gene copy number	Promotes Treg function. Inhibits T _H 17 differentiation.	Wu et al., 2009
miR-182	Association with C allele of the rs76481776 variant	Evidence indirectly suggests a protective effect in VKH.	Liu et al., 2016
miR-301a	Decreased gene copy number	Promotes T _H 17 and TNF- α expression.	Wu et al., 2009
let-7g-3p	Good predictor of VKH	Unknown.	Park et al., 2011

TABLE 2 | miRNAs involved in response to pharmacological treatment in VKH and corticosteroid resistance.

Corticosteroid response		
miRNA	Regulation by corticosteroids	References
miR-17-92 cluster (miR-20a)	Downregulation	Moschos et al., 2007; Molitoris et al., 2011
miR-20a	Downregulation	Moschos et al., 2007
miR-23a	Inhibition of maturation	Hudson et al., 2014b; Kwok et al., 2017
miR-146a	Downregulation	Heier et al., 2016; Lambert et al., 2018
miR-182	Downregulation	Dong et al., 2020
miR-301a	Downregulation	Moschos et al., 2007
Corticosteroid resistance		
miRNA	Contribution to CSR	References
miR-15b-16	Prevent CSR	Rainer et al., 2009
miR-21	Promotes CSR	Wang et al., 2011
miR-29a	Promotes CSR	Glantschnig et al., 2019
miR-124	Controversial	Lv et al., 2012; Kim et al., 2015; Liang et al., 2017
miR-128b	Prevents CSR	Kotani et al., 2009
miR-130b	Promotes CSR	Tessel et al., 2011
miR-182	Promotes CSR	Yang et al., 2012; Hudson et al., 2014a
miR-221	Controversial	Kotani et al., 2009; Xu et al., 2019
miR-222	Promotes CSR	Xu et al., 2019
miR-331-3p	Promotes CSR	Lucafo et al., 2020
IMT		
Drug	Effect	References
Mycophenolate mofetil	Upregulates miR-146a in SLE CD4 ⁺ T cells	Tang et al., 2015
Methotrexate	Downregulates miR-146a-5p but MTX-responsive patients have increased levels compared to non-MTX-responsive patients.	Singh et al., 2019
Cyclosporine A	Upregulates miR-23a and miR-182	Van Den Hof et al., 2014; Yang et al., 2017
Adalimumab	Decreases miR-146a-5p	Prattichizzo et al., 2016; Mensa et al., 2018

increased miR-23a expression in PBMCs from HC, whereas overexpression of miR-23a increases IL-6 production in human retinal pigment epithelial cells (Hou et al., 2016). Conversely, miR-23a has been shown to restrain IL-17-mediated response by inhibiting the nuclear factor κ B pathway (Hu et al., 2017) and to facilitate the expression of the immunoregulatory enzyme HO-1 by targeting its inhibitor Bach-1 (Su et al., 2020). Thus, miR-23a might act as a balancing factor in inflammation with opposing proinflammatory and anti-inflammatory roles. It is possible that the effect of miR-23a depends on the tissue it is expressed or is modified by the inflammatory milieu.

miR-146a: High miR-146a encoding gene copy number has been linked to VKH disease (Hou et al., 2016). However,

no association with several miR-146 single-nucleotide polymorphisms (SNPs) was found in a similar study performed by the same authors (Zhou et al., 2014). The C allele of one of these SNPs (rs2910164 C > G) impairs nuclear processing of the pri-miR-146a, leading to lower mature miR-146a expression in PBMCs (Jazdzewski et al., 2008; Zhou et al., 2014), indicating that it has a functional impact. The lack of association of SNPs with VKH and the increased number of miR-146a encoding gene copies in these patients suggest that an aberrant overexpression of mature miR-146a, not its down-regulation, may have a role in the disease. Evidence supports a tolerogenic effect of miR-146a by enhancing Treg function (Lu et al., 2010; Zhou et al., 2015) and impairing T_H17 differentiation (Liu et al., 2016; Li et al., 2017). How a high CNV of miR-146a gene is linked to VKH is still unknown.

miR-182: The rs76481776 SNP, located in the MIR182 gene, is associated with a limited expression of mature miR-182 in CC in versus TT or CT genotypes (Saus et al., 2010). A significant association with VKH was found for the C allele but not the T allele of the rs76481776 SNP in a Han Chinese cohort (Yu et al., 2014). Accordingly, the authors also report that CD4⁺ T cells from HC with the CC genotype have a lower expression of mature miR-182 compared with cells from donors carrying at least one T allele (Yu et al., 2014). Given the association of the C allele with VKH, the evidence suggests that miR-182 has protective role.

miR-301a: A low copy number of the MIR301A gene is associated with VKH in the Han Chinese population (Hou et al., 2016). Literature shows that miR-301a promotes T_H17 differentiation and TNF- α production by targeting SNIP1 and PIAS3 (Mycko et al., 2012; He et al., 2016). There seems to be a contradiction between the low copy number and the proinflammatory effects of miR-301a in the context of VKH, although the relationship between CNV and expression has not been evaluated. A low copy number could sustain enough miR-301a expression without the activation of compensating negative feedback mechanisms, promoting inflammation.

Let-7g-3p: In one study, the authors identified a predictive panel of 24 miRNA in VKH patients, with let-7g-3p being the best predictor (Asakage et al., 2020), suggesting a strong link with disease development. A decreased expression of circulating let-7g-3p was found in Graves disease patients in remission (Hiratsuka et al., 2016). However, most of the knowledge on the immunoregulatory effects of let-7g is related with let-7g-5p (Yang et al., 2020). The role of let-7g-3p in VKH is still unclear.

miRNA in Therapeutic Response

The current pharmacologic treatment for VKH includes immunosuppressive and immunomodulatory drugs, which are known to modify the expression of some of the previously reported VKH-related miRNA, accordingly to *in vitro*, animal model, and human studies evidence.

Corticosteroids: The expression of miR-20a, or the cluster miR17-92 in which it is located, is down-regulated by CS in mice lung tissue and murine T-cell lymphoma cell line (Moschos et al., 2007; Molitoris et al., 2011). The same effect is seen

in miR-301a expression after CS stimulation (Moschos et al., 2007). Intracellular level of miR-23a is also down-regulated by dexamethasone (Dex) in both human endothelial cells and C2C12 myotubes, although the mechanism seems to be different as the one for miR-20a and miR-301a (Hudson et al., 2014b; Kwok et al., 2017). The use of Dex reverts the up-regulation of miR-146 induced by TNF- α in human bronchial epithelial cells *in vitro* and also in serum of pediatric patients with Crohn disease (Heier et al., 2016; Lambert et al., 2018). Finally, Dex decreases the level of miR-182 in preadipocytes, allowing C/EBP α -driven adipocyte differentiation (Dong et al., 2020).

MMF: The active metabolite of MMF, mycophenolic acid, is known to up-regulate miR-146a in T cells from SLE patients after treatment, according to microarray-based analysis and reverse transcription-quantitative polymerase chain reaction analysis (Tang et al., 2015).

MTX: RA patients who exhibit clinical improvement have higher blood levels of miR-146a-5p and other miRNAs at 4 months after MTX treatment initiation, supporting a mechanistic link between miR-146a expression and therapeutic response to MTX (Singh et al., 2019).

CsA: CsA-induced gingivae growth in rats occurs together with an up-regulation of miR-23a (Yang et al., 2017). The same effects over miR-23a expression are seen in primary mouse hepatocytes treated with CsA *in vitro* (Van Den Hof et al., 2014).

Adalimumab: A significant down-regulation of miR-146a-5p was observed in PBMCs from psoriasis patients after adalimumab treatment, reaching levels compared to that of the HC group (Mensa et al., 2018). Moreover, adalimumab reduced the expression of miR-146a in THP-1 and endothelial cells *in vitro* (Prattichizzo et al., 2016).

It is important to remark that none of the aforementioned publications established a direct relationship between changes of the miRNA expression and the therapeutic actions of the VKH-related drugs. How these drugs modify the levels of miRNAs is still under investigation, although the mechanisms behind might include (i) impairment of miRNA maturation, as CS down-regulates Dicer, Drosha, and DGCR8/Pasha and also induces G3BP1, all of them key miRNA processing enzymes (Smith et al., 2010; Kwok et al., 2017; Clayton et al., 2018); (ii) increasing exocytosis of miRNAs, making them less available intracellularly (Hudson et al., 2014a,b); (iii) histone modification in the promoter of miRNA genes by action of MMF or its active metabolite (Tang et al., 2015; Yang et al., 2015); and (iv) miRNA gene expression by indirect mechanisms that include extracellular adenosine signaling after MTX treatment (Yang et al., 2021). Less known are the mechanisms for CsA and adalimumab, although both drugs modify the profile expression of a number of different miRNAs (Gooch et al., 2017; Wcislo-Dziadecka et al., 2018).

A different but relevant aspect in the pharmacological treatment of VKH is the refractoriness to CS treatment [CS resistance (CSR)]. Recently, our group published a systematic review about CSR, a crucial issue in the management of uveitides such as VKH, which can be broadly described as refractory uveal inflammation despite the administration of high dose of CS (Valenzuela et al., 2020a). The VKH-related

miRNA miR-182 confers CSR inhibiting apoptosis in lymphoma cells (Yang et al., 2012) and prevents CS-induced atrophy of skeletal muscle by targeting FOXO3a (Hudson et al., 2014a). Most data on CSR-related miRNAs involve molecules with unknown relationship with VKH; a summary of these findings is provided next as it could guide future research (Table 2). Evidence shows that a shift in the relative expression of the GR isoforms α and β after CS treatment constitutes a marker for CS sensitivity (Urzua et al., 2017, 2019). In this regard, miR-130b overexpression was found to inhibit GR α expression and conferred CSR to multiple myeloma cells (Tessel et al., 2011). Similarly, transfection of miR-331-3p mimic promotes CS sensitivity in several transformed cell lines by inhibiting JKN phosphorylation (Lucafo et al., 2020). Other pro-CSR miRNAs are miR-21, miR-29a and miR-222; conversely, miR-15b, miR-16, and miR-128b promote CS sensitivity in cancer cells (Kotani et al., 2009; Rainer et al., 2009; Wang et al., 2011; Glantschnig et al., 2019; Xu et al., 2019). Evidence for both pro- and anti-CSR effects of miR-221 and miR-124 has been reported (Kotani et al., 2009; Lv et al., 2012; Kim et al., 2015; Liang et al., 2017; Xu et al., 2019). Although CSR is a slightly different concept in the context of cancer, it also involves impairment of pharmacological response to CS; hence, some of these miRNAs might be involved in CSR in VKH patients as well.

CONCLUSION

VKH is a complex disease with incompletely understood etiopathogenesis that requires aggressive long-term CS treatment with a high risk of wasting side effects. Although scarce, evidence supports a role of miRNAs in the development of VKH disease, therapeutic response, and even therapy resistance. Future research in the subject must aim to not only find the association of miRNAs with VKH and the use of therapy but also determine potential targets and functional changes caused by the differential expression of these regulatory RNAs. Successful progress in this task will contribute to establishing new pharmacological targets and biomarkers for disease activity and therapy response.

AUTHOR CONTRIBUTIONS

FV wrote the manuscript. MB, FV, RV, CU, and LC read, discussed, and revised the manuscript. All authors listed have made a substantial, direct and intellectual contribution to the work, and approved it for publication.

FUNDING

This study was supported by the National Agency for Research and Development (ANID) grant Fondecyt de Iniciación en Investigación No. 11191215 (given to LC) and Fondo de Fomento al Desarrollo Científico y Tecnológico (FONDEF) grant No. IT1710087 (given to CU).

REFERENCES

- Abu El-Asrar, A. M., Dheyab, A., Khatib, D., Struyf, S., Van Damme, J., and Opdenakker, G. (2020). Efficacy of B cell depletion therapy with rituximab in refractory chronic recurrent uveitis associated with vogt-koyanagi-harada disease. *Ocul. Immunol. Inflamm.* doi: 10.1080/09273948.2020.1820531 [Epub ahead of print].
- Abu El-Asrar, A. M., Dosari, M., Hemachandran, S., Gikandi, P. W., and Al-Muammar, A. (2017). Mycophenolate mofetil combined with systemic corticosteroids prevents progression to chronic recurrent inflammation and development of 'sunset glow fundus' in initial-onset acute uveitis associated with Vogt-Koyanagi-Harada disease. *Acta Ophthalmol.* 95, 85–90. doi: 10.1111/aos.13189
- Agarwal, M., Ganesh, S. K., and Biswas, J. (2006). Triple agent immunosuppressive therapy in Vogt-Koyanagi-Harada syndrome. *Ocul. Immunol. Inflamm.* 14, 333–339. doi: 10.1080/09273940600976938
- Asakage, M., Usui, Y., Nezu, N., Shimizu, H., Tsubota, K., Yamakawa, N., et al. (2020). Comprehensive miRNA analysis using serum from patients with noninfectious uveitis. *Invest. Ophthalmol. Vis. Sci.* 61:4. doi: 10.1167/iov.61.11.4
- Chang, R., Yi, S., Tan, X., Huang, Y., Wang, Q., Su, G., et al. (2018). MicroRNA-20a-5p suppresses IL-17 production by targeting OSM and CCL1 in patients with Vogt-Koyanagi-Harada disease. *Br. J. Ophthalmol.* 102, 282–290. doi: 10.1136/bjophthalmol-2017-311079
- Chee, S. P., Jap, A., and Bacsal, K. (2007). Spectrum of Vogt-Koyanagi-Harada disease in Singapore. *Int. Ophthalmol.* 27, 137–142. doi: 10.1007/s10792-006-9009-6
- Chee, S. P., and Win, M. Z. A. (2021). Iris manifestations in inadequately treated chronic recurrent Vogt-Koyanagi-Harada Disease. *Ocul. Immunol. Inflamm.* doi: 10.1080/09273948.2020.1870701 [Epub ahead of print].
- Chen, L., Hou, X., Zhang, M., Zheng, Y., Zheng, X., Yang, Q., et al. (2020). MicroRNA-223-3p modulates dendritic cell function and ameliorates experimental autoimmune myocarditis by targeting the NLRP3 inflammasome. *Mol. Immunol.* 117, 73–83. doi: 10.1016/j.molimm.2019.10.027
- Chi, W., Yang, P., Li, B., Wu, C., Jin, H., Zhu, X., et al. (2007). IL-23 promotes CD4⁺ T cells to produce IL-17 in Vogt-Koyanagi-Harada disease. *J. Allergy Clin. Immunol.* 119, 1218–1224. doi: 10.1016/j.jaci.2007.01.010
- Chi, W., Zhu, X., Yang, P., Liu, X., Lin, X., Zhou, H., et al. (2008). Upregulated IL-23 and IL-17 in Behcet patients with active uveitis. *Invest. Ophthalmol. Vis. Sci.* 49, 3058–3064. doi: 10.1167/iov.07-1390
- Clayton, S. A., Jones, S. W., Kurowska-Stolarska, M., and Clark, A. R. (2018). The role of microRNAs in glucocorticoid action. *J. Biol. Chem.* 293, 1865–1874. doi: 10.1074/jbc.R117.000366
- Commodaro, A. G., Peron, J. P., Genre, J., Arslanian, C., Sanches, L., Muccioli, C., et al. (2010). IL-10 and TGF-beta immunoregulatory cytokines rather than natural regulatory T cells are associated with the resolution phase of Vogt-Koyanagi-Harada (VKH) syndrome. *Scand. J. Immunol.* 72, 31–37. doi: 10.1111/j.1365-3083.2010.02401.x
- Couto, C., Schlaen, A., Frick, M., Khoury, M., Lopez, M., Hurtado, E., et al. (2018). Adalimumab treatment in patients with Vogt-Koyanagi-Harada disease. *Ocul. Immunol. Inflamm.* 26, 485–489. doi: 10.1080/09273948.2016.1236969
- De La Rosa, I. A., Perez-Sanchez, C., Ruiz-Limon, P., Patino-Trives, A., Torres-Granados, C., Jimenez-Gomez, Y., et al. (2020). Impaired microRNA processing in neutrophils from rheumatoid arthritis patients confers their pathogenic profile. Modulation by biological therapies. *Haematologica* 105, 2250–2261. doi: 10.3324/haematol.2018.205047
- Dekkema, G. J., Bijma, T., Jellema, P. G., Van Den Berg, A., Kroesen, B. J., Stegeman, C. A., et al. (2019). Increased miR-142-3p expression might explain reduced regulatory T cell function in granulomatosis with polyangiitis. *Front. Immunol.* 10:2170. doi: 10.3389/fimmu.2019.02170
- Dong, M., Ye, Y., Chen, Z., Xiao, T., Liu, W., and Hu, F. (2020). MicroRNA 182 is a novel negative regulator of adipogenesis by targeting CCAAT/Enhancer-binding protein alpha. *Obesity (Silver Spring)* 28, 1467–1476. doi: 10.1002/oby.22863
- Ei Ei Lin, O., Chee, S. P., Wong, K. K. Y., and Hla Myint, H. (2020). Vogt-Koyanagi-Harada disease managed with immunomodulatory therapy within 3 months of disease onset. *Am. J. Ophthalmol.* 220, 37–44. doi: 10.1016/j.ajo.2020.07.036
- Errera, M. H., Fardeau, C., Cohen, D., Navarro, A., Gaudric, A., Bodaghi, B., et al. (2011). Effect of the duration of immunomodulatory therapy on the clinical features of recurrent episodes in Vogt-Koyanagi-Harada disease. *Acta Ophthalmol.* 89, e357–e366. doi: 10.1111/j.1755-3768.2010.02055.x
- Geng, L., Tang, X., Wang, S., Sun, Y., Wang, D., Tsao, B. P., et al. (2020). Reduced Let-7f in bone marrow-derived mesenchymal stem cells triggers Treg/Th17 imbalance in patients with systemic lupus erythematosus. *Front. Immunol.* 11:233. doi: 10.3389/fimmu.2020.00233
- Glantschnig, C., Koenen, M., Gil-Lozano, M., Karbiener, M., Pickrahn, I., Williams-Dautovich, J., et al. (2019). A miR-29a-driven negative feedback loop regulates peripheral glucocorticoid receptor signaling. *FASEB J.* 33, 5924–5941. doi: 10.1096/fj.201801385RR
- Gooch, J. L., King, C., Francis, C. E., Garcia, P. S., and Bai, Y. (2017). Cyclosporine a alters expression of renal microRNAs: new insights into calcineurin inhibitor nephrotoxicity. *PLoS One* 12:e0175242. doi: 10.1371/journal.pone.0175242
- He, C., Shi, Y., Wu, R., Sun, M., Fang, L., Wu, W., et al. (2016). miR-301a promotes intestinal mucosal inflammation through induction of IL-17A and TNF-alpha in IBD. *Gut* 65, 1938–1950. doi: 10.1136/gutjnl-2015-309389
- He, X., Jing, Z., and Cheng, G. (2014). MicroRNAs: new regulators of Toll-like receptor signalling pathways. *Biomed. Res. Int.* 2014, 945169. doi: 10.1155/2014/945169
- Hegewald, A. B., Breitwieser, K., Ottinger, S. M., Mobarrez, F., Korotkova, M., Rethi, B., et al. (2020). Extracellular miR-574-5p induces osteoclast differentiation via TLR 7/8 in Rheumatoid arthritis. *Front. Immunol.* 11:585282. doi: 10.3389/fimmu.2020.585282
- Heier, C. R., Fiorillo, A. A., Chaisson, E., Gordish-Dressman, H., Hathout, Y., Damsker, J. M., et al. (2016). Identification of pathway-specific serum biomarkers of response to glucocorticoid and infliximab treatment in children with inflammatory bowel disease. *Clin. Transl. Gastroenterol.* 7:e192. doi: 10.1038/ctg.2016.49
- Herbort, C. P. Jr., Abu El Asrar, A. M., Takeuchi, M., Pavesio, C. E., Couto, C., Hedayatfar, A., et al. (2019). Catching the therapeutic window of opportunity in early initial-onset Vogt-Koyanagi-Harada uveitis can cure the disease. *Int. Ophthalmol.* 39, 1419–1425. doi: 10.1007/s10792-018-0949-4
- Herbort, C. P. Jr., Abu El Asrar, A. M., Yamamoto, J. H., Pavesio, C. E., Gupta, V., Khairallah, M., et al. (2017). Reappraisal of the management of Vogt-Koyanagi-Harada disease: sunset glow fundus is no more a fatality. *Int. Ophthalmol.* 37, 1383–1395. doi: 10.1007/s10792-016-0395-0
- Hiratsuka, I., Yamada, H., Munetsuna, E., Hashimoto, S., and Itoh, M. (2016). Circulating microRNAs in Graves' disease in relation to clinical activity. *Thyroid* 26, 1431–1440. doi: 10.1089/thy.2016.0062
- Hiyama, T., Harada, Y., and Kiuchi, Y. (2021). Efficacy and safety of adalimumab therapy for the treatment of non-infectious uveitis: efficacy comparison among uveitis aetiologies. *Ocul. Immunol. Inflamm.* doi: 10.1080/09273948.2020.1857791 [Epub ahead of print].
- Honardoost, M. A., Naghavian, R., Ahmadijanejad, F., Hosseini, A., and Ghaedi, K. (2015). Integrative computational mRNA-miRNA interaction analyses of the autoimmune-deregulated miRNAs and well-known Th17 differentiation regulators: an attempt to discover new potential miRNAs involved in Th17 differentiation. *Gene* 572, 153–162. doi: 10.1016/j.gene.2015.08.043
- Hou, S., Ye, Z., Liao, D., Bai, L., Liu, Y., Zhang, J., et al. (2016). miR-23a, miR-146a and miR-301a confer predisposition to Vogt-Koyanagi-Harada syndrome but not to Behcet's disease. *Sci. Rep.* 6:20057. doi: 10.1038/srep20057
- Hu, J., Qin, Y., Yi, S., Wang, C., Yang, J., Yang, L., et al. (2019). Decreased interleukin(IL)-35 expression is associated with active intraocular inflammation in Vogt-Koyanagi-Harada (VKH) disease. *Ocul. Immunol. Inflamm.* 27, 595–601. doi: 10.1080/09273948.2018.1433306
- Hu, J., Zhai, C., Hu, J., Li, Z., Fei, H., Wang, Z., et al. (2017). MiR-23a inhibited IL-17-mediated proinflammatory mediators expression via targeting IKKalpha in articular chondrocytes. *Int. Immunopharmacol.* 43, 1–6. doi: 10.1016/j.intimp.2016.11.031
- Hudson, M. B., Rahnert, J. A., Zheng, B., Woodworth-Hobbs, M. E., Franch, H. A., and Price, S. R. (2014a). miR-182 attenuates atrophy-related gene expression by targeting FoxO3 in skeletal muscle. *Am. J. Physiol. Cell Physiol.* 307, C314–C319. doi: 10.1152/ajpcell.00395.2013
- Hudson, M. B., Woodworth-Hobbs, M. E., Zheng, B., Rahnert, J. A., Blount, M. A., Gooch, J. L., et al. (2014b). miR-23a is decreased during muscle atrophy by a

- mechanism that includes calcineurin signaling and exosome-mediated export. *Am. J. Physiol. Cell Physiol.* 306, C551–C558. doi: 10.1152/ajpcell.00266.2013
- Jap, A., Luu, C. D., Yeo, I., and Chee, S. P. (2008). Correlation between peripapillary atrophy and corticosteroid therapy in patients with Vogt-Koyanagi-Harada disease. *Eye (Lond.)* 22, 240–245. doi: 10.1038/sj.eye.6702591
- Jazdzewski, K., Murray, E. L., Franssila, K., Jarzab, B., Schoenberg, D. R., and De La Chapelle, A. (2008). Common SNP in pre-miR-146a decreases mature miR expression and predisposes to papillary thyroid carcinoma. *Proc. Natl. Acad. Sci. U.S.A.* 105, 7269–7274. doi: 10.1073/pnas.0802682105
- Kawaguchi, T., Horie, S., Bouchenaki, N., Ohno-Matsui, K., Mochizuki, M., and Herbort, C. P. (2010). Suboptimal therapy controls clinically apparent disease but not subclinical progression of Vogt-Koyanagi-Harada disease. *Int. Ophthalmol.* 30, 41–50. doi: 10.1007/s10792-008-9288-1
- Kim, J., Jeong, D., Nam, J., Aung, T. N., Gim, J. A., Park, K. U., et al. (2015). MicroRNA-124 regulates glucocorticoid sensitivity by targeting phosphodiesterase 4B in diffuse large B cell lymphoma. *Gene* 558, 173–180. doi: 10.1016/j.gene.2015.01.001
- Kim, S. J., Chen, Z., Essani, A. B., Elshabrawy, H. A., Volin, M. V., Volkov, S., et al. (2016). Identification of a novel toll-like receptor 7 endogenous ligand in rheumatoid arthritis synovial fluid that can provoke arthritic joint inflammation. *Arthritis Rheumatol.* 68, 1099–1110. doi: 10.1002/art.39544
- Kitaichi, N., Horie, Y., and Ohno, S. (2008). Prompt therapy reduces the duration of systemic corticosteroids in Vogt-Koyanagi-Harada disease. *Graefes Arch. Clin. Exp. Ophthalmol.* 246, 1641–1642. doi: 10.1007/s00417-008-0869-5
- Kobayashi, H., Kokubo, T., Takahashi, M., Sato, K., Miyokawa, N., Kimura, S., et al. (1998). Tyrosinase epitope recognized by an HLA-DR-restricted T-cell line from a Vogt-Koyanagi-Harada disease patient. *Immunogenetics* 47, 398–403. doi: 10.1007/s002510050375
- Kotani, A., Ha, D., Hsieh, J., Rao, P. K., Schotte, D., Den Boer, M. L., et al. (2009). miR-128b is a potent glucocorticoid sensitizer in MLL-AF4 acute lymphocytic leukemia cells and exerts cooperative effects with miR-221. *Blood* 114, 4169–4178. doi: 10.1182/blood-2008-12-191619
- Kwok, H. H., Poon, P. Y., Mak, K. H., Zhang, L. Y., Liu, P., Zhang, H., et al. (2017). Role of G3BP1 in glucocorticoid receptor-mediated microRNA-15b and microRNA-23a biogenesis in endothelial cells. *Cell. Mol. Life Sci.* 74, 3613–3630. doi: 10.1007/s00018-017-2540-y
- Lai, T. Y., Chan, R. P., Chan, C. K., and Lam, D. S. (2009). Effects of the duration of initial oral corticosteroid treatment on the recurrence of inflammation in Vogt-Koyanagi-Harada disease. *Eye (Lond)* 23, 543–548. doi: 10.1038/eye.2008.89
- Lambert, K. A., Roff, A. N., Panganiban, R. P., Douglas, S., and Ishmael, F. T. (2018). MicroRNA-146a is induced by inflammatory stimuli in airway epithelial cells and augments the anti-inflammatory effects of glucocorticoids. *PLoS One* 13:e0205434. doi: 10.1371/journal.pone.0205434
- Li, B., Wang, X., Choi, I. Y., Wang, Y. C., Liu, S., Pham, A. T., et al. (2017). miR-146a modulates autoreactive Th17 cell differentiation and regulates organ-specific autoimmunity. *J. Clin. Invest.* 127, 3702–3716. doi: 10.1172/JCI94012
- Li, B., Yang, P., Zhou, H., Huang, X., Jin, H., Chu, L., et al. (2005). Upregulation of T-bet expression in peripheral blood mononuclear cells during Vogt-Koyanagi-Harada disease. *Br. J. Ophthalmol.* 89, 1410–1412. doi: 10.1136/bjo.2005.074062
- Li, W., Kong, L. B., Li, J. T., Guo, Z. Y., Xue, Q., Yang, T., et al. (2014). MiR-568 inhibits the activation and function of CD4(+) T cells and Treg cells by targeting NFAT5. *Int. Immunol.* 26, 269–281. doi: 10.1093/intimm/dxt065
- Li, W., Liu, S., Chen, Y., Weng, R., Zhang, K., He, X., et al. (2020). Circulating exosomal microRNAs as biomarkers of systemic lupus erythematosus. *Clinics (Sao Paulo)* 75:e1528. doi: 10.6061/clinics/2020/e1528
- Liang, Y. N., Tang, Y. L., Ke, Z. Y., Chen, Y. Q., Luo, X. Q., Zhang, H., et al. (2017). MiR-124 contributes to glucocorticoid resistance in acute lymphoblastic leukemia by promoting proliferation, inhibiting apoptosis and targeting the glucocorticoid receptor. *J. Steroid Biochem. Mol. Biol.* 172, 62–68. doi: 10.1016/j.jsbmb.2017.05.014
- Liberman, P., Gaur, F., Berger, O., and Urzua, C. A. (2015). Causes of uveitis in a tertiary center in Chile: a cross-sectional retrospective review. *Ocul. Immunol. Inflamm.* 23, 339–345. doi: 10.3109/09273948.2014.981548
- Liu, L., Hua, M., Liu, C., He, N., Li, Z., and Ma, D. (2016). The aberrant expression of microRNAs and correlations with T cell subsets in patients with immune thrombocytopenia. *Oncotarget* 7, 76453–76463. doi: 10.18632/oncotarget.12949
- Liu, X., Yang, P., Lin, X., Ren, X., Zhou, H., Huang, X., et al. (2009). Inhibitory effect of Cyclosporin a and corticosteroids on the production of IFN-gamma and IL-17 by T cells in Vogt-Koyanagi-Harada syndrome. *Clin. Immunol.* 131, 333–342. doi: 10.1016/j.clim.2008.12.007
- Lu, L. F., Boldin, M. P., Chaudhry, A., Lin, L. L., Taganov, K. D., Hanada, T., et al. (2010). Function of miR-146a in controlling Treg cell-mediated regulation of Th1 responses. *Cell* 142, 914–929. doi: 10.1016/j.cell.2010.08.012
- Lucafo, M., Sicari, D., Chicco, A., Curci, D., Bellazzo, A., Di Silvestre, A., et al. (2020). miR-331-3p is involved in glucocorticoid resistance reversion by rapamycin through suppression of the MAPK signaling pathway. *Cancer Chemother. Pharmacol.* 86, 361–374. doi: 10.1007/s00280-020-04122-z
- Lv, M., Zhang, X., Jia, H., Li, D., Zhang, B., Zhang, H., et al. (2012). An oncogenic role of miR-142-3p in human T-cell acute lymphoblastic leukemia (T-ALL) by targeting glucocorticoid receptor-alpha and cAMP/PKA pathways. *Leukemia* 26, 769–777. doi: 10.1038/leu.2011.273
- Lyszkiewicz, M., Winter, S. J., Witzlau, K., Fohse, L., Brownlie, R., Puchalka, J., et al. (2019). miR-181a/b-1 controls thymic selection of Treg cells and tunes their suppressive capacity. *PLoS Biol.* 17:e2006716. doi: 10.1371/journal.pbio.2006716
- Mensa, E., Recchioni, R., Marcheselli, F., Giuliodori, K., Consales, V., Molinelli, E., et al. (2018). MiR-146a-5p correlates with clinical efficacy in patients with psoriasis treated with the tumour necrosis factor-alpha inhibitor adalimumab. *Br. J. Dermatol.* 179, 787–789. doi: 10.1111/bjd.16659
- Molitoris, J. K., Mccoll, K. S., and Distelhorst, C. W. (2011). Glucocorticoid-mediated repression of the oncogenic microRNA cluster miR-17-92 contributes to the induction of Bim and initiation of apoptosis. *Mol. Endocrinol.* 25, 409–420. doi: 10.1210/me.2010-0402
- Moschos, S. A., Williams, A. E., Perry, M. M., Birrell, M. A., Belvisi, M. G., and Lindsay, M. A. (2007). Expression profiling in vivo demonstrates rapid changes in lung microRNA levels following lipopolysaccharide-induced inflammation but not in the anti-inflammatory action of glucocorticoids. *BMC Genomics* 8:240. doi: 10.1186/1471-2164-8-240
- Mycko, M. P., Cichalewska, M., Machlanska, A., Cwiklinska, H., Mariasiewicz, M., and Selmaj, K. W. (2012). MicroRNA-301a regulation of a T-helper 17 immune response controls autoimmune demyelination. *Proc. Natl. Acad. Sci. U.S.A.* 109, E1248–E1257. doi: 10.1073/pnas.1114325109
- Nahid, M. A., Satoh, M., and Chan, E. K. (2011). MicroRNA in TLR signaling and endotoxin tolerance. *Cell. Mol. Immunol.* 8, 388–403. doi: 10.1038/cmi.2011.26
- Norose, K., and Yano, A. (1996). Melanoma specific Th1 cytotoxic T lymphocyte lines in Vogt-Koyanagi-Harada disease. *Br. J. Ophthalmol.* 80, 1002–1008. doi: 10.1136/bjo.80.11.1002
- Norose, K., Yano, A., Aosai, F., and Segawa, K. (1990). Immunologic analysis of cerebrospinal fluid lymphocytes in Vogt-Koyanagi-Harada disease. *Invest. Ophthalmol. Vis. Sci.* 31, 1210–1216.
- Norose, K., Yano, A., Wang, X. C., Tokushima, T., Umihira, J., Seki, A., et al. (1994). Dominance of activated T cells and interleukin-6 in aqueous humor in Vogt-Koyanagi-Harada disease. *Invest. Ophthalmol. Vis. Sci.* 35, 33–39.
- Ohta, K., and Yoshimura, N. (1998). Expression of Fas antigen on helper T lymphocytes in Vogt-Koyanagi-Harada disease. *Graefes Arch. Clin. Exp. Ophthalmol.* 236, 434–439. doi: 10.1007/s004170050102
- O'keefe, G. A., and Rao, N. A. (2017). Vogt-Koyanagi-Harada disease. *Surv. Ophthalmol.* 62, 1–25. doi: 10.1016/j.survophthal.2016.05.002
- Otani, S., Sakurai, T., Yamamoto, K., Fujita, T., Matsuzaki, Y., Goto, Y., et al. (2006). Frequent immune response to a melanocyte specific protein KU-MEL-1 in patients with Vogt-Koyanagi-Harada disease. *Br. J. Ophthalmol.* 90, 773–777. doi: 10.1136/bjo.2005.086520
- Park, H. S., Nam, K. Y., and Kim, J. Y. (2011). Intravitreal bevacizumab injection for persistent serous retinal detachment associated with Vogt-Koyanagi-Harada disease. *Graefes Arch. Clin. Exp. Ophthalmol.* 249, 133–136. doi: 10.1007/s00417-010-1477-8
- Prattichizzo, F., Giuliani, A., Recchioni, R., Bonafe, M., Marcheselli, F., De Carolis, S., et al. (2016). Anti-TNF-alpha treatment modulates SASP and SASP-related microRNAs in endothelial cells and in circulating angiogenic cells. *Oncotarget* 7, 11945–11958. doi: 10.18632/oncotarget.7858
- Przepiera-Bedzak, H., Fischer, K., and Brzosko, M. (2016). Extra-articular symptoms in constellation with selected serum cytokines and disease activity in spondyloarthritis. *Mediators Inflamm.* 2016:7617954. doi: 10.1155/2016/7617954

- Qi, J., Hou, S., Zhang, Q., Liao, D., Wei, L., Fang, J., et al. (2013). A functional variant of pre-miRNA-196a2 confers risk for Behcet's disease but not for Vogt-Koyanagi-Harada syndrome or AAO in ankylosing spondylitis. *Hum. Genet.* 132, 1395–1404. doi: 10.1007/s00439-013-1346-8
- Rainer, J., Ploner, C., Jesacher, S., Ploner, A., Eduardoff, M., Mansha, M., et al. (2009). Glucocorticoid-regulated microRNAs and mirtrons in acute lymphoblastic leukemia. *Leukemia* 23, 746–752. doi: 10.1038/leu.2008.370
- Ramchandran, R., and Chaluvally-Raghavan, P. (2017). miRNA-mediated RNA activation in mammalian cells. *Adv. Exp. Med. Biol.* 983, 81–89. doi: 10.1007/978-981-10-4310-9_6
- Reddycherla, A. V., Meinert, I., Reinhold, A., Reinhold, D., Schraven, B., and Simeoni, L. (2015). miR-20a inhibits TCR-mediated signaling and cytokine production in human naive CD4+ T cells. *PLoS One* 10:e0125311. doi: 10.1371/journal.pone.0125311
- Rosenbaum, J. T., Bodaghi, B., Couto, C., Zierhut, M., Acharya, N., Pavesio, C., et al. (2019). New observations and emerging ideas in diagnosis and management of non-infectious uveitis: a review. *Semin. Arthritis Rheum.* 49, 438–445. doi: 10.1016/j.semarthrit.2019.06.004
- Saus, E., Soria, V., Escaramis, G., Vivarelli, F., Crespo, J. M., Kagerbauer, B., et al. (2010). Genetic variants and abnormal processing of pre-miR-182, a circadian clock modulator, in major depression patients with late insomnia. *Hum. Mol. Genet.* 19, 4017–4025. doi: 10.1093/hmg/ddq316
- Shen, E., Rathinam, S. R., Babu, M., Kanakath, A., Thundikandy, R., Lee, S. M., et al. (2016). Outcomes of Vogt-Koyanagi-Harada disease: a subanalysis from a randomized clinical trial of antimetabolite therapies. *Am. J. Ophthalmol.* 168, 279–286. doi: 10.1016/j.ajo.2016.06.004
- Singh, A., Patro, P. S., and Aggarwal, A. (2019). MicroRNA-132, miR-146a, and miR-155 as potential biomarkers of methotrexate response in patients with rheumatoid arthritis. *Clin. Rheumatol.* 38, 877–884. doi: 10.1007/s10067-018-4380-z
- Smith, L. K., Shah, R. R., and Cidlowski, J. A. (2010). Glucocorticoids modulate microRNA expression and processing during lymphocyte apoptosis. *J. Biol. Chem.* 285, 36698–36708. doi: 10.1074/jbc.M110.162123
- Starega-Roslan, J., Krol, J., Koscińska, E., Kozłowski, P., Szałachcic, W. J., Sobczak, K., et al. (2011). Structural basis of microRNA length variety. *Nucleic Acids Res.* 39, 257–268. doi: 10.1093/nar/gkq727
- Su, D., Wang, X., Ma, Y., Hao, J., Wang, J., Lu, Y., et al. (2020). Nrf2-induced miR-23a-27a-24-2 cluster modulates damage repair of intestinal mucosa by targeting the Bach1/HO-1 axis in inflammatory bowel diseases. *Free Radic. Biol. Med.* 163, 1–9. doi: 10.1016/j.freeradbiomed.2020.11.006
- Sugita, S., Takase, H., Taguchi, C., Imai, Y., Kamoi, K., Kawaguchi, T., et al. (2006). Ocular infiltrating CD4+ T cells from patients with Vogt-Koyanagi-Harada disease recognize human melanocyte antigens. *Invest. Ophthalmol. Vis. Sci.* 47, 2547–2554. doi: 10.1167/iov.05-1547
- Tang, H., Lai, Y., Zheng, J., Chen, K., Jiang, H., and Xu, G. (2020). MiR-146a promotes tolerogenic properties of dendritic cells and through targeting Notch1 signaling. *Immunol. Invest.* 49, 555–570. doi: 10.1080/08820139.2019.1708385
- Tang, Q., Yang, Y., Zhao, M., Liang, G., Wu, H., Liu, Q., et al. (2015). Mycophenolic acid upregulates miR-142-3P/5P and miR-146a in lupus CD4+T cells. *Lupus* 24, 935–942. doi: 10.1177/0961203315570685
- Tessel, M. A., Benham, A. L., Krett, N. L., Rosen, S. T., and Gunaratne, P. H. (2011). Role for microRNAs in regulating glucocorticoid response and resistance in multiple myeloma. *Horm. Cancer* 2, 182–189. doi: 10.1007/s12672-011-0072-8
- Urzua, C. A., Chen, P., Chaigne-Delalande, B., Liu, B., Anguita, R., Guerrero, J., et al. (2019). Glucocorticoid receptor-alpha and MKP-1 as candidate biomarkers for treatment response and disease activity in Vogt-Koyanagi-Harada disease. *Am. J. Ophthalmol.* 207, 319–325. doi: 10.1016/j.ajo.2019.06.032
- Urzua, C. A., Guerrero, J., Gatica, H., Velasquez, V., and Goecke, A. (2017). Evaluation of the glucocorticoid receptor as a biomarker of treatment response in Vogt-Koyanagi-Harada disease. *Invest. Ophthalmol. Vis. Sci.* 58, 974–980. doi: 10.1167/iov.16-20783
- Valenzuela, R. A., Flores, I., Pujol, M., Llanos, C., Carreno, E., Rada, G., et al. (2020a). Definition of uveitis refractory to treatment: a systematic review in the absence of a consensus. *Ocul. Immunol. Inflamm.* doi: 10.1080/09273948.2020.1793369 [Epub ahead of print].
- Valenzuela, R. A., Flores, I., Urrutia, B., Fuentes, F., Sabat, P. E., Llanos, C., et al. (2020b). New pharmacological strategies for the treatment of non-infectious uveitis. a minireview. *Front. Pharmacol.* 11:655. doi: 10.3389/fphar.2020.00655
- Van Den Hof, W. F., Van Summeren, A., Lommen, A., Coonen, M. L., Brauers, K., Van Herwijnen, M., et al. (2014). Integrative cross-omics analysis in primary mouse hepatocytes unravels mechanisms of cyclosporin A-induced hepatotoxicity. *Toxicology* 324, 18–26. doi: 10.1016/j.tox.2014.06.003
- Velez, G., Roybal, C. N., Colgan, D., Tsang, S. H., Bassuk, A. G., and Mahajan, V. B. (2016). Precision medicine: personalized proteomics for the diagnosis and treatment of idiopathic inflammatory disease. *JAMA Ophthalmol.* 134, 444–448. doi: 10.1001/jamaophthalmol.2015.5934
- Wang, C., Tian, Y., Lei, B., Xiao, X., Ye, Z., Li, F., et al. (2012). Decreased IL-27 expression in association with an increased Th17 response in Vogt-Koyanagi-Harada disease. *Invest. Ophthalmol. Vis. Sci.* 53, 4668–4675. doi: 10.1167/iov.12-9863
- Wang, C., Wang, L., Hu, J., Li, H., Kijlstra, A., and Yang, P. (2018). Increased expression of IL-23 receptor (IL-23R) in Vogt-Koyanagi-Harada (VKH) disease. *Curr. Eye Res.* 43, 1369–1373. doi: 10.1080/02713683.2018.1485952
- Wang, X., Li, C., Ju, S., Wang, Y., Wang, H., and Zhong, R. (2011). Myeloma cell adhesion to bone marrow stromal cells confers drug resistance by microRNA-21 up-regulation. *Leuk. Lymphoma* 52, 1991–1998. doi: 10.3109/10428194.2011.591004
- Wang, Y., and Gaudio, P. A. (2008). Infliximab therapy for 2 patients with Vogt-Koyanagi-Harada syndrome. *Ocul. Immunol. Inflamm.* 16, 167–171. doi: 10.1080/09273940802204527
- Wcislo-Dziadecka, D., Simka, K., Kazmierczak, A., Kruszniewska-Rajs, C., Gola, J., Grabarek, B., et al. (2018). Psoriasis treatment changes the expression profile of selected caspases and their regulatory microRNAs. *Cell Physiol. Biochem.* 50, 525–537. doi: 10.1159/000494166
- Wu, J., Zhang, H., Zheng, Y., Jin, X., Liu, M., Li, S., et al. (2018). The long noncoding RNA MALAT1 induces tolerogenic dendritic cells and regulatory T cells via miR155/dendritic cell-specific intercellular adhesion molecule-3 grabbing nonintegrin/IL10 axis. *Front. Immunol.* 9:1847. doi: 10.3389/fimmu.2018.01847
- Wu, L., Evans, T., Saravia, M., Schlaen, A., and Couto, C. (2009). Intravitreal bevacizumab for choroidal neovascularization secondary to Vogt-Koyanagi-Harada syndrome. *Jpn. J. Ophthalmol.* 53, 57–60. doi: 10.1007/s10384-008-0600-4
- Wu, L., Zhou, H., Zhang, Q., Zhang, J., Ni, F., Liu, C., et al. (2010). DNA methylation mediated by a microRNA pathway. *Mol. Cell* 38, 465–475. doi: 10.1016/j.molcel.2010.03.008
- Xu, J., Su, Y., Xu, A., Fan, F., Mu, S., Chen, L., et al. (2019). miR-221/222-mediated inhibition of autophagy promotes dexamethasone resistance in multiple myeloma. *Mol. Ther.* 27, 559–570. doi: 10.1016/j.ymthe.2019.01.012
- Yang, A., Ma, J., Wu, M., Qin, W., Zhao, B., Shi, Y., et al. (2012). Aberrant microRNA-182 expression is associated with glucocorticoid resistance in lymphoblastic malignancies. *Leuk. Lymphoma* 53, 2465–2473. doi: 10.3109/10428194.2012.693178
- Yang, D., Haemmig, S., Zhou, H., Perez-Cremades, D., Sun, X., Chen, L., et al. (2021). Methotrexate attenuates vascular inflammation through an adenosine-microRNA-dependent pathway. *Elife* 10:e58064. doi: 10.7554/eLife.58064
- Yang, F., Lu, J., Yu, Y., and Gong, Y. (2017). Epithelial to mesenchymal transition in cyclosporine A-induced rat gingival overgrowth. *Arch. Oral Biol.* 81, 48–55. doi: 10.1016/j.archoralbio.2017.04.024
- Yang, P., Ye, Z., Du, L., Zhou, Q., Qi, J., Liang, L., et al. (2018). Novel treatment regimen of Vogt-Koyanagi-Harada disease with a reduced dose of corticosteroids combined with immunosuppressive agents. *Curr. Eye Res.* 43, 254–261. doi: 10.1080/02713683.2017.1383444
- Yang, P., Zhang, M., Wang, X., Xu, A. L., Shen, M., Jiang, B., et al. (2020). MicroRNA let-7g-5p alleviates murine collagen-induced arthritis by inhibiting Th17 cell differentiation. *Biochem. Pharmacol.* 174:113822. doi: 10.1016/j.bcp.2020.113822
- Yang, Y., Tang, Q., Zhao, M., Liang, G., Wu, H., Li, D., et al. (2015). The effect of mycophenolic acid on epigenetic modifications in lupus CD4+T cells. *Clin. Immunol.* 158, 67–76. doi: 10.1016/j.clim.2015.03.005
- Yu, H., Liu, Y., Bai, L., Kijlstra, A., and Yang, P. (2014). Predisposition to Behcet's disease and VKH syndrome by genetic variants of miR-182. *J. Mol. Med. (Berl.)* 92, 961–967. doi: 10.1007/s00109-014-1159-9

- Zhang, D., Qiu, X., Li, J., Zheng, S., Li, L., and Zhao, H. (2019). MiR-23a-3p-regulated abnormal acetylation of FOXP3 induces regulatory T cell function defect in Graves' disease. *Biol. Chem.* 400, 639–650. doi: 10.1515/hsz-2018-0343
- Zhou, Q., Haupt, S., Kreuzer, J. T., Hammitzsch, A., Proft, F., Neumann, C., et al. (2015). Decreased expression of miR-146a and miR-155 contributes to an abnormal Treg phenotype in patients with rheumatoid arthritis. *Ann. Rheum. Dis.* 74, 1265–1274. doi: 10.1136/annrheumdis-2013-204377
- Zhou, Q., Hou, S., Liang, L., Li, X., Tan, X., Wei, L., et al. (2014). MicroRNA-146a and Ets-1 gene polymorphisms in ocular Behcet's disease and Vogt-Koyanagi-Harada syndrome. *Ann. Rheum. Dis.* 73, 170–176. doi: 10.1136/annrheumdis-2012-201627
- Zmuda, M., Tiev, K. P., Knoeri, J., and Heron, E. (2013). Successful use of infliximab therapy in sight-threatening corticosteroid-resistant Vogt-Koyanagi-Harada disease. *Ocul. Immunol. Inflamm.* 21, 310–316. doi: 10.3109/09273948.2013.775312
- Conflict of Interest:** The authors declare that the research was conducted in the absence of any commercial or financial relationships that could be construed as a potential conflict of interest.

Copyright © 2021 Vega-Tapia, Bustamante, Valenzuela, Urzua and Cuitino. This is an open-access article distributed under the terms of the Creative Commons Attribution License (CC BY). The use, distribution or reproduction in other forums is permitted, provided the original author(s) and the copyright owner(s) are credited and that the original publication in this journal is cited, in accordance with accepted academic practice. No use, distribution or reproduction is permitted which does not comply with these terms.



OPEN ACCESS

Edited by:

Jing Zhang,
Shanghai Jiao Tong University, China

Reviewed by:

Qi-En Yang,
Northwest Institute of Plateau
Biology, Chinese Academy of
Sciences (CAS), China
Xiaoyong Li,
Shanghai Jiao Tong University, China

*Correspondence:

Wenxian Zeng
zengwenxian2015@126.com
Yi Zheng
y.zheng@nwfau.edu.cn
orcid.org/0000-0003-0152-2671

[†]These authors have contributed
equally to this work

Specialty section:

This article was submitted to
Epigenomics and Epigenetics,
a section of the journal
Frontiers in Cell and Developmental
Biology

Received: 23 March 2021

Accepted: 06 May 2021

Published: 04 June 2021

Citation:

Lv Y, Li T, Yang M, Su L, Zhu Z,
Zhao S, Zeng W and Zheng Y (2021)
Melatonin Attenuates Chromium
(VI)-Induced Spermatogonial Stem
Cell/Progenitor Mitophagy by
Restoration of
METTL3-Mediated RNA
N⁶-Methyladenosine Modification.
Front. Cell Dev. Biol. 9:684398.
doi: 10.3389/fcell.2021.684398

Melatonin Attenuates Chromium (VI)-Induced Spermatogonial Stem Cell/Progenitor Mitophagy by Restoration of METTL3-Mediated RNA N⁶-Methyladenosine Modification

Yinghua Lv^{1,2†}, Tianjiao Li^{2†}, Manman Yang¹, Lihong Su², Zhendong Zhu³, Sihang Zhao², Wenxian Zeng^{2*} and Yi Zheng^{2*}

¹Shaanxi Key Laboratory of Natural Products & Chemical Biology, College of Chemistry & Pharmacy, Northwest A&F University, Yangling, China, ²Key Laboratory for Animal Genetics, Breeding and Reproduction of Shaanxi Province, College of Animal Science and Technology, Northwest A&F University, Yangling, China, ³College of Animal Science and Technology, Qingdao Agricultural University, Qingdao, China

Spermatogonial stem cells (SSCs) are the basis of spermatogenesis, and any damage to SSCs may result in spermatogenic disorder and male infertility. Chromium (Cr) (VI) is a proven toxin, mutagen, and carcinogen, perpetually detrimental to environmental organisms due to its intricate and enduring detoxification process *in vivo*. Despite this, the deleterious effects of Cr (VI) on SSCs and the underlying mechanisms remain poorly understood. In this study, we identified that Cr (VI) impaired male reproductive system in mouse testes and induced mitochondrial dynamic imbalance and mitophagy in SSCs/progenitors. Cr (VI) also downregulated the RNA N⁶-methyladenosine (m⁶A) modification levels in mitochondrial dynamic balance and mitophagy genes in SSCs/progenitors. Inspiringly, the toxic effects of Cr (VI) could be relieved by melatonin pretreatment. Melatonin alleviated Cr (VI)-induced damage to male reproductive system and autophagy in mouse testes. Melatonin also attenuated Cr (VI)-induced cell viability loss and reactive oxygen species (ROS) generation, as well as mitochondrial dynamic disorders and mitophagy in SSCs/progenitors. The protective roles of melatonin against Cr (VI)-induced mitophagy were exerted by restoration of METTL3-mediated RNA m⁶A modification and activation of mitochondrial fusion proteins MFN2 and OPA1, as well as inhibition of the mitophagy BNIP3/NIX receptor pathway. Thus, our study provides novel insights into the molecular mechanisms for RNA m⁶A modification underlying the gene regulatory network responsible for mitochondrial dynamic balance, and also lays new experimental groundwork for treatment of Cr (VI)-induced damage to male fertility.

Keywords: chromium (VI), spermatogonial stem cells, mitophagy, melatonin, RNA m⁶A modification

INTRODUCTION

Chromium (Cr) is a natural metal element and most frequently detected in soil, ground water, air, rocks, and living organisms. Chromium and chromium-containing compounds are prevalent, mainly due to their extensive industrial applications, such as electroplating, leather tanning, stainless steel production, water cooling, printing inks, textile dyeing, pigment manufacturing of wood, drilling muds, fireworks, wood preservation, and anti-corrosion and conversion coatings (Ukhurebor et al., 2021). Trivalent chromium [Cr (III)] and hexavalent chromium [Cr (VI)] are the two stable valence states typically found in workplace and environment (Kotas and Stasicka, 2000; Costa, 2003). In natural systems, Cr (III) is generally considered as low toxicity and mobility in humans and animals (Chen et al., 2019). By contrast, Cr (VI) is a strong oxidizing agent and one of the most toxic environmental potential carcinogens. Cr (VI) is toxic to both plants and animals, perpetually detrimental to environmental organisms due to its intricate and enduring detoxification process *in vivo* (Zhitkovich, 2011). The well-known cellular toxicity of Cr (VI) can be attributed to reactive oxygen species (ROS) generation that triggers oxidative stress, DNA damage, genomic instability (Zhitkovich, 2005), or epigenetic modulation (DesMarais and Costa, 2019). While the potential toxicity of Cr (VI) has appealed to the public, its deleterious effects on male fertility remain to be explored. For instance, the detrimental influences of Cr (VI) on spermatogonial stem cells (SSCs) warrant systematic investigation. Since SSCs are the cornerstone of spermatogenesis and able to differentiate into sperm thereby transmitting paternal genetic information to the next generation (Kubota and Brinster, 2018; Sharma et al., 2019), studies in this respect would be of great value to male fertility and reproductive health.

Epigenetic events, including DNA methylation and histone modifications, regulate SSC homeostasis (Makela and Hobbs, 2019). Our previous study showed that high dosages of Cr (VI) induced a global increase of H3K9me3 and activated apoptotic signaling pathways in mouse SSCs (Lv et al., 2018). Whether this phenotype also involves changes in other epigenetic markers, e.g., N⁶-methyladenosine (m⁶A) modification of RNA methylation, remains elusive. RNA m⁶A modification is the most abundant and widely distributed RNA modification in eukaryotes, accounting for more than 90% in all RNA modifications (Meyer et al., 2012). It is involved in RNA splicing, translation, stabilization, and degradation, thus playing regulatory roles in many biological processes, including SSC maintenance and spermatogenesis (Hsu et al., 2017; Lin et al., 2017; Xu et al., 2017). Previous studies have shown that activation of stress-response pathways causes global reshaping of the cellular mRNA methylome. More precisely, in the heat shock state, m⁶A residues within the 5' UTR promote cap-independent translation of heat shock factor (HSF) mRNAs, activating the cell heat shock response pathway (Meyer et al., 2015). Additionally, under UV irradiation, RNA m⁶A modification could recruit DNA repair enzyme

pol κ to DNA damage sites to facilitate DNA repair and cell survival (Xiang et al., 2017). These studies suggest that RNA m⁶A modification is involved in regulation of gene expression and in protection of cells under stress conditions. It has also been reported that m⁶A is essential for the well-being of male reproductive system. For instance, the increased m⁶A modification of RNA methylation is related to the inhibition of demethylase FTO thereby contributing to MEHP-induced Leydig cell injury (Zhao et al., 2021). However, it remains unknown whether RNA m⁶A modification is involved in Cr (VI)-induced toxicity in SSCs.

Melatonin is an endogenous indoleamine hormone. As the strongest endogenous free radical scavenger of ROS and inducer of antioxidant systems *in vivo* (Bonnefont-Rousselot et al., 2011), melatonin is involved in various physiological processes, such as apoptosis and autophagy in cancer cells, neurodegeneration and progressions of liver diseases as well as other pathologies (Fernandez et al., 2015). Recent studies by peers and us have shown that melatonin could protect testes against heat-induced damage (Zhang et al., 2020a) and spermatogonia against the stress of chemotherapy and oxidation *via* elimination of ROS (Zhang et al., 2019), and that melatonin also has protective roles against Cr (VI)-induced apoptosis and the global levels of H3K9me3 and H3K27me3 in mouse SSCs (Lv et al., 2018). Nevertheless, whether melatonin has effects on Cr (VI)-induced RNA m⁶A modification in SSCs and, if any, the underlying mechanisms remain to be probed.

In this study, we first demonstrated that Cr (VI) impaired male reproductive system in mouse testes, along with a decrease in cell viability but an increase in ROS generation in SSCs/progenitors. Then, we identified that RNA m⁶A modification was involved in Cr (VI)-induced mitochondrial dynamic disorders and mitophagy. Inspiringly, melatonin alleviated Cr (VI)-induced damage to male reproductive system and autophagy in mouse testes. Melatonin also attenuated Cr (VI)-induced cell viability loss and ROS generation, as well as mitochondrial dynamic disorders and mitophagy in SSCs/progenitors. The protective roles of melatonin against Cr (VI)-induced mitophagy were exerted by restoration of METTL3-mediated RNA m⁶A modification and activation of mitochondrial fusion proteins MFN2 and OPA1, as well as inhibition of the mitophagy BNIP3/NIX receptor pathway. Thus, our study provides novel insights into the molecular mechanisms for RNA m⁶A modification underlying the gene regulatory network responsible for mitochondrial dynamic balance, and also lays new experimental groundwork for treatment of Cr (VI)-induced damage to male fertility.

MATERIALS AND METHODS

Chemicals and Antibodies

Na₂CrO₄ (98% of purity; 307,831) and melatonin (98% of purity; M5250) were purchased from Sigma-Aldrich (St. Louis, MO, United States). The detailed antibody information is shown in **Table 1**.

TABLE 1 | The detailed antibody information.

Antibody	Species source	Supplier	Identifier	Dilution	
				WB	IHC
LIN28	Rabbit	Abcam	ab46020		1:200
CDH1	Rabbit	Proteintech	20874-1-AP		1:200
m ⁶ A	Rabbit	Synaptic systems	202003	1:1,000	
Beclin1	Rabbit	Cell signaling technology	3738s	1:1,000	
p-Beclin1	Rabbit	Cell signaling technology	13825s	1:1,000	
LC3B	Rabbit	Sigma-Aldrich	L-7543	1:1,000	
β-actin	Mouse	CWBIO	CW0096	1:2,000	
Tom20	Rabbit	Proteintech	11802-1-AP	1:1,000	
MT1	Mouse	Abnova	H00004543-A01	1:1,000	
NOX4	Rabbit	NOVUS	NB110-58849	1:1,000	
METTL3	Rabbit	Cell signaling technology	15073-1-AP	1:1,000	

WB, western blot; IHC, immunohistochemistry.

Cells and Treatment

Immortalized mouse SSCs/progenitors (the C18-4 cell line) were established from type A spermatogonia in testes from 6-day-old mice (Hofmann et al., 2005). The cells were cultured with the medium comprising DMEM (high glucose, Hyclone), 10% FBS (BI) and 1% penicillin-streptomycin (Invitrogen, 15140122). Cells were maintained at 37°C in an atmosphere of 5% CO₂ in air. Cells were pretreated with vehicle or 50 μM melatonin for 2 h, followed by treatment with 10 μM Cr (VI) for 1 or 4 h, unless otherwise stated.

Animals and Treatment

C57BL/6J mice were purchased from the laboratory animal center of the Fourth Military Medical University, Xi'an, China. Adult male mice aged 8–10 weeks, with the body weight (*b.w.*) 22–25 g, were fed with the basal diet and kept at 20 ± 2°C and 50 ± 5% humidity under a 12-h light-dark cycle. Forty mice were divided into four groups at random, with 10 mice in each group: the control group (intraperitoneal injection with an equal volume of physiological saline daily), the Cr (VI) group [intraperitoneal injection with 16.2 mg/kg *b.w.*/day Cr (VI)], the melatonin + Cr (VI) group [intraperitoneal injection with 25 mg/kg *b.w.*/day melatonin at 4 h before intraperitoneal injection with 16.2 mg/kg *b.w.*/day Cr (VI)] and the melatonin group (intraperitoneal injection with 25 mg/kg *b.w.*/day melatonin). Melatonin and Cr (VI) treatment lasted for 14 consecutive days, followed by 14 days of recovery before sacrifice. All animal procedures were in accordance with and approved by the Institutional Animal Care and Use Committee of Northwest A&F University (DK-314020038).

Hematoxylin and Eosin Staining

Hematoxylin and eosin (H&E) staining was performed as previously reported (Zheng et al., 2019). Briefly, after deparaffinization and rehydration, testis sections were stained with hematoxylin and eosin, and then sealed with neutral gum and examined under a light microscope. To quantify the ratios of only 1–3 layers of germ cell, empty and abnormal tubules, 300 seminiferous tubules from five mice were analyzed in each group.

Immunohistochemistry

Mouse testes were collected, fixed in diluted Bouin's solution and embedded in paraffin. Testis sections were sliced at a thickness of 6 μm. After deparaffinization and rehydration, testis sections were permeabilized with 0.5% Triton X-100 (Solarbio) for 10 min and subjected to heat-induced antigen retrieval in 10 mM sodium citrate buffer (pH = 6.0), followed by blocking with 10% donkey serum for 2 h at room temperature. Testis sections were then incubated with primary antibodies (Table 1) at 4°C overnight. Next day, testis sections were washed with PBS and incubated with the corresponding secondary antibody anti-rabbit-Alexa Fluor 488 (1:300; 711-545-152, Jackson ImmunoResearch) or anti-rabbit-Alexa Fluor 594 (1:300; 711-585-152, Jackson ImmunoResearch) for 1 h at 37°C. After washing, testis sections were stained with DAPI (1:1,000; BioWorld) and examined under a fluorescence microscope (Nikon Eclipse 80i, Tokyo, Japan).

Assays of Sperm Number, Progressive Motility, and Morphological Abnormality

Sperm progressive motility was determined by computer-assisted sperm analysis (CASA; HVIEW, China), as previously reported (Li et al., 2020a). In brief, the sample (0.5 ml) was pre-incubated at 37°C for 5 min, and the sperm progressive motility was defined as the percentage of spermatozoa with straight line velocity (VSL) > 25 μm/s and straightness of path (STR) ≥ 75%. The standard parameter was set at 30 frames/s. A minimum of 300 spermatozoa were observed from at least five randomly selected fields with 20 μm CELL-VU® DRM-600 sperm count slides (Millennium Sciences, United States) and a microscopic stage warmer (KITAZATO, Japan). Later, the sample was fixed with ethanol, and the sperm number was evaluated using CASA and 20 μm CELL-VU® DRM-600 sperm count slides. Then, the mouse semen sample was fixed in 4% paraformaldehyde for 24 h and subsequently spread on slides. H&E staining was conducted for sperm morphology examination. Over 1,000 spermatozoa were examined for morphological abnormality under a light microscope, and assessment of sperm morphological abnormality was referred to a previous report (Gotoh et al., 2012).

Depletion of *Mettl3* by Lentivirus-Mediated shRNA Targeting

To stably deplete *Mettl3* in mouse SSCs/progenitors, lentiviruses harboring shRNA targeting mouse *Mettl3* were packaged, produced, and delivered to cells, following a previous article (Zheng et al., 2020). In brief, lentiviruses were produced by co-transfecting the cloned shRNA expressing vectors (backbone: pGreenPuro; System Biosciences) and the 2nd generation packaging vectors psPAX2 and pMD2.G into HEK293T cells, and were concentrated using ultracentrifugation. Mouse SSCs/progenitors exposed to 10 µg/ml polybrene (Sigma-Aldrich) and the concentrated virus supernatant at a multiplicity of infection (MOI) of 20 were centrifuged at 3,000 g for 1 h at 32°C, followed by 16 h of incubation at 37°C. About 5 days after lentiviral transduction, cells were harvested for validation or downstream experiments. For construction of the shRNA expressing vectors, a sequence specific to the mouse *Mettl3* cDNA (5'-GCTACCGTATGGGACATTA-3') or a scramble sequence (5'-GACACCTACGCAAAACCCT-3') was used.

CCK-8 Assay

Cell viability was determined using a Cell Counting Kit-8 (CCK-8) assay kit (Beyotime, Beijing, China). Mouse SSCs/progenitors were prepared and dispersed in 96-well cell culture plates at a density of 1.0×10^4 cells/well. After overnight incubation, cells were either exposed to Cr (VI) at the dose of 0, 2.5, 5, 10, 25, or 50 µM for 12 h, or to 10 µM Cr (VI) for 0, 1, 4, 8, 12, 16, 20, or 24 h, unless otherwise stated. Then, about 10 µl of the CCK-8 solution diluted in DMEM was added to each well and incubated for 1.5 h at 37°C. The optical density of each well was measured at 490 nm with a microplate reader. Three independent experiments were performed, and in each independent experiment, at least three parallel measurements were performed.

MTT Assay

Mouse SSCs/progenitors were prepared and dispersed in 96-well cell culture plates at a density of 1.0×10^4 cells/well. After overnight incubation, cells were treated with Cr (VI) at the dose of 0, 2.5, 5, 10, 25 or 50 µM for 24 h. Then, the cells were washed with PBS, and the fresh medium containing MTT [3-(4,5)-dimethylthiazol-2-yl-4-methyl-5-phenyltetrazolium bromide] was added to each well, followed by 4 h of incubation. Later, the medium containing MTT was removed, and dimethyl sulfoxide (100 µl) was added to each well. The plate was then gently shaken for 10 min to dissolve formazan crystals. Finally, the absorbance at 490 nm in each well was recorded with a microplate reader. Three independent experiments were performed, and in each independent experiment, at least three parallel measurements were performed.

EdU Assay

Mouse SSCs were prepared and dispersed in 96-well cell culture plates at a density of 1.0×10^4 cells/well. After overnight incubation, cells were exposed to Cr (VI) at the dose of 0,

2.5, 5, 10, 25, or 50 µM for 24 h. Then, the cells were washed with PBS, and subjected to an EdU assay, as previously reported (Zheng et al., 2017). Three independent experiments were performed.

MDC Incorporation Assay

A fluorescent compound, namely monodansylcadaverine (MDC; Solarbio), has been proposed as a tracer for autophagic vacuoles. Thus, autophagic vacuoles can be detected by MDC staining. After the melatonin and/or Cr (VI) treatment, cells were incubated with 50 µM MDC in a serum-free medium for 30 min at 37°C. Then the cells were washed with PBS for three times and fluorescence micrographs were captured using an inverted fluorescence microscope (Olympus IX71, Tokyo, Japan).

m⁶A Dot-Blot Assay

Total RNAs were extracted from cells with Trizol reagent (Takara) and mRNAs were purified using PolyAtract® mRNA Isolation Systems (Promega, Z5310) following the manufacturer's instructions. Briefly, mRNA samples were loaded onto a Hybond-N⁺ membrane (GE HealthCare, RPN303B) and crosslinked to the membrane with UV radiation. Then, the membrane was blocked with 5% non-fat milk (Bio-Rad) for 2 h, followed by incubation with a rabbit anti-m⁶A polyclone antibody (Synaptic Systems, 202003) at 4°C overnight. Next day, the membrane was incubated with an HRP-conjugated goat anti-rabbit IgG (CWbio, CW0156) antibody for 2 h at room temperature. The immunocomplex was visualized and captured by a Bio-Rad Chemidoc XRS with a Western Bright ECL Kit (Bio-Rad, Berkeley, CA, United States). Finally, the membrane was stained with 0.02% methylene blue to eliminate the difference in mRNA amount.

Mito and Lyso Tracker Staining

Cells were pretreated with vehicle or 50 µM melatonin for 2 h, followed by treatment with 10 µM Cr (VI) for 1 or 4 h. Then, the cells were refreshed and incubated with 200 nM Mito-Tracker Green (Beyotime, Beijing, China) and 75 nM Lyso-Tracker Red (Beyotime, Beijing, China) for 45 min. Subsequently, the cells were washed twice and visualized under an inverted microscope (Olympus IX71, Tokyo, Japan). To quantify the ratio of cells double positive for both Mito and Lyso staining, 100 cells were analyzed in each group and three independent experiments were performed.

Mitochondrial Membrane Potential Assay

Mitochondrial membrane potential (MMP) was determined by using the lipophilic cationic dye JC-1 (Beyotime, Beijing, China). Cells were seeded into 96-well plates with a density of 1×10^4 cells/well. After overnight plating, cells were pretreated with vehicle or 50 µM melatonin for 2 h, followed by treatment with 10 µM Cr (VI) for 1 or 4 h. After washing, the cells were incubated with JC-1 for 20 min at 37°C. Then a microplate reader was employed to detect the fluorescence

intensity. The ratio of red/green fluorescence density indicated mitochondrial polarization.

Analysis of the ROS Level

The intracellular ROS accumulation was detected by the ROS Assay Kit (Beyotime, Beijing, China). Cells were seeded to 6-well plates and treated with Cr (VI). Then the cells were incubated with 10 μ M DCFH-DA for 20 min at 37°C, dissociated by trypsin, and collected after centrifugation. The same number of cells were seeded into 96-well plates, and detected by a microplate reader.

m⁶A-IP-qPCR Analysis

Quantitative real-time PCR (qPCR) analyses were performed to detect the relative abundance of the selected mRNA in the m⁶A antibody IP sample and in the input sample. Briefly, total RNAs were extracted from cells using the RNAiso plus reagent (Takara, Dalian, China). mRNAs were purified from total RNAs using the PolyAtract mRNA Isolation Systems (Promega, Z5310) and then fragmented using RNA Fragmentation reagent (Invitrogen, AM8740) for 1 min at 94°C. Protein A beads were washed and diluted into 500 μ l IP buffer (150 mM NaCl, 0.1% NP-40, 10 mM Tris, pH = 7.4, 100 U RNase inhibitor) and incubated with a m⁶A antibody (Synaptic Systems, 202003) for 1 h at 4°C. About 10% of the fragmented RNAs were left aside as input RNAs, whereas the remaining RNAs were added to the mixture and incubated for 4 h at 4°C with rotation. The mRNAs harboring m⁶A were eluted using 100 μ l elution buffer (IP buffer, 6.7 mM m⁶A) for 1 h at 4°C and precipitated with 5 mg glycogen (Life Technologies, AM9510) and one-tenth volume of 3 M sodium acetate (Solarbio) in 2.5 volumes of 100% ethanol at -80°C overnight. The same numbers of the concentrated IP RNAs or input RNAs from each sample were used for cDNA synthesis. The m⁶A enrichment was finally determined by qPCR analysis.

qPCR Analysis

Total RNAs were extracted from cells with Trizol reagent (Takara, Dalian, China), according to the manufacturer's protocol. For each sample, 1 μ g total RNAs were subjected to reverse transcription into cDNAs using the PrimeScript™ RT reagent Kit with gDNA Eraser (Takara, Dalian, China). qPCR analyses were conducted with an IQ5 (Bio-Rad, Berkeley, CA, United States). Reactions were run in triplicates, and three independent experiments were performed. The geometric mean of the housekeeping gene β -actin was used as an internal reference and the data were analyzed using the $2^{-\Delta\Delta C_t}$ method. Primer sequences for qPCR analyses were shown in Table 2.

Western Blot Analysis

Cells were lysed in RIPA buffer (Solarbio, Beijing, China) for 30 min on ice, and then centrifuged at 12,000 g for 10 min at 4°C. The concentrations of proteins were measured with a BCA kit (Takara, Dalian, China). About 30 μ g total proteins from each sample were separated by polyacrylamide gel electrophoresis in the presence of sodium dodecyl sulfate (SDS-PAGE) and transferred onto the poly-vinylidene fluoride (PVDF) membrane at 10 V using the Bio-Rad semidry transfer system. The blot-transferred membranes were blocked with 5% fat-free dry milk dissolved in Tris-buffered saline containing 0.1% tween-20 (TBST) for 2 h and then incubated with primary antibodies (Table 1) on the shaker at 4°C overnight. Blots were washed with TBST, followed by incubation with a horseradish peroxidase (HRP)-conjugated anti-rabbit or anti-mouse IgG antibody (Millipore). Protein bands were visualized under a Bio-Rad Chemidoc XRS with a Western Bright ECL Kit (Bio-Rad, Berkeley, CA, United States) and digital images were captured. Finally, the gray scale analysis was performed by comparing the signals of target proteins with those of the housekeeper β -actin.

TABLE 2 | Primer sequences for qPCR analyses.

Gene	Forward primer (5'→3')	Reverse primer (5'→3')	Product size, bp
<i>Mfn1</i>	AGAGCCCATCTTTTCAGGTCC	TTAGTTTCCAGCCCACTGTTTTC	197
<i>Mfn2</i>	AGCAGATTACGGAGGAAGTGGA	GAGCAGCGGTCAGACAGGTT	190
<i>Opa1</i>	GCTTCAAGGTCGTCTCAAGGATA	TCGTTCTTGTTTCGTTGTGA	129
<i>Drp1</i>	CAGTGTCCCAAAGGCAGTAATG	CGCTGCTTCTTTTCTTCGTTG	151
<i>Bnip3</i>	TTCAGCAATGGCAATGGGA	TTGTGGTGTCTGGGAGCGA	153
<i>Nix</i>	GCAATGAGAATGGAATGGGA	TTCTTGTGGTGAAGGGCTGTC	164
<i>Mettl3</i>	GAGGTTCTGTTCCACAGTCATAA	TAGGTTTAGAGATGATGCCGTCC	217
<i>Wtap</i>	AGTTATGGCACGGGATGAGTTA	TCCTGCTGTGTCTGCTTTAGTT	147
<i>Fto</i>	CTGAGGATGAAAGTGAGGACGAG	TGGAACATAACCGAGGCTGTG	204
<i>Ythdf2</i>	CCTCTTGGAGCAGAGACCAAA	TTATTCGGCCTTGCCCTGTGG	123
β -actin	TCTTTTCCAGCCTTCTCTTCTTG	GTTGGCATAGAGGTCTTTACGGA	109
<i>Mfn2</i> -IP	ATGTGTCTGTGTCTGCTCCTCA	TGTGCTCAGGCTGGAGAAAGTA	149
<i>Opa1</i> -IP	AGGTCATCAGTCTGAGCCAGGT	CTGTGGTGTAAATGTTCCTGA	147
<i>Bnip3</i> -IP	CTGCCCTGCTACCTCTCG	AGGTTCTCTCCCGCTCT	100
<i>Nix</i> -IP	CTTCTCTGCTTCCATCCACA	CATGATCTGCCCATCTTCTTGT	134

Statistics

Experimental data were analyzed with the Graph Pad Prism 6 software and presented as the mean \pm SEM. A Student's *t*-test (two-sided) or one-way ANOVA followed by a Duncan's multiple range test (SPSS 19.0; Chicago, IL, United States) was performed to determine the significant value. A value of $p < 0.05$ was considered statistically significant. * $p < 0.05$; ** $p < 0.01$.

RESULTS

Cr (VI) Damaged Male Reproductive System and SSCs/Progenitors in Mouse Testes

To systematically investigate the toxic effects of Cr (VI) on male reproductive system, we randomly divided 20 male C57/BL6 mice into two groups: control and Cr (VI), with 10 mice in each group. Mice in the Cr (VI) treatment group were intraperitoneally injected with Cr (VI) (16.2 mg/kg *b.w.*/day) for 14 consecutive days. The dosage was based on previous reports (Kart et al., 2016; Ogbomida et al., 2018) and our preliminary experiment (data not shown). All mice in both groups were sacrificed on the 14th day after the last administration, and the testes were removed for examination. H&E staining results showed that seminiferous tubules were clearly diminished after Cr (VI) administration. Cr (VI) administration also triggered nuclear pyknosis and exfoliation of spermatogenic cells, as well as the emergence of different sizes of vacuoles and even cavities in some seminiferous tubules. Quantification analyses revealed markedly higher ratios of only 1–3 layers of germ cell, empty and abnormal tubules in the Cr (VI) treatment group (Figures 1A–D). In addition, despite no significant difference in body weight (Figure 1E), Cr (VI) treatment clearly decreased the testicular index (the ratio of testis weight to body weight, Figure 1F), the sperm number (Figure 1G), and progressive motility (Figure 1H), along with an increase of abnormal epididymal spermatozoa (Figure 1I).

Next, we performed immunofluorescence staining on testis sections with SSC/progenitor markers LIN28 (Zheng et al., 2009; Figure 1J) and CDH1 (Tokuda et al., 2007; Figure 1K). After quantification, we identified that the numbers of LIN28⁺ and CDH1⁺ cells per seminiferous tubule were significantly reduced after Cr (VI) treatment (Figures 1L,M), suggesting that Cr (VI) also induces damage to SSCs/progenitors.

Cr (VI) Impaired Cell Viability and Induced ROS Generation in SSCs/Progenitors

Previous articles described that the cell survival rate was significantly decreased when exposed to 12.5 μ M or higher concentrations of Cr (VI) (Hu et al., 2016, 2018). To investigate the influence of Cr (VI) on SSC viability, we employed an immortalized mouse SSC/progenitor line, i.e., C-184 (Hofmann et al., 2005). These cells were exposed

to different dosages of Cr (VI), and then subjected to a CCK-8 assay. As shown in Figure 2A, treatment of Cr (VI) for 12 h decreased the percentages of viable cells in a concentration-dependent manner, with an approximately 50% of decrease in the 10 μ M Cr (VI) treatment group. MTT (Figure 2B) and EdU assays (Figures 2C,D) generated similar results. We also detected ROS generation under different Cr (VI) dosages. Consistently, the ROS level was significantly increased after 1 h of 10 μ M Cr (VI) treatment (Figure 2E). We further incubated the cells with 10 μ M Cr (VI) for different time. As expected, the cell viability was decreased in a time-dependent manner (Figure 2F). Thus, we applied 10 μ M Cr (VI) treatment in subsequent *in vitro* experiments, unless otherwise stated. The overall data demonstrate that Cr (VI) impairs cell viability and induces ROS generation in SSCs/progenitors.

Cr (VI) Induced Mitochondrial Dynamic Imbalance and Mitophagy in SSCs/Progenitors

Monodansylcadaverine, a fluorescent pigment, is typically used to detect the occurrence of autophagy (Weiss-Sadan et al., 2019; de Campos et al., 2020). We identified that the fluorescence intensity of MDC was clearly increased after 10 μ M Cr (VI) treatment (Figures 3A,B), suggestive of Cr (VI)-induced autophagy in SSCs/progenitors. We then investigated whether autophagy-associated genes were also activated by Cr (VI). To this end, we incubated mouse SSCs/progenitors with 10 μ M Cr (VI) for different time. As shown in Figures 3C,D, p-Beclin1 and LC3-II, two autophagy markers, were upregulated by Cr (VI) in a time-dependent manner.

In addition to ROS generation (Figure 2E), we found that treatment with 10 μ M Cr (VI) for 4 h also decreased mitochondrial membrane potential (Figure 3E). Excessive ROS production and decreased MMP could indicate malfunctioned mitochondria. Hence, we performed Mito Tracker staining, and found that Cr (VI) caused mitochondrial aggregation and displaying the short rod morphology (Figure 3F). We assumed that Cr (VI) might disturb the balance between mitochondrial fusion and fission. To this end, we performed a qPCR analysis for mitochondrial fusion- (*Mfn1*, *Mfn2*, and *Opa1*) and fission-related genes (*Drp1*; Varuzhanyan and Chan, 2020). The qPCR result showed significant downregulation of *Mfn1*, *Mfn2*, and *Opa1* but upregulation of *Drp1* at the mRNA level (Figure 3G). Besides, the mitochondrial marker Tom20, a protein that localizes on the mitochondrial outer membrane (OMM) and responsible for the first step of mitochondrial protein transportation (Di Maio et al., 2016), was substantially downregulated after 4 h of 10 μ M Cr (VI) treatment, as demonstrated by the Western blot (WB) analysis (Figures 3H,I).

To investigate whether Cr (VI) induces mitophagy to clear damaged mitochondria in SSCs, we conducted a qPCR analysis for mitophagy activation genes *Bnip3* and *Nix* (Lampert et al., 2019). As shown in Figures 3J,K, *Bnip3* and *Nix* were significantly upregulated after 4 h of 10 μ M

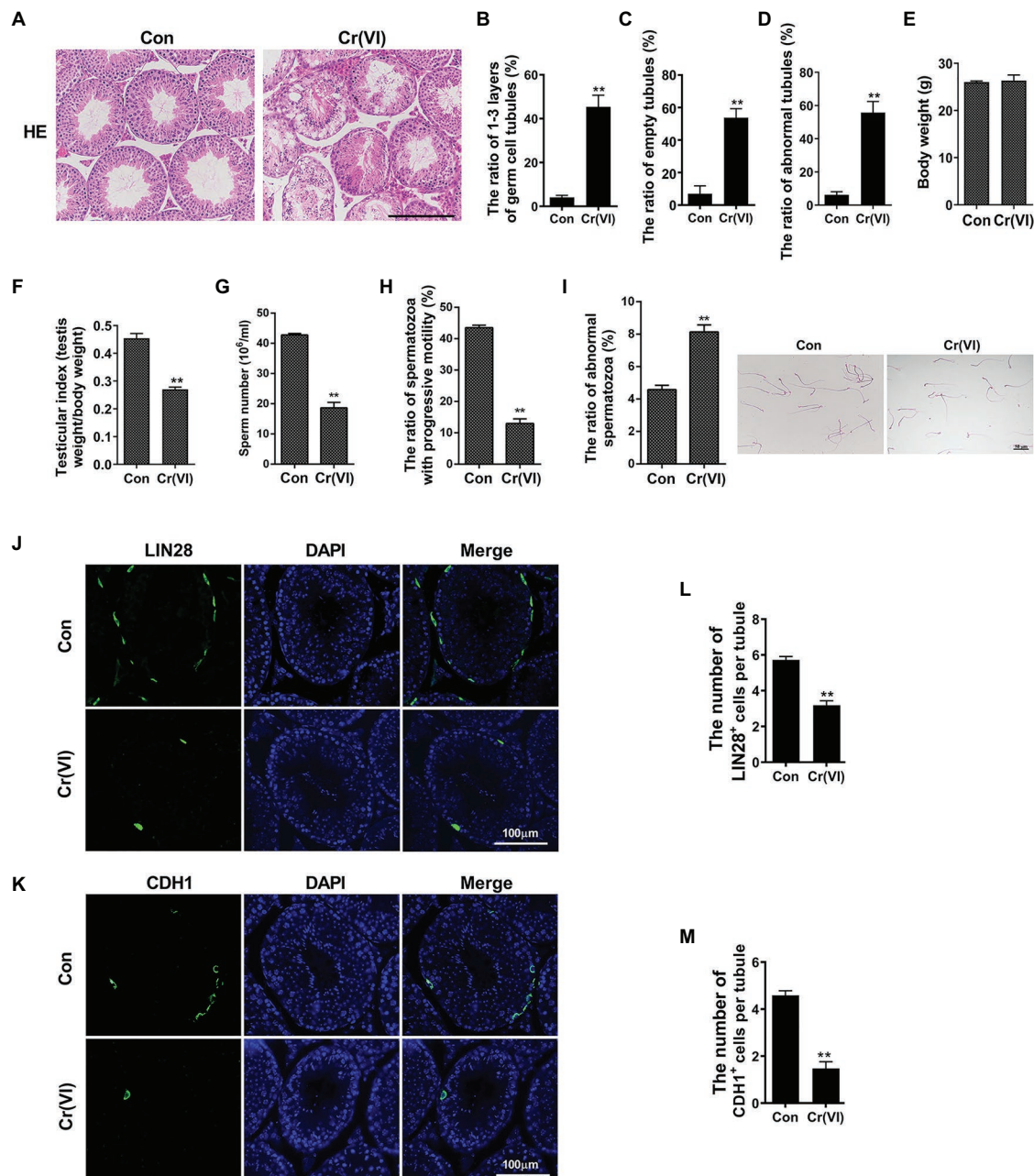


FIGURE 1 | Chromium (Cr) (VI) damaged male reproductive system and spermatogonial stem cells (SSCs)/progenitors in mouse testes. **(A)** Hematoxylin and eosin (H&E) staining of testis sections from control and Cr (VI)-treated mice. Bar = 200 μ m. **(B–D)** The ratios of only 1–3 layers of germ cell **(B)**, empty **(C)**, and abnormal **(D)** seminiferous tubules in control and Cr (VI)-treated mouse testes. **(E)** The average body weight in control and Cr (VI)-treated mice. **(F)** The average testicular index (testis weight/body weight) in control and Cr (VI)-treated mice. **(G)** The average sperm number (10^6 /ml) in control and Cr (VI)-treated mice. **(H)** The ratio of spermatozoa with progressive motility in control and Cr (VI)-treated mice. **(I)** Left: the ratio of abnormal spermatozoa in control and Cr (VI)-treated mice; Right: images of spermatozoa from the control and Cr (VI)-treated mice. Bar = 50 μ m. **(J,K)** Immunofluorescence staining for LIN28 **(J)** and CDH1 **(K)** in testis sections from control and Cr (VI)-treated mice. Bar = 100 μ m. **(L,M)** The numbers of LIN28⁺ **(L)** and CDH1⁺ cells **(M)** per seminiferous tubule in control and Cr (VI)-treated mouse testes. Data are presented as the mean \pm SEM from five mice, and 300 seminiferous tubules from five mice were analyzed in each group. ** $p < 0.01$.

Cr (VI) treatment. We further detected the ratio of autophagic lysosome (AL)-engulfed mitochondria, with Mito and Lyso Tracker staining to label mitochondria and lysosomes, respectively. As shown in **Figures 3L,M**, 4 h of 10 μ M

Cr (VI) treatment considerably increased the ratio of cells double positive for both Mito and Lyso staining, suggesting the elevated number of cells with impaired mitochondria that are engulfed by ALs.

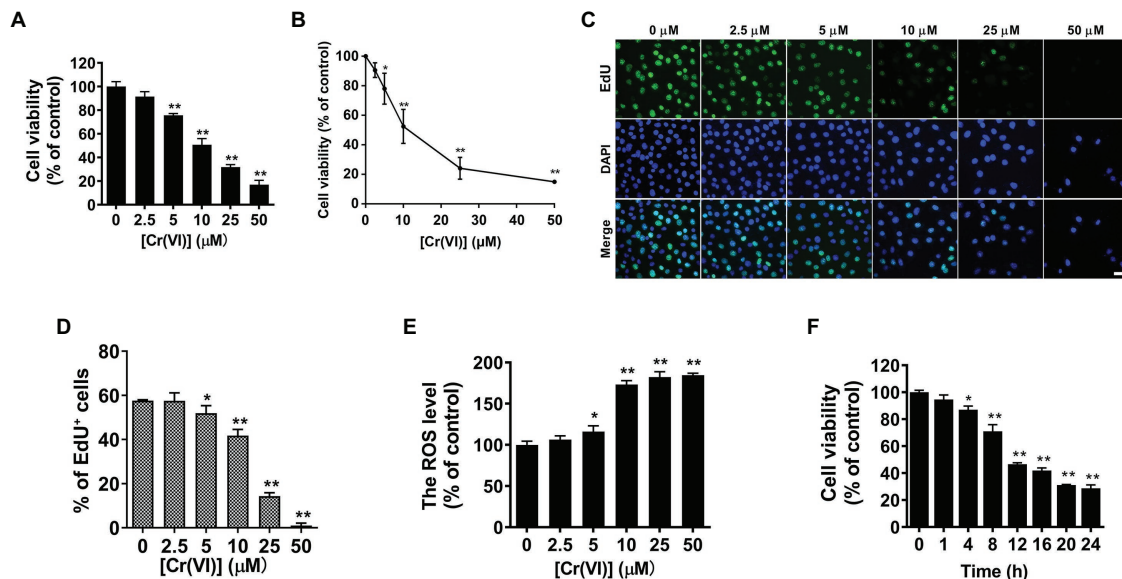


FIGURE 2 | Chromium (VI) impaired cell viability and induced reactive oxygen species (ROS) generation in SSCs/progenitors. **(A,B)** A Cell Counting Kit-8 (CCK-8; **A**) and MTT assay **(B)** for the viability of SSCs/progenitors treated with different concentrations of Cr (VI) for 12 h. **(C)** Representative images of cells in different treatment groups that incorporate EdU. Bar = 20 μm. **(D)** Quantification of cells in different treatment groups that incorporate EdU. At least 300 cells were analyzed in each group. **(E)** DCFH-DA detection of the intracellular ROS accumulation in SSCs/progenitors treated with different concentrations of Cr (VI) for 1 h. **(F)** A CCK-8 assay for the viability of SSCs/progenitors treated with 10 μM Cr (VI) for different time. Data are presented as the mean ± SEM of three independent experiments. **p* < 0.05; ***p* < 0.01.

Cr (VI) Downregulated the RNA m⁶A Modification Levels in Mitochondrial Dynamic Balance and Mitophagy Genes in SSCs/Progenitors

Next, we investigated whether Cr (VI) affects the m⁶A modification in SSCs. To this end, we treated mouse SSCs/progenitors with 10 μM Cr (VI), followed by RNA extraction and m⁶A dot-blot to detect the m⁶A level. As shown in **Figure 4A**, the RNA m⁶A modification level showed a clear decrease after 1 h of Cr (VI) treatment, and then remained stable. To investigate whether RNA m⁶A modification is involved in Cr (VI)-induced mitochondrial dynamic imbalance and mitophagy in SSCs, we additionally performed a m⁶A-IP-qPCR assay for mitochondrial fusion and mitophagy genes. The result uncovered that 4 h of 10 μM Cr (VI) treatment reduced the m⁶A modification levels in mitochondrial fusion genes *Mfn2* and *Opa1* (**Figure 4B**), as well as in mitophagy genes *Bnip3* and *Nix* (**Figure 4C**), suggesting potential roles of RNA m⁶A modification in Cr (VI)-induced mitochondrial abnormality in SSCs/progenitors.

Melatonin Alleviated Cr (VI)-Induced Damage to Male Reproductive System and Autophagy in Mouse Testes

Melatonin is a strong endogenous free radical scavenger of ROS and inducer of antioxidant systems *in vivo* (Bonnefont-Rousselot et al., 2011). To explore whether

melatonin has protective roles against Cr (VI)-induced testicular damage, we randomly divided 40 male C57/BL6 mice into four groups: control, Cr (VI), melatonin + Cr (VI), melatonin, with 10 mice in each group. In the melatonin + Cr (VI) group, the mice were pre-intraperitoneally injected with melatonin (25 mg/kg *b.w./day*), followed by intraperitoneal injection with Cr (VI; 16.2 mg/kg *b.w./day*). Melatonin and Cr (VI) treatment lasted for 14 consecutive days. The mice were sacrificed on the 14th day after the last treatment, and the testes were removed for examination. H&E staining results showed that melatonin treatment effectively attenuated Cr (VI)-induced damage to testes, characterized by alleviated vacuolization of seminiferous tubules, reduced ratios of only 1–3 layers of germ cell, empty and abnormal tubules (**Figures 5A–D**). In addition, despite no significant difference in body weight (**Figure 5E**), melatonin pretreatment restored the testicular index (**Figure 5F**), sperm number (**Figure 5G**), and progressive motility (**Figure 5H**), along with diminished abnormal epididymal spermatozoa (**Figure 5I**).

The subsequent immunofluorescence staining analysis uncovered that melatonin treatment also attenuated Cr (VI)-induced decrease of LIN28⁺ cells per seminiferous tubule (**Figures 5J,K**), suggesting the preservation of SSCs/progenitors by melatonin. Besides, the autophagy marker LC3-II was less induced with melatonin treatment (**Figure 5L**). The overall data therefore suggest that melatonin could alleviate Cr (VI)-induced damage to male reproductive system and autophagy in mouse testes.

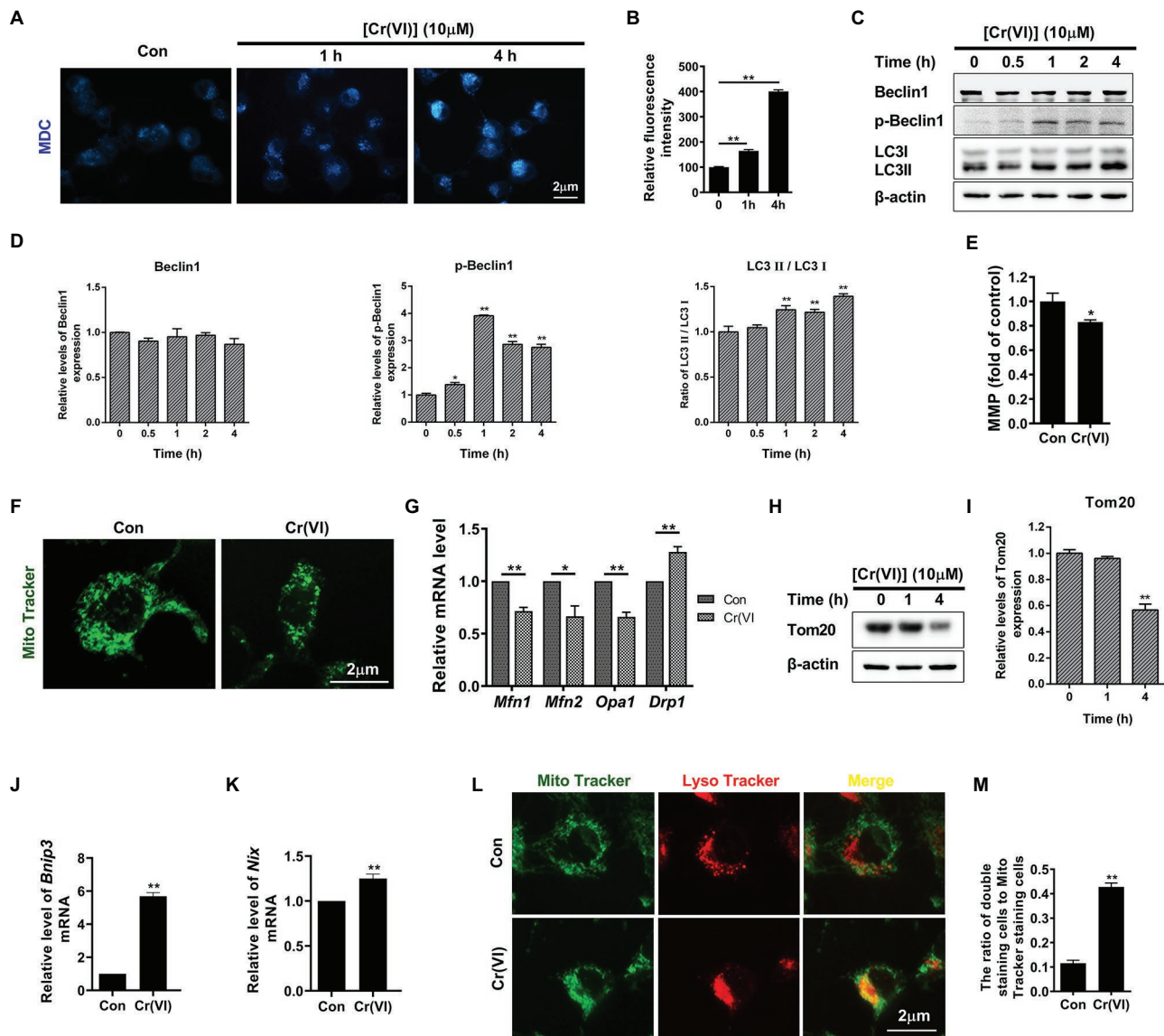


FIGURE 3 | Chromium (VI) induced mitochondrial dynamic imbalance and mitophagy in SSCs/progenitors. **(A)** Monodansylcadaverine (MDC) staining for autophagic vacuoles. Bar = 2 μm. **(B)** The relative fluorescence intensity of MDC in SSCs/progenitors treated with 10 μM Cr (VI) for different time. **(C)** Western blot analysis of the expression levels of autophagy markers Beclin1, p-Beclin1, and LC3 in SSCs/progenitors treated with 10 μM Cr (VI) for different time. β-actin is used as a loading control. **(D)** The relative band intensities of Beclin1, p-Beclin1, and LC3-II in different cell treatment groups. **(E)** Mitochondrial membrane potential (MMP) in SSCs/progenitors treated with vehicle or 10 μM Cr (VI) for 4 h, as detected by the lipophilic cationic dye JC-1. **(F)** Mito Tracker staining for mitochondria in SSCs/progenitors treated with vehicle or 10 μM Cr (VI) for 4 h. Bar = 2 μm. **(G)** qPCR analysis of *Mfn1*, *Mfn2*, *Opa1*, and *Drp1* in SSCs/progenitors treated with vehicle or 10 μM Cr (VI) for 4 h. **(H)** Western blot analysis of Tom20 in SSCs/progenitors treated with 10 μM Cr (VI) for different time. β-actin is used as a loading control. **(I)** The relative band intensities of Tom20 in different cell treatment groups. **(J,K)** qPCR analysis of *Bnip3* **(J)** and *Nix* **(K)** in SSCs/progenitors treated with vehicle or 10 μM Cr (VI) for 4 h. **(L)** Mito and Lyso Tracker co-staining analysis in SSCs/progenitors treated with vehicle or 10 μM Cr (VI) for 4 h. Bar = 2 μm. **(M)** The ratios of double staining cells to Mito Tracker staining cells in the control and 4 h of 10 μM Cr (VI) treatment group. Data are presented as the mean ± SEM of three independent experiments. **p* < 0.05; ***p* < 0.01.

Melatonin Attenuated Cr (VI)-Induced Cell Viability Loss and ROS Generation in SSCs/Progenitors

Then, we explored the protective roles of melatonin against Cr (VI)-induced oxidative damage in SSCs. Mouse SSCs/progenitors were pretreated with 50 μM melatonin for 2 h,

followed by treatment with 10 μM Cr (VI) for 1 or 4 h. By WB analysis, we found that while 1 h of Cr (VI) treatment downregulated melatonin receptor 1 (MT1), pre-treatment with melatonin could alleviate this (Figures 6A,B). In addition, NADPH oxidase 4 (NOX4), a protein that is expressed in mitochondria and mediates ROS production (Kuroda et al., 2010),

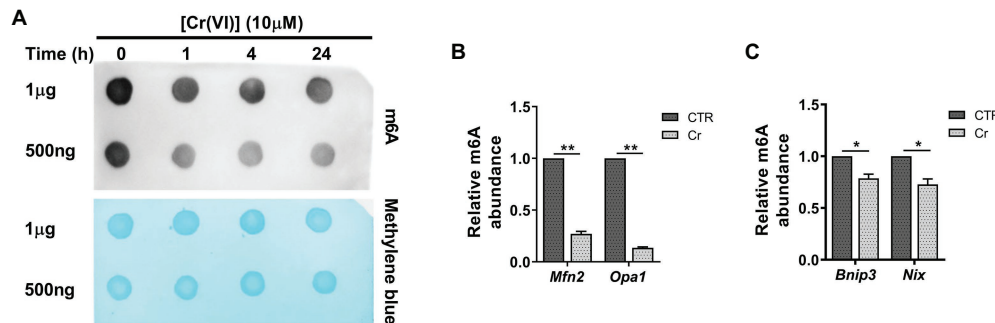


FIGURE 4 | Chromium (VI) downregulated the RNA N⁶-methyladenosine (m⁶A) modification levels in mitochondrial dynamic balance and mitophagy genes in SSCs/progenitors. **(A)** The m⁶A dot-blot assay showing the global RNA m⁶A modification levels in SSCs/progenitors treated with 10 μM Cr (VI) for different time. About 1 μg means 1 μg mRNAs, and 500 ng means 500 ng extracted and purified mRNAs from SSCs/progenitors. Methylene blue is used as a loading control to eliminate the difference in mRNA amount. **(B,C)** The m⁶A-IP-qPCR analysis showing the relative m⁶A abundance in mitochondrial fusion genes *Mfn2*, *Opa1* **(B)** and in mitophagy genes *Bnip3*, *Nix* **(C)** in SSCs/progenitors treated with vehicle or 10 μM Cr (VI) for 4 h. Data are presented as the mean ± SEM of three independent experiments. **p* < 0.05; ***p* < 0.01.

was upregulated after 4 h of Cr (VI) treatment, but pretreatment with melatonin relieved its upregulation (Figures 6C,D). Similarly, cell viability loss and ROS generation, both of which were induced by 4 h of Cr (VI) treatment, could be attenuated by pretreatment with melatonin (Figures 6E,F).

Melatonin Attenuated Cr (VI)-Induced Mitochondrial Dynamic Disorders and Mitophagy via RNA m⁶A Modification in SSCs/Progenitors

Next, we probed the influence of melatonin on Cr (VI)-induced mitochondrial abnormality in SSCs. Mouse SSCs/progenitors were still pretreated with 50 μM melatonin for 2 h, followed by treatment with 10 μM Cr (VI) for 4 h. The qPCR result showed that pretreatment with melatonin maintained the mRNA levels of mitochondrial fusion genes *Mfn1*, *Mfn2*, and *Opa1*, while counteracted Cr (VI)-induced upregulation of mitophagy genes *Bnip3* and *Nix* (Figure 7A). MMP was also restored by melatonin pretreatment (Figure 7B). Moreover, pretreatment with melatonin attenuated Cr (VI)-induced increase of the MDC fluorescence intensity (Figures 7C,D) and upregulation of autophagy markers p-Beclin1 and LC3-II (Figures 7E,F), as revealed by MDC staining for autophagic vacuoles and Western blot analysis, respectively. In addition, melatonin pretreatment attenuated Cr (VI)-induced increase of cells double positive for both Mito and Lyso staining (Figures 7G,H), i.e., cells with impaired mitochondria that are engulfed by ALs. Melatonin pretreatment was also found to maintain the protein level of the mitochondrial marker Tom20 (Figures 7I,J).

Later, we performed a m⁶A dot-blot analysis to investigate whether melatonin affects RNA m⁶A modification in SSCs. The m⁶A dot-blot result showed that melatonin pretreatment restored the RNA m⁶A level that was decreased after 1 h of Cr (VI) treatment (Figure 7K). We further conducted a m⁶A-IP-qPCR assay for mitochondrial fusion and mitophagy genes. Interestingly, it was identified that melatonin pretreatment

reversed the Cr (VI)-induced decrease of m⁶A modification levels in mitochondrial fusion genes *Mfn2* and *Opa1*, as well as in mitophagy genes *Bnip3* and *Nix* (Figure 7L). Therefore, the overall data suggest that melatonin could attenuate Cr (VI)-induced mitochondrial dynamic disorders and mitophagy via RNA m⁶A modification in SSCs/progenitors.

Melatonin Attenuated Cr (VI)-Induced Decrease of the RNA m⁶A Modification Level via METTL3 in SSCs/Progenitors

We subsequently delved into the mechanisms underlying melatonin-restored RNA m⁶A modification levels that were reduced by Cr (VI). To this end, we carried out a qPCR analysis for m⁶A-associated genes, i.e., *Mettl3*, *Wtap*, *Fto*, and *Ythdf2*, encoding methyltransferases METTL3, WTAP (the m⁶A writers), the demethylase FTO (the m⁶A eraser) and the m⁶A-binding protein YTHDF2 (the m⁶A reader), respectively (Shi et al., 2019). By qPCR analysis, we found that *Mettl3* was decreased at the mRNA level after 4 h of Cr (VI) treatment, but that pretreatment with melatonin attenuated the Cr (VI)-induced downregulation of *Mettl3* (Figures 8A,B).

METTL3 is a major component of the m⁶A methyltransferase complex (Shi et al., 2019). As Cr (VI) downregulated the global RNA m⁶A modification level and *Mettl3*, but both could be maintained by melatonin pretreatment in SSCs/progenitors, we then explored whether melatonin attenuates the Cr (VI)-decreased RNA m⁶A modification level via METTL3. To this end, we constructed a *Mettl3*-depleted mouse SSC/progenitor line by lentivirus-mediated shRNA targeting. qPCR and Western blot results demonstrated significant downregulation of METTL3 (Figures 8C–E). Subsequently, the *Mettl3*-depleted and control cell lines were pretreated with 50 μM melatonin, followed by treatment with 10 μM Cr (VI) for 1 or 4 h. The qPCR analysis revealed that while the Cr (VI)-induced downregulation of *Mettl3* was attenuated by melatonin pretreatment in control cells, the *Mettl3* expression level was neither significantly reduced by Cr (VI) treatment nor restored by melatonin pretreatment in

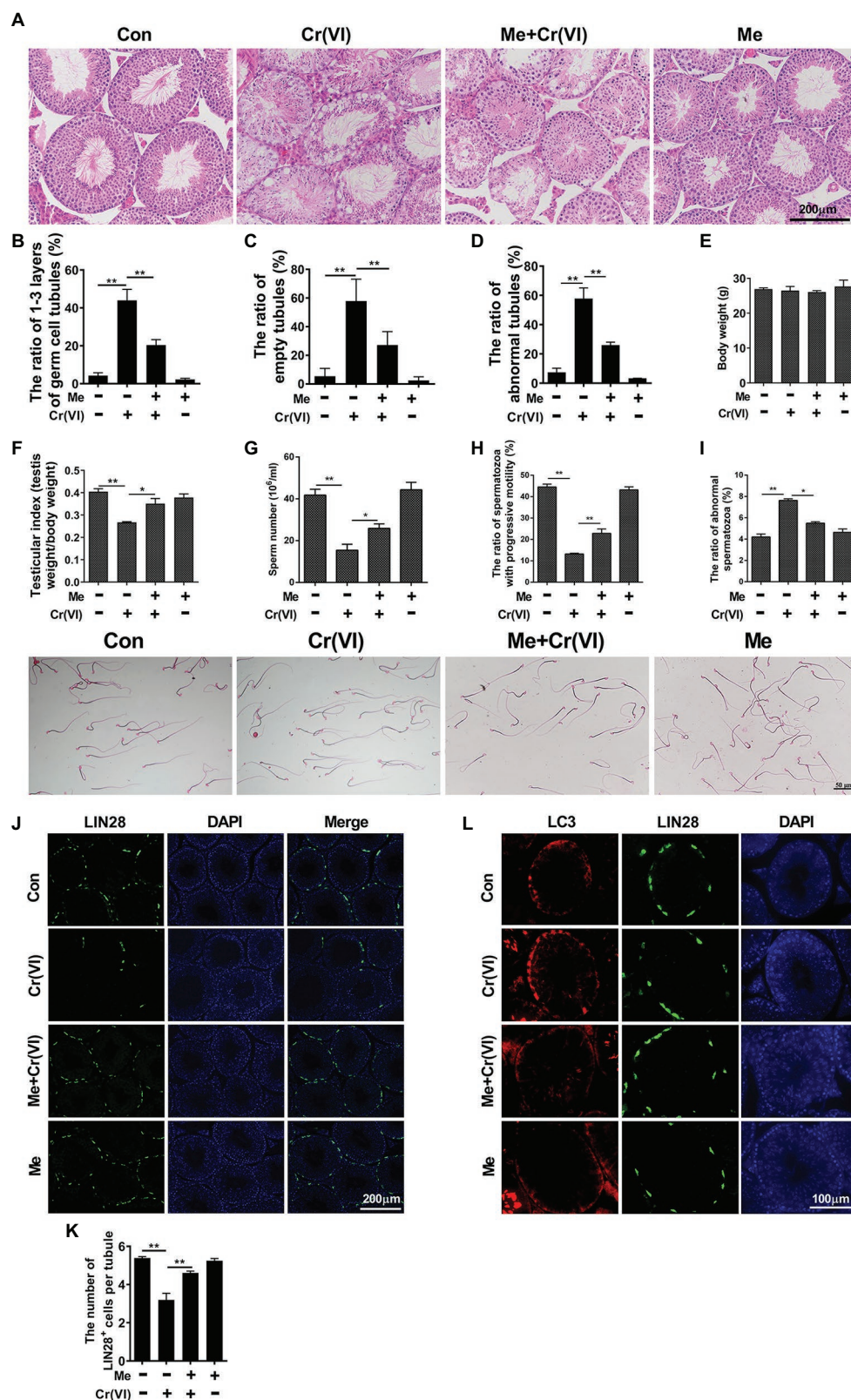


FIGURE 5 | Melatonin alleviated Cr(VI)-induced damage to male reproductive system and autophagy in mouse testes. **(A)** H&E staining of testis sections from the control, Cr(VI), melatonin + Cr(VI), and melatonin-treated mice. Bar = 200 μ m. **(B–D)** The ratios of only 1–3 layers of germ cell **(B)**, empty **(C)**, and abnormal **(D)** tubules. **(E–I)** Body weight **(E)**, testicular index **(F)**, sperm number **(G)**, and progressive motility **(H)** of spermatozoa. **(I)** The ratio of abnormal spermatozoa. **(J–L)** Immunofluorescence for LIN28 **(J)**, LC3 **(L)**, and DAPI **(K)**. Scale bar = 200 μ m. **(K)** The number of LIN28⁺ cells per tubule. **(Continued)**

FIGURE 5 | (D) seminiferous tubules in testes from the control, Cr (VI), melatonin + Cr (VI), and melatonin-treated mice. **(E)** The average body weight in different mouse groups. **(F)** The average testicular index (testis weight/body weight) in different mouse groups. **(G)** The average sperm number ($10^6/\text{ml}$) in different mouse groups. **(H)** The ratio of spermatozoa with progressive motility in different mouse groups. **(I)** The upper panel: the ratio of abnormal spermatozoa in different mouse groups; The lower panel: images of spermatozoa from different groups of mice. Bar = 50 μm . **(J)** Immunofluorescence staining for LIN28 in testis sections from the control, Cr (VI), melatonin + Cr (VI), and melatonin-treated mice. Bar = 200 μm . **(K)** The numbers of LIN28⁺ cells per seminiferous tubule in testes from the control, Cr (VI), melatonin + Cr (VI), and melatonin-treated mice. **(L)** Co-staining analysis for LC3 and LIN28 in testis sections from the control, Cr (VI), melatonin + Cr (VI), and melatonin-treated mice. Bar = 100 μm . Data are presented as the mean \pm SEM from five mice, and 300 seminiferous tubules from five mice were analyzed in each group. * $p < 0.05$; ** $p < 0.01$.

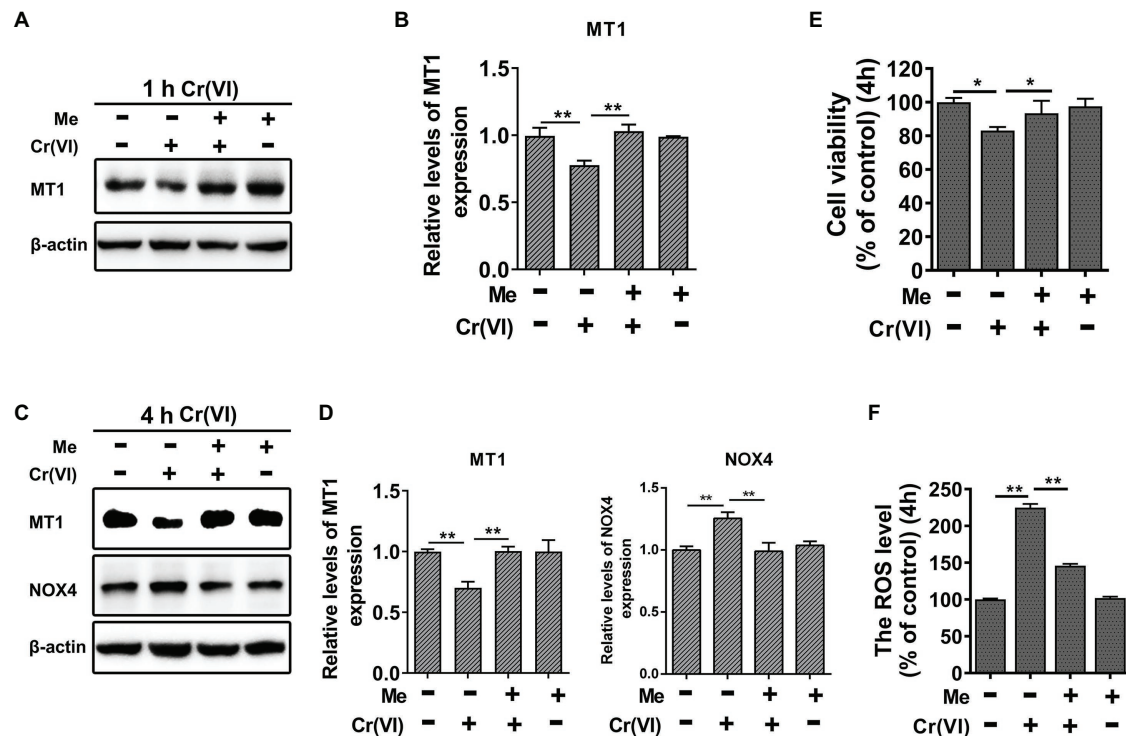


FIGURE 6 | Melatonin attenuated Cr (VI)-induced cell viability loss and ROS generation in SSCs/progenitors. **(A)** Western blot analysis of melatonin receptor 1 (MT1) in the control, Cr (VI), melatonin + Cr (VI), and melatonin-treated SSCs/progenitors. Of these, Cr (VI) treatment lasted for 1 h. β -actin is used as a loading control. **(B)** The relative expression of MT1 in different cell groups after 1 h of Cr (VI) treatment. **(C)** Western blot analysis of MT1 and NADPH oxidase 4 (NOX4) in the control, Cr (VI), melatonin + Cr (VI), and melatonin-treated SSCs/progenitors. Of these, Cr (VI) treatment lasted for 4 h. β -actin is used as a loading control. **(D)** The relative expression of MT1 and NOX4 in different cell groups after 4 h of Cr (VI) treatment. **(E)** A CCK-8 assay for SSC/progenitor viability in the control, Cr (VI), melatonin + Cr (VI), and melatonin treatment group. Of these, Cr (VI) treatment lasted for 4 h. **(F)** DCFH-DA detection of the intracellular ROS accumulation in the control, Cr (VI), melatonin + Cr (VI), and melatonin-treated SSCs/progenitors. Of these, Cr (VI) treatment lasted for 4 h. Data are presented as the mean \pm SEM of three independent experiments. * $p < 0.05$; ** $p < 0.01$.

Mettl3-depleted cells (Figures 8F,G). The m⁶A dot-blot result demonstrated the overall reduced m⁶A modification level by *Mettl3* depletion and, notably, that while the Cr (VI)-induced decrease of the RNA m⁶A modification level was attenuated by melatonin pretreatment in control cells, this could not be recapitulated in *Mettl3*-depleted cells (Figures 8H,I). Hence, the overall data suggest that melatonin could attenuate Cr (VI)-induced decrease of the RNA m⁶A modification level via METTL3 in SSCs/progenitors.

Melatonin Attenuated Cr (VI)-Induced Mitophagy by Restoration of METTL3-Mediated RNA m⁶A Modification in SSCs/Progenitors

Finally, we investigated whether melatonin could attenuate Cr (VI)-induced mitophagy in SSCs in the same way, i.e., by

restoration of METTL3-mediated RNA m⁶A modification. Still, the *Mettl3*-depleted and control cell lines were pretreated with 50 μM melatonin, followed by treatment with 10 μM Cr (VI) for 1 h or 4 h. Western blot analysis revealed that while the expression level of MT1 was maintained by melatonin pretreatment in both cell lines, Cr (VI)-induced autophagy markers p-Beclin1 and LC3-II were only minimally downregulated in melatonin-pretreated *Mettl3*-depleted cells (Figures 9A–D). Similarly, melatonin pretreatment relatively less attenuated Cr (VI)-induced increase of cells double positive for both Mito and Lyso staining (cells with impaired mitochondria that are engulfed by ALs) in *Mettl3*-depleted cells (Figures 9E,F). Together, these data suggest that melatonin could attenuate Cr (VI)-induced mitophagy by restoration of METTL3-mediated RNA m⁶A modification in SSCs/progenitors.

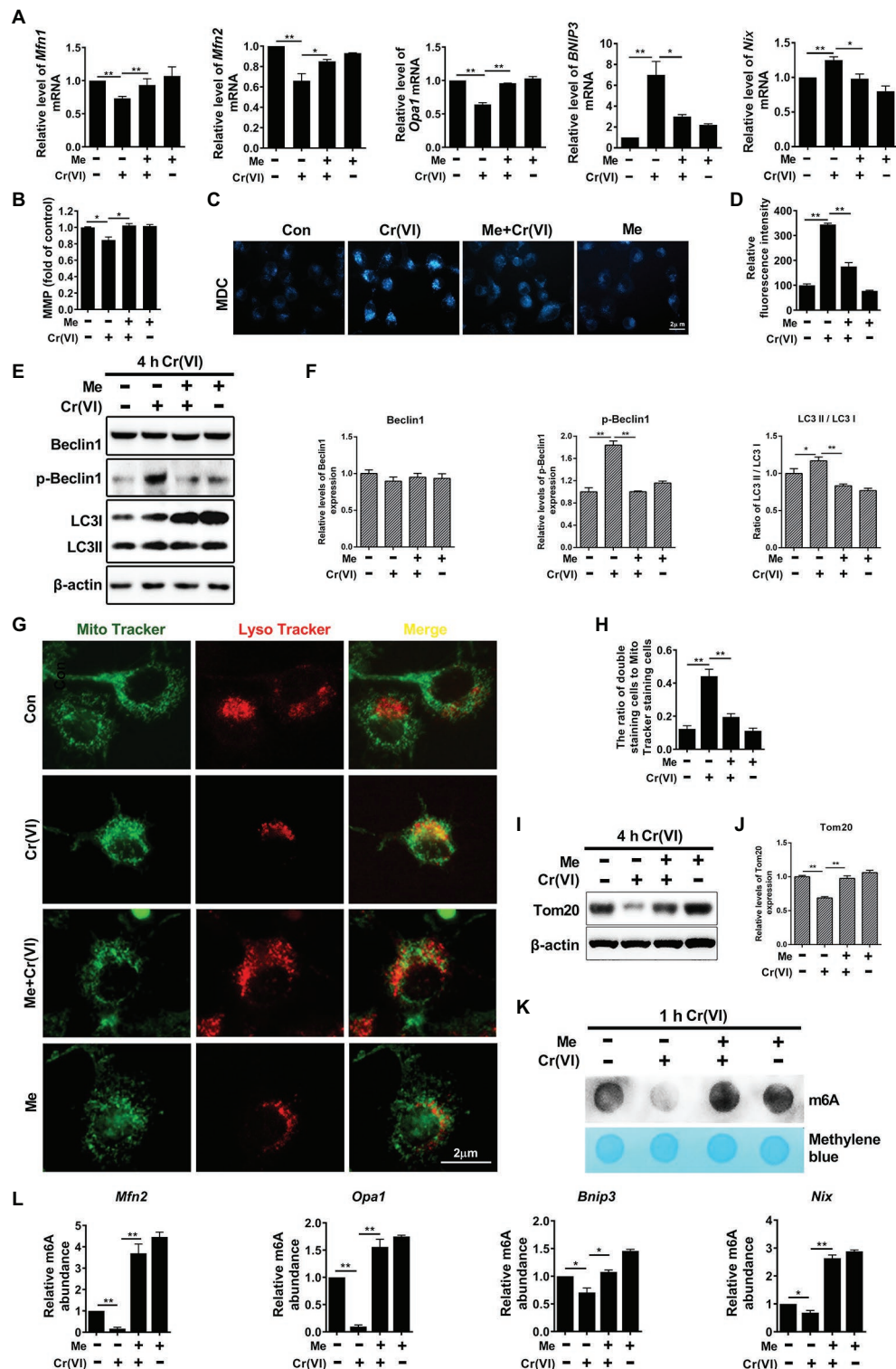


FIGURE 7 | Melatonin attenuated Cr(VI)-induced mitochondrial dynamic disorders and mitophagy via RNA m⁶A modification in SSCs/progenitors. **(A)** qPCR analysis of *Mfn1*, *Mfn2*, *Opa1*, *Bnip3*, and *Nix* in the control, Cr(VI), melatonin + Cr(VI), and melatonin-treated SSCs/progenitors. **(B)** MMP in the control, Cr(VI), melatonin + Cr(VI), and melatonin-treated SSCs/progenitors, as detected by the lipophilic cationic dye JC-1. **(C)** MDC staining for autophagic vacuoles in the control, Cr(VI), melatonin + Cr(VI), and melatonin-treated SSCs/progenitors. Bar = 2 μ m. **(D)** The relative fluorescence intensity of MDC in the control, Cr(VI), melatonin + Cr(VI), and melatonin-treated SSCs/progenitors. **(E)** Western blot analysis of the expression levels of autophagy markers Beclin1, p-Beclin1, and LC3 in (Continued)

FIGURE 7 | the control, Cr (VI), melatonin + Cr (VI), and melatonin-treated SSCs/progenitors. Of these, Cr (VI) treatment lasted for 4 h. β -actin is used as a loading control. **(F)** The relative band intensities of Beclin1, p-Beclin1, and LC3-II in different cell treatment groups. **(G)** Mito and Lyso Tracker co-staining analysis in the control, Cr (VI), melatonin + Cr (VI), and melatonin-treated SSCs/progenitors. Bar = 2 μ m. **(H)** The ratios of double staining cells to Mito Tracker staining cells in the control, Cr (VI), melatonin + Cr (VI), and melatonin-treated SSCs/progenitors. **(I)** Western blot analysis of Tom20 in the control, Cr (VI), melatonin + Cr (VI), and melatonin-treated SSCs/progenitors. Of these, Cr (VI) treatment lasted for 4 h. β -actin is used as a loading control. **(J)** The relative band intensities of Tom20 in different cell treatment groups. **(K)** The m⁶A dot-blot assay showing the global RNA m⁶A modification levels in the control, Cr (VI), melatonin + Cr (VI), and melatonin-treated SSCs/progenitors. Of these, Cr (VI) treatment lasted for 1 h. Methylene blue is used as a loading control to eliminate the difference in mRNA amount. **(L)** The m⁶A-IP-qPCR analysis showing the relative m⁶A abundance in mitochondrial fusion genes *Mfn2*, *Opa1* and in mitophagy genes *Bnip3*, *Nix* in the control, Cr (VI), melatonin + Cr (VI), and melatonin-treated SSCs/progenitors. Data are presented as the mean \pm SEM of three independent experiments. * $p < 0.05$; ** $p < 0.01$.

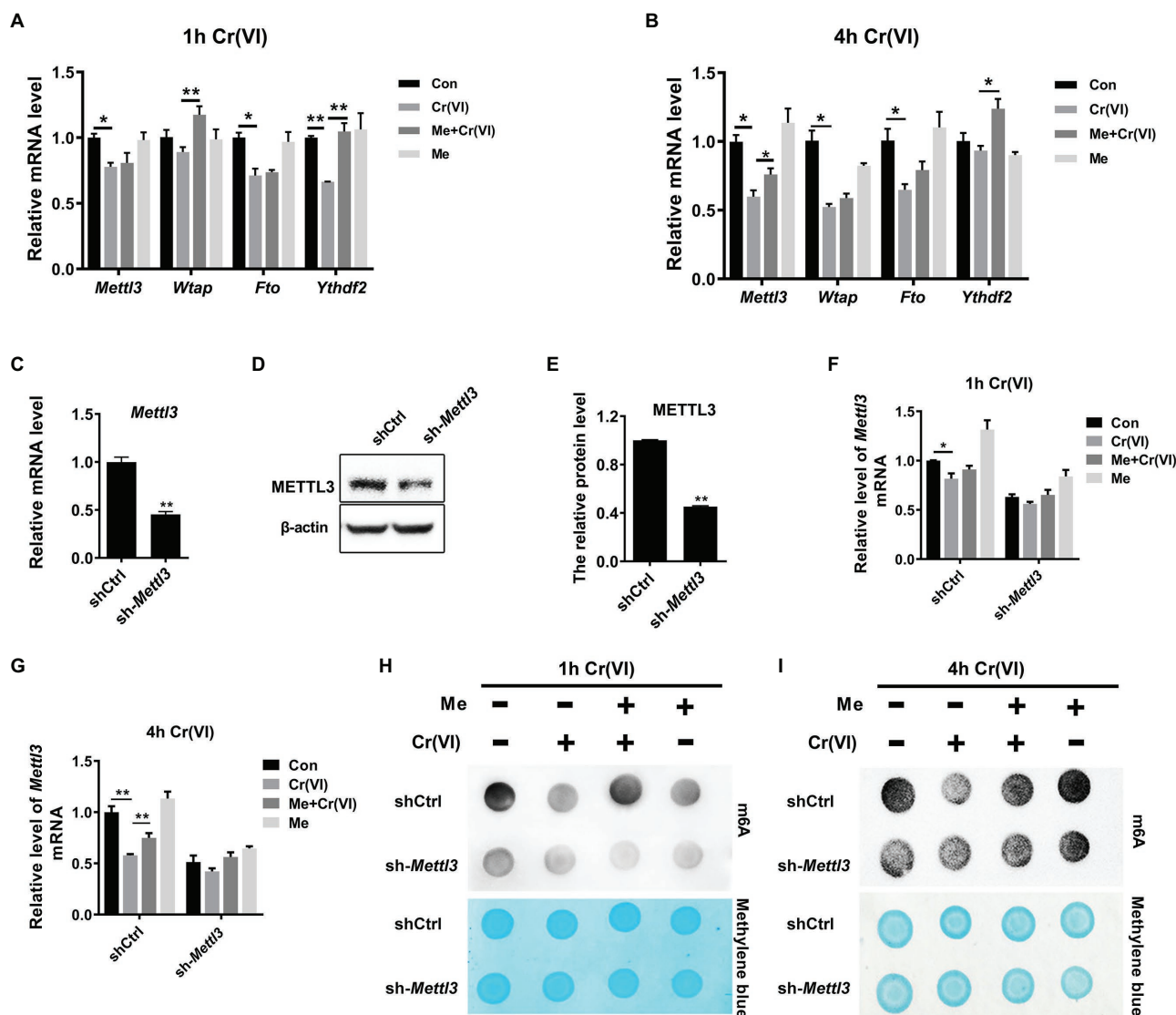


FIGURE 8 | Melatonin attenuated Cr (VI)-induced decrease of the RNA m⁶A modification level via METTL3 in SSCs/progenitors. **(A,B)** qPCR analysis of *Mettl3*, *Wtap*, *Fto*, and *Ythdf2* in the control, Cr (VI), melatonin + Cr (VI), and melatonin-treated SSCs/progenitors. Of these, Cr (VI) treatment lasted for 1 h **(A)** or 4 h **(B)**. **(C,D)** qPCR **(C)** and Western blot analysis **(D)** of METTL3 in the scramble control and *Mettl3*-shRNA SSC/progenitor group. β -actin is used as a loading control. **(E)** The METTL3 band intensities relative to β -actin in the scramble control and *Mettl3*-shRNA SSC/progenitor group. **(F,G)** qPCR analysis of *Mettl3* in the scramble control and *Mettl3*-shRNA SSCs/progenitors treated with vehicle, Cr (VI), melatonin + Cr (VI), or melatonin. Of these, Cr (VI) treatment lasted for 1 h **(F)** or 4 h **(G)**. **(H,I)** The m⁶A dot-blot assay showing the global RNA m⁶A modification levels in the scramble control and *Mettl3*-shRNA SSCs/progenitors treated with vehicle, Cr (VI), melatonin + Cr (VI), or melatonin. Of these, Cr (VI) treatment lasted for 1 h **(H)** or 4 h **(I)**. Methylene blue is used as a loading control to eliminate the difference in mRNA amount. Data are presented as the mean \pm SEM of three independent experiments. * $p < 0.05$; ** $p < 0.01$.

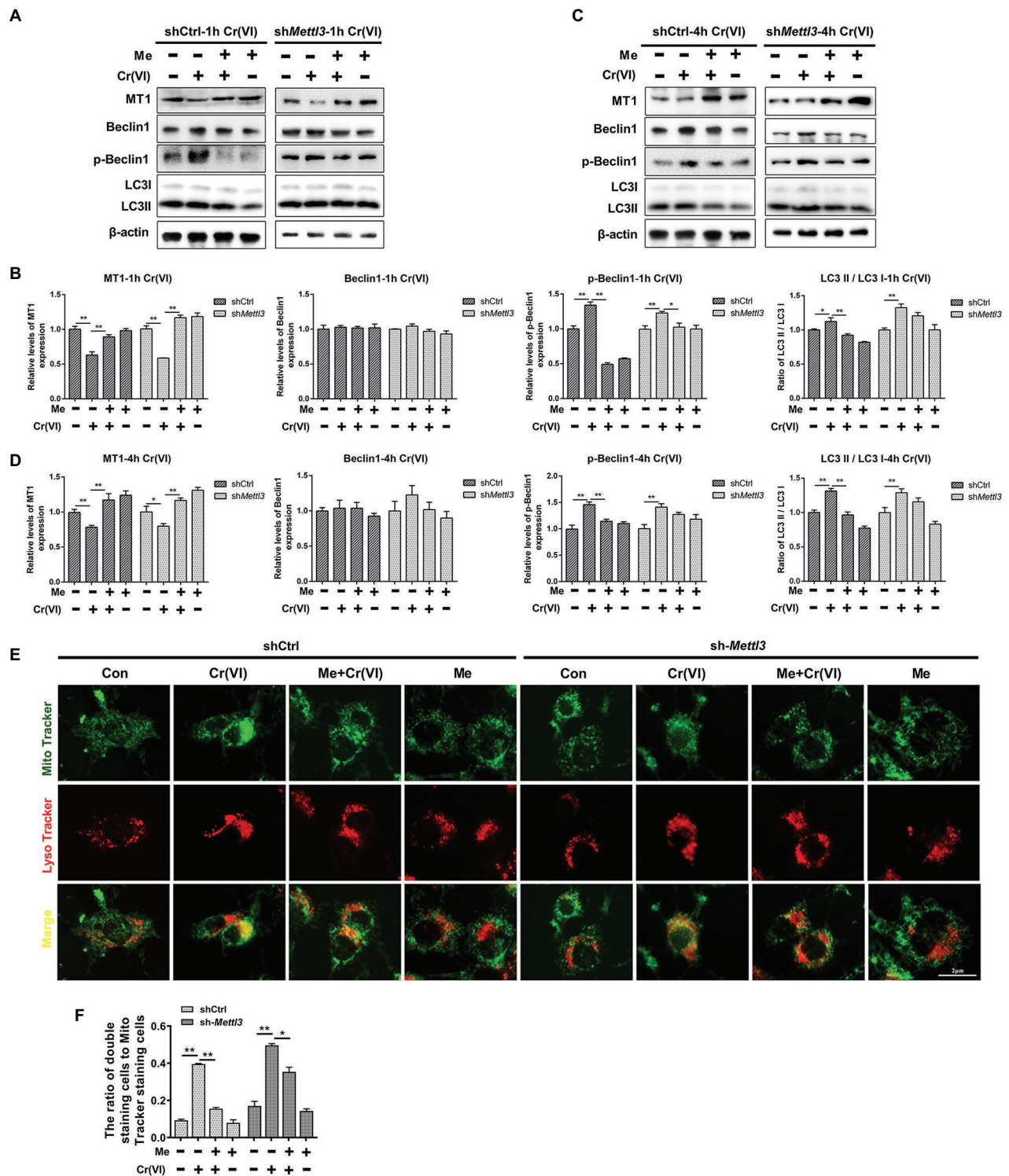


FIGURE 9 | Melatonin attenuated Cr (VI)-induced mitophagy by restoration of METTL3-mediated RNA m⁶A modification in SSCs/progenitors. **(A,C)** Western blot analysis of MT1, Beclin1, p-Beclin1, and LC3 in the scramble control and *Mettl3*-shRNA SSCs/progenitors treated with vehicle, Cr (VI), melatonin + Cr (VI), or melatonin. Of these, Cr (VI) treatment lasted for 1 **(A)** or 4 h **(C)**. β-actin is used as a loading control. **(B,D)** The relative expression of MT1, Beclin1, p-Beclin1, and LC3-II in different cell groups after 1 **(B)** or 4 h **(D)** of Cr (VI) treatment. **(E)** Mito and Lyso Tracker co-staining analysis in the scramble control and *Mettl3*-shRNA SSCs/progenitors treated with vehicle, Cr (VI), melatonin + Cr (VI), or melatonin. Of these, Cr (VI) treatment lasted for 4 h. Bar = 2 μm. **(F)** The ratios of double staining cells to Mito Tracker staining cells in the scramble control and *Mettl3*-shRNA SSCs/progenitors treated with vehicle, Cr (VI), melatonin + Cr (VI), or melatonin. Data are presented as the mean ± SEM of three independent experiments. **p* < 0.05; ***p* < 0.01.

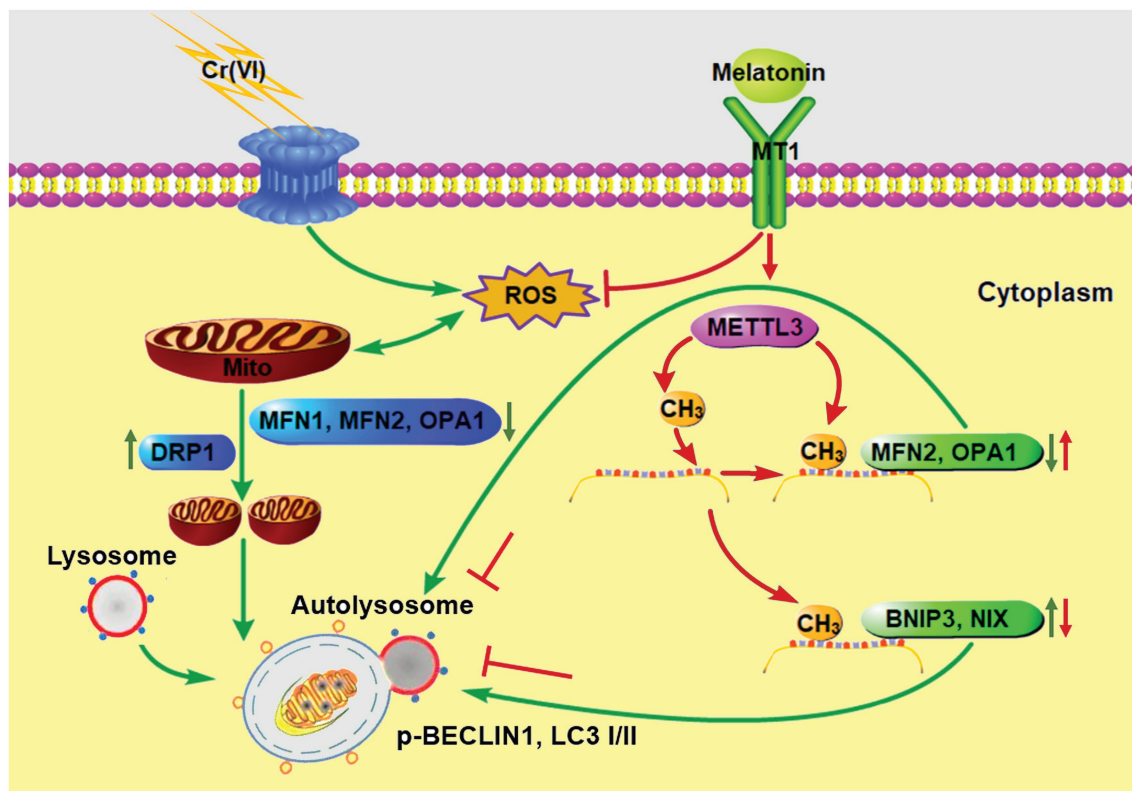


FIGURE 10 | A schematic overview illustrating melatonin-mediated attenuation of Cr (VI)-induced mitochondrial dynamic disorders and mitophagy in SSCs. Cr (VI) exposure induces ROS generation and oxidative stress, and downregulates mitochondrial fusion proteins MFN1, MFN2, and OPA1, while upregulates the mitochondrial fission protein DRP1, resulting in mitochondrial dynamic disorders. The fragmented mitochondria fuse with lysosomes to form autolysosomes, causing aberrant mitophagy. Melatonin can inhibit ROS production and restore METTL3-mediated RNA m⁶A modification levels in mitochondrial fusion genes *Mfn2* and *Opa1*, as well as in mitophagy genes *Bnip3* and *Nix*, resulting in upregulation of MFN2 and OPA1 and downregulation of BNIP3 and NIX. In this way, autolysosomal formation and mitophagy are repressed. Green and red arrows point to Cr (VI)- and melatonin-induced biological processes, respectively.

DISCUSSION

Chromium (VI) is a proven toxin, mutagen, and carcinogen. Although the adverse effects of Cr (VI) on fitness have appealed to the public, its deleterious effects on male fertility in particular SSCs remain poorly understood. In this study, we identified that exposure of SSCs/progenitors to 10 μ M Cr (VI) for 4 h upregulated LC3-II and p-Beclin1. LC3-II and p-Beclin1 are two well-known markers for autophagy. Autophagy is a universal event occurring in eukaryotic cells to maintain homeostasis and metabolic balance (Mizushima et al., 2008). Technically, it is a conservative autophagic lysosomal degradation process characterized by transporting toxic proteins and damaged organelles into lysosomes to form autophagosomes, indispensable for cell elimination, reconstruction, growth, and development (Klionsky and Emr, 2000). During this process, the cytosolic LC3 (LC3-I) is converted to the autophagosomal membrane type (LC3-II). The presence of LC3 in autophagosomes and the conversion of LC3-I to LC3-II have thus been used as indicators of autophagy (Kabeya et al., 2000, 2004). In addition, phosphorylation of Beclin1 (p-Beclin1), a mammalian autophagy effector involved in autophagic vesicle nucleation, is important

to sufficient autophagy induction (Aita et al., 1999; Liang et al., 1999). Therefore, upregulation of LC3-II and p-Beclin1 after Cr (VI) treatment indicates Cr (VI)-induced autophagy in SSCs/progenitors.

Mitochondria are highly dynamic organelles. In response to external stimuli, mitochondria frequently undergo fusion and fission (mitochondrial dynamics) to maintain dynamic balance thereby safeguarding normal cellular functions in various biological processes (Varuzhanyan and Chan, 2020). Mitochondrial fusion occurs *via* two distinct steps, both mediated by the large GTP-hydrolyzing enzymes of the dynamin superfamily. Of these, MFN1 and MFN2 mediate fusion of the mitochondrial OMM, while OPA1 mediates fusion of the inner membrane (IMM). Mitochondrial fusion is counterbalanced by fission that is regulated by DRP1 (Varuzhanyan and Chan, 2020). The appropriate dynamic balance between mitochondrial fusion and fission maintains the mitochondrial size, quantity, shape, and length. A recent article reported that clusterin relieved Cr (VI)-induced mitochondrial apoptosis in L02 hepatocytes by repressing the Ca²⁺-ROS-Drp1-mitochondrial fission axis (Tang et al., 2020). Despite that, little is known about the Cr (VI)-induced changes in mitochondrial dynamics in SSCs, if any. Here, we found

that following Cr (VI) treatment, mitochondrial fusion genes *Mfn1*, *Mfn2*, and *Opa1* were significantly downregulated, while the key mitochondrial fission gene *Drp1* was upregulated. Besides, the short rod-like morphology indicative of mitochondrial aggregation was observed after Cr (VI) treatment. These, along with downregulation of the mitochondrial marker Tom20, excessive ROS production and decreased MMP, well demonstrate that Cr (VI) perturbs mitochondrial dynamics and homeostasis.

Typically, damaged mitochondria require elimination to maintain the cellular homeostasis, which is attained by mitophagy. Mitophagy, namely mitochondrial autophagy, is a targeted defense against mitochondrial impairment, playing critical roles in selective degradation of damaged or redundant mitochondria (Zhang et al., 2020b). There are two well-known routes for mitophagy: (1) the phosphatase and tensin homolog (PTEN) induced kinase I (PINK1)-Parkin pathway; and (2) the receptor (NIX/BNIP3L, BNIP3 and FUNDC1)-mediated pathway (Kubli and Gustafsson, 2012). Here, we found that exposure of SSCs/progenitors to 10 μ M Cr (VI) for 4 h did not activate the PINK1-Parkin pathway. Instead, Cr (VI) treatment upregulated *Bnip* and *Nix*, suggesting induction of the receptor-mediated mitophagy pathway.

N⁶-methyladenosine is the most abundant internal modification of mRNAs in eukaryotes. In mammals, each mRNA contains an average of 3–5 m⁶A modifications within a consensus sequence (Meyer et al., 2012). The methylation and demethylation of m⁶A are dynamically regulated by m⁶A writers (methyltransferases, e.g., METTL3/14 and WTAP, responsible for catalyzing the m⁶A modification of adenosine acid on mRNAs), erasers (demethylases, e.g., FTO and ALKBH5, responsible for demethylation of m⁶A modified bases), and readers (m⁶A-binding proteins, e.g., YTHDF2, responsible for recognition of the base of m⁶A modification and for activation of downstream regulatory pathways involved in RNA degradation and miRNA processing; Shi et al., 2019). RNA m⁶A modification plays important regulatory roles in various biological processes, such as the response to inflammatory, DNA damage, cell proliferation, and survival (Shi et al., 2019). Despite this, the influence of RNA m⁶A modification on the response to Cr (VI)-induced toxicity in SSCs has so far not been studied. Here, we identified that Cr (VI) treatment induced autophagy in SSCs/progenitors, along with a decrease in the global RNA m⁶A level, suggesting that RNA m⁶A modification may play a regulatory role in Cr (VI)-induced SSC/progenitor autophagy. Indeed, the m⁶A-IP-qPCR assay uncovered that Cr (VI) treatment reduced the m⁶A modification levels in mitochondrial fusion genes *Mfn2* and *Opa1*, as well as in mitophagy genes *Bnip3* and *Nix*, lending support to potential roles of RNA m⁶A modification in Cr (VI)-induced mitochondrial abnormality in SSCs/progenitors.

Melatonin is the strongest endogenous free radical scavenger, implicated in antioxidant systems and prevention of oxidative damage in cells. Melatonin can directly act on testes and alleviate testicular damage caused by oxidative stress, apoptosis, hyperthermia, and inflammation (Dong et al., 2020; Li et al., 2020b; Zhang et al., 2020a). In addition, melatonin has been

reported to protect mitochondria by scavenging ROS, inhibiting the mitochondrial permeability transition pore (MPTP), activating uncoupling proteins (UCPs), and maintaining the optimal MMP, together maintaining mitochondrial homeostasis and preserving mitochondrial functions (Tan et al., 2016). Since one of the main reasons for Cr (VI)-induced cytotoxicity is elevated ROS that trigger oxidative stress, we assumed that melatonin might have protective roles against Cr (VI)-induced cytotoxicity in SSCs. As expected, melatonin pretreatment downregulated the Cr (VI)-induced increase of NOX4 via MT1, thereby alleviating ROS overproduction and preserving cell viability. Also, our results demonstrated that melatonin pretreatment attenuated Cr (VI)-induced mitochondrial dynamic disorders and mitophagy, providing novel insights into the mechanisms underlying the protective roles of melatonin against Cr (VI)-induced cytotoxicity in SSCs/progenitors. Yet, a point that should not be overlooked is that the SSC niche and testosterone secretion may change after Cr (VI) and/or melatonin treatment. This, and the roles it plays, if any, are stimulating topics in future research.

Intriguingly, our results suggest that the protective roles of melatonin against Cr (VI)-induced mitochondrial dynamic disorders and mitophagy in SSCs/progenitors also involve RNA m⁶A modification. To gain more knowledge in this respect, we analyzed the expression levels of four well-known m⁶A-associated genes, i.e., *Mettl3*, *Wtap*, *Fto*, and *Ythdf2*, which encode the m⁶A writer, eraser, or reader, and found that melatonin pretreatment attenuated the Cr (VI)-induced downregulation of *Mettl3*. METTL3 is a key component of the m⁶A methyltransferase complex (Shi et al., 2019). We thus presumed that melatonin could exert its protective roles via METTL3-mediated RNA m⁶A modification. To this end, we constructed a *Mettl3*-depleted mouse SSC/progenitor line. As expected, *Mettl3* depletion reduced the overall RNA m⁶A level, and weakened the protective roles of melatonin against the Cr (VI)-induced decrease of the RNA m⁶A level and mitophagy. Thus, our study has for the first time demonstrated that melatonin could attenuate Cr (VI)-induced mitophagy by restoration of METTL3-mediated RNA m⁶A modification in SSCs/progenitors.

In this study, we reported the involvement of METTL3-mediated RNA m⁶A modification in the protective roles of melatonin against Cr (VI)-induced mitophagy in SSCs/progenitors. Indeed, apart from METTL3, other methyltransferases, demethylases, or RNA-binding proteins may also function in this process, which warrants systematic investigation in future. Besides, we identified that both the m⁶A abundance and mRNA levels of mitochondrial fusion genes *Mfn2* and *Opa1* were reduced by Cr (VI) treatment. Differently, Cr (VI) decreased the m⁶A abundance but increased the mRNA levels of receptor-mediated mitophagy pathway genes *Bnip3* and *Nix*. Given that m⁶A is a ubiquitous RNA modification, orchestrating mRNA splicing, translation, stability, and degradation (Niu et al., 2013), it would be stimulating to delve into the m⁶A-mediated transcriptional regulation in these genes. Future studies in these regards would extend the knowledge about the roles of RNA m⁶A modification in

mitochondrial physiology, providing clues for treatment of disorders resulted from mitochondrial malfunction.

To sum up, we identified that melatonin could attenuate Cr (VI)-induced mitochondrial dynamic disorders and mitophagy in SSCs/progenitors, *via* a mechanism illustrated in **Figure 10**. Our study does provide novel insights into the molecular mechanisms for RNA m⁶A modification underlying the gene regulatory network responsible for mitochondrial dynamic balance. Moreover, since SSCs are the cornerstone of spermatogenesis and able to differentiate into sperm thereby transmitting paternal genetic information to the next generation, our study, providing knowledge about the response of SSCs to environmental toxicant Cr (VI) and the underlying mechanisms for the protective roles of melatonin, would contribute to development of tailored therapies for Cr (VI)-induced damage to male fertility.

DATA AVAILABILITY STATEMENT

The original contributions presented in the study are included in the article/supplementary material; further inquiries can be directed to the corresponding authors.

REFERENCES

- Aita, V. M., Liang, X. H., Murty, V. V., Pincus, D. L., Yu, W., Cayanis, E., et al. (1999). Cloning and genomic organization of beclin 1, a candidate tumor suppressor gene on chromosome 17q21. *Genomics* 59, 59–65. doi: 10.1006/geno.1999.5851
- Bonnefont-Rousselot, D., Collin, F., Jore, D., and Gardes-Albert, M. (2011). Reaction mechanism of melatonin oxidation by reactive oxygen species in vitro. *J. Pineal Res.* 50, 328–335. doi: 10.1111/j.1600-079X.2010.00847.x
- Chen, Q. Y., Murphy, A., Sun, H., and Costa, M. (2019). Molecular and epigenetic mechanisms of Cr(VI)-induced carcinogenesis. *Toxicol. Appl. Pharmacol.* 377:114636. doi: 10.1016/j.taap.2019.114636
- Costa, M. (2003). Potential hazards of hexavalent chromate in our drinking water. *Toxicol. Appl. Pharmacol.* 188, 1–5. doi: 10.1016/S0041-008X(03)00011-5
- de Campos, C. B., Zhu, Y. X., Sepetov, N., Romanov, S., Bruins, L. A., Shi, C. X., et al. (2020). Identification of PIKfyve kinase as a target in multiple myeloma. *Haematologica* 105, 1641–1649. doi: 10.3324/haematol.2019.222729
- DesMarais, T. L., and Costa, M. (2019). Mechanisms of chromium-induced toxicity. *Curr. Opin. Toxicol.* 14, 1–7. doi: 10.1016/j.cotox.2019.05.003
- Di Maio, R., Barrett, P. J., Hoffman, E. K., Barrett, C. W., Zharikov, A., Borah, A., et al. (2016). Alpha-synuclein binds to TOM20 and inhibits mitochondrial protein import in parkinson's disease. *Sci. Transl. Med.* 8:342ra378. doi: 10.1126/scitranslmed.aaf3634
- Dong, Y., Zhao, J., Zhu, Q., Liu, H., Wang, J., and Lu, W. (2020). Melatonin inhibits the apoptosis of rooster leydig cells by suppressing oxidative stress via AKT-Nrf2 pathway activation. *Free Radic. Biol. Med.* 160, 1–12. doi: 10.1016/j.freeradbiomed.2020.06.024
- Fernandez, A., Ordonez, R., Reiter, R. J., Gonzalez-Gallego, J., and Mauriz, J. L. (2015). Melatonin and endoplasmic reticulum stress: relation to autophagy and apoptosis. *J. Pineal Res.* 59, 292–307. doi: 10.1111/jpi.12264
- Gotoh, H., Hirawatari, K., Hanzawa, N., Miura, I., and Wakana, S. (2012). QTL on mouse chromosomes 1 and 4 causing sperm-head morphological abnormality and male subfertility. *Mamm. Genome* 23, 399–403. doi: 10.1007/s00335-012-9395-1
- Hofmann, M. C., Braydich-Stolle, L., Dettin, L., Johnson, E., and Dym, M. (2005). Immortalization of mouse germ line stem cells. *Stem Cells* 23, 200–210. doi: 10.1634/stemcells.2003-0036

ETHICS STATEMENT

The animal study was reviewed and approved by Institutional Animal Care and Use Committee of Northwest A&F University.

AUTHOR CONTRIBUTIONS

YL and YZ conceived the study and designed the experiments. YL, TL, MY, LS, ZZ, and SZ performed the experiments. YL, TL, and YZ analyzed the data and wrote the manuscript. WZ and YZ supervised the study and approved the final submission. All authors contributed to the article and approved the submitted version.

FUNDING

This study was supported by National Natural Science Foundation of China (81703193, 32002178, and 31772605), Natural Science Foundation of Shaanxi Province, China (2019JQ-643), the Undergraduate Training Program for Innovation and Entrepreneurship (S202010712699), and a startup fund from Northwest A&F University (2452019001).

- Hsu, P. J., Zhu, Y., Ma, H., Guo, Y., Shi, X., Liu, Y., et al. (2017). Ythdc2 is an N(6)-methyladenosine binding protein that regulates mammalian spermatogenesis. *Cell Res.* 27, 1115–1127. doi: 10.1038/cr.2017.99
- Hu, G., Li, P., Cui, X., Li, Y., Zhang, J., Zhai, X., et al. (2018). Cr(VI)-induced methylation and down-regulation of DNA repair genes and its association with markers of genetic damage in workers and 16HBE cells. *Environ. Pollut.* 238, 833–843. doi: 10.1016/j.envpol.2018.03.046
- Hu, G., Li, P., Li, Y., Wang, T., Gao, X., Zhang, W., et al. (2016). Methylation levels of P16 and TP53 that are involved in DNA strand breakage of 16HBE cells treated by hexavalent chromium. *Toxicol. Lett.* 249, 15–21. doi: 10.1016/j.toxlet.2016.03.003
- Kabeya, Y., Mizushima, N., Ueno, T., Yamamoto, A., Kirisako, T., Noda, T., et al. (2000). LC3, a mammalian homologue of yeast Apg8p, is localized in autophagosome membranes after processing. *EMBO J.* 19, 5720–5728. doi: 10.1093/emboj/19.21.5720
- Kabeya, Y., Mizushima, N., Yamamoto, A., Oshitani-Okamoto, S., Ohsumi, Y., and Yoshimori, T. (2004). LC3, GABARAP and GATE16 localize to autophagosomal membrane depending on form-II formation. *J. Cell Sci.* 117, 2805–2812. doi: 10.1242/jcs.01131
- Kart, A., Koc, E., Dalginli, K. Y., Gulmez, C., Sertcelik, M., and Atakisi, O. (2016). The therapeutic role of glutathione in oxidative stress and oxidative DNA damage caused by hexavalent chromium. *Biol. Trace Elem. Res.* 174, 387–391. doi: 10.1007/s12011-016-0733-0
- Klionsky, D. J., and Emr, S. D. (2000). Autophagy as a regulated pathway of cellular degradation. *Science* 290, 1717–1721. doi: 10.1126/science.290.5497.1717
- Kotas, J., and Stasicka, Z. (2000). Chromium occurrence in the environment and methods of its speciation. *Environ. Pollut.* 107, 263–283. doi: 10.1016/S0269-7491(99)00168-2
- Kubli, D. A., and Gustafsson, A. B. (2012). Mitochondria and mitophagy: the yin and yang of cell death control. *Circ. Res.* 111, 1208–1221. doi: 10.1161/CIRCRESAHA.112.265819
- Kubota, H., and Brinster, R. L. (2018). Spermatogonial stem cells. *Biol. Reprod.* 99, 52–74. doi: 10.1093/biolre/boy077
- Kuroda, J., Ago, T., Matsushima, S., Zhai, P., Schneider, M. D., and Sadoshima, J. (2010). NADPH oxidase 4 (Nox4) is a major source of oxidative stress in the failing heart. *Proc. Natl. Acad. Sci. U. S. A.* 107, 15565–15570. doi: 10.1073/pnas.1002178107

- Lampert, M. A., Orogo, A. M., Najor, R. H., Hammerling, B. C., Leon, L. J., Wang, B. J., et al. (2019). BNIP3L/NIX and FUNDC1-mediated mitophagy is required for mitochondrial network remodeling during cardiac progenitor cell differentiation. *Autophagy* 15, 1182–1198. doi: 10.1080/15548627.2019.1580095
- Li, Z., Zhao, J., Liu, H., Wang, J., and Lu, W. (2020b). Melatonin inhibits apoptosis in mouse Leydig cells via the retinoic acid-related orphan nuclear receptor alpha/p53 pathway. *Life Sci.* 246:117431. doi: 10.1016/j.lfs.2020.117431
- Li, R. N., Zhu, Z. D., Zheng, Y., Lv, Y. H., Tian, X. E., Wu, D., et al. (2020a). Metformin improves boar sperm quality via 5'-AMP-activated protein kinase-mediated energy metabolism in vitro. *Zool. Res.* 41, 527–538. doi: 10.24272/j.issn.2095-8137.2020.074
- Liang, X. H., Jackson, S., Seaman, M., Brown, K., Kempkes, B., Hibshoosh, H., et al. (1999). Induction of autophagy and inhibition of tumorigenesis by beclin 1. *Nature* 402, 672–676. doi: 10.1038/45257
- Lin, Z., Hsu, P. J., Xing, X., Fang, J., Lu, Z., Zou, Q., et al. (2017). Mettl3-/Mettl14-mediated mRNA N(6)-methyladenosine modulates murine spermatogenesis. *Cell Res.* 27, 1216–1230. doi: 10.1038/cr.2017.117
- Lv, Y., Zhang, P., Guo, J., Zhu, Z., Li, X., Xu, D., et al. (2018). Melatonin protects mouse spermatogonial stem cells against hexavalent chromium-induced apoptosis and epigenetic histone modification. *Toxicol. Appl. Pharmacol.* 340, 30–38. doi: 10.1016/j.taap.2017.12.017
- Makela, J. A., and Hobbs, R. M. (2019). Molecular regulation of spermatogonial stem cell renewal and differentiation. *Reproduction* 158, R169–R187. doi: 10.1530/REP-18-0476
- Meyer, K. D., Patil, D. P., Zhou, J., Zinoviev, A., Skabkin, M. A., Elemento, O., et al. (2015). 5' UTR m(6)A promotes cap-independent translation. *Cell* 163, 999–1010. doi: 10.1016/j.cell.2015.10.012
- Meyer, K. D., Saletore, Y., Zumbo, P., Elemento, O., Mason, C. E., and Jaffrey, S. R. (2012). Comprehensive analysis of mRNA methylation reveals enrichment in 3' UTRs and near stop codons. *Cell* 149, 1635–1646. doi: 10.1016/j.cell.2012.05.003
- Mizushima, N., Levine, B., Cuervo, A. M., and Klionsky, D. J. (2008). Autophagy fights disease through cellular self-digestion. *Nature* 451, 1069–1075. doi: 10.1038/nature06639
- Niu, Y., Zhao, X., Wu, Y. S., Li, M. M., Wang, X. J., and Yang, Y. G. (2013). N6-methyl-adenosine (m6A) in RNA: an old modification with a novel epigenetic function. *Genomics Proteomics Bioinformatics* 11, 8–17. doi: 10.1016/j.gpb.2012.12.002
- Ogbomida, E. T., Omofonmwan, K., Aganmwonyi, I., Fasipe, I. P., Enuneku, A., and Ezemonye, L. I. N. (2018). Bioactive profiling and therapeutic potential of mushroom (*Pleurotus tuberregium*) extract on Wistar albino rats (*Ratus norvegicus*) exposed to arsenic and chromium toxicity. *Toxicol. Rep.* 5, 401–410. doi: 10.1016/j.toxrep.2018.03.004
- Sharma, S., Wistuba, J., Pock, T., Schlatt, S., and Neuhaus, N. (2019). Spermatogonial stem cells: updates from specification to clinical relevance. *Hum. Reprod. Update* 25, 275–297. doi: 10.1093/humupd/dmz006
- Shi, H., Wei, J., and He, C. (2019). Where, when, and how: context-dependent functions of RNA methylation writers, readers, and erasers. *Mol. Cell* 74, 640–650. doi: 10.1016/j.molcel.2019.04.025
- Tan, D. X., Manchester, L. C., Qin, L., and Reiter, R. J. (2016). Melatonin: a mitochondrial targeting molecule involving mitochondrial protection and dynamics. *Int. J. Mol. Sci.* 17:2124. doi: 10.3390/ijms17122124
- Tang, S., Ye, S., Ma, Y., Liang, Y., Liang, N., and Xiao, F. (2020). Clusterin alleviates Cr(VI)-induced mitochondrial apoptosis in L02 hepatocytes via inhibition of Ca(2+)-ROS-Drp1-mitochondrial fission axis. *Ecotoxicol. Environ. Saf.* 205:111326. doi: 10.1016/j.ecoenv.2020.111326
- Tokuda, M., Kadokawa, Y., Kurahashi, H., and Marunouchi, T. (2007). CDH1 is a specific marker for undifferentiated spermatogonia in mouse testes. *Biol. Reprod.* 76, 130–141. doi: 10.1095/biolreprod.106.053181
- Ukhurebor, K. E., Aigbe, U. O., Onyancha, R. B., Nwankwo, W., Osibote, O. A., Paumo, H. K., et al. (2021). Effect of hexavalent chromium on the environment and removal techniques: a review. *J. Environ. Manag.* 280:111809. doi: 10.1016/j.jenvman.2020.111809
- Varuzhanyan, G., and Chan, D. C. (2020). Mitochondrial dynamics during spermatogenesis. *J. Cell Sci.* 133:jcs235937. doi: 10.1242/jcs.235937
- Weiss-Sadan, T., Maimoun, D., Oelschlagel, D., Kaschani, F., Misiak, D., Gaikwad, H., et al. (2019). Cathepsins drive anti-inflammatory activity by regulating autophagy and mitochondrial dynamics in macrophage foam cells. *Cell. Physiol. Biochem.* 53, 550–572. doi: 10.33594/000000157
- Xiang, Y., Laurent, B., Hsu, C. H., Nachtergaele, S., Lu, Z., Sheng, W., et al. (2017). RNA m(6)A methylation regulates the ultraviolet-induced DNA damage response. *Nature* 543, 573–576. doi: 10.1038/nature21671
- Xu, K., Yang, Y., Feng, G. H., Sun, B. F., Chen, J. Q., Li, Y. F., et al. (2017). Mettl3-mediated m(6)A regulates spermatogonial differentiation and meiosis initiation. *Cell Res.* 27, 1100–1114. doi: 10.1038/cr.2017.100
- Zhang, Y., Bian, H., Ma, Y., Xiao, Y., and Xiao, F. (2020b). Cr(VI)-induced overactive mitophagy contributes to mitochondrial loss and cytotoxicity in L02 hepatocytes. *Biochem. J.* 477, 2607–2619. doi: 10.1042/BCJ20200262
- Zhang, X., Xia, Q., Wei, R., Song, H., Mi, J., Lin, Z., et al. (2019). Melatonin protects spermatogonia from the stress of chemotherapy and oxidation via eliminating reactive oxidative species. *Free Radic. Biol. Med.* 137, 74–86. doi: 10.1016/j.freeradbiomed.2019.04.009
- Zhang, P., Zheng, Y., Lv, Y., Li, F., Su, L., Qin, Y., et al. (2020a). Melatonin protects the mouse testis against heat-induced damage. *Mol. Hum. Reprod.* 26, 65–79. doi: 10.1093/molehr/gaaa002
- Zhao, T., Wang, J., Wu, Y., Han, L., Chen, J., Wei, Y., et al. (2021). Increased m6A modification of RNA methylation related to the inhibition of demethylase FTO contributes to MEHP-induced leydig cell injury. *Environ. Pollut.* 268:115627. doi: 10.1016/j.envpol.2020.115627
- Zheng, Y., Feng, T., Zhang, P., Lei, P., Li, F., and Zeng, W. (2020). Establishment of cell lines with porcine spermatogonial stem cell properties. *J. Anim. Sci. Biotechnol.* 11:33. doi: 10.1186/s40104-020-00439-0
- Zheng, Y., Jongejan, A., Mulder, C. L., Mastenbroek, S., Repping, S., Wang, Y., et al. (2017). Trivial role for NSMCE2 during in vitro proliferation and differentiation of male germline stem cells. *Reproduction* 154, 181–195. doi: 10.1530/REP-17-0173
- Zheng, K., Wu, X., Kaestner, K. H., and Wang, P. J. (2009). The pluripotency factor LIN28 marks undifferentiated spermatogonia in mouse. *BMC Dev. Biol.* 9:38. doi: 10.1186/1471-213X-9-38
- Zheng, Y., Zhang, P., Zhang, C., and Zeng, W. (2019). Surgery-induced cryptorchidism induces apoptosis and autophagy of spermatogenic cells in mice. *Zygote* 27, 101–110. doi: 10.1017/S096719941900011X
- Zhitkovich, A. (2005). Importance of chromium-DNA adducts in mutagenicity and toxicity of chromium(VI). *Chem. Res. Toxicol.* 18, 3–11. doi: 10.1021/tx049774+
- Zhitkovich, A. (2011). Chromium in drinking water: sources, metabolism, and cancer risks. *Chem. Res. Toxicol.* 24, 1617–1629. doi: 10.1021/tx200251t

Conflict of Interest: The authors declare that the research was conducted in the absence of any commercial or financial relationships that could be construed as a potential conflict of interest.

Copyright © 2021 Lv, Li, Yang, Su, Zhu, Zhao, Zeng and Zheng. This is an open-access article distributed under the terms of the Creative Commons Attribution License (CC BY). The use, distribution or reproduction in other forums is permitted, provided the original author(s) and the copyright owner(s) are credited and that the original publication in this journal is cited, in accordance with accepted academic practice. No use, distribution or reproduction is permitted which does not comply with these terms.



LOC550643, a Long Non-coding RNA, Acts as Novel Oncogene in Regulating Breast Cancer Growth and Metastasis

Kuo-Wang Tsai^{1*}, Kian-Hwee Chong², Chao-Hsu Li^{2,3}, Ya-Ting Tu¹, Yi-Ru Chen¹, Ming-Cheng Lee¹, Shih-Hsuan Chan^{4*}, Lu-Hai Wang^{4,5,6*} and Yao-Jen Chang^{2,7*}

¹ Department of Research, Taipei Tzu Chi Hospital, Buddhist Tzu Chi Medical Foundation, New Taipei City, Taiwan, ² Division of General Surgery, Department of Surgery, Taipei Tzu Chi Hospital, Buddhist Tzu Chi Medical Foundation, New Taipei City, Taiwan, ³ Graduate Institute of Clinical Medicine, College of Medicine, National Taiwan University, Taipei, Taiwan, ⁴ Graduate Institute of Integrated Medicine, China Medical University, Taichung, Taiwan, ⁵ Chinese Medicine Research Center, China Medical University, Taichung, Taiwan, ⁶ Institute of Molecular Medicine, College of Life Science, National Tsing Hua University, Hsinchu, Taiwan, ⁷ School of Medicine, Tzu Chi University, Hualien, Taiwan

OPEN ACCESS

Edited by:

Nejat Dalay,
Istanbul University, Turkey

Reviewed by:

Olga Hernández De La Cruz,
National Autonomous University
of Mexico, Mexico
Ye Liang,
The Affiliated Hospital of Qingdao
University, China

*Correspondence:

Yao-Jen Chang
yjchang@tzuchi.com.tw
Lu-Hai Wang
luhaiwang@mail.cmu.edu.tw
Shih-Hsuan Chan
jamesc27@mail.cmu.edu.tw
Kuo-Wang Tsai
kwtsai6733@gmail.com

Specialty section:

This article was submitted to
Epigenomics and Epigenetics,
a section of the journal
Frontiers in Cell and Developmental
Biology

Received: 16 April 2021

Accepted: 27 June 2021

Published: 20 July 2021

Citation:

Tsai K-W, Chong K-H, Li C-H,
Tu Y-T, Chen Y-R, Lee M-C,
Chan S-H, Wang L-H and Chang Y-J
(2021) LOC550643, a Long
Non-coding RNA, Acts as Novel
Oncogene in Regulating Breast
Cancer Growth and Metastasis.
Front. Cell Dev. Biol. 9:695632.
doi: 10.3389/fcell.2021.695632

Metastatic disease is responsible for over 90% of death in patients with breast cancer. Therefore, identifying the molecular mechanisms that regulate metastasis and developing useful therapies are crucial tasks. Long non-coding RNAs (lncRNAs), which are non-coding transcripts with >200 nucleotides, have recently been identified as critical molecules for monitoring cancer progression. This study examined the novel lncRNAs involved in the regulation of tumor progression in breast cancer. This study identified 73 metastasis-related lncRNA candidates from comparison of paired isogenic high and low human metastatic breast cancer cell lines, and their expression levels were verified in clinical tumor samples by using The Cancer Genome Atlas. Among the cell lines, a novel lncRNA, LOC550643, was highly expressed in breast cancer cells. Furthermore, the high expression of LOC550643 was significantly correlated with the poor prognosis of breast cancer patients, especially those with triple-negative breast cancer. Knockdown of LOC550643 inhibited cell proliferation of breast cancer cells by blocking cell cycle progression at S phase. LOC550643 promoted important *in vitro* metastatic traits such as cell migration and invasion. Furthermore, LOC550643 could inhibit miR-125b-2-3p expression to promote breast cancer cell growth and invasiveness. In addition, by using a xenograft mouse model, we demonstrated that depletion of LOC550643 suppressed the lung metastatic potential of breast cancer cells. Overall, our study shows that LOC550643 plays an important role in breast cancer cell metastasis and growth, and LOC550643 could be a potential diagnosis biomarker and therapeutic target for breast cancer.

Keywords: breast cancer, ncRNA, metastasis, lncRNA, microRNA

INTRODUCTION

Breast cancer is the most common cancer and the second leading cause of cancer deaths among women worldwide (Bray et al., 2018). Unlike other malignancies, breast cancer is considered a heterogeneous disease consisting of at least four molecular subtypes, namely luminal A, luminal B, HER2, and triple negative (or basal-like) subtypes, which are determined on the basis of hormone

receptor status and HER2 expression (Yeo et al., 2014). Among breast cancer subtypes, triple negative breast cancer (TNBC) is the most aggressive one, it has the poorest 5-year survival rate, and has the shortest recurrence intervals because of the lack of effective treatments and targeted therapy (Bertucci et al., 2012). Therefore, developing useful prognostic biomarkers and alternative therapeutic approaches for patients with TNBC is urgently required.

Long non-coding RNAs (lncRNAs) are an emerging class of ncRNAs with an estimated number of 15,000 human genome transcripts, and these RNAs have been demonstrated to play a crucial role in tumor development (Derrien et al., 2011; Serviss et al., 2014). Abundant evidence indicates that lncRNAs exert their function by interacting with cellular macromolecules such as chromatin, RNAs and proteins to regulate genes important for cell proliferation, motility, invasiveness, and angiogenesis (Serviss et al., 2014; Kumar and Goyal, 2017; Zhang et al., 2020). lncRNAs can also act as decoys to titrate cancer-related miRNAs to regulate the aforementioned cellular activities (Yoon et al., 2014; Chan and Tay, 2018). Despite numerous efforts being made to identify the role of lncRNA in tumor progression, the function of most lncRNAs remains largely unknown.

In this study, we compared the lncRNA expression profiles between the highly metastatic MDA-MB-231-IV2-1 subline and its parental line MDA-MB-231 to identify clinically relevant metastasis-related lncRNAs that can be found in The Cancer Genome Atlas (TCGA) database. We demonstrated that *LOC550643* promoted *in vitro* metastasis-traits such as cell growth, migration, and invasion through inhibiting miR-125b-2-3p. High *LOC550643* expression was significantly correlated with poor overall survival (OS) when compared with low *LOC550643* expression in TNBC patients.

MATERIALS AND METHODS

Cell Line

Eight human cell lines, namely MCF-10A, MCF-7, T-47D, SK-BR-3, BT-549, Hs578T, MDA-MB-231, and MDA-MB-453, were originally obtained from the American Type Culture Collection and maintained in Dulbecco's modified Eagle medium (DMEM) supplemented with 10% inactivated fetal bovine serum (FBS) (Invitrogen, Carlsbad, CA, United States). The highly metastatic MDA-MB-231-IV2-1 and MDA-MB-231-IV2-2 cells were isolated using an *in vivo* mouse model, as in our previous study (Chan et al., 2014). Breast cancer cell total RNA was prepared using TRIZOL (Invitrogen, Carlsbad, CA, United States) in accordance with the manufacturer's instructions. Total RNA was incubated with DNase I (20 mg/ml) at 37°C for 30 min followed by phenol-chloroform extraction. RNA was then precipitated with isopropanol at 4°C for 30 min followed by centrifugation at 12,500 rpm. RNA pellets were washed with 70% ethanol three times and dissolved in DEPC-treated water.

Microarray Analysis

MDA-MB-231-P and MDA-MB-231-IV2-1 cells were cultured in DMEM supplemented with 10% inactivated FBS. The cells were subjected to RNA extraction after 70% confluence was reached. Breast cancer cell total RNA was prepared using TRIZOL approach. Next, 0.2 µg of total RNA was subjected to amplification by using a Low Input Quick-Amp Labeling kit (Agilent Technologies, United States) and labeled with Cy3 (CyDye, Agilent Technologies, United States). Finally, 0.6 µg of Cy3-labeled cRNA was fragmented and hybridized using an Agilent SurePrint G3 Human V2 GE 8 × 60K microarray (Agilent Technologies, United States) at 65°C for 17 h. After hybridization, the microarray image was scanned and analyzed using Feature Extraction 10.5.1.1 (Agilent Technologies, United States). We performed microarray experiments by using the Agilent oligonucleotide ChIP-on-chip protocol, then data analysis were analyzing by Welgene Biotech (Taipei, Taiwan). We submitted all microarray raw data to the National Center for Biotechnology Information (NCBI) Gene Expression Omnibus (GEO), and they are freely available (accession number: GSE175513).

Pathway Enrichment Analysis

The differentially expressed gene-associated networks were analyzed with *Kyoto Encyclopedia of Genes and Genomes* (KEGG) pathways. Altered gene expressions were selected from microarray data and were subsequently fed into the KEGG pathways using the R package SubPathwayMiner (version 3.1). Enriched pathways were extracted by Hypergeometric testing the false discovery rate-corrected *q*-value were calculated.

Reverse Transcription and Real-Time Polymerase Chain Reaction (PCR) Analysis

Total RNA was reverse-transcribed with random primers and SuperScript III Reverse Transcriptase in accordance with the relevant user manual (Invitrogen, Carlsbad, CA, United States). The RT reaction was carried out at 42°C for 1 h followed by inactivation at 70°C for 10 min. The cDNA was used for the subsequent PCR reaction with gene-specific primers, and gene expression analysis was conducted using a SYBR Green I assay (Applied Biosystems, Foster City, CA, United States). Delta-delta Ct values were used to determine their relative expressions as fold changes using GAPDH as an internal control. The primers used are listed in **Supplementary Table 1**.

Clinical Samples

The data and specimens used in this study were collected from 36 breast cancer patients who underwent surgery at the Department of Surgery, Kaohsiung Veterans General Hospital (KSVGH), Taiwan. Informed consent forms were obtained from all patients by the KSVGH biobank. This study was approved by the ethics committees of KSVGH (VGHKS16-CT10-08).

LOC550643 Expression Analysis and Clinical Impact of TCGA Database

In this study, we downloaded TCGA data on RNA sequences in breast cancer tissue samples from the TCGA online database¹. The RNA-seq data of 1092 breast cancer tissue samples and 113 corresponding adjacent normal tissue samples were fetched from TCGA public domain. Among them are expression profiles of 56 paired normal/tumor tissues from the breast cancer patients. We identified lncRNAs differentially expressed in cancer tissues versus their adjacent normal tissues from the 56 breast cancer patients. The clinical information of the patients was also downloaded. In this study, the Kaplan–Meier survival analysis was applied for evaluating *LOC550643* relevant overall survival in 1070 breast cancer patients.

RNA Ligase–Mediated Rapid Amplification of the 5′ and 3′ Rapid Amplified cDNA Ends for Full-Length Determination

To map the full *LOC550643* sequence, RNA ligase–mediated rapid amplification of cDNA ends (RACE) was performed using the GeneRacer kit (Invitrogen, Carlsbad, CA, United States) in accordance with the manufacturer's instructions. The 5′ RACE was conducted to obtain the complete sequence of the lncRNA transcript. The 5′ end sequence of the lncRNA transcript was generated using GeneRacer 5′ primer and reverse primers. In addition, the 3′ end sequence of the lncRNA transcript was obtained using the GeneRacer 3′ primer and forward primers. The complete sequence of the lncRNA transcript was obtained by merging the 5′ end and 3′ end sequences. PCR products were gel-purified and cloned into a pCR4 TOPO vector (Invitrogen, Carlsbad, CA, United States) for sequencing. The primers used in the RNA ligase–mediated RACE are presented in **Supplementary Table 1**.

LOC550643 Knockdown

MDA-MB-231-IV2-1 cells with approximately 70% confluence were cultured in 60-mm cell culture dishes with DMEM supplemented with 10% FBS for 24 h prior to transient transfection. For *LOC550643* knockdown, *LOC550643* siRNAs (10 nmol/L) transfection was conducted using lipofectamine RNAiMAX (Invitrogen) in Opti-MEM (Invitrogen). The sequences of siRNAs purchased from Gene Discovery are presented in **Supplementary Table 2**.

Cell Proliferation Assay

Cells were transfected with either si-*LOC550643* or siNC and plated onto 96-well plates. Cell proliferation was determined at the time point of 0, 1, 2, 3, and 4 days. Cell viability was analyzed by MTS assay (Promega Corporation, United States) in accordance with the manufacturer's instructions.

Colony Formation Assay

A total of 4000 cells were plated in 6-well plates and incubated at 37°C for 10 days. The cultured medium was replaced every 3 days. Cells were fixed with 4% formaldehyde for 2 min, and colonies were stained with 0.5% crystal violet solution for 2 h. The 6-well plates were washed with H₂O and air-dried. The crystal violet-stained cells were then lysed with 1 mL of 10% acetic acid followed by analysis of 595 nm the absorbance using a spectrophotometer.

Cell Synchronization

MDA-MB-231-IV2-1 cells were synchronized at the late G1/early S phase by using a double thymidine block in accordance with a previous study (Chen and Deng, 2018). MDA-MB-231-IV2-1 cells with approximately 70% confluence were seeded in 6-cm dishes and transfected with si-*LOC550643* as previously described. After 24 h of siRNA transfection, the first thymidine block was initiated through the addition of thymidine (Sigma) to the wells at a final concentration of 2 mM for 16 h. Cells were then washed with 1X phosphate-buffered saline (PBS) and further cultured in normal cell maintenance media for 8 h to release the cell cycle. The second 16-h thymidine (2 mM) block was initiated immediately following the 8-h cell cycle release. After the second thymidine block, the cells were washed with 1X PBS to release the cell cycle and further incubated in a medium containing nocodazole (1 µg/mL) to arrest cells in the G2/M phase. The cell cycle progression of the cells was analyzed using flow cytometry every hour for 8 h following the release. The cell cycle profiles were analyzed using NucleoView NC-3000 to determine the percentages of cells in the G1, S, and G2/M phases.

Image Flow Cytometry Assay

The cell cycle of MDA-MB-231-IV2-1 with *LOC550643* knockdown was determined using the fluorescence image cytometer NucleoCounter NC-3000 (ChemoMetec, Gydevang, Lillerød, Denmark). After transfection with siRNA for 48 h, the cells were trypsinized and the number of cells was determined. A total of 1×10^6 cells were fixed with 70% ethanol at 4°C overnight. The cells were then stained with 1 µg/mL DAPI (4',6-diamidino-2-phenylindole) solution containing DAPI and 0.1% triton X-100 in PBS at 37°C for 5 min. Finally, the stained cells were analyzed using the NucleoView NC-300 software program (ChemoMetec, Gydevang, Lillerød, Denmark).

Western Blotting

The cells were harvested 48 h after transient transfection followed by PBS wash, and treated with lysis buffer (50 mM Tris-HCl at pH 8.0, 150 mM NaCl, 1% NP-40, 0.02% sodium azide, 1 µg/mL aprotinin, 1 mM PMSF) at 4°C for 30 min. The relevant details are described in our previous study (Tsai et al., 2018). Detailed information regarding the primary antibodies used in this study is presented in **Supplementary Table 3**.

Cell Invasion

For the invasion assay, 3×10^5 cells were suspended in 200 µL of DMEM with 2% FBS and plated onto BD BioCoat

¹<https://tcga-data.nci.nih.gov/tcga/dataAccessMatrix.htm>

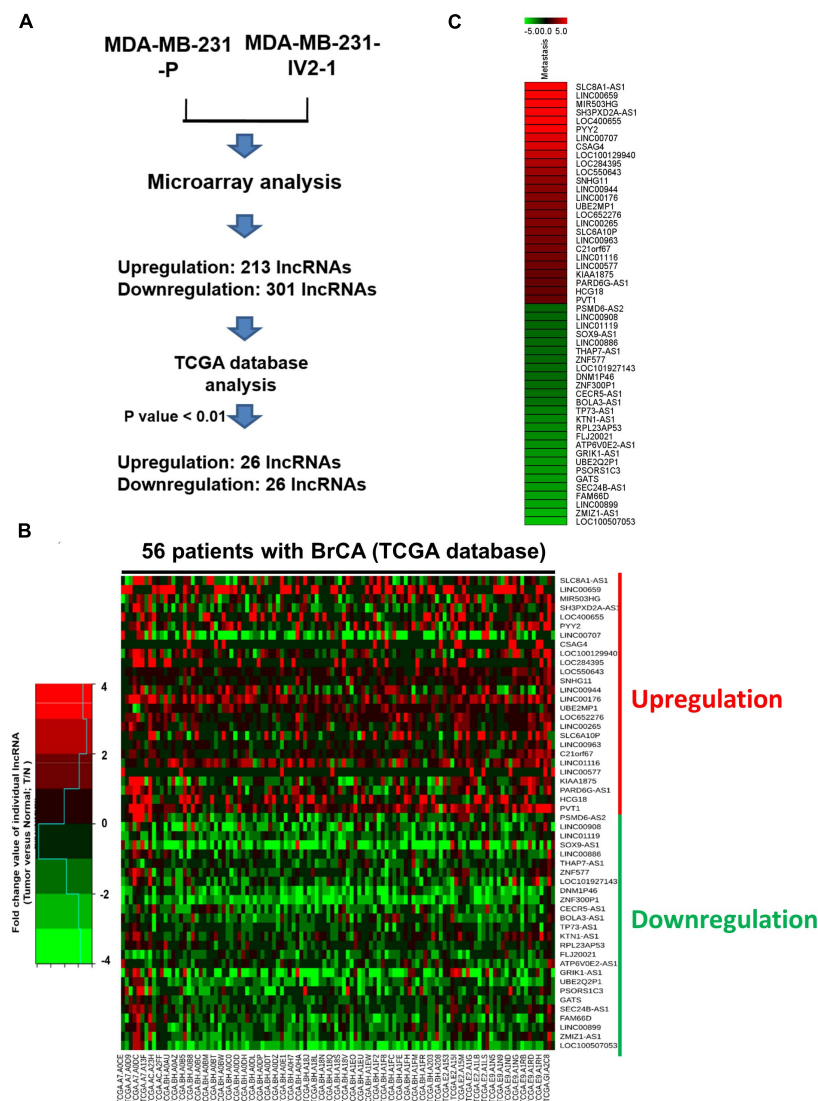


FIGURE 1 | Comparison of MDA-MB-231-P and MDA-MB-231-IV2-1 lncRNA profiles. **(A)** Flowchart for the microarray approach to screening lncRNA candidates and the use of TCGA database to examine their expression levels. **(B)** The 56 expression profiles of normal/tumor tissue pairs from patients with breast cancer obtained from TCGA database. The fold change values of the individual lncRNAs were calculated using the lncRNA expression levels of tumor cells compared with non-tumor cells. A heatmap of the differential expression of the 52 lncRNA candidates in 56 patients with breast cancer is presented. **(C)** Heatmap of selected putative metastasis-associated lncRNAs in MDA-MB-231-P cells compared with MDA-MB-IV2-1 cells.

Matrigel Invasion Chambers (24-well insert; pore size, 8 μ m; BD Biosciences) precoated with 100 μ L Matrigel (0.5 μ g/ μ L) per insert and incubated in a humidified chamber for 2 h at 37°C. The lower chamber was filled with DMEM containing 10% FBS. After being cultured for 24 h, the transwell inserts were fixed and stained with crystal violet solution (0.5% crystal violet, 5% formaldehyde, 50% ethanol, and 0.85% sodium chloride). Cells that did not invade were erased with a cotton swab. The invaded cells were imaged under a microscope at 100 \times magnification.

Animal Model

A xenograft mouse model was performed in this study, 10 mice were used for the lung metastasis assay (five controls and five

for LOC550643 knockdown). A total of 1×10^6 cells were transfected with the indicated siRNAs 24 h before injection, and then they were suspended in 100 μ L of 1X PBS and were injected into C.B-17 severe combined immunodeficient (SCID) mice via tail vein. The lung metastasis status of the mice was investigated 3 weeks after injection. The mice were intravenously injected with 200 μ L of luciferin (20 mg/mL) and anesthetized with isoflurane. The mice were then transferred to the imaging chamber of the *in vivo* imaging system (IVIS) spectrum to obtain the luminescent signals (Perkin Elmer Inc., MA, United States). The luminescent signals were measured and analyzed using Living Image 4.4 (Perkin Elmer Inc., MA, United States).

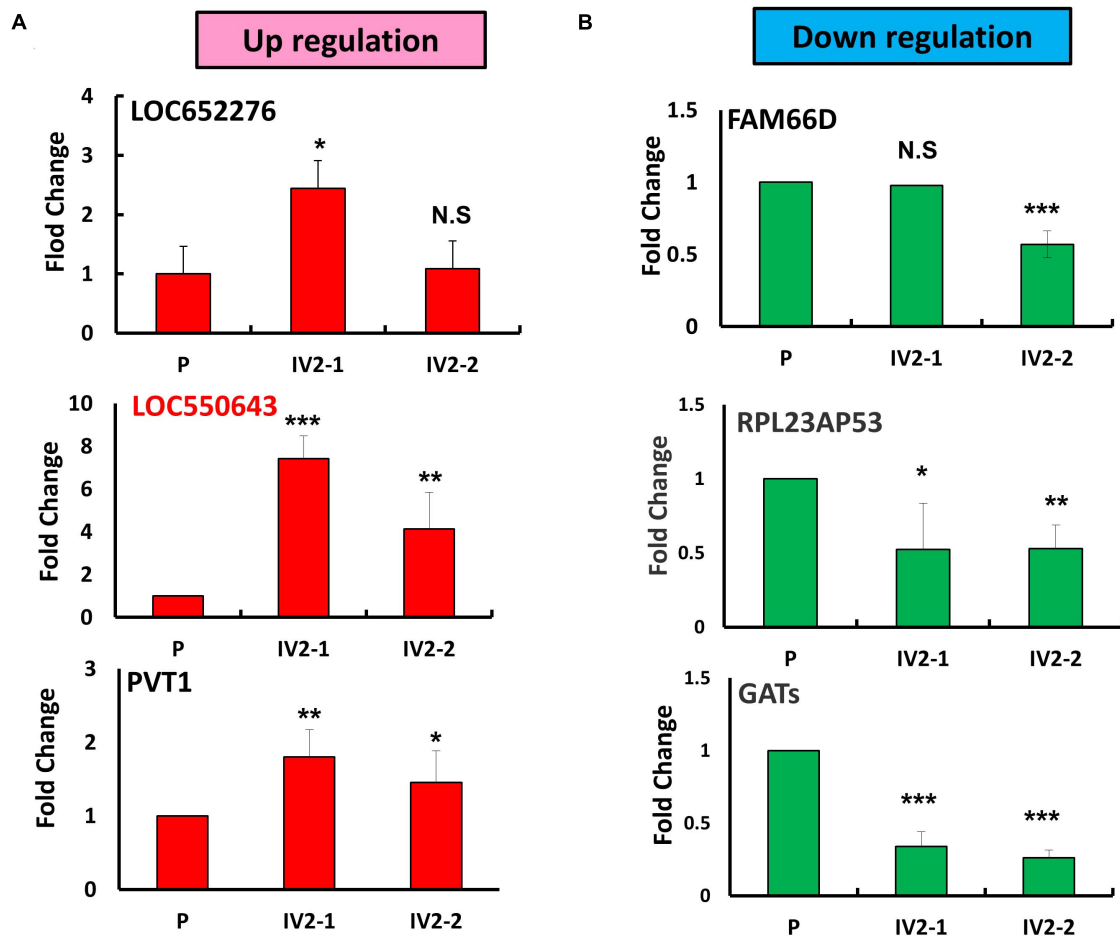


FIGURE 2 | Identification of metastasis-related lncRNA candidates in MDA-MB-231-IV2 cells. **(A)** Expression levels of the three putative oncogenic lncRNA candidates examined in the parental MDA-MB-231, MDA-MB-231-IV2-1, and MDA-MB-231-IV2-2 cells. **(B)** Expression levels of the three tumor-suppressive lncRNA candidates examined in the parental MDA-MB-231-P, MDA-MB-231-IV2-1, and MDA-MB-231-IV2-2 cells. All experiments were carried out in triplicate. Using Student's *t*-test to analyze our data and $p < 0.05$ was considered significant (* $p < 0.05$, ** $p < 0.01$, and *** $p < 0.001$).

In vivo Imaging System

The mice were injected intravenously with 200 μ L of luciferin (20 mg/mL) at a dose of 200 mg/kg and then euthanized using CO₂. The mouse lungs were surgically removed and placed in the IVIS chamber for IVIS imaging between 5 and 15 min after sacrifice. The bioluminescence images were acquired using the IVIS SpectrumCT and were analyzed using Living Image 4.4 (Perkin Elmer Inc., CA, United States).

Hematoxylin and Eosin Staining

Samples were fixed in 4% paraformaldehyde for 1 h at room temperature and then embedded in paraffin. The 6- μ m tissue sections were prepared using a microtome followed by deparaffinization with xylene. The tissue sections were slowly rehydrated by immersing them into decreasing concentrations of ethanol and then placing them in deionized water for the subsequent hematoxylin and eosin (H&E) staining. The tissue sections were then stained with hematoxylin solution (Merck, CA, United States) for 3 min followed by washing with water

for 5 min. Finally, the tissue sections were stained with eosin (Merck, CA, United States) for 30 s followed by dehydration using increasing concentrations of ethanol. The sections were finally maintained in xylene. The tissue sections were mounted using Micromount (Leica, CA, United States) for 1 h at room temperature.

Small RNA Transcriptome Analysis Through Next-Generation Sequencing

After the MDA-MB-231-IV2-1 cells were transfected with si-LOC550643 and the scrambled control for 48 h, the total RNA was extracted from two samples by using TRIZOL reagent. The small RNA library was prepared using the NEBNext small RNA library prep kit (New England Biolabs). The library preparation process is described in details in our previous study (Tseng et al., 2017). Finally, the small RNA profiles of the MDA-MB-231-IV2-control and MDA-MB-231-IV2-LOC550643 knockdown were performed using the MiSeq V2 reagent kit (150 cycles; Illumina, San Diego, CA, United States). The sequencing data were

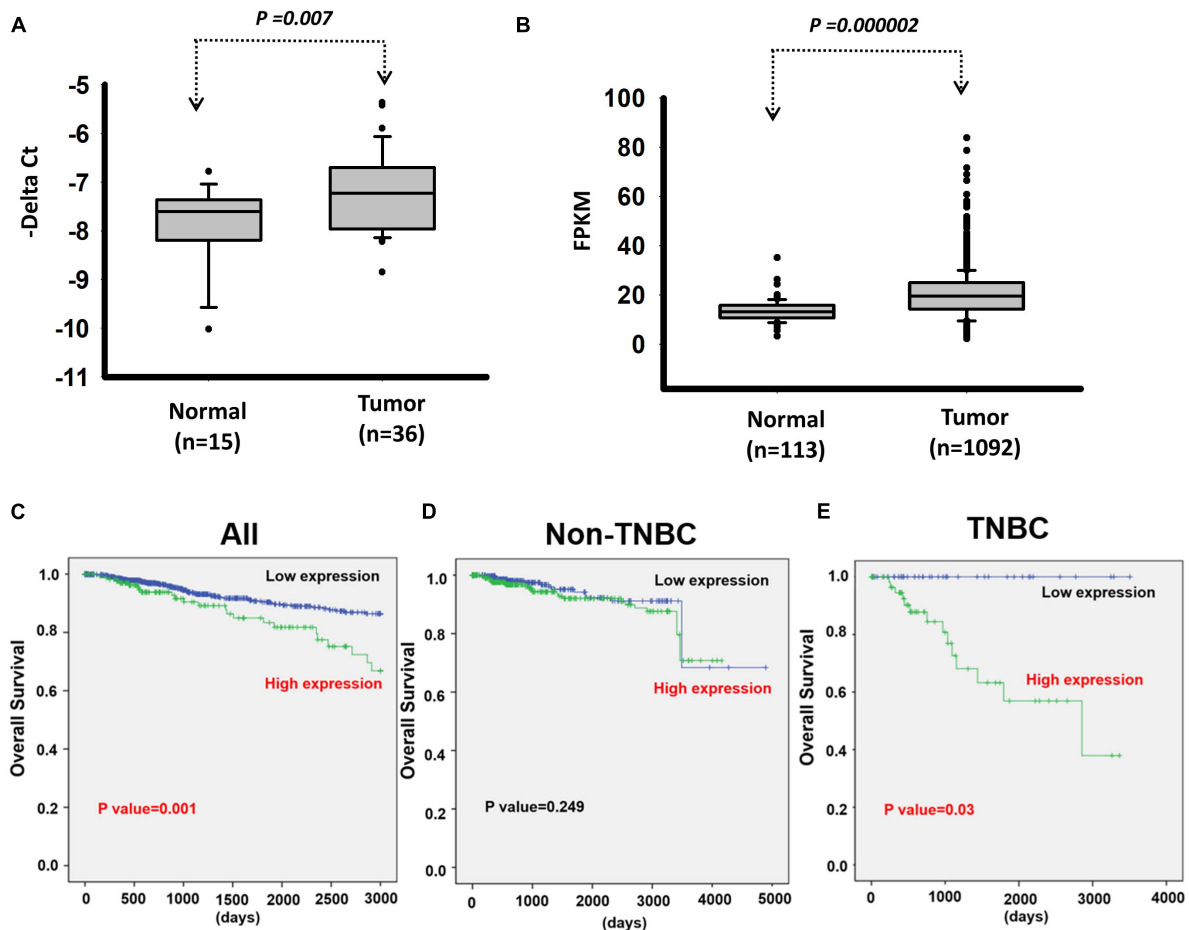


FIGURE 3 | Analysis of *LOC550643* expression levels in breast cancer tissues. **(A)** Expression levels of *LOC550643* in breast cancer tissues and corresponding adjacent normal tissues (real-time PCR). **(B)** Expression levels of *LOC550643* in human breast cancer tissues versus normal tissues (TCGA database). **(C-E)** Impacts of *LOC550643* expression on the OS of TNBC patients versus non-TNBC patients.

analyzed using our own tool (Pan et al., 2014). All microarray raw data were deposited in the NCBI GEO, and they are all accessible (accession number: GSE175514).

MicroRNA Expression Analysis and Clinical Impacts of TCGA Database

We downloaded small RNA expression data for breast cancer tissues from TCGA database. The expression profiles of 778 breast cancer tissue samples and 87 matched normal parts were fetched from TCGA portal. The clinical information of breast cancer patients was also downloaded. Small RNA and RNA sequencing were performed simultaneously for 757 breast cancer patients. The small RNA transcriptome profiles were subject to an OS analysis by using the Kaplan-Meier method.

Stem-Loop Reverse Transcription PCR

The PCR process is described in detail in our previous study (Liu et al., 2018). The miR-125b-2-3p expression levels were normalized to those

of U6 small RNA ($\Delta Ct = \text{target miR-125b-2-3p Ct} - \text{U6 Ct}$). The primers used are presented in **Supplementary Table 1**.

Ectopic Expression of miRNAs

Breast cancer cells were transfected with 10 nM miRNA-125b-2-3p mimics or a scrambled control (GenDiscovery Biotechnology Inc., Taiwan) by using lipofectamine RNAiMAX reagent. After 24 h of transfection, the miR-125b-2-3p expression levels were confirmed using stem-loop reverse transcription quantitative PCR.

Candidate miRNA Targets and Luciferase Activity Assay

The putative miRNAs targeting LOC550643 (Genebank ID: MH892397) were predicted using TargetScan. In this study, 189 miRNAs were predicted to bind to LOC550643. The full lengths of LOC550643-wt (Genebank ID: MH892397) and LOC550643-mut (mutated miR-125b-2-3p binding site) were synthesized using Invitrogen (Invitrogen, Waltham, MA,

United States). The fragments were cloned into the pMIR-REPORT vector. During synthesis, a *SpeI* cutting site was added at the 5' end, and *HindIII* was added at the 3' end of the LOC550643-wt and LOC550643-mut fragments, which were then cloned into the pMIR-REPORT vector. Subsequently, the pMIR-LOC550643-wt or pMIR-LOC550643-mut vectors were cotransfected separately with miR-125b-2-3p mimics or scrambled controls into breast cancer cells by using lipofectamine RNAiMAX reagent. 24 h post transfection, cells were harvested with lysis buffer and luciferase activity was measured by using the Dual-Glo Luciferase Reporter Assay System (Promega Corporation, Madison, WI, United States).

Statistical Analysis

The clinical impacts of *LOC550643* on breast cancer were evaluated using Fisher's test and a chi-squared test. *LOC550643* expression levels were tested in triplicate for clinical samples, cell growth, invasion ability, colony formation, cell cycle, and reporter experiments. The histograms present the mean values, and the error bars indicate the standard deviation. The *in vitro* and animal experiment data were analyzed using Student *t*-tests. OS was determined using the log-rank test or the Kaplan–Meier method. A *p*-value of < 0.05 was considered significant for the experiments.

RESULTS

Identification of Metastasis-Related lncRNA Candidates in TNBC

To explore the role of lncRNAs in breast cancer metastasis, we first generated expression profiles of human lncRNAs in MDA-MB-231-P and MDA-MB-231-IV2-1 cells by using a microarray approach (Agilent SurePrint G3 Human V2 GE; 34092 protein-coding genes and 8715 lncRNAs). The highly metastatic MDA-MB-231-IV2-1 cells were isolated using an *in vivo* mouse model; therefore, the MDA-MB-231-IV2-1 cells exhibited higher metastatic ability than did the MDA-MB-231-P cells (Chan et al., 2014). After the microarray profiling process, several protein-coding genes with differential expression were identified between the MDA-MB-231-P and MDA-MB-231-IV2-1 cells (2926 upregulated genes and 2989 downregulated genes; fold change > 2 and < 0.5 , $p < 0.01$; **Supplementary Figures 1A,B**). These raw microarray data were uploaded to the NCBI GEO database and are freely available (accession number: GSE175513). Through pathway enrichment analysis, we observed that these differentially expressed genes were significantly involved in cell migration and motility signaling pathways (**Supplementary Figure 1C**). We also identified several differentially expressed lncRNA candidates between the MDA-MB-231-P and IV2-1 cells (213 upregulated lncRNAs and 301 downregulated lncRNAs; fold change: > 2 and < 0.5 , respectively, $p < 0.01$; **Figure 1A**). We further examined the expression levels of these lncRNA candidates (514 differentially expressed lncRNAs) in breast cancer cells by using TCGA database. A total of 52 lncRNA candidates had significant differential expression

in breast cancer cells when compared with adjacent normal cells (**Figure 1B**). Among them, we first randomly selected 6 lncRNA candidates to confirm their expression levels by using real-time PCR with MDA-MB-231-P, MDA-MB-231-IV2-1, and MDA-MB-231-IV2-2 cells. Similar to the MDA-MB-231-IV2-1 cells, the MDA-MB-231-IV2-2 cells were derived from MDA-MB-231-P cells by using an *in vivo* mouse model (Chan et al., 2014). Our data revealed that the expression levels of LOC550643 and PVT1 were significantly upregulated in MDA-MB-231-IV2-1 and MDA-MB-231-IV2-2 cells (**Figure 2A**), whereas the expression levels of *LOC652276* were significantly increased in MDA-MB-231-IV2-1 cells but not in MDA-MB-231-IV2-2 cells when compared with MDA-MB-231-P cells. In addition, the expression levels of *PRL23AP53* and *GATS* were significantly lower in the MDA-MB-231-IV2-1 and MDA-MB-231-IV2-2 cells, but those of *FAM66D* were significantly lower only in MDA-MB-231-IV2-2 cells (**Figure 2B**).

Correlation of LOC550643 Expression With Poor Prognosis in Breast Cancer Patients

We next investigated the clinical impacts of the 52 metastasis-associated lncRNAs by analyzing TCGA data. Among them, a novel lncRNA, *LOC550643*, was correlated with a survival curve in patients with breast cancer (**Supplementary Figure 2**). As presented in **Figures 3A,B**, the expression levels of *LOC550643* were significantly upregulated in breast cancer tissue when compared with adjacent normal tissues. Moreover, high *LOC550643* expression levels were associated with pathological stages ($p = 0.009$) and weakly associated with pN stage ($p = 0.053$) (**Table 1**). The Kaplan–Meier analysis revealed that high *LOC550643* expression levels were significantly correlated with a poor OS curve (effect of *LOC550643* on OS: $p = 0.003$, **Table 2** and **Figure 3C**). A multivariate Cox regression model indicated a significant association between high *LOC550643* expression levels and poor OS (*LOC550643*: adjusted hazard ratio, 2.00; 95% CI, 1.24–3.23; $p = 0.004$; **Table 2**). Stratified by molecular subtypes, the Kaplan–Meier survival analysis indicated that when compared with non-TNBC patients, high *LOC550643* expression was significantly associated with poor OS in patients with TNBC (**Figures 3D,E**). Therefore, we surmised that *LOC550643* might participate in the cellular machinery responsible for regulating growth and metastasis of breast cancer.

Identification of the Full Length LOC550643 in Breast Cancer Cells

According to the University of Santa Cruz (UCSC) database, *LOC550643* comprises three exons (**Supplementary Figure 3A**). However, the real length of the *LOC550643* sequence is unclear; therefore, we identified their full lengths by performing 5' and 3' RACE. The RACE results revealed three *LOC550643* transcripts of varying lengths (V1: 718 bp; V2: 581 bp; and V3: 476 bp) (**Supplementary Figure 3B** and **Supplementary Table 4**). Details on the gene structures of the three *LOC550643* isoforms are presented in **Supplementary Figures 3C,D**.

TABLE 1 | The relationship between expression levels of *LOC550643* and clinicopathologic data of BC patients.

Variables	Expression level of <i>LOC550643</i> (n = 1073)		P-value
	Low expression	Highly expression	
	Number (%)	Number (%)	
AJCC pathological stage			
I	243 (89.0)	30 (11.0)	0.009 ^b
II	451 (81.3)	104 (18.7)	
III	191 (84.9)	34 (15.1)	
IV	14 (70.0)	6 (30.0)	
pT stage			
T1	308 (86.5)	48 (13.5)	0.267 ^b
T2	463 (82.5)	98 (17.5)	
T3	105 (83.3)	21 (16.7)	
T4	23 (76.7)	7 (23.3)	
pN stage (n = 1067)			
N0	494 (85.3)	85 (14.7)	0.053 ^a
N1	246 (79.4)	64 (20.6)	
N2	92 (85.2)	16 (14.8)	
N3	63 (90.0)	7 (10.0)	
pM stage			
M0	885 (84.0)	168 (16.0)	0.118 ^b
M1	14 (70.0)	6 (30.0)	

^ap-value is estimated by chi-square test.^bp-value is estimated by Fisher's test.**TABLE 2 |** Univariate and multivariate Cox's regression analysis of *LOC550643* and expression for overall survival of 1070 patients with breast cancer.

Characteristic	No. (%)	OS			
		CHR (95% CI)	P-value	AHR (95% CI)	P-value
<i>LOC550643</i>	(n=)				
Low	896 (83.7)	1.00		1.00	
High	174 (16.3)	2.15 (1.34–3.46)	0.003	2.00 (1.24–3.23)	0.004

Abbreviation: OS, overall survival; CHR, crude hazard ratio; AHR, adjusted hazard ratio.

AHR were adjusted for AJCC pathological stage (II, III, and IV VS. I).

Despite the aforementioned discovery, the detailed roles of *LOC550643* and its isoforms in breast cancer metastasis are unclear. We also examined *LOC550643* expression among breast cancer cell lines with different molecular subtypes and invasive capabilities (**Supplementary Figure 4A**). To address the function of *LOC550643* in breast cancer cells, we designed two siRNAs targeting *LOC550643* with sequences complementary to the second and third exons, respectively (**Supplementary Figure 4B**). After siRNA transfection, the knockdown efficiency of *LOC550643* in the MDA-MB-231-IV2-1 cells was confirmed using real-time PCR. The endogenous expression levels of *LOC550643* in scramble siRNA-transfected cells (N.C) were similar to that of in the mock control group (**Supplementary Figure 4C**). However, the *LOC550643* mRNA levels in the MDA-MB-231-IV2-1 cells markedly decreased after si-*LOC550643*#301 or si-*LOC550643*#543 transfection (**Supplementary Figure 4C**).

Suppression of Breast Cancer Cell Growth Through the Impairment of Cell Cycle Progression by *LOC550643* Knockdown

As shown above, high *LOC550643* expression was correlated with poor OS in breast cancer patients, particularly in those with TNBC (**Figure 3E**). Furthermore, we pooled two siRNAs (siRNA#301 and siRNA#543), which could reduce the overall concentration and prevent off-target effects for examining the biological function of *LOC550643* in TNBC cell lines. After transfection with the pooled siRNAs, *LOC550643* expression levels were obviously reduced in MDA-MB-231-IV2-1, BT549, and Hs578T cells (**Figures 4A–C**). Our data indicated that *LOC550643* knockdown significantly suppressed colony formation capability in the three breast cancer cell lines (**Figures 4D–I**). Furthermore, *LOC550643* knockdown

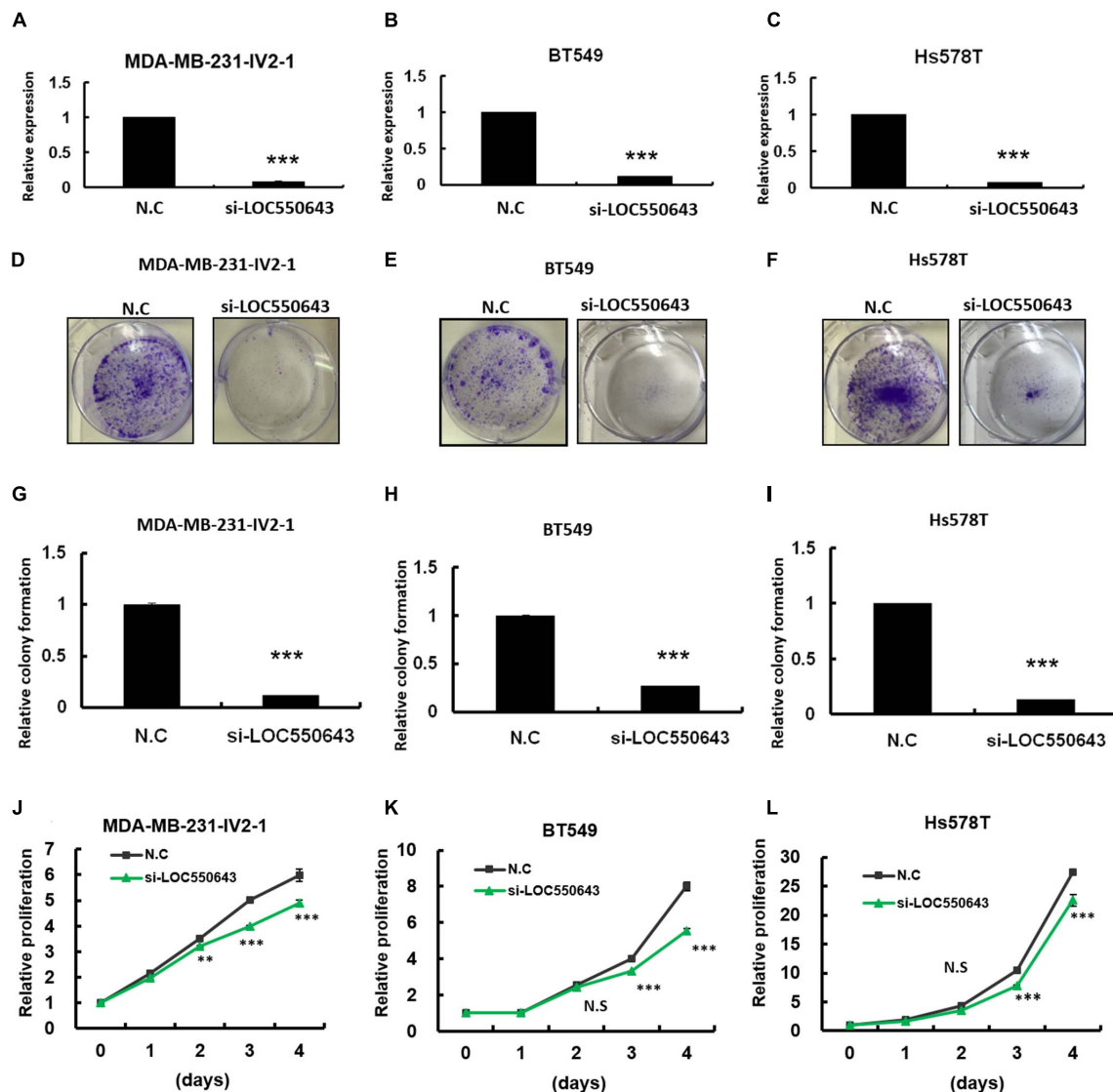


FIGURE 4 | Examination of *LOC550643* cellular function in breast cancer cell lines. The siRNAs (N.C, si-*LOC550643*-pool) were individually transfected into breast cancer cells (MDA-MB-231-IV2-1, BT549, and Hs578T) followed by cellular function examination. **(A–C)** Relative expression of *LOC550643* in three breast cancer cell lines after siRNA transfection (real-time PCR). **(D–F)** Colony formation assay performed for MDA-MB-231-IV2-1, BT549, and Hs578T cells after transfection with si-*LOC550643* or a scramble control. The cells were fixed and stained with crystal violet solution. **(G–I)** Relative colony formation ability quantified using a 595-nm optical density. **(J–L)** Cell proliferation measured using the CellTiter-Glo assay at various time points following *LOC550643* knockdown (0, 1, 3, and 4 days) as compared with the scramble control. All experiments were carried out in triplicate. Using Student's *t*-test to analyze our data and $p < 0.05$ was considered significant (* $p < 0.05$, ** $p < 0.01$, and *** $p < 0.001$).

also slightly inhibited the proliferation of breast cancer cells (Figures 4J–L). These results implied that *LOC550643* might be involved in breast cancer cell growth. To more thoroughly understand the detail mechanism of the involvement of *LOC550643* in breast cancer cell growth, we investigated the effects of *LOC550643* on cell cycle by using an image flow cytometry assay. Our data revealed a significantly increase in the S phase (13% increase, $p < 0.001$) accompanied by a 17% decrease ($p < 0.001$) of MDA-MB-231-IV2-1 G1-phase cells upon *LOC550643* knockdown (Figures 5A,B). We further checked cell cycle progression over time following release from

a double thymidine block. As shown in Figure 5C, most control cells entered the G2/M phase from the late G1/early S phase 8 h after release, whereas the *LOC550643* knockdown cells were blocked in the S phase and delayed entry into the G2/M phase. We also examined the cell cycle-related genes and observed that *LOC550643* knockdown resulted in lower Cyclin B1, Cyclin A2, and CDK2 protein levels in MDA-MB-231-IV2-1 cells and increased P21 and P27 protein levels in MDA-MB-231-IV2-1 cells (Figures 5D,E). These data indicate that *LOC550643* knockdown could suppress cell growth by promoting cell cycle S phase arrest.

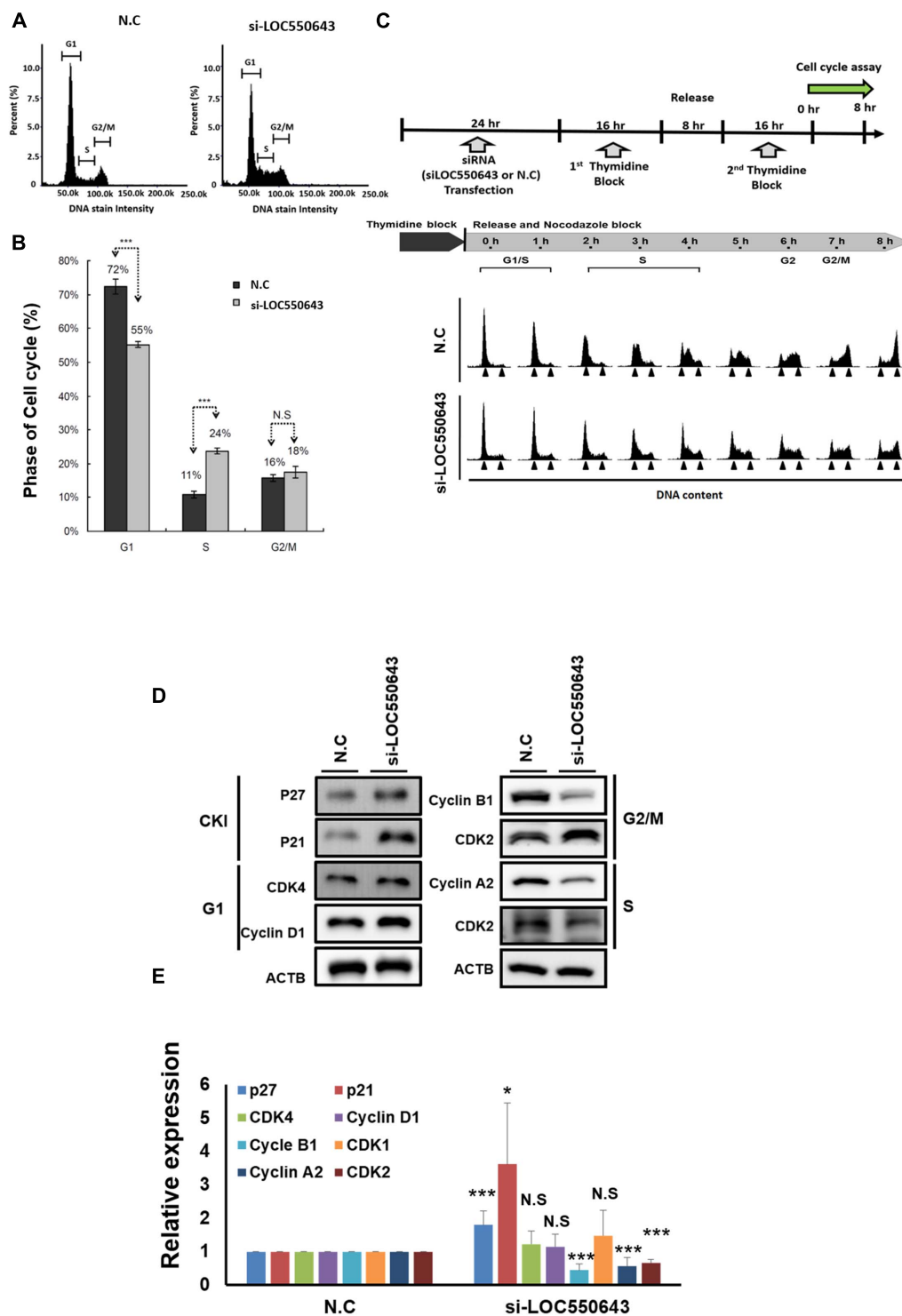
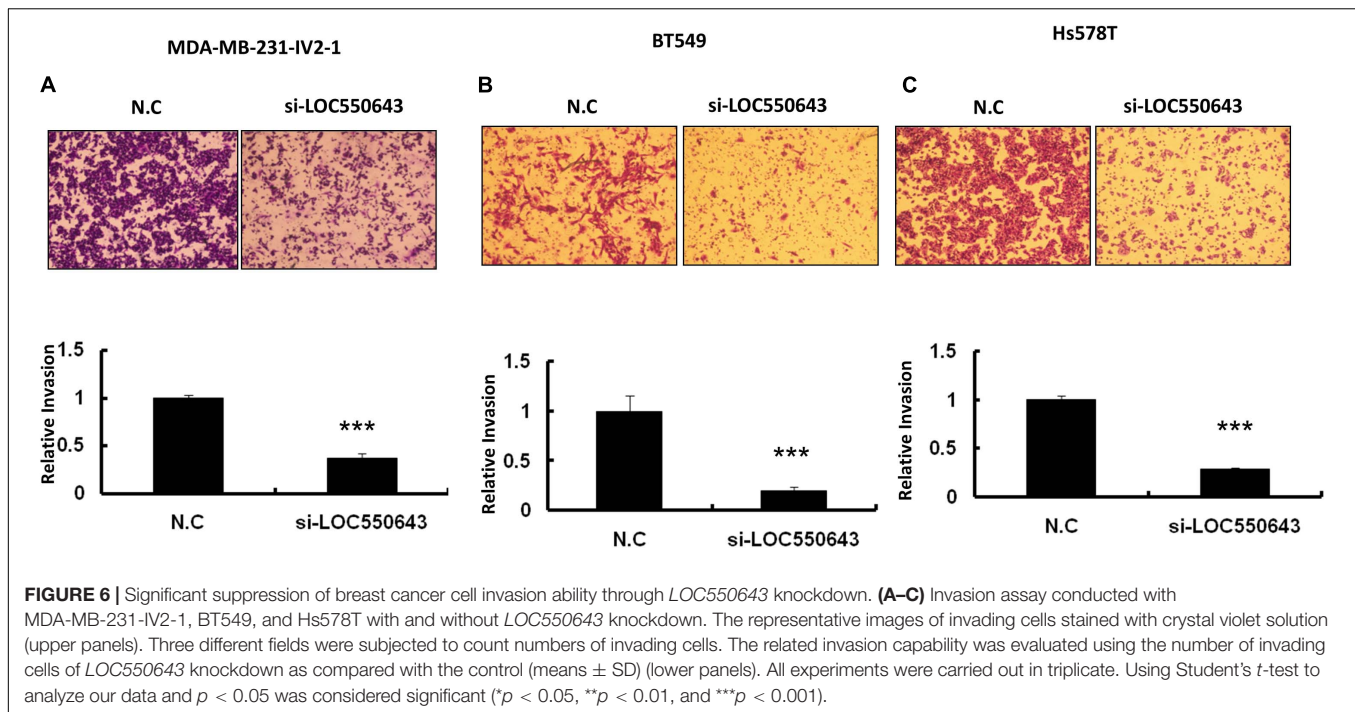


FIGURE 5 | Suppression of breast cancer cell growth through the induction of cell cycle arrest at the S phase following *LOC550643* depletion. **(A)** Cell cycle of MDA-MB-231-IV2-1 cells after 48 h of *LOC550643* knockdown. **(B)** Experiments were performed in triplicate and data were quantified and analyzed using Student's *t*-test. **(C)** Cell cycle of MDA-MB-231-IV2-1 cells synchronized using a double thymidine block and released into nocodazole medium for the indicated times. At each time point, the cells were subjected to cell cycle analysis. **(D)** Expression levels of cell cycle-related genes examined using Western blotting assays following 48 h of siRNA transfection. **(E)** Western blotting assays were done in triplicate, then all experiment data were further quantified. Using Student's *t*-test to analyze our data and $p < 0.05$ was considered significant (* $p < 0.05$, ** $p < 0.01$, and *** $p < 0.001$).



Suppression of Breast Cancer Cell Lung Metastasis Potential Through *LOC550643* Depletion

Furthermore, *LOC550643* knockdown also suppressed breast cancer cell invasion ability in three TNBC cell lines, namely MDA-MB-231-IV2-1 (Figure 6A), BT549 (Figure 6B), and Hs578T (Figure 6C). To validate our *in vitro* findings, we employed a mouse model to determine whether *LOC550643* would affect the lung metastasis potential of the MDA-MB-231-IV2-1 cells. One million *LOC550643*-depleted MDA-MB-231-IV2-1 cells labeled with luciferase and the control MDA-MB-231-IV2-1 cells labeled with luciferase were, separately, intravenously injected into SCID mice. Three weeks after injection, the mice were sacrificed, and lung metastasis were examined using IVIS imaging. The lungs of mice injected with *LOC550643*-depleted MDA-MB-231-IV2-1 cells displayed reduced luminescence signals when compared with the control group (Figures 7A,B). After IVIS imaging, the mouse lungs were fixed with 3.5% formaldehyde and embedded with paraffin to form tissue blocks. H&E staining of lung sections confirmed that the *LOC550643*-depleted MDA-MB-231-IV2-1 cells formed smaller metastases than did the control cells (Figures 7C,D). Taken together, the results revealed that *LOC550643* knockdown could suppress breast cancer cell metastasis.

Direct Interaction of *LOC550643* With miR-125b-2-3p to Suppress Breast Cancer Cell Growth and Motility

To further explore the mechanism of how *LOC550643* modulates breast cancer cell growth and motility, we performed miRNA transcriptome analysis using breast cancer cells with and without

LOC550643 knockdown. The transcriptome data analysis revealed 181 downregulated and 104 upregulated miRNAs in MDA-MB-231-IV2-1 cells upon *LOC550643* knockdown (Figure 8A). In addition, target prediction tools identified 189 miRNAs directly bound to *LOC550643* sequences (Figure 8A). Relevant studies have revealed that the target-directed miRNA degradation mechanism (TDMD) could modulate miRNA stability by binding target genes. Furthermore, the transcripts of target genes with highly complementary miRNA-binding sites could induce miRNA degradation (Bitetti et al., 2018; Ghini et al., 2018). In accordance with TDMD theory, we suggest that *LOC550643* knockdown could increase abundance of target miRNA candidates by reducing *LOC550643*–miRNA interactions in MDA-MB-231-IV2-1 cells. We identified 5 miRNAs, namely miR-29b-5p, miR-34b-3p, miR-125b-2-3p, miR-629-3p, and miR-6515-5p, that could be sponged by *LOC550643*. We further analyzed the expression levels of miR-29b-5p, miR-34b-3p, miR-125b-2-3p, and miR-629-3p in breast cancer cells and observed that only miR-125b-2-3p was significantly lower in breast cancer tissues compared with the normal tissues (Supplementary Figure 5). Moreover, miR-125b-2-3p expression was greatly decreased in breast cancer cells upon *LOC550643* overexpression, whereas miR-125b-2-3p expression levels were significantly higher in *LOC550643*-depleted breast cancer cells (Figures 8B,C). Therefore, we examined whether miR-125b-2-3p would directly interact with *LOC550643*. To do so, the full length *LOC550643* was cloned immediately downstream of the luciferase reporter, and the luciferase activity was measured in the presence of miR-125b-2-3p or a scramble sequence. As presented in Figure 8E, luciferase reporter assay revealed that the luciferase activity levels of 293T cells cotransfected with miR-125b-2-3p mimics and the luciferase reporter plasmid were

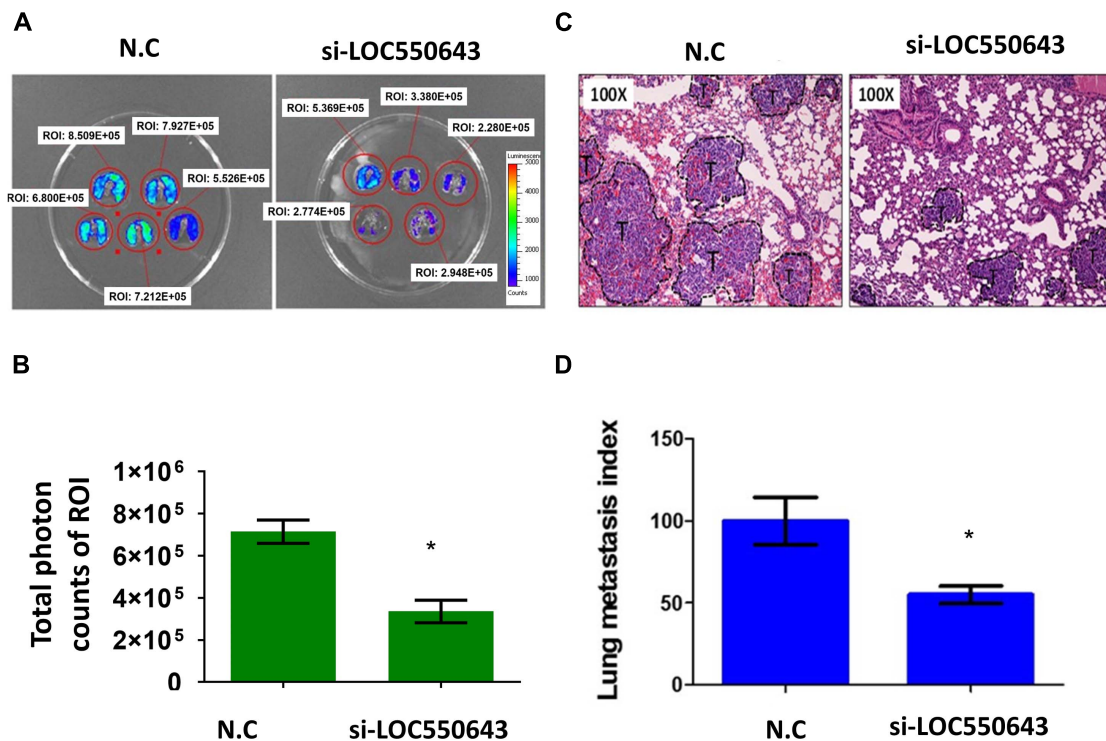


FIGURE 7 | Suppression of the lung metastasis potential of MDA-MB-231-IV2-1 cells through *LOC550643* depletion. **(A)** Lung metastatic ability of si-*LOC550643* and N.C control MDA-MB-231-IV2-1 cells examined using the SCID mice model through intravenous injection. Ten SCID mice were used (five as controls and five with *LOC550643* knockdown). Three weeks after injection, lung metastasis status was assessed using IVIS. **(B)** ROI intensity calculated and analyzed using Student's *t*-test. **(C)** Metastatic lungs examined using H&E staining. **(D)** Lung metastasis index assessed using Student's *t*-test. **p* < 0.05.

significantly lower than those of cells cotransfected with the control miRNA mimics. The miR-125b-2-3p mimics had no inhibitory effect on the luciferase activity of the reporter plasmid containing *LOC550643* with mutated miR-125b-2-3p binding sites (Figure 8F). On the basis of these findings, we concluded that *LOC550643* is a miRNA sponge for miR-125b-2-3p in breast cancer cells. Next, we examined the role of miR-125b-2-3p in breast cancer cells and observed that miR-125b-2-3p expression significantly suppressed cell proliferation, colony formation, and invasion ability (Figures 9A–D). Low miR-125b-2-3p expression is associated with poor survival in patients with breast cancer (Supplementary Figure 6A). Because *LOC550643* exerts its oncogenic function through miR-125b-2-3p sponging, we explored the impact of *LOC550643*–miR-125b-2-3p axis activity in breast cancer cells. Patients were classified into three groups according to *LOC550643* and miR-125b-2-3p expression. The first group comprised patients with low *LOC550643* and high miR-125b-2-3p expression, the second group comprised patients with both high or both low *LOC550643* and miR-125b-2-3p expression, and the third group comprised patients with high *LOC550643* and low miR-125b-2-3p expression. As presented in Supplementary Figure 6B, breast cancer patients with high *LOC550643* and low miR-125b-2-3p expression had the poorest survival rate among the three groups. Therefore, we conclude that *LOC550643* promotes breast cancer cell growth and metastasis through miR-125b-2-3p sponging.

DISCUSSION

lncRNA is no longer considered “transcription noise,” and its abnormal expression was revealed to be meaningful to the onset and development of human malignancies (Schmitt and Chang, 2016). Thus, lncRNA has become one of the major topic in cancer research. A number of studies have recently indicated that numerous lncRNAs are associated with breast cancer progression, including *GAS5* (Mourtada-Maarabouni et al., 2009; Zheng et al., 2020), *H19* (Adriaenssens et al., 1998), *HOTAIR* (Rinn et al., 2007), *MALAT1* (Loi et al., 2007), *NEAT1* (Silva et al., 2011), *UCA1* (Wang et al., 2008), *XIST* (Benoît et al., 2007), and *BCAR4* (Peng et al., 2021). In our study, we performed transcriptome analysis of MDA-MB-231-P and MDA-MB-231-IV2-1 cells and identified several metastasis-associated lncRNAs in breast cancer cells. Herein, we report a novel functional lncRNA, *LOC550643*, which is highly expressed in patients with breast cancer. In addition, high *LOC550643* expression levels are significantly correlated with poor survival in breast cancer patients. *LOC550643* is located on chromosome X (p11.21), and three alternative isoforms can be generated in breast cancer cells. Relevant studies have indicated that a known lncRNA termed *XIST* (X inactive specific transcript), which is located in the X inactivation center, and its product are transcribed from the inactive X chromosome (Yang et al., 2017). *XIST* is one of the first known examples of lncRNA with a prominent role in regulating X

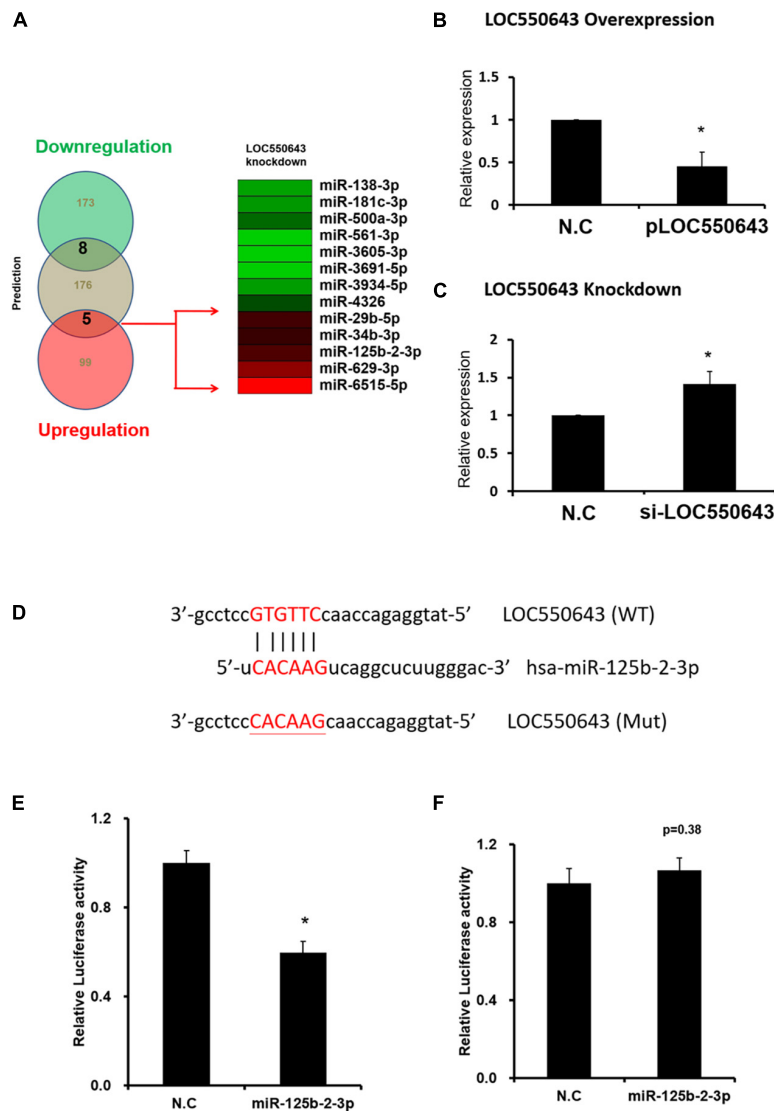


FIGURE 8 | Regulation of miR-125b-2-3p expression through direct interaction with *LOC550643*. **(A)** Identification of *LOC550643*-sponged miRNA candidates through TargetScan and small RNA profiles. **(B)** Expression levels of miR-125b-2-3p examined in MDA-MB-231-P cells with ectopic *LOC550643* expression (real-time PCR). **(C)** Expression levels of miR-125b-2-3p assessed in MDA-MB-231-IV2-1 cells with si-*LOC550643* transfection by real-time PCR. **(D)** Schema of luciferase constructs. The miR-125b-2-3p targeting sequence in the *LOC550643* sequence is represented in the upper panel, and the mutated sequence of its binding region is in red. **(E,F)** Relative luciferase activity of pMIR-*LOC550643*-wt and pMIR-*LOC550643*-mut identified in breast cancer cells transfected with miR-125b-2-3p mimics and scramble control. All experiments were carried out in triplicate. Using Student's *t*-test to analyze our data and $p < 0.05$ was considered significant (* $p < 0.05$, ** $p < 0.01$, and *** $p < 0.001$).

chromosome inactivation. In mammals, the majority of genes are silenced in one of the X-chromosomes in each cell, accounting for a similar level of gene expression between the sexes (Dey et al., 2014). *XIST* is typically expressed by all female somatic cells but not in female breast, ovarian, or cervical cancer cell lines (Kawakami et al., 2004; Benoît et al., 2007). *XIST* also plays a crucial role in ovarian cancer (Ren et al., 2015), non-small cell lung cancer (Tantai et al., 2015), and glioblastoma (Yao et al., 2015).

Zhu et al. (2015) first discovered *LOC550643* as a novel non-coding RNA mapped to Xp11.21. They observed that *LOC550643*

was a susceptibility locus for systemic lupus erythematosus (SLE) and that it played a critical role in X-linked genetic variants in the pathogenesis of SLE in Han Chinese populations (Zhu et al., 2015). In order to avoid abnormal overexpression of X-linked genes, epigenetic modification participates to X chromosome inactivation in female cells (Brooks and Renaudineau, 2015). Zhu et al. (2015) hypothesized that *LOC550643* may maintain the X inactivation that prevents X-linked gene overexpression through dosage compensation in women. However additional studies are needed to determine how this locus influences the etiology of SLE (Zhu et al., 2015). Yang et al. (2017) discovered that

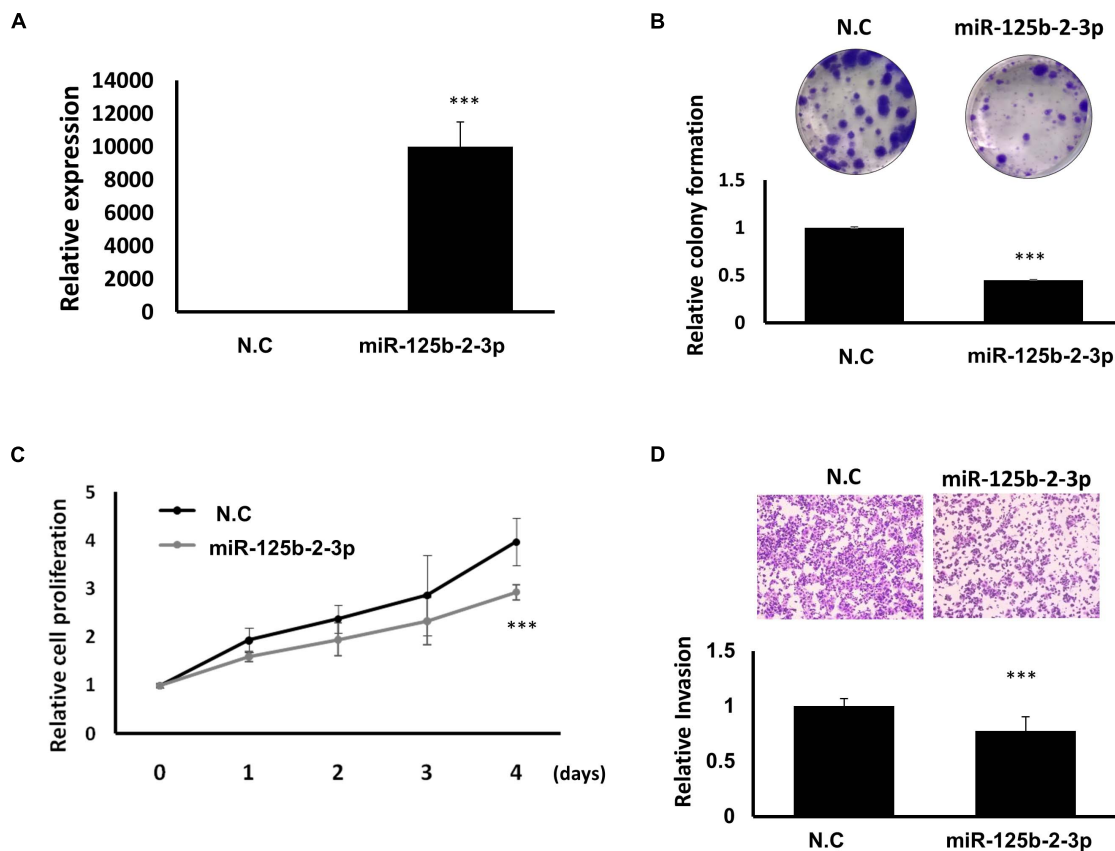


FIGURE 9 | Suppression of breast cancer cell growth and motility through miR-125b-2-3p expression. **(A)** Expression levels of miR-125b-2-3p examined in MDA-MB-231-IV2-1 cells after miR-125b-2-3p mimics transfection (real-time PCR). **(B)** Colony formation ability examined and quantified in MDA-MB-231-IV2-1 cells with or without miR-125b-2-3p overexpression. **(C)** Cell proliferation of MDA-MB-231-IV2-1 cells assessed after miR-125b-2-3p transfection for various time periods. **(D)** Invasion capability assessed using the transwell assay in MDA-MB-231-IV2-1 cells transfected with miR-125b-2-3p and the scramble control. The cell images of a representative experiment are displayed. The values quantified using Ascent are in the graph. Data are reported as the numbers of invading cells relative to the controls (means \pm SD). All experiments were carried out in triplicate. Using Student's *t*-test to analyze our data and $p < 0.05$ was considered significant (* $p < 0.05$, ** $p < 0.01$, and *** $p < 0.001$).

LOC550643 was highly expressed in nasopharyngeal carcinoma (NPC) and greatly associated with distant metastasis in patients with NPC. The researchers also observed that male patients with NPC had a higher tendency to express *LOC550643* than did female patients with NPC. Yang et al. (2017) suggested that high expression levels of *LOC550643* may act as a crucial role in NPC progression and its expression levels may use as a potential prognostic biomarker in NPC patients. Zhai et al. (2020) reported that high *LOC550643* expression contributed to pancreatic cancer progression by enhancing *KRAS* expression. Furthermore, *LOC550643* knockdown could suppress pancreatic cancer cell growth and invasion capability through releasing miR-494-3p sponging. Relevant studies have also investigated the role of *LOC550643* in thyroid cancer, revealing significantly higher levels of *LOC550643* expression in thyroid cancer cells and that *LOC550643* knockdown inhibited cancer cell growth by impairing cell cycle progression (Luo et al., 2020). By contrast, Konina et al. (2019) reported an opposite role, in which *LOC550643* inhibited melanoma cell

migration ability but did not influence cell growth. An increasing number of studies have revealed that *LOC550643* is frequently overexpressed in human cancer cells and plays an oncogenic role in modulating cancer growth and metastasis. However, *LOC550643* expression might also suppress tumors in different cancer types, such as melanoma.

Our data indicate that *LOC550643* knockdown could suppress breast cancer cell proliferation by inducing cell cycle arrest in the S phase. The S phase (synthesis phase) is the part of the cell cycle in which DNA is replicated. The central machines that promote cell cycle progression are cyclin-dependent kinases (CDKs). Cyclin-binding enables inactive CDKs to become active (Barnum and O'Connell, 2014). Two types of cyclin are crucial for mitosis in animal cells: cyclin A, which is known mainly for its role in the S phase, in which it has been implicated in DNA replication, and cyclin B (De Boer et al., 2008; Gavet and Pines, 2010). In eukaryotes, cyclin B/CDK1 is essential for both entry and progression through mitosis (Gavet and Pines, 2010). Cyclin A/CDK2 expression is elevated at the onset of the

S phase, and further activation occurs early in the G2 phase to regulate G2 phase progression (De Boer et al., 2008). CDK2 is considered a key CDK in the control of DNA replication in the S phase, even though CDK1 can compensate if CDK2 is disabled (Santamaría et al., 2007). Our data indicate that *LOC550643* knockdown resulted in lower cyclin B1, cyclin A2, and CDK2 protein levels in MDA-MB-231-IV2-1 cells and inhibited cell growth via promoting cell cycle arrest at the S phase. In addition, the current study indicated that *LOC550643* can sponge miR-125b-2-3p through direct interaction in breast cancer cells. Through a bioinformatics analysis, Shi et al. (2018) suggested that cyclin A2 is a potential target of miR-125b-2-3p. However, few studies have reported that miR-125b-2-3p contributes to cancer progression. Murray et al. (2014) revealed that serum levels of miR-125a-3p and miR-125b-2-3p increased before chemotherapy and subsequently decreased early following treatment in patients with pleuropulmonary blastoma (PPB). According to these results, miR-125b-2-3p may be useful as a serum biomarker for the early detection of PPB in patients with known germline *DICER1* mutations and for potential disease monitoring in patients with PPB (Murray et al., 2014). In addition, Lu et al. (2018) reported that miR-125b-2-3p sensitized colorectal cancer (CRC) to first-line chemotherapeutic therapy. Furthermore, the two-miRNA-based signatures (miR-125b-2-3p and miR-933) were a good prognostic and predictive biomarkers for tumor progression in advanced CRC, and they could be useful for providing standard first-line chemotherapy to patients with CRC (Lu et al., 2018). Meng et al. (2020) reported that high miR-125b-2-3p expression was correlated with metastasis and poor survival in patients with clear cell renal cell carcinoma. However, the biological function of miR-125b-2-3p in human cancer cells remains unknown. We identified that miR-125b-2-3p can suppress cell proliferation, colony formation, migration, and invasion capability in human breast cancer cells.

In summary, we identified a novel lncRNA, *LOC550643*, which acts as an oncogene in promoting breast cancer cell growth and metastasis. We also revealed that *LOC550643* expression can serve as a useful molecular biomarker for cancer diagnosis and as a potential therapeutic target for patients with breast cancer.

DATA AVAILABILITY STATEMENT

The original contributions presented in the study are publicly available. This data can be found here: <https://www.ncbi.nlm.nih.gov/geo/>, accession numbers: GSE175513 and GSE175514.

ETHICS STATEMENT

The studies involving human participants were reviewed and approved by the Institutional Review Board of the Taipei Tzu Chi Hospital. Written informed consent for participation was not required for this study in accordance with the national legislation and the institutional requirements. The animal study was reviewed and approved by Animal Center and the Use Committee of Kaohsiung Veterans General Hospital (No. VGHKS-2017-2020-A042).

AUTHOR CONTRIBUTIONS

K-WT, Y-JC, and S-HC executed this study and drafted the manuscript. Y-TT and M-CL performed the biological function assay for the gastric cancer cells. Y-JC, K-HC, and Y-RC assisted in collecting clinical samples and analysis. K-WT, Y-JC, and L-HW supervised the study and edited the manuscript.

FUNDING

This study was supported by grants from the Ministry of Science and Technology (MOST 106-2320-B-075B-004, MOST 107-2320-B-003-MY2, and MOST 109-2320-B-039-062-MY2), Taipei Tzu Chi Hospital, Buddhist Tzu Chi Medical Foundation (TCRD-TPE-109-66 and TCRD-TPE-MOST-108-17), and China Medical University intramural grant (CMU110-Z-06).

ACKNOWLEDGMENTS

The authors thank the Core Laboratory, Department of Research, Taipei Tzu Chi Hospital, Buddhist Tzu Chi Medical Foundation, for technical and core facility support. This manuscript was edited by Wallace Academic Editing.

SUPPLEMENTARY MATERIAL

The Supplementary Material for this article can be found online at: <https://www.frontiersin.org/articles/10.3389/fcell.2021.695632/full#supplementary-material>

Supplementary Figure 1 | Comparison of MDA-MB-231-P and MDA-MB-231-IV2-1 transcriptome profiles. **(A)** Results of differentially expressed protein-coding genes with twofold change (2926 upregulated and 2989 downregulated) in MDA-MB-231-IV2-1 cells compared with MDA-MB-231-P cells. **(B)** Scatter plot of total gene expressions in MDA-MB-231-P versus MDA-MB-231-IV2-1. **(C)** Gene ontology analysis of the twofold change in the protein-coding gene list revealing a significant enrichment in cell motility-related function.

Supplementary Figure 2 | Kaplan–Meier analysis of the 52 metastasis-associated lncRNAs from TCGA data. Upper panel indicates the hazard ratio, and the lower panel is the $\log^{(p\text{ value})}$. The $\log^{(p\text{ value})}$ of <-1.3 is significant and marked in red ($p < 0.05$).

Supplementary Figure 3 | Identification of the *LOC550643* gene structure in breast cancer cells by using RACE. **(A)** Genomic location of the *LOC550643* in the UCSC human genome database (upper panels). EST transcripts are in the lower panel. **(B)** Identification of the full length of *LOC550643* through 3' and 5' RACE. **(C)** Three transcripts of alternative splicing variants. **(D)** Three *LOC550643* isoforms aligned using a multiple alignment tool (<http://www.ebi.ac.uk/Tools/msa/clustalo/>).

Supplementary Figure 4 | Expression levels and knockdown efficiency of *LOC550643* assessed in human breast cancer cells. **(A)** Expression levels of *LOC550643* assessed in human breast cancer cell lines by real-time PCR. **(B)** Schema of interaction sites of the two siRNA (si-*LOC550643*#301 and si-*LOC550643*#543) sequences designed for *LOC550643* knockdown. **(C)** After 48 h of individual siRNA of transfection (si-*LOC550643*#301, si-*LOC550643*#543, and N.C control) into MDA-MB-231-IV2-1 cells, *LOC550643* expression levels

were examined using real-time PCR. Mock indicated a non-transfection control. The efficiency of si-LOC550643#301, si-LOC550643#543 LOC550643 knockdown and mock was evaluated through comparisons with the control group.

Supplementary Figure 5 | Expression levels of miRNA candidates assessed in human breast cancer cells from TCGA database. The expression levels of **(A)** miR-29b-5p, **(B)** miR-34b-3p, **(C)** miR-125b-2-3p, and **(D)** miR-629-3p were

assessed in breast cancer tissue samples ($n = 778$) compared with adjacent normal tissue samples ($n = 87$; TCGA database).

Supplementary Figure 6 | (A) Impacts of miR-125b-2-3p expression on the OS of patients with breast cancer. **(B)** Combination of LOC550643 and miR-125b-2-3p expression levels was correlated with the survival curve of patients with breast cancer.

REFERENCES

- Adriaenssens, E., Dumont, L., Lottin, S., Bolle, D., Leprêtre, A., Delobelle, A., et al. (1998). H19 overexpression in breast adenocarcinoma stromal cells is associated with tumor values and steroid receptor status but independent of p53 and Ki-67 expression. *Am. J. Pathol.* 153, 1597–1607. doi: 10.1016/s0002-9440(10)65748-3
- Barnum, K. J., and O'Connell, M. J. (2014). Cell cycle regulation by checkpoints. *Cell Cycle Control Mech. Protoc.* 1170, 29–40. doi: 10.1007/978-1-4939-0888-2_2
- Benoit, M.-H., Hudson, T. J., Maire, G., Squire, J. A., Arcand, S. L., Provencher, D., et al. (2007). Global analysis of chromosome X gene expression in primary cultures of normal ovarian surface epithelial cells and epithelial ovarian cancer cell lines. *Int. J. Oncol.* 30, 5–18.
- Bertucci, F., Finetti, P., and Birnbaum, D. (2012). Basal breast cancer: a complex and deadly molecular subtype. *Curr. Mol. Med.* 12, 96–110. doi: 10.2174/156652412798376134
- Bitetti, A., Mallory, A. C., Golini, E., Carrieri, C., Carreno Gutierrez, H., Perlas, E., et al. (2018). MicroRNA degradation by a conserved target RNA regulates animal behavior. *Nat. Struct. Mol. Biol.* 25, 244–251. doi: 10.1038/s41594-018-0032-x
- Bray, F., Ferlay, J., Soerjomataram, I., Siegel, R. L., Torre, L. A., and Jemal, A. (2018). Global cancer statistics 2018: GLOBOCAN estimates of incidence and mortality worldwide for 36 cancers in 185 countries. *CA Cancer J. Clin.* 68, 394–424. doi: 10.3322/caac.21492
- Brooks, W. H., and Renaudineau, Y. (2015). Epigenetics and autoimmune diseases: the X chromosome-nucleolus nexus. *Front. Genet.* 6:22. doi: 10.3389/fgene.2015.00022
- Chan, J. J., and Tay, Y. (2018). Noncoding RNA:RNA regulatory networks in cancer. *Int. J. Mol. Sci.* 19:1310.
- Chan, S. H., Huang, W. C., Chang, J. W., Chang, K. J., Kuo, W. H., Wang, M. Y., et al. (2014). MicroRNA-149 targets GIT1 to suppress integrin signaling and breast cancer metastasis. *Oncogene* 33, 4496–4507. doi: 10.1038/onc.2014.10
- Chen, G., and Deng, X. (2018). Cell synchronization by double thymidine block. *Bio. Protoc.* 8:e2994.
- De Boer, L., Oakes, V., Beamish, H., Giles, N., Stevens, F., Somodevilla-Torres, M., et al. (2008). Cyclin A/cdk2 coordinates centrosomal and nuclear mitotic events. *Oncogene* 27, 4261–4268. doi: 10.1038/onc.2008.74
- Derrien, T., Guigo, R., and Johnson, R. (2011). The long non-coding RNAs: a new (P)layer in the “Dark Matter”. *Front. Genet.* 2:107. doi: 10.3389/fgene.2011.00107
- Dey, B. K., Mueller, A. C., and Dutta, A. (2014). Long non-coding RNAs as emerging regulators of differentiation, development, and disease. *Transcription* 5:e944014. doi: 10.4161/21541272.2014.944014
- Gavet, O., and Pines, J. (2010). Progressive activation of CyclinB1-Cdk1 coordinates entry to mitosis. *Developmental cell* 18, 533–543. doi: 10.1016/j.devcel.2010.02.013
- Ghini, F., Rubolino, C., Climent, M., Simeone, I., Marzi, M. J., and Nicassio, F. (2018). Endogenous transcripts control miRNA levels and activity in mammalian cells by target-directed miRNA degradation. *Nat. Commun.* 9:3119.
- Kawakami, T., Zhang, C., Taniguchi, T., Kim, C. J., Okada, Y., Sugihara, H., et al. (2004). Characterization of loss-of-inactive X in Klinefelter syndrome and female-derived cancer cells. *Oncogene* 23, 6163–6169. doi: 10.1038/sj.onc.1207808
- Konina, D. O., Filatova, A. Y., and Skoblov, M. Y. (2019). LINC01420 RNA structure and influence on cell physiology. *BMC Genomics* 20:298.
- Kumar, M. M., and Goyal, R. (2017). LncRNA as a therapeutic target for angiogenesis. *Curr. Top. Med. Chem.* 17, 1750–1757. doi: 10.2174/1568026617666161116144744
- Liu, W. S., Chan, S. H., Chang, H. T., Li, G. C., Tu, Y. T., Tseng, H. H., et al. (2018). Isocitrate dehydrogenase 1-snail axis dysfunction significantly correlates with breast cancer prognosis and regulates cell invasion ability. *Breast Cancer Res.* 20:25.
- Loi, S., Haibe-Kains, B., Desmedt, C., Lallemand, F., Tutt, A. M., Gillet, C., et al. (2007). Definition of clinically distinct molecular subtypes in estrogen receptor-positive breast carcinomas through genomic grade. *J. Clin. Oncol.* 25, 1239–1246. doi: 10.1200/jco.2006.07.1522
- Lu, J. H., Zuo, Z. X., Wang, W., Zhao, Q., Qiu, M. Z., Luo, H. Y., et al. (2018). A two-microRNA-based signature predicts first-line chemotherapy outcomes in advanced colorectal cancer patients. *Cell Death Discov.* 4:116.
- Luo, J. Z., Qin, L., and Zhang, L. J. (2020). Expression and function of long non-coding RNA LINC01420 in thyroid cancer. *Oncol. Lett.* 19, 399–405.
- Meng, X., Liu, K., Xiang, Z., Yu, X., Wang, P., and Ma, Q. (2020). MiR-125b-2-3p associates with prognosis of ccRCC through promoting tumor metastasis via targeting EGR1. *Am. J. Transl. Res.* 12, 5575–5585.
- Mourtada-Maarabouni, M., Pickard, M., Hedge, V., Farzaneh, F., and Williams, G. (2009). GAS5, a non-protein-coding RNA, controls apoptosis and is downregulated in breast cancer. *Oncogene* 28, 195–208. doi: 10.1038/onc.2008.373
- Murray, M. J., Bailey, S., Raby, K. L., Saini, H. K., De Kock, L., Burke, G. A., et al. (2014). Serum levels of mature microRNAs in DICER1-mutated pleuropulmonary blastoma. *Oncogenesis* 3:e87. doi: 10.1038/oncsis.2014.1
- Pan, C. T., Tsai, K. W., Hung, T. M., Lin, W. C., Pan, C. Y., Yu, H. R., et al. (2014). miRSeq: a user-friendly standalone toolkit for sequencing quality evaluation and miRNA profiling. *Biomed. Res. Int.* 2014:462135.
- Peng, R., Cao, J., Guo, Q., Sun, Q., Xu, L., Xie, X., et al. (2021). Variant in BCAR4 gene correlated with the breast cancer susceptibility and mRNA expression of lncRNA BCAR4 in Chinese Han population. *Breast Cancer* 28, 424–433. doi: 10.1007/s12282-020-01174-0
- Ren, C., Li, X., Wang, T., Wang, G., Zhao, C., Liang, T., et al. (2015). Functions and mechanisms of long noncoding RNAs in ovarian cancer. *Int. J. Gynecol. Cancer* 25, 566–569.
- Rinn, J. L., Kertesz, M., Wang, J. K., Squazzo, S. L., Xu, X., Bruggmann, S. A., et al. (2007). Functional demarcation of active and silent chromatin domains in human HOX loci by noncoding RNAs. *Cell* 129, 1311–1323. doi: 10.1016/j.cell.2007.05.022
- Santamaria, D., Barrière, C., Cerqueira, A., Hunt, S., Tardy, C., Newton, K., et al. (2007). Cdk1 is sufficient to drive the mammalian cell cycle. *Nature* 448, 811–815. doi: 10.1038/nature06046
- Schmitt, A. M., and Chang, H. Y. (2016). Long noncoding RNAs in cancer pathways. *Cancer Cell* 29, 452–463. doi: 10.1016/j.ccell.2016.03.010
- Serviss, J. T., Johnsson, P., and Grandner, D. (2014). An emerging role for long non-coding RNAs in cancer metastasis. *Front. Genet.* 5:234. doi: 10.3389/fgene.2014.00234
- Shi, J., Ye, G., Zhao, G., Wang, X., Ye, C., Thammaravong, K., et al. (2018). Coordinative control of G2/M phase of the cell cycle by non-coding RNAs in hepatocellular carcinoma. *PeerJ* 6:e5787. doi: 10.7717/peerj.5787
- Silva, J. M., Boczek, N. J., Berres, M. W., Ma, X., and Smith, D. I. (2011). LINC01420 is over expressed in breast and ovarian cancer and affects cellular proliferation. *RNA Biol.* 8, 496–505. doi: 10.4161/rna.8.3.14800
- Tantai, J., Hu, D., Yang, Y., and Geng, J. (2015). Combined identification of long non-coding RNA XIST and HIF1A-AS1 in serum as an effective screening for non-small cell lung cancer. *Int. J. Clin. Exp. Pathol.* 8:7887.

- Tsai, K. W., Lo, Y. H., Liu, H., Yeh, C. Y., Chen, Y. Z., Hsu, C. W., et al. (2018). Linc00659, a long noncoding RNA, acts as novel oncogene in regulating cancer cell growth in colorectal cancer. *Mol. Cancer* 17:72.
- Tseng, H. H., Tseng, Y. K., You, J. J., Kang, B. H., Wang, T. H., Yang, C. M., et al. (2017). Next-generation sequencing for microRNA profiling: MicroRNA-21-3p promotes oral cancer metastasis. *Anticancer Res.* 37, 1059–1066. doi: 10.21873/anticancer.11417
- Wang, F., Li, X., Xie, X., Zhao, L., and Chen, W. (2008). UCA1, a non-protein-coding RNA up-regulated in bladder carcinoma and embryo, influencing cell growth and promoting invasion. *FEBS Lett.* 582, 1919–1927. doi: 10.1016/j.febslet.2008.05.012
- Yang, L., Tang, Y., He, Y., Wang, Y., Lian, Y., Xiong, F., et al. (2017). High expression of LINC01420 indicates an unfavorable prognosis and modulates cell migration and invasion in nasopharyngeal carcinoma. *J. Cancer* 8:97. doi: 10.7150/jca.16819
- Yao, Y., Ma, J., Xue, Y., Wang, P., Li, Z., Liu, J., et al. (2015). Knockdown of long non-coding RNA XIST exerts tumor-suppressive functions in human glioblastoma stem cells by up-regulating miR-152. *Cancer Lett.* 359, 75–86. doi: 10.1016/j.canlet.2014.12.051
- Yeo, B., Turner, N. C., and Jones, A. (2014). An update on the medical management of breast cancer. *BMJ* 348:g3608. doi: 10.1136/bmj.g3608
- Yoon, J. H., Abdelmohsen, K., and Gorospe, M. (2014). Functional interactions among microRNAs and long noncoding RNAs. *Semin. Cell Dev. Biol.* 34, 9–14. doi: 10.1016/j.semcdb.2014.05.015
- Zhai, H., Zhang, X., Sun, X., Zhang, D., and Ma, S. (2020). Long non-coding RNA LINC01420 contributes to pancreatic cancer progression through targeting KRAS proto-oncogene. *Dig. Dis. Sci.* 65, 1042–1052. doi: 10.1007/s10620-019-05829-7
- Zhang, R., Zhu, Q., Yin, D., Yang, Z., Guo, J., Zhang, J., et al. (2020). Identification and validation of an autophagy-related lncRNA signature for patients with breast cancer. *Front. Oncol.* 10:597569. doi: 10.3389/fonc.2020.597569
- Zheng, S., Li, M., Miao, K., and Xu, H. (2020). lncRNA GAS5-promoted apoptosis in triple-negative breast cancer by targeting miR-378a-5p/SUFU signaling. *J. Cell Biochem.* 121, 2225–2235. doi: 10.1002/jcb.29445
- Zhu, Z., Liang, Z., Liany, H., Yang, C., Wen, L., Lin, Z., et al. (2015). Discovery of a novel genetic susceptibility locus on X chromosome for systemic lupus erythematosus. *Arthritis Res. Ther.* 17:349.

Conflict of Interest: The authors declare that the research was conducted in the absence of any commercial or financial relationships that could be construed as a potential conflict of interest.

Copyright © 2021 Tsai, Chong, Li, Tu, Chen, Lee, Chan, Wang and Chang. This is an open-access article distributed under the terms of the Creative Commons Attribution License (CC BY). The use, distribution or reproduction in other forums is permitted, provided the original author(s) and the copyright owner(s) are credited and that the original publication in this journal is cited, in accordance with accepted academic practice. No use, distribution or reproduction is permitted which does not comply with these terms.



N6-Methyladenosine Modification Opens a New Chapter in Circular RNA Biology

Jun Wu^{1,2†}, Xin Guo^{3†}, Yi Wen¹, Shangqing Huang^{1,2}, Xiaohui Yuan^{1,2}, Lijun Tang^{1,2*} and Hongyu Sun^{1,2,3*}

¹ Department of General Surgery and Pancreatic Injury and Repair Key Laboratory of Sichuan Province, The General Hospital of Western Theater Command, Chengdu, China, ² College of Medicine, Southwest Jiaotong University, Chengdu, China, ³ Laboratory of Basic Medicine, The General Hospital of Western Theater Command, Chengdu, China

OPEN ACCESS

Edited by:

Jing Zhang,
Shanghai Jiao Tong University, China

Reviewed by:

Xiao-Yu Chen,
Shanghai Sixth People's Hospital,
China
Peifeng Li,
Qingdao University, China

*Correspondence:

Lijun Tang
tanglj2016@163.com
Hongyu Sun
shongyu2008@163.com

[†] These authors have contributed
equally to this work

Specialty section:

This article was submitted to
Epigenomics and Epigenetics,
a section of the journal
Frontiers in Cell and Developmental
Biology

Received: 13 May 2021

Accepted: 06 July 2021

Published: 23 July 2021

Citation:

Wu J, Guo X, Wen Y, Huang S,
Yuan X, Tang L and Sun H (2021)
N6-Methyladenosine Modification
Opens a New Chapter in Circular
RNA Biology.
Front. Cell Dev. Biol. 9:709299.
doi: 10.3389/fcell.2021.709299

As the most abundant internal modification in eukaryotic cells, N6-methyladenosine (m6A) in mRNA has shown widespread regulatory roles in a variety of physiological processes and disease progressions. Circular RNAs (circRNAs) are a class of covalently closed circular RNA molecules and play an essential role in the pathogenesis of various diseases. Recently, accumulating evidence has shown that m6A modification is widely existed in circRNAs and found its key biological functions in regulating circRNA metabolism, including biogenesis, translation, degradation and cellular localization. Through regulating circRNAs, studies have shown the important roles of m6A modification in circRNAs during immunity and multiple diseases, which represents a new layer of control in physiological processes and disease progressions. In this review, we focused on the roles played by m6A in circRNA metabolism, summarized the regulatory mechanisms of m6A-modified circRNAs in immunity and diseases, and discussed the current challenges to study m6A modification in circRNAs and the possible future directions, providing a comprehensive insight into understanding m6A modification of circRNAs in RNA epigenetics.

Keywords: N6-methyladenosine, circular RNAs, metabolism, immunity, diseases

INTRODUCTION

Epigenetic modifications in RNA have been found to play important regulatory roles in a variety of physiological processes and disease progressions. To date, over 160 types of chemical modifications have been identified in RNA molecules, such as N6-methyladenosine (m6A), 5-methylcytosine (m5C), N1-methyladenosine (m1A), 5-hydroxymethylcytosine (5hmC), N6, 2'-Odimethyladenosine (m6Am), 7-methylguanine (m7G), and so on (Roundtree et al., 2017a; Frye et al., 2018). Among them, m6A has been considered as the most abundant internal modification in RNA, which was discovered from methylated nucleosides in mRNA of Novikoff hepatoma cells in the early 1970s (Desrosiers et al., 1974; Roundtree et al., 2017a). With the development of next-generation sequencing and bioinformatics, a large number of m6A modifications in the transcriptome were discovered and annotated, including mRNAs and non-coding RNAs (Zhou et al., 2017; Frye et al., 2018; He et al., 2020; Sekar and Lakshmanan, 2020; Zhu et al., 2020). In mRNA, the m6A modification has been extensively studied and reviewed by several excellent reviews (Roundtree et al., 2017a; Zaccara et al., 2019; Zhu et al., 2020; Jiang et al., 2021).

Up to now, accumulating evidence has demonstrated that circular RNAs (circRNAs) play important roles in the occurrence, development and prognosis of various diseases, such as cardiovascular diseases (Aufiero et al., 2019; Zhang and Huang, 2020), immune diseases (Chen X. et al., 2019), tumors (Meng S. et al., 2017), skin diseases (Wu et al., 2020), and so on. However, the regulatory role of m6A in circRNAs remains unclear. It was not until 2017 that circRNAs were found to be modified by m6A (Zhou et al., 2017). Based on the important roles of m6A in RNA epigenetic modifications, predictably and rapidly, a large number of recent studies have demonstrated that m6A acts as a key regulator to affect circRNAs functions, thereby participating in development and disease progressions. Therefore, in this review, we focused on the roles of m6A modification in circRNAs during circRNA metabolism and discussed their biological consequences in human development and diseases based on current studies. Importantly, this review will provide a comprehensive understanding of m6A in circRNA biology.

BIOGENESIS, CHARACTERISTICS AND FUNCTIONS OF circRNAs

circRNAs are a class of covalently closed circular RNA molecules that lack 5' caps and 3' tails, which were discovered in the 1970s (Hsu and Coca-Prados, 1979; Chen and Yang, 2015). In a long time afterward, they were thought to be byproducts of splicing (Sanger et al., 1976; Panda et al., 2017). In recent years, a large number of circRNAs have been discovered and annotated with the development of next-generation sequencing technologies and bioinformatic approaches (Xia et al., 2017). The circRNAs are mainly generated by the back-splicing of pre-mRNAs. Currently, three mechanisms were proposed regarding the biogenesis of circRNAs, namely lariat-driven circularization (Zaphiropoulos, 1996; Jeck et al., 2013), intron pairing-driven circularization (Jeck et al., 2013; Zhang et al., 2014; Ivanov et al., 2015) and RBP-driven circularization (Conn et al., 2015; Kramer et al., 2015). In addition, circRNAs are also generated by pre-transfer ribonucleic acid (tRNA), and pre-ribosomal ribonucleic acid (rRNA) molecules (Zhang et al., 2017). According to their origin, the formed circRNAs can be classified into four categories (Zhang et al., 2017): intronic circRNAs (CiRNAs), exon-intron circRNAs (EIciRNAs), exonic circRNAs (EcRNAs), and others (such as the circRNAs that are derived from tRNA and rRNA).

circRNAs were expressed widely in tissue, cell, and developmental stage-specific manners (Memczak et al., 2013; Nicolet et al., 2018) and existed in most mammals (Memczak et al., 2013), plants (Wang et al., 2014), and virus (Nahand et al., 2020). For example, in human heart, about 9% of the expressed genes can produce circRNAs (Aufiero et al., 2018), while in brain, 20% of the genes can produce circRNAs (Rybak-Wolf et al., 2015). In addition, different circular junctions can be generated from the same gene (Nicolet et al., 2018). These discoveries indicated the important regulatory roles of circRNAs. Another characteristic is that circRNAs are more stable than the linear RNAs and have long half-lives than 48 h (Jeck et al., 2013). Due to the covalently closed circular structure without 5'

caps and 3' tails, circRNAs can resist the foreign chemicals or exonucleases (Jeck et al., 2013; Aufiero et al., 2019). Therefore, despite the low expression level, circRNAs can be accumulated to the relatively high levels.

A large number of studies have revealed the functions of circRNAs. (1) microRNA (miRNA) sponges. Cytoplasmic circRNAs can bind specific miRNAs by miRNA response elements to prevent the interplays with target mRNAs (Thomson and Dinger, 2016; Cheng et al., 2019). (2) Interaction with proteins. Some circRNAs that contain protein binding sites have the protein binding abilities to regulate their activity and localization (Du W. W. et al., 2016; Barbagallo et al., 2019). (3) Templates for protein synthesis. Due to the lack of 5'-end, the translation of circRNAs only is initiated by the cap-independent mechanisms. This function of circRNAs will be discussed in detail in following section. (4) Regulation of gene transcription. Some circRNAs located in nucleus, such as circ-EIF3J and circ-PAIP2, can combine with the U1 snRNP to further interact with RNA Pol II and enhance the expression of their parental genes in HeLa and HEK293 cells (Li et al., 2015).

m6A MODIFICATION OF circRNA

Widely Existed m6A Modification of circRNAs

Through depletion of rRNA, treatment with RNase R to digest linear RNAs and m6A-modified RNA immunoprecipitation sequencing (MeRIP-seq), m6A modification of circRNAs has been found to exist widely. In plant, Wang et al. (2020) found that about 10% of the EcRNAs contained m6A sites in moso bamboo. In human embryonic stem cells (hESCs) and HeLa cells, Zhou et al. (2017) identified 1,404 m6A circRNAs and 987 m6A circRNAs, respectively, and they found that m6A circRNAs were expressed in cell-type-specific methylation patterns. In a rat model of hypoxia mediated pulmonary hypertension (HPH), Su et al. (2020) identified 1130 m6A circRNAs in total. In the lens epithelium cells from age-related cataract (ARC), Li et al. (2020) identified 4876 m6A peaks within circRNAs. Besides, in HPH, 80% of m6A circRNAs were derived from protein-coding genes, while in ARC, over 70% of circRNAs were derived from sense overlapping. These studies suggested that m6A modification of circRNAs was widely existed and might play important roles in diseases. In addition, the m6A sites in circRNAs may be distinct from the corresponding mRNAs. In hESCs cells, Zhou et al. (2017) reported that 33% of m6A circRNAs were produced from genes that encode m6A mRNAs methylated on different exons, while 26% of m6A circRNAs were produced from genes that encode mRNAs without detectable m6A modification (Zhou et al., 2017). Another phenomenon is that m6A sites in mRNAs are most common in the last exon (Meyer et al., 2012), while circularization of the last exon of genes is uncommon (Zhang et al., 2014). These evidence suggested that circRNAs exhibit the patterns of m6A modification that are distinct from those of mRNAs.

m6A Regulators of circRNA

As the most abundant mRNA internal modification, the functions of m6A on mRNA are mediated through three homologous factors (Zaccara et al., 2019), namely so called “writers” (methyltransferase), “erasers” (demethylase), and “readers” (recognition). In circRNAs, m6A modification was found to be written, read and erased by the same regulators with mRNA (Zhou et al., 2017).

m6A Writers

The m6A is installed by a multi-subunit complex (Zaccara et al., 2019). This complex consists of two core components (methyltransferase-like 3 protein (METTL3) and METTL14) and other accessory regulatory subunits [Wilm’s tumor-1-associated protein (WTAP), VIRMA (Virilizer), E3 ubiquitin-protein ligase HAKAI, RNA recognition motif 15/15B (RBM15/15B), Zinc finger CCCH domain-containing protein 13 (ZC3H13)] (Zaccara et al., 2019; Gu et al., 2021; Jiang et al., 2021). METTL3 is the catalytic core of the multi-subunit complex (Bokar et al., 1997; Liu et al., 2014). METTL14 contains the RNA-binding site and is an allosteric activator of the enzymatic activity of METTL3 (Liu et al., 2014; Zaccara et al., 2019). WTAP is essential for m6A formation and it is responsible for localizing METTL3–METTL14 heterodimers to transcription sites (Ping et al., 2014). VIRMA may modulate region-selective methylation of sites in 3′ UTR and location near stop codons (Yue et al., 2018). RBM15/15B are the mediators of methylation specificity, which facilitate the recruitment of the writer complex to specific sites (Patil et al., 2016; Zaccara et al., 2019). ZC3H13 is a WTAP interactor, which acts as a bridge between RBM15 and WTAP (Knuckles et al., 2018). HAKAI functions as an E3 ubiquitin ligase, which was first identified in the WTAP interaction proteome (Horiuchi et al., 2013). Deletion of HAKAI results in a partial reduction in global m6A levels (Růžička et al., 2017). Notably, METTL16 is the new identified methyltransferase that can regulate S-adenosylmethionine homeostasis and can methylate long non-coding RNA and U6 small nuclear RNA (Brown et al., 2016; Pendleton et al., 2017; Warda et al., 2017). Currently, only few m6A residues in poly(A) RNA were found to be catalyzed by METTL16 (Brown et al., 2016; Pendleton et al., 2017; Warda et al., 2017).

m6A Erasers

m6A is a reversible process, which can be removed by demethylases. There are two demethylases, namely obesity-associated protein (FTO) and AlkB homolog 5 (ALKBH5). Both of them belong to the α -ketoglutarate-dependent dioxygenase AlkB-like superfamily and they remove m6A through Fe^{2+} and α -ketoglutarate-dependent manner (Jia et al., 2011; Zheng et al., 2013). Under physiological conditions, the demethylases appear to have a limited role, indicating that they function in specific tissues, or under specific stress and disease-relevant conditions (Zhao et al., 2017).

m6A Readers

m6A readers are a class of RNA binding proteins, which can recognize and bind to m6A sites, thereby resulting in different

downstream effects, such as splicing, export and translation of m6A RNAs (Xiao et al., 2016; Roundtree et al., 2017b; Yang et al., 2017). In YT521-B homology (YTH) domain family, there are five m6A readers identified, namely YTHDC1, YTHDC2, YTHDF1, YTHDF2, and YTHDF3 (Liu et al., 2015). Among them, YTHDF1, YTHDF2, and YTHDF3 are mainly located in the cytoplasm. YTHDC1 is mainly found in the nucleus and YTHDC2 is located in both cytoplasm and nucleus. YTHDC1 affects their splicing (Kasowitz et al., 2018) and export (Roundtree et al., 2017b); YTHDC2 affects their degradation and translation (Hsu et al., 2017); YTHDF1 promotes translation (Wang et al., 2015); YTHDF2 promotes degradation (Du H. et al., 2016) and YTHDF3 promotes the translation and degradation (Shi et al., 2017). The other m6A readers include insulin-like growth factor 2 mRNA binding proteins 1-3 (IGF2BP1-3), heterogeneous nuclear ribonucleoprotein (HNRNP) family (HNRNPC, HNRNPA2B1, and HNRNPG), fragile X mental retardation protein (FMRP) and eukaryotic initiation factor 3 (eIF3). IGF2BPs can regulate gene expression by enhancing the stability of target RNAs (Huang H. et al., 2018). FMRP can promote nuclear export (Edens et al., 2019). eIF3 can facilitate cap-independent translation (Meyer et al., 2015).

ROLES OF m6A IN circRNA METABOLISM

Currently, several studies have found that m6A modification can affect the “fate” of m6A-modified circRNAs (Figure 1), including circRNAs biogenesis, translation, degradation and cellular localization, indicating that m6A plays important roles in circRNA metabolism. Through participating in circRNA metabolism, m6A can regulate many physiological and pathological processes. For example, during the nuclear phase, m6A can be read by specific nuclear readers and promote the nuclear export of circRNAs. Upon exporting to the cytoplasm, m6A can be read by specific cytosolic reader proteins, thereby affecting the function of circRNAs. Therefore, this section aimed to discuss the roles of m6A in circRNA metabolism comprehensively.

m6A and Biogenesis of circRNA

circRNA is conserved evolutionarily and is expressed in cell, tissue and developmental stage-specific expression patterns (Memczak et al., 2013; Hsiao et al., 2017; Nicolet et al., 2018), suggesting that circRNAs play an important regulatory role in different physiological and pathological processes. Therefore, it is essential to understand the regulation regarding the biogenesis of circRNAs. The biogenesis of circRNA is distinct from canonical splicing, and it is generated through a back-splicing orchestrated by the spliceosome machinery (Aufiero et al., 2019). Recently, Tang et al. (2020) reported that m6A could promote the biogenesis of circRNA in male germ cells. They found that, for open reading frames (ORFs)-containing circRNAs during murine spermatogenesis, the back splicing occurred mostly at m6A enriched sites, while these m6A sites were usually located around the start and stop codons in linear mRNAs. To

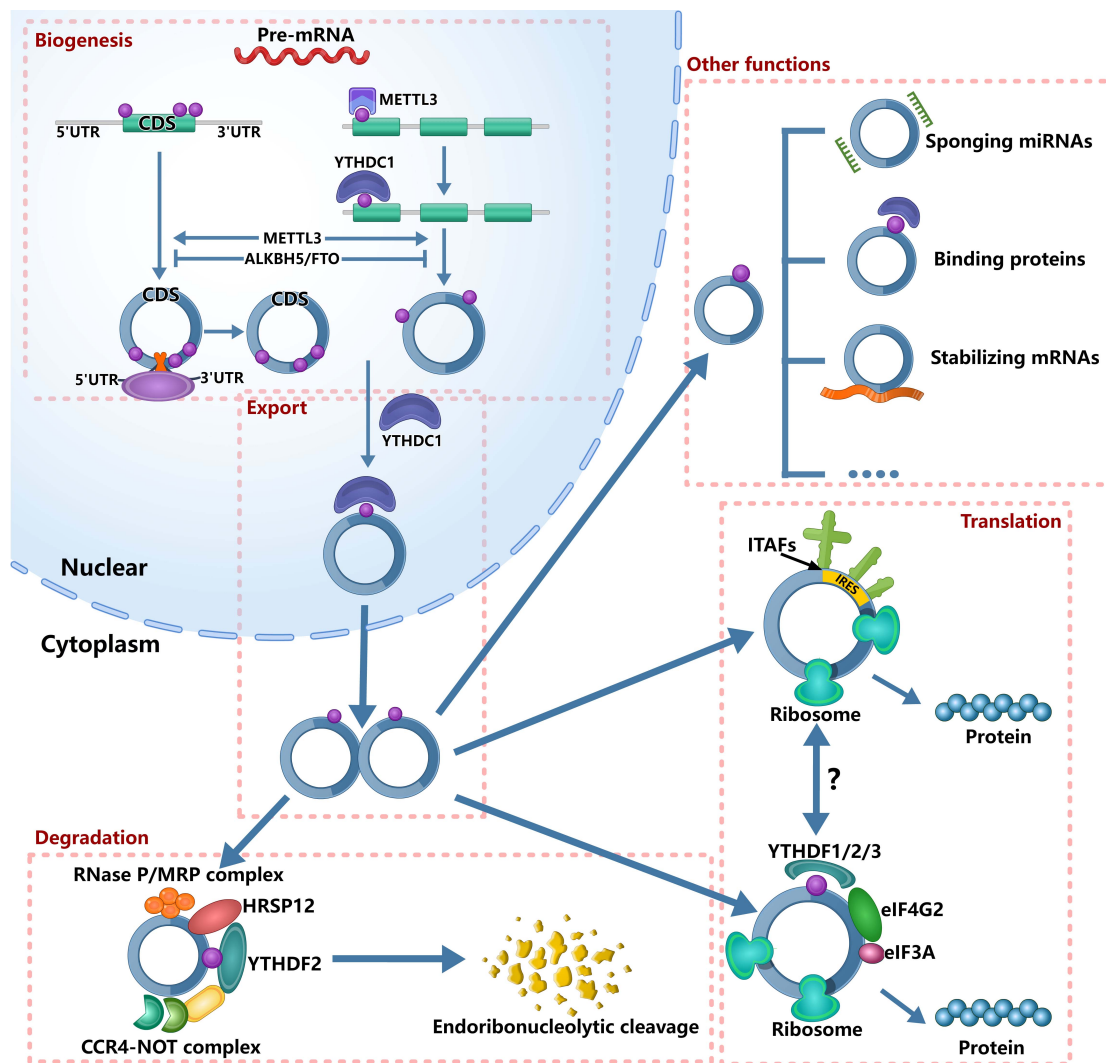


FIGURE 1 | Roles of m6A in circRNA metabolism. It's has confirmed that m6A can regulate circRNA metabolism, including circRNAs biogenesis, translation, degradation and cellular localization. On the one hand, m6A sites located around the start and stop codons in linear mRNAs can recruit spliceosome, leading to back splicing and circRNA production. On the other hand, m6A deposition and YTHDC1 binding to exons can regulate circularization. In the nucleus, the m6A can bind specific nuclear reader proteins, mainly YTHDC1, which can promote the export of circRNAs. Upon circRNAs export to the cytoplasm, m6A binds to specific reader proteins and other proteins to stabilize some mRNAs. The nuclear export of circRNAs also affects its miRNA sponges. The translation of circRNAs is only in cap-independent translation initiation mechanisms: IRES-dependent initiation of translation and m6A-dependent initiation of translation. m6A-driven translation of circRNA requires eIF4G2 and YTHDF3 and is enhanced by METTL3/14, inhibited by FTO. IRES-driven translation and m6A-driven translation may have interplays. Finally, m6A-modified circRNAs are endoribonuclease-cleaved via the YTHDF2-HRSP12-RNase P/MRP axis.

further establish the cause-effect relationship between m6A and circRNAs, Tang et al. (2020) knocked out ALKBH5 and METTL3, respectively. After knocking out ALKBH5 in spermatogenic cells, the m6A level was significantly increased compared with wild-type controls. Consistently, the circRNAs abundance was increased in *Alkbh5*-null spermatogenic cells. After knocking out METTL3, they identified much fewer circRNAs. Similarly, Di Timoteo et al. (2020) also reported that the level of circRNA was decreased in HeLa cells after knocking out METTL3. Interestingly, they found the consistent decrease of circ-ZNF609 after knocking out YTHDC1 in HeLa, RD, RH4, and HEK293T cells. Further analysis found that m6A deposition and YTHDC1

binding to exons that undergo circularization were significantly correlative, and circRNAs containing total-only m6As were more represented among those decreasing upon depletion of both YTHDC1 and METTL3 compared with those affected by either METTL3 or YTHDC1 knockdown alone. These evidence indicated that m6A regulated the biogenesis of circRNAs in an METTL3/YTHDC1-dependent manner. In colorectal cancer, METTL3 could increase the expression of circ1662 (Chen et al., 2021). Therefore, based on the above evidence, we can confirm that m6A modification can increase the biogenesis of circRNAs. However, more detailed information is needed to understand how m6A regulates the biogenesis of circRNAs.

m6A and Translation of circRNA

Although circRNA is considered as non-coding RNA for a long time, accumulating evidence has shown that some circRNAs have protein-coding potential and can be translated (Legnini et al., 2017; Pamudurti et al., 2017; Yang et al., 2017, 2018; Zhang et al., 2018a,b; Liang et al., 2019). More recently, Huang et al. (2021) reported a database, TransCirc,¹ to help investigate the circRNAs that have translation capacity. However, the mechanisms about the translation of circRNAs remain largely unknown. As we all know, the translation initiation of mRNA is dependent on the cap structure of 5'-end, which contains a 7-methyl guanosine (m7G) that can be recognized by the eukaryotic translation initiation factor 4E (eIF4E) (Gross et al., 2003). However, circRNA is a covalently closed RNA molecule without 5' caps and 3' tails (Meng X. et al., 2017), so that circRNA is translated in cap-independent translation initiation mechanisms. Currently, two mechanisms are reported in translation initiation of circRNA: internal ribosome entry site (IRES)-dependent initiation of translation and m6A-dependent initiation of translation. IRESs are sequences that form secondary structures on RNA and can initiate translation through recruiting ribosomes by IRES-transacting factors (ITAFs) in the absence of canonical translation initiation factors (Godet et al., 2019). At first, the fact that circRNAs can be translated is proved by IRES-driven pathway (Chen and Sarnow, 1995). Afterward, more and more circRNAs that can be translated by IRES-driven pathway were reported, such as circZNF609 (Legnini et al., 2017), circMbl (Pamudurti et al., 2017), circSHPRH (Zhang et al., 2018a), circFBXW7 (Yang et al., 2018), circLINC-PINT (Zhang et al., 2018b), circb-catenin (Liang et al., 2019).

Interestingly, the discovery of m6A that can initiate the translation of circRNA expands the coding landscape of human transcriptome (Yang et al., 2017). Yang et al. (2017) found that the m6A-driven translation of circRNAs was widespread, with hundreds of endogenous circRNAs having translation potential, by the analysis of polysome profiling, computational prediction and mass spectrometry. Mechanistically, they found that the m6A-driven translation of circRNA required initiation factor eIF4G2 and m6A reader YTHDF3, and was enhanced by methyltransferase METTL3/14, inhibited by demethylase FTO (Yang et al., 2017). When inserting a short fragment (19nt) containing different copies of consensus m6A motifs (RRACH) before the start codon of circRNA reporter in 293 cells, the protein could be detected. Moreover, single m6A site has similar translation efficiency compared to circRNA with two m6A sites (Yang et al., 2017). These evidence suggested that m6A motif was essential for initiating translation. In human papillomavirus (HPV), m6A-modified circE7 could be translated to produce E7 oncoprotein (Zhao et al., 2019).

In addition to initiating the translation of circRNAs, m6A may also regulate the translation of circRNAs (Yang et al., 2017). For example, circZNF609 could be translated by IRES-driven pathway (Legnini et al., 2017). A recent study reported that two mutant at m6A sites displayed approximately 50% reduction of circ-ZNF609 translation (Di Timoteo et al., 2020).

Further analysis found that m6A regulated its translation through recognition by YTHDF3 and eIF4G2 (Di Timoteo et al., 2020). This study suggested that the two cap-independent translation of circRNA might have interplays. However, the relationships between the two cap-independent translations need further investigations.

In mRNAs, studies have shown that m6A regulates their translation under stress response (Zhou et al., 2015, 2018). Yang et al. (2017) found that m6A-mediated circRNA translation was increased under the heat shock condition and its mechanism might be the translocation of YTHDF2 from cytosol into nucleus upon heat shock to block the m6A "eraser" FTO (Zhou et al., 2015; Yang et al., 2017). These evidence suggested that m6A-mediated circRNA translation played important roles in cellular stress response. In the future, to broaden our understanding regarding the significance of circRNA translation in the specific conditions, it is essential to explore the conditions that affect the m6A-mediated circRNA translation.

m6A and Degradation of circRNA

Due to the covalently closed circular structure without 5' caps and 3' tails, circRNAs can resist the foreign chemicals or exonucleases (Jeck et al., 2013; Aufiero et al., 2019). Therefore, circRNAs are more stable than the linear RNAs and are not degraded readily by RNase R, resulting in their long half-lives exceeding 48 h (Jeck et al., 2013; Suzuki and Tsukahara, 2014). Thus, there are few studies that reported the degradation of circRNA.

Hansen et al. (2011) reported that circRNAs with near perfect complementary miRNA target sites could be degraded in an Ago2-slicer-dependent manner. Ago2 is a member of the Argonaute protein family, which is important for RNA interference (Suzuki and Tsukahara, 2014) and can mediate the degradation of circRS-7 (Hansen et al., 2011). However, only a few circRNAs have miRNA sponge function or specific miRNA target sites. Jia et al. (2019) found that the depletion of GW182 (a key component of the P-body and RNA interference machine) could lead to the accumulation of endogenous circular transcripts. However, the depletion of other P-body components or RNAi complex factors did not have similar effects. So, there are more studies to explain this phenomenon.

A recent study reported that m6A-containing circRNAs could be degraded through YTHDF2-HRSP12-RNase P/MRP axis (Park et al., 2019). Mechanistically, human heat-responsive protein 12 (HRSP12) acted as an adaptor protein that linked YTHDC2 and RNase P/MRP to form YTHDF2-HRSP12-RNase P/MRP complex. Notably, after downregulating the expression YTHDF2, HRSP12, or POP1, Park et al. (2019) observed only three out of all tested 11 circRNAs commonly increased, indicating that this mechanism could only cleave a subset of m6A-containing circRNAs.

m6A and Cellular Localization of circRNA

As we all know, a large number of circRNAs function in cytoplasm, such as miRNA sponges (Thomson and Dinger, 2016). Thus, it is essential to understand how the circRNAs export from the nucleus to the cytoplasm. Huang C. et al. (2018) found that *Drosophila* Hel25E and its human homologs,

¹<https://www.biosino.org/transcirc/>

UAP56/URH49, could regulate circRNAs localization and control the efficiency of nuclear export by measuring the lengths of mature circRNAs. Chen et al. (2021) reported that YTHDC1 could bind to the m6A motif GAACU of circNSUN2 and facilitate circNSUN2 export from the nucleus to the cytoplasm, further promote colorectal liver metastasis by stabilizing HMGA2 (Chen R. X. et al., 2019). In addition, the m6A-modified circ1662 could bind to YAPI and accelerate its nuclear transport (Chen et al., 2021). However, more studies are required to investigate the details that m6A regulates the cellular localization of circRNAs.

m6A circRNAs AND IMMUNITY

m6A in mRNA can control various aspects of immunity, including immune recognition, activation of innate and adaptive immune responses (Shulman and Stern-Ginossar, 2020). However, its roles in circRNA immunity are unknown. Several recent studies have discovered that m6A can also control circRNA immunity (Figure 2), including the roles in innate immune and anti-tumor immunity.

The innate immune system relies on pattern recognition receptors (PRRs) recognizing pathogen associated molecular patterns (PAMPs) to recognize “non-self” (Reikine et al., 2014; Wu and Chen, 2014). The PRRs, such as RIG-I and MDA5, can sense foreign nucleic acids. MDA5 can detect long double-stranded RNA (dsRNA) and RIG-I can recognize 5′ triphosphate on short dsRNAs (Schlee, 2013; Reikine et al., 2014; Wu and Chen, 2014). Reportedly, some exogenous circRNAs can activate antiviral and immune gene expression (Chen et al., 2017), while some endogenous circRNAs can inhibit protein kinase R and set the threshold for innate immunity upon virus infection (Liu et al., 2019). However, the mechanisms that the innate immune system recognizes self and non-self circRNAs remain unclear. Chen et al. (2021) found that m6A can mark circRNA as “self” and these endogenous circRNAs inhibited innate immune responses (Chen Y. G. et al., 2019). This immunosuppression was mediated by binding to YTHDF2 directly and inhibiting RIG-I activation. In addition, exogenous circRNAs activated innate immunity by directly binding RIG-I and K63-polyubiquitin chain and they together formed a three-component signaling-competent complex for immune signaling (Chen Y. G. et al., 2019). These evidence suggested that, for human circRNAs, m6A modification was essential for the recognition function of innate immunity.

Besides participating in the recognition of innate immunity, m6A-modified circRNAs can inhibit the tumor growth by inducing anti-tumor immunity. Chen et al. (2021) reported that circFOREIGN could induce CD8⁺ T cell responses, and after receiving circFOREIGN, the growth of tumor in mice model was lower than the negative control, indicating that circFOREIGN would can induce adaptive immunity against OVA-expressing tumors. Notably, Li et al. (2021) reported that the immune responses induced by m6A-modified circNDUFB2 could inhibit NSCLC progression. The overexpression of circNDUFB2 markedly inhibited the tumorigenicity of LLC1 cells (a murine lung carcinoma cell line) *in vivo*, and the level of IFN- β in serum was significantly increased in the

mice with circNDUFB2-overexpressed LLC1 cells. Moreover, the infiltration of CD8⁺ T cells and DCs in the tumor tissues were significantly increased. These results suggested that m6A-modified circNDUFB2 inhibited tumor progression by activating anti-tumor immunity. However, more studies are needed to explore the roles of m6A modification in circRNAs in the field of tumor immunity.

These evidence demonstrated the roles of m6A modification in circRNAs during recognizing innate immunity and inducing anti-tumor immunity, but major knowledge gaps in field of immunity remain to be filled, such as its specific roles in different immune diseases and immune cells.

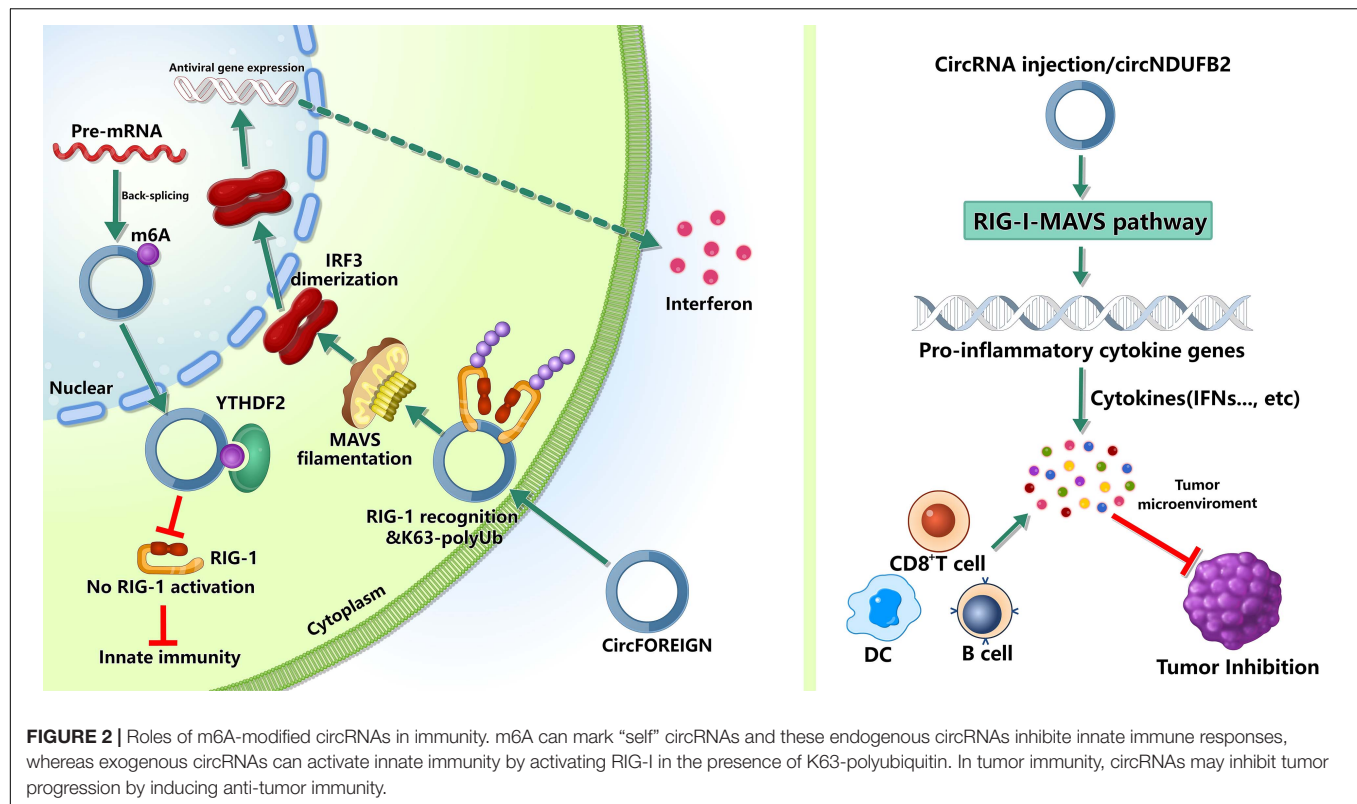
m6A circRNA AND DISEASES

Although it was not until 2017 that circRNAs were found to be modified by m6A, many studies have shown that m6A modification of circRNAs plays important roles in physiological processes and disease progressions (Figure 3), such as tumors (Chen R. X. et al., 2019; Chen et al., 2021; Li et al., 2021), acute coronary syndrome (Guo et al., 2020), pulmonary hypertension (Su et al., 2020), and age-related cataract (Li et al., 2020). In this section, we focused on the roles of m6A-modified circRNAs in physiological processes and disease progressions.

m6A circRNA and Tumor

m6A modification of circRNAs has been shown to be involved in the progression of many tumors. In patients with colorectal carcinoma (CRC), metastasis is the overwhelming cause of death, and the liver is the most frequent distant metastatic site (Hofheinz and Stintzing, 2019). Recently, Chen R. X. et al. (2019) reported a novel metastatic mechanism to liver of CRC. First, YTHDC1 binds to the m6A motif of circNSUN2 and facilitates circNSUN2 export from the nucleus to the cytoplasm. Next, IGF2BP2 binds to the CAUCAU motif of circNSUN2 through the KH3-4 di-domain and the AAACA site inside of circNSUN2 can directly bind to the 3′UTR of HMGA2 with AU-Rich Elements, ultimately forming circNSUN2/IGF2BP2/HMGA2 RNA-protein ternary complex to stabilize HMGA2 mRNA, thereby promoting colorectal liver metastasis. This study provided the comprehensive evidence that m6A modification of circRNAs may contribute to cancer therapy (He et al., 2021). Another study found that m6A could increase the expression of circ1662 in CRC and circ1662 directly bound to yes-associated protein 1 (YAP1) and accelerated its nuclear accumulation to regulate the SMAD3 pathway, thereby promoting the invasion and migration of CRC cells (Chen et al., 2021).

In Hepatitis B virus (HBV)-associated hepatocellular carcinoma (HCC), circARL3 was upregulated in HBV positive HCC tissues and knockdown of circARL3 inhibited the proliferation and invasion of HBV + HCC cells (Rao et al., 2021). Rao et al. (2021) found that HBx protein could upregulate the expression of METTL3, increasing the m6A modification of circARL3. m6A-modified circARL3 can be read by YTHDC1 and regulate its biogenesis. Finally, circARL3 promoted HBV + HCC progression by sponging miR-1305.



In non-small cell lung cancer (NSCLC), circNDUFB2 was downregulated and elevated circNDUFB2 could inhibit growth and metastasis of NSCLC cells (Li et al., 2021). circNDUFB2 functions as a scaffold to enhance the interaction between TRIM25 and IGF2BPs and can form a TRIM25/circNDUFB2/IGF2BPs ternary complex. By the way, TRIM25 is an RNA-binding protein and belongs to the Tripartite Motif (TRIM) family of E3 ubiquitin ligases, which catalyzes the addition of polyubiquitin chains to its substrates for degradation (Lee et al., 2018). This ternary complex facilitates ubiquitination and degradation of IGF2BPs during NSCLC progression. m6A modification of circNDUFB2 can enhance this effect by regulating the interactions between circNDUFB2 and IGF2BPs. In addition, circNDUFB2 participates in the activation of anti-tumor immunity during NSCLC progression by activating the RIG-I-MAVS pathway (Li et al., 2021), indicating that circNDUFB2 inhibits NSCLC progression in a dual-role pattern.

In cervical cancer, Zhou et al. (2017) identified a large number of m6A-modified circRNAs in HeLa cells, indicating that m6A-modified circRNAs may play an important regulatory role in cervical cancer. As we all know, human papillomavirus (HPV) infection is the main cause that leads to the occurrence of cervical cancer (Chibwesha and Stringer, 2019). Zhao et al. (2019) reported that HPV could generate the circE7, which was an oncoprotein-encoding circRNA. circE7 is m6A-modified and can be translated to produce E7 oncoprotein in an m6A-independent manner. Specific disruption of circE7 can reduce E7 protein levels in CaSki cervical carcinoma cells and can inhibit cancer cell growth both *in vitro* and in tumor xenografts.

In poorly differentiated gastric adenocarcinoma (PDGA), Zhang et al. (2020) identified 20 differentially expressed m6A-modified circRNAs by SRAMP analysis, m6A-immunoprecipitation and real-time quantitative PCR. They found that the trend of m6A modification alteration was mainly consistent with the expression level of circRNAs. However, the roles of these m6A-modified circRNAs in PDGA remain unclear and need to be explored extensively.

In human ameloblastoma, Niu et al. (2020) investigated the global m6A modification, including in mRNAs, lncRNAs and circRNAs. They found 3,673 differentially methylated m6A sites in mRNAs, 4,975 differentially methylated m6A sites in lncRNAs and 364 differentially methylated m6A sites within circRNAs. Although a global data of m6A in ameloblastoma was provided, their roles and the relationships among these m6A-modified mRNAs, lncRNAs and circRNAs need to be further explored.

Based on the above analysis, we can confirm that m6A modification of circRNAs plays critical roles in occurrence, development and metastasis of tumors. Of note, besides the above roles, m6A modification of circRNAs is also related to resistance of chemotherapy and radiotherapy. In sorafenib-resistant HCC, m6A could increase the expression of circRNA-SORE and increased circRNA-SORE sequestered miR-103a-2-5p and miR-660-3p by acting as a miRNA sponge, thereby competitively activating the Wnt/ β -catenin pathway and inducing sorafenib resistance (Xu et al., 2020). In hypopharyngeal squamous cell carcinoma (HPSCC), m6A could stabilize the expression of circCUX1 and knocking down circCUX1 promoted the sensitivity of hypopharyngeal cancer cells to

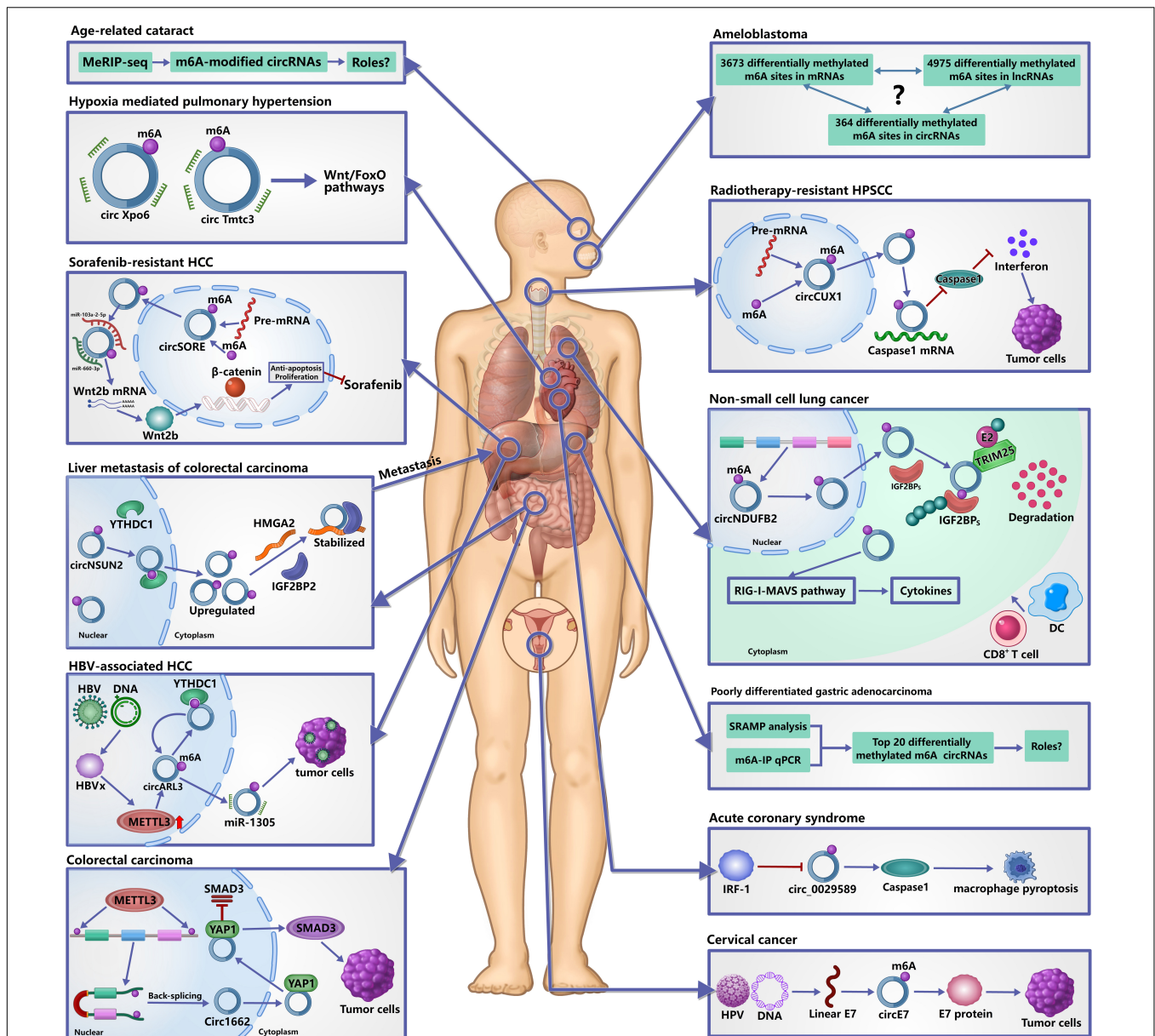


FIGURE 3 | Roles of m6A-modified circRNAs in diseases. It has confirmed that m6A modification of circRNAs plays important roles in the occurrence and development of human diseases. In tumors, m6A-modified circRNAs are not only involved in their occurrence, development and metastasis, but also in the resistance of chemotherapy and radiotherapy by regulating the metabolism and functions of circRNAs. In acute coronary syndrome, IRF-1 facilitates macrophage pyroptosis and inflammation by inhibiting m6A-modified circ_0029589, thereby promoting the formation of necrotic core. In hypoxia mediated pulmonary hypertension, m6A may affect the interaction between circRNAs and miRNAs to participate in its development. In age-related cataract, many differentially expressed m6A-modified circRNAs are identified, but the specific roles remain unclear.

radiotherapy. Mechanistically, circCUX1 bound to caspase1 and inhibited its expression, leading to a decrease in the release of inflammatory factors, thereby developing tolerance to radiotherapy (Wu et al., 2021). As a key inflammation-related molecule, caspase1 can affect the occurrence, development, invasion, and metastasis of tumors by regulating the tumor inflammatory microenvironment (Hu et al., 2010), and caspase-1 actively induced tumor cell programmed death and anti-tumor immune surveillance (Zitvogel et al., 2012). Therefore,

these evidence provided the new insights into understanding the resistant to radiotherapy.

m6A circRNA and Acute Coronary Syndrome

Reportedly, macrophage death plays a key role in promoting the formation of necrotic core and plaque disruption in late atherosclerotic lesions (Hizir et al., 2017; Xu et al., 2018;

TABLE 1 | m6A-modified circRNAs as the potential therapeutic target of different diseases based on current reports.

Target	Disease types	Expression	Function	References
circNSUN2	CRC	Up	Stabilize HMGA2 mRNA, and promote colorectal liver metastasis.	Chen R. X. et al., 2019
circ1662	CRC	Up	Bind to YAP1 and accelerate its nuclear accumulation to regulate the SMAD3 pathway.	Chen et al., 2021
circARL3	HBV + HCC	Up	Sponge miR-1305 and promote HBV + HCC progression.	Rao et al., 2021
circNDUFB2	NSCLC	Down	(1) Function as a scaffold to enhance the interaction between TRIM25 and IGF2BPs, from a TRIM25/circNDUFB2/IGF2BPs ternary complex and facilitate ubiquitination and degradation of IGF2BPs. (2) Participate in the activation of anti-tumor immunity by activating the RIG-I-MAVS pathway	Li et al., 2021
circE7	Cervical cancer	Up	Can be translated to produce E7 oncoprotein and promote the growth of cervical cancer.	Zhao et al., 2019
circRNA-SORE	Sorafenib-resistant HCC	Up	Sponge miR-103a-2-5p and miR-660-3p, thereby competitively activating the Wnt/ β -catenin pathway and inducing sorafenib resistance.	Xu et al., 2020
circCUX1	Radiotherapy-resistant HPSCC	Up	Bind to caspase1 and inhibit its expression, leading to a decrease in the release of inflammatory factors.	Wu et al., 2021
circ_0029589	ACS	Down	Decrease caspase-1 activity.	Guo et al., 2020
circXpo6	HPH	Up	Sponge miRNA.	Su et al., 2020
circTmtc3	HPH	Up	Sponge miRNA.	Su et al., 2020

CRC, colorectal carcinoma; HCC, hepatocellular carcinoma; HBV, Hepatitis B virus; NSCLC, non-small cell lung cancer; HPSCC, hypopharyngeal squamous cell carcinoma; ACS, acute coronary syndrome; HPH, hypoxia mediated pulmonary hypertension; YAP1, yes-associated protein 1; HMGA2, high mobility group AT-hook 2; TRIM25, Tripartite Motif 25; SMAD3, SMAD family member 3; RIG-I, retinoic acid-inducible gene-I; MAVS, mitochondrial anti-viral signaling protein; IGF2BPs, insulin-like growth factor 2 mRNA-binding proteins.

Guo et al., 2019). Pyroptosis is a newly identified inflammatory programmed cell death with the activation of caspase-1 and the consequent release of inflammatory cytokines (Liu et al., 2016), and has been found to have a strong correlation with ox-LDL-induced human macrophage death and aggravates the instability of atherosclerotic lesions (Yan et al., 2016; Martinet et al., 2019). Guo et al. (2019) found that IFN regulatory factor (IRF)-1 could activate ox-LDL-induced macrophage pyroptosis in atherosclerosis (AS) and acute coronary syndrome (ACS). However, the underlying mechanism is unknown. A recent study found that the expression of hsa_circ_0029589 was significantly decreased in ACS and the relative m6A level of circ_0029589 was obviously elevated (Guo et al., 2020). Inhibition of IRF-1 obviously induced the expression of circ_0029589 and reduced the m6A level of circ_0029589, and knocking down the expression of METTL3 markedly increased circ_0029589 expression and decreased the m6A level of circ_0029589 and caspase-1 activity in AS and ACS (Guo et al., 2020). These results suggested that IRF-1 facilitated macrophage pyroptosis and inflammation in ACS by inhibiting circ_0029589 through promoting its m6A modification.

m6A circRNA and Pulmonary Hypertension

Pulmonary hypertension is a lethal disease and hypoxia mediated pulmonary hypertension (HPH) belongs to group III pulmonary hypertension, which is induced by chronic hypoxia (Pugliese et al., 2015; Galiè et al., 2016). To investigate the significance of m6A circRNAs in HPH, Su et al. (2020) analyzed transcriptome-wide map of m6A circRNAs in a rat model by high-throughput m6A and circRNAs sequencing. They found that m6A abundance in circRNAs was significantly reduced under hypoxia *in vitro* and m6A-modified circXpo6 and circTmtc3 might be involved

in HPH through regulating Wnt and FoxO signaling pathways by influencing the interactions between circRNAs and miRNAs. However, there are more evidence to explore the roles of m6A-modified circXpo6 and circTmtc3 in HPH and their bindings to miRNAs need to be validated by dual-luciferase reporter assay.

m6A circRNA and Age-Related Cataract

Age-related cataract (ARC) is one of the leading causes of vision impairment and accounts for the majority of senile blindness worldwide (Khairallah et al., 2015). However, the pathogenesis of ARC remains unclear. A recent study found that there are a lot of m6A circRNAs in the lens epithelium cells from the patients with ARC (Li et al., 2020). The level of m6A abundance in total circRNAs was decreased compared with the controls and ALKBH5 was significantly upregulated in ARCs. The authors predicted the potential functions of m6A modified circRNAs and found the relevant pathways that may be associated with m6A modified circRNAs. These results indicated that m6A modification of circRNAs may play an important role in ARC. However, a large number of studies are needed to investigate their roles and validate the predicted the potential functions of m6A modified circRNAs.

Based on the above analysis regarding the roles of m6A modified circRNAs in different diseases, we can deduce that m6A modification in circRNAs has following common mechanisms to participate in disease progression. (1) Under pathological conditions, the expression of methyltransferases and/or demethylases is upregulated or downregulated, leading to the changes in m6A levels of circRNAs. (2) Through recognizing m6A motif by different m6A readers, m6A modification can regulate the metabolism and functions of circRNAs, thereby participating in disease progression (**Figures 2, 3**). However, the relationships among m6A modification, circRNA functions

and diseases remain largely unclear. It is confirmed that m6A modification is as the upstream regulatory mechanism to affect downstream molecules by regulating circRNAs directly. In the future, the conjoint analysis of MeRIP-seq and RNA-seq may be helpful for seeking disease-specific m6A modified circRNAs. After that, qRT-PCR, RIP, RNA pull down, and dual-luciferase reporter assay may be used for exploring the mechanism of selected m6A modified circRNAs.

CONCLUSION AND FUTURE DIRECTIONS

No doubt, increasing number of studies have validated that circRNAs play key roles in human development and disease progressions; and epigenetic modification, especially m6A in mRNA, has emerged as widespread regulatory mechanisms that control gene expression in diverse physiological and pathological processes. However, the roles of epigenetic modifications in circRNAs remain largely unknown. Despite there are only 4 years regarding the researches of m6A in circRNAs, accumulating studies have identified numerous m6A-modified circRNAs and have found their important regulatory roles in development and diseases. In conclusion, current studies have found that these m6A-modified circRNAs are expressed in cell-type and disease-specific methylation patterns. In functions, m6A modification can regulate circRNAs metabolism, including circRNAs biogenesis, translation, degradation and cellular localization. Importantly, these m6A-modified circRNAs participate in diverse physiological and pathological processes, such as immunity, tumors, acute coronary syndrome, pulmonary hypertension and age-related cataract, by regulating circRNAs metabolism and functions. In general, the discovery of m6A modification in circRNAs broadened our horizons in RNA epigenetics and we provided a comprehensive understanding about the m6A modification of circRNAs and their roles based on current reports.

In addition, m6A-modified circRNAs may become the potential therapeutic target of diseases. For example, m6A-modified circNSUN2 has been found to play a key role in promoting colorectal liver metastasis (Chen R. X. et al., 2019; He et al., 2021). Targeted inhibition of circNSUN2 may block colorectal liver metastasis. Here, we listed the prospect targets that may be used for clinical treatment in the future in **Table 1** based on current reports. However, the research regarding targeting m6A-modified circRNAs in diseases is still

in infancy and many studies are needed to seek disease-specific targets and to develop effective methods for detection of m6A-modified circRNAs.

Currently, many questions are about when and how m6A is added on or removed from circRNAs, and about how m6A regulates circRNAs metabolism and disease progressions. For example, Tang et al. (2020) found that, during murine spermatogenesis, for a subset of circRNAs, the back splicing occurs mostly at m6A enriched sites, which are usually located around the start and stop codons in linear mRNAs. Zhou et al. (2017) found that numerous m6A circRNAs were generated from exons that didn't contain m6A peaks in corresponding mRNAs. The question is whether m6A was added before or after the circRNAs were formed. In addition, the causes that lead to the change of m6A modification in circRNAs are unclear.

Another challenge is the technologies to study m6A modification. For example, MeRIP-Seq is the main method to identify m6A modifications using m6A-specific antibodies. A limitation of this method is that it cannot provide the precise location of m6A at single-nucleotide resolution. Ho-Xuan et al. (2020) found that endogenous proteins could not be detected when they constructed the overexpression of circZNF609. Comprehensive mutational analysis found that deletion constructs, which were deficient in producing circZNF609, still generated the observed protein products, suggesting that the apparent circZNF609 translation originated from transsplicing byproducts of the overexpression plasmids. Therefore, the overexpression construction of circRNAs need to be evaluated carefully. In the future, studies should overcome and solve these challenges and questions in order to better understand the roles of m6A in circRNAs biology further.

AUTHOR CONTRIBUTIONS

HS and LT designed and executed the study. JW and XG collected and analyzed the data, and wrote the manuscript. YW and SH made the figures. XY was responsible for language quality. All authors contributed to the article and approved the submitted version.

FUNDING

This work was supported by the National Natural Science Foundation of China (Grant No. 81772001) and the National Clinical Key Subject of China (Grant No. 41732113).

REFERENCES

- Aufiero, S., Reckman, Y. J., Pinto, Y. M., and Creemers, E. E. (2019). Circular RNAs open a new chapter in cardiovascular biology. *Nat. Rev. Cardiol.* 16, 503–514. doi: 10.1038/s41569-019-0185-2
- Aufiero, S., Van Den Hoogenhof, M. M. G., Reckman, Y. J., Beqqali, A., Van Der Made, I., Kluin, J., et al. (2018). Cardiac circRNAs arise mainly from constitutive exons rather than alternatively spliced exons. *RNA* 24, 815–827. doi: 10.1261/rna.064394.117
- Barbagallo, D., Caponnetto, A., Brex, D., Mirabella, F., Barbagallo, C., Lauro, G., et al. (2019). CircSMARCA5 regulates VEGFA mRNA splicing and angiogenesis in glioblastoma multiforme through the binding of SRSF1. *Cancers (Basel)* 11:194. doi: 10.3390/cancers11020194
- Bokar, J. A., Shambaugh, M. E., Polayes, D., Matera, A. G., and Rottman, F. M. (1997). Purification and cDNA cloning of the AdoMet-binding subunit of the human mRNA (N6-adenosine)-methyltransferase. *RNA* 3, 1233–1247.
- Brown, J. A., Kinzig, C. G., Degregorio, S. J., and Steitz, J. A. (2016). Methyltransferase-like protein 16 binds the 3'-terminal triple helix of MALAT1

- long noncoding RNA. *Proc. Natl. Acad. Sci. U.S.A.* 113, 14013–14018. doi: 10.1073/pnas.1614759113
- Chen, C., Yuan, W., Zhou, Q., Shao, B., Guo, Y., Wang, W., et al. (2021). N6-methyladenosine-induced circ1662 promotes metastasis of colorectal cancer by accelerating YAP1 nuclear localization. *Theranostics* 11, 4298–4315. doi: 10.7150/thno.51342
- Chen, C. Y., and Sarnow, P. (1995). Initiation of protein synthesis by the eukaryotic translational apparatus on circular RNAs. *Science* 268, 415–417. doi: 10.1126/science.7536344
- Chen, L. L., and Yang, L. (2015). Regulation of circRNA biogenesis. *RNA Biol* 12, 381–388. doi: 10.1080/15476286.2015.1020271
- Chen, R. X., Chen, X., Xia, L. P., Zhang, J. X., Pan, Z. Z., Ma, X. D., et al. (2019). N(6)-methyladenosine modification of circNSUN2 facilitates cytoplasmic export and stabilizes HMGA2 to promote colorectal liver metastasis. *Nat. Commun.* 10:4695. doi: 10.1038/s41467-019-12651-2
- Chen, X., Yang, T., Wang, W., Xi, W., Zhang, T., Li, Q., et al. (2019). Circular RNAs in immune responses and immune diseases. *Theranostics* 9, 588–607. doi: 10.7150/thno.29678
- Chen, Y. G., Chen, R., Ahmad, S., Verma, R., Kasturi, S. P., Amaya, L., et al. (2019). N6-Methyladenosine modification controls circular RNA immunity. *Mol. Cell* 76, 96.e9–109.e9.
- Chen, Y. G., Kim, M. V., Chen, X., Batista, P. J., Aoyama, S., Wilusz, J. E., et al. (2017). Sensing self and foreign circular RNAs by intron identity. *Mol. Cell* 67, 228.e5–238.e5.
- Cheng, Z., Yu, C., Cui, S., Wang, H., Jin, H., Wang, C., et al. (2019). circTP63 functions as a ceRNA to promote lung squamous cell carcinoma progression by upregulating FOXM1. *Nat. Commun.* 10:3200.
- Chibwesha, C. J., and Stringer, J. S. A. (2019). Cervical cancer as a global concern: contributions of the dual epidemics of HPV and HIV. *JAMA* 322, 1558–1560. doi: 10.1001/jama.2019.16176
- Conn, S. J., Pillman, K. A., Toubia, J., Conn, V. M., Salamanidis, M., Phillips, C. A., et al. (2015). The RNA binding protein quaking regulates formation of circRNAs. *Cell* 160, 1125–1134. doi: 10.1016/j.cell.2015.02.014
- Desrosiers, R., Friderici, K., and Rottman, F. (1974). Identification of methylated nucleosides in messenger RNA from Novikoff hepatoma cells. *Proc. Natl. Acad. Sci. U.S.A.* 71, 3971–3975. doi: 10.1073/pnas.71.10.3971
- Di Timoteo, G., Dattilo, D., Centrón-Broco, A., Colantoni, A., Guarnacci, M., Rossi, F., et al. (2020). Modulation of circRNA metabolism by m(6)A modification. *Cell Rep.* 31:107641. doi: 10.1016/j.celrep.2020.107641
- Du, H., Zhao, Y., He, J., Zhang, Y., Xi, H., Liu, M., et al. (2016). YTHDF2 destabilizes m(6)A-containing RNA through direct recruitment of the CCR4-NOT deadenylase complex. *Nat. Commun.* 7:12626.
- Du, W. W., Yang, W., Liu, E., Yang, Z., Dhaliwal, P., and Yang, B. B. (2016). Foxo3 circular RNA retards cell cycle progression via forming ternary complexes with p21 and CDK2. *Nucleic Acids Res.* 44, 2846–2858. doi: 10.1093/nar/gkw027
- Edens, B. M., Vissers, C., Su, J., Arumugam, S., Xu, Z., Shi, H., et al. (2019). FMRP modulates neural differentiation through m(6)A-Dependent mRNA nuclear export. *Cell Rep.* 28, 845.e5–854.e5.
- Frye, M., Harada, B. T., Behm, M., and He, C. (2018). RNA modifications modulate gene expression during development. *Science* 361, 1346–1349. doi: 10.1126/science.aau1646
- Galiè, N., Humbert, M., Vachieri, J. L., Gibbs, S., Lang, I., Torbicki, A., et al. (2016). 2015 ESC/ERS guidelines for the diagnosis and treatment of pulmonary hypertension. *Rev. Esp. Cardiol. (Engl Ed)* 69:177. doi: 10.1016/j.rec.2016.01.002
- Godet, A. C., David, F., Hantelys, F., Tatin, F., Lacazette, E., Garmy-Susini, B., et al. (2019). IRES trans-acting factors, key actors of the stress response. *Int. J. Mol. Sci.* 20:924. doi: 10.3390/ijms20040924
- Gross, J. D., Moerke, N. J., Von Der Haar, T., Lugovskoy, A. A., Sachs, A. B., McCarthy, J. E., et al. (2003). Ribosome loading onto the mRNA cap is driven by conformational coupling between eIF4G and eIF4E. *Cell* 115, 739–750. doi: 10.1016/s0092-8674(03)00975-9
- Gu, J., Zhan, Y., Zhuo, L., Zhang, Q., Li, G., Li, Q., et al. (2021). Biological functions of m(6)A methyltransferases. *Cell Biosci.* 11:15.
- Guo, M., Yan, R., Ji, Q., Yao, H., Sun, M., Duan, L., et al. (2020). IFN regulatory Factor-1 induced macrophage pyroptosis by modulating m6A modification of circ_0029589 in patients with acute coronary syndrome. *Int. Immunopharmacol.* 86:106800. doi: 10.1016/j.intimp.2020.106800
- Guo, M., Yan, R., Yao, H., Duan, L., Sun, M., Xue, Z., et al. (2019). IFN regulatory factor 1 mediates macrophage pyroptosis induced by oxidized low-density lipoprotein in patients with acute coronary syndrome. *Mediators Inflamm.* 2019:2917128.
- Hansen, T. B., Wiklund, E. D., Bramsen, J. B., Villadsen, S. B., Statham, A. L., Clark, S. J., et al. (2011). miRNA-dependent gene silencing involving Ago2-mediated cleavage of a circular antisense RNA. *EMBO J.* 30, 4414–4422. doi: 10.1038/emboj.2011.359
- He, R. Z., Jiang, J., and Luo, D. X. (2020). The functions of N6-methyladenosine modification in lncRNAs. *Genes Dis.* 7, 598–605. doi: 10.1016/j.gendis.2020.03.005
- He, R. Z., Jiang, J., and Luo, D. X. (2021). M6A modification of circNSUN2 promotes colorectal liver metastasis. *Genes Dis.* 8, 6–7. doi: 10.1016/j.gendis.2019.12.002
- Hizir, Z., Bottini, S., Grandjean, V., Trabucchi, M., and Repetto, E. (2017). RNY (YRNA)-derived small RNAs regulate cell death and inflammation in monocytes/macrophages. *Cell Death Dis.* 8:e2530. doi: 10.1038/cddis.2016.429
- Hofheinz, R. D., and Stintzing, S. (2019). Study evidence confirms current clinical practice in refractory metastatic colorectal cancer: the ReDOS trial. *Lancet Oncol.* 20, 1036–1037. doi: 10.1016/s1470-2045(19)30390-0
- Horiuchi, K., Kawamura, T., Iwanari, H., Ohashi, R., Naito, M., Kodama, T., et al. (2013). Identification of Wilms' tumor 1-associating protein complex and its role in alternative splicing and the cell cycle. *J. Biol. Chem.* 288, 33292–33302. doi: 10.1074/jbc.m113.500397
- Ho-Xuan, H., Glazar, P., Latini, C., Heizler, K., Haase, J., Hett, R., et al. (2020). Comprehensive analysis of translation from overexpressed circular RNAs reveals pervasive translation from linear transcripts. *Nucleic Acids Res.* 48, 10368–10382. doi: 10.1093/nar/gkaa704
- Hsiao, K. Y., Sun, H. S., and Tsai, S. J. (2017). Circular RNA - New member of noncoding RNA with novel functions. *Exp. Biol. Med. (Maywood)* 242, 1136–1141. doi: 10.1177/1535370217708978
- Hsu, M. T., and Coca-Prados, M. (1979). Electron microscopic evidence for the circular form of RNA in the cytoplasm of eukaryotic cells. *Nature* 280, 339–340. doi: 10.1038/280339a0
- Hsu, P. J., Zhu, Y., Ma, H., Guo, Y., Shi, X., Liu, Y., et al. (2017). Ythdc2 is an N(6)-methyladenosine binding protein that regulates mammalian spermatogenesis. *Cell Res.* 27, 1115–1127. doi: 10.1038/cr.2017.99
- Hu, B., Elinav, E., Huber, S., Booth, C. J., Strowig, T., Jin, C., et al. (2010). Inflammation-induced tumorigenesis in the colon is regulated by caspase-1 and NLR4. *Proc. Natl. Acad. Sci. U.S.A.* 107, 21635–21640. doi: 10.1073/pnas.1016814108
- Huang, C., Liang, D., Tatomer, D. C., and Wilusz, J. E. (2018). A length-dependent evolutionarily conserved pathway controls nuclear export of circular RNAs. *Genes Dev.* 32, 639–644. doi: 10.1101/gad.314856.118
- Huang, H., Weng, H., Sun, W., Qin, X., Shi, H., Wu, H., et al. (2018). Recognition of RNA N(6)-methyladenosine by IGF2BP proteins enhances mRNA stability and translation. *Nat. Cell Biol.* 20, 285–295. doi: 10.1038/s41556-018-0045-z
- Huang, W., Ling, Y., Zhang, S., Xia, Q., Cao, R., Fan, X., et al. (2021). TransCirc: an interactive database for translatable circular RNAs based on multi-omics evidence. *Nucleic Acids Res.* 49, D236–D242.
- Ivanov, A., Memczak, S., Wyler, E., Torti, F., Porath, H. T., Orejuela, M. R., et al. (2015). Analysis of intron sequences reveals hallmarks of circular RNA biogenesis in animals. *Cell Rep.* 10, 170–177. doi: 10.1016/j.celrep.2014.12.019
- Jeck, W. R., Sorrentino, J. A., Wang, K., Slevin, M. K., Burd, C. E., Liu, J., et al. (2013). Circular RNAs are abundant, conserved, and associated with ALU repeats. *RNA* 19, 141–157. doi: 10.1261/rna.035667.112
- Jia, G., Fu, Y., Zhao, X., Dai, Q., Zheng, G., Yang, Y., et al. (2011). N6-methyladenosine in nuclear RNA is a major substrate of the obesity-associated FTO. *Nat. Chem. Biol.* 7, 885–887. doi: 10.1038/nchembio.687
- Jia, R., Xiao, M. S., Li, Z., Shan, G., and Huang, C. (2019). Defining an evolutionarily conserved role of GW182 in circular RNA degradation. *Cell Discov.* 5:45.
- Jiang, X., Liu, B., Nie, Z., Duan, L., Xiong, Q., Jin, Z., et al. (2021). The role of m6A modification in the biological functions and diseases. *Signal Transduct. Target Ther.* 6:74.
- Kasowitz, S. D., Ma, J., Anderson, S. J., Leu, N. A., Xu, Y., Gregory, B. D., et al. (2018). Nuclear m6A reader YTHDC1 regulates alternative polyadenylation and splicing during mouse oocyte development. *PLoS Genet.* 14:e1007412. doi: 10.1371/journal.pgen.1007412

- Khairallah, M., Kahloun, R., Bourne, R., Limburg, H., Flaxman, S. R., Jonas, J. B., et al. (2015). Number of people blind or visually impaired by cataract worldwide and in world regions, 1990 to 2010. *Invest. Ophthalmol. Vis. Sci.* 56, 6762–6769. doi: 10.1167/iops.15-17201
- Knuckles, P., Lence, T., Haussmann, I. U., Jacob, D., Kreim, N., Carl, S. H., et al. (2018). Zc3h13/Flacc is required for adenosine methylation by bridging the mRNA-binding factor Rbm15/Spenito to the m(6)A machinery component Wtap/Fl(2)d. *Genes Dev.* 32, 415–429. doi: 10.1101/gad.309146.117
- Kramer, M. C., Liang, D., Tatomer, D. C., Gold, B., March, Z. M., Cherry, S., et al. (2015). Combinatorial control of Drosophila circular RNA expression by intronic repeats, hnRNPs, and SR proteins. *Genes Dev.* 29, 2168–2182. doi: 10.1101/gad.270421.115
- Lee, J. M., Choi, S. S., Lee, Y. H., Khim, K. W., Yoon, S., Kim, B. G., et al. (2018). The E3 ubiquitin ligase TRIM25 regulates adipocyte differentiation via proteasome-mediated degradation of PPAR γ . *Exp. Mol. Med.* 50, 1–11. doi: 10.1038/s12276-018-0162-6
- Legnini, I., Di Timoteo, G., Rossi, F., Morlando, M., Briganti, F., Sthandier, O., et al. (2017). Circ-ZNF609 is a circular RNA that can be translated and functions in myogenesis. *Mol. Cell* 66, 22.e9–37.e9.
- Li, B., Zhu, L., Lu, C., Wang, C., Wang, H., Jin, H., et al. (2021). circNDUFB2 inhibits non-small cell lung cancer progression via destabilizing IGF2BPs and activating anti-tumor immunity. *Nat. Commun.* 12:295.
- Li, P., Yu, H., Zhang, G., Kang, L., Qin, B., Cao, Y., et al. (2020). Identification and characterization of N6-Methyladenosine CircRNAs and methyltransferases in the lens epithelium cells from age-related cataract. *Invest. Ophthalmol. Vis. Sci.* 61:13. doi: 10.1167/iops.61.10.13
- Li, Z., Huang, C., Bao, C., Chen, L., Lin, M., Wang, X., et al. (2015). Exon-intron circular RNAs regulate transcription in the nucleus. *Nat. Struct. Mol. Biol.* 22, 256–264. doi: 10.1038/nsmb.2959
- Liang, W. C., Wong, C. W., Liang, P. P., Shi, M., Cao, Y., Rao, S. T., et al. (2019). Translation of the circular RNA circ β -catenin promotes liver cancer cell growth through activation of the Wnt pathway. *Genome Biol.* 20:84.
- Liu, C. X., Li, X., Nan, F., Jiang, S., Gao, X., Guo, S. K., et al. (2019). Structure and degradation of circular RNAs regulate PKR activation in innate immunity. *Cell* 177, 865.e1–880.e1. doi: 10.1016/j.cell.2019.03.046
- Liu, J., Yue, Y., Han, D., Wang, X., Fu, Y., Zhang, L., et al. (2014). A METTL3-METTL14 complex mediates mammalian nuclear RNA N6-adenosine methylation. *Nat. Chem. Biol.* 10, 93–95. doi: 10.1038/nchembio.1432
- Liu, N., Dai, Q., Zheng, G., He, C., Parisien, M., and Pan, T. (2015). N(6)-methyladenosine-dependent RNA structural switches regulate RNA-protein interactions. *Nature* 518, 560–564. doi: 10.1038/nature14234
- Liu, X., Zhang, Z., Ruan, J., Pan, Y., Magupalli, V. G., Wu, H., et al. (2016). Inflammasome-activated gasdermin D causes pyroptosis by forming membrane pores. *Nature* 535, 153–158. doi: 10.1038/nature18629
- Martinet, W., Coornaert, I., Puylaert, P., and De Meyer, G. R. Y. (2019). Macrophage death as a pharmacological target in atherosclerosis. *Front. Pharmacol.* 10:306. doi: 10.3389/fphar.2019.00306
- Memczak, S., Jens, M., Elefsinioti, A., Torti, F., Krueger, J., Rybak, A., et al. (2013). Circular RNAs are a large class of animal RNAs with regulatory potency. *Nature* 495, 333–338. doi: 10.1038/nature11928
- Meng, S., Zhou, H., Feng, Z., Xu, Z., Tang, Y., Li, P., et al. (2017). CircRNA: functions and properties of a novel potential biomarker for cancer. *Mol. Cancer* 16:94.
- Meng, X., Li, X., Zhang, P., Wang, J., Zhou, Y., and Chen, M. (2017). Circular RNA: an emerging key player in RNA world. *Brief Bioinform.* 18, 547–557. doi: 10.1093/bib/bbw045
- Meyer, K. D., Patil, D. P., Zhou, J., Zinoviev, A., Skabkin, M. A., Elemento, O., et al. (2015). 5' UTR m(6)A promotes cap-independent translation. *Cell* 163, 999–1010. doi: 10.1016/j.cell.2015.10.012
- Meyer, K. D., Saletore, Y., Zumbo, P., Elemento, O., Mason, C. E., and Jaffrey, S. R. (2012). Comprehensive analysis of mRNA methylation reveals enrichment in 3' UTRs and near stop codons. *Cell* 149, 1635–1646. doi: 10.1016/j.cell.2012.05.003
- Nahand, J. S., Jamshidi, S., Hamblin, M. R., Mahjoubin-Tehran, M., Vosough, M., Jamali, M., et al. (2020). Circular RNAs: new epigenetic signatures in viral infections. *Front. Microbiol.* 11:1853. doi: 10.3389/fmicb.2020.01853
- Nicolet, B. P., Engels, S., Aglialoro, F., Van Den Akker, E., Von Lindern, M., and Wolkers, M. C. (2018). Circular RNA expression in human hematopoietic cells is widespread and cell-type specific. *Nucleic Acids Res.* 46, 8168–8180. doi: 10.1093/nar/gky721
- Niu, X., Xu, J., Liu, J., Chen, L., Qiao, X., and Zhong, M. (2020). Landscape of N(6)-Methyladenosine modification patterns in human ameloblastoma. *Front. Oncol.* 10:556497. doi: 10.3389/fonc.2020.556497
- Pamudurti, N. R., Bartok, O., Jens, M., Ashwal-Fluss, R., Stottmeister, C., Ruhe, L., et al. (2017). Translation of CircRNAs. *Mol. Cell* 66, 9.e7–21.e7.
- Panda, A. C., Grammatikakis, I., Munk, R., Gorospe, M., and Abdelmohsen, K. (2017). Emerging roles and context of circular RNAs. *Wiley Interdiscip. Rev. RNA* 8:10.1002/wrna.1386. doi: 10.1002/wrna.1386
- Park, O. H., Ha, H., Lee, Y., Boo, S. H., Kwon, D. H., Song, H. K., et al. (2019). Endoribonucleolytic cleavage of m(6)A-Containing RNAs by RNase P/MRP complex. *Mol. Cell* 74, 494.e8–507.e8. doi: 10.1016/j.molcel.2019.02.034
- Patil, D. P., Chen, C. K., Pickering, B. F., Chow, A., Jackson, C., Guttman, M., et al. (2016). m(6)A RNA methylation promotes XIST-mediated transcriptional repression. *Nature* 537, 369–373. doi: 10.1038/nature19342
- Pendleton, K. E., Chen, B., Liu, K., Hunter, O. V., Xie, Y., Tu, B. P., et al. (2017). The U6 snRNA m(6)A Methyltransferase METTL16 regulates SAM synthetase intron retention. *Cell* 169, 824.e4–835.e4.
- Ping, X. L., Sun, B. F., Wang, L., Xiao, W., Yang, X., Wang, W. J., et al. (2014). Mammalian WTAP is a regulatory subunit of the RNA N6-methyladenosine methyltransferase. *Cell Res.* 24, 177–189. doi: 10.1038/cr.2014.3
- Pugliese, S. C., Poth, J. M., Fini, M. A., Olschewski, A., El Kasmi, K. C., and Stenmark, K. R. (2015). The role of inflammation in hypoxic pulmonary hypertension: from cellular mechanisms to clinical phenotypes. *Am. J. Physiol. Lung Cell Mol. Physiol.* 308, L229–L252.
- Rao, X., Lai, L., Li, X., Wang, L., Li, A., and Yang, Q. (2021). N(6)-methyladenosine modification of circular RNA circ-ARL3 facilitates Hepatitis B virus-associated hepatocellular carcinoma via sponging miR-1305. *IUBMB Life* 73, 408–417. doi: 10.1002/iub.2438
- Reikine, S., Nguyen, J. B., and Modis, Y. (2014). Pattern recognition and signaling mechanisms of RIG-I and MDA5. *Front. Immunol.* 5:342. doi: 10.3389/fimmu.2014.00342
- Roundtree, I. A., Evans, M. E., Pan, T., and He, C. (2017a). Dynamic RNA modifications in gene expression regulation. *Cell* 169, 1187–1200. doi: 10.1016/j.cell.2017.05.045
- Roundtree, I. A., Luo, G. Z., Zhang, Z., Wang, X., Zhou, T., Cui, Y., et al. (2017b). YTHDC1 mediates nuclear export of N(6)-methyladenosine methylated mRNAs. *Elife* 6:e31311.
- Růžicka, K., Zhang, M., Campilho, A., Bodi, Z., Kashif, M., Saleh, M., et al. (2017). Identification of factors required for m(6) A mRNA methylation in Arabidopsis reveals a role for the conserved E3 ubiquitin ligase HAKAI. *New Phytol.* 215, 157–172. doi: 10.1111/nph.14586
- Rybak-Wolf, A., Stottmeister, C., Glažar, P., Jens, M., Pino, N., Giusti, S., et al. (2015). Circular RNAs in the mammalian brain are highly abundant, conserved, and dynamically expressed. *Mol. Cell* 58, 870–885. doi: 10.1016/j.molcel.2015.03.027
- Sanger, H. L., Klotz, G., Riesner, D., Gross, H. J., and Kleinschmidt, A. K. (1976). Viroids are single-stranded covalently closed circular RNA molecules existing as highly base-paired rod-like structures. *Proc. Natl. Acad. Sci. U.S.A.* 73, 3852–3856. doi: 10.1073/pnas.73.11.3852
- Schlee, M. (2013). Master sensors of pathogenic RNA - RIG-I like receptors. *Immunobiology* 218, 1322–1335. doi: 10.1016/j.imbio.2013.06.007
- Sekar, D., and Lakshmanan, G. (2020). Methylation of N6-adenosine (m6A) modification in miRNAs and its implications in immunity. *Epigenomics* 12, 1083–1085. doi: 10.2217/epi-2020-0131
- Shi, H., Wang, X., Lu, Z., Zhao, B. S., Ma, H., Hsu, P. J., et al. (2017). YTHDF3 facilitates translation and decay of N(6)-methyladenosine-modified RNA. *Cell Res.* 27, 315–328. doi: 10.1038/cr.2017.15
- Shulman, Z., and Stern-Ginossar, N. (2020). The RNA modification N(6)-methyladenosine as a novel regulator of the immune system. *Nat. Immunol.* 21, 501–512. doi: 10.1038/s41590-020-0650-4
- Su, H., Wang, G., Wu, L., Ma, X., Ying, K., and Zhang, R. (2020). Transcriptome-wide map of m(6)A circRNAs identified in a rat model of hypoxia mediated pulmonary hypertension. *BMC Genomics* 21:39. doi: 10.1186/s12864-020-6462-y

- Suzuki, H., and Tsukahara, T. (2014). A view of pre-mRNA splicing from RNase R resistant RNAs. *Int. J. Mol. Sci.* 15, 9331–9342. doi: 10.3390/ijms15069331
- Tang, C., Xie, Y., Yu, T., Liu, N., Wang, Z., Woolsey, R. J., et al. (2020). m(6)A-dependent biogenesis of circular RNAs in male germ cells. *Cell Res.* 30, 211–228. doi: 10.1038/s41422-020-0279-8
- Thomson, D. W., and Dinger, M. E. (2016). Endogenous microRNA sponges: evidence and controversy. *Nat. Rev. Genet.* 17, 272–283. doi: 10.1038/nrg.2016.20
- Wang, P. L., Bao, Y., Yee, M. C., Barrett, S. P., Hogan, G. J., Olsen, M. N., et al. (2014). Circular RNA is expressed across the eukaryotic tree of life. *PLoS One* 9:e90859. doi: 10.1371/journal.pone.0090859
- Wang, X., Zhao, B. S., Roundtree, I. A., Lu, Z., Han, D., Ma, H., et al. (2015). N(6)-methyladenosine modulates messenger RNA translation efficiency. *Cell* 161, 1388–1399. doi: 10.1016/j.cell.2015.05.014
- Wang, Y., Wang, H., Xi, F., Wang, H., Han, X., Wei, W., et al. (2020). Profiling of circular RNA N(6)-methyladenosine in moso bamboo (*Phyllostachys edulis*) using nanopore-based direct RNA sequencing. *J. Integr. Plant Biol.* 62, 1823–1838. doi: 10.1111/jipb.13002
- Warda, A. S., Kretschmer, J., Hackert, P., Lenz, C., Urlaub, H., Höbartner, C., et al. (2017). Human METTL16 is a N(6)-methyladenosine (m(6)A) methyltransferase that targets pre-mRNAs and various non-coding RNAs. *EMBO Rep.* 18, 2004–2014. doi: 10.15252/embr.201744940
- Wu, J., and Chen, Z. J. (2014). Innate immune sensing and signaling of cytosolic nucleic acids. *Annu. Rev. Immunol.* 32, 461–488. doi: 10.1146/annurev-immunol-032713-120156
- Wu, P., Fang, X., Liu, Y., Tang, Y., Wang, W., Li, X., et al. (2021). N6-methyladenosine modification of circCUX1 confers radioresistance of hypopharyngeal squamous cell carcinoma through caspase1 pathway. *Cell Death Dis.* 12:298.
- Wu, X., Xiao, Y., Ma, J., and Wang, A. (2020). Circular RNA: a novel potential biomarker for skin diseases. *Pharmacol Res* 158, 104841. doi: 10.1016/j.phrs.2020.104841
- Xia, S., Feng, J., Lei, L., Hu, J., Xia, L., Wang, J., et al. (2017). Comprehensive characterization of tissue-specific circular RNAs in the human and mouse genomes. *Brief Bioinform.* 18, 984–992. doi: 10.1093/bib/bbw081
- Xiao, W., Adhikari, S., Dahal, U., Chen, Y. S., Hao, Y. J., Sun, B. F., et al. (2016). Nuclear m(6)A reader YTHDC1 regulates mRNA splicing. *Mol. Cell* 61, 507–519. doi: 10.1016/j.molcel.2016.01.012
- Xu, J., Wan, Z., Tang, M., Lin, Z., Jiang, S., Ji, L., et al. (2020). N(6)-methyladenosine-modified CircRNA-SORE sustains sorafenib resistance in hepatocellular carcinoma by regulating β -catenin signaling. *Mol. Cancer* 19:163.
- Xu, Y. J., Zheng, L., Hu, Y. W., and Wang, Q. (2018). Pyroptosis and its relationship to atherosclerosis. *Clin. Chim. Acta* 476, 28–37. doi: 10.1016/j.cca.2017.11.005
- Yan, H., Li, Y., Peng, X., Huang, D., Gui, L., and Huang, B. (2016). Resistance of mitochondrial DNA-depleted cells against oxidized low-density lipoprotein-induced macrophage pyroptosis. *Mol. Med. Rep.* 13, 4393–4399. doi: 10.3892/mmr.2016.5077
- Yang, Y., Fan, X., Mao, M., Song, X., Wu, P., Zhang, Y., et al. (2017). Extensive translation of circular RNAs driven by N(6)-methyladenosine. *Cell Res.* 27, 626–641. doi: 10.1038/cr.2017.31
- Yang, Y., Gao, X., Zhang, M., Yan, S., Sun, C., Xiao, F., et al. (2018). Novel role of FBXW7 circular RNA in repressing glioma tumorigenesis. *J. Natl. Cancer Inst.* 110, 304–315. doi: 10.1093/jnci/djx166
- Yue, Y., Liu, J., Cui, X., Cao, J., Luo, G., Zhang, Z., et al. (2018). VIRMA mediates preferential m(6)A mRNA methylation in 3'UTR and near stop codon and associates with alternative polyadenylation. *Cell Discov.* 4:10.
- Zaccara, S., Ries, R. J., and Jaffrey, S. R. (2019). Reading, writing and erasing mRNA methylation. *Nat. Rev. Mol. Cell Biol.* 20, 608–624. doi: 10.1038/s41580-019-0168-5
- Zaphiropoulos, P. G. (1996). Circular RNAs from transcripts of the rat cytochrome P450 2C24 gene: correlation with exon skipping. *Proc. Natl. Acad. Sci. U.S.A.* 93, 6536–6541. doi: 10.1073/pnas.93.13.6536
- Zhang, C., Wang, J., Geng, X., Tu, J., Gao, H., Li, L., et al. (2020). Circular RNA expression profile and m6A modification analysis in poorly differentiated adenocarcinoma of the stomach. *Epigenomics* 12, 1027–1040. doi: 10.2217/epi-2019-0153
- Zhang, M., Huang, N., Yang, X., Luo, J., Yan, S., Xiao, F., et al. (2018a). A novel protein encoded by the circular form of the SHPRH gene suppresses glioma tumorigenesis. *Oncogene* 37, 1805–1814. doi: 10.1038/s41388-017-0019-9
- Zhang, M., Zhao, K., Xu, X., Yang, Y., Yan, S., Wei, P., et al. (2018b). A peptide encoded by circular form of LINC-PINT suppresses oncogenic transcriptional elongation in glioblastoma. *Nat. Commun.* 9:4475.
- Zhang, T. R., and Huang, W. Q. (2020). Angiogenic circular RNAs: a new landscape in cardiovascular diseases. *Microvasc. Res.* 129:103983. doi: 10.1016/j.mvr.2020.103983
- Zhang, X. O., Wang, H. B., Zhang, Y., Lu, X., Chen, L. L., and Yang, L. (2014). Complementary sequence-mediated exon circularization. *Cell* 159, 134–147. doi: 10.1016/j.cell.2014.09.001
- Zhang, Y., Liang, W., Zhang, P., Chen, J., Qian, H., Zhang, X., et al. (2017). Circular RNAs: emerging cancer biomarkers and targets. *J. Exp. Clin. Cancer Res.* 36:152.
- Zhao, B. S., Roundtree, I. A., and He, C. (2017). Post-transcriptional gene regulation by mRNA modifications. *Nat. Rev. Mol. Cell Biol.* 18, 31–42. doi: 10.1038/nrm.2016.132
- Zhao, J., Lee, E. E., Kim, J., Yang, R., Chamseddin, B., Ni, C., et al. (2019). Transforming activity of an oncoprotein-encoding circular RNA from human papillomavirus. *Nat. Commun.* 10:2300.
- Zheng, G., Dahl, J. A., Niu, Y., Fedorcsak, P., Huang, C. M., Li, C. J., et al. (2013). ALKBH5 is a mammalian RNA demethylase that impacts RNA metabolism and mouse fertility. *Mol. Cell* 49, 18–29. doi: 10.1016/j.molcel.2012.10.015
- Zhou, C., Molin, B., Daneshvar, K., Pondick, J. V., Wang, J., Van Wittenberghe, N., et al. (2017). Genome-wide maps of m6A circRNAs identify widespread and cell-type-specific methylation patterns that are distinct from mRNAs. *Cell Rep.* 20, 2262–2276. doi: 10.1016/j.celrep.2017.08.027
- Zhou, J., Wan, J., Gao, X., Zhang, X., Jaffrey, S. R., and Qian, S. B. (2015). Dynamic m(6)A mRNA methylation directs translational control of heat shock response. *Nature* 526, 591–594. doi: 10.1038/nature15377
- Zhou, J., Wan, J., Shu, X. E., Mao, Y., Liu, X. M., Yuan, X., et al. (2018). N(6)-Methyladenosine guides mRNA alternative translation during integrated stress response. *Mol. Cell* 69, 636.e7–647.e7.
- Zhu, Z. M., Huo, F. C., and Pei, D. S. (2020). Function and evolution of RNA N6-methyladenosine modification. *Int. J. Biol. Sci.* 16, 1929–1940. doi: 10.7150/ijbs.45231
- Zitvogel, L., Kepp, O., Galluzzi, L., and Kroemer, G. (2012). Inflammasomes in carcinogenesis and anticancer immune responses. *Nat. Immunol.* 13, 343–351. doi: 10.1038/ni.2224

Conflict of Interest: The authors declare that the research was conducted in the absence of any commercial or financial relationships that could be construed as a potential conflict of interest.

Publisher's Note: All claims expressed in this article are solely those of the authors and do not necessarily represent those of their affiliated organizations, or those of the publisher, the editors and the reviewers. Any product that may be evaluated in this article, or claim that may be made by its manufacturer, is not guaranteed or endorsed by the publisher.

Copyright © 2021 Wu, Guo, Wen, Huang, Yuan, Tang and Sun. This is an open-access article distributed under the terms of the Creative Commons Attribution License (CC BY). The use, distribution or reproduction in other forums is permitted, provided the original author(s) and the copyright owner(s) are credited and that the original publication in this journal is cited, in accordance with accepted academic practice. No use, distribution or reproduction is permitted which does not comply with these terms.



KIAA1429 and ALKBH5 Oppositely Influence Aortic Dissection Progression *via* Regulating the Maturation of Pri-miR-143-3p in an m6A-Dependent Manner

OPEN ACCESS

Edited by:

Jing Zhang,
Shanghai Jiao Tong University, China

Reviewed by:

Xiao-Yu Chen,
Shanghai Sixth People's Hospital,
China
Guihai Feng,
Institute of Zoology, Chinese
Academy of Sciences (CAS), China

*Correspondence:

Zhiwei Wang
wangzhiwei@whu.edu.cn

†ORCID:

Peng Wang
orcid.org/0000-0001-6013-7146
Zhiwei Wang
orcid.org/0000-0001-5643-9344

Specialty section:

This article was submitted to
Epigenomics and Epigenetics,
a section of the journal
Frontiers in Cell and Developmental
Biology

Received: 16 February 2021

Accepted: 15 July 2021

Published: 19 August 2021

Citation:

Wang P, Wang Z, Zhang M,
Wu Q, Shi F and Yuan S (2021)
KIAA1429 and ALKBH5 Oppositely
Influence Aortic Dissection
Progression *via* Regulating
the Maturation of Pri-miR-143-3p
in an m6A-Dependent Manner.
Front. Cell Dev. Biol. 9:668377.
doi: 10.3389/fcell.2021.668377

Peng Wang^{1,2,3†}, Zhiwei Wang^{1,2*†}, Min Zhang^{1,2}, Qi Wu^{1,2,3}, Feng Shi^{1,2,3} and Shun Yuan^{1,2,3}

¹ Department of Cardiovascular Surgery, Renmin Hospital of Wuhan University, Wuhan, China, ² Cardiovascular Surgery Laboratory, Renmin Hospital of Wuhan University, Wuhan, China, ³ Central Laboratory, Renmin Hospital of Wuhan University, Wuhan, China

Despite decades of study into aortic dissection (AD), a lethal cardiovascular emergency due to a tear in the aorta intima or bleeding within the aortic wall, leading to the separation of the different layers of it, the factors that influence its progression and the deeper regulatory mechanisms remain poorly understood. Nowadays, with the maturity of N6-methyladenosine (m6A) sequence technology, m6A modification, one type of RNA epigenesis, has gradually become a new research hotspot for epigenetic molecular regulation. Especially recently, increasing evidence has revealed that m6A modification functions as a pivotal post-transcriptional modification to influence the progression of multiple diseases. Based on these findings, it is reasonable to speculate that m6A modification may affect the onset and progression of AD. To explore the validity of our conjecture and to elucidate its underlying molecular mechanism of action, we conducted the present study. In this study, we found that KIAA1429 is downregulated while ALKBH5 is upregulated in aortic tissues from AD patients. Furthermore, gain- and loss-of-function studies showed that KIAA1429 and ALKBH5 can oppositely regulate HASMC proliferation, HAEC apoptosis, and AD progression in AngII-infused mice. Mechanistically, we demonstrated that KIAA1429/ALKBH5-mediated m6A modifications can regulate the processing of pri-miR-143-3p through interacting with the microprocessor protein DGCR8, thus indirectly regulating the downstream target gene of mature miR-143-3p, DDX6, to perform their biological functions *in vitro* and *in vivo*. Our findings have revealed a novel connection between m6A modification and AD progression and may provide a novel molecular basis for subsequent researchers to search for novel therapeutic approaches to improve the health of patients struggling with AD.

Keywords: aortic dissection, m6A, KIAA1429, ALKBH5, miR-143-3p

INTRODUCTION

Aortic dissection (AD) is a lethal cardiovascular emergency due to a tear in the aorta intima or bleeding within the aortic wall, leading to the separation of the different layers of the aortic wall (Gawinecka et al., 2017; Tchana-Sato et al., 2018). Despite decades of study into AD, the factors that influence its progression and the deeper regulatory mechanisms remain poorly understood. Therefore, one of the prerequisites to the development of novel coping strategies for AD is to elucidate the underlying molecular mechanisms involved.

According to the results of available studies, both decreased cell proliferation capacity of human aortic smooth muscle cells (HASMCs) and excessive apoptosis of human aortic endothelial cells (HAECs) in the arterial vascular wall are closely related to the development of AD (Lai et al., 2019; Song et al., 2019; Sun et al., 2020). Although numerous studies have confirmed this conclusion, the molecular regulatory mechanisms involved in HASMC and HAEC dysfunction are not well investigated, especially epigenetic studies. Epigenetic abnormalities mainly occur at the following levels: DNA (Cantara et al., 2011), RNA (Berger, 2002), and histone modification (Akhavan-Niaki and Samadani, 2013). At the RNA level, diverse types of posttranscriptional modifications have been recognized, among which N6-methyladenosine (m6A) RNA methylation is one of the most common modifications in eukaryote messenger RNAs (Desrosiers et al., 1974; Dominissini et al., 2012; Meyer et al., 2012).

Nowadays, with the maturity of m6A sequencing technology, m6A modification, one type of RNA epigenesis, has gradually become a new research hotspot for epigenetic molecular regulation (Frye et al., 2018; He et al., 2019). M6A modification has been confirmed to be a dynamic and reversible process modulated by m6A WERs (writers, readers, and erasers). The methyltransferase complex that catalyzes the formation of m6A methylation is called “writers,” among which methyltransferase like 3 (METTL3), methyltransferase like 14 (METTL14), Vir-like methyltransferase-associated (KIAA1429), and WT1-associated protein (WTAP) play vital roles (Lan et al., 2019). In turn, demethylase, fat mass and obesity-associated protein (FTO), and alkylation repair homolog protein 5 (ALKBH5) function as “erasers” to remove the m6A methylation (Meyer and Jaffrey, 2017). Meanwhile, several m6A-binding proteins, including YTHDC1/2, YTHDF1/2/3, and HNRNP, act as the “readers” to decode m6A methylation (Roundtree et al., 2017).

Recently, accumulating evidence has revealed that m6A modification influences the progression of multiple diseases through regulating non-coding RNA biogenesis. For instance, Zhang et al. (2019b) found that ALKBH5 could promote invasion and metastasis of gastric cancer *via* decreasing methylation of the lncRNA NEAT1. Zuo et al. (2020) reported that M6A-mediated upregulation of LINC00958 exacerbates hepatocellular carcinoma progression. Zhang et al. (2019a) demonstrated that excessive miR-25-3p expression induced by m6A promotes pancreatic cancer progression. However, the above findings mainly focus on the field of oncology, and whether m6A modification is also involved in human cardiovascular diseases

by regulating non-coding RNAs biogenesis has been less reported (Su et al., 2020).

This study aims to explore the role of m6A modification in the development of AD and elucidate the underlying mechanisms by which m6A modification influences AD progression.

MATERIALS AND METHODS

Clinical Samples

The collection and usage of clinical specimens in this study were approved by the Clinical Research Ethics Committees of Renmin Hospital of Wuhan University, China. Meanwhile, informed written consent of all participants was obtained. Aortic tissues ($n = 25$) were collected from acute thoracic AD patients who underwent emergency aortic replacement surgery from April 2018 to December 2019. Normal aorta tissues ($n = 25$) were obtained from heart donors declared brain dead. The clinical data of all donors and AD patients are present in **Supplementary Table 1**.

Cell Culture and Cell Transfection

HAECs were purchased from ATCC (#PCS-100-011TM, Manassas, VA, United States) and cultured in Endothelial Cell Growth Basal Medium-2 (Lonza, Basel, CHE). HASMCs were purchased from ATCC (#PCS-100-012TM) and cultured in DMEM (HyClone, Logan, UT, United States). All media were supplemented with endothelial cell growth factors, 5% fetal bovine serum (Invitrogen, Carlsbad, CA, United States), and 1% penicillin/streptomycin (Sigma, Darmstadt, DEU). The external conditions for cell culture were as follows: 37°C, humidified atmosphere containing 5% CO₂.

To obtain stable transfection cell lines, we transfected cells with diverse lentivirus vector (Genechem, Shanghai, China) carrying overexpression plasmids (termed as LV-KIAA1429/LV-ALKBH5), a negative control (termed as LV-NC), interfering RNA (termed as sh-KIAA1429/sh-ALKBH5), or scramble control (termed as sh-NC). Stable cell clones were selected by using puromycin (4 µg/ml) for 1 week. To interfere with miR-143-3p and DDX6 expression, miR-143-3p mimics, inhibitor, pcDNA3.1-DDX6, si-DDX6, or their respective negative controls (NC) were synthesized by GeneChem Co., Ltd. (Shanghai, China) and transiently transfected into cells using Lipofectamine 3000 reagent (Invitrogen).

AngII Infusion AD Model and Adenovirus Vector Transfection

The Ethical Committee of the Renmin Hospital of Wuhan University approved the animal experiments, which were designed in accordance with the Wuhan Directive for Animal Research and the Current Guidelines for the Care and Use of Laboratory Animals published by the National Institutes of Health (NIH). Male C57BL/6N mice were purchased from the Guangdong Medical Laboratory Animal Center (Foshan, China). The angiotensin II (AngII)-infusion mouse AD model was established as described in our previous study

(Wang et al., 2021). Concretely, osmotic mini-pumps (Alzet, Cupertino, CA, United States) containing AngII (1 μ g/kg/min, Enzo Biochem, New York, NY, United States) were implanted in 7-week-old male mice. Moreover, to interfere with the expression of KIAA1429, ALKBH5, or DDX6 *in vivo*, adeno-associated virus 9 (AAV9) vectors carrying a variety of overexpression plasmids or interfering RNA were randomly injected through the tail vein to C57BL/6N mice. All mice were monitored daily to record their survival time and death reasons. The experimental endpoint was mouse death from aortic rupture or treatment time up to 28 days. The aortas of mice were collected to confirm the formation of AD.

RNA Extraction and qRT-PCR

Total RNA was extracted from tissues and cells using Trizol Reagent (Invitrogen). Subsequent concentration determination of samples, reverse transcription, and qRT-PCR were performed as reported in our previous work (Wang et al., 2017). The expression of pri-miR-143-3p and pri-miR-3129 was examined using a TaqMan pri-miRNA assay. The primer sequences used in the present study are listed in **Supplementary Table 2**.

Western Blot

Cells or tissue samples were lysed by RIPA lysis buffer containing 1% protease inhibitors (Sigma). The protein extractions were quantified by BCA Protein Assay Kit (Beyotime, Shanghai, China). Western blot assays were performed as described in our previous work (Wang et al., 2017). Primary antibodies used in this study are shown in **Supplementary Table 3**.

Cell Proliferation Assays

The cell proliferation was detected by Cell Counting Kit-8 (CCK8, Dojindo, Kumamoto, Japan) and 5-ethynyl-2'-deoxyuridine (EdU; Ribobio, Guangzhou, China) assays. CCK8 assay was conducted as described in our previous work (Wang et al., 2017).

5-ethynyl-2'-deoxyuridine assay was performed in accordance with the protocol for the Click-iT[®] EdU Imaging Kit (Invitrogen). Cells were hatched with EdU for 2 h, then fixed in 4% paraformaldehyde for 1 h, and incubated with glycine. Subsequently, the cells were washed with TBS after being submerged into the cocktail for 0.5 h in darkness and further covered in Hoechst for 30 min. Images were captured by a fluorescence microscope (BX63, Olympus, Japan).

Cell Apoptosis Assays

In the TUNEL assay, cells were fixed in paraformaldehyde for 15 min and then stained by *in situ* Cell Death Detection Kit (TMR red) (Roche, Basel, CHE). We randomly chose six visual fields from each group to count the positive TUNEL-stained cells. Apoptotic cells were presented as percentages (cell count with positive TUNEL staining/cell count with positive DAPI staining) and we obtained images using a fluorescence microscope (BX63, Olympus).

In flow cytometry analysis, cells were collected, resuspended, and double-stained with Annexin V-FITC (#556547, BD Biosciences, Franklin, NJ, United States) as well as propidium

iodide (PI; Solarbio, Beijing, China) at room temperature for 10 min in darkness. Subsequently, cell apoptosis was analyzed using the FACScan flow cytometer installed with Cell Quest software (BD Biosciences).

RNA m6A Dot Blots

The Poly(A)⁺ RNAs (100 and 250 ng, respectively) were denatured and spotted onto a nylon membrane (Sigma) with a Bio-Dot apparatus (Bio-Rad, Hercules, CA, United States). Then, membranes were ultraviolet (UV) crosslinked, blocked, incubated with m6A antibody (#202003, Synaptic Systems, Canoga Park, CA, United States) overnight at 4°C, and hatched with HRP-conjugated anti-mouse IgG (Proteintech, Rosemont, IL, United States). After extensive washing, membranes were visualized by chemiluminescence system (Bio-Rad). Meanwhile, the membrane stained with 0.02% methylene blue (MB) in 0.3 M sodium acetate (pH 5.2) was used to show the consistency between groups.

Dual-Luciferase Reporter Assay

The 3'-UTR of DDX6 was amplified and then inserted into the *Xba*I restriction enzyme site of a pMiR-REPORTTM Luciferase vector (Promega, Madison, WI, United States). We mutated the binding site of miR-143-3p in the 3'-UTR-loading vectors using the QuikChange site-directed mutagenesis kit (Promega). The activity of firefly luciferase was detected by Dual-Luciferase Reporter Assay (Promega), being normalized to Renilla luciferase activity (Wang et al., 2017).

Ectopic Reporter Constructs

We recomposed a previously described ectopic reporter construct (Auyeung et al., 2013; Alarcón et al., 2015) to analyze the pri-miR-143-3p processing. Concretely, we displaced pri-miR-1-1, the miRNA control, with its modified version in which the adenosine [A] of the potential RRACH m6A sequence motif was mutated. We next placed it downstream of the query miRNA, either wild-type (WT) version (WT) or mutant version (Mut) pri-miR-143-3p in which the adenosine [A] of the RRACH m6A sequence motif was mutated to thymidine [T]. Then, these two constructs were transfected into cells utilizing Lipofectamine 3000 (Invitrogen), and qRT-PCR was used to determine the production of mature miR-1-1 and miR-143-3p.

RNA Immunoprecipitation Assay

RNA immunoprecipitation (RIP) assay was conducted using the Magna RIPTM RNA-Binding Protein Immunoprecipitation Kit (Millipore, MA, United States). After cells were lysed and centrifuged, the supernatant was incubated with magnetic beads conjugated with antibodies against Argonaute-2 (anti-Ago2) or anti-Immunoglobulin G (anti-IgG) at 4°C overnight. The precipitated RNAs were eluted, purified, and then detected by qRT-PCR.

m6A RNA Immunoprecipitation Assay

The RNAs isolated from cells were treated with DNase I (Thermo Fisher Scientific, United States) and then chemically fragmented

to 100 nt on the ice. The anti-m6A antibody (1:1,000, Abcam, United States) previously combined with magnetic Dynabeads (Thermo Fisher Scientific) was used for immunoprecipitations in the RIP Immunoprecipitation buffer (Magna RIP Kit, Millipore) and incubated with DNA-free fragmented RNAs. Then, the beads were treated with Proteinase K (25 mg/ml) at 42°C for 2 h. RNAs were extracted and subjected to qRT-PCR.

Co-immunoprecipitation Assay

Cell lysates were centrifuged and the supernatant was preincubated with 20 µg of protein A-Sepharose beads (Thermo Fisher Scientific) with vibrating for 2 h at 4°C. The samples were then centrifuged again and transferred to a new 2-ml EP tube. The samples were incubated with the primary antibodies for 1.5 h and then incubated with protein A-Sepharose beads to capture the immunocomplex. Next, the beads were washed three times, dissolved in electrophoresis sample loading buffer, and incubated for 15 min at 95°C.

Bioinformatics Database

We screened out candidate miRNAs whose expression might be regulated by KIAA1429 or ALKBH5 using the LinkedOmics database. We searched m6AVar database for the predicted m6A sites in pri-miR-143-3p. TargetScan (context score < -0.2), miRanda (score < -0.5), and PicTar (total context ++ score < -0.6) databases were used to predict the target genes of miRNA. The available addresses for the above databases are presented in **Supplementary Table 4**.

Statistical Analysis

All statistical analyses were performed by using GraphPad Prism 8.0 (GraphPad, United States) and SPSS 24.0 (IBM, United States), and two-tailed Student's *t*-test and Pearson's correlation coefficient analysis were, respectively, adopted to analyze differences between groups or the correlations between KIAA1429, ALKBH5, miR-143-3p, and DDX6. Kaplan–Meier curve with log-rank test was utilized to analyze the survival time. A two-sided *p*-value < 0.05 was considered to be statistically significant. Each experiment was performed in triplicate, and all data are expressed as mean ± standard error of the mean (SEM).

RESULTS

KIAA1429 Is Downregulated While ALKBH5 is Upregulated in Aorta Samples From AD Patients

To identify whether m6A modification was involved in AD development, we initially measured the expression levels of multiple key genes related to m6A, as described in section “Introduction,” in 25 pairs of aorta tissues derived from donors and AD patients. It was observed that KIAA1429 was significantly downregulated while ALKBH5 was upregulated in the aorta specimens of AD patients compared to donors (**Figure 1A** and **Supplementary Figure 1**). Subsequently, when the expression levels of KIAA1429 and ALKBH5 were further detected in 25

pairs of aorta samples from normal and AngII-induced AD mice, the same change trends emerged (**Figures 1B,C**). Furthermore, the protein levels of KIAA1429 and ALKBH5 in aorta specimens from AD patients were significantly lower and higher than in aorta tissues from donors, respectively (**Figures 1D,E**). Taken together, the aberrant expression of KIAA1429 and ALKBH5 in aortas of AD patients indicated that m6A modification mediated by methyltransferase or demethylase might be indeed involved in AD progression.

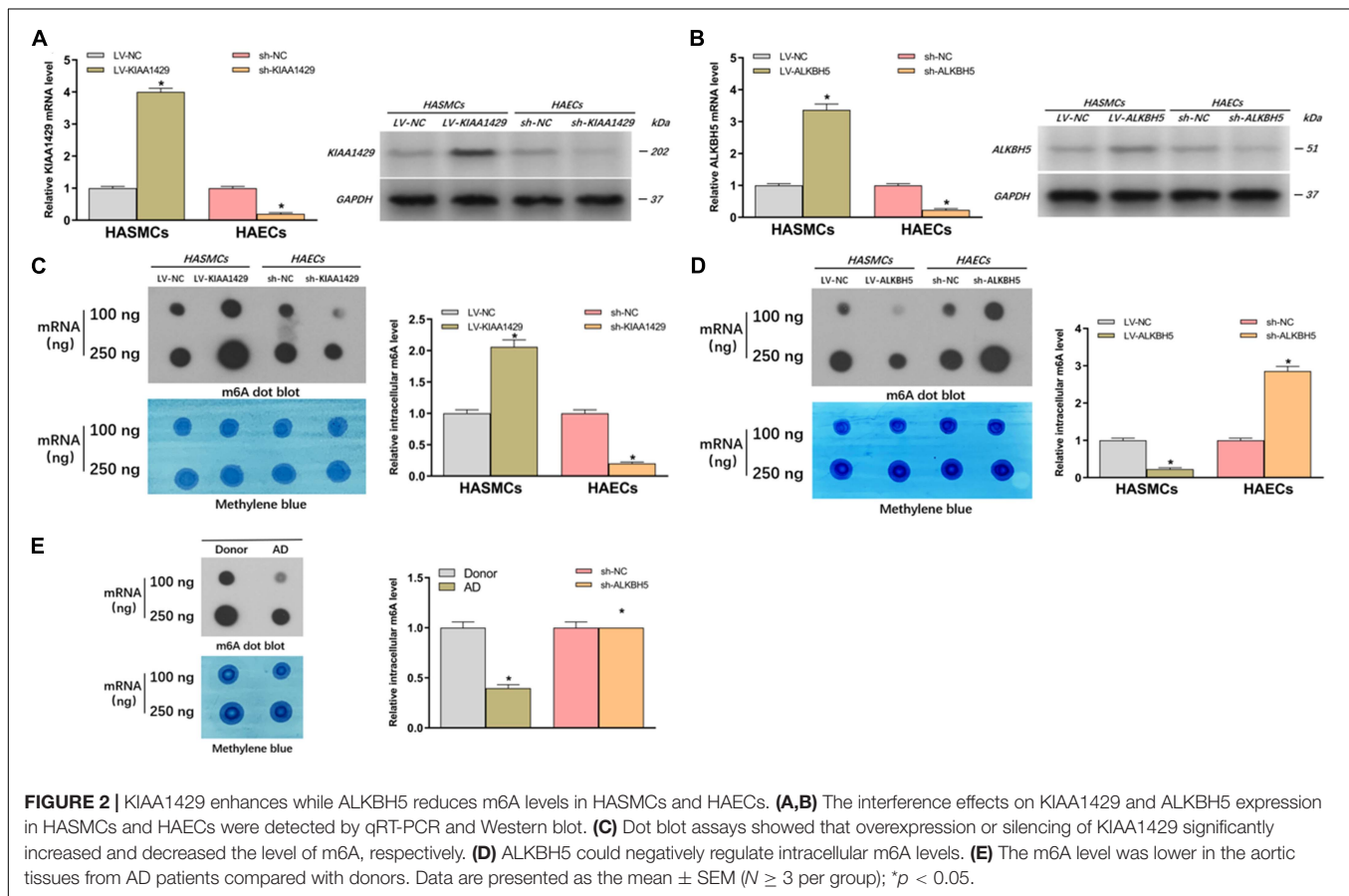
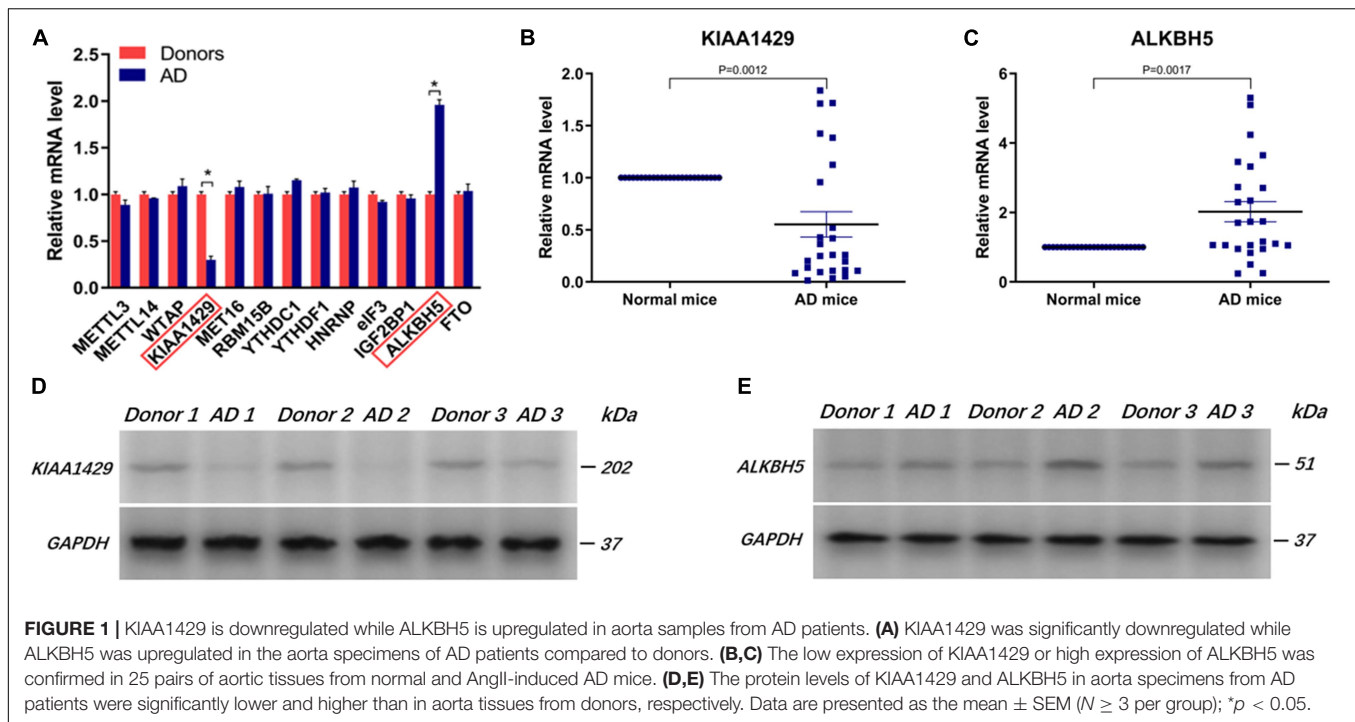
KIAA1429 Enhances While ALKBH5 Reduces m6A Levels in HASMCs and HAECS

To further clarify whether m6A modification is indeed related to AD progression, we investigated the effects of abnormally expressed KIAA1429 and ALKBH5 on m6A levels in HASMCs and HAECS. Firstly, cells were stably transfected with interfering lentiviral vectors and the corresponding control vectors. The interference effects were subsequently measured with qRT-PCR and Western blot (**Figures 2A,B**). Then, we measured the changes in intracellular levels by performing dot blot assays and observed that overexpression or silencing of KIAA1429 significantly increased and decreased the level of m6A, respectively (**Figure 2C**). On the contrary, we found that ALKBH5 could negatively regulate intracellular m6A levels (**Figure 2D**). Moreover, we explored whether there were differences between the m6A levels of AD patients and donors. The results showed that the m6A level was lower in the aortic tissues from AD patients compared with donors (**Figure 2E**). Collectively, our findings revealed that KIAA1429 and ALKBH5 could influence the development of AD by regulating m6A levels in HASMCs and HAECS.

KIAA1429 Can Promote HASMC Proliferation, Inhibit HAEC Apoptosis, and Inhibit AD Progression in AngII-Infused Mice

Because the aberrant expression of KIAA1429 in AD tissues had been identified by us, we then assessed the influences of KIAA1429 on the development of AD, including the effects on HASMC proliferation, HAEC apoptosis, and the incidence of AD in AngII-infused mice. Firstly, CCK8 and EdU assays were performed to investigate whether KIAA1429 is involved in HASMC proliferation. Both results indicated that KIAA1429 overexpression led to markedly enhanced HASMC proliferation while its knockdown resulted in significantly decreased HASMC proliferation (**Figures 3A,B** and **Supplementary Figure 7A**). Furthermore, the flow cytometry analysis revealed that overexpression of KIAA1429 notably promoted HAEC apoptosis while knockdown of it significantly inhibited HAEC apoptosis (**Figure 3C**).

To examine whether KIAA1429 affects the development of AD *in vivo*, we interfered with KIAA1429 expression in AngII-infused C57BL/6J mice by injecting AAV9 vectors harboring overexpression plasmids (termed as LV-KIAA1429), shRNA (termed as sh-KIAA1429), or corresponding NC through the



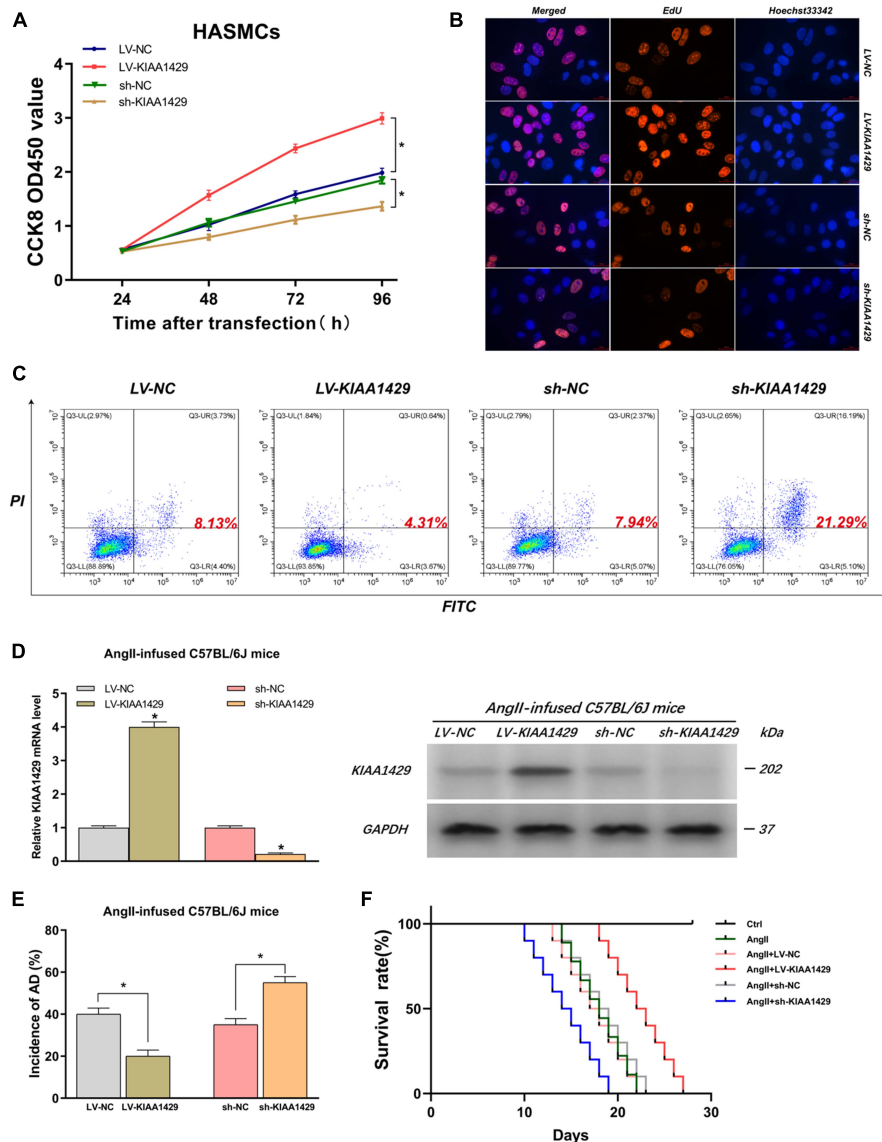


FIGURE 3 | KIAA1429 can promote HASMC proliferation, inhibit HAEC apoptosis, and inhibit AD progression in AngII-infused mice. **(A,B)** KIAA1429 overexpression led to markedly enhanced HASMC proliferation while its knockdown resulted in significantly decreased HASMC proliferation. **(C)** Flow cytometry analysis revealed that overexpression of KIAA1429 notably promoted HAEC apoptosis while knockdown of it significantly inhibited HAEC apoptosis. **(D)** The interference effects on KIAA1429 expression in AngII-infused C57BL/6J mice were detected by qRT-PCR and Western blot. **(E)** KIAA1429 overexpression reduced incidence while its knockdown increased the incidence of AD in AngII-infused mice. **(F)** Mice in the LV-KIAA1429 group and sh-KIAA1429 group had longer and shorter survival times compared to the control group, respectively. Data are presented as the mean \pm SEM ($N \geq 3$ per group); * $p < 0.05$.

tail vein and confirmed interference effect by measuring the mRNA and protein levels of KIAA1429 in arterial tissues of mice (Figure 3D). At 28 days after AngII infusion, the incidence of AD and the survival time of mice in different groups were counted and analyzed. The results indicated that KIAA1429 overexpression reduced the incidence while its knockdown increased the incidence of AD in AngII-infused mice (Figure 3E). Moreover, survival analysis results showed that mice in the LV-KIAA1429 group ($n = 25$) and sh-KIAA1429 group ($n = 25$) had longer and shorter survival times compared to the control group ($n = 25$), respectively (Figure 3F). Taken together, these

data revealed that KIAA1429 can promote the development of AD *in vivo* and *in vitro*.

ALKBH5 Can Suppress HASMC Proliferation, Promote HAEC Apoptosis, and Facilitate AD Progression in AngII-Infused Mice

By the same token, we explored the impacts of ALKBH5 on AD progression. Firstly, we performed CCK8 and EdU assays and found that overexpression of ALKBH5 significantly

inhibited HASMC proliferation while knockdown of ALKBH5 led to increased HASMC proliferation (Figures 4A,B and Supplementary Figure 7B). Subsequently, the flow cytometry

analysis showed that ALKBH5 overexpression notably promoted HAEC apoptosis while its knockdown significantly suppressed HAEC apoptosis (Figure 4C). Furthermore,

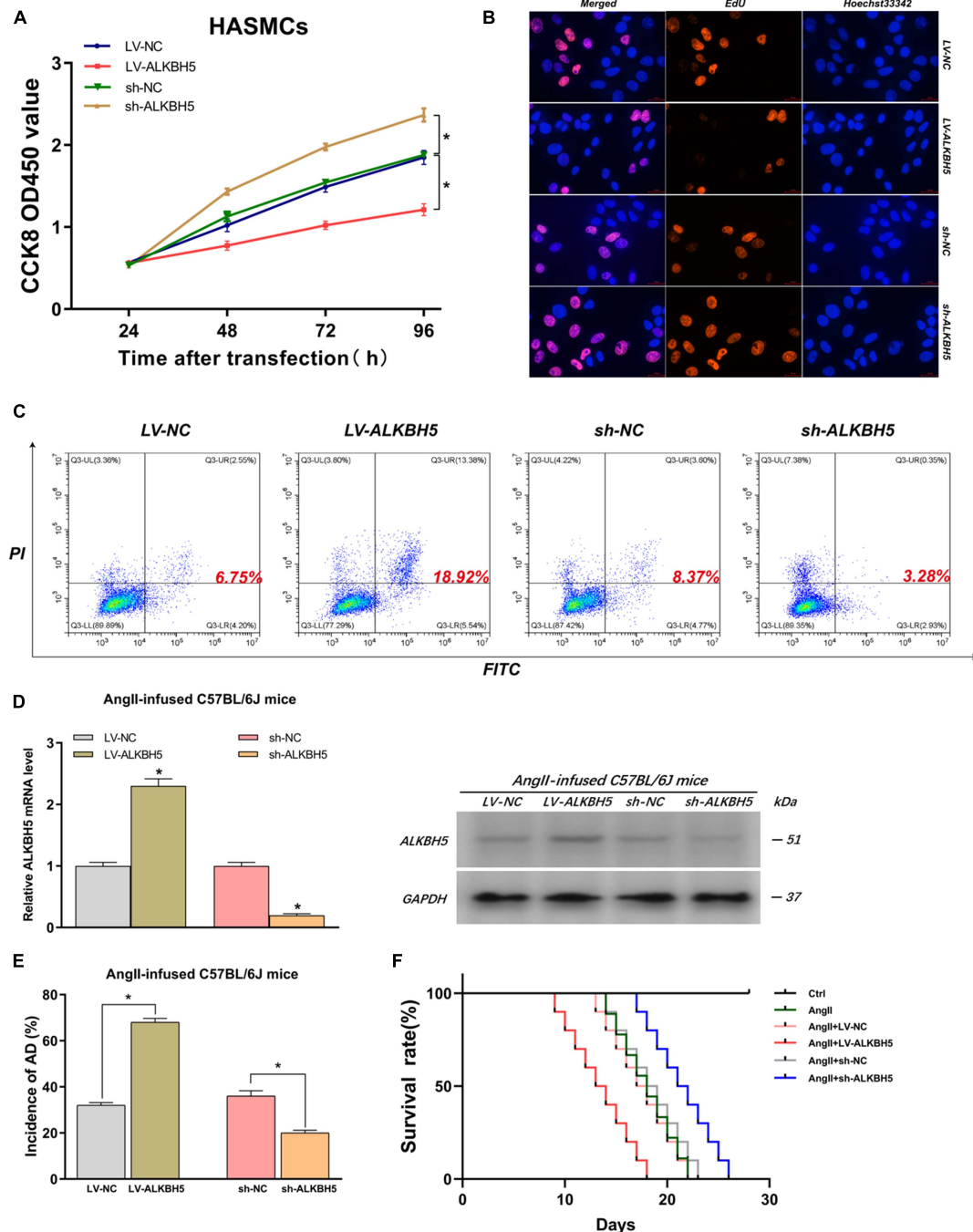


FIGURE 4 | ALKBH5 can suppress HASMC proliferation, promote HAEC apoptosis, and facilitate AD progression in AngII-infused mice. **(A,B)** Both CCK8 and EdU assays found that overexpression of ALKBH5 significantly inhibited HASMC proliferation while knockdown of ALKBH5 led to increased HASMC proliferation. **(C)** Flow cytometry analysis showed that ALKBH5 overexpression notably promoted HAEC apoptosis while its knockdown significantly suppressed HAEC apoptosis. **(D)** The interference effects on ALKBH5 expression in AngII-infused C57BL/6J mice were examined. **(E)** KIAA1429 overexpression reduced the incidence while its knockdown increased the incidence of AD in AngII-infused mice. **(F)** Mice in the sh-ALKBH5 group and LV-ALKBH5 group had longer and shorter survival times compared to the control group, respectively. Data are presented as the mean \pm SEM ($N \geq 3$ per group); * $p < 0.05$.

in animal experiments, we first confirmed the effect of interference on ALKBH5 expression and then found that ALKBH5 overexpression could increase the incidence of AD in mice and shorten the survival time of mice (Figures 4D–F). Collectively, these data suggested that ALKBH5 could promote the development of AD *in vivo* and *in vitro*.

KIAA1429 and ALKBH5 Oppositely Regulate the Processing of miR-143-3p via m6A Modification

Two recent studies have shown that m6A modification can influence tumor progression by affecting the binding of DGCR8 to pri-miRNAs (Lai et al., 2019; Song et al., 2019). Therefore, we herein assessed whether KIAA1429 and ALKBH5 also regulate the combination of DGCR8 and pri-miRNAs in HASMCs and HAECs. Given that enhanced m6A levels can cause the upregulation of miRNAs through facilitating the corresponding pri-miRNA processing (Lai et al., 2019; Song et al., 2019), and that KIAA1429 can improve the m6A levels in HASMCs and HAECs (Figure 2C), we inferred that the levels of KIAA1429/m6A-dependent miRNAs should be positively correlated with KIAA1429. Conversely, the levels of ALKBH5/m6A-dependent miRNAs should be negatively correlated with ALKBH5. Through searching the LinkedOmics database, we found 13 miRNAs positively associated in expression with KIAA1429 and 12 miRNAs negatively associated with ALKBH5 (Figures 5A,B). To confirm whether these candidate miRNAs are regulated by KIAA1429 or ALKBH5 in HASMCs and HAECs, we first measured the changes in their expression levels and found that only miR-26b, miR-143-3p, and miR-145 increased when KIAA1429 was overexpressed and decreased when KIAA1429 was silenced (Figure 5C and Supplementary Figure 2A). Similarly, we observed that only the levels of miR-320d, miR-143-3p, and miR-582 were negatively regulated by ALKBH5 (Figure 5D and Supplementary Figure 2B). We then selected miR-143-3p, the intersection of the above results, for further study.

Subsequently, we determined the level of variation of immature miRNA, pri-miR-143-3p, when the level of KIAA1429 or ALKBH5 changed and observed that unprocessed pri-miRNA-143-3p was accumulated in KIAA1429-knockdown or ALKBH5-overexpression cells and significantly decreased in KIAA1429-overexpression or ALKBH5-silence cells (Figure 5E). To explore the specific mechanisms of this phenomenon, we first searched the m6AVar database for the predicted m6A sites in pri-miR-143-3p, and two RRACH m6A sequence motifs, (GGAC) base sequence, in the pri-miR-143-3p region (only one sequence motif presents outside the pre-miRNA region) were found (Supplementary Figure 3). Then, we recomposed a previously described ectopic reporter construct (Sun et al., 2020). In one reporter, a WT version of pri-miR-143-3p was introduced. In the other reporter, the adenosine [A] of the RRACH m6A sequence motif located in the pri-miR-143-3p region outside the pre-miR-143-3p sequence was mutated to thymidine [T] (Figure 5F). Our findings demonstrated that mutation of the RRACH m6A

motif in pri-miR-143-3p significantly reduced its processing to the mature form (Figure 5G).

We next performed the RIP assay to determine the influences of m6A modification on the binding of DGCR8 to pri-miR-143-3p. The results revealed that the levels of pri-miR-143-3p bound to DGCR8 were significantly enhanced or reduced by overexpression of KIAA1429 or ALKBH5, respectively (Figures 5H,I). Moreover, we performed m6A RNA immunoprecipitation (MeRIP) assay and found that overexpressing KIAA1429 or silencing ALKBH5 notably increased the quantity of pri-miR-143-3p modified by m6A (Figure 5J). Taken together, our findings revealed that KIAA1429 could facilitate pri-miR-143-3p processing by enhancing the binding of DGCR8 to it, and ALKBH5 could hinder the processing in the same way.

MiR-143-3p Is a Downstream Target of KIAA1429 and ALKBH5

To investigate the underlying mechanism of miR-143-3p function in AD development as a downstream target of KIAA1429 and ALKBH5, we first examined its expression level in 25 pairs of aorta samples derived from donors and AD patients and found that miR-143-3p was significantly downregulated in tissues from AD patients (Figure 6A). Meanwhile, a positive correlation between miR-143-3p and KIAA1429 ($R = 0.4314$, $p = 0.0313$) and a negative correlation between miR-143-3p and ALKBH5 ($R = -0.4105$, $p = 0.0415$) were identified by Pearson's correlation coefficient analysis (Figure 6B).

Subsequently, we found that miR-143-3p upregulation could partly restore the cell proliferation suppressed by KIAA1429 knockdown. Accordingly, downregulation of miR-143-3p could partly decrease cell multiplication promoted by KIAA1429 overexpression (Figure 6C). Moreover, TUNEL apoptosis assay showed that enrichment of miR-143-3p could partly attenuate HAEC apoptosis induced by the silence of KIAA1429 (Figure 6D and Supplementary Figure 7C). We then applied the same methods to confirm that increased miR-143-3p could enhance the pro-proliferative effect of ALKBH5 knockdown on HASMCs and decreased miR-143-3p could weaken the anti-apoptotic effect of ALKBH5 knockdown on HAECs (Figures 6E,F and Supplementary Figure 7D).

MiR-143-3p Directly Targets DDX6 in HASMCs and HAECs

To identify the target genes of miR-143-3p in HASMCs and HAECs, we first searched for putative targets using three databases (TargetScan, miRanda, and PicTar) and obtained 11 candidate genes in their intersection (Figure 7A). Subsequently, we validated the prediction results by qRT-PCR and found that only the levels of DDX6, TUB, and PGK1 both changed after the upregulation and downregulation of miR-143-3p (Figure 7B and Supplementary Figure 4). We next explored whether their levels were affected by KIAA1429 and ALKBH5. The results showed that only the expressions of DDX6 and TUB were reduced or elevated after the overexpression or silence of KIAA1429, respectively (Figure 7C). Meanwhile, only the levels of DDX6

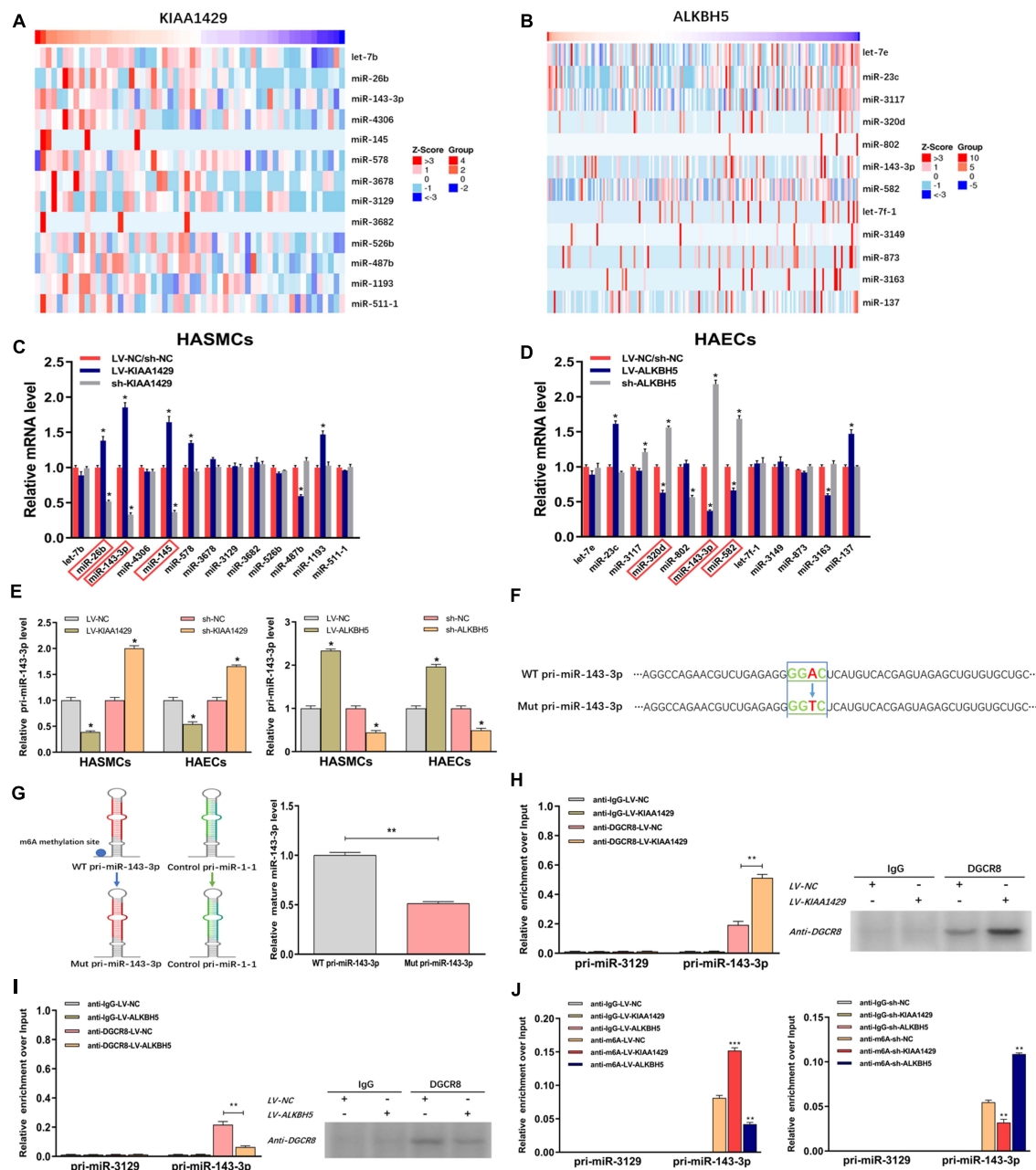


FIGURE 5 | KIAA1429 and ALKBH5 oppositely regulate the processing of miR-143-3p via m6A modification. **(A,B)** Through searching in the LinkedOmics database, we found 13 miRNAs positively associated in expression with KIAA1429 and 12 miRNAs negatively associated with ALKBH5. **(C)** The levels of miR-26b, miR-143-3p, and miR-145 increased when KIAA1429 was overexpressed and decreased when KIAA1429 was silenced. **(D)** The levels of miR-320d, miR-143-3p, and miR-582 were negatively regulated by ALKBH5. **(E)** The unprocessed pri-miRNA-143-3p was accumulated in KIAA1429-knockdown or ALKBH5-overexpression cells and significantly decreased in KIAA1429-overexpression or ALKBH5-silence cells. **(F)** In one reporter, the adenosine [A] of the RRACH m6A sequence motif located in the pri-miR-143-3p region outside the pre-miR-143-3p sequence was mutated to thymidine [T]. **(G)** The mutation of the RRACH m6A motif in pri-miR-143-3p significantly reduced its processing to the mature form. **(H,I)** The levels of pri-miR-143-3p bound to DGCR8 were significantly enhanced or reduced by overexpression of KIAA1429 or ALKBH5, respectively. **(J)** MeRIP assay showed that overexpressing KIAA1429 or silencing ALKBH5 notably increased the quantity of pri-miR-143-3p modified by m6A. Data are presented as the mean \pm SEM ($N \geq 3$ per group); * $p < 0.05$, ** $p < 0.01$, and *** $p < 0.001$.

and PGK1 changed with the upregulation or downregulation of ALKBH5 (Figure 7D). Therefore, we choose DDX6, the intersection of these results, as our research object in this study. Consistent with the above qRT-PCR results, subsequent

Western blot assays confirmed the regulatory effects of miR-143-3p, KIAA1429, and ALKBH5 on the expression levels of DDX6 (Figures 7E–G). Moreover, we also found the high expression of DDX6 in aorta samples from AD patients, which was negatively

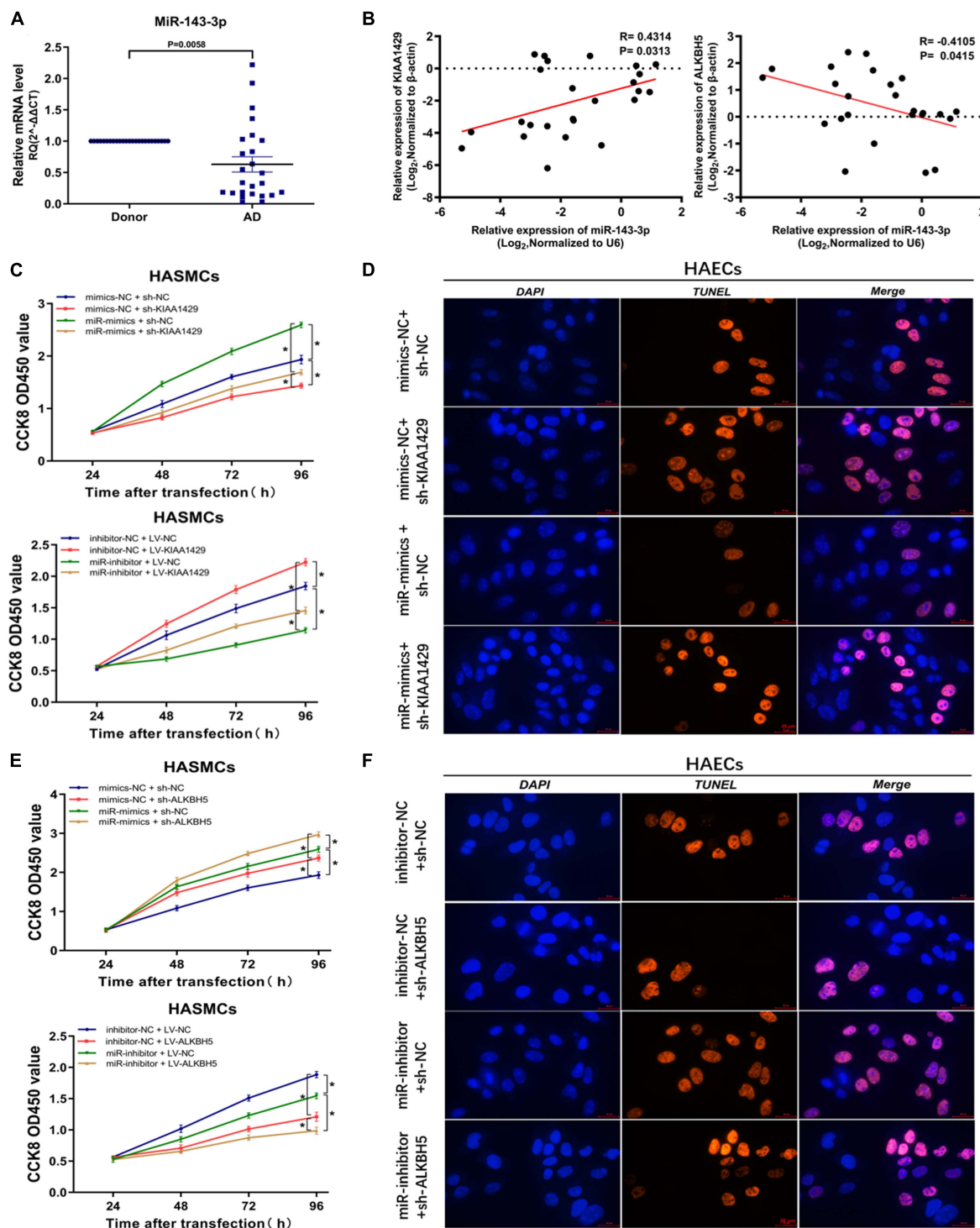
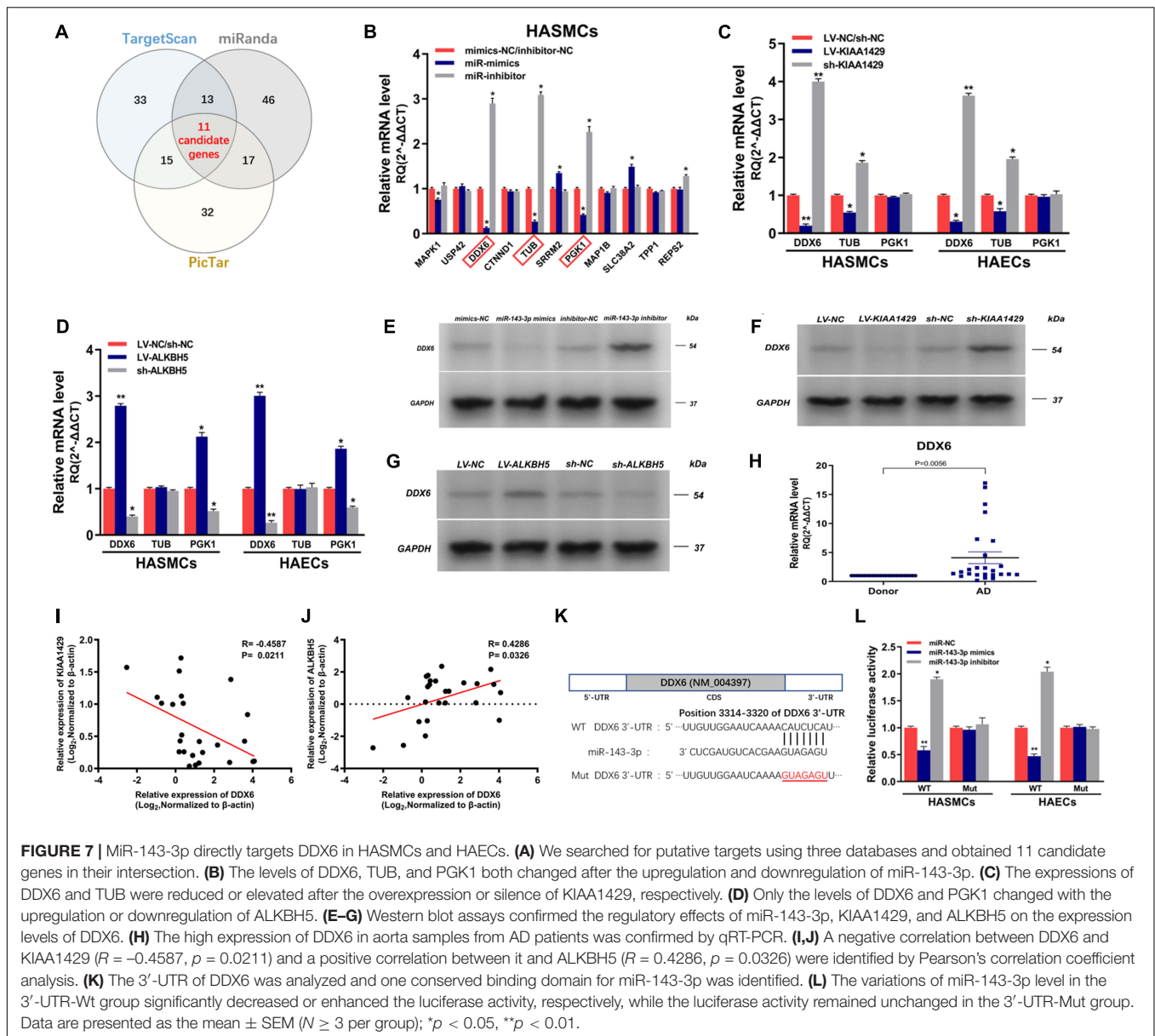


FIGURE 6 | MiR-143-3p is a downstream target of KIAA1429 and ALKBH5. **(A)** MiR-143-3p is significantly downregulated in aortic tissues from AD patients. **(B)** A positive correlation between miR-143-3p and KIAA1429 ($R = 0.4314$, $p = 0.0313$) and a negative correlation between miR-143-3p and ALKBH5 ($R = -0.4105$, $p = 0.0415$) were identified by Pearson's correlation coefficient analysis. **(C)** MiR-143-3p upregulation could partly restore the cell proliferation suppressed by KIAA1429 knockdown and downregulation of miR-143-3p could partly decrease cell multiplication promoted by KIAA1429 overexpression. **(D)** TUNEL apoptosis assay showed that enrichment of miR-143-3p could partly attenuate HAEC apoptosis induced by the silence of KIAA1429. **(E,F)** Upregulation of miR-143-3p could enhance the pro-proliferative effect of ALKBH5 knockdown on HASMCs and downregulation of miR-143-3p could weaken the anti-apoptotic effect of ALKBH5 knockdown on HAECs. Data are presented as the mean \pm SEM ($N \geq 3$ per group); * $p < 0.05$.



correlated with the expression levels of KIAA1429 and positively correlated with ALKBH5 (Figures 7H–J).

Lastly, dual-luciferase reporter assay was performed to substantiate the direct interaction between miR-143-3p and DDX6. The 3'-UTR of DDX6 was analyzed and one conserved binding domain for miR-143-3p was identified (Figure 7K). Then, the wild-type 3'-UTR (Wt) and the mutant 3'-UTR sequence (Mut) of DDX6 were cloned to construct reporter plasmids and mutant vectors, respectively. We found that upregulation or downregulation of miR-143-3p in the 3'-UTR-Wt group significantly decreased or enhanced the luciferase activity, respectively, while the luciferase activity remained unchanged in the 3'-UTR-Mut group, which revealed the targeted binding relationship between miR-143-3p and DDX6 (Figure 7L). Collectively, our findings demonstrated that DDX6

is a direct target gene of miR-143-3p and regulated by both KIAA1429 and ALKBH5.

KIAA1429 and ALKBH5 Affect AD Progression via the miR-143-3p/DDX6 Pathway

Since we had demonstrated that KIAA1429 or ALKBH5 could regulate DDX6 indirectly by modulating miR-143-3p, we intended to further explore whether they could directly regulate DDX6. We performed a luciferase reporter assay and MeRIP assay after the binding site of the 3'-UTR region of DDX6 was mutated. Results indicated that there was no significant change in luciferase activity between groups Wt and Mut, and the amount of DDX6 precipitated

by m6A and IgG also did not change significantly when KIAA1429 or ALKBH5 was disturbed (**Figures 8A,B** and **Supplementary Figure 5**). These data suggested that neither KIAA1429 nor ALKBH5 may directly regulate DDX6 mRNA in HASMCs and HAECs.

Given that we had clarified the expression relationship between DDX6 and KIAA1429 or ALKBH5, we further explored the functional relationship between them. Through elevating the level of DDX6 in KIAA1429-overexpressing HASMCs, HAECs, and AngII-infused mice (**Figures 8C,D**), we found that the enrichment of DDX6 could partly counteract the effect of pro-proliferative effect on HASMCs, the anti-apoptotic effect on HAECs, and the inhibitory effect on AD progression in mice induced by KIAA1429 overexpression (**Figures 8E–I** and **Supplementary Figure 7E**). Similarly, by reducing the level of DDX6 (**Figures 8J,K**), we found that DDX6 knockdown also partially neutralized the role of ALKBH5 overexpression in the progression of AD *in vitro* and *in vivo* (**Figures 8L–P** and **Supplementary Figure 7F**). Furthermore, we also explored whether KIAA1429 and ALKBH5 also exert their functions through direct binding to DDX6 by performing the co-immunoprecipitation (Co-IP) assay. The results showed that neither KIAA1429 nor ALKBH5 could directly bind to DDX6 (**Figures 8Q,R**). Taken together, our findings indicated that the miR-143-3p/DDX6 pathway is the downstream effector of KIAA1429 and ALKBH5 affecting AD progression.

DISCUSSION

The biological functions and mechanisms of various chemical modifications of DNA and protein have been extensively investigated and elucidated (Gawinecka et al., 2017; Tchanasato et al., 2018; Song et al., 2019). Nonetheless, the role of RNA modifications remains mostly undiscovered, among which m6A methylation is the most prevalent modification on eukaryotic RNAs. With the advancement of m6A sequence technology, m6A modification has gained increasing attention in recent years (Lai et al., 2019; Sun et al., 2020). Numerous studies revealed that dynamic m6A modifications closely involve multiple physiological and biochemical processes, including maturation of pri-miRNA, transcription splicing, RNA stability, fate and functions of lncRNAs, and RNA–protein interactions (Berger, 2002; Cantara et al., 2011). Based on these findings, it is reasonable to speculate that m6A modification may affect the onset and progression of AD. To confirm the validity of our conjecture and to elucidate its underlying molecular mechanism of action, we conducted the present study.

In our study, we initially measured the expression levels of multiple key genes related to m6A, including “writers,” “readers,” and “erasers,” in aortic tissues derived from donors and AD patients to identify the presence or absence of differentially expressed genes. Results showed the significant low expression of KIAA1429, m6A “writer,” and significant high expression of ALKBH5, m6A “eraser,” in aortas from AD patients.

Moreover, we also demonstrated that KIAA1429 enhanced while ALKBH5 reduced the m6A levels in HASMCs and HAECs by using m6A dot blot assay. These findings implied that m6A modification mediated by methyltransferase and demethylase is indeed involved in AD progression. Subsequently, results of a series of *in vitro* and *in vivo* functional experiments uncovered an opposite role of KIAA1429 and ALKBH5 in affecting the progression of AD. KIAA1429 can promote HASMC proliferation, suppress HAEC apoptosis, and facilitate AD progression in AngII-infused mice, while ALKBH5 plays the exact opposite role.

Given that we had revealed the role of KIAA1429 and ALKBH5 in AD development, we next intended to elucidate the potential mechanism by which they function. The findings of two recent studies that METTL14 suppresses the metastasis of hepatocellular carcinoma by modulating pri-miRNA processing *via* interacting with DGCR8 (Song et al., 2019), and that METTL3 could positively modulate the pri-miRNA process through interacting with the microprocessor protein DGCR8 (Lai et al., 2019), suggest that m6A modification can influence disease progression by affecting the binding of DGCR8 to pri-miRNAs. Therefore, we herein assessed whether KIAA1429 and ALKBH5 influence AD progression also through the same mechanism. We first screened out several candidate miRNAs whose expression was regulated by KIAA1429 or ALKBH5 using bioinformatics analysis and expression level detection, from which miR-143-3p was selected as the target in this study because its expression was both positively regulated by KIAA1429 and negatively regulated by ALKBH5. Subsequently, we demonstrated that KIAA1429 could enhance the binding of DGCR8 to pri-miR-143-3p, resulting in the overall increase of mature miR-143-3p and the consequent reduction of unprocessed primary miR-143-3p. On the contrary, ALKBH5 attenuated the binding of DGCR8 to pri-miR-143-3p and thus inhibited pri-miR-143-3p processing, leading to the overall decline of mature miR-143-3p. Furthermore, to clarify the functional mechanism of miR-143-3p more clearly, we predicted and verified its target gene and finally identified DDX6 as a direct target gene of miR-143-3p.

To further strengthen the persuasiveness of signaling pathways revealed in this study, we then directly explored the relationship between DDX6 and KIAA1429 or ALKBH5 at the expression and functional levels. In terms of expression level, KIAA1429 and ALKBH5 could down- or upregulate DDX6, respectively, and it was worth noting here that they indirectly regulated DDX6 levels through modulating pri-miR-143-3p processing, rather than through direct binding to DDX6. In terms of the influence on AD progression *in vitro* and *in vivo*, DDX6 was found to be negatively positively correlated with KIAA1429 and positively correlated with ALKBH5. These data demonstrated that KIAA1429 and ALKBH5 could affect AD progression *via* regulating the miR-143-3p/DDX6 pathway.

In addition, we explored whether two common epigenetic mechanisms other than m6A modification are also associated with the abnormal downregulation of miR-143-3p in aorta tissues of AD patients. Firstly, we treated cells with multiple DNA methyltransferase inhibitors and determined their effects on miR-143-3p expression, whereas no significant difference

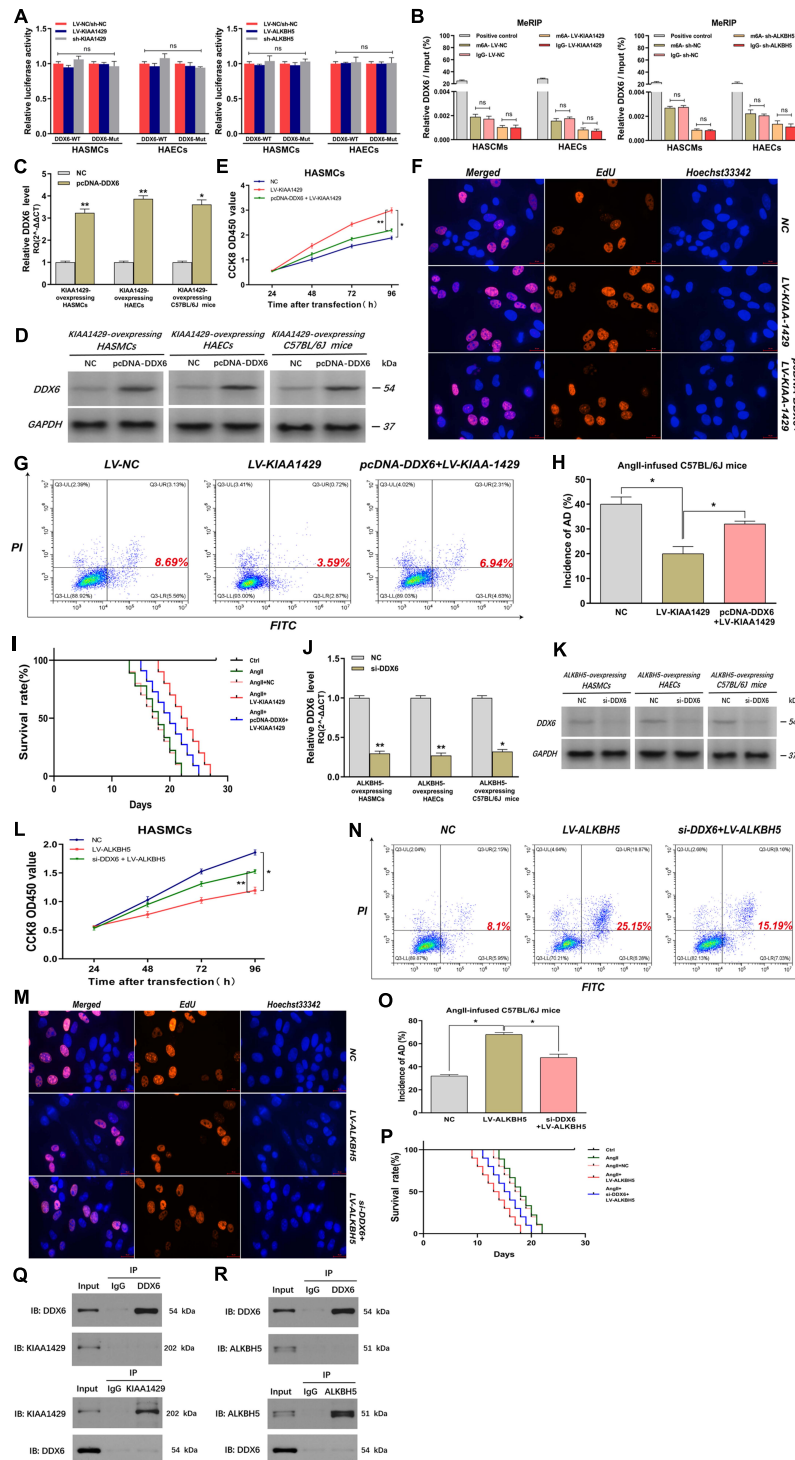


FIGURE 8 | KIAA1429 and ALKBH5 affect AD progression via the miR-143-3p/DDX6 pathway. (A,B) After the binding site of the 3'-UTR region of DDX6 was mutated, both the luciferase activity and the amount of DDX6 precipitated by m6A and IgG did not change significantly when KIAA1429 or ALKBH5 was disturbed. **(C,D)** The effect of elevating DDX6 level in KIAA1429-overexpressing HASMCs, HAECs, and AngII-infused mice was detected. **(E-I)** The enrichment of DDX6 could partly counteract the effect of the pro-proliferative effect on HASMCs, the anti-apoptotic effect on HAECs, and the inhibitory effect on AD progression in mice induced by KIAA1429 overexpression. **(J,K)** The effect of reducing DDX6 level in ALKBH5-overexpressing HASMCs, HAECs, and AngII-infused mice was examined. **(L-P)** The reduction of DDX6 could partly counteract the effect of the anti-proliferative effect on HASMCs, the pro-apoptotic effect on HAECs, and the promotional effect on AD progression in mice induced by KIAA1429 overexpression. **(Q,R)** Neither KIAA1429 nor ALKBH5 could directly bind to DDX6. Data are presented as the mean \pm SEM ($N \geq 3$ per group); * $p < 0.05$, ** $p < 0.01$, and ns $p > 0.05$.

was observed, suggesting that DNA methylation might not be related to miR-143-3p expression in HASMCs and HAECs (**Supplementary Figure 6A**). Subsequently, we investigated the role of histone acetylation in miR-143-3p expression *via* treating cells with various histone deacetylase (HDAC) inhibitors. The results revealed that these HDAC inhibitors had no significant influence on miR-143-3p level (**Supplementary Figure 6B**). This conclusion was further confirmed by results showing that the overexpression of HDAC also had no impact on miR-143-3p expression (**Supplementary Figure 6C**). These findings suggested that neither DNA methylation nor histone acetylation is related to the decline of miR-143-3p, which further highlighted the importance of m6A modification in influencing the onset and progression of AD.

Although we tried our best to design our study as rigorously and completely as possible, there are still limitations. One limitation is that the clinical tissue specimen size needs to be further expanded for reducing the likelihood of bias, such as gender bias and age bias. A major obstacle to overcoming this deficiency is that normal aorta samples are derived from donations in China and the number of heart donors declared brain dead is in short supply. Another shortcoming is that we only investigated the function and mechanism of m6A modification in two cell types with the highest relevance to AD development in this study, HASMCs and HAECs. Its role and potential function mechanism in other cell types in the arterial vessel wall need to be further explored in future studies.

In summary, our findings have revealed a novel connection between m6A modification and AD progression. Concretely, we found that KIAA1429 is downregulated while ALKBH5 is upregulated in aortic tissues from AD patients. We demonstrated that KIAA1429/ALKBH5-mediated m6A modifications can regulate the processing of pri-miR-143-3p through interacting with the microprocessor protein DGCR8. Furthermore, KIAA1429 and ALKBH5 can oppositely regulate HASMC proliferation, HAEC apoptosis, and AD progression in AngII-infused mice *via* the miR-143-3p/DDX6 pathway. The findings presented here reveal the role of m6A modification in AD progression for the first time and may provide a novel molecular basis for subsequent researchers to search for novel therapeutic approaches to improve the health of patients struggling with AD.

REFERENCES

- Akhavan-Niaki, H., and Samadani, A. A. (2013). DNA methylation and cancer development: molecular mechanism. *Cell Biochem. Biophys.* 67, 501–513. doi: 10.1007/s12013-013-9555-2
- Alarcón, C. R., Lee, H., Goodarzi, H., Halberg, N., and Tavazoie, S. F. (2015). N6-methyladenosine marks primary microRNAs for processing. *Nature* 519, 482–485. doi: 10.1038/nature14281
- Auyeung, V. C., Ulitsky, I., McGeary, S. E., and Bartel, D. P. (2013). Beyond secondary structure: primary-sequence determinants license pri-miRNA hairpins for processing. *Cell* 152, 844–858. doi: 10.1016/j.cell.2013.01.031
- Berger, S. L. (2002). Histone modifications in transcriptional regulation. *Curr. Opin. Genet. Dev.* 12, 142–148. doi: 10.1016/s0959-437x(02)00279-4

DATA AVAILABILITY STATEMENT

The original contributions presented in the study are included in the article/**Supplementary Material**, further inquiries can be directed to the corresponding author/s.

ETHICS STATEMENT

The studies involving human participants were reviewed and approved by Clinical Research Ethics Committees of Renmin Hospital of Wuhan University. The patients/participants provided their written informed consent to participate in this study. The animal study was reviewed and approved by The Ethical Committee of the Renmin Hospital of Wuhan University.

AUTHOR CONTRIBUTIONS

PW designed the project plan, completed the main experiment, and drafted the manuscript. ZW contributed to the resources and supervised the implementation of the whole project. MZ organized the experimental data and revised the manuscript. QW and FS established the AngII infusion animal model. SY completed the bioinformatics analysis. All authors have read and approved the final version of the manuscript.

FUNDING

This work was supported by grants from the National Natural Science Foundation of China (Nos. 81570428 and 81600367), the Key Support Project of Health Commission of Hubei Province (No. WJ2019Z012), and the Guiding Fund of Renmin Hospital of Wuhan University (No. RMYD2018Z07).

SUPPLEMENTARY MATERIAL

The Supplementary Material for this article can be found online at: <https://www.frontiersin.org/articles/10.3389/fcell.2021.668377/full#supplementary-material>

- Cantara, W. A., Crain, P. F., Rozenski, J., McCloskey, J. A., Harris, K. A., Zhang, X., et al. (2011). The RNA Modification Database, RNAMDB: 2011 update. *Nucleic Acids Res.* 39, D195–D201.
- Desrosiers, R., Friderici, K., and Rottman, F. (1974). Identification of methylated nucleosides in messenger RNA from Novikoff hepatoma cells. *Proc. Natl. Acad. Sci. U.S.A.* 71, 3971–3975. doi: 10.1073/pnas.71.10.3971
- Dominissini, D., Moshitch-Moshkovitz, S., Schwartz, S., Salmon-Divon, M., Ungar, L., Osenberg, S., et al. (2012). Topology of the human and mouse m6A RNA methylomes revealed by m6A-seq. *Nature* 485, 201–206. doi: 10.1038/nature11112
- Frye, M., Harada, B. T., Behm, M., and He, C. (2018). RNA modifications modulate gene expression during development. *Science* 361, 1346–1349. doi: 10.1126/science.aau1646

- Gawinecka, J., Schönrrath, F., and von Eckardstein, A. (2017). Acute aortic dissection: pathogenesis, risk factors and diagnosis. *Swiss Med. Wkly.* 147:w14489.
- He, L., Li, H., Wu, A., Peng, Y., Shu, G., Yin, G., et al. (2019). Functions of N6-methyladenosine and its role in cancer. *Mol. Cancer* 18:176.
- Lai, Y., Li, J., Zhong, L., He, X., Si, X., Sun, Y., et al. (2019). The pseudogene PTENP1 regulates smooth muscle cells as a competing endogenous RNA. *Clin. Sci.* 133, 1439–1455. doi: 10.1042/cs20190156
- Lan, T., Li, H., Zhang, D., Xu, L., Liu, H., Hao, X., et al. (2019). KIAA1429 contributes to liver cancer progression through N6-methyladenosine-dependent post-transcriptional modification of GATA3. *Mol. Cancer* 18:186.
- Meyer, K. D., and Jaffrey, S. R. (2017). Rethinking m(6)A readers, writers, and erasers. *Annu. Rev. Cell Dev. Biol.* 33, 319–342. doi: 10.1146/annurev-cellbio-100616-060758
- Meyer, K. D., Saletore, Y., Zumbo, P., Elemento, O., Mason, C. E., Jaffrey, S. R., et al. (2012). Comprehensive analysis of mRNA methylation reveals enrichment in 3' UTRs and near stop codons. *Cell* 149, 1635–1646. doi: 10.1016/j.cell.2012.05.003
- Roundtree, I. A., Evans, M. E., Pan, T., and He, C. (2017). Dynamic RNA modifications in gene expression regulation. *Cell* 169, 1187–1200. doi: 10.1016/j.cell.2017.05.045
- Song, Y., Yang, L., Guo, R., Lu, N., Shi, Y., Wang, X., et al. (2019). Long noncoding RNA MALAT1 promotes high glucose-induced human endothelial cells pyroptosis by affecting NLRP3 expression through competitively binding miR-22. *Biochem. Biophys. Res. Commun.* 509, 359–366. doi: 10.1016/j.bbrc.2018.12.139
- Su, H., Wang, G., Wu, L., Ma, X., Ying, K., Zhang, R., et al. (2020). Transcriptome-wide map of m(6)A circRNAs identified in a rat model of hypoxia mediated pulmonary hypertension. *BMC Genomics* 21:39. doi: 10.1186/s12864-020-6462-y
- Sun, L., Wang, C., Yuan, Y., Guo, Z., He, Y., Ma, W., et al. (2020). Downregulation of HDAC1 suppresses media degeneration by inhibiting the migration and phenotypic switch of aortic vascular smooth muscle cells in aortic dissection. *J. Cell Physiol.* 235, 8747–8756. doi: 10.1002/jcp.29718
- Tchana-Sato, V., Sakalihan, N., and Defraigne, J. O. (2018). [Aortic dissection]. *Rev. Med. Liege* 73, 290–295.
- Wang, P., Deng, Y., and Fu, X. (2017). MiR-509-5p suppresses the proliferation, migration, and invasion of non-small cell lung cancer by targeting YWHAG. *Biochem. Biophys. Res. Commun.* 482, 935–941. doi: 10.1016/j.bbrc.2016.11.136
- Wang, P., Wang, Z., Zhang, M., Wu, Q., and Shi, F. (2021). Lnc-OIP5-AS1 exacerbates aorta wall injury during the development of aortic dissection through upregulating TUB via sponging miR-143-3p. *Life Sci.* 271:119199. doi: 10.1016/j.lfs.2021.119199
- Zhang, J., Bai, R., Li, M., Ye, H., Wu, C., Wang, C., et al. (2019a). Excessive miR-25-3p maturation via N(6)-methyladenosine stimulated by cigarette smoke promotes pancreatic cancer progression. *Nat. Commun.* 10:1858.
- Zhang, J., Guo, S., Piao, H. Y., Wang, Y., Wu, Y., Meng, X. Y., et al. (2019b). ALKBH5 promotes invasion and metastasis of gastric cancer by decreasing methylation of the lncRNA NEAT1. *J. Physiol. Biochem.* 75, 379–389. doi: 10.1007/s13105-019-00690-8
- Zuo, X., Chen, Z., Gao, W., Zhang, Y., Wang, J., Wang, J., et al. (2020). M6A-mediated upregulation of LINC00958 increases lipogenesis and acts as a nanotherapeutic target in hepatocellular carcinoma. *J. Hematol. Oncol.* 13:5.

Conflict of Interest: The authors declare that the research was conducted in the absence of any commercial or financial relationships that could be construed as a potential conflict of interest.

Publisher's Note: All claims expressed in this article are solely those of the authors and do not necessarily represent those of their affiliated organizations, or those of the publisher, the editors and the reviewers. Any product that may be evaluated in this article, or claim that may be made by its manufacturer, is not guaranteed or endorsed by the publisher.

Copyright © 2021 Wang, Wang, Zhang, Wu, Shi and Yuan. This is an open-access article distributed under the terms of the Creative Commons Attribution License (CC BY). The use, distribution or reproduction in other forums is permitted, provided the original author(s) and the copyright owner(s) are credited and that the original publication in this journal is cited, in accordance with accepted academic practice. No use, distribution or reproduction is permitted which does not comply with these terms.



LncRNA RNA Component of Mitochondrial RNA-Processing Endoribonuclease Promotes AKT-Dependent Breast Cancer Growth and Migration by Trapping MicroRNA-206

Yingdan Huang^{1,2†}, Bangxiang Xie^{3,4†}, Mingming Cao^{1,2}, Hua Lu⁵, Xiaohua Wu^{2,6}, Qian Hao^{1,2*} and Xiang Zhou^{1,2,7,8*}

¹ Fudan University Shanghai Cancer Center and Institutes of Biomedical Sciences, Fudan University, Shanghai, China, ² Department of Oncology, Shanghai Medical College, Fudan University, Shanghai, China, ³ Beijing Institute of Hepatology, Beijing You An Hospital, Capital Medical University, Beijing, China, ⁴ Beijing Engineering Research Center for Precision Medicine and Transformation of Hepatitis and Liver Cancer, Beijing, China, ⁵ Department of Biochemistry & Molecular Biology, Tulane Cancer Center, Tulane University School of Medicine, New Orleans, LA, United States, ⁶ Department of Gynecologic Oncology, Fudan University Shanghai Cancer Center, Fudan University, Shanghai, China, ⁷ Key Laboratory of Breast Cancer in Shanghai, Fudan University Shanghai Cancer Center, Fudan University, Shanghai, China, ⁸ Shanghai Key Laboratory of Medical Epigenetics, International Co-Laboratory of Medical Epigenetics and Metabolism, Ministry of Science and Technology, Institutes of Biomedical Sciences, Fudan University, Shanghai, China

OPEN ACCESS

Edited by:

Jing Zhang,
Shanghai Jiao Tong University, China

Reviewed by:

Zhiqian Zhang,
Southern University of Science
and Technology, China
Narendra Singh,
Stowers Institute for Medical
Research, United States

*Correspondence:

Qian Hao
haoqian@fudan.edu.cn
Xiang Zhou
xiangzhou@fudan.edu.cn

[†] These authors have contributed
equally to this work

Specialty section:

This article was submitted to
Epigenomics and Epigenetics,
a section of the journal
Frontiers in Cell and Developmental
Biology

Received: 25 June 2021

Accepted: 30 August 2021

Published: 21 September 2021

Citation:

Huang Y, Xie B, Cao M, Lu H,
Wu X, Hao Q and Zhou X (2021)
LncRNA RNA Component of
Mitochondrial RNA-Processing
Endoribonuclease Promotes
AKT-Dependent Breast Cancer
Growth and Migration by Trapping
MicroRNA-206.
Front. Cell Dev. Biol. 9:730538.
doi: 10.3389/fcell.2021.730538

The RNA component of mitochondrial RNA-processing endoribonuclease (RMRP) was recently shown to play a role in cancer development. However, the function and mechanism of RMRP during cancer progression remain incompletely understood. Here, we report that RMRP is amplified and highly expressed in various malignant cancers, and the high level of RMRP is significantly associated with their poor prognosis, including breast cancer. Consistent with this, ectopic RMRP promotes proliferation and migration of TP53-mutated breast cancer cells, whereas depletion of RMRP leads to inhibition of their proliferation and migration. RNA-seq analysis reveals AKT as a downstream target of RMRP. Interestingly, RMRP indirectly elevates AKT expression by preventing AKT mRNA from miR-206-mediated targeting via a competitive sequestering mechanism. Remarkably, RMRP endorses breast cancer progression in an AKT-dependent fashion, as knockdown of AKT completely abolishes RMRP-induced cancer cell growth and migration. Altogether, our results unveil a novel role of the RMRP-miR-206-AKT axis in breast cancer development, providing a potential new target for developing an anti-breast cancer therapy.

Keywords: non-coding RNA, RMRP, miR-206, AKT, breast cancer

INTRODUCTION

The past decade has witnessed the growing importance of the non-coding RNAs (ncRNA) as critical regulators of almost all biological aspects of human cancer (Esteller, 2011; Wolin and Maquat, 2019). Long non-coding RNAs (lncRNA) and microRNAs (miRNA) constitute the majority of ncRNA (Garzon et al., 2009; Gibb et al., 2011). LncRNAs are a group of ncRNAs with >200 nucleotides (Schmitt and Chang, 2016), while miRNAs represent a group of small regulatory RNAs with 18-23 nucleotides in length (Garneau et al., 2007; Fabian et al., 2010). Three modes of action

have been proposed to illustrate how lncRNAs might function in cancer (Schmitt and Chang, 2016; He et al., 2019). First, the nuclear lncRNAs can modulate gene expression by controlling local chromatin remodeling or directing the recruitment of regulatory factors to specific promoter regions on chromosomes. One prominent example is the p53-inducible large intergenic non-coding RNA (lincRNA)-p21 that recruits hnRNP-K to the proper genomic locations to globally repress gene transcription (Huarte et al., 2010). Also, lncRNAs can interact with multiple proteins to facilitate the formation of functional complexes or perturb molecule interactions. For instance, lncRNA-ROR was shown to inhibit p53 translation by binding to hnRNP-I and preventing the interaction of the latter with p53 mRNA (Zhang et al., 2013). Moreover, lncRNAs can associate with different RNA molecules, such as mRNAs and microRNAs, to regulate mRNA turnover and translation. It has been shown that a number of highly expressed lncRNAs are able to act as competitive endogenous RNAs (ceRNAs) to sequester microRNAs (miRNAs) away from their mRNA targets (Tay et al., 2014). Because of the increasingly complex network with the addition of ncRNAs in cancer, more efforts are needed to thoroughly dissect the molecular basis underlying the role of lncRNAs in disease development.

The PI3K/AKT signaling pathway plays an important role in cell fate decisions, including growth and proliferation, survival, angiogenesis, metabolic remodeling, and chemoresistance (Hoxhaj and Manning, 2020; Liu et al., 2020). Recently, lncRNAs have been shown to play a critical role in the AKT pathway (Peng et al., 2017; Revathidevi and Munirajan, 2019). lncRNA AK023948 was found to functionally interact with DHX9 and the regulatory subunit of PI3K, p85, leading to AKT activation (Koirala et al., 2017). LINK-A could facilitate AKT and Phosphatidylinositol 3,4,5-trisphosphate [PtdIns(3,4,5)P₃] interaction and, as thus, induce enzymatic activation of AKT by forming a trimeric complex (Lin et al., 2017). PCAT1 interacted directly with FKBP51, thus perturbing the PHLPP/FKBP51 complex that is required for dephosphorylation of AKT at Ser-473 (Shang et al., 2019). In this study, we identified a lncRNA, the RNA component of mitochondrial RNA-processing endoribonuclease (RMRP), as an additional regulator of the AKT pathway as described below.

RMRP was found to be involved in the cleavage of the RNA primer for mitochondrial DNA replication (Chang and Clayton, 1987) and the precursor of ribosomal RNA (rRNA) (Goldfarb and Cech, 2017). Mutation of RMRP was identified in patients with cartilage-hair hypoplasia, a human ribosomopathy characterized by metaphyseal dysplasia, anemia, and immune dysregulation (Ridanpää et al., 2001; Narla and Ebert, 2010). RMRP also plays a role in cancer development. Mutations in the *RMRP* promoter led to enhanced nuclear protein binding to the promoter, consequently elevating transcription of *RMRP*, which might be associated with cancer progression (Rheinbay et al., 2017; Son et al., 2019). Moreover, RMRP has been shown to act as a sponge for microRNAs and promote gastric and lung cancer development (Meng et al., 2016; Shao et al., 2016; Hussien et al., 2021). We recently found that RMRP interacts with and sequesters SNRPA1 in

the nucleus, where the latter binds to wild type p53 (wt p53) and promotes MDM2-mediated proteasomal degradation of wt p53 in colorectal cancer (Chen et al., 2021). In breast cancer, upregulation of RMRP partially resulted from its promoter mutation (Rheinbay et al., 2017) or Wnt/Hippo activation (Park and Jeong, 2015), but its biological function and the underlying mechanism in this cancer remain unclear. Herein, we report the wt p53-independent tumor-promoting function of RMRP. We found that the RMRP gene is amplified and overexpressed in a variety of human cancers, and the high level of RMRP is significantly associated with poor prognosis of multiple cancers, including breast cancer. Remarkably, RMRP promoted proliferation and migration of *TP53*-mutated breast cancer cells by activating the AKT signaling pathway. It did so by preventing miRNA-206 from binding to its target AKT mRNA. Our study establishes a role of the RMRP-miR-206-AKT axis in breast cancer development, and provides these molecules as potential biomarkers and therapeutic targets for future developing treatments of the disease.

MATERIALS AND METHODS

Cell Culture and Transient Transfection

Human breast cancer cell lines JIMT-1 and BT549 were cultured in Dulbecco's modified Eagle's medium supplemented with 10% fetal bovine serum, 100 U/ml penicillin, and 100 µg/ml streptomycin. All cells were cultured at 37°C in an incubator containing 5% carbon dioxide. Cells were seeded on the dish at appropriate density one day before transfection, and then transfected plasmids, siRNAs or the miRNA mimic/inhibitor according to the manufacturer's protocol of the Hieff Trans liposomal transfection reagent (Yeasen, Shanghai, China). Cells were harvested at 24–48 h post transfection for immunoblotting or RT-quantitative PCR (qPCR) analyses.

Plasmids, siRNAs, and miRNA Mimics and Inhibitor

The plasmid expressing RMRP was purchased from Shanghai Genechem (Shanghai, China). The pcDNA3-luc-mcs Dual-Luciferase miRNA Target Expression Vector was a gift from Shenglin Huang. pcDNA3-luc-mcs-AKT-3'UTR reporter plasmids were generated by inserting the AKT 3'UTR amplified by PCR into the pcDNA3-luc-mcs vector. siRNAs targeting RMRP and AKT were designed by the BLOCK-iTTM RNAi Designer¹ and synthesized by Genepharma (Shanghai, China). The siRNA sequences are as follows, siNC: UUCUCCGAACGUGUCACGU, siRMRP-1: CCUAG GCUACACACUGAGGACU, siRMRP-2: GUUCGUGCUGAA GGCCUGUAU, siAKT-1: GCACCUUCAUUGGCUACAA, siAKT-2: GCGUGACCAUGAACGAGUU. The miRNA mimics and inhibitors were designed and synthesized by Genepharma. The sequences are as follows, double-stranded hsa-miR-206 mimics: UGGAAUGUAAGGAAGUGUGUGG

¹<http://rnaidesigner.thermofisher.com/rnaexpress/design.do>

and ACACACUCCUUAUCCAUAU; and hsa-miR-206 inhibitor: CCACACUCCUUAUCCAUAU.

Generation of Lentiviral Particles

The PWPXL-RMRP plasmid was generated by inserting the full-length sequence of RMRP into the lentivirus-based PWPXL vector. HEK293T cells were transfected with PWPXL-vector or PWPXL-RMRP, along with the packaging plasmid psPAX2 and the envelope plasmid pMD2.G. The virus particles were collected 48 h after transfection. The supernatant of 2–4 ml containing virus particles was added to breast cancer cells, JIMT-1 and BT549, for 24–36 h.

CRISPR/Cas9-Mediated Gene Editing

The CRISPR/Cas9 targeting vector lentiCRISPR v2 was purchased from Addgene (Cambridge, MA, United States). The sgRNA for RMRP was designed at <http://crispr.mit.edu/>, and was cloned into the lentiCRISPR v2 vector at the BsmBI site. The combination of sgRNAs was used to achieve the best efficiency as previously described (Chen et al., 2021), and two different clones, RMRP-KO#1 and RMRP-KO#2, were selected for future experiments. The cells were infected with the lentiviruses encoding the sgRNAs and selected by 1 μ g/ml puromycin for a week.

Reverse Transcription and Quantitative PCR Analysis

Total RNAs were isolated from cells using RNAiso Plus (Takara, Dalian, China) following the manufacturer's protocol. Total RNAs of 0.5 to 1 μ g were used as templates for reverse transcription using the PrimeScriptTM RT reagent Kit with gDNA Eraser (Takara, Dalian, China). Quantitative RT-PCR (RT-qPCR) was conducted using TB GreenTM Premix according to the manufacturer's protocol (Takara, Dalian, China). The RT-qPCR primers GAPDH, U6, RMRP and AKT are as follows, GAPDH: 5'-GGAGCGAGATCCCTCCAAAAT-3' and 5'-GGCTGTTGTCATACTTCTCATGG-3', U6: 5'-GCTTCGG CAGCACATATACTAAAAT-3' and 5'-CGCTTCACGAATTTG CGTGTCAT-3', RMRP: 5'-TGCTGAAGGCCTGTATCCT-3' and 5'-TGAGAATGAGCCCCGTGT-3', and AKT: 5'-AGCGA CGTGGCTATTGTGAAG-3' and 5'-GCCATCATTTCTTGAG GAGGAAGT-3'.

Immunoblotting

Cells were harvested and lysed in lysis buffer consisting of 50 mM Tris/HCl (pH7.5), 0.5% Nonidet P-40 (NP-40), 1 mM EDTA, 150 mM NaCl, 1 mM dithiothreitol (DTT), 0.2 mM phenylmethylsulfonyl fluoride (PMSF), 10 μ M pepstatin A and 1 μ g/ml leupeptin. Equal amounts of clear cell lysate (20–80 μ g) were used for immunoblotting (IB) analysis as described previously (Zhou et al., 2013). anti-GAPDH (Catalog No. 60004-1, Proteintech), anti-AKT (Catalog No. #9272, Cell Signaling Technology, Danvers, MA, United States), anti-pAKT (Thr-308) (Catalog No. #4056, Cell Signaling Technology, Danvers, MA, United States), and the secondary antibodies for rabbit (Catalog No. ARG65351, Arigo) and mouse (Catalog No. ARG65350, Arigo) were commercially purchased.

Cell Viability Assay

To detect cell proliferation, the Cell Counting Kit-8 (CCK-8) (Dojindo Molecular Technologies, Japan) was used according to the manufacturer's instructions. Cells (2000–5000) were seeded per well in 96-well culture plates at 12 h post transfection. Cell viability was determined by adding WST-8 at a final concentration of 10% to each well, and the absorbance of the samples was measured at 450 nm using a Microplate Reader every 24 h for 4–5 days.

Transwell Invasion Assay

The assay was performed using the transwell chamber inserts in a 24-well plate. Briefly, 5×10^4 cells suspended in 200 μ l of serum-free medium were added to the upper chamber after 12 h post transfection. The lower chambers were filled with the culture medium with 20% fetal bovine serum. After culture for 24–36 h at 37°C, the cells on the upper surface were scraped and washed away, while the cells on the lower surface were fixed with methanol and stained with 0.1% crystal violet. The number of invasive cells was counted in at least three randomly selected fields under an optical microscope by image J software.

Luciferase Reporter Assay

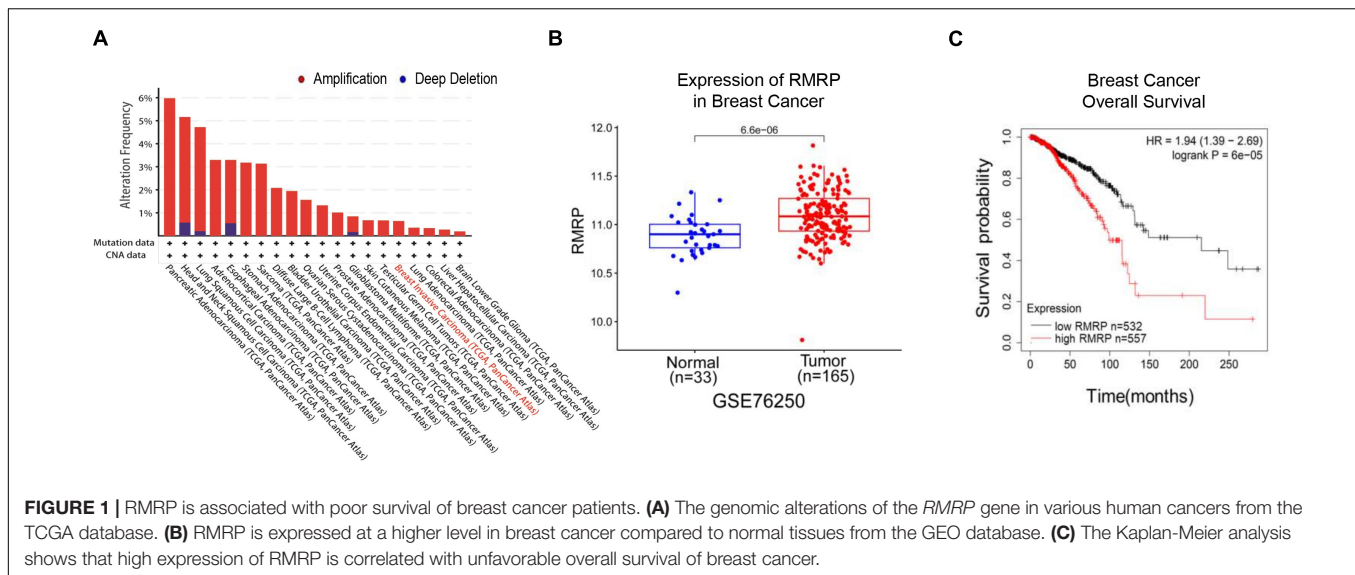
HEK293T cells were seeded at 5×10^3 cells per well in 96 well plates. The cells were then co-transfected with the combinations of the Renilla plasmid, the pcDNA3-luc-mcs-AKT-3'UTR reporter plasmid, PWPXL or PWPXL-RMRP plasmid, and the control or miR-206 mimics as indicated in the figure. At 48 h post transfection, cells were lysed using passive lysis buffer, and the Firefly and Renilla luciferase activities were measured by the dual-luciferase assay kit (Promega, Madison, WI, United States).

Databases of Cancer Patients

The cBioPortal website was used for analyzing the mutation and copy number variations of RMRP based on the TCGA database (Cerami et al., 2012; Gao et al., 2013). The raw data of gene expression were available in Gene Expression Omnibus database (GSE76250) (Jiang et al., 2016). Cancer patient survival was analyzed by the Kaplan-Meier Plotter website (Nagy et al., 2021).

Statistics

Statistical analyses were performed using GraphPad Prism 6 software or SPSS 19.0 software. Data of experiments are expressed as mean \pm standard deviation (SD) of at least three independent experiments. The Student's *t* test or one-way analysis of variance was performed to evaluate the differences between two groups or more than two groups. The Kaplan-Meier statistics were used to analyze the significant difference of patient survival. *p* < 0.05 was considered statistically significant, and the asterisks represent significance in the following way: **p* < 0.05, ***p* < 0.01, and ****p* < 0.001.



RESULTS

RNA Component of Mitochondrial RNA-Processing Endoribonuclease Is Associated With Unfavorable Prognosis in Different Cancers

To explore the clinical relevance of RMRP in human cancers, we analyzed the TCGA database and found that the *RMRP* gene is amplified in multiple cancers (Figure 1A). Consistently, the expression of RMRP was preferentially upregulated in cancerous tissues compared to normal tissues (Figure 1B and Supplementary Figure 1A) by mining the Gene Expression Omnibus (GEO) and UALCAN databases (Chandrashekar et al., 2017). In addition, the Kaplan-Meier analysis revealed that the increased expression of RMRP is significantly associated with unfavorable prognosis of various human cancers, including breast cancer, head-neck carcinoma, lung adenocarcinoma, pancreatic ductal adenocarcinoma, stomach adenocarcinoma, and uterine corpus endometrial carcinoma (Figure 1C and Supplementary Figure 1B). Therefore, these findings suggest that RMRP may play an oncogenic role in cancer.

RNA Component of Mitochondrial RNA-Processing Endoribonuclease Promotes Proliferation and Migration of Breast Cancer Cells

Since we previously showed that RMRP endorses cancer cell growth by inhibiting the wt p53 pathway (Chen et al., 2021), we wanted to determine if RMRP can function independently of wt p53 or not. To do so, we selected the *TP53*-mutated breast cancer cell lines, JIMT-1 and BT549, as the model systems here by generating RMRP-stably overexpressing cell lines (Figure 2A). Interestingly, ectopic RMRP still significantly promoted the survival of these breast cancer cells (Figure 2C).

Conversely, using RMRP-knockout or -knockdown JIMT-1 and BT549 cells (Figure 2B), we found that depletion of RMRP significantly suppresses the growth of these cells (Figure 2D). Of note, knockout of RMRP via CRISPR-Cas9 achieved a more profound inhibitory effect on cancer cell growth (Figure 2D), because RMRP expression was more markedly depleted in JIMT-1 cells (Figure 2B). Furthermore, we found that ectopic expression of RMRP dramatically promotes, while depletion of RMRP prohibits, breast cancer cell migration (Figures 2E,F). Finally, we examined RMRP's function in wt p53-harboring breast cancer cells. As shown in Supplementary Figure 2, overexpression of RMRP significantly boosted, while knockdown of RMRP repressed, growth and migration of MCF-7 (Supplementary Figures 2A,B) and CAL-51 cells (Supplementary Figures 2C,D). Together, these results demonstrate that RMRP can promote proliferation and migration of breast cancer cells independently of wt p53.

RNA Component of Mitochondrial RNA-Processing Endoribonuclease Activates the AKT Pathway by Upregulating Its Expression

To explore the molecular mechanism underlying the wt p53-independent oncogenic effects of RMRP, we re-analyzed the RNA-seq results from HCT116 cells as reported in our previous study (Chen et al., 2021) and found that a myriad of genes are dysregulated in response to RMRP knockout (Figure 3A). The Kyoto Encyclopedia of Genes and Genomes (KEGG) analysis revealed the AKT signaling pathway as the most significantly downregulated in RMRP-depleted cells (Figure 3B). To validate this result, we determined if RMRP regulates the mRNA expression of AKT by RT-qPCR in breast cancer cells. Indeed, as shown in Figure 3C, overexpression of RMRP increased the level of AKT mRNA. Consistently, depletion of RMRP reduced the AKT mRNA level (Figure 3D). Consistently, ectopic

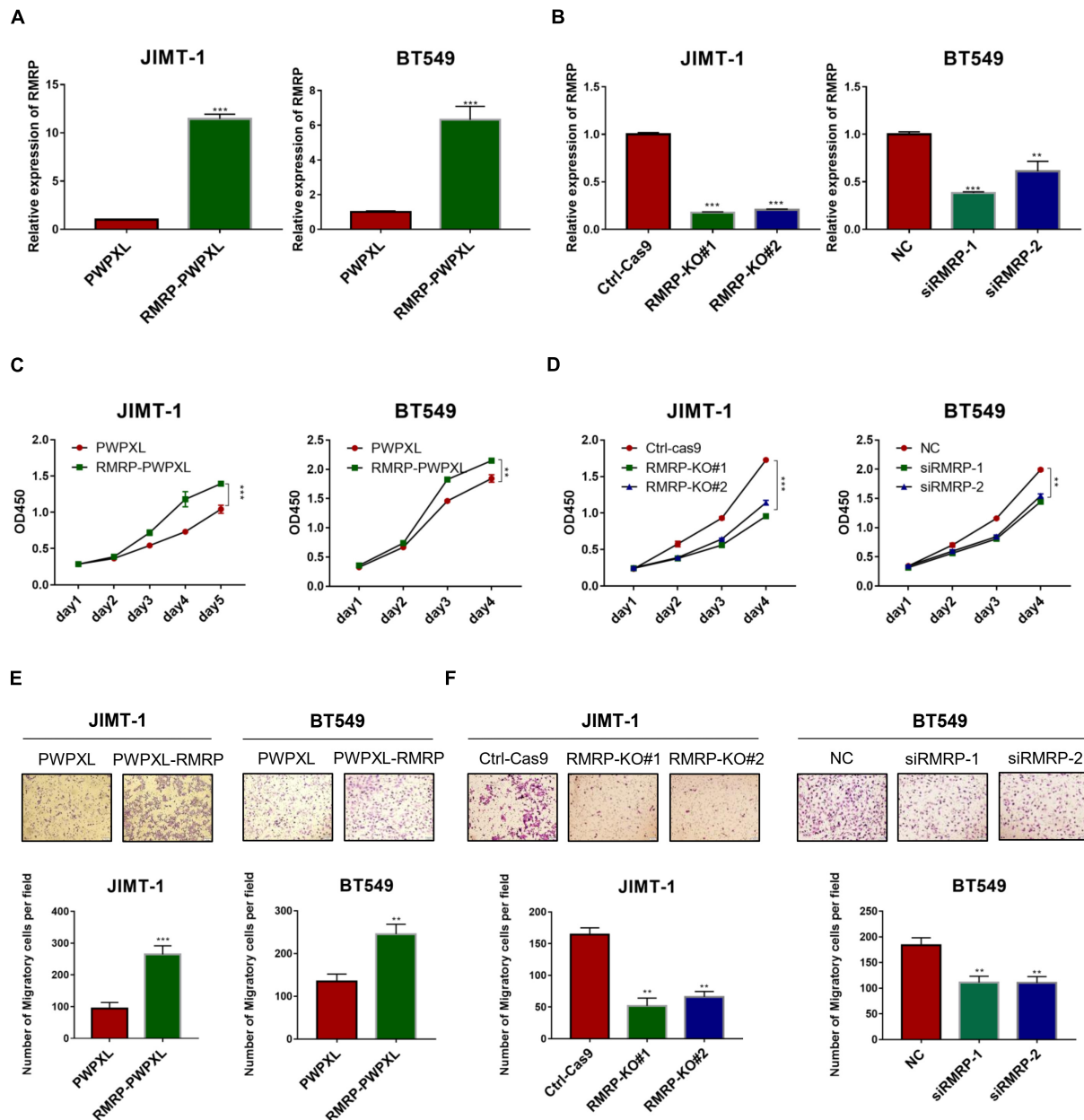


FIGURE 2 | RMRP promotes proliferation and migration of breast cancer cells. **(A)** Efficiency of RMRP-PWPXL overexpression in JIMT-1 and BT549 cells was evaluated by RT-qPCR. **(B)** Efficiency of CRISPR-Cas9-mediated knockout or RNAi-mediated knockdown of RMRP in JIMT-1 and BT549 cells was evaluated by RT-qPCR. **(C)** Overexpression of RMRP prompts JIMT-1 and BT549 cell proliferation determined by the CCK-8 assay. **(D)** Depletion of RMRP represses JIMT-1 and BT549 cell proliferation determined by the CCK-8 assay. **(E)** Overexpression of RMRP prompts JIMT-1 and BT549 cell migration determined by the Transwell assay. **(F)** Depletion of RMRP prompts JIMT-1 and BT549 cell migration determined by the Transwell assay. ** $p < 0.01$, *** $p < 0.001$.

RMRP dramatically increased the level of AKT protein as well as its phosphorylated form in JIMT-1 and BT549 cells (Figure 3E), while knockout or knockdown of RMRP resulted in the significant reduction of AKT and phosphorylated AKT in both breast cancer cell lines (Figure 3F). Collectively, these results demonstrate that RMRP can activate the AKT signaling pathway, which might account for its tumor-promoting functions in breast cancer cells.

RNA Component of Mitochondrial RNA-Processing Endoribonuclease Induces AKT Expression by Sequestering miR-206

Next, we wanted to determine how RMRP promotes AKT expression. Since miRNAs have been documented to target mRNAs for degradation and/or inhibit their translation (Bartel,

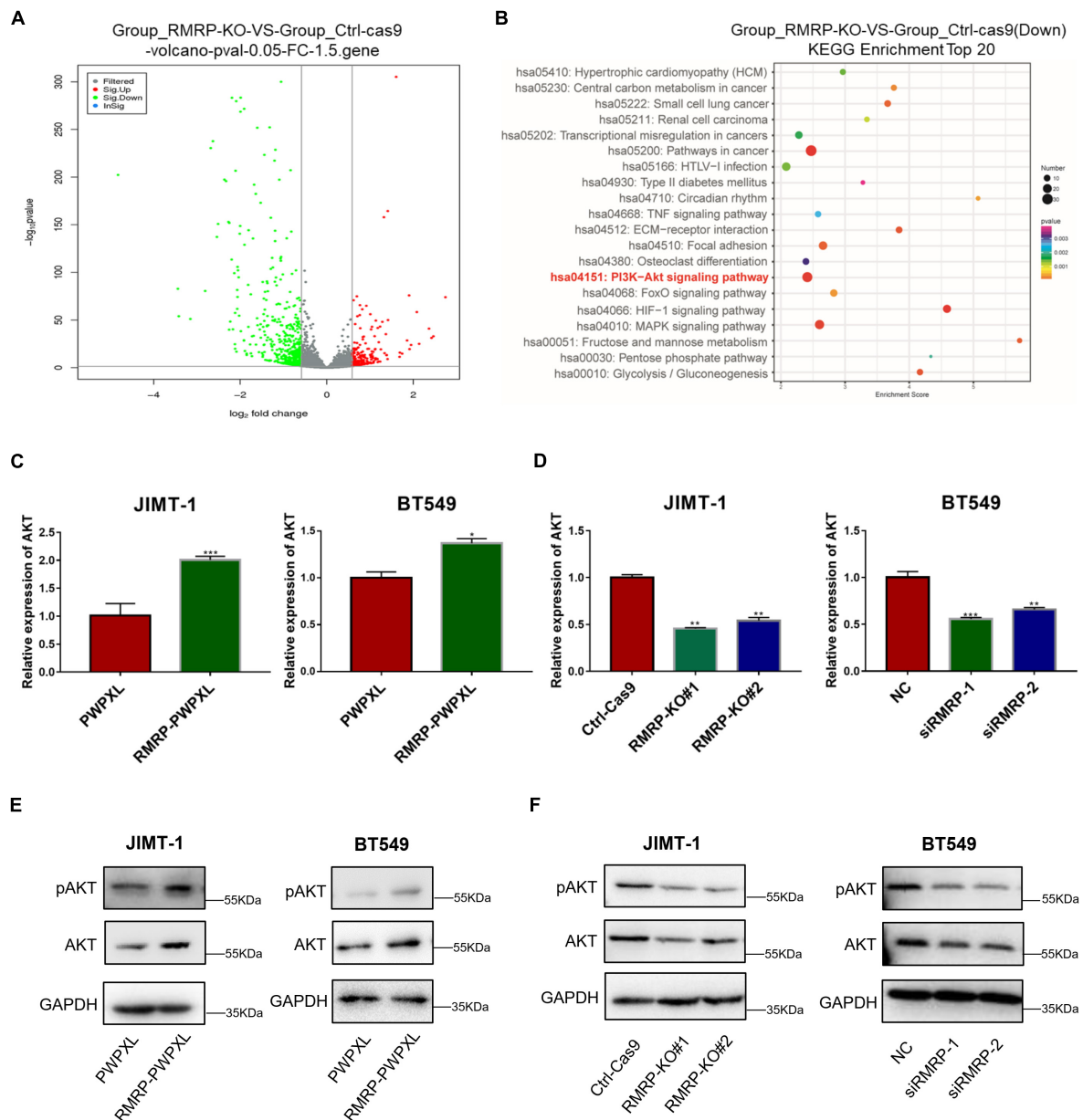


FIGURE 3 | RMRP upregulates AKT expression. (A) Differentially expressed gene profile in response to RMRP knockout revealed by the volcano-map. **(B)** Downregulated cancer-related pathways in response to RMRP knockout revealed by KEGG enrichment. **(C)** Overexpression of RMRP elevates AKT mRNA expression in JIMT-1 and BT549 cells. **(D)** Depletion of RMRP reduces AKT mRNA expression in JIMT-1 and BT549 cells. **(E)** Overexpression of RMRP elevates AKT protein expression and phosphorylated AKT in JIMT-1 and BT549 cells. **(F)** Depletion of RMRP reduces AKT protein expression and phosphorylated AKT in JIMT-1 and BT549 cells. * $p < 0.05$, ** $p < 0.01$, *** $p < 0.001$.

2009), and also, lncRNAs can derepress mRNA expression by sequestering these inhibitory miRNAs (Tay et al., 2014), we decided to test if RMRP might also utilize this mechanism to activate the expression of AKT. By searching the microRNA-target interaction database, miRTarBase (Huang et al., 2020), we identified miR-206 as a potential binder for both RMRP and AKT (Figure 4A). To test this, we ectopically expressed miR-206 mimics in JIMT-1 cells, and found that the levels of AKT and phosphorylated AKT are indeed reduced (Figure 4B).

Remarkably, overexpression of RMRP completely abrogated miR-206-mediated AKT inhibition (Figure 4B). Moreover, miR-206 mimics significantly repressed the expression of the luciferase reporter gene harboring the AKT 3'-UTR (Figure 4C). Consistently, overexpression of RMRP abolished miR-206 inhibition of the luciferase activity (Figure 4C). Taken together, these results demonstrate that RMRP induces AKT protein levels by overcoming miR-206's inhibition of its expression.

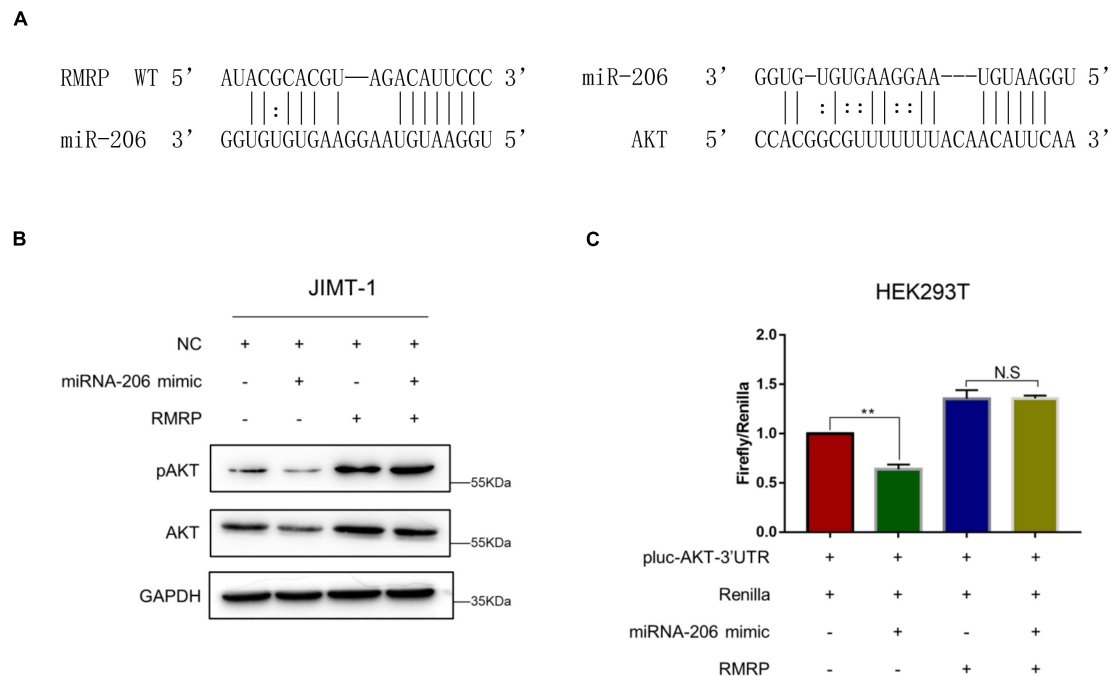


FIGURE 4 | RMRP upregulates AKT expression by sponging miR-206. **(A)** Both RMRP and AKT are potentially targeted by miR-206 through the miRTarBase. **(B)** miR-206 mimics-induced inhibition of AKT can be completely restored by RMRP overexpression. **(C)** The luciferase reporter assay was performed to show that RMRP overexpression completely abrogates miR-206 mimics-induced inhibition of the reporter gene fused with the AKT 3'-UTR. ** $p < 0.01$.

RNA Component of Mitochondrial RNA-Processing Endoribonuclease Negates miR-206-Mediated Repression of Breast Cancer Cell Growth and Migration

Given that miR-206 inhibits AKT expression (Figures 4B,C), we next tested if miR-206 suppresses breast cancer cell growth and migration. Delivery of the miR-206 inhibitor into JIMT-1 and BT549 cells significantly triggered their proliferation (Figure 5A). Consistently, the miR-206 inhibitor promoted JIMT-1 and BT549 cell migration (Figure 5B). Also, miR-206 mimics significantly reduced JIMT-1 and BT549 cell proliferation and migration (Figures 5C,D), indicating that miR-206 plays a tumor suppressive role in breast cancer. Importantly, RMRP overexpression completely abolished miR-206's tumor suppressive activity (Figures 5C,D). These results demonstrate that RMRP endorses breast cancer development by counteracting the tumor suppression function of miR-206.

RNA Component of Mitochondrial RNA-Processing Endoribonuclease Promotes Breast Cancer Cell Survival and Migration in an AKT-Dependent Fashion

Finally, we determined if RMRP promotes breast cancer cell growth and migration through activation of the AKT pathway.

The cell viability assay revealed that ectopic RMRP significantly increases cancer cell growth, while knockdown of AKT by two independent siRNAs blocks the tumor-promoting function of RMRP in JIMT-1 and BT549 cells (Figures 6A,B). In addition, the migratory potential of cancer cells was also evaluated through the transwell assay. Consistently, ectopic RMRP dramatically enhanced spread of JIMT-1 and BT549 cells, whereas depletion of AKT completely abrogated RMRP-induced cancer cell migration (Figures 6C,D). Taken together, these results demonstrate that activation of the AKT pathway is required for RMRP-mediated breast cancer survival and migration independently of wt p53.

DISCUSSION

RMRP has been shown to promote progression of various cancers, including colorectal cancer (Chen et al., 2021), gastric cancer (Shao et al., 2016), lung cancer (Meng et al., 2016), and cholangiocarcinoma (Tang et al., 2019). Recently, it was reported that recurrent mutations in the RMRP promoter are associated with higher expression level of RMRP in breast cancer, suggesting that this lncRNA may play a role in breast carcinogenesis (Rheinbay et al., 2017). In this study, we found that RMRP is amplified and overexpressed in numerous human cancers including breast cancer, and its high expression level is significantly associated with unfavorable cancer prognosis (Figure 1 and Supplementary Figure 1). We then verified RMRP as an oncogenic lncRNA, because it could drive breast cancer cell growth and migration (Figure 2 and Supplementary Figure 2).

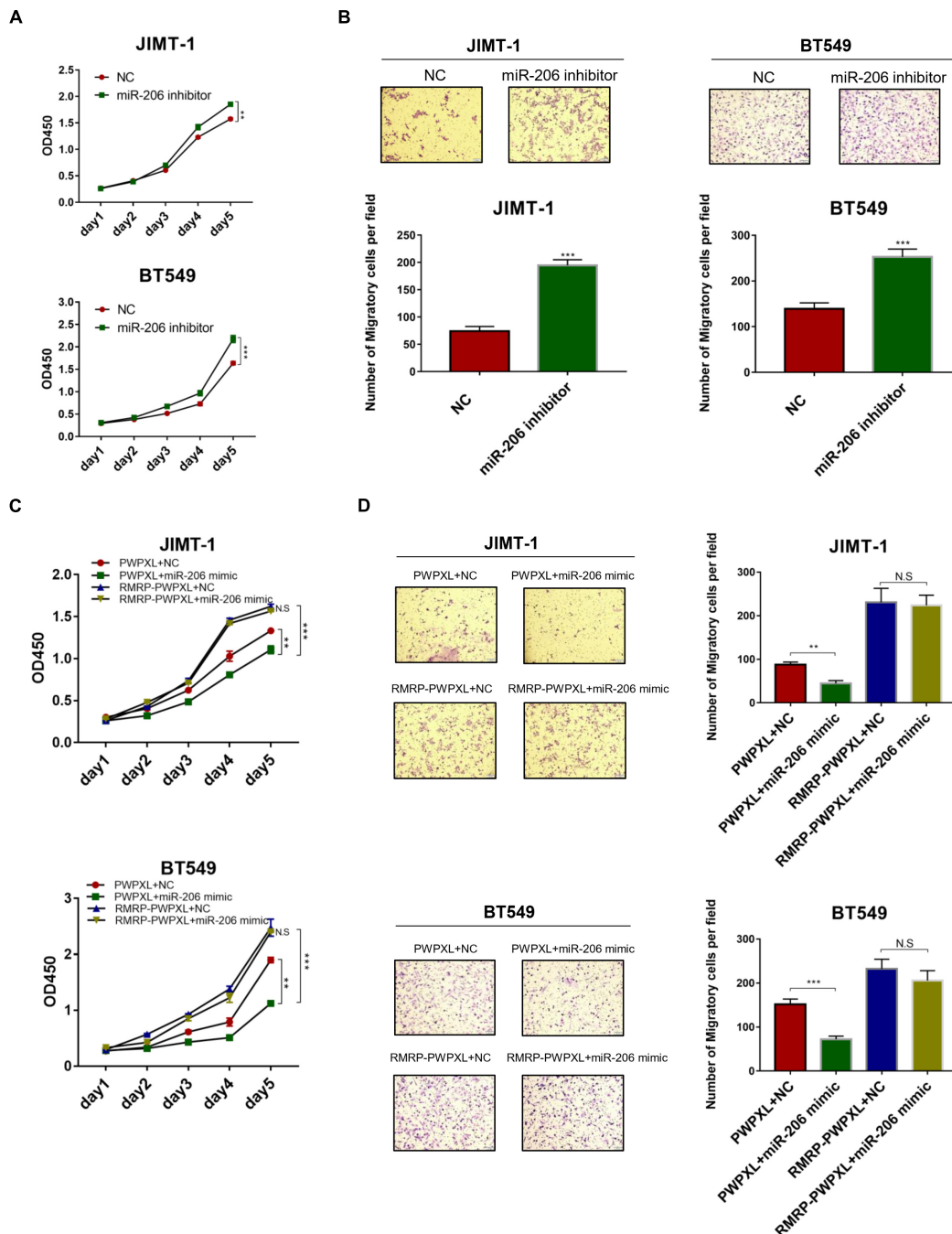


FIGURE 5 | RMRP negates the tumor suppressive function of miR-206. **(A)** Inhibition of miR-206 promotes JIMT-1 and BT549 cell proliferation determined by the CCK-8 assay. **(B)** Inhibition of miR-206 promotes JIMT-1 and BT549 cell migration determined by the Transwell assay. **(C)** RMRP overexpression abrogates miR-206 inhibition of cell proliferation determined by the CCK-8 assay. **(D)** RMRP overexpression abrogates miR-206 inhibition of cell migration determined by the Transwell assay. ** $p < 0.01$, *** $p < 0.001$.

Mechanistically, RMRP can activate the AKT signaling pathway as demonstrated by RNA-seq, RT-qPCR and immunoblotting analyses (Figure 3). Remarkably, RMRP induces AKT level and activity by preventing miR-206-mediated inhibition of AKT mRNA expression (Figure 4). Hence, our study as presented

above unveils a critical role of the RMRP-miR-206-AKT cascade in breast cancer cell growth and migration (Figures 5–7).

Activation of the PI3K/AKT pathway is crucial to tumor growth and propagation. In response to insulin, growth factors or cytokines, the lipid kinase PI3K can be recruited to the plasma

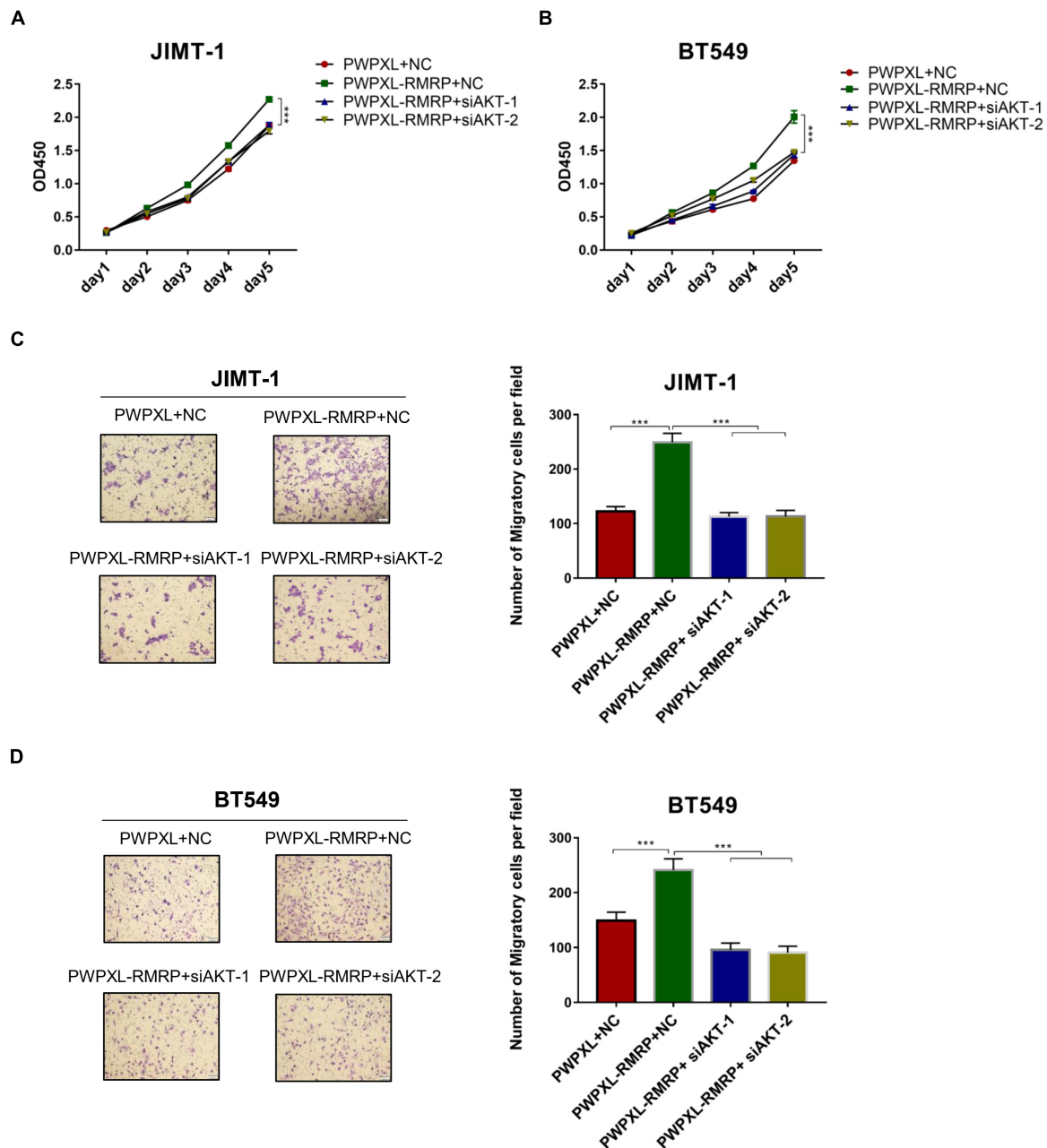
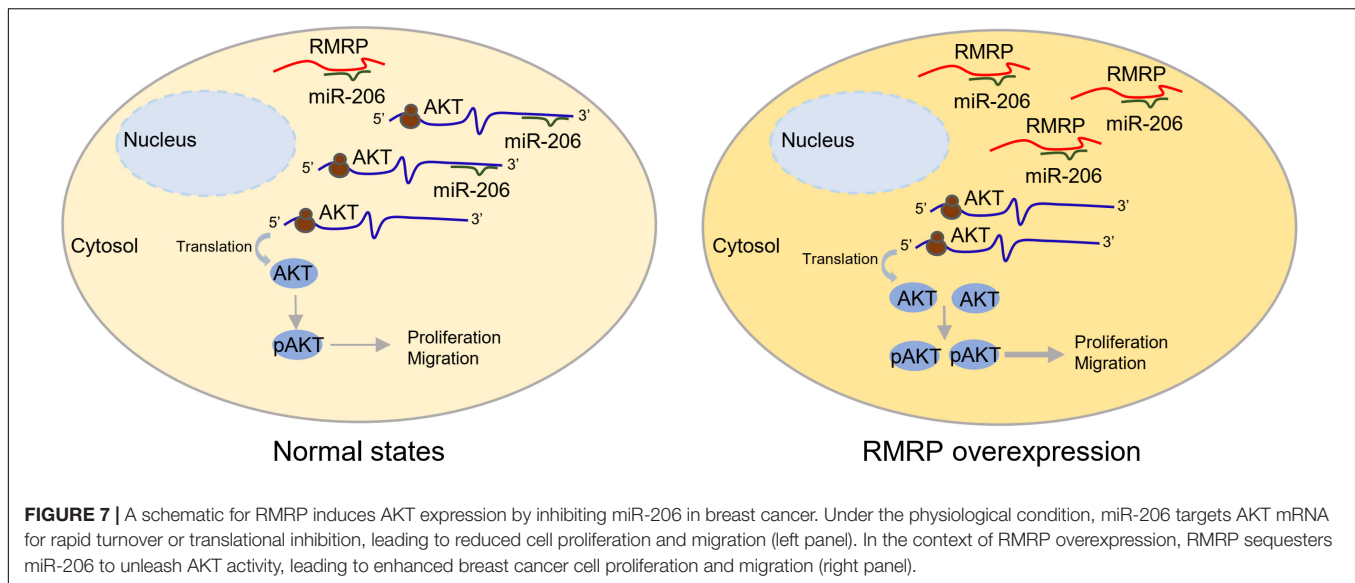


FIGURE 6 | Ectopic RMRP promotes breast cancer cell growth and migration dependently of AKT. **(A)** Knockdown of AKT restores RMRP-induced JIMT-1 cell proliferation determined by the CCK-8 assay. **(B)** Knockdown of AKT restores RMRP-induced BT549 cell proliferation determined by the CCK-8 assay. **(C)** Knockdown of AKT abolishes RMRP-induced JIMT-1 cell migration determined by the Transwell assay. **(D)** Knockdown of AKT abolishes RMRP-induced BT549 cell migration determined by the Transwell assay. *** $p < 0.001$.

membrane. PI3K then phosphorylates phosphatidylinositol 4,5-bisphosphate [PtdIns(4,5)P₂] to produce PtdIns(3,4,5)P₃ that serves as a second messenger to recruit AKT to the membrane, where it is fully activated through phosphorylation at Thr-308 and Ser-473 (Alessi et al., 1996, 1997). In general, activated AKT promotes cancer development via phosphorylation and inhibition of the three key downstream effectors, GSK3 (Cross et al., 1995), TSC2 (Menon et al., 2014), and FOXO

(Brunet et al., 1999). The first identified AKT substrate, GSK3, was found to mediate phosphorylation of c-MYC, SREBP, NRF2, and HIF1 α , leading to proteasomal degradation of these oncoproteins. GSK3 is inactivated through phosphorylation by AKT, which leads to derepression of these oncogenic transcription factors and consequent cancer growth and progression (Hoxhaj and Manning, 2020). Phosphorylation of TSC2 by AKT activated the mTORC1-S6K/4E-BP pathway that



is regarded as an energy-sensor to monitor metabolic changes and support cancer cell growth (Valvezan and Manning, 2019), while phosphorylation of FOXO transcription factors enhanced tumorigenesis by influencing glycolysis, redox homeostasis, and many other cell growth-associated pathways (Hornsveld et al., 2018). Thus, our finding has emphasized the important role of RMRP by activating AKT in breast cancer.

RMRP was originally identified as a causative gene for cartilage-hair hypoplasia, because numerous mutations in the *RMRP* gene caused the disease by affecting multiple organ systems (Ridanpää et al., 2001, 2002; Bonafe et al., 2002). Later studies revealed that mutation or loss of expression of RMRP results in the impairment of ribosome biogenesis and deregulation of the cyclin-dependent cell cycle progression, eventually leading to growth inhibition of the chondrocytic and lymphocytic cell lineages (Hermanns et al., 2005; Thiel et al., 2005). Indeed, genetic mouse models further verified the essential role of RMRP during early embryonic development, as homozygous inactivation of RMRP caused embryonic lethality (Rosenbluh et al., 2011). Additionally, it was found that human telomerase reverse transcriptase (hTERT) associates with RMRP to form a distinct ribonucleoprotein complex that has RNA-dependent RNA polymerase (RdRP) activity (Maida et al., 2009). RMRP could be thus processed into a double-stranded RNA with a hairpin structure and consequently endogenous siRNAs that are important for proper development and differentiation of skeletal, hair, and hematopoietic cells (Maida et al., 2013; Rogler et al., 2014). Recently, RMRP was also found to be involved in cancer development. The oncogenic transcription factors, such as β -catenin, YAP, and c-MYC, can activate the transcription of RMRP (Park and Jeong, 2015; Xiao et al., 2019) that promotes tumor cell survival and propagation by regulating the expression of, for example, Cyclin D2 and KRAS (Meng et al., 2016; Shao et al., 2016). Importantly, the existence of RMRP in the blood plasma exhibits a diagnostic value for detection of lung cancer (Leng et al.,

2018; Yuan et al., 2020). However, the role of RMRP in breast cancer remains unclear. We previously found that RMRP can moderately promote proliferation of p53-deficient HCT116 cells, suggesting a p53-independent role of RMRP, but the underlying mechanism was elusive. In this study, we demonstrate that this role is executed by sequestering miR-206 from targeting AKT mRNA for degradation, consequently leading to AKT-dependent breast cancer cell growth and migration. Similarly, RMRP can act as a sponge of miR-206 in other types of cancer (Meng et al., 2016; Shao et al., 2016). Although recent studies suggested a potential role of RMRP in regulating AKT in the ischemic models (Kong et al., 2019; Li and Sui, 2020), our study demonstrates for the first time that RMRP can promote breast cancer cell growth and migration via AKT activation.

miR-206 is a vertebrate-specific microRNA that is involved in a variety of human diseases, including skeletal and muscular developmental disorders, heart failure, chronic obstructive pulmonary disease, Alzheimer's disease, and numerous types of cancer (Novak et al., 2014). Studies showed that miR-206 can target estrogen receptor α (ER α), leading to inhibition of the estrogen signaling pathway and as thus cell growth and proliferation in breast cancer (Adams et al., 2007, 2009). miR-206 also suppresses stem-like and metastatic features of breast cancer by regulating the TWF1- MKL1-IL11 pathway (Samaeekia et al., 2017). In line with these findings, we also showed that miR-206 mimics repress JIMT-1 and BT549 cell growth and migration (Figures 5C,D), while the miR-206 inhibitor drives proliferation and migration of these cells (Figures 5A,B). Although a few studies suggested that miR-206 indirectly regulates the PI3K/AKT pathway by targeting c-Met or HDAC6 (Liu et al., 2017; Tang et al., 2017; Dai et al., 2018), our study identified AKT as a direct target gene of miR-206, because miR-206 mimics via its seed region significantly reduced the expression of AKT and the luciferase reporter gene fused with the 3'-UTR of AKT (Figures 4B,C). Therefore, these results reveal an

uncharacterized tumor suppressive role of miR-206 by targeting the AKT pathway.

Our results indicate that the oncogenic effect of RMRP on JIMT-1 and BT549 cells largely relies on AKT activation. Given the fact that the expression of miR-206 can be repressed by ER α (Adams et al., 2007), both JIMT-1 and BT549 that were derived from ER- or triple-negative breast cancer patients (Tanner et al., 2004; Grigoriadis et al., 2012; Tian and Zhang, 2018) should have high expression level of miR-206. Also, because the expression of ER is extremely low in both breast cancer cell lines, miR-206 may preferentially target AKT for rapid turnover, as evidenced by the immunoblotting analysis above (Figure 4B). In this scenario, miR-206 thereby plays a critical role in restricting the AKT activity. Remarkably, our data clearly demonstrate that RMRP can overcome miR-206 inhibition of AKT (Figures 4B,C, 5C,D) and, as thus, trigger AKT-dependent growth and migration of breast cancer cells (Figure 6).

CONCLUSION

RMRP was recently found to play a role in cancer development, but its function and the underlying mechanism in breast cancer are largely unknown. Our study uncovers the RMRP-miR-206-AKT regulatory axis as a new pathway that plays a critical role in promoting the growth and migration of aggressive breast cancer cells, which could serve as a potential target pathway for future development of prognostic biomarkers or therapeutic strategies for this type of cancer.

DATA AVAILABILITY STATEMENT

The original contributions presented in the study are included in the article/**Supplementary Material**, further inquiries can be directed to the corresponding authors.

REFERENCES

- Adams, B. D., Cowee, D. M., and White, B. A. (2009). The role of miR-206 in the epidermal growth factor (EGF) induced repression of estrogen receptor- α (ER α) signaling and a luminal phenotype in MCF-7 breast cancer cells. *Mol. Endocrinol.* 23, 1215–1230. doi: 10.1210/me.2009-0062
- Adams, B. D., Furneaux, H., and White, B. A. (2007). The micro-ribonucleic acid (miRNA) miR-206 targets the human estrogen receptor- α (ER α) and represses ER α messenger RNA and protein expression in breast cancer cell lines. *Mol. Endocrinol.* 21, 1132–1147. doi: 10.1210/me.2007-0022
- Alessi, D. R., Andjelkovic, M., Caudwell, B., Cron, P., Morrice, N., Cohen, P., et al. (1996). Mechanism of activation of protein kinase B by insulin and IGF-1. *EMBO J.* 15, 6541–6551. doi: 10.1002/j.1460-2075.1996.tb01045.x
- Alessi, D. R., James, S. R., Downes, C. P., Holmes, A. B., Gaffney, P. R., Reese, C. B., et al. (1997). Characterization of a 3-phosphoinositide-dependent protein kinase which phosphorylates and activates protein kinase B α . *Curr. Biol.* 7, 261–269.
- Bartel, D. P. (2009). MicroRNAs: target recognition and regulatory functions. *Cell* 136, 215–233.

ETHICS STATEMENT

The study was approved by the Ethics Committee of Fudan University Shanghai Cancer Center.

AUTHOR CONTRIBUTIONS

YH conducted and analyzed most of the experiments. BX conducted and analyzed part of the experiments and provided critical reagents and materials. MC performed part of IB analysis. HL and XW provided important instructions. QH and XZ conceived, designed and supervised the study, and analyzed the data. XZ drafted and edited the manuscript. HL edited the manuscript. All authors contributed to the article and approved the submitted version.

FUNDING

XZ was supported by the National Natural Science Foundation of China (Nos. 81874053 and 82072879), QH was supported by the National Natural Science Foundation of China (No. 81702352), and HL was in part supported by the Reynolds and Ryan Families Chair in Translational Cancer Fund.

ACKNOWLEDGMENTS

We thank the laboratory members for active and helpful discussion, and the innovative research team of high-level local university in Shanghai.

SUPPLEMENTARY MATERIAL

The Supplementary Material for this article can be found online at: <https://www.frontiersin.org/articles/10.3389/fcell.2021.730538/full#supplementary-material>

- Bonafe, L., Schmitt, K., Eich, G., Giedion, A., and Superti-Furga, A. (2002). RMRP gene sequence analysis confirms a cartilage-hair hypoplasia variant with only skeletal manifestations and reveals a high density of single-nucleotide polymorphisms. *Clin. Genet.* 61, 146–151.
- Brunet, A., Bonni, A., Zigmond, M. J., Lin, M. Z., Juo, P., Hu, L. S., et al. (1999). Akt promotes cell survival by phosphorylating and inhibiting a Forkhead transcription factor. *Cell* 96, 857–868. doi: 10.1016/s0092-8674(00)80595-4
- Cerami, E., Gao, J., Dogrusoz, U., Gross, B. E., Sumer, S. O., Aksoy, B. A., et al. (2012). The cBio cancer genomics portal: an open platform for exploring multidimensional cancer genomics data. *Cancer Discov.* 2, 401–404. doi: 10.1158/2159-8290.CD-12-0095
- Chandrasekar, D. S., Bashel, B., Balasubramanya, S. A. H., Creighton, C. J., Ponce-Rodriguez, I., Chakravarthi, B., et al. (2017). UALCAN: a portal for facilitating tumor subgroup gene expression and survival analyses. *Neoplasia* 19, 649–658. doi: 10.1016/j.neo.2017.05.002
- Chang, D. D., and Clayton, D. A. (1987). A novel endoribonuclease cleaves at a priming site of mouse mitochondrial DNA replication. *EMBO J.* 6, 409–417. doi: 10.1002/j.1460-2075.1987.tb04770.x

- Chen, Y., Hao, Q., Wang, S., Cao, M., Huang, Y., Weng, X., et al. (2021). Inactivation of the tumor suppressor p53 by long noncoding RNA RMRP. *Proc. Natl. Acad. Sci. U.S.A.* 118:e2026813118.
- Cross, D. A., Alessi, D. R., Cohen, P., Andjelkovich, M., and Hemmings, B. A. (1995). Inhibition of glycogen synthase kinase-3 by insulin mediated by protein kinase B. *Nature* 378, 785–789. doi: 10.1038/378785a0
- Dai, C., Xie, Y., Zhuang, X., and Yuan, Z. (2018). MiR-206 inhibits epithelial ovarian cancer cells growth and invasion via blocking c-Met/AKT/mTOR signaling pathway. *Biomed. Pharmacother.* 104, 763–770. doi: 10.1016/j.biopha.2018.05.077
- Esteller, M. (2011). Non-coding RNAs in human disease. *Nat. Rev. Genet.* 12, 861–874.
- Fabian, M. R., Sonenberg, N., and Filipowicz, W. (2010). Regulation of mRNA translation and stability by microRNAs. *Annu. Rev. Biochem.* 79, 351–379.
- Gao, J., Aksoy, B. A., Dogrusoz, U., Dresdner, G., Gross, B., Sumer, S. O., et al. (2013). Integrative analysis of complex cancer genomics and clinical profiles using the cBioPortal. *Sci. Signal.* 6:pl1. doi: 10.1126/scisignal.2004088
- Garneau, N. L., Wilusz, J., and Wilusz, C. J. (2007). The highways and byways of mRNA decay. *Nat. Rev. Mol. Cell Biol.* 8, 113–126. doi: 10.1038/nrm2104
- Garzon, R., Calin, G. A., and Croce, C. M. (2009). MicroRNAs in cancer. *Annu. Rev. Med.* 60, 167–179.
- Gibb, E. A., Brown, C. J., and Lam, W. L. (2011). The functional role of long non-coding RNA in human carcinomas. *Mol. Cancer* 10:38. doi: 10.1186/1476-4598-10-38
- Goldfarb, K. C., and Cech, T. R. (2017). Targeted CRISPR disruption reveals a role for RNase MRP RNA in human preribosomal RNA processing. *Genes Dev.* 31, 59–71. doi: 10.1101/gad.286963.116
- Grigoriadis, A., Mackay, A., Noel, E., Wu, P. J., Natrajan, R., Frankum, J., et al. (2012). Molecular characterisation of cell line models for triple-negative breast cancers. *BMC Genomics* 13:619. doi: 10.1186/1471-2164-13-619
- He, R. Z., Luo, D. X., and Mo, Y. Y. (2019). Emerging roles of lncRNAs in the post-transcriptional regulation in cancer. *Genes Dis.* 6, 6–15. doi: 10.1016/j.gendis.2019.01.003
- Hermanns, P., Bertuch, A. A., Bertin, T. K., Dawson, B., Schmitt, M. E., Shaw, C., et al. (2005). Consequences of mutations in the non-coding RMRP RNA in cartilage-hair hypoplasia. *Hum. Mol. Genet.* 14, 3723–3740. doi: 10.1093/hmg/ddi403
- Hornsveld, M., Dansen, T. B., Derksen, P. W., and Burgering, B. M. T. (2018). Re-evaluating the role of FOXOs in cancer. *Semin. Cancer Biol.* 50, 90–100. doi: 10.1016/j.semcancer.2017.11.017
- Hoxhaj, G., and Manning, B. D. (2020). The PI3K-AKT network at the interface of oncogenic signalling and cancer metabolism. *Nat. Rev. Cancer* 20, 74–88. doi: 10.1038/s41568-019-0216-7
- Huang, H. Y., Lin, Y. C., Li, J., Huang, K. Y., Shrestha, S., Hong, H. C., et al. (2020). miRTarBase 2020: updates to the experimentally validated microRNA-target interaction database. *Nucleic Acids Res.* 48, D148–D154.
- Huarte, M., Guttman, M., Feldser, D., Garber, M., Koziol, M. J., Kenzelmann-Broz, D., et al. (2010). A large intergenic noncoding RNA induced by p53 mediates global gene repression in the p53 response. *Cell* 142, 409–419. doi: 10.1016/j.cell.2010.06.040
- Hussen, B. M., Azimi, T., Hidayat, H. J., Taheri, M., and Ghafouri-Fard, S. (2021). Long non-coding RNA RMRP in the pathogenesis of human disorders. *Front. Cell Dev. Biol.* 9:676588. doi: 10.3389/fcell.2021.676588
- Jiang, Y. Z., Liu, Y. R., Xu, X. E., Jin, X., Hu, X., Yu, K. D., et al. (2016). Transcriptome analysis of triple-negative breast cancer reveals an integrated mRNA-lncRNA signature with predictive and prognostic value. *Cancer Res.* 76, 2105–2114. doi: 10.1158/0008-5472.CAN-15-3284
- Koirala, P., Huang, J., Ho, T. T., Wu, F., Ding, X., and Mo, Y. Y. (2017). LncRNA AK023948 is a positive regulator of AKT. *Nat. Commun.* 8:14422.
- Kong, F., Jin, J., Lv, X., Han, Y., Liang, X., Gao, Y., et al. (2019). Long noncoding RNA RMRP upregulation aggravates myocardial ischemia-reperfusion injury by sponging miR-206 to target ATG3 expression. *Biomed. Pharmacother.* 109, 716–725. doi: 10.1016/j.biopha.2018.10.079
- Leng, Q., Lin, Y., Zhan, M., and Jiang, F. (2018). An integromic signature for lung cancer early detection. *Oncotarget* 9, 24684–24692. doi: 10.18632/oncotarget.25227
- Li, X., and Sui, Y. (2020). Valproate improves middle cerebral artery occlusion-induced ischemic cerebral disorders in mice and oxygen-glucose deprivation-induced injuries in microglia by modulating RMRP/PI3K/Akt axis. *Brain Res.* 1747:147039. doi: 10.1016/j.brainres.2020.147039
- Lin, A., Hu, Q., Li, C., Xing, Z., Ma, G., Wang, C., et al. (2017). The LINK-A lncRNA interacts with PtdIns(3,4,5)P3 to hyperactivate AKT and confer resistance to AKT inhibitors. *Nat. Cell Biol.* 19, 238–251. doi: 10.1038/ncb3473
- Liu, F., Zhao, X., Qian, Y., Zhang, J., Zhang, Y., and Yin, R. (2017). MiR-206 inhibits head and neck squamous cell carcinoma cell progression by targeting HDAC6 via PTEN/AKT/mTOR pathway. *Biomed. Pharmacother.* 96, 229–237. doi: 10.1016/j.biopha.2017.08.145
- Liu, R., Chen, Y., Liu, G., Li, C., Song, Y., Cao, Z., et al. (2020). PI3K/AKT pathway as a key link modulates the multidrug resistance of cancers. *Cell Death Dis.* 11:797.
- Maida, Y., Kyo, S., Lassmann, T., Hayashizaki, Y., and Masutomi, K. (2013). Off-target effect of endogenous siRNA derived from RMRP in human cells. *Int. J. Mol. Sci.* 14, 9305–9318. doi: 10.3390/ijms14059305
- Maida, Y., Yasukawa, M., Furuuchi, M., Lassmann, T., Possemato, R., Okamoto, N., et al. (2009). An RNA-dependent RNA polymerase formed by TERT and the RMRP RNA. *Nature* 461, 230–235. doi: 10.1038/nature08283
- Meng, Q., Ren, M., Li, Y., and Song, X. (2016). LncRNA-RMRP acts as an oncogene in lung cancer. *PLoS One* 11:e0164845. doi: 10.1371/journal.pone.0164845
- Menon, S., Dibble, C. C., Talbott, G., Hoxhaj, G., Valvezan, A. J., Takahashi, H., et al. (2014). Spatial control of the TSC complex integrates insulin and nutrient regulation of mTORC1 at the lysosome. *Cell* 156, 771–785. doi: 10.1016/j.cell.2013.11.049
- Nagy, Á., Munkácsy, G., and Gyorffy, B. (2021). Pancancer survival analysis of cancer hallmark genes. *Sci Rep.* 11:6047. doi: 10.1038/s41598-021-84787-5
- Narla, A., and Ebert, B. L. (2010). Ribosomopathies: human disorders of ribosome dysfunction. *Blood* 115, 3196–3205. doi: 10.1182/blood-2009-10-178129
- Novak, J., Kruzliak, P., Bienertova-Vasku, J., Slaby, O., and Novak, M. (2014). MicroRNA-206: a promising theranostic marker. *Theranostics* 4, 119–133. doi: 10.7150/thno.7552
- Park, J., and Jeong, S. (2015). Wnt activated beta-catenin and YAP proteins enhance the expression of non-coding RNA component of RNase MRP in colon cancer cells. *Oncotarget* 6, 34658–34668. doi: 10.18632/oncotarget.5778
- Peng, W. X., Koirala, P., and Mo, Y. Y. (2017). LncRNA-mediated regulation of cell signaling in cancer. *Oncogene* 36, 5661–5667. doi: 10.1038/onc.2017.184
- Revathidevi, S., and Munirajan, A. K. (2019). Akt in cancer: mediator and more. *Semin. Cancer Biol.* 59, 80–91. doi: 10.1016/j.semcancer.2019.06.002
- Rheinbay, E., Parasuraman, P., Grimsby, J., Tiao, G., Engreitz, J. M., Kim, J., et al. (2017). Recurrent and functional regulatory mutations in breast cancer. *Nature* 547, 55–60.
- Ridanpää, M., Sistonen, P., Rockas, S., Rimoin, D. L., Makitie, O., and Kaitila, I. (2002). Worldwide mutation spectrum in cartilage-hair hypoplasia: ancient founder origin of the major 70A→G mutation of the untranslated RMRP. *Eur. J. Hum. Genet.* 10, 439–447. doi: 10.1038/sj.ejhg.5200824
- Ridanpää, M., van Eenennaam, H., Pelin, K., Chadwick, R., Johnson, C., Yuan, B., et al. (2001). Mutations in the RNA component of RNase MRP cause a pleiotropic human disease, cartilage-hair hypoplasia. *Cell* 104, 195–203. doi: 10.1016/s0092-8674(01)00205-7
- Rogler, L. E., Kosmyrna, B., Moskowitz, D., Bebaee, R., Rahimzadeh, J., Kutchko, K., et al. (2014). Small RNAs derived from lncRNA RNase MRP have gene-silencing activity relevant to human cartilage-hair hypoplasia. *Hum. Mol. Genet.* 23, 368–382. doi: 10.1093/hmg/ddt427
- Rosenbluh, J., Nijhawand, D., Chen, Z., Wong, K. K., Masutomi, K., and Hahn, W. C. (2011). RMRP is a non-coding RNA essential for early murine development. *PLoS One* 6:e26270. doi: 10.1371/journal.pone.0026270
- Samaeekia, R., Adorno-Cruz, V., Bockhorn, J., Chang, Y. F., Huang, S., Prat, A., et al. (2017). miR-206 inhibits stemness and metastasis of breast cancer by targeting MKL1/IL11 pathway. *Clin. Cancer Res.* 23, 1091–1103. doi: 10.1158/1078-0432.ccr-16-0943
- Schmitt, A. M., and Chang, H. Y. (2016). Long noncoding RNAs in cancer pathways. *Cancer Cell* 29, 452–463. doi: 10.1016/j.ccell.2016.03.010
- Shang, Z., Yu, J., Sun, L., Tian, J., Zhu, S., Zhang, B., et al. (2019). LncRNA PCAT1 activates AKT and NF-kappaB signaling in castration-resistant prostate cancer

- by regulating the PHLPP/FKBP51/IKKalpha complex. *Nucleic Acids Res.* 47, 4211–4225. doi: 10.1093/nar/gkz108
- Shao, Y., Ye, M., Li, Q., Sun, W., Ye, G., Zhang, X., et al. (2016). LncRNA-RMRP promotes carcinogenesis by acting as a miR-206 sponge and is used as a novel biomarker for gastric cancer. *Oncotarget* 7, 37812–37824. doi: 10.18632/oncotarget.9336
- Son, H. J., Choi, E. J., Yoo, N. J., and Lee, S. H. (2019). Somatic mutations in long-non-coding RNA RMRP in acute leukemias. *Pathol. Res. Pract.* 215:152647. doi: 10.1016/j.prp.2019.152647
- Tang, L., Wang, Y., Wang, H., Xu, B., Ji, H., Xu, G., et al. (2019). Long noncoding-RNA component of mitochondrial RNA processing endoribonuclease is involved in the progression of cholangiocarcinoma by regulating microRNA-217. *Cancer Sci.* 110, 2166–2179. doi: 10.1111/cas.14074
- Tang, R., Ma, F., Li, W., Ouyang, S., Liu, Z., and Wu, J. (2017). miR-206-3p Inhibits 3T3-L1 cell adipogenesis via the c-Met/PI3K/Akt pathway. *Int. J. Mol. Sci.* 18:1510. doi: 10.3390/ijms18071510
- Tanner, M., Kapanen, A. I., Junttila, T., Raheem, O., Grenman, S., Elo, J., et al. (2004). Characterization of a novel cell line established from a patient with Herceptin-resistant breast cancer. *Mol. Cancer Ther.* 3, 1585–1592.
- Tay, Y., Rinn, J., and Pandolfi, P. P. (2014). The multilayered complexity of ceRNA crosstalk and competition. *Nature* 505, 344–352. doi: 10.1038/nature12986
- Thiel, C. T., Horn, D., Zabel, B., Ekici, A. B., Salinas, K., Gebhart, E., et al. (2005). Severely incapacitating mutations in patients with extreme short stature identify RNA-processing endoribonuclease RMRP as an essential cell growth regulator. *Am. J. Hum. Genet.* 77, 795–806. doi: 10.1086/497708
- Tian, X., and Zhang, Z. (2018). miR-191/DAB2 axis regulates the tumorigenicity of estrogen receptor-positive breast cancer. *IUBMB Life* 70, 71–80. doi: 10.1002/iub.1705
- Valvezan, A. J., and Manning, B. D. (2019). Molecular logic of mTORC1 signalling as a metabolic rheostat. *Nat. Metab.* 1, 321–333.
- Wolin, S. L., and Maquat, L. E. (2019). Cellular RNA surveillance in health and disease. *Science* 366, 822–827. doi: 10.1126/science.aax2957
- Xiao, X., Gu, Y., Wang, G., and Chen, S. (2019). c-Myc, RMRP, and miR-34a-5p form a positive-feedback loop to regulate cell proliferation and apoptosis in multiple myeloma. *Int. J. Biol. Macromol.* 122, 526–537. doi: 10.1016/j.ijbiomac.2018.10.207
- Yuan, S., Xiang, Y., Guo, X., Zhang, Y., Li, C., Xie, W., et al. (2020). Circulating long noncoding RNAs act as diagnostic biomarkers in non-small cell lung cancer. *Front. Oncol.* 10:537120. doi: 10.3389/fonc.2020.537120
- Zhang, A., Zhou, N., Huang, J., Liu, Q., Fukuda, K., Ma, D., et al. (2013). The human long non-coding RNA-RoR is a p53 repressor in response to DNA damage. *Cell Res.* 23, 340–350. doi: 10.1038/cr.2012.164
- Zhou, X., Hao, Q., Liao, J., Zhang, Q., and Lu, H. (2013). Ribosomal protein S14 unties the MDM2-p53 loop upon ribosomal stress. *Oncogene* 32, 388–396. doi: 10.1038/onc.2012.63

Conflict of Interest: The authors declare that the research was conducted in the absence of any commercial or financial relationships that could be construed as a potential conflict of interest.

Publisher's Note: All claims expressed in this article are solely those of the authors and do not necessarily represent those of their affiliated organizations, or those of the publisher, the editors and the reviewers. Any product that may be evaluated in this article, or claim that may be made by its manufacturer, is not guaranteed or endorsed by the publisher.

Copyright © 2021 Huang, Xie, Cao, Lu, Wu, Hao and Zhou. This is an open-access article distributed under the terms of the Creative Commons Attribution License (CC BY). The use, distribution or reproduction in other forums is permitted, provided the original author(s) and the copyright owner(s) are credited and that the original publication in this journal is cited, in accordance with accepted academic practice. No use, distribution or reproduction is permitted which does not comply with these terms.



OPEN ACCESS

Edited by:

Tao Zeng,
University of Chinese Academy
of Sciences, Chinese Academy
of Sciences (CAS), China

Reviewed by:

Abhijit Shukla,
Memorial Sloan Kettering Cancer
Center, United States
Jutang Li,
Shanghai Jiao Tong University School
of Medicine, China
Rongbin Wang,
Anhui College of Traditional Chinese
Medicine, China

***Correspondence:**

Jun Xu
jun_xu@fudan.edu.cn
Xiaofan Yin
yxf_mh2011@163.com

[†] These authors have contributed
equally to this work

Specialty section:

This article was submitted to
Epigenomics and Epigenetics,
a section of the journal
Frontiers in Cell and Developmental
Biology

Received: 03 June 2021

Accepted: 11 August 2021

Published: 30 September 2021

Citation:

Gu H, Huang Z, Zhou K, Chen G,
Bian C, Xu J and Yin X (2021)
Expression Profile Analysis of Long
Non-coding RNA in OVX
Models-Derived BMSCs
for Postmenopausal Osteoporosis
by RNA Sequencing
and Bioinformatics.
Front. Cell Dev. Biol. 9:719851.
doi: 10.3389/fcell.2021.719851

Expression Profile Analysis of Long Non-coding RNA in OVX Models-Derived BMSCs for Postmenopausal Osteoporosis by RNA Sequencing and Bioinformatics

Huijie Gu[†], Zhongyue Huang[†], Kaifeng Zhou[†], Guangnan Chen, Chong Bian, Jun Xu* and Xiaofan Yin*

Department of Orthopedics, Minhang Hospital, Fudan University, Shanghai, China

Osteoporosis (OP) has the characteristics of a systematically impaired bone mass, strength, and microstructure. Long non-coding RNAs (lncRNAs) are longer than 200 nt, and their functions in osteoporosis is yet not completely understood. We first harvested the bone marrow mesenchymal stem cells (BMSCs) from ovariectomy (OVX) and sham mice. Then, we systematically analyzed the differential expressions of lncRNAs and messenger RNAs (mRNAs) and constructed lncRNA-mRNA coexpression network in order to identify the function of lncRNA in osteoporosis. Totally, we screened 743 lncRNAs (461 upregulated lncRNAs and 282 downregulated lncRNAs) and 240 mRNAs (128 upregulated and 112 downregulated) with significantly differential expressions in OP compared to normal. We conducted Gene Ontology (GO) and Kyoto Encyclopedia of Genes and Genomes (KEGG) functional analyses to investigate the functions and pathways of the differential expression of messenger RNAs (mRNAs), a coexpressed network of lncRNA/mRNA. Quantitative PCR (qPCR) validated that the expressions of NONMMUT096150.1, NONMMUT083450.1, and NONMMUT029743.2 were all downregulated, whereas NONMMUT026970.2, NONMMUT051734.2, NONMMUT003617.2, and NONMMUT034049.2 were all upregulated in the OVX group. NONMMUT096150.1, as a key lncRNA in OP, was identified to modulate the adipogenesis of BMSCs. Further analysis suggested that NONMMUT096150.1 might modulate the adipogenesis of BMSCs via the peroxisome proliferator-activated receptor (PPAR) signaling pathway, AMPK signaling pathway, and the lipolysis regulation in adipocyte and adipocytokine signaling pathway. Our study expands the understanding of lncRNA in the pathogenesis of OP.

Keywords: osteoporosis, lncRNA, BMSCs, OVX model, differentially expressed, NONMMUT0961501

INTRODUCTION

Osteoporosis (OP) has the characteristics of a systematically impaired bone mass, strength and microstructure, which generates fracture risk and exhibits an association with substantial pain, disability, and even death (Kanis et al., 2019). Postmenopausal osteoporosis (PMOP) is the most common primary osteoporosis (POP) and results from estrogen deficiency (Rosen, 2000). Several studies indicate that the imbalance differentiation of BMSCs plays a basic role in PMOP. Nonetheless, it is yet elusive toward the underlining mechanisms toward PMOP (Noh et al., 2020).

lncRNAs, a sort of non-coding RNAs with > 200 nt, are largely reported to have an association with various diseases, including osteoporosis (He et al., 2020; He and Chen, 2021). lncRNA itself does not encode protein and regulates gene expression at epigenetic, transcription, and posttranscriptional levels (Dykes and Emanueli, 2017; Wang et al., 2019). lncRNA regulates the expression of mRNA encoding protein by binding to microRNAs (miRNAs) of specific sequences, so lncRNA is called miRNA sponge (Yoon et al., 2014). Li et al. (2018) identified that lncRNA Bmncr mediates age-related bone loss via reversing the age-related alteration between osteogenesis and adipogenic differentiation of BMSCs. Yin et al. (2021) reported that lncRNAs (AK039312 and AK079370) exerted an inhibition effect on the differentiation of osteoblast and the formation of bone by suppressing osteogenic transcription factors via targeting miR-199b-5p, then activating GSK-3 β and in-depth inhibiting the Wnt/ β -catenin pathway. Knockdown of LNC_000052 could promote osteogenesis and inhibit apoptosis of BMSCs via the PI3K/Akt signaling pathway (Li et al., 2020). Increasing study indicates that lncRNAs exhibit importantly in BMSCs differentiation and osteoporosis. Nevertheless, it is not clear on the roles of most lncRNAs in osteoporosis.

Here, we utilized RNA-sequencing to identify the differentially expressed lncRNAs (DElncRNA) and mRNAs (DEmRNAs) of BMSCs from sham and OVX mice. Subsequently, we constructed a protein-protein interaction (PPI) network of DEmRNAs and coexpressed networks of DElncRNA/DEmRNA and analyzed the function of networks by GO and KEGG. We determined sectional DElncRNAs expression by quantitative real-time PCR (qRT-PCR). Our findings gave a new insight into clarifying lncRNAs' regulatory role in PMOP.

MATERIALS AND METHODS

Ovariectomy Mouse Model

The animal experimental protocols got the approval of the Animal Care and Experiment Committee of Fudan University. Six-week-old C57BL female mice (about 20–24 g of weight) were obtained from the Shanghai Model Organisms Center (Shanghai, China). No obvious difference existed in mice's weight at the start. Twelve mice received an ovariectomy operation (OVX), while another 12 mice received sham operation, after anesthesia with intraperitoneal injection of pentobarbital sodium (50 mg/kg

body weight). We executed ovariectomy as previously described (Gu et al., 2020).

Bone Mineral Density Measurement and Micro-CT Analysis

At 6 weeks postoperation, we harvested the left femurs to determine the bone mineral density (BMD) via dual-energy X-ray absorptiometry (DXA; GE Healthcare, Piscataway, NJ, United States). Then, we fixed the left femur with 4% paraformaldehyde for 24 h and analyzed it by SkyScan-1176 microcomputed tomography (μ CT) (Bruker microCT, Kontich, Germany). The trabecular bone volume/tissue volume ratio (BV/TV) of the distal femur was measured.

mBMSCs Culture

According to previous reports, bone marrow was flushed from the femur and tibia and then isolated mBMSCs (Gu et al., 2020). Taken briefly, at 6-week postoperation, the mice were euthanized. We harvested the femur and tibia and removed the epiphyses of individual bones. Bone marrow was washed from the diaphysis by medium containing low-glucose Dulbecco's modified Eagle's medium (DMEM) (LG-DMEM; Gibco BRL, United States), 10% fetal bovine serum (FBS) (Gibco BRL, United States), 2 mM glutamine, 1% streptomycin/penicillin. We obtained cell suspension by repeatedly aspirating cells with the use of 20-gauge needle. Cells (1×10^6) with indicated culture medium were inoculated in 60 mm culture dish under 37°C incubator containing 5% CO₂. We changed the medium twice 1 week and utilized the cells with well status after three or five passages.

RNA Extraction, RNA-Sequencing, and Analysis of Differentially Expressed Genes

MiRNA isolation kit (Ambion, Austin, TX, United States) was applied to extract the whole RNA from BMSCs of three mice in an individual group. TruSeq stranded total RNA with Ribo-Zero Gold (Illumina, San Diego, CA, United States) was employed to generate the libraries as the manual described. RNA was sequenced on the Illumina sequencing platform (HiSeqTM 2500; Shanghai Oebiotech Co., Ltd., Shanghai, China). Paired-end reads (125 bp/150 bp) were generated. Then, lncRNAs and mRNAs with the differential expression between the sham and OVX mice were identified by DESeq software packages.¹ The differentially expressed genes were identified with the criteria of fold change > 2; $p < 0.05$. TBtools was used to analyze the distribution of DElncRNAs and DEmRNAs on chromosomes (Chen et al., 2020).

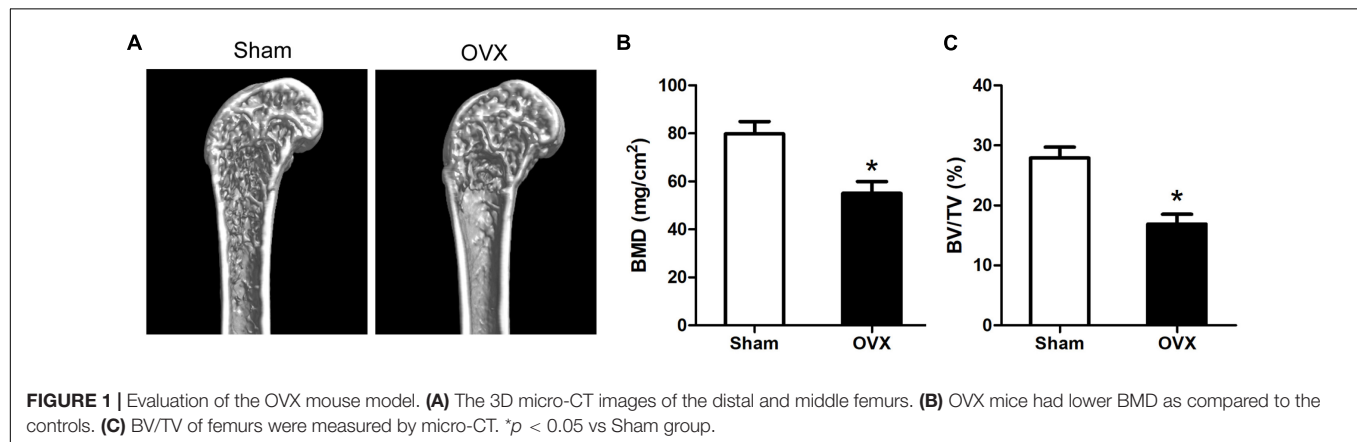
Functional Annotation of DEmRNA and DElncRNA-Related mRNAs

The Gene Ontology (GO) was conducted to explore DEmRNAs and lncRNA coexpressed mRNAs' biological functions. Kyoto Encyclopedia of Genes and Genomes (KEGG) was employed to uncover the pathways of DEmRNAs and lncRNA coexpressed

¹<http://bioconductor.org/packages/release/bioc/html/DESeq.html>

TABLE 1 | Primers for qRT-PCR in the experiment.

Gene symbol	Forward primer	Reverse primer
NONMMUT096150.1	GCGTCCTTACAGGAGTGAA	GGTTCCGCACGGGATGTA
NONMMUT083450.1	TTTGAGGGCCTCTCTAGCCT	CAGACCTAGCAGATGGAGCG
NONMMUT029743.2	GAGCAAGTTGTGTGTGCCAG	CAAAACCCCTGACCTTGCAGC
NONMMUT026970.2	TTCTCCCTCGTTACCCGACT	CCTCAACGGAGACACACTCC
NONMMUT051734.2	ACTGCCTTTCCTTGTCCCTG	TGTGCTGTGAACCAAGCTGA
NONMMUT003617.2	TTAGAAGCATCCCGTGGTCC	TTCTCAGACTGTCCTCGGGT
NONMMUT030409.2	CGCACCATTGCACCTTGTGA	AACAAAGCCTGCCTCTCTCC
β -actin	ATCATGTTTGAGACCTTCAA	CATCTCTTGCTCGAAGTCCA



mRNAs. $p < 0.05$ means there is a statistically significant difference regarding the GO terms and pathways.

DElncRNA–DEmRNA Coexpression Analysis

DElncRNA–DEmRNA coexpression analysis was taken to investigate DElncRNAs' roles in osteoporosis. We analyzed DElncRNAs and DEmRNAs referring to the criteria of fold change > 2 , $p < 0.05$. DElncRNA–DEmRNA pairs with correlation coefficient ≥ 0.98 and $p < 0.05$ were selected in the analysis. We visualized the coexpression network utilizing the software Cytoscape 3.7.0, and we measured the nodes' centrality in the coexpression network by K-core analysis.

DElncRNAs Validation

Seven DElncRNAs were validated by qPCR. The cDNAs were reversed transcribed from RNA utilizing the NCodeTM EXPRESS SYBR[®] GreenERTM miRNA qPCR kit (Invitrogen, Carlsbad, CA, United States). We conducted qPCR reaction on the GeneAmp PCR system 9600 (Perkin Elmer, United States). All primers were obtained from Sangon Biotech (Shanghai, China), and their sequences are shown in **Table 1**. The relative lncRNAs expression was obtained after normalization to β -actin. $2^{-\Delta \Delta C_t}$ method was applied to calculate the expression level of each lncRNA.

Statistical Analysis

All representative data was analyzed by SPSS 22.0 (IBM Corp., Armonk, NY, United States). The data were shown as the

mean \pm standard deviation (SD). The difference existing in two and more groups were determined by Student's t -test and one-way analysis of variance (ANOVA), respectively. The fold change of each lncRNA expression was shown after calculation by the $2^{-\Delta \Delta C_t}$ method. $p < 0.05$ means that there is a significant difference in compared groups.

RESULTS

Ovariectomy Mice Model Evaluation

We evaluated the OVX mice model as the methods described before. We harvested left femurs after 6 weeks of operation and tested them. A reduced bone formation was indicated by micro-CT in the OVX group (**Figure 1A**). The BMD and bone volume (BV)/total volume (TV) of OVX mice were shown to reduce in comparison with the sham group (**Figures 1B,C**).

DElncRNAs and DEmRNAs in Bone Marrow Mesenchymal Stem Cells of Ovariectomy Mice

The gene expression variation between OVX and sham groups was assessed by heat map analysis and volcano plots (**Figure 2**). In this study, the DElncRNAs and DEmRNAs were identified. In total, 743 DElncRNAs were identified in OVX mice, including 461 upregulated lncRNAs, and 282 downregulated lncRNAs; the top 10 DElncRNAs were NONMMUT026970.2, NONMMUT010789.2, NONMMUT016319.2, NONMMUT0

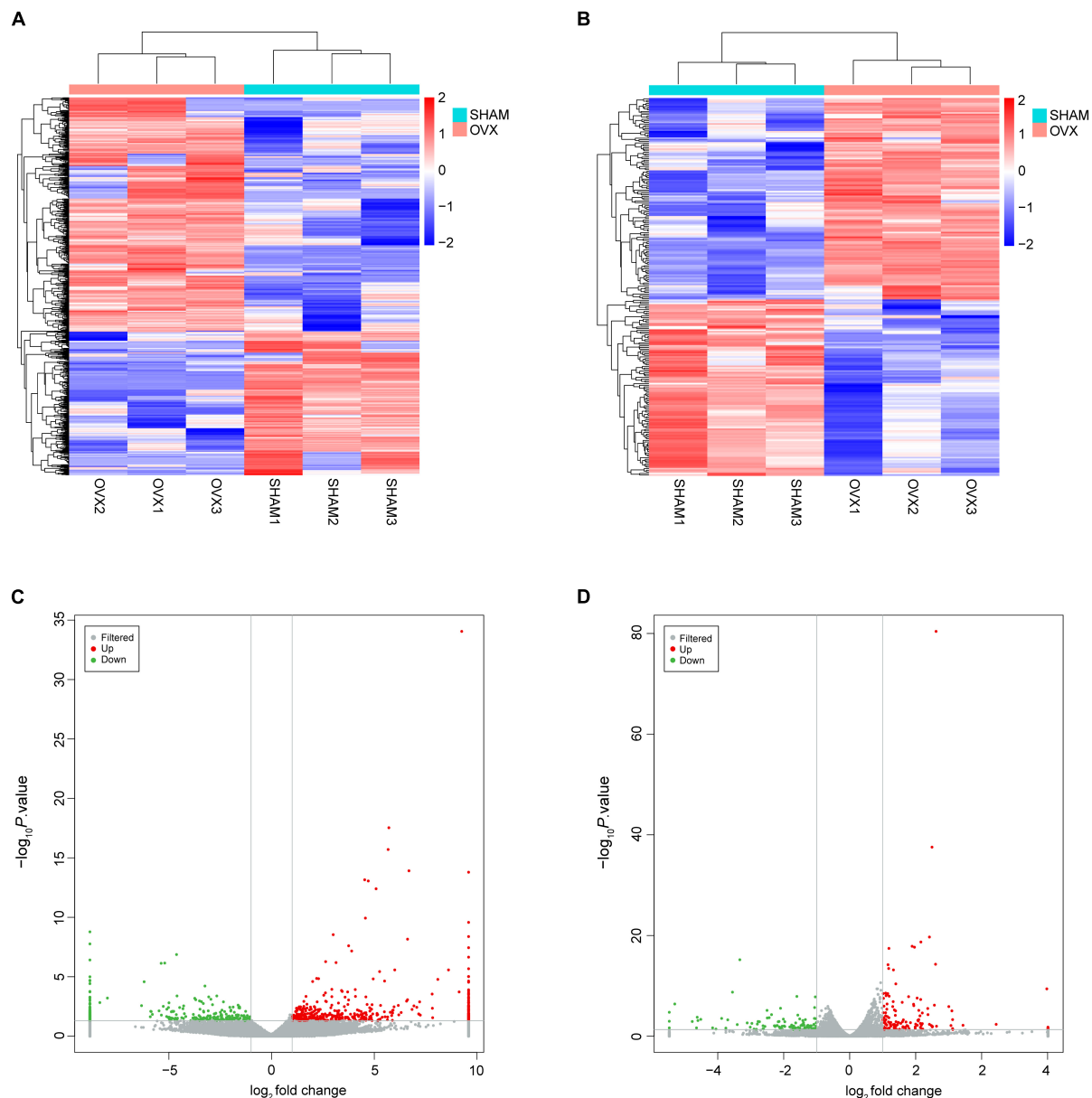


FIGURE 2 | Expression profiles of lncRNAs and mRNAs. **(A)** Cluster analysis of differentially expressed lncRNAs. **(B)** Cluster analysis of differentially expressed mRNAs. Red indicates increased expression, and blue denotes decreased expression. **(C)** The volcano plot of differentially expressed lncRNAs. **(D)** The volcano plot of differentially expressed mRNAs.

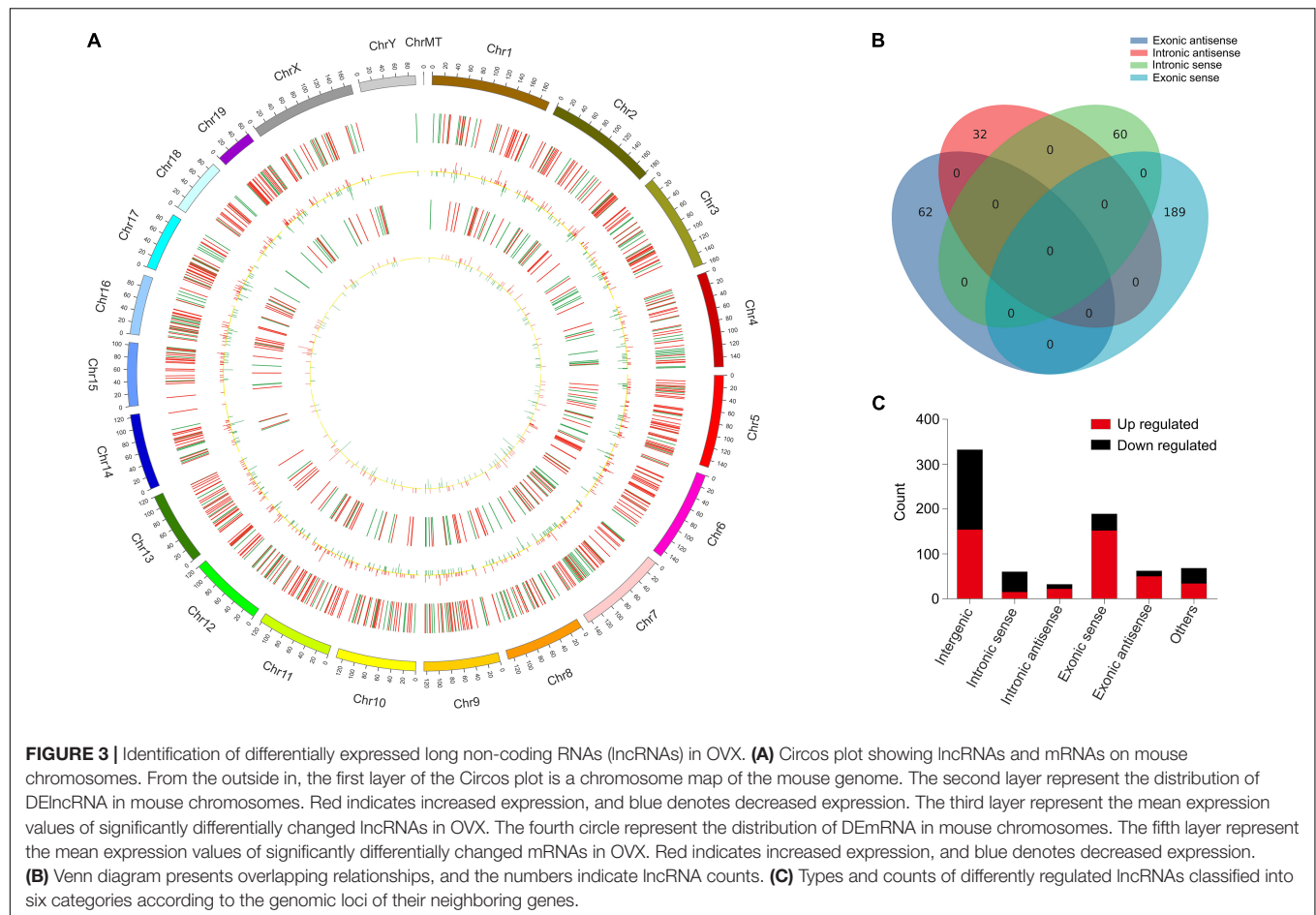
51734.2, NONMMUT036562.2, NONMMUT015053.2, NONMMUT069358.2, NONMMUT034071.2, NONMMUT038202.2, and NONMMUT026990.2 (**Supplementary Table 1**). Two hundred forty DEMRNAs were identified in OVX mice, including 128 upregulated and 112 downregulated; the top 10 DEMRNAs were *Scd1*, *Plin1*, *Cyp2f2*, *Cfd*, *Cidec*, *Thrsp*, *Fabp4*, *A2m*, *Glb1l2*, and *Cxcl14* (**Supplementary Table 2**).

These DELncRNAs and DEMRNAs were distributed in all chromosomes including chromosomes X and Y (**Figure 3A**). The DELncRNAs (totally 743) were classified into six categories: 332 were intergenic, 60 were intronic sense, 32 were intronic

antisense, 189 were exonic sense, 62 were exonic antisense, and 68 were others. There were no overlaps between the four categories, including intronic and antisense, and exonic sense and antisense (**Figure 3B**). Intergenic and exonic sense lncRNAs constituted the largest number in all DELncRNAs and comprised 44.7 and 25.4%, respectively (**Figure 3C**).

Functional Analysis of DEMRNAs

In order to forecast the function of DELncRNAs in osteoporosis, we first analyzed the functions of DEMRNAs via GO and KEGG pathway analyses, which provided a clue about



osteoporosis. The significantly enriched GO targeted by mRNAs with up- and downregulation primarily participated in cardiac muscle contraction, skeletal muscle contraction, the transition between fast and slow fiber, and brown fat cell differentiation (Figures 4A,B and Supplementary Tables 3, 4). The KEGG pathway analysis revealed that mRNAs with up- and downregulation were mostly enriched in the peroxisome proliferator-activated receptor (PPAR) signaling pathway and cardiac muscle contraction, respectively (Figures 4C,D and Supplementary Tables 5, 6). The top 20 significantly enriched pathways were employed to construct a pathway network to expound the important pathways in the development of osteoporosis. The PPAR signaling pathway, lipolysis regulation in adipocyte, adipocytokine signaling pathway, and mitogen-activated protein kinase (MAPK) signaling pathway, which were involved in osteogenesis and adipogenesis of BMSCs, were included in the network and exchanged with each other (Figure 4E). We constructed DEmRNAs network by Search Tool for the Retrieval of Interacting Genes/Proteins (STRING) database to further unearth genes' function at the protein level. The interactions among DEmRNAs were evaluated by the medium confidence score (0.4). One hundred sixty-eight nodes and 440 edges were included in the network (Figure 5A). The k-core of nodes was calculated, and the 30 highest k-core DEmRNAs are shown in Figure 5B. The top 10 hub DEmRNAs

include Cfd, Adipoq, Tnni1, Lep, Myl2, Casq2, Csrp3, Myl3, Myoz2, and Actn2. These 30 DEmRNAs constituted two important subnetworks, which were enriched in the PPAR signaling pathway, adipocytokine signaling pathway, and AMPK signaling pathway, involving in the differentiation of BMSCs (Figures 5C,D).

lncRNA-mRNA Coexpression Network in Osteoporosis

We performed lncRNA-mRNAs coexpression analysis and constructed the coexpression networks to identify the function of lncRNAs in osteoporosis. The coexpression network of lncRNA-mRNA (correlation coefficient ≥ 0.98) was constructed using Cytoscape3.5.1 (Figure 6) and included 608 network nodes and 1,125 connections. The k-core of network nodes was calculated, and the results ($k\text{-core} \geq 5$) are shown in Supplementary Table 7. The three highest k-core lncRNAs were NONMMUT054704.2, NONMMUT005069.2, and NONMMUT096150.1.

Functional Analysis of the Coexpression Network

To elucidate DElncRNA's biological role, we illustrated mRNAs coexpressed with lncRNA by GO (Supplementary Table 8) and KEGG (Supplementary Table 9). The top 30 GOs are

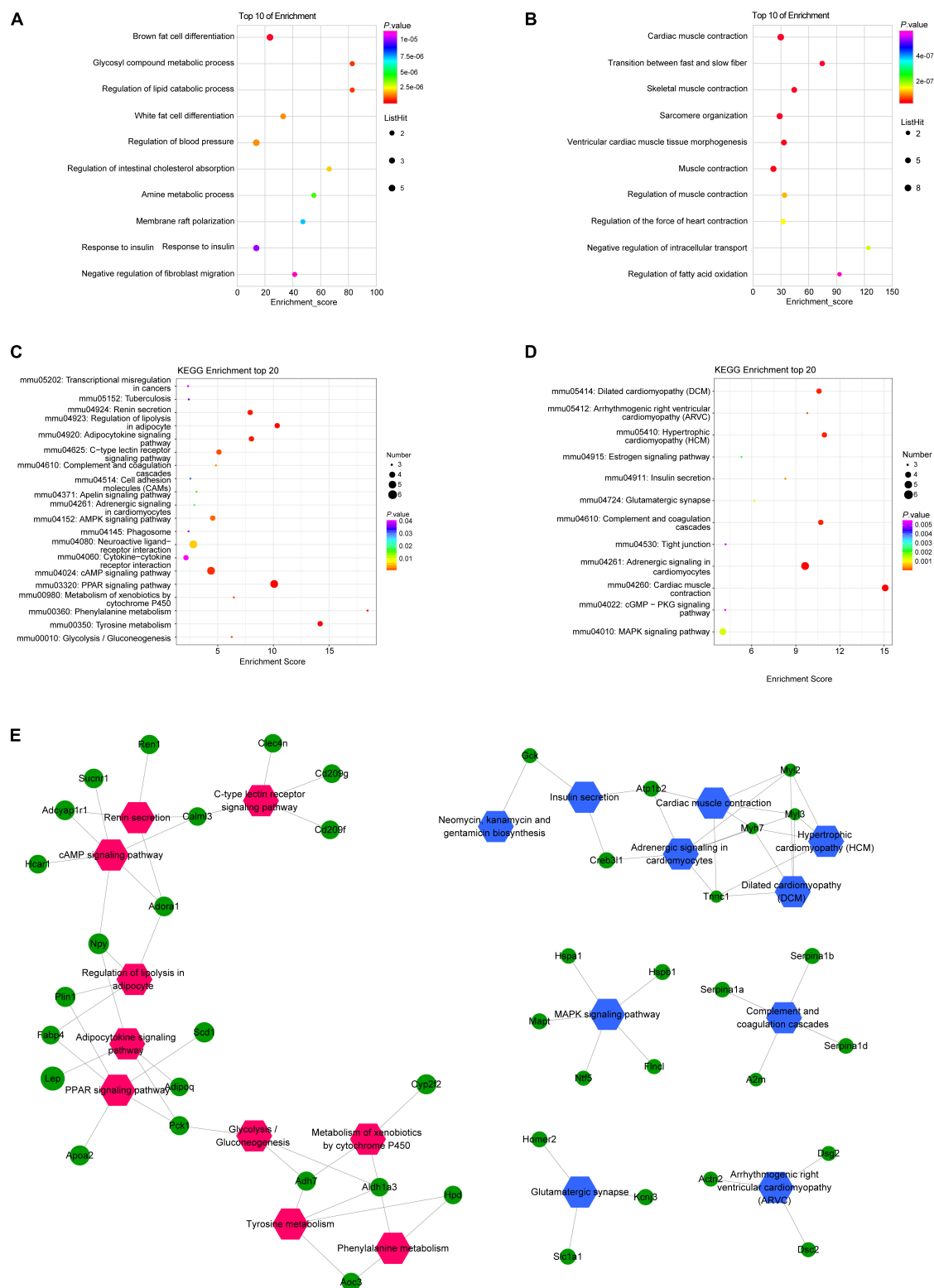


FIGURE 4 | Gene Ontology (GO) and Kyoto Encyclopedia of Genes and Genomes (KEGG) pathway analyses of mRNAs in OVX. GO annotations of up (A) and down (B) regulated mRNAs with top 10 enrichment scores of biological processes. KEGG pathway enrichment analysis of up (C) and down (D) regulated mRNAs with top 20 enrichment scores. Interaction and overlapping of associated molecules among significant pathways (E). Hexagons represent the most significantly enriched pathways; ellipses indicate mRNAs that act as the link hinge between the pathways.

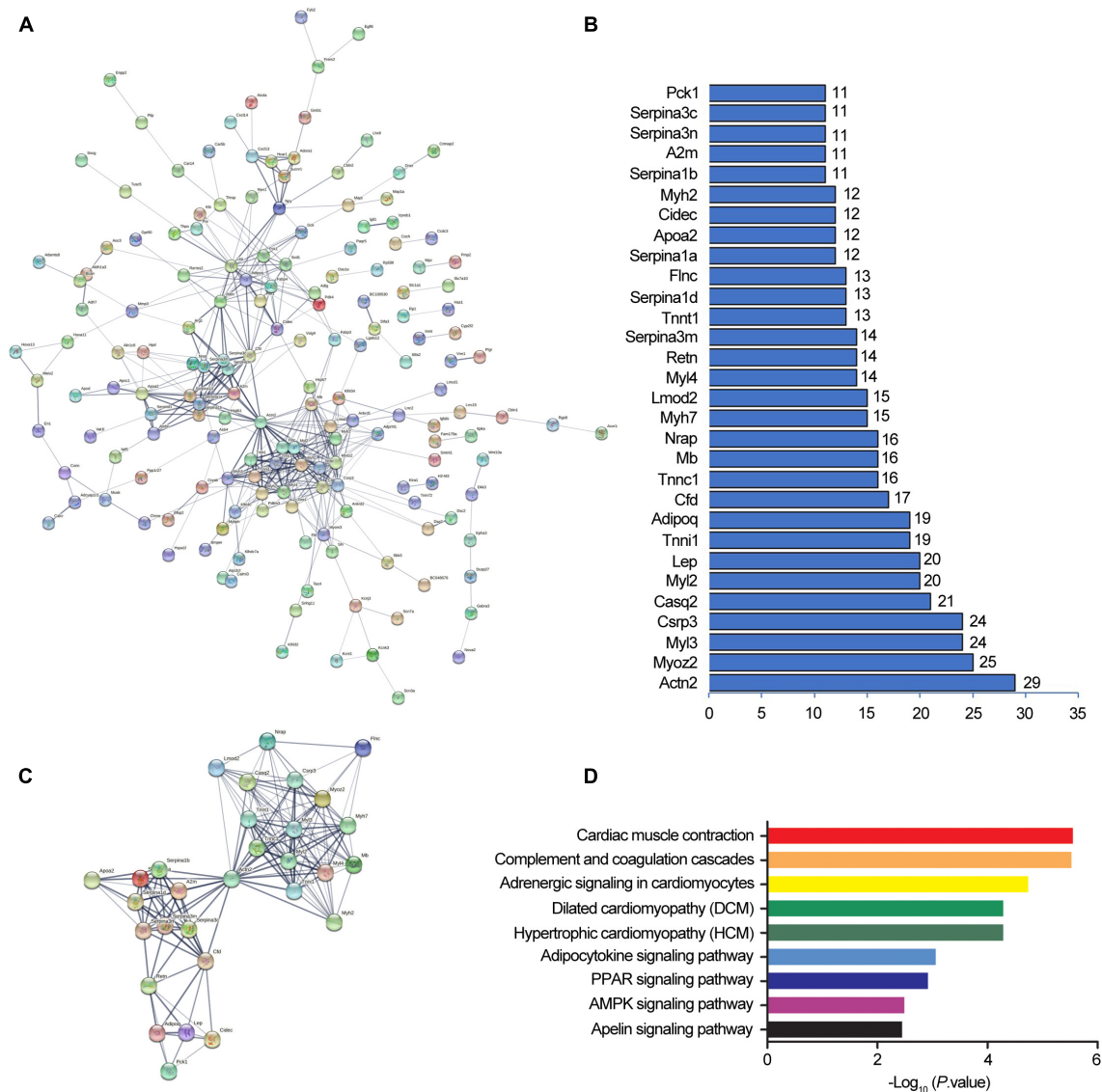


FIGURE 5 | Protein-protein interaction networks by Search Tool for the Retrieval of Interacting Genes/Proteins (STRING). STRING software constructed the differentially expressed mRNAs (fold change ≥ 2 , and $P < 0.05$) network based on protein-protein interactions (A). A confidence score that calculated for all protein interactions based on experimentally and computationally interaction was set as the medium (>0.4). Thirty top k-score genes involved in the network (B). Thirty top k-score genes constitute the subnetworks (C). KEGG pathway annotations of the network (D).

shown in **Figure 7A**. GO terms, such as positive regulation of inflammatory response to an antigenic stimulus, protein localization to nuclear pore, and megakaryocyte differentiation, were significantly enriched. The enriched signaling pathways ($p < 0.05$) can be a reflector of lncRNAs' function in osteoporosis. NONMMUT096150.1 was shown as an example by flow chart analysis (**Figures 7B,C**). mRNAs that coexpressed with NONMMUT096150.1 are shown in **Figure 7B**. The function of NONMMUT096150.1 was annotated by their connections with mRNAs. The top 20 enriched KEGG pathways were identified in these DEmRNAs coexpressed with NONMMUT096150.1 ($p < 0.05$, **Figure 7C**), including PPAR signaling pathway, lipolysis regulation in adipocyte, and adipocytokine signaling

pathway. The functional annotation indicates that the lncRNA may have multiple functions in osteoporosis.

Validation of Differentially Expressed lncRNA in Ovariectomy vs. Sham Control

Seven DELncRNAs were validated by qPCR in this study. We chose three lncRNAs with downregulated expression in the OVX group, namely, NONMMUT096150.1, NONMMUT083450.1, and NONMMUT029743.2, and four lncRNAs with upregulated expression in OVX group, namely, NONMMUT026970.2, NONMMUT051734.2, NONMMUT003617.2, and NONMMUT034049.2 for qPCR validation.

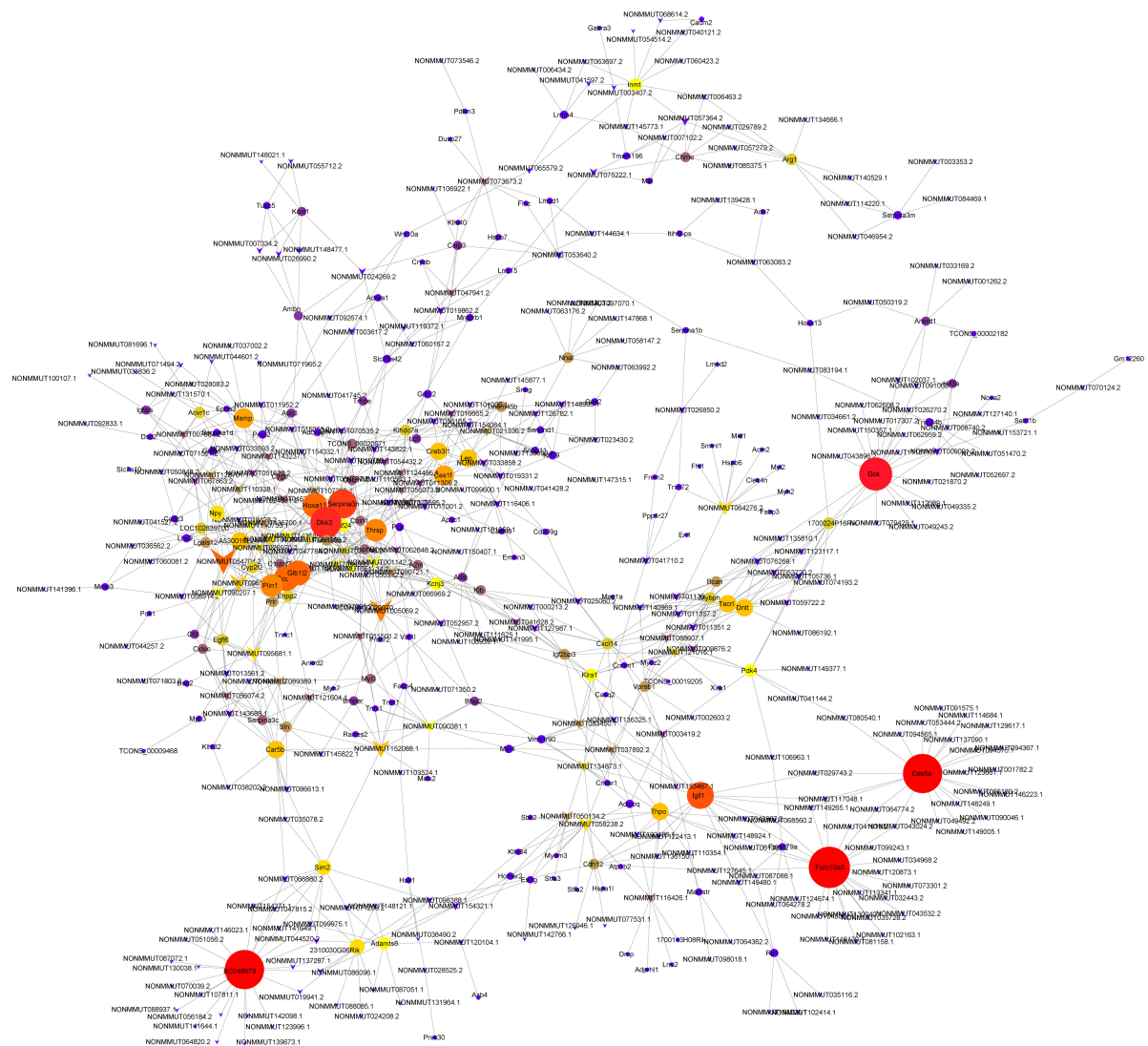


FIGURE 6 | Coexpression networks constructed by weighted correlation network analysis. Circle, mRNA; diamond, long non-coding RNA; line, correlative relationship. Different sizes and colors represent the corresponding k-core scoring.

Consistent with the sequencing findings, we verified that NONMMUT096150.1, NONMMUT083450.1, and NONMMUT029743.2 were all downregulated, whereas NONMMUT026970.2, NONMMUT051734.2, NONMMUT003617.2, and NONMMUT034049.2 were all upregulated in the OVX group, as shown in **Figure 8**. Thus, the qPCR results fully supported the reliability of lncRNA expression profiles of OVX by sequencing analysis.

lncRNA NONMMUT096150.1 Involved in the Adipogenesis Through Transcription Factor Association Analysis

The GO and KEGG analysis showed that NONMMUT096150.1 was involved in the adipogenesis of BMSCs. Furthermore, the qPCR results validated that NONMMUT096150.1 was

downregulated in BMSCs from OVX mice. In order to understand how lncRNA NONMMUT096150.1 functioned in osteoporosis, we had the deeper analysis of NONMMUT096150.1 through transcription factor association analysis. In this study, we identified five coexpressions between NONMMUT096150.1 and transcription factors (TFs), including Hoxa13, Pax6, Nr0b2, Prdm16, Msx1, and Pitx1, and 156 relations between TFs and mRNAs. **Figure 9A** shows that Cytoscape 3.5.1 was employed to construct the coexpression network of NONMMUT096150.1-TFs-mRNAs. The mRNAs in this network were annotated by GO and KEGG pathway analysis to investigate in-depth NONMMUT096150.1's functions in osteoporosis. GO analysis showed that GO terms (calcium ion binding, troponin complex, and cardiac muscle contraction) were greatly enriched. The top 30 terms are shown in **Figure 9B**. A total of 17 enriched KEGG pathways exhibited great enrichment ($p < 0.05$,

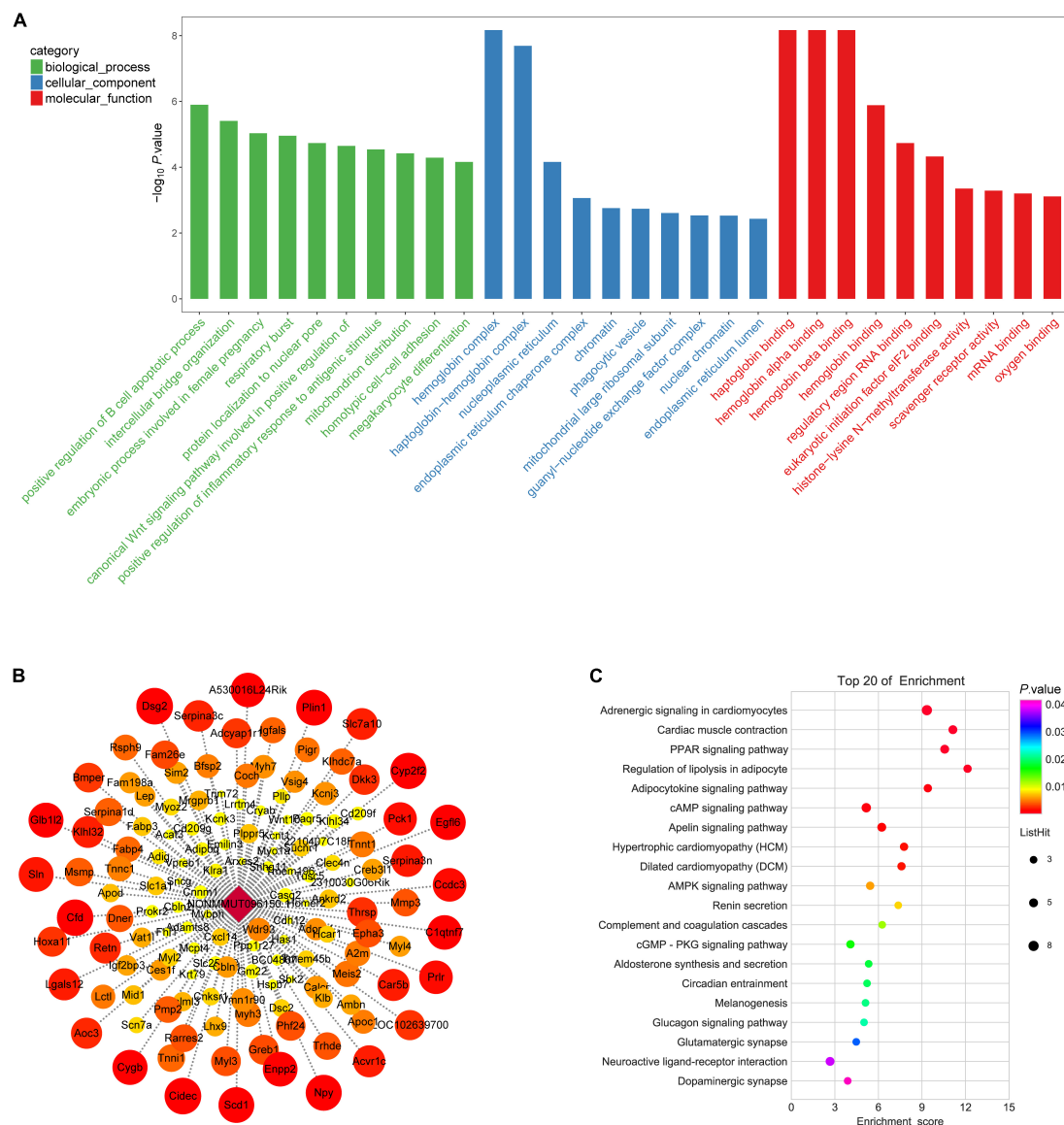


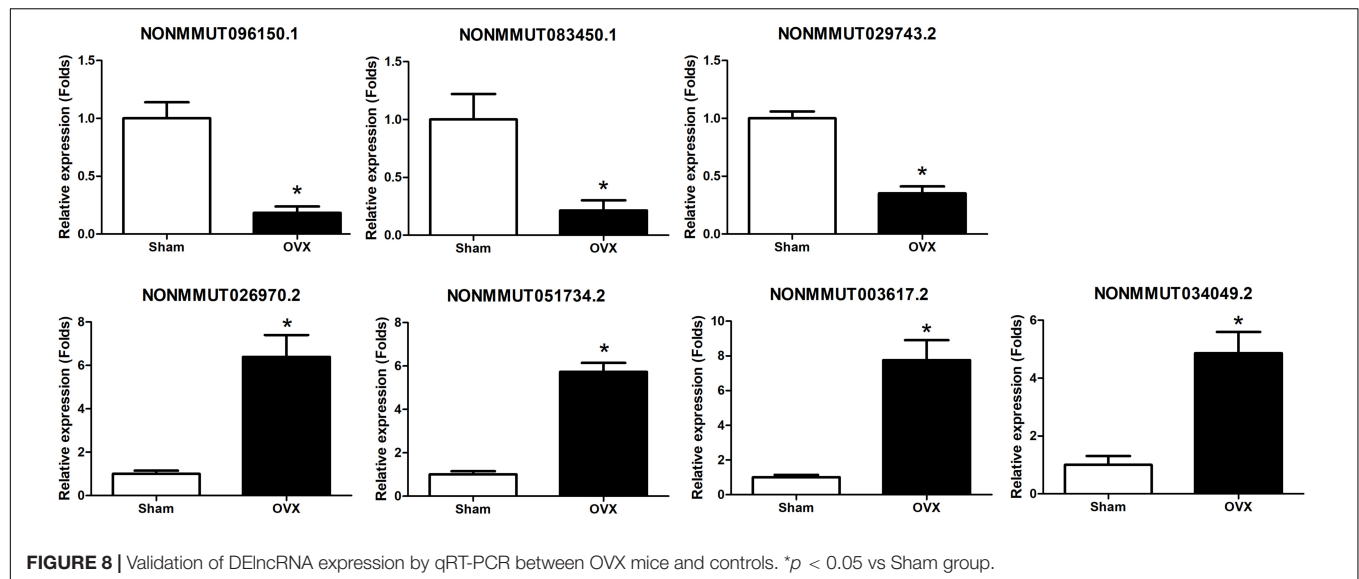
FIGURE 7 | Gene Ontology (GO) annotations for long non-coding RNAs (lncRNAs) in OVX. **(A)** The figure shows top 10 most enriched GO for DelncRNA in ontologies of biological processes, cellular component, and molecular function. **(B)** mRNAs that coexpressed with lncRNA RP11-222K16.2. Weighted correlation network analysis based on Pearson's correlation was used to estimate the correlation coefficient between the lncRNA and coding genes, and the soft threshold was set at 0.8. **(C)** KEGG pathway annotations of the lncRNA NONMMUT096150.1.

Supplementary Table 10). The top 10 pathways are displayed in **Figure 9C**, including the PPAR signaling pathway, AMPK signaling pathway, and lipolysis regulation in adipocyte and adipocytokine signaling pathway. The functional annotation indicates that the lncRNA NONMMUT096150.1 may function as an adipogenesis regulatory in OP.

DISCUSSION

The imbalanced bone formation and resorption induced by various factors, such as genetic interaction, epigenetic, and

environmental, was the basic pathogenesis of OP (Bristow et al., 2014). Several studies have explored the molecular mechanisms of OP; however, the role of lncRNAs in OP has just begun to be understood, and most of them have not yet been investigated. Here, we identified the DELncRNAs and DEMRNAs between OVX and sham mice using RNA-sequencing. Subsequently, we constructed the coexpression network of lncRNA/mRNA and performed GO and KEGG pathway analyses to uncover lncRNAs' biological functions in the pathogenesis of OP. We verified the primary lncRNAs expression by qPCR and also explored their function by functional experiments. Our work indicates a coexpression lncRNA/mRNA



network involved in the development of OP, indicating that lncRNAs functioned importantly.

In the present study, we identify 240 DEMRNAs in OVX, compared with control mice, via RNA-seq. Some of the DEMRNAs are reported to be involved in OP in previous studies. Adig, as an adipocyte-enriched transmembrane protein, is essential for adipogenesis (Kim et al., 2005). The deficiency of Adig-reduced plasma leptin levels regulated by fat mass and exposed an impairment of leptin secretion from adipose explants (Alvarez-Guaita et al., 2021). Fabp3 is reported to promote adipogenesis and inhibit osteogenesis of BMSCs. Accumulation of Fabp3 leads to the occurrence of OP through impaired osteogenesis of BMSCs, while knockdown of Fabp3 reduces bone loss in aged mice (Liu et al., 2020). DKK3 is reported to negatively regulate the osteogenesis of rat dental follicle cells (Zhang et al., 2017). Ambn is reported to modulate the osteogenic capacity of BMSCs (Stakkestad et al., 2017). Lu et al. (2016) found that Ambn stimulates long bone growth and increases osteogenic gene expression and proliferation of osteoblast via modulating the production of extracellular matrix and the properties of cell adhesion in the long bone growth plate. The GO and KEGG pathway analyses indicated that the DEMRNAs participated in the OP pathogenesis. The upregulated DEMRNAs were involved in adipocytokine signaling pathway, apelin signaling pathway, AMPK signaling pathway, and PPAR signaling pathway, while the downregulated DEMRNAs were involved in the estrogen signaling pathway and MAPK signaling pathway. There was crosstalk between each signaling pathway via several mRNAs. Furthermore, we constructed the PPI network of DEMRNAs via STRING. The top 30 highest k-core nodes were selected and constructed to the subnetwork. The KEGG analyses of this subnetwork revealed that the 30 nodes took part in adipogenesis signaling pathways, including adipocytokine signaling pathway, PPAR signaling pathway, AMPK signaling pathway, and apelin signaling pathway. Previous studies have shown that ginsenoside Rg3 reduces osteoporosis caused by

ovariectomy through the AMPK/mTOR signaling pathway (Zhang et al., 2020). Exosomes derived from bone marrow mesenchymal stem cells promote the proliferation of osteoblasts through the MAPK pathway to improve osteoporosis (Zhao et al., 2018). Isopsoralen regulates PPAR- γ /Wnt to inhibit oxidative stress in osteoporosis (Wang et al., 2018). In summary, DEMRNAs may participate in the development of osteoporosis by regulating related signal pathways.

We identified 743 DElncRNAs in OVX mice, with 461 upregulation, and 282 downregulation. The biological functions of lncRNAs are closely related to the mRNAs that they regulate. We constructed the coexpression network of DElncRNAs and DEMRNAs and analyzed the function by bioinformatics. The results indicated that this coexpression network was involved in the differentiation of BMSCs. Four lncRNAs might have been validated in BMSCs of OVX. Among them, NONMMUT096150.1 gained our attention, as its k-core was high in the coexpression network, and its expression is downexpressed in OVX. One hundred thirty-nine mRNAs coexpressed with NONMMUT096150.1; furthermore, KEGG analysis showed that the lncRNA may regulate the adipogenesis of BMSCs. In our previous study, we have indicated that the adipogenesis of BMSCs in OVX mice is upregulated (Gu et al., 2020).

The lncRNAs mediated mRNAs expression regulation by modulating the expression and/or function of TFs (Wang et al., 2021). Therefore, we further define the function of lncRNA NONMMUT096150.1 through transcription factor association analysis. The coexpression network of NONMMUT096150.1-TFs-mRNAs is constructed. There are six TFs, including Hoxa13, Pax6, Nr0b2, Prdm16, Msx1, and Pitx1, in this coexpression network. Overexpression of Hoxa13 stimulates the osteogenic differentiation of MC3T3-E1 via increasing the protein level of β -catenin (Li et al., 2021). Pax6 is reported to be a negative regulator of osteoclastogenesis and attenuates the OC differentiation via activation of Acp5 gene (Kogawa et al., 2013). Another study shows that p38/ β -catenin/Pax6 axis could

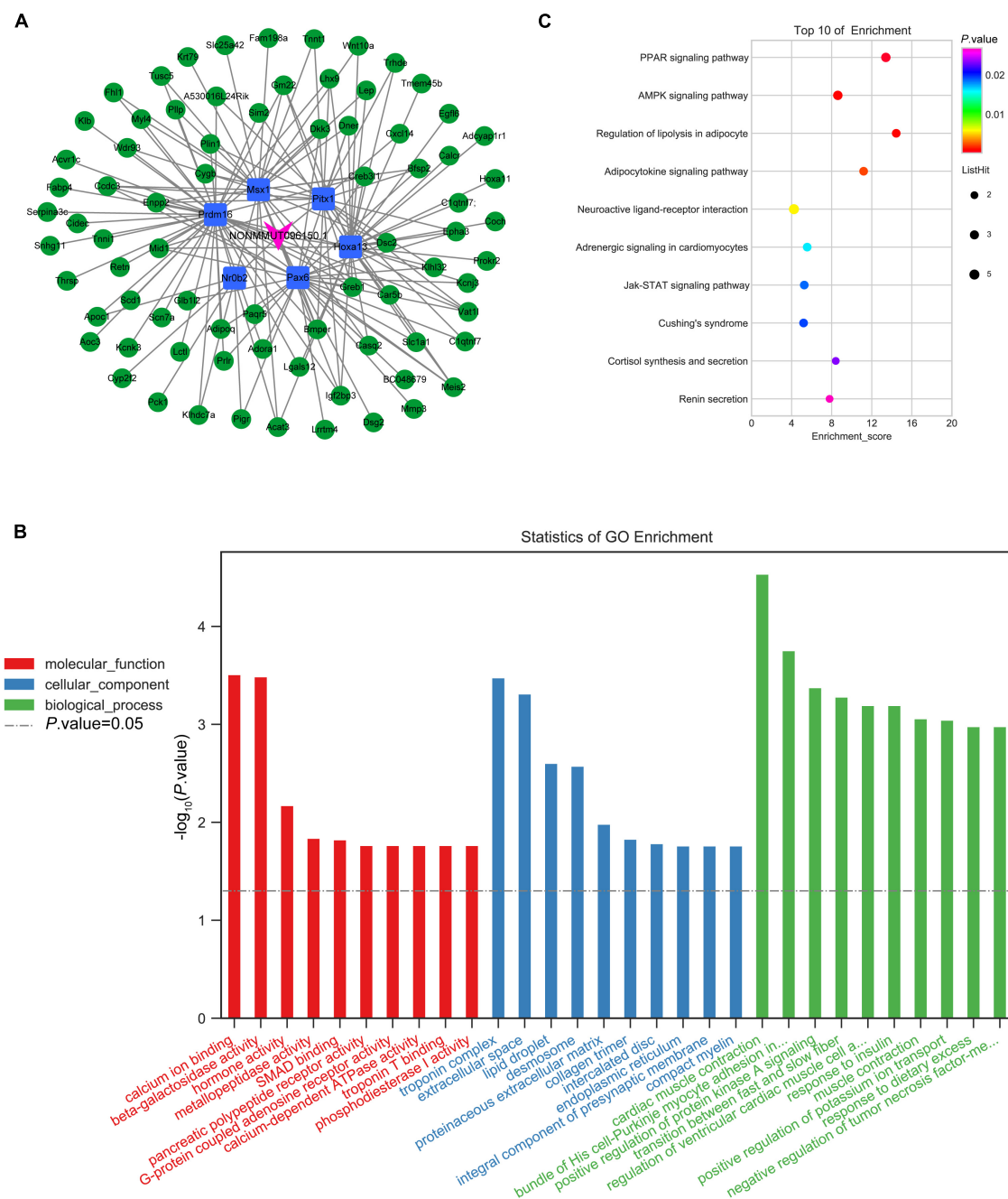


FIGURE 9 | Coexpression network of NONMMUT096150.1-TFs-mRNAs in the OVX mouse model. **(A)** NONMMUT096150.1-TFs-mRNAs networks in OVX mice. **(B)** The top 10 GO enrichment analyses of cellular component, molecular function and biological process. **(C)** KEGG pathway annotations of the network.

inhibit osteoclastogenesis (Jie et al., 2019). Nr0b2 is proved to regulate the transcriptional activity of Runx2 and promote osteoblast differentiation and bone formation (Jeong et al., 2010). MiR-23a cluster mediated osteogenic differentiation regulation by modulating the transforming growth factor beta (TGF- β) signaling pathway after targeting Prdm16 (Zeng et al., 2017). Msx1 is reported to enhance the osteogenic differentiation of multipotent muscle satellite cells and human dental pulp

stem cells (Goto et al., 2016; Ding et al., 2017). Pitx1, which inhibits Wnt pathway and the self-renewal of mesenchymal stem cells, induced senile osteoporosis in mice (Karam et al., 2019). The GO terms of this network, including calcium ion binding, hormone activity, and extracellular space, regulated the pathological process of OP. KEGG pathway analyses show that this network is involved in PPAR signaling pathway, AMPK signaling pathway, and lipolysis regulation in adipocyte and

adipocytokine signaling pathway. These results indicate that the lncRNA NONMMUT096150.1 might directly or indirectly regulate the adipogenesis of BMSCs. Further work needs to be carried out to explore the lncRNA's biological functions.

This study has some limitations. First, the expression level of key DE mRNAs needs to be verified by qRT-PCR. Second, the prognostic value of key lncRNAs and genes and their role in the development of PMOP need to be further explored through experiments. In future research, we will further explore the relationship between the expression levels of key lncRNAs and genes and the prognosis of OP patients, and the specific regulatory mechanisms of key lncRNAs and genes.

In this study, we first systematically identified OP-associated lncRNAs in OVX mice and constructed lncRNAs/mRNAs coexpression network. The lncRNAs played crucial roles in the differentiation of BMSCs during OP. The NONMMUT096150.1 was verified by network and bioinformatics to be a key lncRNA in OP, regulating the adipogenesis of BMSCs. The data further deepened our understanding of lncRNAs along with their functions in the pathogenesis of OP. Nevertheless, more and more verification is needed to explore the detailed mechanism of lncRNAs under OP.

DATA AVAILABILITY STATEMENT

The datasets presented in this study can be found in online repositories. The names of the repository/repositories and accession number(s) can be found below: <https://www.ncbi.nlm.nih.gov/sra/PRJNA737522>, BioProject accession: PRJNA737522.

REFERENCES

- Alvarez-Guaita, A., Patel, S., Lim, K., Haider, A., Dong, L., Conway, O. J., et al. (2021). Phenotypic characterization of *Adig* null mice suggests roles for adipogenin in the regulation of fat mass accrual and leptin secretion. *Cell Rep.* 34:108810. doi: 10.1016/j.celrep.2021.108810
- Bristow, S. M., Gamble, G. D., Stewart, A., Horne, L., House, M. E., Aati, O., et al. (2014). Acute and 3-month effects of microcrystalline hydroxyapatite, calcium citrate and calcium carbonate on serum calcium and markers of bone turnover: a randomised controlled trial in postmenopausal women. *Br. J. Nutr.* 112, 1611–1620. doi: 10.1017/s0007114514002785
- Chen, C., Chen, H., Zhang, Y., Thomas, H. R., Frank, M. H., He, Y., et al. (2020). TBtools: an integrative toolkit developed for interactive analyses of big biological data. *Mol. Plant* 13, 1194–1202. doi: 10.1016/j.molp.2020.06.009
- Ding, K., Liu, W. Y., Zeng, Q., Hou, F., Xu, J. Z., and Yang, Z. (2017). Msx1-modulated muscle satellite cells retain a primitive state and exhibit an enhanced capacity for osteogenic differentiation. *Exp. Cell Res.* 352, 84–94. doi: 10.1016/j.yexcr.2017.01.016
- Dykes, I. M., and Emanuel, C. (2017). Transcriptional and post-transcriptional gene regulation by long non-coding RNA. *Genomics Proteomics Bioinformatics* 15, 177–186. doi: 10.1016/j.gpb.2016.12.005
- Goto, N., Fujimoto, K., Fujii, S., Ida-Yonemochi, H., Ohshima, H., Kawamoto, T., et al. (2016). Role of MSX1 in osteogenic differentiation of human dental pulp stem cells. *Stem Cells Int.* 2016:8035759.
- Gu, H., Shi, S., Xiao, F., Huang, Z., Xu, J., Chen, G., et al. (2020). MiR-1-3p regulates the differentiation of mesenchymal stem cells to prevent osteoporosis by targeting secreted frizzled-related protein 1. *Bone* 137:115444. doi: 10.1016/j.bone.2020.115444

ETHICS STATEMENT

The animal study was reviewed and approved by the animal experimental protocols got the approval of the Animal Care and Experiment Committee of Fudan University.

AUTHOR CONTRIBUTIONS

HG, KZ, and XY: conception and design. HG, ZH, and JX: development of methodology. HG and GC: sample collection. ZH and CB: analysis and interpretation of data. HG, KZ, and JX: writing, review, and revision of the manuscript. All authors contributed to the article and approved the submitted version.

FUNDING

This work was financially supported by the National Natural Science Foundation of China (Grant Nos. 81301335 and 81772433) and National Natural Science Foundation of Minhang, Shanghai (Grant No. 2021MHZ037).

SUPPLEMENTARY MATERIAL

The Supplementary Material for this article can be found online at: <https://www.frontiersin.org/articles/10.3389/fcell.2021.719851/full#supplementary-material>

- He, T., Liu, W., Cao, L., Liu, Y., Zou, Z., Zhong, Y., et al. (2020). CircRNAs and lncRNAs in osteoporosis. *Differentiation* 116, 16–25. doi: 10.1016/j.diff.2020.10.002
- He, Y., and Chen, Y. (2021). The potential role of lncRNAs in osteoporosis. *J. Bone Miner. Metab.* 39, 341–352. doi: 10.1007/s00774-021-01205-6
- Jeong, B. C., Lee, Y. S., Bae, I. H., Lee, C. H., Shin, H. I., Ha, H. J., et al. (2010). The orphan nuclear receptor SHP is a positive regulator of osteoblastic bone formation. *J. Bone Miner. Res.* 25, 262–274. doi: 10.1359/jbmr.090718
- Jie, Z., Shen, S., Zhao, X., Xu, W., Zhang, X., Huang, B., et al. (2019). Activating β -catenin/Pax6 axis negatively regulates osteoclastogenesis by selectively inhibiting phosphorylation of p38/MAPK. *FASEB J.* 33, 4236–4247. doi: 10.1096/fj.201801977r
- Kanis, J. A., Cooper, C., Rizzoli, R., and Reginster, J. Y. (2019). European guidance for the diagnosis and management of osteoporosis in postmenopausal women. *Osteoporos Int.* 30, 3–44. doi: 10.1007/s00198-018-4704-5
- Karam, N., Lavoie, J. F., St-Jacques, B., Bouhanik, S., Franco, A., Ladoul, N., et al. (2019). Bone-Specific Overexpression of PITX1 induces senile osteoporosis in mice through deficient self-renewal of mesenchymal progenitors and Wnt pathway inhibition. *Sci. Rep.* 9:3544.
- Kim, J. H., Do, H. J., Choi, S. J., Cho, H. J., Park, K. H., Yang, H. M., et al. (2005). Efficient gene delivery in differentiated human embryonic stem cells. *Exp. Mol. Med.* 37, 36–44.
- Kogawa, M., Hisatake, K., Atkins, G. J., Findlay, D. M., Enoki, Y., Sato, T., et al. (2013). The paired-box homeodomain transcription factor Pax6 binds to the upstream region of the TRAP gene promoter and suppresses receptor activator of NF- κ B ligand (RANKL)-induced osteoclast differentiation. *J. Biol. Chem.* 288, 31299–31312.
- Li, C. J., Xiao, Y., Yang, M., Su, T., Sun, X., Guo, Q., et al. (2018). Long noncoding RNA Bmncr regulates mesenchymal stem cell fate during skeletal aging. *J. Clin. Invest.* 128, 5251–5266. doi: 10.1172/jci99044

- Li, M., Cong, R., Yang, L., Yang, L., Zhang, Y., and Fu, Q. (2020). A novel lncRNA LNC_000052 leads to the dysfunction of osteoporotic BMSCs via the miR-96-5p-PIK3R1 axis. *Cell Death Dis.* 11:795.
- Li, R., Dong, Y., and Li, F. E. T. S. (2021). Proto-Oncogene 1 Suppresses MicroRNA-128 transcription to promote osteogenic differentiation through the HOXA13/ β -catenin axis. *Front. Physiol.* 12:626248. doi: 10.3389/fphys.2021.626248
- Liu, Z. Z., Hong, C. G., Hu, W. B., Chen, M. L., Duan, R., Li, H. M., et al. (2020). Autophagy receptor OPTN (optineurin) regulates mesenchymal stem cell fate and bone-fat balance during aging by clearing FABP3. *Autophagy*. doi: 10.1080/15548627.2020.1839286
- Lu, X., Fukumoto, S., Yamada, Y., Evans, C. A., Diekwisch, T. G., and Luan, X. (2016). Ameloblastin, an extracellular matrix protein, affects long bone growth and mineralization. *J. Bone Miner. Res.* 31, 1235–1246. doi: 10.1002/jbmr.2788
- Noh, J. Y., Yang, Y., and Jung, H. (2020). Molecular mechanisms and emerging therapeutics for osteoporosis. *Int. J. Mol. Sci.* 21:7623. doi: 10.3390/ijms21207623
- Rosen, C. J. (2000). "The epidemiology and pathogenesis of osteoporosis," in *Endotext*, eds K. R. Feingold, B. Anawalt, A. Boyce, G. Chrousos, W. W. de Herder, K. Dungan et al. (South Dartmouth, MA: MDText.com, Inc).
- Stakkestad, Ø., Lyngstadaas, S. P., Vondrasek, J., Gordeladze, J. O., and Reseland, J. E. (2017). Ameloblastin peptides modulates the osteogenic capacity of human mesenchymal stem cells. *Front. Physiol.* 8:58. doi: 10.3389/fphys.2017.00058
- Wang, D., Wan, X., Zhang, Y., Kong, Z., Lu, Y., Sun, X., et al. (2019). A novel androgen-reduced prostate-specific lncRNA, PSLNR, inhibits prostate-cancer progression in part by regulating the p53-dependent pathway. *Prostate* 79, 1362–1377.
- Wang, J., Wang, G., Gong, L., Sun, G., Shi, B., Bao, H., et al. (2018). Isopsoralen regulates PPARGgamma/WNT to inhibit oxidative stress in osteoporosis. *Mol. Med. Rep.* 17, 1125–1131.
- Wang, L., Zhu, P., Mo, Q., Luo, W., Du, Z., Jiang, J., et al. (2021). Comprehensive analysis of full-length transcriptomes of *Schizothorax prenanti* by single-molecule long-read sequencing. *Genomics*. doi: 10.1016/j.ygeno.2021.01.009
- Yin, C., Tian, Y., Yu, Y., Li, D., Miao, Z., Su, P., et al. (2021). Long noncoding RNA AK039312 and AK079370 inhibits bone formation via miR-199b-5p. *Pharmacol. Res.* 163:105230. doi: 10.1016/j.phrs.2020.105230
- Yoon, J. H., Abdelmohsen, K., and Gorospe, M. (2014). Functional interactions among microRNAs and long noncoding RNAs. *Semin. Cell Dev. Biol.* 34, 9–14. doi: 10.1016/j.semcdb.2014.05.015
- Zeng, H. C., Bae, Y., Dawson, B. C., Chen, Y., Bertin, T., Munivez, E., et al. (2017). MicroRNA miR-23a cluster promotes osteocyte differentiation by regulating TGF- β signalling in osteoblasts. *Nat. Commun.* 8:15000.
- Zhang, X., Du, Y., Ling, J., Li, W., Liao, Y., and Wei, X. (2017). Dickkopf-related protein 3 negatively regulates the osteogenic differentiation of rat dental follicle cells. *Mol. Med. Rep.* 15, 1673–1681. doi: 10.3892/mmr.2017.6165
- Zhang, X., Huang, F., Chen, X., Wu, X., and Zhu, J. (2020). Ginsenoside Rg3 attenuates ovariectomy-induced osteoporosis via AMPK/mTOR signaling pathway. *Drug Dev. Res.* 81, 875–884. doi: 10.1002/ddr.21705
- Zhao, P., Xiao, L., Peng, J., Qian, Y. Q., and Huang, C. C. (2018). Exosomes derived from bone marrow mesenchymal stem cells improve osteoporosis through promoting osteoblast proliferation via MAPK pathway. *Eur. Rev. Med. Pharmacol. Sci.* 22, 3962–3970.

Conflict of Interest: The authors declare that the research was conducted in the absence of any commercial or financial relationships that could be construed as a potential conflict of interest.

Publisher's Note: All claims expressed in this article are solely those of the authors and do not necessarily represent those of their affiliated organizations, or those of the publisher, the editors and the reviewers. Any product that may be evaluated in this article, or claim that may be made by its manufacturer, is not guaranteed or endorsed by the publisher.

Copyright © 2021 Gu, Huang, Zhou, Chen, Bian, Xu and Yin. This is an open-access article distributed under the terms of the Creative Commons Attribution License (CC BY). The use, distribution or reproduction in other forums is permitted, provided the original author(s) and the copyright owner(s) are credited and that the original publication in this journal is cited, in accordance with accepted academic practice. No use, distribution or reproduction is permitted which does not comply with these terms.



Crosstalk Between MicroRNAs and Circular RNAs in Human Diseases: A Bibliographic Study

Yu-Meng Chen¹, Yi-Li Zheng¹, Xuan Su¹ and Xue-Qiang Wang^{1,2*}

¹ Department of Sport Rehabilitation, Shanghai University of Sport, Shanghai, China, ² Shanghai Shangti Orthopaedic Hospital, Shanghai, China

OPEN ACCESS

Edited by:

Jing Zhang,
Shanghai Jiao Tong University, China

Reviewed by:

Walter Erwin Kaufmann,
Emory University, United States
Yulong Bai,
Fudan University, China

*Correspondence:

Xue-Qiang Wang
wangxueqiang@sus.edu.cn

Specialty section:

This article was submitted to
Epigenomics and Epigenetics,
a section of the journal
Frontiers in Cell and Developmental
Biology

Received: 07 August 2021

Accepted: 28 September 2021

Published: 18 October 2021

Citation:

Chen Y-M, Zheng Y-L, Su X and
Wang X-Q (2021) Crosstalk Between
MicroRNAs and Circular RNAs
in Human Diseases: A Bibliographic
Study.
Front. Cell Dev. Biol. 9:754880.
doi: 10.3389/fcell.2021.754880

Background: Crosstalk of circular RNAs (circRNAs) and microRNAs (miRNAs) refers to the communication and co-regulation between them. circRNAs can act as miRNAs sponges, and miRNAs can mediate circRNAs. They interact to regulate gene expression and participate in the occurrence and development of various human diseases.

Methods: Publications on the crosstalk between miRNAs and circRNAs in human diseases were collected from Web of Science. The collected material was limited to English articles and reviews. CiteSpace and Microsoft Excel were used for bibliographic analysis.

Results: A total of 1,013 papers satisfied the inclusion criteria. The publication outputs and types of researched diseases were analyzed, and bibliographic analysis was used to characterize the most active journals, countries, institutions, keywords, and references. The annual number of publications remarkably increased from 2011 to 2020. Neoplasm was the main research hotspot ($n = 750$ publications), and *Biochemical and Biophysical Research Communications* published the largest number of papers ($n = 64$) on this topic. Nanjing Medical University ranked first among institutions actively engaged in this field by publishing 72 papers, and China contributed 96.84% of the 1,013 papers ($n = 981$ publications) analyzed. Burst keywords in recent years included glioblastoma, miR-7, skeletal muscle, and non-coding RNA.

Conclusion: Crosstalk between miRNAs and circRNAs in human diseases is a popular research topic. This study provides important clues on research trends and frontiers.

Keywords: microRNA, circular RNA, crosstalk, bibliography, cancer

INTRODUCTION

MicroRNAs (miRNAs) are endogenous non-coding RNAs (ncRNAs) measuring ~22 nucleotides in length; they were first discovered in 1993 (Lee et al., 1993; Bartel, 2004). Lee et al. (1993) reported that lin-4 negatively regulates the expression of lin-14 protein by binding to the 3'-untranslated region (3'UTR) of lin-14 messenger RNA (mRNA) in *Caenorhabditis elegans*. miRNAs are crucial post-transcriptional regulators of gene expression and known to pair with the 3'UTR of

target mRNAs to either induce mRNA degradation or inhibit translation (Bartel, 2009). Moreover, these RNAs have been reported to be involved in the processes of various diseases, such as cancer (Iacona and Lutz, 2019; Iqbal et al., 2019), chronic pain (Lopez-Gonzalez et al., 2017; Tramullas et al., 2018), and cardiac diseases (Colpaert and Calore, 2019; Fitzsimons et al., 2020).

Circular RNAs (circRNAs) are endogenous ncRNAs with covalent closed-loop structures that were first discovered in viral RNA by Sanger et al. (1976). circRNAs possess high stability on account of their unique structure, which protects them from degradation by exonucleases (Jeck et al., 2013). This type of RNA has been confirmed to modulate gene expression by acting as miRNA sponges (Hansen et al., 2013a; Memczak et al., 2013) or RNA binding protein regulators (Li et al., 2015). Similar to miRNAs, circRNAs are involved in a number of human diseases, such as cancer (Wang et al., 2017; Patop and Kadener, 2018), neurodegenerative disorders

(Floris et al., 2017; Huang et al., 2020), and cardiovascular diseases (Aufiero et al., 2019; Zhang et al., 2020).

Crosstalk of circRNAs and miRNAs refers to the communication and co-regulation between them. As two important gene-expression regulators, circRNAs interact with miRNAs and participate in regulating mRNA expression in various human diseases (Hansen et al., 2013a; Kristensen et al., 2019). Crosstalk between miRNAs and circRNAs has been extensively studied, but the relevant mechanisms remain incompletely understood. To date, two mechanisms have been identified: (1) circRNAs act as miRNA inhibitors/sponges. ciRS-7 (circular RNA sponge for miR-7), one of the most typical circRNAs, has been observed to show overlapping co-expression with miR-7 in mouse brain. ciRS-7 can sponge miR-7 to inhibit miR-7 activity extensively, thereby increasing the levels of miR-7 target genes (Hansen et al., 2013a). (2) miRNAs mediate circRNAs. ciRS-7, also known as CDR1as, has been confirmed

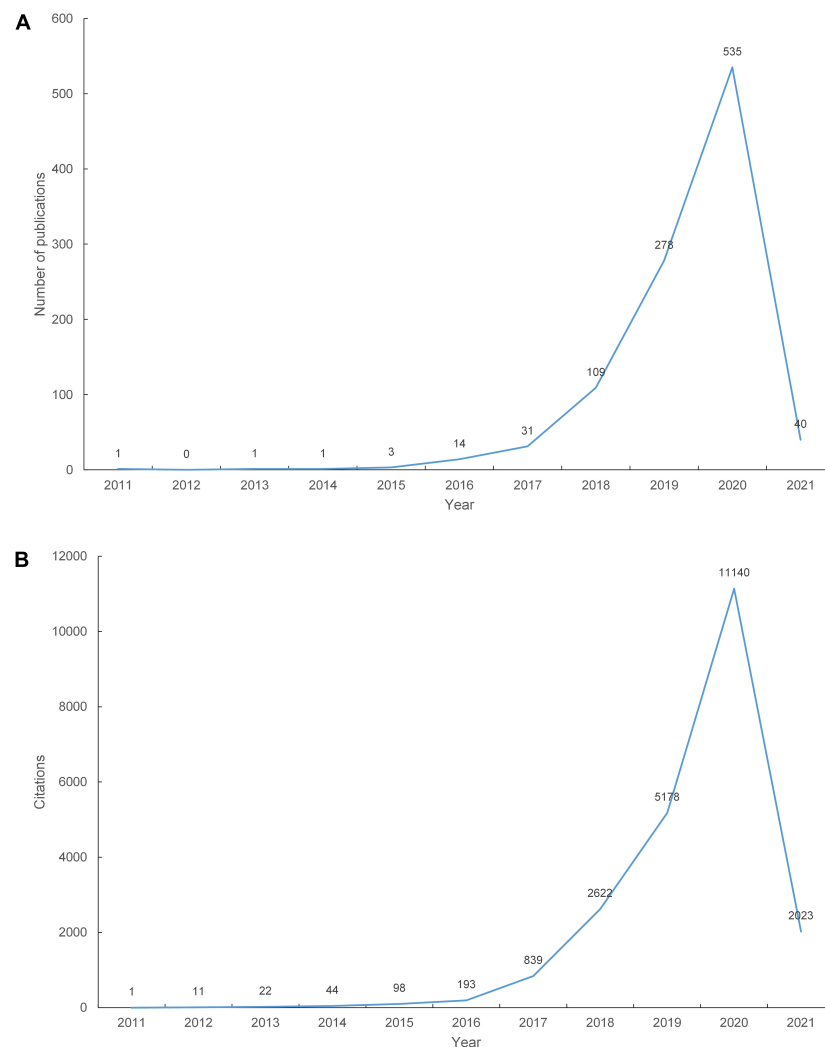


FIGURE 1 | The number of publications and citations. **(A)** The number of annual publications on the crosstalk between microRNAs and circular RNAs from 2011 to 2021; **(B)** The number of annual citations on the crosstalk between microRNAs and circular RNAs from 2011 to 2021.

to be cleaved by Argonaute 2 via miR-671 mediation in cultured cells (Hansen et al., 2011) and mouse brain (Kleaveland et al., 2018). Furthermore, ciRS-7 and its crosstalk with miRNAs have been found to exert a significant effect on sensorimotor gating and synaptic transmission (Piwecka et al., 2017).

Crosstalk between circRNAs and miRNAs may provide new avenues through which the mechanisms, diagnosis, and treatment of human diseases could be explored. Thus, in the present work, we provide a bibliographic analysis of the related literature to identify current global research trends and emerging topics in this field.

MATERIALS AND METHODS

Data Acquisition and Inclusion Criteria

This bibliographic analysis included published articles and reviews that related to research on the crosstalk between circRNAs and miRNAs, and these publications focused on the occurrence and development of human diseases or might be beneficial for studying human diseases. Data were extracted from Science Citation Index Expanded (SCI-Expanded) of Web of Science (WoS) in March 2021. Searches were conducted using the following keywords: TI = (circRNA* or "circ RNA*" OR "circular RNA*" OR circularRNA*) AND TI = (microRNA* OR mir* OR miRNA* OR "micro RNA*" OR "small non-coding RNAs" OR "small non-coding RNA" OR "small RNA*").

Supplementary Figure 1 shows the process of literature selection. Language was restricted to English, and no species limitation was implemented. We selected articles and reviews, and excluded all other publication types, such as meeting abstracts and corrections. Studies focusing on human diseases were included, while research on other subjects, such as plants, were excluded. The search and screening process was performed by two authors; in the event of disagreement, the final decision was made by the corresponding author.

Analytical Tools and Key Indicators

Microsoft Excel 2019 and CiteSpace V (version: 5.6.R5; Drexel University) were used for bibliographic analysis, and SPSS 22.0 (SPSS Inc., Chicago, IL, United States) was used for statistical analysis. CiteSpace is often used for bibliographic analysis with data derived from WoS (Liu et al., 2019; Xu and Sun, 2020; Yan et al., 2020). International Classification of Diseases 11th Revision (ICD-11) was used to classify the diseases evaluated in the 1,013 papers we obtained (World Health Organization [WHO], 2021).

The number of publications and citations, journal impact factor (JIF, 2019), h-index, category and JIF quartile were collected from WoS. The productivity of an individual or group was reflected by the number of articles published. The number of citations, IF and h-index were collected to assess the impact of individuals or groups on publications in this field. IF values were acquired from Journal Citation Reports (2021), which is a highly suitable index for evaluating the influence of journals (Garfield, 2006). The h-index characterizes the scientific output of a researcher. If the h-index of a researcher is h , the researcher published at least h papers and each of these papers was cited

at least h times (Hirsch, 2005). Each journal was assigned to at least one category in descending order according to JIF, and the top 25% of JIF distribution were Q1, 25–50% were Q2 and 50–75% were Q3. Centrality is an indicator calculated by CiteSpace to evaluate the importance of nodes in a network; nodes with high centrality indicate pivotal points (Chen, 2006).

RESULTS

Publication Output

A total of 1,013 papers were included in our study. **Figure 1A** shows the number of articles published by year. The first paper related to the crosstalk between miRNAs and circRNAs in human diseases was published in 2011. The number of publications increased from 1 in 2011 to 535 in 2020. As of February 28, 2021, 40 papers on this topic have been published in 2021. **Figure 1B** shows the total number of citations of the 1,013 papers per year. Linear regression analysis showed that the number of publications ($t = 3.376$, $P = 0.01 < 0.05$, data of 2021 were not included because they are incomplete) and citations ($t = 3.413$, $P = 0.009 < 0.05$, data of 2021 were not included) increased remarkably each year from 2011 to 2020.

Distribution of Diseases

The research directions of the 1,013 papers were classified and summarized according to ICD-11. **Table 1** shows the top 10 diseases studied. Neoplasm was the most popular research topic related to the crosstalk between miRNAs and circRNAs ($n = 750$ publications; 74.04% of the total number of publications) and had an h-index of 56; this topic was followed by diseases of the circulatory system ($n = 62$ publications; h-index = 17) and musculoskeletal system or connective tissue ($n = 57$ publications; h-index = 15).

Distribution by Journals

A total of 244 journals contributed the 1,013 papers included in this study. Among the top 10 journals ranked by number

TABLE 1 | The top 10 diseases ranked by number of publications.

Rank	Disease	Publication	Citations	H-index
1	Neoplasms	750	15435	56
2	Diseases of the circulatory system	62	1756	17
3	Diseases of the musculoskeletal system or connective tissue	57	1031	15
4	Diseases of the nervous system	21	557	10
5	Diseases of the visual system	12	120	5
6	Diseases of the respiratory system	12	56	4
7	Diseases of the digestive system	11	141	4
8	Certain infectious or parasitic diseases	10	78	4
9	Endocrine, nutritional or metabolic diseases	10	425	5
10	Symptoms, signs or clinical findings, not elsewhere classified	10	64	3

of publications (**Table 2**), *Biochemical and Biophysical Research Communications* contributed the greatest number of publications ($n = 64$) and had the highest h-index (33), followed by *European Review for Medical and Pharmacological Sciences* ($n = 43$ publications) and *Journal of Cellular Biochemistry* ($n = 38$ publications). The IF of the top 10 journals ranged from 2.886 to 15.302 (mean = 5.4113). Among the journals contributing publications on the crosstalk between miRNAs and circRNAs in human diseases, *Molecular Cancer* ($n = 26$ publications) had the highest IF (IF 2019 = 15.302), followed by *Molecular Therapy-Nucleic Acids* ($n = 28$ publications; IF 2019 = 7.032) and *Cell*

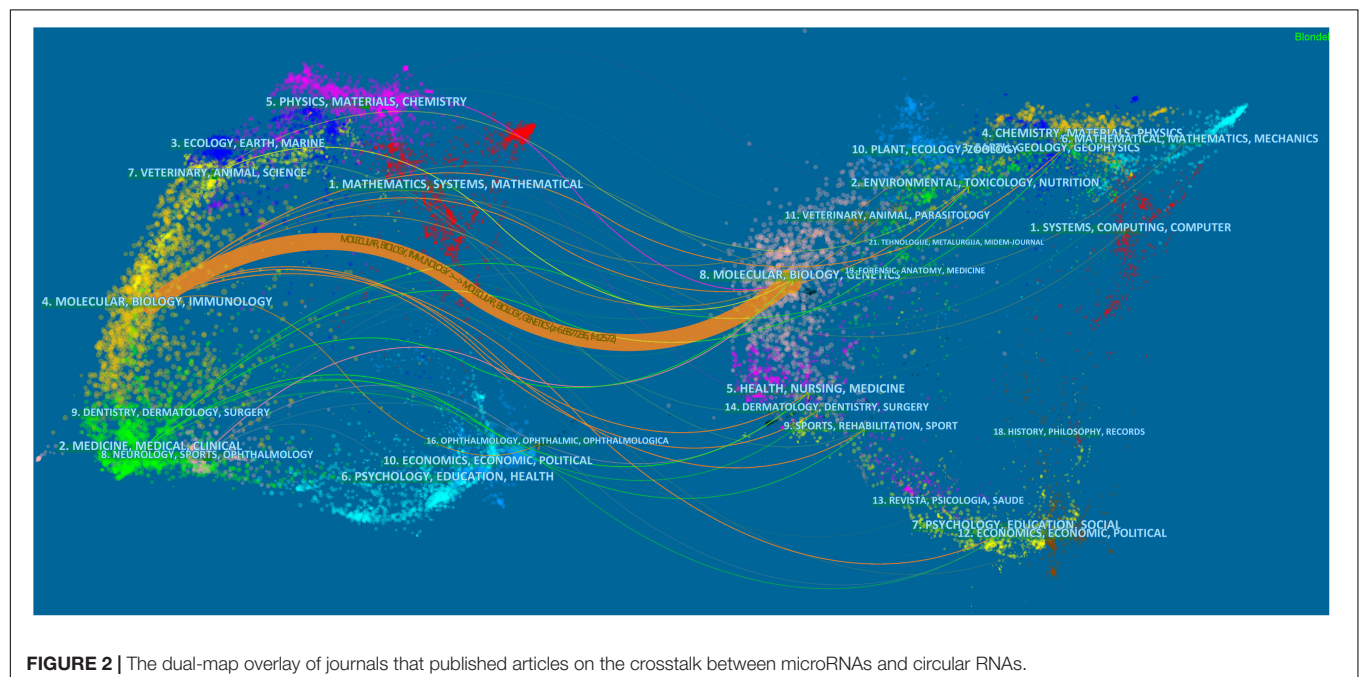
Death and Disease ($n = 25$ publications; IF 2019 = 6.304). Among the top 10 journals, 33.33% JIF quartile were Q1, 46.67% were Q2 and 20% were Q3.

A dual map of journals presenting contributions and connections between disciplines is shown in **Figure 2**. The left-hand side of the map presents citing journals, whereas the right-hand side presents cited journals. The 1,013 papers obtained from our database search were mostly published in journals dedicated to molecular, biology and immunology field, and cited journal publications on molecular, biology, and genetics field.

TABLE 2 | The top 10 journals ranked by number of publications.

Rank	Journal	Publication	H-index	JIF (2019)	Category (Web of Science)	JIF Quartile (2019)
1	Biochemical and Biophysical Research Communications	64	33	2.985	Biochemistry and molecular biology biophysics	Q3; Q2
2	European Review for Medical and Pharmacological Sciences	43	8	3.024	Pharmacology and pharmacy	Q2
3	Journal of Cellular Biochemistry	38	13	4.237	Cell biology biochemistry and molecular biology	Q2; Q2
4	Oncotargets and Therapy	35	6	3.337	Oncology biotechnology and applied microbiology	Q3; Q2
5	Cancer Cell International	33	8	4.175	Oncology	Q2
6	Aging-US	32	10	4.831	Geriatrics and gerontology cell biology	Q1; Q2
7	Cancer Management and Research	32	8	2.886	Oncology	Q3
8	Molecular Therapy-Nucleic Acids	28	12	7.032	Medicine, research and experimental	Q1
9	Molecular Cancer	26	18	15.302	Oncology biochemistry and molecular biology	Q1; Q1
10	Cell Death and Disease	25	10	6.304	Cell biology	Q1

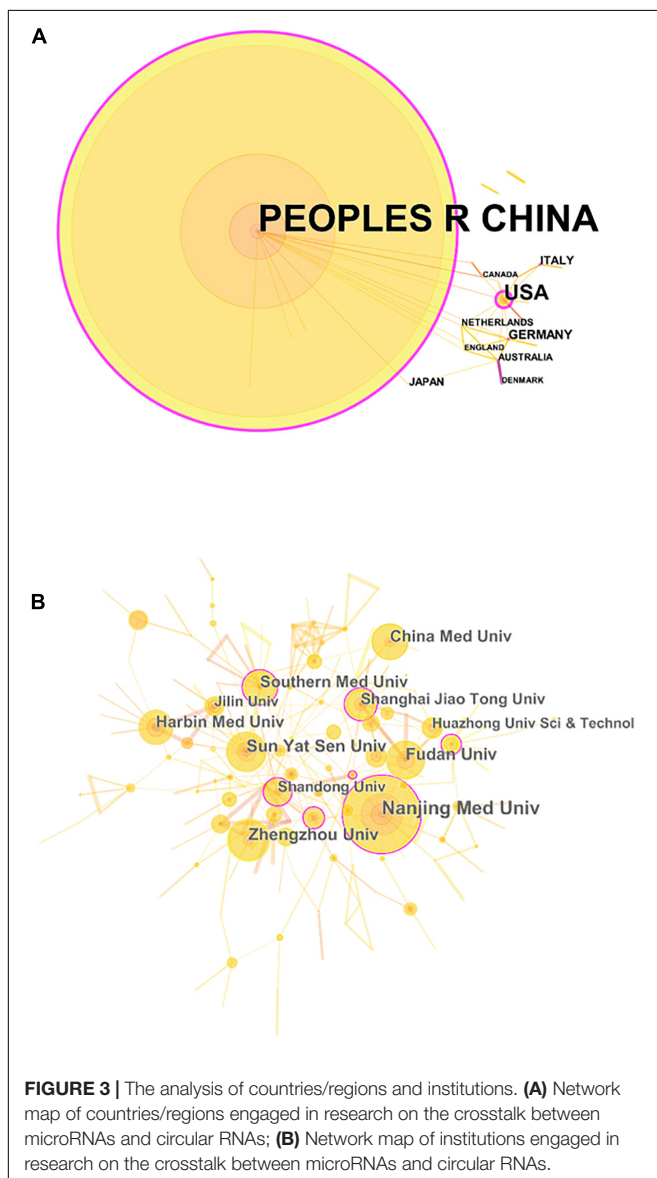
JIF, journal impact factor.



Distribution by Countries and Institutions

In total, 30 countries and 748 institutions contributed to the related research, and the details of each item can be found in **Supplementary Tables 1, 2. Figures 3A,B**, respectively, show the contributions and collaborations by country and by institution. The distribution of countries is presented in **Figure 4. Table 3** shows the top 10 countries ranked by distribution of publications. China contributed 96.84% of the 1,013 papers ($n = 981$ publications), with a high centrality of 0.57. The United States revealed the highest centrality (0.59) and contributed the second highest number of publications ($n = 42$).

The top 10 institutions ranked by number of publications were all universities in China (**Table 4**). Among these institutions, Nanjing Medical University ranked first ($n = 72$ publications), followed by Zhengzhou University ($n = 43$ publications) and Sun Yat-sen University ($n = 41$ publications).



Analysis of Keywords

The top 20 keywords with the strongest citation bursts at different time periods are shown in **Figure 5**. Messenger RNA was the first keyword with the strongest citation burst, which began in 2011 and ended in 2016. Glioblastoma, mir-7, skeletal muscle, and ncRNA were keywords with strong citation bursts that lasted until 2020. Among these four keywords, glioblastoma revealed the highest strength (3.5635) and was the first to burst (in 2013).

Analysis of References

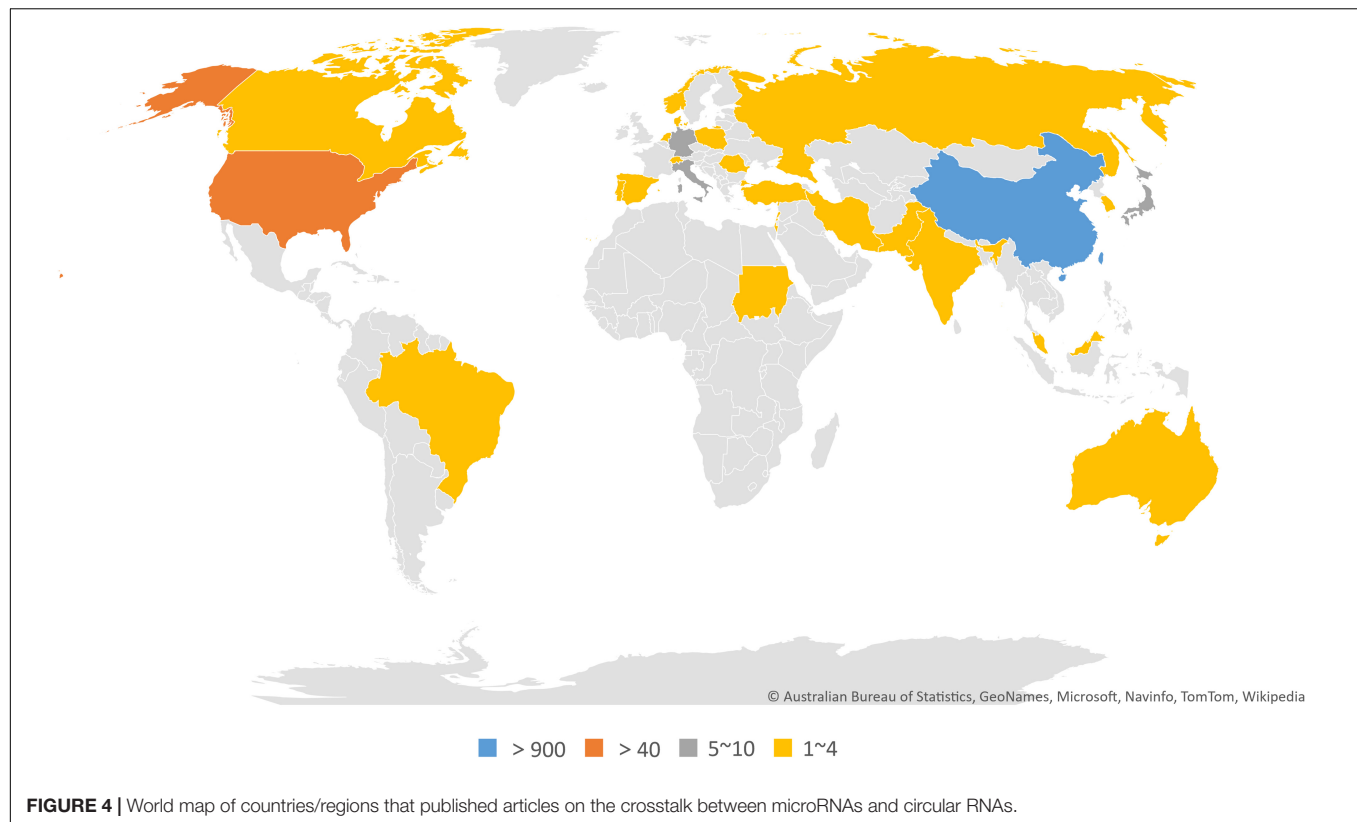
References are an indispensable part of publications. **Figure 6** illustrates a timeline view of references in the 1,013 publications related to the crosstalk between microRNAs and circRNAs in human diseases. The timeline view was constructed using CiteSpace, and the cluster labels were extracted from the keywords. **Figure 6** shows the top 8 clusters, the first of which is marked #0. Gastric cancer revealed the largest cluster, followed by miRNA sponge (#1), ovarian cancer (#2), and glioma (#3).

DISCUSSION

In this study, we performed a bibliographic analysis of studies on the crosstalk between miRNAs and circRNAs and found that research on this topic is well underway. circRNAs can communicate and co-regulate with miRNAs to regulate gene expression. Hansen and his colleagues published the first paper on the crosstalk between ciRS-7 and miR-671 in 2011 (Hansen et al., 2011). However, the number of publications on this subject exceeded 10 per year until 2016. Thereafter, publications exceeded 100 papers per year in 2018 and reached 535 papers per year in 2020.

The mechanisms of crosstalk between miRNAs and circRNAs are incompletely understood. miRNAs and circRNAs have been proven to interact in the pathological process of many human diseases, including cancer, osteoarthritis (OA) and neuropathic pain (NP). circRNAs sponging miRNAs was a frequently mentioned mechanism of the crosstalk between circRNAs and miRNAs in human diseases. Zheng et al. (2016) revealed that circHIPK3, a circRNAs differently expresses between cancer and normal tissues, has 18 potential binding sites and can sponge 9 miRNAs to modulate human cell proliferation. Liu et al. (2016) reported that circRNA-CER competitively binds miR-136 to regulated MMP13 expression and participated in the degradation of chondrocyte extracellular matrix. Several circRNAs have been confirmed to regulate mRNA expression by sponge miRNAs, and then involved in neuroinflammation, neuronal autophagy, cell proliferation, and central sensitization in NP (Song et al., 2020). About the mechanisms of cancer, Hanse found miR-671 can directionally cleave ciRS-7 to release miR-7 that sponged by ciRS-7 (Hansen et al., 2013b). However, few studies researched the mechanism of miRNAs mediating circRNAs.

Neoplasms are the most common condition associated with research on the crosstalk between miRNAs and circRNAs; indeed, articles discussing neoplasms made up 74.04% of the total number of publications obtained, with a high h-index (56). Han and his colleagues revealed that circMTO1 inhibits the process of



hepatocellular carcinoma by sponging miR-9 (Han et al., 2017). Zhang and his colleagues found that circFGFR1 upregulates the expression of CXCR4, the miR-381-3p target gene, to promote the progression of non-small cell lung cancer by miR-381-3p (Zhang et al., 2019b). The research findings of Zhang et al. (2017) were published in *Molecular Cancer*, which had the highest IF among the top 10 journals ranked by number of publications. Interactions between miRNAs and circRNAs have also been explored in other types of neoplasms, such as gastric cancer, breast cancer (Yang et al., 2019) and glioma (Xu et al., 2018). Most of the related research focuses on malignant tumors and the mechanism of circRNA as a miRNA sponge.

Biochemical and Biophysical Research Communications contributed the most to research on the crosstalk between miRNAs and circRNAs by publishing 64 articles with the highest h-index (33). However, in terms of IF, this journal placed ninth among the top 10 journals ranked by number of publications. *Molecular Cancer*, the IF of which was 15.302, was the only journal with an IF greater than 10 among the top 10 journals. Although the IF of the top 10 journals was not high, JIF Quartile shown that these journals ranked well in corresponding categories (33.33% of Q1 and 46.67% of Q2). These results suggest that the quality of most publications was reliable, but more high quality and ground-breaking researches are needed

TABLE 3 | The top 10 countries ranked by number of publications.

Rank	Country	Publication	Centrality
1	China*	981	0.57
2	United States	42	0.59
3	Germany	8	0.10
4	Italy	6	0.10
5	Japan	5	0.00
6	Australia	4	0.13
7	Netherlands	4	0.00
8	Canada	3	0.04
9	Denmark	3	0.00
10	England	3	0.00

*Includes the data of Taiwan (5 publications).

TABLE 4 | The top 10 institutions ranked by number of publications.

Rank	Institution	Publication	Country
1	Nanjing Medical University	72	China
2	Zhengzhou University	43	China
3	Sun Yat-sen University	41	China
4	Fudan University	40	China
5	China Medical University	37	China
6	Harbin Medical University	36	China
7	Southern Medical University	34	China
8	Shanghai Jiao Tong University	32	China
9	Shandong University	30	China
10	Huazhong University of Science and Technology	24	China

Top 20 Keywords with the Strongest Citation Bursts

Keywords	Year	Strength	Begin	End	2011 - 2020
messenger rna	2011	1.8941	2011	2016	
glioblastoma	2011	2.1654	2013	2020	
microrna 7	2011	3.5635	2013	2018	
growth factor receptor	2011	1.5258	2013	2018	
stem cell	2011	1.7601	2013	2018	
identification	2011	2.7494	2015	2016	
microrna	2011	2.4509	2015	2016	
gene expression	2011	2.2935	2015	2017	
reveal	2011	5.7158	2015	2018	
carcinoma	2011	1.8382	2015	2018	
biogenesis	2011	1.7011	2016	2017	
long noncoding rna	2011	3.0054	2016	2017	
circrna biogenesis	2011	1.5442	2016	2018	
circular rna (circrna)	2011	1.7022	2016	2018	
gene	2011	1.6104	2016	2017	
abundant	2011	3.327	2017	2018	
insight	2011	1.9711	2017	2018	
mir-7	2011	1.4583	2018	2020	
skeletal muscle	2011	1.7503	2018	2020	
non-coding rna	2011	1.4583	2018	2020	

FIGURE 5 | The top 20 keywords with the strongest citation bursts of publications on the crosstalk between microRNAs and circular RNAs.

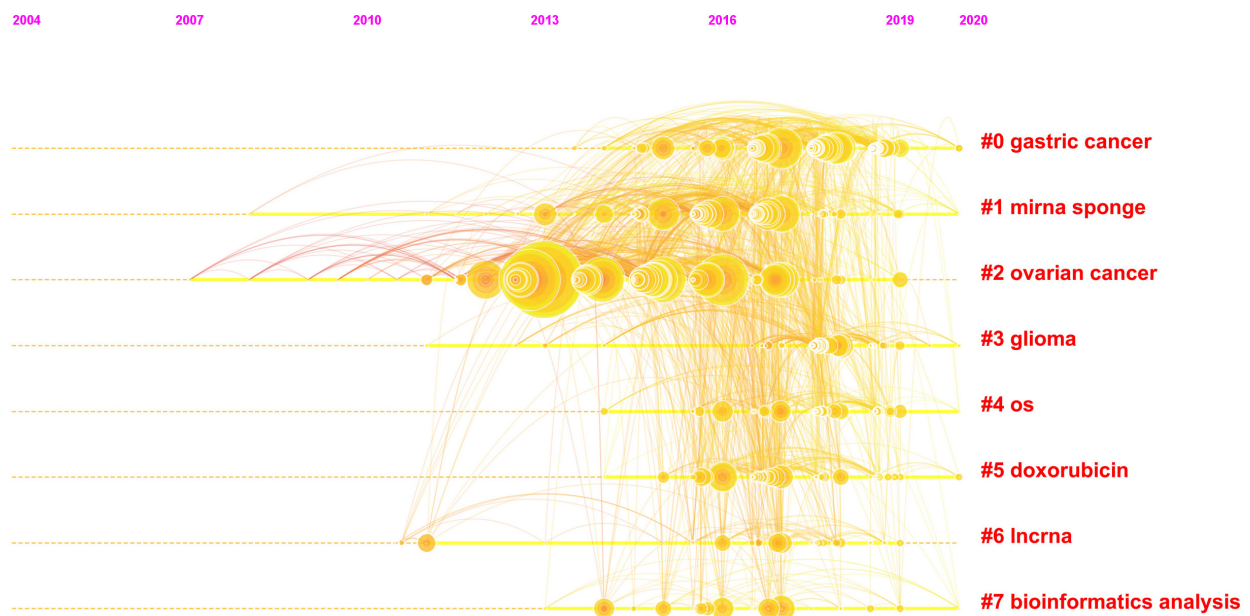


FIGURE 6 | The analysis of references. Co-citation map (timeline view) of references from publications on the crosstalk between microRNAs and circular RNAs.

in this field. Furthermore, the crosstalk between circRNAs and miRNAs is a relatively new field, and it may be a possible reason for these results.

China is the major country contributing research on the crosstalk between miRNAs and circRNAs in human diseases. The country published 981 papers (96.84% of the total number of articles included in this work) and showed fairly high centrality (0.57). The United States ranked second in terms of countries with the greatest number of publications; the country published 42 papers and demonstrated the highest centrality (0.59) among the countries compared. Interestingly, China noticeably contributed more publications than the United States, but the centrality of the former was lower than that of the latter. This finding may be explained by the vast number of articles published by China alone, which could result in low centrality. The top 10 institutions ranked by number of publications were all Chinese universities, among which Nanjing Medical University ranked first, with 72 publications. Therefore, China is the leading country in research on the crosstalk between miRNAs and circRNAs in human diseases, and universities are the main institutional form in this field.

According to CiteSpace V, “glioblastoma,” “miR-7,” “skeletal muscle,” and “non-coding RNA” are the most popular keywords in the related research; these terms indicate potential research hotspots and frontiers. The four potential frontiers of research on the crosstalk between miRNAs and circRNAs in human diseases are as follows:

- (1) Glioblastoma: Glioblastoma multiforme (GBM), the most common type of brain cancer, is also known as grade IV glioma; the disease has a short overall survival time and high malignancy (Westphal and Lamszus, 2011; Louis et al., 2016). Although therapeutic strategies for this disease have been improved, GBM remains difficult to treat (Omuro and DeAngelis, 2013). circRNAs and miRNAs play important roles in many malignancies, and their crosstalk in GBM remains unclear. Thus, research on this field has great potential therapeutic significance.
- (2) MiR-7: miR-7 can modulate the expression of several oncogenes, and changes in miR-7 activity can affect the progression of cancer (Hansen et al., 2013b). The mechanism underlying the crosstalk between circRNAs and miR-7 in human diseases is a research hotspot.
- (3) Skeletal muscle: Skeletal muscle, which contains 50–75% of all proteins in the human body, accounts for approximately 40% of the human body weight. Skeletal muscle is closely related to human locomotion and metabolism, and skeletal muscle diseases can severely affect a patient's quality of life (Frontera and Ochala, 2015). circRNAs and miRNAs can regulate the development of skeletal muscle, and the crosstalk between these RNAs is a research frontier (Ge and Chen, 2011; Zhang et al., 2019a).
- (4) Non-coding RNA: Research conducted over the last decade has reported that ncRNAs are involved in several physiological and pathological processes. circRNAs and miRNAs are two types of ncRNAs that do not code proteins but can regulate gene expression. The effect of crosstalk between circRNAs and

miRNAs on the complex and unknown regulatory networks of ncRNA must be further investigated (Panni et al., 2020).

According to our analysis of keywords and references, research on the crosstalk between circRNAs and miRNAs mainly focuses on cancer, including glioma, gastric cancer, and ovarian cancer, and the related sponge mechanism. Journals in molecular, biology and genetics field were the main source of references for the published research. Most publications were published in journals dedicated to molecular, biology and immunology field.

To the best of our knowledge, this study is the first to use CiteSpace to perform a bibliographic analysis of publications on the crosstalk between miRNAs and circRNAs. However, this study presents some limitations. First, SCI-E of WoS, although an authoritative and comprehensive database in the medical field, was the only resource we selected for data acquisition; thus, some important findings published in other databases may have been missed. Second, the contributions and collaborations of authors were not analyzed because most of the authors were from China and different Chinese names could be translated to the same English name. Third, this study lacked an assessment of the overall quality of publications.

CONCLUSION

A total of 1,013 papers on the crosstalk between miRNAs and circRNAs in human diseases were published. The first paper was published in 2011 and initiated research in this field. The quality of most publications was relatively well in this field, but high-impact researches were needed. *Biochemical and Biophysical Research Communications* contributed the most to this field in terms of number of publications, and China produced the largest amount of research on this topic. In terms of institution, Nanjing Medical University published the largest number of related articles. At present, cancer is the most popular research area related to the crosstalk between miRNAs and circRNAs in human diseases. The latest burst keywords are “glioblastoma,” “miR-7,” “skeletal muscle,” and “non-coding RNA.” As far as we know, no bibliographic analysis has been conducted for publications on the crosstalk between circRNAs and miRNAs before. This study may provide researchers important clues on research trends and frontiers in this field.

DATA AVAILABILITY STATEMENT

The original contributions presented in the study are included in the article/**Supplementary Material**, further inquiries can be directed to the corresponding author.

AUTHOR CONTRIBUTIONS

Y-MC and X-QW: conceptualization and visualization. Y-MC: data curation, formal analysis, methodology, and writing – original draft. X-QW: funding acquisition and supervision. Y-MC, Y-LZ, XS, and X-QW: validation. Y-MC, Y-LZ, and XS:

writing, review, and editing. All authors contributed to the article and approved the submitted version.

FUNDING

This research was funded by the National Natural Science Foundation of China, grant number 81871844; Shuguang Program supported by Shanghai Education Development Foundation and Shanghai Municipal Education Commission, grant number 18SG48; the Shanghai Municipal Commission of Health and Family Planning, grant number 201840346; the Shanghai Key Lab of Human Performance (Shanghai

University of Sport), grant number 11DZ2261100; and Shanghai Frontiers Science Research Base of Exercise and Metabolic Health.

SUPPLEMENTARY MATERIAL

The Supplementary Material for this article can be found online at: <https://www.frontiersin.org/articles/10.3389/fcell.2021.754880/full#supplementary-material>

Supplementary Figure 1 | Flowchart of literature selection on the crosstalk between microRNAs and circular RNAs in human diseases.

REFERENCES

- Aufiero, S., Reckman, Y. J., Pinto, Y. M., and Creemers, E. E. (2019). Circular RNAs open a new chapter in cardiovascular biology. *Nat. Rev. Cardiol.* 16, 503–514. doi: 10.1038/s41569-019-0185-2
- Bartel, D. P. (2004). MicroRNAs: genomics, biogenesis, mechanism, and function. *Cell* 116, 281–297. doi: 10.1016/s0092-8674(04)00045-5
- Bartel, D. P. (2009). MicroRNAs: target recognition and regulatory functions. *Cell* 136, 215–233. doi: 10.1016/j.cell.2009.01.002
- Chen, C. (2006). CiteSpace II: detecting and visualizing emerging trends and transient patterns in scientific literature. *J. Am. Soc. Inform. Sci. Technol.* 57, 359–377. doi: 10.1002/asi.20317
- Colpaert, R. M. W., and Calore, M. (2019). MicroRNAs in cardiac diseases. *Cells* 8:737. doi: 10.3390/cells8070737
- Fitzsimons, S., Oggero, S., Bruen, R., McCarthy, C., Strowitzki, M. J., Mahon, N. G., et al. (2020). microRNA-155 is decreased during atherosclerosis regression and is increased in urinary extracellular vesicles during atherosclerosis progression. *Front. Immunol.* 11:576516. doi: 10.3389/fimmu.2020.576516
- Floris, G., Zhang, L., Follesa, P., and Sun, T. (2017). Regulatory role of circular RNAs and neurological disorders. *Mol. Neurobiol.* 54, 5156–5165. doi: 10.1007/s12035-016-0055-4
- Frontera, W. R., and Ochala, J. (2015). Skeletal muscle: a brief review of structure and function. *Calcif Tissue Int.* 96, 183–195. doi: 10.1007/s00223-014-9915-y
- Garfield, E. (2006). The history and meaning of the journal impact factor. *JAMA* 295, 90–93. doi: 10.1001/jama.295.1.90
- Ge, Y., and Chen, J. (2011). MicroRNAs in skeletal myogenesis. *Cell Cycle* 10, 441–448. doi: 10.4161/cc.10.3.14710
- Han, D., Li, J., Wang, H., Su, X., Hou, J., Gu, Y., et al. (2017). Circular RNA circMTO1 acts as the sponge of microRNA-9 to suppress hepatocellular carcinoma progression. *Hepatology* 66, 1151–1164. doi: 10.1002/hep.29270
- Hansen, T. B., Jensen, T. I., Clausen, B. H., Bramsen, J. B., Finsen, B., Damgaard, C. K., et al. (2013a). Natural RNA circles function as efficient microRNA sponges. *Nature* 495, 384–388. doi: 10.1038/nature11993
- Hansen, T. B., Kjems, J., and Damgaard, C. K. (2013b). Circular RNA and miR-7 in cancer. *Cancer Res.* 73, 5609–5612. doi: 10.1158/0008-5472.CAN-13-1568
- Hansen, T. B., Wiklund, E. D., Bramsen, J. B., Villadsen, S. B., Statham, A. L., Clark, S. J., et al. (2011). miRNA-dependent gene silencing involving Ago2-mediated cleavage of a circular antisense RNA. *EMBO J.* 30, 4414–4422. doi: 10.1038/emboj.2011.359
- Hirsch, J. E. (2005). An index to quantify an individual's scientific research output. *Proc. Natl. Acad. Sci. U. S. A.* 102, 16569–16572. doi: 10.1073/pnas.0507655102
- Huang, J. L., Su, M., and Wu, D. P. (2020). Functional roles of circular RNAs in Alzheimer's disease. *Ageing Res. Rev.* 60:101058. doi: 10.1016/j.arr.2020.101058
- Iacona, J. R., and Lutz, C. S. (2019). miR-146a-5p: expression, regulation, and functions in cancer. *Wiley Interdiscip. Rev. RNA* 10:e1533. doi: 10.1002/wrna.1533
- Iqbal, M. A., Arora, S., Prakasam, G., Calin, G. A., and Syed, M. A. (2019). MicroRNA in lung cancer: role, mechanisms, pathways and therapeutic relevance. *Mol. Aspects Med.* 70, 3–20. doi: 10.1016/j.mam.2018.07.003
- Jeck, W. R., Sorrentino, J. A., Wang, K., Slevin, M. K., Burd, C. E., Liu, J., et al. (2013). Circular RNAs are abundant, conserved, and associated with ALU repeats. *RNA* 19, 141–157. doi: 10.1261/rna.035667.112
- Journal Citation Reports (2021). *Sign in to Continue with Journal Citation Reports*. Available online at: <https://jcr.clarivate.com/jcr/home> (accessed September 19, 2021).
- Kleaveland, B., Shi, C. Y., Stefano, J., and Bartel, D. P. (2018). A Network of noncoding regulatory RNAs acts in the mammalian brain. *Cell* 174, 350–362.e17. doi: 10.1016/j.cell.2018.05.022
- Kristensen, L. S., Andersen, M. S., Stagsted, L. V. W., Ebbesen, K. K., Hansen, T. B., and Kjems, J. (2019). The biogenesis, biology and characterization of circular RNAs. *Nat. Rev. Genet.* 20, 675–691. doi: 10.1038/s41576-019-0158-7
- Lee, R. C., Feinbaum, R. L., and Ambros, V. (1993). The C. elegans heterochronic gene lin-4 encodes small RNAs with antisense complementarity to lin-14. *Cell* 75, 843–854. doi: 10.1016/0092-8674(93)90529-y
- Li, Z., Huang, C., Bao, C., Chen, L., Lin, M., Wang, X., et al. (2015). Exon-intron circular RNAs regulate transcription in the nucleus. *Nat. Struct. Mol. Biol.* 22, 256–264. doi: 10.1038/nsmb.2959
- Liu, Q., Zhang, X., Hu, X., Dai, L., Fu, X., Zhang, J., et al. (2016). Circular RNA related to the chondrocyte ECM regulates MMP13 expression by functioning as a MiR-136 'Sponge' in human cartilage degradation. *Sci. Rep.* 6:22572. doi: 10.1038/srep22572
- Liu, S., Sun, Y. P., Gao, X. L., and Sui, Y. (2019). Knowledge domain and emerging trends in Alzheimer's disease: a scientometric review based on citespaces analysis. *Neural. Regen. Res.* 14, 1643–1650. doi: 10.4103/1673-5374.255995
- Lopez-Gonzalez, M. J., Landry, M., and Favereaux, A. (2017). MicroRNA and chronic pain: from mechanisms to therapeutic potential. *Pharmacol. Ther.* 180, 1–15. doi: 10.1016/j.pharmthera.2017.06.001
- Louis, D. N., Perry, A., Reifemberger, G., von Deimling, A., Figarella-Branger, D., Cavenee, W. K., et al. (2016). The 2016 World Health Organization classification of tumors of the central nervous system: a summary. *Acta Neuropathol.* 131, 803–820. doi: 10.1007/s00401-016-1545-1
- Memczak, S., Jens, M., Elefsinioti, A., Torti, F., Krueger, J., Rybak, A., et al. (2013). Circular RNAs are a large class of animal RNAs with regulatory potency. *Nature* 495, 333–338. doi: 10.1038/nature11928
- Omuro, A., and DeAngelis, L. M. (2013). Glioblastoma and other malignant gliomas: a clinical review. *JAMA* 310, 1842–1850. doi: 10.1001/jama.2013.280319
- Panni, S., Lovering, R. C., Porras, P., and Orchard, S. (2020). Non-coding RNA regulatory networks. *Biochim. Biophys. Acta Gene Regul. Mech.* 1863:194417. doi: 10.1016/j.bbagrm.2019.194417
- Patop, I. L., and Kadener, S. (2018). circRNAs in Cancer. *Curr. Opin. Genet. Dev.* 48, 121–127. doi: 10.1016/j.gde.2017.11.007
- Piwecka, M., Glazar, P., Hernandez-Miranda, L. R., Memczak, S., Wolf, S. A., Rybak-Wolf, A., et al. (2017). Loss of a mammalian circular RNA locus causes miRNA deregulation and affects brain function. *Science* 357:eaam8526. doi: 10.1126/science.aam8526
- Sanger, H. L., Klotz, G., Riesner, D., Gross, H. J., and Kleinschmidt, A. K. (1976). Viroids are single-stranded covalently closed circular RNA molecules existing as highly base-paired rod-like structures. *Proc. Natl. Acad. Sci. U. S. A.* 73, 3852–3856. doi: 10.1073/pnas.73.11.3852

- Song, G., Yang, Z., Guo, J., Zheng, Y., Su, X., and Wang, X. (2020). Interactions among lncRNAs/circRNAs, miRNAs, and mRNAs in neuropathic pain. *Neurotherapeutics* 17, 917–931. doi: 10.1007/s13311-020-00881-y
- Tramullas, M., Frances, R., de la Fuente, R., Velategui, S., Carcelen, M., Garcia, R., et al. (2018). MicroRNA-30c-5p modulates neuropathic pain in rodents. *Sci. Transl. Med.* 10:eaa06299. doi: 10.1126/scitranslmed.aao6299
- Wang, Y., Mo, Y., Gong, Z., Yang, X., Yang, M., Zhang, S., et al. (2017). Circular RNAs in human cancer. *Mol. Cancer* 16:25. doi: 10.1186/s12943-017-0598-7
- Westphal, M., and Lamszus, K. (2011). The neurobiology of gliomas: from cell biology to the development of therapeutic approaches. *Nat. Rev. Neurosci.* 12, 495–508. doi: 10.1038/nrn3060
- World Health Organization [WHO] (2021). *International Classification of Diseases 11th Revision [Online]*. Available online at: <https://icd.who.int/en/> (accessed July 9, 2021).
- Xu, A. H., and Sun, Y. X. (2020). Research hotspots and effectiveness of repetitive transcranial magnetic stimulation in stroke rehabilitation. *Neural Regen. Res.* 15, 2089–2097. doi: 10.4103/1673-5374.282269
- Xu, H., Zhang, Y., Qi, L., Ding, L., Jiang, H., and Yu, H. (2018). NFIX circular RNA promotes glioma progression by regulating miR-34a-5p via notch signaling pathway. *Front. Mol. Neurosci.* 11:225. doi: 10.3389/fnmol.2018.00225
- Yan, W., Zheng, K., Weng, L., Chen, C., Kiartivich, S., Jiang, X., et al. (2020). Bibliometric evaluation of 2000–2019 publications on functional near-infrared spectroscopy. *Neuroimage* 220:117121. doi: 10.1016/j.neuroimage.2020.117121
- Yang, R., Xing, L., Zheng, X., Sun, Y., Wang, X., and Chen, J. (2019). The circRNA circAGFG1 acts as a sponge of miR-195-5p to promote triple-negative breast cancer progression through regulating CCNE1 expression. *Mol. Cancer* 18:4. doi: 10.1186/s12943-018-0933-7
- Zhang, J., Liu, H., Hou, L., Wang, G., Zhang, R., Huang, Y., et al. (2017). Circular RNA_LARP4 inhibits cell proliferation and invasion of gastric cancer by sponging miR-424-5p and regulating LATS1 expression. *Mol. Cancer* 16:151. doi: 10.1186/s12943-017-0719-3
- Zhang, L., Zhang, Y., Wang, Y., Zhao, Y., Ding, H., and Li, P. (2020). Circular RNAs: functions and clinical significance in cardiovascular disease. *Front. Cell Dev. Biol.* 8:584051. doi: 10.3389/fcell.2020.584051
- Zhang, P., Chao, Z., Zhang, R., Ding, R., Wang, Y., Wu, W., et al. (2019a). Circular RNA regulation of myogenesis. *Cells* 8:885. doi: 10.3390/cells8080885
- Zhang, P. F., Pei, X., Li, K. S., Jin, L. N., Wang, F., Wu, J., et al. (2019b). Circular RNA circFGFR1 promotes progression and anti-PD-1 resistance by sponging miR-381-3p in non-small cell lung cancer cells. *Mol. Cancer* 18:179. doi: 10.1186/s12943-019-1111-2
- Zheng, Q., Bao, C., Guo, W., Li, S., Chen, J., Chen, B., et al. (2016). Circular RNA profiling reveals an abundant circHIPK3 that regulates cell growth by sponging multiple miRNAs. *Nat. Commun.* 7:11215. doi: 10.1038/ncomms11215

Conflict of Interest: The authors declare that the research was conducted in the absence of any commercial or financial relationships that could be construed as a potential conflict of interest.

Publisher's Note: All claims expressed in this article are solely those of the authors and do not necessarily represent those of their affiliated organizations, or those of the publisher, the editors and the reviewers. Any product that may be evaluated in this article, or claim that may be made by its manufacturer, is not guaranteed or endorsed by the publisher.

Copyright © 2021 Chen, Zheng, Su and Wang. This is an open-access article distributed under the terms of the Creative Commons Attribution License (CC BY). The use, distribution or reproduction in other forums is permitted, provided the original author(s) and the copyright owner(s) are credited and that the original publication in this journal is cited, in accordance with accepted academic practice. No use, distribution or reproduction is permitted which does not comply with these terms.



Expression Profile and Potential Function of Circular RNAs in Peripheral Blood Mononuclear Cells in Male Patients With Primary Gout

Fei Dai^{1,2†}, Quan-Bo Zhang^{1,3†}, Yi-Ping Tang^{1,2}, Yi-Xi He^{1,2}, Ting Yi^{1,2} and Yu-Feng Qing^{1,2*}

¹Research Center of Hyperuricemia and Gout, Affiliated Hospital of North Sichuan Medical College, North Sichuan Medical College, Nanchong, China, ²Department of Rheumatology and Immunology, Affiliated Hospital of North Sichuan Medical College, North Sichuan Medical College, Nanchong, China, ³Department of Geriatrics, Affiliated Hospital of North Sichuan Medical College, North Sichuan Medical College, Nanchong, China

OPEN ACCESS

Edited by:

Jing Zhang,
Shanghai Jiao Tong University, China

Reviewed by:

Abhijit Shukla,
Memorial Sloan Kettering Cancer
Center, United States

Yedi Zhou,
Second Xiangya Hospital, Central
South University, China

*Correspondence:

Yu-Feng Qing
qingyufengqq@163.com

[†]These authors have contributed
equally to this work and share first
authorship

Specialty section:

This article was submitted to
Epigenomics and Epigenetics,
a section of the journal
Frontiers in Genetics

Received: 20 June 2021

Accepted: 11 October 2021

Published: 26 October 2021

Citation:

Dai F, Zhang Q-B, Tang Y-P, He Y-X,
Yi T and Qing Y-F (2021) Expression
Profile and Potential Function of
Circular RNAs in Peripheral Blood
Mononuclear Cells in Male Patients
With Primary Gout.
Front. Genet. 12:728091.
doi: 10.3389/fgene.2021.728091

Circular RNAs (circRNAs) are non-coding RNAs (ncRNAs) with a single-stranded covalently closed-loop structure, and their abnormal expression may participate in the pathogenesis of various human diseases. Currently, knowledge of circRNAs in gout is limited. In this case-control study, human circRNA microarrays were used to identify differentially expressed circRNAs in peripheral blood mononuclear cells (PBMCs) from patients with primary gout ($n = 5$) and healthy controls (HC; $n = 3$). Bioinformatics methods were used to analyze significantly different circRNAs (fold change >1.5 , $p < 0.05$). In addition, four significantly differentially expressed circRNAs were selected for quantitative real-time polymerase chain reaction to detect expression levels in 90 gout patients and 60 HC. Subsequently, circRNA-miRNA-mRNA network was established to predict the function of circRNAs of interest. Microarray analysis indicated that 238 circRNAs were upregulated and 41 circRNAs were down-regulated in the gout group (fold change >1.5 , $p < 0.05$). Bioinformatics analysis showed that differentially expressed circRNAs were involved in the pathogenesis of gout via various pathways. Moreover, the expression levels of hsa_circRNA_103657 and hsa_circRNA_000241 were significantly higher in the gout group than those in the HC group, and both correlated significantly with lipid metabolism parameters. Furthermore, the area under the curve of hsa_circRNA_103657 was 0.801 (95% confidence interval (CI): 0.730–0.871; $p < 0.001$). Our results provide novel insights into the pathogenesis of primary gout. Differentially expressed circRNAs were identified in the PBMCs of gout patients, and these differential circRNAs may play important roles in the development and progression of gout.

Keywords: gout, circular RNA, microarray analysis, peripheral blood mononuclear cells, biomarker

INTRODUCTION

Gout is a common metabolic disease characterized by disturbances in purine metabolism and (or) decreased excretion of uric acid, which lead to increased uric acid in the blood and deposits of urate crystals in tissues (Dalbeth et al., 2016). The main manifestations of primary gout include hyperuricemia, acute arthritis, tophi, joint deformities, urinary tract stones, and kidney disease. Recent epidemiological studies have shown that the global prevalence and incidence of gout are

increasing, with a prevalence of <1–6.8% and an incidence of 0.58–2.89 per 1,000 person years (Dehlin et al., 2020). However, the specific pathogenesis of gout remains unclear. Studies have reported that genetics, immunity, eating habits, and traumatic stress, are likely involved in the occurrence and development of gout (Dalbeth et al., 2016; Dalbeth et al., 2019; Clebak et al., 2020; Dehlin et al., 2020). Although elevated serum uric acid levels are considered an important risk factor for the development of gout, only approximately 10% of hyperuricemia patients suffer from gout (Zhang, 2021). The typical onset of joint symptoms and the discovery of urate crystals in the joint cavity are important indicators for the diagnosis of primary gout (Dalbeth et al., 2016), at which point urate crystals have been deposited into the joint cavity or caused joint deformities, which results in serious consequences for patients' quality of life (Dalbeth et al., 2019). In addition, patients with gout often have comorbid diabetes, hypertension, hyperlipidemia, and cardiovascular and cerebrovascular diseases, which significantly threaten human health (Dalbeth et al., 2016; Dalbeth et al., 2019; Clebak et al., 2020; Dehlin et al., 2020). Therefore, clarifying the exact pathogenesis of gout and identifying biomarkers of primary gout is crucial to develop methods that enable early diagnosis and treatment of gout.

As an important element of epigenetics, non-coding RNA participates in the development of diseases by regulating gene expression and other functions; this is currently a research hotspot in the field of life sciences. Circular RNAs (circRNAs) are a new type of non-coding RNA molecule, which are composed of exons, introns, or fragments of the two, and are highly resistant to degradation because of their distinct circular structure (Zhou et al., 2020). Emerging evidence suggests that circRNAs are potential candidates for diagnostic biomarkers and therapeutic targets for a variety of diseases, including tumors (Wang J. et al., 2021), cardiovascular diseases (Ward et al., 2021), and nervous system diseases (Li M.-L. et al., 2021). However, at present, knowledge of circRNAs in gout remains limited. Therefore, in this study, microarray technology was used to screen and analyze the differential expression of circRNAs in peripheral blood mononuclear cells (PBMCs) between patients with primary gout and healthy controls (HC). We aimed to explore the role of circRNAs in gout, provide new insights into the pathogenesis of gout, and identify biomolecules for the diagnosis and treatment of gout from a genetic perspective.

MATERIALS AND METHODS

Patients and Sample Collection

Male patients with primary gout and healthy volunteers were recruited from the Affiliated Hospital of North Sichuan Medical College from March 2020 to March 2021. All patients met the American College of Rheumatology/European League Against Rheumatism 2015 gout classification criteria (Neogi et al., 2015) and were subdivided into acute gout flare (AG) and intercritical gout (IG) groups according to their clinical manifestations. Specifically, gout patients with symptoms of joint swelling, heat, and pain during the previous 3 days were classified into

the AG group, whereas those who had not experienced joint symptoms for at least 2 weeks and had normal inflammatory indicators, such as erythrocyte sedimentation rate (ESR), high-sensitivity C-reactive protein (CRP), and white blood cell (WBC) count, were classified into the IG group. During the same period, age- and sex-matched healthy volunteers with no hyperuricemia, metabolic syndrome, or other chronic diseases were recruited as the HC group from the Physical Examination Center of Affiliated Hospital of Sichuan North Medical University.

The study was conducted in two phases. Firstly, we selected six primary gout patients (three AG and three IG) and three HC and isolated total RNAs from their PBMCs for microarray analysis using a human circRNA microarray (Arraystar Inc., Rockville, MD, United States). Secondly, target circRNAs were detected in 90 primary gout patients (45 AG and 45 IG) and 60 HC using quantitative real-time polymerase chain reaction (qRT-PCR). Exclusion criteria for gout patients included 1) serious diseases of major organs, such as the heart and kidneys, 2) other serious conditions, such as malignant tumors and autoimmune diseases, 3) infection-related disorders, and 4) secondary gout due to other diseases.

The clinical data of all subjects including age, sex, body mass index, and laboratory indicators, such as serum uric acid (sUA) levels, blood glucose (GLU) levels, inflammation indicators, and lipid metabolism indicators were recorded. Inflammation indicators included ESR, CRP, WBC count, neutrophil granule count (GR), lymphocyte count (LY), and monocyte count (Mo), and lipid metabolism indicators included plasma total cholesterol (TC), triglycerides (TG), high-density lipoprotein cholesterol (HDL), low-density lipoprotein cholesterol (LDL), and very-low-density lipoprotein (VLDL). All laboratory indicators were measured by the Clinical Laboratory Department of the Affiliated Hospital of North Sichuan Medical College. All participants provided written informed consent and patient data were analyzed anonymously. The study was approved by the Ethics Committee of the Affiliated Hospital of North Sichuan Medical College (Ethics approval number: 2019 ER(A)040) and was conducted following the ethical code of the Declaration of Helsinki of 1975.

Sample Preparation

In each subject, 4 ml of fasting peripheral venous blood were collected in a heparin anticoagulation tube. PBMCs were isolated from blood samples by Ficoll-Hypaque density gradient centrifugation and stored at -80°C for subsequent analysis.

RNA Extraction

The total RNA in PMBCs was extracted according to manufacturer instructions of the TRIzol reagent (Invitrogen, Grand Island, NY, United States). The integrity of RNA was evaluated by standard denaturing agarose gel electrophoresis, and the concentration and purity of RNA were measured by NanoDrop ND-1000.

Circular RNAs Microarray

Samples of age- and sex-matched six gout patients (three AG and three IG) and three HC were selected for the microarray analysis.

We used the Arraystar Human circRNA Array v2 chip (8×15 K) (Arraystar, Rockville, MD, United States), which contains 13,617 human circRNA probes. Sample preparation and microarray hybridization were performed according to Arraystar's standard protocols (Agilent Technology). Briefly, 2000 ng of the total RNA were digested with rnaase R (Epicentre, Illumina, Inc., Madison, WI, United States) to remove linear RNAs and enrich circRNAs. Then, the enriched circRNAs were amplified and transcribed into fluorescent cRNA using a random priming method (Arraystar Super RNA Labeling Kit; Arraystar). The labeled cRNAs were hybridized onto the Arraystar Human circRNA Array v2 (8×15 K, Arraystar). After washing the slides, the arrays were scanned using the Agilent Scanner G2505C (Agilent Technologies, Inc., Santa Clara, CA, United States).

Data Analysis and Differentially Expressed Circular RNAs Identification

The Agilent Feature Extraction software (version 11.0.1.1) was used to analyze the acquired array images. Quantile normalization and subsequent data processing were performed using the R software (R Project for Statistical Computing, Vienna, Austria) limma package. Differentially expressed circRNAs that differed significantly between the gout group and the HC group were identified using scatter plot and volcano plot filtering (p -value calculated from an unpaired t -test; $p < 0.05$). Differentially expressed circRNAs between the two groups were identified using fold change filtering (fold change >1.5). Hierarchical clustering was performed to determine distinguishable circRNA expression patterns among samples.

Quantitative real-time polymerase chain reaction Amplification

Four significantly more highly expressed circRNAs (hsa_circRNA_100632, hsa_circRNA_405646, hsa_circRNA_000241, and hsa_circRNA_103657) and two significantly more lowly expressed circRNAs (hsa_circRNA_104917, hsa_circRNA_001594) were selected from the microarray results for the qRT-PCR experiments.

According to the instructions of the reverse transcription reagent (TaKaRa, Japan), 2 μ l (600 ng) of total RNA was reverse transcribed into cDNA. The PCR reaction was then performed using the LightCycle®96 PCR machine (Roche,

Switzerland). The reaction system included TB Green Premix Ex Taq II (Takara Bio, Inc.): 5 μ l, the forward primer: 0.1 μ l (10 pmol/L), the reverse primer: 0.1 μ l (10 pmol/L), cDNA: 1.0 μ l, and ddH₂O: 3.8 μ l. The thermocycling conditions were as follows: 95°C for 10 min, followed by 40 cycles of denaturation at 95°C for 10 s, and annealing/extension at 60°C for 1 min. All reactions were performed in triplicate. The expression of the housekeeping gene (β -actin) was used as the internal control to normalize the expression of each target gene. Relative quantification with the $2^{-\Delta\Delta C_q}$ method (Livak and Schmittgen, 2001) was used to evaluate the relative expression of circRNAs. The β -actin and the six circRNA primer sequences used for qRT-PCR (Shanghai Shenggong Bioengineering Co., Ltd., Shanghai, China) are listed in Table 1.

Bioinformatics Analysis: Gene Ontology and Pathway Analysis

The gene ontology (GO) project provides a controlled vocabulary to describe gene and gene product attributes of any organism (<http://www.geneontology.org>) (Huntley et al., 2014). The ontology covers three domains: Biological Process (BP), Cellular Component (CC), and Molecular Function (MF). Fisher's exact test in the Bioconductor's top GO was used to establish whether there was more overlap between the differential genes and the GO annotation list than would be expected by chance. The p -value produced by the top GO denotes the significance of the GO items' enrichment in the differential genes, where a lower p -value indicated a more significant GO item ($p \leq 0.05$ was recommended).

Pathway analysis is a functional analysis that maps genes to Kyoto Encyclopedia of Genes and Genomes (KEGG) pathways (<http://www.genome.jp/kegg/>) (Kanehisa et al., 2014). The p -value (EASE-score, Fisher's p -value, or hypergeometric p -value) denotes the significance of the pathway correlated to the conditions, where the lower the p -value, the more significant the pathway ($p < 0.05$ was considered statistically significant).

Construction of Competitive Endogenous RNA Regulatory Network

CircRNA-miRNA interactions were predicted using Arraystar's homemade miRNA target prediction software (Rockville, MD, United States) based on TargetScan (http://www.targetscan.org/vert_72/) (Enright et al., 2003) and miRanda ([**TABLE 1 |** Primer sequences used in the validation of circRNAs.](http://www.</p>
</div>
<div data-bbox=)

gene name	Forward primers sequence(5'-3')	Reverse primers sequence(5'-3')
β -actin	GAGCTACGAGCTGCCTGACG	GTAGTTTCGTGGATGCCACAG
hsa_circRNA_000241	GTGCGCTGCAATCCAGACAG	AGGACAAGCCGACTGCATTGG
hsa_circRNA_103657	ATGGACCCAAGAGTCAGCGG	TGCTTGGCCATTTCGGTTCC
hsa_circRNA_405646	ACGAGCTGGTTAGGAGGCAC	TACATCCACTCCACGGCACC
hsa_circRNA_100632	TTGTGACCTCCCTCTCCGTG	GCGGCGAATGCAGAGTTGAT
hsa_circRNA_104917	TTCAGCTCTGAGACCAACCGC	TCATCTGCGAGAGGTCCCT
hsa_circRNA_001594	GGTGCTCCTGACTGCAGAA	ACTCGAGGGTGGAGGAGAGT

miranda.org/) (Pasquinelli, 2012). Then, the target genes of these miRNAs were predicted using the TargetScan, miRDB (<http://mirdb.org/>) (Chen and Wang, 2020), and mirtarbase (<https://mirtarbase.cuhk.edu.cn/>) (Huang et al., 2020) databases. Only the miRNA-mRNA predicted by these three databases were retained. Finally, according to the predicted relationship of circRNA-miRNA-mRNA, the ceRNA network was constructed using the Cytoscape software version 3.7.2 (<http://www.cytoscape.org/index.html>) (Shannon et al., 2003).

Statistical Analysis

IBM SPSS Statistics 23.0 and GraphPad Prism 8.0 statistical software were used for analysis. Quantitative data with approximately normal distributions are described as means \pm standard deviations, and data with non-normal distributions are described as medians (interquartile ranges). Statistical analysis of demographics, clinical, and laboratory indicators were performed using independent samples t-tests, Mann-Whitney U-tests, and one-way analyses of variance, followed by LSD posthoc tests. Fisher's exact test was used for the GO enrichment and KEGG pathway analysis. Correlations were calculated using Spearman's rank correlation test. The receiver operating characteristic (ROC) curve was used to evaluate the diagnostic efficacy of the candidate biomarker. A $p < 0.05$ was considered statistically significant.

RESULTS

Circular RNAs Expression Profiles

Arraystar Human circRNA Array v2 (8 \times 15 K) was used to detect and analyze circRNAs in the PBMCs of six gout patients (including three AG and three IG) and three HC. When data of nine subjects were analyzed and processed, the results of one IG case were found to be significantly biased. Through a retrospective review, the patient was found to have possible early rheumatoid arthritis at enrollment into the study, which was missed at that time of recruitment. Thus, the data of this case was excluded and the data of eight cases (three AG, two IG, and three HC) were retained for subsequent analyses. The demographic and clinical features of the eight subjects are summarized in **Supplementary Material S1**. To ensure rigor, all subjects were reconfirmed that they met inclusion criteria.

We found 279 differentially expressed circRNAs (fold change >1.5 and $p < 0.05$) between gout and HC groups, of which 238 had higher and 41 had lower expression levels in the gout group than those in the HC group. Microarray data have been uploaded to the Gene Expression Omnibus database under the accession number GSE178825. The top 15 upregulated and top 15 downregulated circRNAs for the gout group are listed in **Table 2**. Scatter plots in **Figure 1A**

TABLE 2 | The top 15 upregulated and 15 downregulated circRNAs in gout patients compared with healthy control subjects.

circRNA	Regulation	Fold Change	P-value	Alias	chrom	circRNA_type
hsa_circRNA_100914	up	10.2022483	0.003146809	hsa_circ_0023903	chr11	exonic
hsa_circRNA_100632	up	5.163444	0.012600554	hsa_circ_0018905	chr10	exonic
hsa_circRNA_091000	up	4.790979	0.028191498	hsa_circ_0091000	chrX	exonic
hsa_circRNA_403982	up	4.4366415	0.005949389	—	chr8	exonic
hsa_circRNA_405646	up	4.0272268	0.000118818	—	chr17	exonic
hsa_circRNA_000992	up	3.4618	0.012692591	hsa_circ_0000992	chr2	exonic
hsa_circRNA_007352	up	3.3827085	0.008540683	hsa_circ_0007352	chrX	exonic
hsa_circRNA_100332	up	3.2688998	0.043596282	hsa_circ_0014130	chr1	exonic
hsa_circRNA_100912	up	3.0983479	0.008225714	hsa_circ_0003695	chr11	exonic
hsa_circRNA_000241	up	3.0679421	0.020358477	hsa_circ_0000241	chr10	sense overlapping
hsa_circRNA_405746	up	2.9812781	0.022371618	—	chr19	exonic
hsa_circRNA_100925	up	2.9686745	0.04539817	hsa_circ_0023940	chr11	exonic
hsa_circRNA_103657	up	2.9388912	0.005663491	hsa_circ_0069977	chr4	exonic
hsa_circRNA_100923	up	2.9170916	0.031237871	hsa_circ_0023936	chr11	exonic
hsa_circRNA_103667	up	2.8591439	0.021060797	hsa_circ_0070039	chr4	exonic
hsa_circRNA_101287	down	3.5782171	0.028296353	hsa_circ_0008274	chr13	exonic
hsa_circRNA_101144	down	2.3865965	0.01677349	hsa_circ_0028196	chr12	exonic
hsa_circRNA_102339	down	2.233307	0.016725147	hsa_circ_0047351	chr18	exonic
hsa_circRNA_104917	down	2.1808263	0.000840297	hsa_circ_0088494	chr9	exonic
hsa_circRNA_407330	down	2.1543414	0.025214642	—	chrX	exonic
hsa_circRNA_001038	down	2.125022	0.037949687	hsa_circ_0000453	chr12	antisense
hsa_circRNA_007215	down	2.0316255	0.022281484	hsa_circ_0007215	chr4	sense overlapping
hsa_circRNA_047641	down	2.0271657	0.037410987	hsa_circ_0047641	chr18	exonic
hsa_circRNA_405498	down	1.973957	0.01876855	—	chr16	exonic
hsa_circRNA_100269	down	1.873869	0.011762548	hsa_circ_0013048	chr1	exonic
hsa_circRNA_102579	down	1.8471502	0.013598646	hsa_circ_0002311	chr19	exonic
hsa_circRNA_001594	down	1.846286	0.013111066	hsa_circ_0001343	chr3	antisense
hsa_circRNA_400100	down	1.7992879	0.012928107	hsa_circ_0092364	chr9	intronic
hsa_circRNA_066113	down	1.7671692	0.008504126	hsa_circ_0066113	chr3	exonic
hsa_circRNA_101501	down	1.7645955	0.001811216	hsa_circ_0034953	chr15	exonic

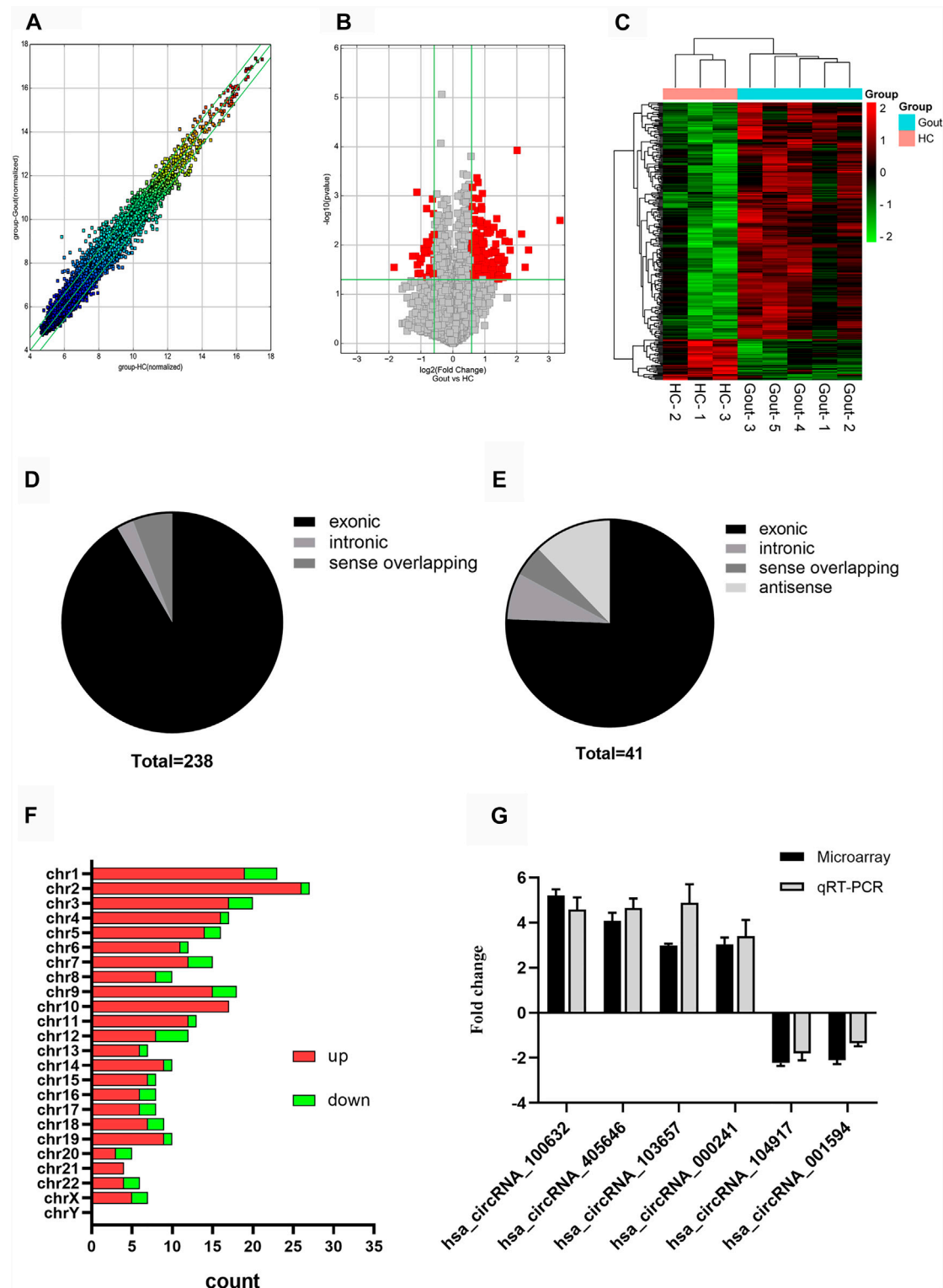


FIGURE 1 | Expression profiles of circRNAs in gout patients compared with healthy controls. **(A)** Scatter plot demonstrating the heterogeneity of the expression of circRNAs in the gout and HC groups. The values of the X and Y axes represent the averaged normalized signal values of the groups (log2-scaled). The green line represents 1.5-fold changes. The expression of circRNAs above the top green line and below the bottom green line indicates changes by > 2-fold between the two groups. **(B)** Volcano plots visualizing differentially expressed circRNAs between the two groups. The vertical lines correspond to 1.5-fold up- and downregulated circRNA expression. The horizontal line represents a p -value of 0.05. The red point in the plot represents significantly differentially expressed circRNAs. **(C)** Clustered

(Continued)

FIGURE 1 | heatmap showing the relationships among the expression levels of samples. Expression values are represented by the color scale. The intensity increases from green (relatively low expression) to red (relatively high expression). Each column represents one sample, and each row represents a single circRNA. **(D)** Genomic region distribution of upregulated circRNAs. **(E)** Genomic region distribution of downregulated circRNAs. **(F)** Distribution of significantly dysregulated circRNAs in chromosomes. **(G)** Relative expression levels of the six circRNAs in five gout patients and three healthy control (HC) subjects. The Y-axis represents the ratio of the relative expression level of circRNAs in the gout group to that of the HC group. Gout: primary gout; HC: healthy controls.

show the heterogeneity of circRNA expression in the PBMCs of the gout and HC groups. The expression change of circRNAs above the top reference line and below the bottom reference line was >1.5-fold. Volcano plots (**Figure 1B**) were used to visualize the significantly differentially expressed circRNAs between the gout and HC groups. Hierarchical cluster analysis (**Figure 1C**) was used to show distinct circRNAs expression profiling between the gout and HC groups. We summarized the classification of significantly differentially expressed circRNAs (fold change >1.5, $p < 0.05$): 218 exons, 6 introns, 14 sense overlappings were included in the up-regulated circRNAs (**Figure 1D**); 31 exons, 3 introns, 2 sense overlappings, and 5 antisenses were contained in the downregulated circRNAs (**Figure 1E**). The transcripts of these significantly differentially expressed circRNAs were widely distributed in all chromosomes except the Y chromosome. The top two chromosomes that upregulated the distribution of circRNAs transcripts were chr1 (7.98%) and chr2 (10.92%), whereas in the downregulated circRNAs, chr1 and chr12 both accounted for 9.76%, and the other chromosomes were less than 8% (**Figure 1F**).

Four circRNAs (hsa_circRNA_100632, hsa_circRNA_405646, hsa_circRNA_000241, hsa_circRNA_103657) were randomly selected from the top 15 upregulated circRNAs, and two circRNAs (hsa_circRNA_104917, hsa_circRNA_001594) were randomly selected from the top 15 downregulated circRNAs for further analysis. The expression levels of six circRNAs in eight samples previously used for microarray detection were analyzed by qRT-PCR to verify the reliability of the microarray results. In the microarray analysis, the fold changes of the normalized levels of the six circRNAs between the gout and HC groups were 5.16, 4.03, 3.08, 2.94, 2.18, and 1.85. In the qRT-PCR analysis, the fold changes in the expression levels of the six circRNAs between the two groups were 4.59, 4.65, 3.39, 4.82, 1.80, and 1.36, respectively. Therefore, the qRT-PCR results were consistent with the trend of the microarray data (**Figure 1G**).

Gene Ontology and Encyclopedia of Genes and Genomes Pathway Analyses of Differentially Expressed Circular RNAs

In this study, GO and KEGG pathway analyses were performed for the parental genes with significant differential expression of circRNAs in the microarray expression profile to explore the potential function and possible biological pathways of circRNAs in the PBMCs of gout patients. In the GO analysis, the histograms represent the top 10 items of enrichment scores in the upregulated (**Supplementary Material S2A**) and downregulated genes (**Supplementary**

Material S2B). Differential genes were primarily related to the “cAMP biosynthetic process,” “enzyme binding,” “adenylate cyclase activity,” and the “nuclear ubiquitin ligase complex.” In the KEGG pathway analysis, the numbers of pathway items that differentially expressed higher and lower circRNAs in the gout group were 34 and 43, respectively. The KEGG pathway analysis showed the circRNAs more highly expressed in the gout group than those in the HC group mainly involved “mitophagy,” “ubiquitin-mediated proteolysis,” and the “FoxO signaling pathway” (**Supplementary Material S2C**; top 10 pathways), whereas circRNAs with lower expression levels in the gout group were significantly involved in “platelet activation,” the “apelin signaling pathway,” and the “cGMP-PKG signaling pathway” (**Supplementary Material S2D**; top 10 pathways).

Expression Levels of the Four Circular RNAs in Gout Patients and Healthy Controls Subjects

In the verification phase, the expression levels of the four upregulated circRNAs were significantly different between the gout and HC groups. Therefore, we detected the expression levels of the four upregulated circRNAs in 150 samples (45 AG, 45 IG, and 60 HC) by qRT-PCR to identify the most suitable clinical biomarkers and determine the role of circRNAs in gout. The demographic and clinical features of all the subjects are summarized in **Table 3**. As shown in **Figure 2**, the expression levels of hsa_circRNA_103657 and hsa_circRNA_000241 in the gout group were significantly higher than those in the HC group ($p < 0.05$; **Figures 2A,B**). The expression levels of hsa_circRNA_100632 and hsa_circRNA_405646 were not statistically different between the two groups ($p > 0.05$; **Figures 2C,D**).

In addition, the expression levels of the four circRNAs in the AG, IG, and HC groups are shown separately. The expression levels of hsa_circRNA_103657 and hsa_circRNA_000241 in the AG and IG groups were significantly higher than those in the HC group ($p < 0.05$) but did not differ significantly between the AG and IG groups (**Figures 2E,F**). The expression levels of hsa_circRNA_100632 and hsa_circRNA_405646 among the three groups were not statistically significant (**Figures 2G,H**).

Prediction and Annotation of hsa_Circular RNAs_103657 and hsa_circRNA_000241 Circular RNAs Mechanism

Since some circRNAs can perform the function of “miRNA sponge” by efficiently binding and inhibiting miRNA transcription, which would further influence downstream

TABLE 3 | Clinical and laboratory data of subjects studied.

	Gout group (n=90)	AG group (n=45)	IG group (n=45)	HC group (n=60)
Age (years)	40.90 ± 12.42	41.31 ± 12.76	40.49 ± 12.20	42.63 ± 10.94
Gender F/M	0/90	0/45	0/45	0/60
Disease duration, median (range) (months)	37.50 (23.75–49.25)	24 (2.00–66.00)	39 (31.50–47.50)	—
BMI (kg/m ²) (\bar{x} ±SD)	25.15 ± 3.47 ^a	24.76 ± 3.63 ^a	25.54 ± 3.29 ^a	22.23 ± 2.06
CRP (mg/L) (\bar{x} ±SD)	15.06 ± 29.10	27.45 ± 37.31 ^b	2.67 ± 2.57	—
ESR (mm/h) (\bar{x} ±SD)	15.90 ± 20.35	24.93 ± 25.49 ^b	6.87 ± 4.58	—
WBC (×10 ⁹ /L) (\bar{x} ±SD)	7.92 ± 2.79 ^a	9.02 ± 3.08 ^{ab}	6.83 ± 1.96 ^a	5.54 ± 1.24
GR (×10 ⁹ /L) (\bar{x} ±SD)	5.24 ± 2.48 ^a	6.23 ± 2.75 ^{ab}	4.24 ± 1.69 ^a	3.38 ± 0.89
LY (×10 ⁹ /L) (\bar{x} ±SD)	1.99 ± 0.68	2.00 ± 0.80 ^b	1.98 ± 0.53	1.76 ± 0.59
Mo (×10 ⁹ /L) (\bar{x} ±SD)	0.48 ± 0.21 ^a	0.56 ± 0.23 ^a	0.40 ± 0.16 ^a	0.32 ± 0.08
sUA (μmol/L) (\bar{x} ±SD)	463.96 ± 142.45 ^a	477.71 ± 140.47 ^a	450.21 ± 144.65 ^a	363.45 ± 51.66
GLU (mmol/L) (\bar{x} ±SD)	5.72 ± 1.12 ^a	5.68 ± 1.07 ^a	5.76 ± 1.17 ^a	4.90 ± 0.41
TG (mmol/L) (\bar{x} ±SD)	2.43 ± 1.78 ^a	2.18 ± 1.41 ^{ab}	2.68 ± 2.09 ^a	1.18 ± 0.33
TC (mmol/L) (\bar{x} ±SD)	4.83 ± 0.85 ^a	4.61 ± 0.79	5.05 ± 0.87 ^a	4.50 ± 0.64
HDL (mmol/L) (\bar{x} ±SD)	1.12 ± 0.26 ^a	1.11 ± 0.26	1.13 ± 0.26	1.18 ± 0.20
LDLC (mmol/L) (\bar{x} ±SD)	2.78 ± 0.62	2.68 ± 0.59	2.89 ± 0.65	2.61 ± 0.58
VLDL (mmol/L) (\bar{x} ±SD)	0.95 ± 0.42 ^a	0.89 ± 0.34 ^a	1.02 ± 0.47 ^a	0.64 ± 0.15

Gout: primary gout, including acute gout flare and intercritical gout; AG: patients with acute gout flare; IG: patients with intercritical gout; HC: healthy controls; \bar{x} ±SD: mean ± standard deviation; BMI: Body Mass Index; CRP: reactive protein; ESR: erythrocyte sedimentation rate; WBC: white blood cell counts; GR: neutrophile granulocyte counts; LY: lymphocyte counts; Mo: monocyte counts; sUA: serum uric acid; GLU: serum glucose; TG: triglycerides; TC: Total Cholesterol; HDL: high-density lipoprotein; LDL: low-density lipoprotein; VLDL: very low-density lipoprotein.

One-way ANOVA, T test or Mann Whitney test. *p*-value < 0.05 was considered to denote statistical significance

^ain comparison with HC group

^bin comparison with IG group.

mRNA expression and finally involved in various diseases, so we predicted the downstream miRNAs of severely dysregulated hsa_circRNA_103657 and hsa_circRNA_000241. Ranked by mirSVRscore, the top-5 miRNAs related to hsa_circRNA_103657 were hsa-miR-329-5p, hsa-miR-556-5p, hsa-miR-452-5p, hsa-miR-345-5p, hsa-miR-22-5p, and the top-5 miRNAs related to hsa_circRNA_000241 were hsa-miR-1303, hsa-miR-619-5p, hsa-miR-645, hsa-miR-4452, hsa-miR-5787. MiRNA-targeted mRNAs were predicted by TargetScan, miRanda and mirtarbase. Finally, the predicted hsa_circRNA_103657 and hsa_circRNA_000241 targeted circRNA-miRNA-mRNA network was established based on sequence-pairing prediction, and a total of 10 miRNAs and 525 mRNAs were predicted to have an interaction with these two circRNAs (Figure 3A). Among them, hsa_circRNA_000241-miRNAs exhibited a relatively large interaction network, especially with hsa-miR-1303, hsa-miR-619-5p, hsa-miR-4452. To gain further insights into the functions of these two circRNAs, all predicted mRNAs were subjected to GO and KEGG enrichment analysis. In the ceRNA regulatory network, GO analysis showed that mRNAs of 525 were mainly concentrated in “endomembrane system organization,” “COPII-coated vesicle budding” (categorized as BPs), “spindle,” “COPII vesicle coat” (categorized as CCs), “alpha-tubulin binding,” “kinesin binding” (categorized as MFs) (Supplementary Material S3). KEGG pathway analysis results show mainly enrichment in the ‘PI3K-Akt signaling pathway’ (Figure 3B) (Supplementary Material S4).

Association Between hsa_Circular RNAs_103657 and hsa_Circular RNAs_000241 Expression Levels and Laboratory Data in Patients With Gout

In the gout group, we assessed correlations between the expression levels of circRNAs (hsa_circRNA_103657 and hsa_circRNA_000241) and plasma lipid, sUA, and GLU levels. Additionally, we evaluated correlations between the expression levels of circRNAs (hsa_circRNA_103657 and hsa_circRNA_000241) and inflammation indicators in the AG group. Results suggested that the expression level of hsa_circRNA_103657 was positively correlated with GLU and TG ($R = 0.419$, $p < 0.001$; $R = 0.263$, $p = 0.013$, respectively; Figures 4A,B), negatively correlated with HDL ($R = -0.210$, $p = 0.048$; Figure 4C), and not correlated with sUA, TC, LDL, or VLDL. The expression level of hsa_circRNA_000241 was positively correlated with TG ($R = 0.339$, $p = 0.001$; Figure 4D) but not correlated with sUA, GLU, TC, HDL, LDL, or VLDL. There were no significant correlations between the expression levels of circRNAs (hsa_circRNA_103657 and hsa_circRNA_000241) and inflammation indicators in the AG group.

Diagnostic Value of hsa_Circular RNAs_103,657 and hsa_Circular RNAs_000241 for Gout

ROC curves were generated to determine the diagnostic value of hsa_circRNA_103657 and hsa_circRNA_000241 in PBMCs for

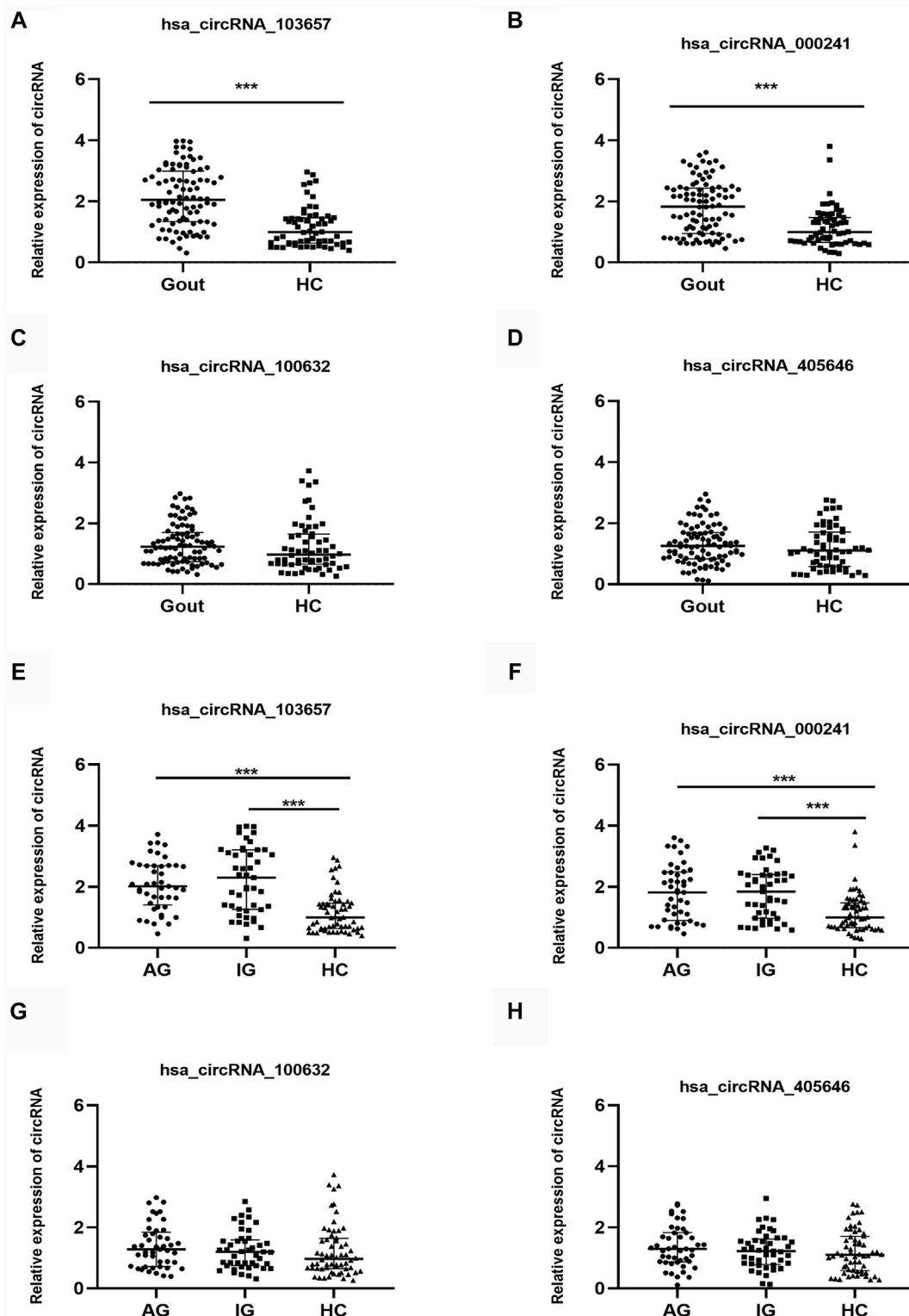
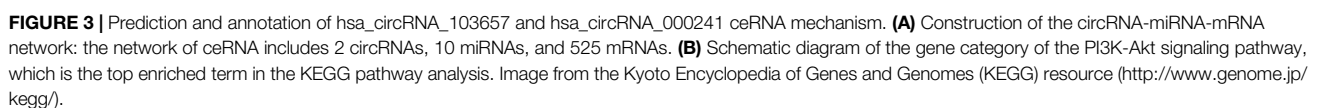


FIGURE 2 | Expression levels of the four circRNAs in gout patients and healthy control subjects. **(A, B, C, D)** Relative expression levels of the four circRNAs in 90 gout patients and 60 healthy control (HC) subjects. **(E, F, G, H)** Relative expression levels of the four circRNAs in 45 acute gout flare (AG) patients, 45 intercritical gout (IG) patients, and 60 HC. Gout: primary gout, including acute gout flare and intercritical gout; AG: patients with acute gout flare; IG: patients with intercritical gout; HC: healthy controls; *** $p < 0.001$.



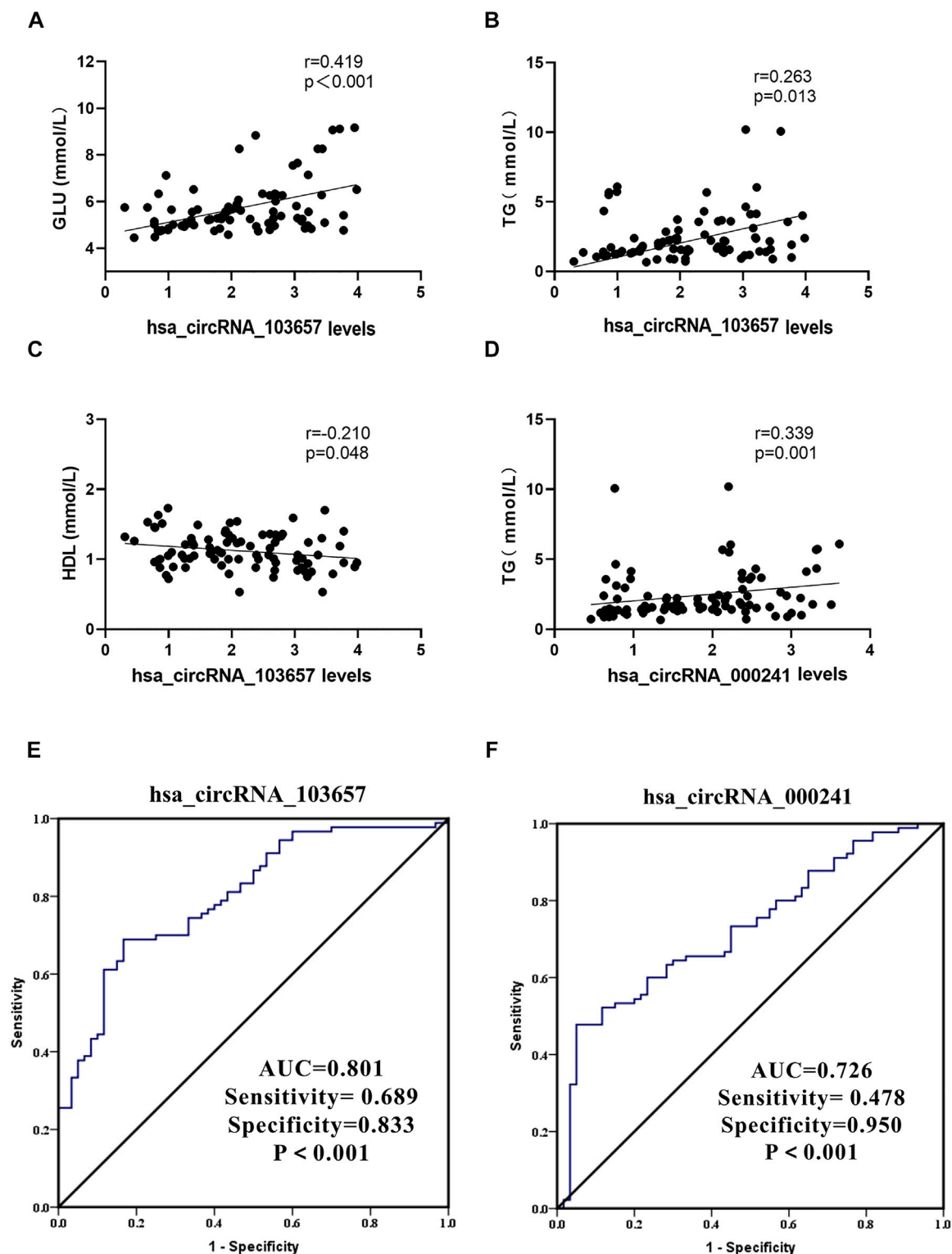


FIGURE 4 | Clinical significance of hsa_circRNA_103657 and hsa_circRNA_000241 in primary gout (**A,B,C,D**) Correlations between the expression levels of circRNAs (hsa_circRNA_103657 and hsa_circRNA_000241) and laboratory data of gout, analyzed using Spearman's coefficient. (**E, F**) Receiver operating characteristic (ROC) curve for the analysis of the diagnostic value of hsa_circRNA_103657 and hsa_circRNA_000241 for primary gout. AUC: area under the curve.

the diagnosis of primary gout (**Figures 3E,F**). The areas under the curve (AUC) of *hsa_circRNA_103657* and *hsa_circRNA_000241* for diagnosing primary gout were 0.801 (95% confidence interval (CI), 0.730–0.871; $p < 0.001$; sensitivity = 68.9%, specificity = 83.3%) and 0.726 (95% CI, 0.646–0.807; $p < 0.001$; sensitivity = 47.8%, specificity = 95.0%), respectively.

DISCUSSION

CircRNAs can act as miRNA sponges, interact with RNA binding proteins, affect protein translation, regulate protein recruitment, and modulate protein assembly (Zhou et al., 2020). Therefore, the multi-functionality of circRNAs makes them ideal for researching and predicting disease. In recent years, increasing numbers of studies have shown that the abnormal expression of circRNAs is closely related to the development of a variety of rheumatism, such as systemic lupus erythematosus (Wang X. et al., 2021), rheumatoid arthritis (Cai et al., 2021), and osteoarthritis (Liu et al., 2021), etc. However, the role of circRNAs in gout is not well understood. In this study, genome-wide microarrays were used to analyze the circRNA expression profile in the PBMCs of gout patients. Compared with the HC group, the gout group had 238 upregulated and 41 downregulated circRNAs. This indicated that there were abnormally expressed circRNAs in the PBMCs of patients with gout, and these abnormally expressed circRNAs play a role in the pathogenesis of gout. According to the genomic regions, the general characteristics of differential circRNAs were further summarized, and most differentially expressed circRNAs were derived from exons. This indicated that circRNAs generate additional transcripts from a gene locus, which is consistent with recent research (Kelly et al., 2015) demonstrating that most circRNAs originate from the exons of protein-coding genes. These significantly different circRNAs were widely distributed in most chromosomes, including the X chromosome, which may be related to the biological mechanism underlying gout. QRT-PCR was used to detect the expression levels of six circRNAs in the PBMCs of eight subjects used in the initial microarray, and their expression levels were entirely consistent with the subsequent microarray results, which confirmed the reliability of the gene microarray data.

The analysis of the GO and KEGG pathways further explored the biological functions and potential mechanisms of the differentially expressed circRNAs in gout. Our results revealed that the biological functions of high- and low-expressed genes in gout differed significantly. Previous studies have confirmed that Toll-like receptor and NOD-like receptor signal transduction pathways are related to the pathogenesis of gout inflammation (Dalbeth et al., 2016; So and Martinon, 2017). Interestingly, our KEGG analysis found that the different circRNAs in the gout group mainly participated in “FoxO signaling pathway,” “apelin signaling pathway,” and “cGMP-PKG signaling pathway,” except for the Toll-like receptor and NOD-like receptor signaling pathways. These data indicated that circRNAs may be involved in the pathogenesis of gout via various signaling pathways.

The cause of gout is complex. Numerous studies (Dalbeth et al., 2016; So and Martinon, 2017; Dalbeth et al., 2019; Clebak et al., 2020; Dehlin et al., 2020; Zhang, 2021) have highlighted that the environment, diet, genetics, immunity, and other aspects participate in the development of the disease in varying degrees, and gout is more prevalent in the male population. We detected the expression levels of *hsa_circRNA_100632*, *hsa_circRNA_405646*, *hsa_circRNA_103657*, and *hsa_circRNA_000241* in 150 male subjects (45 AG, 45 IG, and 60 HC) using qRT-PCR and confirmed that *hsa_circRNA_103657* and *hsa_circRNA_000241* were significantly upregulated in the PBMCs of gout patients. These circRNAs have not been reported to date. To gain further insight, we constructed a circRNA-miRNA-mRNA network based on *hsa_circRNA_103657* and *hsa_circRNA_000241*, and conducted bioinformatics analysis on its downstream targets. The 10 predicted miRNAs have been reported in multiple diseases, especially *hsa-miR-1303*. It has been reported that *hsa-miR-1303* plays an important role in osteosarcoma progression (Han et al., 2021), non-small cell lung cancer (Chen et al., 2020), breast cancer (Liang et al., 2020), Neuroblastoma (Li et al., 2016) and other diseases. KEGG enrichment analysis also pointed out effective signaling pathways, such as the PI3K-Akt signaling pathway, 18 predicted mRNAs participated in this pathway in our research. The dysfunction of PI3K-Akt signaling pathway was related to a variety of pathological conditions, including metabolic diseases (Zhang et al., 2021a), autoimmune inflammatory diseases (Song et al., 2019), cancers (Hoxhaj and Manning, 2020), and neurological diseases (Fu et al., 2020). There are also reports suggesting that the imbalance of the PI3K-Akt signaling pathway can affect uric acid metabolism (Zhang et al., 2021b) or gout inflammation (Paré et al., 2021). Our results indirectly indicate that the dysregulated *hsa_circRNA_103657* and *hsa_circRNA_000241* may participate in the pathogenesis of gout by affecting this pathway. This provides a theoretical basis for us to further explore the potential pathogenesis of circRNA-miRNA-mRNA regulatory network in gout.

Epidemiological investigations have shown that gout is closely related to hyperuricemia, hyperlipidemia, and hyperglycemia (Dalbeth et al., 2019). Moreover, elevated sUA levels are considered an important risk factor for gout, and hyperuricemia is one of the independent risk factors for metabolic diseases such as hypertension, diabetes, and coronary heart disease (Dalbeth et al., 2016; Zhang, 2021). Based on these findings, we analyzed the correlations between sUA, lipid, and glucose metabolism and the expression level of circRNAs and revealed that the expression level of *hsa_circRNA_000241* was positively correlated with TG, and the expression of *hsa_circRNA_103657* was positively correlated with TG and GLU and negatively correlated with HDL. This suggests that *hsa_circRNA_000241* and *hsa_circRNA_103657* are involved in the regulation of lipid or glucose metabolism in patients with gout and that increased expression levels are dangerous for patients with gout.

Gout is a metabolic disease that seriously affects people's health. Although most patients with AG also have hyperuricemia, some gout patients exhibit sUA levels in the normal range. A retrospective cohort study in South Korea showed that sUA

levels did not increase during an acute flare in approximately 40% of gout patients (Lee et al., 2020). Currently, the gold standard diagnostic test for gout is the identification of monosodium urate (MSU) crystals using polarized light microscopy in synovial fluid cells or a tophus (Neogi et al., 2015). However, because of the invasive nature of the operation, its clinical application has certain limitations, especially in gout patients without hyperuricemia, in whom the detection rate of MSU is extremely low. Therefore, it is vital to identify more effective diagnostic markers and therapeutic targets to prevent malignant development of the disease.

The ideal biomarker should possess the following characteristics: high specificity, high sensitivity, non-invasive, convenient, cheap, and reproducible. Because of their unique structure, high stability, and specific expression, circRNAs are being increasingly recognized as new diagnostic markers of diseases in recent years (Zhou et al., 2020; Wang J. et al., 2021; Ward et al., 2021). For example, circ-PSD3 in tissue samples may be a potential diagnostic biomarker or molecular therapy target for papillary thyroid carcinoma (Li Z. et al., 2021). Moreover, circFKBP8 and circMBNL1 are abnormally expressed in peripheral blood and may be potential diagnostic biomarkers for major depressive disorder (Shi et al., 2021). Luo et al. (Luo et al., 2021) have revealed that hsa_circ_0082688 and hsa_circ_0082689 in whole blood could be used as diagnostic biomarkers for systemic lupus erythematosus. However, there have not been any reports regarding the use of circRNAs as biomarkers for gout. In this study, the expression levels of hsa_circRNA_103657 and hsa_circRNA_000241 in the gout group were significantly higher than those in the HC group. As known to all, the ROC curve is generated using an analysis method that reflects the sensitivity and specificity of disease diagnosis indicators (Mandrekar, 2010). The AUC indicates the diagnostic efficacy of the indicator. The value of AUC ranges from 0.5 to 1.0, and values close to 1.0 indicate better diagnostic efficacy. The ROC analysis showed that the AUC of hsa_circRNA_103657 was more than 0.8, which indicated that it could distinguish gout patients from healthy individuals. Thus, hsa_circRNA_103657 may be offered as a potential diagnostic biomarker for gout. However, further validation is necessary to establish this biomarker for clinical use.

There are several limitations to the present study. First is the relatively small sample size and the inclusion of only male subjects. The findings need to be confirmed in large-scale studies conducted in populations with different ethnicities and from other regions. Second, to determine whether hsa_circRNA_103657 can be used as a diagnostic biomarker, it must be evaluated for its ability to accurately differentiate gout from other similar diseases. Cases with other conditions should be included in future studies to provide further evidence supporting hsa_circRNA_103657 as a diagnostic biomarker for gout. Third, we could only speculate that hsa_circRNA_103657 is involved in lipid and sugar metabolism in primary gout; the

specific pathogenesis of hsa_circRNA_103657 in gout remains uncertain. Therefore, functional experimental studies are required to establish the causal relationship between aberrantly expressed hsa_circRNA_103657 and gout.

In conclusion, our study is the first to measure circRNA expression in the PBMCs of gout patients and HC using microarray technology and qRT-PCR. Our findings enhance our understanding of the role played by circRNAs in primary gout, especially hsa_circRNA_103657 and hsa_circRNA_000241, which has potential functional and clinical significance in gout. However, the molecular mechanism and specific functions of these circRNAs in gout require further study.

DATA AVAILABILITY STATEMENT

We have uploaded the raw data to GEO accession number GSE178825: <https://www.ncbi.nlm.nih.gov/geo/query/acc.cgi?acc=GSE178825>.

ETHICS STATEMENT

The studies involving human participants were reviewed and approved by the Ethics Committee of the Affiliated Hospital of North Sichuan Medical College. The patients/participants provided their written informed consent to participate in this study.

AUTHOR CONTRIBUTIONS

Conceptualization : Y-FQ, Q-BZ. Data curation: Y-FQ, Q-BZ. Formal analysis: Y-FQ, FD. Funding acquisition: Q-BZ. Investigation: FD, Q-BZ, Y-XH, TY. Methodology: Y-FQ, FD, Y-PT, TY. Project administration: Y-FQ. Software: FD, Y-PT. Validation: Y-XH. Writing—original draft: FD. Writing—review & editing: Y-FQ, Y-PT, Y-XH.

FUNDING

This work was supported by funding from the National Natural Science Foundation of China (Grant Number: 81974250); Science and Technology Project of Nanchong City (Grant Number: 20SXCTD0002); Science and Technology Plan Project of Sichuan Province (Grant Number: 2018JY0257).

SUPPLEMENTARY MATERIAL

The Supplementary Material for this article can be found online at: <https://www.frontiersin.org/articles/10.3389/fgene.2021.728091/full#supplementary-material>

REFERENCES

- Cai, Y., Liang, R., Xiao, S., Huang, Q., Zhu, D., Shi, G.-P., et al. (2021). Circ_0088194 Promotes the Invasion and Migration of Rheumatoid Arthritis Fibroblast-like Synoviocytes via the miR-766-3p/MMP2 Axis. *Front. Immunol.* 12, 628654. doi:10.3389/fimmu.2021.628654
- Chen, Y., and Wang, X. (2020). miRDB: an Online Database for Prediction of Functional microRNA Targets. *Nucleic Acids Res.* 48, D127–D131. doi:10.1093/nar/gkz757
- Chen, J., Jiang, T., Yu, B., Li, T., Zhao, P., Yuan, L., et al. (2020). Upregulation of microRNA-1303 Is a Potential Prognostic Marker of Non-small Cell Lung Cancer. *Cancer Biomark* 28 (4), 439–446. doi:10.3233/CBM-201461
- Clebak, K. T., Morrison, A., and Croad, J. R. (2020). Gout: Rapid Evidence Review. *Am. Fam. Physician* 102 (9), 533–538.
- Dalbeth, N., Merriman, T. R., and Stamp, L. K. (2016). Gout. *Lancet* 388 (10055), 2039–2052. doi:10.1016/S0140-6736(16)00346-9
- Dalbeth, N., Choi, H. K., Joosten, L. A. B., Khanna, P. P., Matsuo, H., Perez-Ruiz, F., et al. (2019). Gout. *Nat. Rev. Dis. Primers* 5 (1), 69. doi:10.1038/s41572-019-0115-y
- Dehlin, M., Jacobsson, L., and Roddy, E. (2020). Global Epidemiology of Gout: Prevalence, Incidence, Treatment Patterns and Risk Factors. *Nat. Rev. Rheumatol.* 16 (7), 380–390. doi:10.1038/s41584-020-0441-1
- Enright, A. J., John, B., Gaul, U., Tuschl, T., Sander, C., Marks, D. S., et al. (2003). MicroRNA Targets in *Drosophila*. *Genome Biol.* 5 (1), R1. doi:10.1186/gb-2003-5-1-r1
- Fu, S., Luo, X., Wu, X., Zhang, T., Gu, L., Wang, Y., et al. (2020). Activation of the Melanocortin-1 Receptor by NDP-MSH Attenuates Oxidative Stress and Neuronal Apoptosis through PI3K/Akt/Nrf2 Pathway after Intracerebral Hemorrhage in Mice. *Oxid. Med. Cell Longev.* 2020, 1–13. doi:10.1155/2020/8864100
- Han, G., Guo, Q., Ma, N., Bi, W., Xu, M., Jia, J., et al. (2021). LncRNA BCRT1 Facilitates Osteosarcoma Progression via Regulating miR-1303/FGF7 axis. *Aging* 13 (11), 15501–15510. doi:10.18632/aging.203106
- Hoxhaj, G., and Manning, B. D. (2020). The PI3K-AKT Network at the Interface of Oncogenic Signalling and Cancer Metabolism. *Nat. Rev. Cancer* 20 (2), 74–88. doi:10.1038/s41568-019-0216-7
- Huang, H.-Y., Lin, Y.-C., Li, J., Huang, K.-Y., Shrestha, S., Hong, H.-C., et al. (2020). miRTarBase 2020: Updates to the Experimentally Validated microRNA-Target Interaction Database. *Nucleic Acids Res.* 48, D148–D154. doi:10.1093/nar/gkz896
- Huntley, R. P., Harris, M. A., Alam-Faruque, Y., Blake, J. A., Carbon, S., Dietze, H., et al. (2014). A Method for Increasing Expressivity of Gene Ontology Annotations Using a Compositional Approach. *BMC Bioinformatics* 15, 155. doi:10.1186/1471-2105-15-155
- Kanehisa, M., Goto, S., Sato, Y., Kawashima, M., Furumichi, M., and Tanabe, M. (2014). Data, Information, Knowledge and Principle: Back to Metabolism in KEGG. *Nucl. Acids Res.* 42, D199–D205. doi:10.1093/nar/gkt1076
- Kelly, S., Greenman, C., Cook, P. R., and Papantonis, A. (2015). Exon Skipping Is Correlated with Exon Circularization. *J. Mol. Biol.* 427 (15), 2414–2417. doi:10.1016/j.jmb.2015.02.018
- Lee, J. S., Kwon, O. C., Oh, J. S., Kim, Y.-G., Lee, C.-K., Yoo, B., et al. (2020). Clinical Features and Recurrent Attack in Gout Patients According to Serum Urate Levels during an Acute Attack. *Korean J. Intern. Med.* 35 (1), 240–248. doi:10.3904/kjim.2018.205
- Li, Z., Xu, Z., Xie, Q., Gao, W., Xie, J., and Zhou, L. (2016). miR-1303 Promotes the Proliferation of Neuroblastoma Cell SH-SY5Y by Targeting GSK3 β and SFRP1. *Biomed. Pharmacother.* 83, 508–513. doi:10.1016/j.biopha.2016.07.010
- Li, M.-L., Wang, W., and Jin, Z.-B. (2021a). Circular RNAs in the Central Nervous System. *Front. Mol. Biosci.* 8, 629593. doi:10.3389/fmolb.2021.629593
- Li, Z., Huang, X., Liu, A., Xu, J., Lai, J., Guan, H., et al. (2021b). Circ_PSD3 Promotes the Progression of Papillary Thyroid Carcinoma via the miR-637/HEMGN axis. *Life Sci.* 264, 118622. doi:10.1016/j.lfs.2020.118622
- Liang, Y., Song, X., Li, Y., Chen, B., Zhao, W., Wang, L., et al. (2020). LncRNA BCRT1 Promotes Breast Cancer Progression by Targeting miR-1303/PTBP3 axis. *Mol. Cancer* 19 (1), 85. doi:10.1186/s12943-020-01206-5
- Liu, D., Liang, Y. H., Yang, Y. T., He, M., Cai, Z. J., Xiao, W. F., et al. (2021). Circular RNA in Osteoarthritis: an Updated Insight into the Pathophysiology and Therapeutics. *Am. J. Transl. Res.* 13 (1), 11–23.
- Livak, K. J., and Schmittgen, T. D. (2001). Analysis of Relative Gene Expression Data Using Real-Time Quantitative PCR and the 2 $^{-\Delta\Delta CT}$ Method. *Methods* 25 (4), 402–408. doi:10.1006/meth.2001.1262
- Luo, Q., Li, X., Fu, B., Zhang, L., Fang, L., Qing, C., et al. (2021). Expression Profile and Diagnostic Value of circRNAs in Peripheral Blood from Patients with Systemic Lupus Erythematosus. *Mol. Med. Rep.* 23 (1), 1. doi:10.3892/mmr.2020.11639
- Mandrek, J. N. (2010). Receiver Operating Characteristic Curve in Diagnostic Test Assessment. *J. Thorac. Oncol.* 5 (9), 1315–1316. doi:10.1097/JTO.0b013e3181ec173d
- Neogi, T., Jansen, T. L. T. A., Dalbeth, N., Fransen, J., Schumacher, H. R., Berendsen, D., et al. (2015). 2015 Gout Classification Criteria: an American College of Rheumatology/European League against Rheumatism Collaborative Initiative. *Ann. Rheum. Dis.* 74 (10), 1789–1798. doi:10.1136/annrheumdis-2015-208237
- Paré, G., Vitry, J., Merchant, M. L., Vaillancourt, M., Murru, A., Shen, Y., et al. (2021). The Inhibitory Receptor CLEC12A Regulates PI3K-Akt Signaling to Inhibit Neutrophil Activation and Cytokine Release. *Front. Immunol.* 12, 650808. doi:10.3389/fimmu.2021.650808
- Pasquinelli, A. E. (2012). MicroRNAs and Their Targets: Recognition, Regulation and an Emerging Reciprocal Relationship. *Nat. Rev. Genet.* 13 (4), 271–282. doi:10.1038/nrg3162
- Shannon, P., Markiel, A., Ozier, O., Baliga, N. S., Wang, J. T., Ramage, D., et al. (2003). Cytoscape: a Software Environment for Integrated Models of Biomolecular Interaction Networks. *Genome Res.* 13 (11), 2498–2504. doi:10.1101/gr.1239303
- Shi, Y., Song, R., Wang, Z., Zhang, H., Zhu, J., Yue, Y., et al. (2021). Potential Clinical Value of Circular RNAs as Peripheral Biomarkers for the Diagnosis and Treatment of Major Depressive Disorder. *EBioMedicine* 66, 103337. doi:10.1016/j.ebiom.2021.103337
- So, A. K., and Martinon, F. (2017). Inflammation in Gout: Mechanisms and Therapeutic Targets. *Nat. Rev. Rheumatol.* 13 (11), 639–647. doi:10.1038/nrrheum.2017.155
- Song, B., Li, X.-F., Yao, Y., Xu, Q.-Q., Meng, X.-M., Huang, C., et al. (2019). BMP9 Inhibits the Proliferation and Migration of Fibroblast-like Synoviocytes in Rheumatoid Arthritis via the PI3K/AKT Signaling Pathway. *Int. Immunopharmacol.* 74, 105685. doi:10.1016/j.intimp.2019.105685
- Wang, J., Zhang, Y., Liu, L., Yang, T., and Song, J. (2021a). Circular RNAs: New Biomarkers of Chemoresistance in Cancer. *Cancer Biol. Med.* 18, 421–436. doi:10.20892/j.issn.2095-3941.2020.0312
- Wang, X., Ma, R., Shi, W., Wu, Z., and Shi, Y. (2021b). Emerging Roles of Circular RNAs in Systemic Lupus Erythematosus. *Mol. Ther. Nucleic Acids* 24, 212–222. doi:10.1016/j.omtn.2021.02.028
- Ward, Z., Pearson, J., Schmeier, S., Cameron, V., and Pilbrow, A. (2021). Insights into Circular RNAs: Their Biogenesis, Detection, and Emerging Role in Cardiovascular Disease. *RNA Biol.* 1, 1–18. doi:10.1080/15476286.2021.1891393
- Zhang, X., Zhao, S., Yuan, Q., Zhu, L., Li, F., Wang, H., et al. (2021a). TXNIP, a Novel Key Factor to Cause Schwann Cell Dysfunction in Diabetic Peripheral Neuropathy, under the Regulation of PI3K/Akt Pathway Inhibition-Induced DNMT1 and DNMT3a Overexpression. *Cell Death Dis.* 12 (7), 642. doi:10.1038/s41419-021-03930-2
- Zhang, Y., Tan, X., Lin, Z., Li, F., Yang, C., Zheng, H., et al. (2021b). Fucoidan from Laminaria Japonica Inhibits Expression of GLUT9 and URAT1 via PI3K/Akt, JNK and NF- κ B Pathways in Uric Acid-Exposed HK-2 Cells. *Mar. Drugs* 19 (5), 238. doi:10.3390/md19050238
- Zhang, W.-Z. (2021). Why Does Hyperuricemia Not Necessarily Induce Gout? *Biomolecules* 11 (2), 280. doi:10.3390/biom11020280
- Zhou, W.-Y., Cai, Z.-R., Liu, J., Wang, D.-S., Ju, H.-Q., and Xu, R.-H. (2020). Circular RNA: Metabolism, Functions and Interactions with Proteins. *Mol. Cancer* 19 (1), 172. doi:10.1186/s12943-020-01286-3

Conflict of Interest: The authors declare that the research was conducted in the absence of any commercial or financial relationships that could be construed as a potential conflict of interest.

Publisher's Note: All claims expressed in this article are solely those of the authors and do not necessarily represent those of their affiliated organizations, or those of the publisher, the editors, and the reviewers. Any product that may be evaluated in this article, or claim that may be made by its manufacturer, is not guaranteed or endorsed by the publisher.

Copyright © 2021 Dai, Zhang, Tang, He, Yi and Qing. This is an open-access article distributed under the terms of the Creative Commons Attribution License (CC BY). The use, distribution or reproduction in other forums is permitted, provided the original author(s) and the copyright owner(s) are credited and that the original publication in this journal is cited, in accordance with accepted academic practice. No use, distribution or reproduction is permitted which does not comply with these terms.



Research Progress of circRNAs in Glioblastoma

Xu Guo and Haozhe Piao *

Department of Neurosurgery, Liaoning Cancer Hospital and Institute, Cancer Hospital of China Medical University, Shenyang, China

Circular RNAs (circRNAs) are a class of single-stranded covalently closed non-coding RNAs without a 5' cap structure or 3' terminal poly (A) tail, which are expressed in a variety of tissues and cells with conserved, stable and specific characteristics. Glioblastoma (GBM) is the most aggressive and lethal tumor in the central nervous system, characterized by high recurrence and mortality rates. The specific expression of circRNAs in GBM has demonstrated their potential to become new biomarkers for the development of GBM. The specific expression of circRNAs in GBM has shown their potential as new biomarkers for GBM cell proliferation, apoptosis, migration and invasion, which provides new ideas for GBM treatment. In this paper, we will review the biological properties and functions of circRNAs and their biological roles and clinical applications in GBM.

OPEN ACCESS

Edited by:

Jing Zhang,
Shanghai Jiao Tong University, China

Reviewed by:

Hernando Lopez Berton,
Johns Hopkins Medicine,
United States
Fabiana Passaro,
University of Naples Federico II, Italy

*Correspondence:

Haozhe Piao
piaohaozhe@cancerhosp-In-
cmu.com

Specialty section:

This article was submitted to
Epigenomics and Epigenetics,
a section of the journal
Frontiers in Cell and Developmental
Biology

Received: 09 October 2021

Accepted: 02 November 2021

Published: 22 November 2021

Citation:

Guo X and Piao H (2021) Research
Progress of circRNAs in Glioblastoma.
Front. Cell Dev. Biol. 9:791892.
doi: 10.3389/fcell.2021.791892

Keywords: circRNAs, non-coding RNAs, biomarker, glioblastoma, miRNAs sponge

INTRODUCTION

Glioblastoma (GBM) is one of the most malignant primary brain tumors in adults, characterized by an expansile and infiltrative growth pattern (Jackson et al., 2019; Tan et al., 2020; McKinnon et al., 2021). According to the World Health Organization (WHO) classification for central nervous system (CNS) tumors, GBM is classified as the highest grade IV (Broekman et al., 2018; Caragher et al., 2018). Currently, the standard of therapy for GBM is surgical resection with maximum safety followed by concurrent radiotherapy and adjuvant chemotherapy (Aliferis and Trafalis, 2015; Karachi et al., 2018; Choi et al., 2019; Geraldo et al., 2019). However, the efficacy of this regimen is limited, and the median survival of patients after treatment is only 15 months (Touat et al., 2017; Lim et al., 2018; Balca-Silva et al., 2019). To better treat GBM patients and improve their survival time and quality of life remains a huge challenge. Therefore, the study of mechanisms regulating the malignant progression of GBM and the explore for early GBM biomarkers are important for the early diagnosis, treatment and prognosis of GBM.

Circular RNAs (circRNAs) are covalently contiguous closed loops without 5' and 3' ends, and are structurally more stable than linear RNAs and less susceptible to degradation by nucleic acid exonucleases (Jakobi and Dieterich, 2019; Huang and Zhu, 2021). Initially circRNAs were thought to be products of missplicing or intermediates escaping from the lasso structure of introns (Chen and

Abbreviations: CircRNAs, circular RNAs; GBM, glioblastoma; CNS, central nervous system; Exonic circRNAs, E-circRNAs; ciRNAs, intron circRNAs; eicRNAs, exon-intron circRNAs; miRNAs, microRNAs; NSCLC, non-small-cell lung cancer; EMT, epithelial mesenchymal transition; PDAC, pancreatic ductal adenocarcinoma; RBP, RNA binding protein; 3'-UTR, 3' untranslated regions; NPC, nasopharyngeal carcinoma; CRC, colorectal cancer; IRES, internal ribosome entry site; ORF, open reading frame; EIF4A3, Eukaryotic initiation factor 4A3; ceRNA, competitive endogenous RNA; EDF, epidermal growth factor; E-box binding zinc finger protein, ZEB; MUC, Mucin; VEGF, vascular endothelial growth factor; GSCs, glioma stem cells; TMZ, temozolomide; OS, overall survival; DFS, disease-free survival; PFS, progress-free survival.

Huang, 2018; Tsitsipatis and Gorospe, 2021). With the widespread use of transcriptome sequencing technologies, numerous studies have identified circRNAs as a class of endogenous, numerous molecules that are stably present in mammalian cells with certain organizational, temporal, and disease properties and are no longer considered a class of RNA molecules with no role in the human body (Han et al., 2018; Wu J. et al., 2021; Choudhary et al., 2021). CircRNAs present in mammalian cells, there are over 400 circRNAs in normal humans whose abnormal expression can induce tumorigenesis (Ebbesen et al., 2017; Zhou et al., 2020; Zhang et al., 2021a; Shao et al., 2021).

Studies have showed that circRNAs are involved in the occurrence and development of GBM due to their highly stable ring structure, high abundance in cancer tissues and relative tissue specificity, and their altered expression is expected to become a new marker for early diagnosis and prognostic assessment of GBM or a new target for effective treatment. This review summarized the research progress of circRNAs in GBM in recent years, including the mechanism of circRNAs occurrence, function and application research in GBM.

BIOGENESIS AND CLASSIFICATION OF CIRCULAR RNAs

CircRNAs were first identified in RNA viruses in 1976, and in 1979, Hsu et al. discovered a ring-like molecule with covalently linked 3 and 5' ends in HeLa cells by electron microscopy (Hsu and Coca-Prados, 1979). Because of its special structure, it was often ignored as an abnormal shear by-product. It was not until 1993 that the existence of this structurally unique closed-loop noncoding RNA was confirmed in humans (Farooqi et al., 2021; Wang X. et al., 2021; Lauretti et al., 2021; Sempere et al., 2021). In recent years, with the widespread application of transcriptomic gene sequencing and biophysical techniques, the biological functions of circRNAs and their roles in the development of human diseases are gradually being better understood with the help of high-throughput sequencing technologies. The circRNAs are mainly formed by processing protein-coding genes by RNA polymerase II (Ashwal-Fluss et al., 2014; Li et al., 2019; Ali et al., 2021; Sinha et al., 2021). Meanwhile circRNAs biosynthesis is mediated by RNA binding proteins, intron pair driven and lasso driven, and thus has an important role in regulating adjacent splice sites and promoting circular biosynthesis (Wu et al., 2021a; van Zonneveld et al., 2021; Zhao et al., 2021). Currently circRNAs have also been shown to have many characteristics. Diversity and abundance, circRNAs are widely found in eukaryotic cells and are very diverse (Glazar et al., 2014; Liu et al., 2020; Han et al., 2021). Stability, unlike linear RNA, circRNAs is a single-stranded, covalent closed-loop structure without a 5' cap structure and a 3' terminal poly(A) tail. This structure may protect it from degradation by RNA exonuclease (RNase) and thus has higher stability than linear RNA (Suzuki and Tsukahara, 2014; Di Timoteo et al., 2020; Wang et al., 2021h). Conservative, circRNAs is highly conserved across species (AbouHaidar

et al., 2014; Mao et al., 2021; Meyer et al., 2021). Specificity, mainly in terms of cell type specificity and tissue specificity (Shang et al., 2019; Gokool et al., 2020; Huang and Zhu, 2021).

CircRNAs can be divided into three categories according to the composition of splicing (Figure 1). Exonic circRNAs (E-circRNAs) are composed of backward-sheared exons, intron circRNAs (ciRNAs) are composed of introns only, exon-intron circRNAs (eiciRNAs). Contains both exons and introns. Jeck et al., (Jeck et al., 2013), proposed two different exon cyclization modes, lariat-driven cyclization mode and intron pairing-driven cyclization mode.

BIOLOGICAL FUNCTIONS OF CIRCULAR RNAs

CircRNAs are functionally diverse and are often found to function as microRNAs (miRNAs) sponges because they are rich in miRNAs binding sites. In addition, circRNAs also have roles in regulating parent gene expression, regulating parent gene selective splicing, translating protein functions and participating in intercellular communication by entering exosomes (Figure 2).

MicroRNAs Sponge

Through miRNAs response elements, non-coding RNAs and coding RNAs form a large-scale regulatory network in the transcriptome. MiRNAs are negative regulators of gene expression, reducing the stability of target genes or limiting their translational function (Salmena et al., 2011; Su and Lv, 2020; Shen et al., 2021). CircRNAs are rich in miRNAs binding sites and competitively repress transcriptional regulation of miRNAs, a new class of highly expressed and stable ceRNAs (Shi et al., 2013). The cyclic RNA hsa_circ_0043280 can reduce PAQR3 levels by competitively absorbing miR-203a-3p and blocking miR-203a-3p, and can function as a tumor suppressor to inhibit tumor growth and metastasis in cervical cancer (Zhang et al., 2021b). Hsa_circ_0006349 promotes MKP1 expression through uptake of miR-98, which enhances proliferation and glycolysis of non-small-cell lung cancer (NSCLC) cells and promotes malignant progression of tumors (Qin et al., 2021). Circ-PPP1CB is downregulated in bladder cancer and negatively correlates with clinical stage and histological grade. Circ-PPP1CB regulates cell growth, metastasis and epithelial mesenchymal transition (EMT) by interacting with the miR-1307-3p/SMG1 axis (Wang F. et al., 2021). Circ-EYA3 is elevated in pancreatic ductal adenocarcinoma (PDAC) tissues and cells, and higher levels of circ-EYA3 are significantly associated with poorer prognosis in PDAC patients. Circ-EYA3 can enhance c-Myc expression by acting as an endogenous miR-1294 sponge, which in turn promotes ATP synthesis to increase energy production and promote malignant progression of PDAC (Rong et al., 2021a).

Interaction with RNA-Binding Proteins

CircRNAs can alter splicing patterns or RNA stability by binding to RNA binding protein (RBP) (Huang A. et al., 2020; Zhou et al., 2020; He A. T. et al., 2021; Li J. et al.,

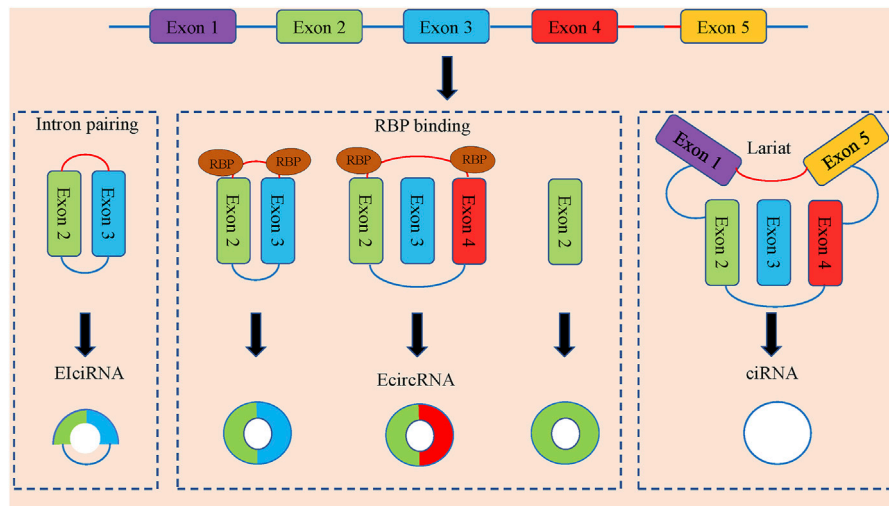


FIGURE 1 | The formation and classification of circRNAs. CircRNAs are commonly divided into EIciRNAs, EcircRNAs and ciRNAs in accordance with their components, which were derived from exons and introns, and both of them in pre-mRNAs, respectively. Latant ecircRNAs can be generated from one pre-mRNA via alternative splicing. The red segment and blue segment between Exon 4 and Exon 5 represented a 7-nt GU-rich motif near the 5' splice site and an 11-nt C-rich motif at the branchpoint site, respectively, which promoted the generation of ciRNAs.

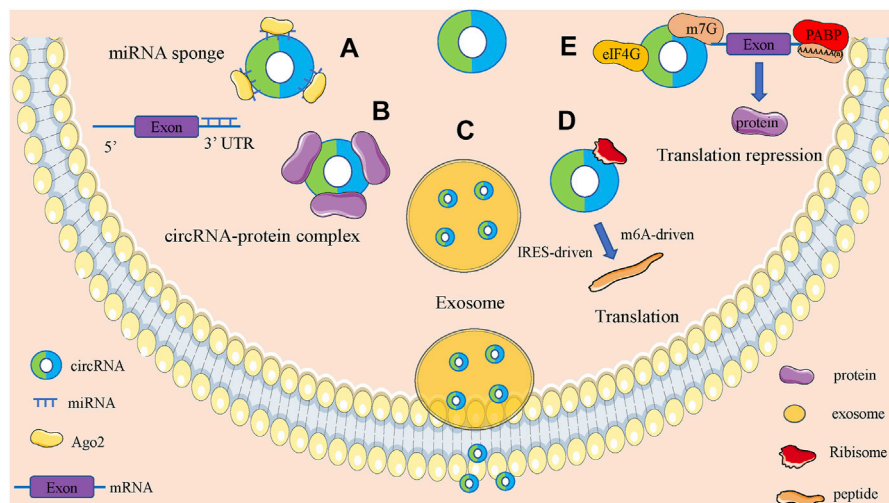


FIGURE 2 | Biological function of circRNAs. (A). CircRNAs can act as miRNA sponges to regulate the expression of downstream genes. (B). CircRNAs can bind to RNA binding protein and regulate parental gene expression. (C). Some circRNAs can be carried by exosomes and involved in the process of cell-cell communication. (D). CircRNAs can encode proteins based on IRES-driven and m6A-driven models. (E). CircRNAs can bind with proteins to establish circRNA-protein complexes and alter the functions of some proteins.

2021). Muscleblind (MBL) is a muscleblind-like 1 (mbnl1) MBL promotes the production of circmb1, which has a specific MBL binding site, and circmb1 has a strong direct interaction with MBL protein (Kristensen et al., 2019). Circ-Mbl regulates MBL protein levels and reduces its own mRNA production by promoting circmb1 production when MBL is in excess. Circmb1 can also eliminate excess MBL by binding to MBL (Ashwal-Fluss et al., 2014). Circrna can facilitate the interaction between DNA, RNA, and RBP to perform biological functions

by binding to related proteins (Qi et al., 2021). Circ-RNF13 prolongs the half-life of SUMO2 by binding to the 3' untranslated regions (3'-UTR) of SUMO2 gene, which leads to sumoylation of GLUT1 and ubiquitination to regulate the AMPK-mTOR pathway, ultimately promoting proliferation and metastasis of nasopharyngeal carcinoma (NPC) (Mo et al., 2021). Circ-RHOBTB3 expression is reduced in colorectal cancer tissues, and lower circ-RHOBTB3 levels are significantly associated with advanced clinical stage and

greater risk of metastasis. Circ-RHOBTB3 binds to hur to promote β -Trcp1-mediated hur ubiquitination, which in turn inhibits the invasive effects of CRC (Chen J. et al., 2021).

Involved in Intercellular Communication Through Exosomes

The main function of exosomes is to mediate intercellular communication through their contents under physiological and pathological conditions (Wang J. et al., 2021; Chen Q. et al., 2021; Shahzad et al., 2021). In addition, exosomes play a role in coagulation, antigen presentation, immune regulation, and viral replication. Exosome contents, such as proteins, mRNAs, and miRNAs, have been shown to act in receptor cells, thereby activating multiple signaling pathways (Kalluri and LeBleu, 2020; Wen et al., 2020; Rong et al., 2021b; Wang et al., 2021e; Reese and Dhayat, 2021; Tian et al., 2021). Tumor cells can secrete more exosomes than normal cells with some variation in contents, and tumor cell-derived exosomes can provide a suitable microenvironment for tumor development, such as cell proliferation, angiogenesis and metastasis, drug resistance and formation of pre-metastatic microenvironment (Li and Wang, 2017; Yan and Chen, 2020). It has been shown that circRNAs can be encapsulated into exosomes and thus participate in tumorigenesis and progression. Exosome-derived hsa_circ_0000337 accelerates Chemoresistance resistance in esophageal cancer cells by regulating the miR-377-3p/JAK2 axis (Zang et al., 2021). Plasma exosomes from colorectal cancer (CRC) patients are enriched in circ-133. Exosomes circ-133 from hypoxic cells are transmitted to normoxic cells and promote CRC metastasis by acting on the miR-133a/GEF-H1/rhoa axis (Yang H. et al., 2020).

Peptide Translation

Normally circRNAs cannot be flipped, but with deeper research, it was found that exon sequences of some circRNAs can be translated into proteins (Chen and Shan, 2021; Dodbele et al., 2021). Some circRNAs contain internal ribosome entry site (IRES) sequences and can bind directly to ribosomes and can be translated in eukaryotic cells (Abe et al., 2015; He L. et al., 2021). The 40S subunit of eukaryotic ribosomes binds to circRNAs and can directly initiate translation (Wang and Wang, 2015). CircRNAs can also be efficiently translated in an *E. Coli* cell-free translation system with an open reading frame (ORF) (Thompson, 2012). It has also been shown that eukaryotic endogenous circRNAs can drive protein translation through m6a methylation (Yang et al., 2017; Dai et al., 2020).

Regulation of Gene Expression

CircRNAs can interact with RNA to participate in post-transcriptional regulation. CircRNAs are formed with a balance between competitive complementary pairing between introns and linear RNAs, which affects mRNA expression and translation (Shao et al., 2021). The ORF-containing circRNAs produced by COL6A3 encodes a novel 198-aa functional peptide, and hsa_circ_0006401–198-aa promotes the stability of the host gene COL6A3 mRNA, thereby facilitating CRC proliferation and

translocation (Zhang et al., 2021c). Circ-PTEN can promote CRC proliferation and translocation by acting as a miR-155 sponge. Circ-PTEN can increase the expression of its host gene PTEN by acting as a sponge for miR-155 and miR-330-3p, which in turn regulates the PI3K/AKT signaling pathway (Wang et al., 2021i). Regulation of parent genes through RNA polymerase II and epigenetic modifications. Some intron derived circRNAs are mainly localized in the nucleus and can interact with RNA polymerase II to promote transcription of their own coding genes (Li et al., 2015). CircRNAs can also regulate parent gene expression through epigenetic modifications. Recently, some circRNAs were also found to have m6a modifications, which affect the stability of the parent gene (Zhou et al., 2017). Thus, circRNAs can be used to regulate the transcription of disease-related parent genes, which in turn affect the expression of the parent gene and its target genes, providing new ideas for the treatment of corresponding diseases.

BIOLOGICAL FUNCTION AND MOLECULAR MECHANISM OF CIRCULAR RNAs IN GLIOBLASTOMA

Studies have shown that circRNAs have important roles in a variety of tumors, and they can be involved in tumorigenesis and progression through many different mechanisms and are closely associated with the clinical features of tumors (Goodall and Wickramasinghe, 2020). Here, we briefly summarize the circRNAs involved in GBM tumorigenesis and progression and analyze their correlation with the clinical features of GBM.

Circular RNAs are associated with Proliferation in Glioblastoma

CircRNAs can regulate the cell proliferation ability of GBM by regulating gene expression or downstream signaling pathways (Table 1). A total of 417 aberrantly expressed circRNAs were found in GBM tissues compared with adjacent normal brains by second-generation sequencing, with hsa_circ_0008344 being the most differentially expressed. Overexpression of hsa_circ_0008344 significantly promoted proliferation, colony formation and decreased apoptosis in GBM cells (Zhou et al., 2018). Eukaryotic initiation factor 4A3 (EIF4A3) bound to MMP9 mRNA transcripts induced circ-MMP9 cyclization and promoted circ-MMP9 expression in GBM. MMP9 promotes the proliferative capacity of GBM cells by targeting miR-124 to regulate the expression of CDK4 and AURKA (Wang et al., 2018b). Hsa_circ_0074027 expression is significantly upregulated in GBM and is associated with clinical features. Hsa_circ_0074027 promotes IL17RD expression through sponge binding of miR-518a-5p, which in turn promotes the proliferative capacity of cells (Qian et al., 2019). Circ-PITX1 enhances MAP3K2 expression by binding miR-379-5p as a competitive endogenous RNA (ceRNA) sponge, which promotes cell proliferation and inhibits apoptosis in GBM (Lv et al., 2019). In addition, Cao et al., also found that circ-PITX1 was significantly overexpressed in GBM tissues and cells, and

TABLE 1 | The proliferation-related circular RNAs in GBM.

circRNAs	Expression	Mechanism	Biological function	Ref.PMID
hsa_circ_0008344	Up	—	Promote cell proliferation, colony formation and inhibit cell apoptotic rate	29687495
circ-MMP9	Up	miR-124/CDK4	Promote cell proliferation	30470262
hsa_circ_0029426	Up	miR-197	Promote cell proliferation and inhibit cell apoptosis	30548670
hsa_circ_0074027	Up	miR-518a-5p/IL17RD	Promote cell proliferation, colony formation and inhibit cell apoptotic rate	30738578
hsa_circ_0067934	Up	PI3K-AKT	Promote cell proliferation	31081099
circ-PITX1	Up	miR-379-5p/MAP3K2	Promote cell proliferation and inhibit cell apoptosis	31493405
circ-FOXO3	Up	miR-138-5p/miR-432-5p/NFAT5	Promote cell proliferation	31504797
hsa_circ_0001801	Up	miR-628-5p/HMGB3	Promote cell proliferation	31858556
circ-EPB41L5	Up	miR-19a/EPB41L5	Promote cell proliferation and colony formation	31905344
circ-ENTPD7	Up	miR-101-3p/ROS1	Promote cell proliferation	32308563
hsa_circ_0043278	Up	miR-638/HOXA9	Promote cell proliferation	33154193
circ-SMO	Up	SMO-193aa	Promote cell proliferation	33446260
circ-SKA3	Up	miR-1	Promote cell proliferation	33500664
circ-PARP4	Up	miR-125a-5p	Promote cell proliferation	33520365
circ-PITX1	Up	miR-584-5p/KPNB1	Promote cell proliferation	33763840
circ-ABCC3	Up	miR-770-5p/SOX2	Promote cell proliferation and inhibit cell apoptosis	33811842
hsa_circ_0006168	Up	miR-628-5p/IGF1R	Promote cell proliferation, colony formation and inhibit cell apoptotic rate	34024251
hsa_circ_0001588	Up	miR-211-5p/YY1	Promote cell proliferation	34105224
circ-FLN1	Up	miR-199-3p	Promote cell proliferation	34498720
circ-SERPINE2	Up	miR-361-3p/miR-324-5p/BCL2	Promote cell proliferation, colony formation and inhibit cell apoptotic rate	34553034
—	—	—	—	—
circ-LGMN	Up	miR-127-3p/LGMN	Promote cell proliferation	34582975
circ-NF1	Up	miR-340	Promote cell proliferation	34589042
circ-NT5E	Down	miR-422a	Inhibit cell proliferation	29967262
hsa_circ_0001946	Down	miR-671-5p/CDR1	Inhibit cell proliferation and promote cell apoptosis	30663767
circ-MTO1	Down	miR-92/WWOX	Inhibit cell proliferation	31456594
circ-AKT3	Down	AKT3-174aa/PI3K/AKT	Inhibit cell proliferation	31470874
hsa_circ_01844	Down	—	Inhibit cell proliferation and promote cell apoptosis	32804726
circ-CDR1as	Down	p53/MDM2	Inhibit cell proliferation	32894144

knockdown of circpitx1 inhibited cell proliferation and tumor growth. Circ-PITX1/miR-584-5p/KPNB1 axis may be a potential therapeutic target for GBM (Cao et al., 2021). Hsa_circ_0001801 upregulates HMGB3 expression in GBM through sponge binding of miR-628-5p, thereby promoting cell proliferation (Chen et al., 2019). Zhu et al., Found that circntpd7 (circbase ID: hsa_circ_0019421) was upregulated in GBM tissues, and knockdown of circntpd7 significantly inhibited GBM cell motility and proliferation (Zhu et al., 2020). Hsa_circ_0043278-miR-638/-HOXA9 regulatory axis has an important role in GBM progression by regulating miR-638/-HOXA9. Hsa_circ_0043278-miR-638/-HOXA9 regulatory axis has an important role in GBM progression and can be involved in GBM tumorigenesis and progression by regulating cell proliferation (Wu et al., 2020). Circ-ABCC3 acts as a sponge for miR-770-5p, which targets SOX2, and knockdown of Circ-ABCC3 significantly inhibits tumor growth *in vivo* (Zhang and Xu, 2021). Wang et al., Found that hsa_circ_0006168 may promote tumor growth in GBM by acting as a competitive endogenous RNA for miR-628-5p and regulating the IGF1R/Ras/Erk pathway (Wang T. et al., 2021). Circ_0001588 may promote the proliferative capacity of GBM cells by regulating the miR-211-5p/YY1 signaling pathway (Wang Q. et al., 2021).

Moreover, circRNAs can also be involved in regulating cell proliferation by binding multiple miRNAs to regulate the expression of downstream genes. Found that circ-FOXO3 can bind both miR-138-5p and miR-432-5p to regulate NFAT5

expression and thus promote cell proliferation (Zhang S. et al., 2019). Li et al., Found that the circ-SERPINE2-miR-361-3p/miR-324-5p/BCL2 signaling pathway plays an important role in the tumor growth process of GBM (Li D. et al., 2021). Besides, hsa_circ_0008344 (Zhou et al., 2018), hsa_circ_0029426 (Zhang G. et al., 2019), hsa_circ_0067934 (Xin et al., 2019), circ-SKA3 (Zhou M. et al., 2021), circ-PARP4 (Zhou J. et al., 2021), circ-FLN1 (Sun et al., 2021) and circ-NF1 (Liu L. et al., 2021) were also shown to significantly promote the proliferative capacity and tumor growth of GBM cells, but the specific molecular mechanisms remain to be further explored.

Hsa_circ_0001946 inhibits cell proliferation and promotes apoptosis by binding to miR-671-5p and regulating CDR1 expression (Li and Diao, 2019). Circ-MTO1 inhibits tumor growth of GBM through miR-92/WWOX regulatory axis (Zhang X. et al., 2019). Circ-NT5E inhibits cell proliferation of GBM by binding miR-422a (Wang et al., 2018a). Circ-CDR1as regulates the malignant growth of GBM by modulating the p53/MDM2 signaling pathway (Lou et al., 2020).

In recent years, circRNAs have been found to be involved in disease processes by encoding peptides. Found that circ-SMO encodes a peptide of length 193aa SMO-199aa. Knockdown deprivation of SMO-193aa in GBM stem cells significantly attenuated Hedgehog signaling and inhibited self-renewal, proliferation *in vitro* and tumorigenicity *in vivo* (Wu X. et al., 2021). Xia et al., Found that circ-AKT3 encodes a novel 174 aa protein, AKT3-174aa, and overexpression of AKT3-174aa

TABLE 2 | The migration and invasion-related circular RNAs in GBM.

circRNAs	Expression	Mechanism	Biological function	Ref.PMID
hsa_circ_0008344	Up	—	Promote cell migration and invasion	29687495
circ-MMP9	Up	miR-124/CDK4	Promote cell migration and invasion	30470262
hsa_circ_0029426	Up	miR-197	Promote cell migration and invasion	30548670
hsa_circ_0074027	Up	miR-518a-5p/IL17RD	Promote cell migration and invasion	30738578
hsa_circ_0067934	Up	PI3K-AKT	Promote cell migration and invasion	31081099
circ-FOXO3	Up	miR-138-5p/miR-432-5p/NFAT5	Promote cell migration and invasion	31504797
hsa_circ_0001801	Up	miR-628-5p/HMGB3	Promote cell migration and invasion	31858556
circ-EPB41L5	Up	miR-19a/EPB41L5	Promote cell migration and invasion	31905344
circ-ENTPD7	Up	miR-101-3p/ROS1	Promote cell migration and invasion	32308563
hsa_circ_0043278	Up	miR-638/HOXA9	Promote cell migration and invasion	33154193
circ-PARP4	Up	miR-125a-5p	Promote cell migration and invasion	33520365
circ-SMARCA5	Up	—	Promote cell migration and invasion	33562358
circ-PITX1	Up	miR-584-5p/KPNB1	Promote cell migration and invasion	33763840
circ-ABCC3	Up	miR-770-5p/SOX2	Promote cell migration and invasion	33811842
hsa_circ_0006168	Up	miR-628-5p/IGF1R	Promote cell migration and invasion	34024251
hsa_circ_0001588	Up	miR-211-5p/YY1	Promote cell migration and invasion	34105224
circ-MELK	Up	miR-593/EphB2	Promote cell migration and invasion	34168916
circ-FLN1	Up	miR-199-3p	Promote cell migration and invasion	34498720
circ-LGMN	Up	miR-127-3p/LGMN	Promote cell migration and invasion	34582975
circ-NT5E	Down	miR-422a	Inhibit cell migration and invasion	29967262
hsa_circ_0001946	Down	miR-671-5p/CDR1	Inhibit cell migration and invasion	30663767
circ-MTO1	Down	miR-92/WWOX	Inhibit cell migration and invasion	31456594

TABLE 3 | Utility of circRNAs for clinical of GBM.

circRNAs	Expression	Clinical Sample	Diagnostic	Utility Prognostic	Predictive	Ref.PMID
has_circ_0029426	Up	Tissues	—	✓	✓	30548670
has_circ_0074027	Up	Tissues	—	—	✓	30738578
has_circ_0067934	Up	Tissues	—	✓	—	31081099
circ-ENTPD7	Up	Tissues	—	✓	✓	32308563
circ-SMO	Up	Tissues	—	✓	—	33446260
circSKA3	Up	Tissues	—	✓	—	33500664
hsa_circ_0001588	Up	Tissues	—	✓	—	34105224
circ-FLNA	Up	Tissues	—	✓	✓	34498720
circ-SERPINE2	Up	Tissues	—	✓	—	34553034
circ-LGMN	Up	Tissues	—	✓	—	34582975
circ-NF1	Up	Tissues	—	✓	✓	34589042
circ-ASAP1	Up	Tissues	—	✓	—	32,926,734
circ-MTO1	Down	Tissues	—	✓	—	31456594
circ-EPB41L5	Down	Tissues	—	✓	✓	31905344
hsa_circ_0006168	Down	Tissues	—	—	✓	34024251

significantly reduced cell proliferation, radioresistance and tumorigenicity of GBM cells *in vivo*, while overexpression of circ-AKT3 suppressed the malignant phenotype of GBM(Xia et al., 2019).

Circular RNAs are associated with Invasion and Metastasis in Glioblastoma

Invasion and metastasis of tumor cells are the main cause of death in most patients with malignant tumors (Asif et al., 2021). This ability to invade and metastasize allows tumor cells to leave their primary location within tissues, enter lymphatic vessels and blood vessels, and colonize distant organs with the blood circulation. Metastasis of tumor cells is a complex, dynamic process that occurs through cytoskeletal remodeling to form leading edge

protrusions, thereby generating mechanical forces that retract and separate the cell tails from the extracellular matrix. CircRNAs have vital roles in the invasion and metastasis of GBM. Hsa_circ_0008344 (Zhou et al., 2018), circ-MMP9(Wang et al., 2018b), hsa_circ_0029426 (Zhang G. et al., 2019), hsa_circ_0074027 (Qian et al., 2019), hsa_circ_0067934 (Xin et al., 2019), circ-FOXO3 (Zhang S. et al., 2019), hsa_circ_0001801 (Chen et al., 2019), circ-EPB41L5 (Lv et al., 2020), circ-ENTPD7 (Zhu et al., 2020), hsa_circ_0043278 (Wu et al., 2020), circ-PARP4 (Zhou J. et al., 2021), circ-SMARCA5 (Barbagallo et al., 2021), circ-PITX1 (Cao et al., 2021), circ-ABCC3(Zhang and Xu, 2021), hsa_circ_0006168 (Wang T. et al., 2021), hsa_circ_0001588 (Wang Q. et al., 2021), circ-MELK (Zhou F. et al., 2021), circ-FLN1 (Sun et al., 2021), circ-LGMN(Chen B. et al., 2021), circ-NT5E (Wang et al.,

2018a), hsa_circ_0001946 (Li and Diao, 2019) and circ-MTO1 (Zhang X. et al., 2019) are involved in the regulation of GBM invasion and metastasis (Table 2).

Epithelial-mesenchymal transition (EMT) is mainly involved in embryogenesis, organogenesis, and tissue healing in humans, but also in tumorigenesis and metastasis, promoting tumor cell invasion and motility by altering intercellular interactions and cell-matrix interactions (Inoue et al., 2015; Wu N. et al., 2021; Satcher and Zhang, 2021; Xiong et al., 2021). About 90% of tumor patient deaths result from tumor invasion and metastasis, which suggests that regulation of the EMT process is important for tumor prevention and treatment. E-cadherin expression is suppressed upon EMT activation, resulting in the loss of the typical polygonal cobblestone morphology of epithelial cells, while cells acquire a spindle-shaped mesenchymal morphology and express markers associated with the mesenchymal cell state, particularly N-cadherin, wave proteins and fibronectin (Cristofanilli and Mendelsohn, 2006; Cai et al., 2021; Zhang N. et al., 2021), therefore, the activation status of EMT can be assessed by changes in the expression of E-cadherin and N-cadherin. It has been shown that growth factors such as epidermal growth factor (EGF), transcription factors such as Snail, Slug, Twist, E-box binding zinc finger protein (ZEB) and signaling pathways such as TGF, Wnt, Notch and Hedgehog can mediate the EMT. Mucin (MUC) acts as an inducer to activate various signaling pathways that also contribute to EMT (Ponnusamy et al., 2013). We found that among the circRNAs involved in GBM, circ-MMP9 (Wang et al., 2018b), hsa_circ_0067934 (Xin et al., 2019), hsa_circ_0001801 (Chen et al., 2019), circ-PARP4 (Zhou J. et al., 2021), circ-PITX1 (Cao et al., 2021), hsa_circ_0006168 (Wang T. et al., 2021), hsa_circ_0001588 (Wang Q. et al., 2021) and circ-MELK (Zhou F. et al., 2021) can regulate GBM invasion and metastasis by modulating the EMT process. Hsa_circ_0067934 (Xin et al., 2019), circ-EPB41L5 (Lv et al., 2020) and circ-ABCC3 (Zhang and Xu, 2021) can participate in the invasion and metastasis of GBM by regulating the PI3K/Akt/mTOR signaling pathway.

Circular RNAs are associated with angiogenesis in Glioblastoma

Tumor development, invasion and metastasis are highly dependent on neovascularization (Goncalves et al., 2021; Rimini and Casadei-Gardini, 2021). Under physiological conditions, angiogenesis is intricately and precisely regulated by multiple molecules and mechanisms that allow the formation of highly tissue-specific, structured and hierarchical vascular networks to sustain the physiological processes of embryonic development, growth and tissue repair (Lai et al., 2021; Martin and Gurevich, 2021; Narasimhan et al., 2021). However, tumor cells are able to release large amounts of vascular endothelial growth factor (VEGF) and inhibit the secretion of angiogenesis inhibitory factor, which unbalances the regulatory mechanism of angiogenesis, resulting in rapid, uncontrolled proliferation of tumor neovascularization and a large, abnormally disordered replenishment network (Liu Y.

et al., 2021; Uemura et al., 2021; Zhu et al., 2021). CircRNAs can also be involved in the malignant invasion and metastasis of GBM by affecting angiogenesis (Figure 3A). Barbagallo et al., Found that circ-SMARCA5 regulates VEGFA mRNA splicing and angiogenesis through binding to SRSF1, which in turn leads to malignant progression of GBM (Barbagallo et al., 2019). In addition, they demonstrated that the GAUGAA motif is a key sequence for binding of circ-SMARCA5 to SRSF1 (Barbagallo et al., 2021). Cao et al., The circ-PITX1/miR-584-5p/KPNB1 regulatory axis was found to be an important molecular mechanism mediating GBM angiogenesis (Cao et al., 2021). Circ-ABCC3 regulates GBM angiogenesis and tumor malignancy progression through PI3K/AKT signaling pathway and miR-770-5p/SOX2 axis (Zhang and Xu, 2021).

Circular RNAs are associated with Tumor Stemness in Glioblastoma

Stem cells are widely involved in body growth and development and organ formation, and have the ability of self-renewal, infinite proliferation and multidirectional differentiation (Jing et al., 2021; Mehraj et al., 2021; Mirzadeh Azad et al., 2021; Otero-Albiol and Carnero, 2021). The strong self-renewal ability, inherent high proliferative capacity and multidirectional differentiation together constitute the basic characteristics of malignant stem cells, among which the self-renewal ability is closely related to tumorigenesis and malignancy (Ferragut et al., 2021; Mehraj et al., 2021; Yue et al., 2021). Over the past three to 4 decades, numerous studies have noted a potential link between stem cell systems and certain tumors, and a small proportion of tumor-initiating cells with stem cell properties, also known as tumor stem cells, have been identified in a variety of organs (Cermenio and Garcia, 2016; Hass et al., 2020; Pan et al., 2021; Ryskalin et al., 2021). Tumor stem cells of glioma tissue origin have the capacity for self-renewal, homotransplantation into tumors, and differentiation into neurons and glial cells; it is now thought that they may be derived from genetically mutated neural stem cells, transiently expanded cells, neural progenitor cells, and even highly differentiated astrocytes and oligodendrocytes in normal brain tissue. It has been found that circRNAs also play an important role in GBM cell stemness (Figure 3B). Zhou et al., Found that circ-MELK expression was significantly increased in GBM tissues and that circ-MELK could regulate GBMEMT progression and glioma stem cells (GSCs) maintenance by binding to miR-593 to promote ephb2 expression (Zhou F. et al., 2021). Gao et al., Demonstrated that circ-E-cadherin encodes a 14 amino acid peptide that binds to the CR2 structural domain of EGFR and activates EGFR-STAT3 signalling, thereby maintaining the tumorigenicity of glioma stem cells (Gao et al., 2021).

Circular RNAs are associated with Temozolomide Resistance in Glioblastoma

TMZ is an alkylating agent with nearly 100% oral bioavailability and easily crosses the blood-brain barrier, and is currently the first-line chemotherapeutic agent for the treatment of GBM (Al-

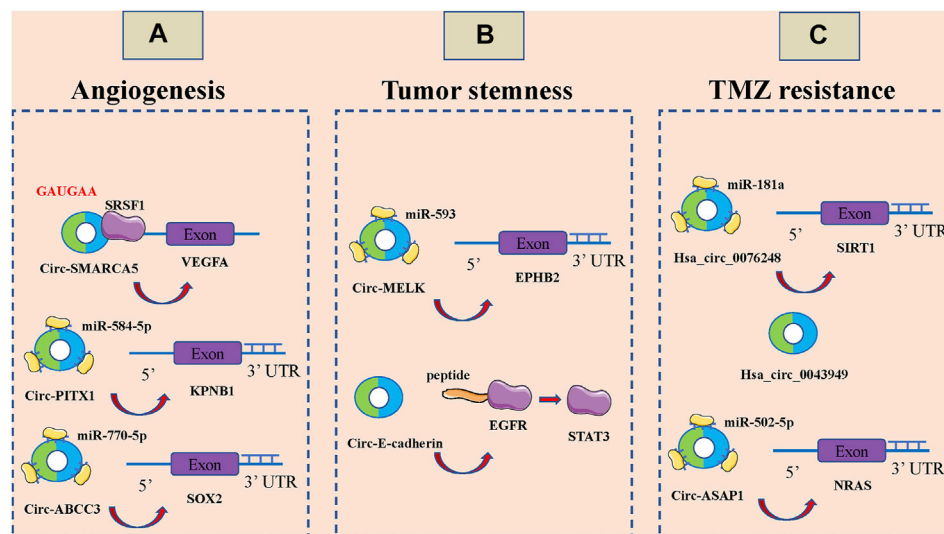


FIGURE 3 | CircRNAs associated with the angiogenesis, tumor stemness and temozolomide (TMZ) resistance of glioblastoma (GBM). **(A)** CircRNAs associated with the angiogenesis of GBM, including circ-SMARCA5, circ-PITX1 and circ-ABCC3. **(B)** CircRNAs associated with the tumor stemness of GBM, including circ-MELK and circ-E-cadherin. **(C)** CircRNAs associated with the temozolomide (TMZ) resistance of glioblastoma GBM, including hsa_circ_0076248, hsa_circ_0043949 and circ-ASAP1.

Toubah et al., 2021; Li F. et al., 2021; Soni et al., 2021). The breakdown products of TMZ can cause DNA methylation after entering tumor cells, which can interfere with cellular DNA replication and cause DNA damage to inhibit the proliferation of tumor cells (Tomar et al., 2021; Winkler, 2021). However, there is a strong DNA damage repair system and complex damage repair mechanisms in GBM cells, which are important in mediating the development of resistance to TMZ in GBM (Trillo Aliaga et al., 2021; Zhang X.-N. et al., 2021). It has been shown that circRNAs are also involved in TMZ resistance of GBM (Figure 3C). Lei et al., Hsa_circ_0076248 was found to be involved in the malignant progression of glioma by binding miR-181a to promote SIRT1 expression, and upregulation of hsa_circ_0076248 significantly inhibited temozolomide chemotherapy sensitivity (Lei et al., 2019). Zhao et al., The expression profiles of circRNAs in three pairs of secondary temozolomide-resistant GBM and the corresponding primary GBM tissues were examined by microarray. The high expression of hsa_circ_0043949 was found to be closely associated with the resistance of TMZ (Zhao et al., 2020). Wei et al., Inhibition of circ-ASAP1 was found to be effective in restoring the sensitivity of TMZ-resistant xenografts to TMZ treatment *in vivo*, possibly by regulating NRAS expression through binding to miR-502-5p (Wei et al., 2021).

Relationships Between Circular RNAs Levels and Clinicopathologic Characteristics in Glioblastoma

Studies have shown that the expression levels of circRNAs significantly correlate with many clinicopathological features of GBM, including tumor size, grading, differentiation and staging,

and tumor recurrence. Found that the expression of hsa_circ_0029426 was correlated with tumor size and WHO classification (Zhang G. et al., 2019). The expression of hsa_circ_0074027 was found to be closely associated with larger tumor size and higher WHO grade (Qian et al., 2019). It was found that high levels of circ-ENTPD7 correlated with advanced GBM classification and tumor size (Zhu et al., 2020). Sun et al., Demonstrated that the expression level of circ-FLNA correlated significantly with the presence of necrosis in MRI scans (Sun et al., 2021) (34498720). Liu et al., A multivariate Cox regression analysis revealed that circnfl expression was an independent prognostic factor for GBM patients (Liu L. et al., 2021). Lv et al., The analysis found that the expression of circ-EPB41L5 correlated with age, number of lesions, necrotic changes, recurrence and survival in GBM patients (Lv et al., 2020). Wang et al., found that hsa_circ_0006168 expression significantly correlated with WHO classification, T-stage, N-stage and M-stage (Wang T. et al., 2021).

Circular RNAs as Prognostic Biomarkers for Glioblastoma

The expression levels of circRNAs were found to be used to predict the prognosis of tumor patients. To further analyze the prognostic value of circRNAs in GBM, we evaluated the association of circRNAs expression levels with the overall survival (OS) rate of GBM patients. Twelve upregulated circRNAs were reported to predict poorer OS in GBM patients (Zhang G. et al., 2019; Qian et al., 2019; Xin et al., 2019; Zhu et al., 2020; Chen B. et al., 2021; Li D. et al., 2021; Liu L. et al., 2021; Wang Q. et al., 2021; Wu X. et al., 2021; Zhou M. et al., 2021; Sun et al., 2021), and three downregulated circRNAs predicted poorer OS in GBM patients (Zhang X. et al., 2019; Lv et al., 2020; Wang

T. et al., 2021). It was shown that lower expression of *has_circ_0067934* was associated with longer disease-free survival (DFS) (Xin et al., 2019). Higher expression of *circ-EPB41L5* was associated with longer progress-free survival (PFS) (Lv et al., 2020). Kaplan-Meier analysis showed that GBM patients with low *circ-ASAP1* expression showed better OS after TMZ treatment compared to GBM patients with high *circ-ASAP1* expression (Wei et al., 2021) (Table 3).

CONCLUSION AND FUTURE PROSPECTS

CircRNAs are highly stable, richly expressed, and functionally diverse, and have begun to attract the attention of researchers in recent years, but research on circRNAs is currently in its infancy (Ducoli and Detmar, 2021; Winkle et al., 2021). Nevertheless, the almost complete sequence overlap between circRNAs and linear RNAs makes the accurate assessment of the expression and function of circRNAs still challenging (Yang X. et al., 2020; Jusic et al., 2020). For example, if exonic circRNAs are formed by reverse splicing, how does the spliceosome specifically recognize the exons of circRNAs, but not those of linear RNAs. Recent studies have found that m6a-modified circRNAs are usually derived from exons that are not methylated in mRNAs, and circRNAs from methylated mRNA exons are less stable, and it is still unclear whether m6a modification affects the stability of circRNAs. CircRNAs are degraded, and the loop structure may confer different properties to their corresponding linear RNAs. The functional implications of circRNAs have only been tentatively explored, probably due to the limitations of the research tools.

Recent studies on circRNAs have focused on their miRNAs sponge function, researchers have verified the binding sites of circRNAs and miRNAs by luciferase reporter system, pull-down experiments using biotin-labeled probes to capture miRNAs, Ago2 immunoprecipitation can also further investigate miRNAs regulatory targets, co-localization of circRNAs and miRNAs in cells can be verified using FISH technique, and these mature experimental techniques now demonstrate the miRNAs sponge function of circRNAs, making the whole RNA network more complete and complex.

Nowadays, there are more and more researches on the mechanism of circRNAs generation. In addition to RBP can bind to circRNAs to reduce the regulation of RBP on target genes and affect tumorigenesis (Huang C.-K. et al., 2020; Li et al., 2020; Yang J. et al., 2021; Song et al., 2021), some RBP can also regulate the generation of circRNAs, which also has an important role in tumor development (2016; Li H. et al., 2021; Liu Z. et al., 2021; Wang et al., 2021d; Wang and Lei, 2021; Yang T. et al., 2021). The translation function of circRNAs is also becoming a hot topic, and the translation initiation mechanism of circRNAs mainly includes cap-dependent, IRES-dependent, m6a-dependent and small ORF-dependent translation initiation (He L. et al., 2021; Wang X. et al., 2021), and circRNAs encode proteins with the function of suppressing tumor activity and protecting proteins from degradation (Chen C.-K. et al., 2021; Wang et al., 2021d; Ma et al., 2021; Qi et al., 2021). In summary,

the interactions between circRNAs and proteins and its translation function are of great significance for the study of tumors, and more in-depth studies should be conducted in this area in the future.

CircRNAs are highly stable and widely expressed in a variety of tissues and body fluids, and thus can be used as potential diagnostic and prognostic biomarkers. Studies have shown that circRNAs are abundant and stable in exosomes, and some circRNAs are more highly expressed in blood than in tissues (D'Ambrosi et al., 2021; Reese and Dhayat, 2021; Tian et al., 2021; van Zonneveld et al., 2021). The high expression and stability of circRNAs in body fluids would be more beneficial for their clinical applications (Bu et al., 2021; Fontemaggi et al., 2021; Wang et al., 2021h; Zhao et al., 2021). However, despite the identification of thousands of tissue- and disease-specific circRNAs by RNA-seq (Kaushik et al., 2021; Tian-Zhao et al., 2021), the understanding of the mechanism of circRNAs generation and biological functions is limited at this stage. Further research is needed to explore the circRNAs associated with GBM, with the aim of being able to be used in combination with traditional biological diagnostic indicators for clinical adjuvant screening of GBM at an early stage, thus indirectly improving the survival rate of GBM patients and achieving early detection and treatment. It is believed that as more and more GBM-related and structurally diverse circRNAs are discovered, the elucidation of complex molecular regulatory mechanisms of GBM and the application of circRNAs-based GBM diagnosis and treatment will have a broad prospect.

In summary, circRNAs are important regulators of GBM genesis and can act as endogenous RNAs or miRNAs sponges competitively repressing miRNAs, thereby altering target gene expression and participating in the development of GBM. Although the exact role of circRNAs in GBM genesis and prognosis is unknown, it is speculated that aberrant expression of circRNAs and their biased distribution in tumors may be common, with different circRNAs expressed up- or down-regulated in GBM cells and tissues, acting through different mechanisms of action.

DATA AVAILABILITY STATEMENT

The data in the current study are available from the corresponding authors on reasonable request.

AUTHOR CONTRIBUTIONS

Original draft preparation, allocation, revision, supplement and edition: XG and HP. All authors have read and agreed to the published version of the manuscript.

ACKNOWLEDGMENTS

We thank the generous support by Liaoning Cancer Hospital and Institute (Shenyang).

REFERENCES

- Abe, N., Matsumoto, K., Nishihara, M., Nakano, Y., Shibata, A., Maruyama, H., et al. (2015). Rolling Circle Translation of Circular RNA in Living Human Cells. *Sci. Rep.* 5, 16435. doi:10.1038/srep16435
- AbouHaidar, M. G., Venkataraman, S., Golshani, A., Liu, B., and Ahmad, T. (2014). Novel Coding, Translation, and Gene Expression of a Replicating Covalently Closed Circular RNA of 220 Nt. *Proc. Natl. Acad. Sci. USA* 111 (40), 14542–14547. doi:10.1073/pnas.1402814111
- Al-Toubah, T., Pelle, E., Valone, T., Haider, M., and Strosberg, J. R. (2021). Efficacy and Toxicity Analysis of Capecitabine and Temozolomide in Neuroendocrine Neoplasms. *J. Natl. Compr. Canc. Netw.*, 1–8. doi:10.6004/jncn.2021.7017
- Ali, S. A., Peffers, M. J., Ormseth, M. J., Jurisica, I., and Kapoor, M. (2021). The Non-coding RNA Interactome in Joint Health and Disease. *Nat. Rev. Rheumatol.* 17, 692–705. doi:10.1038/s41584-021-00687-y
- Aliferis, C., and Trafalis, D. T. (2015). Glioblastoma Multiforme: Pathogenesis and Treatment. *Pharmacol. Ther.* 152, 63–82. doi:10.1016/j.pharmthera.2015.05.005
- Ashwal-Fluss, R., Meyer, M., Pamudurti, N. R., Ivanov, A., Bartok, O., Hanan, M., et al. (2014). circRNA Biogenesis Competes with Pre-mRNA Splicing. *Mol. Cell* 56 (1), 55–66. doi:10.1016/j.molcel.2014.08.019
- Asif, P. J., Longobardi, C., Hahne, M., and Medema, J. P. (2021). The Role of Cancer-Associated Fibroblasts in Cancer Invasion and Metastasis. *Cancers* 13 (18), 4720. doi:10.3390/cancers13184720
- Balça-Silva, J., Matias, D., Carmo, A. d., Sarmiento-Ribeiro, A. B., Lopes, M. C., and Moura-Neto, V. (2019). Cellular and Molecular Mechanisms of Glioblastoma Malignancy: Implications in Resistance and Therapeutic Strategies. *Semin. Cancer Biol.* 58, 130–141. doi:10.1016/j.semcancer.2018.09.007
- Barbagallo, D., Caponnetto, A., Barbagallo, C., Battaglia, R., Mirabella, F., Brex, D., et al. (2021). The GAUGAA Motif Is Responsible for the Binding between circSMARCA5 and SRSF1 and Related Downstream Effects on Glioblastoma Multiforme Cell Migration and Angiogenic Potential. *Ijms* 22 (4), 1678. doi:10.3390/ijms22041678
- Barbagallo, D., Caponnetto, A., Brex, D., Mirabella, F., Barbagallo, C., Lauretta, G., et al. (2019). CircSMARCA5 Regulates VEGFA mRNA Splicing and Angiogenesis in Glioblastoma Multiforme through the Binding of SRSF1. *Cancers* 11 (2), 194. doi:10.3390/cancers11020194
- Broekman, M. L., Maas, S. L. N., Abels, E. R., Mempel, T. R., Krichevsky, A. M., and Breakefield, X. O. (2018). Multidimensional Communication in the Microenvirons of Glioblastoma. *Nat. Rev. Neurol.* 14 (8), 482–495. doi:10.1038/s41582-018-0025-8
- Bu, T., Qiao, Z., Wang, W., Yang, X., Zhou, J., Chen, L., et al. (2021). Diagnostic Biomarker Hsa_circ_0126218 and Functioning Prediction in Peripheral Blood Mononuclear Cells of Female Patients with Major Depressive Disorder. *Front. Cell Dev. Biol.* 9, 651803. doi:10.3389/fcell.2021.651803
- Cai, J., Cui, Y., Yang, J., and Wang, S. (2021). Epithelial-mesenchymal Transition: When Tumor Cells Meet Myeloid-Derived Suppressor Cells. *Biochim. Biophys. Acta (Bba) - Rev. Cancer* 1876 (1), 188564. doi:10.1016/j.bbcan.2021.188564
- Cao, Y., Wang, F., Chen, Y., Wang, Y., Song, H., and Long, J. (2021). CircPITX1 Regulates Proliferation, Angiogenesis, Migration, Invasion, and Cell Cycle of Human Glioblastoma Cells by Targeting miR-584-5p/KPNB1 Axis. *J. Mol. Neurosci.* 71 (8), 1683–1695. doi:10.1007/s12031-021-01820-y
- Caragher, S. P., Hall, R. R., Ahsan, R., and Ahmed, A. U. (2018). Monoamines in Glioblastoma: Complex Biology with Therapeutic Potential. *Neuro Oncol.* 20 (8), 1014–1025. doi:10.1093/neuonc/nox210
- Cermeño, E. A., and García, A. J. (2016). Tumor-Initiating Cells: Emerging Biophysical Methods of Isolation. *Curr. Stem Cell Rep* 2 (1), 21–32. doi:10.1007/s40778-016-0036-6
- Chen, B., and Huang, S. (2018). Circular RNA: An Emerging Non-coding RNA as a Regulator and Biomarker in Cancer. *Cancer Lett.* 418, 41–50. doi:10.1016/j.canlet.2018.01.011
- Chen, B., Wang, M., Huang, R., Liao, K., Wang, T., Yang, R., et al. (2021a). Circular RNA circLGMN Facilitates Glioblastoma Progression by Targeting miR-127-3p/LGMN axis. *Cancer Lett.* 522, 225–237. doi:10.1016/j.canlet.2021.09.030
- Chen, C.-K., Cheng, R., Demeter, J., Chen, J., Weingarten-Gabbay, S., Jiang, L., et al. (2021b). Structured Elements Drive Extensive Circular RNA Translation. *Mol. Cell* 81, 4300–4318. doi:10.1016/j.molcel.2021.07.042
- Chen, J., Wu, Y., Luo, X., Jin, D., Zhou, W., Ju, Z., et al. (2021c). Circular RNA circRHOTB3 Represses Metastasis by Regulating the HuR-Mediated mRNA Stability of PTBP1 in Colorectal Cancer. *Theranostics* 11 (15), 7507–7526. doi:10.7150/thno.59546
- Chen, L., and Shan, G. (2021). CircRNA in Cancer: Fundamental Mechanism and Clinical Potential. *Cancer Lett.* 505, 49–57. doi:10.1016/j.canlet.2021.02.004
- Chen, Q., Li, Y., Liu, Y., Xu, W., and Zhu, X. (2021d). Exosomal Non-coding RNAs-Mediated Crosstalk in the Tumor Microenvironment. *Front. Cell Dev. Biol.* 9, 646864. doi:10.3389/fcell.2021.646864
- Chen, W. L., Jiang, L., Wang, J. S., and Liao, C. X. (2019). Circ-0001801 Contributes to Cell Proliferation, Migration, Invasion and Epithelial to Mesenchymal Transition (EMT) in Glioblastoma by Regulating miR-628-5p/HMGB3 axis. *Eur. Rev. Med. Pharmacol. Sci.* 23 (24), 10874–10885. doi:10.26355/eurev_201912_19791
- Choi, B. D., Maus, M. V., June, C. H., and Sampson, J. H. (2019). Immunotherapy for Glioblastoma: Adoptive T-Cell Strategies. *Clin. Cancer Res.* 25 (7), 2042–2048. doi:10.1158/1078-0432.CCR-18-1625
- Choudhary, A., Madbhagat, P., Sreepadmanabh, M., Bhardwaj, V., and Chande, A. (2021). Circular RNA as an Additional Player in the Conflicts between the Host and the Virus. *Front. Immunol.* 12, 602006. doi:10.3389/fimmu.2021.602006
- Cristofanilli, M., and Mendelsohn, J. (2006). Circulating Tumor Cells in Breast Cancer: Advanced Tools for "tailored" Therapy? *Proc. Natl. Acad. Sci.* 103 (46), 17073–17074. doi:10.1073/pnas.0608651103
- Dai, F., Wu, Y., Lu, Y., An, C., Zheng, X., Dai, L., et al. (2020). Crosstalk between RNA m6A Modification and Non-coding RNA Contributes to Cancer Growth and Progression. *Mol. Ther. - Nucleic Acids* 22, 62–71. doi:10.1016/j.omtn.2020.08.004
- D'Ambrosi, S., Visser, A., Antunes-Ferreira, M., Poutsma, A., Giannoukakos, S., Sol, N., et al. (2021). The Analysis of Platelet-Derived circRNA Repertoire as Potential Diagnostic Biomarker for Non-small Cell Lung Cancer. *Cancers* 13 (18), 4644. doi:10.3390/cancers13184644
- Di Timoteo, G., Rossi, F., and Bozzoni, I. (2020). Circular RNAs in Cell Differentiation and Development. *Development* 147 (16). doi:10.1242/dev.182725
- Dodbele, S., Mutlu, N., and Wilusz, J. E. (2021). Best Practices to Ensure Robust Investigation of Circular RNAs: Pitfalls and Tips. *EMBO Rep.* 22 (3), e52072. doi:10.15252/embr.202052072
- Ducoli, L., and Detmar, M. (2021). Beyond PROX1: Transcriptional, Epigenetic, and Noncoding RNA Regulation of Lymphatic Identity and Function. *Developmental Cell* 56 (4), 406–426. doi:10.1016/j.devcel.2021.01.018
- Ebbesen, K. K., Hansen, T. B., and Kjems, J. (2017). Insights into Circular RNA Biology. *RNA Biol.* 14 (8), 1035–1045. doi:10.1080/15476286.2016.1271524
- Farooqi, A. A., Attar, R., Yulaevna, I. M., and Berardi, R. (2021). Interaction of Long Non-coding RNAs and Circular RNAs with microRNAs for the Regulation of Immunological Responses in Human Cancers. *Semin. Cell Developmental Biol.* S1084–9521 (21), 00138–5. doi:10.1016/j.semcdb.2021.05.029
- Ferragut, F., Vachetta, V. S., Troncoso, M. F., Rabinovich, G. A., and Elola, M. T. (2021). ALCAM/CD166: A Pleiotropic Mediator of Cell Adhesion, Stemness and Cancer Progression. *Cytokine Growth Factor. Rev.* 61, 27–37. doi:10.1016/j.cytogfr.2021.07.001
- Fontemaggi, G., Turco, C., Esposito, G., and Di Agostino, S. (2021). New Molecular Mechanisms and Clinical Impact of circRNAs in Human Cancer. *Cancers* 13 (13), 3154. doi:10.3390/cancers13133154
- Gao, X., Xia, X., Li, F., Zhang, M., Zhou, H., Wu, X., et al. (2021). Circular RNA-Encoded Oncogenic E-Cadherin Variant Promotes Glioblastoma Tumorigenicity through Activation of EGFR-STAT3 Signalling. *Nat. Cell Biol.* 23 (3), 278–291. doi:10.1038/s41556-021-00639-4
- Geraldo, L. H. M., Garcia, C., da Fonseca, A. C. C., Dubois, L. G. F., de Sampaio e Spohr, T. C. L., Matias, D., et al. (2019). Glioblastoma Therapy in the Age of Molecular Medicine. *Trends Cancer* 5 (1), 46–65. doi:10.1016/j.trecan.2018.11.002
- Glazar, P., Papavasiliou, P., and Rajewsky, N. (2014). circBase: a Database for Circular RNAs. *RNA* 20 (11), 1666–1670. doi:10.1261/rna.043687.113
- Gokool, A., Loy, C. T., Halliday, G. M., and Voineagu, I. (2020). Circular RNAs: The Brain Transcriptome Comes Full Circle. *Trends Neurosciences* 43 (10), 752–766. doi:10.1016/j.tins.2020.07.007
- Gonçalves, R. C., Banfi, A., Oliveira, M. B., and Mano, J. F. (2021). Strategies for Re-vascularization and Promotion of Angiogenesis in Trauma and Disease. *Biomaterials* 269, 120628. doi:10.1016/j.biomaterials.2020.120628

- Goodall, G. J., and Wickramasinghe, V. O. (2020). RNA in Cancer. *Nat. Rev. Cancer* 21, 22–36. doi:10.1038/s41568-020-00306-0
- Han, B., Chao, J., and Yao, H. (2018). Circular RNA and its Mechanisms in Disease: From the Bench to the Clinic. *Pharmacol. Ther.* 187, 31–44. doi:10.1016/j.pharmthera.2018.01.010
- Han, Y., Zhang, H., Bian, C., Chen, C., Tu, S., Guo, J., et al. (2021). Circular RNA Expression: Its Potential Regulation and Function in Abdominal Aortic Aneurysms. *Oxidative Med. Cell Longevity* 2021, 1–21. doi:10.1155/2021/9934951
- Hass, R., von der Ohe, J., and Ungefroren, H. (2020). Impact of the Tumor Microenvironment on Tumor Heterogeneity and Consequences for Cancer Cell Plasticity and Stemness. *Cancers* 12 (12), 3716. doi:10.3390/cancers12123716
- He, A. T., Liu, J., Li, F., and Yang, B. B. (2021a). Targeting Circular RNAs as a Therapeutic Approach: Current Strategies and Challenges. *Sig Transduct Target. Ther.* 6 (1), 185. doi:10.1038/s41392-021-00569-5
- He, L., Man, C., Xiang, S., Yao, L., Wang, X., and Fan, Y. (2021b). Circular RNAs' Cap-independent Translation Protein and its Roles in Carcinomas. *Mol. Cancer* 20 (1), 119. doi:10.1186/s12943-021-01417-4
- Hsu, M.-T., and Coca-Prados, M. (1979). Electron Microscopic Evidence for the Circular Form of RNA in the Cytoplasm of Eukaryotic Cells. *Nature* 280 (5720), 339–340. doi:10.1038/280339a0
- Huang, A., Zheng, H., Wu, Z., Chen, M., and Huang, Y. (2020a). Circular RNA-Protein Interactions: Functions, Mechanisms, and Identification. *Theranostics* 10 (8), 3503–3517. doi:10.7150/thno.42174
- Huang, C.-K., Kafert-Kasting, S., and Thum, T. (2020b). Preclinical and Clinical Development of Noncoding RNA Therapeutics for Cardiovascular Disease. *Circ. Res.* 126 (5), 663–678. doi:10.1161/CIRCRESAHA.119.315856
- Huang, Y., and Zhu, Q. (2021). Mechanisms Regulating Abnormal Circular RNA Biogenesis in Cancer. *Cancers* 13 (16), 4185. doi:10.3390/cancers13164185
- Inoue, T., Umezawa, A., Takenaka, T., Suzuki, H., and Okada, H. (2015). The Contribution of Epithelial-Mesenchymal Transition to Renal Fibrosis Differs Among Kidney Disease Models. *Kidney Int.* 87 (1), 233–238. doi:10.1038/ki.2014.235
- Jackson, C. M., Choi, J., and Lim, M. (2019). Mechanisms of Immunotherapy Resistance: Lessons from Glioblastoma. *Nat. Immunol.* 20 (9), 1100–1109. doi:10.1038/s41590-019-0433-y
- Jakobi, T., and Dieterich, C. (2019). Computational Approaches for Circular RNA Analysis. *WIREs RNA* 10 (3), e1528. doi:10.1002/wrna.1528
- Jeck, W. R., Sorrentino, J. A., Wang, K., Slevin, M. K., Burd, C. E., Liu, J., et al. (2013). Circular RNAs Are Abundant, Conserved, and Associated with ALU Repeats. *RNA* 19 (2), 141–157. doi:10.1261/rna.035667.112
- Jing, N., Gao, W.-Q., and Fang, Y.-X. (2021). Regulation of Formation, Stemness and Therapeutic Resistance of Cancer Stem Cells. *Front. Cell Dev. Biol.* 9, 641498. doi:10.3389/fcell.2021.641498
- Jusic, A., Devaux, Y., and Devaux, Y. (2020). Mitochondrial Noncoding RNA-Regulatory Network in Cardiovascular Disease. *Basic Res. Cardiol.* 115 (3), 23. doi:10.1007/s00395-020-0783-5
- Kalluri, R., and LeBleu, V. S. (2020). The Biology, Function, and Biomedical Applications of Exosomes. *Science* 367 (6478). doi:10.1126/science.aau6977
- Karachi, A., Dastmalchi, F., Mitchell, D. A., and Rahman, M. (2018). Temozolomide for Immunomodulation in the Treatment of Glioblastoma. *Neuro Oncol.* 20 (12), 1566–1572. doi:10.1093/neuonc/nyy072
- Kaushik, A. C., Wu, Q., Lin, L., Li, H., Zhao, L., Wen, Z., et al. (2021). Exosomal ncRNAs Profiling of Mycobacterial Infection Identified miRNA-185-5p as a Novel Biomarker for Tuberculosis. *Brief Bioinform* 22 (6), bbab210. doi:10.1093/bib/bbab210
- Kristensen, L. S., Andersen, M. S., Stagsted, L. V. W., Ebbesen, K. K., Hansen, T. B., and Kjems, J. (2019). The Biogenesis, Biology and Characterization of Circular RNAs. *Nat. Rev. Genet.* 20 (11), 675–691. doi:10.1038/s41576-019-0158-7
- Lai, V., Neshat, S. Y., Rakoski, A., Pitingolo, J., and Doloff, J. C. (2021). Drug Delivery Strategies in Maximizing Anti-angiogenesis and Anti-tumor Immunity. *Adv. Drug Deliv. Rev.* 113920. doi:10.1016/j.addr.2021.113920
- Lauretti, E., Dabrowski, K., and Praticò, D. (2021). The Neurobiology of Non-coding RNAs and Alzheimer's Disease Pathogenesis: Pathways, Mechanisms and Translational Opportunities. *Ageing Res. Rev.* 71, 101425. doi:10.1016/j.arr.2021.101425
- Lei, B., Huang, Y., Zhou, Z., Zhao, Y., Thapa, A. J., Li, W., et al. (2019). Circular RNA Hsa_circ_0076248 Promotes Oncogenesis of Glioma by Sponging miR-181a to Modulate SIRT1 Expression. *J. Cell Biochem* 120 (4), 6698–6708. doi:10.1002/jcb.27966
- Li, D., Li, L., Chen, X., Yang, W., and Cao, Y. (2021a). Circular RNA SERPINE2 Promotes Development of Glioblastoma by Regulating the miR-361-3p/miR-324-5p/BCL2 Signaling Pathway. *Mol. Ther. - Oncolytics* 22, 483–494. doi:10.1016/j.omto.2021.07.010
- Li, F., Chen, S., Yu, J., Gao, Z., Sun, Z., Yi, Y., et al. (2021b). Interplay of M6A and Histone Modifications Contributes to Temozolomide Resistance in Glioblastoma. *Clin. Translational Med.* 11 (9), e553. doi:10.1002/ctm2.553
- Li, H., Deng, Z., Yang, H., Pan, X., Wei, Z., Shen, H.-B., et al. (2021c). circRNA-binding Protein Site Prediction Based on Multi-View Deep Learning, Subspace Learning and Multi-View Classifier. *Brief Bioinform*, bbab394. doi:10.1093/bib/bbab394
- Li, H. M., Ma, X. L., and Li, H. G. (2019). Intriguing Circles: Conflicts and Controversies in Circular RNA Research. *WIREs RNA* 10 (5), e1538. doi:10.1002/wrna.1538
- Li, J., Wei, M., Liu, X., Xiao, S., Cai, Y., Li, F., et al. (2021d). The Progress, Prospects, and Challenges of the Use of Non-coding RNA for Diabetic Wounds. *Mol. Ther. - Nucleic Acids* 24, 554–578. doi:10.1016/j.omtn.2021.03.015
- Li, X., and Diao, H. (2019). Circular RNA Circ_0001946 Acts as a Competing Endogenous RNA to Inhibit Glioblastoma Progression by Modulating miR-671-5p and CDR1. *J. Cell Physiol* 234 (8), 13807–13819. doi:10.1002/jcp.28061
- Li, X., and Wang, X. (2017). The Emerging Roles and Therapeutic Potential of Exosomes in Epithelial Ovarian Cancer. *Mol. Cancer* 16 (1), 92. doi:10.1186/s12943-017-0659-y
- Li, Y., Ge, Y.-z., Xu, L., and Jia, R. (2020). Circular RNA ITCH: A Novel Tumor Suppressor in Multiple Cancers. *Life Sci.* 254, 117176. doi:10.1016/j.lfs.2019.117176
- Li, Z., Huang, C., Bao, C., Chen, L., Lin, M., Wang, X., et al. (2015). Exon-intron Circular RNAs Regulate Transcription in the Nucleus. *Nat. Struct. Mol. Biol.* 22 (3), 256–264. doi:10.1038/nsmb.2959
- Lim, M., Xia, Y., Bettgowda, C., and Weller, M. (2018). Current State of Immunotherapy for Glioblastoma. *Nat. Rev. Clin. Oncol.* 15 (7), 422–442. doi:10.1038/s41571-018-0003-5
- Liu, C., Wu, Y., and Ma, J. (2020). Interaction of Non-coding RNAs and Hippo Signaling: Implications for Tumorigenesis. *Cancer Lett.* 493, 207–216. doi:10.1016/j.canlet.2020.08.012
- Liu, L., Jia, L., Shao, J., Liu, H., Wu, Q., and Wu, X. (2021a). Circular RNA circNF1 siRNA Silencing Inhibits Glioblastoma Cell Proliferation by Promoting the Maturation of miR-340. *Front. Neurol.* 12, 658076. doi:10.3389/fneur.2021.658076
- Liu, Y., Huang, N., Liao, S., Rothzger, E., Yao, F., Li, Y., et al. (2021b). Current Research Progress in Targeted Anti-angiogenesis Therapy for Osteosarcoma. *Cell Prolif* 54 (9), e13102. doi:10.1111/cpr.13102
- Liu, Z., Wang, T., She, Y., Wu, K., Gu, S., Li, L., et al. (2021c). N6-methyladenosine-modified circIGF2BP3 Inhibits CD8+ T-Cell Responses to Facilitate Tumor Immune Evasion by Promoting the Deubiquitination of PD-L1 in Non-small Cell Lung Cancer. *Mol. Cancer* 20 (1), 105. doi:10.1186/s12943-021-01398-4
- Lou, J., Hao, Y., Lin, K., Lyu, Y., Chen, M., Wang, H., et al. (2020). Circular RNA CDR1as Disrupts the p53/MDM2 Complex to Inhibit Gliomagenesis. *Mol. Cancer* 19 (1), 138. doi:10.1186/s12943-020-01253-y
- Lv, T., Miao, Y., Xu, T., Sun, W., Sang, Y., Jia, F., et al. (2020). Circ-EPB41L5 Regulates the Host Gene EPB41L5 via Sponging miR-19a to Repress Glioblastoma Tumorigenesis. *Ageing* 12 (1), 318–339. doi:10.18632/ageing.102617
- Lv, X., Wang, M., Qiang, J., and Guo, S. (2019). Circular RNA Circ-PITX1 Promotes the Progression of Glioblastoma by Acting as a Competing Endogenous RNA to Regulate miR-379-5p/MAP3K2 axis. *Eur. J. Pharmacol.* 863, 172643. doi:10.1016/j.ejphar.2019.172643
- Ma, J., Du, W. W., Zeng, K., Wu, N., Fang, L., Lyu, J., et al. (2021). An Antisense Circular RNA circSCRIB Enhances Cancer Progression by Suppressing Parental Gene Splicing and Translation. *Mol. Ther.* 29 (9), 2754–2768. doi:10.1016/j.ymthe.2021.08.002
- Mao, X., Cao, Y., Guo, Z., Wang, L., and Xiang, C. (2021). Biological Roles and Therapeutic Potential of Circular RNAs in Osteoarthritis. *Mol. Ther. - Nucleic Acids* 24, 856–867. doi:10.1016/j.omtn.2021.04.006
- Martin, P., and Gurevich, D. B. (2021). Macrophage Regulation of Angiogenesis in Health and Disease. *Semin. Cell Developmental Biol.* 119, 101–110. doi:10.1016/j.semcdb.2021.06.010

- McKinnon, C., Nandhabalan, M., Murray, S. A., and Plaha, P. (2021). Glioblastoma: Clinical Presentation, Diagnosis, and Management. *BMJ* 374, n1560. doi:10.1136/bmj.n1560
- Mehraj, U., Ganai, R. A., Macha, M. A., Hamid, A., Zargar, M. A., Bhat, A. A., et al. (2021). The Tumor Microenvironment as Driver of Stemness and Therapeutic Resistance in Breast Cancer: New Challenges and Therapeutic Opportunities. *Cell Oncol.* doi:10.1007/s13402-021-00634-9
- Meyer, T., Sand, M., Schmitz, L., and Stockfleth, E. (2021). The Role of Circular RNAs in Keratinocyte Carcinomas. *Cancers* 13 (16), 4240. doi:10.3390/cancers13164240
- Mirzadeh Azad, F., Polignano, I. L., Proserpio, V., and Oliviero, S. (2021). Long Noncoding RNAs in Human Stemness and Differentiation. *Trends Cell Biol.* 31 (7), 542–555. doi:10.1016/j.tcb.2021.02.002
- Mo, Y., Wang, Y., Zhang, S., Xiong, F., Yan, Q., Jiang, X., et al. (2021). Circular RNA circRNF13 Inhibits Proliferation and Metastasis of Nasopharyngeal Carcinoma via SUMO2. *Mol. Cancer* 20 (1), 112. doi:10.1186/s12943-021-01409-4
- Narasimhan, B., Narasimhan, H., Lorente-Ros, M., Romeo, F. J., Bhatia, K., and Aronow, W. S. (2021). Therapeutic Angiogenesis in Coronary Artery Disease: a Review of Mechanisms and Current Approaches. *Expert Opin. Investig. Drugs* 30 (9), 947–963. doi:10.1080/13543784.2021.1964471
- Otero-Albiol, D., and Carnero, A. (2021). Cellular Senescence or Stemness: Hypoxia Flips the coin. *J. Exp. Clin. Cancer Res.* 40 (1), 243. doi:10.1186/s13046-021-02035-0
- Pan, G., Liu, Y., Shang, L., Zhou, F., and Yang, S. (2021). EMT-associated microRNAs and Their Roles in Cancer Stemness and Drug Resistance. *Cancer Commun.* 41 (3), 199–217. doi:10.1002/cac2.12138
- Ponnusamy, M., Seshacharyulu, P., Lakshmanan, I., Vaz, A., Chugh, S., and Batra, S. (2013). Emerging Role of Mucins in Epithelial to Mesenchymal Transition. *Ccdt* 13 (9), 945–956. doi:10.2174/15680096113136660100
- Qi, Y., Han, W., Chen, D., Zhao, J., Bai, L., Huang, F., et al. (2021). Engineering Circular RNA Regulators to Specifically Promote Circular RNA Production. *Theranostics* 11 (15), 7322–7336. doi:10.7150/thno.56990
- Qian, L., Guan, J., Wu, Y., and Wang, Q. (2019). Upregulated Circular RNA Circ_0074027 Promotes Glioblastoma Cell Growth and Invasion by Regulating miR-518a-5p/IL17RD Signaling Pathway. *Biochem. Biophysical Res. Commun.* 510 (4), 515–519. doi:10.1016/j.bbrc.2019.01.140
- Qin, C., Lu, R., Yuan, M., Zhao, R., Zhou, H., Fan, X., et al. (2021). Circular RNA 0006349 Augments Glycolysis and Malignance of Non-small Cell Lung Cancer Cells through the microRNA-98/MKPI Axis. *Front. Cell Dev. Biol.* 9, 690307. doi:10.3389/fcell.2021.690307
- Reese, M., and Dhayat, S. A. (2021). Small Extracellular Vesicle Non-coding RNAs in Pancreatic Cancer: Molecular Mechanisms and Clinical Implications. *J. Hematol. Oncol.* 14 (1), 141. doi:10.1186/s13045-021-01149-4
- Rimini, M., and Casadei-Gardini, A. (2021). Angiogenesis in Biliary Tract Cancer: Targeting and Therapeutic Potential. *Expert Opin. Investig. Drugs* 30 (4), 411–418. doi:10.1080/13543784.2021.1881479
- Rong, Z., Shi, S., Tan, Z., Xu, J., Meng, Q., Hua, J., et al. (2021a). Circular RNA CircEYA3 Induces Energy Production to Promote Pancreatic Ductal Adenocarcinoma Progression through the miR-1294/c-Myc axis. *Mol. Cancer* 20 (1), 106. doi:10.1186/s12943-021-01400-z
- Rong, Z., Xu, J., Shi, S., Tan, Z., Meng, Q., Hua, J., et al. (2021b). Circular RNA in Pancreatic Cancer: a Novel Avenue for the Roles of Diagnosis and Treatment. *Theranostics* 11 (6), 2755–2769. doi:10.7150/thno.56174
- Ryskalin, L., Biagioni, F., Busceti, C. L., Giambelluca, M. A., Morelli, L., Frati, A., et al. (2021). The Role of Cellular Prion Protein in Promoting Stemness and Differentiation in Cancer. *Cancers* 13 (2), 170. doi:10.3390/cancers13020170
- Salmena, L., Poliseno, L., Tay, Y., Kats, L., and Pandolfi, P. P. (2011). A ceRNA Hypothesis: the Rosetta Stone of a Hidden RNA Language? *Cell* 146 (3), 353–358. doi:10.1016/j.cell.2011.07.014
- Satcher, R. L., and Zhang, X. H.-F. (2021). Evolving Cancer-Niche Interactions and Therapeutic Targets during Bone Metastasis. *Nat. Rev. Cancer.* doi:10.1038/s41568-021-00406-5
- Sempere, L. F., Powell, K., Rana, J., Brock, A. A., and Schmittgen, T. D. (2021). Role of Non-coding RNAs in Tumor Progression and Metastasis in Pancreatic Cancer. *Cancer Metastasis Rev.* 40, 761–776. doi:10.1007/s10555-021-09995-x
- Shahzad, U., Krumholtz, S., Rutka, J. T., and Das, S. (2021). Noncoding RNAs in Glioblastoma: Emerging Biological Concepts and Potential Therapeutic Implications. *Cancers* 13 (7), 1555. doi:10.3390/cancers13071555
- Shang, Q., Yang, Z., Jia, R., and Ge, S. (2019). The Novel Roles of circRNAs in Human Cancer. *Mol. Cancer* 18 (1), 6. doi:10.1186/s12943-018-0934-6
- Shao, T., Pan, Y.-h., and Xiong, X.-d. (2021). Circular RNA: an Important Player with Multiple Facets to Regulate its Parental Gene Expression. *Mol. Ther. - Nucleic Acids* 23, 369–376. doi:10.1016/j.omtn.2020.11.008
- Shen, H., Liu, B., Xu, J., Zhang, B., Wang, Y., Shi, L., et al. (2021). Circular RNAs: Characteristics, Biogenesis, Mechanisms and Functions in Liver Cancer. *J. Hematol. Oncol.* 14 (1), 134. doi:10.1186/s13045-021-01145-8
- Shi, X., Sun, M., Liu, H., Yao, Y., and Song, Y. (2013). Long Non-coding RNAs: a New Frontier in the Study of Human Diseases. *Cancer Lett.* 339 (2), 159–166. doi:10.1016/j.canlet.2013.06.013
- Sinha, T., Panigrahi, C., Das, D., and Panda, A. (2021). Circular RNA Translation, a Path to Hidden Proteome. *Wiley Interdiscip. Rev. RNA*, e1685. doi:10.1002/wrna.1685
- Song, C., Zhang, Y., Huang, W., Shi, J., Huang, Q., Jiang, M., et al. (2021). Circular RNA Cwc27 Contributes to Alzheimer's Disease Pathogenesis by Repressing Pur- α Activity. *Cell Death Differ.* doi:10.1038/s41418-021-00865-1
- Soni, V., Adhikari, M., Simonyan, H., Lin, L., Sherman, J. H., Young, C. N., et al. (2021). *In Vitro* and *In Vivo* Enhancement of Temozolomide Effect in Human Glioblastoma by Non-invasive Application of Cold Atmospheric Plasma. *Cancers* 13 (17), 4485. doi:10.3390/cancers13174485
- Su, Q., and Lv, X. (2020). Revealing New Landscape of Cardiovascular Disease through Circular RNA-miRNA-mRNA axis. *Genomics* 112 (2), 1680–1685. doi:10.1016/j.ygeno.2019.10.006
- Sun, Y., Ma, G., Xiang, H., Wang, X., Wang, H., Zhang, Y., et al. (2021). circFLNA Promotes Glioblastoma Proliferation and Invasion by Negatively Regulating miR1993p Expression. *Mol. Med. Rep.* 24 (5). doi:10.3892/mmr.2021.12426
- Suzuki, H., and Tsukahara, T. (2014). A View of Pre-mRNA Splicing from RNase R Resistant RNAs. *Ijms* 15 (6), 9331–9342. doi:10.3390/ijms15069331
- Tan, A. C., Ashley, D. M., López, G. Y., Malinzak, M., Friedman, H. S., and Khasraw, M. (2020). Management of Glioblastoma: State of the Art and Future Directions. *CA A. Cancer J. Clin.* 70 (4), 299–312. doi:10.3322/caac.21613
- Thompson, S. R. (2012). So You Want to Know if Your Message Has an IRES? *WIREs RNA* 3 (5), 697–705. doi:10.1002/wrna.1129
- Tian, T., Zhao, Y., Zheng, J., Jin, S., Liu, Z., and Wang, T. (2021). Circular RNA: A Potential Diagnostic, Prognostic, and Therapeutic Biomarker for Human Triple-Negative Breast Cancer. *Mol. Ther. - Nucleic Acids* 26, 63–80. doi:10.1016/j.omtn.2021.06.017
- Tian-Zhao, D., Yang, Y., Xing-Xuan, W., Yu-Xin, C., and Xue-Lian, W. (2021). Profiling of Circular RNAs and circTPCN/miR-634/mTOR Regulatory Pathway in Cervical Cancer. *Genomics* 113 (4), 2253–2263. doi:10.1016/j.ygeno.2021.05.026
- Tomar, M. S., Kumar, A., Srivastava, C., and Shrivastava, A. (2021). Elucidating the Mechanisms of Temozolomide Resistance in Gliomas and the Strategies to Overcome the Resistance. *Biochim. Biophys. Acta (Bba) - Rev. Cancer* 1876 (2), 188616. doi:10.1016/j.bbcan.2021.188616
- Touat, M., Idbaih, A., Sanson, M., and Ligon, K. L. (2017). Glioblastoma Targeted Therapy: Updated Approaches from Recent Biological Insights. *Ann. Oncol.* 28 (7), 1457–1472. doi:10.1093/annonc/mdx106
- Trillo Aliaga, P., Spada, F., Peveri, G., Bagnardi, V., Fumagalli, C., Laffi, A., et al. (2021). Should Temozolomide Be Used on the Basis of O6-Methylguanine DNA Methyltransferase Status in Patients with Advanced Neuroendocrine Tumors? A Systematic Review and Meta-Analysis. *Cancer Treat. Rev.* 99, 102261. doi:10.1016/j.ctrv.2021.102261
- Tsitsipatis, D., and Gorospe, M. (2021). Practical Guide for Circular RNA Analysis: Steps, Tips, and Resources. *WIREs RNA* 12 (1), e1633. doi:10.1002/wrna.1633
- Uemura, A., Fruttiger, M., D'Amore, P. A., De Falco, S., Jousen, A. M., Sennlaub, F., et al. (2021). VEGFR1 Signaling in Retinal Angiogenesis and Microinflammation. *Prog. Retin. Eye Res.* 84, 100954. doi:10.1016/j.preteyeres.2021.100954
- van Zonneveld, A. J., Kölling, M., Bijkerk, R., and Lorenzen, J. M. (2021). Circular RNAs in Kidney Disease and Cancer. *Nat. Rev. Nephrol.* doi:10.1038/s41581-021-00465-9
- Wang, F., Zhang, Y., Zhou, X., Chen, X., Xiang, J., Fan, M., et al. (2021a). Circular RNA CircPPP1CB Suppresses Tumorigenesis by Interacting with the MiR-

- 1307-3p/SMG1 Axis in Human Bladder Cancer. *Front. Cell Dev. Biol.* 9, 704683. doi:10.3389/fcell.2021.704683
- Wang, J., Zhang, Y., Liu, L., Yang, T., and Song, J. (2021b). Circular RNAs: New Biomarkers of Chemoresistance in Cancer. *Cancer Biol. Med.* 18, 421–436. doi:10.20892/j.issn.2095-3941.2020.0312
- Wang, Q., Zheng, D., Li, Y., Zhang, Y., Sui, R., Chen, Y., et al. (2021c). Circular RNA Circ_0001588 Sponges miR-211-5p to Facilitate the Progression of Glioblastoma via Up-regulating YY1 Expression. *J. Gene Med.* 23 (10), e3371. doi:10.1002/jgm.3371
- Wang, R., Zhang, S., Chen, X., Li, N., Li, J., Jia, R., et al. (2018a). CircNT5E Acts as a Sponge of miR-422a to Promote Glioblastoma Tumorigenesis. *Cancer Res.* 78 (17), 4812–4825. doi:10.1158/0008-5472.CAN-18-0532
- Wang, R., Zhang, S., Chen, X., Li, N., Li, J., Jia, R., et al. (2018b). EIF4A3-induced Circular RNA MMP9 (circMMP9) Acts as a Sponge of miR-124 and Promotes Glioblastoma Multiforme Cell Tumorigenesis. *Mol. Cancer* 17 (1), 166. doi:10.1186/s12943-018-0911-0
- Wang, S., Latallo, M. J., Zhang, Z., Huang, B., Bobrovnikov, D. G., Dong, D., et al. (2021d). Nuclear export and Translation of Circular Repeat-Containing Intronic RNA in C9ORF72-ALS/FTD. *Nat. Commun.* 12 (1), 4908. doi:10.1038/s41467-021-25082-9
- Wang, S., Zhang, K., Tan, S., Xin, J., Yuan, Q., Xu, H., et al. (2021e). Circular RNAs in Body Fluids as Cancer Biomarkers: the New Frontier of Liquid Biopsies. *Mol. Cancer* 20 (1), 13. doi:10.1186/s12943-020-01298-z
- Wang, T., Mao, P., Feng, Y., Cui, B., Zhang, B., Chen, C., et al. (2021f). Blocking Hsa_circ_0006168 Suppresses Cell Proliferation and Motility of Human Glioblastoma Cells by Regulating hsa_circ_0006168/miR-628-5p/IGF1R ceRNA axis. *Cell Cycle* 20 (12), 1181–1194. doi:10.1080/15384101.2021.1930357
- Wang, X., Ma, R., Zhang, X., Cui, L., Ding, Y., Shi, W., et al. (2021g). Crosstalk between N6-Methyladenosine Modification and Circular RNAs: Current Understanding and Future Directions. *Mol. Cancer* 20 (1), 121. doi:10.1186/s12943-021-01415-6
- Wang, Y., He, W., Ibrahim, S. A., He, Q., and Jin, J. (2021h). Circular RNAs: Novel Players in the Oxidative Stress-Mediated Pathologies, Biomarkers, and Therapeutic Targets. *Oxidative Med. Cell Longevity* 2021, 1–14. doi:10.1155/2021/6634601
- Wang, Y., and Wang, Z. (2015). Efficient Backsplicing Produces Translatable Circular mRNAs. *RNA* 21 (2), 172–179. doi:10.1261/rna.048272.114
- Wang, Y., Wang, Z., Lu, J., and Zhang, H. (2021i). Circular RNA Circ-PTEN Elevates PTEN Inhibiting the Proliferation of Non-small Cell Lung Cancer Cells. *Hum. Cell* 34 (4), 1174–1184. doi:10.1007/s13577-021-00526-y
- Wang, Z., and Lei, X. (2021). Prediction of RBP Binding Sites on circRNAs Using an LSTM-Based Deep Sequence Learning Architecture. *Brief Bioinform* 22 (6), bbab342. doi:10.1093/bib/bbab342
- Wei, Y., Lu, C., Zhou, P., Zhao, L., Lyu, X., Yin, J., et al. (2021). EIF4A3-induced Circular RNA ASAP1 Promotes Tumorigenesis and Temozolomide Resistance of Glioblastoma via NRAS/MEK1/ERK1-2 Signaling. *Neuro Oncol.* 23 (4), 611–624. doi:10.1093/neuonc/noaa214
- Wen, G., Zhou, T., and Gu, W. (2020). The Potential of Using Blood Circular RNA as Liquid Biopsy Biomarker for Human Diseases. *Protein Cell.* doi:10.1007/s13238-020-00799-3
- Winkle, M., El-Daly, S. M., Fabbri, M., and Calin, G. A. (2021). Noncoding RNA Therapeutics - Challenges and Potential Solutions. *Nat. Rev. Drug Discov.* 20 (8), 629–651. doi:10.1038/s41573-021-00219-z
- Winkler, F. (2021). Silencing Glioblastoma Networks to Make Temozolomide More Effective. *Neuro Oncol.* 23, 1807–1809. doi:10.1093/neuonc/noab186
- Wu, J., Guo, X., Wen, Y., Huang, S., Yuan, X., Tang, L., et al. (2021a). N6-Methyladenosine Modification Opens a New Chapter in Circular RNA Biology. *Front. Cell Dev. Biol.* 9, 709299. doi:10.3389/fcell.2021.709299
- Wu, N., Li, Z., Wang, J., Geng, L., Yue, Y., Deng, Z., et al. (2021b). Low Molecular Weight Fucoidan Attenuating Pulmonary Fibrosis by Relieving Inflammatory Reaction and Progression of Epithelial-Mesenchymal Transition. *Carbohydr. Polym.* 273, 118567. doi:10.1016/j.carbpol.2021.118567
- Wu, X., Xiao, S., Zhang, M., Yang, L., Zhong, J., Li, B., et al. (2021c). A Novel Protein Encoded by Circular SMO RNA Is Essential for Hedgehog Signaling Activation and Glioblastoma Tumorigenicity. *Genome Biol.* 22 (1), 33. doi:10.1186/s13059-020-02250-6
- Wu, Z., Zheng, M., Zhang, Y., Xie, M., Tian, S., Ding, T., et al. (2020). Hsa_circ_0043278 Functions as Competitive Endogenous RNA to Enhance Glioblastoma Multiforme Progression by Sponging miR-638. *Aging* 12 (21), 21114–21128. doi:10.18632/aging.103603
- Xia, X., Li, X., Li, F., Wu, X., Zhang, M., Zhou, H., et al. (2019). A Novel Tumor Suppressor Protein Encoded by Circular AKT3 RNA Inhibits Glioblastoma Tumorigenicity by Competing with Active Phosphoinositide-dependent Kinase-1. *Mol. Cancer* 18 (1), 131. doi:10.1186/s12943-019-1056-5
- Xin, J., Zhang, X. Y., Sun, D. K., Tian, L. Q., and Xu, P. (2019). Up-regulated Circular RNA Hsa_circ_0067934 Contributes to Glioblastoma Progression through Activating PI3K-AKT Pathway. *Eur. Rev. Med. Pharmacol. Sci.* 23 (8), 3447–3454. doi:10.26355/eurev.201904.17709
- Xiong, L., Ye, X., Chen, Z., Fu, H., Li, S., Xu, P., et al. (2021). Advanced Maternal Age-associated SIRT1 Deficiency Compromises Trophoblast Epithelial-Mesenchymal Transition through an Increase in Vimentin Acetylation. *Aging Cell* 20, e13491. doi:10.1111/acel.13491
- Yan, L., and Chen, Y. G. (2020). Circular RNAs in Immune Response and Viral Infection. *Trends Biochem. Sci.* 45 (12), 1022–1034. doi:10.1016/j.tibs.2020.08.006
- Yang, H., Zhang, H., Yang, Y., Wang, X., Deng, T., Liu, R., et al. (2020a). Hypoxia Induced Exosomal circRNA Promotes Metastasis of Colorectal Cancer via Targeting GEF-H1/RhoA axis. *Theranostics* 10 (18), 8211–8226. doi:10.7150/thno.44419
- Yang, J., Zhang, X., Cao, J., Xu, P., Chen, Z., Wang, S., et al. (2021a). Circular RNA UBE2Q2 Promotes Malignant Progression of Gastric Cancer by Regulating Signal Transducer and Activator of Transcription 3-mediated Autophagy and Glycolysis. *Cell Death Dis* 12 (10), 910. doi:10.1038/s41419-021-04216-3
- Yang, T., Shen, P., Chen, Q., Wu, P., Yuan, H., Ge, W., et al. (2021b). FUS-induced circRHOBTB3 Facilitates Cell Proliferation via miR-600/NACCC1 Mediated Autophagy Response in Pancreatic Ductal Adenocarcinoma. *J. Exp. Clin. Cancer Res.* 40 (1), 261. doi:10.1186/s13046-021-02063-w
- Yang, X., Liu, M., Li, M., Zhang, S., Hiju, H., Sun, J., et al. (2020b). Epigenetic Modulations of Noncoding RNA: a Novel Dimension of Cancer Biology. *Mol. Cancer* 19 (1), 64. doi:10.1186/s12943-020-01159-9
- Yang, Y., Fan, X., Mao, M., Song, X., Wu, P., Zhang, Y., et al. (2017). Extensive Translation of Circular RNAs Driven by N6-Methyladenosine. *Cell Res* 27 (5), 626–641. doi:10.1038/cr.2017.31
- Yue, J., Wu, Y., Qiu, L., Zhao, R., Jiang, M., and Zhang, H. (2021). LncRNAs Link Cancer Stemness to Therapy Resistance. *Am. J. Cancer Res.* 11 (4), 1051–1068.
- Zang, R., Qiu, X., Song, Y., and Wang, Y. (2021). Exosomes Mediated Transfer of Circ_0000337 Contributes to Cisplatin (CDDP) Resistance of Esophageal Cancer by Regulating JAK2 via miR-377-3p. *Front. Cell Dev. Biol.* 9, 673237. doi:10.3389/fcell.2021.673237
- Zhang, C., Ding, R., Sun, Y., Huo, S. T., He, A., Wen, C., et al. (2021a). Circular RNA in Tumor Metastasis. *Mol. Ther. - Nucleic Acids* 23, 1243–1257. doi:10.1016/j.omtn.2021.01.032
- Zhang, C., Liu, P., Huang, J., Liao, Y., Pan, C., Liu, J., et al. (2021b). Circular RNA Hsa_circ_0043280 Inhibits Cervical Cancer Tumor Growth and Metastasis via miR-203a-3p/PAQR3 axis. *Cell Death Dis* 12 (10), 888. doi:10.1038/s41419-021-04193-7
- Zhang, C., Zhou, X., Geng, X., Zhang, Y., Wang, J., Wang, Y., et al. (2021c). Circular RNA Hsa_circ_0006401 Promotes Proliferation and Metastasis in Colorectal Carcinoma. *Cell Death Dis* 12 (5), 443. doi:10.1038/s41419-021-03714-8
- Zhang, G., Sun, W., Zhu, L., Feng, Y., Wu, L., and Li, T. (2019a). Overexpressed Circ_0029426 in Glioblastoma Forecasts Unfavorable Prognosis and Promotes Cell Progression by Sponging miR-197. *J. Cell Biochem* 120 (6), 10295–10302. doi:10.1002/jcb.28313
- Zhang, H., and Xu, W. (2021). CircABCC3 Knockdown Inhibits Glioblastoma Cell Malignancy by Regulating miR-770-5p/SOX2 axis through PI3K/AKT Signaling Pathway. *Brain Res.* 1764, 147465. doi:10.1016/j.brainres.2021.147465
- Zhang, N., Ng, A. S., Cai, S., Li, Q., Yang, L., and Kerr, D. (2021d). Novel Therapeutic Strategies: Targeting Epithelial-Mesenchymal Transition in Colorectal Cancer. *Lancet Oncol.* 22 (8), e358–e368. doi:10.1016/S1470-2045(21)00343-0
- Zhang, S., Liao, K., Miao, Z., Wang, Q., Miao, Y., Guo, Z., et al. (2019b). CircFOXO3 Promotes Glioblastoma Progression by Acting as a Competing

- Endogenous RNA for NFAT5. *Neuro Oncol.* 21 (10), 1284–1296. doi:10.1093/neuonc/noz128
- Zhang, X.-N., Yang, K.-D., Chen, C., He, Z.-C., Wang, Q.-H., Feng, H., et al. (2021e). Pericytes Augment Glioblastoma Cell Resistance to Temozolomide through CCL5-CCR5 Paracrine Signaling. *Cell Res* 31 (10), 1072–1087. doi:10.1038/s41422-021-00528-3
- Zhang, X., Zhong, B., Zhang, W., Wu, J., and Wang, Y. (2019c). Circular RNA CircMTO1 Inhibits Proliferation of Glioblastoma Cells via miR-92/WWOX Signaling Pathway. *Med. Sci. Monit.* 25, 6454–6461. doi:10.12659/MSM.918676
- Zhao, B., Li, Z., Qin, C., Li, T., Wang, Y., Cao, H., et al. (2021). Mobius Strip in Pancreatic Cancer: Biogenesis, Function and Clinical Significance of Circular RNAs. *Cell. Mol. Life Sci.* 78 (17-18), 6201–6213. doi:10.1007/s00018-021-03908-5
- Zhao, C., Gao, Y., Guo, R., Li, H., and Yang, B. (2020). Microarray Expression Profiles and Bioinformatics Analysis of mRNAs, lncRNAs, and circRNAs in the Secondary Temozolomide-Resistant Glioblastoma. *Invest. New Drugs* 38 (5), 1227–1235. doi:10.1007/s10637-019-00884-3
- Zhou, C., Molinier, B., Daneshvar, K., Pondick, J. V., Wang, J., Van Wittenberghe, N., et al. (2017). Genome-Wide Maps of m6A circRNAs Identify Widespread and Cell-type-specific Methylation Patterns that Are Distinct from mRNAs. *Cell Rep.* 20 (9), 2262–2276. doi:10.1016/j.celrep.2017.08.027
- Zhou, F., Wang, B., Wang, H., Hu, L., Zhang, J., Yu, T., et al. (2021a). circMELK Promotes Glioblastoma Multiforme Cell Tumorigenesis through the miR-593/EphB2 axis. *Mol. Ther. - Nucleic Acids* 25, 25–36. doi:10.1016/j.omtn.2021.05.002
- Zhou, J., Wang, H., Hong, F., Hu, S., Su, X., Chen, J., et al. (2021b). CircularRNA circPARP4 Promotes Glioblastoma Progression through Sponging miR-125a-5p and Regulating FUT4. *Am. J. Cancer Res.* 11 (1), 138–156.
- Zhou, J., Wang, H., Chu, J., Huang, Q., Li, G., Yan, Y., et al. (2018). Circular RNA Hsa_circ_0008344 Regulates Glioblastoma Cell Proliferation, Migration, Invasion, and Apoptosis. *J. Clin. Lab. Anal.* 32 (7), e22454. doi:10.1002/jcla.22454
- Zhou, M., Li, H., Chen, K. e., Ding, W., Yang, C., and Wang, X. (2021c). CircSKA3 Downregulates miR-1 through Methylation in Glioblastoma to Promote Cancer Cell Proliferation. *Cmar* 13, 509–514. doi:10.2147/CMAR.S279097
- Zhou, W.-Y., Cai, Z.-R., Liu, J., Wang, D.-S., Ju, H.-Q., and Xu, R.-H. (2020). Circular RNA: Metabolism, Functions and Interactions with Proteins. *Mol. Cancer* 19 (1), 172. doi:10.1186/s12943-020-01286-3
- Zhu, F., Cheng, C., Qin, H., Wang, H., and Yu, H. (2020). A Novel Circular RNA circENTPD7 Contributes to Glioblastoma Progression by Targeting ROS1. *Cancer Cell Int* 20, 118. doi:10.1186/s12935-020-01208-9
- Zhu, L., Lama, S., Tu, L., Dusting, G. J., Wang, J.-H., and Liu, G.-S. (2021). TAK1 Signaling Is a Potential Therapeutic Target for Pathological Angiogenesis. *Angiogenesis* 24 (3), 453–470. doi:10.1007/s10456-021-09787-5

Conflict of Interest: The authors declare that the research was conducted in the absence of any commercial or financial relationships that could be construed as a potential conflict of interest.

Publisher's Note: All claims expressed in this article are solely those of the authors and do not necessarily represent those of their affiliated organizations, or those of the publisher, the editors and the reviewers. Any product that may be evaluated in this article, or claim that may be made by its manufacturer, is not guaranteed or endorsed by the publisher.

Copyright © 2021 Guo and Piao. This is an open-access article distributed under the terms of the Creative Commons Attribution License (CC BY). The use, distribution or reproduction in other forums is permitted, provided the original author(s) and the copyright owner(s) are credited and that the original publication in this journal is cited, in accordance with accepted academic practice. No use, distribution or reproduction is permitted which does not comply with these terms.



Crosstalk Among circRNA/lncRNA, miRNA, and mRNA in Osteoarthritis

Hui Kong¹, Ming-Li Sun¹, Xin-An Zhang^{1*} and Xue-Qiang Wang^{2,3*}

¹College of Kinesiology, Shenyang Sport University, Shenyang, China, ²Department of Sport Rehabilitation, Shanghai University of Sport, Shanghai, China, ³Department of Rehabilitation Medicine, Shanghai Shangti Orthopaedic Hospital, Shanghai, China

OPEN ACCESS

Edited by:

Jing Zhang,
Shanghai Jiao Tong University, China

Reviewed by:

Lei Zhao,
University of Wisconsin-Madison,
United States
Amy Osborne,
University of Canterbury, New Zealand

*Correspondence:

Xin-An Zhang
zhangxa2725@163.com
Xue-Qiang Wang
qiang897@163.com

Specialty section:

This article was submitted to
Epigenomics and Epigenetics,
a section of the journal
Frontiers in Cell and Developmental
Biology

Received: 11 September 2021

Accepted: 29 November 2021

Published: 15 December 2021

Citation:

Kong H, Sun M-L, Zhang X-A and
Wang X-Q (2021) Crosstalk Among
circRNA/lncRNA, miRNA, and mRNA
in Osteoarthritis.
Front. Cell Dev. Biol. 9:774370.
doi: 10.3389/fcell.2021.774370

Osteoarthritis (OA) is a joint disease that is pervasive in life, and the incidence and mortality of OA are increasing, causing many adverse effects on people's life. Therefore, it is very vital to identify new biomarkers and therapeutic targets in the clinical diagnosis and treatment of OA. ncRNA is a nonprotein-coding RNA that does not translate into proteins but participates in protein translation. At the RNA level, it can perform biological functions. Many studies have found that miRNA, lncRNA, and circRNA are closely related to the course of OA and play important regulatory roles in transcription, post-transcription, and post-translation, which can be used as biological targets for the prevention, diagnosis, and treatment of OA. In this review, we summarized and described the various roles of different types of miRNA, lncRNA, and circRNA in OA, the roles of different lncRNA/circRNA-miRNA-mRNA axis in OA, and the possible prospects of these ncRNAs in clinical application.

Keywords: osteoarthritis, miRNA, lncRNA, circRNA, lncRNA/circRNA-miRNA-mRNA axis

INTRODUCTION

Osteoarthritis (OA) is a joint disease that is pervasive in life. It is largely caused by cartilaginous injury and affects the whole joint tissue (Pereira et al., 2015). Nearly half of people over 65 suffer from OA. (Sakalauskiene and Jauniskienė, 2010; Glyn-Jones et al., 2015). Globally, the incidence and mortality of OA are increasing (Bijlsma et al., 2011). Arthrodynia, swelling, and inability to move freely are the main symptoms of OA and cause many adverse effects on people's lives. Several risk factors (Prieto-Alhambra et al., 2014), including age, sex, obesity, genetics, and joint damage, have been linked to OA progression (Felson et al., 2000; Vincent, 2019; Abramoff and Caldera, 2020). Articular cartilage degeneration and secondary osteogenesis are the main pathological manifestations of OA (Burr and Gallant, 2012). The long-term development of OA will not only affect people's behaviors and activities but also cause depression, anxiety, and other negative emotions (Litwic et al., 2013). To provide more perfect, targeted treatment for patients with OA, the progression of OA needs to be studied. The specific pathogenesis of OA may be related to metalloproteinases (Mehana et al., 2019), cytokines (Boehme and Rolaufts, 2018), signaling pathways (Rigoglou and Papavassiliou, 2013), and noncoding RNA (ncRNA) (Sondag and Haqqi, 2016).

ncRNA is a nonprotein-coding RNA that does not translate into proteins but participates in protein translation. At the RNA level, it can perform biological functions (Wu et al., 2019). microRNA (miRNA), long ncRNA (lncRNA), circular RNA (circRNA), ribosomal RNA (rRNA), transfer RNA (tRNA), small nuclear RNA (snRNA), small nucleolar RNA (snoRNA), small interfering RNA (siRNA), short hairpin RNA (shRNA) and Piwi-interactingRNA (piRNA) are the main ncRNAs (Chen et al., 2021). Studies have found that ncRNA is closely related to the occurrence of several diseases for the past few years (Esteller, 2011; Wang et al., 2019b). For example,

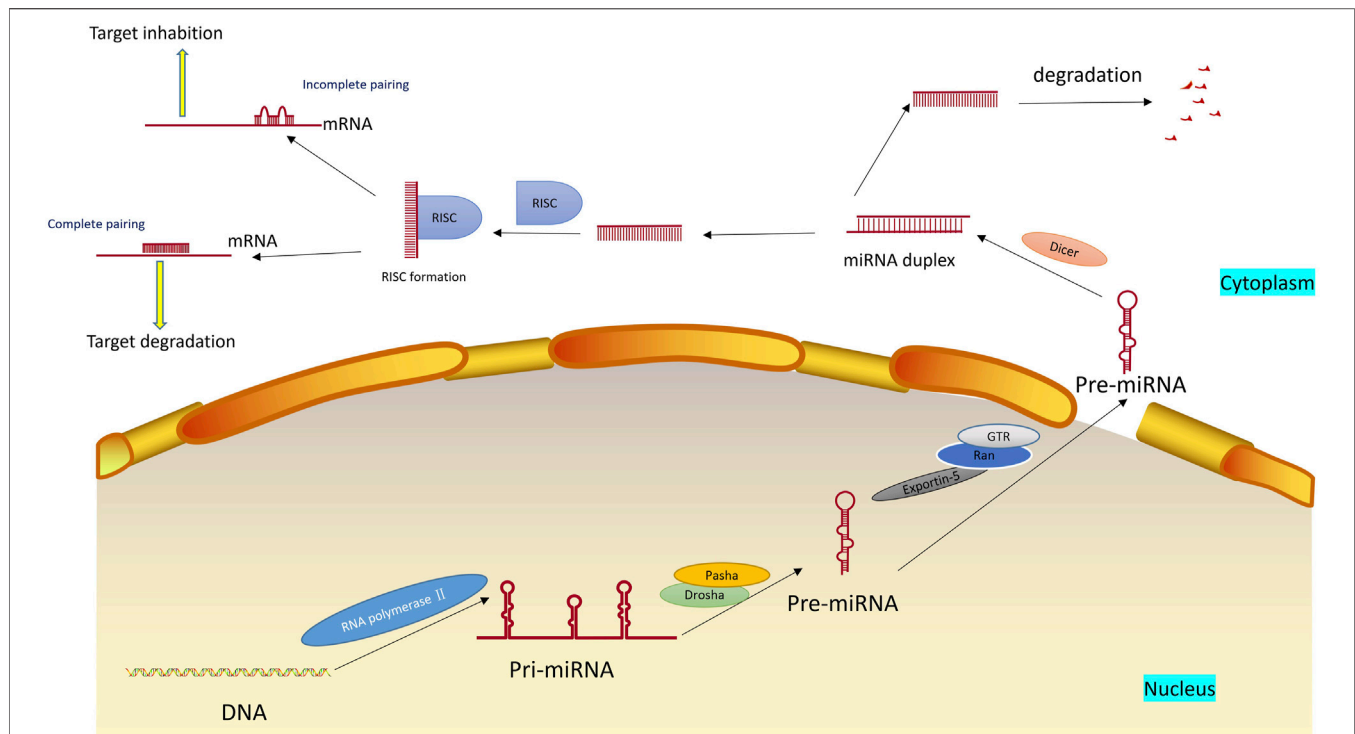


FIGURE 1 | Formation and mechanism of miRNA. miRNAs are first transcribed into longer primary miRNAs in the nucleus and then processed into hairpin RNAs of 60–70 nucleotides in the nucleus by Drosha, Pasha et al. The precursor miRNAs are transported out of the cell nucleus with the help of the Ran-GTP-dependent nucleoplasmic/cell transporter Exportin-5 and split into 21–25 nucleotide length double-stranded miRNAs in the cytoplasm by Dicer. Subsequently, the double helix is derotated by the action of the derotation enzyme, and one of the strands is integrated into the RNA-induced silencing complex (RISC), an asymmetric RISC assembly is formed, and the other chain is immediately degraded.

promoter CpG methylation of two genes encoding members of the miR-200 family can easily lead to the occurrence and development of breast and colorectal cancer (Lim et al., 2013); miR-34b/c is a critical tumor suppressor. The methylation of miR-34b/c CpG island leads to the silence of miR-34b/c, thus increasing the incidence of tumors (Toyota et al., 2008); the decreased expression of miR-133 may induce myocardial hypertrophy by targeting the beta-1 adrenergic receptor pathway (Castaldi et al., 2014). Many studies have also found that miRNA, lncRNA, and circRNA are closely related to the course of OA, and play important regulatory roles in transcription, post-transcription, and post-translation (Li et al., 2019b; Zhang et al., 2021e). The interaction between lncRNA/circRNA, miRNA, and mRNA has attracted increasing attention. For example, lncRNA/circRNA can bind to miRNA, reduce the inhibitory effect of miRNA on mRNA, participate in regulating the progress of chondrocyte proliferation and apoptosis, extracellular matrix (ECM) degradation and inflammatory response in the progress of OA. Furthermore, lncRNA-p21 could induce chondrocyte apoptosis and slow the process of OA by binding to miR-451 and promoting the expression of downstream target gene mRNA (Tang et al., 2018a). This review describes the roles of miRNA, lncRNA, and circRNA in OA and the role of the lncRNA/circRNA-miRNA-mRNA axis in OA.

MIRNAS AND OA

miRNA is a single-stranded RNA molecule with a length of about 20–24 nucleotides (Correia de Sousa et al., 2019). It belongs to one type of ncRNA and widely exists in eukaryotes to regulate the expression of other genes. miRNA regulates gene expression based on complete or incomplete pairing with mRNA. In most cases, the single-stranded miRNA in the complex is paired with the 3'UTR of the target mRNA in an incomplete complementary manner, blocking the translation of the gene and regulating gene expression. This process, called translation inhibition, is mainly found in animal cells. When the miRNA is completely complementary to the 3'UTR of the target mRNA, the mRNA in the complementary region would be specifically broken, eventually leading to gene silencing, and the process called post-transcriptional gene silencing, which will eventually lead to the degradation of target mRNA, mainly exists in plant cells (Liu et al., 2014a). The same gene can be regulated by multiple miRNAs, and multiple target genes can be regulated by the same miRNA (Iacona and Lutz, 2019). The formation and mechanism of miRNA are shown in Figure 1.

With the deepening of research, miRNAs have been discovered and studied increasingly, and they have become a potential target in disease prevention and treatment. miRNA has many functions roles in human diseases, such as regulating cell

autophagy (Li et al., 2019h), epigenesis (Yao et al., 2019), glucose metabolism (Fu et al., 2015). Chen et al. (2018c) developed a computational model for disease association prediction to detect potential miRNA-disease associations accurately and efficiently. By studying three common human cancers (Zhang et al., 2021b), namely, colon cancer, esophagus cancer, and kidney cancer, many miRNAs were confirmed to be connected with the three kinds of cancer. In addition, many studies have proven that miRNA is related to the pathological processes of intervertebral disc degeneration (Shi et al., 2021b), muscle atrophy (Zhang et al., 2021a), and cardiovascular diseases (Liu et al., 2021a).

Currently, growing findings reveal that miRNA expression level changes exist in various tissues of patients with OA, leading to abnormal target gene expression. miRNA has many functions in OA, such as regulating cell autophagy and apoptosis (Yu et al., 2019b), inflammatory reaction (Sui et al., 2019), and cartilage degradation (Guo et al., 2020). Changes in miRNA expression levels in different tissues can be experimented with by gene sequencing. Gene sequencing is a new type of gene detection technology, which can analyze and determine the whole sequence of genes from blood or saliva to predict the possibility of suffering from various diseases and lock in individual diseased genes for early prevention and treatment. Zhou et al. (2020b) revealed 21 differentially expressed miRNAs in synovial tissues from OA patients compared with normal controls by gene sequencing technology. The expression levels of the first two DE miRNAs (hsa-miR-17-5p and hsa-miR-20b-5p), which cover most of the DE miRNAs, were analyzed and found to be down-regulated in OA, which was also confirmed by qRT-PCR verification. Ntoumou et al. (2017) assessed differential miRNA expression by microarray analysis in the serum of patients with OA. Compared with the control group, 279 miRNAs were differentially expressed in OA. This study focused on analyzing and studying three differentially expressed miRNAs: hsa-miR-140-3p, hsa-miR-671-3p, and hsa-miR-33b-3p. We found that the expression of these three miRNAs was down-regulated in the serum of OA patients. Through serum microRNA array analysis and bioinformatics analysis, they determined that these three miRNAs were potential OA biomarkers involved in the metabolic processes of insulin and cholesterol. OA is a metabolic disease, and insulin resistance plays a vital role in metabolic syndrome. Therefore, the metabolic processes of insulin and cholesterol in the body are closely related to OA. In addition, based on RNA sequencing and miRNA analysis, Wu et al. (2021a) identified that miR-210-5p is highly enriched in the exosomes of OA sclerotic subchondral osteoblasts, triggering the expression of genes associated with catabolism in articular chondrocytes. Therefore, the abnormal up-regulation of miR-210-5p in exosomes could serve as a marker for OA. Notably, miRNA show obvious tissue specificity in different OA tissues. For example, the expression of miR-125b-5p in synovial fluid and chondrocytes is different in OA patients. Ge et al. (2017) found by PCR that miR-125b-5p in synovial fluid was significantly up-regulated in OA patients compared with normal subjects, promoting synovial cell apoptosis by targeting *syn1*. Rasheed et al. (2019) treated chondrocytes with IL-1 β to construct OA cell models and

determined the expression of miR-125b-5p using Taqman analysis. They found that miR-125b-5p in chondrocytes was significantly down-regulated compared to healthy individuals and regulated inflammatory genes in OA chondrocytes by targeting TRAF6. Our appeal study found that expression levels of multiple miRNAs in the synovial membrane, cartilage, and subchondral bone were altered in OA patients compared to healthy individuals. In addition, even in the same tissue, if in different stages of development, the expression of miRNAs may be different. For example, in different stages of the knee joint cartilage of rats, Sun et al. (2011) used Solexa sequencing and RT-qPCR detection for the expression of miRNAs. They tested the miRNAs in the rat knee joint cartilage at the starting point, on Day 21 and Day 42, and found that the expression of miRNAs was different at each stage. Among them, 4 representative miRNAs were selected for further analysis. Compared with the initial stage, the expressions of aggrecan, *col1a1*, and *ColXa1* were up-regulated on day 21. The expression of *ColXa1* was up-regulated on day 42, whereas those of aggrecan and *col1a1* were down-regulated. The expression of *Sox9* showed minimal change during the three stages. Gabler et al. (2015) found that miRNA could control the differentiation of chondrocytes and regulate the occurrence of OA. During the development of human bone marrow mesenchymal stem cells (HMSCs), the expression of miRNA in different development stages is also different. By microarray analysis, the miR spectra of HMSCs in patients with OA at different development time points were measured. Among the 1,349 detected miRNAs, 553 were expressed in cartilage formation, they further performed miRNAs detection at 7, 14, 21, and 42 days after cartilage formation and found that their expression of miRNAs was also different. In summary, the expression of miRNAs in OA patients is different in different tissues and between different stages of development of the same tissue.

It is well known that many intracellular signaling pathways, such as nuclear factor-kappaB (NF- κ B) and transforming growth factor β (TGF- β) played an vital roles in the pathogenesis of OA (Nishimura et al., 2020). In recent years, more studies discovered that miRNA can delay the pathological process of OA by promoting or inhibiting these pathways (Xu et al., 2016). NF- κ B is an essential nuclear transcription factor in cells participating in the inflammatory and immune response of the body and apoptosis regulation (Lawrence, 2009). For example, as the 3'UTR of NF- κ B contains the binding site of miR-143 and miR-124, when the DNA methylation degree of miR-143 and miR-124 promoters is reduced, the expression of miR-143 and miR-124 is up-regulated, and the transcription process is activated, thereby inhibiting the NF- κ B signaling pathway, inhibiting apoptosis and delaying the progression of OA (Qiu et al., 2020). Similarly, When the expression levels of miR-34a and miR-181a were decreased, the expression of the BCL2 gene was increased, thereby limiting the term of NF- κ B translocation into the nucleus in OA Chondrocytes cultures and eventually reducing apoptosis and oxidative stress (Cheleschi et al., 2019). The TGF- β signaling pathway is involved in many cellular processes in mature organisms and developing embryos, including cell

TABLE 1 | Functional characterization of the miRNAs in OA.

miRNA	Expression	Target gene(s)	Tissue/cell source	Region	Model	Functions	Reference
miR-103	Up	SPHK1	Cartilage tissue	knee joint, hip joint	OA rat model	Apoptosis	Li et al. (2019a)
	Up	Sox6	Cartilage tissue	knee joint	OA cell model	Apoptosis	Chen and Wu, (2019)
miR-34a	Up	TGIF2	Synovial fluid	knee joint	OA cell model	Apoptosis	Luo et al. (2019a)
	Up	DLL1	Cartilage tissue	knee joint, hip joint	OA rat model	Apoptosis	Zhang et al. (2018d)
	Up	<i>SIRT1/p53</i>	Cartilage tissue	knee joint	OA rat model	Apoptosis	Yan et al. (2016)
	Up	Cyr61	Cartilage tissue	knee joint	OA cell model	Apoptosis	Yang et al. (2018a)
	Up	—	Cartilage tissue	knee joint	OA rat model	Apoptosis	Tao et al. (2020)
	Up	—	Cartilage tissue	knee joint	OA rat model	Apoptosis	Abouheif et al. (2010)
miR-486-5p	Up	SMAD2	Cartilage tissue	knee joint	OA cell model	Apoptosis	Shi et al. (2018)
miR-375	Up	<i>JAK2</i>	Cartilage tissue	knee joint	OA mouse model	Apoptosis	Zou et al. (2019)
	Up	ATG2B	Cartilage tissue	knee joint	OA mouse model	Autophagy	Li et al. (2020c)
miR-29b	Up	PTH1H	Cartilage tissue	knee joint	OA mouse model	Apoptosis	Dou et al. (2020)
	Up	<i>Wnt5a</i>	—	—	OA mouse model	cartilage degradation	Sun et al. (2020)
	Up	COL2A1, COL1A2	Cartilage tissue	knee joint, hip joint	OA mouse model	Apoptosis	Moulin et al. (2017)
	Up	COL1A1, COL3A1	Cartilage tissue	knee joint, hip joint	OA cell model	Apoptosis	Mayer et al. (2017)
miR-29b-3p	Up	PGRN	Cartilage tissue	knee joint	OA rat model	Apoptosis	Chen et al. (2017)
miR-124A	Up	QKI, MAP 1B	Cartilage tissue	knee joint	OA rat model	cartilage degradation	Jiang et al. (2020b)
miR-455-3p	Up	PAK2	Cartilage tissue	knee joint	OA mouse model	cartilage degradation	Hu et al. (2019b)
	Up	COL2A1	Cartilage tissue	—	OA cell model	Apoptosis, Inflammation	Cheng et al. (2020)
	Up	PTEN	Bone marrow, Cartilage tissue	—	OA mouse model	Apoptosis, Inflammation	Wen et al. (2020)
miR-30b	Up	ERG	Cartilage tissue	knee joint	OA cell model	cartilage degradation	Li et al. (2015)
miR-181	Up	PTEN	Cartilage tissue	knee joint	OA cell model	Apoptosis	Wu et al. (2017b)
miR-324-5p	Up	Gpc1	Cartilage tissue	—	OA cell model	—	Woods et al. (2019)
miR-146a	Up	TRAF6	Cartilage tissue	knee joint, hip joint	OA cell model	Apoptosis	Zhong et al. (2017)
	Up	Camk2d, Ppp3r2	Cartilage tissue	knee joint	OA mouse model	cartilage degradation	Zhang et al. (2017)
	Up	Smad4	Cartilage tissue	knee joint	OA rat model	Apoptosis	Li et al. (2012)
	Up	CXCR4	Cartilage tissue	—	OA mouse model	nflammation	Sun et al. (2017)
miR-146a-5p	Up	TRAF6	Cartilage tissue	hip joint	OA cell model	Apoptosis	Shao et al. (2020)
	Up	TXNIP	SW1353 and C28/I2 cells	—	—	Apoptosis, Inflammation	Zhao and Gu, (2020)
	Up	—	Cartilage tissue, Blood	—	OA cell model	cartilage degradation, Inflammation	Skrzypa et al. (2019)
miR-146b	Up	A2M	Cartilage tissue	knee joint	OA mouse model	Apoptosis, cartilage degradation	Liu et al. (2019d)
	Up	—	Bone marrow, Cartilage tissue	—	OA cell model	Apoptosis	Budd et al. (2017)
miR-1236	Up	rs4246215	Cartilage tissue	knee joint	OA cell model	Apoptosis	Wang et al. (2020b)
miR-10a-5p	Up	HOXA3	Cartilage tissue, Blood	—	OA mouse model	Apoptosis, cartilage degradation	Li et al. (2020b)
	Up	HOXA1	Cartilage tissue	hip joint	OA mouse model	Apoptosis	Ma et al. (2019b)

(Continued on following page)

TABLE 1 | (Continued) Functional characterization of the miRNAs in OA.

miRNA	Expression	Target gene(s)	Tissue/cell source	Region	Model	Functions	Reference
miR-27b-3p	Up	KDM4B	Cartilage tissue	knee joint	OA rat model	Inflammation	Zhang et al. (2020c)
miR-483-5p	Up	Matn3, Timp2	Cartilage tissue	knee joint	OA mouse model	cartilage degradation	Wang et al. (2017b)
miR-340-5p	Up	FMOD	Cartilage tissue	knee joint	OA mouse model	Apoptosis	Zhang et al. (2018c)
miR-195	Up	PTHrP	Cartilage tissue	knee joint	OA rat model	Apoptosis	Cao et al. (2019b)
miR-195-5p	Up	REGγ	Cartilage tissue	— —	OA mouse model	Apoptosis	Shu et al. (2019)
miR-23b-3p	Up	COL11A2	Cartilage tissue	knee joint	OA mouse model	inflammation	Yang et al. (2019b)
miR-448	Up	matrilin-3	Cartilage tissue	knee joint	OA cell model	Apoptosis, cartilage degradation	Yang et al. (2018b)
miR-203	Up	ERα	Blood, Cartilage tissue	— —	OA rat model	cartilage degradation	Tian et al. (2019)
	Up	MCL-1	Cartilage tissue	— —	OA cell model	Apoptosis, cartilage degradation, Inflammation	Zhao et al. (2017)
miR-203a	Up	Smad3	Cartilage tissue	knee joint	OA cell model	cartilage degradation, Inflammation	An et al. (2020)
miR-21	Up	GDF-5	Cartilage tissue	— —	OA cell model	Apoptosis	Zhang et al. (2014)
miR-21-5p	Up	FGF18	Cartilage tissue	knee joint	OA mouse model	Apoptosis, cartilage degradation	Wang et al. (2019e)
miR-218-5p	Up	PIK3C2A	Cartilage tissue	knee joint	OA mouse model	cartilage degradation, Apoptosis	Lu et al. (2017)
miR-449a	Up	GDF5	Cartilage tissue	— —	OA cell model	cartilage degradation	Wu et al. (2018a)
miR-125b-5p	Up	SYVN1	Synovial fluid	— —	OA cell model	Apoptosis	Ge et al. (2017)
miR-384-5p	Up	SOX9	Cartilage tissue	knee joint	OA mouse model	Apoptosis	Zhang et al. (2020i)
miR-23a-3p	Up	SMAD3	Cartilage tissue	— —	OA cell model	cartilage degradation	Kang et al. (2016a)
miR-139	Up	MCPIP1	Cartilage tissue	— —	OA cell model	Apoptosis	Makki and Haqqi, (2015)
miR-206	Up	— —	Cartilage tissue	knee joint	OA cell model	Apoptosis	Ni et al. (2018)
miR-382-3p	Up	CX43	Cartilage tissue	knee joint	OA cell model	Inflammation	Lei et al. (2019)
miR-101	Up	Sox9	Synovial fluid	knee joint	OA rat model	cartilage degradation	Dai et al. (2015)
miR-30a	Up	Sox9	Cartilage tissue	knee joint	OA cell model	cartilage degradation, Inflammation	Chang et al. (2016)
	Up	DLL4	bone marrow	— —	OA rat model	Cell differentiation	Tian et al. (2016)
miR-216b	Up	Smad3	Cartilage tissue	knee joint	OA cell model	cartilage degradation	He et al. (2017)
miR-128a	Up	Atg12	Cartilage tissue	knee joint	OA rat model	Autophagy	Lian et al. (2018)
miR-20a	Up	IκBβ	Cartilage tissue, blood	— —	OA rat model	Inflammation	Zhao and Gong, (2019)
miR-136	Up	Mcl-1	Cartilage tissue	— —	OA cell model	Apoptosis, cartilage degradation, Inflammation	Wang and Kong, (2018)
miR-130b	Up	SOX9	Bone marrow, Cartilage tissue	— —	OA rat model	Cell differentiation	Zhang et al. (2021c)
miR-132-3p	Up	ADAMTS-5	Bone marrow, Cartilage tissue	— —	OA rat model	Cell differentiation	Zhou et al. (2018c)
miR-1246	Up	HNF4γ	Cartilage tissue	— —	OA mouse model	Inflammation	Wu et al. (2017a)
miR-9	Up	— —	Cartilage tissue	— —	OA mouse model	Apoptosis, cartilage degradation, Inflammation	Zhang et al. (2019e)
miR-222	Up	HDAC-4	Cartilage tissue	knee joint	OA mouse model	Apoptosis	Song et al. (2015)
miR-155	Up	PIK3R1	Cartilage tissue	knee joint	OA cell model	Apoptosis	Fan et al. (2020)
miR-33a	Up	Smad7	Cartilage tissue	knee joint	OA cell model	Cell differentiation	Kostopoulou et al. (2015)

(Continued on following page)

TABLE 1 | (Continued) Functional characterization of the miRNAs in OA.

miRNA	Expression	Target gene(s)	Tissue/cell source	Region	Model	Functions	Reference
miR-93	Down	TLR4	Cartilage tissue, Synovial fluid	knee joint	OA mouse model	Apoptosis, inflammation	Ding et al. (2019)
miR-93-5p	Down	TCF4	Cartilage tissue	knee joint	OA rat model	Apoptosis	Xue et al. (2019)
miR-92a-3p	Down	WNT5A	Bone marrow, Cartilage tissue	— —	OA mouse model	cartilage degradation	Mao et al. (2018b)
miR-92a-3p	Down	HDAC2	Bone marrow, Cartilage tissue	— —	OA cell model	cartilage degradation	Mao et al. (2017b)
miR-92a-3p	Down	ADAMTS-4, ADAMTS-5	Cartilage tissue	knee joint	OA cell model	cartilage degradation, Inflammation	Mao et al. (2017a)
miR-107	Down	TRAF3	Cartilage tissue	knee joint	OA rat model	Autophagy and apoptosis	Zhao et al. (2019b)
miR-101a-3p	Down	UBE2D1, FZD4	Cartilage tissue	— —	OA rat model	Apoptosis	Mao et al. (2021a)
miR-671	Down	— —	Cartilage tissue	knee joint	OA mouse model	Apoptosis	Zhang et al. (2019a)
miR-671-3p	Down	TRAF3	Cartilage tissue	knee joint	OA cell model	cartilage degradation, Inflammation, Apoptosis	Liu et al. (2019e)
miR-140	Down	— —	Synovial fluid, Cartilage tissue	knee joint	OA cell model	cartilage degradation	Si et al. (2016)
	Down	RALA	Cartilage tissue	knee joint	OA cell model	Cell differentiation	Karlsen et al. (2014)
	Down	IGFBP-5	Cartilage tissue	knee joint	OA cell model	cartilage degradation	Tardif et al. (2009)
	Down	IGFBP5	Cartilage tissue	knee joint	OA cell model	inflammation	Karlsen et al. (2016)
	Down	ADAMTS5	Cartilage tissue	— —	OA mouse model	cartilage degradation	Miyaki et al. (2010)
	Down	MMP-13	Cartilage tissue	— —	OA cell model	cartilage degradation	(Liang et al., 2012; Liang et al., 2016)
	Down	SMAD1	Cartilage tissue	— —	OA cell model	Apoptosis	Li et al. (2018a)
	Down	NFAT3, SMAD3	Cartilage tissue	knee joint	OA cell model	inflammation	Tardif et al. (2013)
miR-140-3p	Down	CXCR4	Cartilage tissue	knee joint	OA cell model	Apoptosis	Ren et al. (2020)
miR-140-5p	Down	SMAD3	— —	— —	OA mouse model	inflammation	Li et al. (2019d)
	Down	HMGB1	Cartilage tissue	knee joint	OA cell model	inflammation	Wang et al. (2020d)
	Down	FUT1	Cartilage tissue	knee joint	OA cell model	Apoptosis	Wang et al. (2018b)
miR-33b-3p	Down	DNMT3A	Cartilage tissue	knee joint	OA cell model	Apoptosis	Ma et al. (2019a)
miR-766-3p	Down	AIFM1	Cartilage tissue	— —	OA cell model	cartilage degradation	Li et al. (2020g)
miR-26a	Down	— —	Cartilage tissue	knee joint	OA rat model	inflammation	Zhao et al. (2019c)
miR-26a/	Down	FUT4	Cartilage tissue	knee joint	OA rat model	Apoptosis	Hu et al. (2018a)
miR-26b							
miR-26a-5p	Down	PTGS2	Bone marrow, Synovial fluid	— —	OA rat model	Apoptosis, Inflammation	Jin et al. (2020)
miR-377-3p	Down	ITGA6	Cartilage tissue	knee joint	OA cell model	Apoptosis	Tu et al. (2020)
miR-410-3p	Down	HMGB1	Synovial fluid, Cartilage tissue	knee joint	OA mouse model	Apoptosis, Inflammation	Pan et al. (2020)
miR-142-3p	Down	HMGB1	Cartilage tissue	knee joint	OA mouse model	Apoptosis, Inflammation	Wang et al. (2016c)
miR-210	Down	HIF-3 α	Cartilage tissue	knee joint	OA cell model	Apoptosis, cartilage degradation	Li et al. (2016)
	Down	DR6	Cartilage tissue	knee joint	OA rat model	Apoptosis, Inflammation	Zhang et al. (2015)
miR-122	Down	SIRT1	Cartilage tissue	knee joint	OA cell model	cartilage degradation	Bai et al. (2020a)
miR-337-3p	Down	PTEN	Cartilage tissue	knee joint	OA cell model	Apoptosis	Huang et al. (2017)
miR-129-3p	Down	CPEB1	Cartilage tissue	knee joint	OA rat model	Apoptosis	Chen et al. (2020d)

(Continued on following page)

TABLE 1 | (Continued) Functional characterization of the miRNAs in OA.

miRNA	Expression	Target gene(s)	Tissue/cell source	Region	Model	Functions	Reference
miR-675-3p	Down	GN5	Cartilage tissue	knee joint	OA cell model	Apoptosis, cartilage degradation	Shen et al. (2020b)
miR-132	Down	PTEN	Cartilage tissue, Blood	— —	OA rat model	Apoptosis	Zhang et al. (2021d)
miR-137	Down	TCF4	Cartilage tissue	knee joint	OA rat model	Apoptosis, inflammation	Wang et al. (2020a)
miR-320c	Down	β -catenin	Cartilage tissue	knee joint	OA mouse model	Apoptosis	Hu et al. (2019a)
miR-29a	Down	Bax	Cartilage tissue	— —	OA cell model	Apoptosis	Miao et al. (2019)
	Down	VEGF	Synovial fluid	knee joint	OA cell model	cartilage degradation, Inflammation	Ko et al. (2017)
miR-193b-3p	Down	MMP-19	Cartilage tissue	knee joint	OA cell model	Inflammation	Chang et al. (2018)
miR-193b-3p	Down	HDAC3	Cartilage tissue	knee joint	OA mouse model	cartilage degradation	Meng et al. (2018)
miR-193b-5p	Down	HDAC7	Cartilage tissue	knee joint, hip joint	OA cell model	Inflammation	Zhang et al. (2019b)
miR-136-5p	Down	ELF3	Bone marrow, Cartilage tissue	— —	OA mouse model	Apoptosis, cartilage degradation	Chen et al. (2020e)
miR-374a-3p	Down	WNT5B	— —	— —	OA cell model	Apoptosis	Shi and Ren, (2020)
miR-19b-3p	Down	GRK6	Cartilage tissue	knee joint, hip joint	OA cell model	cartilage degradation, Inflammation	Duan et al. (2019a)
miR-221-3p	Down	SDF1/CXCR4	Cartilage tissue	knee joint	OA cell model	cartilage degradation	Zheng et al. (2017)
miR-502-5p	Down	TRAF2	Cartilage tissue	knee joint, hip joint	OA cell model	cartilage degradation, Inflammation	Zhang et al. (2016b)
miR-31	Down	CXCL12	Cartilage tissue	— —	OA cell model	Apoptosis	Dai et al. (2019)
miR-488	Down	ZIP-8	Cartilage tissue	knee joint	OA mouse model	cartilage degradation	Song et al. (2013)
miR-125b	Down	ADAMTS-4	Cartilage tissue	knee joint	OA cell model	— —	Matsukawa et al. (2013)
miR-181c	Down	NEAT1	Synovial fluid	— —	OA cell model	Apoptosis, Inflammation	Wang et al. (2017d)
miR-615-3p	Down	— —	bone marrow	— —	OA rat model	Inflammation	Zhou et al. (2018a)
miR-211-5p	Down	Fibulin-4	Cartilage tissue	— —	OA rat model	cartilage degradation, Inflammation	Liu and Luo, (2019)
miR-19a	Down	SOX9	Cartilage tissue	knee joint	OA cell model	Apoptosis	Yu and Wang, (2018)
miR-503-5p	Down	SGK1	Cartilage tissue	knee joint	OA rat model	Apoptosis, Inflammation	Wang et al. (2021b)
miR-33	Down	CCL2	Cartilage tissue	— —	OA mouse model	Inflammation	Wei et al. (2016)
miR-27	Down	Leptin	Cartilage tissue	— —	OA rat model	Inflammation	Zhou et al. (2017)
miR-186	Down	SPP1	Cartilage tissue	— —	OA mouse model	Apoptosis	Lin et al. (2019)
miR-149	Down	TAK1	Cartilage tissue	— —	OA cell model	Inflammation	Chen et al. (2018a)
miR-204-5p	Down	Runx2	Cartilage tissue	knee joint	OA rat model	Apoptosis	Cao et al. (2018a)
miR-128-3p	Down	WISP1	Cartilage tissue	knee joint	OA cell model	Apoptosis, cartilage degradation, Inflammation	Chen and Li, (2020)
miR-320	Down	MMP-13	Cartilage tissue	— —	OA mouse model	Inflammation	Meng et al. (2016)
miR-558	Down	COX-2	Cartilage tissue	knee joint	OA cell model	Inflammation	Park et al. (2013)
miR-634	Down	PIK3R1	Cartilage tissue	— —	OA cell model	cartilage degradation	Cui et al. (2016)
miR-24	Down	C-myc	Cartilage tissue	knee joint	OA rat model	Apoptosis	Wu et al. (2018b)
miR-365	Down	HIF-2 α	Cartilage tissue	knee joint	OA cell model	Apoptosis	Hwang et al. (2017)
miR-126-3p	Down	— —	Synovial fluid	knee joint	OA rat model	cartilage degradation, Inflammation	Zhou et al. (2021d)
miR-520c-3p	Down	GAS2	Cartilage tissue	hip joint	OA cell model	Apoptosis, cartilage degradation	Peng et al. (2021)

(Continued on following page)

TABLE 1 | (Continued) Functional characterization of the miRNAs in OA.

miRNA	Expression	Target gene(s)	Tissue/cell source	Region	Model	Functions	Reference
miR-1207-5p	Down	CX3CR1	Cartilage tissue	— —	OA cell model	Apoptosis, cartilage degradation	Liu et al. (2020b)
miR-152	Down	TCF-4	Cartilage tissue	knee joint, hip joint	OA rat model	Apoptosis	Wan et al. (2020)
miR-296-5p	Down	TGF- β	Cartilage tissue	knee joint	OA cell model	Apoptosis, cartilage degradation	Cao et al. (2020)
miR-373	Down	P2X7R	Cartilage tissue, Blood	— —	OA cell model	cartilage degradation, Inflammation	Zhang et al. (2018e)
miR-25-3p	Down	IGFBP7	Cartilage tissue	— —	OA rat model	Apoptosis	He and Deng, (2021)
miR-95-5p	Down	HDAC2, HDAC8	Bone marrow, Cartilage tissue	— —	OA cell model	cartilage degradation	Mao et al. (2018a)
miR-181a	Down	GPD1L	Cartilage tissue	knee joint	OA cell model	Apoptosis	Zhai et al. (2017)
miR-411	Down	HIF-1 α	Cartilage tissue	— —	OA cell model	autophagy	Yang et al. (2020b)
miR-98	Down	Bcl-2	Cartilage tissue	— —	OA mouse model	Apoptosis	Wang et al. (2017c)
	Down	Bcl-2	Cartilage tissue	— —	OA rat model	cartilage degradation, Apoptosis	Wang et al. (2016b)
	Down	— —	Cartilage tissue	knee joint	OA rat model	Apoptosis	Wang et al. (2016a)
miR-125b-5p	Down	TRAF6	Cartilage tissue	knee joint, hip joint	OA cell model	Inflammation	Rasheed et al. (2019)
miR-27a	Down	TLR4	Cartilage tissue	knee joint, hip joint	OA rat model	cartilage degradation, Inflammation	Qiu et al. (2019)
	Down	NF- κ B	Cartilage tissue	knee joint	OA rabbit model	Apoptosis, Inflammation	Zhang et al. (2019c)
	Down	PLK2	Cartilage tissue	knee joint	OA rat model	Apoptosis	Liu et al. (2019c)
miR-15a-5p	Down	PTHrP	Cartilage tissue	knee joint	OA cell model	Apoptosis	Duan et al. (2019b)
miR-9-5p	Down	Tnc	Cartilage tissue	knee joint, hip joint	OA mouse model	Apoptosis	Chen et al. (2019a)
miR-145	Down	BNIP3	Cartilage tissue	knee joint	OA mouse model	Apoptosis	Wang et al. (2020c)
miR-145	Down	MKK4	Cartilage tissue	— —	OA rat model	cartilage degradation	Hu et al. (2017)
miR-145	Down	TNFRSF11B	Cartilage tissue	knee joint	OA cell model	Apoptosis	Wang et al. (2017a)

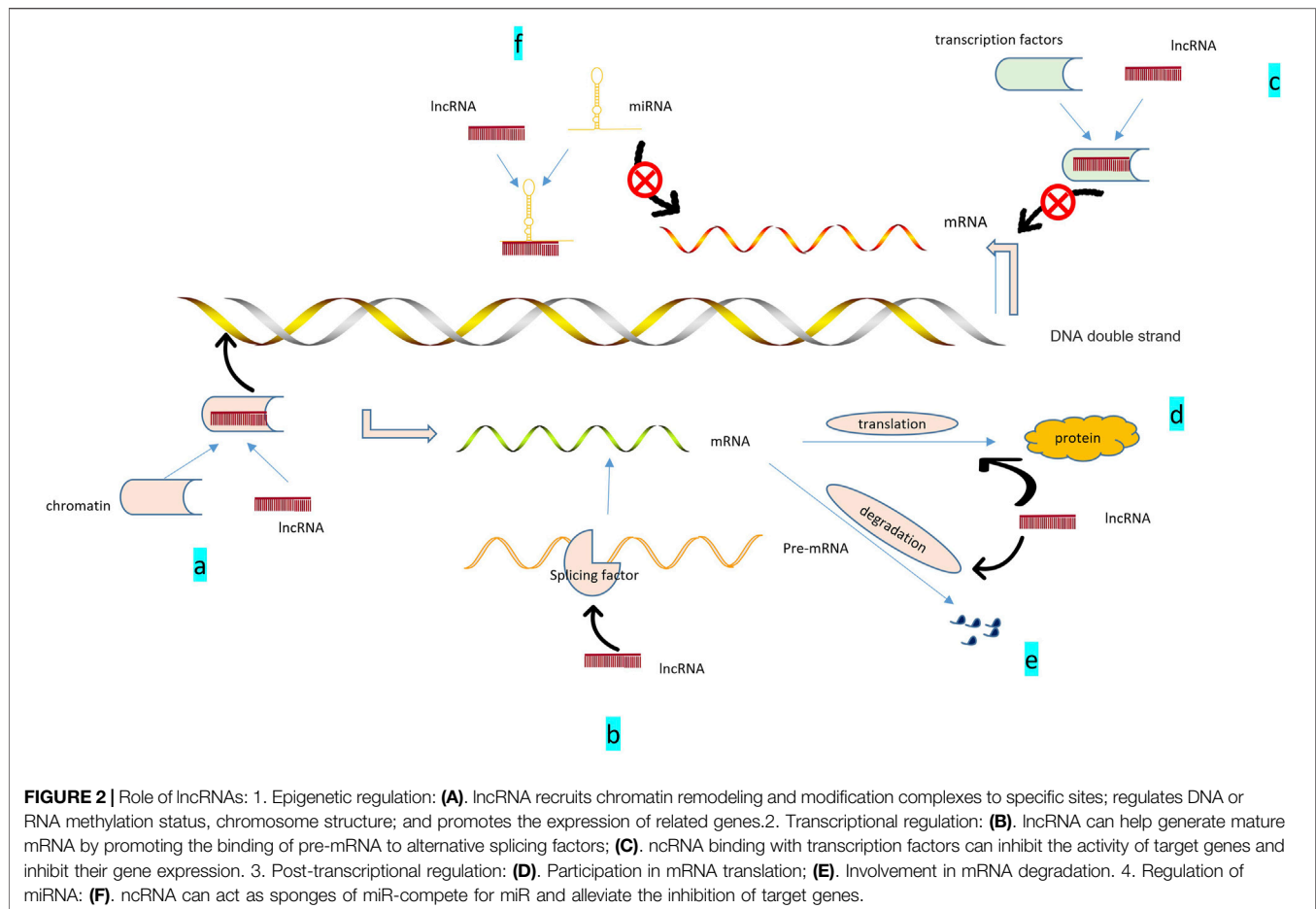
Abbreviations: SPHK1, sphingosine kinase-1; SOX9, SRY-Box 9; DLL1, delta-like protein 1; SIRT1, silent information regulator 1; SMAD2, SMAD, family member 2; PTHLH, parathyroid hormone-like hormone; Wnt5a, wnt family member 5A; PGRN, progranulin; MAP, 1B, microtubule associated protein 1B; Gpc1, glypican 1; Ppp3r2, calcineurin B, type II, protein phosphatase 3; TXNIP, thioredoxin-interacting protein; A2M, alpha-2-macroglobulin; KDM4B, lysine demethylase 4B; Matn3, cartilage matrix protein matrilin 3; Timp2, tissue inhibitor of metalloproteinase 2; PTHrP, parathyroid hormone-related protein; MCL-1, myeloid cell leukemia-1; GDF-5, growth differentiation factor 5; FGF18, fibroblast growth factor 18; GDF5, growth differentiation factor 5; SYVN1, synoviolin 1; CX43, connexin 43; TLR4, toll-like receptor 4; TCF4, transcription factor 4; HDAC2, histone deacetylase 2; ADAMTS-4, aggrecanase-1; TRAF3, TNF, receptor-associated factor 3; UBE2D1, ubiquitin-conjugating enzyme 2D1; FZD4, frizzled class receptor 4; MMP-13, matrix metalloproteinase-13; FUT1, fucosyltransferase 1; DNMT3A, DNA, methyltransferase 3A; DR6, death receptor 6; GNG5, G-protein subunit g 5; HDAC7, histone deacetylase 7; HDAC3, histone deacetylase 3; ELF3, E74-like factor 3; TRAF2, TNF, receptor-associated factor 2; SPP1, phosphoprotein 1; COX-2, cyclooxygenase-2; HIF-2 α , hypoxia-inducible factor-2 α ; GAS2, Growth arrest-specific 2; P2X7R, P2X7 receptor; IGFBP7, insulin-like growth factor-binding protein 7; HIF-1 α , hypoxia-inducible factor 1 alpha; Bcl-2, B-cell lymphoma 2; PLK2, polo-like kinase 2.

growth, differentiation, apoptosis, dynamic cell balance, and other cellular functions. By promoting or inhibiting the TGF- β signaling pathway, we can regulate the cellular processes, thereby inducing or delaying the progression of OA (Shen et al., 2014). Hu et al. (2019b) established OA mouse models. QPCR and Western blot were used to compare the expression of miR-455-3p and PAK2 in the cartilage of healthy individuals and patients with OA, and the luciferase reporter gene was used to analyze the interaction between them. The results showed that miR-455-3p could inhibit the expression of pak 2, promote the TGF- β signaling pathway, and ultimately inhibit OA by directly targeting PAK2 3'UTR. In summary, various miRNAs are involved in regulating OA progression by handling a variety of

intracellular signaling pathways. In addition, increasing evidence also emphasizes that changes in the expression of many miRNAs can also directly regulate the development of OA. The specific information of these miRNAs is listed in **Table 1**.

LNCRNAs AND OA

lncRNAs are ncRNAs with a length of more than 200 nucleotides that have little or no protein-coding potential, and account for more than 80% of total lncRNAs (Ponting et al., 2009). At first, lncRNA was considered the “noise” of genome transcription, with no biological function, and its mechanism of action was only *in*



situ regulation, through recruitment and formation of chromatin modification complexes [such as IGF2RRNA antisense (AIR), XIST] to silence the transcription of neighboring genes. As more detection techniques were applied to RNA studies, such as microarray, RNA sequencing (RNA-seq), Northern blot, and real-time quantitative reverse transcription-polymerase chain reaction (qRT-PCR) (Zhu et al., 2013), more biological functions of lncRNAs gradually being discovered. Recent studies have discovered several mechanisms of action of lncRNA, which can interact with proteins, DNA, and RNA to regulate many biological processes (Zhu et al., 2013). For example, lncRNA MALAT1 acts on miR-150-5P and AKT3 to regulate cell proliferation and apoptosis (Zhang et al., 2019g), thus participating in the growth and development of the body and the pathological process of diseases (Kopp and Mendell, 2018) (Figure 2).

lncRNA is closely related to cell growth, differentiation, and senescence. In addition, lncRNA has a special relationship with some human diseases, such as cardiovascular diseases (Huang, 2018), nervous system diseases (Zhang et al., 2019f), and immune-mediated diseases (Zhou et al., 2018b). In the recently updated database of lncRNA-related diseases, more than 200,000 lncRNAs have been recorded in their association with diseases (Bao et al., 2019).

lncRNA can regulate chondrocyte proliferation and apoptosis, inflammatory response, and extracellular matrix degradation, and promote the repair and stability of articular cartilage. Recent studies have shown an essential relationship between some changes or disorders of lncRNAs and the occurrence and development of OA. There are many studies to detect the expression of lncRNA in OA patients. Yang et al. (2021a) examined the lncRNA profiles of patients with OA and healthy individuals by RNA sequencing. They found that 25 lncRNAs are differentially expressed in patients with OA compared with the control group. Through microarray analysis, Xing et al. (2014) detected the expression of lncRNA in KOA cartilage and normal cartilage and further verified it by real-time polymerase chain reaction (RT-PCR). They found that the expression of 121 lncRNAs in KOA is different from normal cartilage: 73 up-regulated lncRNAs and 48 down-regulated lncRNAs. Among the up-regulated lncRNAs, HOTAIR is the most up-regulated. Pearson et al. (2016) separated OA chondrocytes through collagenase digestion and analyzed lncRNA expression through RNA sequencing (RNAseq) and qPCR. Finally, 983 lncRNAs were identified in OA chondrocytes. A total of 125 differentially expressed lncRNAs were identified after interleukin-1B (IL-1B) stimulation. Through microarray and qPCR analysis, Liu et al. (2014b) compared the

TABLE 2 | Functional characterization of the lncRNAs in OA.

lncRNA	Expression	Target genes	Related genes	Tissue/cell source	Region	Model	Functions	Reference
ANRIL	Up	miRNA-122-5p	DUSP4	Cartilage tissue, synoviocytes	knee joint	OA cell model	Cell proliferation and apoptosis	Li et al. (2019e)
CASC2	Up	—	IL-17	Blood, Synovial fluid, chondrocyte	—	OA cell model	Cell proliferation and apoptosis	Huang et al. (2019d)
CIR	Up	—	—	Cartilage tissue	hip joint	OA rat model	Cell autophagy	Wang et al. (2018a)
	Up	miR-130a	Bim	Cartilage tissue	knee joint	OA cell model	Cell proliferation and apoptosis	Lu et al. (2018)
	Up	miR-27b	—	Cartilage tissue	knee joint	OA cell model	Degradation of extracellular matrix	Li et al. (2017b)
HOTAIR	Up	—	MMP	Cartilage tissue, Synovial fluid	temporomandibular	OA rabbit model	Cell proliferation and apoptosis	Zhang et al. (2016a)
	Up	—	WIF-1	SW1353 cells	knee joint	OA cell model	Degradation of extracellular matrix	Yang et al. (2020c)
	Up	—	—	Synovial fluid, Cartilage tissue	knee joint	OA cell model	Cell proliferation and apoptosis	Liang et al. (2021)
	Up	—	—	Synovial tissue	knee joint	OA rat model	Cell proliferation and apoptosis, inflammation	Mao et al. (2019b)
	Up	miR-20b	PTEN	Cartilage tissue	knee joint	OA mouse model	Cell proliferation and apoptosis, Degradation of extracellular matrix	Chen et al. (2020f)
	Up	miR-130a-3p	—	Cartilage tissue	—	OA human model	Cell proliferation and apoptosis, Cell autophagy	He and Jiang, (2020)
	Up	miR-17-5p	FUT2	Cartilage tissue	knee joint	OA rat model	Cell proliferation and apoptosis, Degradation of extracellular matrix	Hu et al. (2018b)
LOC101928134	Up	—	IFNA1	Synovial fluid, Cartilage tissue	knee joint	OA rat model	Cell proliferation and apoptosis, Degradation of extracellular matrix	Yang et al. (2019a)
LINC00671	Up	—	Smurf2	Cartilage tissue	knee joint	OA mouse model	Degradation of extracellular matrix	Chen and Xu, (2021)
TM1P3	Up	—	—	Cartilage tissue	knee joint	OA cell model	Degradation of extracellular matrix	Li et al. (2019g)
GAS5	Up	miR-144	mTOR	Cartilage tissue	knee joint	OA rat model	Cell proliferation and apoptosis	Ji et al. (2021)
	Up	miR-137	—	Blood, cartilage tissues	—	OA cell model	Cell proliferation and apoptosis	Gao et al. (2020)
	Up	miR-21	—	Cartilage tissue	knee joint	OA cell model	Cell proliferation and apoptosis	Song et al. (2014)
SAMD14-4	Up	—	COL1A1, COL1A2	Cartilage tissue	knee joint	OA cell model	inflammation	Zhang et al. (2019d)
KLF3-AS1	Up	miR-206	GIT1	Cartilage tissue	knee joint	OA mouse model	Cell proliferation and apoptosis	Liu et al. (2018)
CTBP1-AS2	Up	miR-130a	—	Cartilage tissue, Synovial fluid	knee joint, hip joint	OA cell model	Cell proliferation and apoptosis	Zhang et al. (2020d)
H19	Up	miR-140-5p	—	Cartilage tissue	knee joint	OA cell model	Degradation of extracellular matrix	Yang et al. (2020a)
	Up	miR-675	—	Cartilage tissue	knee joint	OA cell model	Degradation of extracellular matrix	Steck et al. (2012)
	Up	miR-106b-5p	TIMP2	Cartilage tissue, Synovial fluid	knee joint	OA cell model	Degradation of extracellular matrix	Tan et al. (2020)
	Up	miR-29a-3p	FOS	Astrocytes	—	OA rat model	inflammation	Yang et al. (2021b)
PART1	Up	miR-373-3p	SOX4	Cartilage tissue	—	OA cell model	Cell proliferation and apoptosis, Degradation of extracellular matrix	Zhu and Jiang, (2019)
LOXL1-AS1	Up	miR-423-5p	KDM5C	Cartilage tissue	knee joint, hip joint	OA cell model	Cell proliferation and apoptosis	Chen et al. (2020c)

(Continued on following page)

TABLE 2 | (Continued) Functional characterization of the lncRNAs in OA.

lncRNA	Expression	Target genes	Related genes	Tissue/cell source	Region	Model	Functions	Reference
MALAT1	Up	miR-145	ADAMTS5	Cartilage tissue	— —	OA cell model	Degradation of extracellular matrix	Liu et al. (2019a)
	Up	miR-146a-PI3K	— —	Cartilage tissue	— —	OA rat model	Degradation of extracellular matrix	Li et al. (2020d)
TUG1	Up	miR-195	MMP-13	Cartilage tissue	knee joint	OA cell model	Degradation of extracellular matrix	Tang et al. (2018b)
	Up	miR-320c	MMP-13	Cartilage tissue	knee joint	OA cell model	Degradation of extracellular matrix, Cell proliferation and apoptosis	Han and Liu, (2021)
XIST	Up	miR-211	CXCR4	Cartilage tissue	knee joint	OA cell model	Cell proliferation and apoptosis	Li et al. (2018b)
	Up	miR-149-5p	DNMT3A	Cartilage tissue	knee joint	OA cell model	Degradation of extracellular matrix	Liu et al. (2020c)
	Up	miR-1277-5p	— —	Cartilage tissue	knee joint, hip joint	OA rat model	Degradation of extracellular matrix	Wang et al. (2019d)
FOXO2-AS1	Up	miR-27a-3p	TLR4	Cartilage tissue	knee joint	OA cell model	Cell proliferation and apoptosis	Wang et al. (2019f)
	Up	miR-206	CCND1	Cartilage tissue	knee joint	OA cell model	Cell proliferation and apoptosis	Cao et al. (2018b)
NEAT1	Up	miR-543	PLA2G4A	Cartilage tissue	knee joint	OA cell model	Cell proliferation and apoptosis	Xiao et al. (2021)
	Up	miR-16-5p	— —	ATDC5	knee joint	OA cell model	Cell proliferation and apoptosis	Li et al. (2020a)
	Up	miR-193a-3p	SOX5	Cartilage tissue	knee joint	OA cell model	Degradation of extracellular matrix	Liu et al. (2020a)
IGHCγ1	Up	miR-6891-3p	TLR4	PBMCs	— —	OA cell model	inflammation	Zhang et al. (2020g)
LINC00511	Up	miR-150-5p	SP1	ATDC5	— —	OA cell model	Cell proliferation and apoptosis	Zhang et al. (2020m)
PVT1	Up	miR-488-3p	— —	Cartilage tissue	knee joint	OA cell model	Cell proliferation and apoptosis	Li et al. (2017c)
	Up	miR-27b-3p	TRAF3	Cartilage tissue	— —	OA cell model	inflammation	Lu et al. (2020)
	Up	miR-26b	— —	Cartilage tissue	knee joint	OA cell model	Degradation of extracellular matrix	Ding et al. (2020)
	Up	miR-149	— —	Cartilage tissue	knee joint	OA cell model	inflammation	Zhao et al. (2018)
	Up	miR-211-3p	— —	SW982 cells, Chondrocytes	— —	OA rat model	Cell proliferation and apoptosis	Xu et al. (2020)
CASC19	Up	miR-152-3p	DDX6	Cartilage tissue	— —	OA cell model	inflammation	Zhou et al. (2021a)
CHRF	Up	miR-146a	— —	ATDC5	— —	OA cell model	inflammation	Yu et al. (2019a)
HOTTIP	Up	miR-663a	— —	Cartilage tissue	knee joint	OA cell model	Cell proliferation and apoptosis	He et al. (2021b)
	Up	miR-455-3p	CCL3	Chondrocytes, Bone marrow	knee joint, hip joint	OA cell model	Degradation of extracellular matrix	Mao et al. (2019a)
DANCR	Up	miR-216a-5p	JAK2, STAT3	Cartilage tissue	knee joint	OA cell model	Cell proliferation and apoptosis	Zhang et al. (2018b)
	Up	miR-1275	MMP-13	SFMSCs, Synovial fluid	— —	OA cell model	Cell proliferation and apoptosis	Fang et al. (2019)
	Up	miR-577	— —	Cartilage tissue	knee joint, hip joint	OA cell model	Cell proliferation and apoptosis	Fan et al. (2018)
TNFSF10	Up	miR-376-3p	FGFR1	Cartilage tissue	knee joint	OA cell model	Cell proliferation and apoptosis	Huang et al. (2019a)
ARFRP1	Up	miR-15a-5p	TLR4	Cartilage tissue	knee joint	OA cell model	inflammation	Zhang et al. (2020b)
LINC00461	Up	miR-30a-5p	— —	Cartilage tissue	— —	OA cell model	Cell proliferation and apoptosis	Zhang et al. (2020n)
BLACAT1	Up	miR-142-5p	— —	BMSCs, Bone marrow	— —	OA rat model	Cell proliferation and apoptosis	Ji et al. (2020)

(Continued on following page)

TABLE 2 | (Continued) Functional characterization of the lncRNAs in OA.

lncRNA	Expression	Target genes	Related genes	Tissue/cell source	Region	Model	Functions	Reference
MCM3AP-AS1	Up	miR-1423p	HMGB1	Synovial fluid, chondrocyte	knee joint, hip joint	OA cell model	Cell proliferation and apoptosis	Gao et al. (2019b)
MCM3AP-AS1	Down	miR-138-5p	SIRT1	Cartilage tissue	knee joint	OA cell model	inflammation	Shi et al. (2021a)
PCAT-1	Up	miR-27b-3p	—	Cartilage tissue	knee joint, hip joint	OA cell model	Cell proliferation and apoptosis	Zhou et al. (2021c)
PMS2L2	Up	miR-203	—	ATDC5	—	OA cell model	inflammation	Li et al. (2019f)
LINC01534	Up	miR-140-5p	—	Cartilage tissue	knee joint	OA cell model	inflammation	Wei et al. (2019)
MIR22HG	Up	miR-9-3p	ADAMTS5	Cartilage tissue	knee joint	OA cell model	Degradation of extracellular matrix	Long et al. (2021)
PCGEM1	Up	miR-770	—	Synovial fluid	—	OA mouse model	Cell proliferation and apoptosis	Kang et al. (2016b)
DILC	Down	—	IL-6	Blood, Synovial fluid	—	OA cell model	inflammation	Huang et al. (2019b)
PACER	Down	—	HOTAIR	Blood	—	OA cell model	Cell proliferation and apoptosis	Jiang et al. (2019)
MIR4435-2HG	Down	—	—	Blood, Synovial fluid	knee joint	OA cell model	Cell proliferation and apoptosis	Xiao et al. (2019b)
HAND2-AS1	Down	—	IL-6	Blood, Synovial fluid	knee joint	OA cell model	inflammation	Si et al. (2021)
ANCR	Down	—	TGF- β 1	Blood	—	OA cell model	Cell proliferation and apoptosis	Li et al. (2019c)
ROR	Down	—	—	Cartilage tissue	knee joint	OA cell model	Cell proliferation and apoptosis	Yang et al. (2018c)
FAS-AS1	Down	—	—	Cartilage tissue	knee joint	OA cell model	Degradation of extracellular matrix	Zhu et al. (2018)
lncRNA-NR024118	Down	—	—	ATDC5	—	OA mouse model	inflammation	Mei et al. (2019)
FER1L4	Down	—	IL-6	Blood, Synovial fluid	—	OA cell model	inflammation	He et al. (2021a)
ZFAS1	Down	—	—	Cartilage tissue	knee joint	OA cell model	Cell proliferation and apoptosis	Ye et al. (2018)
MEG3	Down	—	VEGF	Cartilage tissue	knee joint	OA cell model	Degradation of extracellular matrix	Su et al. (2015)
	Down	—	TRIB2	Synovial fluid	knee joint	OA cell model	Cell proliferation and apoptosis	You et al. (2019)
	Down	miR-361-5p	FOXO1	Cartilage tissue	knee joint	OA cell model	Cell proliferation and apoptosis	Wang et al. (2019a)
	Down	miR-16	SMAD7	Cartilage tissue	—	OA rat model	Cell proliferation and apoptosis	Xu and Xu, (2017)
	Down	miR-93	TGFBR2	Cartilage tissue	knee joint	OA rat model	Degradation of extracellular matrix	Chen et al. (2019b)
MALAT-1	Down	—	—	Cartilage tissue	knee joint	OA rat model	Cell proliferation and apoptosis	Gao et al. (2019a)
SNHG7	Down	miR-34a-5p	SYVN1	Cartilage tissue	knee joint	OA cell model	Cell proliferation and apoptosis	Tian et al. (2020)
	Down	miR-214-5p	PPARGC1B	Cartilage tissue	knee joint	OA cell model	inflammation	Xu et al. (2021)
SNHG9	Down	miR-34a	—	Cartilage tissue, Synovial fluid	knee joint	OA cell model	Cell proliferation and apoptosis	Zhang et al. (2020e)
NKILA	Down	miR-145	SP1	Cartilage tissue	—	OA cell model	Cell proliferation and apoptosis	Xue et al. (2020)
SNHG5	Down	miR-10a-5p	H3F3B	Cartilage tissue	knee joint	OA cell model	Cell proliferation and apoptosis	Jiang et al. (2020a)
	Down	miR-26a	SOX2	Cartilage tissue	knee joint	OA cell model	Cell proliferation and apoptosis	Shen et al. (2018)
PART-1	Down	miR-590-3p	TGFBR2/Smad3	Cartilage tissue	knee joint, hip joint	OA cell model	Cell proliferation and apoptosis	Lu et al. (2019)

(Continued on following page)

TABLE 2 | (Continued) Functional characterization of the lncRNAs in OA.

lncRNA	Expression	Target genes	Related genes	Tissue/cell source	Region	Model	Functions	Reference
OIP5-AS1	Down	miR-29b-3p	PGRN	Cartilage tissue	knee joint	OA cell model	inflammation	Zhi et al. (2020)
	Down	miR-30a-5p	— —	Cartilage tissue	— —	OA cell model	Cell proliferation and apoptosis	Qin et al. (2021)
DNM3OS	Down	miR-126	CHON-001	Cartilage tissue	knee joint	OA cell model	Cell proliferation and apoptosis	
LINC00623	Down	miR-101	HRAS	Cartilage tissue	knee joint	OA cell model	Cell proliferation and apoptosis	Lü et al. (2020)
ATB	Down	miR-223	— —	ATDC5	— —	OA mouse model	inflammation	Ying et al. (2019)
HOTAIRM1-1	Down	miR-125b	BMPR2	Cartilage tissue	knee joint	OA cell model	Cell proliferation and apoptosis	Xiao et al. (2019c)
HULC	Down	miR-101	— —	Cartilage tissue	knee joint	OA cell model	inflammation	Chu et al. (2019)
SNHG15	Down	miR-141-3p	BCL2L13	Cartilage tissue	knee joint	OA rat model	Cell proliferation and apoptosis	Zhang et al. (2020k)
LINC00662	Down	miR-15b-5p	GPR120	Cartilage tissue	knee joint	OA rat model	inflammation	Lu and Zhou, (2020)
LUADT1	Down	miR-34a	SIRT1	Synovial fluid, chondrocytes	knee joint, hip joint	OA cell model	Cell proliferation and apoptosis	Ni et al. (2020b)
UFC1	Down	miR-34a	— —	Cartilage tissue	knee joint	OA cell model	Cell proliferation and apoptosis	Zhang et al. (2016c)

Abbreviations: PBMCs, peripheral blood mononuclear cells; MMP, metalloproteinases; WIF-1, Wnt inhibitory factor 1; FUT2, fucosyltransferase 2; KDM5C, lysine demethylase 5C; DNMT3A, DNA methyltransferase 3A; SIRT1, silent information regulator-1; TRIB2, Tribbles homolog 2; TGFBR2, transforming growth factor β receptor type II; KLF4, Krüppel-like factor 4; PPARGC1B, PPARG, coactivator 1 beta; H3F3B, H3 histone family 3B; Smad3, SMAD, family member 3; PGRN=progranulin; DNM3OS, dynamin 3 opposite strand; HRAS, Harvey rat sarcoma viral oncogene homolog; BMPR2, bone morphogenetic protein receptor 2.

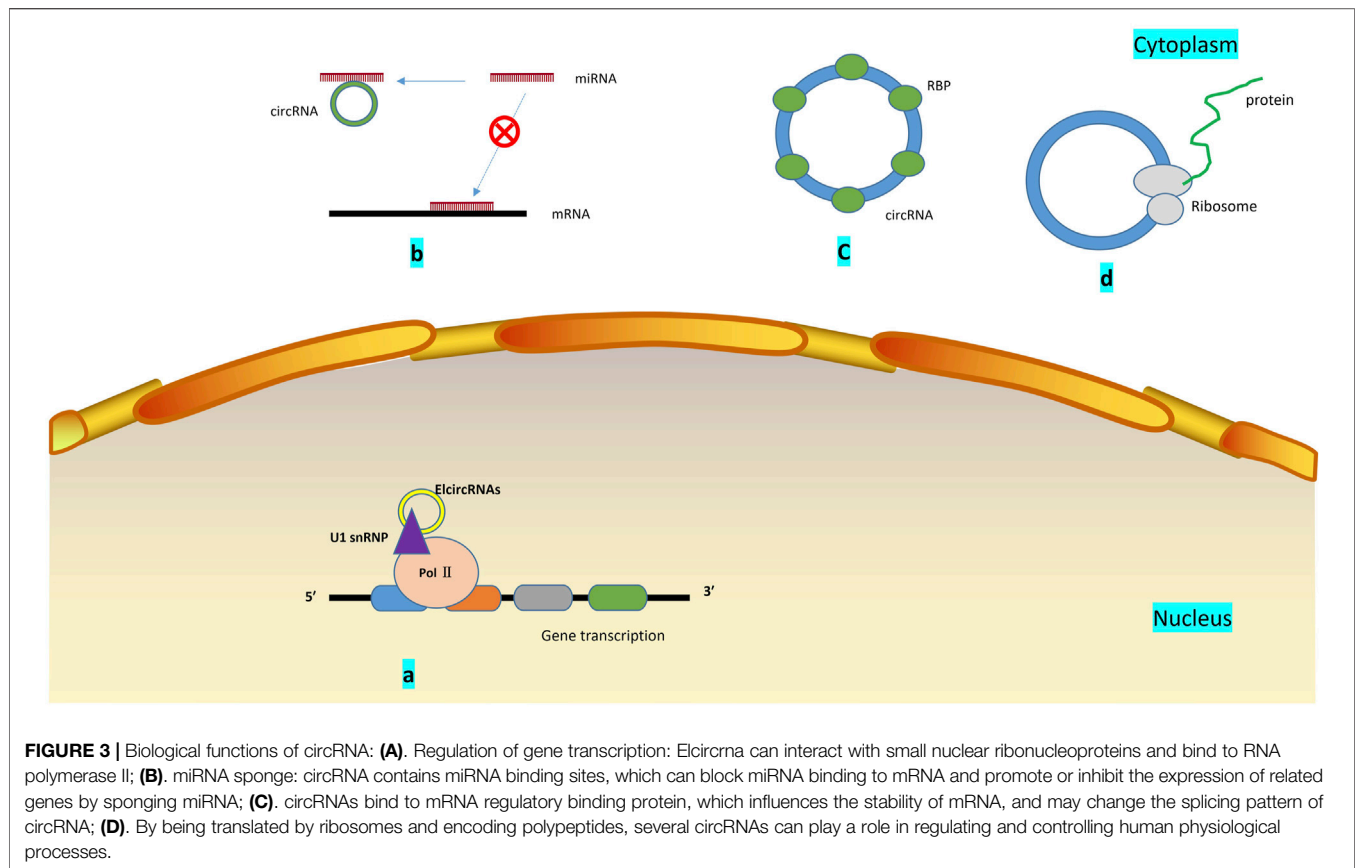
expression of lncRNA in OA cartilage and normal cartilage, and found 152 differentially expressed lncRNAs in OA cartilage. Compared with normal cartilage, 82 increased lncRNAs and 70 decreased lncRNAs were in OA cartilage. Using mRNA and lncRNA microarray analysis, Zhang et al. (2020a) found that 990 lncRNAs were different in OA chondrocytes compared with the control group: 666 up-regulated, 324 down-regulated. In addition, 546 mRNAs had a different expression: 419 up-regulated, 127 down-regulated. Six lncRNAs (ENST00000606283.1, ENST00000436872.1, ENST00000488584.1, ENST00000603682.1, XR-245446.2, and ENST00000605586.1) were tested by qPCR. The results were consistent with the test results. In summary, through the detection of lncRNA expression levels in the chondrocytes of OA patients and healthy individuals, we can finally find that there are differences in the expression of a variety of lncRNAs. In addition to the lncRNAs of appeal, several lncRNAs are closely related to the progress of OA, as shown in **Table 2**.

CIRC RNA AND OA

The circRNA molecule is in a closed-loop structure and is not affected by RNA exonuclease. They are mainly in the cytoplasm or stored in exosomes. They are stable and not easily degradable, and widely exist in many eukaryotes. circRNAs are formed by reverse splicing through nonclassical splicing. One model believes that in the transcription of pre-RNA, due to the partial folding of RNA, the originally nonadjacent exons are pulled closer, and

exon jumping occurs, resulting in the formation of circular RNA intermediates in the region to be crossed. Moreover, ring RNA molecules composed of exons are formed by lasso splicing. Another model suggests that the reverse complementary sequence located in the intron region leads to intron region pairing mediated reverse splicing, resulting in the formation of circular RNA molecules (Chen and Yang, 2015). To date, the biological functions of circRNAs that have been discovered mainly include interactions with miRNAs (Cao et al., 2019a), binding of regulatory proteins (Zang et al., 2020), transcription of regulatory genes (Zhang, 2020), and coding functions (Lei et al., 2020) (**Figure 3**). For example, circRNA.33186 increased MMP-13 expression by interacting with miR-127-5p to regulate cell proliferation and apoptosis (Zhou et al., 2019b).

Bipartite Network Projection allocates resources according to the known associations between different miRNAs and diseases, entirely using the similarity information of miRNA and diseases to predict various conditions accurately (Chen et al., 2018b). KATZ Measure is a graph-based calculation method, which converts the calculation of the similarity between lncRNA and diseases into the problem of similarity calculation between nodes in heterogeneous networks to predict the correlation between lncRNA and conditions. The integration of the two can recognize the association of circRNA with the disease (Chen, 2015). Through Bipartite Network Projection and KATZ Measure (Zhao et al., 2019a), many circRNAs related to diseases have been discovered, and circRNAs are involved in the diagnosis and treatment of atherosclerosis (Zhang et al., 2018a), cancer (Li et al., 2020f), cardiac hyperplasia (Li et al., 2020e), and other diseases. There



are many experimental studies related to circRNA and diseases, and the main research types are cell experiments or animal experiments. Through these experiments, we have found multiple action mechanisms of circRNA on various conditions. For example, circRNA_100367 acts as a signaling molecule that regulates esophageal squamous cell carcinoma through the Wnt3 signaling pathway (Liu et al., 2019b); circRNA_0016624 regulates gene-based expression of interest in osteoporosis patients *via* sponge miR-98 (Yang et al., 2020d); circRNA_100395 mitigates the progression of breast cancer by directly targeting MAPK6 (Yu et al., 2020).

In addition, several circRNAs participate in the development of OA and the OA of the abnormal expression in various tissues. For example, Xiao et al. (2019a) used illumina sequencing platform to detect circRNA expression in patients with mild and severe KOA. In this paper, 197 differentially expressed circRNAs were identified. Among them, the up-regulation amplitude of Hg38_circ_0007474 is the largest, and the down-regulation amplitude of hg38_circ_0000118 is the largest. Further analysis of the three circRNAs selected from hsa_circ_0045714, hsa_circ_0005567, and hsa_circ_0002485 found that all three circRNAs can inhibit the function of the corresponding miRNA by serving as a sponge for miRNAs and indirectly promote its downstream process, thereby participating in the development of OA. Wang et al. (2019h) used microarray analysis to screen for circRNA expression in healthy and KOA articular cartilage. They found 1,380 circRNAs differentially expressed in the articular cartilage of knee joints of

healthy individuals and patients with OA. Meanwhile, constructing a circRNA-miRNA network verified the ten most likely target genes related to circRNA. It was finally discovered that hsa_circRNA_003231 might be involved in the occurrence and progression of OA. Zhou et al. (2018e) established OA models in interleukin-1 β (IL1 β)-treated mouse articular chondrocytes (MACs) to study the expression and function of circRNAs in OA using new sequencing methods and bioinformatic analysis. Compared with the control group, 255 circRNAs were differentially expressed in MACs treated with IL-1 β : 119 up-regulated, 136 down-regulated. Mmu-circRNA-30365 and Mmu-circRNA36866 were two substantially different circRNAs, and their specific expression changes in patients with OA and normal individuals were verified by QRT-PCR. Liu et al. (2016) analyzed circRNA expression between OA and normal cartilage samples by hierarchical clustering analysis and found that compared with normal cartilage, 71 circRNAs were differentially expressed (16 were increased, and 55 were decreased) in OA cartilage. In this study, we focused on the research of circRNA-CER. We found that this circRNA could compete with MMP13 for miR-136 and participate in the degradation of the extracellular matrix of chondrocytes. The above examples fully prove that the expression levels of circRNA in OA patients and healthy individuals are different, and these differentially expressed circRNA has a special relationship with the progression of OA.

Several studies have reported the functions and mechanisms of several circRNAs in OA, but relevant studies are few. Zhou et al. (2018d) established rat OA models, predicted the function of

TABLE 3 | Functional characterization of the circRNAs in OA.

CircRNA	Expression	Target genes	Related genes	Tissue/cell source	Region	Model	Functions	Reference
CircVCAN	Up	--	--	Cartilage tissue	--	OA cell model	Cell proliferation and apoptosis	Ma et al. (2020)
hsa_circ_0000448	Up	--	--	Synovial tissues	Temporomandibular joint	OA cell model	Degradation of extracellular matrix	Hu et al. (2019c)
hsa_circ_0037658	Up	--	--	Cartilage tissue	--	OA cell model	Cell autophagy	Sui et al. (2021)
hsa_circ_0032131	Up	--	--	Blood	--	OA cell model	Cell proliferation and apoptosis	Wang et al. (2019g)
	Up	miR-502-5p	PRDX3	Cartilage tissue	--	OA rat model	Cell proliferation and apoptosis	Xu and Ma, (2021)
CircRNA.33186	Up	miR-127-5p	--	Cartilage tissue	knee joint	OA mouse model	Cell proliferation and apoptosis	Zhou et al. (2019b)
CircRNA_0092516	Up	miR-337-3p	PTEN	Cartilage tissue	knee joint	OA mouse model	Cell proliferation and apoptosis	Huang et al. (2021)
CircGCN1L1	Up	miR-330-3p	TNF- α	Synovial fluid	Temporomandibular joint	OA rat model	Cell proliferation and apoptosis	Zhu et al. (2020)
CircRNA-UBE2G1	Up	miR-373	HIF-1a	Cartilage tissue	knee joint	OA cell model	Cell proliferation and apoptosis	Chen et al. (2020b)
CircRNA HIPK3	Up	miR-124	SOX8	Cartilage tissue	--	OA cell model	Cell proliferation and apoptosis	Wu et al. (2020)
CircTMBIM6	Up	miR-27a	MMP13	Cartilage tissue	knee joint	OA cell model	Degradation of extracellular matrix	Bai et al. (2020b)
CircPSM3	Up	miRNA-296-5p	--	Cartilage tissue	--	OA cell model	Cell proliferation and apoptosis	Ni et al. (2020a)
hsa_circ_0005105	Up	miR-26a	NAMPT	Cartilage tissue	--	OA cell model	Degradation of extracellular matrix	Wu et al. (2017c)
CircRNA-CDR1as	Up	miRNA-641	--	Cartilage tissue	knee joint	OA cell model	Degradation of extracellular matrix	Zhang et al. (2020j)
CircRNA Atp9b	Up	miR-138-5p	--	Cartilage tissue	knee joint	OA mouse model	Degradation of extracellular matrix	Zhou et al. (2018d)
Circ_0116061	Up	miR-200b-3p	SMURF2	Cartilage tissue	knee joint	OA cell model	Cell proliferation and apoptosis, inflammation	Zheng et al. (2021)
Circ-BRWD1	Up	miR-1277	TRAF6	Cartilage tissue	knee joint	OA cell model	Cell proliferation and apoptosis, Degradation of extracellular matrix, inflammation	Guo et al. (2021)
Circ-SPG11	Up	miR-337-3p	ADAMTS5	Cartilage tissue	knee joint	OA cell model	Cell proliferation and apoptosis, Degradation of extracellular matrix, inflammation	Liu et al. (2021b)
Circ_SLC39A8	Up	miR-591	IRAK3	Cartilage tissue	knee joint	OA cell model	Cell proliferation and apoptosis, Degradation of extracellular matrix, inflammation	Yu et al. (2021)
Circ-PRKCH	Up	miR-140-3p	ADAM10	Cartilage tissue	knee joint	OA cell model	Degradation of extracellular matrix	Zhao et al. (2021)
CircCDH13	Up	miR-296-3p	PTEN	Cartilage tissue	hip joint	OA mouse model	Cell proliferation and apoptosis, Degradation of extracellular matrix	Zhou et al. (2021e)
Circ-IQGAP1	Up	miR-671-5p	TCF4	Cartilage tissue	knee joint, hip joint	OA cell model	Cell proliferation and apoptosis, Degradation of extracellular matrix, inflammation	Xi et al. (2021)
Circ_0136,474	Up	miR-127-5p	MMP-13	Cartilage tissue	knee joint	OA cell model	Cell proliferation and apoptosis	Li et al. (2019i)
Circ_RUNX2	Up	--	RUNX2	Blood	--	OA cell model	Degradation of extracellular matrix	Wang et al. (2021a)
CircRSU1	Up	miR-93-5p	MAP3K8	Cartilage tissue	knee joint	OA mouse model	Degradation of extracellular matrix	Yang et al. (2021c)
CircRNA3503	Down	--	--	Synovial fluid	--	OA cell model	Degradation of extracellular matrix	Tao et al. (2021)

(Continued on following page)

TABLE 3 | (Continued) Functional characterization of the circRNAs in OA.

CircRNA	Expression	Target genes	Related genes	Tissue/cell source	Region	Model	Functions	Reference
CircPDE4B	Down	— —	RIC8A, MID1	Cartilage tissue	— —	OA mouse model	Degradation of extracellular matrix	Shen et al. (2021)
CircSERPINE2	Down	miR-1271	— —	Cartilage tissue	— —	OA cell model	Degradation of extracellular matrix, Cell proliferation and apoptosis	Shen et al. (2019)
	Down	miR-495	TGFBR2	Cartilage tissue	knee joint	OA cell model	Cell proliferation and apoptosis	Zhang et al. (2020h)
CiRS-7	Down	miR-7	— —	Cartilage tissue	— —	OA rat model	Inflammation	Zhou et al. (2020a)
	Down	miR-7	— —	Blood	— —	OA cell model	Cell proliferation and apoptosis	Zhou et al. (2019a)
CircCDK14	Down	miR-125a-5p	Smad2	Cartilage tissue	knee joint	OA rabbit model	Cell proliferation and apoptosis	Shen et al. (2020a)
CircPDE4D	Down	miR-103a-3p	FGF18	Cartilage tissue	knee joint	OA mouse model	Degradation of extracellular matrix	Wu et al. (2021b)
CircRNA_0001236	Down	miR-3677-3p	Sox9	Bone marrow, Cartilage tissue	— —	OA mouse model	Degradation of extracellular matrix	Mao et al. (2021b)
CircRNA-9119	Down	miRNA-26a	PTEN	Cartilage tissue	— —	OA cell model	Cell proliferation and apoptosis	Chen et al. (2020a)
Hsa_circ_0005567	Down	miR-495	ATG14	Cartilage tissue	— —	OA cell model	Cell autophagy and apoptosis	Zhang et al. (2020f)
CircRNA-CER	Up	miR-136	MMP13	— —	knee joint	OA cell model	Degradation of extracellular matrix	Liu et al. (2016)
CircHYBID	Down	hsa-miR-29b-3p	TGF- β 1	Cartilage tissue	knee joint	OA cell model	Degradation of extracellular matrix	Liao et al. (2021)
CircADAMTS6	Down	miR-431-5p	— —	Cartilage tissue	— —	OA cell model	Cell proliferation and apoptosis	Fu et al. (2021)
Hsa_circ_0045714	Down	miR-193b	IGF1R	Cartilage tissue	knee joint	OA cell model	Cell proliferation and apoptosis	Li et al. (2017a)
Circ_0020093	Down	miR-23b	SPRY1	Cartilage tissue	— —	OA cell model	Degradation of extracellular matrix	Feng et al. (2021)
CircANKRD36	Down	miR-599	Cas21	Cartilage tissue	— —	OA cell model	Cell proliferation and apoptosis	Zhou et al. (2021b)
CircSLC7A2	Down	miR-4498	TIMP3	Cartilage tissue	— —	OA mouse model	Degradation of extracellular matrix, Cell proliferation and apoptosis, inflammation	Ni et al. (2021)

Abbreviations: TNF- α , tumor necrosis factor- α ; LEF1, lymphoid enhancer-binding factor 1; NAMPT, nicotinamide phosphoribosyltransferase; SMURF2, Smad ubiquitin regulatory factor 2; TRAF6, TNF, receptor-associated factor 6; ADAM10, a-disintegrin and metalloproteinase domain 10; PTEN, phosphatase and tensin homolog; MID1, midline 1; TGFBR2, transforming growth factor- β receptor 2; SPRY1, sprouty 1.

circRNA_ATP9b in rat knee chondrocytes through bioinformatic analysis, and finally found that circRNA_ATP9b regulated the degradation of extracellular matrix through sponge miR-138-5p, thereby controlling the progression of OA. Moreover, circRNA_ATP9b expression was increased, and miR-138-5p expression was down-regulated in IL-1 β -induced chondrocytes. circRNA_ATP9b regulated the expression of related genes by targeting miR-138-5p. Li et al. (2017a) analyzed the dual-luciferase reporter genes and found that the transcriptional activity of miR-193b can be inhibited by overexpression of hsa_circ_0045714. Overexpression of hsa_circ_0045714 can also up-regulate the expression of insulin-like growth factor 1 receptor (IGF1R) because IGF1R is a crucial target gene of miR-193b. It is associated with cell proliferation and apoptosis. Further studies on the progression of circRNA in OA are presented in **Table 3**.

INTERACTIONS BETWEEN LNCRNAs, MIRNAS AND MRNAS IN OA

Studies have shown that lncRNA-miRNA-mRNA axis plays a vital control effect in the progression of several diseases, such as cardiovascular disease and cancer (He et al., 2018; Wang et al., 2019c). The mechanisms of interaction of lncRNAs, miRNAs, and mRNAs in various diseases are as follows: 1) The structure of most lncRNAs is similar to mRNAs, and miRNAs binding to mRNAs can reduce the expression of lncRNAs. lncRNA and miRNA compete to bind the 3'-UTR of target gene mRNA, thereby indirectly inhibiting the interaction between miRNA and mRNA. For example, in Alzheimer's disease, the post-transcriptional regulation of BACE1 involves miR-485-5p, and the specific antisense transcription of BACE1 forms lncRNA-BACE1-As, which compete with lncRNA-BACE1-As to bind to the

lncRNAs-miRNAs-mRNAs axis in Cartilage tissue.

lncRNA	miRNA	Target
CIR↑	miR-130a	Bim
HOTAIR↑	miR-20b	PTEN
	miR-17-5p	FUT2
KLF3-AS1↑	miR-206	GIT1
H19↑	miR-106b-5p	TIMP2
PART1↑	miR-373-3p	SOX4
LOXL1-AS1↑	miR-423-5p	KDM5C
MALAT1↑	miR-145	ADAMTS5
TUG1↑	miR-195	MMP-13
	miR-320c	MMP-13
XIST↑	miR-211	CXCR4
	miR-149-5p	DNMT3A
FOXO2-AS1↑	miR-27a-3p	TLR4
	miR-206	CCND1
NEAT1↑	miR-543	PLA2G4A
	miR-193a-3p	SOX5
PVT1↑	miR-27b-3p	TRAF3
CASC19↑	miR-152-3p	DDX6
TNFSF10↑	miR-376-3p	FGFR1
ARFRP1↑	miR-15a-5p	TLR4
MEG3↓	miR-361-5p	FOXO1
	miR-16	SMAD7
	miR-93	TGFB2
SNHG7↓	miR-34a-5p	SYVN1
	miR-214-5p	PPARGC1B
SNHG5↓	miR-10a-5p	H3F3B
	miR-26a	SOX2
OIP5-AS1↓	miR-29b-3p	PGRN
HOTAIRM1-1↓	miR-125b	BMP2

lncRNAs-miRNAs-mRNAs axis in Synovial tissue.

lncRNA	miRNA	Target
DANCR↑	miR-1275	MMP-13

lncRNAs-miRNAs-mRNAs axis in blood.

lncRNA	miRNA	Target
H19↑	miR-29a-3p	FOS
IGHCγ1↑	miR-6891-3p	TLR4

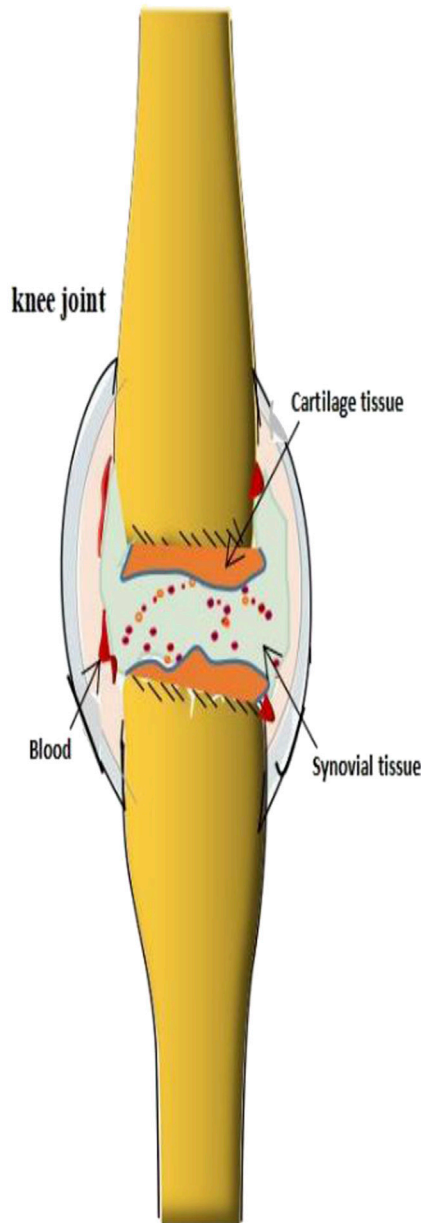


FIGURE 4 | lncRNA-miRNA-mRNA axis in OA. lncRNA can combine with miRNA to promote the expression of related target genes. PTEN = phosphatase and tensin homolog; FUT2 = fucosyltransferase 2; TIMP2 = tissue inhibitor of metalloproteinase 2; KDM5C = lysine demethylase 5C; DNMT3A = DNA methyltransferase 3A; TLR4 = toll-like receptor 4; CCND1 = cyclin D1; KLF4 = Krüppel-like factor 4; SYVN1 = synoviolin 1; PPARGC1B = PPARG coactivator 1 beta; H3F3B = H3 histone family 3B; PGRN = progranulin; DNMT3OS = dynamin 3 opposite strand; BMP2 = bone morphogenetic protein receptor 2.

binding sites of related mRNAs (Faghihi et al., 2010). 2) lncRNAs sponge miRNAs as competitive endogenous RNAs (ceRNAs). lncRNA molecules contain miRNA binding sites, which can bind

to miRNA, inhibit the interaction between miRNA and mRNA, improve the expression level of related mRNA, and regulate the expression of target genes. For example, Zhang et al. (2020l)

constructed a complete mRNA-lncRNA-miRNA ceRNA regulatory network; lncRNAs ENST00000326237.3, ENST00000399702.5, and ENST00000463727.1 were found to regulate related genes through competitive binding of the same miRNA has-miR-1260a. Kong et al. (2019) demonstrated that lncRNA—CDC6 can further regulate CDC6 expression through direct uptake of miR-215 as a ceRNA. Luan et al. (Luan and Wang, 2018) found that in cervical cancer, XLOC_006390 may act as ceRNA and bind with miR-331-3p and miR-338-3p, thus regulating the expression of genes related to cervical cancer. 3) miRNAs mediate the degradation of lncRNAs. For example, miRNA-150 is the target gene for lncRNA CASC11 in human plasma, and increased concentrations of miRNA-150 decrease the activity of lncRNA CASC11 (Luo et al., 2019b). 4) lncRNAs act as miRNAs precursors. For example, Tao et al. (2017) found that miR-869a and miR-160c could be clipped from lncRNAs npc83 and npc521. However, in OA, lncRNA mainly binds to miRNA as a competitive endogenous RNA (ceRNA), inhibiting its target genes' expression and regulating OA's progression by regulating cell proliferation, apoptosis, autophagy and extracellular matrix (ECM) degradation (Figure 4).

There are many examples where lncRNA functions as a binding of ceRNA to miRNA in OA. For example, Zhang et al. (2020m) took IL -1 β -induced OA chondrocytes as the research object to study the molecular mechanism of LINC00511 in regulating OA. The study found that the expression of LINC00511 was up-regulated, and the lncRNA could be used as a sponge of miR-150-5p and combined with 3'-UTR of transcription factor inhibit the proliferation of chondrocytes, promote apoptosis and degradation of ECM, and finally regulate OA. Liu et al. (2018) established an OA chondrocyte model induced by IL -1 β and an OA mouse model caused by collagenase. The experiments were performed *in vivo* and *in vitro* at two levels, and the cell state was examined by the CCK-8 method and flow cytometry. Studies have found that KLF3-AS1, as a ceRNA interacting with miR-206, promotes the expression of GIT1 and then promotes the proliferation of chondrocytes and inhibits apoptosis, ultimately alleviating the progression of OA. Likewise, Tian et al. (2020) studied the relationship between SNHG7, miR-34a-5p, and SYVN1 in human chondrocytes. It has been found that in OA tissues, SNHG7 is down-regulated, and SNHG7 can regulate SYVN1 by sponging miR-34a-5p, thereby promoting cell proliferation and inhibiting apoptosis and autophagy. In addition, studies have found that lncRNA XIST is up-regulated in OA articular cartilage. Like a sponge, XIST regulates the target proteins miR-211, miR-17-5p, miR-149-5p, and miR-27b-3p, thereby promoting the proliferation and apoptosis of chondrocytes and finally inducing OA (Li et al., 2018b; Zhu et al., 2021). These results suggest that lncRNAs can act as miRNA sponges in the interaction of lncRNAs, miRNAs, and mRNA in OA.

Interactions Between circRNAs, miRNAs and mRNAs in OA

Currently, research on the mechanism of interactions between circRNAs, miRNAs, and mRNAs is growing (Peng et al., 2020).

circRNAs and miRNAs are closely related to the expression of disease-related mRNAs, and interactions between circRNAs, miRNAs, and mRNAs may be involved in the pathological mechanism of OA (Figure 5). At present, research on the interaction mechanism of circRNAs, miRNAs, and mRNAs is not comprehensive. Relevant research has three main types: 1) circRNAs interact with miRNAs. miRNA interacts with mRNA to inhibit mRNA expression. circRNA molecules contain miRNA binding sites, which can sponge miRNA and release miRNA's inhibitory effect on target genes. For example, Hansen et al. (2013) found that CiRS-7 could sponge miR-7, inhibit the binding of miR-7 and its target genes, and indirectly promote the expression of related mRNA. Other research suggests that hsa_circ_101237, like a sponge for miRNA490-3p, promotes the expression of its target gene MAPK1. In patients with lung cancer, hsa_circ_101237 expression is up-regulated, thereby promoting the proliferation, differentiation, and migration of lung cancer cells (Zhang et al., 2020o). 2) circRNA can regulate the splicing of pre-mRNA, thus affecting the production of protein. 3) circRNA can pair with targeted mRNA directly through local bases. As the circRNA molecule is rich in miRNA binding sites, the circ RNA molecule functions as a miRNA sponge in cells so that the inhibition effect of the miRNA on target genes can be released, and the expression level of the target genes is increased. Therefore, in OA, the interaction mechanism of circRNA, miRNA, and mRNA is mainly circRNA sponging miRNA (Kulcheski et al., 2016). Many circRNA expressions in OA have been changed, and OA is regulated by adsorbing a specific miRNA. For example, hsa_circ_0005567 is down-regulated in OA patients and, by competitively binding to miR-495, terminates Atg14 expression and eventually induces human chondrocyte apoptosis (Zhang et al., 2020f); hsa_circ_0032131 is up-regulated in the human body, and knocking out hsa_circ_0032131 inactivates the STAT3 signaling pathway by sponging miR-502-5p, thereby relieving symptoms of OA in the body (Xu and Ma, 2021); circPSM3 is up-regulated in OA chondrocytes, and its low expression promotes chondrogenesis and OA development. circPSM3 can inhibit OA chondrogenesis by sponging miRNA-296-5p (Ni et al., 2020a). All these results prove the mechanism of circRNA sponge miRNA in osteoarthritis.

Other studies have found interactions between circRNA, miRNA, and mRNA. Shen et al. (2020a) established a rabbit model of OA and studied the role and mechanism of circCDK14 in OA by quantitative reverse transcriptase-polymerase chain reaction (RT-PCR) and other methods. miR-125a-5p is a downstream target protein of circCDK14, while Smad2 is an mRNA target protein of circCDK14. The mechanism of action of circCDK14 in OA is to down-regulate the expression of Smad2 through the sponge action of miR-125a-5p, resulting in dysfunction of the TGF- β signaling pathway. Chen et al. (2020a) studied the expression and action mechanism of circRNA-9119 in OA patients using bioinformatics prediction and double luciferase reporter gene detection. They found that the expression of circRNA-9119 was down-regulated to provide a sponge effect on miR-26a. At the same time, miR-26a targeted the 3'-UTR of PTEN to promote cell proliferation and inhibit

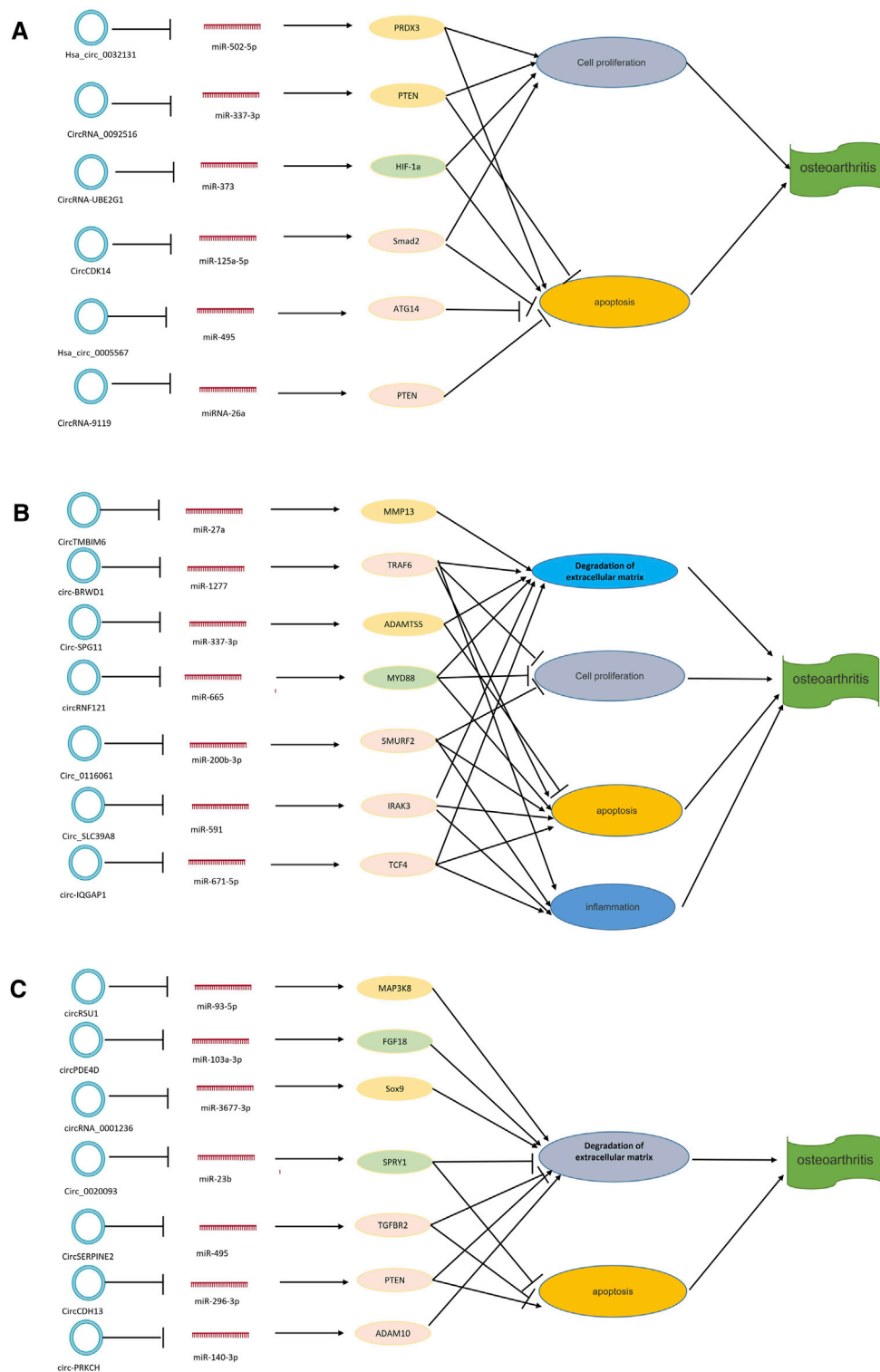


FIGURE 5 | circRNA-miRNA-mRNA axis in OA. circRNAs can combine with miRNAs to promote the expression of related target genes. **(A)** circRNAs that play a role in cell proliferation and apoptosis. **(B)** circRNAs that play a role in degradation of the extracellular matrix and apoptosis. **(C)** circRNAs that play a role in degradation of the extracellular matrix, cell proliferation, apoptosis, and inflammation. NAMPT = nicotinamide phosphoribosyltransferase; MMP13 = matrix metalloproteinase.

apoptosis. Their results all demonstrated the mechanism of the interaction between circRNAs, miRNAs, and mRNAs in OA.

CLINICAL IMPLICATIONS

At present, the incidence of OA is very high, and its pathogenesis is still unclear. Studying the specific pathological process and molecular pathway of OA is of great clinical significance (Duan et al., 2020). First, ncRNA can be used to diagnose OA. The expression of many ncRNAs between patients with OA and normal individuals have remarkable differences, which can be seen in humans and animals. For example, Huang et al. (2019c) showed that miRNA-204 and miRNA-211 are decreased in OA, resulting in Runx2 accumulation in multiple types of joint cells and elevated OA markers, and leading to total joint degeneration. Second, several ncRNAs are associated with the prognosis of OA. Rousseau et al. (2020) took the miRNAs in the serum of female patients with KOA as the research objects. He first made a preliminary screening of the research objects through next-generation sequencing and then further analyzed the research objects through RT-QPCR. He found that miR-146A-5p is up-regulated in patients with mild OA, and the prognosis of OA caused by the up-regulation of miRNA is relatively good. In addition, the increase of miR-186-5p in an individual means that the individual might have the imaging changes of OA in the past 4 years, which could be prevented in advance to avoid the occurrence of OA as much as possible. Finally, several ncRNAs can be used for the treatment of OA. Several new drugs can be developed to promote or inhibit several ncRNAs, or change the pathway of action of ncRNA to treat OA. For example, miR-93 is down-regulated in mice with OA and lipopolysaccharide-treated chondrocytes, and acts directly on TLR4 to exert biological effects. miR-93 regulates OA by inhibiting the TLR4/NF- κ B pathway, lipopolysaccharide-induced inflammation, and apoptosis. In patients with OA and down-regulation of miR-93, corresponding drugs can be developed to promote its up-regulation and inhibit the aggravation of OA (Ding et al., 2019). These studies indicate that ncRNA has great potential for clinical use in OA. At present,

most of the tissue comes from cartilage and is found in the knee joint, and the chondrocytes are cultured to construct the OA cell model. Further research is needed, and more clinical trials must be explored to find biomarkers associated with OA while developing the immense potential of ncRNA.

CONCLUSION

In recent years, ncRNAs have become one of the most widely studied fields in the development of OA. However, the studies on the regulation of miRNA, lncRNA, and circRNA in diseases and their use as indicators for diagnosis or treatment of OA are still in the early stages, and the mechanism of action of OA, which may involve multiple signaling pathways, is still unclear. This study reviews the interactions between lncRNA/circRNA and miRNA in OA. Through high-throughput sequencing technologies such as microarray analysis and RNA sequencing, the findings reveal that a large number of miRNA, lncRNA, and circRNA are dysregulated in patients with OA, and the clinical trials related to ncRNA and OA are summarized. The present research progress of ncRNA in the prevention, diagnosis, and treatment of OA is illustrated, which provides a basis for the treatment of OA by ncRNA in the future.

AUTHOR CONTRIBUTIONS

X-AZ and X-QW: conceptualization, project administration, and funding acquisition. HK, X-AZ, and X-QW: writing—review and editing. All authors contributed to the article and approved the submitted version.

FUNDING

This work was supported by the Innovative Talents Support Program for Universities of Liaoning Province, No. WR2019024; Shanghai Frontiers Science Research Base of Exercise and Metabolic Health.

REFERENCES

- Abouheif, M. M., Nakasa, T., Shibuya, H., Niimoto, T., Kongcharoensombat, W., and Ochi, M. (2010). Silencing microRNA-34a Inhibits Chondrocyte Apoptosis in a Rat Osteoarthritis Model *In Vitro*. *Rheumatology* 49 (11), 2054–2060. doi:10.1093/rheumatology/keq247
- Abramoff, B., and Caldera, F. E. (2020). Osteoarthritis. *Med. Clin. North America* 104 (2), 293–311. doi:10.1016/j.mcna.2019.10.007
- An, Y., Wan, G., Tao, J., Cui, M., Zhou, Q., and Hou, W. (2020). Down-regulation of microRNA-203a Suppresses IL-1 β -induced Inflammation and Cartilage Degradation in Human Chondrocytes through Smad3 Signaling. *Biosci. Rep.* 40 (3), BSR20192723. doi:10.1042/BSR20192723
- Bai, Y., Chen, K., Zhan, J., and Wu, M. (2020a). miR-122/SIRT1 axis Regulates Chondrocyte Extracellular Matrix Degradation in Osteoarthritis. *Biosci. Rep.* 40 (6), BSR20191908. doi:10.1042/BSR20191908
- Bai, Z. M., Kang, M. M., Zhou, X. F., and Wang, D. (2020b). CircTMBIM6 Promotes Osteoarthritis-Induced Chondrocyte Extracellular Matrix Degradation via miR-27a/MMP13 axis. *Eur. Rev. Med. Pharmacol. Sci.* 24 (15), 7927–7936. doi:10.26355/eurrev_202008_22475
- Bao, Z., Yang, Z., Huang, Z., Zhou, Y., Cui, Q., and Dong, D. (2019). LncRNADisease 2.0: an Updated Database of Long Non-coding RNA-Associated Diseases. *Nucleic Acids Res.* 47 (D1), D1034–D1037. doi:10.1093/nar/gky905
- Bijlsma, J. W., Berenbaum, F., and Lefeber, F. P. (2011). Osteoarthritis: an Update with Relevance for Clinical Practice. *The Lancet* 377 (9783), 2115–2126. doi:10.1016/S0140-6736(11)60243-2
- Boehme, K. A., and Rolauffs, B. (2018). Onset and Progression of Human Osteoarthritis—Can Growth Factors, Inflammatory Cytokines, or Differential miRNA Expression Concomitantly Induce Proliferation, ECM Degradation, and Inflammation in Articular Cartilage? *Int. J. Mol. Sci.* 19 (8), 2282. doi:10.3390/ijms19082282
- Budd, E., de Andrés, M. C., Sanchez-Elsner, T., and Oreffo, R. O. C. (2017). MiR-146b Is Down-Regulated during the Chondrogenic Differentiation of Human Bone Marrow Derived Skeletal Stem Cells and Up-Regulated in Osteoarthritis. *Sci. Rep.* 7, 46704. doi:10.1038/srep46704

- Burr, D. B., and Gallant, M. A. (2012). Bone Remodelling in Osteoarthritis. *Nat. Rev. Rheumatol.* 8 (11), 665–673. doi:10.1038/nrrheum.2012.130
- Cao, J., Han, X., Qi, X., Jin, X., and Li, X. (2018a). miR-204-5p Inhibits the Occurrence and Development of Osteoarthritis by Targeting Runx2. *Int. J. Mol. Med.* 42 (5), 2560–2568. doi:10.3892/ijmm.2018.3811
- Cao, L., Wang, Y., Wang, Q., and Huang, J. (2018b). LncRNA FOXD2-AS1 Regulates Chondrocyte Proliferation in Osteoarthritis by Acting as a Sponge of miR-206 to Modulate CCND1 Expression. *Biomed. Pharmacother.* 106, 1220–1226. doi:10.1016/j.biopha.2018.07.048
- Cao, M., Zhang, L., Wang, J.-H., Zeng, H., Peng, Y., Zou, J., et al. (2019a). Identifying circRNA-Associated-cerRNA Networks in Retinal Neovascularization in Mice. *Int. J. Med. Sci.* 16 (10), 1356–1365. doi:10.7150/ijms.35149
- Cao, X., Duan, Z., Yan, Z., Li, Y., Li, L., Sun, J., et al. (2019b). miR-195 Contributes to Human Osteoarthritis via Targeting PTHrP. *J. Bone Miner. Metab.* 37 (4), 711–721. doi:10.1007/s00774-018-0973-5
- Cao, Z., Liu, W., Qu, X., Bi, H., Sun, X., Yu, Q., et al. (2020). miR-296-5p Inhibits IL-1 β -induced Apoptosis and Cartilage Degradation in Human Chondrocytes by Directly Targeting TGF- β 1/CTGF/p38MAPK Pathway. *Cell Cycle* 19 (12), 1443–1453. doi:10.1080/15384101.2020.1750813
- Castaldi, A., Zaglia, T., Di Mauro, V., Carullo, P., Viggiani, G., Borile, G., et al. (2014). MicroRNA-133 Modulates the β 1-Adrenergic Receptor Transduction Cascade. *Circ. Res.* 115 (2), 273–283. doi:10.1161/CIRCRESAHA.115.303252
- Chang, T., Xie, J., Li, H., Li, D., Liu, P., and Hu, Y. (2016). MicroRNA-30a Promotes Extracellular Matrix Degradation in Articular Cartilage via downregulation of Sox9. *Cell Prolif.* 49 (2), 207–218. doi:10.1111/cpr.12246
- Chang, Z. k., Meng, F. g., Zhang, Z. q., Mao, G. p., Huang, Z. y., Liao, W. m., et al. (2018). MicroRNA-193b-3p Regulates Matrix Metalloproteinase 19 Expression in Interleukin-1 β -induced Human Chondrocytes. *J. Cel. Biochem.* 119 (6), 4775–4782. doi:10.1002/jcb.26669
- Chesleschi, S., Tenti, S., Mondanelli, N., Corallo, C., Barbarino, M., Giannotti, S., et al. (2019). MicroRNA-34a and MicroRNA-181a Mediate Visfatin-Induced Apoptosis and Oxidative Stress via NF-Kb Pathway in Human Osteoarthritic Chondrocytes. *Cells* 8 (8), 874. doi:10.3390/cells8080874
- Chen, C., and Xu, Y. (2021). Long Noncoding RNA LINC00671 Exacerbates Osteoarthritis by Promoting ONECUT2-Mediated Smurf2 Expression and Extracellular Matrix Degradation. *Int. Immunopharmacology* 90, 106846. doi:10.1016/j.intimp.2020.106846
- Chen, C., Yin, P., Hu, S., Sun, X., and Li, B. (2020a). Circular RNA-9119 Protects IL-1 β -treated Chondrocytes from Apoptosis in an Osteoarthritis Cell Model by Intercepting the microRNA-26a/PTEN axis. *Life Sci.* 256, 117924. doi:10.1016/j.lfs.2020.117924
- Chen, G., Liu, T., Yu, B., Wang, B., and Peng, Q. (2020b). CircRNA-UBE2G1 Regulates LPS-Induced Osteoarthritis through miR-373/HIF-1 α axis. *Cell Cycle* 19 (13), 1696–1705. doi:10.1080/15384101.2020.1772545
- Chen, H., Yang, J., and Tan, Z. (2019a). Upregulation of microRNA-9-5p Inhibits Apoptosis of Chondrocytes through Downregulating Tnc in Mice with Osteoarthritis Following Tibial Plateau Fracture. *J. Cel Physiol* 234 (12), 23326–23336. doi:10.1002/jcp.28900
- Chen, J., and Wu, X. (2019). MicroRNA-103 Contributes to Osteoarthritis Development by Targeting Sox6. *Biomed. Pharmacother.* 118, 109186. doi:10.1016/j.biopha.2019.109186
- Chen, K., Fang, H., and Xu, N. (2020c). LncRNA LOXL1-AS1 Is Transcriptionally Activated by JUND and Contributes to Osteoarthritis Progression via Targeting the miR-423-5p/KDM5C axis. *Life Sci.* 258, 118095. doi:10.1016/j.lfs.2020.118095
- Chen, K., Zhu, H., Zheng, M.-Q., and Dong, Q.-R. (2019b). LncRNA MEG3 Inhibits the Degradation of the Extracellular Matrix of Chondrocytes in Osteoarthritis via Targeting miR-93/TGFBR2 Axis. *Cartilage* 2019, 194760351985575. doi:10.1177/1947603519855759
- Chen, L.-L., and Yang, L. (2015). Regulation of circRNA Biogenesis. *RNA Biol.* 12 (4), 381–388. doi:10.1080/15476286.2015.1020271
- Chen, L., Li, Q., Wang, J., Jin, S., Zheng, H., Lin, J., et al. (2017). MiR-29b-3p Promotes Chondrocyte Apoptosis and Facilitates the Occurrence and Development of Osteoarthritis by Targeting PGRN. *J. Cel. Mol. Med.* 21 (12), 3347–3359. doi:10.1111/jcmm.13237
- Chen, Q., Wu, S., Wu, Y., Chen, L., and Pang, Q. (2018a). MiR-149 Suppresses the Inflammatory Response of Chondrocytes in Osteoarthritis by Down-Regulating the Activation of TAK1/NF-Kb. *Biomed. Pharmacother.* 101, 763–768. doi:10.1016/j.biopha.2018.02.133
- Chen, R., Ye, B., Xie, H., Huang, Y., Wu, Z., Wu, H., et al. (2020d). miR-129-3p Alleviates Chondrocyte Apoptosis in Knee Joint Fracture-Induced Osteoarthritis through CPEB1. *J. Orthop. Surg. Res.* 15 (1), 552. doi:10.1186/s13018-020-02070-1
- Chen, S., and Li, B. (2020). MiR-128-3p Post-Transcriptionally Inhibits WISP1 to Suppress Apoptosis and Inflammation in Human Articular Chondrocytes via the PI3K/AKT/NF- κ B Signaling Pathway. *Cel Transpl.* 29, 096368972093913. doi:10.1177/0963689720939131
- Chen, X., Guo, D.-Y., Yin, T.-L., and Yang, J. (2021). Non-Coding RNAs Regulate Placental Trophoblast Function and Participate in Recurrent Abortion. *Front. Pharmacol.* 12, 646521. doi:10.3389/fphar.2021.646521
- Chen, X. (2015). KATZLDA: KATZ Measure for the lncRNA-Disease Association Prediction. *Sci. Rep.* 5, 16840. doi:10.1038/srep16840
- Chen, X., Shi, Y., Xue, P., Ma, X., Li, J., and Zhang, J. (2020e). Mesenchymal Stem Cell-Derived Exosomal microRNA-136-5p Inhibits Chondrocyte Degeneration in Traumatic Osteoarthritis by Targeting ELF3. *Arthritis Res. Ther.* 22 (1), 256. doi:10.1186/s13075-020-02325-6
- Chen, X., Xie, D., Wang, L., Zhao, Q., You, Z.-H., and Liu, H. (2018b). BNPMDA: Bipartite Network Projection for MiRNA-Disease Association Prediction. *Bioinformatics (Oxford, England)* 34 (18), 3178–3186. doi:10.1093/bioinformatics/bty333
- Chen, X., Zhou, Z., and Zhao, Y. (2018c). ELLPMDA: Ensemble Learning and Link Prediction for miRNA-Disease Association Prediction. *RNA Biol.* 15 (6), 1–12. doi:10.1080/15476286.2018.1460016
- Chen, Y., Zhang, L., Li, E., Zhang, G., Hou, Y., Yuan, W., et al. (2020f). Long-chain Non-coding RNA HOTAIR Promotes the Progression of Osteoarthritis via Sponging miR-20b/PTEN axis. *Life Sci.* 253, 117685. doi:10.1016/j.lfs.2020.117685
- Cheng, F., Hu, H., Sun, K., Yan, F., and Geng, Y. (2020). miR-455-3p Enhances Chondrocytes Apoptosis and Inflammation by Targeting COL2A1 in the In Vitro Osteoarthritis Model. *Biosci. Biotechnol. Biochem.* 84 (4), 695–702. doi:10.1080/09168451.2019.1690974
- Chu, P., Wang, Q., Wang, Z., and Gao, C. (2019). Long Non-coding RNA Highly Up-Regulated in Liver Cancer Protects Tumor Necrosis Factor-Alpha-Induced Inflammatory Injury by Down-Regulation of microRNA-101 in ATDC5 Cells. *Int. Immunopharmacology* 72, 148–158. doi:10.1016/j.intimp.2019.04.004
- Correia de Sousa, M., Gjorgjieva, M., Dolicka, D., Sobolewski, C., and Foti, M. (2019). Deciphering miRNAs' Action through miRNA Editing. *Int. J. Mol. Sci.* 20 (24), 6249. doi:10.3390/ijms20246249
- Cui, X., Wang, S., Cai, H., Lin, Y., Zheng, X., Zhang, B., et al. (2016). Overexpression of microRNA-634 Suppresses Survival and Matrix Synthesis of Human Osteoarthritis Chondrocytes by Targeting PIK3R1. *Sci. Rep.* 6, 23117. doi:10.1038/srep23117
- Dai, L., Zhang, X., Hu, X., Liu, Q., Man, Z., Huang, H., et al. (2015). Silencing of miR-101 Prevents Cartilage Degradation by Regulating Extracellular Matrix-Related Genes in a Rat Model of Osteoarthritis. *Mol. Ther.* 23 (8), 1331–1340. doi:10.1038/mt.2015.61
- Dai, Y., Liu, S., Xie, X., Ding, M., Zhou, Q., and Zhou, X. (2019). MicroRNA-31 Promotes C-hondrocyte Proliferation by Targeting C-X-C Motif Chemokine Ligand 12. *Mol. Med. Rep.* 19 (3), 2231–2237. doi:10.3892/mmr.2019.9859
- Ding, L.-B., Li, Y., Liu, G.-Y., Li, T.-H., Li, F., Guan, J., et al. (2020). Long Non-coding RNA PVT1, a Molecular Sponge of miR-26b, Is Involved in the Progression of Hyperglycemia-Induced Collagen Degradation in Human Chondrocytes by Targeting CTGF/TGF- β Signal Ways. *Innate Immun.* 26 (3), 204–214. doi:10.1177/1753425919881778
- Ding, Y., Wang, L., Zhao, Q., Wu, Z., and Kong, L. (2019). MicroRNA-93 Inhibits Chondrocyte Apoptosis and Inflammation in Osteoarthritis by Targeting the TLR4/NF- κ B Signaling Pathway. *Int. J. Mol. Med.* 43 (2), 779–790. doi:10.3892/ijmm.2018.4033
- Dou, P., He, Y., Yu, B., and Duan, J. (2020). Downregulation of microRNA-29b by DNMT3B Decelerates Chondrocyte Apoptosis and the Progression of Osteoarthritis via PTHLH/CDK4/RUNX2 axis. *Aging* 13 (5), 7676–7690. doi:10.18632/aging.103778
- Duan, L., Duan, D., Wei, W., Sun, Z., Xu, H., Guo, L., et al. (2019a). MiR-19b-3p Attenuates IL-1 β Induced Extracellular Matrix Degradation and Inflammatory

- Injury in Chondrocytes by Targeting GRK6. *Mol. Cel Biochem* 459 (1-2), 205–214. doi:10.1007/s11010-019-03563-2
- Duan, L., Liang, Y., Xu, X., Wang, J., Li, X., Sun, D., et al. (2020). Noncoding RNAs in Subchondral Bone Osteoclast Function and Their Therapeutic Potential for Osteoarthritis. *Arthritis Res. Ther.* 22 (1), 279. doi:10.1186/s13075-020-02374-x
- Duan, Z.-X., Huang, P., Tu, C., Liu, Q., Li, S.-Q., Long, Z.-L., et al. (2019b). MicroRNA-15a-5p Regulates the Development of Osteoarthritis by Targeting PTHrP in Chondrocytes. *Biomed. Research International* 2019, 1–11. doi:10.1155/2019/3904923
- Esteller, M. (2011). Non-coding RNAs in Human Disease. *Nat. Rev. Genet.* 12 (12), 861–874. doi:10.1038/nrg3074
- Faghihi, M. A., Zhang, M., Huang, J., Modarresi, F., Van der Brug, M. P., Nalls, M. A., et al. (2010). Evidence for Natural Antisense Transcript-Mediated Inhibition of microRNA Function. *Genome Biol.* 11 (5), R56. doi:10.1186/gb-2010-11-5-r56
- Fan, X., Yuan, J., Xie, J., Pan, Z., Yao, X., Sun, X., et al. (2018). Long Non-protein Coding RNA DANCER Functions as a Competing Endogenous RNA to Regulate Osteoarthritis Progression via miR-577/SphK2 axis. *Biochem. biophysical Res. Commun.* 500 (3), 658–664. doi:10.1016/j.bbrc.2018.04.130
- Fan, Z., Liu, Y., Shi, Z., Deng, K., Zhang, H., Li, Q., et al. (2020). MiR-155 Promotes Interleukin-1 β -induced Chondrocyte Apoptosis and Catabolic Activity by Targeting PIK3R1-mediated PI3K/Akt Pathway. *J. Cel Mol Med* 24 (15), 8441–8451. doi:10.1111/jcmm.15388
- Fang, P., Zhang, L. X., Hu, Y., Zhang, L., and Zhou, L. W. (2019). Long Non-coding RNA DANCER Induces Chondrogenesis by Regulating the miR-1275/MMP-13 axis in Synovial Fluid-Derived Mesenchymal Stem Cells. *Eur. Rev. Med. Pharmacol. Sci.* 23 (23), 10459–10469. doi:10.26355/eurrev_201912_19685
- Felson, D. T., Lawrence, R. C., Dieppe, P. A., Hirsch, R., Helmick, C. G., Jordan, J. M., et al. (2000). Osteoarthritis: New Insights. Part 1: the Disease and its Risk Factors. *Ann. Intern. Med.* 133 (8), 635–646. doi:10.7326/0003-4819-133-8-200010170-00016
- Feng, M., Jing, L., Cheng, J., An, S., Huang, J., and Yan, Q. (2021). Circ_0020093 Ameliorates IL-1 β -induced Apoptosis and Extracellular Matrix Degradation of Human Chondrocytes by Upregulating SPRY1 via Targeting miR-23b. *Mol. Cel Biochem* 476 (10), 3623–3633. doi:10.1007/s11010-021-04186-2
- Fu, Q., Li, L., Wang, B., Wu, J., Li, H., Han, Y., et al. (2021). CircADAMTS6/miR-431-5p axis Regulate Interleukin-1 β Induced Chondrocyte Apoptosis. *J. Gene Med.* 23 (2), e3304. doi:10.1002/jgm.3304
- Fu, X., Dong, B., Tian, Y., Lefebvre, P., Meng, Z., Wang, X., et al. (2015). MicroRNA-26a Regulates Insulin Sensitivity and Metabolism of Glucose and Lipids. *J. Clin. Invest.* 125 (6), 2497–2509. doi:10.1172/JCI75438
- Gabler, J., Ruetze, M., Kynast, K. L., Grossner, T., Diederichs, S., and Richter, W. (2015). Stage-Specific miRs in Chondrocyte Maturation: Differentiation-dependent and Hypertrophy-Related miR Clusters and the miR-181 Family. *Tissue Eng. A* 21 (23-24), 2840–2851. doi:10.1089/ten.TEA.2015.0352
- Gao, G. C., Cheng, X. G., Wei, Q. Q., Chen, W. C., and Huang, W. Z. (2019a). Long Noncoding RNA MALAT-1 Inhibits Apoptosis and Matrix Metabolism Disorder in Interleukin-1 β -induced Inflammation in Articular Chondrocytes via the JNK Signaling Pathway. *J. Cel Biochem* 120 (10), 17167–17179. doi:10.1002/jcb.28977
- Gao, S. T., Yu, Y. M., Wan, L. P., Liu, Z. M., and Lin, J. X. (2020). LncRNA GAS5 Induces Chondrocyte Apoptosis by Down-Regulating miR-137. *Eur. Rev. Med. Pharmacol. Sci.* 24 (21), 10984–10991. doi:10.26355/eurrev_202011_23582
- Gao, Y., Zhao, H., and Li, Y. (2019b). LncRNA MCM3AP-AS1 Regulates miR-142-3p/HMGB1 to Promote LPS-Induced Chondrocyte Apoptosis. *BMC Musculoskelet. Disord.* 20 (1), 605. doi:10.1186/s12891-019-2967-4
- Ge, F.-X., Li, H., and Yin, X. (2017). Upregulation of microRNA-125b-5p Is Involved in the Pathogenesis of Osteoarthritis by Downregulating SYVN1. *Oncol. Rep.* 37 (4), 2490–2496. doi:10.3892/or.2017.5475
- Glyn-Jones, S., Palmer, A. J. R., Agricola, R., Price, A. J., Vincent, T. L., Weinans, H., et al. (2015). Osteoarthritis. *The Lancet* 386 (9991), 376–387. doi:10.1016/S0140-6736(14)60802-3
- Guo, Y., Tian, L., Du, X., and Deng, Z. (2020). MiR-203 Regulates Estrogen Receptor α and Cartilage Degradation in IL-1 β -stimulated Chondrocytes. *J. Bone Miner Metab.* 38 (3), 346–356. doi:10.1007/s00774-019-01062-4
- Guo, Z., Wang, H., Zhao, F., Liu, M., Wang, F., Kang, M., et al. (2021). Exosomal Circ-BRWD1 Contributes to Osteoarthritis Development through the Modulation of miR-1277/TRAF6 axis. *Arthritis Res. Ther.* 23 (1), 159. doi:10.1186/s13075-021-02541-8
- Han, H., and Liu, L. (2021). Long Noncoding RNA TUG1 Regulates Degradation of Chondrocyte Extracellular Matrix via miR-320c/MMP-13 axis in Osteoarthritis. *Open Life Sci.* 16 (1), 384–394. doi:10.1515/biol-2021-0037
- Hansen, T. B., Jensen, T. I., Clausen, B. H., Bramsen, J. B., Finsen, B., Damgaard, C. K., et al. (2013). Natural RNA Circles Function as Efficient microRNA Sponges. *Nature* 495 (7441), 384–388. doi:10.1038/nature11993
- He, B., and Jiang, D. (2020). HOTAIR-induced Apoptosis Is Mediated by Sponging miR-130a-3p to Repress Chondrocyte Autophagy in Knee Osteoarthritis. *Cell Biol Int* 44 (2), 524–535. doi:10.1002/cbin.11253
- He, J.-H., Han, Z.-P., Zou, M.-X., Wang, L., Lv, Y. B., Zhou, J. B., et al. (2018). Analyzing the LncRNA, miRNA, and mRNA Regulatory Network in Prostate Cancer with Bioinformatics Software. *J. Comput. Biol.* 25 (2), 146–157. doi:10.1089/cmb.2016.0093
- He, J., Wang, L., Ding, Y., Liu, H., and Zou, G. (2021a). LncRNA FER1L4 Is Dysregulated in Osteoarthritis and Regulates IL-6 Expression in Human Chondrocyte Cells. *Sci. Rep.* 11 (1), 13032. doi:10.1038/s41598-021-92474-8
- He, J., Zhang, J., and Wang, D. (2017). Down-regulation of microRNA-216b Inhibits IL-1 β -induced Chondrocyte Injury by Up-Regulation of Smad3. *Biosci. Rep.* 37 (2), BSR20160588. doi:10.1042/BSR20160588
- He, X., and Deng, L. (2021). Potential of miR-25-3p in protection of Chondrocytes: Emphasis on Osteoarthritis. *Folia Histochem. Cytobiol.* 59 (1), 30–39. doi:10.5603/FHC.a2021.0004
- He, X., Gao, K., Lu, S., and Wu, R. (2021b). LncRNA HOTTIP Leads to Osteoarthritis Progression via Regulating miR-663a/Fyn-Related Kinase axis. *BMC Musculoskelet. Disord.* 22 (1), 67. doi:10.1186/s12891-020-03861-7
- Hu, G., Zhao, X., Wang, C., Geng, Y., Zhao, J., Xu, J., et al. (2017). MicroRNA-145 Attenuates TNF- α -Driven Cartilage Matrix Degradation in Osteoarthritis via Direct Suppression of MKK4. *Cell Death Dis* 8 (10), e3140. doi:10.1038/cddis.2017.522
- Hu, J., Wang, Z., Pan, Y., Ma, J., Miao, X., Qi, X., et al. (2018a). MiR-26a and miR-26b Mediate Osteoarthritis Progression by Targeting FUT4 via NF-Kb Signaling Pathway. *Int. J. Biochem. Cel Biol.* 94, 79–88. doi:10.1016/j.biocel.2017.12.003
- Hu, J., Wang, Z., Shan, Y., Pan, Y., Ma, J., and Jia, L. (2018b). Long Non-coding RNA HOTAIR Promotes Osteoarthritis Progression via miR-17-5p/FUT2/ β -Catenin axis. *Cel Death Dis* 9 (7), 711. doi:10.1038/s41419-018-0746-z
- Hu, S., Mao, G., Zhang, Z., Wu, P., Wen, X., Liao, W., et al. (2019a). MicroRNA-320c Inhibits Development of Osteoarthritis through Downregulation of Canonical Wnt Signaling Pathway. *Life Sci.* 228, 242–250. doi:10.1016/j.lfs.2019.05.011
- Hu, S., Zhao, X., Mao, G., Zhang, Z., Wen, X., Zhang, C., et al. (2019b). MicroRNA-455-3p Promotes TGF- β Signaling and Inhibits Osteoarthritis Development by Directly Targeting PAK2. *Exp. Mol. Med.* 51 (10), 1–13. doi:10.1038/s12276-019-0322-3
- Hu, Y., Zhu, H., Bu, L., and He, D. (2019c). Expression Profile of Circular RNA S in TMJ Osteoarthritis Synovial Tissues and Potential Functions of Hsa_circ_0000448 with Specific Back-Spliced junction. *Am. J. Transl Res.* 11 (9), 5357–5374.
- Huang, B., Yu, H., Li, Y., Zhang, W., and Liu, X. (2019a). Upregulation of Long Noncoding TNFSF10 Contributes to Osteoarthritis Progression through the miR-376-3p/FGFR1 axis. *J. Cel Biochem* 120 (12), 19610–19620. doi:10.1002/jcb.29267
- Huang, J., Liu, L., Yang, J., Ding, J., and Xu, X. (2019b). LncRNA DILC Is Downregulated in Osteoarthritis and Regulates IL-6 Expression in Chondrocytes. *J. Cel Biochem* 120 (9), 16019–16024. doi:10.1002/jcb.28880
- Huang, J., Zhao, L., Fan, Y., Liao, L., Ma, P. X., Xiao, G., et al. (2019c). The microRNAs miR-204 and miR-211 Maintain Joint Homeostasis and Protect against Osteoarthritis Progression. *Nat. Commun.* 10 (1), 2876. doi:10.1038/s41467-019-10753-5
- Huang, T., Wang, J., Zhou, Y., Zhao, Y., Hang, D., and Cao, Y. (2019d). LncRNA CASC2 Is Up-Regulated in Osteoarthritis and Participates in the Regulation of IL-17 Expression and Chondrocyte Proliferation and Apoptosis. *Biosci. Rep.* 39 (5), BSR20182454. doi:10.1042/BSR20182454
- Huang, Y. (2018). The Novel Regulatory Role of lncRNA-miRNA-mRNA axis in Cardiovascular Diseases. *J. Cel Mol Med* 22 (12), 5768–5775. doi:10.1111/jcmm.13866

- Huang, Z., Ma, W., Xiao, J., Dai, X., and Ling, W. (2021). CircRNA_0092516 Regulates Chondrocyte Proliferation and Apoptosis in Osteoarthritis through the miR-337-3p/PTEN axis. *J. Biochem.* 169 (4), 467–475. doi:10.1093/jb/mvaa119
- Huang, Z., Zhang, N., Ma, W., Dai, X., and Liu, J. (2017). MiR-337-3p Promotes Chondrocytes Proliferation and Inhibits Apoptosis by Regulating PTEN/AKT axis in Osteoarthritis. *Biomed. Pharmacother.* 95, 1194–1200. doi:10.1016/j.biopha.2017.09.016
- Hwang, H. S., Park, S. J., Lee, M. H., and Kim, H. A. (2017). MicroRNA-365 Regulates IL-1 β -induced Catabolic Factor Expression by Targeting HIF-2 α in Primary Chondrocytes. *Sci. Rep.* 7 (1), 17889. doi:10.1038/s41598-017-18059-6
- Iacona, J. R., and Lutz, C. S. (2019). miR-146a-5p: Expression, Regulation, and Functions in Cancer. *WIREs RNA* 10 (4), e1533. doi:10.1002/wrna.1533
- Ji, Q., Qiao, X., Liu, Y., and Wang, D. (2021). Expression of Long-Chain Noncoding RNA GAS5 in Osteoarthritis and its Effect on Apoptosis and Autophagy of Osteoarthritis Chondrocytes. *Histol. Histopathol* 36 (4), 475–484. doi:10.14670/HH-18-312
- Ji, Y., Fang, Q. Y., Wang, S. N., Zhang, Z. W., Hou, Z. J., Li, J. N., et al. (2020). LncRNA BLACAT1 Regulates Differentiation of Bone Marrow Stromal Stem Cells by Targeting miR-142-5p in Osteoarthritis. *Eur. Rev. Med. Pharmacol. Sci.* 24 (6), 2893–2901. doi:10.26355/eurev_202003_20653
- Jiang, H., Pang, H., Wu, P., Cao, Z., Li, Z., and Yang, X. (2020a). LncRNA SNHG5 Promotes Chondrocyte Proliferation and Inhibits Apoptosis in Osteoarthritis by Regulating miR-10a-5p/H3F3B axis. *Connect. Tissue Res.* 2020, 1–10. doi:10.1080/03008207.2020.1825701
- Jiang, L., Sun, X., and Kong, H. (2020b). microRNA-9 Might Be a Novel Protective Factor for Osteoarthritis Patients. *Hereditas* 157 (1), 15. doi:10.1186/s41065-020-00128-y
- Jiang, M., Liu, J., Luo, T., Chen, Q., Lu, M., and Meng, D. (2019). LncRNA PACER Is Down-Regulated in Osteoarthritis and Regulates Chondrocyte Apoptosis and lncRNA HOTAIR Expression. *Biosci. Rep.* 39 (6), BSR20190404. doi:10.1042/BSR20190404
- Jin, Z., Ren, J., and Qi, S. (2020). Human Bone Mesenchymal Stem Cells-Derived Exosomes Overexpressing microRNA-26a-5p Alleviate Osteoarthritis via Down-Regulation of PTGS2. *Int. Immunopharmacology* 78, 105946. doi:10.1016/j.intimp.2019.105946
- Kang, L., Yang, C., Song, Y., Liu, W., Wang, K., Li, S., et al. (2016a). MicroRNA-23a-3p Promotes the Development of Osteoarthritis by Directly Targeting SMAD3 in Chondrocytes. *Biochem. biophysical Res. Commun.* 478 (1), 467–473. doi:10.1016/j.bbrc.2016.06.071
- Kang, Y., Song, J., Kim, D., Ahn, C., Park, S., Chun, C.-H., et al. (2016b). PCGEM1 Stimulates Proliferation of Osteoarthritic Synoviocytes by Acting as a Sponge for miR-770. *J. Orthop. Res.* 34 (3), 412–418. doi:10.1002/jor.23046
- Karlsen, T. A., de Souza, G. A., Ødegaard, B., Engebretsen, L., and Brinchmann, J. E. (2016). microRNA-140 Inhibits Inflammation and Stimulates Chondrogenesis in a Model of Interleukin 1 β -Induced Osteoarthritis. *Mol. Ther. - Nucleic Acids* 5 (10), e373. doi:10.1038/mtna.2016.64
- Karlsen, T. A., Jakobsen, R. B., Mikkelsen, T. S., and Brinchmann, J. E. (2014). microRNA-140 Targets RALA and Regulates Chondrogenic Differentiation of Human Mesenchymal Stem Cells by Translational Enhancement of SOX9 and ACAN. *Stem Cell Dev.* 23 (3), 290–304. doi:10.1089/scd.2013.0209
- Ko, J.-Y., Lee, M. S., Lian, W.-S., Weng, W.-T., Sun, Y.-C., Chen, Y.-S., et al. (2017). MicroRNA-29a Counteracts Synovitis in Knee Osteoarthritis Pathogenesis by Targeting VEGF. *Sci. Rep.* 7 (1), 3584. doi:10.1038/s41598-017-03616-w
- Kong, X., Duan, Y., Sang, Y., Li, Y., Zhang, H., Liang, Y., et al. (2019). LncRNA-CDC6 Promotes Breast Cancer Progression and Function as ceRNA to Target CDC6 by Sponging microRNA-215. *J. Cel Physiol* 234 (6), 9105–9117. doi:10.1002/jcp.27587
- Kopp, F., and Mendell, J. T. (2018). Functional Classification and Experimental Dissection of Long Noncoding RNAs. *Cell* 172 (3), 393–407. doi:10.1016/j.cell.2018.01.011
- Kostopoulou, F., Malizos, K. N., Papatheanasiou, I., and Tsezou, A. (2015). MicroRNA-33a Regulates Cholesterol Synthesis and Cholesterol Efflux-Related Genes in Osteoarthritic Chondrocytes. *Arthritis Res. Ther.* 17, 42. doi:10.1186/s13075-015-0556-y
- Kulcheski, F. R., Christoff, A. P., and Margis, R. (2016). Circular RNAs Are miRNA Sponges and Can Be Used as a New Class of Biomarker. *J. Biotechnol.* 238, 42–51. doi:10.1016/j.jbiotec.2016.09.011
- Lawrence, T. (2009). The Nuclear Factor NF- κ B Pathway in Inflammation. *Cold Spring Harbor Perspect. Biol.* 1 (6), a001651. doi:10.1101/cshperspect.a001651
- Lei, J., Fu, Y., Zhuang, Y., Zhang, K., and Lu, D. (2019). miR-382-3p Suppressed IL-1 β Induced Inflammatory Response of Chondrocytes via the TLR4/MyD88/NF- κ B Signaling Pathway by Directly Targeting CX43. *J. Cel Physiol* 234 (12), 23160–23168. doi:10.1002/jcp.28882
- Lei, M., Zheng, G., Ning, Q., Zheng, J., and Dong, D. (2020). Translation and Functional Roles of Circular RNAs in Human Cancer. *Mol. Cancer* 19 (1), 30. doi:10.1186/s12943-020-1135-7
- Li, B.-F., Zhang, Y., Xiao, J., Wang, F., Li, M., Guo, X.-Z., et al. (2017a). Hsa_circ_0045714 Regulates Chondrocyte Proliferation, Apoptosis and Extracellular Matrix Synthesis by Promoting the Expression of miR-193b Target Gene IGF1R. *Hum. Cel.* 30 (4), 311–318. doi:10.1007/s13577-017-0177-7
- Li, C., Hu, Q., Chen, Z., Shen, B., Yang, J., Kang, P., et al. (2018a). MicroRNA-140 Suppresses Human Chondrocytes Hypertrophy by Targeting SMAD1 and Controlling the Bone Morphogenetic Protein Pathway in Osteoarthritis. *Am. J. Med. Sci.* 355 (5), 477–487. doi:10.1016/j.amjms.2018.01.004
- Li, D., Sun, Y., Wan, Y., Wu, X., and Yang, W. (2020a). LncRNA NEAT1 Promotes Proliferation of Chondrocytes via Down-regulation of miR-16-5p in Osteoarthritis. *J. Gene Med.* 22 (9), e3203. doi:10.1002/jgm.3203
- Li, F., Yao, J., Hao, Q., and Duan, Z. (2019a). miRNA-103 Promotes Chondrocyte Apoptosis by Down-Regulation of Sphingosine Kinase-1 and Ameliorates PI3K/AKT Pathway in Osteoarthritis. *Biosci. Rep.* 39 (10), BSR20191255. doi:10.1042/BSR20191255
- Li, H.-Z., Xu, X.-H., Lin, N., Wang, D.-W., Lin, Y.-M., Su, Z.-Z., et al. (2020b). Overexpression of miR-10a-5p Facilitates the Progression of Osteoarthritis. *Aging* 12 (7), 5948–5976. doi:10.18632/aging.102989
- Li, H., Li, Z., Pi, Y., Chen, Y., Mei, L., Luo, Y., et al. (2020c). MicroRNA-375 Exacerbates Knee Osteoarthritis through Repressing Chondrocyte Autophagy by Targeting ATG2B. *Aging* 12 (8), 7248–7261. doi:10.18632/aging.103073
- Li, H., Xie, S., Li, H., Zhang, R., and Zhang, H. (2020d). LncRNA MALAT1 Mediates Proliferation of LPS Treated-Articular Chondrocytes by Targeting the miR-146a-PI3K/Akt/mTOR axis. *Life Sci.* 254, 116801. doi:10.1016/j.lfs.2019.116801
- Li, H., Xu, J.-D., Fang, X.-H., Zhu, J.-N., Yang, J., Pan, R., et al. (2020e). Circular RNA circRNA_000203 Aggravates Cardiac Hypertrophy via Suppressing miR-26b-5p and miR-140-3p Binding to Gata4. *Cardiovasc. Res.* 116 (7), 1323–1334. doi:10.1093/cvr/cvz215
- Li, H., Yang, H. H., Sun, Z. G., Tang, H. B., and Min, J. K. (2019b). Whole-transcriptome Sequencing of Knee Joint Cartilage from Osteoarthritis Patients. *Bone Jt. Res.* 8 (7), 290–303. doi:10.1302/2046-3758.87.BJR-2018-0297.R1
- Li, J., Huang, J., Dai, L., Yu, D., Chen, Q., Zhang, X., et al. (2012). miR-146a, an IL-1 β Responsive miRNA, Induces Vascular Endothelial Growth Factor and Chondrocyte Apoptosis by Targeting Smad4. *Arthritis Res. Ther.* 14 (2), R75. doi:10.1186/ar3798
- Li, L., Lv, G., Wang, B., and Kuang, L. (2018b). The Role of lncRNA XIST/miR-211 axis in Modulating the Proliferation and Apoptosis of Osteoarthritis Chondrocytes through CXCR4 and MAPK Signaling. *Biochem. biophysical Res. Commun.* 503 (4), 2555–2562. doi:10.1016/j.bbrc.2018.07.015
- Li, L., Yang, C., Liu, X., Yang, S., Ye, S., Jia, J., et al. (2015). Elevated Expression of microRNA-30b in Osteoarthritis and its Role in ERG Regulation of Chondrocyte. *Biomed. Pharmacother.* 76, 94–99. doi:10.1016/j.biopha.2015.10.014
- Li, Q., Zhang, Z., Guo, S., Tang, G., Lu, W., and Qi, X. (2019c). LncRNA ANCR Is Positively Correlated with Transforming Growth Factor- β 1 in Patients with Osteoarthritis. *J. Cel Biochem* 120 (9), 14226–14232. doi:10.1002/jcb.28881
- Li, W., Zhao, S., Yang, H., Zhang, C., Kang, Q., Deng, J., et al. (2019d). Potential Novel Prediction of TMJ-OA: MiR-140-5p Regulates Inflammation through Smad/TGF β Signaling. *Front. Pharmacol.* 10, 15. doi:10.3389/fphar.2019.00015
- Li, X., Huang, T. L., Zhang, G. D., Jiang, J. T., and Guo, P. Y. (2019e). LncRNA ANRIL Impacts the Progress of Osteoarthritis via Regulating Proliferation and Apoptosis of Osteoarthritis Synoviocytes. *Eur. Rev. Med. Pharmacol. Sci.* 23 (22), 9729–9737. doi:10.26355/eurev_201911_19535
- Li, X., Ding, J., Wang, X., Cheng, Z., and Zhu, Q. (2020f). NUDT21 Regulates circRNA Cyclization and ceRNA Crosstalk in Hepatocellular Carcinoma. *Oncogene* 39 (4), 891–904. doi:10.1038/s41388-019-1030-0

- Li, X., Yu, M., Chen, L., Sun, T., Wang, H., Zhao, L., et al. (2019f). RETRACTED: LncRNA PMS2L2 Protects ATDC5 Chondrocytes against Lipopolysaccharide-Induced Inflammatory Injury by Sponging miR-203. *Life Sci.* 217, 283–292. doi:10.1016/j.lfs.2018.12.020
- Li, Y.-F., Li, S.-H., Liu, Y., and Luo, Y.-T. (2017b). Long Noncoding RNA CIR Promotes Chondrocyte Extracellular Matrix Degradation in Osteoarthritis by Acting as a Sponge for Mir-27b. *Cell Physiol Biochem* 43 (2), 602–610. doi:10.1159/000480532
- Li, Y., Li, S., Luo, Y., Liu, Y., and Yu, N. (2017c). LncRNA PVT1 Regulates Chondrocyte Apoptosis in Osteoarthritis by Acting as a Sponge for miR-488-3p. *DNA Cel. Biol.* 36 (7), 571–580. doi:10.1089/dna.2017.3678
- Li, Y., Li, Z., Li, C., Zeng, Y., and Liu, Y. (2019g). Long Noncoding RNA TM1P3 Is Involved in Osteoarthritis by Mediating Chondrocyte Extracellular Matrix Degradation. *J. Cel Biochem* 120 (8), 12702–12712. doi:10.1002/jcb.28539
- Li, Y., Zhou, D., Ren, Y., Zhang, Z., Guo, X., Ma, M., et al. (2019h). Mir223 Restrains Autophagy and Promotes CNS Inflammation by Targeting ATG16L1. *Autophagy* 15 (3), 478–492. doi:10.1080/15548627.2018.1522467
- Li, Z., Cheng, J., and Liu, J. (2020g). Baicalin Protects Human OA Chondrocytes against IL-1 β -Induced Apoptosis and ECM Degradation by Activating Autophagy via MiR-766-3p/AIFM1 Axis. *Drug Des. Devel Ther.* 14, 2645–2655. doi:10.2147/DDDT.S255823
- Li, Z., Meng, D., Li, G., Xu, J., Tian, K., and Li, Y. (2016). Overexpression of microRNA-210 Promotes Chondrocyte Proliferation and Extracellular Matrix Deposition by Targeting HIF-3 α in Osteoarthritis. *Mol. Med. Rep.* 13 (3), 2769–2776. doi:10.3892/mmr.2016.4878
- Li, Z., Yuan, B., Pei, Z., Zhang, K., Ding, Z., Zhu, S., et al. (2019i). Circ_0136474 and MMP-13 Suppressed Cell Proliferation by Competitive Binding to miR-127-5p in Osteoarthritis. *J. Cel Mol Med* 23 (10), 6554–6564. doi:10.1111/jcmm.14400
- Lian, W.-S., Ko, J.-Y., Wu, R.-W., Sun, Y.-C., Chen, Y.-S., Wu, S.-L., et al. (2018). MicroRNA-128a Represses Chondrocyte Autophagy and Exacerbates Knee Osteoarthritis by Disrupting Atg12. *Cel Death Dis* 9 (9), 919. doi:10.1038/s41419-018-0994-y
- Liang, Q., Asila, A., Deng, Y., Liao, J., Liu, Z., and Fang, R. (2021). Osteopontin-induced lncRNA HOTAIR Expression Is Involved in Osteoarthritis by Regulating Cell Proliferation. *BMC Geriatr.* 21 (1), 57. doi:10.1186/s12877-020-01993-y
- Liang, Y., Duan, L., Xiong, J., Zhu, W., Liu, Q., Wang, D., et al. (2016). E2 Regulates MMP-13 via Targeting miR-140 in IL-1 β -induced Extracellular Matrix Degradation in Human Chondrocytes. *Arthritis Res. Ther.* 18 (1), 105. doi:10.1186/s13075-016-0997-y
- Liang, Z.-J., Zhuang, H., Wang, G.-X., Li, Z., Zhang, H.-T., Yu, T.-Q., et al. (2012). MiRNA-140 Is a Negative Feedback Regulator of MMP-13 in IL-1 β -stimulated Human Articular Chondrocyte C28/I2 Cells. *Inflamm. Res.* 61 (5), 503–509. doi:10.1007/s00011-012-0438-6
- Liao, H.-X., Zhang, Z.-H., Chen, H.-L., Huang, Y.-M., Liu, Z.-L., and Huang, J. (2021). CircHYBID Regulates Hyaluronan Metabolism in Chondrocytes via Hsa-miR-29b-3p/TGF- β 1 axis. *Mol. Med.* 27 (1), 56. doi:10.1186/s10020-021-00319-x
- Lim, Y., Wright, J. A., Attema, J. L., Gregory, P. A., Bert, A. G., Smith, E., et al. (2013). Epigenetic Modulation of the miR-200 Family Is Associated with Transition to a Breast Cancer Stem Cell-like State. *J. Cel. Sci.* 126 (Pt 10), 2256–2266. doi:10.1242/jcs.122275
- Lin, Z., Tian, X. Y., Huang, X. X., He, L. L., and Xu, F. (2019). microRNA-186 Inhibition of PI3K-AKT Pathway via SPP1 Inhibits Chondrocyte Apoptosis in Mice with Osteoarthritis. *J. Cel Physiol* 234 (5), 6042–6053. doi:10.1002/jcp.27225
- Litwic, A., Edwards, M. H., Dennison, E. M., and Cooper, C. (2013). Epidemiology and burden of Osteoarthritis. *Br. Med. Bull.* 105, 185–199. doi:10.1093/bmb/lds038
- Liu, B., Li, J., and Cairns, M. J. (2014a). Identifying miRNAs, Targets and Functions. *Brief. Bioinformatics* 15 (1), 1–19. doi:10.1093/bib/bbs075
- Liu, C., Ren, S., Zhao, S., and Wang, Y. (2019a). LncRNA MALAT1/MiR-145 Adjusts IL-1 β -Induced Chondrocytes Viability and Cartilage Matrix Degradation by Regulating ADAMTS5 in Human Osteoarthritis. *Yonsei Med. J.* 60 (11), 1081–1092. doi:10.3349/ymj.2019.60.11.1081
- Liu, F., Liu, X., Yang, Y., Sun, Z., Deng, S., Jiang, Z., et al. (2020a). NEAT1/miR-193a-3p/SOX5 axis Regulates Cartilage Matrix Degradation in Human Osteoarthritis. *Cel Biol Int* 44 (4), 947–957. doi:10.1002/cbin.11291
- Liu, H., and Luo, J. (2019). miR-211-5p Contributes to Chondrocyte Differentiation by Suppressing Fibulin-4 Expression to Play a Role in Osteoarthritis. *J. Biochem.* 166 (6), 495–502. doi:10.1093/jb/mvz065
- Liu, J., Liu, Y., Wang, F., and Liang, M. (2021a). miR-204: Molecular Regulation and Role in Cardiovascular and Renal Diseases. *Hypertension* 78 (2), 270–281. doi:10.1161/HYPERTENSIONAHA.121.14536
- Liu, J., Xue, N., Guo, Y., Niu, K., Gao, L., Zhang, S., et al. (2019b). CircRNA_100367 Regulated the Radiation Sensitivity of Esophageal Squamous Cell Carcinomas through miR-217/Wnt3 Pathway. *Aging* 11 (24), 12412–12427. doi:10.18632/aging.102580
- Liu, Q., Zhang, X., Dai, L., Hu, X., Zhu, J., Li, L., et al. (2014b). Long Noncoding RNA Related to Cartilage Injury Promotes Chondrocyte Extracellular Matrix Degradation in Osteoarthritis. *Arthritis Rheumatol.* 66 (4), 969–978. doi:10.1002/art.38309
- Liu, Q., Zhang, X., Hu, X., Dai, L., Fu, X., Zhang, J., et al. (2016). Circular RNA Related to the Chondrocyte ECM Regulates MMP13 Expression by Functioning as a MiR-136 'Sponge' in Human Cartilage Degradation. *Sci. Rep.* 6, 22572. doi:10.1038/srep22572
- Liu, W., Zha, Z., and Wang, H. (2019c). Upregulation of microRNA-27a Inhibits Synovial Angiogenesis and Chondrocyte Apoptosis in Knee Osteoarthritis Rats through the Inhibition of PLK2. *J. Cel Physiol* 234 (12), 22972–22984. doi:10.1002/jcp.28858
- Liu, X. C., Xu, L., Cai, Y. L., Zheng, Z. Y., Dai, E. N., and Sun, S. (2020b). MiR-1207-5p/CX3CR1 axis Regulates the Progression of Osteoarthritis via the Modulation of the Activity of NF- κ B Pathway. *Int. J. Rheum. Dis.* 23 (8), 1057–1065. doi:10.1111/1756-185X.13898
- Liu, X., Liu, L., Zhang, H., Shao, Y., Chen, Z., Feng, X., et al. (2019d). MiR-146b Accelerates Osteoarthritis Progression by Targeting Alpha-2-Macroglobulin. *Aging* 11 (16), 6014–6028. doi:10.18632/aging.102160
- Liu, Y., Li, Q., Gao, Z., Lei, F., and Gao, X. (2021b). Circ-SPG11 Knockdown Hampers IL-1 β -induced Osteoarthritis Progression via Targeting miR-337-3p/ADAMTS5. *J. Orthop. Surg. Res.* 16 (1), 392. doi:10.1186/s13018-021-02526-y
- Liu, Y., Lin, L., Zou, R., Wen, C., Wang, Z., and Lin, F. (2018). MSC-derived Exosomes Promote Proliferation and Inhibit Apoptosis of Chondrocytes via lncRNA-KLF3-AS1/miR-206/GIT1 axis in Osteoarthritis. *Cell Cycle* 17 (21–22), 2411–2422. doi:10.1080/15384101.2018.1526603
- Liu, Y., Liu, K., Tang, C., Shi, Z., Jing, K., and Zheng, J. (2020c). Long Non-coding RNA XIST Contributes to Osteoarthritis Progression via miR-149-5p/DNMT3A axis. *Biomed. Pharmacother.* 128, 110349. doi:10.1016/j.biopha.2020.110349
- Liu, Z., Chen, S., Yang, Y., Lu, S., Zhao, X., Hu, B., et al. (2019e). MicroRNA-671-3p Regulates the Development of K-neo Osteoarthritis by Targeting TRAF3 in Chondrocytes. *Mol. Med. Rep.* 20 (3), 2843–2850. doi:10.3892/mmr.2019.10488
- Long, H., Li, Q., Xiao, Z., and Yang, B. (2021). LncRNA MIR22HG Promotes Osteoarthritis Progression via Regulating miR-9-3p/ADAMTS5 Pathway. *Bioengineered* 12 (1), 3148–3158. doi:10.1080/21655979.2021.1945362
- Lu, C., Li, Z., Hu, S., Cai, Y., and Peng, K. (2019). LncRNA PART-1 Targets TGFBR2/Smad3 to Regulate Cell Viability and Apoptosis of Chondrocytes via Acting as miR-590-3p Sponge in Osteoarthritis. *J. Cel Mol Med* 23 (12), 8196–8205. doi:10.1111/jcmm.14690
- Lü, G., Li, L., Wang, B., and Kuang, L. (2020). LINC00623/miR-101/HRAS axis Modulates IL-1 β -mediated ECM Degradation, Apoptosis and Senescence of Osteoarthritis Chondrocytes. *Aging* 12 (4), 3218–3237. doi:10.18632/aging.102801
- Lu, J., Ji, M.-L., Zhang, X.-J., Shi, P.-L., Wu, H., Wang, C., et al. (2017). MicroRNA-218-5p as a Potential Target for the Treatment of Human Osteoarthritis. *Mol. Ther.* 25 (12), 2676–2688. doi:10.1016/j.ymthe.2017.08.009
- Lu, M., and Zhou, E. (2020). Long Noncoding RNA LINC00662-miR-15b-5p Mediated GPR120 Dysregulation Contributes to Osteoarthritis. *Pathol. Int.* 70 (3), 155–165. doi:10.1111/pin.12875
- Lu, X., Yu, Y., Yin, F., Yang, C., Li, B., Lin, J., et al. (2020). Knockdown of PVT1 Inhibits IL-1 β -induced Injury in Chondrocytes by Regulating miR-27b-3p/TRAF3 axis. *Int. immunopharmacology* 79, 106052. doi:10.1016/j.intimp.2019.106052
- Lu, Z., Luo, M., and Huang, Y. (2018). lncRNA-CIR Regulates Cell Apoptosis of Chondrocytes in Osteoarthritis. *J. Cel Biochem* 120, 7229–7237. doi:10.1002/jcb.27997

- Luan, X., and Wang, Y. (2018). LncRNA XLOC_006390 Facilitates Cervical Cancer Tumorigenesis and Metastasis as a ceRNA Against miR-331-3p and miR-338-3p. *J. Gynecol. Oncol.* 29 (6), e95. doi:10.3802/jgo.2018.29.e95
- Luo, C., Liang, J. S., Gong, J., Zhang, H. L., Feng, Z. J., Yang, H. T., et al. (2019a). The Function of microRNA-34a in Osteoarthritis. *Bratisl Lek Listy* 120 (5), 386–391. doi:10.4149/BLL_2019_063
- Luo, H., Xu, C., Le, W., Ge, B., and Wang, T. (2019b). LncRNA CASC11 Promotes Cancer Cell Proliferation in Bladder Cancer through miRNA-150. *J. Cel Biochem* 120 (8), 13487–13493. doi:10.1002/jcb.28622
- Ma, F., Li, G., Yu, Y., Xu, J., and Wu, X. (2019a). MiR-33b-3p Promotes Chondrocyte Proliferation and Inhibits Chondrocyte Apoptosis and Cartilage ECM Degradation by Targeting DNMT3A in Osteoarthritis. *Biochem. biophysical Res. Commun.* 519 (2), 430–437. doi:10.1016/j.bbrc.2019.09.022
- Ma, H. R., Mu, W. B., Zhang, K. Y., Zhou, H. K., Jiang, R. D., and Cao, L. (2020). CircVCAN Regulates the Proliferation and Apoptosis of Osteoarthritis Chondrocyte through NF-Kb Signaling Pathway. *Eur. Rev. Med. Pharmacol. Sci.* 24 (12), 6517–6525. doi:10.26355/eurrev_202006_21635
- Ma, Y., Wu, Y., Chen, J., Huang, K., Ji, B., Chen, Z., et al. (2019b). miR-10a-5p Promotes Chondrocyte Apoptosis in Osteoarthritis by Targeting HOXA1. *Mol. Ther. - Nucleic Acids* 14, 398–409. doi:10.1016/j.omtn.2018.12.012
- Makki, M. S., and Haqqi, T. M. (2015). miR-139 Modulates MCP1/IL-6 Expression and Induces Apoptosis in Human OA Chondrocytes. *Exp. Mol. Med.* 47, e189. doi:10.1038/emmm.2015.66
- Mao, D., Wu, M., Wei, J., Zhou, X., Yang, L., and Chen, F. (2021a). MicroRNA-101a-3p Could Be Involved in the Pathogenesis of Temporomandibular Joint Osteoarthritis by Mediating UBE2D1 and FZD4. *J. Oral Pathol. Med.* 50 (2), 236–243. doi:10.1111/jop.13131
- Mao, G., Hu, S., Zhang, Z., Wu, P., Zhao, X., Lin, R., et al. (2018a). Exosomal miR-95-5p Regulates Chondrogenesis and Cartilage Degradation via Histone Deacetylase 2/8. *J. Cel Mol Med* 22 (11), 5354–5366. doi:10.1111/jcmm.13808
- Mao, G., Kang, Y., Lin, R., Hu, S., Zhang, Z., Li, H., et al. (2019a). Long Non-coding RNA HOTTIP Promotes CCL3 Expression and Induces Cartilage Degradation by Sponging miR-455-3p. *Front. Cel Dev. Biol.* 7, 161. doi:10.3389/fcell.2019.00161
- Mao, G., Wu, P., Zhang, Z., Zhang, Z., Liao, W., Li, Y., et al. (2017a). MicroRNA-92a-3p Regulates Aggrecanase-1 and Aggrecanase-2 Expression in Chondrogenesis and IL-1 β -Induced Catabolism in Human Articular Chondrocytes. *Cel Physiol Biochem* 44 (1), 38–52. doi:10.1159/000484579
- Mao, G., Xu, Y., Long, D., Sun, H., Li, H., Xin, R., et al. (2021b). Exosome-transported circRNA_0001236 Enhances Chondrogenesis and Suppress Cartilage Degradation via the miR-3677-3p/Sox9 axis. *Stem Cel Res Ther* 12 (1), 389. doi:10.1186/s13287-021-02431-5
- Mao, G., Zhang, Z., Hu, S., Zhang, Z., Chang, Z., Huang, Z., et al. (2018b). Exosomes Derived from miR-92a-3p-Overexpressing Human Mesenchymal Stem Cells Enhance Chondrogenesis and Suppress Cartilage Degradation via Targeting WNT5A. *Stem Cel Res Ther* 9 (1), 247. doi:10.1186/s13287-018-1004-0
- Mao, G., Zhang, Z., Huang, Z., Chen, W., Huang, G., Meng, F., et al. (2017b). MicroRNA-92a-3p Regulates the Expression of Cartilage-specific Genes by Directly Targeting Histone Deacetylase 2 in Chondrogenesis and Degradation. *Osteoarthritis and cartilage* 25 (4), 521–532. doi:10.1016/j.joca.2016.11.006
- Mao, T., He, C., Wu, H., Yang, B., and Li, X. (2019b). Silencing lncRNA HOTAIR Declines Synovial Inflammation and Synovocyte Proliferation and Promotes Synovocyte Apoptosis in Osteoarthritis Rats by Inhibiting Wnt/ β -Catenin Signaling Pathway. *Cell Cycle* 18 (22), 3189–3205. doi:10.1080/15384101.2019.1671716
- Matsukawa, T., Sakai, T., Yonezawa, T., Hiraiwa, H., Hamada, T., Nakashima, M., et al. (2013). MicroRNA-125b Regulates the Expression of Aggrecanase-1 (ADAMTS-4) in Human Osteoarthritic Chondrocytes. *Arthritis Res. Ther.* 15 (1), R28. doi:10.1186/ar4164
- Mayer, U., Benditz, A., and Grässel, S. (2017). miR-29b Regulates Expression of Collagens I and III in Chondrogenically Differentiating BMSC in an Osteoarthritic Environment. *Sci. Rep.* 7 (1), 13297. doi:10.1038/s41598-017-13567-x
- Mehana, E.-S. E., Khafaga, A. F., and El-Blehi, S. S. (2019). The Role of Matrix Metalloproteinases in Osteoarthritis Pathogenesis: An Updated Review. *Life Sci.* 234, 116786. doi:10.1016/j.lfs.2019.116786
- Mei, X., Tong, J., Zhu, W., and Zhu, Y. (2019). LncRNA-NR024118 O-verexpression R-everse LPS-induced I-nflammatory I-njury and A-poptosis via NF- κ B/Nrf2 S-signaling in ATDC5 C-hondrocytes. *Mol. Med. Rep.* 20 (4), 3867–3873. doi:10.3892/mmr.2019.10639
- Meng, F., Li, Z., Zhang, Z., Yang, Z., Kang, Y., Zhao, X., et al. (2018). MicroRNA-193b-3p Regulates Chondrogenesis and Chondrocyte Metabolism by Targeting HDAC3. *Theranostics* 8 (10), 2862–2883. doi:10.7150/thno.23547
- Meng, F., Zhang, Z., Chen, W., Huang, G., He, A., Hou, C., et al. (2016). MicroRNA-320 Regulates Matrix Metalloproteinase-13 Expression in Chondrogenesis and Interleukin-1 β -Induced Chondrocyte Responses. *Osteoarthritis and cartilage* 24 (5), 932–941. doi:10.1016/j.joca.2015.12.012
- Miao, G., Zang, X., Hou, H., Sun, H., Wang, L., Zhang, T., et al. (2019). Bax Targeted by miR-29a Regulates Chondrocyte Apoptosis in Osteoarthritis. *Biomed. Research International* 2019, 1–9. doi:10.1155/2019/1434538
- Miyaki, S., Sato, T., Inoue, A., Otsuki, S., Ito, Y., Yokoyama, S., et al. (2010). MicroRNA-140 Plays Dual Roles in Both Cartilage Development and Homeostasis. *Genes Dev.* 24 (11), 1173–1185. doi:10.1101/gad.1915510
- Moulin, D., Salone, V., Koufany, M., Clément, T., Behm-Ansmant, I., Branlant, C., et al. (2017). MicroRNA-29b Contributes to Collagens Imbalance in Human Osteoarthritic and Dedifferentiated Articular Chondrocytes. *Biomed. Research International* 2017, 1–12. doi:10.1155/2017/9792512
- Ni, J. L., Dang, X. Q., and Shi, Z. B. (2020a). CircPSM3 Inhibits the Proliferation and Differentiation of OA Chondrocytes by Targeting miRNA-296-5p. *Eur. Rev. Med. Pharmacol. Sci.* 24 (7), 3467–3475. doi:10.26355/eurrev_202004_20805
- Ni, S., Xu, C., Zhuang, C., Zhao, G., Li, C., Wang, Y., et al. (2020b). LncRNA LUADT1 Regulates miR-34a/SIRT1 to Participate in Chondrocyte Apoptosis. *J. Cel Biochem* 122, 1003–1008. doi:10.1002/jcb.29637
- Ni, W., Jiang, C., Wu, Y., Zhang, H., Wang, L., Yik, J. H. N., et al. (2021). CircSLC7A2 Protects against Osteoarthritis through Inhibition of the miR-4498/TIMP3 axis. *Cell Prolif* 54 (6), e13047. doi:10.1111/cpr.13047
- Ni, Z., Shang, X., Tang, G., and Niu, L. (2018). Expression of miR-206 in Human Knee Articular Chondrocytes and Effects of miR-206 on Proliferation and Apoptosis of Articular Chondrocytes. *Am. J. Med. Sci.* 355 (3), 240–246. doi:10.1016/j.amjms.2017.11.003
- Nishimura, R., Hata, K., Takahata, Y., Murakami, T., Nakamura, E., Ohkawa, M., et al. (2020). Role of Signal Transduction Pathways and Transcription Factors in Cartilage and Joint Diseases. *Int. J. Mol. Sci.* 21 (4), 1340. doi:10.3390/ijms21041340
- Ntoumou, E., Tzetis, M., Braoudaki, M., Lambrou, G., Poulou, M., Malizos, K., et al. (2017). Serum microRNA Array Analysis Identifies miR-140-3p, miR-33b-3p and miR-671-3p as Potential Osteoarthritis Biomarkers Involved in Metabolic Processes. *Clin. Epigenet* 9, 127. doi:10.1186/s13148-017-0428-1
- Pan, H., Dai, H., Wang, L., Lin, S., Tao, Y., Zheng, Y., et al. (2020). MicroRNA-410-3p Modulates Chondrocyte Apoptosis and Inflammation by Targeting High Mobility Group Box 1 (HMGB1) in an Osteoarthritis Mouse Model. *BMC Musculoskelet. Disord.* 21 (1), 486. doi:10.1186/s12891-020-03489-7
- Park, S. J., Cheon, E. J., and Kim, H. A. (2013). MicroRNA-558 Regulates the Expression of Cyclooxygenase-2 and IL-1 β -induced Catabolic Effects in Human Articular Chondrocytes. *Osteoarthritis and cartilage* 21 (7), 981–989. doi:10.1016/j.joca.2013.04.012
- Pearson, M. J., Philp, A. M., Heward, J. A., Roux, B. T., Walsh, D. A., Davis, E. T., et al. (2016). Long Intergenic Noncoding RNAs Mediate the Human Chondrocyte Inflammatory Response and Are Differentially Expressed in Osteoarthritis Cartilage. *Arthritis Rheumatol.* 68 (4), 845–856. doi:10.1002/art.39520
- Peng, L., Deng, M., Ma, Y., Hu, W., and Liang, F. (2021). miR-520c-3p Regulates IL-1 β -stimulated Human Chondrocyte Apoptosis and Cartilage Degradation by Targeting GAS2. *J. Orthop. Surg. Res.* 16 (1), 347. doi:10.1186/s13018-021-02466-7
- Peng, P., Zhang, B., Huang, J., Xing, C., Liu, W., Sun, C., et al. (2020). Identification of a circRNA-miRNA-mRNA Network to Explore the Effects of circRNAs on Pathogenesis and Treatment of Spinal Cord Injury. *Life Sci.* 257, 118039. doi:10.1016/j.lfs.2020.118039
- Ponting, C. P., Oliver, P. L., and Reik, W. (2009). Evolution and Functions of Long Noncoding RNAs. *Cell* 136 (4), 629–641. doi:10.1016/j.cell.2009.02.006
- Prieto-Alhambra, D., Judge, A., Javadi, M. K., Cooper, C., Diez-Perez, A., and Arden, N. K. (2014). Incidence and Risk Factors for Clinically Diagnosed Knee,

- Hip and Hand Osteoarthritis: Influences of Age, Gender and Osteoarthritis Affecting Other Joints. *Ann. Rheum. Dis.* 73 (9), 1659–1664. doi:10.1136/annrheumdis-2013-203355
- Qin, G. H., Yang, W. C., Yao, J. N., Zhao, Y., and Wu, X. J. (2021). LncRNA OIP5-AS1 Affects the Biological Behaviors of Chondrocytes of Patients with Osteoarthritis by Regulating Micro-30a-5p. *Eur. Rev. Med. Pharmacol. Sci.* 25 (3), 1215–1224. doi:10.26355/eurrev_202102_24825
- Qiu, B., Xu, X., Yi, P., and Hao, Y. (2020). Curcumin Reinforces MSC-derived Exosomes in Attenuating Osteoarthritis via Modulating the miR-124/NF- κ B and miR-143/ROCK1/TLR9 Signalling Pathways. *J. Cel Mol Med* 24 (18), 10855–10865. doi:10.1111/jcmm.15714
- Qiu, W.-J., Xu, M.-Z., Zhu, X.-D., and Ji, Y.-H. (2019). MicroRNA-27a Alleviates IL-1 β -induced Inflammatory Response and Articular Cartilage Degradation via TLR4/NF-Kb Signaling Pathway in Articular Chondrocytes. *Int. immunopharmacology* 76, 105839. doi:10.1016/j.intimp.2019.105839
- Rasheed, Z., Rasheed, N., Abdulmonem, W. A., and Khan, M. I. (2019). Author Correction: MicroRNA-125b-5p Regulates IL-1 β Induced Inflammatory Genes via Targeting TRAF6-Mediated MAPKs and NF-Kb Signaling in Human Osteoarthritic Chondrocytes. *Sci. Rep.* 9 (1), 14729. doi:10.1038/s41598-019-50844-3
- Ren, T., Wei, P., Song, Q., Ye, Z., Wang, Y., and Huang, L. (2020). MiR-140-3p Ameliorates the Progression of Osteoarthritis via Targeting CXCR4. *Biol. Pharm. Bull.* 43 (5), 810–816. doi:10.1248/bpb.b19-00959
- Rigoglou, S., and Papavassiliou, A. G. (2013). The NF-Kb Signalling Pathway in Osteoarthritis. *Int. J. Biochem. Cel Biol.* 45 (11), 2580–2584. doi:10.1016/j.biocel.2013.08.018
- Rousseau, J.-C., Millet, M., Croset, M., Sornay-Rendu, E., Borel, O., and Chapurlat, R. (2020). Association of Circulating microRNAs with Prevalent and Incident Knee Osteoarthritis in Women: the OFELY Study. *Arthritis Res. Ther.* 22 (1), 2. doi:10.1186/s13075-019-2086-5
- Sakalauskiene, G., and Jauniškiene, D. (2010). Osteoarthritis: Etiology, Epidemiology, Impact on the Individual and Society and the Main Principles of Management. *Medicina (Kaunas)* 46 (11), 790–797.
- Shao, J., Ding, Z., Peng, J., Zhou, R., Li, L., Qian, Q., et al. (2020). MiR-146a-5p Promotes IL-1 β -induced Chondrocyte Apoptosis through the TRAF6-Mediated NF- κ B Pathway. *Inflamm. Res.* 69 (6), 619–630. doi:10.1007/s00011-020-01346-w
- Shen, H., Wang, Y., Shi, W., Sun, G., Hong, L., and Zhang, Y. (2018). LncRNA SNHG5/miR-26a/SOX2 Signal axis Enhances Proliferation of Chondrocyte in Osteoarthritis. *Acta Biochim. Biophys. Sinica* 50 (2), 191–198. doi:10.1093/abbs/gmx141
- Shen, J., Li, S., and Chen, D. (2014). TGF- β Signaling and the Development of Osteoarthritis. *Bone Res.* 2, 14002. doi:10.1038/boneres.2014.2
- Shen, P., Yang, Y., Liu, G., Chen, W., Chen, J., Wang, Q., et al. (2020a). CircCDK14 Protects against Osteoarthritis by Sponging miR-125a-5p and Promoting the Expression of Smad2. *Theranostics* 10 (20), 9113–9131. doi:10.7150/thno.45993
- Shen, S., Wu, Y., Chen, J., Xie, Z., Huang, K., Wang, G., et al. (2019). CircSERPINE2 Protects against Osteoarthritis by Targeting miR-1271 and ETS-Related Gene. *Ann. Rheum. Dis.* 78 (6), 826–836. doi:10.1136/annrheumdis-2018-214786
- Shen, S., Yang, Y., Shen, P., Ma, J., Fang, B., Wang, Q., et al. (2021). circPDE4B Prevents Articular Cartilage Degeneration and Promotes Repair by Acting as a Scaffold for RIC8A and MID1. *Ann. Rheum. Dis.* 80 (9), 1209–1219. doi:10.1136/annrheumdis-2021-219969
- Shen, X.-F., Cheng, Y., Dong, Q.-R., and Zheng, M.-Q. (2020b). MicroRNA-675-3p Regulates IL-1 β -stimulated Human Chondrocyte Apoptosis and Cartilage Degradation by Targeting GNG5. *Biochem. biophysical Res. Commun.* 527 (2), 458–465. doi:10.1016/j.bbrc.2020.04.044
- Shi, F.-L., and Ren, L.-X. (2020). Up-regulated miR-374a-3p Relieves Lipopolysaccharides Induced Injury in CHON-001 Cells via Regulating Wingless-type MMTV Integration Site Family Member 5B. *Mol. Cell. probes* 51, 101541. doi:10.1016/j.mcp.2020.101541
- Shi, J., Cao, F., Chang, Y., Xin, C., Jiang, X., Xu, J., et al. (2021a). Long Non-coding RNA MCM3AP-AS1 Protects Chondrocytes ATDC5 and CHON-001 from IL-1 β -induced Inflammation via Regulating miR-138-5p/SIRT1. *Bioengineered* 12 (1), 1445–1456. doi:10.1080/21655979.2021.1905247
- Shi, J., Guo, K., Su, S., Li, J., and Li, C. (2018). miR-486-5p I-s U-pregulated in O-steoarthritis and I-nhibits C-hondrocyte P-roliferation and M-igration by S-uppressing SMAD2. *Mol. Med. Rep.* 18 (1), 502–508. doi:10.3892/mmr.2018.8931
- Shi, J., Wang, S., He, Q., Liu, K., Zhao, W., Xie, Q., et al. (2021b). TNF- α Induces Up-regulation of MicroRNA-27a via the P38 Signalling Pathway, Which Inhibits Intervertebral Disc Degeneration by Targeting FSTL1. *J. Cel Mol Med* 25 (15), 7146–7156. doi:10.1111/jcmm.16745
- Shu, Y., Long, J., Guo, W., and Ye, W. (2019). MicroRNA-195-5p I-nhibitor P-revents the D-evelopment of O-steoarthritis by T-argeting REGy. *Mol. Med. Rep.* 19 (6), 4561–4568. doi:10.3892/mmr.2019.10124
- Si, H.-b., Zeng, Y., Zhou, Z.-k., Pei, F.-x., Lu, Y.-r., Cheng, J.-q., et al. (2016). Expression of miRNA-140 in Chondrocytes and Synovial Fluid of Knee Joints in Patients with Osteoarthritis. *Chin. Med. Sci. J.* 31 (4), 207–212. doi:10.1016/s1001-9294(17)30002-0
- Si, Z., Zhou, S., Shen, Z., Luan, F., and Yan, J. (2021). LncRNA HAND2-AS1 Is Downregulated in Osteoarthritis and Regulates IL-6 Expression in Chondrocytes. *J. Orthop. Surg. Res.* 16 (1), 68. doi:10.1186/s13018-021-02216-9
- Skrzypa, M., Szala, D., Gablo, N., Czech, J., Pajak, J., Kopanska, M., et al. (2019). miRNA-146a-5p Is Upregulated in Serum and Cartilage Samples of Patients with Osteoarthritis. *Pol. Przegl Chir* 91 (3), 1–5. doi:10.5604/01.3001.0013.0135
- Sondag, G. R., and Haqqi, T. M. (2016). The Role of MicroRNAs and Their Targets in Osteoarthritis. *Curr. Rheumatol. Rep.* 18 (8), 56. doi:10.1007/s11926-016-0604-x
- Song, J., Ahn, C., Chun, C.-H., and Jin, E.-J. (2014). A Long Non-coding RNA, GAS5, Plays a Critical Role in the Regulation of miR-21 during Osteoarthritis. *J. Orthop. Res.* 32 (12), 1628–1635. doi:10.1002/jor.22718
- Song, J., Jin, E.-H., Kim, D., Kim, K. Y., Chun, C.-H., and Jin, E.-J. (2015). MicroRNA-222 Regulates MMP-13 via Targeting HDAC-4 during Osteoarthritis Pathogenesis. *BBA Clin.* 3, 79–89. doi:10.1016/j.bbacli.2014.11.009
- Song, J., Kim, D., Lee, C. H., Lee, M. S., Chun, C.-H., and Jin, E.-J. (2013). MicroRNA-488 Regulates Zinc Transporter SLC39A8/ZIP8 during Pathogenesis of Osteoarthritis. *J. Biomed. Sci.* 20, 31. doi:10.1186/1423-0127-20-31
- Steck, E., Boeuf, S., Gabler, J., Werth, N., Schnatzer, P., Diederichs, S., et al. (2012). Regulation of H19 and its Encoded microRNA-675 in Osteoarthritis and under Anabolic and Catabolic In Vitro Conditions. *J. Mol. Med.* 90 (10), 1185–1195. doi:10.1007/s00109-012-0895-y
- Su, W., Xie, W., Shang, Q., and Su, B. (2015). The Long Noncoding RNA MEG3 Is Downregulated and Inversely Associated with VEGF Levels in Osteoarthritis. *Biomed. Research International* 2015, 1–5. doi:10.1155/2015/356893
- Sui, C., Liu, D., Que, Y., Xu, S., and Hu, Y. (2021). Knockdown of Hsa_circ_0037658 Inhibits the Progression of Osteoarthritis via Inducing Autophagy. *Hum. Cel.* 34 (1), 76–85. doi:10.1007/s13577-020-00440-9
- Sui, C., Zhang, L., and Hu, Y. (2019). MicroRNA-let-7a I-nhibition I-nhibits LPS-induced I-nflammatory I-njury of C-hondrocytes by T-argeting IL6R. *Mol. Med. Rep.* 20 (3), 2633–2640. doi:10.3892/mmr.2019.10493
- Sun, J. L., Yan, J. F., Yu, S. B., Zhao, J., Lin, Q. Q., and Jiao, K. (2020). MicroRNA-29b Promotes Subchondral Bone Loss in TMJ Osteoarthritis. *J. Dent Res.* 99 (13), 1469–1477. doi:10.1177/0022034520937617
- Sun, J., Zhong, N., Li, Q., Min, Z., Zhao, W., Sun, Q., et al. (2011). MicroRNAs of Rat Articular Cartilage at Different Developmental Stages Identified by Solexa Sequencing. *Osteoarthritis and cartilage* 19 (10), 1237–1245. doi:10.1016/j.joca.2011.07.002
- Sun, T., Li, X., Song, H., Gao, F., Zhou, G., Li, X., et al. (2017). MiR-146a Aggravates LPS-Induced Inflammatory Injury by Targeting CXCR4 in the Articular Chondrocytes. *Cel Physiol Biochem* 44 (4), 1282–1294. doi:10.1159/000485488
- Tan, F., Wang, D., and Yuan, Z. (2020). The Fibroblast-like Synoviocyte Derived Exosomal Long Non-coding RNA H19 Alleviates Osteoarthritis Progression through the miR-106b-5p/TIMP2 Axis. *Inflammation* 43 (4), 1498–1509. doi:10.1007/s10753-020-01227-8
- Tang, L., Ding, J., Zhou, G., and Liu, Z. (2018a). LncRNA-p21 P-romotes C-hondrocyte A-poptosis in O-steoarthritis by A-cting as a S-ponge for miR-451. *Mol. Med. Rep.* 18 (6), 5295–5301. doi:10.3892/mmr.2018.9506
- Tang, L. P., Ding, J. B., Liu, Z. H., and Zhou, G. J. (2018b). LncRNA TUG1 Promotes Osteoarthritis-Induced Degradation of Chondrocyte Extracellular Matrix via miR-195/MMP-13 axis. *Eur. Rev. Med. Pharmacol. Sci.* 22 (24), 8574–8581. doi:10.26355/eurrev_201812_16620

- Tao, H., Cheng, L., and Yang, R. (2020). Downregulation of miR-34a Promotes Proliferation and Inhibits Apoptosis of Rat Osteoarthritic Cartilage Cells by Activating PI3K/Akt Pathway. *Clin. Interv. Aging* 15, 373–385. doi:10.2147/CIA.S241855
- Tao, S.-C., Huang, J.-Y., Gao, Y., Li, Z.-X., Wei, Z.-Y., Dawes, H., et al. (2021). Small Extracellular Vesicles in Combination with Sleep-Related circRNA3503: A Targeted Therapeutic Agent with Injectable Thermosensitive Hydrogel to Prevent Osteoarthritis. *Bioactive Mater.* 6 (12), 4455–4469. doi:10.1016/j.bioactmat.2021.04.031
- Tao, S.-C., Yuan, T., Zhang, Y.-L., Yin, W.-J., Guo, S.-C., and Zhang, C.-Q. (2017). Exosomes Derived from miR-140-5p-Overexpressing Human Synovial Mesenchymal Stem Cells Enhance Cartilage Tissue Regeneration and Prevent Osteoarthritis of the Knee in a Rat Model. *Theranostics* 7 (1), 180–195. doi:10.7150/thno.17133
- Tardif, G., Hum, D., Pelletier, J.-P., Duval, N., and Martel-Pelletier, J. (2009). Regulation of the IGFBP-5 and MMP-13 Genes by the microRNAs miR-140 and miR-27a in Human Osteoarthritic Chondrocytes. *BMC Musculoskelet. Disord.* 10, 148. doi:10.1186/1471-2474-10-148
- Tardif, G., Pelletier, J.-P., Fahmi, H., Hum, D., Zhang, Y., Kapoor, M., et al. (2013). NFAT3 and TGF- β /smad3 Regulate the Expression of miR-140 in Osteoarthritis. *Arthritis Res. Ther.* 15 (6), R197. doi:10.1186/ar4387
- Tian, F., Wang, J., Zhang, Z., and Yang, J. (2020). LncRNA SNHG7/miR-34a-5p/SYVN1 axis Plays a Vital Role in Proliferation, Apoptosis and Autophagy in Osteoarthritis. *Biol. Res.* 53 (1), 9. doi:10.1186/s40659-020-00275-6
- Tian, L., Su, Z., Ma, X., Wang, F., and Guo, Y. (2019). Inhibition of miR-203 Ameliorates Osteoarthritis Cartilage Degradation in the Postmenopausal Rat Model: Involvement of Estrogen Receptor α . *Hum. Gene Ther. Clin. Develop.* 30 (4), 160–168. doi:10.1089/humc.2019.101
- Tian, Y., Guo, R., Shi, B., Chen, L., Yang, L., and Fu, Q. (2016). MicroRNA-30a Promotes Chondrogenic Differentiation of Mesenchymal Stem Cells through Inhibiting Delta-like 4 Expression. *Life Sci.* 148, 220–228. doi:10.1016/j.lfs.2016.02.031
- Toyota, M., Suzuki, H., Sasaki, Y., Maruyama, R., Imai, K., Shinomura, Y., et al. (2008). Epigenetic Silencing of microRNA-34b/c and B-Cell Translocation Gene 4 Is Associated with CpG Island Methylation in Colorectal Cancer. *Cancer Res.* 68 (11), 4123–4132. doi:10.1158/0008-5472.CAN-08-0325
- Tu, Y., Ma, T., Wen, T., Yang, T., Xue, L., Cai, M., et al. (2020). MicroRNA-377-3p Alleviates IL-1 β -caused Chondrocyte Apoptosis and Cartilage Degradation in Osteoarthritis in Part by Downregulating ITGA6. *Biochem. biophysical Res. Commun.* 523 (1), 46–53. doi:10.1016/j.bbrc.2019.11.186
- Vincent, T. L. (2019). Mechanoflamination in Osteoarthritis Pathogenesis. *Semin. Arthritis Rheum.* 49 (3S), S36–S38. doi:10.1016/j.semarthrit.2019.09.018
- Wan, D., Qu, Y., Ai, S., and Cheng, L. (2020). miR-152 Attenuates Apoptosis in Chondrocytes and Degeneration of Cartilages in Osteoarthritis Rats via TCF-4 Pathway. *Dose-Response* 18 (4), 155932582094691. doi:10.1177/1559325820946918
- Wang, A., Hu, N., Zhang, Y., Chen, Y., Su, C., Lv, Y., et al. (2019a). MEG3 Promotes Proliferation and Inhibits Apoptosis in Osteoarthritis Chondrocytes by miR-361-5p/FOXO1 axis. *BMC Med. Genomics* 12 (1), 201. doi:10.1186/s12920-019-0649-6
- Wang, C.-L., Peng, J.-P., and Chen, X.-D. (2018a). LncRNA-CIR Promotes Articular Cartilage Degeneration in Osteoarthritis by Regulating Autophagy. *Biochem. biophysical Res. Commun.* 505 (3), 692–698. doi:10.1016/j.bbrc.2018.09.163
- Wang, C., Li, N., Liu, Q., Su, L., Wang, S., Chen, Y., et al. (2021a). The Role of circRNA Derived from RUNX2 in the Serum of Osteoarthritis and its Clinical Value. *J. Clin. Lab. Anal.* 35 (7), e23858. doi:10.1002/jcla.23858
- Wang, G.-D., Zhao, X.-W., Zhang, Y.-G., Kong, Y., Niu, S.-S., Ma, L.-F., et al. (2017a). Effects of miR-145 on the Inhibition of Chondrocyte Proliferation and Fibrosis by Targeting TNFRSF11B in Human Osteoarthritis. *Mol. Med. Rep.* 15 (1), 75–80. doi:10.3892/mmr.2016.5981
- Wang, G.-L., Wu, Y.-B., Liu, J.-T., and Li, C.-Y. (2016a). Upregulation of miR-98 Inhibits Apoptosis in Cartilage Cells in Osteoarthritis. *Genet. Test. Mol. biomarkers* 20 (11), 645–653. doi:10.1089/gtmb.2016.0011
- Wang, H., Zhang, H., Sun, Q., Wang, Y., Yang, J., Yang, J., et al. (2017b). Intracellular Delivery of Antago-miR-483-5p Inhibits Osteoarthritis by Modulating Matrilin 3 and Tissue Inhibitor of Metalloproteinase 2. *Mol. Ther.* 25 (3), 715–727. doi:10.1016/j.jymthe.2016.12.020
- Wang, J., Chen, L., Jin, S., Lin, J., Zheng, H., Zhang, H., et al. (2017c). Altered Expression of microRNA-98 in IL-1 β -induced Cartilage Degradation and its Role in Chondrocyte Apoptosis. *Mol. Med. Rep.* 16 (3), 3208–3216. doi:10.3892/mmr.2017.7028
- Wang, J., Chen, L., Jin, S., Lin, J., Zheng, H., Zhang, H., et al. (2016b). MiR-98 Promotes Chondrocyte Apoptosis by Decreasing Bcl-2 Expression in a Rat Model of Osteoarthritis. *Acta Biochim. Biophys. Sin.* 48 (10), 923–929. doi:10.1093/abbs/gmw084
- Wang, J., Fang, L., Ye, L., Ma, S., Huang, H., Lan, X., et al. (2020a). miR-137 Targets the Inhibition of TCF4 to Reverse the Progression of Osteoarthritis through the AMPK/NF- κ B Signaling Pathway. *Biosci. Rep.* 40 (6), BSR20200466. doi:10.1042/BSR20200466
- Wang, J., Zhu, S., Meng, N., He, Y., Lu, R., and Yan, G.-R. (2019b). ncRNA-Encoded Peptides or Proteins and Cancer. *Mol. Ther.* 27 (10), 1718–1725. doi:10.1016/j.jymthe.2019.09.001
- Wang, L., Cho, K. B., Li, Y., Tao, G., Xie, Z., and Guo, B. (2019c). Long Noncoding RNA (lncRNA)-Mediated Competing Endogenous RNA Networks Provide Novel Potential Biomarkers and Therapeutic Targets for Colorectal Cancer. *Int. J. Mol. Sci.* 20 (22), 5758. doi:10.3390/ijms20225758
- Wang, Q., Wang, W., Zhang, F., Deng, Y., and Long, Z. (2017d). NEAT1/miR-181c Regulates Osteopontin (OPN)-Mediated Synovial Cell Proliferation in Osteoarthritis. *J. Cel. Biochem.* 118 (11), 3775–3784. doi:10.1002/jcb.26025
- Wang, T., Liu, Y., Wang, Y., Huang, X., Zhao, W., and Zhao, Z. (2019d). Long Non-coding RNA XIST Promotes Extracellular Matrix Degradation by Functioning as a Competing Endogenous RNA of miR-1277-5p in Osteoarthritis. *Int. J. Mol. Med.* 44 (2), 630–642. doi:10.3892/ijmm.2019.4240
- Wang, W.-T., Huang, Z.-P., Sui, S., Liu, J.-H., Yu, D.-M., and Wang, W.-B. (2020b). microRNA-1236 Promotes Chondrocyte Apoptosis in Osteoarthritis via Direct Suppression of PIK3R3. *Life Sci.* 253, 117694. doi:10.1016/j.lfs.2020.117694
- Wang, W. F., Liu, S. Y., Qi, Z. F., Lv, Z. H., Ding, H. R., and Zhou, W. J. (2020c). MiR-145 Targeting BNIP3 Reduces Apoptosis of Chondrocytes in Osteoarthritis through Notch Signaling Pathway. *Eur. Rev. Med. Pharmacol. Sci.* 24 (16), 8263–8272. doi:10.26355/eurrev_202008_22622
- Wang, X.-B., Zhao, F.-C., Yi, L.-H., Tang, J.-L., Zhu, Z.-Y., Pang, Y., et al. (2019e). MicroRNA-21-5p as a Novel Therapeutic Target for Osteoarthritis. *Rheumatology (Oxford)* 58, 1485–1497. doi:10.1093/rheumatology/kez102
- Wang, X., Guo, Y., Wang, C., Yu, H., Yu, X., and Yu, H. (2016c). MicroRNA-142-3p Inhibits Chondrocyte Apoptosis and Inflammation in Osteoarthritis by Targeting HMGB1. *Inflammation* 39 (5), 1718–1728. doi:10.1007/s10753-016-0406-3
- Wang, Y., Cao, L., Wang, Q., Huang, J., and Xu, S. (2019f). LncRNA FOXD2-AS1 Induces Chondrocyte Proliferation through Sponging miR-27a-3p in Osteoarthritis. *Artif. Cell nanomedicine, Biotechnol.* 47 (1), 1241–1247. doi:10.1080/21691401.2019.1596940
- Wang, Y., and Kong, D. (2018). Retracted : MicroRNA-136 Promotes Lipopolysaccharide-induced ATDC5 Cell Injury and Inflammatory Cytokine Expression by Targeting Myeloid Cell Leukemia 1. *J. Cel Biochem* 119 (11), 9316–9326. doi:10.1002/jcb.27208
- Wang, Y., Shen, S., Li, Z., Li, W., and Weng, X. (2020d). MIR-140-5p Affects Chondrocyte Proliferation, Apoptosis, and Inflammation by Targeting HMGB1 in Osteoarthritis. *Inflamm. Res.* 69 (1), 63–73. doi:10.1007/s00111-019-01294-0
- Wang, Y., Wu, C., Yang, Y., Ren, Z., Lammi, M. J., and Guo, X. (2019g). Preliminary Exploration of Hsa_circ_0032131 Levels in Peripheral Blood as a Potential Diagnostic Biomarker of Osteoarthritis. *Genet. Test. Mol. biomarkers* 23 (10), 717–721. doi:10.1089/gtmb.2019.0036
- Wang, Y., Wu, C., Zhang, F., Zhang, Y., Ren, Z., Lammi, M. J., et al. (2019h). Screening for Differentially Expressed Circular RNAs in the Cartilage of Osteoarthritis Patients for Their Diagnostic Value. *Genet. Test. Mol. biomarkers* 23 (10), 706–716. doi:10.1089/gtmb.2019.0108
- Wang, Z., Hu, J., Pan, Y., Shan, Y., Jiang, L., Qi, X., et al. (2018b). miR-140-5p/miR-149 Affects Chondrocyte Proliferation, Apoptosis, and Autophagy by Targeting FUT1 in Osteoarthritis. *Inflammation* 41 (3), 959–971. doi:10.1007/s10753-018-0750-6
- Wang, Z., Zhou, N., Wang, W., Yu, Y., Xia, L., and Li, N. (2021b). HDAC2 Interacts with microRNA-503-5p to Regulate SGK1 in Osteoarthritis. *Arthritis Res. Ther.* 23 (1), 78. doi:10.1186/s13075-020-02373-y

- Wei, M., Xie, Q., Zhu, J., Wang, T., Zhang, F., Cheng, Y., et al. (2016). MicroRNA-33 Suppresses CCL2 Expression in Chondrocytes. *Biosci. Rep.* 36 (3), BSR20160068. doi:10.1042/BSR20160068
- Wei, W., He, S., Wang, Z., Dong, J., Xiang, D., Li, Y., et al. (2019). LINC01534 Promotes the Aberrant Metabolic Dysfunction and Inflammation in IL-1 β -Simulated Osteoarthritic Chondrocytes by Targeting miR-140-5p. *Cartilage* 2019, 194760351988878. doi:10.1177/1947603519888787
- Wen, X., Li, H., Sun, H., Zeng, A., Lin, R., Zhao, J., et al. (2020). MiR-455-3p Reduces Apoptosis and Alleviates Degeneration of Chondrocyte through Regulating PI3K/AKT Pathway. *Life Sci.* 253, 117718. doi:10.1016/j.lfs.2020.117718
- Woods, S., Barter, M. J., Elliott, H. R., McGillivray, C. M., Birch, M. A., Clark, I. M., et al. (2019). miR-324-5p Is up Regulated in End-Stage Osteoarthritis and Regulates Indian Hedgehog Signalling by Differing Mechanisms in Human and Mouse. *Matrix Biol.* 77, 87–100. doi:10.1016/j.matbio.2018.08.009
- Wu, D.-P., Zhang, J.-L., Wang, J.-Y., Cui, M.-X., Jia, J.-L., Liu, X.-H., et al. (2017a). MiR-1246 Promotes LPS-Induced Inflammatory Injury in Chondrogenic Cells ATDC5 by Targeting HNF4 γ . *Cel Physiol Biochem* 43 (5), 2010–2021. doi:10.1159/000484162
- Wu, J., Zou, M., Ping, A., Deng, Z., and Cai, L. (2018a). MicroRNA-449a Upregulation Promotes Chondrocyte Extracellular Matrix Degradation in Osteoarthritis. *Biomed. Pharmacother.* 105, 940–946. doi:10.1016/j.biopha.2018.06.074
- Wu, Q., Yuan, Z. H., Ma, X. B., and Tang, X. H. (2020). Low Expression of CircRNA HIPK3 Promotes Osteoarthritis Chondrocyte Apoptosis by Serving as a Sponge of miR-124 to Regulate SOX8. *Eur. Rev. Med. Pharmacol. Sci.* 24 (15), 7937–7945. doi:10.26355/eurrev_202008_22476
- Wu, X.-F., Zhou, Z.-H., and Zou, J. (2017b). MicroRNA-181 Inhibits Proliferation and Promotes Apoptosis of Chondrocytes in Osteoarthritis by Targeting PTEN. *Biochem. Cel Biol.* 95 (3), 437–444. doi:10.1139/bcb-2016-0078
- Wu, X., Crawford, R., Xiao, Y., Mao, X., and Prasad, I. (2021a). Osteoarthritic Subchondral Bone Release Exosomes that Promote Cartilage Degeneration. *Cells* 10 (2), 251. doi:10.3390/cells10020251
- Wu, Y. H., Liu, W., Zhang, L., Liu, X. Y., Wang, Y., Xue, B., et al. (2018b). Retracted : Effects of microRNA-24 Targeting C-myc on Apoptosis, Proliferation, and Cytokine Expressions in Chondrocytes of Rats with Osteoarthritis via MAPK Signaling Pathway. *J. Cel. Biochem.* 119 (10), 7944–7958. doi:10.1002/jcb.26514
- Wu, Y., Hong, Z., Xu, W., Chen, J., Wang, Q., Chen, J., et al. (2021b). Circular RNA circPDE4D Protects against Osteoarthritis by Binding to miR-103a-3p and Regulating FGF18. *Mol. Ther.* 29 (1), 308–323. doi:10.1016/j.ymthe.2020.09.002
- Wu, Y., Lu, X., Shen, B., and Zeng, Y. (2019). The Therapeutic Potential and Role of miRNA, lncRNA, and circRNA in Osteoarthritis. *Curr. Gene Ther.* 19 (4), 255–263. doi:10.2174/1566523219666190716092203
- Wu, Y., Zhang, Y., Zhang, Y., and Wang, J.-J. (2017c). CircRNA Hsa_circ_0005105 Upregulates NAMPT Expression and Promotes Chondrocyte Extracellular Matrix Degradation by Sponging miR-26a. *Cel Biol Int* 41 (12), 1283–1289. doi:10.1002/cbin.10761
- Xi, P., Zhang, C. I., Wu, S. y., Liu, L., Li, W. j., and Li, Y. m. (2021). CircRNA circ-IQGAP1 Knockdown Alleviates Interleukin-1 β -Induced Osteoarthritis Progression via Targeting miR-671-5p/TCF4. *Orthop. Surg.* 13 (3), 1036–1046. doi:10.1111/os.12923
- Xiao, K., Xia, Z., Feng, B., Bian, Y., Fan, Y., Li, Z., et al. (2019a). Circular RNA Expression Profile of Knee Condyle in Osteoarthritis by Illumina HiSeq Platform. *J. Cel Biochem* 120 (10), 17500–17511. doi:10.1002/jcb.29014
- Xiao, P., Zhu, X., Sun, J., Zhang, Y., Qiu, W., Li, J., et al. (2021). LncRNA NEAT1 Regulates Chondrocyte Proliferation and Apoptosis via Targeting miR-543/PLA2G4A axis. *Hum. Cel.* 34 (1), 60–75. doi:10.1007/s13577-020-00433-8
- Xiao, Y., Bao, Y., Tang, L., and Wang, L. (2019b). LncRNA MIR4435-2HG Is Downregulated in Osteoarthritis and Regulates Chondrocyte Cell Proliferation and Apoptosis. *J. Orthop. Surg. Res.* 14 (1), 247. doi:10.1186/s13018-019-1278-7
- Xiao, Y., Yan, X., Yang, Y., and Ma, X. (2019c). Downregulation of Long Noncoding RNA HOTAIRM1 Variant 1 Contributes to Osteoarthritis via Regulating miR-125b/BMP2 axis and Activating JNK/MAPK/ERK Pathway. *Biomed. Pharmacother.* 109, 1569–1577. doi:10.1016/j.biopha.2018.10.181
- Xing, D., Liang, J.-q., Li, Y., Lu, J., Jia, H.-b., Xu, L.-y., et al. (2014). Identification of Long Noncoding RNA Associated with Osteoarthritis in Humans. *Orthopaedic Surg.* 6 (4), 288–293. doi:10.1111/os.12147
- Xu, B., Li, Y.-y., Ma, J., and Pei, F.-x. (2016). Roles of microRNA and Signaling Pathway in Osteoarthritis Pathogenesis. *J. Zhejiang Univ. Sci. B* 17 (3), 200–208. doi:10.1631/jzus.B1500267
- Xu, J., and Ma, X. (2021). Hsa_circ_0032131 Knockdown Inhibits Osteoarthritis Progression via the miR-502-5p/PRDX3 axis. *Aging* 13 (11), 15100–15113. doi:10.18632/aging.203073
- Xu, J., Pei, Y., Lu, J., Liang, X., Li, Y., Wang, J., et al. (2021). LncRNA SNHG7 Alleviates IL-1 β -induced Osteoarthritis by Inhibiting miR-214-5p-Mediated PPARGC1B Signaling Pathways. *Int. immunopharmacology* 90, 107150. doi:10.1016/j.intimp.2020.107150
- Xu, J., and Xu, Y. (2017). The lncRNA MEG3 Downregulation Leads to Osteoarthritis Progression via miR-16/SMAD7 axis. *Cell Biosci* 7, 69. doi:10.1186/s13578-017-0195-x
- Xu, K., Meng, Z., Xian, X.-M., Deng, M.-H., Meng, Q.-G., Fang, W., et al. (2020). LncRNA PVT1 Induces Chondrocyte Apoptosis through Upregulation of TNF- α in Synoviocytes by Sponging miR-211-3p. *Mol. Cell. probes* 52, 101560. doi:10.1016/j.mcp.2020.101560
- Xue, H., Yu, P., Wang, W. Z., Niu, Y. Y., and Li, X. (2020). The Reduced lncRNA NKILA Inhibited Proliferation and Promoted Apoptosis of Chondrocytes via miR-145/sp1/nf-Kb Signaling in Human Osteoarthritis. *Eur. Rev. Med. Pharmacol. Sci.* 24 (2), 535–548. doi:10.26355/eurrev_202001_20030
- Xue, H., Tu, Y., Ma, T., Wen, T., Yang, T., Xue, L., et al. (2019). miR-93-5p Attenuates IL-1 β -induced Chondrocyte Apoptosis and Cartilage Degradation in Osteoarthritis Partially by Targeting TCF4. *Bone* 123, 129–136. doi:10.1016/j.bone.2019.03.035
- Yan, S., Wang, M., Zhao, J., Zhang, H., Zhou, C., Jin, L., et al. (2016). MicroRNA-34a Affects Chondrocyte Apoptosis and Proliferation by Targeting the SIRT1/p53 Signaling Pathway during the Pathogenesis of Osteoarthritis. *Int. J. Mol. Med.* 38 (1), 201–209. doi:10.3892/ijmm.2016.2618
- Yang, B., Ni, J., Long, H., Huang, J., Yang, C., and Huang, X. (2018a). IL-1 β -induced miR-34a Up-regulation Inhibits Cyr61 to Modulate Osteoarthritis Chondrocyte Proliferation through ADAMTS-4. *J. Cel. Biochem.* 119 (10), 7959–7970. doi:10.1002/jcb.26600
- Yang, B., Xu, L., and Wang, S. (2020a). Regulation of lncRNA-H19/miR-140-5p in Cartilage Matrix Degradation and Calcification in Osteoarthritis. *Ann. Palliat. Med.* 9 (4), 1896–1904. doi:10.21037/apm-20-929
- Yang, D. W., Zhang, X., Qian, G. B., Jiang, M. J., Wang, P., and Wang, K. Z. (2019a). Downregulation of Long Noncoding RNA LOC101928134 Inhibits the Synovial Hyperplasia and Cartilage Destruction of Osteoarthritis Rats through the Activation of the Janus Kinase/signal Transducers and Activators of Transcription Signaling Pathway by Upregulating IFNA1. *J. Cel Physiol* 234 (7), 10523–10534. doi:10.1002/jcp.27730
- Yang, F., Huang, R., Ma, H., Zhao, X., and Wang, G. (2020b). miRNA-411 Regulates Chondrocyte Autophagy in Osteoarthritis by Targeting Hypoxia-Inducible Factor 1 Alpha (HIF-1 α). *Med. Sci. Monit.* 26, e921155. doi:10.12659/MSM.921155
- Yang, G., Tang, K., Qiao, L., Li, Y., and Sun, S. (2021a). Identification of Critical Genes and lncRNAs in Osteolysis after Total Hip Arthroplasty and Osteoarthritis by RNA Sequencing. *Biomed. Research International* 2021, 1–13. doi:10.1155/2021/6681925
- Yang, H., Wu, D., Li, H., Chen, N., and Shang, Y. (2018b). Downregulation of microRNA-448 Inhibits IL-1 β -induced Cartilage Degradation in Human Chondrocytes via Upregulation of Matrilin-3. *Cell Mol Biol Lett* 23, 7. doi:10.1186/s11658-018-0072-6
- Yang, Q., Yao, Y., Zhao, D., Zou, H., Lai, C., Xiang, G., et al. (2021b). LncRNA H19 Secreted by Umbilical Cord Blood Mesenchymal Stem Cells through microRNA-29a-3p/FOS axis for central Sensitization of Pain in Advanced Osteoarthritis. *Am. J. Transl. Res.* 13 (3), 1245–1256.
- Yang, Q., Zhou, Y., Cai, P., Fu, W., Wang, J., Wei, Q., et al. (2019b). Downregulation of microRNA-23b-3p Alleviates IL-1 β -induced Injury in Chondrogenic CHON-001 Cells. *Drug Des. Devel Ther.* 13, 2503–2512. doi:10.2147/DDDT.S211051
- Yang, Y., Shen, P., Yao, T., Ma, J., Chen, Z., Zhu, J., et al. (2021c). Novel Role of circRSU1 in the Progression of Osteoarthritis by Adjusting Oxidative Stress. *Theranostics* 11 (4), 1877–1900. doi:10.7150/thno.53307
- Yang, Y., Xing, D., Wang, Y., Jia, H., Li, B., and Li, J. J. (2020c). A Long Non-coding RNA, HOTAIR, Promotes Cartilage Degradation in Osteoarthritis by

- Inhibiting WIF-1 Expression and Activating Wnt Pathway. *BMC Mol. Cel Biol* 21 (1), 53. doi:10.1186/s12860-020-00299-6
- Yang, Y., Yujiao, W., Fang, W., Linhui, Y., Ziqi, G., Zhichen, W., et al. (2020d). The Roles of miRNA, lncRNA and circRNA in the Development of Osteoporosis. *Biol. Res.* 53 (1), 40. doi:10.1186/s40659-020-00309-z
- Yang, Z., Tang, Y., Lu, H., Shi, B., Ye, Y., Xu, G., et al. (2018c). Retracted : Long Non-coding RNA Reprogramming (lncRNA-ROR) Regulates Cell Apoptosis and Autophagy in Chondrocytes. *J. Cel. Biochem.* 119 (10), 8432–8440. doi:10.1002/jcb.27057
- Yao, Q., Chen, Y., and Zhou, X. (2019). The Roles of microRNAs in Epigenetic Regulation. *Curr. Opin. Chem. Biol.* 51, 11–17. doi:10.1016/j.cbpa.2019.01.024
- Ye, D., Jian, W., Feng, J., and Liao, X. (2018). Role of Long Noncoding RNA ZFAS1 in Proliferation, Apoptosis and Migration of Chondrocytes in Osteoarthritis. *Biomed. Pharmacother.* 104, 825–831. doi:10.1016/j.biopha.2018.04.124
- Ying, H., Wang, Y., Gao, Z., and Zhang, Q. (2019). Long Non-coding RNA Activated by Transforming Growth Factor Beta Alleviates Lipopolysaccharide-Induced Inflammatory Injury via Regulating microRNA-223 in ATDC5 Cells. *Int. Immunopharmacology* 69, 313–320. doi:10.1016/j.intimp.2019.01.056
- You, D., Yang, C., Huang, J., Gong, H., Yan, M., and Ni, J. (2019). Long Non-coding RNA MEG3 Inhibits Chondrogenic Differentiation of Synovium-Derived Mesenchymal Stem Cells by Epigenetically Inhibiting TRIB2 via Methyltransferase EZH2. *Cell Signal.* 63, 109379. doi:10.1016/j.cellsig.2019.109379
- Yu, C., Shi, D., Li, Z., Wan, G., and Shi, X. (2019a). Retracted : Long Noncoding RNA CHRF Exacerbates IL-6-induced Inflammatory Damages by Downregulating microRNA-146a in ATDC5 Cells. *J. Cel Physiol* 234 (12), 21851–21859. doi:10.1002/jcp.28749
- Yu, C., and Wang, Y. (2018). RETRACTED: MicroRNA-19a Promotes Cell Viability and Migration of Chondrocytes via Up-Regulating SOX9 through NF-Kb Pathway. *Biomed. Pharmacother.* 98, 746–753. doi:10.1016/j.biopha.2017.11.132
- Yu, J., Qin, Y., and Zhou, N. (2021). Knockdown of Circ_SLC39A8 Protects against the Progression of Osteoarthritis by Regulating miR-591/IRAK3 axis. *J. Orthop. Surg. Res.* 16 (1), 170. doi:10.1186/s13018-021-02323-7
- Yu, Q., Zhao, B., He, Q., Zhang, Y., and Peng, X. B. (2019b). microRNA-206 Is Required for Osteoarthritis Development through its Effect on Apoptosis and Autophagy of Articular Chondrocytes via Modulating the Phosphoinositide 3-kinase/protein Kinase B-mTOR Pathway by Targeting Insulin-like Growth Factor-1. *J. Cel Biochem* 120 (4), 5287–5303. doi:10.1002/jcb.27803
- Yu, X. P., Liu, C. G., Qiu, F., Xu, Y. Q., Xing, F., Yin, J. Q., et al. (2020). CircRNA_100395 Protects Breast Carcinoma Deterioration by Targeting MAPK6. *Eur. Rev. Med. Pharmacol. Sci.* 24 (23), 12216–12223. doi:10.26355/eurrev_202012_24012
- Zang, J., Lu, D., and Xu, A. (2020). The Interaction of circRNAs and RNA Binding Proteins: An Important Part of circRNA Maintenance and Function. *J. Neurosci. Res.* 98 (1), 87–97. doi:10.1002/jnr.24356
- Zhai, X., Meng, R., Li, H., Li, J., Jing, L., Qin, L., et al. (2017). miR-181a Modulates Chondrocyte Apoptosis by Targeting Glycerol-3-Phosphate Dehydrogenase 1-Like Protein (GPD1L) in Osteoarthritis. *Med. Sci. Monit.* 23, 1224–1231. doi:10.12659/msm.899228
- Zhang, B., Sun, M., Wang, J., Ma, C., Hao, T., Liu, G., et al. (2019a). MiR-671 Ameliorates the Progression of Osteoarthritis *In Vitro* and *In Vivo*. *Pathol. - Res. Pract.* 215 (7), 152423. doi:10.1016/j.prp.2019.04.015
- Zhang, C.-Y., Yang, C.-Q., Chen, Q., Liu, J., Zhang, G., Dong, C., et al. (2021a). miR-194-Loaded Gelatin Nanospheres Target MEF2C to Suppress Muscle Atrophy in a Mechanical Unloading Model. *Mol. Pharmaceutics* 18 (8), 2959–2973. doi:10.1021/acs.molpharmaceut.1c00121
- Zhang, C., Wang, P., Jiang, P., Lv, Y., Dong, C., Dai, X., et al. (2016a). Upregulation of lncRNA HOTAIR Contributes to IL-1 β -induced MMP Overexpression and Chondrocytes Apoptosis in Temporomandibular Joint Osteoarthritis. *Gene* 586 (2), 248–253. doi:10.1016/j.gene.2016.04.016
- Zhang, C., Zhang, Z., Chang, Z., Mao, G., Hu, S., Zeng, A., et al. (2019b). miR-193b-5p Regulates Chondrocytes Metabolism by Directly Targeting Histone Deacetylase 7 in Interleukin-1 β -induced Osteoarthritis. *J. Cel Biochem* 120 (8), 12775–12784. doi:10.1002/jcb.28545
- Zhang, D., Cao, X., Li, J., and Zhao, G. (2015). MiR-210 Inhibits NF-Kb Signaling Pathway by Targeting DR6 in Osteoarthritis. *Sci. Rep.* 5, 12775. doi:10.1038/srep12775
- Zhang, D., Wang, K., Wei, W., Liu, Y., and Liu, S. (2021b). Multifunctional Plasmonic Core-Satellites Nanoprobe for Cancer Diagnosis and Therapy Based on a Cascade Reaction Induced by MicroRNA. *Anal. Chem.* 93 (27), 9521–9530. doi:10.1021/acs.analchem.1c01539
- Zhang, F. e., Lammi, M. J., Tan, S., Meng, P., Wu, C., and Guo, X. (2020a). Cell Cycle-Related lncRNAs and mRNAs in Osteoarthritis Chondrocytes in a Northwest Chinese Han Population. *Medicine* 99 (24), e19905. doi:10.1097/MD.00000000000019905
- Zhang, F. Q., Wang, Z., Zhang, H., Liu, L., Luo, X. L., and Liu, W. W. (2019c). MiR-27a Alleviates Osteoarthritis in Rabbits via Inhibiting Inflammation. *Eur. Rev. Med. Pharmacol. Sci.* 23 (3 Suppl. I), 89–95. doi:10.26355/eurrev_201908_18634
- Zhang, F., Zhang, R., Zhang, X., Wu, Y., Li, X., Zhang, S., et al. (2018a). Comprehensive Analysis of circRNA Expression Pattern and circRNA-miRNA-mRNA Network in the Pathogenesis of Atherosclerosis in Rabbits. *Aging* 10 (9), 2266–2283. doi:10.18632/aging.101541
- Zhang, G., Sun, Y., Wang, Y., Liu, R., Bao, Y., and Li, Q. (2016b). MiR-502-5p Inhibits IL-1 β -induced Chondrocyte Injury by Targeting TRAF2. *Cell Immunol.* 302, 50–57. doi:10.1016/j.cellimm.2016.01.007
- Zhang, G., Wu, Y., Xu, D., and Yan, X. (2016c). Long Noncoding RNA UFC1 Promotes Proliferation of Chondrocyte in Osteoarthritis by Acting as a Sponge for miR-34a. *DNA Cel. Biol.* 35 (11), 691–695. doi:10.1089/dna.2016.3397
- Zhang, G., Zhang, Q., Zhu, J., Tang, J., and Nie, M. (2020b). LncRNA ARFRP1 Knockdown Inhibits LPS-Induced the Injury of Chondrocytes by Regulation of NF-Kb Pathway through Modulating miR-15a-5p/TLR4 axis. *Life Sci.* 261, 118429. doi:10.1016/j.lfs.2020.118429
- Zhang, G., Zhou, Y., Su, M., Yang, X., and Zeng, B. (2020c). Inhibition of microRNA -27b-3p Relieves Osteoarthritis Pain via Regulation of KDM4B-dependent DLX5. *BioFactors* 46 (5), 788–802. doi:10.1002/biof.1670
- Zhang, H., Chen, C., Cui, Y., Li, Y., Wang, Z., Mao, X., et al. (2019d). lnc-SAMD14-4 Can Regulate Expression of the COL1A1 and COL1A2 in Human Chondrocytes. *PeerJ* 7, e7491. doi:10.7717/peerj.7491
- Zhang, H., Li, J., Shao, W., and Shen, N. (2020d). LncRNA CTBP1-AS2 Is Upregulated in Osteoarthritis and Increases the Methylation of miR-130a Gene to Inhibit Chondrocyte Proliferation. *Clin. Rheumatol.* 39 (11), 3473–3478. doi:10.1007/s10067-020-05113-4
- Zhang, H., Li, J., Shao, W., and Shen, N. (2020e). LncRNA SNHG9 Is Downregulated in Osteoarthritis and Inhibits Chondrocyte Apoptosis by Downregulating miR-34a through Methylation. *BMC Musculoskelet. Disord.* 21 (1), 511. doi:10.1186/s12891-020-03497-7
- Zhang, J., Cheng, F., Rong, G., Tang, Z., and Gui, B. (2020f). Hsa_circ_0005567 Activates Autophagy and Suppresses IL-1 β -Induced Chondrocyte Apoptosis by Regulating miR-495. *Front. Mol. Biosci.* 7, 216. doi:10.3389/fmolb.2020.00216
- Zhang, L. L. (2020). CircRNA-PTPRA Promoted the Progression of Atherosclerosis through Sponging with miR-636 and Upregulating the Transcription Factor SP1. *Eur. Rev. Med. Pharmacol. Sci.* 24 (23), 12437–12449. doi:10.26355/eurrev_202012_24039
- Zhang, L., Zhang, P., Sun, X., Zhou, L., and Zhao, J. (2018b). Long Non-coding RNA DANCER Regulates Proliferation and Apoptosis of Chondrocytes in Osteoarthritis via miR-216a-5p-JAK2-STAT3 axis. *Biosci. Rep.* 38 (6), BSR20181228. doi:10.1042/BSR20181228
- Zhang, P., Gao, G., Zhou, Z., and He, X. (2021c). microRNA-130b Downregulation Potentiates Chondrogenic Differentiation of Bone Marrow Mesenchymal Stem Cells by Targeting SOX9. *Braz. J. Med. Biol. Res.* 54 (4), e10345. doi:10.1590/1414-431X202010345
- Zhang, P., Sun, J., Liang, C., Gu, B., Xu, Y., Lu, H., et al. (2020g). lncRNA IGHCy1 Acts as a ceRNA to Regulate Macrophage Inflammation via the miR-6891-3p/TLR4 Axis in Osteoarthritis. *Mediators Inflamm.* 2020, 1–11. doi:10.1155/2020/9743037
- Zhang, Q., Qiao, X., and Xia, W. (2020h). CircSERPINE2 Weakens IL-1 β -caused Apoptosis and Extracellular Matrix Degradation of Chondrocytes by Regulating miR-495/TGFBR2 axis. *Biosci. Rep.* 40 (11), BSR20201601. doi:10.1042/BSR20201601
- Zhang, Q., Wang, Y., Zhang, M., and Ying, H. (2019e). Retracted : Green tea Polyphenols Attenuate LPS-induced Inflammation through Upregulating microRNA-9 in Murine Chondrogenic ATDC5 Cells. *J. Cel Physiol* 234 (12), 22604–22612. doi:10.1002/jcp.28826
- Zhang, W., Cheng, P., Hu, W., Yin, W., Guo, F., Chen, A., et al. (2020i). Correction: Inhibition of microRNA-384-5p Alleviates Osteoarthritis through its Effects on

- Inhibiting Apoptosis of Cartilage Cells via the NF-Kb Signaling Pathway by Targeting SOX9. *Cancer Gene Ther.* 27 (10-11), 836–837. doi:10.1038/s41417-020-0202-y
- Zhang, W., Cheng, P., Hu, W., Yin, W., Guo, F., Chen, A., et al. (2018c). Downregulated microRNA-340-5p Promotes Proliferation and Inhibits Apoptosis of Chondrocytes in Osteoarthritis Mice through Inhibiting the Extracellular Signal-regulated Kinase Signaling Pathway by Negatively Targeting the FMOD Gene. *J. Cel Physiol* 234 (1), 927–939. doi:10.1002/jcp.26921
- Zhang, W., Hsu, P., Zhong, B., Guo, S., Zhang, C., Wang, Y., et al. (2018d). MiR-34a Enhances Chondrocyte Apoptosis, Senescence and Facilitates Development of Osteoarthritis by Targeting DLL1 and Regulating PI3K/AKT Pathway. *Cel Physiol Biochem* 48 (3), 1304–1316. doi:10.1159/000492090
- Zhang, W., Hu, C., Zhang, C., Luo, C., Zhong, B., and Yu, X. (2021d). MiRNA-132 Regulates the Development of Osteoarthritis in Correlation with the Modulation of PTEN/PI3K/AKT Signaling. *BMC Geriatr.* 21 (1), 175. doi:10.1186/s12877-021-02046-8
- Zhang, W., Qi, L., Chen, R., He, J., Liu, Z., Wang, W., et al. (2021e). Circular RNAs in Osteoarthritis: Indispensable Regulators and Novel Strategies in Clinical Implications. *Arthritis Res. Ther.* 23 (1), 23. doi:10.1186/s13075-021-02420-2
- Zhang, W., Zhang, C., Hu, C., Luo, C., Zhong, B., and Yu, X. (2020j). Circular RNA-CDRIAs Acts as the Sponge of microRNA-641 to Promote Osteoarthritis Progression. *J. Inflamm.* 17, 8. doi:10.1186/s12950-020-0234-y
- Zhang, W., Zhong, B., Zhang, C., Luo, C., and Zhan, Y. (2018e). miR-373 Regulates Inflammatory Cytokine-Mediated Chondrocyte Proliferation in Osteoarthritis by Targeting the P2X7 Receptor. *FEBS open bio* 8 (3), 325–331. doi:10.1002/2211-5463.12345
- Zhang, X., Huang, C.-R., Pan, S., Pang, Y., Chen, Y.-S., Zha, G.-C., et al. (2020k). Long Non-coding RNA SNHG15 Is a Competing Endogenous RNA of miR-141-3p that Prevents Osteoarthritis Progression by Upregulating BCL2L13 Expression. *Int. immunopharmacology* 83, 106425. doi:10.1016/j.intimp.2020.106425
- Zhang, X., Liang, H., Kourkoulis, N., Wu, Z., Li, G., and Shang, X. (2020l). Comprehensive Analysis of lncRNA and miRNA Expression Profiles and ceRNA Network Construction in Osteoporosis. *Calcif Tissue Int.* 106 (4), 343–354. doi:10.1007/s00223-019-00643-9
- Zhang, X., Wang, C., Zhao, J., Xu, J., Geng, Y., Dai, L., et al. (2017). miR-146a Facilitates Osteoarthritis by Regulating Cartilage Homeostasis via Targeting Camk2d and Ppp3r2. *Cel Death Dis* 8 (4), e2734. doi:10.1038/cddis.2017.146
- Zhang, X., Zhu, X.-L., Ji, B.-Y., Cao, X., Yu, L.-J., Zhang, Y., et al. (2019f). LncRNA-1810034E14Rik Reduces Microglia Activation in Experimental Ischemic Stroke. *J. Neuroinflammation* 16 (1), 75. doi:10.1186/s12974-019-1464-x
- Zhang, Y., Dong, Q., and Sun, X. (2020m). Positive Feedback Loop LINC00511/miR-150-5p/SP1 Modulates Chondrocyte Apoptosis and Proliferation in Osteoarthritis. *DNA Cel. Biol.* 39 (9), 1506–1512. doi:10.1089/dna.2020.5718
- Zhang, Y., Jia, J., Yang, S., Liu, X., Ye, S., and Tian, H. (2014). MicroRNA-21 Controls the Development of Osteoarthritis by Targeting GDF-5 in Chondrocytes. *Exp. Mol. Med.* 46, e79. doi:10.1038/emmm.2013.152
- Zhang, Y., Ma, L., Wang, C., Wang, L., Guo, Y., and Wang, G. (2020n). Long Noncoding RNA LINC00461 Induced Osteoarthritis Progression by Inhibiting miR-30a-5p. *Aging* 12 (5), 4111–4123. doi:10.18632/aging.102839
- Zhang, Y., Wang, F., Chen, G., He, R., and Yang, L. (2019g). LncRNA MALAT1 Promotes Osteoarthritis by Modulating miR-150-5p/AKT3 axis. *Cel Biosci* 9, 54. doi:10.1186/s13578-019-0302-2
- Zhang, Z.-Y., Gao, X.-H., Ma, M.-Y., Zhao, C.-L., Zhang, Y.-L., and Guo, S.-S. (2020o). CircRNA_101237 Promotes NSCLC Progression via the miRNA-490-3p/MAPK1 axis. *Sci. Rep.* 10 (1), 9024. doi:10.1038/s41598-020-65920-2
- Zhao, C., Wang, Y., Jin, H., and Yu, T. (2017). Knockdown of microRNA-203 Alleviates LPS-Induced Injury by Targeting MCL-1 in C28/I2 Chondrocytes. *Exp. Cel. Res.* 359 (1), 171–178. doi:10.1016/j.yexcr.2017.07.034
- Zhao, G., and Gu, W. (2020). Effects of miR-146a-5p on Chondrocyte Interleukin-1 β -Induced Inflammation and Apoptosis Involving Thioredoxin Interacting Protein Regulation. *J. Int. Med. Res.* 48 (11), 030006052096955. doi:10.1177/0300060520969550
- Zhao, H., and Gong, N. (2019). miR-20a Regulates Inflammation in Osteoarthritis by Targeting the IkB β and Regulates NK-Kb Signaling Pathway Activation. *Biochem. biophysical Res. Commun.* 518 (4), 632–637. doi:10.1016/j.bbrc.2019.08.109
- Zhao, J., Li, T., and Luo, W. (2021). Silencing of Circ-PRKCH Protects against Lipopolysaccharide (LPS)-evoked Chondrocyte Damage and Extracellular Matrix Loss by the miR-140-3p/ADAM10 axis. *Gen. Physiol. Biophys.* 40 (2), 89–101. doi:10.4149/gpb_2021001
- Zhao, Q., Yang, Y., Ren, G., Ge, E., and Fan, C. (2019a). Integrating Bipartite Network Projection and KATZ Measure to Identify Novel CircRNA-Disease Associations. *IEEE Trans.on Nanobioscience* 18 (4), 578–584. doi:10.1109/TNB.2019.2922214
- Zhao, X., Li, H., and Wang, L. (2019b). MicroRNA-107 Regulates Autophagy and Apoptosis of Osteoarthritis Chondrocytes by Targeting TRAF3. *Int. immunopharmacology* 71, 181–187. doi:10.1016/j.intimp.2019.03.005
- Zhao, Y., Zhao, J., Guo, X., She, J., and Liu, Y. (2018). Long Non-coding RNA PVT1, a Molecular Sponge for miR-149, Contributes Aberrant Metabolic Dysfunction and Inflammation in IL-1 β -simulated Osteoarthritic Chondrocytes. *Biosci. Rep.* 38 (5), BSR20180576. doi:10.1042/BSR20180576
- Zhao, Z., Dai, X.-S., Wang, Z.-Y., Bao, Z.-Q., and Guan, J.-Z. (2019c). MicroRNA-26a Reduces Synovial Inflammation and Cartilage Injury in Osteoarthritis of Knee Joints through Impairing the NF-Kb Signaling Pathway. *Biosci. Rep.* 39 (4), BSR20182025. doi:10.1042/BSR20182025
- Zheng, W., Hou, G., and Li, Y. (2021). Circ_0116061 Regulated the Proliferation, Apoptosis, and Inflammation of Osteoarthritis Chondrocytes through Regulating the miR-200b-3p/SMURF2 axis. *J. Orthop. Surg. Res.* 16 (1), 253. doi:10.1186/s13018-021-02391-9
- Zheng, X., Zhao, F.-C., Pang, Y., Li, D.-Y., Yao, S.-C., Sun, S.-S., et al. (2017). Downregulation of miR-221-3p Contributes to IL-1 β -induced Cartilage Degradation by Directly Targeting the SDF1/CXCR4 Signaling Pathway. *J. Mol. Med.* 95 (6), 615–627. doi:10.1007/s00109-017-1516-6
- Zhi, L., Zhao, J., Zhao, H., Qing, Z., Liu, H., and Ma, J. (2020). Downregulation of LncRNA OIP5-AS1 Induced by IL-1 β Aggravates Osteoarthritis via Regulating miR-29b-3p/PGRN. *Cartilage* 2020, 194760351990080. doi:10.1177/1947603519900801
- Zhong, J.-H., Li, J., Liu, C.-F., Liu, N., Bian, R.-X., Zhao, S.-M., et al. (2017). Effects of microRNA-146a on the Proliferation and Apoptosis of Human Osteoarthritis Chondrocytes by Targeting TRAF6 through the NF-Kb Signalling Pathway. *Biosci. Rep.* 37 (2), BSR20160578. doi:10.1042/BSR20160578
- Zhou, B., Li, H., and Shi, J. (2017). miR-27 Inhibits the NF-Kb Signaling Pathway by Targeting Leptin in Osteoarthritic Chondrocytes. *Int. J. Mol. Med.* 40 (2), 523–530. doi:10.3892/ijmm.2017.3021
- Zhou, C., He, T., and Chen, L. (2021a). LncRNA CASC19 Accelerates Chondrocytes Apoptosis and Proinflammatory Cytokine Production to Exacerbate Osteoarthritis Development through Regulating the miR-152-3p/DDX6 axis. *J. Orthop. Surg. Res.* 16 (1), 399. doi:10.1186/s13018-021-02543-x
- Zhou, J. L., Deng, S., Fang, H. S., Du, X. j., Peng, H., and Hu, Q. j. (2021b). Circular RNA circANKRD36 Regulates Casz1 by Targeting miR-599 to Prevent Osteoarthritis Chondrocyte Apoptosis and Inflammation. *J. Cel. Mol. Med.* 25 (1), 120–131. doi:10.1111/jcmm.15884
- Zhou, J. X., Tian, Z. G., Zhu, L. F., Wu, W. D., Zhou, S. L., Zhao, Y. T., et al. (2018a). MicroRNA-615-3p Promotes the Osteoarthritis Progression by Inhibiting Chondrogenic Differentiation of Bone Marrow Mesenchymal Stem Cells. *Eur. Rev. Med. Pharmacol. Sci.* 22 (19), 6212–6220. doi:10.26355/eurev_201810_16027
- Zhou, L., Gu, M., Ma, X., Wen, L., Zhang, B., Lin, Y., et al. (2021c). Long Non-coding RNA PCAT-1 Regulates Apoptosis of Chondrocytes in Osteoarthritis by Sponging miR-27b-3p. *J. Bone Miner Metab.* 39 (2), 139–147. doi:10.1007/s00774-020-01128-8
- Zhou, M., Zhang, Z., Zhao, H., Bao, S., Cheng, L., and Sun, J. (2018b). An Immune-Related Six-lncRNA Signature to Improve Prognosis Prediction of Glioblastoma Multiforme. *Mol. Neurobiol.* 55 (5), 3684–3697. doi:10.1007/s12035-017-0572-9
- Zhou, X., Jiang, L., Fan, G., Yang, H., Wu, L., Huang, Y., et al. (2019a). Role of the ciRS-7/miR-7 axis in the Regulation of Proliferation, Apoptosis and Inflammation of Chondrocytes Induced by IL-1 β . *Int. immunopharmacology* 71, 233–240. doi:10.1016/j.intimp.2019.03.037
- Zhou, X., Li, J., Zhou, Y., Yang, Z., Yang, H., Li, D., et al. (2020a). Down-regulated ciRS-7/up-Regulated miR-7 axis Aggravated Cartilage Degradation and Autophagy Defection by PI3K/AKT/mTOR Activation Mediated by IL-17A in Osteoarthritis. *Aging* 12 (20), 20163–20183. doi:10.18632/aging.103731
- Zhou, X., Luo, D., Sun, H., Qi, Y., Xu, W., Jin, X., et al. (2018c). MiR-132-3p Regulates ADAMTS-5 Expression and Promotes Chondrogenic Differentiation

- of Rat Mesenchymal Stem Cells. *J. Cel. Biochem.* 119 (3), 2579–2587. doi:10.1002/jcb.26421
- Zhou, Y., Ming, J., Li, Y., Li, B., Deng, M., Ma, Y., et al. (2021d). Exosomes Derived from miR-126-3p-Overexpressing Synovial Fibroblasts Suppress Chondrocyte Inflammation and Cartilage Degradation in a Rat Model of Osteoarthritis. *Cell Death Discov.* 7 (1), 37. doi:10.1038/s41420-021-00418-y
- Zhou, Y., Wang, Z., Chen, X., Zhang, J., Yang, L., Liu, S., et al. (2020b). Identification of Differentially Expressed miRNAs and mRNAs in Synovial of Osteoarthritis via RNA-Sequencing. *BMC Med. Genet.* 21 (1), 46. doi:10.1186/s12881-020-0978-5
- Zhou, Z.-B., Du, D., Huang, G.-X., Chen, A., and Zhu, L. (2018d). Circular RNA Atp9b, a Competing Endogenous RNA, Regulates the Progression of Osteoarthritis by Targeting miR-138-5p. *Gene* 646, 203–209. doi:10.1016/j.gene.2017.12.064
- Zhou, Z.-B., Huang, G.-X., Fu, Q., Han, B., Lu, J.-J., Chen, A.-M., et al. (2019b). circRNA.33186 Contributes to the Pathogenesis of Osteoarthritis by Sponging miR-127-5p. *Mol. Ther.* 27 (3), 531–541. doi:10.1016/j.ymthe.2019.01.006
- Zhou, Z., Du, D., Chen, A., and Zhu, L. (2018e). Circular RNA Expression Profile of Articular Chondrocytes in an IL-1 β -induced Mouse Model of Osteoarthritis. *Gene* 644, 20–26. doi:10.1016/j.gene.2017.12.020
- Zhou, Z., Ma, J., Lu, J., Chen, A., and Zhu, L. (2021e). Circular RNA CircCDH13 Contributes to the Pathogenesis of Osteoarthritis via CircCDH13/miR-296-3p/PTEN axis. *J. Cel Physiol* 236 (5), 3521–3535. doi:10.1002/jcp.30091
- Zhu, H., Hu, Y., Wang, C., Zhang, X., and He, D. (2020). CircGNC1L1 Promotes Synovial Proliferation and Chondrocyte Apoptosis by Targeting miR-330-3p and TNF- α in TMJ Osteoarthritis. *Cel Death Dis* 11 (4), 284. doi:10.1038/s41419-020-2447-7
- Zhu, J., Fu, H., Wu, Y., and Zheng, X. (2013). Function of lncRNAs and Approaches to lncRNA-Protein Interactions. *Sci. China Life Sci.* 56 (10), 876–885. doi:10.1007/s11427-013-4553-6
- Zhu, J. K., He, T. D., Wei, Z. X., and Wang, Y. M. (2018). lncRNA FAS-AS1 Promotes the Degradation of Extracellular Matrix of Cartilage in Osteoarthritis. *Eur. Rev. Med. Pharmacol. Sci.* 22 (10), 2966–2972. doi:10.26355/eurrev_201805_15051
- Zhu, Y. J., and Jiang, D. M. (2019). lncRNA PART1 Modulates Chondrocyte Proliferation, Apoptosis, and Extracellular Matrix Degradation in Osteoarthritis via Regulating miR-373-3p/SOX4 axis. *Eur. Rev. Med. Pharmacol. Sci.* 23 (19), 8175–8185. doi:10.26355/eurrev_201910_19124
- Zhu, Y., Li, R., and Wen, L.-M. (2021). Long Non-coding RNA XIST Regulates Chondrogenic Differentiation of Synovium-Derived Mesenchymal Stem Cells from Temporomandibular Joint via miR-27b-3p/ADAMTS-5 axis. *Cytokine* 137, 155352. doi:10.1016/j.cyto.2020.155352
- Zou, L.-X., Yu, L., Zhao, X.-M., Liu, J., Lu, H.-G., Liu, G.-W., et al. (2019). MiR-375 Mediates Chondrocyte Metabolism and Oxidative Stress in Osteoarthritis Mouse Models through the JAK2/STAT3 Signaling Pathway. *Cells Tissues Organs* 208 (1-2), 13–24. doi:10.1159/000504959

Conflict of Interest: The authors declare that the research was conducted in the absence of any commercial or financial relationships that could be construed as a potential conflict of interest.

Publisher's Note: All claims expressed in this article are solely those of the authors and do not necessarily represent those of their affiliated organizations, or those of the publisher, the editors and the reviewers. Any product that may be evaluated in this article, or claim that may be made by its manufacturer, is not guaranteed or endorsed by the publisher.

Copyright © 2021 Kong, Sun, Zhang and Wang. This is an open-access article distributed under the terms of the Creative Commons Attribution License (CC BY). The use, distribution or reproduction in other forums is permitted, provided the original author(s) and the copyright owner(s) are credited and that the original publication in this journal is cited, in accordance with accepted academic practice. No use, distribution or reproduction is permitted which does not comply with these terms.



Potential Prognostic Value of a Seven m6A-Related LncRNAs Signature and the Correlative Immune Infiltration in Colon Adenocarcinoma

Xiu-kun Chai¹, Wei Qi¹, Chun-Yan Zou², Chen-Xi He³, Miao Su⁴ and Dong-Qiang Zhao^{1*}

¹Department of Gastroenterology, The Second Hospital of Hebei Medical University, Shijiazhuang, China, ²Department of Gastroenterology, Qinhuangdao First Hospital, Qinhuangdao, China, ³Department of Gastroenterology, Xingtai City People's Hospital, Xingtai, China, ⁴Department of Gastroenterology, Harrison International Peace Hospital, Hengshui, China

OPEN ACCESS

Edited by:

Xiang Zhang,
The Chinese University of Hong Kong,
China

Reviewed by:

Qin An,
Salk Institute for Biological Studies,
United States
Lei Zhao,
University of Wisconsin-Madison,
United States

*Correspondence:

Dong-Qiang Zhao
drzhaodq_1124@163.com

Received: 10 September 2021

Accepted: 22 November 2021

Published: 22 December 2021

Citation:

Chai X-k, Qi W, Zou C-Y, He C-X, Su M
and Zhao D-Q (2021) Potential
Prognostic Value of a Seven m6A-
Related LncRNAs Signature and the
Correlative Immune Infiltration in
Colon Adenocarcinoma.
Front. Genet. 12:774010.
doi: 10.3389/fgene.2021.774010

Long non-coding RNAs (lncRNAs) and their N6-methyladenosine (m6A) modifications play an essential role in tumorigenesis and cancer progression. This study was designed to explore the value of m6A-related lncRNAs in prognosis and therapeutic applications of immune infiltration of colon adenocarcinoma (COAD). We downloaded the COAD gene expression and clinical data from The Cancer Genome Atlas project. By co-expression analysis, Lasso Cox regression analysis, and univariate and multivariate Cox regression, we constructed an independent prognostic signature of seven m6A-related lncRNAs. The prognostic lncRNAs were divided into two clusters by consistent clustering analysis, as well as into two groups of low–high risk based on the signature. Then we identified the relationship between the different groups with clinical features and immune cell infiltration. Cluster 2 had a higher risk score with a lower survival rate. The risk score was higher in groups with advanced clinical features, such as stage III–IV, N1–3, and M1. The expression of AC156455.1 was increased in tumor tissues and cluster 2, and the lncRNA ZEB1–AS1 was notably higher in the high-risk group. Five types of immune cells showed differences in two clusters, and most were upregulated in type 2. The expression of memory B cells was positively correlated with the risk score. The prognostic model was verified by the Gene Expression Omnibus (GEO) dataset. Besides, we found that the expression of these seven lncRNAs in tumor tissues was significantly higher than that in normal tissues, which verified the feasibility of the model. Thus, the signature of seven m6A-related lncRNAs can independently predict the prognosis of COAD. This signature is also closely associated with immune cell infiltration, and new therapeutic targets can be explored from this field.

Keywords: lncRNA, m6A, bioinformatics analysis, immune cell infiltration, COAD

INTRODUCTION

Colorectal cancer (CRC) is one of the most common and malignant tumors, ranking third in incidence and second in mortality from cancer-related deaths worldwide (Siegel et al., 2021). Colon adenocarcinoma (COAD) accounts for more than 90% of different pathological subtypes of it. So far, the general treatment of surgical resection and combination therapy, such as radiotherapy, chemotherapy, and immunotherapy, remains the only effective therapy for COAD.

Treatment techniques are improving, but the results are unsatisfactory, with a 5-year relative survival rate of 90% of localized CRC to 14% of metastasized (Kweon, 2018). First, more than 50% of the patients with CRC have liver metastasis for the late diagnosis (Banerjee et al., 2017). Second, the recurrence rate remains high after surgery. Third, the benefits of radiation and chemotherapy remain low, resulting in few effective treatments for patients in an advanced stage. Therefore, new and efficient prognostic markers and therapeutic targets must be discovered urgently.

The occurrence and development of tumors are closely related to the changes of genes and epigenetic changes. As the most abundant apparent epigenetic modification, N⁶-methyladenosine plays a crucial part in nearly all stages of RNA transcription, processing, degradation, and translation. There exist three types of m⁶A regulators, including methyltransferase “writers” (such as METTL3, METTL14, etc.), demethylase “erasers” (FTO and ALKBH5), and m⁶A binding protein “readers” (YTHDC, YTHDF1/2/3, etc.) (Zaccara et al., 2019). Recently, increasing studies have demonstrated that aberrant m⁶A modifications play an important role in the occurrence and progression of tumors, including COAD, and act as the tumor suppressor (Li et al., 2019; Yue et al., 2019). Gu et al. discovered that through an m⁶A-dependent manner DMDRMR could interact with IGF2BP3 to regulate target genes and act as a prognostic and therapeutic target for clear cell renal cell carcinoma (ccRCC) (Gu et al., 2021).

Researchers found that, consisting of more than 200 nucleotides, long non-coding RNAs (lncRNAs) significantly impact the epigenetic modifications, regulation, and splicing (Li et al., 2017). They can regulate physiological processes such as cell differentiation, immune response, and apoptosis (Liu et al., 2016). With more and more lncRNAs identified, 14,826 lncRNAs have been annotated by the GENCODE consortium (v22; <https://www.encodegenes.org/>). Emerging evidence suggests that lncRNAs participate in regulating proliferation and metastasis of various tumor cells and could be used as diagnostic and prognostic markers (Zhu et al., 2017; Kong et al., 2019; Poursheikhani et al., 2020). Gutschner et al. found the lncRNA MALAT1 could act as a prognostic marker of lung cancer and the knockout of MALAT1 related to little metastasis (Gutschner et al., 2013). Cen et al. discovered that lncRNA IGFL2-AS1 could result in a pretty poor prognosis for the patients of COAD (Cen et al., 2021).

In recent years, research on the relationship between m⁶A methylation and lncRNA in tumors has become a hotspot, showing that m⁶A-related lncRNA can serve as novel potential prognostic targets for multiple cancers (Jin et al., 2021; Li et al., 2021b; Liu et al., 2021). Romanowska et al. identified a risk signature including four m⁶A-related lncRNAs for head and neck squamous cell carcinoma (HNSCC) patients (Romanowska et al., 2021). Yu et al. constructed a prognostic signature based on m⁶A-related lncRNAs to predict the prognosis accurately of renal clear cell carcinoma patients (Yu et al., 2021). However, the study of COAD-related m⁶A methylation based on lncRNA remains relatively few.

Multiple studies have shown that the tumor microenvironment (TME) relates closely to the prognosis and treatment effect of tumors, for playing a vital role in the

progression (Danaher et al., 2018; Toor et al., 2020), as well as in immunotherapies of COAD (Koi and Carethers., 2017). Although therapies are improving, the 5-year survival rate of advanced COAD is only 10% for chemotherapeutic drug resistance and disease recurrence.

Therefore, the finding of novel therapeutic markers and strategies for COAD is crucial. Thus, we performed the study to explore the relationship between m⁶A-related lncRNA and COAD to find new prognostic markers and therapeutic drug targets.

MATERIALS AND METHODS

Acquisition and Preprocessing of COAD Data

We obtained the RNA sequencing (RNA-seq) of COAD from the database of The Cancer Genome Atlas (TCGA) (<https://portal.gdc.cancer.gov/>), including 39 healthy samples and 398 tumor samples. Meanwhile, we collected clinical data grouped according to survival time, survival status, gender, age, stage, and TMN stages. Then, using Perl software, we obtained the mRNA expression matrix and the gene expression matrix based on the human genome annotation data downloaded from the GENCODE website (<https://www.encodegenes.org/human/>). Then we got the RNA and lncRNA expression as well as the m⁶A-related gene expression based on the m⁶A-related genes on the web and R language software. Finally, the m⁶A-related lncRNA expression was obtained by co-expression analysis of lncRNA and the m⁶A-related gene expression using the R package (limma, corFilter = 0.4, $p = 0.001$). The workflow is shown in **Figure 1**.

Identification of Prognostic m⁶A-Related lncRNAs

The clinical survival data, containing only survival time and survival state data, were combined with m⁶A-related lncRNA expression data. Then using the R survival package and the univariate Cox analysis (if $p < 0.05$, there were too many lncRNAs, set $p < 0.001$), prognostic m⁶A-related lncRNAs would be obtained. The confidence interval and the hazard ratio were calculated using the survival package and visualized by forest plots. Differences in prognostic m⁶A-related lncRNAs in normal and tumor samples were analyzed by differential analysis. The results were obtained through R packages (limma, pheatmap, reshape2, ggpubr), and a boxplot and heat map were prepared to visualize the results.

Relationship Between Clusters With Clinicopathological Features and Immune Cell Infiltration

Firstly, the prognostic m⁶A-related lncRNAs were classified into two clusters based on the packages, Limma and ConsensusClusterPlus, according to the lncRNAs expression. By the consistent cluster analysis, we calculated the cluster Max K value = 9, clusterNum = 2. Using survival and survminer packages, survival analysis of the two prognostic m⁶A-related

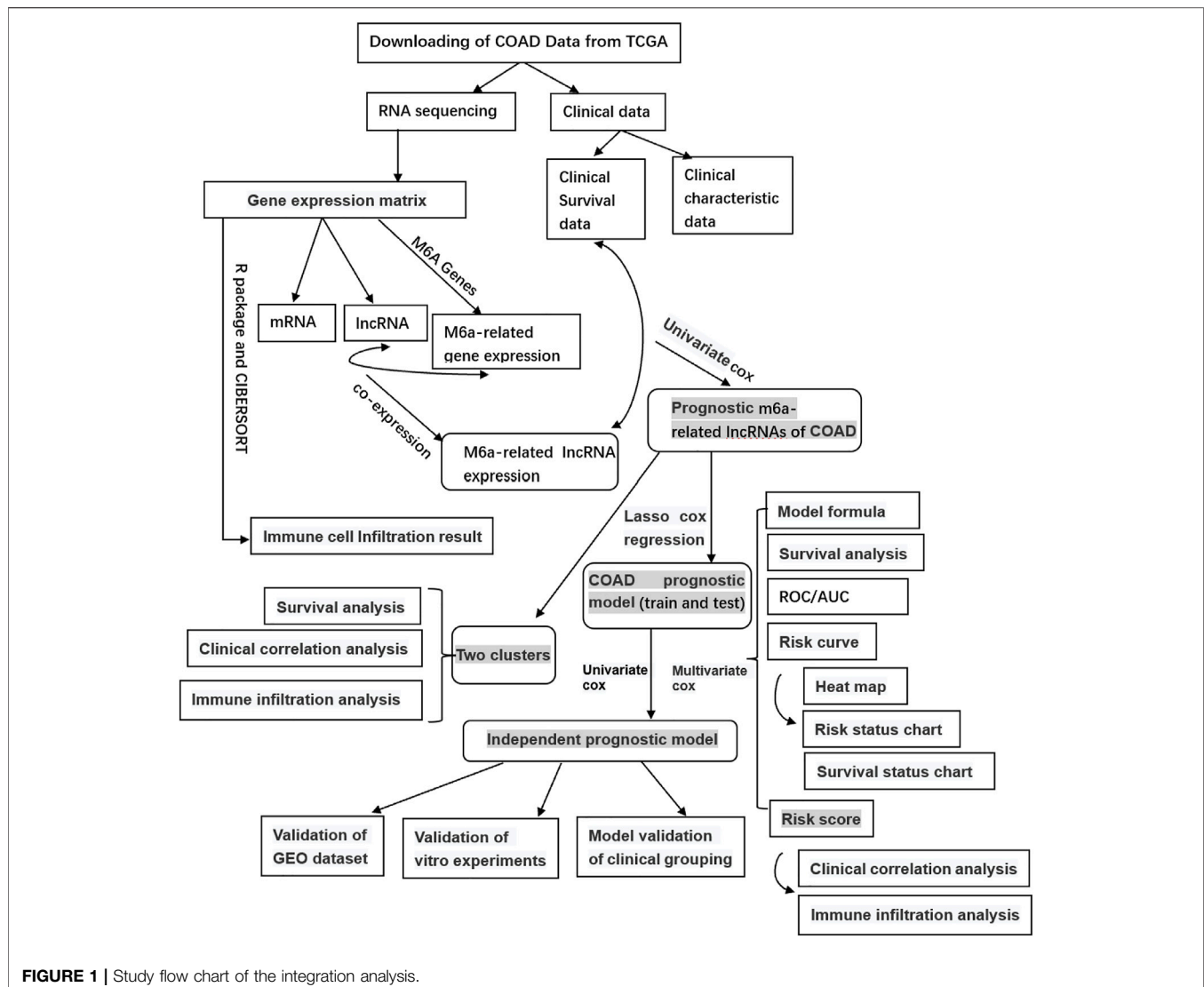


FIGURE 1 | Study flow chart of the integration analysis.

lncRNAs types was performed, and the survival curves were drawn. Subsequently, we analyzed the correlation between the two subtypes and clinical characteristics and visualized them by drawing heat maps. The immune cell infiltration results were obtained using CIBERSOERT, and the R packages BiocManager, Limma, PreprocessCore, and E1071. The TME was scored using the estimate, limma, and BiocManager packages. Then we obtained the immune cell, stromal, and estimate score files and compared their differences in two clusters. Explore differences of the immune cells in different types by Limma and Vioplot packages.

Construction of Independent Prognostic Model and the Risk Groupings

Prognostic m⁶A-related lncRNA samples were divided into training and testing datasets. By using caret, glmnet, survminer, and timeROC packages, also applying Lasso regression, the optimal prognostic model and model formula were obtained. The two groups were sorted into two groups of

high and low risk, according to the median risk score of the training dataset. Then, survival analysis of the two groups was performed by survival and survminer packages. All *p*-values were less than 0.01, indicating differences in survival, suggesting that the model can divide patients into high- and low-risk groups. Setting the prediction time at 1 year, we drew the receiver operating characteristic (ROC) curves by survival, survminer, and timeROC packages. Then, risk graphs of risk state, survival state, and risk heat map were obtained. Through univariate and multivariate Cox regression analysis, we confirmed whether the risk score was an independent indicator of the prognosis and whether the prognostic model was independent.

Relationship Between Risk Score With Clinicopathological Features and Immune Cell Infiltration

The model would be verified to be applied to patients in different clinical groups by survival and the survminer R package. We

applied limma, ggpub, and pheatmap packages to explore differences between risk scores with clinicopathological characteristics, immune scores, different clusters, and even the seven lncRNAs, visualized by the R package ($p < 0.001^{***}$, 0.01^{**} , 0.05^{*}). Then we used limma, ggplot2, ggpubr, and ggextra packages to identify the correlation between immune cells and the risk score. Samples with $p > 0.05$ would be filtered out before analysis, and the sum of all immune cells in a sample is equal to 1. The correlation coefficient and p -value were obtained by the Spearman test, visualized by scatter plots.

Validation of the Prognostic Value of Seven Screened m⁶A-Related lncRNAs by Gene Expression Omnibus Dataset

To verify the prognostic values of the seven m⁶A-lncRNAs signature, we gained external cohort (GSE39582) from Gene Expression Omnibus (GEO) (<https://www.ncbi.nlm.nih.gov/geo/query/acc.cgi>). Calculating the risk-score of every patient based on the signature, we classified the subjects into high- and low-risk groups with the median score of the training dataset of TCGA data. Through the survival package of R, we performed the survival probability. Therefore, the prediction model could be validated.

Validation of the Expression Level of Seven m⁶A-Related lncRNAs in Tissue Specimens by Quantitative Reverse Transcription-PCR

We collected 20 paired COAD samples and tumor-adjacent normal tissues from the Second Hospital of Hebei Medical University. All the fresh samples were frozen in liquid nitrogen immediately and stored at -80°C . All tissues were confirmed histopathologically by pathologists and did not receive preoperative radiotherapy or chemotherapy. All patients signed the informed consent before the operation, and the ethics committees approved the consent procedure. The expression levels of the seven lncRNAs were examined by quantitative reverse transcription (qRT)-PCR. The $2^{-\Delta\Delta\text{Ct}}$ method was used to calculate the relative expression level.

Statistics

All analyses were performed by R software v4.1 (<https://www.r-project.org/>) and Perl v5.30 (<https://www.perl.org/>). The p -value used in the analysis was two-sided, and a p -value < 0.05 was regarded as statistically significant. Univariate Cox regression, multivariate Cox regression, and Lasso regression were utilized. Quantitative data were expressed as mean \pm SD and analyzed for significant difference in two groups by Student's t -test. All data with p -values less than 0.05 were recognized as statistically significant.

RESULTS

Nine Prognostic m⁶A-Related lncRNAs

By combining the m⁶A-related lncRNA expression data with the survival data, then using univariate Cox regression, we obtained nine prognostic m⁶A-related lncRNAs: LINC02657,

NSMCE1-DT, AC139149.1, ZKSCAN2-DT, AC156455.1, ZEB1-AS1, AP001619.1, AL391422.4, and ATP2B1-AS1 ($p < 0.001$; if $p < 0.05$, there were too many lncRNAs). All of them were high-risk lncRNAs (Supplementary Table S1). The expression of AC156455.1 in tumor tissue was significantly higher than that of the normal group. The results were visualized by forest plots, box plots, and heat maps (Figures 2A–C).

The Independent Prognostic Model of Seven m⁶A-Related lncRNAs

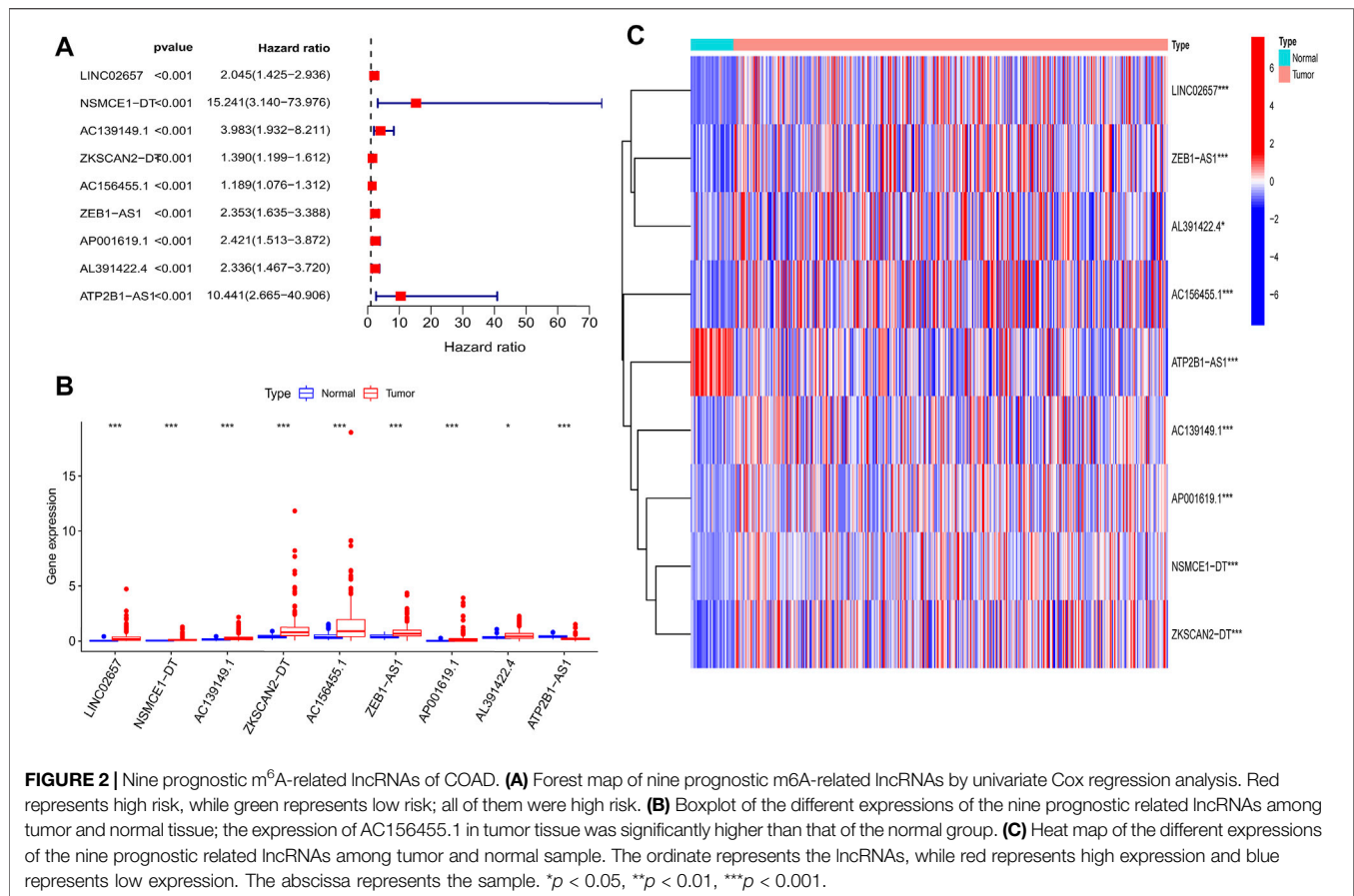
Prognostic m⁶A-related lncRNA samples were divided into training and test datasets (50% in each group). Through the R packages and Lasso regression, using the cross-validation method to optimize the model, we finally obtained the independent prognostic model consisting of seven lncRNAs, model formula: risk score = LINC02657 * 0.246632699492067 + AC139149.1 * 0.276937064691493 + ZKSCAN2-DT * 0.016797173163626 + AC156455.1 * 0.187570142850178 + ZEB1-AS1 * 0.569626111717306 + AL391422.4 * 0.537921082314907 + ATP2B1-AS1 * 0.555444251652824 (Supplementary Figures S1A, B). There were survival differences between the high- and low-risk groups in the training and test groups, with the survival curve drawn by the R package ($p < 0.05$). The high-risk group had a low survival rate (Figures 3A, B). In addition, the area under the curve (AUC) was 0.733 and 0.673 in the training dataset and testing dataset for overall survival (OS) at 1 year (Figures 3C, D), revealing the high accuracy of this model in predicting the prognosis. Through the risk curve of heat map, survival state, and risk state map, we found that more deaths occurred in the high-risk group (Figures 4A–D). The expression of the all prognostic lncRNAs was higher in the high-risk group among both training and testing datasets. The expression of the lncRNA ZEB1-AS1 was significantly higher in the high-risk groups (Figures 5A, B). By univariate and multivariate Cox regression, the risk score was identified as an independent prognostic indicator (Figures 6A–D), verifying the independence of the model.

Relationship Between Different Clusters or High-Low Risk Groups With Clinicopathological Features

Prognostic m⁶A-related lncRNAs were divided into two types through consistent clustering analysis (Supplementary Figures S2A–D). Differences in survival analysis were found between the two groups ($p < 0.01$).

The survival rate of type 2 was low, suggesting a poor prognosis (Figure 7A). We analyzed the correlation between the two subtypes with clinical characteristics, visualized by Figure 7B. AC156455.1 expression was found to be significantly higher in type 2, suggesting that AC156455.1 may be predominantly related to the occurrence and development of COAD.

By verifying the prognostic model on the clinical traits, it was found that the model applied to clinical characteristics such as age, gender, stage, and T and N staging (Figures 8A–J).



Analyzing differences of different clusters, clinicopathological characteristics, immune scores, and the lncRNA expression of the high- and low-risk groups, we discovered differences in clusters and clinical traits (stages, N and M staging) in the high- and low-risk groups (**Figures 9A–E**). The proportion of cluster two in the high-risk group was high, while the low survival rate indicated that the high-risk group was accompanied by a poor prognosis. Advanced clinical features such as stage III–IV, N1–3, and M1 occupied more in the high-risk groups, showing the higher risk attached to the worse clinical stage. The results of the heat map indicated that all prognostic lncRNAs were high-risk markers. The expression of ZEB1-AS1 was significantly increased in the high-risk group both on the risk curve and on the heat map. Hence, further studies should be conducted to explore the prognostic value of lncRNA ZEB1-AS1 in COAD.

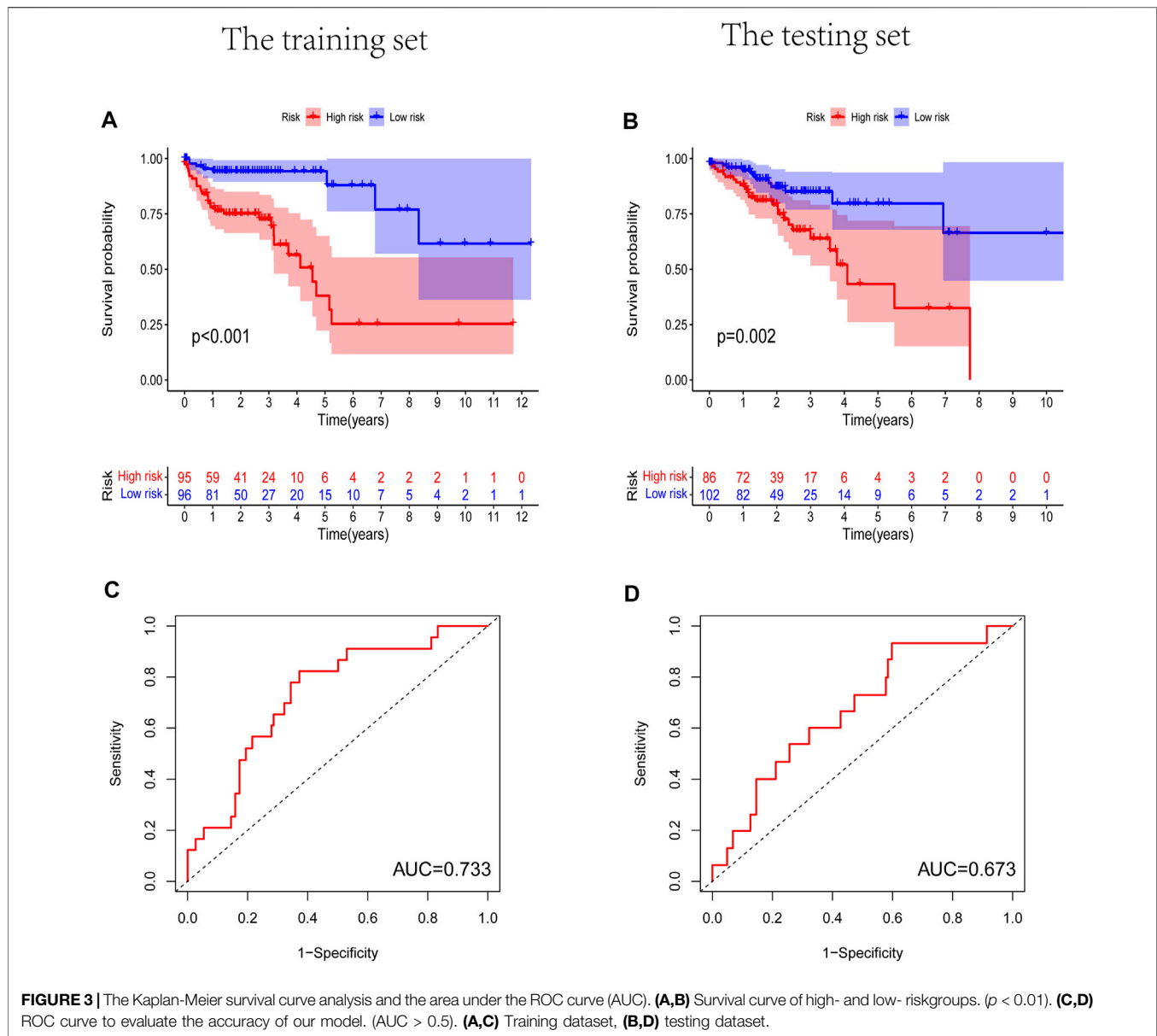
Relationship Between Different Clusters or High-Low Risk Groups With Immune Cell Infiltration

There were five types of immune cells expressed differently in two different clusters: CD4 memory activated T cells, follicular helper T cells, activated natural killer (NK) cells, CD4 memory T cells, and memory B cells (**Supplementary Table S2**). The first three were upregulated in type 2, which had a low

survival rate. They may be relevant to poor prognosis and provide some reference for immunotherapy. T cells CD4 memory resting was upregulated in type 1 (**Figures 10A–F**). There were differences in the immune score, stromal score, and estimate score between type 1 and type 2; all had low scores in type 2. The lower the score was, the higher the tumor purity was, which may correlate with poor prognosis (**Figures 11A–C**). We got risk scores of the samples according to the prognostic model formula. We explored which immune cells were associated with patients' risk using limma, ggplot2, ggpubr, ggextra packages, and Spearman test. Finally, memory B cells were correlated with the risk score ($p < 0.05$, $R > 0$), indicating that its content was positively correlated with the risk of the patients. The higher the content of memory B cells, the higher risk the patient had ($R = 0.17$, $p = 0.043$), visualized by a scatter diagram (**Figure 12**).

Validation of GEO Dataset

We obtained the GSE39582 data set from GEO database which contained 579 samples and then obtained the expression levels of seven m⁶A-related lncRNAs as well as the survival data of the samples. According to the model, we calculated the risk score and obtained the high- and low-risk groups based on the median risk scores of the training dataset of TCGA data. Finally, we found there were survival differences between the high- and low-risk



groups, $p < 0.001$ (Figure 13). Our model was validated in the GEO dataset.

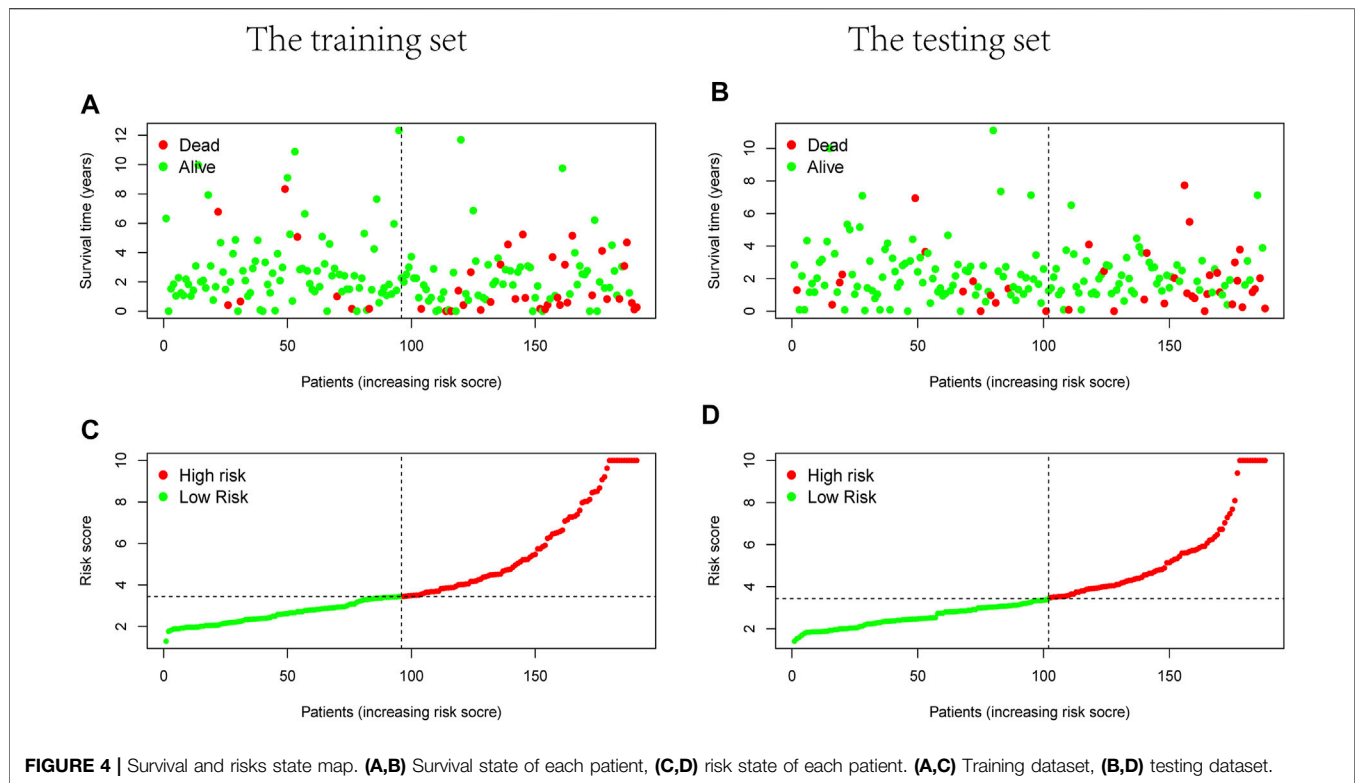
Validation of the Expression Level of Screened m⁶A-Related lncRNAs by qRT-PCR

In order to further validate the feasibility of the prognostic signature, we performed qRT-PCR experiment to identify the expression levels of the seven lncRNAs in clinical tissue samples. Finally, we found the expression of these seven lncRNAs in tumor tissues was significantly higher than that in tumor-adjacent normal tissues (Figure 14), especially ZKSCAN2-DT and AC156455.1, consistent with the TCGA dataset. Collectively, this further validated the stability and

reliability of the m⁶A-related lncRNAs prognostic signature. β -Actin was chosen as the internal control. The primers used are listed in Table 1.

DISCUSSION

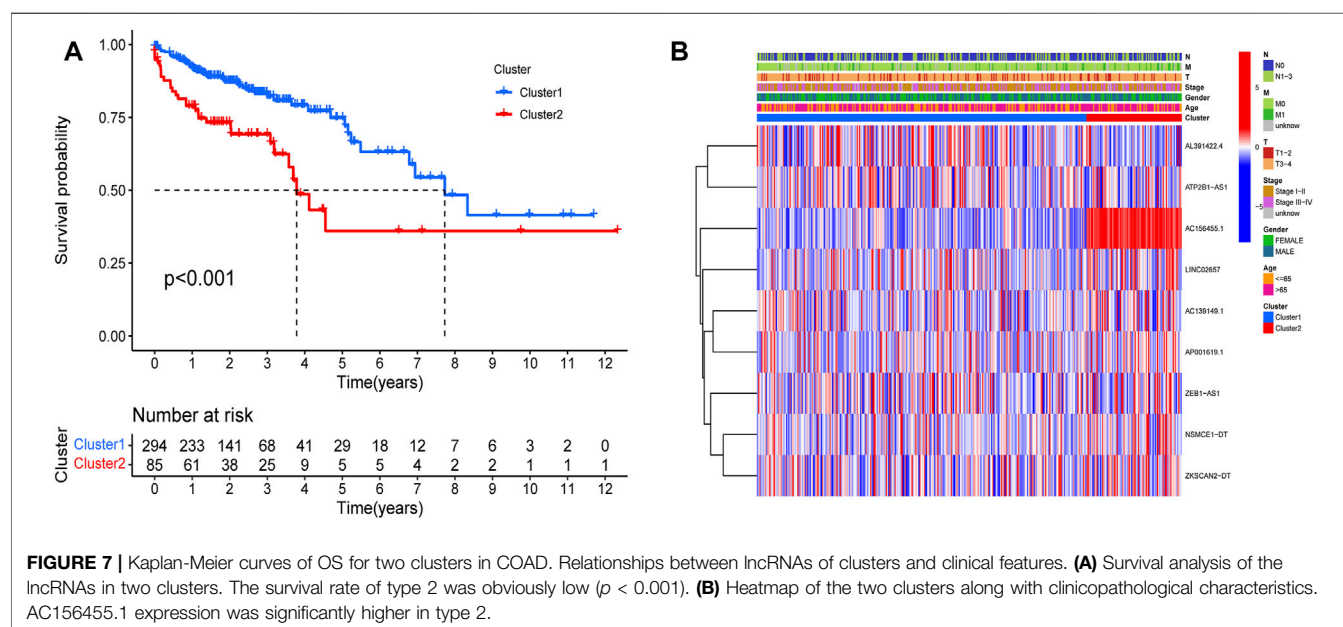
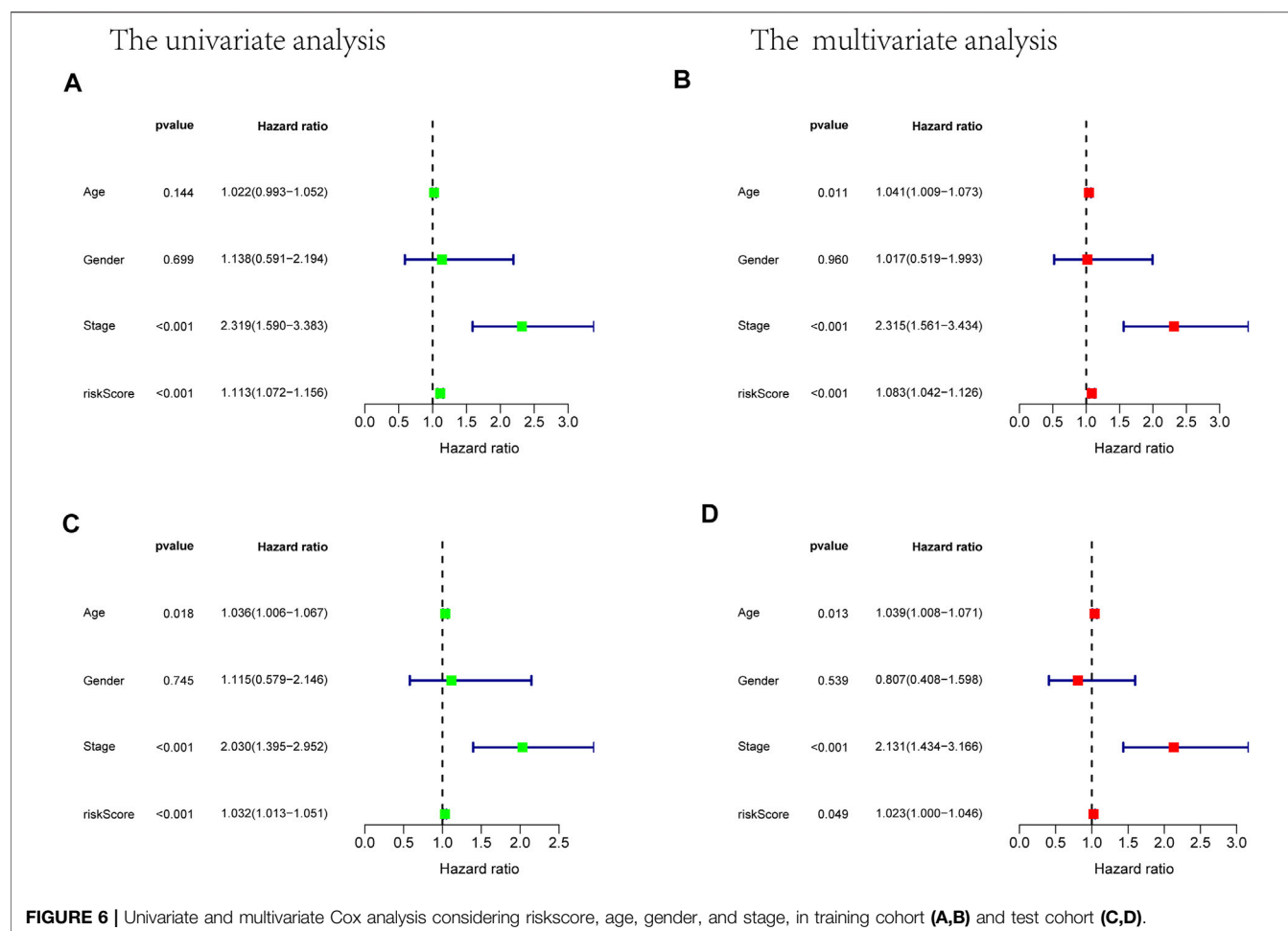
Aberrant m⁶A modifications are closely related to the onset and progression of various cancers, including CRC (Liu et al., 2018; Gong et al., 2019; Wang et al., 2020; Wang et al., 2021; Zhang and Zhang., 2021). Nowadays, lncRNAs are reported to act essential roles in the development of tumors, especially in epigenetic regulation, protein interaction, and RNA metabolism. Emerging researches on N⁶-methyladenosine of lncRNA are performed to provide prognosis-related biomarkers and novel



therapeutic targets for various carcinomas (Li et al., 2021a; Chen et al., 2021; Han et al., 2021). In our study, we obtained nine prognostic m⁶A-related lncRNA of COAD. All of them were high risk, meaning that the genes with higher expression have a worse prognosis. We finally got the independent prognostic model consisting of seven m⁶A lncRNAs. There was a difference in survival probability between high- and low-risk group samples, in both

training and testing groups. The high-risk group has a low survival rate. Moreover, the AUC showed that the model accurately predicts the prognosis. Through the risk curve, we found that more deaths occurred in the high-risk group.

Furthermore, we explored the relationship between risk score and clinical characteristics and found that advanced clinical features such as stage III–IV, N1–3, and M1 occupied more



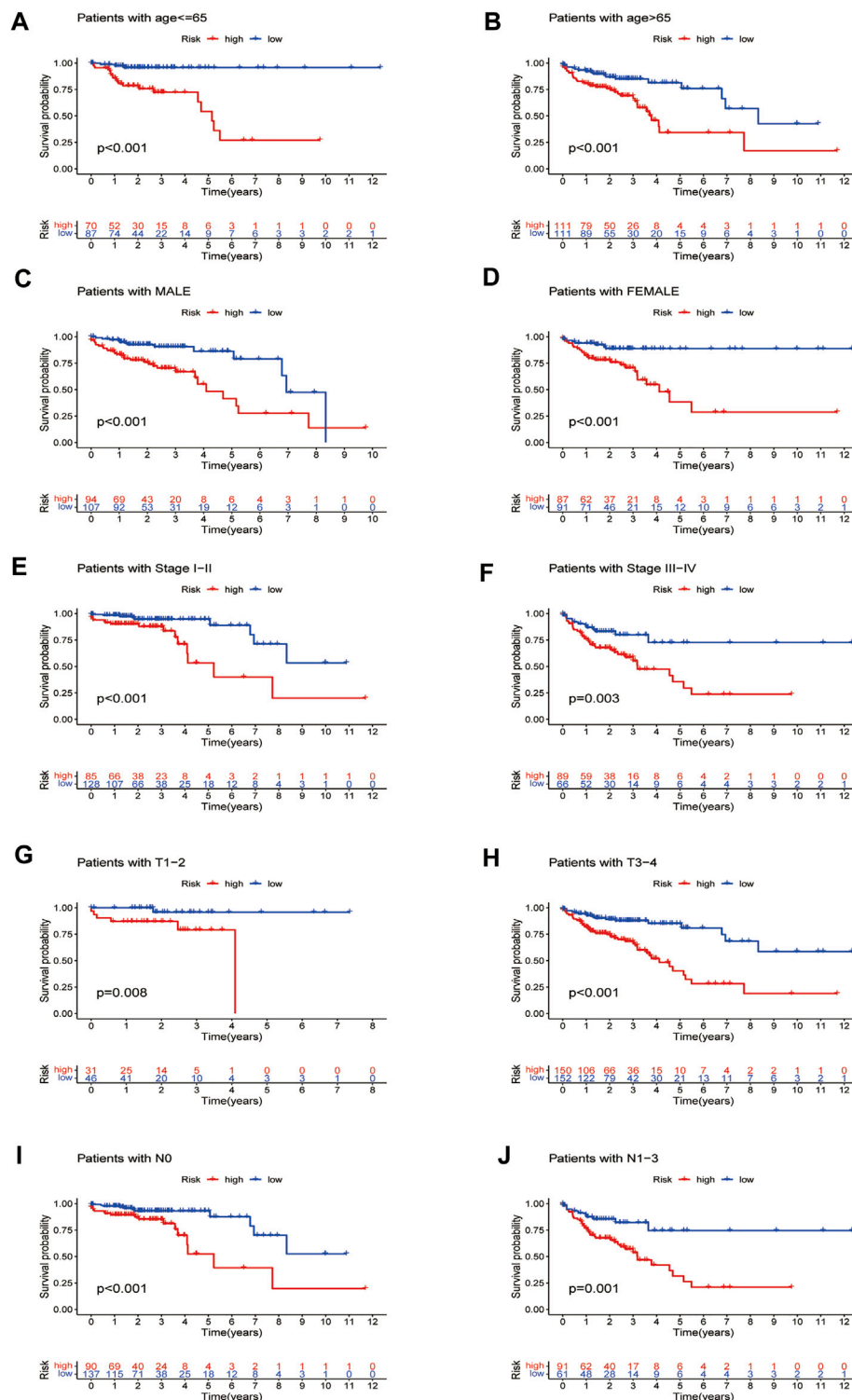


FIGURE 8 | Survival curves for model validation (our prognostic model applied to different clinical groups: age, gender, stage, and T and N staging, $p < 0.05$).

in the high-risk groups. It showed that the high-risk score was highly correlated with malignant clinical characteristics. Therefore, the model can be used as a new potential prognostic biomarker of COAD.

In the study, we found two special lncRNAs, AC156455.1 and ZEB1-AS1. Yang et al. constructed a risk signature of seven lncRNAs (LINC00460, AL139351.1, AC156455.1, AL035446.1, LINC02471, AC022509.2, and LINC01606) for

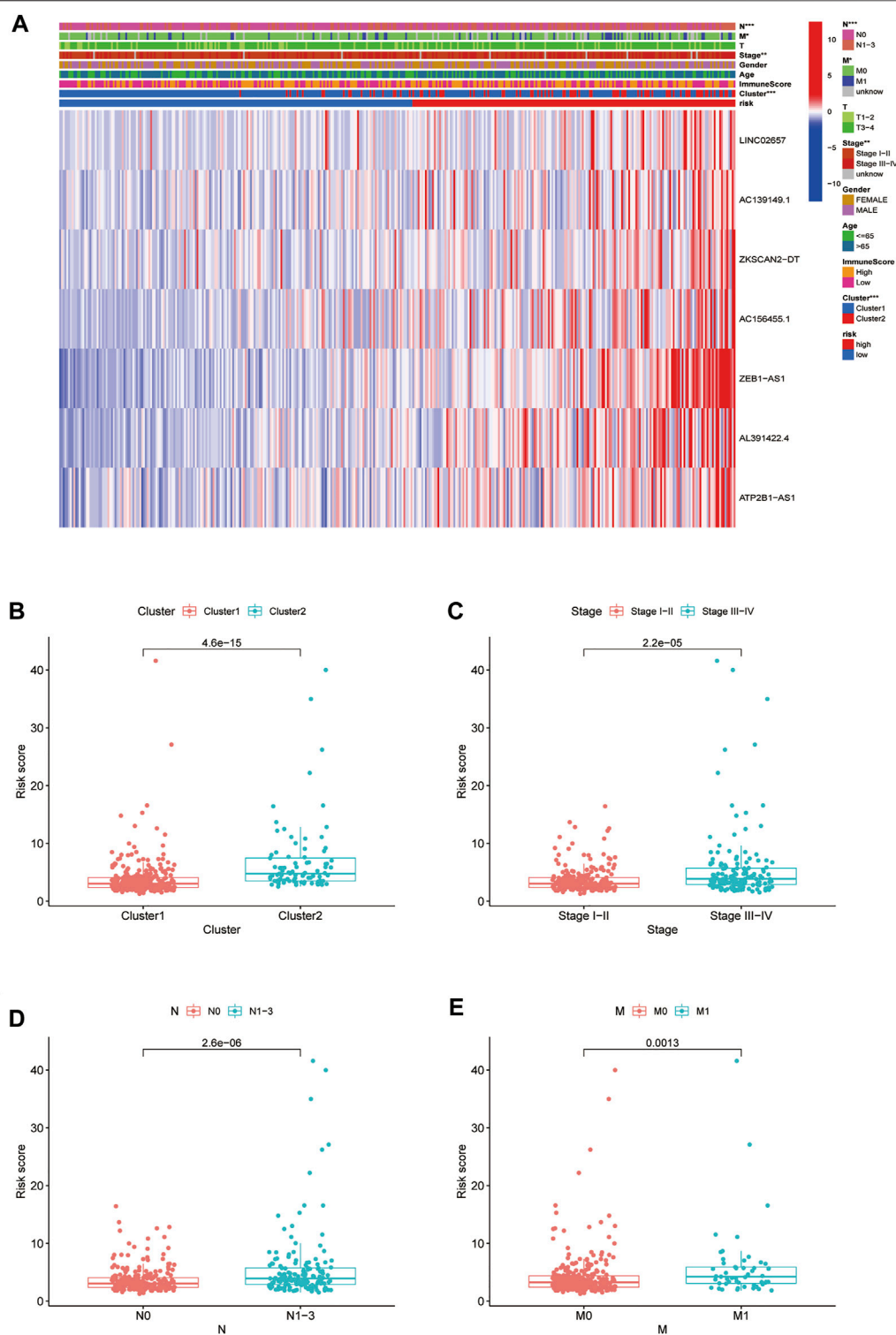


FIGURE 9 | Relationship between high-low risk groups and clinicopathological features. **(A)** Heatmap of correlation analysis between riskscore and clinical traits; **(B-E)** boxplot of relationship analysis of riskscore and clinical features (clusters, clinical traits such as stage, and N and M staging were closely related to riskscore, $p < 0.05$).

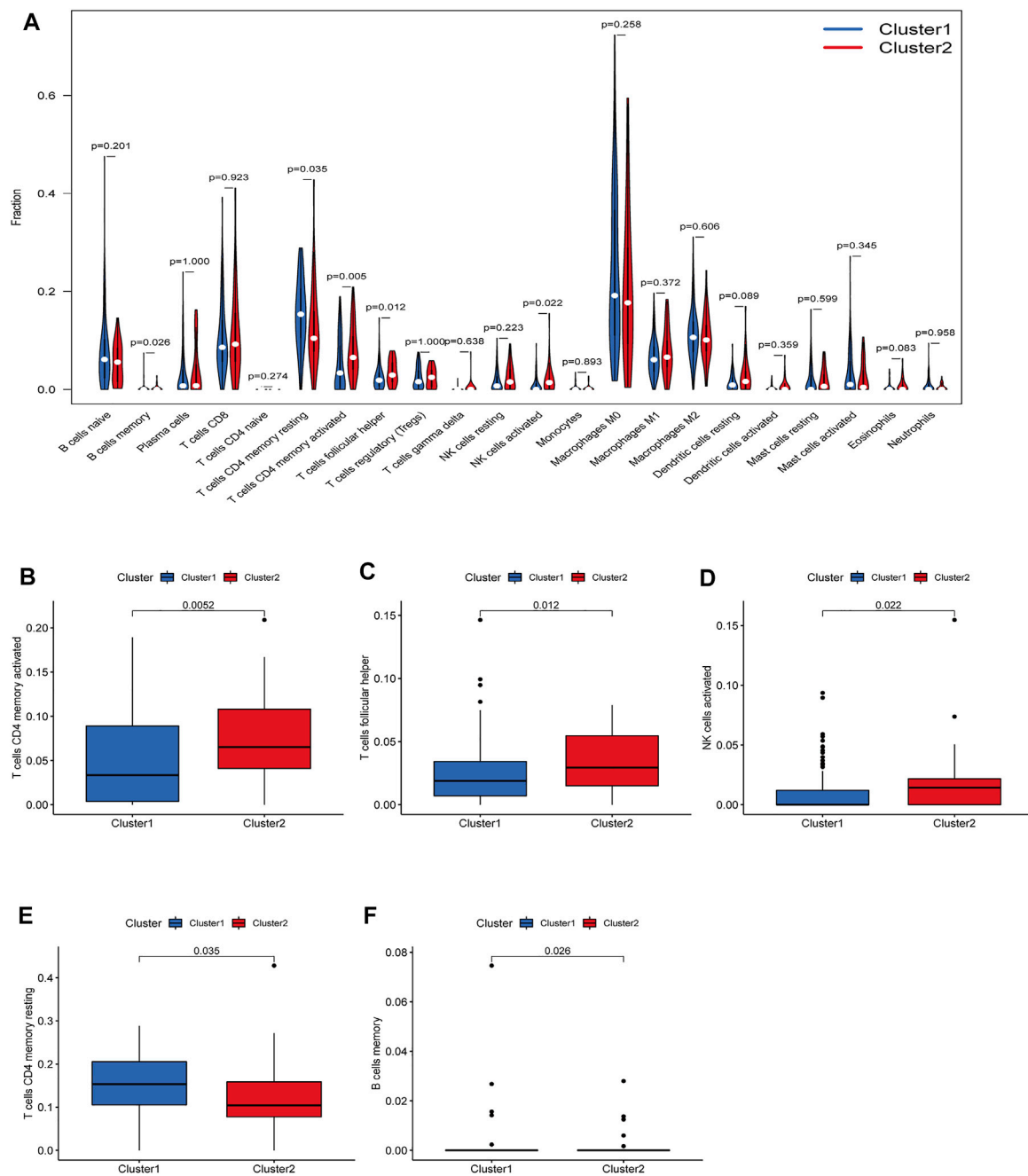
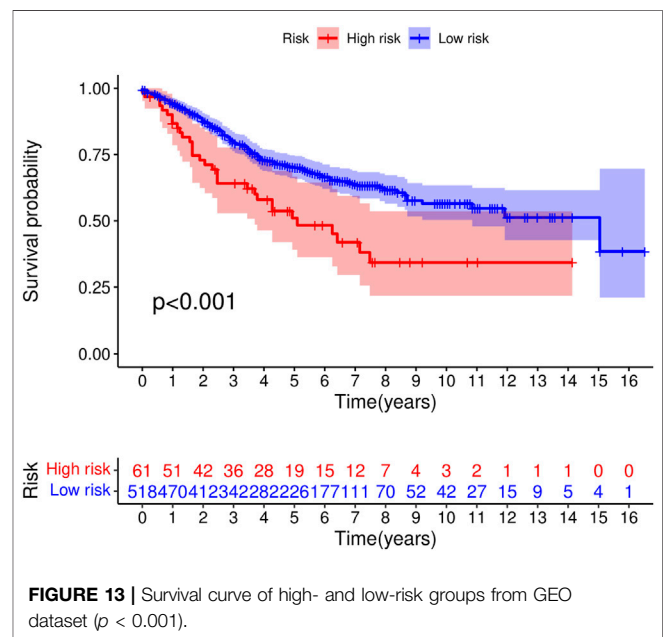
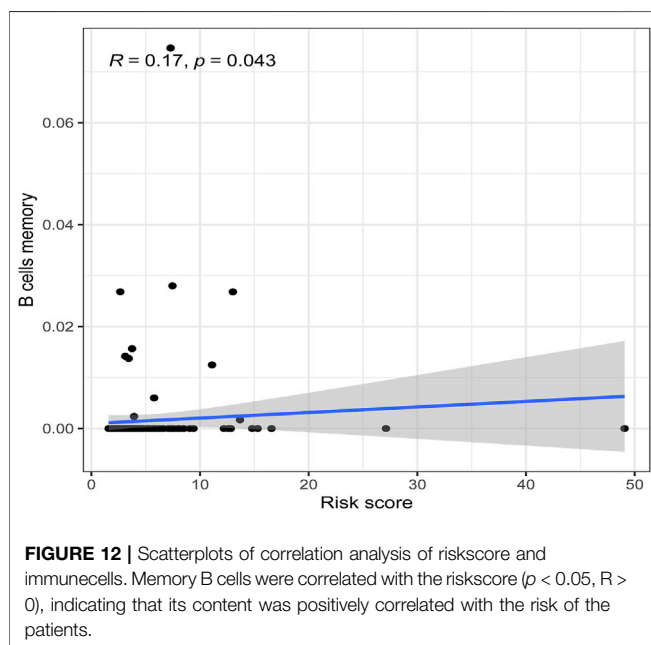
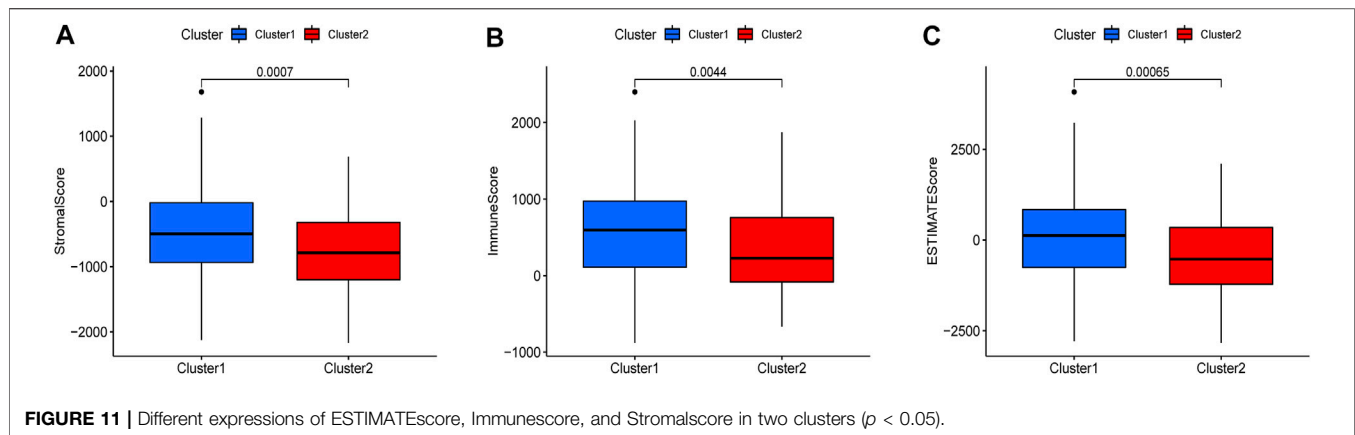


FIGURE 10 | Different analysis of immune cell infiltration in the two clusters. **(A)** Violinplot; **(B–F)** Boxplot. CD4 memory activated T cells, follicular helper T cells and a1186ctivated NK cells were upregulated in type 2, which had a low survival rate.

clear cell renal cell carcinoma patients (Yang et al., 2021). AC156455.1 was included in Yang's signature and also existed in our model. The level of AC156455.1 expression in tumor tissues was significantly higher than that of the normal group. Meanwhile, the expression level of AC156455.1 was significantly higher in type 2, which had a low survival rate. Being of high risk, AC156455.1 was associated with the malignancy of COAD, suggesting that it could be further studied for specific prognostic value. The other identified

lncRNA was ZEB1-AS1, the expression of which was significantly higher in high-risk groups of both test and training samples and could also be further studied for the prognosis of COAD.

Zheng et al. identified a risk model of four m⁶A-related lncRNA predicting the OS and therapeutic value of ovarian cancer (OC). lncRNA CACNA1G-AS1 was identified to be upregulated in 30 OC specimens and 3 OC cell lines, while its knockdown restrained the multiplication capacity



of OC cells (Zheng et al., 2021). Zheng and collages verified this lncRNA in OC samples, and tumor cell lines revealed its potential prognostic and therapeutic value. In the same way, we could conduct further research on ZEB1-AS1 and AC156455.1, which we found to be closely correlated with COAD.

Yang et al. found that through the m⁶A modification of METTL3-mediated MYC mRNA, HBXIP can lead to tumorigenesis of GC (Yang Z. et al., 2020). Different enzymes that participate in m⁶A modifications can lead to progression in different cancers (Yang et al., 2020a), while the underlying mechanisms, such as the involved signaling pathways, need further research.

In addition, methylation is a reversible process, and demethylation can be used in tumor therapy. ALKBH5, one of the demethylases, could affect tumor progression by regulating lncRNA demethylation. In a research about pancreatic cancer, the

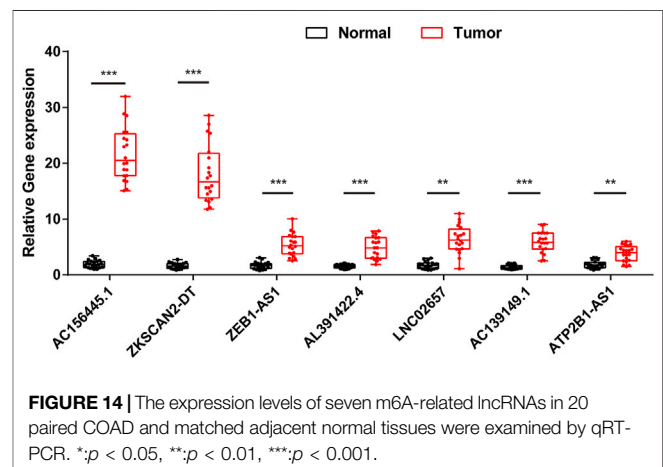


TABLE 1 | Primers used in qRT-PCR.

Primer	Sequence	Primer length	Tm	Product size
AL391422.4-F-H	GTGTGAGTGTGGTATGGCTGTGTC	24	60.4	134 bp
AL391422.4-R-H	TGGAAGGCGGAGGTTGTAGTGAG	23	61.5	
ATP2B1-AS1-F-H	ACGCCCTCCCTTTCTTCCTTC	22	62.3	146 bp
H ATP2B1-AS1-R-H	CCTCTGCACCAACACGTCATG	22	61.5	
AC156455.1-F-H	TCATCTGACCTCCTGGCAACCC	22	62.1	135 bp
AC156455.1-R-H	TCCGAAGCCTCCTTCACTGAGTC	23	61.2	
ZKSCAN2-DT-F-H	TCATCTGACCTCCTGGCAACCC	25	59.4	132 bp
ZKSCAN2-DT-R-H	TCCGAAGCCTCCTTCACTGAGTC	23	60.9	
AC139149.1-F-H	TGTAATCAGTAGAGCAGGGCAGAGG	25	60.4	88 bp
AC139149.1-R-H	AGAGACAGAGAACCAGGACGGAAG	24	60.4	
ZEB1-AS1-F-H	TGGCAGGACTCAGAGCTAAGGTATC	25	60.2	105 bp
ZEB1-AS1-R-H	ACATCTGTGAGCCGATGCTTCTTG	24	59.7	
LNC02657-F-H	GCAAGAGAGAAGACAGTGGGTGAAG	25	59.8	135 bp
LNC02657-R-H	ATTTGTGCCGTGACTCTGGGAAC	23	60.2	
β -actin-F	GGCTGTATTCCCTCCATCG	20	61.8	154 bpzz
β -actin-R	CCAGTTGGTAACAATGCCATGT	22	61.1	

expression of ALKBH5 was found downregulated in tumor cells and could inhibit cells by demethylating the lncRNA KCN15-AS1, which can be used in prognostics and therapy strategies (He et al., 2018).

When it comes to the point above, by what methylation mechanism does our prognostic lncRNAs act in, whether it can be mediated by MettL3, and what the signaling pathway is, whether it can be demethylated, all these need further research.

Yu and Zhu found immune cell infiltration related to m⁶A-correlated lncRNA in GC can provide novel therapeutic value. The high-risk scores indicated a lower purity of tumor cells, as well as a higher density of immune-related cells (Yu and Zhu, 2021). Gaudreau et al. investigated the correlation between neoadjuvant chemotherapy (NCT) and the immune microenvironment (IME) in resectable NSCLC (non-small cell lung cancer) and discovered NCT was closely related to the cell infiltration increase of cytotoxic CD8⁺ T cells and CD20⁺ B cells (Gaudreau et al., 2021). In our study, we found five kinds of immune cells expressed differently in different types of lncRNA, that is, CD4 memory activated T cells, follicular helper T cells, activated NK cells, CD4 memory T cells, and memory B cells. The first three were upregulated in type 2, which had a low survival rate. They may be relevant to poor prognosis. There were differences in the immune score, stromal score, and estimate score between type 1 and type 2, all of which had low scores in type 2. The lower the score was, the higher the tumor purity was. This may be correlated with a poor prognosis. Memory B cells were correlated with the risk score. We found that m⁶A-related lncRNAs were associated with immune cell infiltration in COAD, which could assist us in exploring new therapeutic targets. Although tumor immunotherapy has made rapid progress in recent years, the overall therapeutic effect of COAD is not satisfactory. So it is necessary to develop multimode therapy and biointegration targets. Further investigation is needed between m⁶A-related lncRNAs and COAD.

In summary, in this study, we obtained seven m⁶A lncRNAs signature and immune infiltration results. Besides, we have verified the prognostic model by GEO dataset, and the expression level of lncRNAs was further verified by in vitro experiments. This suggests the signature could be used as a new potential and promising biomarker and provide an

individual treatment strategy for COAD. Nevertheless, the m⁶A methylation mechanism of these lncRNAs is still unknown. Furthermore, the specific correlation between m⁶A-related lncRNA and immune cells should be thoroughly explored.

DATA AVAILABILITY STATEMENT

Publicly available datasets were analyzed in this study. These data can be found here: The Cancer Genome Atlas (TCGA) (<https://portal.gdc.cancer.gov/>).

ETHICS STATEMENT

Ethical review and approval was not required for the study on human participants in accordance with the local legislation and institutional requirements. Written informed consent for participation was not required for this study in accordance with the national legislation and the institutional requirements.

AUTHOR CONTRIBUTIONS

All authors listed have made a substantial, direct, and intellectual contribution to the work and approved it for publication.

ACKNOWLEDGMENTS

The authors would like to thank the TCGA database for the availability of the data.

SUPPLEMENTARY MATERIAL

The Supplementary Material for this article can be found online at: <https://www.frontiersin.org/articles/10.3389/fgene.2021.774010/full#supplementary-material>

REFERENCES

- Banerjee, A., Pathak, S., Subramaniam, V. D., G., D., Murugesan, R., and Verma, R. S. (2017). Strategies for Targeted Drug Delivery in Treatment of Colon Cancer: Current Trends and Future Perspectives. *Drug Discov. Today* 22 (8), 1224–1232. doi:10.1016/j.drudis.2017.05.006
- Cen, X., Huang, Y., Lu, Z., Shao, W., Zhuo, C., Bao, C., et al. (2021). lncRNA IGF2-AS1 Promotes the Proliferation, Migration, and Invasion of Colon Cancer Cells and Is Associated with Patient Prognosis. *Cmar* 13, 5957–5968. doi:10.2147/CMAR.S313775
- Chen, Y.-t., Xiang, D., Zhao, X.-y., and Chu, X.-y. (2021). Upregulation of lncRNA NIFK-AS1 in Hepatocellular Carcinoma by m6A Methylation Promotes Disease Progression and Sorafenib Resistance. *Hum. Cell* 34, 1800–1811. doi:10.1007/s13577-021-00587-z
- Danaher, P., Warren, S., Lu, R., Samayoa, J., Sullivan, A., Pekker, I., et al. (2018). Pan-cancer Adaptive Immune Resistance as Defined by the Tumor Inflammation Signature (TIS): Results from the Cancer Genome Atlas (TCGA). *J. Immunotherapy Cancer* 6 (1), 63. doi:10.1186/s40425-018-0367-1
- Gaudreau, P.-O., Negrao, M. V., Mitchell, K. G., Reuben, A., Corsini, E. M., Li, J., et al. (2021). Neoadjuvant Chemotherapy Increases Cytotoxic T Cell, Tissue Resident Memory T Cell, and B Cell Infiltration in Resectable NSCLC. *J. Thorac. Oncol.* 16 (1), 127–139. doi:10.1016/j.jtho.2020.09.027
- Gong, D., Zhang, J., Chen, Y., Xu, Y., Ma, J., Hu, G., et al. (2019). The m6A-Suppressed P2RX6 Activation Promotes Renal Cancer Cells Migration and Invasion through ATP-Induced Ca²⁺ Influx Modulating ERK1/2 Phosphorylation and MMP9 Signaling Pathway. *J. Exp. Clin. Cancer Res.* 38 (1), 233. doi:10.1186/s13046-019-1223-y
- Gu, Y., Niu, S., Wang, Y., Duan, L., Pan, Y., Tong, Z., et al. (2021). DMDRMR-mediated Regulation of m6A-Modified CDK4 by m6A Reader IGF2BP3 Drives ccRCC Progression. *Cancer Res.* 81 (4), 923–934. doi:10.1158/0008-5472.CAN-20-1619
- Gutschner, T., Hämmerle, M., Eissmann, M., Hsu, J., Kim, Y., Hung, G., et al. (2013). The Noncoding RNA MALAT1 Is a Critical Regulator of the Metastasis Phenotype of Lung Cancer Cells. *Cancer Res.* 73 (3), 1180–1189. doi:10.1158/0008-5472.CAN-12-2850
- Han, T., Xu, D., Zhu, J., Li, J., Liu, L., and Deng, Y. (2021). Identification of a Robust Signature for Clinical Outcomes and Immunotherapy Response in Gastric Cancer: Based on N6-Methyladenosine Related Long Noncoding RNAs. *Cancer Cell Int* 21 (1), 432. doi:10.1186/s12935-021-02146-w
- He, Y., Hu, H., Wang, Y., Yuan, H., Lu, Z., Wu, P., et al. (2018). ALKBH5 Inhibits Pancreatic Cancer Motility by Decreasing Long Non-coding RNA KCNK15-AS1 Methylation. *Cell Physiol Biochem* 48 (2), 838–846. doi:10.1159/000491915
- Jin, Y., Wang, Z., He, D., Zhu, Y., Hu, X., Gong, L., et al. (2021). Analysis of m6A-Related Signatures in the Tumor Immune Microenvironment and Identification of Clinical Prognostic Regulators in Adrenocortical Carcinoma. *Front. Immunol.* 12, 637933. doi:10.3389/fimmu.2021.637933
- Koi, M., and Carethers, J. M. (2017). The Colorectal Cancer Immune Microenvironment and Approach to Immunotherapies. *Future Oncol.* 13 (18), 1633–1647. doi:10.2217/fon-2017-0145
- Kong, X., Duan, Y., Sang, Y., Li, Y., Zhang, H., Liang, Y., et al. (2019). lncRNA-CDC6 Promotes Breast Cancer Progression and Function as ceRNA to Target CDC6 by Sponging microRNA-215. *J. Cell Physiol* 234 (6), 9105–9117. doi:10.1002/jcp.27587
- Kweon, S.-S. (2018). Updates on Cancer Epidemiology in Korea, 2018. *Chonnam Med. J.* 54 (2), 90–100. doi:10.4068/cmj.2018.54.2.90
- Li, H., Ma, S.-Q., Huang, J., Chen, X.-P., and Zhou, H.-H. (2017). Roles of Long Noncoding RNAs in Colorectal Cancer Metastasis. *Oncotarget* 8 (24), 39859–39876. doi:10.18632/oncotarget.16339
- Li, N., Chen, X., Liu, Y., Zhou, T., and Li, W. (2021a). Gene Characteristics and Prognostic Values of m6A RNA Methylation Regulators in Non-small Cell Lung Cancer. *J. Healthc. Eng.* 2021, 2257066. doi:10.1155/2021/2257066
- Li, T., Hu, P.-S., Zuo, Z., Lin, J.-F., Li, X., Wu, Q.-N., et al. (2019). METTL3 Facilitates Tumor Progression via an m6A-igf2bp2-dependent Mechanism in Colorectal Carcinoma. *Mol. Cancer* 18 (1), 112. doi:10.1186/s12943-019-1038-7
- Li, Z., Li, Y., Zhong, W., and Huang, P. (2021b). m6A-Related lncRNA to Develop Prognostic Signature and Predict the Immune Landscape in Bladder Cancer. *J. Oncol.* 2021, 7488188. doi:10.1155/2021/7488188
- Liu, J., Eckert, M. A., Harada, B. T., Liu, S.-M., Lu, Z., Yu, K., et al. (2018). m6A mRNA Methylation Regulates AKT Activity to Promote the Proliferation and Tumorigenicity of Endometrial Cancer. *Nat. Cell Biol* 20 (9), 1074–1083. doi:10.1038/s41556-018-0174-4
- Liu, X., Xiao, Z.-D., Han, L., Zhang, J., Lee, S.-W., Wang, W., et al. (2016). lncRNA NBR2 Engages a Metabolic Checkpoint by Regulating AMPK under Energy Stress. *Nat. Cell Biol* 18 (4), 431–442. doi:10.1038/ncb3328
- Liu, Z., Li, S., Huang, S., Wang, T., and Liu, Z. (2021). N6-Methyladenosine Regulators and Related lncRNAs Are Potential to Be Prognostic Markers for Uveal Melanoma and Indicators of Tumor Microenvironment Remodeling. *Front. Oncol.* 11, 704543. doi:10.3389/fonc.2021.704543
- Poursheikhani, A., Abbaszadegan, M. R., Nokhandani, N., and Kerachian, M. A. (2020). Integration Analysis of Long Non-coding RNA (lncRNA) Role in Tumorigenesis of colon Adenocarcinoma. *BMC Med. Genomics* 13 (1), 108. doi:10.1186/s12920-020-00757-2
- Romanowska, K., Rąwłuszko-Wieczorek, A. A., Marczak, Ł., Kosińska, A., Suchorska, W. M., and Golusiński, W. (2021). The m6A RNA Modification Quantity and mRNA Expression Level of RNA Methylation-Related Genes in Head and Neck Squamous Cell Carcinoma Cell Lines and Patients. *Biomolecules* 11 (6), 908. doi:10.3390/biom11060908
- Siegel, R. L., Miller, K. D., Fuchs, H. E., and Jemal, A. (2021). Cancer Statistics, 2021. *CA A. Cancer J. Clin.* 71 (1), 7–33. doi:10.3322/caac.21654
- Toor, S. M., Sasidharan Nair, V., Decock, J., and Elkord, E. (2020). Immune Checkpoints in the Tumor Microenvironment. *Semin. Cancer Biol.* 65, 1–12. doi:10.1016/j.semcancer.2019.06.021
- Wang, Q., Chen, C., Ding, Q., Zhao, Y., Wang, Z., Chen, J., et al. (2020). METTL3-mediated m6A Modification of HDGF mRNA Promotes Gastric Cancer Progression and Has Prognostic Significance. *Gut* 69 (7), 1193–1205. doi:10.1136/gutjnl-2019-319639
- Wang, S., Gan, M., Chen, C., Zhang, Y., Kong, J., Zhang, H., et al. (2021). Methyl CpG Binding Protein 2 Promotes Colorectal Cancer Metastasis by Regulating N6-methyladenosine Methylation through Methyltransferase-like 14. *Cancer Sci.* 112 (8), 3243–3254. doi:10.1111/cas.15011
- Yang, H., Xiong, X., and Li, H. (2021). Development and Interpretation of a Genomic Instability Derived lncRNAs Based Risk Signature as a Predictor of Prognosis for Clear Cell Renal Cell Carcinoma Patients. *Front. Oncol.* 11, 678253. doi:10.3389/fonc.2021.678253
- Yang, J., Chen, J., Fei, X., Wang, X., and Wang, K. (2020a). N6-methyladenine RNA M-odification and C-ancer (Review). *Oncol. Lett.* 20 (2), 1504–1512. doi:10.3892/ol.2020.11739
- Yang, Z., Jiang, X., Li, D., and Jiang, X. (2020b). HBXIP Promotes Gastric Cancer via METTL3-Mediated MYC mRNA m6A Modification. *Aging* 12 (24), 24967–24982. doi:10.18632/aging.103767
- Yu, J., Mao, W., Sun, S., Hu, Q., Wang, C., Xu, Z., et al. (2021). Identification of an m6A-Related lncRNA Signature for Predicting the Prognosis in Patients with Kidney Renal Clear Cell Carcinoma. *Front. Oncol.* 11, 663263. doi:10.3389/fonc.2021.663263
- Yu, Z. L., and Zhu, Z. M. (2021). N6-Methyladenosine Related Long Non-coding RNAs and Immune Cell Infiltration in the Tumor Microenvironment of Gastric Cancer. *Biol. Proced. Online* 23 (1), 15. doi:10.1186/s12575-021-00152-w
- Yue, B., Song, C., Yang, L., Cui, R., Cheng, X., Zhang, Z., et al. (2019). METTL3-mediated N6-Methyladenosine Modification Is Critical for Epithelial-Mesenchymal Transition and Metastasis of Gastric Cancer. *Mol. Cancer* 18 (1), 142. doi:10.1186/s12943-019-1065-4
- Zaccara, S., Ries, R. J., and Jaffrey, S. R. (2019). Reading, Writing and Erasing mRNA Methylation. *Nat. Rev. Mol. Cell Biol* 20 (10), 608–624. doi:10.1038/s41580-019-0168-5
- Zhang, Z., and Zhang, X. (2021). Identification of m6A-Related Biomarkers Associated with Prognosis of Colorectal Cancer. *Med. Sci. Monit.* 27, e932370. doi:10.12659/MSM.932370

- Zheng, J., Guo, J., Cao, B., Zhou, Y., and Tong, J. (2021). Identification and Validation of lncRNAs Involved in m6A Regulation for Patients with Ovarian Cancer. *Cancer Cell Int* 21 (1), 363. doi:10.1186/s12935-021-02076-7
- Zhu, H., Zhao, H., Zhang, L., Xu, J., Zhu, C., Zhao, H., et al. (2017). Dandelion Root Extract Suppressed Gastric Cancer Cells Proliferation and Migration through Targeting lncRNA-CCAT1. *Biomed. Pharmacother.* 93, 1010–1017. doi:10.1016/j.biopha.2017.07.007

Conflict of Interest: The authors declare that the research was conducted in the absence of any commercial or financial relationships that could be construed as a potential conflict of interest.

Publisher's Note: All claims expressed in this article are solely those of the authors and do not necessarily represent those of their affiliated organizations or those of the publisher, the editors, and the reviewers. Any product that may be evaluated in this article, or claim that may be made by its manufacturer, is not guaranteed or endorsed by the publisher.

Copyright © 2021 Chai, Qi, Zou, He, Su and Zhao. This is an open-access article distributed under the terms of the Creative Commons Attribution License (CC BY). The use, distribution or reproduction in other forums is permitted, provided the original author(s) and the copyright owner(s) are credited and that the original publication in this journal is cited, in accordance with accepted academic practice. No use, distribution or reproduction is permitted which does not comply with these terms.



Non-Coding RNAs and Brain Tumors: Insights Into Their Roles in Apoptosis

Omid Reza Tamtaji¹, Maryam Derakhshan², Fatemeh Zahra Rashidi Noshabad³, Javad Razaviyan⁴, Razie Hadavi¹, Hamed Jafarpour⁵, Ameneh Jafari^{6,7}, Ali Rajabi^{3,8}, Michael R. Hamblin⁹, Mahmood Khaksary Mahabady^{10*}, Mohammad Taghizadieh^{11*} and Hamed Mirzaei^{12*}

¹Students' Scientific Research Center, Tehran University of Medical Sciences, Tehran, Iran, ²Department of Pathology, Isfahan University of Medical Sciences, Isfahan, Iran, ³Student Research Committee, Kashan University of Medical Sciences, Kashan, Iran, ⁴Student Research Committee, School of Medicine, Shahid Beheshti University of Medical Sciences, Tehran, Iran, ⁵Student Research Committee, School of Medicine, Mazandaran University of Medical Sciences, Sari, Iran, ⁶Advanced Therapy Medicinal Product (ATMP) Department, Breast Cancer Research Center, Motamed Cancer Institute, ACECR, Tehran, Iran, ⁷Proteomics Research Center, Shahid Beheshti University of Medical Sciences, Tehran, Iran, ⁸School of Medicine, Kashan University of Medical Sciences, Kashan, Iran, ⁹Laser Research Centre, Faculty of Health Science, University of Johannesburg, Johannesburg, South Africa, ¹⁰Anatomical Sciences Research Center, Institute for Basic Sciences, Kashan University of Medical Sciences, Kashan, Iran, ¹¹Department of Pathology, School of Medicine, Center for Women's Health Research Zahra, Tabriz University of Medical Sciences, Tabriz, Iran, ¹²Research Center for Biochemistry and Nutrition in Metabolic Diseases, Institute for Basic Sciences, Kashan University of Medical Sciences, Kashan, Iran

OPEN ACCESS

Edited by:

Jing Zhang,
Shanghai Jiao Tong University, China

Reviewed by:

Youliang Wang,
Beijing Institute of Technology, China
Giovanni Nigita,
The Ohio State University,
United States

*Correspondence:

Mahmood Khaksary Mahabady
mkhaksarymahabady@gmail.com
Mohammad Taghizadieh
MohammadTaghizadieh@gmail.com
Hamed Mirzaei
h.mirzaei2002@gmail.com

Specialty section:

This article was submitted to
Epigenomics and Epigenetics,
a section of the journal
Frontiers in Cell and Developmental
Biology

Received: 09 October 2021

Accepted: 08 December 2021

Published: 17 January 2022

Citation:

Tamtaji OR, Derakhshan M, Rashidi Noshabad FZ, Razaviyan J, Hadavi R, Jafarpour H, Jafari A, Rajabi A, Hamblin MR, Mahabady MK, Taghizadieh M and Mirzaei H (2022) Non-Coding RNAs and Brain Tumors: Insights Into Their Roles in Apoptosis. *Front. Cell Dev. Biol.* 9:792185. doi: 10.3389/fcell.2021.792185

A major terrifying ailment afflicting the humans throughout the world is brain tumor, which causes a lot of mortality among pediatric and adult solid tumors. Several major barriers to the treatment and diagnosis of the brain tumors are the specific micro-environmental and cell-intrinsic features of neural tissues. Absence of the nutrients and hypoxia trigger the cells' mortality in the core of the tumors of humans' brains: however, type of the cells' mortality, including apoptosis or necrosis, has been not found obviously. Current studies have emphasized the non-coding RNAs (ncRNAs) since their crucial impacts on carcinogenesis have been discovered. Several investigations suggest the essential contribution of such molecules in the development of brain tumors and the respective roles in apoptosis. Herein, we summarize the apoptosis-related non-coding RNAs in brain tumors.

Keywords: brain tumors, non-coding RNAs, apoptosis, microRNA, long non-coding (lnc) RNA

INTRODUCTION

Cancer is specified as uncontrolled cell growth and proliferation resulting in an imbalance between division and death of the cells as a result of many different factors including physicochemical or biological agents (Evan and Vousden, 2001; Jafari et al., 2021a). Today in the world, cancer is still one of the paramount health issues (Nikolaou et al., 2018; Jafari et al., 2020). Brain tumors are almost specified with great morbidity and mortality rate (Weller et al., 2015). Glioma is the most common and aggressive diagnosed tumor of the central nervous system (CNS) with low survival and high recurrence rate (Khani et al., 2019; Xu et al., 2020). Among all tumors, glioma represents just 1–2%, whereas approximately 30% of all preliminary and 80% of every malignant tumor of the brain are affiliated with glioma, which responsible for many brain disease-related deaths. It is thought neurological stem and/or progenitor cells are responsible for brain tumors. Based on morphological resemblance to the normal neuroglial cells, these heterogeneous tumors histologically are classified into oligodendrogliomas, astrocytomas, and ependymomas (Weller et al., 2015). Based on classification by WHO, there are two classes of glioma with four distinct

grades including low- (I and II) and high- (III and IV) grades. Classification of glioma based upon molecular characteristics including genetics, gene expression, DNA methylation, and so on plays a pivotal role in diagnosis, prognosis, and treatment (Li et al., 2019a). Despite much research and clinical investigation in recent years, the prognosis and treatment of glioma are not so desirable (Xu et al., 2020). Great proliferation rate with high resistance to therapies, sensitivity of the CNS and low ability to repair itself, and inability of most drugs to pass the blood brain barrier (BBB) prevent impressive treatment of glioma (So et al., 2021). One of the malignant glioma's hallmarks is its ability to infiltrate the brain, leads to avoidable recurrence post local therapy (So et al., 2021). Nowadays, existing therapeutic approaches include resection surgery, chemotherapy, radiotherapy, and combination therapies. However, contrary to considerable progress in treatment options, after initial resection, frequently quick progression and a high rate of recurrence are shown in patients with glioma (Aldape et al., 2019). Discovering new, innovative, and effective therapies for brain tumors depends on the improved perception of the molecular aspects of this disorder (Aldape et al., 2019).

Several studies have indicated the contribution of apoptosis in the pathophysiology of brain tumors (Mellai and Schiffer, 2007; Fernald and Kurokawa, 2013; Mohamed Yusoff, 2015). Apoptosis is a physiological process during aging and development which led to programmed cell death (Majtnerová and Roušar, 2018; Wang, 2020). The term of apoptosis was first used in a paper published in 1972 by Kerr, Wyllie and Currie to describe a hemostatic process which maintains cell populations by removing damaged and unnecessary cells (Majtnerová and Roušar, 2018). Apoptosis is controlled genetically and is an eventually conserved process among multicellular organisms (D'Arcy, 2019; Jafari et al., 2021b). The mediators of apoptosis are enzymes named caspases. Caspases are cytosolic proteases with the proteolytic activity and they are expressed as pro-enzymes in most cells. When a caspase is activated, it can also activate other procaspases and can induce a cascade of activated caspases which can finally led to cellular death (D'Arcy, 2019; Elmore, 2007). A wide range of conditions and stimuli can initiate apoptosis (Elmore, 2007; Majtnerová and Roušar, 2018). Today three main pathways are described in apoptosis including extrinsic, intrinsic and perforin/granzyme-mediated pathways (Majtnerová and Roušar, 2018). The intrinsic pathway is mitochondrial and initiate with death signals like DNA damage and withdrawal of trophic factors. The response to death signals is disruption of the mitochondrial membrane permeability which led to activation of a series of caspases (Wang, 2020). The extrinsic pathway is induced *via* death receptors placed on plasma membrane such as TNF and Fas receptors. This pathway also eventually leads to the activation of caspases (Wang, 2020). In perforin/granzyme pathway, apoptosis can be caused by each of the granzyme A or granzyme B. Both extrinsic and intrinsic pathway in addition to granzyme B pathway led to apoptosis via cleavage of caspase-3. But granzyme A pathway is initiated via single stranded DNA damage and induce apoptosis via a caspase independent pathway (Elmore, 2007). A variety of morphological and

biochemical changes occurs in cells during apoptosis (Majtnerová and Roušar, 2018). Morphological changes contain cellular shrinkage, nuclear fragmentation and chromatin condensation. The cytoplasmic membrane undergoes changes including budding, blebbing, loss of integrity and transfer of phosphatidylserine (PS) to the extracellular part of membrane. The exposure of PS in outer membrane helps recognition and swallowing apoptotic cells by macrophages. These changes can be observed by light and electron microscopes but electron microscopy give more valuable information and show us more morphological changes (Elmore, 2007; Pistritto et al., 2016; Xu et al., 2019a). Some of the biochemical features which are observed in apoptotic cells contain protein cross-linking, DNA segmentation, and nuclear and cytoskeletal proteins cleavage. Apoptotic cells also form apoptotic bodies and express the ligands necessary for recognition by phagocytic cells and finally, they are identified and removed by phagocytic cells (Elmore, 2007).

It has been shown that different cellular/molecular mechanisms are associated with apoptosis-related processes in brain tumors. Along with genetic mechanisms, epigenetic mechanisms (e.g., non-coding RNAs networks) greatly affect the regulation of apoptosis-related processes. The non-coding RNAs (ncRNAs) belong to a class of RNAs, which function at the RNA level (Nicoloso and Calin, 2008; Pop et al., 2018). ncRNAs are highly heterogeneous in length, structure and cellular function (Hashemian et al., 2020; Mirzaei and Hamblin, 2020; Balandeh et al., 2021; Dashti et al., 2021; Mahjoubin-Tehran et al., 2021). They can be classified into two main classes: structural non-coding RNA and regulatory non-coding RNA. Structural ncRNA include ribosomal RNA (rRNA) and transfer RNA (tRNA). Regulatory ncRNAs are divided into three subclasses based on the length, and include different types from small nucleolar/nuclear RNA (snoRNA/snRNA), small interfering RNAs (siRNA), microRNA (miRNA), and piwiRNA (PiRNA) to Xist and circRNA (Zhang et al., 2019a) (Figure 1).

In this study, we describe the structure and biogenesis of miRNA, lncRNA, and circRNA, then summarize the apoptosis-related non-coding RNAs in brain tumors.

NON-CODING RNAs AND BRAIN TUMORS

MicroRNAs Biogenesis

MiRNAs are small single stranded non-coding RNAs, with the mean length of nearly 22 nucleotides, which play important roles in regulating gene expression at the post-transcriptional level and RNA silencing (Shabaninejad et al., 2019). In 1993, lin-4, the discovery of the first miRNA, lin-4, by the Ambros and Ruvkun team led to a revolution in molecular biology (Lee et al., 1993; Achkar et al., 2016; Gebert and MacRae, 2019; O'Brien et al., 2018).

Generally, miRNA is critical for normal animal development and is capable of regulating a variety of biological processes and signaling pathways like metabolism and differentiation as well as rapid growth or proliferation. Increasing evidence have shown the correlation between miRNA deregulation and numerous kinds of human diseases, including heart disease, metabolic

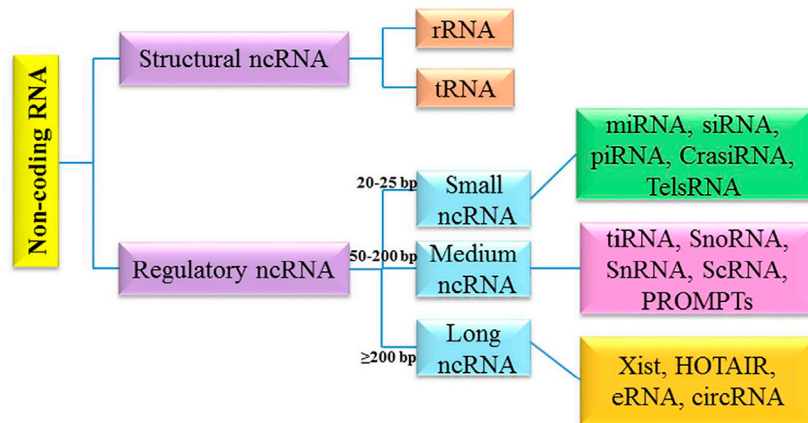


FIGURE 1 | Classification of non-coding RNAs.

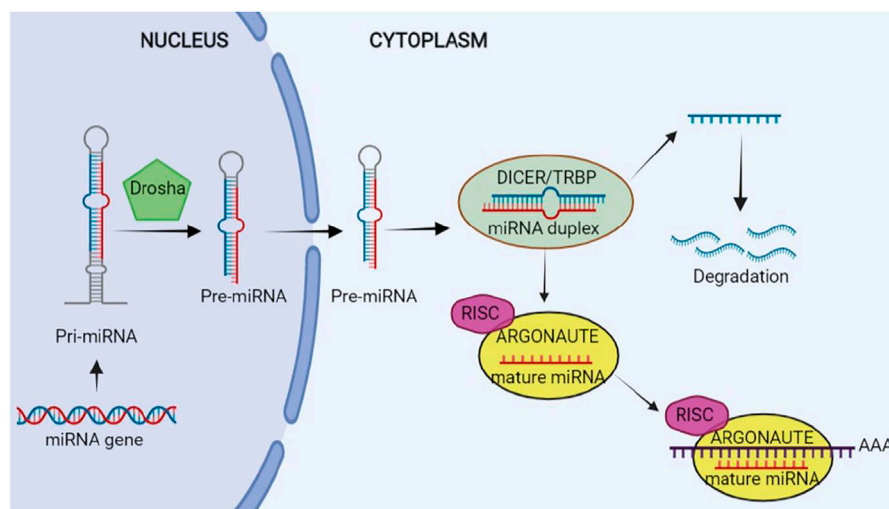


FIGURE 2 | Biogenesis of microRNA (miRNA). This figure is created by www.BioRender.com.

disorder, and cancer. In addition, miRNAs contribute importantly to invasion, metastasis and the tumor angiogenesis and are capable of exiting from the cells through vesicles and entering the extra-cellular fluids (O'Brien et al., 2018; Lin and Gregory, 2015).

RNA polymerase II (Pol. II) enzyme begins miRNAs biogenesis in the nucleus and approximately half of the miRNAs have been identified to be intragenic, largely derived from the introns, whereas the others to be intergenic with their specific promoters (Gebert and MacRae, 2019).

Therefore, a long transcript referred to as the primary microRNA (pri-miRNA) is generated after the transcription by Pol. II and hence Pri-miRNA may create a cluster of two or more miRNAs or a miRNA. Furthermore, it has a local stem loop structure, undergoing several steps of maturation like splicing, polyadenylation, as well as capping. Scission of Pri-miRNA to pre-miRNA is conducted by a micro-processor complex which

has two parts: the double-strand RNase DROSHA and its crucial cofactor; that is, DiGeorge syndrome critical region 8 (DGCR8) (Lee et al., 1993; Ha and Kim, 2014; Lin and Gregory, 2015; Gebert and MacRae, 2019).

Research has shown a length of nearly 65 nucleotides of pre-miRNAs with a hairpin-like structure that is the same as the pri-miRNA. Then, Exportin 5 translocates pre-miRNA into cytoplasm, wherein its maturity ends. Pre-miRNA is converted to a mature ~22 nucleotide miRNA duplex by RNase III DICER1 enzyme and its binding protein, and transactivation response element RNA-binding protein (TRBP) in the cytoplasm. A strand works as one of the guide miRNAs and the other is loaded to Argonaute (AGO) for making a complex: RNA-induced silencing complex (RISC). The complex is assembled by two steps of loading and unwinding of RNA duplex. RISC is capable of binding to the 3'-UTR of the target mRNAs from 5'-UTR of miRNA that may repress translation or degrade mRNA (Ha and

Kim, 2014; Lin and Gregory, 2015). The schematic steps of biogenesis of miRNA is illustrated in **Figure 2**.

MiRNAs may target and regulate a majority of the protein-coding genes due to the existence of one conserved binding site for miRNAs in the above genes. Additionally, numerous mRNAs may be targeted by a miRNA (Ha and Kim, 2014).

MicroRNAs and Apoptosis in Brain Tumors

The miRNA-342 is elevated in glioblastoma cell, and could directly modulate BCL2 expression, suggesting a possible role in apoptosis induction (Ghaemi et al., 2020). The miRNA-16 can promote apoptosis by targeting BCL2 in glioblastoma cell (Yang et al., 2014). The miR-148a is elevated in glioblastoma cell. miR-148a inhibition could induce apoptosis *via* pro-apoptotic molecule BIM in glioblastoma (Kim et al., 2014). The elevated level of miR-330-5p in glioblastoma could induce cell apoptosis *via* targeting ITGA5 expression in glioblastoma cells (Feng et al., 2017). The miR-758-5p was up-regulated in glioblastoma. It can promote apoptosis by decreasing ZBTB20 in glioblastoma cell (Liu et al., 2018a). There is a downregulation of miR-543 in glioblastoma and its upregulation can induce apoptosis by targeting ADAM9 (Ji et al., 2017). MiR-152-3p affected the apoptosis of glioblastoma cells *via* NF2 overexpression (Sun et al., 2017). The inhibition of increased miR-210 in glioblastoma can increase ROD1 expression and apoptosis (Zhang et al., 2015). The overexpression of miR-125a-3p leads to decreased Nrg1 and increased apoptosis in glioblastoma cell (Yin et al., 2015). In another study, miR-500a-5p inhibited apoptosis in glioblastoma through targeting CHD5 mRNA 3'-UTR (Liu et al., 2018b). MiR-146a was down regulated in glioblastoma. In addition, upregulation of miR-146a suppresses Notch1 and stimulate in glioblastoma (Hu et al., 2016). MiR-125b was markedly up-regulated in glioma. MiR-125b regulates cell apoptosis by different signaling pathways (Wu et al., 2013). Elevated levels of miR-374b are reported in glioma. MiR-374b is implicated in the glioma progression by regulating apoptosis *via* targeting GATA3 and SEMA3B (Gao et al., 2019a). Upregulation of decreased miR-378a-3p in glioblastoma decreased the expression of TSPAN17 and increased apoptosis (Guo et al., 2019). MiR-152-3p induced glioma cell apoptosis *via* decreasing DNMT1 (Sun et al., 2017). In astrocytoma tumor cells, miRNA-124-3p was up-regulated and its over-expression leads to increasing apoptosis *via* targeting 3'-UTR of PIM1 (Deng et al., 2016). Furthermore, the over-expression of miRNA-160a-5p is able to enhance apoptosis in astrocytoma cells *via* decreasing Fas-activated serine/threonine kinase (FASTK), an anti-apoptotic agent (Zhi et al., 2013). The induction of an increase in MiR-181b-5p level in astrocytoma showed an increase in apoptosis through targeting NOVA1 in astrocytoma (Zhi et al., 2014). A study revealed a significant down-regulation of miR-106a-5p in astrocytoma. The Over-expression of miR-106a-5p leads to decrease in FASTK expression and increase in apoptosis (Zhi et al., 2013). Besides, miRNA-10b was up-regulated in medulloblastoma cell. miRNA-10b inhibition could also decrease the expression of BCL2 and MCL-1 protein expression in medulloblastoma cell lines (Pal and Greene, 2015). Xu et al. (2014) found that over-expression of miR-22

stimulated apoptosis *via* inhibiting PAPST1 in medulloblastoma cell. MiR-378 was down-regulated in medulloblastoma. The over-expression of miR-378 showed promoting apoptosis through targeting UHRF1 in medulloblastoma (Zhang et al., 2017). MiR-383 negatively regulated PRDX3. The over expression of miR-383 and inhibiting PRDX3 could leads to stimulating apoptosis in medulloblastoma (Li et al., 2013).

Meningioma cell lines show a low level miRNA-34a-3p and miRNA-34a-3p upregulation can stimulate cancer cell apoptosis *via* decreasing BCL2 protein (Werner et al., 2017). MiR-29c-3p was up-regulated in meningioma cell. MiR-29c-3p induces apoptosis *via* targeting PTX3 (Dalan et al., 2017). Apoptosis-related miRNAs in brain tumors and their expression were summarized in **Table 1**.

Biogenesis of lncRNAs

ncRNAs ability to regulate gene expression at transcriptional and post-transcriptional levels explains their house-keeping functions in numerous biological processes (Statello et al., 2021). Overall, researchers have described lncRNAs as long RNA transcripts of ≥ 200 nucleotides, which do not result in protein production (Nam et al., 2016). Moreover, they contribute importantly to the adjustment of the translation machineries and in its modulation *via* regulating the essential performance of other ncRNAs like small nucleolar RNA (snoRNA), miRNAs, and so forth. Several scholars presented many regulatory patterns that are under the control of numerous lncRNAs influencing different cellular activities that are correlated to the normal development and pathophysiology of some diseases like different kinds of cancers, neurological and cardio-vascular conditions, as well as metabolic and immunological dysfunctions (Maass et al., 2014). Therefore, it is important to know lncRNAs biogenesis for its differentiation from other kinds of RNA and deciphering its applicable prominence. Studies have also demonstrated transcription of numerous groups of lncRNAs from numerous DNA elements like enhancers, intergenic regions, and promoters in the eukaryotic genomes (Maass et al., 2014; Fang and Fullwood, 2016). In addition, they revealed the contribution of several mechanisms to the biogenesis of lncRNA like cleavage through ribonuclease P (RNaseP) for generating mature ends and forming protein (snoRNP) complex caps at their ends, snoRNA, and circular structures. However, there are not enough information of the action of synthesis and modulation of various lncRNAs (Dahariya et al., 2019).

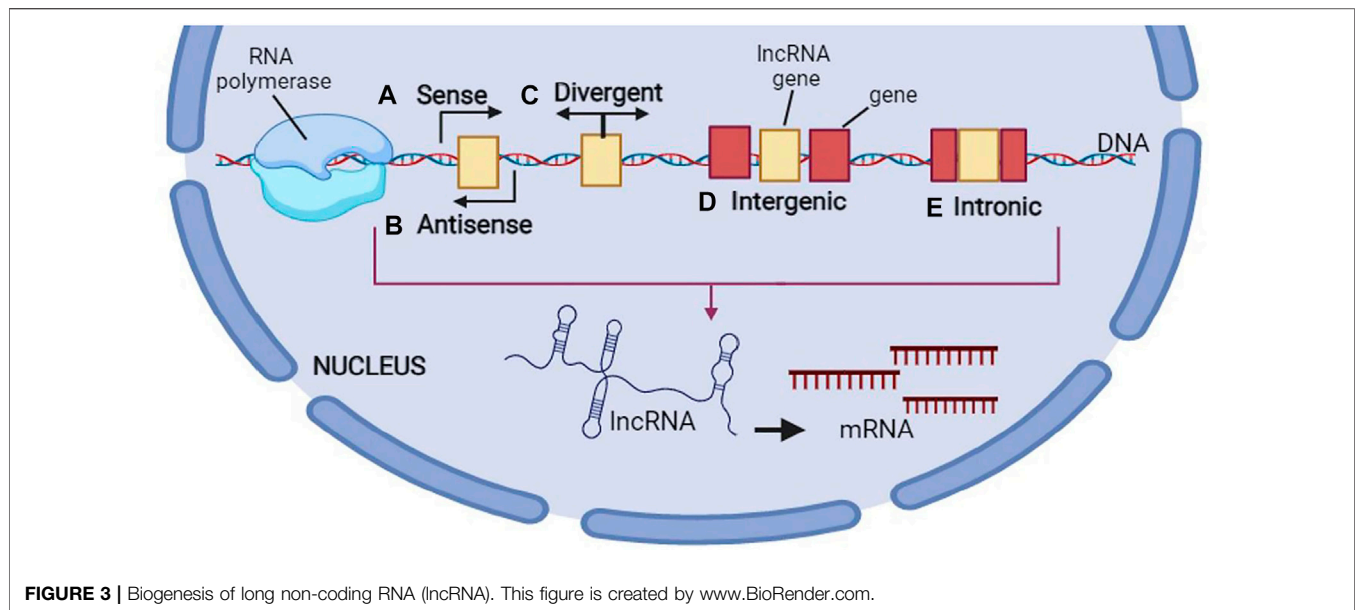
Besides the dimension of the other classes of ncRNAs (e.g., siRNAs, miRNAs, and small sno/sn RNAs), lncRNAs enjoy the secondary and 3D structures that empower them for having protein-like and RNA functions (Cabili et al., 2015). Several studies determined the location of lncRNAs in the nucleus (Derrien et al., 2012), with the contribution of many lncRNAs to the cytoplasm (Cabili et al., 2015). In addition, it is possible for many lncRNAs to be transmitted to the near cells or serum *via* exosome trafficking. Earlier researchers have regarded lncRNAs as the by-products of transcription process. Nonetheless, lncRNAs contribute to the cell differentiation process, growth as well as pathogenesis of numerous illnesses like cancers (Maass et al., 2014). lncRNAs can modulate gene expression at the time

TABLE 1 | Apoptosis-related miRNAs in brain tumors.

	Genomic coordinates	Brain tumors	miRNAs	Targets	Model	Type of cell line	Ref
Up regulated miRNA expression	q32.2 chr1: 207801852–207801939 (-)	Meningioma	miRNA-29c-3p	PTX3	<i>In vitro</i>	Human tissues and meningioma cell line MEN-117 and MEN-141	Dalan et al. (2017)
	q31.1 chr2: 176150303–176150412 (+)	Medulloblastoma	miRNA-10b	Bcl2-MCL1	<i>In vitro</i>	medulloblastoma cell lines DAOY and UW228 and human sample	Pal and Greene, (2015)
	p15.2 chr7: 25949919–25949986 (-)	Glioblastoma	miRNA-148a	BIM	<i>In vitro</i>	GBM cell lines U87, U373, A172, T98G, SNB-19 and U251	Kim et al. (2014)
	p23.1 chr8: 9903388–9903472 (-)	Astrocytoma	Mirna-124-3p	PIM1	<i>In vitro</i>	Human astrocytoma cell line u251 and human tissues	Deng et al. (2016)
	p15.5 chr11: 568089–568198 (-)	Glioblastoma	miRNA-210	ROD1	<i>In vitro</i>	Tumor tissues and GBM cell line U87MG, U251	Zhang et al. (2015)
	q24.1 chr11: 122099757–122099844 (-)	Glioblastoma	miRNA-125b	P53 P38MAPK	<i>In vitro</i>	U251 and U87 cells, rat GMB C6 cells and human brain tissues	Wu et al. (2013)
	q32.2 chr14: 100109655–100109753 (+)	Gliomoblastoma	miRNA-342	Bcl2	<i>In vitro</i>	Glioblastoma cell line U251 and U87	Ghaemi et al. (2020)
	p11.23 chrX: 50008431–50008514 (+)	Glioblastoma	miRNA-500a-5p	CHD5	<i>In vitro</i> <i>In vivo</i>	Tumor tissues sample Glioblastoma cell lines U-87MG, U251	Liu et al. (2018b)
	q13.2 chrX: 74218547–74218618 (-)	Glioblastoma	miRNA-374b	GATA3 SEMA3B	<i>In vitro</i>	Glioma cell line U251 and human tissues sample	Gao et al. (2019a)
	p36.22 chr1: 9151668–9151777 (-)	Meningioma	Mirna-34a-3p	Bcl2	<i>In vitro</i>	Ben-Men-1	Werner et al. (2017)
	q32.1 chr1: 198858873–198858982 (-)	Astrocytoma	miR-181b-5p	NOVA1	<i>In vitro</i>	Human tissues and astrocytoma cell lines U251 and U87	Zhi et al. (2014)
	q32 chr5: 149732825–149732890 (+)	Glioblastoma	miRNA-378a-3p	TSPAN17		GBM cell lines U87MG and MT-330 and tumor tissues	Guo et al. (2019)
Down regulated miRNA expression	q32 chr5: 149732825–149732890 (+)	Medulloblastoma	miRNA-378	UHRF1	<i>In vivo</i> <i>In vitro</i>	DAOY and HEK 293T cell line Tumor tissues	Zhang et al. (2017)
	q33.3 chr5: 160485352–160485450 (+)	Glioblastoma	miRNA-146a	Notch1	<i>In vitro</i>	GBM tissues, U87, U251, A172	Hu et al. (2016)
	p22 chr8: 14853438–14853510 (-)	Medulloblastoma	miRNA-383	PRDX3	<i>In vitro</i>	Human sample and cell line DAOY, D283 and D341	Li et al. (2013)
	q14.2 chr13: 50048973–50049061 (-)	Glioblastoma	miRNA-16	BCL2	<i>In vitro</i> and <i>in vivo</i>	Glioblastoma cell line U87 and U373 and human sample	Yang et al. (2014)
	q32.31 chr14: 101026020–101026107 (+)	Glioblastoma	miRNA-758-5p	ZBTB20	<i>In vivo</i>	Human tissues and U118, LN-299, H4, A172, U87-MG, and U251	Liu et al. (2018a)
	q32.31 chr14: 101031987–101032064 (+)	Glioblastoma	miRNA-543	ADAM9	<i>In vitro</i> , human	U87, U251, LN229, and T98, human tissues	Ji et al. (2017)
	p13.3 chr17: 1713903–1713987 (-)	Medulloblastoma	miRNA-22	PAPST1	<i>In vivo</i> <i>In vitro</i>	medulloblastoma cell lines D341 and DAOY and tumor tissues	Xu et al. (2014)
	q21.32 chr17: 48037161–48037247 (-)	Glioblastoma	MiRNA-152-3P	DVMT1 NF2	<i>In vitro</i>	U251, U87, T98-G and A172	Sun et al. (2017)
	q13.32 chr19: 45638994–45639087 (-)	Glioblastoma	miRNA-330-5p	ITGA5	<i>In vitro</i>	U87, U251, and U373	Feng et al. (2017)
	q13.41 chr19: 51693254–51693339 (+)	Glioblastoma	miRNA-125a-3p	Nrg1	<i>In vitro</i> <i>In vivo</i>	Animal sample Tumor sample Glioblastoma cell line U251/U87-MG	Yin et al. (2015)
	q26.2 chrX: 134170198–134170278 (-)	Astrocytoma	MiRNA-106a-5p	FASTK	<i>In vitro</i>	Astrocytoma cell line U251 and human tissues samples	Zhi et al. (2013)

of transcription, post-transcription, and even epigenetically (Cabili et al., 2015). Actually, lncRNAs greatly affect gene expression by modifying chromatin and remodeling, modifying histone, as well as changing the nucleosome localization. In comparison to the mRNAs, numerous lncRNAs are situated at the nucleus and researchers have shown the existence of fewer exons in the lncRNA genes in comparison to the mRNAs. Results have demonstrated the less effective splicing of lncRNAs than the mRNAs (Guo et al., 2020; Statello et al., 2021). In fact, they exhibited longer distances

between and the branch point and 3' splice site weaker internal splicing signals. Besides processing and transcription, lncRNAs frequently consist of the embedded sequence motifs with the ability of recruiting specific nuclear factors that enhance the lncRNA nuclear localization and function. Furthermore, researchers observed export of numerous lncRNAs to the cytosol with the similar export and processing pathways to the mRNAs. When the lncRNAs reached the cytoplasm, they experience particular arrangement processes for assigning various lncRNAs to the certain organelles or distribution in



the cytoplasm for associating with several RNA-binding proteins (RBPs) (Statello et al., 2021). According to estimations, 50% of the pools of 70% of cytoplasmic lncRNAs occur in polysome fraction and lncRNAs at multiple level regulate the genes' expression. (Carlevaro-Fita et al., 2016). In fact, through interactions with RNA, proteins, as well as DNA, lncRNAs may modulate the chromatin structure and functions and transcription of the distant and near genes, and influence the RNA splicing, translation, and stability. Research has showed the contribution of lncRNAs to the creation and modulation of nuclear condensates and organelles. They are capable of suppressing the genes' expression via interferences in the transcription machinery and alter recruitment of the transcription factors or Pol II at the suppressed promoter (Pal and Greene, 2015) and histone modification (Pal and Greene, 2015; Lin et al., 2020) and declines the accessibility of chromatin (Statello et al., 2021).

One of the other kinds of lncRNAs classification has been done according to their genomic profile or correlation with the protein coding genes: 1) one or more exons of a coding gene are overlapped by sense lncRNAs, 2) full or partial complementarity to transcripts on the opposite strand exhibits anti-sense transcripts, 3) an intron of a gene produces the intronic lncRNAs, 4) there is a similar promoter in both protein-coding genes and bi-directional transcripts, though their transcription is formed in the opposite direction, 5) inter-genic lncRNAs (lincRNAs) are situated between the protein-coding genes and their transcription occurs individually, 6) enhancer RNAs (eRNAs) have been found to be created from the enhancer regions of the protein-coding genes, and finally 7) the origin of circRNAs is the splicing processes of the protein coding genes that create the covalently-closed loops (Beermann et al., 2016). lncRNA biogenesis occurs in the nucleus resembling synthesizing the protein-coding transcripts. Moreover, histone modifications occur frequently for epigenetic marking of lncRNA promoters that are modulated by transcription factors, which advocate or

hinder the gene expression (Guttman and Rinn, 2012). Like mRNAs, Pol II transcribes numerous lncRNAs whereas other lncRNA promoters protect the structures transcribed by Pol III. Therefore, there is a precise spatial or temporal regulation of lncRNA expression. Generally, there are fewer lncRNAs than mRNAs, though their expression is largely limited to the certain kinds of cells (Cabili et al., 2011; Derrien et al., 2012). Based on the transcriptome-wide investigations, lncRNAs exhibited more certain expression profiles than the mRNAs (Elmore, 2007; Nikolaou et al., 2018). In other words, their expression is done in a cell tissue-, type-, developmental stage or disease state-specific way. For reaching the mature forms, the nascent RNA transcripts experience several processing steps during and after transcription, like splicing, 5'-capping, chemical base modification, as well as poly-adenylation. The schematic steps of biogenesis of lncRNA is shown in **Figure 3**.

Researchers have found the biological contributions of lncRNAs as 1) the transcription regulators in cis or trans, 2) regulator of mRNA processing, protein activity, and posttranscriptional control, and 3) structuring the nuclear domains (Quinn and Chang, 2016). Overall, RNA polymerase II transcribe the lncRNAs, which exhibit hallmarks of the protein-coding genes, including conservation and chromatin structure of promoters, modulation of expression *via* morphogens and transcription factors, ranges of half-life tissue-specific expression, splicing, as well as other splice variants. Several lncRNAs enjoy a 3-helical structure at their 3' end, created by cleavage *via* RnaseP, which helps protecting them against degradation (Yang et al., 2016).

Long Non-coding RNAs and Apoptosis in Brain Tumors

lncRNA EGFR-AS1 expression was notably up-regulated in glioma. EGFR-AS1 inhibition induced apoptosis. MiR-133b is

a target of EGFR-AS1. Lnc-EGFR-AS1 knockdown increased miR-133b expression. MiR-133b was able to decrease RACK1 expression. The over-expression of miR-133b causes glioma cells to increase their apoptosis by reducing N-cadherin, Vimentin, MMP-2 and Bcl-2 and elevating Bax, cleaved Caspase-3 and PARP expression (Dong et al., 2019). There is a remarkable increase in LncRNA HOXA11-AS in glioma. The direct target of LncRNA HOXA11-AS is miRNA-130-5p, i.e., it downregulates miRNA-130-5p. Apoptosis was greatly increased upon miR-130-5p transfection. The oncogenic function of LncRNA HOXA11-AS is partly related to miR-130a-5p-HMGB2 axis. The down-regulation of LncRNA HOXA11-AS leads to increasing apoptosis in glioma (Xu et al., 2019b). Zhang et al. (2020a) showed that glioma cells apoptosis was increased by LPP-AS2 inhibition. LPP-AS2 knockdown leads to decreased EGFR the expression. LPP-AS2 acts as a molecular sponge for miR-7-5p and inhibiting miR-7-5p reverses the cell apoptosis stimulated by LPP-AS2 knockdown. LPPAS2 sponging of miR-7-5p up-regulates EGFR to activate the PI3K/AKT/c-MYC pathway (Zhang et al., 2020a). Human glioma cells have low amounts of lncRNA UBE2R2-AS1. Glioma cells growth is in part regulated by the UBE2R2-AS1/miR-877-3p/TLR4 pathway. Following upregulation of UBE2R2-AS1 in glioma cells, there was a remarkable elevation of caspase-3, caspase-7, and caspase-8, while reduction of Bcl2 (Xu et al., 2019c). LncRNA Gas5 is down-regulated in glioma. The Overexpression of Gas5 promotes the apoptosis. Gas5 and miR-222 expressions are inversely associated. The overexpression of Gas5 upregulates Plexin C1, bmf by lowering the level of miR-222. The down-regulation of miR-222 increases the level of bmf (a pro-apoptotic agent), which increase Bax expression and decrease Bcl-2 expression in glioma (Zhao et al., 2015). LncRNA ZEB1-AS1 is elevated in glioma. Knockdown of ZEB1-AS1 induces apoptosis by increasing Bax and lowering Bcl-2 (Lv et al., 2016). LncRNA H19 expression was up-regulated in glioblastoma cells. H19 knockdown leads to increasing apoptosis in glioblastoma cells under TMZ treatment. H19 knockdown reduces pro-caspase 3 and increases cleaved caspase 3 and Bax, and decreases Bcl-2 in glioblastoma cells under TMZ treatment (Li et al., 2016). High levels of LncRNA SNHG6 are present in glioma cells. The knockdown of SNHG6 increases apoptosis. By regulating miR-101-3p expression, SNHG6 exerts its effect in glioma tumorigenesis (Meng et al., 2018). NEAT1 is downregulated in glioma. Elevating the level of NEAT1 in glioma cells can enhance apoptosis. NEAT1 exerts its tumor suppressor effects by down-regulating miR-92b and up-regulating DKK3 (Liu et al., 2020). LncRNA SNHG16 is elevated in glioma. SNHG16 inhibition leads to apoptosis *via* upregulating caspase-3 and Bax and, down-regulating Bcl-2, Bcl-xl and Mcl-1. In addition, SNHG16 may affect apoptosis via regulation of PI3K/Akt pathway. By binding to MiR-4518 and its inhibition, SNHG16 can regulate PRMT5 expression. SNHG16 could exerts oncogenic function through the SNHG16-miR-4518 axis in glioma cells (Lu et al., 2018). Apoptosis of glioma cells could be enhanced by inhibiting lncRNA EPIC1. The down regulation of EPIC1 reduces the Cdc20 expression which functions as an anti-apoptotic agent in glioma cells (Wang et al., 2020a). LncRNA SOX2OT is present

in high levels in glioma. SOX2OT inhibition upregulates miR-194-5p and miR-122 which in turn enhance the apoptosis of glioblastoma stem cells (Su et al., 2017). Glioblastoma cells have low levels of LncRNA CASC2. LncRNA CASC2 acts as a tumor suppressor by stimulating apoptosis through CASC2-miR-18a axis in glioblastoma (Wang et al., 2020b). LncRNA GAPLINC was significantly up-regulated in glioblastoma tissues. GAPLINC inhibition promoted apoptosis. GAPLINC can target miR-331-3p. GAPLINC could be an oncogenic lncRNA via negative modulation of miR-331-3p in glioblastoma (Chen et al., 2019). The overexpression of LncRNA LINC00657 leads to miR-190a-3p inhibition; Consequently, PTEN expression is stimulated regulating caspase3 through PI3K/Akt/mTOR pathway. Thus, the overexpression of LncRNA LINC00657 induces apoptosis in glioblastoma (Chu et al., 2019). LncRNA SNHG20 was highly expressed in glioblastoma. The knockdown of SNHG20 significantly promotes cell apoptosis. PI3K/Akt/mTOR signaling pathway were inhibited by SNHG20 knockdown, while were stimulated by SNHG20 overexpression. Apoptosis is increased with IGF-1, a PI3K signaling activator, whereas apoptosis is decreased with GDC-094, a PI3K signaling inhibitor. Apoptosis induced by SNHG20 knockdown is efficiently rescued by IGF-1 (Gao et al., 2019b). Glioblastoma stem cells have high amounts of LncRNA NEAT1. LncRNA NEAT1 inhibition promotes glioblastoma stem cells apoptosis. There is a binding region between LncRNA NEAT1 and microRNA let-7e. NEAT1 inhibition increases the level of let-7e which can downregulate NRAS (a pro-oncogenic factor) as its target. In addition, the overexpression of NRAS significantly inhibit apoptosis in glioblastoma stem cells (Gong et al., 2016). LncRNA AGAP2-AS1 is elevated in glioblastoma and its inhibition leads to TFPI2 overexpression and enhanced apoptosis (Luo et al., 2019). LncRNA MANTN1-AS1 was down-regulated in glioblastoma. LncRNA MANTN1-AS1 induce glioblastoma cell apoptosis via regulation of different proteins RELA, ERK1/2, survivin, MMP-9, Bcl-2 and Bax (Han et al., 2019). LncRNA DLEU1 was significantly up-regulated in glioblastoma tissues. DLEU1 knockdown increase Bax and decrease Bcl-2. SP1 is a target of miR-4429 and DLEU1 sponged miR-4429 to induce SP1 expression. Therefore, SP1-DLEU1-miR-4429 pathway could regulate apoptosis in glioblastoma (Liu et al., 2019). LncRNA HOTAIRM1 inhibits apoptosis in glioblastoma through regulation of miR-873-5p/ZEB2 axis. By inactivating miR-873-5p, HOTAIRM1 upregulates ZEB2 (Lin et al., 2020). LncRNA MALAT1 has pivotal role in ZHX1 expression. MALAT1 induce ZHX1 expression through miR-199a in glioblastoma cells. The overexpression of ZHX1 is related to decreased Bax and increased Bcl-2 in glioblastoma (Liao et al., 2019a). In another study showed a significant up-regulation of LncRNA LEF1-AS1 expression in glioblastoma. The Knockdown of *LEF1-AS1* significantly promoted cell apoptosis through regulating p27, Bcl-2, and Bax expression (Wang et al., 2017). LINC01152 was up-regulated in glioblastoma. The silenced LINC01152 decreases the levels of MAML2. The apoptosis of glioblastoma cells is stimulated by MAML2 depletion. LINC01152 and MAML2 3'UTR have binding sites for miR-466. miR-466 inhibition

could in part reverse the enhanced apoptosis observed after LINC01152 silencing (Wu et al., 2021). High levels of LncRNA SNHG3 are observed in glioma. SNHG3 inhibition induces cell apoptosis (Fei et al., 2018). In glioma cells, the silencing of LncRNA PVT1 inhibits EZH2 which in turn increases caspase 3 and Bax and reduces Bcl-2 and as a result, apoptosis is promoted (Yang et al., 2017). LncRNA GATA6-AS was up-regulated in glioma. GATA6-AS overexpression results in TUG1 downregulation and apoptosis inhibition (Liao et al., 2019b). LncRNA UBA6-AS1 expression was enhanced in glioblastoma. Through miR-760/HOXA2 regulation, UBA6-AS1 inhibition can improve apoptosis (Cheng et al., 2021). LncRNA KCNQ1OT1 significantly was Up-Regulated in glioma. LncRNA KCNQ1OT1 down-regulation induces glioma cells apoptosis. KCNQ1OT1 expression inversely correlates with miR-370 expression in glioma cells. Apoptosis is increased by miR-370 upregulation. MiR-370 exerts its anti-oncogenic effects through CCNE2 downregulation (Gong et al., 2017). LncRNA SCAMP1 is observed in high levels in glioma cells. The inhibition of SCAMP1 promotes apoptosis via molecular sponging of miR-499a-5p (Zong et al., 2019). LncRNA HOTAIR expression was up-regulated in glioblastoma. There is positively correlation between HOTAIR with the HK2 expression. HK2 depletion sensitizes the glioblastoma cells to TMZ-induced apoptosis. HK2 absence in glioblastoma cells also enhances the cleavage of caspase-3 following TMZ treatment and induces higher apoptosis. Depletion of HOTAIR also suppresses the expression of HK2 increases the TMZ-induced apoptosis and cleavage caspase-3 in glioblastoma cells. The expression of miR-125 up-regulates by HOTAIR knockdown and miR-125 could be the downstream of HOTAIR for HK2 regulation (Zhang et al., 2020b). Low levels of LncRNA HOTTIP is observed in glioma. HOTTIP upregulation increases cell apoptosis. HOTTIP directly binds to BRE gene and down-regulate BRE expression. Through BRE downregulation which results in cyclin A and CDK2 suppression and P53 elevation, HOTTIP reduces glioma cell growth (Xu et al., 2016). LncRNA LINC00515 was over-expressed in glioma tissues. LINC00515 deficiency increases apoptosis in glioma cells. LINC00515 regulates PRMT5 expression *via* sponging miR-16 (Wu and Lin, 2019). A remarkably low level of LncRNA PART1 is observed in glioma. PART1 inactivates miR-190a-3p which suppresses PTEN/AKT axis and as a result apoptosis is enhanced in glioma cells (Jin et al., 2020a). LncRNA WEE2-AS1 is elevated in glioblastoma. Through miR-520f-3p/SP1 axis, WEE2-AS1 inhibition improves apoptosis in glioblastoma (Lin et al., 2021). LncRNA Linc-00313 is elevated in glioma. Linc-00313 suppression significantly promotes apoptosis in glioma; this effect is due to miR-342-3p and miR-485-5p upregulation (Shao et al., 2019). LncRNA AC003092.1 is lowered in glioblastoma. LncRNA AC003092.1 exerts its effects in TMZ chemosensitivity by regulating miR-195/TFPI-2 pathway (Xu et al., 2018a). Glioma cells have elevated levels of LncRNA SNHG12. The overexpression of LncRNA SNHG12 significantly inhibit the apoptosis in glioma cell *via* targeting Hu antigen R (HuR) (Lei et al., 2018). LncRNA HOTAIRM1 is upregulated in glioma and glioblastoma. HOTAIRM1 inhibited cell apoptosis via regulation

of HOXA1 gene (Li et al., 2018). The overexpression of LncRNA PABPC1 increased apoptosis in glioblastoma cells via BDNF-AS-RAX2-DLG5 axis (Su et al., 2020). Glioblastoma cells show elevated levels of LncRNA PXN-AS1. Apoptosis of glioblastoma cells was promoted by PXN-AS1 inhibition through lowering Bcl-2 and elevating Bax (Chen et al., 2020). There are low levels of TAF15 and LncRNA LINC00665 in glioma, on the contrary, high levels of MTF1, YY2, and GTSE1 are observed. TAF15 upregulation could promotes apoptosis *via* targeting MTF1, YY2, and GTSE1 (Ruan et al., 2020). LncRNA MATN1-AS1 is lowered in glioblastoma. MATN1-AS1 upregulation is able to promote apoptosis through RELA, survivin, ERK1/2, MMP-9, and Bcl-2 inhibition, and Bax elevation (Han et al., 2019).

Medulloblastoma tissues are observed to have elevated levels of LncRNA HOTAIR which binds to miR-1 and miR-206 and inhibits them to upregulate YY1. Through miR-1/miR-206-YY1 pathway, HOTAIR suppression leads to increased apoptosis in medulloblastoma (Zhang et al., 2020c). Medulloblastoma tissues demonstrate high levels of LncRNA LOXL1-AS1. The proliferation and metastasis of medulloblastoma cells are improved by LOXL1-AS1 *via* stimulating PI3K-AKT pathway and therefore, its suppression results in increased apoptosis (Gao et al., 2018). There is an elevated level of LncRNA TP73-AS1 in medulloblastoma cells which binds to miR-494-3p to inhibit it and in turn activate EIF5A2, the pathway that explains promoted apoptosis following TP73-AS1 suppression (Li et al., 2019b). LncRNA CRNDE was up-regulated in medulloblastoma. The knockdown of LncRNA CRNDE induces apoptosis *via* promoting the activity of caspase-3 in medulloblastoma cells (Song et al., 2016). Cleaved-caspase-3, caspase-9, and Bax elevation, and bcl-2 reduction are the results of HOTAIR downregulation in medulloblastoma cells (Zhao et al., 2020). Varon et al. (2019) reported a significant up-regulation of LncRNA TP73-AS1 in medulloblastoma cells. Silencing TP73-AS1 stimulates apoptosis *via* targeting caspase 3 in medulloblastoma cells.

Malignant meningioma shows LncRNA LINC00702 to be upregulated. LINC00702 stimulates tumorigenesis by inactivating miR-4652-3p which consequently activates ZEB1. Therefore, LINC00702 downregulation induces apoptosis (Li et al., 2019c). Astrocytoma cells are shown to have high amounts of LncRNA SNHG17. SNHG17 can bind to miR-876-5p to keep it from sponging ERLIN2. This pathway justifies the enhanced apoptosis observed after SNHG17 inhibition (Du and Hou, 2020). **Table 2** lists apoptosis-related lncRNAs in brain tumors and their expression.

Biogenesis of the Circular RNAs

Circular RNAs (circRNAs) characterize a type of endogenous ncRNA generated by back splicing events, with the ubiquitous presence in numerous species. They have one or more exons with the major location in the cytoplasm so that a few of the circRNAs consisting of intron originate in the nucleus (Guo et al., 2014). In spite of the linear RNAs, circRNAs make a continuous loop formation using covalent bonds and therefore do not have a 5–3' direction or a polyadenylated tail; these features result in their

TABLE 2 | Apoptosis-related lncRNAs in brain tumors.

	Genomic coordinates	Brain tumors	lncRNA	Targets	Model	Type of cell line	Ref
Up regulated lncRNAs expression	p36.32 chr1: 3735510–3745905 (-)	Medulloblastoma	TP73-AS1	miR-494-3p/EIF5A2 E-cadherin, N-cadherin, Vimentin	<i>In vivo</i> <i>In vitro</i>	specimens of medulloblastoma human medulloblastoma cell lines Daoy, D341 animal experiment	Li et al. (2019b)
	p36.32 chr1: 3735510–3745905 (-)	Medulloblastoma	TP73-AS1	Capase-3	<i>In vivo</i> <i>In vitro</i>	cell lines UW228.2, MED8A and ONS76, DAOY/mice	Varon et al. (2019)
	p35.3 chr1: 28505979–28510892 (+)	Glioblastoma	SNHG3		Human, <i>in vitro</i>	glioma tissue/cell lines (A172, U251, U87, and SHG44)	Fei et al. (2018)
	p35.3 chr1: 28578537–28581010 (-)	Glioblastoma	SNHG12	HuR	<i>In vitro</i>	tumor samples U87, LN229, U373, U251	Lei et al. (2018)
	q27.3 chr3: 188151205–188154057 (-)	Glioblastoma	LPP-AS2	miR-7-5p/EGFR/PI3K/AKT/and c-MYC PI3K/AKT pathway	<i>In vitro</i> <i>In vivo</i>	Glioma tissues U251, U87, SHG44, T98G, GOS-3, TJ905, U373	Zhang et al. (2020a)
	q26.33 chr3: 180989761–181117494 (+)	Glioblastoma	SOX2-OT	MiR-194-5p, miR-122	<i>In vivo</i>	U87 and U251 cell lines	Su et al. (2017)
	q13.2 chr4: 67701208–67723914 (+)	Glioblastoma	UBA6-AS1	miR-760/HOXA2	<i>In vivo</i> <i>In vitro</i>	GBM tissues/GBM cell lines A172 and U251	Cheng et al. (2021)
	q25 chr4: 108167524–108176426 (+)	Glioblastoma	LEF1-AS1	ERK1/2 and Akt/mTOR pathway	<i>In vivo</i>	GBM tissues Human U251 and U87 glioma cells	Wang et al. (2017)
	q14.1 chr5: 78360610–78476026 (+)	Glioblastoma	SCAMP1	Bax and Bcl-2 Wnt/ β -catenin	<i>In vitro</i> <i>In vivo</i>	Glioma specimens U87, U251, HEK293T mice	Zong et al. (2019)
	p15.2 chr7: 27184506–27189298 (+)	Glioblastoma	HOXA11-AS	miR-130a-5p/HMGB2	<i>In vitro</i> <i>In vivo</i>	Glioma tissues and U251 and U87MG cells	Xu et al. (2019b)
	p11.2 chr7: 55179749–55188934 (-)	Glioblastoma	EGFR-AS1	miR-133b/RACK1 N-cadherin, Vimentin and MMP-2, Bax, cleaved Caspase-3 and PARP	<i>In vitro</i> <i>In vivo</i>	Human U87, U251 and T Human glioma specimens 98 G	Dong et al. (2019)
	q34 chr7: 141704002–141738230 (-)	Glioblastoma	WEE2-AS1	miR-520f-3p/SP1	<i>In vivo</i> <i>In vitro</i>	GBM tissues/GBM cell lines T98 and U138/mice	Lin et al. (2021)
	p15.2 chr7: 27095646–27096327 (+)	Glioblastoma	HOTAIRM1	HOXA1	<i>In vivo</i> <i>In vitro</i>	U87, U251, and A172 cell lines glioma tissues	Li et al. (2018)
	p15.2 chr7: 27095646–27096327 (+)	Glioblastoma	HOTAIRM1	miR-873-5p/ZEB2 Cyclin A1, Cyclin D1, Bcl-2, Caspase-3	<i>In vitro</i>	U87, LN-229, U-251, and A172	Lin et al. (2020)
	q13.1 chr8: 66921683–66925541 (-)	Glioblastoma	SNHG6	miR-876-5p/ERLIN2 axis	<i>In vitro</i>	LN-215, ADF, U138, A-382	Du and Hou, (2020)
	q24.21 chr8: 127794525–128101256 (+)	Glioblastoma	PVT1	Bax/bcl2/caspase 3	<i>In vivo</i> <i>In vitro</i>	glioma cell lines U87MG and U251/glioma tissue/mice	Yang et al. (2017)
	p11.22 chr10: 31206277–31319691 (-)	Glioblastoma	ZEB1-AS1	Bax/bcl2	<i>In vivo</i> <i>In vitro</i>	HS683, T98G, U87, U251 glioma tissues	Lv et al. (2016)
	p15.1 chr10: 4201140–4243912 (-)	Meningioma	LINC00702	miR-876-5p/ERLIN2 axis	<i>In vitro</i>	LN-215, ADF, U138, A-382	Du and Hou, (2020)
	q13.1 chr11: 65497687–65506431 (+)	Glioblastoma	MALAT1	miR-199a/ZHX1 Bcl-2/Bax	<i>In vivo</i> <i>In vitro</i>	Glioma tissues U87-MG, U251, T98G, and A172	Liao et al. (2019a)
	q13.1 chr11: 65422773–65426457 (+)	Glioblastoma	NEAT1	miRNA let-7e/NRAS	Human, <i>In vitro</i>	glioma tissues U87, T98G, U251, A272 and U373 cell lines	Gong et al. (2016)
	p15.5 chr11: 1995175–1996191 (-)	Glioblastoma	H19	Notch signaling pathway	<i>In vivo</i> <i>In vitro</i>	GBM tissue GBM cell lines (M059K, LN-229, T98G, and U343) mice	Wu et al. (2021)
	p15.5 chr11: 2608327–2699994 (-)	Glioblastoma	KCNQ1OT1	miR-370/CCNE2	<i>In vitro</i> <i>In vivo</i>	cell lines (U87, U251)/glioma tissues/mice	Gong et al. (2017)
	q24.23 chr12: 120201290–120213231 (+)	Glioblastoma	PXN-AS1	Wnt/ β -catenin pathway	<i>In vivo</i>	A172, U251, U87, LN229	Chen et al. (2020)
	q13.13 chr12: 53962307–53974956 (-)	Medulloblastoma	HOTAIR	miR-1/miR-206/YY1	<i>In vivo</i>	Animal sample primary medulloblastoma samples Human cells, Daoy, D283 med and D34	Zhang et al. (2020c)

(Continued on following page)

TABLE 2 | (Continued) Apoptosis-related lncRNAs in brain tumors.

	Genomic coordinates	Brain tumors	lncRNA	Targets	Model	Type of cell line	Ref
	q13.13 chr12: 53962307–53974956 (-)	Medulloblastoma	HOTAIR	caspase-3,9/ bcl2/bax	<i>In vivo</i>	medulloblastoma cell lines Daoy and D341/mice	Zhao et al. (2020)
	q13.13 chr12: 53962307–53974956 (-)	Glioblastoma	HOTAIR	Caspase-3	<i>In vivo</i>	U-87 and A172 cell lines/	Zhang et al. (2020b)
	q14.1 chr12: 57726270–57728356 (+)	Glioblastoma	AGAP2-AS1	TFPI2	<i>In vivo</i> <i>In vitro</i>	GBM samples/mice GBM tumor tissues GBM cell lines (A172, U87/ MG, U251/MG, LN229, and SHG44)	Luo et al. (2019)
	q14.2 chr13: 50082168–50107202 (+)	Glioblastoma	DLEU1	miR-4429 Bcl-2/Bax/ caspase-3	?	U251, U87 and LN229	Liu et al. (2019)
	q24.1 chr15: 73908070–73919870 (-)	Medulloblastoma	LOXL1-AS1	PI3K-AKT	<i>In vivo</i> <i>In vitro</i>	Human tissues Human medulloblastoma cell lines cell lines Daoy, D283, D425, D341, and D458	Gao et al. (2018)
	q12.2 chr16: 54845188–54848278 (-)	Medulloblastoma	CRNDE	miR-101-3p	<i>In vivo</i>	glioma tissues U87, U251, LN229, T98G Mice	Meng et al. (2018)
	q24.3 chr17: 72030290–72036316 (+)	Glioblastoma	LINC01152	caspase-3	<i>In vivo</i> <i>In vitro</i>	cell lines D283, Daoy, D425, D341, and D458/Human Samples/Mouse	Song et al. (2016)
	q25.1 chr17: 76557763–76564689 (+)	Glioblastoma	SNHG16	Bcl/bax/caspase-3/ PI3K/Akt	<i>In vitro</i>	brain glioma specimens/ U251, H4, SW1783 and LN229 cells/	Lu et al. (2018)
	q25.2 chr17: 77086715–77093762 (+)	Glioblastoma	SNHG20	PI3K/Akt/mTOR	<i>in vivo</i>	glioblastoma tissues glioblastoma cell lines (U87MG, U343, U251, LN215)	Gao et al. (2019b)
	p11.31 chr18: 3466249–3473203 (+)	Glioblastoma	GAPLINC	miR-331-3p	<i>in vitro</i> <i>in vivo</i>	GBM cell lines (T98G, U251, LN18, LN229, and A172)	Chen et al. (2019)
	q11.2 chr18: 22164885–22167781 (-)	Glioblastoma	GATA6-AS1	TUG1	<i>In vitro</i>	Tumor tissues glioma cell lines Hs 683 and CCD-25Lu	Liao et al. (2019b)
	q11.23 chr20: 38419637–38435375 (-)	Astrocytoma	SNHG17	Caspase 3/bcl2/bax	<i>In vitro</i>	cell lines U87MG, U251, U343, Hs683, LN215 and A172	Li et al. (2016)
	q21.3 chr21: 25582769–25583326 (-)	Glioblastoma	LINC00515	miR-16/PRMT5	<i>In vivo</i>	Glioma tissue/Human glioma cell lines U251, U87MG, LN229	Wu and Lin, (2019)
	q22.3 chr21: 4,3461959–43478223 (-)	Glioblastoma	Linc-00313	UPF1-Linc-00313- miR-342-3p/miR- 485-5p-Zic4- SHCBP1	<i>In vivo</i>	(GBM) cell lines U87, U251/ glioma tissues/mice	Shao et al. (2019)
	q13.31 chr22: 47630827–48023030 (+)	Glioblastoma	EPIC1 (LOC284930)	Notch signaling pathway	<i>In vivo</i> <i>In vitro</i>	GBM tissue GBM cell lines (M059K, LN-229, T98G, and U343) mice	Wu et al. (2021)
Down regulated lncRNAs expression	p35.2 chr1: 30718503–30726744 (+)	Glioblastoma	MATN1-AS1	RELA ERK1/2, Bcl-2, survivin, andMMP- 9, Bax	<i>in vivo</i> <i>in vitro</i>	U87MG and U251 GBM tissue	Han et al. (2019)
	p35.2 chr1: 30718503–30726744 (+)	Glioblastoma	MATN1-AS1	Bcl/bax	<i>In vivo</i> <i>In vitro</i>	GBM cells U87MG and U251/GBM tissue specimens/mice	Han et al. (2019)
	q25.1 chr1: 173858558–173867045 (-)	Glioblastoma	GAS5	Bcl-2/bax	<i>In vivo</i> <i>In vitro</i>	cell lines (U87 and U251)/ glioma tissues/mice	Zhao et al. (2015)
	q12.1 chr5: 60487712–60491518 (+)	Glioblastoma	PART1	PI3K/AKT Bcl2/bax	<i>In vitro</i> , human	U87MG, LN-18, LN-428 glioma tissues	Jin et al. (2020a)
	p15.2 chr7: 27198574–27201236 (+)	Glioblastoma	HOTTIP	P53	<i>In vivo</i> <i>in vitro</i>	A172, U251, U87-MG, U118-MG glioma tissues mice	Xu et al. (2016)
	q21.3 chr7: 94022832–94064723 (+)	Glioblastoma	AC003092.1	miR-195/TFPI-2 signaling	<i>In vivo</i> <i>In vitro</i>	Human U87 cell line/glioma tissues/mice	Xu et al. (2018a)
	p13.3 chr9: 33775182–33801186 (-)	Glioblastoma	UBE2R2-AS1	miR-877-3p/TLR4 caspase-3/-7/-8 and Bcl2	<i>In vitro</i> <i>In silico</i>	U251, A-172, U87-MG, and U373 glioma samples	Xu et al. (2019c)

(Continued on following page)

TABLE 2 | (Continued) Apoptosis-related lncRNAs in brain tumors.

Genomic coordinates	Brain tumors	lncRNA	Targets	Model	Type of cell line	Ref
q26.11 chr10: 118046278–118206659 (+)	Glioblastoma	CASC2	miRNA-18a	<i>In vitro</i>	glioblastoma tissue	Wang et al. (2020b)
			E-cadherin	<i>In vivo</i>	Human glioblastoma cells (A172 and T98)	
p14.1 chr11: 27506829–27515218 (+)	Glioblastoma	BDNF-AS	PABPC1-BDNF-AS-RAX2-DLG5 pathway	<i>In vivo</i>	U87 and U251 Glioma tissues Mice	Su et al. (2020)
q13.1 chr11: 65422773–65426457 (+)	Glioblastoma	NEAT1	miR-92b/DKK3 pathway		U-87 MG and U251 glioma tissues	Liu et al. (2020)
q13.12 chr19: 36259539–36264788 (-)	Glioblastoma	LINC00665	TAF15/LINC00665/MTF1(Y2)/GTSE1 axis	<i>In vivo</i>	U251 and U87 glioma cells/glioma tissues/mice	Ruan et al. (2020)
q11.23 chr20: 36045617–36051018 (-)	Glioblastoma	LINC00657 (NORAD)	miR-190a-3p/PTEN	<i>In vitro</i> <i>In vivo</i>	U-87 MG, LN-18 and U-118 MG	Chu et al. (2019)
			PI3K/Akt/mTOR	<i>In vitro</i>	Animal cases	

higher stability in the plasma and tissues (Suzuki and Tsukahara, 2014).

Hence, the mentioned specific structural features imply the fact that they are pathologically and physiologically major transcripts. A lot of investigations have confirmed that the abnormal expression of circRNAs is one of the major regulatory elements in expansion and carcinogenesis of some cancers such as hematological malignancies, lung cancer, and liver cancer, revealing the probable targets to diagnosis and prognosis of these cancers by circRNAs. Some recent investigations performed about features and biogenesis of the circRNAs, summarized their functions and mechanisms of action in cancers, and discussed their capacity to diagnose and treat the diseases of interest (Bach et al., 2019; Zhang et al., 2020d; Lei et al., 2020; Shen et al., 2021).

Considering their origins, it is possible to classify circRNAs into 3 groups of circular intron RNAs (ciRNAs), exonic circRNAs (ecircRNAs), and exon–intron circRNAs (EIciRNAs) (Meng et al., 2017) (Figure 4). Various circularization mechanisms regulate circRNA biogenesis, out of which ecircRNA is abundantly found so that it includes most of specified circRNAs (Bolha et al., 2017). In fact, gene transcription is regulated by cirRNAs. Overall, Pol II transcribes a pre-mRNA

which consists of exons and introns as well as a seven-methylguanosine cap and poly-adenosine tail, which is added to its 5'- and 3'-ends. After that, pre-mRNA is spliced at the canonical splice sites (5'-GU & 3'-AG at introns) using spliceosomes for maturity and translatability. In addition, one of the specific splicing manners known as back-splicing generates CircRNA, where the 3'-end of an exon binds to the 5'-end of its own or an upstream exon via a 3', 5'- phosphodiester bond, and establishes a closed structure with a back-splicing junction. Researchers viewed circRNAs as the splicing errors consisting of scrambled exons, and presented and verified two biogenesis models based on the splicing events sequence and various intermediates, including direct backsplicing model and lariat model (Zhang et al., 2020d; Zhou et al., 2020).

Circular RNAs and Apoptosis in Brain Tumors

Glioblastoma cells show a remarkably high level of Circular RNA hsa_circ_0067934. The hsa_circ_0067934 silencing promotes apoptosis in glioblastoma cells via PI3K-AKT pathway (Xin et al., 2019). MiR-181a was down-regulated in glioma, while the circ_0076248 and SIRT1 were up-regulated.

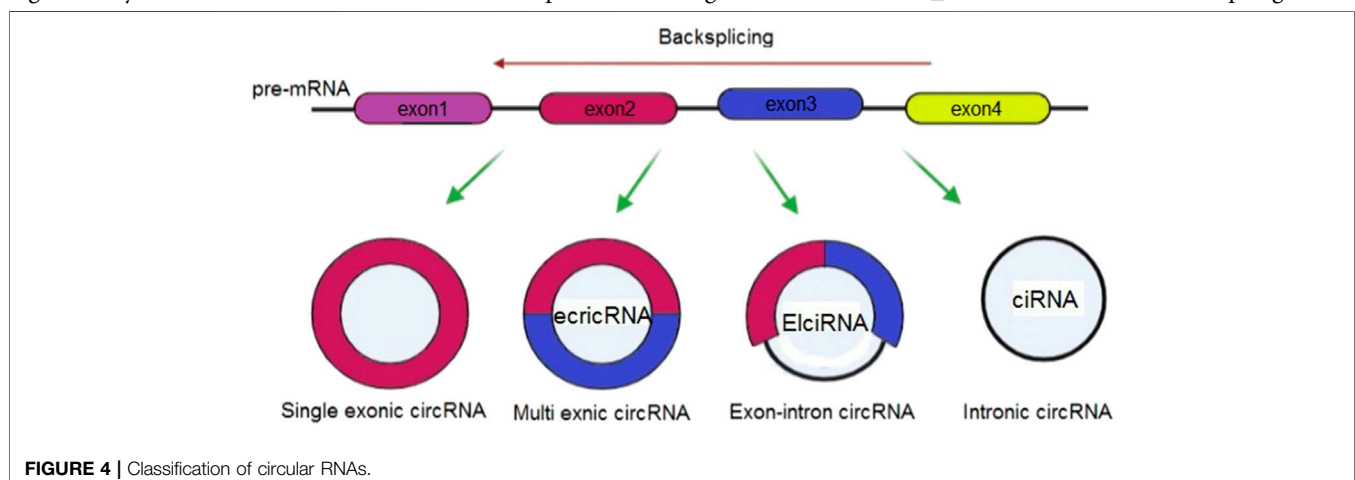


TABLE 3 | Apoptosis-related circular RNAs in brain tumors.

	Genomic coordinate	Brain tumors	Circular RNAs	CircbaseID	Targets	Model	Type of cell line	Ref
Up regulated circular RNA expression	q21.3 chr1: 151206672–151212515 (+)	Glioblastoma	CircPIP5K1A	hsa_circ_0014130	PI3K/AKT	<i>In vivo</i>	U87, TJ861, TJ905, U251, H4, A172 glioma tissues	Zheng et al. (2021)
	q26.2 chr3: 170013698–170015181 (+)	Glioblastoma	CircPRKCI	hsa_circ_0067934	PI3K-AKT pathway	<i>In vitro</i>	mice GBM samples	Xin et al. (2019)
	q26.2 chr3: 170013698–170015181 (+)	Glioblastoma	CircPRKCI	hsa_circ_0067934	caspase-3, caspase-9 and PARP	<i>In vivo</i> <i>In vitro</i>	The LN18, U251, LN229, T98G and A172 cells	Zhang et al. (2019b)
	q14.2 chr5: 82832825–82838087 (+)	glioblastoma	CircVCAN	hsa_circ_0073237	microRNA-1183	<i>In vitro</i>	The 293T, U87, and U251 cells glioma tissues/mice	Zhu et al. (2020)
	p21.2 chr6: 37787306–38084515 (+)	Glioblastoma	CircZFAND3	hsa_circ_0076248	MIR-181a/SIRT1	<i>In vivo</i>	Human GBM samples/U251, U87 cell lines	Lei et al. (2019)
	q14.3 chr6: 86176777–86197207 (+)	Glioblastoma	CircNT5E	hsa_circ_0077231	NT5E, SOX4, PI3KCA, p-Akt, p-Smad2	<i>In vitro</i> <i>In vivo</i> <i>In vitro</i>	Animal studies Tumor tissue samples/GBM cells (U87 and U251)/mice	Wang et al. (2018a)
	q32.1 chr7: 128845043–128846428 (+)	Glioblastoma	CircSMO742	hsa_circ_0001742	miR-338-3p/SMO	<i>In vivo</i> <i>In vitro</i>	10 human gliomas tissues/human glioblastoma A172 and U-87 MG/mice	Xiong et al. (2019)
	q24.21 chr8: 128806778–128903244 (+)	Glioblastoma	CircPVT1	hsa_circ_0085536	miR-199a-5p YAP1 and PI3K/AKT Capase-3 Capase-9 Ncadherin, Vimentin, Zeb1, E-cadherin	<i>In vitro</i>	human GBM tissues U539 and U251 cells	Chi et al. (2020)
	q34.12 chr9: 130914461–130915734 (+)	Glioblastoma	CircLCN2	hsa_circ_0088732	N-cadherin, vimentin, E-cadherin	<i>In vivo</i> <i>In vitro</i>	tumor tissues/glioma cell lines LN229, U87-MG, U251, and A172/mice	Jin et al. (2020b)
	q12.11 chr13: 21735928–21746820 (-)	Medulloblastoma	CircSKA3	hsa_circ_0029696	miR-383-5p/FOXM1 Bcl2 and capase-3	<i>In vivo</i> <i>In vitro</i>	tissue samples/cell lines DAOY and ONS-76	Wang et al. (2020c)
	q13.3 chr13: 38136718–38161065 (-)	Glioblastoma	CircPOSTN	hsa_circ_0030018	Bcl2/bax/caspase 3	<i>In vivo</i>	Human tissue sample/Glioma cell line (U251, LN229)/mice	Long et al. (2020)
	q15.2 chr15: 43120125–43164956 (-)	Glioblastoma	CircTTBK2	hsa_circ_0000594	Mirna-520b/EZH2	<i>In vitro</i> <i>In vivo</i> <i>In vitro</i>	glioma tissues A172 and U251 mice	Yuan et al. (2019)
	q15.2 chr15: 43120125–43164956 (-)	Glioblastoma	CircTTBK2	hsa_circ_0000594	PI3K/AKT and ERK	<i>In vivo</i> <i>In vitro</i>	Human tissues specimens/Human U87 and U251 glioma cell lines mice/	Zheng et al. (2017)
	p13.3 chr16: 765172–767480 (+)	Glioblastoma	CircMETRN	hsa_circ_0037251	miR-1229-3p/mTOR axis	<i>In vivo</i> <i>In vitro</i>	U373, U251 mice	Cao et al. (2019)
	q21.1 chr18: 48189458–48190874 (+)	Glioblastoma	CircMAPK4	hsa_circ_0047688	p38/MAPK	<i>In vitro</i> <i>In vivo</i>	U138, U373 and U87 glioma cell lines/glioma tissues/mice	He et al. (2020)
	p13.13 chr19: 13183860–13192669 (+)	Glioblastoma	CircNFIH	hsa_circ_0049658	Notch signaling pathway	<i>In vivo</i> <i>In vitro</i>	SF-539, SHG-44 U87 glioma tissue from mice	Xu et al. (2018b)

(Continued on following page)

TABLE 3 | (Continued) Apoptosis-related circular RNAs in brain tumors.

	Genomic coordinate	Brain tumors	Circular RNAs	CircbaseID	Targets	Model	Type of cell line	Ref
	p13.13 chr19: 13183860–13192669 (+)	Glioblastoma	CircNFIX	hsa_circ_0049658	miR-378e/ RPN2 axis	<i>In vivo</i>	Patient samples T98, U251, SW1783,A172	Ding et al. (2019)
	q13.1 chrX: 69606467–69607147 (+)	Glioblastoma	CircKIF4A	hsa_circ_0090956	Wnt5a, β-catenin, c-Myc, cyclin D1/bcl2/bax	<i>In vitro</i> <i>In vivo</i>	Mice glioma sample LN229, A172, SHG44, U251s mice	Huo et al. (2020)
Down regulated Circular RNA expression	q11.21 chr20: 33001547–33037285 (+)	Glioblastoma	CircITCH	hsa_circ_0001141	ITCH-Wnt/ β-catenin	<i>In vitro</i> , human	cancer tissues U87, U251, A172, SHG44, LN229, T98G, SHG139	Wang et al. (2018b)

The down-regulation of hsa_circ_0076248 or miR-181a overexpression upregulate p53 and SIRT1. Down regulation of hsa_circ_0076248 leads to inhibiting xenograft tumors' growth and increasing apoptosis (Lei et al., 2019). CircPVT1 was over-expressed in glioblastoma tissues. Silencing circPVT1 increases the number of apoptotic cells by increased cleaved-Caspase-3 and cleavedCaspase-9 expression via targeting miR-199a-5p (Chi et al., 2020). Glioblastoma cells were shown to have a greatly elevated level of circNT5E. circNT5E up-regulation inhibits apoptosis via miR-422a (Wang et al., 2018a). Glioma cells have a high level of Circ-TTBK2 and EZH2. Through miR-520b/EZH2 pathway, circ-TTBK2 suppression is able to improve apoptosis (Yuan et al., 2019). The high level of circSMO742 and SMO can inhibit miR-338-3p which results in increased proliferation, migration and invasion and decreased apoptosis of glioma cells (Xiong et al., 2019). Cir-ITCH is observed in low amounts in glioma. Through miR-214 inactivation and modulation of ITCH-Wnt/β-catenin axis in glioma cells, cir-ITCH upregulation can improve apoptosis (Wang et al., 2018b). Glioma cells have an elevated level of circPOSTN. Via targeting miR-361-5p/TPX2, circPOSTN suppression can lower Bcl-2 and elevate Bax and caspase-3 which result in apoptosis (Long et al., 2020). CircPIP5K1A was up-regulated in glioma cells. The apoptosis increases after the knockdown of circPIP5K1A through TCF12/PI3K/AKT axis regulation by miR-515-5p inactivation (Zheng et al., 2021). Circ-MAPK4 was over-expressed in glioma tissues. Circ-MAPK4 silencing increases apoptosis by elevating caspase-3, caspase-7, caspase-9, and PARP1 via targeting miR-125a-3p and regulating p38/MAPK (Peng et al., 2020). Glioma cells show a greatly high level of circ-TTBK2. circ-TTBK2 regulates miR-217/HNF1β/Derlin-1 pathway which reduces apoptosis (Zheng et al., 2017). Glioma cells show hsa_circ_0088732 to be upregulated. hsa_circ_0088732 inhibition stimulates apoptosis through the miR-661/RAB3D pathway (Jin et al., 2020b). Glioma cells show circNFIX to be overexpressed. circNFIX impedes miR-34a-5p which inhibits apoptosis and therefore, circNFIX knockout can show the opposite effects (Xu et al., 2018b). CircKIF4A

expression was increased in glioma. By targeting miR-139-3p which downregulates cyclin D1, c-Myc and Bcl2, and upregulates Bax, CircKIF4A suppression can improve apoptosis in glioma cells (Huo et al., 2020). Glioma cells show circPRKCI to be overexpressed. CircPRKCI shRNA could induce apoptosis by increasing Annexin V, and cleaving caspase-3, caspase-9 and PARP via targeting miR-545 (Zhang et al., 2019b). circNFIX is present in high amounts in glioma tissues. circNFIX suppression targets miR-378e/RPN2 pathway to induce apoptosis (Ding et al., 2019). hsa_circ_00037251 inhibition promotes apoptosis in glioma via miR-1229-3p/mTOR pathway (Cao et al., 2019). Radioresistant glioma was shown to have notably elevated levels of circ_VCAN. It exerts a carcinogenic role in glioma via regulating microRNA-1183. The knockdown of circ_VCAN stimulated apoptosis in glioma cells (Zhu et al., 2020). CircSKA3 was up-regulated in medulloblastoma tissues. circSKA3 reduces Bcl-2, while elevates caspase-3 in medulloblastoma cells by targeting miR-383-5p (Wang et al., 2020c). **Table 3** illustrates apoptosis-related circular RNAs in brain tumors and their expression.

CONCLUSION

Various cellular functions reveal the contribution of ncRNAs to the cancer development at the transcriptional, translational, as well as epigenetic, level. Hence, ncRNAs can be a hopeful path of molecular medicine, though, patterns of RNAs expression in the brain tumors are not constant and stable, and thus researchers must provide proper alternatives to be utilized as the diagnostic or treatment instruments. With their stable structure, various ncRNAs have shown their capacity to function as regulatory agents. Studies illustrated a few circRNAs, lncRNAs even snoRNAs as the potent treatment, diagnostic, prognostic targets in the tumors of brain. Therefore, there are limited investigations revealing the strict correlation of RNAs with prognosis of the cases with gliomas, WHO grade, as well as their real potential diagnostic value. Nonetheless, multiple investigations largely emphasized the pathological- clinical specimens. A major difficulty is that we must wait for those research that specify circRNAs,

snoRNAs, miRNA, and lncRNAs from the bodily fluids, in particular, CSF and blood of the cases with brain tumors. Hence, it is important to focus on the particular methods about stability, abundance, and longer half-life for identifying ncRNAs molecules associated with the noninvasive diagnosis and classification of the sub-types of gliomas. Hence, such attempts may simplify the evaluation of the initial treatment with higher sensitivity, magnetic resonance imaging (MRI), and or other conventional bio-markers. Thus, expression profile of the regulator RNAs that is identified by analyzing circRNAs, snoRNAs, miRNA, and lncRNA along with studying the respective effects would be of high importance for exploring the molecular pathology of the

tumors in the brain. Finally, more research must be performed for developing one of the new RNA-based approaches for treating any malignant tumor and using their diagnostic and prognostic potency, which may result in promising results for cases with the brain tumors.

AUTHOR CONTRIBUTIONS

OT, FN, JR, RH, HJ, AR, MH, and HM contributed in data collection and manuscript drafting. All authors approved the final version for submission. MD, AJ, MM, and MT, critically revised the manuscript.

REFERENCES

- Achkar, N. P., Cambiagno, D. A., and Manavella, P. A. (2016). miRNA Biogenesis: a Dynamic Pathway. *Trends Plant Sci.* 21 (12), 1034–1044. doi:10.1016/j.tplants.2016.09.003
- Aldape, K., Brindle, K. M., Chesler, L., Chopra, R., Gajjar, A., Gilbert, M. R., et al. (2019). Challenges to Curing Primary Brain Tumours. *Nat. Rev. Clin. Oncol.* 16 (8), 509–520. doi:10.1038/s41571-019-0177-5
- Bach, D.-H., Lee, S. K., and Sood, A. K. (2019). Circular RNAs in Cancer. *Mol. Ther. - Nucleic Acids* 16, 118–129. doi:10.1016/j.omtn.2019.02.005
- Balandeh, E., Mohammadshafie, K., Mahmoudi, Y., Hossein Pourhanif, M., Rajabi, A., Bahabadi, Z. R., et al. (2021). Roles of Non-coding RNAs and Angiogenesis in Glioblastoma. *Front. Cell Dev. Biol.* 9, 716462. doi:10.3389/fcell.2021.716462
- Beermann, J., Piccoli, M.-T., Viereck, J., and Thum, T. (2016). Non-coding RNAs in Development and Disease: Background, Mechanisms, and Therapeutic Approaches. *Physiol. Rev.* 96 (4), 1297–1325. doi:10.1152/physrev.00041.2015
- Bolha, L., Ravnik-Glavac, M., and Glavac, D. (2017). Circular RNAs: Biogenesis, Function, and a Role as Possible Cancer Biomarkers. *Int. J. Genomics* 2017, 6218353. doi:10.1155/2017/6218353
- Cabili, M. N., Dunagin, M. C., McClanahan, P. D., Biesch, A., Padovan-Merhar, O., Regev, A., et al. (2015). Localization and Abundance Analysis of Human lncRNAs at Single-Cell and Single-Molecule Resolution. *Genome Biol.* 16 (1), 20–16. doi:10.1186/s13059-015-0586-4
- Cabili, M. N., Trapnell, C., Goff, L., Koziol, M., Tazon-Vega, B., Regev, A., et al. (2011). Integrative Annotation of Human Large Intergenic Noncoding RNAs Reveals Global Properties and Specific Subclasses. *Genes Dev.* 25 (18), 1915–1927. doi:10.1101/gad.1744661
- Cao, Q., Shi, Y., Wang, X., Yang, J., Mi, Y., Zhai, G., et al. (2019). Circular METRN RNA Hsa_circ_0037251 Promotes Glioma Progression by Sponging miR-1229-3p and Regulating mTOR Expression. *Sci. Rep.* 9 (1), 19791. doi:10.1038/s41598-019-56417-8
- Carlevaro-Fita, J., Rahim, A., Guigó, R., Vardy, L. A., and Johnson, R. (2016). Cytoplasmic Long Noncoding RNAs Are Frequently Bound to and Degraded at Ribosomes in Human Cells. *RNA* 22 (6), 867–882. doi:10.1261/rna.053561.115
- Chen, H. H., Zong, J., and Wang, S. J. (2019). lncRNA GAPLINC Promotes the Growth and Metastasis of Glioblastoma by Sponging miR-331-3p. *Eur. Rev. Med. Pharmacol. Sci.* 23 (1), 262–270. doi:10.26355/eurrev_201901_16772
- Chen, H., Hou, G., Yang, J., Chen, W., Guo, L., Mao, Q., et al. (2020). SOX9-activated PXN-AS1 Promotes the Tumorigenesis of Glioblastoma by EZH2-mediated Methylation of DKK1. *J. Cell Mol Med* 24 (11), 6070–6082. doi:10.1111/jcmm.15189
- Cheng, F., Liu, J., Zhang, Y., You, Q., Chen, B., Cheng, J., et al. (2021). Long Non-coding RNA UBA6-AS1 Promotes the Malignant Properties of Glioblastoma by Competitively Binding to microRNA-760 and Enhancing Homeobox A2 Expression. *Cancer Manag. Res.* 13, 379–392. doi:10.2147/cmar.s287676
- Chi, G., Yang, F., Xu, D., and Liu, W. (2020). Silencing hsa_circ_PVT1 (circPVT1) Suppresses the Growth and Metastasis of Glioblastoma Multiforme Cells by Up-Regulation of miR-199a-5p. *Artif. Cell nanomedicine, Biotechnol.* 48 (1), 188–196. doi:10.1080/21691401.2019.1699825
- Chu, L., Yu, L., Liu, J., Song, S., Yang, H., Han, F., et al. (2019). Long Intergenic Non-coding LINC00657 Regulates Tumorigenesis of Glioblastoma by Acting as a Molecular Sponge of miR-190a-3p. *Aging* 11 (5), 1456–1470. doi:10.18632/aging.101845
- Dahariya, S., Paddibhatla, I., Kumar, S., Raghuwanshi, S., Palapati, A., and Gutti, R. K. (2019). Long Non-coding RNA: Classification, Biogenesis and Functions in Blood Cells. *Mol. Immunol.* 112, 82–92. doi:10.1016/j.molimm.2019.04.011
- Dalan, A. B., Gulluoglu, S., Tuysuz, E. C., Kuskucu, A., Yaltirik, C. K., Ozturk, O., et al. (2017). Simultaneous Analysis of miRNA-mRNA in Human Meningiomas by Integrating Transcriptome: A Relationship between PTX3 and miR-29c. *BMC cancer* 17 (1), 207–209. doi:10.1186/s12885-017-3198-4
- D'Arcy, M. S. (2019). Cell Death: a Review of the Major Forms of Apoptosis, Necrosis and Autophagy. *Cel Biol. Int.* 43 (6), 582–592.
- Dashti, F., Mirazimi, S. M. A., Rabiei, N., Fathazam, R., Rabiei, N., Piroozmand, H., et al. (2021). The Role of Non-coding RNAs in Chemotherapy for Gastrointestinal Cancers. *Mol. Ther. - Nucleic Acids* 26, 892–926. doi:10.1016/j.omtn.2021.10.004
- Deng, D., Wang, L., Chen, Y., Li, B., Xue, L., Shao, N., et al. (2016). MicroRNA-124-3p Regulates Cell Proliferation, Invasion, Apoptosis, and Bioenergetics by Targeting PIM1 in Astrocytoma. *Cancer Sci.* 107 (7), 899–907. doi:10.1111/cas.12946
- Derrien, T., Johnson, R., Bussotti, G., Tanzer, A., Djebali, S., Tilgner, H., et al. (2012). The GENCODE V7 Catalog of Human Long Noncoding RNAs: Analysis of Their Gene Structure, Evolution, and Expression. *Genome Res.* 22 (9), 1775–1789. doi:10.1101/gr.132159.111
- Ding, C., Wu, Z., You, H., Ge, H., Zheng, S., Lin, Y., et al. (2019). CircNFIX promotes progression of glioma through regulating miR-378e/RPN2 axis. *J. Exp. Clin. Cancer Res.* 38 (1), 506–512. doi:10.1186/s13046-019-1483-6
- Dong, Z.-Q., Guo, Z.-Y., and Xie, J. (2019). The lncRNA EGFR-AS1 Is Linked to Migration, Invasion and Apoptosis in Glioma Cells by Targeting miR-133b/RACK1. *Biomed. Pharmacother.* 118, 109292. doi:10.1016/j.biopha.2019.109292
- Du, F., and Hou, Q. (2020). SNHG17 Drives Malignant Behaviors in Astrocytoma by Targeting miR-876-5p/ERLIN2 axis. *BMC cancer* 20 (1), 839. doi:10.1186/s12885-020-07280-8
- Elmore, S. (2007). Apoptosis: a Review of Programmed Cell Death. *Toxicol. Pathol.* 35 (4), 495–516. doi:10.1080/01926230701320337
- Evan, G. I., and Vousden, K. H. (2001). Proliferation, Cell Cycle and Apoptosis in Cancer. *Nature* 411 (6835), 342–348. doi:10.1038/35077213
- Fang, Y., and Fullwood, M. J. (2016). Roles, Functions, and Mechanisms of Long Non-coding RNAs in Cancer. *Genomics, Proteomics & Bioinformatics* 14 (1), 42–54. doi:10.1016/j.gpb.2015.09.006
- Fei, F., He, Y., He, S., He, Z., Wang, Y., Wu, G., et al. (2018). lncRNA SNHG3 Enhances the Malignant Progress of Glioma through Silencing KLF2 and P21. *Biosci. Rep.* 38 (5), BSR20180420. doi:10.1042/BSR20180420
- Feng, L., Ma, J., Ji, H., Liu, Y., and Hu, W. (2017). miR-330-5p Suppresses Glioblastoma Cell Proliferation and Invasiveness through Targeting ITGA5. *Biosci. Rep.* 37 (3), BSR20170019. doi:10.1042/BSR20170019
- Fernald, K., and Kurokawa, M. (2013). Evading Apoptosis in Cancer. *Trends Cell Biology* 23 (12), 620–633. doi:10.1016/j.tcb.2013.07.006

- Gao, J., Bai, S., Wang, Y., Zhao, S., He, Z., and Wang, R. (2019). MiR-374b Targets GATA3 to Promote Progression and Development of Glioblastoma via Regulating SEMA3B. *Neoplasma* 66 (4), 543–554. doi:10.4149/neo_2018_180830N659
- Gao, R., Zhang, R., Zhang, C., Liang, Y., and Tang, W. (2018). LncRNA LOXL1-AS1 Promotes the Proliferation and Metastasis of Medulloblastoma by Activating the PI3K/AKT Pathway. *Anal. Cel Pathol (Amst)* 2018, 9275685. doi:10.1155/2018/9275685
- Gao, X. F., He, H. Q., Zhu, X. B., Xie, S. L., and Cao, Y. (2019). LncRNA SNHG20 Promotes Tumorigenesis and Cancer Stemness in Glioblastoma via Activating PI3K/Akt/mTOR Signaling Pathway. *Neoplasma* 66 (4), 532–542. doi:10.4149/neo_2018_180829N656
- Gebert, L. F. R., and MacRae, I. J. (2019). Regulation of microRNA Function in Animals. *Nat. Rev. Mol. Cel Biol* 20 (1), 21–37. doi:10.1038/s41580-018-0045-7
- Ghaemi, S., Arefian, E., Rezaeadeh Valojerdi, R., Soleimani, M., Moradimotlagh, A., and Jamshidi Adegani, F. (2020). Inhibiting the Expression of Anti-apoptotic Genes BCL2L1 and MCL1, and Apoptosis Induction in Glioblastoma Cells by microRNA-342. *Biomed. Pharmacother.* 121, 109641. doi:10.1016/j.biopha.2019.109641
- Gong, W., Zheng, J., Liu, X., Liu, Y., Guo, J., Gao, Y., et al. (2017). Knockdown of Long Non-coding RNA KCNQ1OT1 Restrained Glioma Cells' Malignancy by Activating miR-370/CCNE2 Axis. *Front. Cel. Neurosci.* 11, 84. doi:10.3389/fncel.2017.00084
- Gong, W., Zheng, J., Liu, X., Ma, J., Liu, Y., and Xue, Y. (2016). Knockdown of NEAT1 restrained the malignant progression of glioma stem cells by activating microRNA let-7e. *Oncotarget* 7 (38), 62208–62223. doi:10.18632/oncotarget.11403
- Guo, C.-J., Ma, X.-K., Xing, Y.-H., Zheng, C.-C., Xu, Y.-F., Shan, L., et al. (2020). Distinct Processing of lncRNAs Contributes to Non-conserved Functions in Stem Cells. *Cell* 181 (3), 621–636. e22. doi:10.1016/j.cell.2020.03.006
- Guo, J. U., Agarwal, V., Guo, H., and Bartel, D. P. (2014). Expanded Identification and Characterization of Mammalian Circular RNAs. *Genome Biol.* 15 (7), 409–414. doi:10.1186/s13059-014-0409-z
- Guo, X. B., Zhang, X. C., Chen, P., Ma, L. M., and Shen, Z. Q. (2019). miR-378a-3p Inhibits Cellular Proliferation and Migration in Glioblastoma Multiforme by Targeting Tetraspanin 17. *Oncol. Rep.* 42 (5), 1957–1971. doi:10.3892/or.2019.7283
- Guttman, M., and Rinn, J. L. (2012). Modular Regulatory Principles of Large Non-coding RNAs. *Nature* 482 (7385), 339–346. doi:10.1038/nature10887
- Ha, M., and Kim, V. N. (2014). Regulation of microRNA Biogenesis. *Nat. Rev. Mol. Cel Biol* 15 (8), 509–524. doi:10.1038/nrm3838
- Han, N., Yang, L., Zhang, X., Zhou, Y., Chen, R., Yu, Y., et al. (2019). LncRNA MATN1-AS1 Prevents Glioblastoma Cell from Proliferation and Invasion via RELA Regulation and MAPK Signaling Pathway. *Ann. Transl. Med.* 7 (23), 784. doi:10.21037/atm.2019.11.36
- Hashemian, S. M., Pourhanif, M. H., Fadaei, S., Velayati, A. A., Mirzaei, H., and Hamblin, M. R. (2020). Non-coding RNAs and Exosomes: Their Role in the Pathogenesis of Sepsis. *Mol. Ther. - Nucleic Acids* 21, 51–74. doi:10.1016/j.omtn.2020.05.012
- He, J., Huang, Z., He, M., Liao, J., Zhang, Q., Wang, S., et al. (2020). Circular RNA MAPK4 (Circ-MAPK4) Inhibits Cell Apoptosis via MAPK Signaling Pathway by Sponging miR-125a-3p in Gliomas. *Mol. Cancer* 19 (1), 17. doi:10.1186/s12943-019-1120-1
- Hu, H.-q., Sun, L.-g., and Guo, W.-j. (2016). Decreased miRNA-146a in Glioblastoma Multiforme and Regulation of Cell Proliferation and Apoptosis by Target Notch1. *Int. J. Biol. Markers* 31 (3), 270–275. doi:10.5301/jbm.5000194
- Huo, L. W., Wang, Y. F., Bai, X. B., Zheng, H. L., and Wang, M. D. (2020). circKIF4A Promotes Tumorigenesis of Glioma by Targeting miR-139-3p to Activate Wnt5a Signaling. *Mol. Med.* 26 (1), 29–15. doi:10.1186/s10020-020-00159-1
- Jafari, A., Rezaei-Tavirani, M., Farhadihosseinabadi, B., Zali, H., and Niknejad, H. (2021). Human Amniotic Mesenchymal Stem Cells to Promote/suppress Cancer: Two Sides of the Same coin. *Stem Cel Res. Ther.* 12 (1), 1–11. doi:10.1186/s13287-021-02196-x
- Jafari, A., Rezaei-Tavirani, M., Niknejad, H., and Zali, H. (2021). Tumor Targeting by Conditioned Medium Derived from Human Amniotic Membrane: New Insight in Breast Cancer Therapy. *Technol. Cancer Res. Treat.* 20, 15330338211036318. doi:10.1177/15330338211036318
- Jafari, A., Rezaei-Tavirani, M., Salimi, M., Tavakkol, R., and Jafari, Z. (2020). Oncological Emergencies from Pathophysiology and Diagnosis to Treatment: A Narrative Review. *Soc. Work Public Health* 35 (8), 689–709. doi:10.1080/19371918.2020.1824844
- Ji, T., Zhang, X., and Li, W. (2017). MicroRNA-543 Inhibits Proliferation, Invasion and Induces Apoptosis of Glioblastoma Cells by Directly Targeting ADAM9. *Mol. Med. Rep.* 16 (5), 6419–6427. doi:10.3892/mmr.2017.7332
- Jin, T., Liu, M., Liu, Y., Li, Y., Xu, Z., He, H., et al. (2020). Lcn2-derived Circular RNA (Hsa_circ_0088732) Inhibits Cell Apoptosis and Promotes EMT in Glioma via the miR-661/RAB3D Axis. *Front. Oncol.* 10, 170. doi:10.3389/fonc.2020.00170
- Jin, Z., Piao, L., Sun, G., Lv, C., Jing, Y., and Jin, R. (2020). Long Non-coding RNA PART1 Exerts Tumor Suppressive Functions in Glioma via Sponging miR-190a-3p and Inactivation of PTEN/AKT Pathway. *Onco Targets Ther.* 13, 1073–1086. doi:10.2147/ott.s232848
- Khani, P., Nasri, F., Khani Chamani, F., Saeidi, F., Sadri Nahand, J., Tabibkhouei, A., et al. (2019). Genetic and Epigenetic Contribution to Astrocytic Gliomas Pathogenesis. *J. Neurochem.* 148 (2), 188–203. doi:10.1111/jnc.14616
- Kim, J., Zhang, Y., Skalski, M., Hayes, J., Kefas, B., Schiff, D., et al. (2014). microRNA-148a Is a Prognostic oncomiR that Targets MIG6 and BIM to Regulate EGFR and Apoptosis in Glioblastoma. *Cancer Res.* 74 (5), 1541–1553. doi:10.1158/0008-5472.can-13-1449
- Lee, R. C., Feinbaum, R. L., and Ambros, V. (1993). The *C. elegans* Heterochronic Gene Lin-4 Encodes Small RNAs with Antisense Complementarity to Lin-14. *cell* 75 (5), 843–854. doi:10.1016/0092-8674(93)90529-y
- Lei, B., Huang, Y., Zhou, Z., Zhao, Y., Thapa, A. J., Li, W., et al. (2019). Circular RNA Hsa_circ_0076248 Promotes Oncogenesis of Glioma by Sponging miR-181a to Modulate SIRT1 Expression. *J. Cel Biochem* 120 (4), 6698–6708. doi:10.1002/jcb.27966
- Lei, M., Zheng, G., Ning, Q., Zheng, J., and Dong, D. (2020). Translation and Functional Roles of Circular RNAs in Human Cancer. *Mol. Cancer* 19 (1), 30–39. doi:10.1186/s12943-020-1135-7
- Lei, W., Wang, Z. L., Feng, H. J., Lin, X. D., Li, C. Z., and Fan, D. (2018). Long Non-coding RNA SNHG12 promotes the Proliferation and Migration of Glioma Cells by Binding to HuR. *Int. J. Oncol.* 53 (3), 1374–1384. doi:10.3892/ijo.2018.4478
- Li, B., Shen, M., Yao, H., Chen, X., and Xiao, Z. (2019). Long Noncoding RNA TP73-AS1 Modulates Medulloblastoma Progression *In Vitro* and *In Vivo* by Sponging miR-494-3p and Targeting EIF5A2. *Onco Targets Ther.* 12, 9873–9885. doi:10.2147/ott.s228305
- Li, K. K.-W., Pang, J. C.-S., Lau, K.-M., Zhou, L., Mao, Y., Wang, Y., et al. (2013). MiR-383 Is Downregulated in Medulloblastoma and Targets Peroxiredoxin 3 (PRDX3). *Brain Pathol.* 23 (4), 413–425. doi:10.1111/bpa.12014
- Li, Q., Dong, C., Cui, J., Wang, Y., and Hong, X. (2018). Over-expressed lncRNA HOTAIRM1 Promotes Tumor Growth and Invasion through Up-Regulating HOXA1 and Sequestering G9a/EZH2/Dnmts Away from the HOXA1 Gene in Glioblastoma Multiforme. *J. Exp. Clin. Cancer Res.* 37 (1), 265. doi:10.1186/s13046-018-0941-x
- Li, T., Ren, J., Ma, J., Wu, J., Zhang, R., Yuan, H., et al. (2019). LINC00702/miR-4652-3p/ZEB1 axis Promotes the Progression of Malignant Meningioma through Activating Wnt/ β -Catenin Pathway. *Biomed. Pharmacother.* 113, 108718. doi:10.1016/j.biopha.2019.108718
- Li, W., Jiang, P., Sun, X., Xu, S., Ma, X., and Zhan, R. (2016). Suppressing H19 Modulates Tumorigenicity and Stemness in U251 and U87MG Glioma Cells. *Cell Mol Neurobiol* 36 (8), 1219–1227. doi:10.1007/s10571-015-0320-5
- Li, Y., Ren, Z., Peng, Y., Li, K., Wang, X., Huang, G., et al. (2019). Classification of Glioma Based on Prognostic Alternative Splicing. *BMC Med. Genomics* 12 (1), 165. doi:10.1186/s12920-019-0603-7
- Liao, K., Lin, Y., Gao, W., Xiao, Z., Medina, R., Dmitriev, P., et al. (2019). Blocking lncRNA MALAT1/miR-199a/ZHX1 axis Inhibits Glioblastoma Proliferation and Progression. *Mol. Ther. - Nucleic Acids* 18, 388–399. doi:10.1016/j.omtn.2019.09.005
- Liao, Y., Zhang, B., Zhang, T., Zhang, Y., and Wang, F. (2019). LncRNA GATA6-AS Promotes Cancer Cell Proliferation and Inhibits Apoptosis in Glioma by Downregulating lncRNA TUG1. *Cancer Biother. Radiopharm.* 34 (10), 660–665. doi:10.1089/cbr.2019.2830

- Lin, H., Zuo, D., He, J., Ji, T., Wang, J., and Jiang, T. (2021). Long Noncoding RNA WEE2-AS1 Plays an Oncogenic Role in Glioblastoma by Functioning as a Molecular Sponge for microRNA-520f-3p. *Oncol. Res. Featuring Preclinical Clin. Cancer Ther.* 28 (6), 591–603.
- Lin, S., and Gregory, R. I. (2015). MicroRNA Biogenesis Pathways in Cancer. *Nat. Rev. Cancer* 15 (6), 321–333. doi:10.1038/nrc3932
- Lin, Y.-H., Guo, L., Yan, F., Dou, Z.-Q., Yu, Q., and Chen, G. (2020). Long Non-coding RNA HOTAIRM1 Promotes Proliferation and Inhibits Apoptosis of Glioma Cells by Regulating the miR-873-5p/ZEB2 axis. *Chin. Med. J.* 133 (2), 174–182. doi:10.1097/cm9.0000000000000615
- Liu, D., Zou, Z., Li, G., Pan, P., and Liang, G. (2020). Long Noncoding RNA NEAT1 Suppresses Proliferation and Promotes Apoptosis of Glioma Cells via Downregulating MiR-92b. *Cancer Control* 27 (1), 1073274819897977. doi:10.1177/1073274819897977
- Liu, J., Jiang, J., Hui, X., Wang, W., Fang, D., and Ding, L. (2018). Mir-758-5p Suppresses Glioblastoma Proliferation, Migration and Invasion by Targeting ZBTB20. *Cell Physiol Biochem* 48 (5), 2074–2083. doi:10.1159/000492545
- Liu, X., Chen, R., and Liu, L. (2019). SP1-DLEU1-miR-4429 Feedback Loop Promotes Cell Proliferative and Anti-apoptotic Abilities in Human Glioblastoma. *Biosci. Rep.* 39 (12), BSR20190994. doi:10.1042/BSR20190994
- Liu, Z., Su, D., Qi, X., and Ma, J. (2018). MiR-500a-5p P-promotes G-lioblastoma C-ell P-roliferation, M-igration and I-nvasion by T-argeting C-hromodomain H-elicase DNA B-inding P-rotein 5. *Mol. Med. Rep.* 18 (3), 2689–2696. doi:10.3892/mmr.2018.9259
- Long, N., Chu, L., Jia, J., Peng, S., Gao, Y., Yang, H., et al. (2020). CircPOSTN/miR-361-5p/TPX2 axis Regulates Cell Growth, Apoptosis and Aerobic Glycolysis in Glioma Cells. *Cancer Cell Int* 20 (1), 374. doi:10.1186/s12935-020-01454-x
- Lu, Y.-F., Cai, X.-L., Li, Z.-Z., Lv, J., Xiang, Y.-a., Chen, J.-J., et al. (2018). LncRNA SNHG16 Functions as an Oncogene by Sponging MiR-4518 and Up-Regulating PRMT5 Expression in Glioma. *Cell Physiol Biochem* 45 (5), 1975–1985. doi:10.1159/000487974
- Luo, W., Li, X., Song, Z., Zhu, X., and Zhao, S. (2019). Long Non-coding RNA AGAP2-AS1 Exerts Oncogenic Properties in Glioblastoma by Epigenetically Silencing TFPI2 through EZH2 and LSD1. *Aging* 11 (11), 3811–3823. doi:10.18632/aging.102018
- Lv, Q.-L., Hu, L., Chen, S.-H., Sun, B., Fu, M.-L., Qin, C.-Z., et al. (2016). A Long Noncoding RNA ZEB1-AS1 Promotes Tumorigenesis and Predicts Poor Prognosis in Glioma. *Int. J. Mol. Sci.* 17 (9), 1431. doi:10.3390/ijms17091431
- Maass, P. G., Luft, F. C., and Bähring, S. (2014). Long Non-coding RNA in Health and Disease. *J. Mol. Med.* 92 (4), 337–346. doi:10.1007/s00109-014-1131-8
- Mahjoubin-Tehran, M., Rezaei, S., Jesmani, A., Birang, N., Morshedi, K., Khanbabaee, H., et al. (2021). New Epigenetic Players in Stroke Pathogenesis: From Non-coding RNAs to Exosomal Non-coding RNAs. *Biomed. Pharmacother.* 140, 111753. doi:10.1016/j.biopha.2021.111753
- Majtnerová, P., and Roušar, T. (2018). An Overview of Apoptosis Assays Detecting DNA Fragmentation. *Mol. Biol. Rep.* 45 (5), 1469–1478.
- Mellai, M., and Schiffer, D. (2007). Apoptosis in Brain Tumors: Prognostic and Therapeutic Considerations. *Anticancer Res.* 27 (1A), 437–448.
- Meng, Q., Yang, B.-Y., Liu, B., Yang, J.-X., and Sun, Y. (2018). Long Non-coding RNA SNHG6 Promotes Glioma Tumorigenesis by Sponging miR-101-3p. *Int. J. Biol. Markers* 33 (2), 148–155. doi:10.1177/1724600817747524
- Meng, X., Li, X., Zhang, P., Wang, J., Zhou, Y., and Chen, M. (2017). Circular RNA: an Emerging Key Player in RNA World. *Brief Bioinform* 18 (4), 547–557. doi:10.1093/bib/bbw045
- Mirzaei, H., and Hamblin, M. R. (2020). Regulation of Glycolysis by Non-coding RNAs in Cancer: Switching on the Warburg Effect. *Mol. Ther. - Oncolytics* 19, 218–239. doi:10.1016/j.omto.2020.10.003
- Mohamed Yusoff, A. (2015). Role of Mitochondrial DNA Mutations in Brain Tumors: A Mini-Review. *J. Can. Res. Ther.* 11 (3), 535. doi:10.4103/0973-1482.161925
- Nam, J. W., Choi, S. W., and You, B. H. (2016). Incredible RNA: Dual Functions of Coding and Noncoding. *Mol. Cell* 39 (5), 367–374. doi:10.14348/molcells.2016.0039
- Nicoloso, M. S., and Calin, G. A. (2008). MicroRNA Involvement in Brain Tumors: from Bench to Bedside. *Brain Pathol.* 18 (1), 122–129. doi:10.1111/j.1750-3639.2007.00119.x
- Nikolaou, M., Pavlopoulou, A., Georgakilas, A. G., and Kyrodimos, E. (2018). The challenge of Drug Resistance in Cancer Treatment: a Current Overview. *Clin. Exp. Metastasis* 35 (4), 309–318. doi:10.1007/s10585-018-9903-0
- O'Brien, J., Hayder, H., Zayed, Y., and Peng, C. (2018). Overview of microRNA Biogenesis, Mechanisms of Actions, and Circulation. *Front. Endocrinol.* 9, 402. doi:10.3389/fendo.2018.00402
- Pal, R., and Greene, S. (2015). microRNA-10b Is Overexpressed and Critical for Cell Survival and Proliferation in Medulloblastoma. *Plos one* 10 (9), e0137845. doi:10.1371/journal.pone.0137845
- Peng, H., Tan, X., Wang, Y., Dai, L., Liang, G., Guo, J., et al. (2020). Clinical Significance of Ki67 and Circulating Tumor Cells with an Epithelial-Mesenchymal Transition Phenotype in Non-small Cell Lung Cancer. *Am. J. Transl. Res.* 12 (6), 2916–2928.
- Pistritto, G., Trisciuglio, D., Ceci, C., Garufi, A., and D'Orazi, G. (2016). Apoptosis as Anticancer Mechanism: Function and Dysfunction of its Modulators and Targeted Therapeutic Strategies. *Aging* 8 (4), 603–619. doi:10.18632/aging.100934
- Pop, S., Enciu, A. M., Necula, L. G., and Tanase, C. (2018). Long Non-coding RNA S in Brain Tumours: Focus on Recent Epigenetic Findings in Glioma. *J. Cel Mol Med* 22 (10), 4597–4610. doi:10.1111/jcmm.13781
- Quinn, J. J., and Chang, H. Y. (2016). Unique Features of Long Non-coding RNA Biogenesis and Function. *Nat. Rev. Genet.* 17 (1), 47–62. doi:10.1038/nrg.2015.10
- Ruan, X., Zheng, J., Liu, X., Liu, Y., Liu, L., Ma, J., et al. (2020). lncRNA LINC00665 Stabilized by TAF15 Impeded the Malignant Biological Behaviors of Glioma Cells via STAU1-Mediated mRNA Degradation. *Mol. Ther. - Nucleic Acids* 20, 823–840. doi:10.1016/j.omtn.2020.05.003
- Shabaninejad, Z., Yousefi, F., Movahedpour, A., Ghasemi, Y., Dokanehiifard, S., Rezaei, S., et al. (2019). Electrochemical-based Biosensors for microRNA Detection: Nanotechnology Comes into View. *Anal. Biochem.* 581, 113349. doi:10.1016/j.ab.2019.113349
- Shao, L., He, Q., Liu, Y., Liu, X., Zheng, J., Ma, J., et al. (2019). UPF1 Regulates the Malignant Biological Behaviors of Glioblastoma Cells via Enhancing the Stability of Linc-00313. *Cell Death Dis* 10 (9), 629. doi:10.1038/s41419-019-1845-1
- Shen, H., Liu, B., Xu, J., Zhang, B., Wang, Y., Shi, L., et al. (2021). Circular RNAs: Characteristics, Biogenesis, Mechanisms and Functions in Liver Cancer. *J. Hematol. Oncol.* 14 (1), 1–16. doi:10.1186/s13045-021-01145-8
- So, J. S., Kim, H., and Han, K. S. (2021). Mechanisms of Invasion in Glioblastoma: Extracellular Matrix, Ca²⁺ Signaling, and Glutamate. *Front. Cel Neurosci* 15, 663092. doi:10.3389/fncel.2021.663092
- Song, H., Han, L. M., Gao, Q., and Sun, Y. (2016). Long Non-coding RNA CRNDE Promotes Tumor Growth in Medulloblastoma. *Eur. Rev. Med. Pharmacol. Sci.* 20 (12), 2588–2597.
- Stattello, L., Guo, C.-J., Chen, L.-L., and Huarte, M. (2021). Gene Regulation by Long Non-coding RNAs and its Biological Functions. *Nat. Rev. Mol. Cel Biol* 22 (2), 96–118. doi:10.1038/s41580-020-00315-9
- Su, R., Cao, S., Ma, J., Liu, Y., Liu, X., Zheng, J., et al. (2017). Knockdown of SOX2OT Inhibits the Malignant Biological Behaviors of Glioblastoma Stem Cells via Up-Regulating the Expression of miR-194-5p and miR-122. *Mol. Cancer* 16 (1), 171. doi:10.1186/s12943-017-0737-1
- Su, R., Ma, J., Zheng, J., Liu, X., Liu, Y., Ruan, X., et al. (2020). PABPC1-induced Stabilization of BDNF-AS Inhibits Malignant Progression of Glioblastoma Cells through STAU1-Mediated Decay. *Cel Death Dis* 11 (2), 81–17. doi:10.1038/s41419-020-2267-9
- Sun, J., Tian, X., Zhang, J., Huang, Y., Lin, X., Chen, L., et al. (2017). Regulation of Human Glioma Cell Apoptosis and Invasion by miR-152-3p through Targeting DNMT1 and Regulating NF2 : MiR-152-3p Regulate Glioma Cell Apoptosis and Invasion. *J. Exp. Clin. Cancer Res.* 36 (1), 100–113. doi:10.1186/s13046-017-0567-4
- Suzuki, H., and Tsukahara, T. (2014). A View of Pre-mRNA Splicing from RNase R Resistant RNAs. *Int. J. Mol. Sci.* 15 (6), 9331–9342. doi:10.3390/ijms15069331
- Varon, M., Levy, T., Mazor, G., Ben David, H., Marciano, R., Krelin, Y., et al. (2019). The Long Noncoding RNA TP73-AS1 Promotes Tumorigenicity of Medulloblastoma Cells. *Int. J. Cancer* 145 (12), 3402–3413. doi:10.1002/ijc.32400

- Wang, H., Li, Y., Hou, J., Jiang, C., Li, D., Lu, J., et al. (2018). Biological Activity and Stability of New Peptide Derivative KW-WK from Bovine Lactoferricin. *Shin Kexue/Food Sci.* 39 (20), 57–62.
- Wang, H. (2020). MicroRNAs and Apoptosis in Colorectal Cancer. *Int. J. Mol. Sci.* 21 (15), 5353. doi:10.3390/ijms21155353
- Wang, J., Qin, C., Zhong, C., Wen, Y., Ke, S., and Liao, B. (2020). Long Non-coding RNA CASC2 Targeting miR-18a Suppresses Glioblastoma Cell Growth, Metastasis and EMT *In Vitro* and *In Vivo*. *J. Biosciences* 45 (1), 1–14. doi:10.1007/s12038-020-00077-8
- Wang, J., Liu, X., Yan, C., Liu, J., Wang, S., Hong, Y., et al. (2017). LEF1-AS1, a Long Non-coding RNA, Promotes Malignancy in Glioblastoma. *Onco Targets Ther.* 10, 4251–4260. doi:10.2147/ott.s130365
- Wang, J., Yang, S., Ji, Q., Li, Q., Zhou, F., Li, Y., et al. (2020). Long Non-coding RNA EPIC1 Promotes Cell Proliferation and Motility and Drug Resistance in Glioma. *Mol. Ther. - Oncolytics* 17, 130–137. doi:10.1016/j.omto.2020.03.011
- Wang, R., Zhang, S., Chen, X., Li, N., Li, J., Jia, R., et al. (2018). CircNTSE Acts as a Sponge of miR-422a to Promote Glioblastoma Tumorigenesis. *Cancer Res.* 78 (17), 4812–4825. doi:10.1158/0008-5472.can-18-0532
- Wang, X., Xu, D., Pei, X., Zhang, Y., Zhang, Y., Gu, Y., et al. (2020). CircSKA3 Modulates FOXM1 to Facilitate Cell Proliferation, Migration, and Invasion while Confine Apoptosis in Medulloblastoma via miR-383-5p. *Cancer Manag. Res.* 12, 13415–13426. doi:10.2147/cmar.s272753
- Weller, M., Wick, W., Aldape, K., Brada, M., Berger, M., Pfister, S. M., et al. (2015). Glioma. *Nat. Rev. Dis. Primers* 1 (1), 15017–15018. doi:10.1038/nrdp.2015.17
- Werner, T. V., Hart, M., Nickels, R., Kim, Y.-J., Menger, M. D., Bohle, R. M., et al. (2017). MiR-34a-3p Alters Proliferation and Apoptosis of Meningioma Cells *In Vitro* and Is Directly Targeting SMAD4, FRAT1 and BCL2. *Aging* 9 (3), 932–954. doi:10.18632/aging.101201
- Wu, J., Wang, N., Yang, Y., Jiang, G., Mu, Q., Zhan, H., et al. (2021). LINC01152 Upregulates MAML2 Expression to Modulate the Progression of Glioblastoma Multiforme via Notch Signaling Pathway. *Cel Death Dis.* 12 (1), 1–14. doi:10.1038/s41419-021-04106-8
- Wu, N., Lin, X., Zhao, X., Zheng, L., Xiao, L., Liu, J., et al. (2013). MiR-125b Acts as an Oncogene in Glioblastoma Cells and Inhibits Cell Apoptosis through P53 and p38MAPK-independent Pathways. *Br. J. Cancer* 109 (11), 2853–2863. doi:10.1038/bjc.2013.672
- Wu, Z., and Lin, Y. (2019). Long Noncoding RNA LINC00515 Promotes Cell Proliferation and Inhibits Apoptosis by Sponging miR-16 and Activating PRMT5 Expression in Human Glioma. *Onco Targets Ther.* 12, 2595–2604. doi:10.2147/ott.s198087
- Xin, J., Zhang, X. Y., Sun, D. K., Tian, L. Q., and Xu, P. (2019). Up-regulated Circular RNA Hsa_circ_0067934 Contributes to Glioblastoma Progression through Activating PI3K-AKT Pathway. *Eur. Rev. Med. Pharmacol. Sci.* 23 (8), 3447–3454. doi:10.26355/eurrev_201904_17709
- Xiong, Z., Zhou, C., Wang, L., Zhu, R., Zhong, L., Wan, D., et al. (2019). Circular RNA SMO Sponges miR-338-3p to Promote the Growth of Glioma by Enhancing the Expression of SMO. *Aging* 11 (24), 12345–12360. doi:10.18632/aging.102576
- Xu, C. H., Xiao, L. M., Liu, Y., Chen, L. K., Zheng, S. Y., Zeng, E. M., et al. (2019). The lncRNA HOXA11-AS Promotes Glioma Cell Growth and Metastasis by Targeting miR-130a-5p/HMGB2. *Eur. Rev. Med. Pharmacol. Sci.* 23 (1), 241–252. doi:10.26355/eurrev_201901_16770
- Xu, H., Zhang, Y., Qi, L., Ding, L., Jiang, H., and Yu, H. (2018). NFIX Circular RNA Promotes Glioma Progression by Regulating miR-34a-5p via Notch Signaling Pathway. *Front. Mol. Neurosci.* 11, 225. doi:10.3389/fnmol.2018.00225
- Xu, L. M., Chen, L., Li, F., Zhang, R., Li, Z. Y., Chen, F. F., et al. (2016). Over-expression of the Long Non-coding RNA HOTTIP Inhibits Glioma Cell Growth by BRE. *J. Exp. Clin. Cancer Res.* 35 (1), 162. doi:10.1186/s13046-016-0431-y
- Xu, N., Liu, B., Lian, C., Doycheva, D. M., Fu, Z., Liu, Y., et al. (2018). Long Noncoding RNA AC003092.1 Promotes Temozolomide Chemosensitivity through miR-195/TFPI-2 Signaling Modulation in Glioblastoma. *Cel Death Dis* 9 (12), 1139. doi:10.1038/s41419-018-1183-8
- Xu, Q.-F., Pan, Y.-W., Li, L.-C., Zhou, Z., Huang, Q.-L., Pang, J. C.-s., et al. (2014). MiR-22 Is Frequently Downregulated in Medulloblastomas and Inhibits Cell Proliferation via the Novel Target PAPST1. *Brain Pathol.* 24 (6), 568–583. doi:10.1111/bpa.12136
- Xu, S., Tang, L., Li, X., Fan, F., and Liu, Z. (2020). Immunotherapy for Glioma: Current Management and Future Application. *Cancer Lett.* 476, 1–12. doi:10.1016/j.canlet.2020.02.002
- Xu, W., Hu, G.-Q., Da Costa, C., Tang, J.-H., Li, Q.-R., Du, L., et al. (2019). Long Noncoding RNA UBE2R2-AS1 Promotes Glioma Cell Apoptosis via Targeting the miR-877-3p/TLR4 axis. *Onco Targets Ther.* 12, 3467–3480. doi:10.2147/ott.s201732
- Xu, X., Lai, Y., and Hua, Z. C. (2019). Apoptosis and Apoptotic Body: Disease Message and Therapeutic Target Potentials. *Biosci. Rep.* 39 (1), BSR20180992. doi:10.1042/BSR20180992
- Yang, A., Wang, H., and Yang, X. (2017). Long Non-coding RNA PVT1 Indicates a Poor Prognosis of Glioma and Promotes Cell Proliferation and Invasion via Target EZH2. *Biosci. Rep.* 37 (6), BSR20170871. doi:10.1042/BSR20170871
- Yang, J. X., Rastetter, R. H., and Wilhelm, D. (2016). Non-coding RNAs: An Introduction. *Adv. Exp. Med. Biol.* 886, 13–32. doi:10.1007/978-94-017-7417-8_2
- Yang, T. Q., Lu, X. J., Wu, T. F., Ding, D. D., Zhao, Z. H., Chen, G. L., et al. (2014). Micro RNA -16 Inhibits Glioma Cell Growth and Invasion through Suppression of BCL 2 and the Nuclear factor- κ B1/MMP 9 Signaling Pathway. *Cancer Sci.* 105 (3), 265–271. doi:10.1111/cas.12351
- Yin, F., Zhang, J. N., Wang, S. W., Zhou, C. H., Zhao, M. M., Fan, W. H., et al. (2015). MiR-125a-3p Regulates Glioma Apoptosis and Invasion by Regulating Nrg1. *PLoS one* 10 (1), e0116759. doi:10.1371/journal.pone.0116759
- Yuan, D. H., Zhao, J., and Shao, G. F. (2019). Circular RNA TTBK2 Promotes the Development of Human Glioma Cells via miR-520b/EZH2 axis. *Eur. Rev. Med. Pharmacol. Sci.* 23 (24), 10886–10898. doi:10.26355/eurrev_201912_19792
- Zhang, C., Ma, L., Niu, Y., Wang, Z., Xu, X., Li, Y., et al. (2020). Circular RNA in Lung Cancer Research: Biogenesis, Functions, and Roles. *Int. J. Biol. Sci.* 16 (5), 803–814. doi:10.7150/ijbs.39212
- Zhang, J., Chen, G., Gao, Y., and Liang, H. (2020). HOTAIR/miR-125 axis-mediated Hexokinase 2 Expression Promotes Chemoresistance in Human Glioblastoma. *J. Cel Mol Med* 24 (10), 5707–5717. doi:10.1111/jcmm.15233
- Zhang, J., Li, N., Fu, J., and Zhou, W. (2020). Long Noncoding RNA HOTAIR Promotes Medulloblastoma Growth, Migration and Invasion by Sponging miR-1/miR-206 and Targeting YY1. *Biomed. Pharmacother.* 124, 109887. doi:10.1016/j.biopha.2020.109887
- Zhang, P., Wu, W., Chen, Q., and Chen, M. (2019). Non-coding RNAs and Their Integrated Networks. *J. Integr. Bioinform* 16 (3). doi:10.1515/jib-2019-0027
- Zhang, S., Lai, N., Liao, K., Sun, J., and Lin, Y. (2015). MicroRNA-210 Regulates Cell Proliferation and Apoptosis by Targeting Regulator of Differentiation 1 in Glioblastoma Cells. *fnr* 3 (3), 236–244. doi:10.5114/fn.2015.54424
- Zhang, X., Niu, W., Mu, M., Hu, S., and Niu, C. (2020). Long Non-coding RNA LPP-AS2 Promotes Glioma Tumorigenesis via miR-7-5p/EGFR/PI3K/AKT/c-MYC Feedback Loop. *J. Exp. Clin. Cancer Res.* 39 (1), 196. doi:10.1186/s13046-020-01695-8
- Zhang, X., Yang, H., Zhao, L., Li, G., and Duan, Y. (2019). Circular RNA PRKCI Promotes Glioma Cell Progression by Inhibiting microRNA-545. *Cel Death Dis* 10 (8), 616. doi:10.1038/s41419-019-1863-z
- Zhang, Z.-Y., Zhu, B., Zhao, X.-W., Zhan, Y.-B., Bao, J.-J., Zhou, J.-Q., et al. (2017). Regulation of UHRF1 by microRNA-378 Modulates Medulloblastoma Cell Proliferation and Apoptosis. *Oncol. Rep.* 38 (5), 3078–3084. doi:10.3892/or.2017.5939
- Zhao, L., Chen, T., Tang, X., Li, S., Liang, R., and Wang, Y. (2020). Medulloblastoma Malignant Biological Behaviors Are Associated with HOTAIR/miR-483-3p/CDK4 axis. *Ann. Transl. Med.* 8 (14), 886. doi:10.21037/atm-20-5006
- Zhao, X., Wang, P., Liu, J., Zheng, J., Liu, Y., Chen, J., et al. (2015). Gas5 Exerts Tumor-Suppressive Functions in Human Glioma Cells by Targeting miR-222. *Mol. Ther.* 23 (12), 1899–1911. doi:10.1038/mt.2015.170
- Zheng, J., Liu, X., Xue, Y., Gong, W., Ma, J., Xi, Z., et al. (2017). TTBK2 Circular RNA Promotes Glioma Malignancy by Regulating miR-217/HNF1 β /Derlin-1 Pathway. *J. Hematol. Oncol.* 10 (1), 52–19. doi:10.1186/s13045-017-0422-2
- Zheng, K., Xie, H., Wu, W., Wen, X., Zeng, Z., and Shi, Y. (2021). CircRNA PIP5K1A Promotes the Progression of Glioma through Upregulation of the TCF12/PI3K/AKT Pathway by Sponging miR-515-5p. *Cancer Cel Int* 21 (1), 27–13. doi:10.1186/s12935-020-01699-6
- Zhi, F., Wang, Q., Deng, D., Shao, N., Wang, R., Xue, L., et al. (2014). MiR-181b-5p Downregulates NOVA1 to Suppress Proliferation, Migration and Invasion and

- Promote Apoptosis in Astrocytoma. *PLoS One* 9 (10), e109124. doi:10.1371/journal.pone.0109124
- Zhi, F., Zhou, G., Shao, N., Xia, X., Shi, Y., Wang, Q., et al. (2013). miR-106a-5p Inhibits the Proliferation and Migration of Astrocytoma Cells and Promotes Apoptosis by Targeting FASTK. *PLoS One* 8 (8), e72390. doi:10.1371/journal.pone.0072390
- Zhou, W.-Y., Cai, Z.-R., Liu, J., Wang, D.-S., Ju, H.-Q., and Xu, R.-H. (2020). Circular RNA: Metabolism, Functions and Interactions with Proteins. *Mol. Cancer* 19 (1), 1–19. doi:10.1186/s12943-020-01286-3
- Zhu, C., Mao, X., and Zhao, H. (2020). The Circ_VCAN with Radioresistance Contributes to the Carcinogenesis of Glioma by Regulating microRNA-1183. *Medicine (Baltimore)* 99 (8), e19171. doi:10.1097/MD.00000000000019171
- Zong, Z., Song, Y., Xue, Y., Ruan, X., Liu, X., Yang, C., et al. (2019). Knockdown of LncRNA SCAMP1 Suppressed Malignant Biological Behaviours of Glioma Cells via Modulating miR-499a-5p/LMX1A/NLR5 Pathway. *J. Cel Mol Med* 23 (8), 5048–5062. doi:10.1111/jcmm.14362

Conflict of Interest: The authors declare that the research was conducted in the absence of any commercial or financial relationships that could be construed as a potential conflict of interest.

Publisher's Note: All claims expressed in this article are solely those of the authors and do not necessarily represent those of their affiliated organizations, or those of the publisher, the editors and the reviewers. Any product that may be evaluated in this article, or claim that may be made by its manufacturer, is not guaranteed or endorsed by the publisher.

Copyright © 2022 Tamtaji, Derakhshan, Rashidi Noshabad, Razaviyan, Hadavi, Jafarpour, Jafari, Rajabi, Hamblin, Mahabady, Taghizadieh and Mirzaei. This is an open-access article distributed under the terms of the Creative Commons Attribution License (CC BY). The use, distribution or reproduction in other forums is permitted, provided the original author(s) and the copyright owner(s) are credited and that the original publication in this journal is cited, in accordance with accepted academic practice. No use, distribution or reproduction is permitted which does not comply with these terms.



Emerging Role and Mechanism of circRNAs in Pediatric Malignant Solid Tumors

Qiyang Shen^{1†}, Xingyu Liu^{2†}, Wei Li^{3†}, Xu Zhao², Tao Li¹, Kai Zhou^{2*} and Jianfeng Zhou^{1*}

¹Department of Pediatric Surgery, Children's Hospital of Nanjing Medical University, Nanjing, China, ²Department of Pediatric Surgery, First Affiliated Hospital of Bengbu Medical College, Bengbu, China, ³Department of ENT, Children's Hospital of Nanjing Medical University, Nanjing, China

Circular RNAs (circRNAs) are non-coding RNAs with covalent closed-loop structures and are widely distributed in eukaryotes, conserved and stable as well as tissue-specific. Malignant solid tumors pose a serious health risk to children and are one of the leading causes of pediatric mortality. Studies have shown that circRNAs play an important regulatory role in the development of childhood malignant solid tumors, hence are potential biomarkers and therapeutic targets for tumors. This paper reviews the biological characteristics and functions of circRNAs as well as the research progress related to childhood malignant solid tumors.

Keywords: pediatric malignant solid tumors, circRNA, epigenetics, biomarkers, biological functions

OPEN ACCESS

Edited by:

Tao Zeng,
Guangzhou Laboratory, China

Reviewed by:

Ying Liu,
Qingdao University, China
Xiujuan Lei,
Shaanxi Normal University, China

*Correspondence:

Jianfeng Zhou
doctorzhoujianfeng@163.com
Kai Zhou
zhoukai0552@163.com

[†]These authors have contributed
equally to this work and share first
authorship

Specialty section:

This article was submitted to
Epigenomics and Epigenetics,
a section of the journal
Frontiers in Genetics

Received: 23 November 2021

Accepted: 21 December 2021

Published: 18 January 2022

Citation:

Shen Q, Liu X, Li W, Zhao X, Li T,
Zhou K and Zhou J (2022) Emerging
Role and Mechanism of circRNAs in
Pediatric Malignant Solid Tumors.
Front. Genet. 12:820936.
doi: 10.3389/fgene.2021.820936

INTRODUCTION

Although rare, childhood malignancies are now the second leading cause of pediatric death (Ollauri-Ibanez and Astigarraga, 2021; Quamine et al., 2021). Furthermore, the incidence of childhood malignancies is increasing worldwide, with less than 40% of children receiving an appropriate diagnosis and treatment (Oyefiade et al., 2021; Sze, 2021). The symptoms of childhood malignancies are often similar to those of other common, benign diseases, so early and accurate diagnosis is difficult, with an untimely diagnosis an important cause of delayed treatment and mortality (Van Paemel et al., 2020; Jain et al., 2021; Lucas et al., 2021). Although significant progress has been made in the treatment of childhood malignancies in recent years, tumor treatment based on surgery and radiotherapy can only kill tumor cells, not effectively control the recurrence and metastasis of some childhood tumors (Weiser et al., 2019; Casey and Cheung, 2020; Cimini et al., 2020; Fair et al., 2020; Greenbaum et al., 2020). Therefore, exploring early diagnostic markers of pediatric tumors to find possible therapeutic targets is important to improve the early diagnosis, treatment, and prognosis of pediatric malignant solid tumors.

Circular RNAs (circRNAs) are a class of non-coding RNAs (ncRNAs) formed by the 3' and 5' ends of mRNAs, which are mainly generated from introns or exons by reverse splicing or lassoing introns (Ebbesen et al., 2017; Huang and Zhu, 2021). Previously, circRNAs were considered as error products in post-transcriptional processing with no important regulatory role in biological processes. However, with the development of sequencing technology, researchers have found that circRNAs are widely distributed in eukaryotic cells and can be stably expressed, playing an important role in the regulation of gene expression in human cells (Qu et al., 2017; Han et al., 2021). An increasing number of studies have shown that circRNAs have important physiopathological functions and are involved in the regulation of cell proliferation, differentiation, and apoptosis, as well as in the development of various diseases including tumors (Altesha et al., 2019; Li Y. et al., 2020; Wu et al., 2020; Xu et al., 2020;

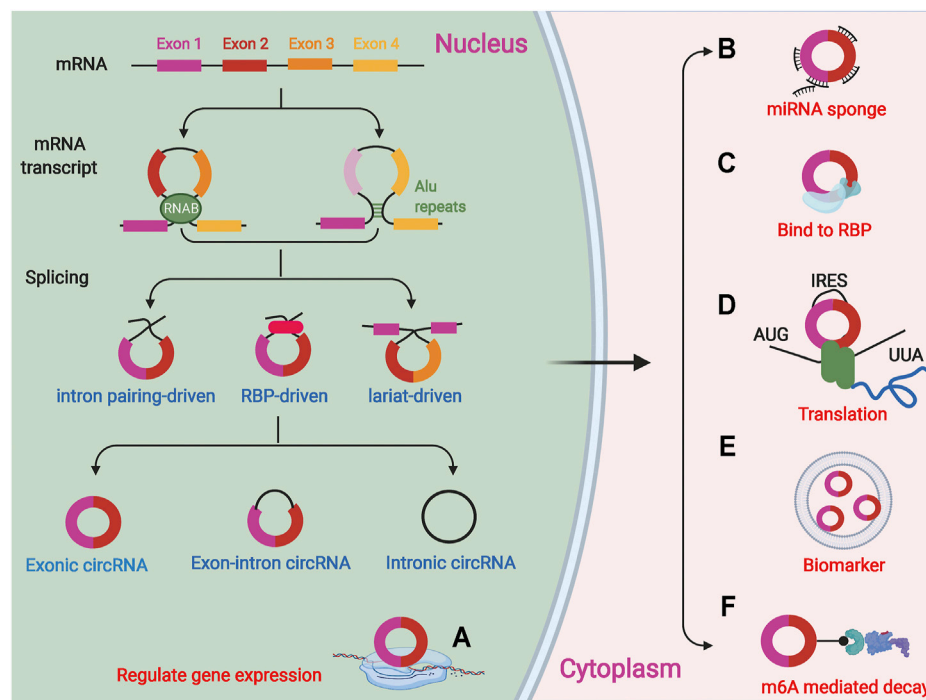


FIGURE 1 | CircRNAs are a covalently closed loops formed by splicing of precursor mRNA (pre-mRNAs). There are three forms of circRNAs: lasso-driven cyclization, intron pairing cyclization and RNA binding proteins (RBPs) mediated cyclization. CircRNAs are classified into three main types, exonic circRNAs, intronic circRNAs, and exon-intron circRNAs. (A) CircRNAs can regulate the expression of related genes in cells; (B) CircRNAs as miRNA sponge can adsorb related miRNAs; (C) The functions of circRNA in interacting with proteins; (D) Several circRNAs have also been reported to encode proteins; (E) CircRNAs in exosomes or microvesicles can be used as specific biomarkers; (F) CircRNAs can be degraded via m6A-mediated decay.

Choudhary et al., 2021; Tian et al., 2021; Zhang et al., 2021). For example, circPRKAR1B regulates FZD4 expression by binding miR-361-3p, promoting the proliferation and migration of osteosarcoma cells as well as tumor susceptibility to chemotherapy resistance (Feng Z.-h. et al., 2021). Circ_0004296 downregulates ETS1 expression by promoting retention of EIF4A3 in the nucleus and inhibiting the nuclear export of ETS1 mRNA, which in turn keeps PCa from malignant growth and metastasis (Mao S. et al., 2021). CircGSK3B directly binds to EZH2 and inhibits the binding of EZH2 and H3K27me3 to the RORA promoter, leading to elevated RORA expression and inhibiting tumor progression by suppressing the growth, invasion, and metastasis of gastric cancer cells (Ma X. et al., 2021).

Recently, circRNAs have been found to have important biological roles in childhood malignant solid tumors, hence the potential to become tumor markers and therapeutic targets. This paper reviews the formation and biological functions of circRNAs, as well as the research on circRNAs in childhood malignant solid tumors to provide new perspectives for the clinical diagnosis and treatment of childhood malignant solid tumors.

OVERVIEW AND BIOLOGICAL PROPERTIES OF CIRCULAR RNA

CircRNAs are formed by splicing of precursor mRNAs (pre-mRNAs) and are mostly endogenous. They have no 3' tail or 5'

cap end and are covalently closed loops (Qu et al., 2015; Meng et al., 2017) formed by lasso-driven cyclization, direct reverse splicing, or exon skipping, or they can be cyclized by intron pairing (Wang et al., 2021e; Xiao et al., 2021). In addition, circRNAs can also be formed by RNA binding proteins (RBPs)-mediated cyclization joining the downstream 5' end donor site to the upstream 3' end acceptor site to form a single-stranded covalent closed-loop that joins the remaining sequence after removal of the intron (Ali et al., 2021; Wang et al., 2021d). Thus, the formation of circRNAs requires the mini-intron at the splice site and the short-chain reverse repeat. Depending on the formation mechanism, circRNAs are classified into three main types, exonic circRNAs (EcircRNAs), intronic circRNAs (ciRNAs), and exon-intron circRNAs (EiRNAs) (Lyu and Huang, 2017; Meng et al., 2017), of which, EcircRNAs are the most abundant and located in the cytoplasm of eukaryotes (Figure 1).

CircRNAs are diverse with more than 25,000 circRNAs detected in human fibroblasts by high-throughput sequencing, and in some cases, circRNA expression even exceeds that of their corresponding linear mRNAs by more than 10-fold (Shen et al., 2021; van Zonneveld et al., 2021). In contrast to mRNAs, circRNAs exist in a covalent closed-loop structure with no cap and tail structure. This unique structure makes circRNAs highly stable and resistant to hydrolysis by RNA exonucleases (Li H. M. et al., 2019), as well as consistently and stably expressed in cells (Wu et al., 2020; Shen et al., 2021). CircRNAs sequences are

evolutionarily conserved not only in mammals but also in the more evolutionarily distant *Drosophila* (Zhao B. et al., 2021; Mao X. et al., 2021). In addition, the expression of the same circRNA can vary greatly over time or in different tissues, as well as in diseased and non-diseased tissues (He A. T. et al., 2021; Verduci et al., 2021). Therefore, circRNAs have the potential to become good diagnostic markers for diseases and therapeutic targets.

Biological Functions of circRNA

CircRNAs are involved in a variety of biological processes by acting as competing endogenous RNAs (ceRNAs), binding RBPs, regulating parental gene expression, and translating proteins or polypeptides.

ACTS AS A COMPETITIVE ENDOGENOUS RNA

CircRNA contains a miRNA response element (MER), which can act as ceRNA to affect gene expression by competitively binding miRNA sites and inhibiting the regulatory effect of miRNA on downstream genes (Cheng et al., 2019; Hong et al., 2020; Luo et al., 2020; Su and Lv, 2020; Wang et al., 2021c). For example, Circ-CD44 is highly expressed in triple-negative breast cancer (TNBC), and high expression of circ-CD44 predicts poor patient prognosis. Circ-CD44 promotes KRAS expression through adsorption of miR-502-5p, thereby promoting TNBC proliferation, migration, and invasion. Circ-SNX6 acts as a molecular “sponge” to attenuate the inhibitory effect of miR-1184 on its target gene GPCPD1, thereby increasing intracellular lysophosphatidic acid levels, ultimately promoting resistance to sunitinib in renal cell carcinoma cells (Huang et al., 2021).

Binding RNA Binding Protein (RBP)

CircRNAs can bind directly to RBPs to form RNA-protein complexes to regulate RBPs and further affect the expression and biology of downstream proteins (Huang et al., 2020; Feng J. et al., 2021; Chen J. et al., 2021; Xu et al., 2021). Muscleblind-like (MBL) binds to exon 2 of its parental gene and induces cyclization to form circMbl, which also binds to MBL to reduce MBL abundance, thereby reducing circMbl production (Ashwal-Fluss et al., 2014). Circ-hHBB3 binds HuR and degrades HuR, whereas Circ-TNPO3 competitively binds IGF2BP3 and inhibits the proliferation and metastasis of gastric cancer by regulating the MYC-SNAIL axis, which leads to malignant progression of GC (Yu et al., 2021). Circ-ACTN4 binds YBX1 and stimulates FZD7 transcription, which in turn promotes intrahepatic cholangiocarcinoma (ICC) proliferation and metastasis, leading to malignant tumor growth and metastasis (Chen et al., 2021c).

Regulation of Parental Gene Expression

Some circRNAs also regulate the transcription of parental genes. Although most circRNAs are located in the cytoplasm, some circRNAs such as ElciRNA are in the nucleus of eukaryotic cells and play an important role at the transcriptional level (Humphreys et al., 2019; Ma N. et al., 2021; Greene et al., 2021). ElciRNA in the nucleus can interact with the U1 small

nuclear ribonucleoprotein particle (snRNP) to contribute to the transcription of its parental genes (Song et al., 2016; Nan et al., 2019) and with the RNA-RNA of U1snRNA to enhance the cis expression of parental genes (Humphreys et al., 2019; Chu et al., 2021). In addition, a fraction of ElciRNAs accumulates in regions outside the nuclear transcription site, suggesting that this fraction may regulate transcription by acting in a trans manner (Ma J. et al., 2021). Introns derived from the Tulp4 gene can be cyclized to form circTulp4, which can interact with U1 snRNP and RNA polymerase II to regulate the transcription of its parental gene, Tulp4, thus participate in the development of Alzheimer's disease (AD) (Ma N. et al., 2021). In summary, circRNAs can regulate parental gene expression through transcriptional regulation, splicing regulation, ceRNA, mRNA trap, translational regulation, and post-translational regulation pathways to regulate parental gene expression (Shao T. et al., 2021).

Translation of Proteins or Peptides

Most circRNAs generated by reverse splicing are found mainly in the cytoplasm, and translation of linear mRNAs usually requires the structure of a 5' end cap and a 3' end poly(A) tail to remain stable. CircRNAs are not normally considered to have a translational function (Marquez-Molins et al., 2021; Yan and Bu, 2021) but they can initiate translation in the cell if they have an internal ribosome entry site (IRES) (He L. et al., 2021; Wang et al., 2021b; Sinha et al., 2021). This approach provides more polypeptide sequences and increases the polypeptide yield because the ribosome does not need to bind to RNA template repeats (Li P. et al., 2021). The cyclic RNA hsa-circ-0000437 can encode a functional peptide called CORO1C-47aa, and overexpression of CORO1C-47aa inhibits endothelial cell proliferation, migration, and differentiation by competing with the transcription factor TACC3 to bind ARNT and inhibit VEGF, which in turn leads to malignant progression of endometrial cancer (Li F. et al., 2021). Circ-RNA circ-FBXW7 encodes the FBXW7-185aa protein that inhibits the proliferation and migratory capacity of TNBC cells by increasing the abundance of FBXW7 and inducing c-Myc degradation (Ye et al., 2019). Circ-FNDC3B encodes a novel protein circFNDC3B-218aa and circFNDC3B-218aa significantly inhibits the proliferation, invasion, and migration of CC by suppressing the expression of Snail and promoting the expression of FBP1 (Pan et al., 2020). The translation of circRNAs and their regulatory role in tumor tissues are likely to provide new ideas for the study of circRNAs.

M6A Methylation Modification Affects the Translation Ability and Nuclear Localization of circRNAs

M6A methylation modification is the most common modification method in eukaryotic RNA, and it mainly affects mRNA splicing, nucleation and translation. Recent studies show that modification of m6A can affect the nuclear localization of circRNA, and circRNA can also bind to the corresponding regulatory protein of m6A to affect its stability. Internal ribosome entry site (IRES) can promote the initiation of circRNA translation, and circRNA

TABLE 1 | Functional characterization of circular RNAs in pediatric malignant solid tumor.

Circular RNAs	Expression	Role	Function role	miRNAs	Related genes	References
Hepatoblastoma						
hsa_circ_0000594	Upregulated	Oncogene	Promote cell proliferation, invasion, and suppress cell apoptosis	miR-217	SIRT1	Song et al. (2019)
circ-STAT3	Upregulated	Oncogene	Promote cell growth, migration and stem-cell characteristics	miR-29a/b/c-3p	GLI2	Liu et al. (2020)
circ-HMGCS1	Upregulated	Oncogene	Promote cell proliferation and inhibit cell apoptosis	miR-503-5p	IGF-PI3K-Akt	Zhen et al. (2019)
Neuroblastoma						
circ-CUX1	Upregulated	Oncogene	Promote aerobic glycolysis, growth, and aggressiveness	-	EWSR1/MAZ	Li et al. (2019a)
hsa_circ_0132,817	Upregulated	Oncogene	Promote cell proliferation, migration, invasion and glycolysis	miR-432-5p	NOL4L	Fang et al. (2021)
circ-DGKB	Upregulated	Oncogene	Promote the proliferation, migration, invasion, and tumorigenesis	miR-873	GLI1	Yang et al. (2020)
circ-CUX1	Upregulated	Oncogene	Promote tumor progression and glycolysis	miR-338-3p	PHF20	Wang et al. (2021f)
circ-KIF2A	Upregulated	Oncogene	Promote cell proliferation, migration, invasion and glycolysis	miR-129-5p	PLK4	Yang et al. (2021)
Circ-CUX1	Upregulated	Oncogene	Promote cell proliferation, migration, invasion and glycolysis	miR-16-5p	DMRT2	Zhang et al. (2020)
Wilms tumors						
hsa_circ_0093740	Upregulated	Oncogene	Promote the growth, migration and metastasis	miR-136/145	DNMT3A	Cao et al. (2021)
circ-CDYL	Upregulated	Oncogene	Promote cell proliferation, migration, and invasion	miR-145-5p	TJP1	Zhou et al. (2021b)
Rhabdomyosarcoma						
circ-ZNF609	Upregulated	Oncogene	Promote cell cycle	-	p-AKT and pRb/Rb	Rossi et al. (2019)
circVAMP3	Upregulated	Oncogene	Promote cell cycle progression	-	AKT-related pathways	Rossi et al. (2021)
Lymphoma						
circ-LAMP1	Upregulated	Oncogene	Promote cell proliferation and inhibit cell apoptosis	miR-615-5p	DDR2	Deng et al. (2019)
circ-APC	Downregulated	Tumor suppressor	Inhibit cell proliferation and tumor growth	miR-888	APC and Wnt/ β -catenin	Hu et al. (2019)
circ-CDYL	Upregulated	Oncogene	Promote cell proliferation	miR-129-5p miR-3163 miR-4662a-5p miR-101-3p miR-186-5p	NOTCH1 FMR1 ABCB1 TWIST1 VEGFA	Mei et al. (2019)
circ-CFL1	Upregulated	Oncogene	Promote cell proliferation, migration and tumor growth	miR-107	HMGB1	Chen et al. (2020)
circ-OTUD7A	Upregulated	Oncogene	Promote cell proliferation, metastasis, inhibit cell cycle arrest and apoptosis	miR-431-5p	FOXP1	Liu et al. (2021b)
circ-NSUN2	Upregulated	Oncogene	Promote cell proliferation and invasion	-	HMGA1/Wnt signaling	Wang et al. (2021a)
Medulloblastoma						
circ-SKA3	Upregulated	Oncogene	Promote cell proliferation, migration, invasion and induced apoptosis and cell cycle arrest	miR-326	ID3	Zhao et al. (2021b)
circ-SKA3 and circ-DTL	Upregulated	Oncogene	Promote cell proliferation, migration, and invasion	-	SKA3 and DTL	Lv et al. (2018)
circ-SKA3	Upregulated	Oncogene	Promote cell proliferation, migration, invasion tumor growth and inhibit cell apoptosis	miR-383-5p	FOXM1	Wang et al. (2020)
Adrenocortical Carcinoma						
circ-CCAC1	Upregulated	Oncogene	Promote cell proliferation, migration, and invasion	miR-514a-5p	C22orf46	Li et al. (2020a)

with single or multiple sites of m6A modification can also initiate translation through IRES, which indicates that the presence of m6A modification may affect the process of circRNA translation (He and He, 2021). CircZNF609 contains an open reading frame, which can translate a segment of mRNA sequence into amino acids, and regulate the translation process by recognizing m6A methylation modification proteins such as YTHD (Legnini et al., 2017). CircNSUN2 can interact with the m6A reading protein YTHDC1 to promote its own export from the nucleus to the cytoplasm in an m6A-dependent manner, and promote nuclear localization. Besides, circNSUN2 can interact with IGF2BP2 and high mobility group protein A2 (HMGA2) combined to form RNA-protein ternary complex circNSUN2/IGF2BP2/HMGA2 in the cytoplasm, enhancing the stability of HMGA2 (Li B. et al., 2021).

ROLES AND SIGNIFICANCE OF CIRC RNAs IN PEDIATRIC MALIGNANT SOLID TUMORS

Many circRNAs are aberrantly expressed in pediatric malignant solid tumors and regulate tumor development. (Table 1). The stability and tissue specificity of circRNAs suggest that they are potential novel biomarkers for the diagnosis and therapeutic targets of pediatric malignant solid tumors.

Hepatoblastoma

Hepatoblastoma (HB) is an embryonal malignancy originating in the liver and is the most common malignant solid tumor of the liver in childhood (Kalish et al., 2017; Munoz et al., 2019; Hager and Sergi, 2021). The incidence of HB has been on the rise in recent years, with a yearly increase of about 4%, and its growth rate far exceeds that of other childhood malignancies, making it one of the major malignancies endangering pediatric health (Calvisi and Solinas, 2020; Prochownik, 2021). Surgery and chemotherapy are the main clinical treatments for HB, with a 3-year survival rate of 72.73% and a 5-year survival rate of 50.0% (Lake et al., 2019; Yang et al., 2019). Currently, the pathogenesis of HB is not clear and may be associated with multiple adverse factors such as genetic factors, immune response, low birth weight, and chromosomal abnormalities (Cristobal et al., 2019; Chen H. et al., 2021).

Circ-STAT3 (hsa_circ_0043800) is upregulated in HB tissues and cells, and inhibition of circ-STAT3 significantly inhibits HB cell growth, migration, and stemness. Circ-STAT3 can act as ceRNA by binding miR-29a/b/c-3p to upregulate Gli2 and STAT3, while Gli2 can activate the transcription of circ_0043800. *In vivo* experiments showed that circ_0043800 promoted HB tumor growth by upregulating Gli2 and STAT3 (Liu et al., 2020). Circ-HMGCS1 expression was significantly increased in HB tissues, and HB patients with high expression of circ-HMGCS1 had reduced overall survival. *In vitro* experiments confirmed that knockdown of circ-HMGCS1 inhibited HB cell proliferation and induced apoptosis. Mechanistic studies revealed that circ-HMGCS1 regulates IGF2 and IGF1R expression by binding to miR-503-5p and affects the downstream PI3K-Akt

signaling pathway to regulate HB cell proliferation and glutamine catabolism (Zhen et al., 2019). Hsa_circ_0000594 expression levels were significantly upregulated in HB tissues and correlated significantly with HB subtypes. Inhibition of hsa_circ_0000594 significantly suppressed the malignant phenotype of HB and bioinformatics analysis indicated that hsa_circ_0000594 may regulate SIRT1 expression by binding miR-217 (Song et al., 2019).

Neuroblastoma

Neuroblastoma (NB) originates from primitive sympathetic ganglion cells (Fetahu and Taschner-Mandl, 2021) and is a common extracranial solid tumor that occurs almost exclusively in children. It is the third most common tumor in children after leukemia and brain tumors (Zafar et al., 2021). Thirty percent of NB tumors occur in the adrenal medulla, about 60% in the abdominal paravertebral ganglia, and the rest in the sympathetic ganglia of the chest, head, neck, and pelvis (Rozen and Shohet, 2021). Currently, many new targeted therapies and immunotherapies have emerged in addition to conventional radiotherapy for NB (Blavier et al., 2020; Bhoopathi et al., 2021; Stanczyk and Westermann, 2021). NB is heterogeneous, and approximately 85–90% of children with low- and intermediate-risk NB can be cured, while the survival rate of children with high-risk NB is less than 50% (Aravindan et al., 2020; Quinn et al., 2021). Children with high-risk NB remain refractory to cure after multiple intensive treatments, and more than 50% of children relapse, with a 5-year survival rate of approximately 40–50% (Brignole et al., 2021). Therefore, it is important to investigate the molecular mechanisms underlying the development of NB.

Circ-CUX1 binds to EWSR1 and promotes interaction with MAZ, leading to transactivation of MAZ and transcriptional alterations of CUX1 and other genes associated with tumor progression. The use of inhibitory peptides that block circ-CUX1-EWSR1 interaction or LV-sh-circ-CUX1 significantly inhibited aerobic glycolysis, growth, and invasiveness of NB cells, suggesting that the circ-CUX1/EWSR1/MAZ axis is a therapeutic target for aerobic glycolysis and NB progression (Li H. et al., 2019). CircRNA hsa_circ_0132817 expression was significantly increased in NB tissues and cell lines, and knockdown of hsa_circ_0132817 inhibited tumor growth *in vivo*. Mechanistic studies suggest that hsa_circ_0132817 can promote tumorigenesis in NB cells by upregulating NOL4L and acting as a sponge for miR-432-5p (Fang et al., 2021). Circ-DGKB (hsa_circ_0133622) expression was upregulated in NB tissues compared to normal dorsal root ganglia and negatively correlated with survival in NB patients. Circ-DGKB overexpression promoted NB cell proliferation, migration, invasion, and tumorigenesis and reduced apoptosis, promoting NB progression by targeting the miR-873/GLI1 axis *in vitro* and *in vivo* (Yang et al., 2020). Circ-CUX1 and PHF20 are upregulated in NB tissues and cells, while miR-338-3p expression is significantly decreased. Mechanistic studies revealed that circ-CUX1 promotes PHF20 expression, thus NB cell progression and glycolysis by binding to miR-338-3p (Wang Y. et al., 2021). Circ-KIF2A levels were increased in NB

tissue samples and cell lines, and inhibition of circ-KIF2A significantly inhibited NB cell proliferation, migration, invasion, and glycolysis. Mechanistic analysis showed that circ-KIF2A could positively regulate PLK4 expression through the sponge miR-129-5p (Yang et al., 2021). Circ-CUX1 promotes NB cell proliferation, migration, invasion, and glycolysis. MiR-16-5p is a direct target of circ-CUX1 and miR-16-5p overexpression-mediated effects in NB cells can be partially alleviated by introducing circ-CUX1 overexpression plasmids. Another study showed that circ-CUX1 accelerates the proliferation, migration, invasion, and glycolysis of NB cells by targeting the miR-16-5p/DMRT2 signaling cascade (Zhang et al., 2020).

Wilms Tumors

Wilms tumor (WT) is the most common primary malignancy of the kidney in children, accounting for 90% of all renal malignancies (Hohenstein et al., 2015). The etiology of WT is unclear and may be related to mutations in genes that regulate normal embryonic development of the urogenital tract (Stock et al., 2002; Fukuzawa and Reeve, 2007). Most patients have a palpable abdominal mass as the first symptom, and some patients may present with symptoms of hematuria, fever, urinary tract infection, varicocele, and anemia (Zhang et al., 2014). Currently, WT is treated with a multidisciplinary combination of surgical, chemotherapy, radiotherapy, and targeted therapy, with an overall cure rate of approximately 90% (Anvar et al., 2019; Palmisani et al., 2021; Pelosi et al., 2021).

The expression of circ-CDYL is significantly downregulated in WT tissues compared to adjacent non-tumor tissues and upregulation of circ-CDYL inhibited cell proliferation, migration, and invasion. Circ-CDYL acts as a miRNA sponge reducing the expression of miR-145-5p and further upregulating TJP1 expression (Zhou R. et al., 2021). Cao et al. found that hsa_circ_0093740 expression was significantly increased in WT and inhibition of hsa_circ_0093740 significantly suppressed the proliferation and migration of WT by high-throughput microarray sequencing. Mechanistic studies revealed that the hsa_circ_0093740-miR-136/145-DNMT3A axis plays an important regulatory role in WT growth and metastasis (Cao et al., 2021).

Rhabdomyosarcoma

Rhabdomyosarcoma (RMS) is a malignant tumor arising from embryonic mesenchymal tissue, accounting for 15% of solid tumors and 50% of soft tissue sarcomas in children (Arndt et al., 2018; Skapek et al., 2019). The diversity of clinical manifestations, the multiplicity of pathological changes, and the different sites of onset make RMS one of the most complex pediatric tumors (Ramadan et al., 2020; Zoroddu et al., 2021). Surgical resection, chemotherapy, and radiotherapy are the main treatments for RMS (van Erp et al., 2018; Frankart et al., 2021). With the continuous improvement of chemotherapy regimens, the survival rate of RMS patients has increased to 70–80% (Pappo and Dirksen, 2018; Mohammad et al., 2020). Despite aggressive treatment, the 5-year survival rate for patients with metastatic RMS is still only 30% (Kashi et al., 2015; Pal et al., 2019), therefore, there is a need to find new

diagnostic treatments and therapies for RMS to improve the survival rate of RMS patients.

Rossi et al. found that circ-ZNF609 expression was significantly upregulated in biopsies of embryonic RMS (ERMS) and alveolar RMS (ARMS). Knockdown of circ-ZNF609 in ERMS cell lines inhibited the cell cycle and led to a strong reduction in *p*-Akt protein levels and altered pRb/Rb ratios. In contrast, the knockdown of circ-ZNF609 had no significant effect on ARMS-derived cells but the exact reason for this is unclear (Rossi et al., 2019). Circ-VAMP3 expression is significantly increased in ARMS cells, and knockdown of circVAMP3 regulates the CCNB1/CDK1 complex, which controls the G2/M checkpoint by promoting the expression of CDKN1A and WEE1, thus the AKK1 and CDK1 complexes, as well as downregulation of Akt and ERK1, thereby inhibiting the cell cycle (Rossi et al., 2021).

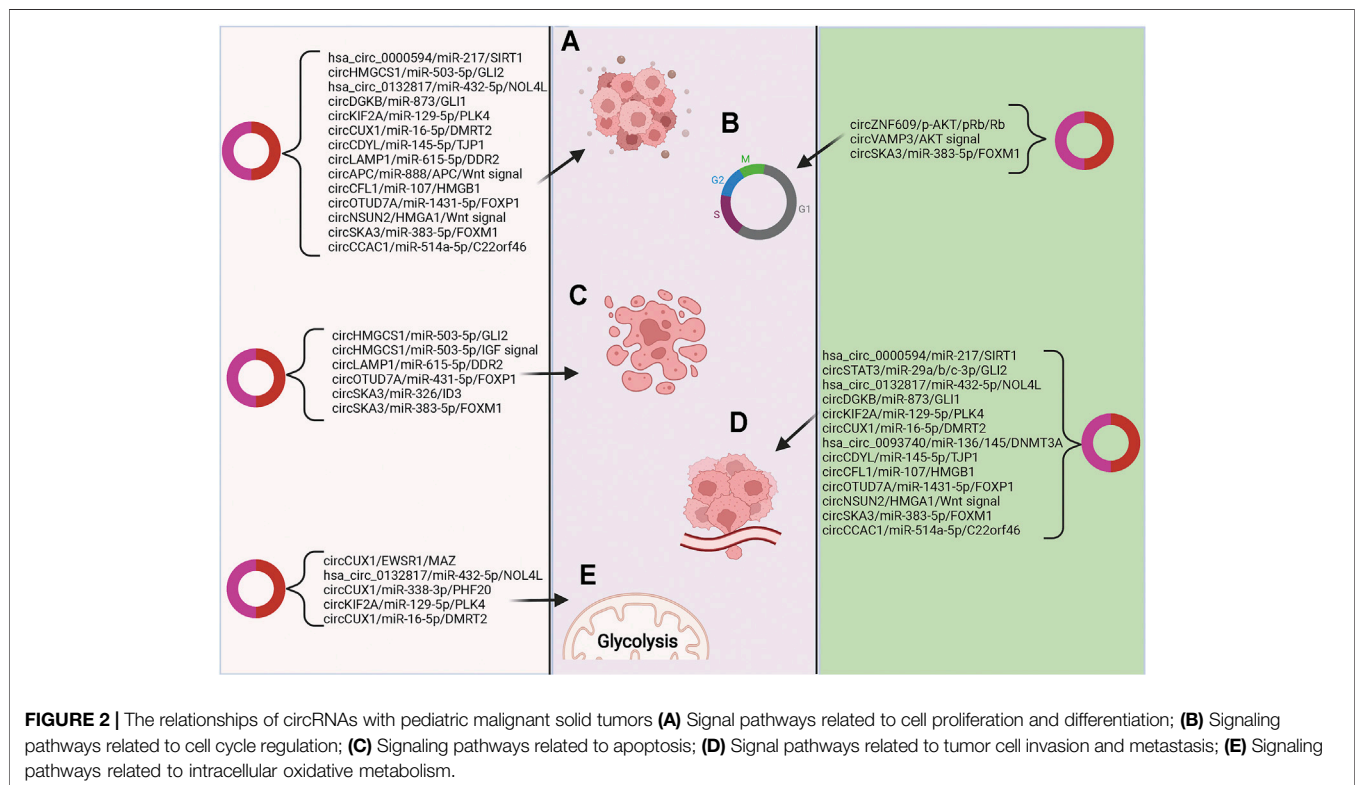
Lymphoma

Lymphoma is a highly heterogeneous disease (Liu M. K. et al., 2021) with increasing morbidity and mortality rates worldwide and is currently treated mainly with conventional radiotherapy (Leslie, 2021). Although the use of rituximab has led to significant improvements in long-term survival in some lymphoma patients, the treatment of relapsed refractory lymphoma remains a challenge (Shao L. et al., 2021; Takiar and Phillips, 2021).

We examined the differentially expressed circRNAs in normal infant thymus and T-cell lymphoblastic lymphoma (T-LBL) and found that circ-LAMP1 was significantly increased in T-LBL. Mechanistic studies revealed that circ-LAMP1 promotes cell proliferation and inhibits apoptosis through the miR-615-5p/DDR2 signaling axis, which in turn leads to malignant progression of T-LBL (Deng et al., 2019). Circ-NSUN2 is aberrantly highly expressed in malignant lymphoma tissues and cell lines, and circ-NSUN2 inhibition reduces the proliferation and invasion of lymphoma cells. Mechanistic studies have demonstrated that circ-NSUN2 can promote lymphoma progression by affecting Wnt pathways through the regulation of HMGA1 (Wang et al., 2021a). The expression of circ-APC (hsa_circ_0127621) is decreased in diffuse large B-cell lymphoma (DLBCL) tissues, cell lines, and plasma by microarray assays. Etoposide expression of circ-APC inhibited cell proliferation *in vitro* and tumor growth *in vivo*. Mechanistic studies revealed that circ-APC acts as a sponge for miR-888 in the cytoplasm to upregulate APC, whereas, in the nucleus, circ-APC binds to the APC promoter and recruits the DNA demethylase TET1, which transcriptionally upregulates APC, thereby inhibiting the typical Wnt/ β -catenin signaling pathway by reducing the accumulation of β -catenin in the nucleus and the catenin signaling pathway by reducing the accumulation of β -catenin in the nucleus, retarding the growth of DLBCL (Hu et al., 2019). In DLBCL, circ-CFL1 directly binds to miR-107 reducing the inhibitory effect on the target gene HMGB1, which promotes enhanced cell migration and proliferation as well as tumor growth (Chen et al., 2020). Circ-OTUD7A is highly expressed in DLBCL, and knockdown of circ-OTUD7A inhibits DLBCL cell proliferation and metastasis, promoting cell cycle arrest and apoptosis. Mechanistic

TABLE 2 | The potential of circRNAs in the diagnosis and prognosis of pediatric malignant solid tumor.

Study	Sample size	circRNAs	Expression	Source	Expression (p value)	Diagnostic value AUC	Sample size	Prognostic value OS (p value)	References
Hepatoblastoma									
Zhen et al.	(Normal: Tumor) (37:37)	circ-HMGC51	Up	Tissues	$p < 0.001$	0.8283	Tumor (n = 33)	$p = 0.0497$	Zhen et al. (2019)
Neuroblastoma									
Yang et al.	(Normal: Tumor) (10:30)	circ-DGKB	Up	Blood	$p < 0.05$	0.7778	Tumor (n = 33)	$p = 0.0324$	Yang et al. (2020)
Zhang et al.	(Normal: Tumor) (50:50)	circ-CUX1	Up	Tissues	$p < 0.05$	-	Tumor (n = 50)	$p = 0.0120$	Zhang et al. (2020)
Lymphoma									
Mei et al.	(Normal: Tumor) (17:18)	circ-CDYL	Up	Tissues	$p < 0.001$	0.856	Tumor (n = 18)	$p = 0.595$	Mei et al. (2019)
Adrenocortical Carcinoma									
Li et al.	(Normal: Tumor) (48:48)	circ-CCAC1	Up	Tissues	$p < 0.01$	-	Tumor (n = 48)	$p = 0.006$	Li et al. (2020a)



experiments showed that circ_OTUD7A uptakes miR-431-5p to promote FOXP1 expression (Liu W. et al., 2021). Circ-NSUN2 is aberrantly highly expressed in malignant lymphoma tissues and cell lines, and circ-NSUN2 inhibition can reduce lymphoma proliferation and invasion. Mechanistic results suggest that circ-NSUN2, regulated by the transcription factor NRF1, can

promote lymphoma progression by stabilizing the HMGA1-activated Wnt pathway (Wang et al., 2021a).

Medulloblastoma

Medulloblastoma (MB) is a highly malignant neuroepithelial tumor of the central nervous system and is a common solid

tumor in children (Li M. et al., 2021; Wen and Hadden, 2021), particularly those under 10 years of age (Hammoud et al., 2020; Danilenko et al., 2021). MB is difficult to treat because of its rapid growth, incomplete surgical excision, and tendency to disseminate with the cerebrospinal fluid (Caimano et al., 2021). The current 5-year survival rate for MB treated with a combination of surgery, radiotherapy, and chemotherapy is 65%. With the improvement of treatment efficacy and prolongation of survival, the toxicities associated with treatment have received increasing attention (Audi et al., 2021), therefore, it is important to search for potential diagnostic markers and therapeutic targets for MB.

Circ-SKA3 expression is elevated in MB tissues and cells, and inhibition of circ-SKA3 significantly inhibits MB cell proliferation, migration, and invasion, inducing apoptosis and cell cycle arrest and circ-SKA3 knockdown inhibits MB growth *in vivo*. Mechanistic analysis suggests that circ-SKA3 directly targets miR-326 to increase ID3 expression (Zhao X. et al., 2021). Differential expression profiles of circRNAs in four normal cerebellum and 4 MB samples using a HiSeq sequencer showed that thirty-three circRNAs were differentially expressed in MB tissue, of which three were upregulated and thirty were downregulated. Upregulated circ-SKA3 and circ-DTL promoted proliferation, migration, and invasion *in vitro* by regulating the expression of host genes as verified by *in vitro* cellular assays, demonstrating that circ-SKA3 and circ-DTL are critical in tumorigenesis and the development of MB (Lv et al., 2018). CircSKA3 and FOXM1 expression levels in MB tissues were significantly elevated, while miR-383-5p expression levels were significantly decreased. CircSKA3 was shown to uptake miR-383-5p and promote the expression of FOXM1. *In vitro* cellular assays confirmed that circSKA3 silencing significantly inhibited cell proliferation, migration, and invasion, promoting MB cell apoptosis (Wang et al., 2020).

Adrenocortical Carcinoma

Adrenocortical adenocarcinoma (ACC) is a malignant endocrine tumor (Georgantzoglou et al., 2021; Kiesewetter et al., 2021) that typically occurs between 0–10 years and 40–50 years, with a higher incidence in children and women (Domenech et al., 2021). Approximately 60–70% of ACC patients exhibit clinical symptoms due to hormonal excess but many patients still have non-significant clinical symptoms (Fay et al., 2014). Common endocrine symptoms include cortisolism, masculinization, or gynecomastia (Ettaieb et al., 2020). The prognosis of ACC is poor, and tumor grade, stage, and hypercortisolism are associated with prognosis (Libe, 2015). Surgical resection is the treatment of choice but postoperative tumor recurrence rates are high and overall survival rates are low (Bedrose et al., 2020), therefore, it is important to identify good early diagnostic markers and therapeutic targets for ACC. Li et al. found that circ-CCAC1 was overexpressed in ACC tissue samples and cell lines and was associated with a poor prognosis. Functional assays showed that circ-CCAC1 enhances C22orf46 expression through uptake of miR-514a-5p promoting ACC progression (Li W. et al., 2020) (Table2).

CircRNAs as Biomarkers of Pediatric Malignant Solid Tumors

Many circRNAs that are highly expressed in blood have relatively low expression of their corresponding linear RNAs (Rahmati et al., 2021; Xiao et al., 2021). The unique functions and properties of circRNAs make them of great clinical potential in life sciences and medicine (Gu et al., 2021; Yi et al., 2021). Recently, many studies have explored the value of circRNAs for clinical application in pediatric malignant solid tumors, suggesting that some circRNAs have great clinical potential in early tumor diagnosis, treatment, and prognosis. (Figure 2).

Zheng et al. analyzed the association between circ-HMGCS1 expression levels and clinical features of HB finding a significant correlation between circ-HMGCS1 and AFP. The subject operating characteristic (ROC) curve was applied to investigate the diagnostic value of circ-HMGCS1 in distinguishing HB tissue from normative tissue showing that circ-HMGCS1 had diagnostic value (Area Under Curve (AUC) = 0.8283), with high expression of circ-HMGCS1 predicting poor prognosis in HB patients by Kaplan-Meier survival curve analysis (Zhen et al., 2019). The expression of circ-DGKB in blood was found to be of clinical importance in the diagnosis of NB by ROC analysis (AUC = 0.7778), with Kaplan-Meier analysis showing that patients with high levels of circ-DGKB expression had a lower survival rate (Yang et al., 2020). Zhang et al. divided NB patients into high and low circ-CUX1 expression groups according to the median value of circ-CUX1 expression for survival analysis revealing that high expression of circ-CUX1 in NB patients was associated with shorter survival times. In addition, high expression of circ-CUX1 was associated with advanced TNM stage, low differentiation grade, and positive lymph node metastasis in NB patients (Zhang et al., 2020). Mei and others reported that the plasma expression of circ-CDYL was significantly different between MCL patients and healthy controls (AUC = 0.856), with no statistically significant difference between circ-CDYL expression levels and prognosis of MCL patients (Mei et al., 2019). Li et al. found that high expression of circ-CCAC1 predicted poorer overall survival in ACC patients (Li W. et al., 2020).

CONCLUSION AND FUTURE PERSPECTIVES

At present, there are few circRNAs studies in pediatric malignant solid tumors with variable results. However, all studies have shown that the expression of multiple circRNAs is dysregulated in pediatric malignant solid tumors, and some of the circRNAs target binding miRNAs that are involved in tumorigenesis and progression. The current exploration of tissue-specific circRNAs and studies of circRNAs-miRNAs-mRNAs networks have revealed the association of circRNAs with childhood malignant solid tumors. In addition, cellular and animal experiments have confirmed that for certain circRNAs that promote tumor growth, reducing their levels by targeted knockdown or RNA interference can inhibit further tumor growth and metastasis, suggesting that circRNAs are novel therapeutic approaches and drug targets for malignant tumors.

However, the main mechanism currently revolves around circRNA as ceRNA to regulate the function of tumor cells. Whether circRNA may affect the occurrence and progression of childhood solid tumors through other mechanisms The regulation is still unclear, and this needs to be further explored. In addition, most of the discoveries of circRNAs were not screened by next-generation sequencing technology, but were studied by referring to other articles, which lacked novelty. More importantly, only through high-throughput sequencing technology, the establishment of circRNAs expression profiles in childhood solid tumors is conducive to in-depth exploration of possible mechanisms.

Currently, the detection of circRNAs in tumors is mainly focused on tissue samples, which are more invasive and not suitable for early clinical tumor diagnosis (Zhou Q. et al., 2021; Lu et al., 2021; Shen et al., 2021) compared to other clinical samples such as serum, urine, and body fluids. CircRNAs are potential novel tumor biomarkers due to their high stability, conservatism, prevalence, tissue, and disease specificity (Ali et al., 2021; Tian et al., 2021; Vakhshiteh et al., 2021). Furthermore, the detection of free circRNAs in tumor tissues and the circulation of pediatric patients with malignant solid tumors is of great significance and value in terms of diagnostic accuracy, clinical staging, differential diagnosis, prognosis, and evaluation of treatment response. The identification of tumor biomarkers with high specificity and sensitivity among candidate circRNAs may improve the diagnostic accuracy and specificity of malignant solid tumors in children by combining them with other biomarkers or imaging examinations. In addition, it may also reduce the need for invasive procedures while helping to address the low organ specificity of existing tumor markers. At present, there are few studies on the clinical application of circRNAs in children with malignant solid tumors, and the sample size of included articles is also small, and there is a lack of multi-center studies. These are all problems that need to be solved urgently.

Moreover, the application of circRNAs as biomarkers for the diagnosis of malignant solid tumors in children is challenging.

REFERENCES

- Ali, S. A., Peffers, M. J., Ormseth, M. J., Jurisica, I., and Kapoor, M. (2021). The Non-coding RNA Interactome in Joint Health and Disease. *Nat. Rev. Rheumatol.* 17 (11), 692–705. doi:10.1038/s41584-021-00687-y
- Altesha, M. A., Ni, T., Khan, A., Liu, K., and Zheng, X. (2019). Circular RNA in Cardiovascular Disease. *J. Cel Physiol* 234 (5), 5588–5600. doi:10.1002/jcp.27384
- Anvar, Z., Acuzio, B., Roma, J., Cerrato, F., and Verde, G. (2019). Origins of DNA Methylation Defects in Wilms Tumors. *Cancer Lett.* 457, 119–128. doi:10.1016/j.canlet.2019.05.013
- Aravindan, N., Herman, T., and Aravindan, S. (2020). Emerging Therapeutic Targets for Neuroblastoma. *Expert Opin. Ther. Targets* 24 (9), 899–914. doi:10.1080/14728222.2020.1790528
- Arndt, C. A. S., Bisogno, G., and Koscielniak, E. (2018). Fifty Years of Rhabdomyosarcoma Studies on Both Sides of the Pond and Lessons Learned. *Cancer Treat. Rev.* 68, 94–101. doi:10.1016/j.ctrv.2018.06.013
- Ashwal-Fluss, R., Meyer, M., Pamudurti, N. R., Ivanov, A., Bartok, O., Hanan, M., et al. (2014). circRNA Biogenesis Competes with Pre-mRNA Splicing. *Mol. Cel* 56 (1), 55–66. doi:10.1016/j.molcel.2014.08.019

Although circRNAs are a promising biomarker due to their high organ-tissue specificity, current studies have not demonstrated that the sensitivity of candidate circRNAs is superior to that of known classical serum biomarkers. Compared to tissue biopsies, liquid biopsies have the advantages of non-invasiveness and reproducibility, however, circRNAs are low in body fluids, clinical data from peripheral blood studies are limited, and most circRNAs have not been shown to have excellent prognostic or diagnostic significance in large samples. Further studies should be conducted to evaluate the expression of circRNAs in serum and disease-related body fluids and there should be a consensus regarding sample handling, detection methods, and threshold values to enable the development of circRNAs as clinical diagnostic biomarkers. In addition, co-detection of tumors may lead to higher sensitivity and accuracy of diagnostic results.

In summary, although much is now known about the formation of circRNAs and their biological role and clinical application in childhood malignant solid tumors, the use of circRNAs for the treatment of pediatric malignant solid tumors requires further investigation. In addition, since many reviews on circRNAs in osteosarcoma have been published, osteosarcoma-related circRNAs were not included in the present review.

AUTHOR CONTRIBUTIONS

QS: Conceptualization, Formal analysis, Data curation, Writing-original draft. XL and WL: Formal analysis, Data curation, Writing-original draft, Writing-Editing. TL and XZ: Project administration, Date curation. KZ and JZ: Supervision.

ACKNOWLEDGMENTS

All graphic figures were made with biorender.com.

- Audi, Z. F., Saker, Z., Rizk, M., Harati, H., Fares, Y., Bahmad, H. F., et al. (2021). Immunosuppression in Medulloblastoma: Insights into Cancer Immunity and Immunotherapy. *Curr. Treat. Options. Oncol.* 22 (9), 83. doi:10.1007/s11864-021-00874-9
- Bedrose, S., Daher, M., Altameemi, L., and Habra, M. A. (2020). Adjuvant Therapy in Adrenocortical Carcinoma: Reflections and Future Directions. *Cancers* 12 (2), 508. doi:10.3390/cancers12020508
- Bhoopathi, P., Mannangatti, P., Emdad, L., Das, S. K., and Fisher, P. B. (2021). The Quest to Develop an Effective Therapy for Neuroblastoma. *J. Cel Physiol* 236 (11), 7775–7791. doi:10.1002/jcp.30384
- Blavier, L., Yang, R.-M., and DeClerck, Y. A. (2020). The Tumor Microenvironment in Neuroblastoma: New Players, New Mechanisms of Interaction and New Perspectives. *Cancers* 12 (10), 2912. doi:10.3390/cancers12102912
- Brignole, C., Pastorino, F., Perri, P., Amoroso, L., Bensa, V., Calarco, E., et al. (2021). Bone Marrow Environment in Metastatic Neuroblastoma. *Cancers* 13 (10), 2467. doi:10.3390/cancers13102467
- Caimano, M., Lospinoso Severini, L., Loricchio, E., Infante, P., and Di Marcotullio, L. (2021). Drug Delivery Systems for Hedgehog Inhibitors in the Treatment of SHH-Medulloblastoma. *Front. Chem.* 9, 688108. doi:10.3389/fchem.2021.688108

- Calvisi, D. F., and Solinas, A. (2020). Hepatoblastoma: Current Knowledge and Promises from Preclinical Studies. *Transl Gastroenterol. Hepatol.* 5, 42. doi:10.21037/tgh.2019.12.03
- Cao, J., Huang, Z., Ou, S., Wen, F., Yang, G., Miao, Q., et al. (2021). circ0093740 Promotes Tumor Growth and Metastasis by Sponging miR-136/145 and Upregulating DNMT3A in Wilms Tumor. *Front. Oncol.* 11, 647352. doi:10.3389/fonc.2021.647352
- Casey, D. L., and Cheung, N.-K. V. (2020). Immunotherapy of Pediatric Solid Tumors: Treatments at a Crossroads, with an Emphasis on Antibodies. *Cancer Immunol. Res.* 8 (2), 161–166. doi:10.1158/2326-6066.CIR-19-0692
- Chen, H., Guan, Q., Guo, H., Miao, L., and Zhuo, Z. (2021a). The Genetic Changes of Hepatoblastoma. *Front. Oncol.* 11, 690641. doi:10.3389/fonc.2021.690641
- Chen, J., Gu, J., Tang, M., Liao, Z., Tang, R., Zhou, L., et al. (2021b). Regulation of Cancer Progression by circRNA and Functional Proteins. *J. Cel. Physiol.* 16, 1–16. doi:10.1002/jcp.30608
- Chen, Q., Wang, H., Li, Z., Li, F., Liang, L., Zou, Y., et al. (2022c). Circular RNA ACTN4 Promotes Intrahepatic Cholangiocarcinoma Progression by Recruiting YBX1 to Initiate FZD7 Transcription. *J. Hepatol.* 76, 135–147. doi:10.1016/j.jhep.2021.08.027
- Chen, X., Xie, X., and Zhou, W. (2020). CircCFL1/MiR-107 Axis Targeting HMGB1 Promotes the Malignant Progression of Diffuse Large B-Cell Lymphoma Tumors. *Cmar Vol.* 12, 9351–9362. doi:10.2147/CMAR.S263222
- Cheng, Z., Yu, C., Cui, S., Wang, H., Jin, H., Wang, C., et al. (2019). circTP63 Functions as a ceRNA to Promote Lung Squamous Cell Carcinoma Progression by Upregulating FOXM1. *Nat. Commun.* 10 (1), 3200. doi:10.1038/s41467-019-11162-4
- Choudhary, A., Madbhagat, P., Sreepadmanabh, M., Bhardwaj, V., and Chande, A. (2021). Circular RNA as an Additional Player in the Conflicts between the Host and the Virus. *Front. Immunol.* 12, 602006. doi:10.3389/fimmu.2021.602006
- Chu, Q., Ding, Y., Xu, X., Ye, C. Y., Zhu, Q. H., Guo, L., et al. (2021). Recent Origin of Circular RNAs in Plants. *New Phytol.* 233, 515–525. doi:10.1111/nph.17798
- Cimini, A., Ricci, M., Chiaravallotti, A., Filippi, L., and Schillaci, O. (2020). Theragnostic Aspects and Radioimmunotherapy in Pediatric Tumors. *Ijms* 21 (11), 3849. doi:10.3390/ijms21113849
- Cristóbal, I., Sanz-Álvarez, M., Luque, M., Caramés, C., Rojo, F., and García-Foncillas, J. (2019). The Role of MicroRNAs in Hepatoblastoma Tumors. *Cancers* 11 (3), 409. doi:10.3390/cancers11030409
- Danilenko, M., Clifford, S. C., and Schwalbe, E. C. (2021). Inter and Intra-tumoral Heterogeneity as a Platform for Personalized Therapies in Medulloblastoma. *Pharmacol. Ther.* 228, 107828. doi:10.1016/j.pharmthera.2021.107828
- Deng, L., Liu, G., Zheng, C., Zhang, L., Kang, Y., and Yang, F. (2019). Circ-LAMP1 Promotes T-Cell Lymphoblastic Lymphoma Progression via Acting as a ceRNA for miR-615-5p to Regulate DDR2 Expression. *Gene* 701, 146–151. doi:10.1016/j.gene.2019.03.052
- Domènech, M., Grau, E., Solanes, A., Izquierdo, A., Del Valle, J., Carrato, C., et al. (2021). Characteristics of Adrenocortical Carcinoma Associated with Lynch Syndrome. *J. Clin. Endocrinol. Metab.* 106 (2), 318–325. doi:10.1210/clinem/dgaa833
- Ebbesen, K. K., Hansen, T. B., and Kjems, J. (2017). Insights into Circular RNA Biology. *RNA Biol.* 14 (8), 1035–1045. doi:10.1080/15476286.2016.1271524
- Ettaieb, M., Kerkhofs, T., van Engeland, M., and Haak, H. (2020). Past, Present and Future of Epigenetics in Adrenocortical Carcinoma. *Cancers* 12 (5), 1218. doi:10.3390/cancers12051218
- Fair, D., Potter, S. L., and Venkatramani, R. (2020). Challenges and Solutions to the Study of Rare Childhood Tumors. *Curr. Opin. Pediatr.* 32 (1), 7–12. doi:10.1097/MOP.0000000000000857
- Fang, Y., Yao, Y., Mao, K., Zhong, Y., and Xu, Y. (2021). Circ_0132817 Facilitates Cell Proliferation, Migration, Invasion and Glycolysis by Regulating the miR-432-5p/NOL4L axis in Neuroblastoma. *Exp. Brain Res.* 239 (6), 1841–1852. doi:10.1007/s00221-021-06091-y
- Fay, A. P., Elfiky, A., Teló, G. H., McKay, R. R., Kaymakçalan, M., Nguyen, P. L., et al. (2014). Adrenocortical Carcinoma: the Management of Metastatic Disease. *Crit. Rev. Oncology/Hematology* 92 (2), 123–132. doi:10.1016/j.critrevonc.2014.05.009
- Feng, J., Chen, W., Dong, X., Wang, J., Mei, X., Deng, J., et al. (2021a). CSCD2: an Integrated Interactional Database of Cancer-specific Circular RNAs. *Nucleic Acids Res.* 50 (D1), D1179–D1183. doi:10.1093/nar/gkab830
- Feng, Z.-h., Zheng, L., Yao, T., Tao, S.-y., Wei, X.-a., Zheng, Z.-y., et al. (2021b). EIF4A3-induced Circular RNA PRKAR1B Promotes Osteosarcoma Progression by miR-361-3p-Mediated Induction of FZD4 Expression. *Cell Death Dis* 12 (11), 1025. doi:10.1038/s41419-021-04339-7
- Fetahu, I. S., and Taschner-Mandl, S. (2021). Neuroblastoma and the Epigenome. *Cancer Metastasis Rev.* 40 (1), 173–189. doi:10.1007/s10555-020-09946-y
- Frankart, A. J., Breneman, J. C., and Pater, L. E. (2021). Radiation Therapy in the Treatment of Head and Neck Rhabdomyosarcoma. *Cancers* 13 (14), 3567. doi:10.3390/cancers13143567
- Fukuzawa, R., and Reeve, A. E. (2007). Molecular Pathology and Epidemiology of Nephrogenic Rests and Wilms Tumors. *J. Pediatr. Hematol. Oncol.* 29 (9), 589–594. doi:10.1097/01.mph.0000212981.67114.ec
- Georgantzoglou, N., Kokkali, S., Tsourouflis, G., and Theocharis, S. (2021). Tumor Microenvironment in Adrenocortical Carcinoma: Barrier to Immunotherapy Success? *Cancers* 13 (8), 1798. doi:10.3390/cancers13081798
- Greenbaum, U., Yalniz, F. F., Srour, S. A., Rezvani, K., Singh, H., Olson, A., et al. (2020). Chimeric Antigen Receptor Therapy: How Are We Driving in Solid Tumors? *Biol. Blood Marrow Transplant.* 26 (10), 1759–1769. doi:10.1016/j.bbmt.2020.06.020
- Greene, J., Baird, A.-M., Lim, M., Flynn, J., McNeven, C., Brady, L., et al. (2021). Differential CircRNA Expression Signatures May Serve as Potential Novel Biomarkers in Prostate Cancer. *Front. Cel. Dev. Biol.* 9, 605686. doi:10.3389/fcell.2021.605686
- Gu, Q., Liu, H., Ma, J., Yuan, J., Li, X., and Qiao, L. (2021). A Narrative Review of Circular RNAs in Brain Development and Diseases of Preterm Infants. *Front. Pediatr.* 9, 706012. doi:10.3389/fped.2021.706012
- Hager, J., and Sergi, C. M. (2021). “Hepatoblastoma,” in *Liver Cancer*. Editor C. M. Sergi (Brisbane, AU: Exon Publications). doi:10.36255/exonpublications.livercancer.2021.ch8
- Hammoud, H., Saker, Z., Harati, H., Fares, Y., Bahmad, H. F., and Nabha, S. (2020). Drug Repurposing in Medulloblastoma: Challenges and Recommendations. *Curr. Treat. Options. Oncol.* 22 (1), 6. doi:10.1007/s11864-020-00805-0
- Han, Y., Zhang, H., Bian, C., Chen, C., Tu, S., Guo, J., et al. (2021). Circular RNA Expression: Its Potential Regulation and Function in Abdominal Aortic Aneurysms. *Oxidative Med. Cell Longevity* 2021, 1–21. doi:10.1155/2021/9934951
- He, A. T., Liu, J., Li, F., and Yang, B. B. (2021a). Targeting Circular RNAs as a Therapeutic Approach: Current Strategies and Challenges. *Sig Transduct Target. Ther.* 6 (1), 185. doi:10.1038/s41392-021-00569-5
- He, L., Man, C., Xiang, S., Yao, L., Wang, X., and Fan, Y. (2021b). Circular RNAs’ Cap-independent Translation Protein and its Roles in Carcinomas. *Mol. Cancer* 20 (1), 119. doi:10.1186/s12943-021-01417-4
- He, P. C., and He, C. (2021). m 6 A RNA Methylation: from Mechanisms to Therapeutic Potential. *EMBO J.* 40 (3), e105977. doi:10.15252/emboj.2020105977
- Hohenstein, P., Pritchard-Jones, K., and Charlton, J. (2015). The Yin and Yang of Kidney Development and Wilms’ Tumors. *Genes Dev.* 29 (5), 467–482. doi:10.1101/gad.256396.114
- Hong, X., Liu, N., Liang, Y., He, Q., Yang, X., Lei, Y., et al. (2020). Circular RNA CRIM1 Functions as a ceRNA to Promote Nasopharyngeal Carcinoma Metastasis and Docetaxel Chemoresistance through Upregulating FOXQ1. *Mol. Cancer* 19 (1), 33. doi:10.1186/s12943-020-01149-x
- Hu, Y., Zhao, Y., Shi, C., Ren, P., Wei, B., Guo, Y., et al. (2019). A Circular RNA from APC Inhibits the Proliferation of Diffuse Large B-Cell Lymphoma by Inactivating Wnt/ β -Catenin Signaling via Interacting with TET1 and miR-888. *Aging* 11 (19), 8068–8084. doi:10.18632/aging.102122
- Huang, A., Zheng, H., Wu, Z., Chen, M., and Huang, Y. (2020). Circular RNA-Protein Interactions: Functions, Mechanisms, and Identification. *Theranostics* 10 (8), 3503–3517. doi:10.7150/thno.42174
- Huang, K.-B., Pan, Y.-H., Shu, G.-N., Yao, H.-H., Liu, X., Zhou, M., et al. (2021). Circular RNA circSNX6 Promotes Sunitinib Resistance in Renal Cell Carcinoma through the miR-1184/GPCPD1/Lysophosphatidic Acid axis. *Cancer Lett.* 523, 121–134. doi:10.1016/j.canlet.2021.10.003
- Huang, Y., and Zhu, Q. (2021). Mechanisms Regulating Abnormal Circular RNA Biogenesis in Cancer. *Cancers* 13 (16), 4185. doi:10.3390/cancers13164185
- Humphreys, D. T., Fossat, N., Demuth, M., Tam, P. P. L., and Ho, J. W. K. (2019). Ularcirc: Visualization and Enhanced Analysis of Circular RNAs via Back and

- Canonical Forward Splicing. *Nucleic Acids Res.* 47 (20), e123. doi:10.1093/nar/gkz718
- Jain, J., Sutton, K. S., and Hong, A. L. (2021). Progress Update in Pediatric Renal Tumors. *Curr. Oncol. Rep.* 23 (3), 33. doi:10.1007/s11912-021-01016-y
- Kalish, J. M., Doros, L., Helman, L. J., Hennekam, R. C., Kuiper, R. P., Maas, S. M., et al. (2017). Surveillance Recommendations for Children with Overgrowth Syndromes and Predisposition to Wilms Tumors and Hepatoblastoma. *Clin. Cancer Res.* 23 (13), e115–e122. doi:10.1158/1078-0432.CCR-17-0710
- Kashi, V. P., Hatley, M. E., and Galindo, R. L. (2015). Probing for a Deeper Understanding of Rhabdomyosarcoma: Insights from Complementary Model Systems. *Nat. Rev. Cancer* 15 (7), 426–439. doi:10.1038/nrc3961
- Kiesewetter, B., Riss, P., Scheuba, C., Mazal, P., Kretschmer-Chott, E., Haug, A., et al. (2021). Management of Adrenocortical Carcinoma: Are We Making Progress? *Ther. Adv. Med. Oncol.* 13, 175883592110384. doi:10.1177/17588359211038409
- Lake, C. M., Tiao, G. M., and Bondoc, A. J. (2019). Surgical Management of Locally-Advanced and Metastatic Hepatoblastoma. *Semin. Pediatr. Surg.* 28 (6), 150856. doi:10.1016/j.sempedsurg.2019.150856
- Legnini, I., Di Timoteo, G., Rossi, F., Morlando, M., Briganti, F., Sthandier, O., et al. (2017). Circ-ZNF609 Is a Circular RNA that Can Be Translated and Functions in Myogenesis. *Mol. Cell* 66 (1), 22–37. e29. doi:10.1016/j.molcel.2017.02.017
- Leslie, L. A. (2021). Novel Therapies for Follicular Lymphoma and Other Indolent Non-hodgkin Lymphomas. *Curr. Treat. Options. Oncol.* 22 (12), 111. doi:10.1007/s11864-021-00909-1
- Li, B., Zhu, L., Lu, C., Wang, C., Wang, H., Jin, H., et al. (2021a). circNDUFB2 Inhibits Non-small Cell Lung Cancer Progression via Destabilizing IGF2BPs and Activating Anti-tumor Immunity. *Nat. Commun.* 12 (1), 295. doi:10.1038/s41467-020-20527-z
- Li, F., Cai, Y., Deng, S., Yang, L., Liu, N., Chang, X., et al. (2021b). A Peptide CORO1C-47aa Encoded by the Circular Noncoding RNA Circ-0000437 Functions as a Negative Regulator in Endometrium Tumor Angiogenesis. *J. Biol. Chem.* 297 (5), 101182. doi:10.1016/j.jbc.2021.101182
- Li, H. M., Ma, X. L., and Li, H. G. (2019b). Intriguing Circles: Conflicts and Controversies in Circular RNA Research. *WIREs RNA* 10 (5), e1538. doi:10.1002/wrna.1538
- Li, H., Yang, F., Hu, A., Wang, X., Fang, E., Chen, Y., et al. (2019a). Therapeutic Targeting of Circ- CUX 1/EWSR 1/MAZ axis Inhibits Glycolysis and Neuroblastoma Progression. *EMBO Mol. Med.* 11 (12), e10835. doi:10.15252/emmm.201910835
- Li, M., Deng, Y., and Zhang, W. (2021c). Molecular Determinants of Medulloblastoma Metastasis and Leptomeningeal Dissemination. *Mol. Cancer Res.* 19 (5), 743–752. doi:10.1158/1541-7786.MCR-20-1026
- Li, P., Song, R., Yin, F., Liu, M., Liu, H., Ma, S., et al. (2021d). circMRPS35 Promotes Malignant Progression and Cisplatin Resistance in Hepatocellular Carcinoma. *Mol. Ther.* 30 (1), 431–447. doi:10.1016/j.yimthe.2021.08.027
- Li, W., Liu, R., Wei, D., Zhang, W., Zhang, H., Huang, W., et al. (2020a). Circular RNA Circ-CCAC1 Facilitates Adrenocortical Carcinoma Cell Proliferation, Migration, and Invasion through Regulating the miR-514a-5p/C22orf46 Axis. *Biomed. Res. Int.* 2020, 1–13. doi:10.1155/2020/3501451
- Li, Y., Ge, Y.-Z., Xu, L., and Jia, R. (2020b). Circular RNA ITCH: A Novel Tumor Suppressor in Multiple Cancers. *Life Sci.* 254, 117176. doi:10.1016/j.lfs.2019.117176
- Libé, R. (2015). Adrenocortical Carcinoma (ACC): Diagnosis, Prognosis, and Treatment. *Front. Cel Dev. Biol.* 3, 45. doi:10.3389/fcell.2015.00045
- Liu, M. K., Sun, X. J., Gao, X. D., Qian, Y., Wang, L., and Zhao, W. L. (2021a). Methylation Alterations and advance of Treatment in Lymphoma. *Front. Biosci. (Landmark Ed.)* 26 (9), 602–613. doi:10.52586/4970
- Liu, W., Lei, L., Liu, X., and Ye, S. (2021b). CircRNA_OTUD7A Upregulates FOXP1 Expression to Facilitate the Progression of Diffuse Large B-Cell Lymphoma via Acting as a Sponge of miR-431-5p. *Genes Genom* 43 (6), 653–667. doi:10.1007/s13258-021-01094-z
- Liu, Y., Song, J., Liu, Y., Zhou, Z., and Wang, X. (2020). Transcription Activation of Circ-STAT3 Induced by Gli2 Promotes the Progression of Hepatoblastoma via Acting as a Sponge for miR-29a/b/c-3p to Upregulate STAT3/Gli2. *J. Exp. Clin. Cancer Res.* 39 (1), 101. doi:10.1186/s13046-020-01598-8
- Lu, Y., Li, K., Gao, Y., Liang, W., Wang, X., and Chen, L. (2021). CircRNAs in Gastric Cancer: Current Research and Potential Clinical Implications. *FEBS Lett.* 595 (21), 2644–2654. doi:10.1002/1873-3468.14196
- Lucas, B., Ravishankar, S., and Pateva, I. (2021). Pediatric Primary Hepatic Tumors: Diagnostic Considerations. *Diagnostics* 11 (2), 333. doi:10.3390/diagnostics11020333
- Luo, Z., Rong, Z., Zhang, J., Zhu, Z., Yu, Z., Li, T., et al. (2020). Circular RNA circCCDC9 Acts as a miR-6792-3p Sponge to Suppress the Progression of Gastric Cancer through Regulating CAV1 Expression. *Mol. Cancer* 19 (1), 86. doi:10.1186/s12943-020-01203-8
- Lv, T., Miao, Y.-F., Jin, K., Han, S., Xu, T.-Q., Qiu, Z.-L., et al. (2018). Dysregulated Circular RNAs in Medulloblastoma Regulate Proliferation and Growth of Tumor Cells via Host Genes. *Cancer Med.* 7 (12), 6147–6157. doi:10.1002/cam4.1613
- Lyu, D., and Huang, S. (2017). The Emerging Role and Clinical Implication of Human Exonic Circular RNA. *RNA Biol.* 14 (8), 1000–1006. doi:10.1080/15476286.2016.1227904
- Ma, J., Du, W. W., Zeng, K., Wu, N., Fang, L., Lyu, J., et al. (2021a). An Antisense Circular RNA circSCRIB Enhances Cancer Progression by Suppressing Parental Gene Splicing and Translation. *Mol. Ther.* 29 (9), 2754–2768. doi:10.1016/j.yimthe.2021.08.002
- Ma, N., Pan, J., Wen, Y., Wu, Q., Yu, B., Chen, X., et al. (2021b). circTulp4 Functions in Alzheimer's Disease Pathogenesis by Regulating its Parental Gene, Tulp4. *Mol. Ther.* 29 (6), 2167–2181. doi:10.1016/j.yimthe.2021.02.008
- Ma, X., Chen, H., Li, L., Yang, F., Wu, C., and Tao, K. (2021c). CircGSK3B Promotes RORA Expression and Suppresses Gastric Cancer Progression through the Prevention of EZH2 Trans-inhibition. *J. Exp. Clin. Cancer Res.* 40 (1), 330. doi:10.1186/s13046-021-02136-w
- Mao, S., Zhang, W., Yang, F., Guo, Y., Wang, H., Wu, Y., et al. (2021a). Hsa_circ_0004296 Inhibits Metastasis of Prostate Cancer by Interacting with EIF4A3 to Prevent Nuclear export of ETS1 mRNA. *J. Exp. Clin. Cancer Res.* 40 (1), 336. doi:10.1186/s13046-021-02138-8
- Mao, X., Cao, Y., Guo, Z., Wang, L., and Xiang, C. (2021b). Biological Roles and Therapeutic Potential of Circular RNAs in Osteoarthritis. *Mol. Ther. - Nucleic Acids* 24, 856–867. doi:10.1016/j.omtn.2021.04.006
- Marquez-Molins, J., Navarro, J. A., Seco, L. C., Pallas, V., and Gomez, G. (2021). Might Exogenous Circular RNAs Act as Protein-Coding Transcripts in Plants? *RNA Biol.* 18, 98–107. doi:10.1080/15476286.2021.1962670
- Mei, M., Wang, Y., Wang, Q., Liu, Y., Song, W., and Zhang, M. (2019). CircCDYL Serves as a New Biomarker in Mantle Cell Lymphoma and Promotes Cell Proliferation. *Cmar Vol.* 11, 10215–10221. doi:10.2147/CMAR.S232075
- Meng, X., Li, X., Zhang, P., Wang, J., Zhou, Y., and Chen, M. (2017). Circular RNA: an Emerging Key Player in RNA World. *Brief Bioinform* 18 (4), bbw045–557. doi:10.1093/bib/bbw045
- Mohammad, K., Baratang Junio, J. A., Tafakori, T., Orfanos, E., and Titorenko, V. I. (2020). Mechanisms that Link Chronological Aging to Cellular Quiescence in Budding Yeast. *Ijms* 21 (13), 4717. doi:10.3390/ijms21134717
- Muñoz, M., Rosso, M., and Coveñas, R. (2019). Neurokinin-1 Receptor Antagonists against Hepatoblastoma. *Cancers* 11 (9), 1258. doi:10.3390/cancers11091258
- Nan, A., Chen, L., Zhang, N., Jia, Y., Li, X., Zhou, H., et al. (2019). Circular RNA circNOL10 Inhibits Lung Cancer Development by Promoting SCLM1-Mediated Transcriptional Regulation of the Humanin Polypeptide Family. *Adv. Sci.* 6 (2), 1800654. doi:10.1002/advs.201800654
- Ollauri-Ibáñez, C., and Astigarraga, I. (2021). Use of Antiangiogenic Therapies in Pediatric Solid Tumors. *Cancers* 13 (2), 253. doi:10.3390/cancers13020253
- Oyefiade, A., Paltin, I., De Luca, C. R., Hardy, K. K., Grosshans, D. R., Chintagumpala, M., et al. (2021). Cognitive Risk in Survivors of Pediatric Brain Tumors. *Jco* 39 (16), 1718–1726. doi:10.1200/JCO.20.02338
- Pal, A., Chiu, H. Y., and Taneja, R. (2019). Genetics, Epigenetics and Redox Homeostasis in Rhabdomyosarcoma: Emerging Targets and Therapeutics. *Redox Biol.* 25, 101124. doi:10.1016/j.redox.2019.101124
- Palmisani, F., Kovar, H., Kager, L., Amann, G., Metzelder, M., and Bergmann, M. (2021). Systematic Review of the Immunological Landscape of Wilms Tumors. *Mol. Ther. - Oncolytics* 22, 454–467. doi:10.1016/j.omto.2021.06.016
- Pan, Z., Cai, J., Lin, J., Zhou, H., Peng, J., Liang, J., et al. (2020). A Novel Protein Encoded by circFND3B Inhibits Tumor Progression and EMT through Regulating Snail in colon Cancer. *Mol. Cancer* 19 (1), 71. doi:10.1186/s12943-020-01179-5

- Pappo, A. S., and Dirksen, U. (2018). Rhabdomyosarcoma, Ewing Sarcoma, and Other Round Cell Sarcomas. *Jco* 36 (2), 168–179. doi:10.1200/JCO.2017.74.7402
- Pelosi, A., Fiore, P. F., Di Matteo, S., Veneziani, I., Caruana, I., Ebert, S., et al. (2021). Pediatric Tumors-Mediated Inhibitory Effect on NK Cells: The Case of Neuroblastoma and Wilms' Tumors. *Cancers* 13 (10), 2374. doi:10.3390/cancers13102374
- Prochownik, E. V. (2021). Reconciling the Biological and Transcriptional Variability of Hepatoblastoma with its Mutational Uniformity. *Cancers* 13 (9), 1996. doi:10.3390/cancers13091996
- Qu, S., Yang, X., Li, X., Wang, J., Gao, Y., Shang, R., et al. (2015). Circular RNA: A New star of Noncoding RNAs. *Cancer Lett.* 365 (2), 141–148. doi:10.1016/j.canlet.2015.06.003
- Qu, S., Zhong, Y., Shang, R., Zhang, X., Song, W., Kjems, J., et al. (2017). The Emerging Landscape of Circular RNA in Life Processes. *RNA Biol.* 14 (8), 992–999. doi:10.1080/15476286.2016.1220473
- Quamine, A. E., Olsen, M. R., Cho, M. M., and Capitini, C. M. (2021). Approaches to Enhance Natural Killer Cell-Based Immunotherapy for Pediatric Solid Tumors. *Cancers* 13 (11), 2796. doi:10.3390/cancers13112796
- Quinn, C. H., Beierle, A. M., and Beierle, E. A. (2021). Artificial Tumor Microenvironments in Neuroblastoma. *Cancers* 13 (7), 1629. doi:10.3390/cancers13071629
- Rahmati, Y., Asemami, Y., Aghamiri, S., Ezzatifar, F., and Najafi, S. (2021). CIRS-7/CDR1as; an Oncogenic Circular RNA as a Potential Cancer Biomarker. *Pathol. - Res. Pract.* 227, 153639. doi:10.1016/j.prp.2021.153639
- Ramadan, F., Fahs, A., Ghayad, S. E., and Saab, R. (2020). Signaling Pathways in Rhabdomyosarcoma Invasion and Metastasis. *Cancer Metastasis Rev.* 39 (1), 287–301. doi:10.1007/s10555-020-09860-3
- Rossi, F., Centrón-Broco, A., Dattilo, D., Di Timoteo, G., Guarnacci, M., Colantoni, A., et al. (2021). CircVAMP3: A circRNA with a Role in Alveolar Rhabdomyosarcoma Cell Cycle Progression. *Genes* 12 (7), 985. doi:10.3390/genes12070985
- Rossi, F., Legnini, I., Megiorni, F., Colantoni, A., Santini, T., Morlando, M., et al. (2019). Circ-ZNF609 Regulates G1-S Progression in Rhabdomyosarcoma. *Oncogene* 38 (20), 3843–3854. doi:10.1038/s41388-019-0699-4
- Rozen, E. J., and Shohet, J. M. (2021). Systematic Review of the Receptor Tyrosine Kinase Superfamily in Neuroblastoma Pathophysiology. *Cancer Metastasis Rev.* 20. doi:10.1007/s10555-021-10001-7
- Shao, L., Xu, C., Wu, H., Jamal, M., Pan, S., Li, S., et al. (2021a). Recent Progress on Primary Central Nervous System Lymphoma-From Bench to Bedside. *Front. Oncol.* 11, 689843. doi:10.3389/fonc.2021.689843
- Shao, T., Pan, Y.-h., and Xiong, X.-d. (2021b). Circular RNA: an Important Player with Multiple Facets to Regulate its Parental Gene Expression. *Mol. Ther. - Nucleic Acids* 23, 369–376. doi:10.1016/j.omtn.2020.11.008
- Shen, H., Liu, B., Xu, J., Zhang, B., Wang, Y., Shi, L., et al. (2021). Circular RNAs: Characteristics, Biogenesis, Mechanisms and Functions in Liver Cancer. *J. Hematol. Oncol.* 14 (1), 134. doi:10.1186/s13045-021-01145-8
- Sinha, T., Panigrahi, C., Das, D., and Panda, A. (2021). Circular RNA Translation, a Path to Hidden Proteome. *WIREs RNA* 15, e1685. doi:10.1002/wrna.1685
- Skapek, S. X., Ferrari, A., Gupta, A. A., Lupo, P. J., Butler, E., Shipley, J., et al. (2019). Rhabdomyosarcoma. *Nat. Rev. Dis. Primers* 5 (1), 1. doi:10.1038/s41572-018-0051-2
- Song, H., Bian, Z. X., Li, H. Y., Zhang, Y., Ma, J., Chen, S. H., et al. (2019). Characterization of Hsa_circ_0000594 as a New Biomarker and Therapeutic Target for Hepatoblastoma. *Eur. Rev. Med. Pharmacol. Sci.* 23 (19), 8274–8286. doi:10.26355/eurrev_201910_19138
- Song, X., Zhang, N., Han, P., Moon, B.-S., Lai, R. K., Wang, K., et al. (2016). Circular RNA Profile in Gliomas Revealed by Identification Tool UROBORUS. *Nucleic Acids Res.* 44 (9), e87. doi:10.1093/nar/gkw075
- Stanczyk, S. A., and Westermann, F. (2021). Neuroblastoma-Telomere Maintenance, Deregulated Signaling Transduction and beyond. *Int. J. Cancer* 13. doi:10.1002/ijc.33839
- Stock, C., Ambros, I. M., Lion, T., Zoubek, A., Amann, G., Gadner, H., et al. (2002). Genetic Changes of Two Wilms Tumors with Anaplasia and a Review of the Literature Suggesting a Marker Profile for Therapy Resistance. *Cancer Genet. Cytogenet.* 135 (2), 128–138. doi:10.1016/s0165-4608(01)00647-1
- Su, Q., and Lv, X. (2020). Revealing New Landscape of Cardiovascular Disease through Circular RNA-miRNA-mRNA axis. *Genomics* 112 (2), 1680–1685. doi:10.1016/j.ygeno.2019.10.006
- Sze, S.-G. K. (2021). Neonatal Renal Tumors. *Clin. Perinatology* 48 (1), 71–81. doi:10.1016/j.clp.2020.11.004
- Takiar, R., and Phillips, T. (2021). Non-chemotherapy Options for Newly Diagnosed Mantle Cell Lymphoma. *Curr. Treat. Options. Oncol.* 22 (11), 98. doi:10.1007/s11864-021-00900-w
- Tian, T., Zhao, Y., Zheng, J., Jin, S., Liu, Z., and Wang, T. (2021). Circular RNA: A Potential Diagnostic, Prognostic, and Therapeutic Biomarker for Human Triple-Negative Breast Cancer. *Mol. Ther. - Nucleic Acids* 26, 63–80. doi:10.1016/j.omtn.2021.06.017
- Vakhshiteh, F., Hassani, S., Momenifar, N., and Pakdaman, F. (2021). Exosomal circRNAs: New Players in Colorectal Cancer. *Cancer Cel Int* 21 (1), 483. doi:10.1186/s12935-021-02112-6
- van Erp, A. E. M., Versleijen-Jonkers, Y. M. H., van der Graaf, W. T. A., and Fleuren, E. D. G. (2018). Targeted Therapy-Based Combination Treatment in Rhabdomyosarcoma. *Mol. Cancer Ther.* 17 (7), 1365–1380. doi:10.1158/1535-7163.MCT-17-1131
- Van Paemel, R., Vlug, R., De Preter, K., Van Roy, N., Speleman, F., Willems, L., et al. (2020). The Pitfalls and Promise of Liquid Biopsies for Diagnosing and Treating Solid Tumors in Children: a Review. *Eur. J. Pediatr.* 179 (2), 191–202. doi:10.1007/s00431-019-03545-y
- van Zonneveld, A. J., Kölling, M., Bijkerk, R., and Lorenzen, J. M. (2021). Circular RNAs in Kidney Disease and Cancer. *Nat. Rev. Nephrol.* 17, 814–826. doi:10.1038/s41581-021-00465-9
- Verdici, L., Tarcitano, E., Strano, S., Yarden, Y., and Blandino, G. (2021). CircRNAs: Role in Human Diseases and Potential Use as Biomarkers. *Cel Death Dis* 12 (5), 468. doi:10.1038/s41419-021-03743-3
- Wang, L., Yang, B., Xu, Z., Song, X., Gong, Z., Xue, S., et al. (2021a). NRF1-regulated CircNSUN2 Promotes Lymphoma Progression through Activating Wnt Signaling Pathway via Stabilizing HMGA1. *Cell Cycle* 20 (9), 819–828. doi:10.1080/15384101.2021.1897272
- Wang, L., Zhou, J., Zhang, C., Chen, R., Sun, Q., Yang, P., et al. (2021b). A Novel Tumour Suppressor Protein Encoded by circMAPK14 Inhibits Progression and Metastasis of Colorectal Cancer by Competitively Binding to MKK6. *Clin. Translational Med.* 11 (10), e613. doi:10.1002/ctm2.613
- Wang, L., Zhou, Y., Jiang, L., Lu, L., Dai, T., Li, A., et al. (2021c). CircWAC Induces Chemotherapeutic Resistance in Triple-Negative Breast Cancer by Targeting miR-142, Upregulating WWP1 and Activating the PI3K/AKT Pathway. *Mol. Cancer* 20 (1), 43. doi:10.1186/s12943-021-01332-8
- Wang, X., Ma, R., Zhang, X., Cui, L., Ding, Y., Shi, W., et al. (2021d). Crosstalk between N6-Methyladenosine Modification and Circular RNAs: Current Understanding and Future Directions. *Mol. Cancer* 20 (1), 121. doi:10.1186/s12943-021-01415-6
- Wang, X., Parodi, L., and Hawkins, S. M. (2021e). Translational Applications of Linear and Circular Long Noncoding RNAs in Endometriosis. *Ijms* 22 (19), 10626. doi:10.3390/ijms221910626
- Wang, X., Xu, D., Pei, X., Zhang, Y., Zhang, Y., Gu, Y., et al. (2020). CircSKA3 Modulates FOXM1 to Facilitate Cell Proliferation, Migration, and Invasion while Confine Apoptosis in Medulloblastoma via miR-383-5p. *Cmar Vol.* 12, 13415–13426. doi:10.2147/CMAR.S272753
- Wang, Y., Niu, Q., Dai, J., Shi, H., and Zhang, J. (2021f). circCUX1 Promotes Neuroblastoma Progression and Glycolysis by Regulating the miR-338-3p/PFH20 axis. *Gen. Physiol. Biophys.* 40 (1), 17–29. doi:10.4149/gpb_2020041
- Weiser, D. A., West-Szymanski, D. C., Frait, E., Weiner, S., Rivas, M. A., Zhao, C. W. T., et al. (2019). Progress toward Liquid Biopsies in Pediatric Solid Tumors. *Cancer Metastasis Rev.* 38 (4), 553–571. doi:10.1007/s10555-019-09825-1
- Wen, J., and Hadden, M. K. (2021). Medulloblastoma Drugs in Development: Current Leads, Trials and Drawbacks. *Eur. J. Med. Chem.* 215, 113268. doi:10.1016/j.ejmech.2021.113268
- Wu, X., Xiao, Y., Ma, J., and Wang, A. (2020). Circular RNA: A Novel Potential Biomarker for Skin Diseases. *Pharmacol. Res.* 158, 104841. doi:10.1016/j.phrs.2020.104841
- Xiao, W., Li, J., Hu, J., Wang, L., Huang, J. R., Sethi, G., et al. (2021). Circular RNAs in Cell Cycle Regulation: Mechanisms to Clinical Significance. *Cell Prolif* 54, e13143. doi:10.1111/cpr.13143

- Xu, M., Xie, F., Tang, X., Wang, T., and Wang, S. (2020). Insights into the Role of Circular RNA in Macrophage Activation and Fibrosis Disease. *Pharmacol. Res.* 156, 104777. doi:10.1016/j.phrs.2020.104777
- Xu, Y., Zhang, S., Liao, X., Li, M., Chen, S., Li, X., et al. (2021). Circular RNA circIKBKB Promotes Breast Cancer Bone Metastasis through Sustaining NF- κ B/bone Remodeling Factors Signaling. *Mol. Cancer* 20 (1), 98. doi:10.1186/s12943-021-01394-8
- Yan, H., and Bu, P. (2021). Non-coding RNA in Cancer. *Essays Biochem.* 65 (4), 625–639. doi:10.1042/EBC20200032
- Yang, J., Yu, L., Yan, J., Xiao, Y., Li, W., Xiao, J., et al. (2020). Circular RNA DGKB Promotes the Progression of Neuroblastoma by Targeting miR-873/GLI1 Axis. *Front. Oncol.* 10, 1104. doi:10.3389/fonc.2020.01104
- Yang, T., Whitlock, R. S., and Vasudevan, S. A. (2019). Surgical Management of Hepatoblastoma and Recent Advances. *Cancers* 11 (12), 1944. doi:10.3390/cancers11121944
- Yang, Y., Pan, H., Chen, J., Zhang, Z., Liang, M., and Feng, X. (2021). CircKIF2A Contributes to Cell Proliferation, Migration, Invasion and Glycolysis in Human Neuroblastoma by Regulating miR-129-5p/PLK4 axis. *Mol. Cell Biochem* 476 (6), 2513–2525. doi:10.1007/s11010-021-04096-3
- Ye, F., Gao, G., Zou, Y., Zheng, S., Zhang, L., Ou, X., et al. (2019). circFBXW7 Inhibits Malignant Progression by Sponging miR-197-3p and Encoding a 185-aa Protein in Triple-Negative Breast Cancer. *Mol. Ther. - Nucleic Acids* 18, 88–98. doi:10.1016/j.omtn.2019.07.023
- Yi, Y., Wu, M., Zeng, H., Hu, W., Zhao, C., Xiong, M., et al. (2021). Tumor-Derived Exosomal Non-coding RNAs: The Emerging Mechanisms and Potential Clinical Applications in Breast Cancer. *Front. Oncol.* 11, 738945. doi:10.3389/fonc.2021.738945
- Yu, T., Ran, L., Zhao, H., Yin, P., Li, W., Lin, J., et al. (2021). Circular RNA Circ-TNPO3 Suppresses Metastasis of GC by Acting as a Protein Decoy for IGF2BP3 to Regulate the Expression of MYC and SNAIL. *Mol. Ther. - Nucleic Acids* 26, 649–664. doi:10.1016/j.omtn.2021.08.029
- Zafar, A., Wang, W., Liu, G., Wang, X., Xian, W., McKeon, F., et al. (2021). Molecular Targeting Therapies for Neuroblastoma: Progress and Challenges. *Med. Res. Rev.* 41 (2), 961–1021. doi:10.1002/med.21750
- Zhang, C., Ding, R., Sun, Y., Huo, S. T., He, A., Wen, C., et al. (2021). Circular RNA in Tumor Metastasis. *Mol. Ther. - Nucleic Acids* 23, 1243–1257. doi:10.1016/j.omtn.2021.01.032
- Zhang, X., Zhang, J., Liu, Q., Zhao, Y., Zhang, W., and Yang, H. (2020). Circ-CUX1 Accelerates the Progression of Neuroblastoma via miR-16-5p/DMRT2 Axis. *Neurochem. Res.* 45 (12), 2840–2855. doi:10.1007/s11064-020-03132-w
- Zhang, Y., Sun, L.-L., Li, T., Sun, H., and Mao, G.-J. (2014). Clinical Study on Carboplatin for Treating Pediatric Patients with Wilms Tumors. *Asian Pac. J. Cancer Prev.* 15 (17), 7277–7280. doi:10.7314/apjcp.2014.15.17.7277
- Zhao, B., Li, Z., Qin, C., Li, T., Wang, Y., Cao, H., et al. (2021a). Mobius Strip in Pancreatic Cancer: Biogenesis, Function and Clinical Significance of Circular RNAs. *Cell. Mol. Life Sci.* 78 (17–18), 6201–6213. doi:10.1007/s00018-021-03908-5
- Zhao, X., Guan, J., and Luo, M. (2021b). Circ-SKA3 Upregulates ID3 Expression by Decoying miR-326 to Accelerate the Development of Medulloblastoma. *J. Clin. Neurosci.* 86, 87–96. doi:10.1016/j.jocn.2021.01.020
- Zhen, N., Gu, S., Ma, J., Zhu, J., Yin, M., Xu, M., et al. (2019). CircHMGCS1 Promotes Hepatoblastoma Cell Proliferation by Regulating the IGF Signaling Pathway and Glutaminolysis. *Theranostics* 9 (3), 900–919. doi:10.7150/thno.29515
- Zhou, Q., Ju, L.-L., Ji, X., Cao, Y.-L., Shao, J.-G., and Chen, L. (2021a). Plasma circRNAs as Biomarkers in Cancer. *Cmar* Vol. 13, 7325–7337. doi:10.2147/CMARS330228
- Zhou, R., Jia, W., Gao, X., Deng, F., Fu, K., Zhao, T., et al. (2021b). CircCDYL Acts as a Tumor Suppressor in Wilms' Tumor by Targeting miR-145-5p. *Front. Cell Dev. Biol.* 9, 668947. doi:10.3389/fcell.2021.668947
- Zoroddu, S., Marchesi, I., and Bagella, L. (2021). PRC2: an Epigenetic Multiprotein Complex with a Key Role in the Development of Rhabdomyosarcoma Carcinogenesis. *Clin. Epigenet* 13 (1), 156. doi:10.1186/s13148-021-01147-w

Conflict of Interest: The authors declare that the research was conducted in the absence of any commercial or financial relationships that could be construed as a potential conflict of interest.

Publisher's Note: All claims expressed in this article are solely those of the authors and do not necessarily represent those of their affiliated organizations, or those of the publisher, the editors and the reviewers. Any product that may be evaluated in this article, or claim that may be made by its manufacturer, is not guaranteed or endorsed by the publisher.

Copyright © 2022 Shen, Liu, Li, Zhao, Li, Zhou and Zhou. This is an open-access article distributed under the terms of the Creative Commons Attribution License (CC BY). The use, distribution or reproduction in other forums is permitted, provided the original author(s) and the copyright owner(s) are credited and that the original publication in this journal is cited, in accordance with accepted academic practice. No use, distribution or reproduction is permitted which does not comply with these terms.



OPEN ACCESS

EDITED BY
Tao Zeng,
Guangzhou Laboratory, China

REVIEWED BY
Jiangbo Wei,
The University of Chicago, United States
Chuanhao Zhang,
Chinese Academy of Sciences (CAS),
China

*CORRESPONDENCE
Weixing Wang,
sate.llite@163.com

SPECIALTY SECTION
This article was submitted to
Epigenomics and Epigenetics,
a section of the journal
Frontiers in Genetics

RECEIVED 29 June 2022
ACCEPTED 03 October 2022
PUBLISHED 14 October 2022

CITATION
Li K and Wang W (2022), Establishment
of m7G-related gene pair signature to
predict overall survival in
colorectal cancer.
Front. Genet. 13:981392.
doi: 10.3389/fgene.2022.981392

COPYRIGHT
© 2022 Li and Wang. This is an open-
access article distributed under the
terms of the [Creative Commons
Attribution License \(CC BY\)](#). The use,
distribution or reproduction in other
forums is permitted, provided the
original author(s) and the copyright
owner(s) are credited and that the
original publication in this journal is
cited, in accordance with accepted
academic practice. No use, distribution
or reproduction is permitted which does
not comply with these terms.

Establishment of m7G-related gene pair signature to predict overall survival in colorectal cancer

Kai Li¹ and Weixing Wang^{2*}

¹Department of Gastrointestinal Surgery II, Renmin Hospital of Wuhan University, Wuhan, China,
²Department of General Surgery, Renmin Hospital of Wuhan University, Wuhan, China

Background: N7-methylguanosine (m7G) is an emerging research hotspot in the field of RNA methylation, and its role in tumor regulation is becoming increasingly recognized. However, its role in colorectal cancer (CRC) remains unclear. Hence, our study explored the role of m7G in CRC.

Methods: The mRNA expression data and the corresponding clinical information of the patients with CRC were obtained from The Cancer Genome Atlas (TCGA). A m7G-related gene pair signature was established using the Cox and LASSO regression analyses. A series of *in silico* analyses based on the signature included analysis of prognosis, correlation analysis, immune-related analysis, and estimation of tumor mutational burden (TMB), microsatellite instability (MSI), and response to immunotherapy. A nomogram prediction model was then constructed.

Results: In total, 2156 m7G-related gene pairs were screened based on 152 m7G-related genes. Then, a prognostic signature of seven gene pairs was constructed, and the patients were stratified into high- or low-risk groups. Better overall survival (OS), left-sided tumor, early stage, immune activity, and low proportion of MSI-low and MSI-high were all associated with a low risk score. High-risk patients had a higher TMB, and patients with a high TMB had a poor OS. Furthermore, the risk score was linked to immune checkpoint expression (including PD-L1), the tumor immune dysfunction and exclusion (TIDE) score, and chemotherapy sensitivity. We also created an accurate nomogram to increase the clinical applicability of the risk score.

Conclusion: We identified an m7G pair-based prognostic signature associated with prognosis, immune landscape, immunotherapy, and chemotherapy in CRC. These findings could help us to better understand the role of m7G in CRC, as well as pave the path for novel methods to assess prognosis and design more effective individualized therapeutic strategies.

Abbreviations: CRC, colorectal cancer; m7G, N7-methylguanosine; MSI, microsatellite instability; TMB, tumor mutational burden; OS, overall survival; TIDE, tumor immune dysfunction and exclusion; TME, tumor microenvironment; DEGs, differentially expressed genes.

KEYWORDS

7-methylguanosine, colorectal cancer, prognosis, tumor microenvironment, treatment response

Introduction

Colorectal cancer (CRC) is the third most common tumor and the second leading cause of cancer-related deaths worldwide, with an estimated 1.8 million new cases and approximately 915,880 deaths worldwide in 2020 (Sung et al., 2021). With increasing incidence and high mortality rates, CRC has become a serious threat to human health (Siegel et al., 2021). Although colonoscopy has provided a better screening method for diagnosing early CRC, many people cannot accept this kind of examination because of its price, psychological pressure, and related risks (Kanth and Inadomi, 2021). Most patients were diagnosed in the middle and late stages of the disease. Currently, CRC can be treated with surgery, chemotherapy, radiotherapy, and biotherapy. However, nearly 40% of CRC patients eventually experience tumor relapse or late metastasis, with less than 15% of patients surviving for more than 5 years (Basak et al., 2020). Consequently, it is important to identify new biomarkers that effectively determine the prognosis of CRC.

RNA methylation has been reported to be associated with various physiological processes and diseases, and abnormal methylation can lead to disease and cancer (Zhang et al., 2021a; Song et al., 2021). To date, more than 170 distinct RNA modifications have been identified (Frye et al., 2018). RNA modification plays an important role in regulating gene expression (Frye et al., 2018). Among these, RNA methylations such as N1-methyladenosine (m1A), N6-methyladenosine (m6A), 5-methylcytosine (m5C), and 7-methylguanosine (m7G) have a variety of biological properties (Shi et al., 2019; Shi et al., 2020; Zhang et al., 2021b; Wei and He, 2021). m6A is the most abundant mRNA modification in eukaryotic cells and is regulated by effector proteins, writers, readers, and erasers (Shi et al., 2019). m6A regulators have been reported to play crucial roles in various biological functions *in vivo* (He et al., 2019; An and Duan, 2022). m7G is the most prevalent modification in the 5' cap of mRNA and is catalyzed by the Trm8/Trm82 complex in yeast and by the METTL1 and WDR4 complexes in humans under the action of methyltransferases (Alexandrov et al., 2002; Luo et al., 2022). m7G can be found not only in mRNA caps but also in several internal sites of mRNAs, tRNAs, and rRNAs (Pandolfini et al., 2019; Dai et al., 2021; Ma et al., 2021). Growing evidence suggests that m7G modification can regulate mRNA transcription, nuclear processing, tRNA stability, miRNA biological function, and maturation of 18S rRNA and plays a vital role in oncogenic mRNA translation and cancer development (Luo et al., 2022). The m7G regulators have been shown to be prognostic factors in multiple cancer types. METTL1 and WDR4 are upregulated in various types of cancers, which are associated with poor prognosis in patients with cancers

such as esophageal squamous cell carcinoma (Han et al., 2022), intrahepatic cholangiocarcinoma (Dai et al., 2021), and nasopharyngeal carcinoma (Chen et al., 2022). Currently, most studies have only focused on the role of a single m7G regulator. However, tumorigenesis is determined by multiple genes, and the prognostic role of multiple m7G regulators has not yet been elucidated.

With the development of RNA sequencing and the establishment and improvement of large tumor databases such as The Cancer Genome Atlas (TCGA), it is possible to systematically study the role of m7G regulators in CRC. Therefore, we developed a novel prognostic signature based on seven m7G-related gene pairs. We systematically and comprehensively investigated the potential role of the model in the clinical outcomes and tumor microenvironment (TME) of CRC. Our results provide additional data on prognostic biomarkers and therapeutic targets for CRC.

Materials and methods

Data source and preprocessing

We collected the original gene expression profiling data of 571 CRC and 44 adjacent normal tissues and the clinical characteristics of CRC cohorts from the TCGA database (<https://portal.gdc.cancer.gov/>). Patients without prognostic data were excluded from this study. In addition, data related to 562 patients were obtained from the Gene Expression Omnibus (ID: GSE29582; <http://www.ncbi.nlm.nih.gov/geo/>) databases. The TCGA dataset (training set) was employed to develop a prognostic signature, and the GSE39582 dataset (validation set), which contained data on 403 CRC samples, was used to validate the predictive accuracy of the signature. Additionally, data regarding 152 m7G regulators were obtained from a previous study (Ming and Wang, 2022).

Construction of m7G-related gene pairs

Pairwise comparisons of the overlapping m7G-related gene expression profiles derived from the training and validation sets were performed. Using the R software, we examined the data relating to m7G-related gene A and m7G-related gene B in each CRC sample to determine a score for each pair. The algorithm presents a scoring system in which the score of the m7G-related gene pair is 1 if the expression level of the first m7G-related gene is higher than that of the second m7G-related gene; otherwise, it

is 0, resulting in the construction of a 0-or-1 matrix. An m7G-related gene pair was deemed invalid if its proportion was <20% or >80% of the samples in either the training or validation sets, respectively (Heinäniemi et al., 2013). Following the screening, the remaining pairs were used for subsequent investigations.

Establishment and validation of the prognostic signature based on m7G-related gene pairs

To discover the OS-related m7G-related gene pairs, a univariate Cox regression analysis was conducted based on the m7G-related gene pairs in the training set. A threshold of p -value < 0.05 was set to screen the prognostic variables. LASSO penalized Cox proportional hazards regression was used to further minimize the risk of over-fitting based on m7G prognostic gene pairs. Subsequently, multivariate Cox analysis was used to select the candidate gene pairs required to establish a prognostic signature. Finally, a signature, termed the risk score, was constructed using seven m7G-related gene pairs and their correlative coefficients acquired in the training set. The risk score for each patient was calculated as follows:

Risk score = (gene pair A coefficient \times expression level) + (gene pair B coefficient \times expression level) + ... + (gene pair n coefficient \times expression level). Furthermore, according to the above formula, the risk scores of patients with CRC were calculated separately, and the patients were stratified into low- and high-risk groups based on the median risk score. Kaplan–Meier survival curves were plotted to estimate the OS differences between the two subgroups. A time-dependent ROC (ROC) curve was plotted to assess the accuracy of the signature.

The external cohort GSE39582 was used to verify the m7G-related prognostic model. The risk score for each patient was calculated using the same coefficients and normalized expression microarray data for the m7G pairs. The patients were stratified into low- and high-risk groups based on the median risk score of the training set. Kaplan–Meier and tdROC curves were plotted to evaluate the prognostic value of the risk model.

The prognostic value of the risk score

The associations between the risk score and clinicopathological traits (age, sex, tumor site, stage, and tumor status) were compared. Univariate and multivariate analyses were performed to evaluate whether the risk scores were independent of the other clinical variables. Moreover, we conducted a stratified analysis to determine whether the risk score preserved its predictive capacity in the different subgroups.

Establishment and validation of a nomogram scoring system

Based on the independent indicators, the R software “regplot” package was used to develop a nomogram for OS prediction at three and 5 years. Then, tdROC analysis for 3- and 5-year OS was performed to evaluate the prognostic accuracy, and the calibration curves were drawn to compare nomogram-predicted probability with actual survival.

Immune-related analysis of colorectal cancer patients using the prognostic signature

The fraction of immune cells in the two risk subgroups was assessed using the CIBERSORT algorithm. Differences between the low- and high-risk groups were detected using the Wilcoxon rank-sum test. We also used boxplots to evaluate the differences in the levels of expression of immunological checkpoints between the low- and high-score groups, which were retrieved from the literature. Moreover, we calculated the tumor immune dysfunction and exclusion (TIDE) score to predict the response to immunotherapy in CRC patients (Jiang et al., 2018).

Tumor mutation burden and microsatellite instability analyses

The “maftools” R package was employed to reveal the mutation frequency in patients with CRC belonging to different risk subgroups. Subsequently, we analyzed the relationship between TMB and the risk scores. Using the Kaplan–Meier method, the OS rates derived from data pertaining to the CRC samples from the low- and high-TMB groups were compared. Next, we evaluated the synergistic effect of TMB and risk score on prognostic stratification. In addition, the association between the risk scores and MSI was explored.

Potential drugs for patients with colorectal cancer

We explored the sensitivity of chemotherapy based on the gene expression levels using the “pRRophetic” R package (Geeleher et al., 2014). The chemotherapeutic response was assessed based on the half-maximal inhibitory concentration (IC50) of each sample.

Functional enrichment analysis

The differentially expressed genes (DEGs) were screened using the “limma” package in the R software by

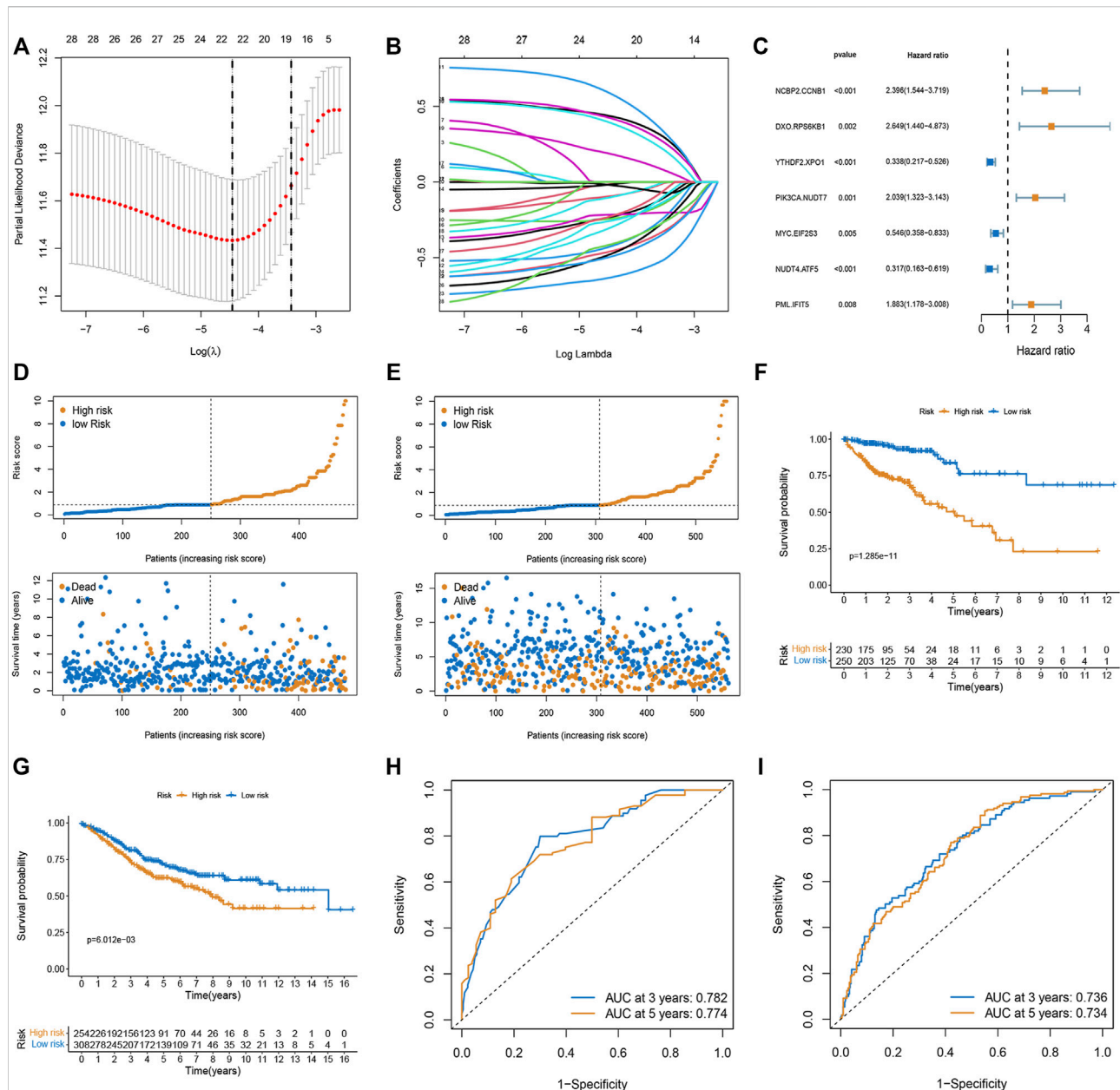


FIGURE 1

Construction and validation of the prognostic model based on m7G-related gene pairs. (A) Plot indicating the optimal λ selection by 10 cross-validated partial likelihood deviance of the LASSO-Cox regression. 10-fold cross-validated partial likelihood deviance was plotted against $\log(\lambda)$. (B) Plot of estimated coefficients from the LASSO-Cox regression against $\log(\lambda)$. Finally, 22 non-zero m7G pairs were selected. (C) Constructing a stepwise Cox proportional hazards model. (D,E) The distribution of each patient's risk score ordered from low to high in training and validation sets. Patients are divided into two risk score level groups. Scatter diagram of the OS-time against the patients' rank of risk score in training and testing sets. (F,G) Overall survival curves of different risk subgroups in the training and validation sets. (H,I) AUC curves to predict the sensitivity and specificity of 3- and 5-year survival according to the risk score in training and validation sets.

setting criteria with $|\log_2(\text{fold change, FC})| > 1$ and adjusted p -value < 0.05 . Subsequently, the "Clusterfiler" R package was employed to perform the Gene Ontology (GO) and Kyoto Encyclopedia of Genes and Genomes (KEGG) pathways.

Statistical analysis

All analyses in this study were performed using the R software (version 4.0.3). Statistical significance was set at $p < 0.05$ unless otherwise stated.

TABLE 1 Multivariate Cox regression analysis of 11 m7G pairs associated with overall survival in patients with CRC.

id	Coef	HR	HR.95L	HR.95H	p-value
NCBP2.CCNB1	0.873933	2.396317	1.543864	3.719457	<0.001
DXO.RPS6KB1	0.974044	2.648634	1.439655	4.872875	0.001
YTHDF2.XPO1	-1.08373	0.338332	0.217453	0.526404	<0.001
PIK3CA.NUDT7	0.712567	2.039219	1.322867	3.143484	0.001
MYC.EIF2S3	-0.60472	0.546229	0.358296	0.832738	0.004
NUDT4.ATF5	-1.14792	0.317297	0.162668	0.618914	<0.001
PML.IFIT5	0.632646	1.882586	1.178223	3.008028	0.008

Results

Establishment and validation of the prognostic signature based on m7G-related gene pairs

The m7G-related genes in the TCGA and GEO datasets were merged into an overlapping gene set, from which 135 m7G-related genes were shared in both sets. Pairwise comparisons were conducted using the algorithm described in the “Methods” section to calculate the risk score for each m7G-related gene pair for subsequent analysis. As a result, 2,156 m7G-related gene pairs were identified. We conducted a univariate Cox regression analysis on these pairs and selected 30 meaningful m7G pairs to generate the models (Supplementary Figure S1). Next, LASSO Cox regression analysis yielded 22 m7G pairs (Figures 1A,B), which were subsequently used to perform multivariate Cox regression analysis. Based on the Akaike information criterion value, we obtained seven m7G pairs to construct risk models, including the NCBP2.CCNB1, DXO. RPS6KB1, YTHDF2. XPO1, PIK3CA.NUDT7, MYC. EIF2S3, NUDT4. ATF5, and PML. IFIT5 gene pairs (Figure 1C). The correlation coefficients are listed in Table 1. A risk score in the training set was assigned to each patient based on the expression levels of the seven m7G pairs multiplied by the regression coefficients obtained from multivariate Cox regression analysis.

Risk score = $(0.873933 \times \text{NCBP2.CCNB1 exp}) + (0.974044 \times \text{DXO. RPS6KB1 exp}) + (-1.08373 \times \text{YTHDF2. XPO1 exp}) + (0.712567 \times \text{PIK3CA.NUDT7 exp}) + (-0.60472 \times \text{MYC. EIF2S3 exp}) + (-1.14792 \times \text{NUDT4. ATF5 exp}) + (0.632646 \times \text{PML. IFIT5 exp})$.

We calculated the risk scores of each sample in the training set and classified the patients into two subgroups (low- and high-risk). In both the training and validation sets, the risk distribution plot demonstrated that survival times increased with the risk score (Figures 1D,E). The Kaplan-Meier curve indicated that low-risk patients had a more favorable survival time than high-risk patients in both the

training and validation sets (Figures 1F,G). The AUC values for three and 5 years in the training set were 0.782 and 0.774, and the AUC values for three and 5 years in the validation set were 0.736 and 0.734 (Figures 1H,I).

Clinical correlation analysis and stratification analysis of the risk score

The relationship between risk score and clinicopathological factors was explored. We found that patients with right-sided CRC and advanced stage (stage III-IV) were associated with high-risk scores, whereas sex and tumor status showed no correlation with risk scores (Figures 2A,B). Further survival analysis revealed that the risk scores could accurately predict the prognosis of patients with all the stratified clinicopathological variants (all $p < 0.05$, Figures 2C-L). Furthermore, we incorporated the risk scores into the corresponding clinical characteristics. Our results from univariate and multivariable Cox regression analyses showed a strong correlation between the risk scores and the prognosis in patients with CRC (Figures 2M,N).

Generation and validation of a nomogram scoring system

To generate personalized predictions for patients with CRC, we integrated the m7G score and clinicopathological parameters (age, tumor site, and stage) to establish a nomogram scoring system (Figure 3A). The predictive accuracy of the nomogram was assessed using receiver operating characteristics and calibration curves. Figure 3B shows that the 3- and 5-year AUC values of the nomogram were 0.845 and 0.831, respectively. The AUC values of the nomogram at years 3 and 5 were all greater than the AUC values for the TNM stage (Figures 3C,D). Lastly, results from the calibration curve analyses showed that the calibration curve of prognostication was close to the standard curve at the 3- and 5-year follow-ups, which again confirmed the inference above (Figure 3E).

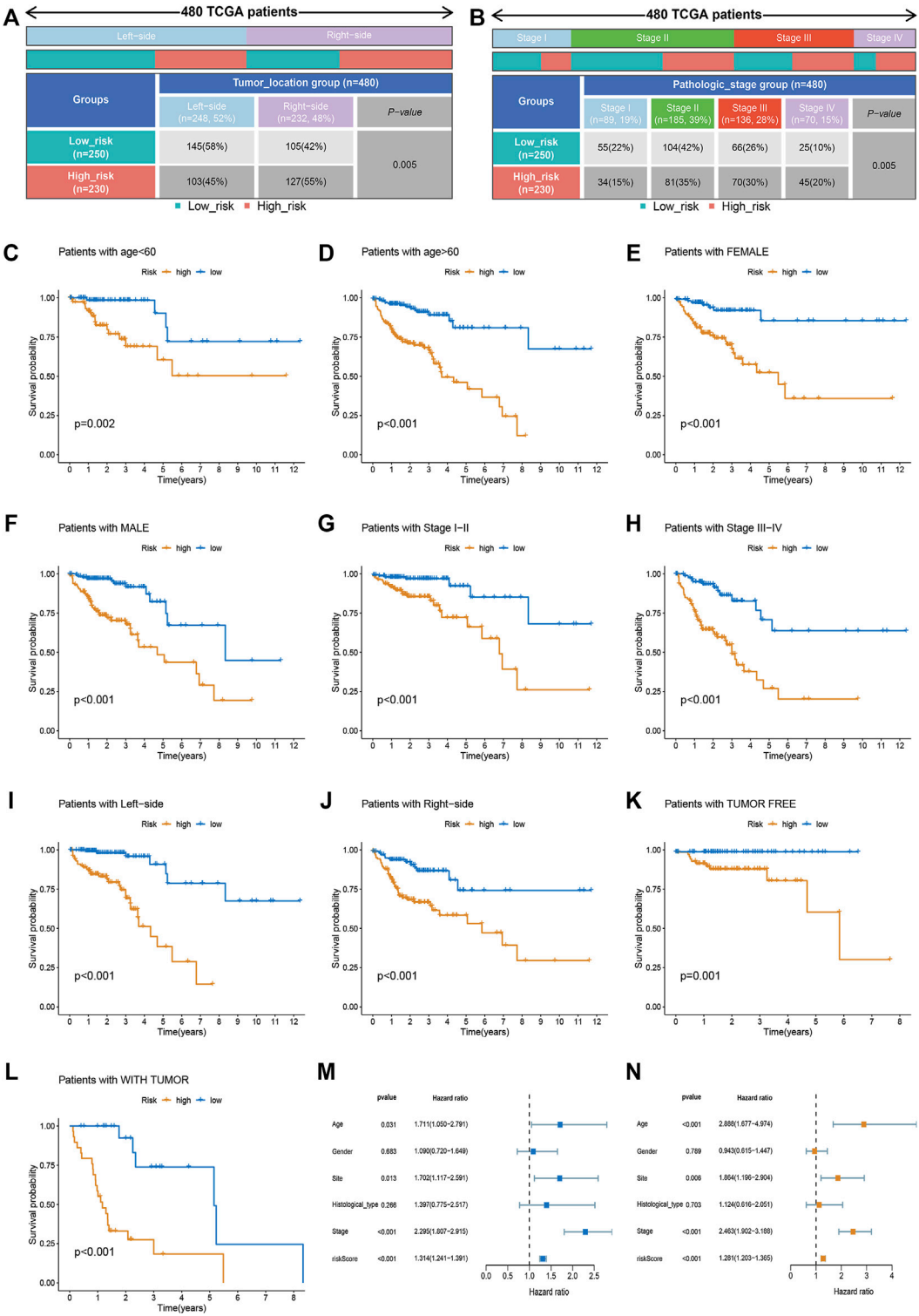


FIGURE 2 Clinical correlation analysis and stratification analysis of the risk score. (A,B) The relationship between the risk score and tumor site and TNM stage. (C–L) The Kaplan-Meier survival curves were stratified by different clinicopathological variants, including age, sex, tumor site, TNM stage, and tumor status. (M) The clinicopathological traits and risk score were analyzed by univariate Cox regression with the OS. (N) Multivariate Cox regression analysis revealing clinicopathological traits and risk scores related to OS.

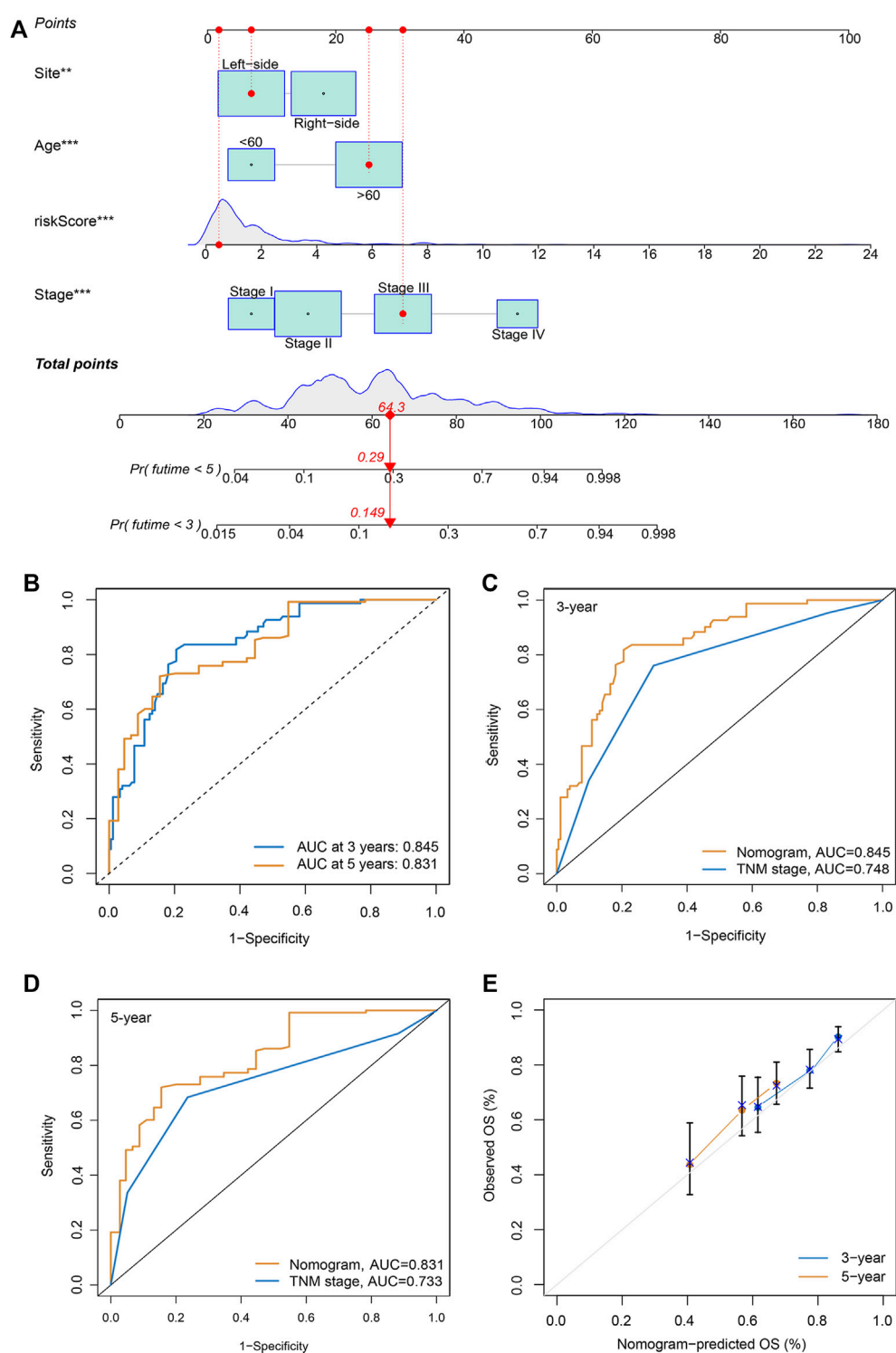


FIGURE 3 Generation and validation of a nomogram scoring system. **(A)** A nomogram for both clinicopathological traits and risk score to predict 3-year and 5-year OS. **(B)** The 3- and 5-year AUC values to evaluate the performance of the nomogram. **(C,D)** Comparison of the AUCs of the nomogram and TNM staging system at 3 and 5 years. **(E)** Calibration curve of the nomogram for predicting 3- and 5-year OS.

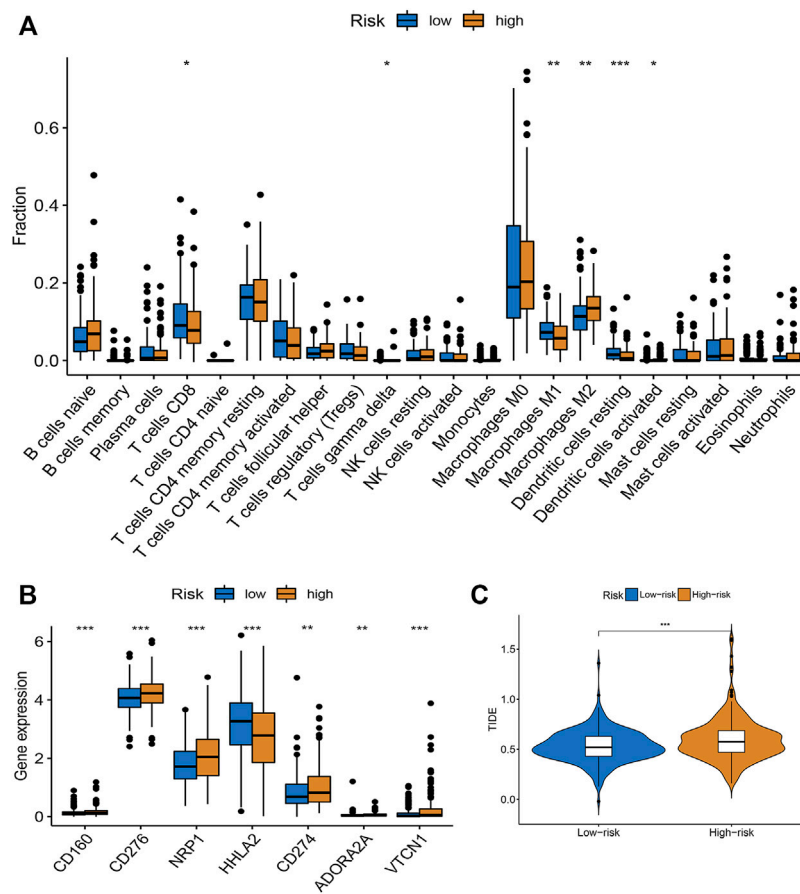


FIGURE 4

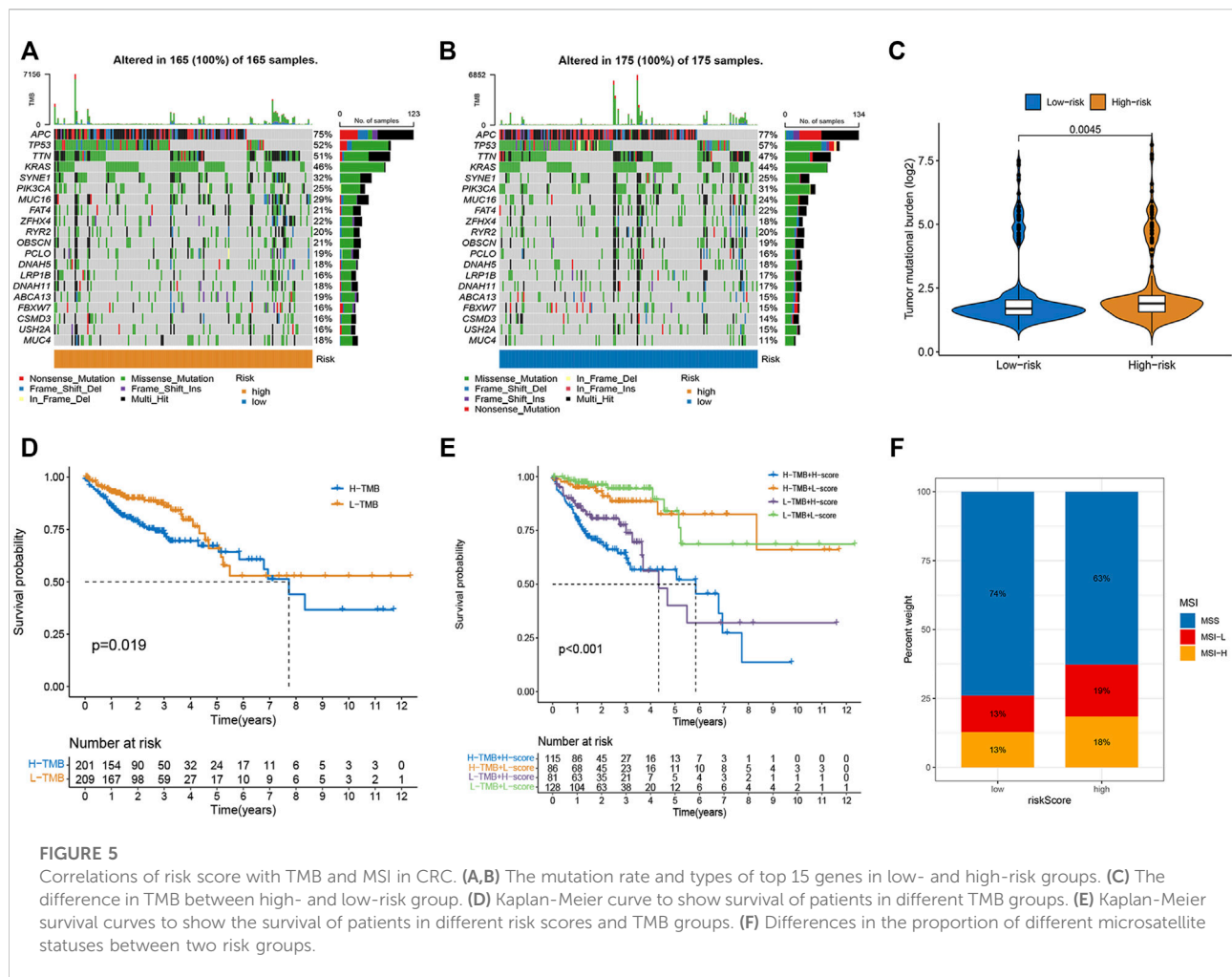
Evaluation of TME and immunotherapy response in different subgroups. (A) Comparison of 22 immune cells between low- and high-risk groups. Median values and IQR for each cell subset were calculated for each patient group and compared between the two groups using the Wilcoxon rank sum test. (B) Expression of common immune checkpoint-related genes in high- and low-risk groups. (C) The difference of stromal score, immune score, and ESTIMATE score between high- and low-risk groups. * $p < 0.05$, ** $p < 0.01$, *** $p < 0.001$.

Evaluation of tumor microenvironment and immunotherapy response

Based on the CIBERSORT algorithm, we noticed a decreased number of activated CD8 + T cells, M1 macrophages, and dendritic cells, as well as resting dendritic cells, and an increased number of M2 macrophages in the high-risk subgroup (Figure 4A). The expression levels of immune checkpoint-related genes in the low- and high-risk subgroups were investigated. We observed that PD-L1 (CD274), CD160, CD276, NRP1, HHLA2, ADORA2A, and VTCN1 levels were increased in the high-risk subgroup (Figure 4B). Moreover, the TIDE algorithm was employed to predict the patient's response to immunotherapy. As illustrated in Figure 4C, higher TIDE scores were observed in the high-risk group than in the low-risk group, indicating that the patients were more prone to immune escape (Figure 4C). Taken together, the risk score may serve as a potential biomarker for predicting the response of patients with CRC to immunotherapy.

Relationship between risk score and tumor mutational burden and microsatellite instability in colorectal cancer

As illustrated in the waterfall charts, the mutated genes in the different risk groups were mainly APC, PIK3CA, SYNE1, KRAS, TTN, TP53, and MUC16, but the mutation rates of these genes were different in the high- and low-risk subgroups (Figures 5A,B). TMB was higher in the high-risk subgroup ($p = 0.004$; Figure 5C), indicating that high-risk patients benefited more from immunotherapy. The Kaplan-Meier survival curve showed that the OS rate was higher in the low TMB group ($p = 0.019$; Figure 5D). A combined analysis of TMB and risk score demonstrated that the risk score was a prognostic factor independent of TMB ($p < 0.001$; Figure 5E). Moreover, higher proportions of MSI-H and MSI-L were observed in the high-risk group than in the low-risk group (Figure 5F).



Exploration of chemotherapy sensitivity

To select potential drugs for patients with CRC, we investigated the correlation between risk scores and drug sensitivity using the “pRRophetic” R package. The IC₅₀ values of doxorubicin, imatinib, JNK Inhibitor VIII, nilotinib, pazopanib, and thapsigargin in the high-risk subgroup were lower, whereas sorafenib and metformin had lower IC₅₀ values in the low-risk subgroup (Figures 6A–H). Taken together, the patients with CRC and high risk scores were more sensitive to doxorubicin, imatinib, JNK inhibitor VIII, nilotinib, pazopanib, and thapsigargin than low risk patients. In contrast, the patients with CRC and low risk scores were more sensitive to sorafenib and metformin.

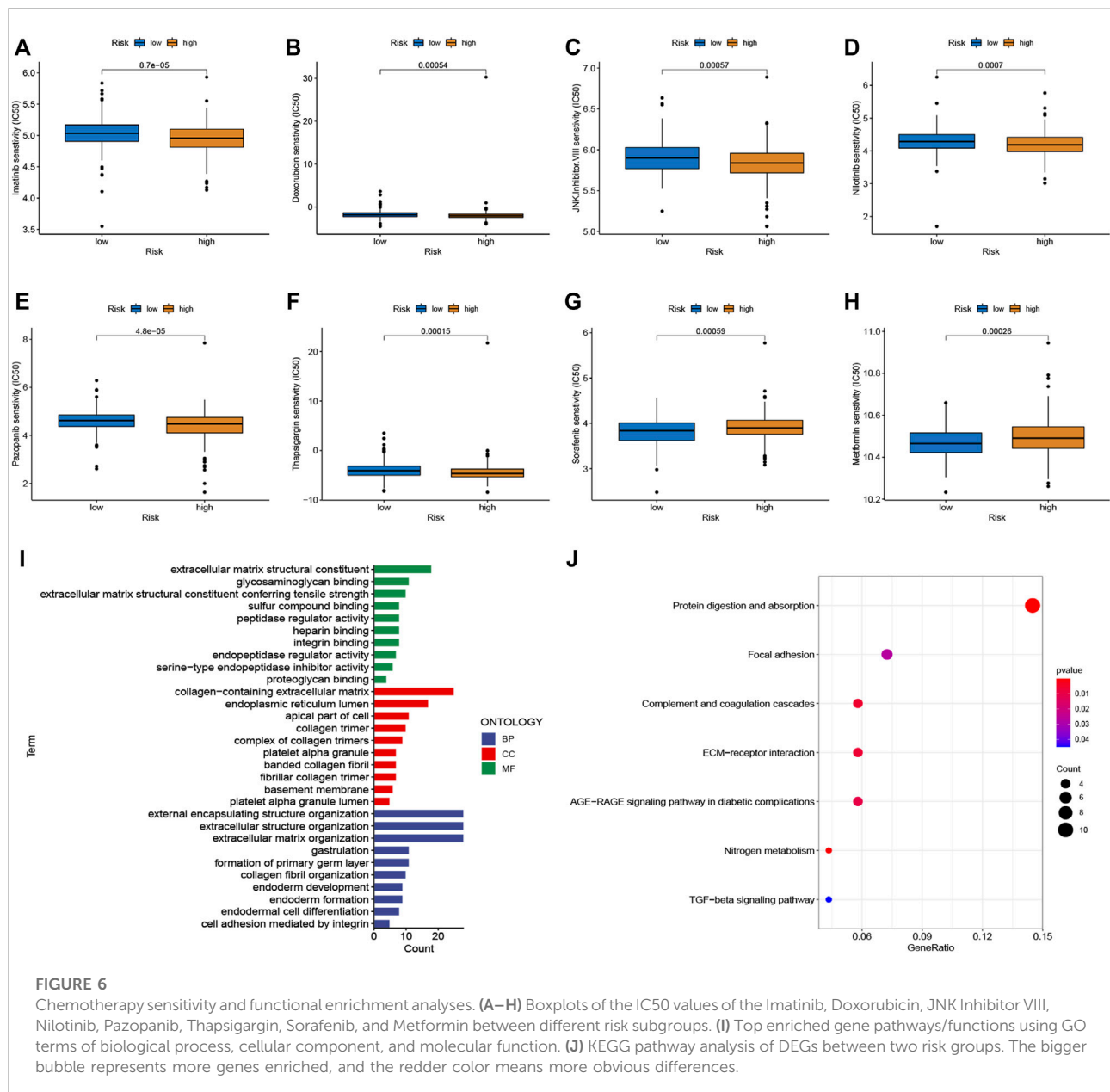
GO and KEGG pathway analysis

We performed functional enrichment analyses to investigate the latent biological processes that affect risk scores. Based on the

criteria of FC > 1.5 and adjusted p-value < 0.05, we screened 262 DEGs in the different risk groups. GO terms indicated enrichment in the collagen-containing extracellular matrix, extracellular matrix structural constituents, and external encapsulating structure organization (Figure 6I). Furthermore, the results of the KEGG pathway analysis, as shown in Figure 6J, suggest that these DEGs were enriched in ECM-receptor interactions, protein digestion, absorption, complement and coagulation cascades, and focal adhesion.

Discussion

CRC is a highly heterogeneous disease, and the difference in heterogeneity provides a complex landscape for the prognosis of patients and their response to immunotherapy. The traditional prognostic evaluation system based on TNM staging has not been able to meet the requirements of precision medicine. Exploring the molecular mechanisms underlying CRC pathogenesis may provide key clues for identifying promising



prognostic biomarkers or developing effective therapeutic targets. A growing number of studies have established that post-transcriptional RNA modifications play a significant role in modulating gene expression, as well as carcinogenesis and development, among which the most common modifications are m6a, m5c, m1a, and m7G (Barbieri and Kouzarides, 2020; Haruehanroengra et al., 2020). Accumulating evidence suggests that m7G modifications actively participate in biological and pathological processes by affecting the metabolism of various RNA molecules. Aberrant m7G levels facilitate tumorigenesis and its progression by regulating multiple oncogenes and tumor suppressor genes (Luo et al.,

2022). However, to the best of our knowledge, few studies have examined the role of m7G regulators and m7G pair-based signatures in CRC as prognostic biomarkers and therapeutic targets. Therefore, the construction of an m7G pair-based signature can not only predict the survival rate of patients but also provide deeper insights into the m7G-mediated immune response and chemoresistance, which will provide novel ideas and methods for determining the pathogenesis and effective treatment modalities for CRC.

In the present study, we developed a novel prognostic signature based on seven m7G gene pairs in patients with CRC using previously identified m7G-related genes with

either higher or lower expression levels. Several m7G-related genes have been reported to be associated with CRC and other cancers. MYC is a master transcription regulator and is one of the most common oncoproteins associated with increased mortality (Castell and Larsson, 2015). MYC activates or represses the transcription of numerous genes involved in cellular processes (Meyer and Penn, 2008). MYC dysregulation occurs in most cancers and is often associated with aggressive disease, treatment resistance, and poor prognosis (Castell and Larsson, 2015). Schmidt et al. (Schmidt et al., 2019) revealed that the MYC-GCN2-eIF2 α negative feedback loop restricts protein synthesis to prevent MYC-dependent apoptosis in CRC (Schmidt et al., 2019). Wu et al. (2021) indicated that MYC could bind to the promoter of the MNX1-AS1 locus and activate its transcription, further promoting CRC progression by stabilizing YB1. XPO1 is a nuclear export protein involved in cancer progression and therapy. Aladhraei et al. (2019) observed that XPO1 expression was elevated in CRC and that XPO1 overexpression was significantly associated with moderately/poorly differentiated tumors and advanced tumor stages. *In vitro* experiments showed that KPT-330, an XPO1 inhibitor, inhibited cancer growth in a dose- and time-dependent manner. Similarly, XPO1 inhibition has been shown to enhance therapeutic response in CRC (Ferreiro-Neira et al., 2016; Inoue et al., 2021). PIK3CA, the gene encoding the alpha catalytic subunit of PI3K, is dysregulated in multiple cancers (Voutsadakis, 2021). It is one of the most frequently mutated oncogenes in CRC. Its mutations are associated with higher gene mutation rates in other important cancer-related pathways, such as the Wnt/ β -catenin and tyrosine kinase receptor/K-Ras/BRAF/MAPK pathways (Voutsadakis, 2021). Additionally, PIK3CA mutations have been reported to be associated with clinicopathological characteristics and prognosis (Mei et al., 2016; Jin et al., 2020).

Infiltrating immune cells are the primary cells in tumor tissues and play vital roles in tumor biology (Hinshaw and Shevde, 2019; Mao et al., 2021). This study investigated the immune status of different risk score groups. The infiltration of immune cells, such as activated CD8⁺ T cell M1 macrophages, activated dendritic cells activated, and resting dendritic cells, in the low-risk group was obviously lower than that of the high-risk subgroup, while the infiltration level of M2 macrophages was increased in the high-risk score group. CD8⁺ T cell infiltration levels are usually associated with favorable clinical outcomes in most solid tumors (van der Leun et al., 2020). The low-risk group was characterized by immune-mediated inflammatory activity, whereas the high-risk group was characterized by immunosuppression. Based on these findings, the worse survival outcomes in high-risk patients may have been caused by the decreased levels of antitumor immunity. Immunotherapy has provided a new perspective on tumor treatment (Riley et al., 2019; Zhang and Zhang, 2020). We assessed the response to immunotherapy in the high- and low-risk groups using the TIDE algorithm (Jiang et al., 2018), and the results showed that the high-risk group had higher TIDE scores,

suggesting a poorer patient response to immunotherapy. Furthermore, we also evaluated the expression of immune checkpoint-related genes and found that PD-L1 (CD274), CD160, CD276, NRP1, HHLA2, ADORA2A, and VTCN1 expression increased in the high-risk score group compared to the low-risk score group, which means that these patients can benefit from ICIs. TMB is a complementary independent biomarker that can predict the efficacy of ICIs (Xiao et al., 2021). In this study, we found that the high-risk group had higher TMB and worse OS. Moreover, the risk score was found to be a prognostic factor independent of TMB. MSI has been used to classify different CRC subtypes (Chen et al., 2018). It is now well-established that patients with MSI-H tend to be more sensitive to ICIs (Lizardo et al., 2020). We found that high-risk scores were associated with MSI-H status in patients with CRC. Research on the sensitivity to chemotherapeutic drugs has always been a hot topic for scientists. We observed that high-risk patients were more sensitive to doxorubicin, imatinib, nilotinib, pazopanib, and thapsigargin, whereas low-risk patients were more sensitive to sorafenib and metformin. Taken together, the m7G pair signature holds promise for predicting the response to immunotherapy and targeted therapy, and it also provides new ideas for the selection of appropriate chemotherapeutic drugs.

Nevertheless, this study has some limitations. First, the signature was conducted based on public databases, which may have been influenced by inherent case selection bias. Second, clinical tissues and CRC cell lines should be employed to validate the expression levels of signature genes, and further investigation and experiments are needed to explore the detailed regulatory effects of m7G-related genes in CRC.

We established a novel m7G pair-based risk signature based on seven m7G-related pairs in CRC. The risk score is closely related to the clinical features and prognosis of patients. The nomogram can serve as a counseling and clinical decision aid for clinicians. Tumor microenvironment analysis established a theoretical framework for future research on the connection between immunity and m7G-related genes in CRC.

Data availability statement

Publicly available datasets were analyzed in this study. This data can be found here: The public datasets were obtained from TCGA (<https://portal.gdc.cancer.gov/>) and GEO (<https://www.ncbi.nlm.nih.gov/geo/>).

Author contributions

All authors listed have made a substantial, direct, and intellectual contribution to the work and approved it for publication.

Conflict of interest

The authors declare that the research was conducted in the absence of any commercial or financial relationships that could be construed as a potential conflict of interest.

Publisher's note

All claims expressed in this article are solely those of the authors and do not necessarily represent those of their affiliated organizations, or those of the publisher, the editors and the reviewers. Any product that may be

evaluated in this article, or claim that may be made by its manufacturer, is not guaranteed or endorsed by the publisher.

Supplementary material

The Supplementary Material for this article can be found online at: <https://www.frontiersin.org/articles/10.3389/fgene.2022.981392/full#supplementary-material>

SUPPLEMENTARY FIGURE S1

Univariate Cox regression analysis of the variables affecting the prognosis of CRC patients.

References

- Aladhraei, M., Kassem Al-Thobhani, A., Pongvarin, N., and Suwannalert, P. (2019). Association of XPO1 overexpression with NF- κ B and Ki67 in colorectal cancer. *Asian Pac. J. Cancer Prev.* 20, 3747–3754. doi:10.31557/apjcp.2019.20.12.3747
- Alexandrov, A., Martzen, M. R., and Phizicky, E. M. (2002). Two proteins that form a complex are required for 7-methylguanosine modification of yeast tRNA. *Rna* 8, 1253–1266. doi:10.1017/s1355838202024019
- An, Y., and Duan, H. (2022). The role of m6A RNA methylation in cancer metabolism. *Mol. Cancer* 21, 14. doi:10.1186/s12943-022-01500-4
- Barbieri, I., and Kouzarides, T. (2020). Role of RNA modifications in cancer. *Nat. Rev. Cancer* 20, 303–322. doi:10.1038/s41568-020-0253-2
- Basak, D., Uddin, M. N., and Hancock, J. (2020). The role of oxidative stress and its counteractive utility in colorectal cancer (CRC). *Cancers (Basel)* 12, E3336. doi:10.3390/cancers12113336
- Castell, A., and Larsson, L. G. (2015). Targeting MYC translation in colorectal cancer. *Cancer Discov.* 5, 701–703. doi:10.1158/2159-8290.Cd-15-0660
- Chen, B., Jiang, W., Huang, Y., Zhang, J., Yu, P., Wu, L., et al. (2022). N(7)-methylguanosine tRNA modification promotes tumorigenesis and chemoresistance through WNT/ β -catenin pathway in nasopharyngeal carcinoma. *Oncogene* 41, 2239–2253. doi:10.1038/s41388-022-02250-9
- Chen, L., Pan, X., Hu, X., Zhang, Y. H., Wang, S., Huang, T., et al. (2018). Gene expression differences among different MSI statuses in colorectal cancer. *Int. J. Cancer* 143, 1731–1740. doi:10.1002/ijc.31554
- Dai, Z., Liu, H., Liao, J., Huang, C., Ren, X., Zhu, W., et al. (2021). N(7)-Methylguanosine tRNA modification enhances oncogenic mRNA translation and promotes intrahepatic cholangiocarcinoma progression. *Mol. Cell* 81, 3339–3355.e8. doi:10.1016/j.molcel.2021.07.003
- Ferreiro-Neira, I., Torres, N. E., Liesenfeld, L. F., Chan, C. H., Penson, T., Landesman, Y., et al. (2016). XPO1 inhibition enhances radiation response in preclinical models of rectal cancer. *Clin. Cancer Res.* 22, 1663–1673. doi:10.1158/1078-0432.Ccr-15-0978
- Frye, M., Harada, B. T., Behm, M., and He, C. (2018). RNA modifications modulate gene expression during development. *Science* 361, 1346–1349. doi:10.1126/science.aau1646
- Geeleher, P., Cox, N., and Huang, R. S. (2014). pRRophetic: an R package for prediction of clinical chemotherapeutic response from tumor gene expression levels. *PLoS One* 9, e107468. doi:10.1371/journal.pone.0107468
- Han, H., Yang, C., Ma, J., Zhang, S., Zheng, S., Ling, R., et al. (2022). N(7)-methylguanosine tRNA modification promotes esophageal squamous cell carcinoma tumorigenesis via the RPTOR/ULK1/autophagy axis. *Nat. Commun.* 13, 1478. doi:10.1038/s41467-022-29125-7
- Haruehanroengra, P., Zheng, Y. Y., Zhou, Y., Huang, Y., and Sheng, J. (2020). RNA modifications and cancer. *RNA Biol.* 17, 1560–1575. doi:10.1080/15476286.2020.1722449
- He, L., Li, H., Wu, A., Peng, Y., Shu, G., and Yin, G. (2019). Functions of N6-methyladenosine and its role in cancer. *Mol. Cancer* 18, 176. doi:10.1186/s12943-019-1109-9
- Heinäniemi, M., Nykter, M., Kramer, R., Wienecke-Baldacchino, A., Sinkkonen, L., Zhou, J. X., et al. (2013). Gene-pair expression signatures reveal lineage control. *Nat. Methods* 10, 577–583. doi:10.1038/nmeth.2445
- Hinshaw, D. C., and Shevde, L. A. (2019). The tumor microenvironment innately modulates cancer progression. *Cancer Res.* 79, 4557–4566. doi:10.1158/0008-5472.Can-18-3962
- Inoue, A., Robinson, F. S., Minelli, R., Tomihara, H., Rizi, B. S., Rose, J. L., et al. (2021). Sequential administration of XPO1 and ATR inhibitors enhances therapeutic response in TP53-mutated colorectal cancer. *Gastroenterology* 161, 196–210. doi:10.1053/j.gastro.2021.03.022
- Jiang, P., Gu, S., Pan, D., Fu, J., Sahu, A., Hu, X., et al. (2018). Signatures of T cell dysfunction and exclusion predict cancer immunotherapy response. *Nat. Med.* 24, 1550–1558. doi:10.1038/s41591-018-0136-1
- Jin, J., Shi, Y., Zhang, S., and Yang, S. (2020). PIK3CA mutation and clinicopathological features of colorectal cancer: A systematic review and meta-analysis. *Acta Oncol.* 59, 66–74. doi:10.1080/0284186x.2019.1664764
- Kanth, P., and Inadomi, J. M. (2021). Screening and prevention of colorectal cancer. *Bmj* 374, n1855. doi:10.1136/bmj.n1855
- Lizardo, D. Y., Kuang, C., Hao, S., Yu, J., Huang, Y., and Zhang, L. (2020). Immunotherapy efficacy on mismatch repair-deficient colorectal cancer: From bench to bedside. *Biochim. Biophys. Acta. Rev. Cancer* 1874, 188447. doi:10.1016/j.bbcan.2020.188447
- Luo, Y., Yao, Y., Wu, P., Zi, X., Sun, N., and He, J. (2022). The potential role of N(7)-methylguanosine (m7G) in cancer. *J. Hematol. Oncol.* 15, 63. doi:10.1186/s13045-022-01285-5
- Ma, J., Han, H., Huang, Y., Yang, C., Zheng, S., Cai, T., et al. (2021). METTL1/WDR4-mediated m(7)G tRNA modifications and m(7)G codon usage promote mRNA translation and lung cancer progression. *Mol. Ther.* 29, 3422–3435. doi:10.1016/j.ymthe.2021.08.005
- Mao, X., Xu, J., Wang, W., Liang, C., Hua, J., Liu, J., et al. (2021). Crosstalk between cancer-associated fibroblasts and immune cells in the tumor microenvironment: New findings and future perspectives. *Mol. Cancer* 20, 131. doi:10.1186/s12943-021-01428-1
- Mei, Z. B., Duan, C. Y., Li, C. B., Cui, L., and Ogino, S. (2016). Prognostic role of tumor PIK3CA mutation in colorectal cancer: A systematic review and meta-analysis. *Ann. Oncol.* 27, 1836–1848. doi:10.1093/annonc/mdw264
- Meyer, R., and Penn, L. Z. (2008). Reflecting on 25 years with MYC. *Nat. Rev. Cancer* 8, 976–990. doi:10.1038/nrc2231
- Ming, J., and Wang, C. (2022). N7-Methylguanosine-Related lncRNAs: Integrated analysis associated with prognosis and progression in clear cell renal cell carcinoma. *Front. Genet.* 13, 871899. doi:10.3389/fgene.2022.871899
- Pandolfini, L., Barbieri, I., Bannister, A. J., Hendrick, A., Andrews, B., Webster, N., et al. (2019). METTL1 promotes let-7 MicroRNA processing via m7G methylation. *Mol. Cell* 74, 1278–1290. doi:10.1016/j.molcel.2019.03.040
- Riley, R. S., June, C. H., Langer, R., and Mitchell, M. J. (2019). Delivery technologies for cancer immunotherapy. *Nat. Rev. Drug Discov.* 18, 175–196. doi:10.1038/s41573-018-0006-z

- Schmidt, S., Gay, D., Uthe, F. W., Denk, S., Paauwe, M., Matthes, N., et al. (2019). A MYC-GCN2-eIF2 α negative feedback loop limits protein synthesis to prevent MYC-dependent apoptosis in colorectal cancer. *Nat. Cell Biol.* 21, 1413–1424. doi:10.1038/s41556-019-0408-0
- Shi, H., Chai, P., Jia, R., and Fan, X. (2020). Novel insight into the regulatory roles of diverse RNA modifications: Re-Defining the bridge between transcription and translation. *Mol. Cancer* 19, 78. doi:10.1186/s12943-020-01194-6
- Shi, H., Wei, J., and He, C. (2019). Where, when, and how: Context-dependent functions of RNA methylation writers, readers, and erasers. *Mol. Cell* 74, 640–650. doi:10.1016/j.molcel.2019.04.025
- Siegel, R. L., Miller, K. D., Fuchs, H. E., and Jemal, A. (2021). Cancer statistics, 2021. *Ca. Cancer J. Clin.* 71, 7–33. doi:10.3322/caac.21654
- Song, P., Tayier, S., Cai, Z., and Jia, G. (2021). RNA methylation in mammalian development and cancer. *Cell Biol. Toxicol.* 37, 811–831. doi:10.1007/s10565-021-09627-8
- Sung, H., Ferlay, J., Siegel, R. L., Laversanne, M., Soerjomataram, I., Jemal, A., et al. (2021). Global cancer statistics 2020: GLOBOCAN estimates of incidence and mortality worldwide for 36 cancers in 185 countries. *Ca. Cancer J. Clin.* 71, 209–249. doi:10.3322/caac.21660
- van der Leun, A. M., Thommen, D. S., and Schumacher, T. N. (2020). CD8(+) T cell states in human cancer: Insights from single-cell analysis. *Nat. Rev. Cancer* 20, 218–232. doi:10.1038/s41568-019-0235-4
- Voutsadakis, I. A. (2021). The landscape of PIK3CA mutations in colorectal cancer. *Clin. Colorectal Cancer* 20, 201–215. doi:10.1016/j.clcc.2021.02.003
- Wei, J., and He, C. (2021). Chromatin and transcriptional regulation by reversible RNA methylation. *Curr. Opin. Cell Biol.* 70, 109–115. doi:10.1016/j.ceb.2020.11.005
- Wu, Q. N., Luo, X. J., Liu, J., Lu, Y. X., Wang, Y., Qi, J., et al. (2021). MYC-activated LncRNA MNX1-AS1 promotes the progression of colorectal cancer by stabilizing YB1. *Cancer Res.* 81, 2636–2650. doi:10.1158/0008-5472.Can-20-3747
- Xiao, J., Li, W., Huang, Y., Huang, M., Li, S., Zhai, X., et al. (2021). A next-generation sequencing-based strategy combining microsatellite instability and tumor mutation burden for comprehensive molecular diagnosis of advanced colorectal cancer. *BMC Cancer* 21, 282. doi:10.1186/s12885-021-07942-1
- Zhang, M., Song, J., Yuan, W., Zhang, W., and Sun, Z. (2021). Roles of RNA methylation on tumor immunity and clinical implications. *Front. Immunol.* 12, 641507. doi:10.3389/fimmu.2021.641507
- Zhang, Q., Liu, F., Chen, W., Miao, H., Liang, H., Liao, Z., et al. (2021). The role of RNA m(5)C modification in cancer metastasis. *Int. J. Biol. Sci.* 17, 3369–3380. doi:10.7150/ijbs.61439
- Zhang, Y., and Zhang, Z. (2020). The history and advances in cancer immunotherapy: Understanding the characteristics of tumor-infiltrating immune cells and their therapeutic implications. *Cell. Mol. Immunol.* 17, 807–821. doi:10.1038/s41423-020-0488-6

Frontiers in Cell and Developmental Biology

Explores the fundamental biological processes of life, covering intracellular and extracellular dynamics.

The world's most cited developmental biology journal, advancing our understanding of the fundamental processes of life. It explores a wide spectrum of cell and developmental biology, covering intracellular and extracellular dynamics.

Discover the latest Research Topics

[See more →](#)

Frontiers

Avenue du Tribunal-Fédéral 34
1005 Lausanne, Switzerland
frontiersin.org

Contact us

+41 (0)21 510 17 00
frontiersin.org/about/contact

